ORNL/TM-2015/588

Effect of Alkali-Silica Reaction on Shear Strength of Reinforced Concrete Structural Members

Victor Saouma
Mohammad Hariri-Ardebili
Yann LePape

September 2015

OAK RIDGE NATIONAL LABORATORY
MANAGED BY UT-BATTELLE FOR THE US DEPARTMENT OF ENERGY

ORNL/TM-2015/588

Light Water Reactors Sustainability Program

Effect of Alkali-Silica Reaction on Shear Strength of Reinforced Concrete Structural Members

Victor Saouma
Mohammad Hariri-Ardebili
Yann Le Pape

September 2015
University of Colorado, Boulder CO 80309-0428

OAK RIDGE NATIONAL LABORATORY
P.O. Box 2008
Oak Ridge, Tennessee 37831-6285
managed by
UT-Battelle, LLC
for the
US DEPARTMENT OF ENERGY
under contract DE-AC05-00OR22725

CONTENTS

LIST OF FIGURES

Figures **Page**

LIST OF TABLES

Tables **Page**

EXECUTIVE SUMMARY

CONTEXT

Alkali-silica reaction (ASR) was discovered in the early 40s by Stanton (1940) of the California Division of Highways. Since, it has been recognized as a major degradation mechanism for concrete dams and transportation infrastructures. Sometimes described as the 'cancer of concrete', this internal swelling mechanism causes expansion, cracking and loss of mechanical properties. There are no known economically viable solutions applicable to massive concrete to prevent the reaction once initiated. The efficiency of the mitigation strategies for ASR subjected structures is limited. Several cases of ASR in nuclear generating stations have been disclosed in Japan (Takatura et al. 2005), Canada at Gentilly 2 NPP (Tcherner and Aziz 2009) [1], and more recently, in the United States for which the U.S. Nuclear Regulatory Commission issued Information Notice (IN) 2011-20, 'Concrete Degradation by Alkali Silica Reaction,' on November 18, 2011, to provide the industry with information related to the ASR identified at Seabrook. Considering that US commercial reactors in operation enter the age when ASR degradation can be visually detected and that numerous non nuclear infrastructures (transportation, energy production) have already experienced ASR in a large majority of the States (e.g., Department of Transportation survey reported by Touma (Touma 2000)), the susceptibility and significance of ASR for nuclear concrete structures must be addressed in the perspective of license renewal and long-term operation beyond 60 years.

STRUCTURAL SIGNIFICANCE OF ASR IN NUCLEAR POWER PLANTS

Because of exposure, dimension and reinforcement ratio differences, the evaluation of the structural significance of ASR on affected concrete in nuclear power plants can not be directly transposed from the transportation infrastructures or concrete dam though the methodological pathways are similar to a large extent. The absence of shear reinforcement (i.e., in the thickness) allowed by ACI 318 (Building Code Requirements for Reinforced Concrete) is common resulting in an absence of confinement that favors the out-of-plane ASR expansion. Hence the shear bearing capacity relies primarily on plain concrete. The residual shear capacity (accidental design scenario) of ASR-affected structures like the biological shield building, the containment building and the fuel handling building will depend on two competitive mechanisms: (i) the extent of the micro-cracking easing the propagation of a shear fracture and (ii) the relative in-plane confinement-induced compression in the direction of the reinforcement potentially limiting the propagation of shear fracture. This question remaining unresolved, further investigation is needed to determine the potential impact of ASR on the structural resistance of nuclear structures.

METHODOLOGY

Structural members representative of portions of Class I-safety concrete nuclear structures, e.g., containment building, internal structures, are studied using the finite element code *Merlin* (**?**). This code has been specifically developed for modeling fracture problems and structures subjected to alkali-silica reaction. It has been validated against various experimental results and has been applied successfully to model hydro-power dams and electricity transportation infrastructures.

Three structural members, namely a beam, a truncated beam and a panel, having similar geometrical characteristics in the zone subjected to shear, in terms of dimensions and reinforcement ratios, have been modeled.

[1] In 2012 however, following an early attempt to extend the life of Gentilly 2 until 2040 (with an approx. $1.9B overhaul), Hydro-Quebec announced its decommissioning after 29 years for economic reasons. (Saouma 2013b)

A parametric study has been conducted by varying the depth of the members, the reinforcement ratio, the boundary conditions (more or less restrained), the residual concrete strength post ASR, the residual Young modulus post ASR and the level of ASR expansion. For each set of parameters, the pre-ASR (reference) and post-ASR, out-of-plane shear resistance are computed and compared. In total, 648 simulations (computation cost between 6 and 60 hours per simulation) were performed and analyzed by statistical methods.

RESULTS

Amongst the full set of 648 analyses, 53% resulted in overall post-ASR shear strength decrease, and 47% in an increase. The range of variation in post-ASR shear strength is particularly wide. Hence, the role of the structural constraint during the development of ASR appears critical to the out-of plane shear resistance of the structures, which results from the competition between the ASR-induced prestressing of reinforced concrete and the degradation of the materials properties. Decrease is more likely to occur when the ASR strain is at its highest value (0.003) for the restrained boundary conditions. These results indicate that each structural configuration needs to be studied specifically. This implies, in particular, that large-scale laboratory test results may not be directly applicable to other in-situ structural configuration. However, these tests provide valuable data for the validation of structural models that can be applied subsequently to analyze the resilience of Class I-safety nuclear concrete structures under accidental scenarios. It is recommended that a full three-dimensional analysis of such structures be undertaken to further confirm this finding.

PERPECTIVES

The features of the ASR model used in Merlin are currently being implemented in GRIZZLY by INL (RISMiC pathway).

The LWRS MaaD pathway has launched a research operation in collaboration between ORNL, the University of Tennessee, the University of Alabama, the University of Colorado, INL (LWRS OLM pathway) and PNNL to build large ASR-mockup subjected to unrestrained and restrained structural effects to study the development of ASR expansion and damage (2016-18), and subsequently, the residual out-of-plane shear capacity (2018-19). These mockups will serve the purpose of validation of the models implemented in GRIZZLY.

Chapter 1

Modeling Strategy

1.1 INTRODUCTION

Whereas alkali-silica reaction (ASR), or alkali-aggregate reaction (AAR), has been reported in numerous dams, only recently has there been evidence of such occurrences in nuclear power plants (NPP): In Japan, Ikata No.1, Shikoku Electric Power (Shimizu et al. 2005), Canada, Gentilly 2 (Sanborn 2015), and the US Seabrook (ML121160422 2012, Haberman 2013). Yet, AAR has seldom, if ever, been investigated in connection with Class I-safety concrete structures (containment building (CCB), internal structures, spent-fuel handling building) damage (as opposed to dams).

Of major importance is the shear strength of the containment vessel when it had been degraded by ASR (Barbosa et al. 2014) and then subjected to an earthquake. This problem may be further aggravated by the lack of shear reinforcement permitted by ACI 318 provision.

The aim of this report is to perform an extensive parametric series of 3D nonlinear finite element analyses of three different "beam-like" geometries, including two different depths, three different types of boundary conditions, and four other parameters: namely, the ASR volumetric expansion, the reinforcement ratio, the loss of elastic modulus induced by ASR and the loss of tensile strength caused by ASR.

In all cases, the structural component are allowed to undertake the full ASR induced expansion (under various boundary conidtions), and then are subjected to a monotonically increasing out-of-plane shear force, i.e. in the perpendicular direction of the reinforcement layers.

The results of the numerical simulations are analyzed in terms of a reduced set of output parameters:

ASR Only without shear load:

- Out of plane ASR induced expansion.
- Longitudinal and lateral reinforcement (corresponding to vertical and hoop) stresses.

ASR+Shear will be compared with identical analyses without ASR, and extracted will be:

- Shear strength reduction.
- Initial stiffness reduction.

The outcome of these 648 analysis are summarized in a database and attempt is being made to answer the following questions:

1. What is the impact of ASR on the shear strength?

2. In case of reduction, under which conditions and by how much?

1.2 MODEL SELECTION

The representativity of the analyzed structural components in regard to an actual CBB geometry is illustrated in Fig. 1.1(a). On the left side, are sketched the beam, truncated beam and the panel under investigation. Correspondingly, the right side shows the concrete model which will be separately tested by the first author within the framework of an NRC grant. Figure 1.1(b) presents in greater details the load support as well as the reinforcement of the container. To facilitate the visualization, the vertical reinforcement will be shown in blue and hoop reinforcement in red, Fig. 1.1(c) and 1.1(d). Because of the large curvature radius of the CBB, reinforcement are considered straight for the sake of simplicity.

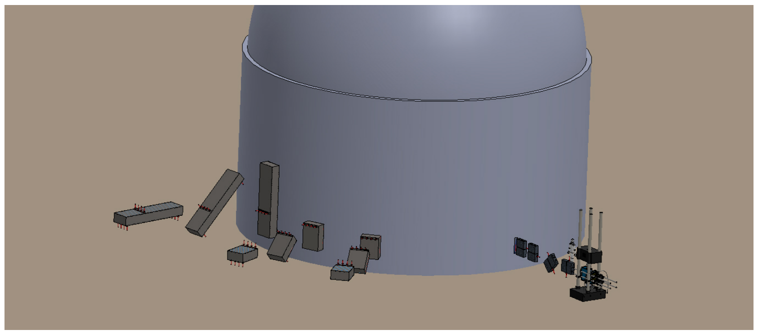

(a) Computational and Laboratory Models

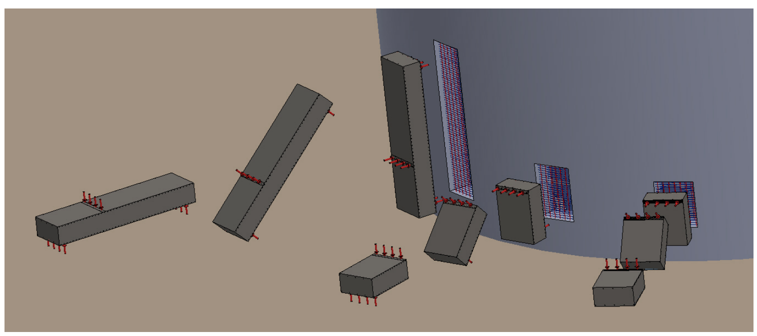

(b) Computational Models;

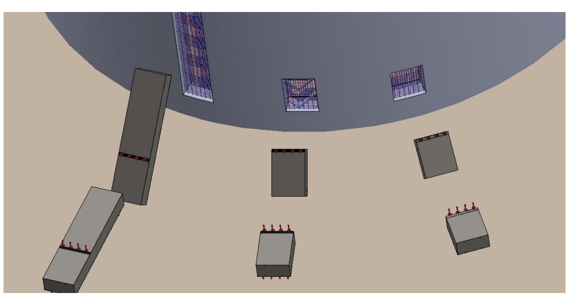

(c) Longitudinal and Circular Reinforcement; Structural Analysis;

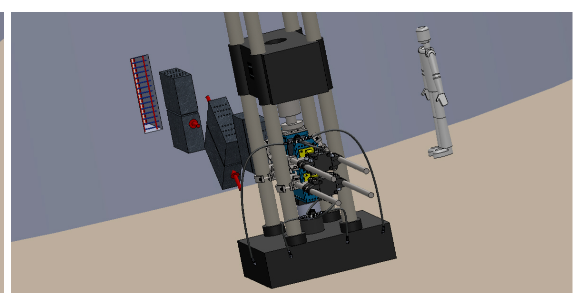

(d) Longitudinal and Circular Reinforcement; Structural Analysis;

Fig. 1.1. From Containment Shell to Concrete Model; Beam, Truncated Beam and Panel (from left to Right)

1.3 BOUNDARY CONDITIONS

As stated earlier, two sets of boundary conditions are considered: those applicable during ASR expansion, and those applicable during the external shear force application. The former is to capture potential ASR strain realignments caused by external constraints (Multon 2004) as implemented in the author's model (Saouma and Perotti 2006).

The choice of the varied geometries (beam, truncated beam and panel) and boundary conditions (unrestrained, restrained and fully restrained) reflects an attempt to model more or less structural restraints as existing in actual Class I-safety concrete structure due to the presence of adjacent or internal structures, as well as, other connecting structural members (basemat, floors, walls).

The boundary conditions are first shown schematically in Fig. 1.5. Details are also provided in Table 1.1.

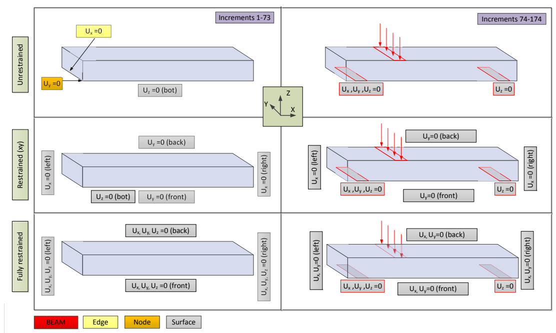

Fig. 1.2. Beam Boundary Conditions

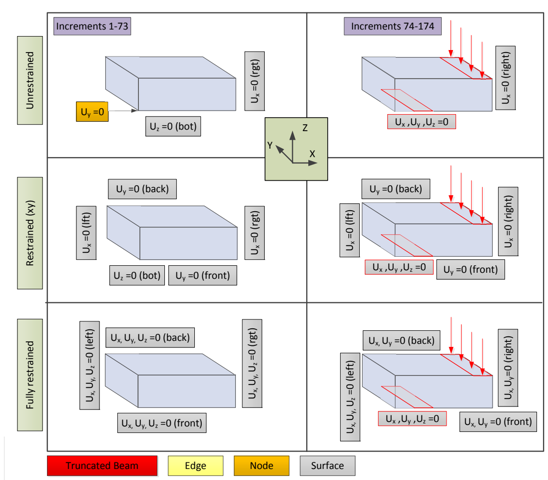

Fig. 1.3. Truncated Beam Boundary Conditions

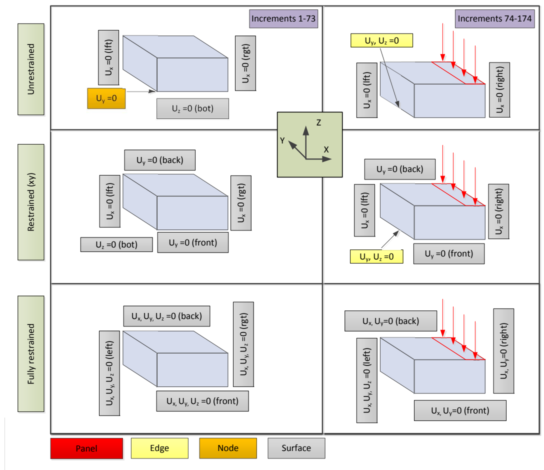

Fig. 1.4. Panel Boundary Conditions

Spec.	BC	Bottom			Front			Back			left			Right		
		x	y	z	x	y	z	x	y	z	x	y	z	x	y	z
AAR Expansion (incr. 1-73)																
B	U	-	-	●	-	-	-	-	-	-		1		-	-	-
	R	-	-	●	-	●	-	-	●	-	●	-	-	●	-	-
	FR	-	-	-	●	●	●	●	●	●	●	●	●	●	●	●
TB	U	-	-	●	-	-	-	-	-	-		2		●	-	-
	R	-	-	●	-	●	-	-	●	-	●	-	-	●	-	-
	FR	-	-	-	●	●	●	●	●	●	●	●	●	●	●	●
P	U	-	-	●	-	-	-	-	-	-	●	3	-	●	-	-
	R	-	-	●	-	●	-	-	●	-	●	-	-	●	-	-
	FR	-	-	-	●	●	●	●	●	●	●	●	●	●	●	●
Shear Load (incr. 74-174)																
B	U		4		-	-	-	-	-	-	-	-	-	-	-	-
	R		4		-	●	-	-	●	●	-	-	●	-	-	-
	FR		4		●	●	-	●	●	-	●	●	-	●	●	-
TB	U		5		-	-	-	-	-	-	-	-	-	●	-	-
	R		5		-	●	-	-	●	-	●	-	-	●	-	-
	FR		5		●	●	-	●	●	-	●	●	●	●	●	-
P	U	-	-	-	-	-	-	-	-	-	●	6	●	-	-	-
	R	-	-	-	-	●	-	-	●	-	●	6	-	●	-	-
	FR	-	-	-	●	●	-	●	●	-	●	●	●	●	●	-

1:xxx;2:xxx; 3:xx;

4:xxx 5:xxx; 6:xx

Table 1.1. Boundary Conditions for AAR Expansion

Finally, given the importance of the BCs, those are better visualized in Fig. 1.6, 1.7 and 1.8, for the beam, the truncated beam and the panel respectively. It should be noted that in all cases components are

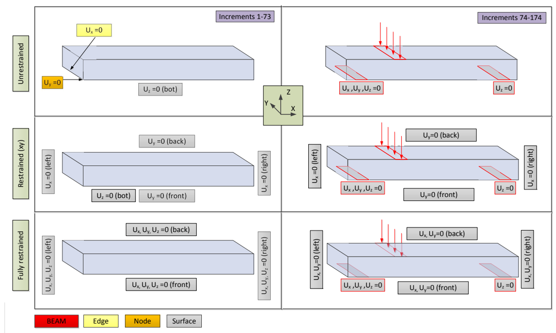

(a) Beam Boundary Conditions

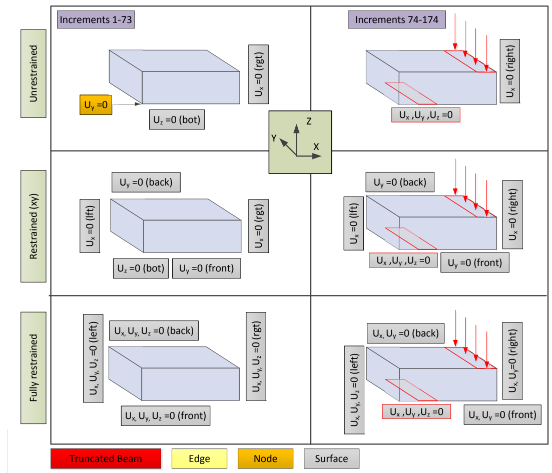

(b) Truncated Beam Boundary Conditions

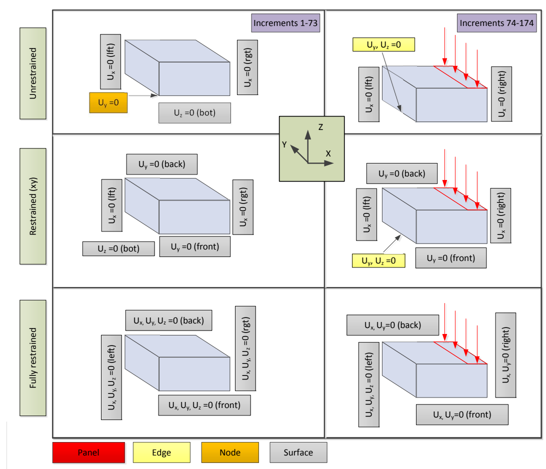

(c) Panel Boundary Conditions

Fig. 1.5. Boundary Conditions

drawn to scale.

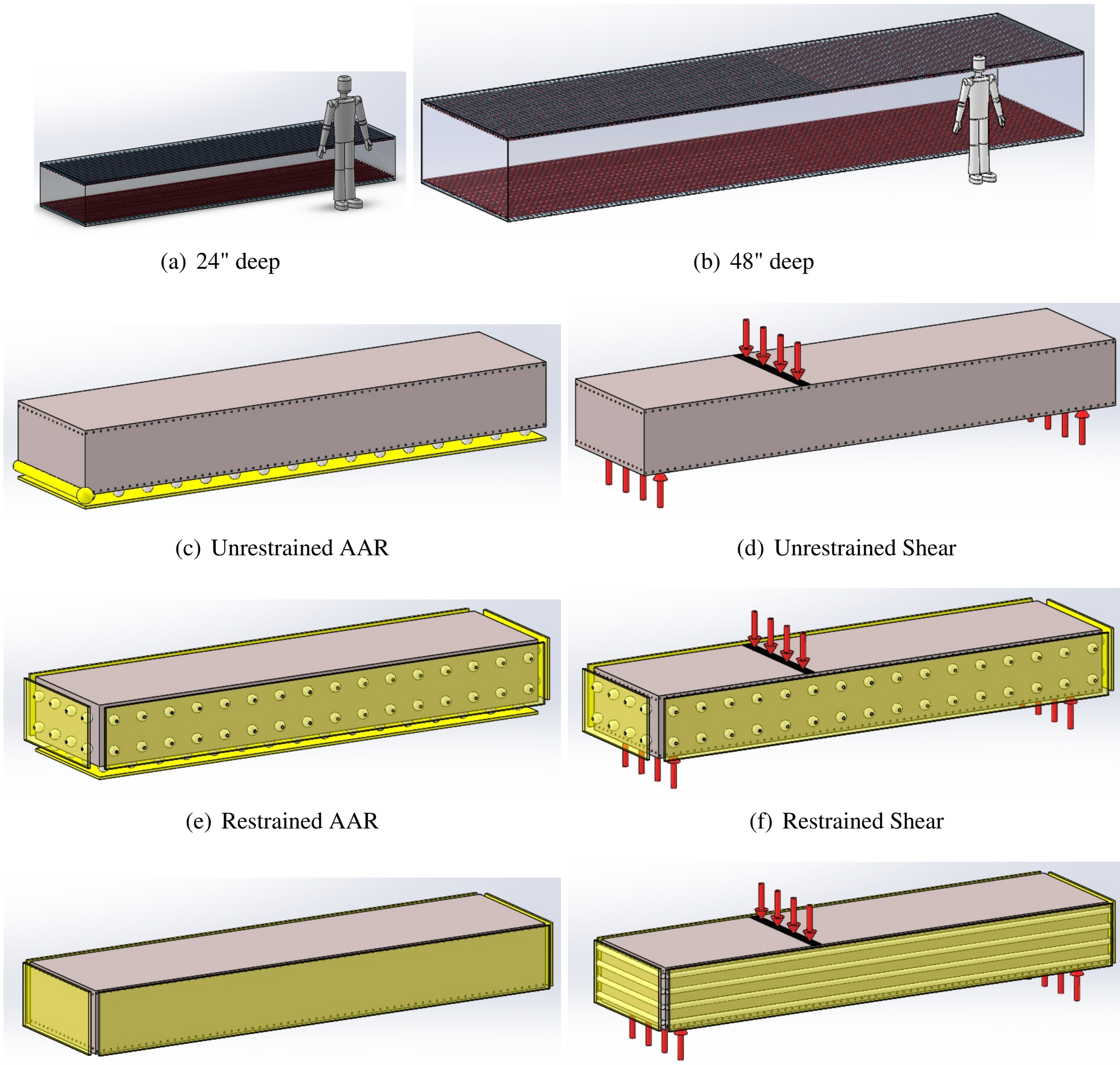

(a) 24" deep

(b) 48" deep

(c) Unrestrained AAR

(d) Unrestrained Shear

(e) Restrained AAR

(f) Restrained Shear

(g) Fully Restrained AAR

(h) Fully Restrained Shear

Fig. 1.6. Boundary Conditions for the Beam

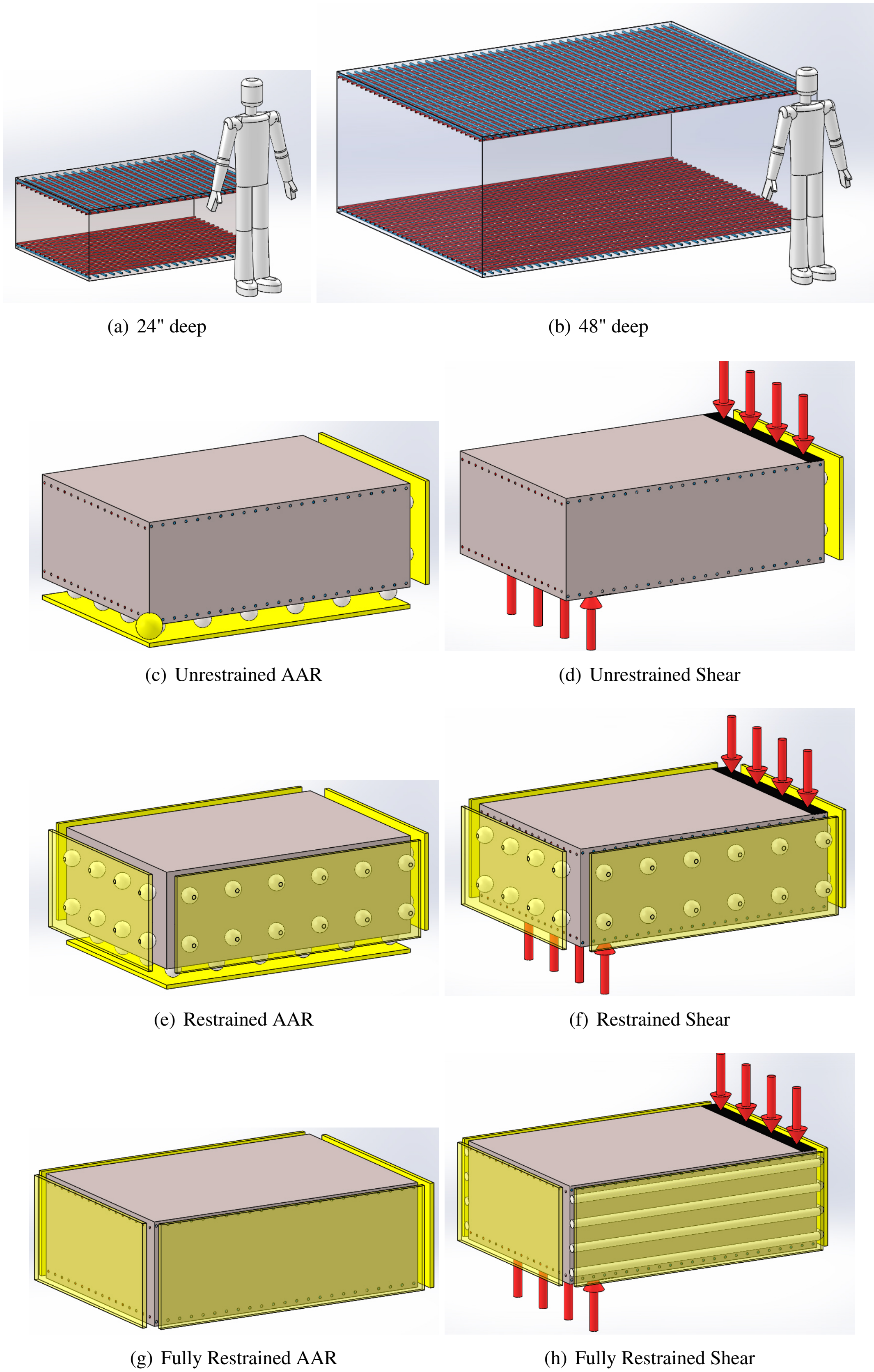

(a) 24" deep

(b) 48" deep

(c) Unrestrained AAR

(d) Unrestrained Shear

(e) Restrained AAR

(f) Restrained Shear

(g) Fully Restrained AAR

(h) Fully Restrained Shear

Fig. 1.7. Boundary Conditions for the Truncated Beam

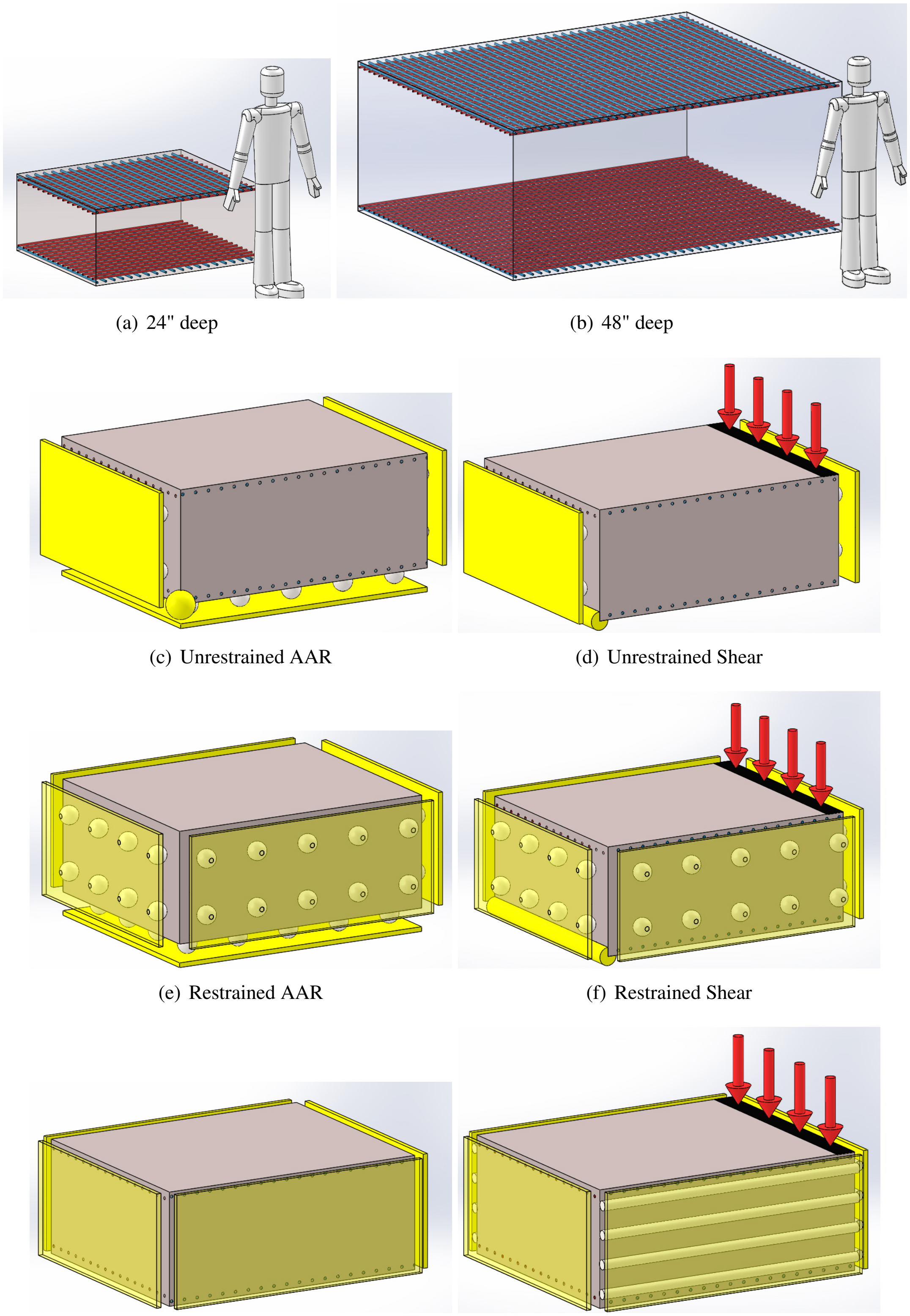

(a) 24" deep (b) 48" deep

(c) Unrestrained AAR (d) Unrestrained Shear

(e) Restrained AAR (f) Restrained Shear

(g) Fully Restrained AAR (h) Fully Restrained Shear

Fig. 1.8. Boundary Conditions for the Panel

1.4 DIMENSIONS

Two different depths are considered: 24 and 48 inches in a attempt to cover the range of Class I-safety reinforced concrete walls in NPPs. In particular, the thickness of the CCB is typically greater than 3 feet. Actual dimensions of the three structural members under consideration in this study are shown in Fig. 1.9 with reference to Table 1.2.

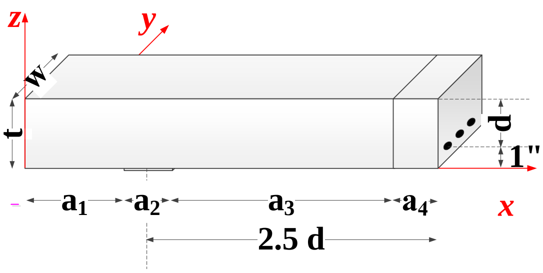

(a) Truncated Beam

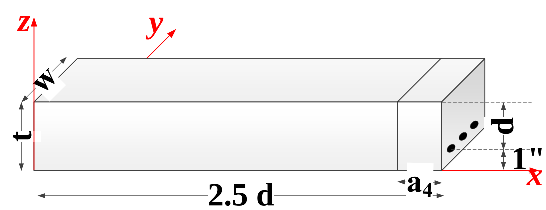

(b) Panel

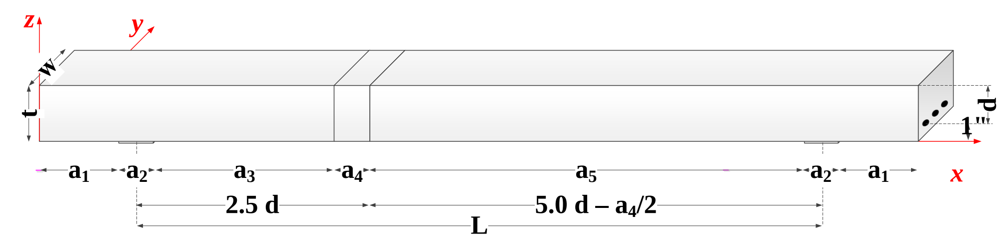

(c) Beam

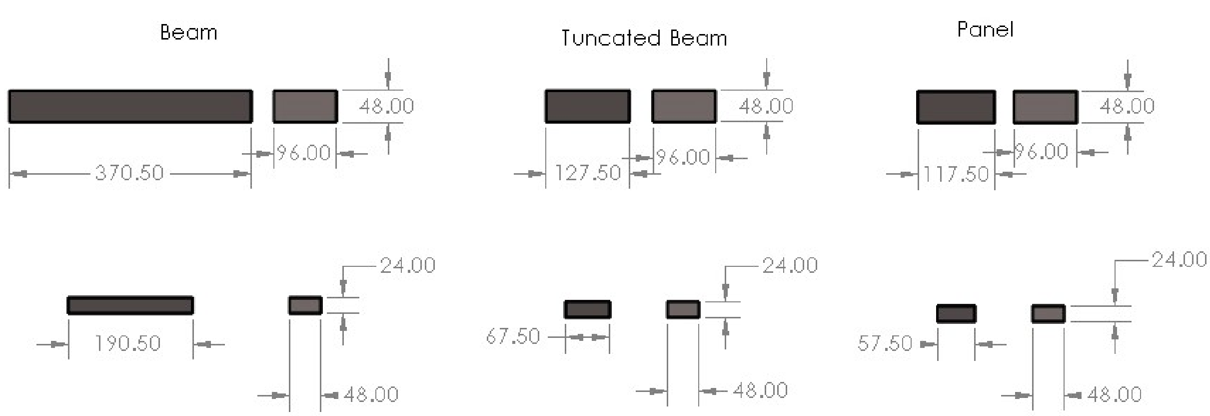

(d) Physical Dimensions (inches)

Fig. 1.9. Dimensions

Table 1.2. Models dimensions (in)

Model	Sub-model	a_1	a_2	a_3	a_4	a_5	d	L_{tot}	w	t
B	B2	8	4	51.5	4	111	23	190.5	48	24
	B4	8	4	111.5	4	231	47	370.5	96	48
TB	TB2	8	4	51.5	4	-	23	67.5	48	24
	TB4	8	4	111.5	4	-	47	127.5	96	48
P	P2	-	-	-	4	-	23	57.5	48	24
	P4	-	-	-	4	-	47	117.5	96	48

1.5 FINITE ELEMENT MESHES AND ANALYSES

The finite element meshes were generated using Kumo (Saouma 2009). The prepared 6 meshes are shown in Fig. 1.10 with the indication of the number of nodes and elements shown (same numbers for 24" and 48") in Table 1.3. 3D eight-node linear continuum elements are used in all cases. Meshes were "optimized" so as to guaranty sufficient refinement, yet to be computationally "affordable". This was achieved by testing various meshes, convergence criteria and comparing displacements. The refined mesh is used at the location of applied load and also support (for the beam and truncated beam models) to capture properly the load transfer mechanism and also possible cracking at these locations.

Geometry	# of Nodes	# of Elements
Beam	1,520	1.036
Truncated Beam	1,323	960
Panel	2,233	1,680

Table 1.3. Finite Element Mesh Characteristics

All analyses were performed with the Merlin finite element code (Saouma et al. 2010) using the Secant Newton algorithm and setting the maximum number of iterations to 300. Convergence criterion for both energy (ratio of the absolute values of the external work done by the applied incremental loads and the residual loads for the current increment) and displacements (ratio of the Euclidean norms of the iterative displacement correction and incremental displacement vectors) was set to 0.01. Though far from ideal, these analyses were compared with others having a tighter convergence criteria and though oscillatory behaviors in the post-shear failure, i.e., post-peak, were observed, they were kept in the interest of computability. A rotating crack model was used.

Four workstations are used to perform the analyses (Intel(R) Xenon(R) 3.6 GHz, RAM 8.00 GB). Each simulation lead a computational cost between 6 and 60 hours. Higher computational time is a results of bad combination of the random variables.

In all AAR simulation followed by a shear test (AAA+Shear), AAR was applied through the first 73 increments), while the incremental shear was applied starting from increment 74 through 174. At the end of the AAR expansion, visualization of results was made to assess that the full expansion was reached.

Finally, it should be noted that a good indicator for discarding results is the out-of-plane displacements. It was arbitrarily assumed that out-of-plane displacement exceeding 5 mm implied automatic discard of the corresponding simulation.

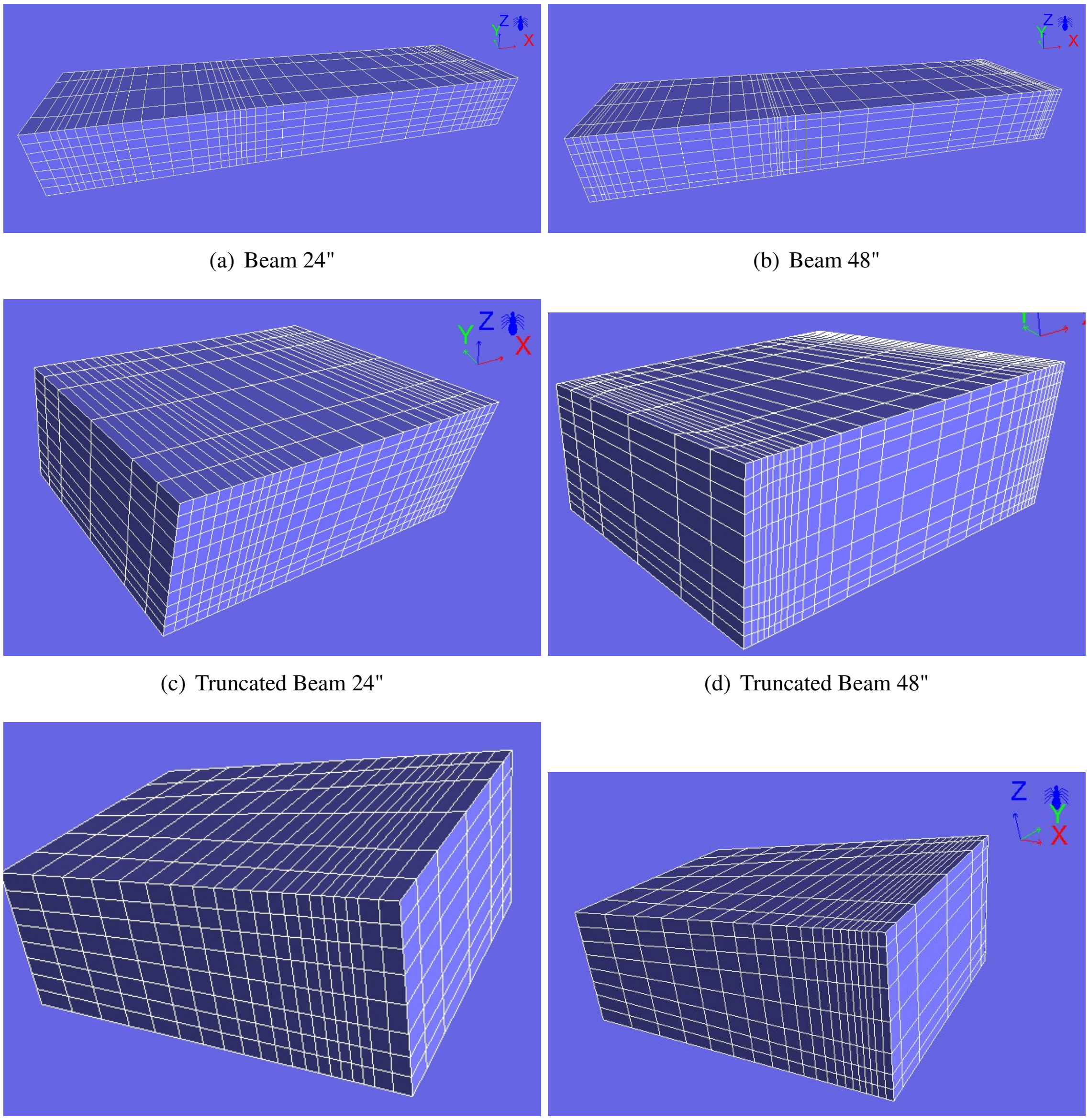

(a) Beam 24"

(b) Beam 48"

(c) Truncated Beam 24"

(d) Truncated Beam 48"

(e) Panel 24"

(f) Panel 48"

Fig. 1.10. Finite Element Meshes

1.6 VARIABLES

Two set of meshes are generated:

ASR + Shear in which seven variables were included in the study, Table 1.4. Thus, for each of the three geometries a total of ($3 \times 2 \times 3 \times 3 \times 2 \times 2$) 216 meshes were generated, i.e. 648 total.

Reference with no ASR modeling. For each of the three geometries a total of ($3 \times 3 \times 2 \times 3$) 54 meshes were generated (or 162 total).

Table 1.4. **Varying Parameters**

Variable	Values
Geometry	Beam (B), Truncated Beam (TB), Panel (P)
Boundary Conditions	Unrestrained, Restrained, Partially Restrained
	AAR+Shear
Thickness	2 ft, 4 ft
AAR Expansion	0.1%, 0.2%, 0.3%
Reinforcement Ratio	0.2%, 0.5%, 1%
Residual Elastic Modulus	0.7, 0.9
Residual Tensile Strength	0.7, 0.9
	AAR
Geometry	Beam (B), Truncated Beam (TB), Panel (P)
Boundary Conditions	Unrestrained, Restrained, Partially Restrained
Thickness	2 ft, 4 ft
Reinforcement Ratio	0.2%, 0.5%, 1%

File names have the following naming convention: **i-A-B-C-D-E-F-G**, where

i Counter
A Geometry (B|TB|P) for beam, truncated beam or panel.
B Depth (2|4) for 24" and 48".
C Boundary Conditions (U|R|FR) for unrestrained, restrained, and fully restrained.
D Final volumetric AAR expansion ε^{∞} (1|2|3) for 0.1%, 0.2% 0.3%.
E Reinforcement ratio ρ (2|5|10) for 0.2% 0.5% and 1%.
F Residual Young modulus relative coefficient β_E (7|9) for 70% and 90%.
G Residual tensile strength relative coefficient β_{ft} (7|9) for 70% and 90%.

The generated meshes are listed in Table 3.1 (Appendix).

1.7 MATERIAL PROPERTIES

The material properties for the nonlinear concrete model (described in Sect. 1.1.2) are given in Table 1.5. The materials properties for reinforcement are provided in Table 1.6. Those of the ASR model (described in Sect. 1.1.1) are shown in Table 1.7. Details of the constitutive model are provided in appendix 1.1, 44.

Table 1.5. Characteristics of concrete (Smeared Crack Model)

Characteristics	Symbol	Unit	Value
Mass density	ρ	kg/m^3	2,250
Modulus of elasticity	E	MPa	26,000
Poisson's ratio	ν	-	0.2
Tensile strength	f_t	MPa	3.1
Exponential softening	G_F	MN/m	1.5e-4
Compressive strength	f_c	MPa	-31.0
Critical displacement in compression	w_d	m	-0.0005
Factor beta for return direction	β	-	0
Factor *e* for roundness of failure surface	e	-	0.55
Onset of nonlinearity in compression	f_{c0}	MPa	-20
Plastic strain at compressive strength	ϵ_{cp}	-	-0.001

Table 1.6. Characteristics of rebar

Characteristics	Symbol	Unit	Value
Cross-sectional area	A_o	mm^2	Variable
Mass per unit length	ρ_l	kg/m	7.924
Elastic modulus	E	MPa	200,000
Poisson's ratio	ν	-	0.3
Yield stress	σ_Y	MPa	248

Table 1.7. Characteristics of the AAR model. ATU: arbitrary time unit

Characteristics	Symbol	Unit	Value
Maximum volumetric strain at temperature T_0^{test}	$\varepsilon_{AAR}^{\infty}$	-	Variable
Characteristic time at temperature θ_0^{test}=273+T_0^{test}	τ_C	ATU	7.58
Latency time at temperature θ_0^{test}=273+T_0^{test}	τ_L	ATU	17.71
Activation energy associated with τ_C	U_C	^{o}K	5,400
Activation energy associated with τ_L	U_L	^{o}K	9,400
Residual reduction factor	Γ_r	-	0.5
Fraction of ε_t prior to reduction of AAR expansion due to macro cracking	γ_t	-	0.5
Compressive strength	f_c'	MPa	-31
Tensile strength	f_t'	MPa	3.1
Shape parameter	a	-	0
Reference temperature	T_0	^{o}C	35
Upper compressive stress beyond which there is no more AAR expansion	σ_U	MPa	-8
Reduction fraction for Young's Modulus when AAR reaction ends	β_E	-	Variable
Reduction faction for tensile strength when AAR reaction ends	β_f	-	Variable

1.8 FILE GENERATION

Given the large number of analyses, the simulations were automated to the extent possible using 5 consecutive Matlab based codes `P1.m, P2.m, P3.m, P4.m` and `P5.m` (See Fig. 1.11 for details).

P1 starts with the mesh generator Kumo to create a generic finite element mesh for a given geometry, depth and boundary conditions (hence a total of 18 files). The created mesh are post-processed by the program `P1.m` to insert the additional features (reinforcement ratio and AAR expansion). This process is performed for all *AAR+Shear* cases, as well as the 6 *Shear* cases only. This will result in the creation of $3 \times (216 + 18) = 702$ input files

P2 run the 702 analyses with Merlin, which represent by far, the most computationally intensive task.

P3 read the Merlin output files (ASCII) and save the relevant results in binary format as individual `.mat` files.

P4 consolidates all the 702 individual `.mat` files into a single master file. Subsequently, it provides a comparison, for each set of parameters, between the case without AAR and the corresponding case with AAR. Finally, it computes:

ASR only (at the end of increment 73):

- Longitudinal and transversal reinforcement maximum stress, strain, mean and standard deviation and outliers.
- Expansion of the middle upper and lower point.

ASR + Shear (increments 74 through 174):

- Evaluation of initial stiffnesses, and corresponding decrease due to ASR.
- Evaluation of peak load and corresponding decrease due to ASR.

P5 performs the final postprocessing:

P5_a generates the 648 individual plots of load displacements, expansion and reinforcement.

P5_b sorts all results and generates LaTeX code included in this report.

P5_c generates 24 3D plots showing the percent reduction in shear strength in terms of maximum AAR expansion and reinforcement ratio. Similarly another 24 plots are generated for the out-of-plane expansion.

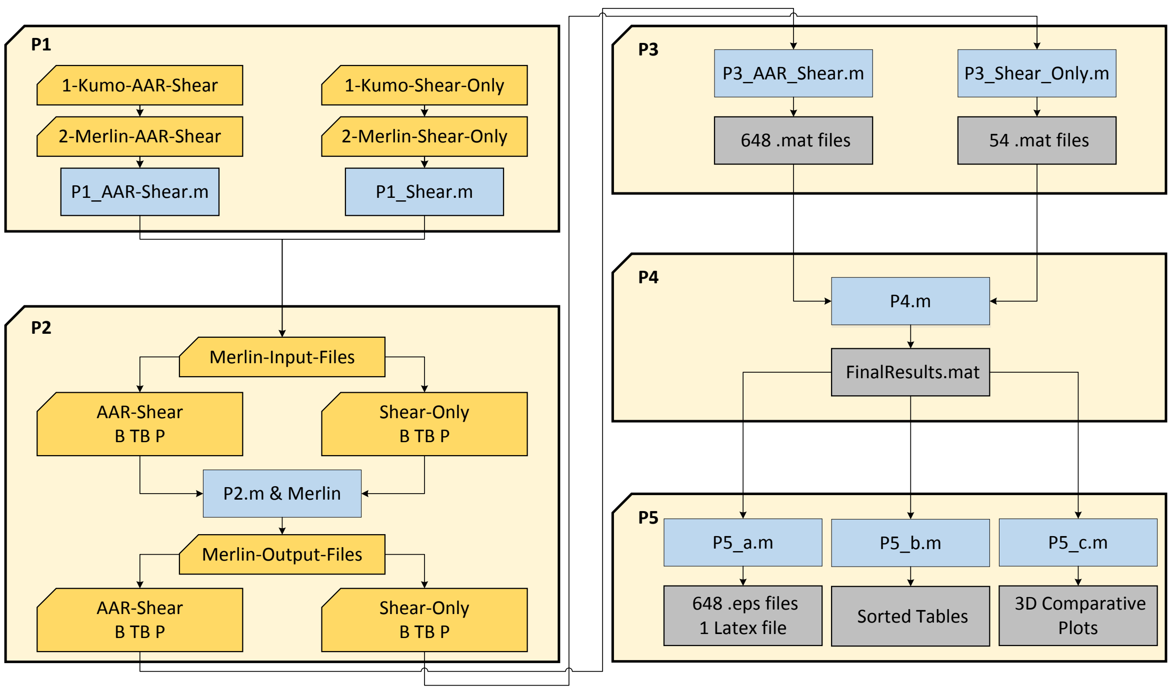

Fig. 1.11. Files generation flowchart.

Chapter 2

Results and Interpretation

2.1 INTRODUCTION

2.1.1 RESULT INTERPRETATION PARADIGM

A compilation of all unsorted results, i.e., sorted by alphabetical file names is initially tabulated in the long table 4.1, p. 85. For each simulation, the variations of the shear capacity and capacity resulting from AAR are presented along with the AAR dimensional change in the unreinforced direction of the structural element, and median and maximum stresses in the reinforcement bars in both directions.

4.2, p. 87, presents the results by sorting the simulations results in terms of variations of structural stiffness. The obtained stiffness variation ranges from a loss of $\approx -100\%$, i.e., full loss, to a gain of $\approx +300\%$. Statistical analysis is discussed later

Similarly, 4.3, p. 89, 4.4, p. 98, and 4.7, p. 112 present similar output tables, obtained by sorting the output data in terms of variation of ultimate shear capacity (range of variation $-100\%/+120\%$), yield shear capacity (range of variation $-100\%/+550\%$) and transverse reinforcement stresses (range of variation $0/+240$ MPa), respectively.

Note that the ultimate shear capacity is the absolute peak of the curve, whereas the yield value is defined as the shear deviating by 15% from the tangent, figure 2.1. Whereas this definition of the yield shear may appear to be arbitrary, it was the most appropriate one to automate for the hundreds of analysis. Results sorted by the ultimate and yield shear stresses are shown in Tables 4.3 and 4.4 respectively.

Furthermore, 2D plots, similar to the one of Fig 2.2 are listed in Figs 4.1.1.1 to 4.1.3.216 for the individual analysis results, and 3D plots, similar to the one in Fig. 2.3 are listed in Fig. 4.2.1 to 4.2.24.

In the 2D plots, the top-left portion shows the shear behavior in term of shear force vs. the shear displacement before ("only shear", solid red line) and after AAR ("AAR+shear". solid blue line). The variation of shear strength and stiffness are also provided in legend. The top-right portion shows the progression of the AAR out-of-plane expansion as a function of the computation increments. Full expansion at the end of the 73$^{\text{rd}}$ is expected. The lower plots correspond to the representation of the stress distribution in the longitudinal and transverse reinforcing bar using *box-and-whisker* diagrams, also known as *boxplots*: the median value is represented by the red line; the 50% confidence intervale by the solid blue box; The upper adjacent value (right bar) is the value of the largest stress that is less than or equal to the upper quartile plus 1.5 the length of the interquartile range. Analogously the lower adjacent value (left mark) is the value of the smallest observation that is greater than or equal to the lower quartile less 1.5 times the length of interquartile range. Outliers (red crosses) are stresses outside lower-upper mark range.

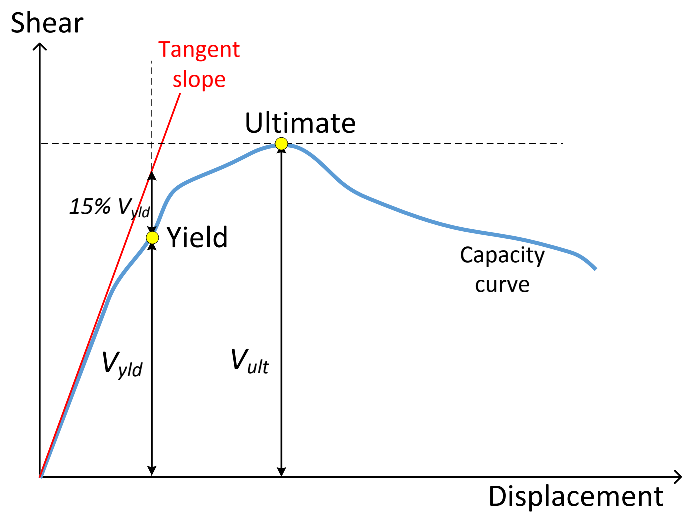

Fig. 2.1. Definition of yield and ultimate points on the capacity curve

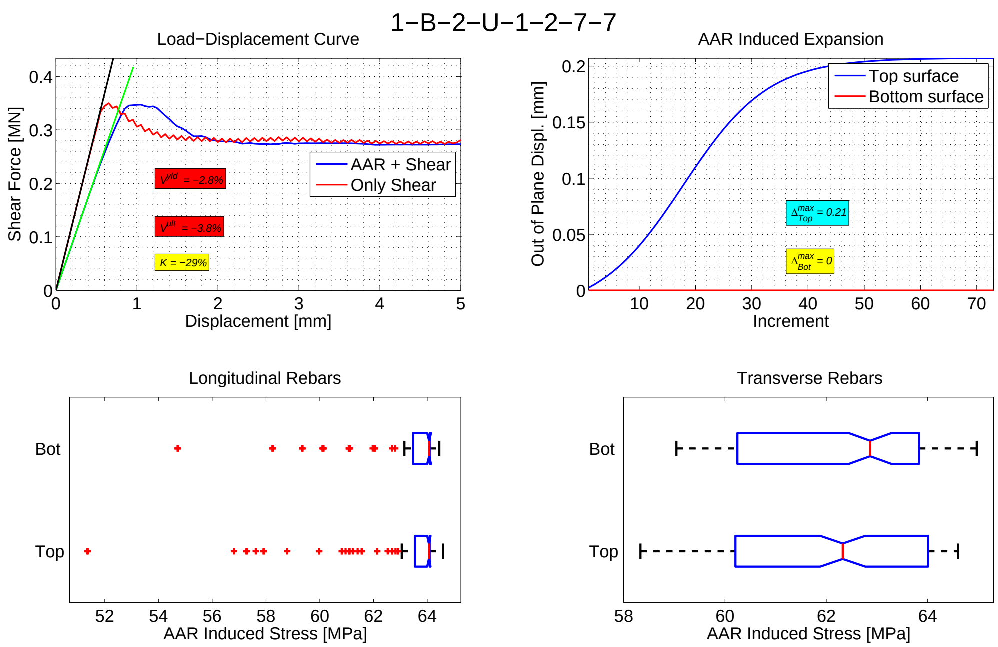

Fig. 2.2. Example of all individual 2D plots in Sect. 4.1

Though we started by looking at individual results, it quickly became clear that such an effort was not only monumental but could easily lead to erroneous interpretation.

As such, it was rapidly concluded that a thorough statistical analysis of results was the only solution, and this was performed with the R statistical analysis package, R Core Team (2015). This analysis will be reported below. For individual analysis results, the reader should consult appendix D.

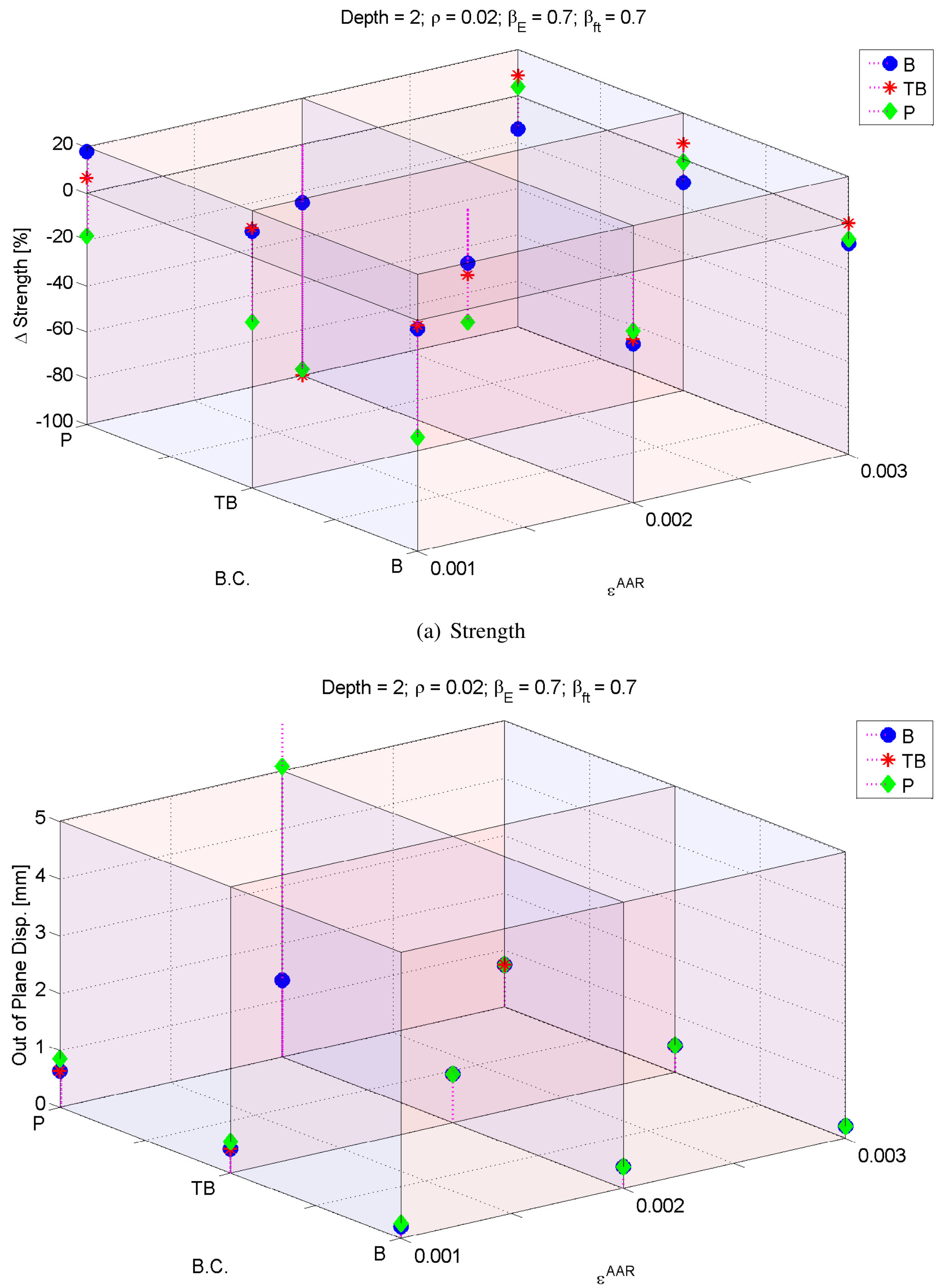

(a) Strength

(b) Displacement

Fig. 2.3. Example of Generated 3D plots in Section 4.2

2.1.2 AAR EFFECTS ON MATERIAL AND STRUCTURES

The interaction of AAR with concrete shear strength is of primary interest. At the material level, the concrete degrades and undoubtedly its shear resistance decreased. On the other hand, at the structural level, AAR induces additional compressive stresses, similar to a prestressing effect, which increase the shear resistance of the structural component. An illustration of this effect is given by the analysis of the simple Mohr-Coulomb equation:

$$\tau = c + \sigma \tan \phi \tag{2.1}$$

For a cohesion of $c = 3$ MPa and an internal friction angle of $\phi = 40^o$, then for a compressive stress σ of 0, 3 and 5 MPa, the resulting shear strength would be 3.0, 5.5 and 7.2 MPa respectively. Furthermore, the AAR expansion is likely to reduce the crack opening due to shear, hence additional aggregate interlock is present, (Blight and Alexander 2008).

The nonlinear numerical model used in Merlin is a fracture-plastic based on the work (and implemented by) Cervenka and Papanikolaou (2008). It combines constitutive models for tensile (fracturing) and compressive (plastic) behavior. The fracture model is based on the classical orthotropic smeared crack formulation and crack band model. It employs Rankine failure criterion, exponential (or user defined) softening, and it can be used as rotated or fixed crack model. The hardening/softening plasticity model is based on (Menétrey and Willam 1995) failure surface. Both models use return mapping algorithm for the integration of constitutive equations. The model can be used to simulate concrete cracking, crushing under high confinement, and crack closure due to crushing in other material directions. Dowel effects are not modeled, while interlocking effects are implicitly accounted for. Hence, the model does take into account the confining effect and will result in higher shear strength.

As such, differentiation will be made between results showing positive or negative shear strength changes. This task is simply achieved by properly filtering the R dataset in terms of the shear strength change. Amongst the full set of 648 analyses, 53% resulted in overall shear strength decrease, and 47% in an increase.

Finally, it must be noted that simulations exhibiting an out-of-plane displacement greater 5 mm are automatically discarded as numerical errors (caused by the limited number of iterations) is very likely to have resulted in a lack of convergence and thus unreliable results.

2.1.3 STATISTICAL ANALYSIS

In this second part of statistical based data interpretation, we seek to develop a model for the shear strength change not to gain a mathematical model *per se* that could be plotted (as it will not make sense as some of the variables are unordered categorical variables), but rather to identify the most relevant parameters amongst those used. In this exercise, each of the 18 sub-variables in Table 2.1 will be separately considered. Multiple Linear Regression analysis, described in some details in Appendix B will be used.

Three fitting models are considered:

1. Full data set.
    - General model: Based on all sub-variables
    - Best model based on Akaike Information Criterion (AIC): Filters the final sub-variables based on AIC
    - Best model based on Bayesian Information Criterion (BIC): Filters the final sub-variables based on BIC
2. Positive Shear Strength Change Data Set.
    - General model

- Best model based on AIC
- Best model based on BIC

3. Negative Shear Strength Change Data Set.

   - General model
   - Best model based on AIC
   - Best model based on BIC

2.2 JOINT STATISTICAL ANALYSIS OF THE FULL DATASET

2.2.1 BOXPLOTS AND HISTOGRAMS

Before any statistical model is built (to assess influence of various parameters), all results are show as boxplots and histograms. However, rather than dealing with the 7 classes of main variables, it was deemed necessary to express the model in terms of each one of their constituents, Table 2.1.

Table 2.1. Main classes of variables and R Sub-variables

Main Variables		Analyses	Normalized R	R Sub-variables
1	Type	B	1	1
		TB	2	2
		P	3	3
2	Depth	24"	2	4
		48"	4	5
3	B.C.	U	1	6
		R	2	7
		FR	3	8
4	ε	0.001	1	9
		0.002	2	10
		0.003	3	11
5	ρ	0.02	1	12
		0.05	2	13
		0.1	3	14
6	β_E	0.7	1	15
		0.9	2	16
7	β_{ft}	0.7	1	17
		0.9	2	18

It should be noted that the R code internally uses normalized/integer values for each of the 18 subvariables.

Boxplots for each of the 18 sub-variables will be presented in the next section. For each specific case, it will be assumed to be a function of that specific sub-variable and the coupled effect of all 17 others.

The analysis separates the simulations for which the shear strength increases form those showing a decrease of the shear strength.

2.2.1.1 Shear Strength Increase

Fig. 2.4 shows the boxplots for the shear strength increase. The following observations can be made:

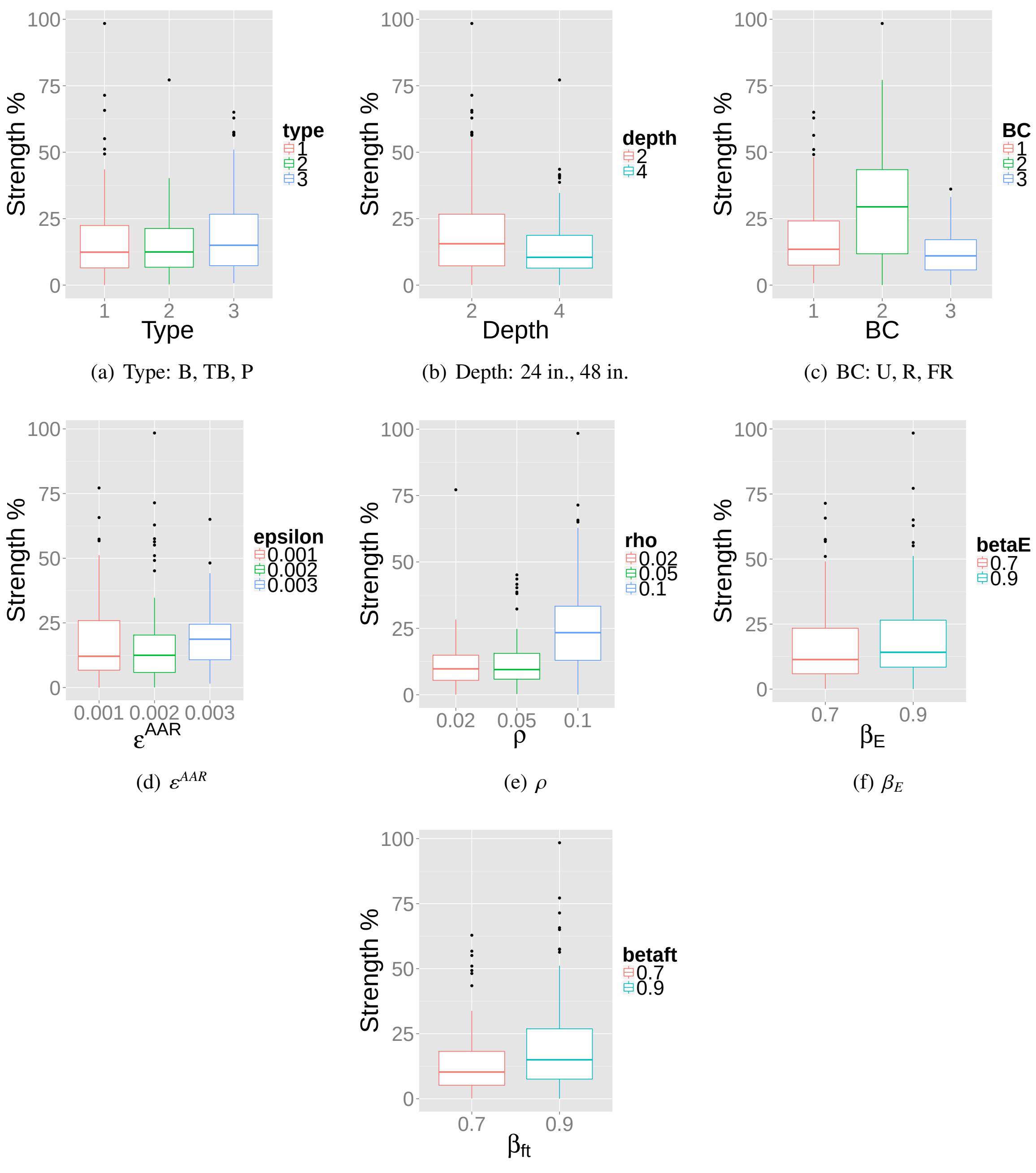

(a) Type: B, TB, P

(b) Depth: 24 in., 48 in.

(c) BC: U, R, FR

(d) ε^{AAR}

(e) ρ

(f) β_E

(g) β_{ft}

Fig. 2.4. Boxplots for Shear Strength Increase in terms of each of the seven variables

- The impact of nature of the structural elements, B and TB geometries, on the shear strength increase is nearly identical; however, P geometry leads to increased variability, Fig. 2.4(a).

- 24"-thick specimens (smaller dimensions) have a slightly larger shear strength increase, possibly attributed to a size effect, than the larger specimens, Fig. 2.4(b).
- Larger reinforcement (higher ρ) leads to larger shear strength increase, Fig. 2.4(e).
- Higher reduction in β_E results in higher reduction in stiffness, Fig. 2.4(f).
- Similarly, a larger decrease in β_{ft} results in smaller increase in strength, Fig. 2.4(g).

It should be noted that in all the above, factors of influence are what one may anticipate, although their quantitative impact may be judged quite limited.

Fig. 2.5(a) shows the histogram of the data set for shear strength increase (due to AAR). The data set follows a lognormal distribution. About 70% of the data falls in the range [0; 20%]. Finally, Fig. 2.5(b) shows the probability distribution function (PDF) of this data set.

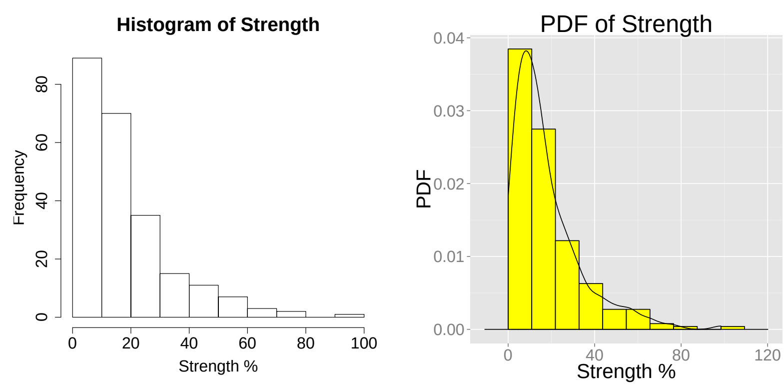

(a) Histogram (b) Probability Distribution Function

Fig. 2.5. Histograms for Shear Strength Increase

Fig. 2.6 shows the strength increase in terms of the AAR induced out-of-plane displacements. The graph has been limited to displacements less than 2.5 mm. Most of the data points fall in the range of [0; 20%] for the strength and [0; 1mm] for the displacement. The scatter plot shows no correlation between the residual strength and the AAR expansion, which can not be used as a direct indicator of the residual structural capacity.

2.2.1.2 Shear Strength Decrease

As above, this subsection seeks to understand the underlying reasons for shear strength decrease at the structural level due to each of the 18 sub-variables. Again, each boxplot is an indicator of the impact of a given subvariable in terms of all 17 others and its impact on shear strength decrease.

Fig. 2.7 shows the boxplots for the shear strength decrease and the following observations can be made:

- P results in higher decreases than B or TB, Fig. 2.7(a). However, based on specific data points, Table 4.3, TB leads to more “large reduction” (reductions greater than 90% or more) cases.

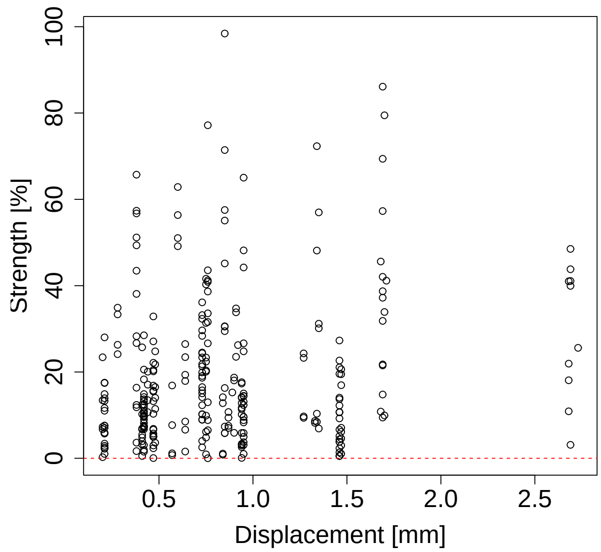

Fig. 2.6. Strength *vs* Displacements for Shear Strength Increase

- Greater depth (48") results in higher shear strength reduction than 24" components, Fig. 2.7(b). Also, the variation of the response for the larger model is smaller.
- The largest shear strength decrease occurs for the restrained (R) situation for which the ou-of-plane expansion is uniform in vertical direction and constrained in the lateral hoop direction only. It is noteworthy that this is the closest case to large structural walls, 2.7(c). Furthermore, the variation associated with (R) boundary conditions is much higher than associated with the (U) and (FR) BCs. 50% of the strength reduction cases associated with the (R) BCs fall in the range of [20%; 95%] (higher reduction). This range for (U) and (FR) BCs are [7%; 27%] and [2%; 7%], respectively.
- Increasing the AAR expansion, ϵ^{AAR}, increases the mean value of the strength reduction in the models. This is consistent with what the intuition would expect, 2.7(d). In addition, for the case with $\epsilon^{AAR} = 0.003$ (the largest expansion in the modeling) variation of the response is much greater than for the two others. In particular, the number of cases with strength reduction of nearly 100% is significantly higher.
- The effect of reinforcement ratio is rather puzzling. Suffice to say that in all three cases the reduction is about the same, i.e. ρ may not have a determining effect for these analyses where the steel may not have yielded, Fig. 2.7(e).
- β_E and β_{ft} do not seem to have large impact on the results. This is understandable as the zone in shear is largely dominated by compression. Their impact would be greater in assessing the out-of-plane displacements, Figs. 2.7(f) and 2.7(g).

Fig. 2.8(a) shows the histogram of the data set for shear strength decrease. About 15% of the data falls in the range [-100% -90%]. Moreover, Fig. 2.8(b) shows the probability distribution function (PDF) of this data set.

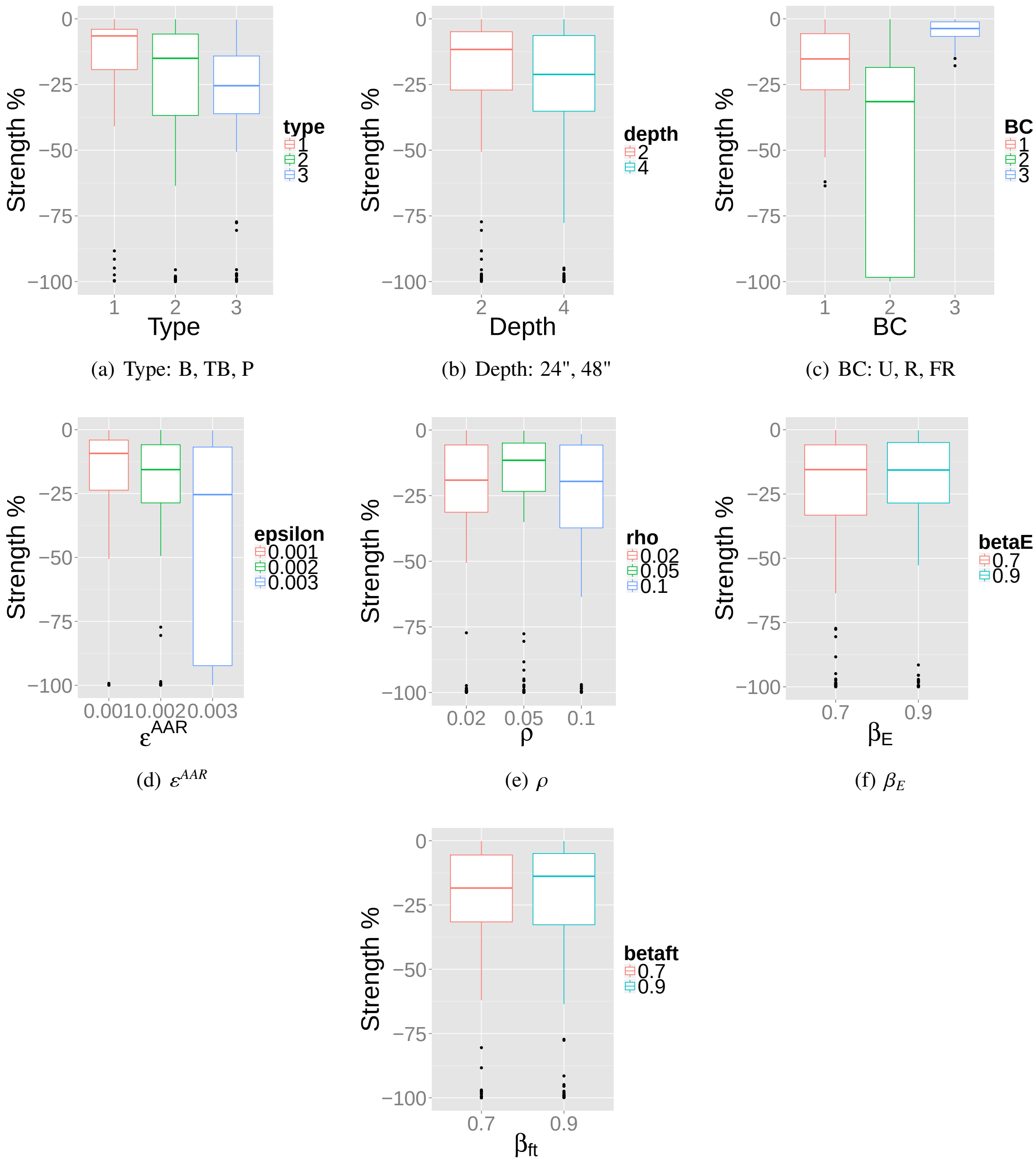

(a) Type: B, TB, P

(b) Depth: 24", 48"

(c) BC: U, R, FR

(d) ε^{AAR}

(e) ρ

(f) β_E

(g) β_{ft}

Fig. 2.7. Boxplots for Shear Strength Decrease in terms of each of the seven variables

Finally, Fig. 2.9 shows the strength *vs* out-of-plane(due to ASR) displacements data points for shear strength decrease. Again, most of the data points fall in the range of [-40; 0]% for the strength and [0; 2mm] for the displacement. No correlation between the residual shear strength and the out-of-plane (due to ASR) displacements is observed.

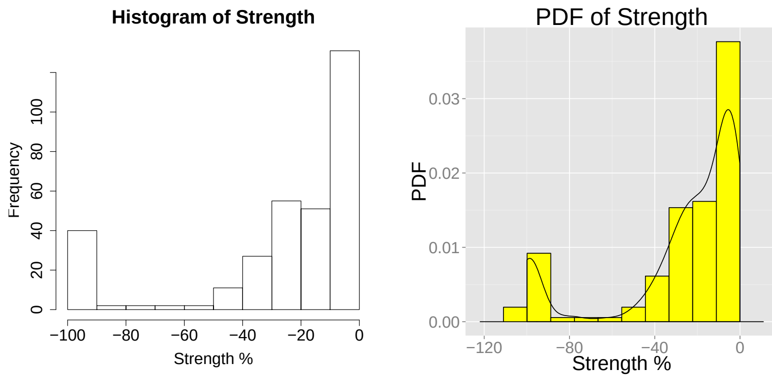

(a) Histogram (b) Probability Distribution Function

Fig. 2.8. Histograms for Shear Strength Decrease

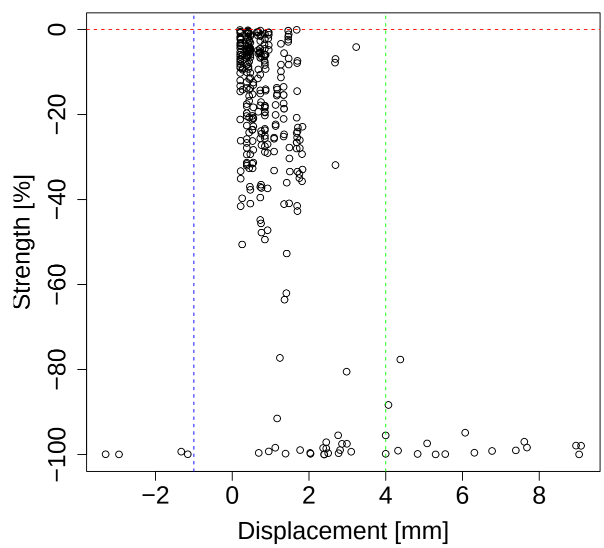

Fig. 2.9. Strength *vs* Displacements for Shear Strength Decrease (truncated at 10 mm)

2.2.2 MODEL FITTING

2.2.2.1 Full Data Set

2.2.2.1.1 General Model

Table 2.2 shows results of linear model fitting based on full data set. We note that BC=FR, $\rho = 0.1$, $\epsilon^{AAR} = 0.003$ and $\beta_{ft} = 0.9$ are the most significant sub-variables. In other words, shear strength variations are mostly dependant on these values. In the following tables, replace TB, 48"... by their actual variable names.

Table 2.2. General Model

Coefficients:	Estimate	Std. error	t value	Pr(>|t|)	
(Intercept)	-9.415	4.329	-2.175	0.030022	*
TB	-9.9358	3.0894	-3.216	0.001368	**
P	-8.3247	3.0756	-2.707	0.006985	**
48"	-1.5465	2.5124	-0.616	0.538432	
R	-7.6516	3.1109	-2.46	0.014184	*
FR	14.5088	3.0273	4.793	2.07E-06	***
$\varepsilon^{\infty} = 0.002$	0.7126	3.0491	0.234	0.81528	
$\varepsilon^{\infty} = 0.003$	-13.3651	3.0902	-4.325	1.78E-05	***
$\rho = 0.05$	4.4008	3.0782	1.43	0.153319	
$\rho = 0.1$	16.297	3.0854	5.282	1.78E-07	***
$\beta_E = 0.9$	3.9798	2.5126	1.584	0.113724	
$\beta_{ft} = 0.9$	8.3452	2.5124	3.322	0.000948	***

2.2.2.1.2 Best Model based on Akaike Information Criterion

Table 2.3 shows the results of best linear model fitting based on full data set and AIC. The number of contributing sub-variables reduces to 10 (compared to the original 11 sub-variables in Table 2.2). Still constraint (FR), $\rho = 0.1$, $\epsilon^{AAR} = 0.003$ and $\beta_{ft} = 0.9$ are the most significant sub-variables.

Table 2.3. Best Model based on Akaike Information Criterion

Coefficients:	Estimate	Std. error	t value	Pr(>|t|)	
(Intercept)	-10.197	4.1363	-2.465	0.013965	*
TB	-9.9279	3.0878	-3.215	0.001372	**
P	-8.324	3.0741	-2.708	0.006961	**
R	-7.6606	3.1093	-2.464	0.014022	*
FR	14.5124	3.0257	4.796	2.03E-06	***
$\varepsilon^{\infty} = 0.002$	0.7163	3.0476	0.235	0.814252	
$\varepsilon^{\infty} = 0.003$	-13.3849	3.0884	-4.334	1.71E-05	***
$\rho = 0.05$	4.3976	3.0767	1.429	0.153414	
$\rho = 0.1$	16.3081	3.0838	5.288	1.72E-07	***
$\beta_E = 0.9$	3.9948	2.5112	1.591	0.112172	
$\beta_{ft} = 0.9$	8.3403	2.5111	3.321	0.000949	***

2.2.2.1.3 Best Model based on Bayesian Information Criterion

Table 2.4 shows the results of best linear model fitting based on full data set and BIC. The number of contributing sub-variables reduces to 7 (compared to the original 11 sub-variables in Table 2.2 and 10 sub-variables in Table 2.3). Still constraint (FR), $\rho = 0.1$, $\epsilon^{AAR} = 0.003$ and $\beta_{ft} = 0.9$ remain the most significant sub-variables.

Table 2.4. Best Model based on Bayesian Information Criterion

Coefficients:	Estimate	Std. error	t value	Pr(>|t|)	
(Intercept)	-14.2853	3.5684	-4.003	7.01E-05	***
R	-7.8177	3.137	-2.492	0.012961	*
FR	14.511	3.0534	4.752	2.50E-06	***
$\varepsilon^{\infty} = 0.002$	0.6537	3.0753	0.213	0.831746	
$\varepsilon^{\infty} = 0.003$	-13.5041	3.1161	-4.334	1.71E-05	***
$\rho = 0.05$	4.414	3.1047	1.422	0.155612	
$\rho = 0.1$	16.3992	3.1119	5.27	1.89E-07	***
$\beta_{ft} = 0.9$	8.3962	2.5339	3.314	0.000975	***

2.2.2.2 Positive Shear Strength Change Data Set

This sub-subsection, repeats all the procedure previously presented but is limited to positive shear strength change data points (i.e. strengh increase). First the general model is fitted, followed by the AIC and BIC best models.

2.2.2.2.1 General Model for Positive Shear Strength Data Set

Table 2.5 shows the results of linear model fitting based on positive shear strength change data points. As seen, constraint (R), $\rho = 0.1$, $\epsilon^{AAR} = 0.003$, $\beta_{ft} = 0.9$ and depth $48''$ are the most significant sub-variables.

Table 2.5. General Model

Coefficients:	Estimate	Std. error	t value	Pr(>|t|)	
(Intercept)	8.0797	2.7794	2.907	0.003931	**
TB	-0.9004	1.9824	-0.454	0.65002	
P	-2.4657	1.9831	-1.243	0.214744	
48"	-5.638	1.6054	-3.512	0.000516	***
R	13.5089	2.2927	5.892	1.06E-08	***
FR	-6.6926	2.0264	-3.303	0.001078	**
$\varepsilon^{\infty} = 0.002$	5.493	1.7703	3.103	0.002106	**
$\varepsilon^{\infty} = 0.003$	6.4055	1.8966	3.377	0.000832	***
$\rho = 0.05$	-2.0508	2.0274	-1.012	0.31261	
$\rho = 0.1$	9.6667	2.0033	4.825	2.26E-06	***
$\beta_E = 0.9$	4.8399	1.488	3.253	0.001279	**
$\beta_{ft} = 0.9$	8.6287	1.4878	5.799	1.74E-08	***

2.2.2.2.2 Best Model based on Akaike Information Criterion

Table 2.6 shows the results of best linear model fitting based on positive shear strength change data points and AIC. The number of contributing sub-variables reduce to 9 (compared to the original 11 sub-variables in Table 2.5). constraints (R) and (FR), $\rho = 0.1$, and $\beta_{ft} = 0.9$ are the most significant sub-variables.

Table 2.6. AIC Model for Positive Shear Strength Data Set

Coefficients:	Estimate	Std. error	t value	Pr(>|t|)	
(Intercept)	7.344	2.673	2.747	0.006382	**
48"	-4.906	1.484	-3.305	0.001068	**
R	13.323	2.238	5.953	7.55E-09	***
FR	-7.15	1.901	-3.762	0.000204	***
$\varepsilon^{\infty} = 0.002$	5.531	1.767	3.13	0.001928	**
$\varepsilon^{\infty} = 0.003$	6.29	1.893	3.323	0.001003	**
$\rho = 0.05$	-2.556	1.985	-1.288	0.19891	
$\rho = 0.1$	9.113	1.951	4.671	4.58E-06	***
$\beta_E = 0.9$	4.774	1.485	3.215	0.001452	**
$\beta_{ft} = 0.9$	8.565	1.486	5.764	2.10E-08	***

2.2.2.2.3 Best Model based on Bayesian Information Criterion

Table 2.7 shows the results of best linear model fitting based on positive shear strength change data points and BIC. The number of contributing sub-variables reduce to 9 (compared to the original 11 sub-variables in Table 2.5 while it does not change with respect to AIC model Table 2.6). Still constraints (R) and (FR), $\rho = 0.1$, and $\beta_{ft} = 0.9$ are the most significant sub-variables.

Table 2.7. BIC Model for Positive Shear Strength Data Set

Coefficients:	Estimate	Std. error	t value	Pr(>|t|)	
(Intercept)	7.344	2.673	2.747	0.006382	**
48"	-4.906	1.484	-3.305	0.001068	**
R	13.323	2.238	5.953	7.55E-09	***
FR	-7.15	1.901	-3.762	0.000204	***
$\varepsilon^{\infty} = 0.002$	5.531	1.767	3.13	0.001928	**
$\varepsilon^{\infty} = 0.003$	6.29	1.893	3.323	0.001003	**
$\rho = 0.05$	-2.556	1.985	-1.288	0.19891	
$\rho = 0.1$	9.113	1.951	4.671	4.58E-06	***
$\beta_E = 0.9$	4.774	1.485	3.215	0.001452	**
$\beta_{ft} = 0.9$	8.565	1.486	5.764	2.10E-08	***

2.2.2.3 Negative Shear Strength Change Data Set

This sub-subsection repeats all the procedure conducted in the previous sub-subsection but limits it analysis to the situations leading to a negative shear strength change. First the general model is fitted, follows the AIC and BIC best models.

2.2.2.3.1 General Model

Table 2.8 shows the results of linear model fitting based on negative shear strength change data points. As seen, constraint (R), $\rho = 0.1$, $\epsilon^{AAR} = 0.003$, and structural member (P) are the most significant sub-variables.

Table 2.8. General Model for Negative Shear Strength Data Set

Coefficients:	Estimate	Std. error	t value	Pr(>|t|)	
(Intercept)	3.233	4.313	0.75	0.454003	
TB	-8.58	3.227	-2.659	0.008242	**
P	-11.502	3.448	-3.336	0.000954	***
48"	-4.672	2.65	-1.763	0.07887	
R	-35.981	2.898	-12.414	0.00E+00	***
FR	8.497	3.584	2.371	0.018345	*
$\varepsilon^{\infty} = 0.002$	-3.649	3.071	-1.188	0.235585	
$\varepsilon^{\infty} = 0.003$	-19.567	2.991	-6.542	2.50E-10	***
$\rho = 0.05$	-3.441	2.912	-1.182	0.238182	
$\rho = 0.1$	-14.238	3.338	-4.265	2.65E-05	***
$\beta_E = 0.9$	4.891	2.502	1.955	0.0515	
$\beta_{ft} = 0.9$	1.134	2.504	0.453	6.51E-01	

2.2.2.3.2 Best Model based on Akaike Information Criterion

Table 2.9 shows the results of best linear model fitting based on negative shear strength change data points and AIC. The number of contributing sub-variables reduce to 10 (compared to the original 11 sub-variables in Table 2.8). Still constraint (R), $\rho = 0.1$, $\epsilon^{AAR} = 0.003$, and structural member (P) are the most significant sub-variables.

Table 2.9. AIC Model for Negative Shear Strength Data Set

Coefficients:	Estimate	Std. error	t value	Pr(>|t|)	
(Intercept)	3.858	4.081	0.945	0.345214	
TB	-8.627	3.221	-2.678	7.79E-03	**
P	-11.565	3.441	-3.361	0.000873	***
48"	-4.714	2.645	-1.782	0.075713	
R	-36.042	2.892	-12.465	0	***
FR	8.275	3.545	2.334	0.020231	*
$\varepsilon^{\infty} = 0.002$	-3.608	3.065	-1.177	2.40E-01	
$\varepsilon^{\infty} = 0.003$	-19.49	2.982	-6.535	2.59E-10	***
$\rho = 0.05$	-3.504	2.905	-1.206	2.29E-01	
$\rho = 0.1$	-14.302	3.331	-4.294	2.35E-05	***
$\beta_E = 0.9$	4.909	2.499	1.965	0.050357	

2.2.2.3.3 Best Model based on Bayesian Information Criterion

Table 2.10 shows the results of best linear model fitting based on negative shear strength change data points and BIC. The number of contributing sub-variables reduce to 8 (compared to the original 11 sub-variables in Table 2.8 and 10 sub-variable with respect to AIC model Table 2.9). Still constraint (R), $\rho = 0.1$, $\epsilon^{AAR} = 0.003$, and structural member (P) are the most significant sub-variables.

Table 2.10. BIC Model for Negative Shear Strength Data Set

Coefficients:	Estimate	Std. error	t value	Pr(>|t|)	
(Intercept)	4.831	3.903	1.238	0.21669	
TB	-9.893	3.171	-3.119	1.98E-03	**
P	-13.776	3.271	-4.212	3.31E-05	***
R	-35.457	2.904	-12.21	0	***
FR	7.428	3.549	2.093	0.03718	*
$\varepsilon^{\infty} = 0.002$	-3.572	3.09	-1.156	0.24855	
$\varepsilon^{\infty} = 0.003$	-19.706	2.993	-6.584	1.92E-10	***
$\rho = 0.05$	-2.969	2.922	-1.016	0.31037	
$\rho = 0.1$	-13.77	3.351	-4.109	5.08E-05	***

2.2.2.4 Preliminary Conclusions

As earlier mentioned, the effect of AAR on the shear strength of concrete structural components is a complex interplay between two effects:

Material degradation, where undoubtedly AAR reduces the tensile strength of the concrete and is very likely to affect the shear strength of concrete.

Structural effect, where steel constrains the concrete expansion, thus putting the later in compression which will *de facto* increase its shear resistance.

Those effects coalesce in the 648 analyses performed, and which interpretation was provided through the statistical approach previously presented.

Table 2.11 summarizes the three sets of results in terms of the 18 sub variables. For each column the top 7 most relevant subvariables are indicated: And the most important preliminary conclusions are:

1. The boundary conditions (R), i.e., “resrained” are the primary cause of shear strength increase or decrease.

2. For shear strength increase the second most important parameter is $\rho = 0.1$, i.e. the highest reinforcement ratio considered.

3. For shear strength decrease the second most important parameter is $\varepsilon = 0.003$.

Table 2.11. Summary of linear model fittinh

		Full Set			Positive Set			Negative Set		
		General	AIC	BIC	General	AIC	BIC	General	AIC	BIC
1	Type B									
2	Type TB	4	4					5	5	5
3	Type P	6	6					4	4	3
4	Depth 2									
5	Depth 4				6	7	7			
6	B.C. U									
7	B.C. R	7	7	5	1	1	1	1	1	1
8	B.C. FR	2	2	2	4	4	4	6	6	6
9	ϵ 0.001									
10	ϵ 0.002			7	7	6	6			7
11	ϵ 0.003	3	3	3	5	5	5	2	2	2
12	ρ 0.02									
13	ρ 0.05			6						
14	ρ 0.10	1	1	1	2	2	2	3	3	4
15	β_E 0.7									
16	β_E 0.9							7	7	
17	β_{ft} 0.7									
18	β_{ft} 0.9	5	5	4	3	3	3			

2.3 STATISTICAL ANALYSIS OF RESTRAINED BOUNDARY CONDITIONS SCENARIO

The preponderant role played by the (R) boundary condition was just demonstrated. To better focus on that scenario, a second "fine grained" investigation on this specific case, and its 216 analyses is performed by filtering out the (FR) and (U) BCs cases.

2.3.1 BOXPLOTS

2.3.1.1 Shear Strength Increase

Fig. 2.10 shows the boxplots for the shear strength increase only for the restrained models. It can be noted:

- The impact of (B) model on shear strength increase is higher than the ones of TB and P models. Variability of TB is more than two other models, Fig. 2.10(a).
- 24" specimens (smaller dimensions) have a slightly larger variability in shear strength increase (size effect?) than the larger specimen, Fig. 2.10(b).
- Larger reinforcement (higher ρ) leads to larger shear strength increase, Fig. 2.10(d).
- Higher reduction in β_E results in smaller shear strength increase, Fig. 2.10(e).
- Similarly, a larger decrease in β_{ft} results in smaller increase in shear strength, Fig. 2.10(f).

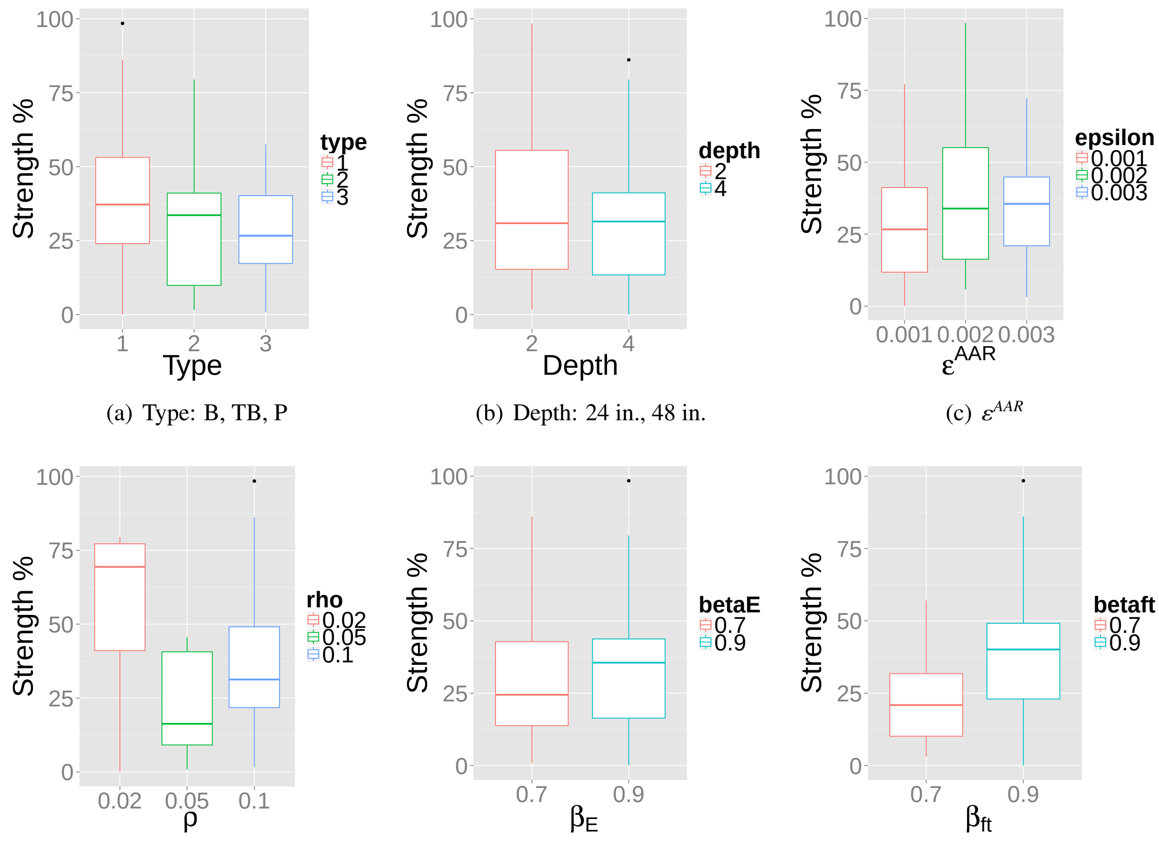

(a) Type: B, TB, P (b) Depth: 24 in., 48 in. (c) ε^{AAR}

(d) ρ (e) β_E (f) β_{ft}

Fig. 2.10. Boxplots for Shear Strength Increase in terms of each of the six variables; only restrained model

Fig. 2.11(a) shows the histogram of the data set for shear strength increase (due to AAR). The data set does not follow a specific distribution. About 80% of the data falls in the range [0 50%] of strength. Finally, Fig. 2.11(b) shows the probability distribution function (PDF) of this data set.

2.3.1.2 Shear Strength Decrease

As above, this subsection seeks to understand the underlying reasons for shear strength decrease at the structural level due to each of the 15 sub-variables. Again, each boxplot is an indicator of the impact of a given sub-variable in terms of all 14 others and its impact on shear strength decrease.

Fig. 2.12 shows the boxplots for the shear strength decrease and only the restrained model. The following observations can be made:

- P results in higher decreases than B and TB, Fig. 2.12(a). However, the variability of the data points are nearly identical.

- Greater depth (48") result in higher shear strength reduction than 24" components, Fig. 2.12(b). The variation of the response is nearly identical in both cases.

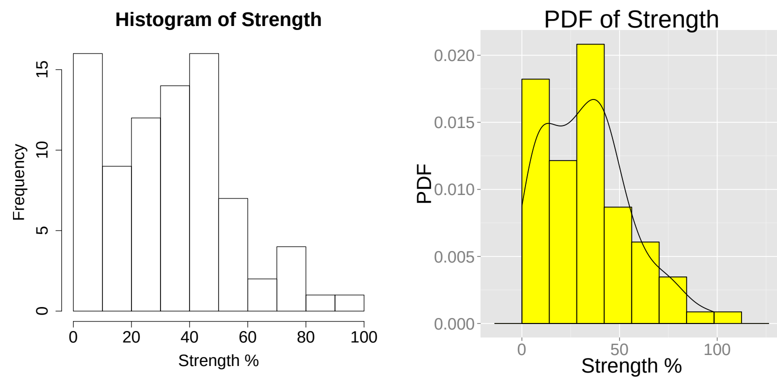

(a) Histogram (b) Probability Distribution Function

Fig. 2.11. Histograms for Shear Strength Increase; only restrained model

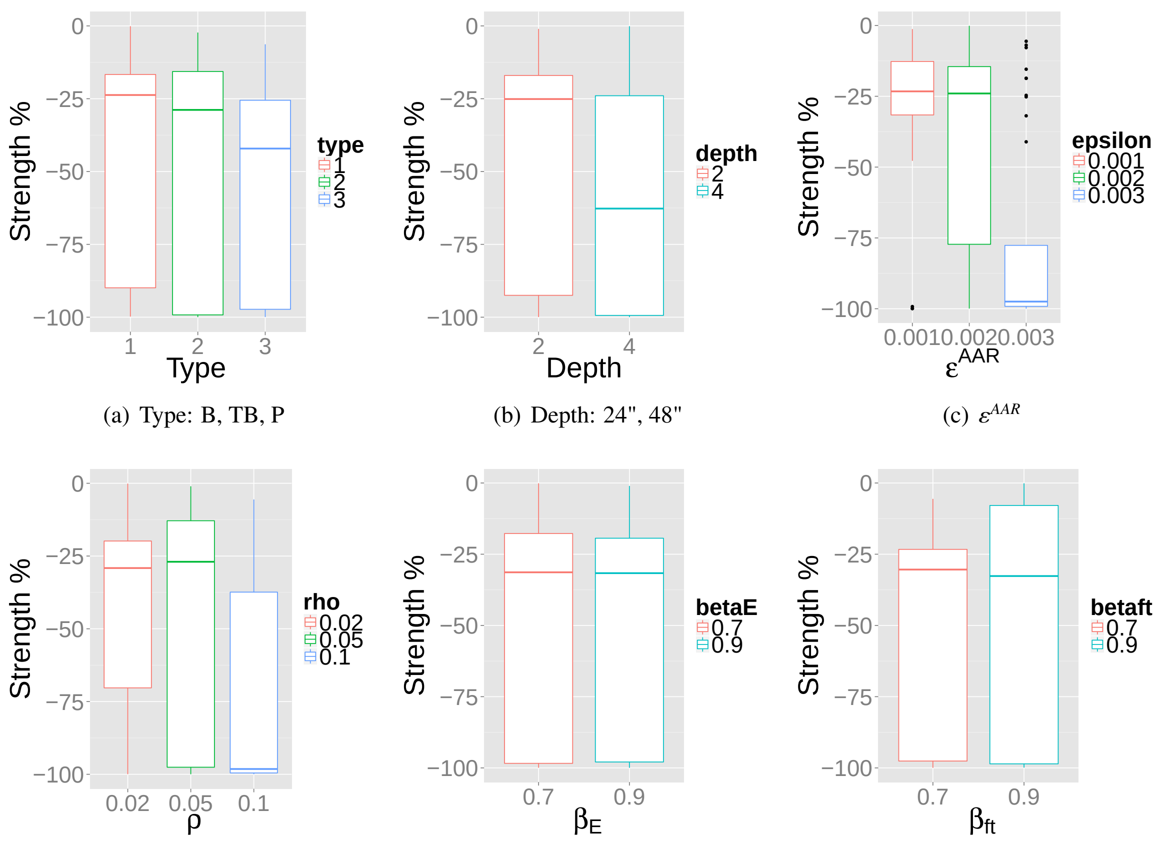

(a) Type: B, TB, P (b) Depth: 24", 48" (c) ε^{AAR}

(d) ρ (e) β_E (f) β_{ft}

Fig. 2.12. Boxplots for Shear Strength Decrease in terms of each of the six variables; only restrained model

- Increasing the AAR expansion, ϵ^{AAR}, increases the mean value of the strength reduction in the models. This is consistent with what one would expect, 2.12(c). In addition, there is considerable gap between the case with $\epsilon^{AAR} = 0.003$ (the largest expansion in the modeling) and the two others. variation of the response in $\epsilon^{AAR} = 0.002$ is greater than the two others.

- β_E and β_{ft} do not seem to have a large impact on the results. This is understandable as the zone in shear is largely under compression. Their impact would be greater in assessing the out of plane displacements, Figs. 2.12(e) and 2.12(f).

Fig. 2.13(a) shows the histogram of the data set for shear strength decrease. About 20% of the data falls in the range [-100% -90%]. Moreover, Fig. 2.13(b) shows the probability distribution function (PDF) of this data set.

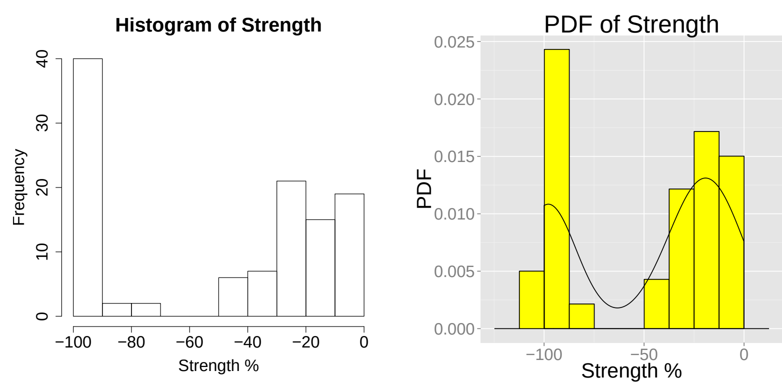

(a) Histogram (b) Probability Distribution Function

Fig. 2.13. Histograms for Shear Strength Decrease; only restrained model

2.3.2 MODEL FITTING: POSITIVE SHEAR STRENGTH CHANGE

This sub-subsection, repeats all the procedure previously presented but is limited to positive shear strength change data points (i.e. strength increase) and is limited to the restrained model. First the general model is fitted, follows by the AIC and BIC best models.

2.3.2.1 General Model for Positive Shear Strength Data Set

Table 2.12 shows the results of linear model fitting based on positive shear strength change data points. As seen, $\rho = 0.05$, $\rho = 0.1$ and $\beta_{ft} = 0.9$ are the most significant sub-variables.

2.3.2.2 Best Model based on Akaike Information Criterion

Table 2.13 shows the results of best linear model fitting based on positive shear strength change data points and AIC. The number of contributing sub-variables reduce to 6 (compared to the original 9 sub-variables in Table 2.12). $\rho = 0.05$, $\rho = 0.1$, and $\beta_{ft} = 0.9$ are the most significant sub-variables.

Table 2.12. General Model; only restrained model

Coefficients:	Estimate	Std. error	t value	Pr(>|t|)	
(Intercept)	48.887	11.795	4.145	9.16E-05	***
TB	-9.443	5.384	-1.754	0.083711	
P	-12.887	5.196	-2.48	0.01546	*
48"	-6.444	4.804	-1.341	0.183982	
$\varepsilon^{\infty} = 0.002$	7.699	4.728	1.628	0.107809	
$\varepsilon^{\infty} = 0.003$	4.478	5.645	0.793	0.430251	
$\rho = 0.05$	-28.164	9.588	-2.937	0.004442	**
$\rho = 0.1$	-16.081	9.585	-1.678	0.097734	
$\beta_E = 0.9$	2.996	4.287	0.699	0.486908	
$\beta_{ft} = 0.9$	15.207	4.277	3.556	0.000671	***

Table 2.13. AIC Model for Positive Shear Strength Data Set; only restrained model

Coefficients:	Estimate	Std. error	t value	Pr(>|t|)	
(Intercept)	56.016	10.688	5.241	1.42E-06	***
TB	-9.993	5.342	-1.871	0.065292	
P	-13.615	5.162	-2.638	0.01014	*
48"	-7.074	4.782	-1.479	0.143296	
$\rho = 0.05$	-29.831	9.413	-3.169	0.002215	**
$\rho = 0.1$	-17.79	9.376	-1.897	0.061634	
$\beta_{ft} = 0.9$	15.598	4.267	3.655	0.000474	***

2.3.2.3 Best Model based on Bayesian Information Criterion

Table 2.14 shows the results of best linear model fitting based on positive shear strength change data points and BIC. The number of contributing sub-variables reduce to 3 (compared to the original 9 sub-variables in Table 2.12). Still $\rho = 0.05$, $\rho = 0.1$, and $\beta_{ft} = 0.9$ are the most significant sub-variables.

Table 2.14. BIC Model for Positive Shear Strength Data Set; only restrained model

Coefficients:	Estimate	Std. error	t value	Pr(>|t|)	
(Intercept)	41.581	9.414	4.417	3.19E-05	***
$\rho = 0.05$	-27.611	9.53	-2.897	0.00488	**
$\rho = 0.1$	-13.706	9.224	-1.486	0.14133	
$\beta_{ft} = 0.9$	14.806	4.417	3.352	0.00124	**

2.3.3 MODEL FITTING: NEGATIVE SHEAR STRENGTH CHANGE DATA SET

This sub-subsection, repeats all the procedure in the previous sub-subsection for the negative shear strength change data points. First the general model is fitted, follows by the AIC and BIC best models.

2.3.3.1 General Model

Table 2.15 shows the results of linear model fitting based on negative shear strength change data points. As seen, ϵ^{AAR} = 0.003, ρ = 0.1, and 48" = 48 are the most significant sub-variables.

Table 2.15. General Model; only restrained model

Coefficients:	Estimate	Std. error	t value	Pr(>|t|)	
(Intercept)	-15.6835	8.7845	-1.785	0.0772	
TB	-12.1158	8.0128	-1.512	0.1336	
P	-10.0268	7.6347	-1.313	0.192	
48"	-13.6526	6.4079	-2.131	0.0355	*
ε^{∞} = 0.002	-9.0327	7.612	-1.187	0.2381	
ε^{∞} = 0.003	-45.1145	7.5992	-5.937	4.04E-08	***
ρ = 0.05	-4.61	6.6249	-0.696	0.4881	
ρ = 0.1	-20.2409	10.1427	-1.996	0.0486	*
β_E = 0.9	5.7823	6.0569	0.955	0.342	
β_{ft} = 0.9	-0.3567	6.0729	-0.059	0.9533	

2.3.3.2 Best Model based on Akaike Information Criterion

Table 2.16 shows the results of best linear model fitting based on negative shear strength change data points and AIC. The number of contributing sub-variables reduce to 5 (compared to the original 9 sub-variables in Table 2.15). Still ϵ^{AAR} = 0.003, ρ = 0.1, and 48" = 48 are the most significant sub-variables.

Table 2.16. AIC Model for Negative Shear Strength Data Set; only restrained model

Coefficients:	Estimate	Std. error	t value	Pr(>|t|)	
(Intercept)	-20.639	6.384	-3.233	0.00163	**
48"	-13.423	6.139	-2.186	0.03098	*
ε^{∞} = 0.002	-9.436	7.569	-1.247	0.21527	
ε^{∞} = 0.003	-45.082	7.557	-5.965	3.27E-08	***
ρ = 0.05	-4.462	6.586	-0.677	0.49956	
ρ = 0.1	-22.453	9.607	-2.337	0.02131	*

2.3.3.3 Best Model based on Bayesian Information Criterion

Table 2.17 shows the results of best linear model fitting based on negative shear strength change data points and BIC. The number of contributing sub-variables reduce to 2 (compared to the original 9 sub-variables in Table 2.15 and 5 sub-variable with respect to AIC model Table 2.16). This time ϵ^{AAR} = 0.003, and ϵ^{AAR} = 0.002 are the most significant sub-variables.

Table 2.17. BIC Model for Negative Shear Strength Data Set; only restrained model

Coefficients:	Estimate	Std. error	t value	Pr(>|t|)	
(Intercept)	-28.141	5.588	-5.036	1.90E-06	***
ε^{∞} = 0.002	-11.857	7.741	-1.532	0.128	
ε^{∞} = 0.003	-50.139	7.558	-6.634	1.31E-09	***

2.3.4 CONCLUSIONS ON MODEL FITTING FOR LEVEL 2

Considering only the restrained model, the following two general conclusions can be made:

- For the positive shear strength data $\rho = 0.05$, $\rho = 0.1$, and $\beta_{ft} = 0.9$ are the most significant sub-variables.
- For the negative shear strength data $\epsilon^{AAR} = 0.003$, and are the most significant sub-variables.

2.4 CONCLUSION FROM ALL ANALYSES

Amongst the full set of 648 analyses, 53% resulted in overall post-ASR shear strength decrease, and 47% in an increase. The range of variation in post-ASR shear strength is particularly wide. Hence, the role of the structural constraint during the development of ASR appears critical to the out-of plane shear resistance of the structures, which results from the competition between the ASR-induced prestressing of reinforced concrete and the degradation of the materials properties. Decrease is more likely to occur when the ASR strain is at its highest value (0.003) for the restrained boundary conditions. These results indicate that each structural configuration needs to be studied specifically. This implies, in particular, that large-scale laboratory test results may not be directly applicable to other in-situ structural configuration. However, these tests provide valuable data for the validation of structural models that can be applied subsequently to analyze the resilience of Class I-safety nuclear concrete structures under accidental scenarios. It is recommended that a full three-dimensional analysis of such structures be undertaken to further confirm this finding.

The features of the ASR model used in Merlin are currently being implemented in GRIZZLY by INL (RISMiC pathway).

The LWRS MaaD pathway has launched a research operation in collaboration between ORNL, the University of Tennessee, the University of Alabama, the University of Colorado, INL (LWRS OLM pathway) and PNNL to build large ASR-mockup subjected to unrestrained and restrained structural effects to study the development of ASR expansion and damage (2016-18), and subsequently, the residual out-of-plane shear capacity (2018-19). These mockups will serve the purpose of validation of the models implemented in GRIZZLY.

Bibliography

Akaike, H.: 1974, A new look at statistical model identification, *IEEE Transactions on Automatic Control* **19**(6), 716–Ű723.

Barbosa, R., Hansen, K., Hoang, L. and Maag, I.: 2014, *Alkali-Silica Reaction in Reinforced Concrete Structures, Part II: Shear Strength of Severe ASR Damaged Concrete Beams*, Norsk Betongforening, pp. 69–72.

Bažant, Z. and Oh, B.-H.: 1983, Crack band theory for fracture of concrete, *Materials and Structures* **16**, 155–177.

Bažant, Z.P. and Zi, G. and Meyer, C.: 2000, Fracture mechanics of aar in concretes with waste glass particles of different sizes, *J. of Engineering Mechanics, ASCE* **126**(3), 226–232.

Blight, G. and Alexander, M. G.: 2008, *Alkali-Aggregate Reaction and Structural Damage to Concrete*, Taylor & Francis.

Capra, B. and Bournazel, J.: 1998, Modeling of induced mechanical effects of alkali-aggregate reactions, *Cement and Concrete Research* **28**(2), 251–260.

CEB: 1983, Concrete under multiaxial states of stress constitutive equations for practical design, *Technical Report Bulletin d'Information 156*, Comité Euro-International du Béton.

Cervenka Consulting: 2010, Atena, `http://www.cervenka.cz/products/atena`.

Cervenka, J. and Papanikolaou, V.: 2008, Three dimensional combined fracture-plastic material model for concrete, *International Journal of Plasticity* **24**(12), 2192–2220.

de Borst, R.: 1986, *Nonlinear Analysis of Frictional Materials*, PhD thesis, Delft University of Technology, Delft.

Haberman, S.: 2013, Seabrook station nuclear plant license advancing, `http://www.seacoastonline.com/articles/20130515-NEWS-305150371`. Retrieved June 2013.

Haha, M.: 2006, *Mechanical effects of alkali silica reaction in concrete studied by SEM-image analysis*, PhD thesis, École Polytechnique Fédérale de Lausanne.

Hordijk, D.: 1991, *Local approach to Fatigue of Concrete*, PhD thesis, Delft University of Technology.

Kolmar, W.: 1986, *Beschreibung der Kraftuebertragung ueber Risse in nichtlinearen Finite-Element-Berechnungen von Stahlbetontragwerken*, PhD thesis, Darmstadt.

Kupfer, B. and Gerstle, K.: 1973, Behavior of concrete under biaxial stresses, *ASCE Journal of the Engineering Mechanics Division* **99**(4), 853–866.

Larive, C.: 1998, *Apports Combinés de l'Experimentation et de la Modélisation à la Comprehension del'Alcali-Réaction et de ses Effets Mécaniques*, PhD thesis, *Laboratoire Central des Ponts et Chaussées*, Paris.

Menétrey, P. and Willam, K.: 1995, Triaxial failure criterion for concrete and its generalization, *ACI Structural Journal* **92**(3), 311–318.

ML121160422: 2012, Impact of alkali silica reaction on seabrook concrete structure, *Technical Report ML121160422*, NextEra.

Multon, S.: 2004, *Evaluation expérimentale et théorique des effets mécaniques de l'alcali-réaction sur des structures modèles*, PhD thesis, Université de Marne la Vallée, France.

R Core Team: 2015, *R: A Language and Environment for Statistical Computing*, R Foundation for Statistical Computing, Vienna, Austria.
URL: *https://www.R-project.org*

Rots, J. G. and Blaauwendraad, J.: 1989, Crack models for concrete: Discrete or smeared? fixed, multi-directional or rotating?, *HERON* **34**(1), 1512–1533.

Sanborn, I.: 2015, Canadian utility closes n-plant plagued by asr, `http://www.newburyportnews.com/opinion/canadian-utility-closes-n-plant-plagued-by-asr/article_7ba05ca3-ad76-5581-aa31-c7b84310d5b3.html`. Retrieved Sept. 2015.

Saouma, V.: 2009, KumoNoSu, a 3d interactive graphics mesh generator for merlin; user's manual, `http://civil.colorado.edu/~saouma/pdf/kumo.pdf`.

Saouma, V.: 2013a, *Numerical Modeling of Alkali Aggregate Reaction*, CRC Press. 320 pages.

Saouma, V.: 2013b, A proposed aging management program for alkali aggregate reactions in a nuclear power plant. personal communication.

Saouma, V. and Perotti, L.: 2006, Constitutive model for alkali aggregate reactions, *ACI Materials Journal* **103**(3), 194–202.

Saouma, V., Perotti, L. and Shimpo, T.: 2007, Stress analysis of concrete structures subjected to alkali-aggregate reactions, *ACI Materials Journal* **104**(5), 532–541.

Saouma, V., Červenka, J. and Reich, R.: 2010, Merlin finite element user's manual, `http://civil.colorado.edu/~saouma/pdf/users.pdf`.

Scrivener: 2003. Personal Communication.

Shimizu, H., Watanabe, Y., Sekimoto, H., Oshima, R., Takiguchi, K., Masuda, Y. and Nishiguchi, I.: 2005, Study on material properties in order to apply for structural analysis of turbine generator foundation affected by alkali-silica reaction, *18th International Conference on Structural Mechanics in Reactor Technology (SMIRT 18)*, Beijing, China, pp. 2055–2060. SMIRT18-H03-5.

Stanton, T.: 1940, Expansion of concrete through reaction between cement and aggregate, *Proceedings of ASCE* **66**, 1781–1811.

Struble, L. and Diamond, S.: 1981, Swelling properties of synthetic alkali silica gels, *Journal of the American Ceramic Society* **64**(11), 652–655.

Takatura, T., Ishikawa, T., Matsumoto, N., Mitsuki, S., Takiguchi, K. and Masuda, Y.: 2005, Investigation of the expanded value of turbine generator foundation affected by alkali-silica reaction, *Proceedings of the 18th International Conference on Structural Mechanics in Reactor Technology (SMIRT18)*, number SMIRT18-H03-7, Beijing, China, pp. 2061–2068.

Tcherner, J. and Aziz, T.: 2009, Effects of aar on seismic assessment of nuclear power plants for life extensions, *Proceedings of the 20th International Conference on Structural Mechanics in Reactor Technology (SMIRT 20)*, number SMIRT20-Division 7 Paper 1789., Espoo, Finland.

Touma, W.: 2000, Alkali-silica reaction in portland cement concrete: Testing methods and mitigation alternatives, *Technical report*, International Center for Aggregate Research.

Ulm, F., Coussy, O., Kefei, L. and Larive, C.: 2000, Thermo-chemo-mechanics of asr expansion in concrete structures, *ASCE J. of Engineering Mechanics* **126**(3), 233–242.

van Mier, J.: 1986, Multi-axial strain softening of concrete; part i: Fracture, *Materials and Structures, RILEM* **19**(111).

Wilkins, M.: 1964, Calculation of elasto-plastic flow, *Methods of Computational Physics* **3**, 211–263.

Wittmann, F., Rokugo, K., Brühwiler, E., Mihashi, H. and Simonin, P.: 1988, Fracture Energy and Strain Softening of Concrete as Determined by Means of Compact Tension Specimens, *Materials and Structures* **21**, 21–32.

Appendix A

Constitutive Models

1.1 ASR AND CONSTITUTIVE MODELS USED IN MERLIN

The ASR model of the author (Saouma and Perotti 2006), Saouma et al. (2007) (Saouma 2013a) is an uncoupled one, that is the constitutive model is in no way affected by the ASR which itself is considered to be an initial strain (akin of temperature), which grafts itself on the mechanical one.

This section will describe first the ASR model yielding to the expression of the ASR strain tensor which is accounted for. Then the nonlinear continuum based constitutive model is described next. This model can be activated whenever the ASR induced strain (or others) may either crack the concrete or initiate its ascent in the nonlinear compressive branch. Finally, the nonlinear discrete interface element is described. Though not directly affected by chemically induced volumetric strain, its presence is of paramount importance to model slot (often cut to relieve stresses) closure due to ASR.

1.1.1 ASR MODEL

1.1.1.1 Premises

Two different aspects of mathematical modelling of ASR in concrete may be distinguished: 1) The kinetics of the chemical reactions and diffusion processes involved, and 2) The mechanics of fracture that affects volume expansion and causes loss of strength, with possible disintegration of the material, (Bažant, Z.P. and Zi, G. and Meyer, C. 2000).

The proposed model, is driven by the following considerations:

1. ASR is a volumetric expansion, and as such can not be addressed individually along a principal direction without due regard to what may occur along the other two orthogonal ones.
2. Kinetics component is taken from the work of (Larive 1998) and (Ulm et al. 2000).
3. ASR is sufficiently influenced by temperature to account its temporal variation in an analysis.
4. ASR expansion is constrained by compression, and is redirected in other less constrained principal directions.This will be accomplished by assigning "weights" to each of the three principal directions.
5. Relatively high compressive or tensile stresses inhibit ASR expansion due to the formation of micro or macro cracks which absorb the expanding gel.
6. High compressive hydrostatic stresses slow down the reaction.

7. Triaxial compressive state of stress reduces but does not eliminate expansion.

8. Accompanying ASR expansion is a reduction in tensile strength and elastic modulus.

1.1.1.2 Expansion Curve

One of the most extensive and rigorous investigation of ASR has been conducted by (Larive 1998) who tested more than 600 specimens with various mixes, ambiental and mechanical conditions. Not only did the author conduct this extensive experimental investigation, but a numerical model has also been proposed for the time expansion of the concrete. In particular, a thermodynamical based model for the expansion evolution is developed, and then calibrated with the experimental data, Fig. 1.1.

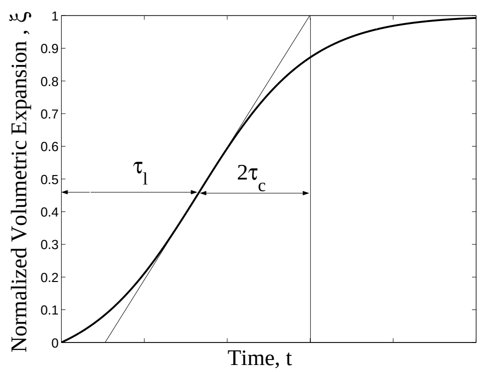

Fig. 1.1. Normalized Expansion Curve ($\xi(t) = \varepsilon^{ASR}_{F,Vol}(t)/\varepsilon^{\infty}_{ASR}$)

$$\xi(t,\theta) = \frac{1 - e^{-\frac{t}{\tau_c(\theta)}}}{1 + e^{-\frac{(t-\tau_l(\theta))}{\tau_c(\theta)}}} \tag{A.1}$$

where τ_l and τ_c are the latency and characteristic times respectively. The first corresponds to the inflexion point, and the second is defined in terms of the intersubsection of the tangent at τ_L with the asymptotic unit value of ξ. In a subsequent work, (Ulm et al. 2000) have shown the thermal dependency of those two coefficients:

$$\begin{aligned} \tau_l(\theta) &= \tau_l(\theta_0)\exp\left[U_l\left(\frac{1}{\theta} - \frac{1}{\theta_0}\right)\right] \\ \tau_c(\theta) &= \tau_c(\theta_0)\exp\left[U_c\left(\frac{1}{\theta} - \frac{1}{\theta_0}\right)\right] \end{aligned} \tag{A.2}$$

expressed in terms of the absolute temperature ($\theta^o K = 273 + T^o C$) and the corresponding activation energies. U_l and U_c are the activation energies minimum energy required to trigger the reaction for the latency and characteristic times respectively, and were determined (for Larive's test) to be

$$U_l = 9,400 \pm 500K \tag{A.3}$$

$$U_c = 5,400 \pm 500K \tag{A.4}$$

To the best of the authors knowledge, the only other tests for these values were performed by (Haha 2006) who obtained values within 20% of Larive's, and dependency on types of aggregates and alkali content of the cement has not been investigated. Hence, in the absence of other tests, those values can be reasonably considered as representative of dam concrete also. The temperature dependance is highlighted by Fig. 1.2 where the expansion curve determined in the laboratory at 38^{o}C is compared with the corresponding one at a dam average temperature of 7^{o}C

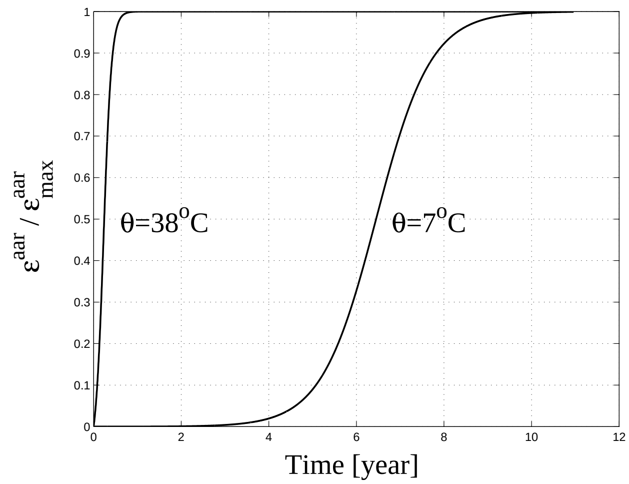

Fig. 1.2. Effect of Temperature on ASR Expansion

1.1.1.3 Volumetric Expansion

Hence, the general (uncoupled) equation for the incremental free volumetric ASR strain is given by

$$\dot{\boldsymbol{\varepsilon}}_V^{ASR}(t) = \Gamma_t(f_t'|w_c, \sigma_I|COD_{max})\Gamma_c(\overline{\sigma}, f_c')g(h)\dot{\xi}(t,\theta)\ \varepsilon^{\infty}\Big|_{\theta=\theta_0} \tag{A.5}$$

where COD is the crack opening displacement, $\xi(t,\theta)$ is a sigmoid curve expressing the volumetric expansion in time as a function of temperature and is given by Eq. A.1, ε^{∞} is the laboratory determined (or predicted) maximum free volumetric expansion at the reference temperature θ_0, Fig. 1.1.

The retardation effect of the hydrostatic compressive stress manifests itself through τ_l. Hence, Eq. A.2 is expanded as follows

$$\tau_l(\theta, \theta_0, I_\sigma, f_c') = f(I_\sigma, f_c')\tau_l(\theta_0)\exp\left[U_l\left(\frac{1}{\theta} - \frac{1}{\theta_0}\right)\right] \tag{A.6}$$

where

$$f(I_\sigma, f_c') = \begin{cases} 1 & \text{if } I_\sigma \geq 0. \\ 1 + \alpha\frac{I_\sigma}{3f_c'} & \text{if } I_\sigma < 0. \end{cases} \tag{A.7}$$

and I_σ is the first invariant of the stress tensor, and f_c' the compressive strength. Based on a careful analysis of (Multon 2004), it was determined that $\alpha = 4/3$. It should be noted, that the stress dependency (through I_σ) of the kinetic parameter τ_l makes the model a truly coupled one between the chemical and mechanical phases. Coupling with the thermal component, is a loose one (hence a thermal analysis can be separately run),

$0 < g(h) \leq 1$ is a reduction function to account for humidity given by

$$g(h) = h^m \tag{A.8}$$

where h is the relative humidity, Capra and Bournazel (1998). Here, it is simply assumed that $g(h) = 1$ for all temperatures.

$\Gamma_t(f_t'|w_c, \sigma_I|COD_{max})$ accounts for ASR reduction due to tensile cracking (in which case gel is absorbed by macro-cracks), Fig. 1.3. A hyperbolic decay, with a non-zero residual value is adopted, Fig.

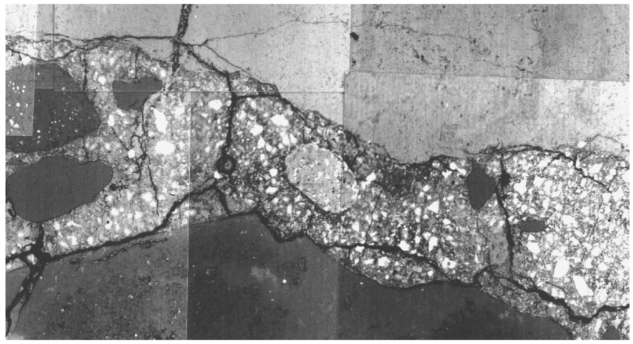

Fig. 1.3. Stress Induced Cracks with Potential Gel Absorption, Scrivener (2003)

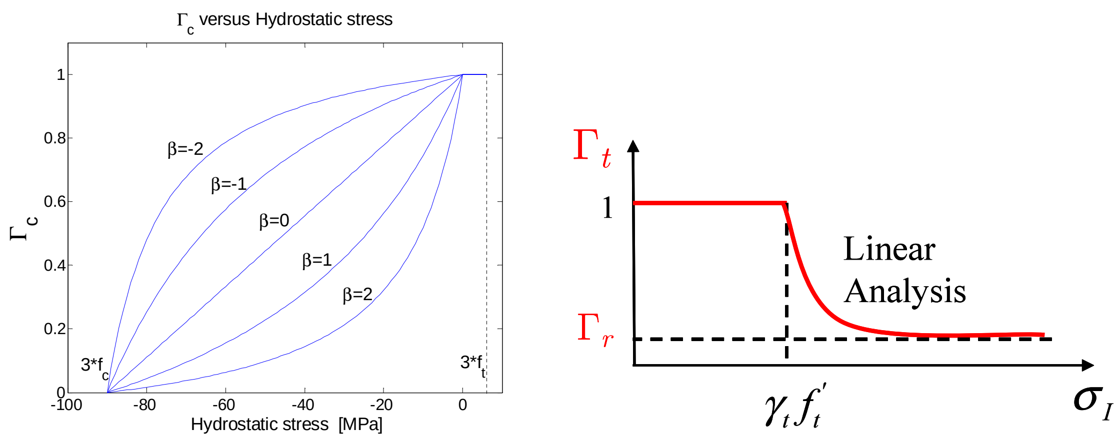

Fig. 1.4. Graphical Representation of Γ_c and Γ_t

1.4:

$$\text{Smeared Crack}\begin{cases} \text{No} \quad \Gamma_t = \begin{cases} 1 & \text{if} \quad \sigma_I \le \gamma_t f_t' \\ \Gamma_r + (1-\Gamma_r)\gamma_t \frac{f_t'}{\sigma_I} & \text{if} \quad \gamma_t f_t' < \sigma_I \end{cases} \\ \text{Yes} \quad \Gamma_t = \begin{cases} 1 & \text{if} \quad \text{COD}_{max} \le \gamma_t w_c \\ \Gamma_r + (1-\Gamma_r)\gamma_t \frac{w_c}{\text{COD}_{max}} & \text{if} \quad \gamma_t w_c < \text{COD}_{max} \end{cases} \end{cases} \tag{A.9}$$

where γ_t is the fraction of the tensile strength beyond which gel is absorbed by the crack, Γ_r is a residual ASR retention factor for ASR under tension. If an elastic model is used, then f_t' is the the tensile strength, σ_I the maximum principal tensile stress. On the other hand, if a smeared crack model is adopted, then COD_{max} is the maximum crack opening displacement at the current Gauss point, and w_c the maximum crack opening displacement in the tensile softening curve, Wittmann et al. (1988). Concrete pores being seldom interconnected, and the gel viscosity relatively high, gel absorption by the pores is not explicitly accounted for. Furthermore, gel absorption by the pores is accounted for by the kinetic equation through the latency time which depends on concrete porosity. The higher the porosity, the larger the latency time.

Γ_c in turns accounts for the reduction in ASR volumetric expansion under compressive stresses (in which case gel is absorbed by diffused micro-cracks), Multon (2004):

$$\Gamma_c = \begin{cases} 1 & \text{if} \quad \overline{\sigma} \leq 0. \quad \text{Tension} \\ 1 - \frac{e^{\beta}\overline{\sigma}}{1+(e^{\beta}-1.)\overline{\sigma}} & \text{if} \quad \overline{\sigma} > 0. \quad \text{Compression} \end{cases} \tag{A.10}$$

$$\overline{\sigma} = \frac{\sigma_I + \sigma_{II} + \sigma_{III}}{3f'_c} \tag{A.11}$$

Whereas this expression will also reduce expansion under uniaxial or biaxial confinement, Fig. 1.4, these conditions are more directly accounted for below through the assignment of weights.

1.1.1.4 ASR Strain Redistribution

The third major premise of the model, is that the volumetric ASR strain must be redistributed to the three principal directions according to their relative propensity for expansion on the basis of a weight which is a function of the respective stresses. Whereas the determination of the weight is relatively straightforward for triaxial ASR expansion under uniaxial confinement (for which some experimental data is available), it is more problematic for biaxially or triaxially confined concrete.

Given principal stress vector defined by $\sigma_k, \sigma_l, \sigma_m$, we need to assign a weight to each of those three principal directions. These weights will control ASR volumetric expansion distribution. For instance, with reference to Fig. 1.5, we consider three scenarios.

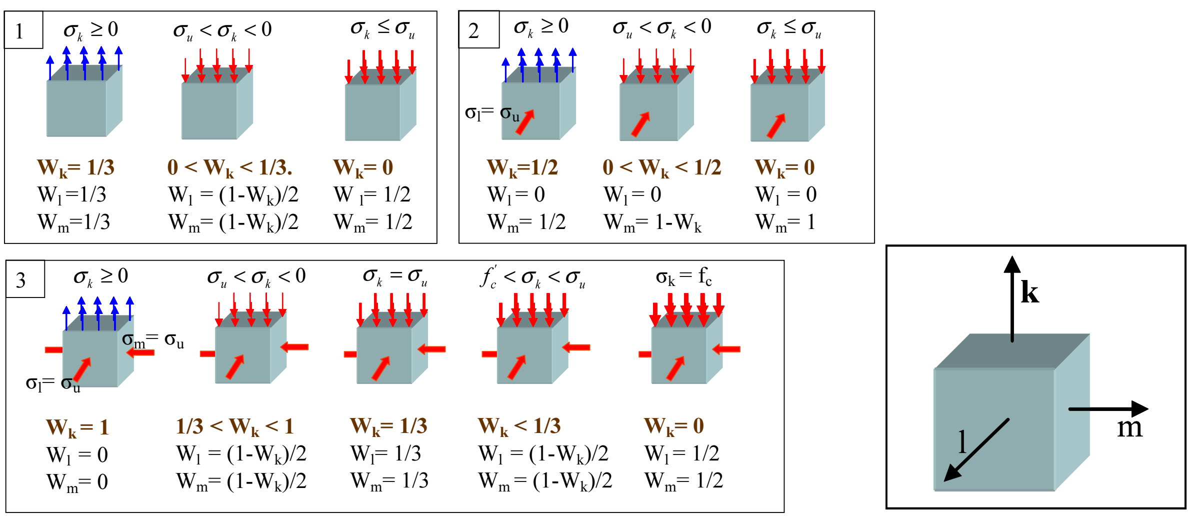

Fig. 1.5. Weight of Volumetric ASR Redistribution in Selected Cases

Uniaxial State of stress, where we distinguish the following three cases:

1. In the first case, we have uniaxial tension, and hence, the volumetric ASR strain is equally redistributed in all three directions.
2. Under a compressive stress greater than the limiting one (σ_u), the weight in the corresponding (k) direction should be less than one third. The remaining ASR has to be equally redistributed in the other two directions.

3. If the compressive stress is lower than σ_u, than ASR expansion in the corresponding direction is prevented (weight equal zero), and thus the other two weights must be equal to one half.

Biaxial state of stress in which we have a compressive stress equal to σ_u in one of the three principal directions. In this case, the corresponding weight will always be equal to zero. As to the possible three combinations:

1. Tension in one direction, equal weights of one half.
2. Compression greater than σ_u in one direction, then the corresponding weight must be less than one half, and the remaining weight is assigned to the third direction.
3. Compression less to σ_u, then the corresponding weight is again zero, and a unit weight is assigned to the third direction.

Triaxial state of stress in which we have σ_u acting on two of the three principle directions. We identify the following five cases:

1. Tension along direction k, then all the expansion is along k.
2. Compressive stress greater than σ_u, then we have a triaxial state of compressive stress, and the corresponding weight will be between one and one third. The remaining complement of the weight is equally distributed in the other two directions.
3. Compression equal to σ_u, hence we have a perfect triaxial state of compressive stress. In this case we have equal weights of one third. It should be noted that the overall expansion is reduced through Γ_c.
4. Compression less than σ_u but greater than the compressive strength. In this case, the weight along k should be less than one third, and the remaining equally distributed along the other two directions.
5. Compression equal to the compressive strength. In this case, the corresponding weight is reduced to zero, and the other two weights are equal to one half each.

Based on the preceding discussion, we generalize this weight allocation scheme along direction k as follows

1. Given σ_k, identify the quadrant encompassing σ_l and σ_m, Fig. 1.6[1]. Weight will be determined through a bilinear interpolation for those four neighboring nodes.

2. Determine the weights of the neighboring nodes from Table 1.1 through proper linear interpolation of σ_k.

3. Compute the weight from:

$$W_k(\sigma_k, \sigma_l, \sigma_m) = \sum_{i=1}^{4} N_i(\sigma_l, \sigma_m) W_i(\sigma_k) \tag{A.12}$$

where N_i is the usual two bilinear shape function used in finite element and is given by

[1] Since compressive stresses are quite low compared to the compressive strength, we ignore the strength gained through the biaxiality or triaxiality of the stress tensor Kupfer and Gerstle (1973). Furthermore, the strength gain is only about 14% for equibiaxial compressive stresses, CEB (1983).

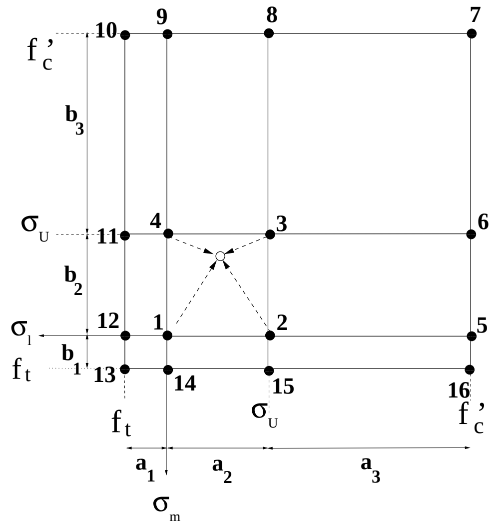

Fig. 1.6. Weight Regions

Node			Weights		
No.	σ_l	σ_m	$\sigma_k \geq 0$	$\sigma_k = \sigma_u$	$\sigma_k = f_c'$
1	0.	0.	1/3	0.	0.
2	σ_u	0.	1/2	0.	0.
3	σ_u	σ_u	1.	1/3	0.
4	0.	σ_u	1/2	0.	0.
5	f_c'	0.	1/2	0.	0.
6	f_c'	σ_u	1.	1/2	0.
7	f_c'	f_c'	1.	1.	1/3
8	σ_u	f_c'	1.	1/2	0.
9	0.	f_c'	1/2	0.	0.
10	f_t'	f_c'	1/2	0.	0.
11	f_t'	σ_u	1/2	0.	0.
12	f_t'	0.	1/3	0.	0.
13	f_t'	f_t'	1/3	0.	0.
14	0.	f_t'	1/3	0.	0.
15	σ_u	f_t'	1/2	0.	0.
16	f_c'	f_t'	1/2	0.	0.

Table 1.1. Triaxial Weights

$$\mathbf{N}(\sigma_l, \sigma_m) = \frac{1}{ab} \lfloor \; (a-\sigma_l)(b-\sigma_m) \quad \sigma_l(b-\sigma_m) \quad \sigma_l\sigma_m \quad (a-\sigma_l)\sigma_m \; \rfloor \tag{A.13}$$

$$\mathbf{W}(k) = \lfloor \; W_1(\sigma_k) \quad W_2(\sigma_k) \quad W_3(\sigma_k) \quad W_4(\sigma_k) \; \rfloor^t \tag{A.14}$$

$$a = (a_1|a_2|a_3) \qquad b = (b_1|b_2|b_3) \tag{A.15}$$

$$\sigma_l = (\sigma_l|f'_c - \sigma_l) \qquad \sigma_m = (\sigma_m|f'_c - \sigma_m) \tag{A.16}$$

The $i - j$ stress space is decomposed into nine distinct regions, Fig. 1.6, where σ_u is the upper (signed) compressive stress below which no ASR expansion can occur along the corresponding direction (except in triaxially loaded cases). Hence, a and b are the dimensions of the quadrant inside which σ_i and σ_j reside.

Weights of the individual nodes are in turn interpolated according to the principal stress component in the third direction σ_k, Table 1.1. It should be noted that those weights are for the most part based on the work of (Larive 1998) and (Multon 2004), but in some cases due to lack of sufficient experimental data, based on simple "engineering common sense".

A simple example for weight determination is shown here. Assuming that the principal stresses are given by $\lfloor\ \sigma_l \quad \sigma_m \quad \sigma_k\ \rfloor = \lfloor\ -5.0 \quad -8.0 \quad -5.0\ \rfloor$ MPa, and that f_c, f'_t and σ_u are equal to -30.0, 2.0, and -10.0 MPa respectively, we seek to determine W_k.

The stress tensors places us inside the quadrant defined by nodes 1-2-3-4 whose respective weights are equal to: $W_1 = \frac{1}{2}\left(\frac{1}{3}\right) = \frac{1}{6}$, $W_2 = \frac{1}{2}\left(\frac{1}{2}\right) = \frac{1}{4}$, $W_3 = \frac{1}{3} + \frac{1}{2}\left(1.0 - \frac{1}{3}\right) = \frac{2}{3}$, and $W_4 = \frac{1}{2}\left(\frac{1}{2}\right) = \frac{1}{4}$ a and b are both equal to -10 MPa, and the "shape factors" will be $N_1 = \frac{1}{100}\left[(-10+5)(-10+8)\right] = \frac{1}{10}$, $N_2 = \frac{1}{100}\left[-5(-10+8)\right] = \frac{1}{10}$, $N_3 = \frac{1}{100}\left[(-5)(-8)\right] = \frac{4}{10}$, $N_4 = \frac{1}{100}\left[-8(-10+5)\right] = \frac{4}{10}$, and finally $W_k = \frac{1}{10} \times \frac{1}{6} + \frac{1}{10} \times \frac{1}{4} + \frac{4}{10} \times \frac{2}{3} + \frac{4}{10} \times \frac{1}{4} = 0.40833$

Based on the earlier work of (Struble and Diamond 1981), in which it was reported that no gel expansion can occur at pressures above 11 MPa (though for a synthetic gel), σ_u is taken as -10 MPa. This value was also confirmed by (Larive 1998). f'_t and f'_c are the concrete tensile and compressive strengths respectively.

Individual strain is given by

$$\dot{\varepsilon}_i^{ASR} = W_i \dot{\varepsilon}_V^{ASR} \tag{A.17}$$

and the resulting relative weights are shown in Fig. 1.7.

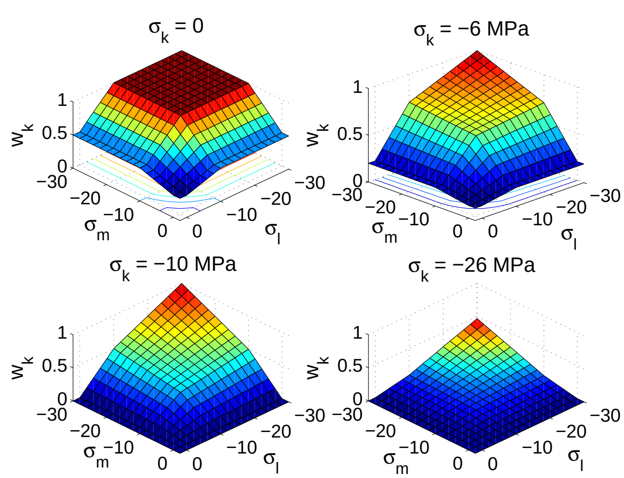

Fig. 1.7. Relative Weights

It should be noted that the proposed model will indeed result in an anisotropic ASR expansion. While not explicitly expressed in tensorial form, the anisotropy stems from the different weights assigned to each of the three principal directions.

1.1.1.5 Degradation

This deterioration being time dependent, the following time dependent nonlinear model is considered, Fig. 1.8.

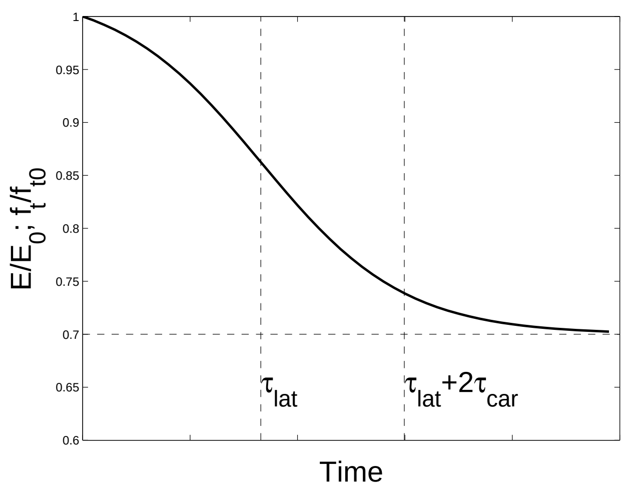

Fig. 1.8. Degradation of E and f_t'

$$E(t,\theta) = E_0\left[1-(1-\beta_E)\,\xi(t,\theta)\right] \tag{A.18}$$

$$f_t'(t,\theta) = f_{t,0}'\left[1-\left(1-\beta_f\right)\xi(t,\theta)\right] \tag{A.19}$$

where E_0 and $f_{t,0}'$ are the original elastic modulus and tensile strength, β_E and β_f are the corresponding residual fractional values when ε_{ASR} tends to $\varepsilon_{ASR}^{\infty}$.

1.1.2 NONLINEAR CONTINUUM MODEL

Since ASR is likely to cause substantial nonlinear deformation, a nonlinear model for the concrete is essential. Given the diffused nature of the ASR induced damage, ASR is on the one hand a prime candidate for a "smeared" crack model, on the other and major structural cracks are likely to develop (specially in dams) for which a "discrete crack" representation is more suitable.

This fracture-plastic model (Cervenka and Papanikolaou 2008) combines constitutive models for tensile (fracturing) and compressive (plastic) behavior. The fracture model is based on the classical orthotropic smeared crack formulation and crack band model. It employs Rankine failure criterion, exponential (or user defined) softening, and it can be used as rotated or fixed crack model. The hardening/softening plasticity model is based on (Menétrey and Willam 1995) failure surface. Both models use return mapping algorithm for the integration of constitutive equations. Special attention is given to the development of an algorithm for the combination of the two models. The combined algorithm is based on a recursive substitution, and it allows for the two models to be developed and formulated separately. The algorithm can handle cases when failure surfaces of both models are active, but also when physical changes such as crack closure occur. The model can be used to simulate concrete cracking, crushing under high confinement, and crack closure due to crushing in other material directions.

The method of strain decomposition, as introduced by (de Borst 1986), is used to combine fracture and plasticity models together. Both models are developed within the framework of return mapping algorithm by (Wilkins 1964). This approach guarantees the solution for all magnitudes of strain increment. From an algorithmic point of view the problem is then transformed into finding an optimal return point on the failure surface. The combined algorithm must determine the separation of strains into plastic and fracturing components, while it must preserve the stress equivalence in both models. The proposed algorithm is based on a recursive iterative scheme. It can be shown that such a recursive algorithm cannot reach convergence in certain cases such as, for instance, softening and dilating materials. For this reason the recursive algorithm is extended by a variation of the relaxation method to stabilize convergence.

1.1.2.1 Material Model Formulation

The material model formulation is based on the strain decomposition into elastic ε^e_{ij}, plastic ε^p_{ij} and fracturing components ε^f_{ij}, de Borst (1986).

$$\varepsilon_{ij} = \varepsilon^e_{ij} + \varepsilon^p_{ij} + \varepsilon^f_{ij} \tag{A.20}$$

The new stress state is then computed from:

$$\sigma^n_{ij} = \sigma^{n-1}_{ij} + E_{ijkl}(\Delta\varepsilon_{kl} - \Delta\varepsilon^p_{kl} - \Delta\varepsilon^f_{kl} \tag{A.21}$$

where the increments of plastic strain $\Delta\varepsilon^p_{kl}$ and fracturing strain $\Delta\varepsilon^f_{kl}$ must be evaluated based on the selected material model.

1.1.2.2 Rankine-Fracturing Model for Concrete Cracking

Rankine criterion is used for concrete cracking

$$F^f_i = \sigma'^t_{ii} - f'^t_i \leq 0 \tag{A.22}$$

where strains and stresses are expressed in material directions. For rotated cracks those correspond to the principal directions, and for the fixed crack model they correspond to the principal ones at the onset of first cracking. Thus, σ'^t_{ii} and f'_{ti} are the trial stress and tensile strength in the local material direction i. Prime symbol denotes quantities in the material directions.

Trial stress is determined from the elastic predictor

$$\sigma'^t_{ij} = \sigma'^{n-1}_{ij} + E_{ijkl}\Delta\varepsilon'_{kl} \tag{A.23}$$

If Equation A.22 is violated (i.e. cracking occurs) then the incremental fracturing strain in direction i can be evaluated under the assumption that the final stress state must satisfy

$$F^f_i = \sigma'^n_{ii} - f'_{ti} = \sigma'^t_{ii} - E_{iikl}\Delta\varepsilon'^f_{kl} - f'_{ti} = 0 \tag{A.24}$$

This equation can be further simplified under the assumption that the increment of fracturing strain is normal to the failure surface, and that always only one failure surface is being checked. Then for surface k the incremental fracturing strain is

$$\Delta\varepsilon'^{f}_{ij} = \Delta\lambda \frac{\partial F^{f}_{k}}{\partial \sigma_{ij}} = \Delta\lambda\delta_{ik} \tag{A.25}$$

substituting into Eq. A.24, the increment of the fracturing multiplier is recovered as

$$\Delta\lambda = \frac{\sigma'^{t}_{kk} - f'_{tk}}{E_{kkkk}} = \frac{\sigma'^{t}_{kk} - \mathrm{f'_t}(w^{max}_{k})}{E_{kkkk}} \tag{A.26}$$

where $\mathrm{f'_t}(w^{max}_{k})$ is the softening curve in terms of w which is the current crack opening. The softening diagram adopted in this model is the exponential decay function of (Hordijk 1991). The crack opening w is determined from

$$w^{max}_{k} = L_t(\hat{\varepsilon}'^{f}_{kk} + \Delta\lambda) \tag{A.27}$$

where $\hat{\varepsilon}'^{f}_{kk}$ is the total fracturing strain in direction k, and L_t is the characteristic dimension of the element as introduced by (Bažant and Oh 1983), Fig. 1.9. L_t is calculated as a size of the element projected into the crack direction, it is a satisfactory solution for low order linear elements. Equation A.26 can be solved by

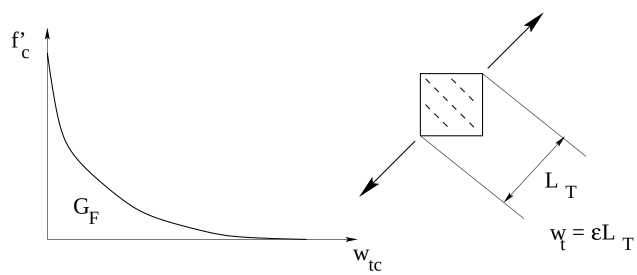

Fig. 1.9. Tensile Softening and Characteristic Length, Cervenka Consulting (2010)

recursive substitution. It can be shown that expanding $\mathrm{f'_t}(w^{max}_{k})$ into a Taylor series, that this iteration scheme converges as long as

$$\left| -\frac{\partial \mathrm{f'_t}(w^{max}_{k})}{\partial w} \right| < \frac{E_{kkkk}}{L_t} \tag{A.28}$$

This equation is violated for softening materials only when snap-back is observed in the stress-strain relationship, which can occur if large finite elements are used. Since in the standard finite element based method, the strain increment is given, therefore, a snap back on the constitutive level can not be captured. Since in the critical region where snap back occurring on the softening curve will be skipped, then the energy dissipated by the system will be over estimated. Because this is undesirable, finite elements smaller than $L < \frac{E_{kkkk}}{\left|\frac{\partial \mathrm{f'_t}(0}{\partial w}\right|}$ should be used, where $\frac{\partial \mathrm{f'_t}(0)}{\partial w}$ is the initial slope of the crack softening curve.

Distinction is made between the total maximum fracturing strain during loading $\hat{\varepsilon}'^{f}_{kk}$ and the current fracturing strain ε'^{f}_{ij} which is determined according to (Rots and Blaauwendraad 1989)

$$\varepsilon'^{f}_{kl} = (E_{ijkl} + E'^{f}_{ijkl})^{-1} E_{klmn}\varepsilon'_{mm} \tag{A.29}$$

$$\sigma'_{ij} = E'^{cr}_{ijkl}\varepsilon'^{f}_{kl} \tag{A.30}$$

where E'^{cr}_{ijkl} is the cracking stiffness in the local material (prime) direction. It is assumed that there is no interaction between normal and shear components thus the crack tensor is given by:

$$E'^{cr}_{ijkl} = 0 \text{ for } i \neq k \text{ and } j \neq l \tag{A.31}$$

The mode I crack stiffness is

$$E'^{cr}_{iiii} = \frac{\text{f't}(w_i^{max})}{\hat{\varepsilon}'^{f}_{ii}} \tag{A.32}$$

and mode II and III crack stiffnesses are assumed to be equal to

$$E'^{cr}_{ijij} = \frac{r_g^{ij} G}{1 - r_g^{ij}} \tag{A.33}$$

where $i \neq j$, $r_g^{ij} = \min(r_g^i, r_g^j)$ is the minimum shear retention factors on cracks for the directions i and j and are given by Kolmar (1986)

$$\begin{aligned} r_g^i &= \frac{-\ln\left(\frac{\varepsilon'_{ii}}{c_1}\right)}{c_2} && \text{(A.34)} \\ c_1 &= 7 + 333(\rho - 0.005) && \text{(A.35)} \\ c_2 &= 10 - 167(\rho - 0.005) && \text{(A.36)} \end{aligned}$$

where ρ is the reinforcement ratio assuming that it is below 0.002. G is the elastic shear modulus.

For the special cases before the onset of cracking, i.e., when expressions approach infinity, large penalty numbers are used for the crack stiffness. The shear retention factor is used only in the case of the fixed crack option.

Finally, the secant constitutive matrix in the material direction is analogous to Eq. A.29 as presented by Rots and Blaauwendraad (1989)

$$\mathbf{E}'^{s} = \mathbf{E} - \mathbf{E}(\mathbf{E}'^{cr} + \mathbf{E})^{-1}\mathbf{E} \tag{A.37}$$

which should then be transformed to the global coordinate system $\mathbf{E}^s = \Gamma_\varepsilon^T \mathbf{E}'^s \Gamma_\varepsilon$ where Γ_ε is the strain vector transformation matrix (i.e. global to local strain transformation matrix).

1.1.2.3 Plasticity Model for Concrete Crushing

Starting with the predictor-corrector formula, the stress is determined from

$$\sigma_{ij}^n = \sigma_{ij}^{n-1} + E_{ijkl}(\Delta\varepsilon_{kl} - \Delta\varepsilon_{kl}^p) = \sigma_{ij}^t - E_{ijkl}\Delta\varepsilon_{kl}^p = \sigma_{ij}^t - \sigma_{ij}^p \tag{A.38}$$

where σ_{ij}^t is the total stress, and σ_{ij}^p is determined from the yield function via the return mapping algorithm

$$F^p(\sigma_{ij}^t - \sigma_{ij}^p) = F^p(\sigma_{ij}^t - \Delta\lambda l_{ij}) \tag{A.39}$$

The critical component of this equation is l_{ij} which is the return direction defined by

$$\begin{aligned} l_{ij} &= E_{ijkl}\frac{\partial G^p(\sigma_{kl}^t)}{\partial \sigma_{kl}} && \text{(A.40)} \\ \Rightarrow \Delta\varepsilon_{ij}^p &= \Delta\lambda \frac{\partial G^p(\sigma_{ij}^t)}{\partial \sigma_{ij}} && \text{(A.41)} \end{aligned}$$

where $G^p(\sigma_{ij})$ is the plastic potential function whose derivative is evaluated at the predictor stress state σ^t_{ij} to determine the return direction.

The adopted failure surface is the one of (Menétrey and Willam 1995) which affords much flexibility in its formulation

$$F^P_{3p} = \left[\sqrt{1.5}\frac{\rho}{f'_c}\right]^2 + m\left[\frac{\rho}{\sqrt{6}f'_c}r(\theta, e) + \frac{\xi}{\sqrt{3}f'_c}\right] - c = 0 \tag{A.42}$$

where

$$m = \sqrt{3}\frac{f'^2_c - f'^2_t}{f'_c f'_t}\frac{e}{e+1} \tag{A.43}$$

$$r(\theta, e) = \frac{4(1-e^2)\cos^2\theta + (2e-1)^2}{2(1-e^2)\cos\theta + (2e-1)\sqrt{4(1-e^2)\cos^2\theta + 5e^2 - 4e}} \tag{A.44}$$

(ξ, ρ, θ) constitute the Heigh-Westerggard coordinates, f'_c and f'_t are the uniaxial compressive and tensile strength respectively. The curvature of the failure surface is controlled by $e \in \langle 0.5, 1.0\rangle$ (sharp corner for $e = 0.5$, and circular for $e = 1.0$, Fig. 1.10.

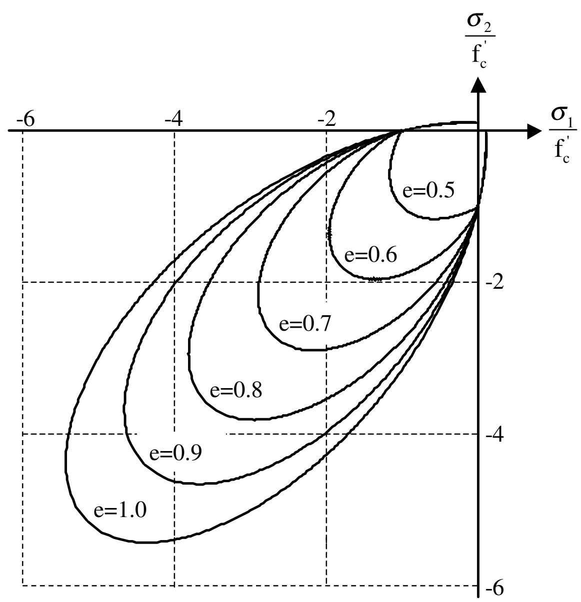

Fig. 1.10. Failure Surface

The position of the failure surface is not fixed, but rather can move depending on the magnitude of the strain hardening/softening parameter. The strain hardening is based on the equivalent plastic strain which is calculated from $\Delta\varepsilon^p_{eq} = \min(\Delta\varepsilon^p_{ij})$.

Hardening/softening is controlled by the parameter $c \in \langle 0, 1\rangle$, which evolved during the yielding/crushing process according to

$$c = \left(\frac{f'_c(\varepsilon^p_{eq})}{f'_c}\right)^2 \tag{A.45}$$

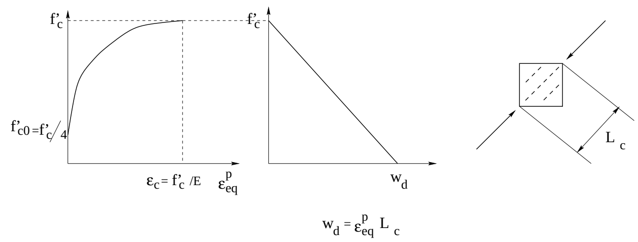

Fig. 1.11. Compressive Hardening and Softening, van Mier (1986)

where $f_c'(\varepsilon_{eq}^p)$ is the hardening/softening law based on uniaxial test, Fig. 1.11. The law shown in Fig. 1.11 has an elliptical ascending branch and a linear postpeak softening branch after the peak. The elliptical ascending part depends on strains

$$\sigma = f_{c0} + (f_c - f_{c0})\sqrt{1 - \left(\frac{\varepsilon_c - \varepsilon_{sq}^p}{\varepsilon_c}\right)^2} \tag{A.46}$$

while the descending part is based on relative displacements. In order to introduce mesh objectivity, the descending branch is based on the work of (van Mier 1986) where the equivalent plastic strain is transformed into displacements through the length scale L_c. This parameter is defined in an analogous manner to the crack band parameter in the fracture model, Fig. 1.9 and it corresponds to the projection of element size into the direction of minimal principal stresses. The square in Eq. A.45 is due to the quadratic nature of the Menétrey-Willam surface.

Return direction is given by the following plastic potential

$$G^p(\sigma_{ij}) = \beta\frac{\sqrt{3}}{I}_1 + \sqrt{2J_2} \tag{A.47}$$

(2.58) where β determines the return direction. If $\beta < 0$ material is being compacted during crushing, if $\beta = 0$ material volume is preserved, and if $\beta > 0$ material is dilating. In general the plastic model is non-associated, since the plastic flow is not perpendicular to the failure surface The return mapping algorithm for the plastic model is based on predictor-corrector approach as shown in Fig. 1.12. During the corrector phase of the algorithm the failure surface moves along the hydrostatic axis to simulate hardening and softening. The final failure surface has the apex located at the origin of the Haigh-Westergaard coordinate system. Secant method based Algorithm 1 is used to determine the stress on the surface, which satisfies the yield condition and also the hardening/softening law.

Algorithm 1: Input: $\sigma_{ij}^{n-1}, \varepsilon_{ij}^{p^{n-1}}, \Delta\varepsilon_{ij}^n$

1. Elastic predictor $\sigma_{ij}^t = \sigma_{ij}^{n-1} + E_{ijkl}\Delta\varepsilon_{kl}^n$
2. Evaluate failure criterion: $f_A^p = F^p\left(\sigma_{ij}^t, \varepsilon_{ij}^{p^{n-1}}\right), \Delta\lambda_A = 0$
3. If failure criterion is violated i.e. $f_A^p > 0$
   (a) Evaluate return direction: $m_{ij} = \frac{\partial G^p(\sigma_{ij}^t)}{\partial\sigma_{ij}}$

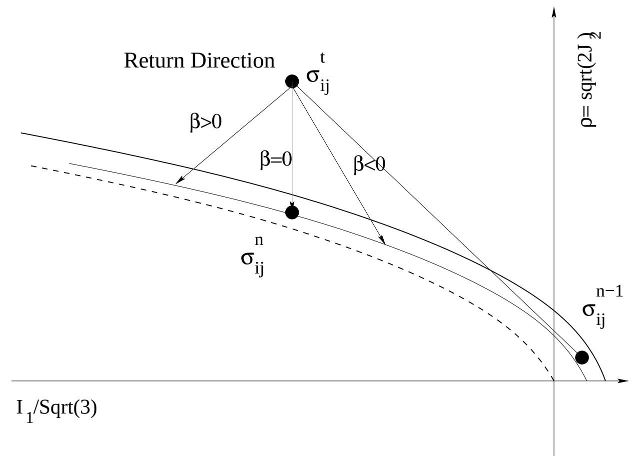

Fig. 1.12. Plastic Predictor-Corrector Algorithm, Cervenka Consulting (2010)

(b) Return mapping: $F^p(\sigma_{ij}^t - \Delta\lambda_B E m_{ij}, \varepsilon_{ij}^{p^{n-1}}) = 0 \Rightarrow \Delta\lambda_B$

(c) Evaluate failure criterion: $f_B^p = F^p(\sigma_{ij}^t - \Delta\lambda_B E m_{ij}, \varepsilon_{ij}^{p^{n-1}}) + \Delta\lambda_B m_{ij}$

(d) Secant iterations as long as $|\Delta\lambda_A - \Delta\lambda_B| < e$

i. New plastic multiplier increment: $\Delta\lambda = \Delta\lambda_A - f_A^p \frac{\Delta\lambda_B - \Delta\lambda_A}{f_B^p - f_A^p}$

ii. New return direction: $m_{ij}^{(i)} = \frac{\partial G^p(\sigma_{ij}^t - \Delta\lambda E m_{ij}^{(i-1)}}{\partial \sigma_{ij}}$

iii. Evaluate failure criterion: $f^p = F^p(\sigma_{ij}^t - \Delta\lambda E m_{ij}^{(i)}, \varepsilon_{ij}^p + \Delta\lambda m_{ij}^{(i)})$

iv. New initial values for secant iterations:

$$* \begin{array}{lll} f_B^p < 0 & \Rightarrow & f_B^p = f^p, \quad \Delta\lambda_B = \Delta\lambda \\ f_B^p \geq 0 & \Rightarrow & f_A^p = f_B^p, \quad \Delta\lambda_A = \Delta\lambda_B, \quad f_B^p = f^p, \quad \Delta\lambda_B = \Delta\lambda \end{array} \tag{A.48}$$

(e) End of secant iteration loop.

4. End of algorithm update stress and plastic strains. $\varepsilon_{ij}^{p^n} = \varepsilon_{ij}^{p^{n-1}} + \Delta\lambda_B mij^{(i)} \qquad ch\sigma_{ij}^n = \sigma_{ij}^t - \Delta\lambda_B E m_{ij}^{(i)}$

1.1.2.4 Combination of Plasticity and Fracture model

The objective is to combine the above models into a single model such that plasticity is used for concrete crushing and the Rankine fracture model for cracking. This problem can be generally stated as a simultaneous solution of the two following inequalities.

$$F^p(\sigma_{ij}^{n-1} + E_{ijkl}(\Delta\varepsilon_{kl} - \Delta\varepsilon_{kl}^f - \Delta\varepsilon_{kl}^p)) \leq 0 \quad \text{solve for} \quad \Delta\varepsilon_{kl}^p \tag{A.49}$$

$$F^f(\sigma_{ij}^{n-1} + E_{ijkl}(\Delta\varepsilon_{kl} - \Delta\varepsilon_{kl}^p - \Delta\varepsilon_{kl}^f)) \leq 0 \quad \text{solve for} \quad \Delta\varepsilon_{kl}^f \tag{A.50}$$

Each inequality depends on the output from the other one, therefore the following iterative scheme is developed.

Algorithm 2:

1. $F^p(\sigma_{ij}^{n-1} + E_{ijkl}(\Delta\varepsilon_{kl} - \Delta\varepsilon_{kl}^{f^{i-1}} + b\Delta\varepsilon_{kl}^{cor^{(i-1)}} - \Delta\varepsilon_{kl}^{p^{(i)}})) \leq 0$solve for$\Delta\varepsilon_{kl}^{p^{(i)}}$

2. $F^p f(\sigma_{ij}^{n-1} + E_{ijkl}(\Delta\varepsilon_{kl} - \Delta\varepsilon_{kl}^{p^{i-1}} - Delta\varepsilon_{kl}^{f^{(i)}})) \leq 0$solve for$\Delta\varepsilon_{kl}^{f^{(i)}}$

3. $\Delta\varepsilon_{ij}^{cor^{(i)}} = \Delta\varepsilon_{ij}^{f^{(i)}} - \Delta\varepsilon_{ij}^{f^{(i-1)}}$

4. Iterative correction of the strain norm between two subsequent iterations can be expressed as $\|\Delta\varepsilon_{ij}^{cor^{(i)}}\| = (1-b)\alpha^f\alpha^p\|\Delta\varepsilon_{ij}^{cor^{(i-1)}}\|$ where $\alpha^f = \frac{\|\Delta\varepsilon_{ij}^{f^{(i)}} - \Delta\varepsilon_{ij}^{f^{(i-1)}}}{\Delta\varepsilon_{ij}^{p^{(i)}}\Delta\varepsilon_{ij}^{p^{(i-1)}}}$ and $\alpha^p = \frac{\|\Delta\varepsilon_{ij}^{p^{(i)}} - \Delta\varepsilon_{ij}^{p^{(i-1)}}}{\Delta\varepsilon_{ij}^{f^{(i)}}\Delta\varepsilon_{ij}^{f^{(i-1)}}}$

b is an iteration correction or relaxation factor, which is introduced in order to guarantee convergence. It is to be determined based on the run-time analysis of α^f and α^p , such that the convergence of the iterative scheme can be assured. The parameters α^f and α^p characterize the mapping properties of each model (i.e. plastic and fracture). It is possible to consider each model as an operator, which maps strain increment on the input into a fracture or plastic strain increment on the output. The product of the two mappings must be contractive in order to obtain a convergence. The necessary condition for the convergence is:

$$|(1-b)\alpha^f\alpha^p| < 1 \tag{A.51}$$

(2.75) If b equals 0, an iterative algorithm based on recursive substitution is obtained. The convergence can be guaranteed only in two cases:

1. One of the models is not activated (i.e. implies α^f or $\alpha^p = 0$

2. There is no softening in either of the two models and dilating material is not used in the plastic part, which for the plastic potential in this work means $\beta < 0$, , (Eq. A.47). This is a sufficient but not necessary condition to ensure that α^f and $\alpha^p < 1$.

It can be shown that the values of α^f and α^p are directly proportional to the softening rate in each model. Since the softening model remains usually constant for a material model and finite element, their values do not change significantly between iterations. It is possible to select the scalar b such that the inequality Eq. A.51 is satisfied always at the end of each iteration based on the current values of α^f and α^p . There are three possible scenarios, which must be handled, for the appropriate calculation of b:

1. $|alpha^f\alpha^p| \leq \chi$, where χ is related to the requested convergence rate. For linear rate it can be set to $\chi = 1/2$. In this case the convergence is satisfactory and $b = -0$.

2. $\chi < |alpha^f\alpha^p|$, then the convergence would be too slow. In this case b can be estimated as $b = 1 - \frac{|alpha^f\alpha^p|}{\chi}$ in order to increase the convergence rate.

3. $1 \leq |alpha^f\alpha^p|$, then the algorithm is diverging. In this case b should be calculated as $b = 1 - \frac{\chi}{|alpha^f\alpha^p|}$ to stabilize the iterations.

This approach guarantees convergence as long as the parameters does not change drastically between the iterations, which should be satisfied for smooth and correctly formulated models. The rate of convergence depends on material brittleness, dilating parameter β and finite element size. It is advantageous to further stabilize the algorithm by smoothing the parameter b during the iterative process:

$$b = \frac{b^{(i)} + b^{(i-1)}}{2} \tag{A.52}$$

where the superscript i denotes values from two subsequent iterations. This will eliminate problems due to the oscillation of the correction parameter b . Important condition for the convergence of the above Algorithm 2 is that the failure surfaces of the two models are intersecting each other in all possible positions even during the hardening or softening. Additional constraints are used in the iterative algorithm. If the stress state at the end of the first step violates the Rankine criterion, the order of the first two steps in Algorithm 2 is reversed. Also in reality concrete crushing in one direction has an effect on the cracking in other directions. It is assumed that after the plasticity yield criterion is violated, the tensile strength in all material directions is set to zero. On the structural level secant matrix is used in order to achieve a robust convergence during the strain localization process. The proposed algorithm for the combination of plastic and fracture models is graphically shown in Fig. 1.13. When both surfaces are activated, the behavior is

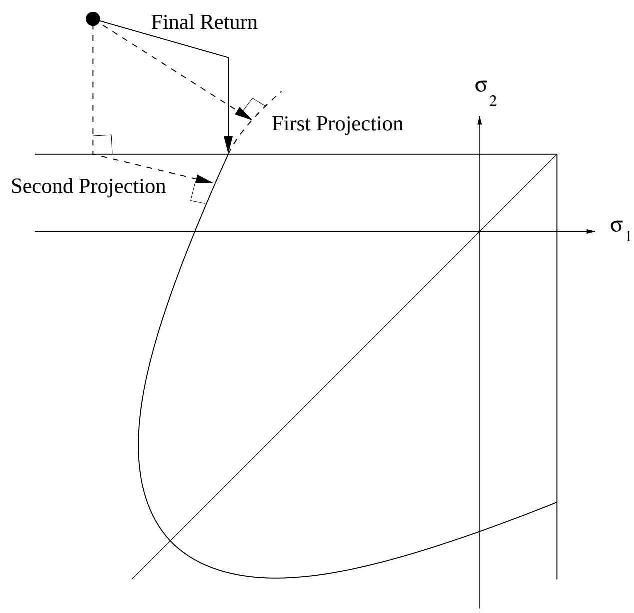

Fig. 1.13. Schematic Description of the Iterative Process in 2D, Cervenka Consulting (2010)

quite similar to the multi-surface plasticity. Contrary to the multi-surface plasticity algorithm the proposed method is more general in the sense that it covers all loading regimes including physical changes such as for instance crack closure. Currently, it is developed only for two interacting models, and its extension to multiple models is not straightforward.

Appendix B

Fundamentals of Multiple Linear Regression

2.1 INTRODUCTION

Multiple linear regression (MLR) is the extension of simple linear regression (SLR) to the case of multiple *explanatory variables* (which may or may not be truly independent). Hence, rather than modeling the mean response as a straight line, as in simple regression, it is now modeled as a function of several explanatory variables.

Multiple explanatory variables are required when scientific knowledge and experience tells us they are likely to be useful. In the problem at hand, this may be the depth of the beam, the maximum AAR expansion or others.

Simply put the model is:

$$y = \beta_0 + \sum_{i=1}^{n} \beta_i x_i + \varepsilon \tag{B.1}$$

where y is the response variable (such as shear strength variation), β_0 the intercept, β_i is the slope coefficient of explanatory variable i, and ε is the remaining unexplained noise in the date (the error), x_i are all the constituents of the 18 variables listed in Table 2.1, and the β_i coefficients are to be determined.

Given the normalized approach taken by R, a higher β coefficient is indicative of a higher "participation factor" or relevant parameter in the shear strength change.

This equation will be solved by minimizing the error between data points and the estimated one ($\hat{\ }$):

$$\hat{y} = \text{argmin}(y - \hat{y})^2 \tag{B.2}$$

2.2 DUMMY VARIABLES

Adapted from
http://www.medicine.mcgill.ca/epidemiology/joseph/courses/EPIB-621/dummy.pdf

A *categorical variable* is one which is not continuous, yet it can take a value that is one of several possible categories.

In the statistical analysis of the results, none of the variables is continuous (such as load), but are rather *dichotomous* (such as depth of 24" or 48"), or (multiple) *categorical variable*, such as Boundary Conditions (U, R, or FR), or type of structure (B, TB or P). Yet internally statistical programs use numbers in all of their calculations, not words. So, even if one did not code dichotomous or multi-categorical variables using numbers, they will be converted by the program into numbers.

We can have R automatically do dummy variable coding, using a “factor” declaration.

2.3 HYPOTHESIS TESTS FOR MULTIPLE REGRESSION

`Adapted from http://pubs.usgs.gov/twri/twri4a3/pdf/chapter11.pdf`

The single most important hypothesis test for MLR is the F test for comparing any two nested models. Let model “s” be the “simpler” MLR model

$$y_s = \beta_0 + \beta_1 x_1 + \beta_2 x_2 + \cdots + \beta_k x_k + \varepsilon_s \tag{B.3}$$

It has $k + 1$ parameters including the intercept, with degrees of freedom (dfs) of $n(k + 1)$. Again, the degrees of freedom equals the number of observation minus the number of parameters estimated, as in SLR. Its sum of squared errors is SSE_s.

Let model “c” be the more complex regression model

$$y_s = \beta_0 + \beta_1 x_1 + \beta_2 x_2 + \cdots + \beta_k x_k + \beta_{k+1} x_{k+1} + \cdots + \beta_m x_m + \varepsilon_s \tag{B.4}$$

It has $m + 1$ parameters and residual degrees of freedom (dfc) of $n(m + 1)$. Its sum of squared errors is SSE_c.

The test of interest is whether the more complex model provides a sufficiently better explanation of the variation in y than does the simpler model. In other words, do the extra explanatory variables x_{k+1} to x_m add any new explanatory power to the equation? The models are “nested” because all of the k explanatory variables in the simpler model are also present in the complex model, and thus the simpler model is nested within the more complex model. The null hypothesis is

$$H_0 \quad : \quad \beta_{k+1} = \beta_{k+2} = \cdots = \beta_m = 0 \qquad \text{versus the alternative} \tag{B.5}$$

$$H_1 \quad : \quad \text{at least one of these } mk \text{ coefficients is not equal to zero.} \tag{B.6}$$

If the slope coefficients for the additional explanatory variables are all not significantly different from zero, the variables are not adding any explanatory power in comparison to the cost of adding them to the model. This cost is measured by the loss in the degrees of freedom = mk, the number of additional variables in the more complex equation.

The test statistic is

$$F = \frac{(\mathrm{SSE}_s - \mathrm{SSE}_c)\,(\mathrm{df}_s - \mathrm{df}_c)}{(\mathrm{SSE}_c/\mathrm{df}_c)} \tag{B.7}$$

where $(\mathrm{df}_s\text{-}\mathrm{df}_c) = m - k$.

If F exceeds the tabulated value of the F distribution with $(\mathrm{df}_s\text{-}\mathrm{df}_c)$ and df_c degrees of freedom for the selected α (say α=0.05), then H_0 is rejected. Rejection indicates that the more complex model should be chosen in preference to the simpler model. If F is small, the additional variables are adding little to the model, and the simpler model would be chosen over the more complex.

2.4 VARIABLE SELECTIONS: AKAIKE AND BAYESIAN MODELS

```
Adapted from http://staff.ustc.edu.cn/ zwp/teach/MVA/select.pdf
```

How can we decide what variables to include? Following Ockham's razor (or in Latin *ex parsimoniae*) "Among competing hypotheses that predict equally well, the one with the fewest assumptions should be selected". In the context of MLR this means that a model with fewer parameters is to be preferred to one with more. However, this needs to be weighed against the ability of the model to actually predict anything.

Or one can say that the cost of adding additional variables is that the degrees of freedom decreases, making it more difficult to find significance in hypothesis tests and increasing the width of confidence intervals. Hence, a "good" model should explain as much of the variance of y as possible with a small number of explanatory variables.

Two particular statistical models are considered:

Akaike Information Criterion (AIC) is one of the most common model selection for model selection procedure that is available in most statistical software packages. It is based on maximum likelihood and a penalty for each parameter, (Akaike 1974). For each model, compute

$$\text{AIC} = n\ln(\text{SSE}) - n\ln(n) + 2p \tag{B.8}$$

where SSE is the usual residual sum of squares from that model, p is the number of parameters in the current model, and n is the sample size. After doing this for all possible models, the "best" model is the one with the smallest AIC.

Note that the AIC is formed from three terms: The first is a measure of fit, since $n\ln(\text{SSE})$ is essentially the sum of squared residuals. The second term, $n\ln(n)$ is a constant, and really plays no role in selecting the model. The third term, $2p$ is a "penalty" term for adding more terms to the model. This is because the first term always decreases as more terms are added into the model, so this is needed for "balance".

Schwartz's Bayesian information criterion (BIC) is similar to AIC but penalizes additional parameters more (**?**). For each model, calculate:

$$\text{BIC} = n\ln(\text{SSE}) - n\ln(n) + \ln(n)p \tag{B.9}$$

where SSE is the usual residual sum of squares from that model, p is the number of parameters in the current model, and n is the sample size. After doing this for all possible models, the"best" model is the one with the smallest BIC. Note the similarity between AIC and BIC, only the last term changes.

2.5 MODELING CONSIDERATIONS

2.5.1 R LISTING AND OUTPUT

The command in R used for linear fitting is "lm". It can be used to carry out regression, single stratum analysis of variance and analysis of covariance. The following short and elegant sample code is at the heart of the procedure.

```
rm(list=ls())
test=read.csv("victor-results.csv",header=T)

## index=1:length(test$disp)
## indexdisp = index[test$disp < 10]
## xx = test$stregth[indexdisp]

index=1:length(test$stregth)
indexstr = index[test$stregth < 0 & test$stregth > -100 & test$disp < 10]
xx = test$stregth[indexstr]
test=test[indexstr,]
```

Listing B.1. Preliminaries

```
## First fit full model - i.e. with all parameters

zzfull = lm(stregth ~ test$type + test$depth + test$BC + test$epsilon +
test$rho + test$betaE + test$betaft, data=test)
# Then type zzfull to show the full model
# or type summary(zzfull)

## best model based on Akaikie Information Criteria, AIC
zbest1 = stepAIC(zzfull)
summary(zbest1)

## best model based on Bayesian Information Criteria, BIC

N1 = log(length(test$stregth))
zbest2 = stepAIC(zbest1, k=N1)
summary(zbest2)
```

Listing B.2. Fitting Code

The results of the linear model fitting are provided in a table including the β_i coefficients for the most relevant sub-variables, their standard deviation, t and $Pr(>|t|)$ (previously defined) are also reported.

Estimated Coefficient: is the value of slope calculated by the regression. It might seem a little confusing that the Intercept also has a value, but should be interpreted as a slope that is always multiplied by 1. This number will obviously vary based on the magnitude of the variable which is going to be an input into the regression, but it is always good practice to spot check this number to evaluate its reasonableness.

Standard Error of the Coefficient Estimate : Measure of the variability in the estimate for the coefficient. Lower means better but this number is relative to the value of the coefficient. As a rule of thumb, this value should to be at least an order of magnitude less than the coefficient estimate.

***t*:** Score that measures whether or not the coefficient for this variable is meaningful for the model.

$Pr(>|t|)$: A predictor that has a low p-value is likely to be a meaningful addition to model because changes in the predictor's value are related to changes in the response variable A large p-value suggests that changes in the predictor are not associated with changes in the response. Hence this number should be as small as possible.

Significance Stars : The stars are shorthand for significance levels, with the number of asterisks displayed according to the p-value computed. $***$ for high significance and $*$ for low significance.

ïż£

Appendix C

File Names

3.1 AAR PLUS SHEAR

Table 3.1. Generated Meshes with AAR

Table 3.1 – *Continued from previous page*

t	BC	$\varepsilon^{\infty}_{AAR}$	ρ	β_E	β_{ft}	Filename	Reference Filename
2 ft	U	0.1 %	0.2 %	0.7	0.7	1-X-2-U-1-2-7-7.inp	*X-2-U-0-2-0-0.inp*
2 ft	U	0.1 %	0.2 %	0.7	0.9	2-X-2-U-1-2-7-9.inp	*X-2-U-0-2-0-0.inp*
2 ft	U	0.1 %	0.2 %	0.9	0.7	3-X-2-U-1-2-9-7.inp	*X-2-U-0-2-0-0.inp*
2 ft	U	0.1 %	0.2 %	0.9	0.9	4-X-2-U-1-2-9-9.inp	*X-2-U-0-2-0-0.inp*
2 ft	U	0.1 %	0.5 %	0.7	0.7	5-X-2-U-1-5-7-7.inp	*X-2-U-0-5-0-0.inp*
2 ft	U	0.1 %	0.5 %	0.7	0.9	6-X-2-U-1-5-7-9.inp	*X-2-U-0-5-0-0.inp*
2 ft	U	0.1 %	0.5 %	0.9	0.7	7-X-2-U-1-5-9-7.inp	*X-2-U-0-5-0-0.inp*
2 ft	U	0.1 %	0.5 %	0.9	0.9	8-X-2-U-1-5-9-9.inp	*X-2-U-0-5-0-0.inp*
2 ft	U	0.1 %	1.0 %	0.7	0.7	9-X-2-U-1-10-7-7.inp	*X-2-U-0-10-0-0.inp*
2 ft	U	0.1 %	1.0 %	0.7	0.9	10-X-2-U-1-10-7-9.inp	*X-2-U-0-10-0-0.inp*
2 ft	U	0.1 %	1.0 %	0.9	0.7	11-X-2-U-1-10-9-7.inp	*X-2-U-0-10-0-0.inp*
2 ft	U	0.1 %	1.0 %	0.9	0.9	12-X-2-U-1-10-9-9.inp	*X-2-U-0-10-0-0.inp*
2 ft	U	0.2 %	0.2 %	0.7	0.7	13-X-2-U-2-2-7-7.inp	*X-2-U-0-2-0-0.inp*
2 ft	U	0.2 %	0.2 %	0.7	0.9	14-X-2-U-2-2-7-9.inp	*X-2-U-0-2-0-0.inp*
2 ft	U	0.2 %	0.2 %	0.9	0.7	15-X-2-U-2-2-9-7.inp	*X-2-U-0-2-0-0.inp*
2 ft	U	0.2 %	0.2 %	0.9	0.9	16-X-2-U-2-2-9-9.inp	*X-2-U-0-2-0-0.inp*
2 ft	U	0.2 %	0.5 %	0.7	0.7	17-X-2-U-2-5-7-7.inp	*X-2-U-0-5-0-0.inp*
2 ft	U	0.2 %	0.5 %	0.7	0.9	18-X-2-U-2-5-7-9.inp	*X-2-U-0-5-0-0.inp*
2 ft	U	0.2 %	0.5 %	0.9	0.7	19-X-2-U-2-5-9-7.inp	*X-2-U-0-5-0-0.inp*
2 ft	U	0.2 %	0.5 %	0.9	0.9	20-X-2-U-2-5-9-9.inp	*X-2-U-0-5-0-0.inp*
2 ft	U	0.2 %	1.0 %	0.7	0.7	21-X-2-U-2-10-7-7.inp	*X-2-U-0-10-0-0.inp*
2 ft	U	0.2 %	1.0 %	0.7	0.9	22-X-2-U-2-10-7-9.inp	*X-2-U-0-10-0-0.inp*
2 ft	U	0.2 %	1.0 %	0.9	0.7	23-X-2-U-2-10-9-7.inp	*X-2-U-0-10-0-0.inp*
2 ft	U	0.2 %	1.0 %	0.9	0.9	24-X-2-U-2-10-9-9.inp	*X-2-U-0-10-0-0.inp*
2 ft	U	0.3 %	0.2 %	0.7	0.7	25-X-2-U-3-2-7-7.inp	*X-2-U-0-2-0-0.inp*
2 ft	U	0.3 %	0.2 %	0.7	0.9	26-X-2-U-3-2-7-9.inp	*X-2-U-0-2-0-0.inp*
2 ft	U	0.3 %	0.2 %	0.9	0.7	27-X-2-U-3-2-9-7.inp	*X-2-U-0-2-0-0.inp*
2 ft	U	0.3 %	0.2 %	0.9	0.9	28-X-2-U-3-2-9-9.inp	*X-2-U-0-2-0-0.inp*
2 ft	U	0.3 %	0.5 %	0.7	0.7	29-X-2-U-3-5-7-7.inp	*X-2-U-0-5-0-0.inp*
2 ft	U	0.3 %	0.5 %	0.7	0.9	30-X-2-U-3-5-7-9.inp	*X-2-U-0-5-0-0.inp*
2 ft	U	0.3 %	0.5 %	0.9	0.7	31-X-2-U-3-5-9-7.inp	*X-2-U-0-5-0-0.inp*

X:[P|B|TB]; U: Unrestrained; R: Restrained; FR: Fully Restrained

Continued on next page

2 ft	U	0.3 %	0.5 %	0.9	0.9	32-X-2-U-3-5-9-9.inp	*X-2-U-0-5-0-0.inp*
2 ft	U	0.3 %	1.0 %	0.7	0.7	33-X-2-U-3-10-7-7.inp	*X-2-U-0-10-0-0.inp*
2 ft	U	0.3 %	1.0 %	0.7	0.9	34-X-2-U-3-10-7-9.inp	*X-2-U-0-10-0-0.inp*
2 ft	U	0.3 %	1.0 %	0.9	0.7	35-X-2-U-3-10-9-7.inp	*X-2-U-0-10-0-0.inp*
2 ft	U	0.3 %	1.0 %	0.9	0.9	36-X-2-U-3-10-9-9.inp	*X-2-U-0-10-0-0.inp*
4 ft	U	0.1 %	0.2 %	0.7	0.7	37-X-4-U-1-2-7-7.inp	*X-4-U-0-2-0-0.inp*
4 ft	U	0.1 %	0.2 %	0.7	0.9	38-X-4-U-1-2-7-9.inp	*X-4-U-0-2-0-0.inp*
4 ft	U	0.1 %	0.2 %	0.9	0.7	39-X-4-U-1-2-9-7.inp	*X-4-U-0-2-0-0.inp*
4 ft	U	0.1 %	0.2 %	0.9	0.9	40-X-4-U-1-2-9-9.inp	*X-4-U-0-2-0-0.inp*
4 ft	U	0.1 %	0.5 %	0.7	0.7	41-X-4-U-1-5-7-7.inp	*X-4-U-0-5-0-0.inp*
4 ft	U	0.1 %	0.5 %	0.7	0.9	42-X-4-U-1-5-7-9.inp	*X-4-U-0-5-0-0.inp*
4 ft	U	0.1 %	0.5 %	0.9	0.7	43-X-4-U-1-5-9-7.inp	*X-4-U-0-5-0-0.inp*
4 ft	U	0.1 %	0.5 %	0.9	0.9	44-X-4-U-1-5-9-9.inp	*X-4-U-0-5-0-0.inp*
4 ft	U	0.1 %	1.0 %	0.7	0.7	45-X-4-U-1-10-7-7.inp	*X-4-U-0-10-0-0.inp*
4 ft	U	0.1 %	1.0 %	0.7	0.9	46-X-4-U-1-10-7-9.inp	*X-4-U-0-10-0-0.inp*
4 ft	U	0.1 %	1.0 %	0.9	0.7	47-X-4-U-1-10-9-7.inp	*X-4-U-0-10-0-0.inp*
4 ft	U	0.1 %	1.0 %	0.9	0.9	48-X-4-U-1-10-9-9.inp	*X-4-U-0-10-0-0.inp*
4 ft	U	0.2 %	0.2 %	0.7	0.7	49-X-4-U-2-2-7-7.inp	*X-4-U-0-2-0-0.inp*
4 ft	U	0.2 %	0.2 %	0.7	0.9	50-X-4-U-2-2-7-9.inp	*X-4-U-0-2-0-0.inp*
4 ft	U	0.2 %	0.2 %	0.9	0.7	51-X-4-U-2-2-9-7.inp	*X-4-U-0-2-0-0.inp*
4 ft	U	0.2 %	0.2 %	0.9	0.9	52-X-4-U-2-2-9-9.inp	*X-4-U-0-2-0-0.inp*
4 ft	U	0.2 %	0.5 %	0.7	0.7	53-X-4-U-2-5-7-7.inp	*X-4-U-0-5-0-0.inp*
4 ft	U	0.2 %	0.5 %	0.7	0.9	54-X-4-U-2-5-7-9.inp	*X-4-U-0-5-0-0.inp*
4 ft	U	0.2 %	0.5 %	0.9	0.7	55-X-4-U-2-5-9-7.inp	*X-4-U-0-5-0-0.inp*
4 ft	U	0.2 %	0.5 %	0.9	0.9	56-X-4-U-2-5-9-9.inp	*X-4-U-0-5-0-0.inp*
4 ft	U	0.2 %	1.0 %	0.7	0.7	57-X-4-U-2-10-7-7.inp	*X-4-U-0-10-0-0.inp*
4 ft	U	0.2 %	1.0 %	0.7	0.9	58-X-4-U-2-10-7-9.inp	*X-4-U-0-10-0-0.inp*
4 ft	U	0.2 %	1.0 %	0.9	0.7	59-X-4-U-2-10-9-7.inp	*X-4-U-0-10-0-0.inp*
4 ft	U	0.2 %	1.0 %	0.9	0.9	60-X-4-U-2-10-9-9.inp	*X-4-U-0-10-0-0.inp*
4 ft	U	0.3 %	0.2 %	0.7	0.7	61-X-4-U-3-2-7-7.inp	*X-4-U-0-2-0-0.inp*
4 ft	U	0.3 %	0.2 %	0.7	0.9	62-X-4-U-3-2-7-9.inp	*X-4-U-0-2-0-0.inp*
4 ft	U	0.3 %	0.2 %	0.9	0.7	63-X-4-U-3-2-9-7.inp	*X-4-U-0-2-0-0.inp*
4 ft	U	0.3 %	0.2 %	0.9	0.9	64-X-4-U-3-2-9-9.inp	*X-4-U-0-2-0-0.inp*
4 ft	U	0.3 %	0.5 %	0.7	0.7	65-X-4-U-3-5-7-7.inp	*X-4-U-0-5-0-0.inp*
4 ft	U	0.3 %	0.5 %	0.7	0.9	66-X-4-U-3-5-7-9.inp	*X-4-U-0-5-0-0.inp*
4 ft	U	0.3 %	0.5 %	0.9	0.7	67-X-4-U-3-5-9-7.inp	*X-4-U-0-5-0-0.inp*
4 ft	U	0.3 %	0.5 %	0.9	0.9	68-X-4-U-3-5-9-9.inp	*X-4-U-0-5-0-0.inp*
4 ft	U	0.3 %	1.0 %	0.7	0.7	69-X-4-U-3-10-7-7.inp	*X-4-U-0-10-0-0.inp*
4 ft	U	0.3 %	1.0 %	0.7	0.9	70-X-4-U-3-10-7-9.inp	*X-4-U-0-10-0-0.inp*
4 ft	U	0.3 %	1.0 %	0.9	0.7	71-X-4-U-3-10-9-7.inp	*X-4-U-0-10-0-0.inp*
4 ft	U	0.3 %	1.0 %	0.9	0.9	72-X-4-U-3-10-9-9.inp	*X-4-U-0-10-0-0.inp*
2 ft	R	0.1 %	0.2 %	0.7	0.7	73-X-2-R-1-2-7-7.inp	*X-2-R-0-2-0-0.inp*
2 ft	R	0.1 %	0.2 %	0.7	0.9	74-X-2-R-1-2-7-9.inp	*X-2-R-0-2-0-0.inp*
2 ft	R	0.1 %	0.2 %	0.9	0.7	75-X-2-R-1-2-9-7.inp	*X-2-R-0-2-0-0.inp*
2 ft	R	0.1 %	0.2 %	0.9	0.9	76-X-2-R-1-2-9-9.inp	*X-2-R-0-2-0-0.inp*
2 ft	R	0.1 %	0.5 %	0.7	0.7	77-X-2-R-1-5-7-7.inp	*X-2-R-0-5-0-0.inp*
2 ft	R	0.1 %	0.5 %	0.7	0.9	78-X-2-R-1-5-7-9.inp	*X-2-R-0-5-0-0.inp*
2 ft	R	0.1 %	0.5 %	0.9	0.7	79-X-2-R-1-5-9-7.inp	*X-2-R-0-5-0-0.inp*
2 ft	R	0.1 %	0.5 %	0.9	0.9	80-X-2-R-1-5-9-9.inp	*X-2-R-0-5-0-0.inp*
2 ft	R	0.1 %	1.0 %	0.7	0.7	81-X-2-R-1-10-7-7.inp	*X-2-R-0-10-0-0.inp*
2 ft	R	0.1 %	1.0 %	0.7	0.9	82-X-2-R-1-10-7-9.inp	*X-2-R-0-10-0-0.inp*
2 ft	R	0.1 %	1.0 %	0.9	0.7	83-X-2-R-1-10-9-7.inp	*X-2-R-0-10-0-0.inp*
2 ft	R	0.1 %	1.0 %	0.9	0.9	84-X-2-R-1-10-9-9.inp	*X-2-R-0-10-0-0.inp*

X:[P|B|TB]; U: Unrestrained; R: Restrained; FR: Fully Restrained

Continued on next page

2 ft	R	0.2 %	0.2 %	0.7	0.7	85-X-2-R-2-2-7-7.inp	*X-2-R-0-2-0-0.inp*
2 ft	R	0.2 %	0.2 %	0.7	0.9	86-X-2-R-2-2-7-9.inp	*X-2-R-0-2-0-0.inp*
2 ft	R	0.2 %	0.2 %	0.9	0.7	87-X-2-R-2-2-9-7.inp	*X-2-R-0-2-0-0.inp*
2 ft	R	0.2 %	0.2 %	0.9	0.9	88-X-2-R-2-2-9-9.inp	*X-2-R-0-2-0-0.inp*
2 ft	R	0.2 %	0.5 %	0.7	0.7	89-X-2-R-2-5-7-7.inp	*X-2-R-0-5-0-0.inp*
2 ft	R	0.2 %	0.5 %	0.7	0.9	90-X-2-R-2-5-7-9.inp	*X-2-R-0-5-0-0.inp*
2 ft	R	0.2 %	0.5 %	0.9	0.7	91-X-2-R-2-5-9-7.inp	*X-2-R-0-5-0-0.inp*
2 ft	R	0.2 %	0.5 %	0.9	0.9	92-X-2-R-2-5-9-9.inp	*X-2-R-0-5-0-0.inp*
2 ft	R	0.2 %	1.0 %	0.7	0.7	93-X-2-R-2-10-7-7.inp	*X-2-R-0-10-0-0.inp*
2 ft	R	0.2 %	1.0 %	0.7	0.9	94-X-2-R-2-10-7-9.inp	*X-2-R-0-10-0-0.inp*
2 ft	R	0.2 %	1.0 %	0.9	0.7	95-X-2-R-2-10-9-7.inp	*X-2-R-0-10-0-0.inp*
2 ft	R	0.2 %	1.0 %	0.9	0.9	96-X-2-R-2-10-9-9.inp	*X-2-R-0-10-0-0.inp*
2 ft	R	0.3 %	0.2 %	0.7	0.7	97-X-2-R-3-2-7-7.inp	*X-2-R-0-2-0-0.inp*
2 ft	R	0.3 %	0.2 %	0.7	0.9	98-X-2-R-3-2-7-9.inp	*X-2-R-0-2-0-0.inp*
2 ft	R	0.3 %	0.2 %	0.9	0.7	99-X-2-R-3-2-9-7.inp	*X-2-R-0-2-0-0.inp*
2 ft	R	0.3 %	0.2 %	0.9	0.9	100-X-2-R-3-2-9-9.inp	*X-2-R-0-2-0-0.inp*
2 ft	R	0.3 %	0.5 %	0.7	0.7	101-X-2-R-3-5-7-7.inp	*X-2-R-0-5-0-0.inp*
2 ft	R	0.3 %	0.5 %	0.7	0.9	102-X-2-R-3-5-7-9.inp	*X-2-R-0-5-0-0.inp*
2 ft	R	0.3 %	0.5 %	0.9	0.7	103-X-2-R-3-5-9-7.inp	*X-2-R-0-5-0-0.inp*
2 ft	R	0.3 %	0.5 %	0.9	0.9	104-X-2-R-3-5-9-9.inp	*X-2-R-0-5-0-0.inp*
2 ft	R	0.3 %	1.0 %	0.7	0.7	105-X-2-R-3-10-7-7.inp	*X-2-R-0-10-0-0.inp*
2 ft	R	0.3 %	1.0 %	0.7	0.9	106-X-2-R-3-10-7-9.inp	*X-2-R-0-10-0-0.inp*
2 ft	R	0.3 %	1.0 %	0.9	0.7	107-X-2-R-3-10-9-7.inp	*X-2-R-0-10-0-0.inp*
2 ft	R	0.3 %	1.0 %	0.9	0.9	108-X-2-R-3-10-9-9.inp	*X-2-R-0-10-0-0.inp*
4 ft	R	0.1 %	0.2 %	0.7	0.7	109-X-4-R-1-2-7-7.inp	*X-4-R-0-2-0-0.inp*
4 ft	R	0.1 %	0.2 %	0.7	0.9	110-X-4-R-1-2-7-9.inp	*X-4-R-0-2-0-0.inp*
4 ft	R	0.1 %	0.2 %	0.9	0.7	111-X-4-R-1-2-9-7.inp	*X-4-R-0-2-0-0.inp*
4 ft	R	0.1 %	0.2 %	0.9	0.9	112-X-4-R-1-2-9-9.inp	*X-4-R-0-2-0-0.inp*
4 ft	R	0.1 %	0.5 %	0.7	0.7	113-X-4-R-1-5-7-7.inp	*X-4-R-0-5-0-0.inp*
4 ft	R	0.1 %	0.5 %	0.7	0.9	114-X-4-R-1-5-7-9.inp	*X-4-R-0-5-0-0.inp*
4 ft	R	0.1 %	0.5 %	0.9	0.7	115-X-4-R-1-5-9-7.inp	*X-4-R-0-5-0-0.inp*
4 ft	R	0.1 %	0.5 %	0.9	0.9	116-X-4-R-1-5-9-9.inp	*X-4-R-0-5-0-0.inp*
4 ft	R	0.1 %	1.0 %	0.7	0.7	117-X-4-R-1-10-7-7.inp	*X-4-R-0-10-0-0.inp*
4 ft	R	0.1 %	1.0 %	0.7	0.9	118-X-4-R-1-10-7-9.inp	*X-4-R-0-10-0-0.inp*
4 ft	R	0.1 %	1.0 %	0.9	0.7	119-X-4-R-1-10-9-7.inp	*X-4-R-0-10-0-0.inp*
4 ft	R	0.1 %	1.0 %	0.9	0.9	120-X-4-R-1-10-9-9.inp	*X-4-R-0-10-0-0.inp*
4 ft	R	0.2 %	0.2 %	0.7	0.7	121-X-4-R-2-2-7-7.inp	*X-4-R-0-2-0-0.inp*
4 ft	R	0.2 %	0.2 %	0.7	0.9	122-X-4-R-2-2-7-9.inp	*X-4-R-0-2-0-0.inp*
4 ft	R	0.2 %	0.2 %	0.9	0.7	123-X-4-R-2-2-9-7.inp	*X-4-R-0-2-0-0.inp*
4 ft	R	0.2 %	0.2 %	0.9	0.9	124-X-4-R-2-2-9-9.inp	*X-4-R-0-2-0-0.inp*
4 ft	R	0.2 %	0.5 %	0.7	0.7	125-X-4-R-2-5-7-7.inp	*X-4-R-0-5-0-0.inp*
4 ft	R	0.2 %	0.5 %	0.7	0.9	126-X-4-R-2-5-7-9.inp	*X-4-R-0-5-0-0.inp*
4 ft	R	0.2 %	0.5 %	0.9	0.7	127-X-4-R-2-5-9-7.inp	*X-4-R-0-5-0-0.inp*
4 ft	R	0.2 %	0.5 %	0.9	0.9	128-X-4-R-2-5-9-9.inp	*X-4-R-0-5-0-0.inp*
4 ft	R	0.2 %	1.0 %	0.7	0.7	129-X-4-R-2-10-7-7.inp	*X-4-R-0-10-0-0.inp*
4 ft	R	0.2 %	1.0 %	0.7	0.9	130-X-4-R-2-10-7-9.inp	*X-4-R-0-10-0-0.inp*
4 ft	R	0.2 %	1.0 %	0.9	0.7	131-X-4-R-2-10-9-7.inp	*X-4-R-0-10-0-0.inp*
4 ft	R	0.2 %	1.0 %	0.9	0.9	132-X-4-R-2-10-9-9.inp	*X-4-R-0-10-0-0.inp*
4 ft	R	0.3 %	0.2 %	0.7	0.7	133-X-4-R-3-2-7-7.inp	*X-4-R-0-2-0-0.inp*
4 ft	R	0.3 %	0.2 %	0.7	0.9	134-X-4-R-3-2-7-9.inp	*X-4-R-0-2-0-0.inp*
4 ft	R	0.3 %	0.2 %	0.9	0.7	135-X-4-R-3-2-9-7.inp	*X-4-R-0-2-0-0.inp*
4 ft	R	0.3 %	0.2 %	0.9	0.9	136-X-4-R-3-2-9-9.inp	*X-4-R-0-2-0-0.inp*
4 ft	R	0.3 %	0.5 %	0.7	0.7	137-X-4-R-3-5-7-7.inp	*X-4-R-0-5-0-0.inp*

X:[P|B|TB]; U: Unrestrained; R: Restrained; FR: Fully Restrained

Continued on next page

4 ft	R	0.3 %	0.5 %	0.7	0.9	138-X-4-R-3-5-7-9.inp	*X-4-R-0-5-0-0.inp*
4 ft	R	0.3 %	0.5 %	0.9	0.7	139-X-4-R-3-5-9-7.inp	*X-4-R-0-5-0-0.inp*
4 ft	R	0.3 %	0.5 %	0.9	0.9	140-X-4-R-3-5-9-9.inp	*X-4-R-0-5-0-0.inp*
4 ft	R	0.3 %	1.0 %	0.7	0.7	141-X-4-R-3-10-7-7.inp	*X-4-R-0-10-0-0.inp*
4 ft	R	0.3 %	1.0 %	0.7	0.9	142-X-4-R-3-10-7-9.inp	*X-4-R-0-10-0-0.inp*
4 ft	R	0.3 %	1.0 %	0.9	0.7	143-X-4-R-3-10-9-7.inp	*X-4-R-0-10-0-0.inp*
4 ft	R	0.3 %	1.0 %	0.9	0.9	144-X-4-R-3-10-9-9.inp	*X-4-R-0-10-0-0.inp*
2 ft	FR	0.1 %	0.2 %	0.7	0.7	145-X-2-FR-1-2-7-7.inp	*X-2-FR-0-2-0-0.inp*
2 ft	FR	0.1 %	0.2 %	0.7	0.9	146-X-2-FR-1-2-7-9.inp	*X-2-FR-0-2-0-0.inp*
2 ft	FR	0.1 %	0.2 %	0.9	0.7	147-X-2-FR-1-2-9-7.inp	*X-2-FR-0-2-0-0.inp*
2 ft	FR	0.1 %	0.2 %	0.9	0.9	148-X-2-FR-1-2-9-9.inp	*X-2-FR-0-2-0-0.inp*
2 ft	FR	0.1 %	0.5 %	0.7	0.7	149-X-2-FR-1-5-7-7.inp	*X-2-FR-0-5-0-0.inp*
2 ft	FR	0.1 %	0.5 %	0.7	0.9	150-X-2-FR-1-5-7-9.inp	*X-2-FR-0-5-0-0.inp*
2 ft	FR	0.1 %	0.5 %	0.9	0.7	151-X-2-FR-1-5-9-7.inp	*X-2-FR-0-5-0-0.inp*
2 ft	FR	0.1 %	0.5 %	0.9	0.9	152-X-2-FR-1-5-9-9.inp	*X-2-FR-0-5-0-0.inp*
2 ft	FR	0.1 %	1.0 %	0.7	0.7	153-X-2-FR-1-10-7-7.inp	*X-2-FR-0-10-0-0.inp*
2 ft	FR	0.1 %	1.0 %	0.7	0.9	154-X-2-FR-1-10-7-9.inp	*X-2-FR-0-10-0-0.inp*
2 ft	FR	0.1 %	1.0 %	0.9	0.7	155-X-2-FR-1-10-9-7.inp	*X-2-FR-0-10-0-0.inp*
2 ft	FR	0.1 %	1.0 %	0.9	0.9	156-X-2-FR-1-10-9-9.inp	*X-2-FR-0-10-0-0.inp*
2 ft	FR	0.2 %	0.2 %	0.7	0.7	157-X-2-FR-2-2-7-7.inp	*X-2-FR-0-2-0-0.inp*
2 ft	FR	0.2 %	0.2 %	0.7	0.9	158-X-2-FR-2-2-7-9.inp	*X-2-FR-0-2-0-0.inp*
2 ft	FR	0.2 %	0.2 %	0.9	0.7	159-X-2-FR-2-2-9-7.inp	*X-2-FR-0-2-0-0.inp*
2 ft	FR	0.2 %	0.2 %	0.9	0.9	160-X-2-FR-2-2-9-9.inp	*X-2-FR-0-2-0-0.inp*
2 ft	FR	0.2 %	0.5 %	0.7	0.7	161-X-2-FR-2-5-7-7.inp	*X-2-FR-0-5-0-0.inp*
2 ft	FR	0.2 %	0.5 %	0.7	0.9	162-X-2-FR-2-5-7-9.inp	*X-2-FR-0-5-0-0.inp*
2 ft	FR	0.2 %	0.5 %	0.9	0.7	163-X-2-FR-2-5-9-7.inp	*X-2-FR-0-5-0-0.inp*
2 ft	FR	0.2 %	0.5 %	0.9	0.9	164-X-2-FR-2-5-9-9.inp	*X-2-FR-0-5-0-0.inp*
2 ft	FR	0.2 %	1.0 %	0.7	0.7	165-X-2-FR-2-10-7-7.inp	*X-2-FR-0-10-0-0.inp*
2 ft	FR	0.2 %	1.0 %	0.7	0.9	166-X-2-FR-2-10-7-9.inp	*X-2-FR-0-10-0-0.inp*
2 ft	FR	0.2 %	1.0 %	0.9	0.7	167-X-2-FR-2-10-9-7.inp	*X-2-FR-0-10-0-0.inp*
2 ft	FR	0.2 %	1.0 %	0.9	0.9	168-X-2-FR-2-10-9-9.inp	*X-2-FR-0-10-0-0.inp*
2 ft	FR	0.3 %	0.2 %	0.7	0.7	169-X-2-FR-3-2-7-7.inp	*X-2-FR-0-2-0-0.inp*
2 ft	FR	0.3 %	0.2 %	0.7	0.9	170-X-2-FR-3-2-7-9.inp	*X-2-FR-0-2-0-0.inp*
2 ft	FR	0.3 %	0.2 %	0.9	0.7	171-X-2-FR-3-2-9-7.inp	*X-2-FR-0-2-0-0.inp*
2 ft	FR	0.3 %	0.2 %	0.9	0.9	172-X-2-FR-3-2-9-9.inp	*X-2-FR-0-2-0-0.inp*
2 ft	FR	0.3 %	0.5 %	0.7	0.7	173-X-2-FR-3-5-7-7.inp	*X-2-FR-0-5-0-0.inp*
2 ft	FR	0.3 %	0.5 %	0.7	0.9	174-X-2-FR-3-5-7-9.inp	*X-2-FR-0-5-0-0.inp*
2 ft	FR	0.3 %	0.5 %	0.9	0.7	175-X-2-FR-3-5-9-7.inp	*X-2-FR-0-5-0-0.inp*
2 ft	FR	0.3 %	0.5 %	0.9	0.9	176-X-2-FR-3-5-9-9.inp	*X-2-FR-0-5-0-0.inp*
2 ft	FR	0.3 %	1.0 %	0.7	0.7	177-X-2-FR-3-10-7-7.inp	*X-2-FR-0-10-0-0.inp*
2 ft	FR	0.3 %	1.0 %	0.7	0.9	178-X-2-FR-3-10-7-9.inp	*X-2-FR-0-10-0-0.inp*
2 ft	FR	0.3 %	1.0 %	0.9	0.7	179-X-2-FR-3-10-9-7.inp	*X-2-FR-0-10-0-0.inp*
2 ft	FR	0.3 %	1.0 %	0.9	0.9	180-X-2-FR-3-10-9-9.inp	*X-2-FR-0-10-0-0.inp*
4 ft	FR	0.1 %	0.2 %	0.7	0.7	181-X-4-FR-1-2-7-7.inp	*X-4-FR-0-2-0-0.inp*
4 ft	FR	0.1 %	0.2 %	0.7	0.9	182-X-4-FR-1-2-7-9.inp	*X-4-FR-0-2-0-0.inp*
4 ft	FR	0.1 %	0.2 %	0.9	0.7	183-X-4-FR-1-2-9-7.inp	*X-4-FR-0-2-0-0.inp*
4 ft	FR	0.1 %	0.2 %	0.9	0.9	184-X-4-FR-1-2-9-9.inp	*X-4-FR-0-2-0-0.inp*
4 ft	FR	0.1 %	0.5 %	0.7	0.7	185-X-4-FR-1-5-7-7.inp	*X-4-FR-0-5-0-0.inp*
4 ft	FR	0.1 %	0.5 %	0.7	0.9	186-X-4-FR-1-5-7-9.inp	*X-4-FR-0-5-0-0.inp*
4 ft	FR	0.1 %	0.5 %	0.9	0.7	187-X-4-FR-1-5-9-7.inp	*X-4-FR-0-5-0-0.inp*
4 ft	FR	0.1 %	0.5 %	0.9	0.9	188-X-4-FR-1-5-9-9.inp	*X-4-FR-0-5-0-0.inp*
4 ft	FR	0.1 %	1.0 %	0.7	0.7	189-X-4-FR-1-10-7-7.inp	*X-4-FR-0-10-0-0.inp*
4 ft	FR	0.1 %	1.0 %	0.7	0.9	190-X-4-FR-1-10-7-9.inp	*X-4-FR-0-10-0-0.inp*

X:[P|B|TB]; U: Unrestrained; R: Restrained; FR: Fully Restrained

Continued on next page

4 ft	FR	0.1 %	1.0 %	0.9	0.7	191-X-4-FR-1-10-9-7.inp	*X-4-FR-0-10-0-0.inp*
4 ft	FR	0.1 %	1.0 %	0.9	0.9	192-X-4-FR-1-10-9-9.inp	*X-4-FR-0-10-0-0.inp*
4 ft	FR	0.2 %	0.2 %	0.7	0.7	193-X-4-FR-2-2-7-7.inp	*X-4-FR-0-2-0-0.inp*
4 ft	FR	0.2 %	0.2 %	0.7	0.9	194-X-4-FR-2-2-7-9.inp	*X-4-FR-0-2-0-0.inp*
4 ft	FR	0.2 %	0.2 %	0.9	0.7	195-X-4-FR-2-2-9-7.inp	*X-4-FR-0-2-0-0.inp*
4 ft	FR	0.2 %	0.2 %	0.9	0.9	196-X-4-FR-2-2-9-9.inp	*X-4-FR-0-2-0-0.inp*
4 ft	FR	0.2 %	0.5 %	0.7	0.7	197-X-4-FR-2-5-7-7.inp	*X-4-FR-0-5-0-0.inp*
4 ft	FR	0.2 %	0.5 %	0.7	0.9	198-X-4-FR-2-5-7-9.inp	*X-4-FR-0-5-0-0.inp*
4 ft	FR	0.2 %	0.5 %	0.9	0.7	199-X-4-FR-2-5-9-7.inp	*X-4-FR-0-5-0-0.inp*
4 ft	FR	0.2 %	0.5 %	0.9	0.9	200-X-4-FR-2-5-9-9.inp	*X-4-FR-0-5-0-0.inp*
4 ft	FR	0.2 %	1.0 %	0.7	0.7	201-X-4-FR-2-10-7-7.inp	*X-4-FR-0-10-0-0.inp*
4 ft	FR	0.2 %	1.0 %	0.7	0.9	202-X-4-FR-2-10-7-9.inp	*X-4-FR-0-10-0-0.inp*
4 ft	FR	0.2 %	1.0 %	0.9	0.7	203-X-4-FR-2-10-9-7.inp	*X-4-FR-0-10-0-0.inp*
4 ft	FR	0.2 %	1.0 %	0.9	0.9	204-X-4-FR-2-10-9-9.inp	*X-4-FR-0-10-0-0.inp*
4 ft	FR	0.3 %	0.2 %	0.7	0.7	205-X-4-FR-3-2-7-7.inp	*X-4-FR-0-2-0-0.inp*
4 ft	FR	0.3 %	0.2 %	0.7	0.9	206-X-4-FR-3-2-7-9.inp	*X-4-FR-0-2-0-0.inp*
4 ft	FR	0.3 %	0.2 %	0.9	0.7	207-X-4-FR-3-2-9-7.inp	*X-4-FR-0-2-0-0.inp*
4 ft	FR	0.3 %	0.2 %	0.9	0.9	208-X-4-FR-3-2-9-9.inp	*X-4-FR-0-2-0-0.inp*
4 ft	FR	0.3 %	0.5 %	0.7	0.7	209-X-4-FR-3-5-7-7.inp	*X-4-FR-0-5-0-0.inp*
4 ft	FR	0.3 %	0.5 %	0.7	0.9	210-X-4-FR-3-5-7-9.inp	*X-4-FR-0-5-0-0.inp*
4 ft	FR	0.3 %	0.5 %	0.9	0.7	211-X-4-FR-3-5-9-7.inp	*X-4-FR-0-5-0-0.inp*
4 ft	FR	0.3 %	0.5 %	0.9	0.9	212-X-4-FR-3-5-9-9.inp	*X-4-FR-0-5-0-0.inp*
4 ft	FR	0.3 %	1.0 %	0.7	0.7	213-X-4-FR-3-10-7-7.inp	*X-4-FR-0-10-0-0.inp*
4 ft	FR	0.3 %	1.0 %	0.7	0.9	214-X-4-FR-3-10-7-9.inp	*X-4-FR-0-10-0-0.inp*
4 ft	FR	0.3 %	1.0 %	0.9	0.7	215-X-4-FR-3-10-9-7.inp	*X-4-FR-0-10-0-0.inp*
4 ft	FR	0.3 %	1.0 %	0.9	0.9	216-X-4-FR-3-10-9-9.inp	*X-4-FR-0-10-0-0.inp*

3.2 AAR

Table 3.2. Generated Meshes without AAR

t	BC	ρ	Filename
2 ft	U	0.2 %	X-2-U-0-2-0-0.inp
2 ft	U	0.5 %	X-2-U-0-5-0-0.inp
2 ft	U	1.0 %	X-2-U-0-10-0-0.inp
4 ft	U	0.2 %	X-4-U-0-2-0-0.inp
4 ft	U	0.5 %	X-4-U-0-5-0-0.inp
4 ft	U	1.0 %	X-4-U-0-10-0-0.inp
2 ft	R	0.2 %	X-2-R-0-2-0-0.inp
2 ft	R	0.5 %	X-2-R-0-5-0-0.inp
2 ft	R	1.0 %	X-2-R-0-10-0-0.inp
4 ft	R	0.2 %	X-4-R-0-2-0-0.inp
4 ft	R	0.5 %	X-4-R-0-5-0-0.inp
4 ft	R	1.0 %	X-4-R-0-10-0-0.inp
2 ft	FR	0.2 %	X-2-FR-0-2-0-0.inp
2 ft	FR	0.5 %	X-2-FR-0-5-0-0.inp
2 ft	FR	1.0 %	X-2-FR-0-10-0-0.inp
4 ft	FR	0.2 %	X-4-FR-0-2-0-0.inp
4 ft	FR	0.5 %	X-4-FR-0-5-0-0.inp
4 ft	FR	1.0 %	X-4-FR-0-10-0-0.inp

Appendix D

Analyses Results

Table 4.1. Unsorted Results

Filename	AAR+Shear			AAR Only				
	K	V_{ult}	V_{yld}	Δ_{ver}	σ^{lan}_{max}	σ^{tra}_{max}	σ^{lan}_{med}	σ^{tra}_{med}
	$\frac{(AAR+x)-x}{x} \times 100$			mm	MPa			
1-B-2-U-1-2-7-7	-28.7 %	-3.8 %	-2.8%	0.207	64.6	65.0	64.1	62.9
2-B-2-U-1-2-7-9	-28.7 %	7.0 %	8.1%	0.207	64.6	65.0	64.1	62.9
3-B-2-U-1-2-9-7	-12.2 %	-2.2 %	-1.2%	0.207	64.8	65.1	64.3	63.2
4-B-2-U-1-2-9-9	-12.2 %	13.9 %	15.1%	0.207	64.8	65.1	64.3	63.2
5-B-2-U-1-5-7-7	-26.9 %	-5.9 %	7.8%	0.213	61.5	62.3	60.5	57.7
6-B-2-U-1-5-7-9	-26.9 %	-0.7 %	17.1%	0.213	61.5	62.3	60.5	57.7
7-B-2-U-1-5-9-7	-8.9 %	-5.3 %	3.7%	0.213	61.9	62.7	61.0	58.4
8-B-2-U-1-5-9-9	-8.9 %	-6.9 %	13.9%	0.213	61.9	62.7	61.0	58.4
9-B-2-U-1-10-7-7	-24.5 %	-2.3 %	35.4%	0.222	56.4	57.8	55.1	50.6
10-B-2-U-1-10-7-9	-24.6 %	-3.1 %	48.0%	0.222	56.4	57.8	55.1	50.6
11-B-2-U-1-10-9-7	-10.6 %	-2.4 %	28.2%	0.222	57.2	58.6	56.0	51.7
12-B-2-U-1-10-9-9	-8.1 %	-4.0 %	35.6%	0.222	57.2	58.6	56.0	51.7
13-B-2-U-2-2-7-7	-28.7 %	11.0 %	12.1%	0.419	128.2	129.2	126.8	124.0
14-B-2-U-2-2-7-9	-28.7 %	13.2 %	14.3%	0.419	128.2	129.2	126.8	124.0
15-B-2-U-2-2-9-7	-12.2 %	11.8 %	12.9%	0.419	128.6	129.5	127.2	124.6
16-B-2-U-2-2-9-9	-12.2 %	14.2 %	15.3%	0.419	128.6	129.5	127.2	124.6
17-B-2-U-2-5-7-7	-26.7 %	-2.8 %	30.1%	0.438	120.2	122.5	117.7	111.6
18-B-2-U-2-5-7-9	-26.6 %	-4.7 %	39.6%	0.438	120.2	122.6	117.7	111.6
19-B-2-U-2-5-9-7	-10.1 %	-7.6 %	23.1%	0.437	121.1	123.4	118.7	112.9
20-B-2-U-2-5-9-9	-11.2 %	-4.5 %	37.8%	0.437	121.1	123.4	118.7	113.0
21-B-2-U-2-10-7-7	-24.1 %	-4.5 %	73.1%	0.467	107.8	110.0	104.5	94.3
22-B-2-U-2-10-7-9	-24.4 %	-4.4 %	84.6%	0.467	107.7	110.4	104.5	94.6
23-B-2-U-2-10-9-7	-8.7 %	-6.0 %	60.3%	0.466	109.3	111.8	106.0	96.3
24-B-2-U-2-10-9-9	-8.1 %	-5.1 %	70.9%	0.466	109.2	112.1	106.0	96.6
25-B-2-U-3-2-7-7	-30.1 %	17.9 %	19.1%	0.636	190.7	192.7	188.2	183.3
26-B-2-U-3-2-7-9	-28.6 %	23.4 %	24.7%	0.636	190.7	192.7	188.2	183.3
27-B-2-U-3-2-9-7	-10.0 %	19.4 %	20.6%	0.635	191.3	193.2	188.9	184.1
28-B-2-U-3-2-9-9	-12.3 %	26.5 %	27.7%	0.635	191.3	193.2	188.9	184.1
29-B-2-U-3-5-7-7	-28.4 %	-5.7 %	38.6%	0.675	176.3	179.8	171.9	161.4
30-B-2-U-3-5-7-9	-26.8 %	-0.5 %	46.2%	0.675	176.3	180.1	171.9	161.4
31-B-2-U-3-5-9-7	-9.1 %	-0.7 %	45.9%	0.674	177.6	181.3	173.2	163.3
32-B-2-U-3-5-9-9	-9.5 %	-1.5 %	44.8%	0.674	177.6	181.5	173.2	163.4
33-B-2-U-3-10-7-7	-26.5 %	-5.6 %	93.9%	0.719	153.8	154.4	146.7	124.1

Continued on next page

Table 4.1 Unsorted Results – *Continued from previous page*

Filename	AAR+Shear			AAR Only				
	K	V_{ult}	V_{yld}	Δ_{ver}	σ^{lan}_{max}	σ^{tra}_{max}	σ^{lan}_{med}	σ^{tra}_{med}
		$\frac{(AAR+x)-x}{x}\times 100$		mm	MPa			
34-B-2-U-3-10-7-9	-24.8 %	-5.6 %	92.3%	0.719	153.8	155.0	147.0	124.5
35-B-2-U-3-10-9-7	-10.7 %	-4.6 %	94.7%	0.721	155.9	157.2	149.0	128.3
36-B-2-U-3-10-9-9	-9.6 %	-5.3 %	95.0%	0.722	155.9	157.9	149.4	129.4
37-B-4-U-1-2-7-7	-28.7 %	-4.1 %	-7.6%	0.413	64.6	65.2	64.0	61.3
38-B-4-U-1-2-7-9	-28.7 %	6.7 %	6.7%	0.413	64.6	65.2	64.0	61.3
39-B-4-U-1-2-9-7	-12.6 %	-8.1 %	-8.1%	0.413	64.8	65.4	64.2	61.7
40-B-4-U-1-2-9-9	-12.6 %	4.0 %	4.0%	0.413	64.8	65.4	64.2	61.7
41-B-4-U-1-5-7-7	-26.3 %	6.7 %	15.1%	0.425	61.5	62.4	60.3	54.9
42-B-4-U-1-5-7-9	-26.3 %	7.1 %	22.2%	0.425	61.5	62.4	60.3	54.9
43-B-4-U-1-5-9-7	-6.4 %	10.3 %	8.0%	0.424	61.9	62.9	60.8	55.7
44-B-4-U-1-5-9-9	-8.6 %	9.0 %	16.2%	0.424	61.9	62.9	60.8	55.7
45-B-4-U-1-10-7-7	-26.3 %	10.7 %	77.8%	0.442	56.4	57.3	54.8	47.1
46-B-4-U-1-10-7-9	-26.4 %	13.5 %	89.8%	0.442	56.4	57.4	54.8	47.1
47-B-4-U-1-10-9-7	-8.8 %	17.1 %	55.2%	0.440	57.3	58.2	55.7	48.2
48-B-4-U-1-10-9-9	-9.3 %	20.1 %	67.9%	0.440	57.2	58.3	55.7	48.2
49-B-4-U-2-2-7-7	-28.5 %	1.1 %	1.1%	0.836	128.2	129.8	126.7	120.2
50-B-4-U-2-2-7-9	-28.6 %	12.8 %	12.8%	0.836	128.2	129.8	126.7	120.2
51-B-4-U-2-2-9-7	-8.3 %	0.8 %	0.8%	0.835	128.6	130.1	127.1	121.0
52-B-4-U-2-2-9-9	-12.9 %	14.2 %	14.2%	0.835	128.6	130.1	127.1	121.0
53-B-4-U-2-5-7-7	-27.3 %	7.5 %	45.6%	0.872	120.2	122.4	117.4	105.0
54-B-4-U-2-5-7-9	-28.2 %	7.0 %	46.4%	0.872	120.1	122.7	117.4	105.1
55-B-4-U-2-5-9-7	-8.0 %	9.4 %	38.8%	0.871	121.1	123.4	118.3	106.5
56-B-4-U-2-5-9-9	-9.0 %	10.7 %	44.6%	0.871	121.0	123.6	118.4	106.6
57-B-4-U-2-10-7-7	-23.0 %	23.5 %	119.6%	0.909	107.3	107.3	102.5	83.8
58-B-4-U-2-10-7-9	-22.3 %	26.2 %	128.6%	0.918	107.6	107.8	103.2	84.3
59-B-4-U-2-10-9-7	-8.2 %	33.8 %	109.6%	0.912	109.0	109.5	104.6	86.5
60-B-4-U-2-10-9-9	-7.8 %	34.7 %	119.3%	0.913	109.0	109.8	104.8	86.5
61-B-4-U-3-2-7-7	-29.1 %	9.4 %	9.4%	1.268	190.8	193.7	188.0	176.8
62-B-4-U-3-2-7-9	-28.6 %	23.3 %	23.3%	1.268	190.7	193.7	188.0	176.8
63-B-4-U-3-2-9-7	-9.6 %	9.7 %	9.7%	1.267	191.4	194.2	188.6	178.1
64-B-4-U-3-2-9-9	-9.7 %	24.3 %	24.3%	1.267	191.4	194.2	188.6	178.1
65-B-4-U-3-5-7-7	-26.2 %	8.2 %	45.4%	1.330	175.9	178.4	170.4	147.8
66-B-4-U-3-5-7-9	-27.7 %	10.4 %	57.8%	1.337	176.1	178.9	170.8	148.2
67-B-4-U-3-5-9-7	-8.9 %	8.7 %	42.3%	1.334	177.3	180.3	172.1	151.4
68-B-4-U-3-5-9-9	-9.4 %	8.4 %	50.8%	1.340	177.4	180.8	172.5	152.4
69-B-4-U-3-10-7-7	21.8 %	-33.4 %	-93.3%	1.497	151.2	149.1	137.8	103.3
70-B-4-U-3-10-7-9	295.6 %	-30.4 %	-75.7%	1.490	151.6	150.9	136.1	103.2
71-B-4-U-3-10-9-7	167.9 %	-27.8 %	-80.7%	1.489	153.2	152.0	141.8	106.4
72-B-4-U-3-10-9-9	166.7 %	-40.9 %	-87.6%	1.482	153.7	152.6	141.8	107.4
73-B-2-R-1-2-7-7	74.3 %	-31.3 %	-43.5%	0.376	0.0	0.0	0.0	0.0
74-B-2-R-1-2-7-9	76.8 %	-18.1 %	-42.9%	0.376	0.0	0.0	0.0	0.0
75-B-2-R-1-2-9-7	115.9 %	-32.0 %	-42.7%	0.381	0.1	0.0	0.0	0.0
76-B-2-R-1-2-9-9	118.3 %	-19.7 %	-42.5%	0.381	0.1	0.0	0.0	0.0
77-B-2-R-1-5-7-7	44.3 %	-19.7 %	-19.7%	0.376	0.0	0.0	0.0	0.0
78-B-2-R-1-5-7-9	44.6 %	-4.6 %	-4.6%	0.376	0.0	0.0	0.0	0.0
79-B-2-R-1-5-9-7	75.4 %	-20.4 %	-25.3%	0.381	0.1	0.0	0.0	0.0
80-B-2-R-1-5-9-9	77.0 %	-6.8 %	-6.8%	0.381	0.1	0.0	0.0	0.0
81-B-2-R-1-10-7-7	27.5 %	28.3 %	28.3%	0.376	0.0	0.0	0.0	0.0
82-B-2-R-1-10-7-9	27.6 %	65.7 %	65.7%	0.376	0.0	0.0	0.0	0.0
83-B-2-R-1-10-9-7	53.4 %	49.3 %	49.3%	0.381	0.1	0.0	0.0	0.0
84-B-2-R-1-10-9-9	54.6 %	51.2 %	51.2%	0.381	0.1	0.0	0.0	0.0

Continued on next page

Table 4.1 Unsorted Results – *Continued from previous page*

Filename	AAR+Shear			AAR Only				
	K	V_{ult}	V_{yld}	Δ_{ver}	σ^{lan}_{max}	σ^{tra}_{max}	σ^{lan}_{med}	σ^{tra}_{med}
	$\frac{(AAR+x)-x}{x}\times 100$			mm	MPa			
85-B-2-R-2-2-7-7	76.7 %	-23.7 %	-37.1%	0.847	0.2	0.0	0.0	0.0
86-B-2-R-2-2-7-9	76.7 %	-17.9 %	-30.4%	0.847	0.2	0.0	0.0	0.0
87-B-2-R-2-2-9-7	-100.0 %	-100.0 %	-100.0 %	26.360	45.7	36.4	-0.1	-0.1
88-B-2-R-2-2-9-9	123.0 %	-20.2 %	-29.3%	0.853	0.3	0.1	0.1	0.0
89-B-2-R-2-5-7-7	-100.0 %	-99.8 %	-100.0%	1.392	22.1	12.0	-1.8	-0.0
90-B-2-R-2-5-7-9	44.6 %	16.3 %	16.3%	0.846	0.1	0.0	0.0	0.0
91-B-2-R-2-5-9-7	-100.0 %	-100.0 %	-100.0 %	32.272	37.5	14.9	-0.4	-0.0
92-B-2-R-2-5-9-9	78.6 %	-1.0 %	-1.0%	0.854	0.3	0.1	0.0	0.0
93-B-2-R-2-10-7-7	27.6 %	30.6 %	30.6%	0.847	0.1	0.0	0.0	-0.0
94-B-2-R-2-10-7-9	27.6 %	71.4 %	71.4%	0.847	0.1	0.0	0.0	-0.0
95-B-2-R-2-10-9-7	53.7 %	55.1 %	55.1%	0.853	0.2	0.1	0.0	0.0
96-B-2-R-2-10-9-9	56.0 %	98.4 %	98.4%	0.853	0.2	0.1	0.0	-0.0
97-B-2-R-3-2-7-7	73.3 %	-25.2 %	-36.1%	1.344	0.4	0.1	0.0	0.0
98-B-2-R-3-2-7-9	73.3 %	-15.4 %	-22.5%	1.344	0.4	0.1	0.0	0.0
99-B-2-R-3-2-9-7	-99.9 %	-94.9 %	-100.0 %	18.180	97.3	46.8	-9.5	0.0
100-B-2-R-3-2-9-9	-99.0 %	-96.1 %	-100.0 %	12.123	67.0	81.5	-0.0	0.1
101-B-2-R-3-5-7-7	-99.1 %	-88.3 %	-99.9%	4.075	100.2	36.5	-11.3	0.6
102-B-2-R-3-5-7-9	-99.7 %	-90.6 %	-100.0 %	12.304	31.9	17.9	-3.2	0.0
103-B-2-R-3-5-9-7	-100.0 %	-99.9 %	-100.0 %	44.691	18.4	11.3	-0.7	-0.1
104-B-2-R-3-5-9-9	-99.5 %	-91.5 %	-99.9%	1.168	17.3	2.5	3.5	0.0
105-B-2-R-3-10-7-7	27.6 %	48.1 %	34.9%	1.344	0.2	0.1	0.0	-0.0
106-B-2-R-3-10-7-9	27.6 %	72.3 %	72.3%	1.344	0.2	0.1	0.0	0.0
107-B-2-R-3-10-9-7	55.7 %	57.0 %	57.0%	1.351	0.4	0.1	0.0	0.0
108-B-2-R-3-10-9-9	-100.0 %	-99.8 %	-100.0%	2.039	21.3	6.0	-1.0	-0.1
109-B-4-R-1-2-7-7	-31.9 %	-23.9 %	442.3%	0.751	0.2	0.2	0.1	0.0
110-B-4-R-1-2-7-9	-31.9 %	-1.3 %	430.9%	0.751	0.2	0.2	0.1	0.0
111-B-4-R-1-2-9-7	-12.5 %	-24.5 %	441.8%	0.759	0.3	0.1	0.1	-0.0
112-B-4-R-1-2-9-9	-12.5 %	0.0 %	459.6%	0.759	0.3	0.1	0.1	-0.0
113-B-4-R-1-5-7-7	-26.6 %	6.1 %	461.4%	0.751	0.2	0.1	0.1	0.0
114-B-4-R-1-5-7-9	-26.6 %	41.6 %	464.7%	0.751	0.2	0.1	0.1	0.0
115-B-4-R-1-5-9-7	-8.8 %	6.5 %	457.7%	0.759	0.3	0.1	0.1	0.0
116-B-4-R-1-5-9-9	-8.8 %	43.6 %	459.5%	0.759	0.3	0.1	0.1	0.0
117-B-4-R-1-10-7-7	-24.6 %	22.4 %	243.4%	0.750	0.2	0.1	0.0	0.0
118-B-4-R-1-10-7-9	-24.6 %	31.4 %	268.5%	0.750	0.2	0.1	0.0	0.0
119-B-4-R-1-10-9-7	-8.1 %	31.6 %	269.2%	0.759	0.2	0.1	0.1	0.0
120-B-4-R-1-10-9-9	-8.1 %	41.2 %	296.2%	0.759	0.2	0.1	0.1	0.0
121-B-4-R-2-2-7-7	-31.9 %	-20.8 %	559.0%	1.684	0.9	0.6	0.1	0.0
122-B-4-R-2-2-7-9	-31.9 %	-0.1 %	559.8%	1.684	0.9	0.6	0.1	0.0
123-B-4-R-2-2-9-7	-12.5 %	-24.0 %	556.3%	1.703	1.6	1.2	0.3	0.0
124-B-4-R-2-2-9-9	-12.5 %	-7.4 %	550.4%	1.703	1.6	1.2	0.3	0.0
125-B-4-R-2-5-7-7	-26.6 %	10.8 %	512.1%	1.685	0.9	0.5	0.1	-0.0
126-B-4-R-2-5-7-9	-26.6 %	45.6 %	573.8%	1.685	0.9	0.5	0.1	-0.0
127-B-4-R-2-5-9-7	-8.9 %	9.9 %	507.1%	1.703	1.3	1.0	0.2	-0.0
128-B-4-R-2-5-9-9	-8.9 %	33.9 %	571.8%	1.703	1.3	1.0	0.2	-0.0
129-B-4-R-2-10-7-7	-24.6 %	31.8 %	269.8%	1.690	0.6	0.5	0.1	0.0
130-B-4-R-2-10-7-9	-24.6 %	86.1 %	308.0%	1.690	0.6	0.5	0.1	-0.0
131-B-4-R-2-10-9-7	-8.1 %	37.2 %	284.9%	1.693	1.1	0.6	0.0	0.0
132-B-4-R-2-10-9-9	-8.1 %	57.3 %	341.3%	1.693	1.1	0.6	0.0	0.0
133-B-4-R-3-2-7-7	-97.0 %	-98.1 %	-100.0 %	13.490	43.3	21.4	14.0	-0.1
134-B-4-R-3-2-7-9	-95.7 %	-98.3 %	-98.1 %	17.384	71.0	19.7	17.0	0.0
135-B-4-R-3-2-9-7	-97.5 %	-99.7 %	-98.8%	2.773	180.2	55.9	5.9	0.4

Continued on next page

Table 4.1 Unsorted Results – *Continued from previous page*

Filename	AAR+Shear			AAR Only				
	K	V_{ult}	V_{yld}	Δ_{ver}	σ^{lan}_{max}	σ^{tra}_{max}	σ^{lan}_{med}	σ^{tra}_{med}
		$\frac{(AAR+x)-x}{x} \times 100$		mm	MPa			
136-B-4-R-3-2-9-9	-98.8 %	-99.7 %	-99.4%	2.502	62.5	29.6	-0.5	-0.1
137-B-4-R-3-5-7-7	-40.9 %	-6.9 %	254.6%	2.690	13.4	11.4	3.1	-0.0
138-B-4-R-3-5-7-9	-97.7 %	-94.8 %	-99.1%	6.072	19.9	12.0	4.0	0.0
139-B-4-R-3-5-9-7	-98.8 %	-99.6 %	-99.5%	2.027	105.5	31.4	18.8	0.1
140-B-4-R-3-5-9-9	-98.8 %	-97.4 %	-99.7%	2.991	17.4	5.0	1.4	-0.0
141-B-4-R-3-10-7-7	-50.8 %	3.1 %	189.3%	2.692	11.4	5.6	5.8	0.0
142-B-4-R-3-10-7-9	-48.5 %	25.6 %	226.1%	2.731	14.2	4.5	6.5	-0.0
143-B-4-R-3-10-9-7	-100.4 %	-100.0 %	-100.0 %	14.468	13.3	5.5	-0.7	-0.0
144-B-4-R-3-10-9-9	-100.0 %	-100.0 %	-100.0 %	484.094	18.7	121.1	-0.2	-0.0
145-B-2-FR-1-2-7-7	-33.5 %	-9.0 %	47.8%	0.206	18.4	3.9	-0.1	-0.1
146-B-2-FR-1-2-7-9	-29.6 %	-6.0 %	57.8%	0.206	18.4	3.9	-0.1	-0.1
147-B-2-FR-1-2-9-7	-9.9 %	-0.5 %	50.3%	0.209	18.9	3.8	-0.1	-0.1
148-B-2-FR-1-2-9-9	-10.2 %	2.2 %	62.0%	0.209	18.9	3.8	-0.1	-0.1
149-B-2-FR-1-5-7-7	-33.2 %	-10.2 %	42.2%	0.206	14.9	3.4	-0.1	-0.1
150-B-2-FR-1-5-7-9	-29.3 %	-7.6 %	54.6%	0.206	14.9	3.4	-0.1	-0.1
151-B-2-FR-1-5-9-7	-9.8 %	-3.7 %	47.0%	0.209	15.5	3.3	-0.1	-0.1
152-B-2-FR-1-5-9-9	-10.1 %	-0.8 %	68.4%	0.209	15.5	3.3	-0.1	-0.1
153-B-2-FR-1-10-7-7	-32.7 %	-13.3 %	28.9%	0.206	11.4	2.9	-0.1	-0.1
154-B-2-FR-1-10-7-9	-28.8 %	-12.0 %	39.9%	0.206	11.4	2.9	-0.1	-0.1
155-B-2-FR-1-10-9-7	-9.7 %	-6.4 %	28.9%	0.209	12.0	2.8	-0.1	-0.0
156-B-2-FR-1-10-9-9	-9.8 %	-4.4 %	46.9%	0.209	12.0	2.8	-0.1	-0.0
157-B-2-FR-2-2-7-7	-33.8 %	-10.2 %	46.1%	0.467	37.4	5.8	-0.2	0.0
158-B-2-FR-2-2-7-9	-36.0 %	-4.9 %	64.2%	0.467	37.4	5.6	-0.2	0.0
159-B-2-FR-2-2-9-7	-16.7 %	5.0 %	59.5%	0.470	37.4	5.8	-0.2	0.0
160-B-2-FR-2-2-9-9	-16.4 %	5.3 %	71.0%	0.470	37.4	5.7	-0.2	-0.0
161-B-2-FR-2-5-7-7	-33.7 %	-11.4 %	41.8%	0.467	29.3	4.9	-0.2	0.0
162-B-2-FR-2-5-7-9	-34.9 %	-6.6 %	59.3%	0.468	29.3	4.7	-0.2	-0.1
163-B-2-FR-2-5-9-7	-15.9 %	-1.5 %	51.3%	0.470	29.7	5.0	-0.2	-0.0
164-B-2-FR-2-5-9-9	-17.0 %	3.0 %	64.3%	0.470	29.7	4.8	-0.2	-0.0
165-B-2-FR-2-10-7-7	-33.7 %	-13.9 %	29.0%	0.468	22.1	3.9	-0.2	-0.0
166-B-2-FR-2-10-7-9	-31.8 %	-4.6 %	40.9%	0.468	22.1	3.8	-0.2	-0.0
167-B-2-FR-2-10-9-7	-16.4 %	-3.1 %	34.8%	0.470	22.8	4.0	-0.2	-0.0
168-B-2-FR-2-10-9-9	-15.7 %	0.1 %	51.4%	0.470	22.8	3.8	-0.2	-0.0
169-B-2-FR-3-2-7-7	-40.9 %	-14.3 %	51.0%	0.729	51.5	9.8	-0.4	-0.0
170-B-2-FR-3-2-7-9	-44.9 %	-4.5 %	68.2%	0.730	51.6	9.7	-0.3	-0.0
171-B-2-FR-3-2-9-7	-25.7 %	-5.5 %	58.4%	0.729	51.1	10.1	-0.3	-0.1
172-B-2-FR-3-2-9-9	-23.1 %	-2.7 %	68.2%	0.729	51.2	10.0	-0.3	-0.0
173-B-2-FR-3-5-7-7	-40.7 %	-15.1 %	-95.4%	0.729	40.4	8.2	-0.3	-0.0
174-B-2-FR-3-5-7-9	-40.1 %	-6.7 %	65.3%	0.730	40.5	8.0	-0.3	0.0
175-B-2-FR-3-5-9-7	-26.3 %	-5.3 %	57.0%	0.729	40.4	8.5	-0.3	-0.0
176-B-2-FR-3-5-9-9	-21.7 %	-0.3 %	65.2%	0.729	40.5	8.4	-0.3	-0.0
177-B-2-FR-3-10-7-7	-42.0 %	-17.9 %	30.6%	0.729	30.1	6.3	-0.3	0.0
178-B-2-FR-3-10-7-9	-37.9 %	-6.6 %	48.5%	0.730	30.2	6.2	-0.3	0.0
179-B-2-FR-3-10-9-7	-24.3 %	-10.6 %	37.6%	0.729	30.3	6.7	-0.3	-0.0
180-B-2-FR-3-10-9-9	-21.0 %	-1.6 %	56.5%	0.729	30.4	6.6	-0.3	0.0
181-B-4-FR-1-2-7-7	-36.1 %	4.8 %	49.9%	0.411	20.3	6.7	-0.0	-0.4
182-B-4-FR-1-2-7-9	-29.9 %	12.4 %	59.8%	0.411	20.3	6.7	-0.0	-0.4
183-B-4-FR-1-2-9-7	-11.3 %	14.9 %	56.6%	0.417	21.0	6.6	-0.0	-0.4
184-B-4-FR-1-2-9-9	-10.7 %	20.6 %	63.5%	0.417	21.0	6.6	-0.0	-0.4
185-B-4-FR-1-5-7-7	-30.4 %	-1.0 %	-94.0%	0.411	15.9	5.7	-0.0	-0.3
186-B-4-FR-1-5-7-9	-29.4 %	0.5 %	50.1%	0.411	15.9	5.7	-0.0	-0.3

Continued on next page

Table 4.1 Unsorted Results – *Continued from previous page*

Filename	AAR+Shear			AAR Only				
	K	V_{ult}	V_{yld}	Δ_{ver}	σ^{lan}_{max}	σ^{tra}_{max}	σ^{lan}_{med}	σ^{tra}_{med}
	$\frac{(AAR+x)-x}{x} \times 100$			mm	MPa			
187-B-4-FR-1-5-9-7	-11.0 %	9.5 %	48.2%	0.417	16.8	5.7	-0.0	-0.3
188-B-4-FR-1-5-9-9	-10.0 %	12.4 %	56.1%	0.417	16.8	5.7	-0.0	-0.3
189-B-4-FR-1-10-7-7	-29.9 %	-2.3 %	42.9%	0.411	11.8	4.6	-0.0	-0.2
190-B-4-FR-1-10-7-9	-28.9 %	5.4 %	55.3%	0.411	11.8	4.6	-0.0	-0.2
191-B-4-FR-1-10-9-7	-10.6 %	3.1 %	45.2%	0.417	12.6	4.7	-0.0	-0.2
192-B-4-FR-1-10-9-9	-9.9 %	9.7 %	59.7%	0.417	12.6	4.7	-0.0	-0.2
193-B-4-FR-2-2-7-7	-41.5 %	5.9 %	54.9%	0.936	43.1	15.4	-0.1	0.0
194-B-4-FR-2-2-7-9	-40.2 %	14.1 %	67.0%	0.936	43.0	15.3	-0.1	0.0
195-B-4-FR-2-2-9-7	-23.4 %	10.2 %	56.6%	0.942	43.3	15.3	-0.1	0.0
196-B-4-FR-2-2-9-9	-20.5 %	17.6 %	72.2%	0.942	43.2	15.3	-0.1	0.1
197-B-4-FR-2-5-7-7	-40.5 %	3.0 %	48.7%	0.937	32.6	12.9	-0.1	-0.0
198-B-4-FR-2-5-7-9	-40.5 %	11.7 %	66.8%	0.937	32.5	12.9	-0.1	-0.0
199-B-4-FR-2-5-9-7	-21.6 %	3.2 %	42.9%	0.942	33.1	13.1	-0.1	-0.0
200-B-4-FR-2-5-9-9	-19.8 %	17.3 %	70.3%	0.943	33.1	13.0	-0.1	-0.0
201-B-4-FR-2-10-7-7	-40.7 %	0.1 %	47.4%	0.937	23.4	10.2	-0.1	-0.1
202-B-4-FR-2-10-7-9	-38.3 %	12.8 %	66.1%	0.938	23.3	10.1	-0.1	-0.1
203-B-4-FR-2-10-9-7	-20.9 %	2.6 %	43.7%	0.943	24.0	10.4	-0.1	-0.0
204-B-4-FR-2-10-9-9	-19.8 %	14.0 %	67.9%	0.944	24.0	10.4	-0.1	-0.0
205-B-4-FR-3-2-7-7	-43.0 %	2.3 %	44.6%	1.460	60.3	29.3	-0.2	0.0
206-B-4-FR-3-2-7-9	-38.0 %	21.1 %	52.8%	1.464	60.3	27.7	-0.2	0.1
207-B-4-FR-3-2-9-7	-26.8 %	19.5 %	53.3%	1.463	60.0	26.9	-0.1	0.2
208-B-4-FR-3-2-9-9	-23.9 %	27.3 %	72.4%	1.464	60.2	28.0	-0.2	0.2
209-B-4-FR-3-5-7-7	-39.3 %	1.0 %	46.9%	1.466	44.7	24.9	-0.1	-0.2
210-B-4-FR-3-5-7-9	-34.8 %	5.2 %	-83.7%	1.462	44.7	25.7	-0.1	-0.2
211-B-4-FR-3-5-9-7	-24.4 %	10.7 %	55.9%	1.462	44.7	22.2	-0.1	-0.2
212-B-4-FR-3-5-9-9	-26.8 %	22.6 %	52.7%	1.464	44.6	22.9	-0.1	-0.2
213-B-4-FR-3-10-7-7	-39.1 %	-2.9 %	38.6%	1.465	31.6	19.0	-0.1	-0.0
214-B-4-FR-3-10-7-9	-38.7 %	3.8 %	52.9%	1.462	31.6	18.8	-0.1	-0.1
215-B-4-FR-3-10-9-7	-21.9 %	4.4 %	53.7%	1.460	31.8	19.5	-0.1	-0.1
216-B-4-FR-3-10-9-9	-42.8 %	-4.1 %	29.9%	3.228	38.2	19.1	0.1	0.4
1-TB-2-U-1-2-7-7	-29.4 %	-2.3 %	-2.5%	0.207	64.5	65.2	64.0	61.7
2-TB-2-U-1-2-7-9	-29.4 %	-8.2 %	0.3%	0.207	64.5	65.2	64.0	61.7
3-TB-2-U-1-2-9-7	-9.6 %	3.4 %	-4.9%	0.207	64.7	65.3	64.3	62.2
4-TB-2-U-1-2-9-9	-9.6 %	-1.8 %	-1.0%	0.207	64.7	65.3	64.3	62.2
5-TB-2-U-1-5-7-7	-27.4 %	-21.2 %	6.5%	0.213	61.3	62.5	60.4	55.6
6-TB-2-U-1-5-7-9	-27.4 %	-8.8 %	8.1%	0.213	61.3	62.5	60.4	55.6
7-TB-2-U-1-5-9-7	-9.6 %	-14.6 %	7.0%	0.213	61.8	62.9	60.9	56.4
8-TB-2-U-1-5-9-9	-9.1 %	-0.6 %	5.5%	0.213	61.8	62.9	60.9	56.4
9-TB-2-U-1-10-7-7	-25.7 %	-41.6 %	-26.6%	0.222	56.2	57.7	55.0	47.6
10-TB-2-U-1-10-7-9	-25.7 %	-33.3 %	-16.2%	0.222	56.2	57.7	55.0	47.6
11-TB-2-U-1-10-9-7	-9.2 %	-35.1 %	-18.5%	0.221	57.0	58.5	55.8	48.8
12-TB-2-U-1-10-9-9	-8.5 %	-26.2 %	-7.3%	0.221	57.0	58.5	55.8	48.8
13-TB-2-U-2-2-7-7	-29.3 %	12.5 %	-2.8%	0.419	128.1	129.7	126.8	121.4
14-TB-2-U-2-2-7-9	-29.3 %	-8.8 %	-5.5%	0.419	128.1	129.8	126.8	121.4
15-TB-2-U-2-2-9-7	-9.8 %	9.9 %	-2.3%	0.419	128.5	130.1	127.2	122.2
16-TB-2-U-2-2-9-9	-9.8 %	-3.5 %	1.6%	0.419	128.5	130.1	127.2	122.2
17-TB-2-U-2-5-7-7	-28.4 %	-20.7 %	-3.4%	0.438	119.8	122.8	117.6	106.7
18-TB-2-U-2-5-7-9	-27.3 %	-11.6 %	-0.2%	0.438	119.8	122.8	117.6	106.7
19-TB-2-U-2-5-9-7	-9.6 %	-15.7 %	-1.6%	0.438	120.8	123.7	118.5	108.2
20-TB-2-U-2-5-9-9	-9.7 %	-2.6 %	4.0%	0.438	120.8	123.7	118.5	108.2
21-TB-2-U-2-10-7-7	-26.7 %	-41.0 %	-25.9%	0.465	107.2	109.6	104.0	87.0

Continued on next page

Table 4.1 Unsorted Results – *Continued from previous page*

Filename	AAR+Shear			AAR Only				
	K	V_{ult}	V_{yld}	Δ_{ver}	σ^{lan}_{max}	σ^{tra}_{max}	σ^{lan}_{med}	σ^{tra}_{med}
	$\frac{(AAR+x)-x}{x} \times 100$			mm	MPa			
22-TB-2-U-2-10-7-9	-27.8 %	-37.7 %	-21.8%	0.466	107.4	110.0	104.1	87.6
23-TB-2-U-2-10-9-7	-9.9 %	-37.0 %	-20.9%	0.465	108.7	111.4	105.6	89.2
24-TB-2-U-2-10-9-9	-9.3 %	-29.3 %	-11.2%	0.465	108.9	111.8	105.7	89.8
25-TB-2-U-3-2-7-7	-29.2 %	6.6 %	-12.1%	0.636	190.5	193.6	188.1	178.9
26-TB-2-U-3-2-7-9	-28.7 %	1.5 %	-9.3%	0.636	190.5	193.6	188.1	178.9
27-TB-2-U-3-2-9-7	-9.8 %	8.5 %	-10.0%	0.635	191.1	194.1	188.7	179.9
28-TB-2-U-3-2-9-9	-9.8 %	-0.6 %	-9.6%	0.635	191.1	194.1	188.7	180.0
29-TB-2-U-3-5-7-7	-27.9 %	-19.4 %	-21.3%	0.675	175.6	180.2	171.4	152.3
30-TB-2-U-3-5-7-9	-28.8 %	-9.4 %	-13.5%	0.676	175.8	180.5	171.6	152.9
31-TB-2-U-3-5-9-7	-10.3 %	-11.5 %	-16.2%	0.674	176.9	181.6	172.7	154.4
32-TB-2-U-3-5-9-9	-9.8 %	-4.9 %	-8.3%	0.675	177.0	181.8	172.8	155.0
33-TB-2-U-3-10-7-7	-30.2 %	-44.8 %	-30.7%	0.726	152.7	153.9	146.9	116.7
34-TB-2-U-3-10-7-9	-27.2 %	-39.6 %	-26.4%	0.728	152.8	154.4	146.9	117.6
35-TB-2-U-3-10-9-7	-12.4 %	-37.0 %	-20.9%	0.726	154.8	156.6	148.9	119.6
36-TB-2-U-3-10-9-9	-11.0 %	-25.6 %	-8.6%	0.728	154.8	157.2	149.1	120.6
37-TB-4-U-1-2-7-7	-29.2 %	-4.2 %	15.7%	0.413	64.7	65.4	64.0	60.8
38-TB-4-U-1-2-7-9	-29.2 %	-6.4 %	21.5%	0.413	64.7	65.4	64.0	60.8
39-TB-4-U-1-2-9-7	-10.3 %	-0.2 %	15.4%	0.413	64.9	65.6	64.2	61.3
40-TB-4-U-1-2-9-9	-9.5 %	-4.5 %	22.2%	0.413	64.9	65.6	64.2	61.3
41-TB-4-U-1-5-7-7	-26.7 %	-9.3 %	20.4%	0.424	61.5	62.8	60.1	53.6
42-TB-4-U-1-5-7-9	-26.7 %	-5.0 %	23.9%	0.424	61.5	62.8	60.1	53.7
43-TB-4-U-1-5-9-7	-8.9 %	-0.7 %	13.5%	0.424	62.0	63.2	60.7	54.5
44-TB-4-U-1-5-9-9	-9.3 %	-3.3 %	20.1%	0.424	62.0	63.2	60.7	54.6
45-TB-4-U-1-10-7-7	-24.9 %	-32.7 %	-20.2%	0.441	56.5	57.8	54.6	44.6
46-TB-4-U-1-10-7-9	-24.8 %	-16.8 %	-1.5%	0.441	56.5	57.8	54.6	44.8
47-TB-4-U-1-10-9-7	-9.7 %	-24.3 %	-10.3%	0.440	57.3	58.6	55.5	45.9
48-TB-4-U-1-10-9-9	-9.1 %	-14.2 %	1.7%	0.440	57.3	58.7	55.5	46.1
49-TB-4-U-2-2-7-7	-29.1 %	-6.4 %	10.3%	0.836	128.4	130.3	126.5	119.0
50-TB-4-U-2-2-7-9	-29.2 %	-7.4 %	19.8%	0.836	128.4	130.3	126.5	119.1
51-TB-4-U-2-2-9-7	-9.5 %	-3.5 %	3.6%	0.835	128.8	130.6	127.0	119.9
52-TB-4-U-2-2-9-9	-9.4 %	-5.9 %	14.9%	0.835	128.8	130.6	127.0	120.0
53-TB-4-U-2-5-7-7	-29.2 %	-14.1 %	19.1%	0.873	120.3	123.2	117.2	100.5
54-TB-4-U-2-5-7-9	-28.6 %	-14.4 %	14.6%	0.873	120.3	123.3	117.2	101.1
55-TB-4-U-2-5-9-7	-10.7 %	-6.0 %	11.4%	0.871	121.3	124.2	118.2	102.4
56-TB-4-U-2-5-9-9	-10.9 %	-9.3 %	14.2%	0.871	121.3	124.2	118.2	103.0
57-TB-4-U-2-10-7-7	-25.6 %	-37.4 %	-25.8%	0.920	107.5	108.7	102.7	76.6
58-TB-4-U-2-10-7-9	-26.8 %	-47.2 %	-37.5%	0.924	107.7	109.2	102.8	77.6
59-TB-4-U-2-10-9-7	-9.7 %	-29.1 %	-16.0%	0.919	109.0	110.8	104.6	79.3
60-TB-4-U-2-10-9-9	-9.9 %	-27.0 %	-13.5%	0.920	109.0	111.2	104.6	80.2
61-TB-4-U-3-2-7-7	-29.4 %	-8.3 %	0.3%	1.269	191.1	194.5	187.9	174.1
62-TB-4-U-3-2-7-9	-28.2 %	-11.3 %	-3.3%	1.269	191.1	194.5	187.7	174.4
63-TB-4-U-3-2-9-7	-9.4 %	-3.4 %	-3.5%	1.268	191.6	195.0	188.5	175.6
64-TB-4-U-3-2-9-9	-9.5 %	-9.9 %	1.9%	1.268	191.6	195.0	188.4	175.8
65-TB-4-U-3-5-7-7	-27.7 %	-21.0 %	-1.1%	1.339	176.1	180.2	170.6	139.6
66-TB-4-U-3-5-7-9	-26.5 %	-17.4 %	-2.5%	1.344	176.3	180.5	170.6	141.1
67-TB-4-U-3-5-9-7	-9.9 %	-15.4 %	-2.3%	1.338	177.5	181.9	171.9	142.6
68-TB-4-U-3-5-9-9	-10.2 %	-13.5 %	-2.6%	1.339	177.5	182.2	172.0	143.8
69-TB-4-U-3-10-7-7	-35.8 %	-62.0 %	-55.0%	1.413	152.2	150.3	137.8	94.1
70-TB-4-U-3-10-7-9	-31.3 %	-63.6 %	-67.0%	1.358	152.2	149.8	135.4	84.9
71-TB-4-U-3-10-9-7	-19.0 %	-52.7 %	-44.0%	1.417	154.4	153.1	142.2	99.9
72-TB-4-U-3-10-9-9	-19.5 %	-36.1 %	-26.7%	1.418	154.1	153.3	142.6	99.7

Continued on next page

Table 4.1 Unsorted Results – *Continued from previous page*

Filename	AAR+Shear			AAR Only				
	K	V_{ult}	V_{yld}	Δ_{ver}	σ^{lan}_{max}	σ^{tra}_{max}	σ^{lan}_{med}	σ^{tra}_{med}
		$\frac{(AAR+x)-x}{x}\times 100$		mm	MPa			
73-TB-2-R-1-2-7-7	-31.4 %	-29.4 %	276.3%	0.376	0.0	0.0	0.0	0.0
74-TB-2-R-1-2-7-9	-31.4 %	-10.1 %	275.6%	0.376	0.0	0.0	0.0	0.0
75-TB-2-R-1-2-9-7	-11.5 %	-27.9 %	287.4%	0.381	0.0	0.0	0.0	0.0
76-TB-2-R-1-2-9-9	-11.5 %	-6.2 %	281.3%	0.381	0.0	0.0	0.0	0.0
77-TB-2-R-1-5-7-7	-27.5 %	-26.7 %	201.3%	0.376	0.0	0.0	0.0	0.0
78-TB-2-R-1-5-7-9	-99.9 %	-99.2 %	-100.0%	0.952	8.0	21.7	1.0	-0.2
79-TB-2-R-1-5-9-7	-11.4 %	-22.6 %	218.2%	0.381	0.0	0.0	0.0	0.0
80-TB-2-R-1-5-9-9	-11.4 %	-5.0 %	275.1%	0.381	0.0	0.0	0.0	0.0
81-TB-2-R-1-10-7-7	-26.0 %	-17.5 %	126.4%	0.376	0.0	0.0	0.0	0.0
82-TB-2-R-1-10-7-9	-26.0 %	1.7 %	179.2%	0.376	0.0	0.0	0.0	0.0
83-TB-2-R-1-10-9-7	-10.2 %	-13.8 %	136.8%	0.381	0.0	0.0	0.0	0.0
84-TB-2-R-1-10-9-9	-10.2 %	3.6 %	184.6%	0.381	0.0	0.0	0.0	0.0
85-TB-2-R-2-2-7-7	-31.4 %	-28.8 %	324.8%	0.847	0.1	0.0	0.0	0.0
86-TB-2-R-2-2-7-9	-31.4 %	-7.8 %	347.1%	0.847	0.0	0.0	0.0	0.0
87-TB-2-R-2-2-9-7	-11.5 %	-25.0 %	347.6%	0.854	0.1	0.0	0.0	0.0
88-TB-2-R-2-2-9-9	-11.5 %	-6.0 %	345.2%	0.855	0.1	0.0	0.0	0.0
89-TB-2-R-2-5-7-7	-27.5 %	-23.4 %	215.0%	0.847	0.0	0.0	0.0	0.0
90-TB-2-R-2-5-7-9	-27.5 %	-4.6 %	292.4%	0.847	0.0	0.0	0.0	0.0
91-TB-2-R-2-5-9-7	-11.4 %	-19.4 %	231.4%	0.855	0.1	0.0	0.0	0.0
92-TB-2-R-2-5-9-9	-11.4 %	-2.3 %	301.8%	0.855	0.1	0.0	0.0	0.0
93-TB-2-R-2-10-7-7	-99.8 %	-98.6 %	-99.9%	2.451	19.8	28.2	1.4	0.9
94-TB-2-R-2-10-7-9	-26.0 %	5.8 %	190.6%	0.847	0.0	0.0	0.0	0.0
95-TB-2-R-2-10-9-7	-10.1 %	-8.4 %	151.6%	0.855	0.1	0.0	0.0	0.0
96-TB-2-R-2-10-9-9	-99.6 %	-99.6 %	-100.0%	0.689	10.7	1.8	0.1	0.0
97-TB-2-R-3-2-7-7	-100.0 %	-100.0 %	-100.0 %	11977.024	198.8	184.6	-0.6	6.3
98-TB-2-R-3-2-7-9	-100.0 %	-100.0 %	-100.0 %	845.807	117.2	104.4	-0.5	0.1
99-TB-2-R-3-2-9-7	-11.5 %	-24.7 %	349.8%	1.352	0.2	0.0	0.0	0.0
100-TB-2-R-3-2-9-9	-98.4 %	-98.4 %	-99.9%	1.122	45.0	43.7	-0.8	0.4
101-TB-2-R-3-5-7-7	-100.3 %	-99.9 %	-100.0%	2.390	11.3	16.0	-1.1	-0.1
102-TB-2-R-3-5-7-9	-99.7 %	-99.0 %	-99.0%	7.393	56.0	36.8	10.3	1.9
103-TB-2-R-3-5-9-7	-11.3 %	-18.7 %	234.4%	1.352	0.1	0.1	0.0	0.0
104-TB-2-R-3-5-9-9	-98.5 %	-95.5 %	-100.0%	3.999	34.4	50.9	0.2	0.9
105-TB-2-R-3-10-7-7	-100.0 %	-100.0 %	-100.0 %	962.240	1.5	13.1	-0.0	0.0
106-TB-2-R-3-10-7-9	-100.0 %	-100.0 %	-100.0 %	7777.896	6.0	57.2	-0.2	-0.0
107-TB-2-R-3-10-9-7	-10.1 %	-5.6 %	159.3%	1.352	0.1	0.0	0.0	0.0
108-TB-2-R-3-10-9-9	-100.2 %	-97.9 %	-100.0%	8.963	38.4	20.4	2.2	1.7
109-TB-4-R-1-2-7-7	-100.1 %	-100.0 %	-100.0%	-2.950	27.2	13.8	-0.5	-0.2
110-TB-4-R-1-2-7-9	-99.7 %	-99.9 %	-99.9%	-3.303	5.5	9.1	-0.7	-0.1
111-TB-4-R-1-2-9-7	-100.0 %	-100.0 %	-100.0 %	194.046	4.7	26.3	-0.4	0.0
112-TB-4-R-1-2-9-9	-12.1 %	77.2 %	385.5%	0.761	0.1	0.1	0.0	0.0
113-TB-4-R-1-5-7-7	-27.2 %	4.8 %	376.3%	0.751	0.1	0.1	0.0	0.0
114-TB-4-R-1-5-7-9	-27.2 %	40.3 %	375.9%	0.751	0.1	0.1	0.0	0.0
115-TB-4-R-1-5-9-7	-9.0 %	8.8 %	376.9%	0.760	0.1	0.1	0.0	0.0
116-TB-4-R-1-5-9-9	-9.0 %	38.7 %	379.0%	0.760	0.1	0.1	0.0	0.0
117-TB-4-R-1-10-7-7	-25.7 %	9.9 %	218.7%	0.751	0.1	0.0	0.0	0.0
118-TB-4-R-1-10-7-9	-25.7 %	23.3 %	257.7%	0.751	0.1	0.0	0.0	0.0
119-TB-4-R-1-10-9-7	-8.4 %	13.0 %	227.6%	0.760	0.1	0.1	0.0	0.0
120-TB-4-R-1-10-9-9	-8.4 %	33.6 %	287.5%	0.760	0.1	0.1	0.0	0.0
121-TB-4-R-2-2-7-7	-98.7 %	-99.3 %	-100.0%	3.100	93.6	22.2	2.4	-0.5
122-TB-4-R-2-2-7-9	-31.7 %	69.4 %	468.1%	1.691	0.3	0.1	0.1	0.0
123-TB-4-R-2-2-9-7	-99.9 %	-100.0 %	-99.9 %	28.224	10.7	8.2	0.1	0.1

Continued on next page

Table 4.1 Unsorted Results – *Continued from previous page*

Filename	AAR+Shear			AAR Only				
	K	V_{ult}	V_{yld}	Δ_{ver}	σ^{lan}_{max}	σ^{tra}_{max}	σ^{lan}_{med}	σ^{tra}_{med}
	$\frac{(AAR+x)-x}{x}\times 100$			mm	MPa			
124-TB-4-R-2-2-9-9	-12.1 %	79.5 %	462.8%	1.700	0.4	0.4	0.1	0.0
125-TB-4-R-2-5-7-7	-27.2 %	9.5 %	403.4%	1.692	0.2	0.1	0.1	0.0
126-TB-4-R-2-5-7-9	-27.2 %	42.1 %	460.4%	1.692	0.2	0.1	0.1	0.0
127-TB-4-R-2-5-9-7	-99.9 %	-100.0 %	-100.0 %	13.595	4.4	0.8	0.0	0.0
128-TB-4-R-2-5-9-9	-9.0 %	41.2 %	457.4%	1.706	0.4	0.2	0.1	0.0
129-TB-4-R-2-10-7-7	-25.7 %	14.8 %	232.9%	1.690	0.2	0.1	0.0	0.0
130-TB-4-R-2-10-7-9	-25.7 %	38.7 %	302.3%	1.690	0.2	0.1	0.0	0.0
131-TB-4-R-2-10-9-7	-99.5 %	-100.0 %	-99.9%	9.040	13.4	3.9	-0.1	-0.0
132-TB-4-R-2-10-9-9	-99.8 %	-100.0 %	-100.0 %	39.806	19.0	1.5	-0.0	-0.0
133-TB-4-R-3-2-7-7	-104.3 %	-98.4 %	-100.0%	7.678	74.9	23.9	6.7	0.8
134-TB-4-R-3-2-7-9	-100.4 %	-99.2 %	-100.0%	6.770	52.1	28.0	-10.3	0.3
135-TB-4-R-3-2-9-7	-12.1 %	41.1 %	488.7%	2.691	1.0	0.7	0.1	0.1
136-TB-4-R-3-2-9-9	-99.2 %	-99.8 %	-99.8%	4.826	54.5	39.8	3.2	0.2
137-TB-4-R-3-5-7-7	-27.2 %	10.9 %	410.0%	2.680	0.3	0.4	0.1	0.0
138-TB-4-R-3-5-7-9	-27.2 %	41.0 %	477.4%	2.679	0.4	0.4	0.1	0.0
139-TB-4-R-3-5-9-7	-100.0 %	-100.0 %	-100.0%	2.400	16.1	11.1	-0.1	-0.0
140-TB-4-R-3-5-9-9	-9.0 %	39.9 %	470.1%	2.686	0.7	0.8	0.1	0.0
141-TB-4-R-3-10-7-7	-25.7 %	18.1 %	242.4%	2.679	0.3	0.4	0.0	0.0
142-TB-4-R-3-10-7-9	-99.3 %	-98.4 %	-100.0%	2.371	8.9	2.4	0.7	0.0
143-TB-4-R-3-10-9-7	-99.6 %	-99.9 %	-99.9%	5.547	12.1	1.4	-0.9	-0.0
144-TB-4-R-3-10-9-9	-8.4 %	43.8 %	317.0%	2.686	0.6	0.6	0.1	0.0
145-TB-2-FR-1-2-7-7	-31.2 %	-0.1 %	46.0%	0.205	17.4	9.5	0.4	1.9
146-TB-2-FR-1-2-7-9	-32.7 %	7.3 %	56.8%	0.205	17.4	9.5	0.4	1.9
147-TB-2-FR-1-2-9-7	-15.3 %	5.7 %	54.6%	0.208	19.0	9.5	0.4	1.8
148-TB-2-FR-1-2-9-9	-14.7 %	14.9 %	68.0%	0.208	19.0	9.5	0.4	1.8
149-TB-2-FR-1-5-7-7	-32.4 %	0.3 %	47.2%	0.205	13.3	7.6	0.4	1.7
150-TB-2-FR-1-5-7-9	-32.0 %	6.7 %	56.6%	0.205	13.3	7.6	0.4	1.7
151-TB-2-FR-1-5-9-7	-15.0 %	2.9 %	51.0%	0.208	14.9	7.8	0.4	1.6
152-TB-2-FR-1-5-9-9	-14.6 %	11.7 %	63.9%	0.208	14.9	7.8	0.4	1.6
153-TB-2-FR-1-10-7-7	-31.9 %	13.4 %	43.6%	0.205	9.7	5.8	0.4	1.7
154-TB-2-FR-1-10-7-9	-31.4 %	23.4 %	56.2%	0.205	9.7	5.8	0.4	1.7
155-TB-2-FR-1-10-9-7	-14.7 %	17.4 %	48.6%	0.208	11.2	5.9	0.4	1.6
156-TB-2-FR-1-10-9-9	-14.3 %	28.0 %	62.0%	0.208	11.2	5.9	0.4	1.6
157-TB-2-FR-2-2-7-7	-30.1 %	6.8 %	56.2%	0.470	52.0	16.6	0.3	1.8
158-TB-2-FR-2-2-7-9	-30.4 %	15.4 %	68.8%	0.470	51.5	16.5	0.3	1.8
159-TB-2-FR-2-2-9-7	-10.6 %	13.2 %	56.6%	0.473	52.7	16.4	0.2	1.8
160-TB-2-FR-2-2-9-9	-13.6 %	22.1 %	78.5%	0.473	52.1	16.4	0.3	1.8
161-TB-2-FR-2-5-7-7	-29.4 %	2.3 %	50.2%	0.471	41.0	12.8	0.3	2.1
162-TB-2-FR-2-5-7-9	-30.5 %	10.3 %	61.9%	0.471	40.5	12.8	0.3	2.1
163-TB-2-FR-2-5-9-7	-11.3 %	5.0 %	54.1%	0.473	42.2	12.9	0.2	2.1
164-TB-2-FR-2-5-9-9	-13.6 %	15.7 %	69.8%	0.473	41.6	12.8	0.2	2.1
165-TB-2-FR-2-10-7-7	-29.0 %	20.4 %	52.4%	0.471	31.1	9.3	0.3	2.3
166-TB-2-FR-2-10-7-9	-30.6 %	27.1 %	60.8%	0.471	30.7	9.3	0.3	2.2
167-TB-2-FR-2-10-9-7	-12.4 %	20.1 %	52.0%	0.473	32.5	9.5	0.3	2.3
168-TB-2-FR-2-10-9-9	-13.8 %	32.9 %	68.1%	0.473	32.0	9.4	0.3	2.2
169-TB-2-FR-3-2-7-7	-27.2 %	8.9 %	-42.4%	0.733	78.1	22.5	0.0	3.0
170-TB-2-FR-3-2-7-9	-28.2 %	16.5 %	63.4%	0.732	76.7	22.6	0.1	2.9
171-TB-2-FR-3-2-9-7	-10.6 %	15.0 %	48.5%	0.731	76.7	22.4	0.1	3.0
172-TB-2-FR-3-2-9-9	-15.0 %	21.3 %	77.4%	0.731	75.2	22.5	0.1	2.9
173-TB-2-FR-3-5-7-7	-36.4 %	2.5 %	-95.4%	0.733	61.1	17.0	0.1	3.2
174-TB-2-FR-3-5-7-9	-38.5 %	10.2 %	61.7%	0.733	59.8	17.1	0.1	3.2

Continued on next page

Table 4.1 Unsorted Results – *Continued from previous page*

Filename	AAR+Shear			AAR Only				
	K	V_{ult}	V_{yld}	Δ_{ver}	σ^{lan}_{max}	σ^{tra}_{max}	σ^{lan}_{med}	σ^{tra}_{med}
		$\frac{(AAR+x)-x}{x} \times 100$		mm	MPa			
175-TB-2-FR-3-5-9-7	-12.7 %	8.9 %	59.9%	0.731	60.5	17.1	0.1	3.4
176-TB-2-FR-3-5-9-9	-10.8 %	19.1 %	67.9%	0.731	59.2	17.2	0.1	3.3
177-TB-2-FR-3-10-7-7	-34.1 %	18.7 %	-95.4%	0.733	46.1	12.0	0.1	3.1
178-TB-2-FR-3-10-7-9	-29.9 %	29.6 %	64.0%	0.733	45.1	12.1	0.1	3.0
179-TB-2-FR-3-10-9-7	-20.0 %	24.5 %	57.6%	0.731	46.2	12.2	0.1	3.2
180-TB-2-FR-3-10-9-9	-10.7 %	36.1 %	64.2%	0.731	45.0	12.3	0.1	3.1
181-TB-4-FR-1-2-7-7	-33.4 %	-5.8 %	72.3%	0.409	18.7	13.8	0.4	3.7
182-TB-4-FR-1-2-7-9	-31.2 %	-0.6 %	81.7%	0.409	18.7	13.8	0.4	3.7
183-TB-4-FR-1-2-9-7	-15.0 %	1.9 %	86.3%	0.415	19.3	14.0	0.4	3.6
184-TB-4-FR-1-2-9-9	-12.5 %	7.3 %	96.1%	0.415	19.3	13.9	0.4	3.6
185-TB-4-FR-1-5-7-7	-32.7 %	-0.6 %	51.5%	0.410	14.8	10.4	0.4	3.1
186-TB-4-FR-1-5-7-9	-30.7 %	6.7 %	62.7%	0.410	14.8	10.4	0.4	3.1
187-TB-4-FR-1-5-9-7	-14.5 %	-1.0 %	50.9%	0.416	15.6	10.7	0.4	3.1
188-TB-4-FR-1-5-9-9	-12.2 %	10.6 %	68.6%	0.416	15.6	10.7	0.4	3.1
189-TB-4-FR-1-10-7-7	-31.8 %	10.2 %	42.6%	0.411	10.9	7.3	0.5	2.9
190-TB-4-FR-1-10-7-9	-29.9 %	25.7 %	62.6%	0.411	10.9	7.3	0.5	2.9
191-TB-4-FR-1-10-9-7	-13.5 %	18.3 %	53.0%	0.417	11.6	7.6	0.4	2.9
192-TB-4-FR-1-10-9-9	-11.9 %	28.5 %	66.2%	0.417	11.6	7.6	0.4	2.9
193-TB-4-FR-2-2-7-7	-34.0 %	-0.7 %	81.5%	0.943	38.2	26.2	0.5	6.0
194-TB-4-FR-2-2-7-9	-31.6 %	3.3 %	88.9%	0.943	38.2	26.1	0.5	6.0
195-TB-4-FR-2-2-9-7	-14.9 %	-3.7 %	76.0%	0.948	38.1	26.2	0.5	6.0
196-TB-4-FR-2-2-9-9	-14.2 %	5.9 %	93.5%	0.948	38.1	26.1	0.5	6.0
197-TB-4-FR-2-5-7-7	-34.7 %	-2.1 %	49.2%	0.944	28.6	18.7	0.6	5.5
198-TB-4-FR-2-5-7-9	-35.2 %	11.4 %	69.8%	0.944	28.7	18.7	0.6	5.5
199-TB-4-FR-2-5-9-7	-12.4 %	-1.2 %	50.5%	0.949	28.9	19.1	0.6	5.4
200-TB-4-FR-2-5-9-9	-13.7 %	9.6 %	67.1%	0.949	29.0	19.1	0.6	5.4
201-TB-4-FR-2-10-7-7	-32.6 %	14.5 %	48.0%	0.946	20.2	12.4	0.5	4.9
202-TB-4-FR-2-10-7-9	-33.8 %	24.8 %	61.4%	0.946	20.2	12.4	0.5	4.9
203-TB-4-FR-2-10-9-7	-11.6 %	14.4 %	47.9%	0.950	20.7	12.8	0.5	4.9
204-TB-4-FR-2-10-9-9	-13.4 %	26.6 %	63.8%	0.950	20.7	12.8	0.6	4.9
205-TB-4-FR-3-2-7-7	-36.6 %	-6.8 %	70.3%	1.467	50.9	37.2	0.7	8.6
206-TB-4-FR-3-2-7-9	-23.9 %	-1.1 %	12.3%	1.467	50.9	37.1	0.8	8.6
207-TB-4-FR-3-2-9-7	-13.4 %	0.5 %	-90.6%	1.462	50.1	37.1	0.8	8.8
208-TB-4-FR-3-2-9-9	-16.4 %	0.5 %	83.8%	1.462	50.1	37.1	0.9	8.8
209-TB-4-FR-3-5-7-7	-34.6 %	-8.3 %	-91.1%	1.469	36.9	25.6	0.7	7.9
210-TB-4-FR-3-5-7-9	-35.5 %	4.6 %	59.4%	1.469	36.9	25.6	0.7	7.9
211-TB-4-FR-3-5-9-7	-16.9 %	-0.3 %	52.0%	1.465	36.7	26.0	0.8	8.0
212-TB-4-FR-3-5-9-9	-22.0 %	6.6 %	62.6%	1.465	36.7	26.0	0.8	7.9
213-TB-4-FR-3-10-7-7	-26.6 %	7.1 %	-79.3%	1.471	25.3	16.1	0.7	6.6
214-TB-4-FR-3-10-7-9	-28.1 %	19.5 %	54.5%	1.471	25.3	16.2	0.8	6.6
215-TB-4-FR-3-10-9-7	-16.5 %	16.9 %	51.2%	1.466	25.5	16.6	0.8	6.9
216-TB-4-FR-3-10-9-9	-6.0 %	20.6 %	56.0%	1.466	25.4	16.7	0.8	6.9
1-P-2-U-1-2-7-7	26.0 %	-50.6 %	-50.6%	0.262	0.2	80.0	-0.0	76.9
2-P-2-U-1-2-7-9	27.9 %	-39.7 %	-39.7%	0.262	0.2	80.0	-0.0	76.9
3-P-2-U-1-2-9-7	-100.1 %	-100.0 %	-100.0%	1.056	10.6	47.3	-1.8	3.3
4-P-2-U-1-2-9-9	-100.0 %	-100.0 %	-100.0 %	69.105	75.7	127.1	2.7	-0.1
5-P-2-U-1-5-7-7	23.6 %	-14.2 %	-35.6%	0.268	0.3	73.7	-0.0	67.8
6-P-2-U-1-5-7-9	23.7 %	-9.5 %	-35.5%	0.268	0.3	73.7	-0.0	67.8
7-P-2-U-1-5-9-7	0.6 %	-9.2 %	-59.1%	0.269	0.3	74.7	-0.0	69.0
8-P-2-U-1-5-9-9	-1.2 %	-6.1 %	-59.1%	0.269	0.3	74.7	-0.0	69.0
9-P-2-U-1-10-7-7	-20.8 %	26.3 %	-44.3%	0.276	0.3	64.8	-0.0	56.5

Continued on next page

Table 4.1 Unsorted Results – *Continued from previous page*

Filename	AAR+Shear			AAR Only				
	K	V_{ult}	V_{yld}	Δ_{ver}	σ^{lan}_{max}	σ^{tra}_{max}	σ^{lan}_{med}	σ^{tra}_{med}
	$\frac{(AAR+x)-x}{x}\times 100$			mm	MPa			
10-P-2-U-1-10-7-9	-20.7 %	24.1 %	-44.3%	0.276	0.3	64.8	-0.0	56.5
11-P-2-U-1-10-9-7	-23.9 %	33.4 %	-28.4%	0.277	0.3	66.2	-0.0	58.2
12-P-2-U-1-10-9-9	-19.7 %	34.9 %	-28.4%	0.277	0.3	66.2	-0.0	58.2
13-P-2-U-2-2-7-7	42.2 %	-28.3 %	-57.3%	0.547	0.5	160.7	-0.0	153.2
14-P-2-U-2-2-7-9	42.2 %	-31.3 %	-55.2%	0.547	0.5	160.7	-0.0	153.2
15-P-2-U-2-2-9-7	56.1 %	-21.0 %	-73.3%	0.548	0.5	161.8	-0.0	154.6
16-P-2-U-2-2-9-9	82.0 %	-22.8 %	-46.5%	0.548	0.5	161.8	-0.0	154.6
17-P-2-U-2-5-7-7	13.7 %	1.2 %	-8.9%	0.571	0.6	143.6	-0.0	129.8
18-P-2-U-2-5-7-9	15.6 %	0.7 %	-7.9%	0.571	0.6	143.6	-0.0	129.8
19-P-2-U-2-5-9-7	13.0 %	16.9 %	-59.1%	0.573	0.7	145.3	-0.0	131.9
20-P-2-U-2-5-9-9	11.0 %	7.7 %	-59.1%	0.573	0.8	145.3	-0.0	132.1
21-P-2-U-2-10-7-7	-2.3 %	51.0 %	53.4%	0.596	1.4	120.5	0.0	96.1
22-P-2-U-2-10-7-9	-0.8 %	49.1 %	54.7%	0.597	1.5	120.5	-0.0	96.4
23-P-2-U-2-10-9-7	-3.2 %	62.9 %	-28.6%	0.599	1.2	122.9	-0.0	99.1
24-P-2-U-2-10-9-9	-1.5 %	56.3 %	-28.4%	0.600	1.2	122.9	0.0	99.8
25-P-2-U-3-2-7-7	36.1 %	-18.4 %	-39.2%	0.847	1.1	239.2	-0.0	226.0
26-P-2-U-3-2-7-9	40.2 %	-25.6 %	-38.1%	0.847	1.1	239.2	-0.0	226.0
27-P-2-U-3-2-9-7	42.9 %	-18.1 %	-73.3%	0.849	1.2	240.6	-0.0	228.0
28-P-2-U-3-2-9-9	62.5 %	-18.0 %	-25.9%	0.849	1.2	240.6	-0.0	228.0
29-P-2-U-3-5-7-7	11.6 %	15.3 %	-10.0%	0.895	2.0	207.1	0.0	175.4
30-P-2-U-3-5-7-9	18.3 %	5.9 %	-6.5%	0.896	2.0	207.1	0.0	176.4
31-P-2-U-3-5-9-7	21.1 %	18.0 %	-59.3%	0.897	2.2	209.4	0.0	179.3
32-P-2-U-3-5-9-9	41.3 %	18.7 %	14.1%	0.898	2.2	209.5	0.0	180.8
33-P-2-U-3-10-7-7	-12.4 %	48.2 %	-44.5%	0.946	4.0	164.7	-0.1	119.8
34-P-2-U-3-10-7-9	-10.5 %	44.2 %	-44.3%	0.946	5.3	165.0	-0.1	120.1
35-P-2-U-3-10-9-7	-1.9 %	-4.8 %	-39.1%	0.949	3.2	168.1	-0.1	124.3
36-P-2-U-3-10-9-9	33.9 %	65.0 %	33.9%	0.949	3.7	168.4	-0.1	125.9
37-P-4-U-1-2-7-7	-28.7 %	-31.6 %	238.0%	0.521	0.3	80.4	-0.0	76.2
38-P-4-U-1-2-7-9	-28.7 %	-21.3 %	268.8%	0.521	0.3	80.4	-0.0	76.2
39-P-4-U-1-2-9-7	-9.6 %	-23.7 %	270.0%	0.522	0.3	80.9	-0.0	77.0
40-P-4-U-1-2-9-9	-9.6 %	-20.3 %	278.9%	0.522	0.3	80.9	-0.0	77.0
41-P-4-U-1-5-7-7	-27.3 %	-32.7 %	135.8%	0.532	0.4	74.5	-0.0	66.3
42-P-4-U-1-5-7-9	-27.3 %	-26.3 %	161.0%	0.532	0.4	74.5	-0.0	66.3
43-P-4-U-1-5-9-7	-9.1 %	-23.6 %	163.1%	0.534	0.4	75.4	-0.0	67.6
44-P-4-U-1-5-9-9	-9.1 %	-15.3 %	157.3%	0.534	0.4	75.4	-0.0	67.6
45-P-4-U-1-10-7-7	-25.9 %	-20.8 %	72.5%	0.547	0.4	65.9	-0.0	54.7
46-P-4-U-1-10-7-9	-25.9 %	-18.3 %	82.7%	0.547	0.4	65.9	-0.0	54.7
47-P-4-U-1-10-9-7	-8.6 %	-12.5 %	93.6%	0.548	0.4	67.2	-0.0	56.4
48-P-4-U-1-10-9-9	-8.6 %	-13.1 %	93.4%	0.548	0.4	67.2	-0.0	56.4
49-P-4-U-2-2-7-7	-28.7 %	-33.2 %	201.8%	1.087	0.8	161.7	0.0	151.3
50-P-4-U-2-2-7-9	-28.7 %	-28.7 %	263.1%	1.087	0.8	161.7	0.0	151.3
51-P-4-U-2-2-9-7	-9.6 %	-25.7 %	246.0%	1.090	0.7	162.7	0.0	152.8
52-P-4-U-2-2-9-9	-9.6 %	-25.5 %	256.8%	1.090	0.7	162.7	0.0	152.8
53-P-4-U-2-5-7-7	-28.3 %	-22.7 %	167.4%	1.125	1.3	145.0	-0.0	120.0
54-P-4-U-2-5-7-9	-28.2 %	-22.3 %	173.6%	1.130	0.7	145.5	0.0	127.1
55-P-4-U-2-5-9-7	-10.2 %	-20.1 %	178.1%	1.130	0.8	146.9	-0.1	123.8
56-P-4-U-2-5-9-9	-9.5 %	-17.8 %	163.7%	1.133	0.9	147.2	-0.0	129.4
57-P-4-U-2-10-7-7	-37.8 %	-13.7 %	103.6%	1.164	2.4	121.3	-0.1	85.8
58-P-4-U-2-10-7-9	-33.3 %	-15.6 %	39.3%	1.164	3.1	121.2	-0.0	85.2
59-P-4-U-2-10-9-7	-20.0 %	-15.2 %	78.8%	1.170	1.6	124.1	-0.1	90.8
60-P-4-U-2-10-9-9	-21.8 %	-14.1 %	103.2%	1.171	2.5	124.0	-0.0	90.0

Continued on next page

Filename	AAR+Shear			AAR Only				
	K	V_{ult}	V_{yld}	Δ_{ver}	σ^{lan}_{max}	σ^{tra}_{max}	σ^{lan}_{med}	σ^{tra}_{med}
	$\frac{(AAR+x)-x}{x} \times 100$			mm	MPa			
61-P-4-U-3-2-7-7	-28.7 %	-28.0 %	230.3%	1.680	2.2	240.9	-0.0	223.2
62-P-4-U-3-2-7-9	-28.7 %	-26.6 %	219.1%	1.680	2.0	240.9	-0.0	223.3
63-P-4-U-3-2-9-7	-9.6 %	-26.6 %	245.2%	1.684	2.7	242.3	-0.0	225.4
64-P-4-U-3-2-9-9	-9.6 %	-24.4 %	248.5%	1.684	2.5	242.4	-0.0	225.4
65-P-4-U-3-5-7-7	-39.0 %	-34.0 %	167.3%	1.751	2.4	208.5	-0.1	162.1
66-P-4-U-3-5-7-9	-38.8 %	-35.0 %	163.4%	1.751	5.6	207.6	-0.1	160.2
67-P-4-U-3-5-9-7	-19.1 %	-26.0 %	170.2%	1.758	2.0	211.1	-0.1	166.1
68-P-4-U-3-5-9-9	-18.2 %	-27.9 %	167.1%	1.761	2.5	211.0	-0.1	166.2
69-P-4-U-3-10-7-7	-43.5 %	-29.3 %	-95.6%	1.823	3.4	166.7	-0.0	106.2
70-P-4-U-3-10-7-9	-39.1 %	-35.7 %	-83.0%	1.817	5.3	166.5	-0.0	106.3
71-P-4-U-3-10-9-7	-34.5 %	-22.9 %	46.3%	1.828	3.2	170.0	-0.1	109.8
72-P-4-U-3-10-9-9	-30.1 %	-33.0 %	30.4%	1.825	3.9	169.8	-0.1	109.8
73-P-2-R-1-2-7-7	32.0 %	-25.8 %	-27.3%	0.376	0.0	0.0	0.0	0.0
74-P-2-R-1-2-7-9	33.0 %	-8.4 %	-27.1%	0.376	0.0	0.0	0.0	0.0
75-P-2-R-1-2-9-7	52.3 %	-31.7 %	-69.5%	0.381	0.0	0.0	0.0	0.0
76-P-2-R-1-2-9-9	54.2 %	-12.3 %	-69.5%	0.381	0.0	0.0	0.0	0.0
77-P-2-R-1-5-7-7	24.6 %	16.4 %	16.4%	0.376	0.0	0.0	0.0	0.0
78-P-2-R-1-5-7-9	23.0 %	38.1 %	38.1%	0.376	0.0	0.0	0.0	0.0
79-P-2-R-1-5-9-7	41.5 %	11.8 %	11.8%	0.381	0.0	0.0	0.0	0.0
80-P-2-R-1-5-9-9	42.9 %	12.4 %	12.4%	0.381	0.0	0.0	0.0	0.0
81-P-2-R-1-10-7-7	14.8 %	56.7 %	64.4%	0.376	0.0	0.0	0.0	0.0
82-P-2-R-1-10-7-9	15.5 %	57.4 %	65.0%	0.376	0.0	0.0	0.0	0.0
83-P-2-R-1-10-9-7	-10.9 %	43.5 %	-31.1%	0.381	0.0	0.0	0.0	0.0
84-P-2-R-1-10-9-9	37.7 %	26.7 %	32.9%	0.381	0.0	0.0	0.0	0.0
85-P-2-R-2-2-7-7	40.3 %	-49.4 %	-34.3%	0.847	0.1	0.0	0.0	0.0
86-P-2-R-2-2-7-9	-76.9 %	-77.2 %	-74.3%	1.236	24.8	9.5	5.5	0.0
87-P-2-R-2-2-9-7	64.7 %	-27.5 %	-13.9%	0.855	0.2	0.0	0.0	0.0
88-P-2-R-2-2-9-9	67.9 %	-19.6 %	-9.3%	0.855	0.1	0.0	0.0	0.0
89-P-2-R-2-5-7-7	-98.4 %	-80.5 %	-99.0%	2.984	25.2	3.8	1.6	0.1
90-P-2-R-2-5-7-9	26.2 %	45.1 %	45.1%	0.847	0.0	0.0	0.0	0.0
91-P-2-R-2-5-9-7	-100.0 %	-99.8 %	-100.0%	3.999	12.4	7.0	-1.3	-0.0
92-P-2-R-2-5-9-9	51.6 %	5.8 %	5.8%	0.855	0.1	0.0	0.0	0.0
93-P-2-R-2-10-7-7	16.6 %	7.3 %	12.6%	0.847	0.0	0.0	0.0	0.0
94-P-2-R-2-10-7-9	17.0 %	57.5 %	65.2%	0.847	0.0	0.0	0.0	0.0
95-P-2-R-2-10-9-7	40.7 %	29.4 %	35.8%	0.855	0.1	0.0	0.0	0.0
96-P-2-R-2-10-9-9	41.8 %	30.5 %	36.9%	0.855	0.1	0.0	0.0	0.0
97-P-2-R-3-2-7-7	-99.9 %	-97.4 %	-100.0%	5.077	30.3	25.8	-5.2	0.0
98-P-2-R-3-2-7-9	-99.6 %	-98.9 %	-99.9%	1.768	89.8	30.4	-0.7	0.2
99-P-2-R-3-2-9-7	67.0 %	-41.1 %	-23.4%	1.352	0.3	0.0	0.0	0.0
100-P-2-R-3-2-9-9	68.2 %	-18.6 %	-8.6%	1.353	0.3	0.0	0.0	0.0
101-P-2-R-3-5-7-7	-100.0 %	-100.0 %	-100.0 %	449.364	43.4	81.5	-24.0	15.4
102-P-2-R-3-5-7-9	-99.9 %	-98.9 %	-99.9%	2.807	18.4	28.2	2.1	0.3
103-P-2-R-3-5-9-7	-99.8 %	-97.1 %	-99.9%	2.451	17.9	21.3	2.0	0.2
104-P-2-R-3-5-9-9	52.8 %	6.9 %	6.9%	1.353	0.1	0.0	0.0	0.0
105-P-2-R-3-10-7-7	-100.1 %	-97.5 %	-100.0%	2.865	12.0	8.5	1.5	0.1
106-P-2-R-3-10-7-9	-100.0 %	-100.0 %	-100.0 %	909.898	6.1	173.3	-14.0	-0.0
107-P-2-R-3-10-9-7	41.4 %	30.1 %	36.5%	1.352	0.2	0.0	0.0	0.0
108-P-2-R-3-10-9-9	42.5 %	31.2 %	37.6%	1.352	0.2	0.0	0.0	0.0
109-P-4-R-1-2-7-7	26.8 %	-45.6 %	-45.6%	0.752	0.1	0.0	0.0	0.0
110-P-4-R-1-2-7-9	25.1 %	-36.5 %	-44.3%	0.752	0.1	0.0	0.0	0.0
111-P-4-R-1-2-9-7	43.7 %	-47.8 %	-77.2%	0.761	0.1	0.0	0.0	0.0

Continued on next page

Table 4.1 Unsorted Results – *Continued from previous page*

Filename	AAR+Shear			AAR Only				
	K	V_{ult}	V_{yld}	Δ_{ver}	σ^{lan}_{max}	σ^{tra}_{max}	σ^{lan}_{med}	σ^{tra}_{med}
	$\frac{(AAR+x)-x}{x} \times 100$			mm	MPa			
112-P-4-R-1-2-9-9	45.5 %	-37.3 %	-76.9%	0.761	0.1	0.0	0.0	0.0
113-P-4-R-1-5-7-7	20.4 %	-17.1 %	-17.1%	0.752	0.1	0.0	0.0	0.0
114-P-4-R-1-5-7-9	21.0 %	0.9 %	0.9%	0.752	0.1	0.0	0.0	0.0
115-P-4-R-1-5-9-7	40.8 %	-27.2 %	-27.2%	0.760	0.1	0.0	0.0	0.0
116-P-4-R-1-5-9-9	40.3 %	-6.3 %	-6.3%	0.760	0.1	0.0	0.0	0.0
117-P-4-R-1-10-7-7	20.1 %	20.1 %	20.1%	0.752	0.1	0.0	0.0	0.0
118-P-4-R-1-10-7-9	20.4 %	20.4 %	20.4%	0.752	0.1	0.0	0.0	0.0
119-P-4-R-1-10-9-7	26.6 %	26.6 %	-23.9%	0.760	0.1	0.0	0.0	0.0
120-P-4-R-1-10-9-9	40.9 %	40.9 %	40.9%	0.760	0.1	0.0	0.0	0.0
121-P-4-R-2-2-7-7	33.6 %	-41.5 %	-41.5%	1.690	0.2	0.1	0.0	0.0
122-P-4-R-2-2-7-9	34.5 %	-25.5 %	-39.1%	1.690	0.3	0.1	0.0	0.0
123-P-4-R-2-2-9-7	57.5 %	-42.7 %	-42.7%	1.704	0.4	0.2	0.1	0.0
124-P-4-R-2-2-9-9	57.2 %	-33.4 %	-33.4%	1.704	0.5	0.2	0.1	0.0
125-P-4-R-2-5-7-7	24.4 %	-14.5 %	-14.5%	1.691	0.3	0.0	0.0	0.0
126-P-4-R-2-5-7-9	24.7 %	-7.9 %	-7.9%	1.691	0.2	0.0	0.0	0.0
127-P-4-R-2-5-9-7	48.8 %	-23.1 %	-23.1%	1.705	0.5	0.1	0.1	0.0
128-P-4-R-2-5-9-9	-99.9 %	-99.9 %	-100.0%	-1.164	51.7	59.2	-1.3	-0.1
129-P-4-R-2-10-7-7	21.7 %	21.7 %	21.7%	1.692	0.2	0.0	0.0	0.0
130-P-4-R-2-10-7-9	21.5 %	21.5 %	21.5%	1.691	0.2	0.0	0.0	0.0
131-P-4-R-2-10-9-7	46.8 %	121.9 %	46.8%	1.705	0.4	0.1	0.0	0.0
132-P-4-R-2-10-9-9	-100.1 %	-99.3 %	-100.0%	-1.333	15.2	6.6	-0.7	0.0
133-P-4-R-3-2-7-7	-99.6 %	-99.6 %	-100.0%	6.311	67.8	46.9	-7.6	0.0
134-P-4-R-3-2-7-9	-99.2 %	-99.1 %	-99.8%	4.324	91.4	24.9	17.8	-0.1
135-P-4-R-3-2-9-7	-100.1 %	-100.0 %	-100.0%	5.299	38.5	22.9	1.2	-0.2
136-P-4-R-3-2-9-9	61.1 %	-31.9 %	-31.9%	2.694	1.2	0.3	0.1	0.0
137-P-4-R-3-5-7-7	25.0 %	-7.8 %	-7.8%	2.684	0.5	0.1	0.0	0.0
138-P-4-R-3-5-7-9	-97.5 %	-77.6 %	-96.9%	4.376	15.4	3.1	2.4	0.0
139-P-4-R-3-5-9-7	-99.7 %	-97.9 %	-100.0%	9.095	28.5	15.8	8.8	0.2
140-P-4-R-3-5-9-9	-99.5 %	-95.5 %	-99.5%	2.762	17.4	22.0	0.2	0.0
141-P-4-R-3-10-7-7	-99.7 %	-97.0 %	-100.0%	7.606	38.1	11.1	-2.4	-0.0
142-P-4-R-3-10-7-9	21.9 %	21.9 %	21.9%	2.684	0.2	0.1	0.0	0.0
143-P-4-R-3-10-9-7	-100.0 %	-100.0 %	-100.0 %	192.624	76.7	46.3	0.0	0.0
144-P-4-R-3-10-9-9	48.5 %	48.5 %	48.5%	2.695	0.6	0.1	0.0	0.0
145-P-2-FR-1-2-7-7	-32.2 %	-7.1 %	69.6%	0.206	14.4	10.6	0.5	0.9
146-P-2-FR-1-2-7-9	-31.3 %	2.5 %	87.0%	0.206	14.4	10.6	0.5	0.9
147-P-2-FR-1-2-9-7	-13.6 %	-3.3 %	76.5%	0.209	14.7	10.7	0.4	0.8
148-P-2-FR-1-2-9-9	-12.7 %	5.7 %	93.0%	0.209	14.7	10.7	0.5	0.8
149-P-2-FR-1-5-7-7	-31.7 %	-1.8 %	45.1%	0.206	12.2	8.6	0.5	1.1
150-P-2-FR-1-5-7-9	-30.7 %	7.6 %	59.0%	0.206	12.1	8.6	0.5	1.1
151-P-2-FR-1-5-9-7	-13.4 %	5.9 %	56.6%	0.209	12.4	8.7	0.4	1.0
152-P-2-FR-1-5-9-9	-12.4 %	13.3 %	67.5%	0.209	12.3	8.7	0.4	1.0
153-P-2-FR-1-10-7-7	-31.0 %	1.0 %	42.3%	0.206	10.0	6.5	0.5	1.0
154-P-2-FR-1-10-7-9	-29.9 %	11.0 %	56.4%	0.206	9.9	6.5	0.5	1.0
155-P-2-FR-1-10-9-7	-13.1 %	7.6 %	51.5%	0.210	10.2	6.6	0.4	0.9
156-P-2-FR-1-10-9-9	-12.0 %	17.5 %	65.5%	0.210	10.1	6.6	0.4	0.9
157-P-2-FR-2-2-7-7	-28.9 %	-1.2 %	80.4%	0.473	27.9	18.9	0.6	0.4
158-P-2-FR-2-2-7-9	-31.7 %	5.7 %	93.0%	0.473	27.9	18.6	0.6	0.4
159-P-2-FR-2-2-9-7	-14.0 %	3.6 %	87.0%	0.475	27.5	18.8	0.5	0.4
160-P-2-FR-2-2-9-9	-13.8 %	16.5 %	112.6%	0.475	27.6	18.6	0.5	0.4
161-P-2-FR-2-5-7-7	-30.5 %	4.9 %	55.2%	0.474	22.0	14.4	0.5	0.9
162-P-2-FR-2-5-7-9	-31.3 %	16.8 %	72.8%	0.474	22.0	14.3	0.5	0.9

Continued on next page

Filename	AAR+Shear			AAR Only				
	K	V_{ult}	V_{yld}	Δ_{ver}	σ^{lan}_{max}	σ^{tra}_{max}	σ^{lan}_{med}	σ^{tra}_{med}
	$\frac{(AAR+x)-x}{x}\times 100$			mm	MPa			
163-P-2-FR-2-5-9-7	-13.8 %	14.0 %	68.6%	0.476	22.0	14.5	0.5	0.9
164-P-2-FR-2-5-9-9	-13.8 %	24.8 %	84.5%	0.476	22.0	14.4	0.5	0.9
165-P-2-FR-2-10-7-7	-30.8 %	6.6 %	49.6%	0.474	16.5	10.3	0.3	1.1
166-P-2-FR-2-10-7-9	-31.0 %	15.6 %	62.8%	0.474	16.4	10.2	0.3	1.0
167-P-2-FR-2-10-9-7	-13.1 %	11.4 %	56.6%	0.476	16.6	10.5	0.4	1.0
168-P-2-FR-2-10-9-9	-13.8 %	21.7 %	71.5%	0.476	16.5	10.4	0.4	1.0
169-P-2-FR-3-2-7-7	-42.1 %	4.0 %	89.8%	0.732	36.5	26.1	0.6	1.4
170-P-2-FR-3-2-7-9	-25.8 %	15.8 %	-0.1%	0.732	36.6	26.0	0.6	1.3
171-P-2-FR-3-2-9-7	-13.4 %	14.2 %	97.4%	0.729	35.9	25.9	0.6	1.4
172-P-2-FR-3-2-9-9	-10.9 %	28.3 %	99.4%	0.729	35.9	25.9	0.6	1.2
173-P-2-FR-3-5-7-7	-40.1 %	10.3 %	-95.6%	0.732	27.8	19.3	0.4	1.6
174-P-2-FR-3-5-7-9	-32.7 %	24.4 %	-94.0%	0.732	27.8	19.3	0.4	1.6
175-P-2-FR-3-5-9-7	-12.0 %	19.9 %	71.9%	0.729	27.5	19.4	0.5	1.7
176-P-2-FR-3-5-9-9	-13.1 %	32.3 %	95.6%	0.729	27.5	19.5	0.5	1.7
177-P-2-FR-3-10-7-7	-38.0 %	12.3 %	58.2%	0.733	20.6	13.4	0.4	1.8
178-P-2-FR-3-10-7-9	-36.7 %	23.4 %	-91.4%	0.733	20.5	13.4	0.4	1.7
179-P-2-FR-3-10-9-7	-16.8 %	21.8 %	67.6%	0.730	20.5	13.6	0.4	1.8
180-P-2-FR-3-10-9-9	-10.6 %	33.2 %	87.5%	0.730	20.5	13.6	0.4	1.8
181-P-4-FR-1-2-7-7	-32.2 %	-6.2 %	-96.9%	0.411	17.9	15.8	0.4	2.7
182-P-4-FR-1-2-7-9	-30.7 %	-0.4 %	-96.7%	0.411	17.8	15.6	0.4	2.7
183-P-4-FR-1-2-9-7	-13.6 %	-0.8 %	-96.1%	0.417	18.4	16.1	0.4	2.6
184-P-4-FR-1-2-9-9	-12.9 %	7.5 %	-95.8%	0.417	18.4	15.9	0.4	2.6
185-P-4-FR-1-5-7-7	-31.9 %	-5.3 %	-97.1%	0.412	15.1	12.0	0.6	2.3
186-P-4-FR-1-5-7-9	-30.1 %	3.2 %	-96.9%	0.412	14.9	11.9	0.5	2.3
187-P-4-FR-1-5-9-7	-14.1 %	1.5 %	-96.4%	0.418	15.4	12.4	0.4	2.2
188-P-4-FR-1-5-9-9	-13.0 %	8.2 %	-96.1%	0.418	15.2	12.3	0.4	2.2
189-P-4-FR-1-10-7-7	-31.5 %	-1.7 %	-97.1%	0.413	11.9	8.5	0.7	1.9
190-P-4-FR-1-10-7-9	-33.2 %	6.9 %	-97.0%	0.413	11.8	8.5	0.7	1.9
191-P-4-FR-1-10-9-7	-13.6 %	7.3 %	-96.4%	0.419	12.4	8.9	0.6	1.9
192-P-4-FR-1-10-9-9	-12.5 %	13.7 %	-96.1%	0.419	12.2	8.9	0.6	1.9
193-P-4-FR-2-2-7-7	-34.0 %	-0.7 %	-93.3%	0.945	35.9	31.9	0.4	4.4
194-P-4-FR-2-2-7-9	-32.5 %	-0.7 %	-97.8%	0.945	35.6	31.9	0.4	4.4
195-P-4-FR-2-2-9-7	-33.8 %	5.0 %	-94.0%	0.949	36.0	31.9	0.5	4.3
196-P-4-FR-2-2-9-9	-25.0 %	9.6 %	-93.1%	0.949	35.5	31.9	0.5	4.3
197-P-4-FR-2-5-7-7	-30.5 %	1.0 %	-93.6%	0.947	28.3	22.7	0.4	4.0
198-P-4-FR-2-5-7-9	-38.3 %	3.7 %	-94.6%	0.947	28.3	22.9	0.4	3.9
199-P-4-FR-2-5-9-7	-15.5 %	8.8 %	-97.5%	0.950	28.5	23.1	0.4	4.0
200-P-4-FR-2-5-9-9	-23.4 %	12.3 %	-93.4%	0.950	28.4	23.3	0.4	3.9
201-P-4-FR-2-10-7-7	-51.3 %	3.1 %	-96.3%	0.948	20.9	15.1	0.7	3.6
202-P-4-FR-2-10-7-9	-38.5 %	8.3 %	-94.9%	0.948	21.0	15.2	0.7	3.6
203-P-4-FR-2-10-9-7	-35.2 %	13.1 %	-94.9%	0.952	21.4	15.5	0.7	3.6
204-P-4-FR-2-10-9-9	-25.2 %	15.0 %	-93.9%	0.952	21.3	15.7	0.7	3.6
205-P-4-FR-3-2-7-7	-42.5 %	-0.3 %	-94.3%	1.463	50.1	47.0	0.7	6.0
206-P-4-FR-3-2-7-9	-38.8 %	-1.7 %	-94.0%	1.463	49.7	47.0	0.7	6.1
207-P-4-FR-3-2-9-7	-27.8 %	1.4 %	-87.9%	1.456	49.9	46.9	0.7	6.1
208-P-4-FR-3-2-9-9	-40.0 %	10.6 %	-94.9%	1.456	49.6	47.0	0.7	6.2
209-P-4-FR-3-5-7-7	-34.2 %	-2.4 %	-93.7%	1.464	37.1	31.9	0.6	6.1
210-P-4-FR-3-5-7-9	-41.6 %	3.8 %	-94.6%	1.464	37.2	32.2	0.6	6.2
211-P-4-FR-3-5-9-7	-10.6 %	9.2 %	-91.4%	1.457	37.2	32.4	0.7	6.2
212-P-4-FR-3-5-9-9	-32.8 %	14.1 %	-94.2%	1.457	37.4	32.7	0.7	6.3
213-P-4-FR-3-10-7-7	-42.6 %	3.0 %	-95.0%	1.466	26.7	19.8	0.7	5.5

Continued on next page

Table 4.1 Unsorted Results – *Continued from previous page*

Filename	AAR+Shear			AAR Only				
	K	V_{ult}	V_{yld}	Δ_{ver}	σ^{lan}_{max}	σ^{tra}_{max}	σ^{lan}_{med}	σ^{tra}_{med}
		$\frac{(AAR+x)-x}{x} \times 100$		mm		MPa		
214-P-4-FR-3-10-7-9	-37.3 %	6.1 %	-94.4%	1.466	26.8	20.3	0.7	5.6
215-P-4-FR-3-10-9-7	-19.3 %	12.2 %	-92.6%	1.459	27.1	20.2	0.8	5.7
216-P-4-FR-3-10-9-9	-46.9 %	13.7 %	-96.3%	1.459	27.1	20.9	0.8	5.7

Table 4.2. Sorted by Stiffness Decrease

Filename	AAR+Shear			AAR Only				
	K	V_{yld}	V_{ult}	Δ_{ver}	σ^{lan}_{max}	σ^{tra}_{max}	σ^{lan}_{med}	σ^{tra}_{med}
		$\frac{(AAR+x)-x}{x} \times 100$		mm		MPa		
133-TB-4-R-3-2-7-7	-104.3 %	-98.4 %	-100.0%	7.678	74.9	23.9	6.7	0.8
143-B-4-R-3-10-9-7	-100.4 %	-100.0 %	-100.0 %	14.468	13.3	5.5	-0.7	-0.0
134-TB-4-R-3-2-7-9	-100.4 %	-99.2 %	-100.0%	6.770	52.1	28.0	-10.3	0.3
101-TB-2-R-3-5-7-7	-100.3 %	-99.9 %	-100.0%	2.390	11.3	16.0	-1.1	-0.1
108-TB-2-R-3-10-9-9	-100.2 %	-97.9 %	-100.0%	8.963	38.4	20.4	2.2	1.7
105-P-2-R-3-10-7-7	-100.1 %	-97.5 %	-100.0%	2.865	12.0	8.5	1.5	0.1
3-P-2-U-1-2-9-7	-100.1 %	-100.0 %	-100.0%	1.056	10.6	47.3	-1.8	3.3
132-P-4-R-2-10-9-9	-100.1 %	-99.3 %	-100.0%	-1.333	15.2	6.6	-0.7	0.0
135-P-4-R-3-2-9-7	-100.1 %	-100.0 %	-100.0%	5.299	38.5	22.9	1.2	-0.2
109-TB-4-R-1-2-7-7	-100.1 %	-100.0 %	-100.0%	-2.950	27.2	13.8	-0.5	-0.2
91-P-2-R-2-5-9-7	-100.0 %	-99.8 %	-100.0%	3.999	12.4	7.0	-1.3	-0.0
139-TB-4-R-3-5-9-7	-100.0 %	-100.0 %	-100.0%	2.400	16.1	11.1	-0.1	-0.0
91-B-2-R-2-5-9-7	-100.0 %	-100.0 %	-100.0 %	32.272	37.5	14.9	-0.4	-0.0
87-B-2-R-2-2-9-7	-100.0 %	-100.0 %	-100.0 %	26.360	45.7	36.4	-0.1	-0.1
4-P-2-U-1-2-9-9	-100.0 %	-100.0 %	-100.0 %	69.105	75.7	127.1	2.7	-0.1
97-TB-2-R-3-2-7-7	-100.0 %	-100.0 %	-100.0 %	11977.024	198.8	184.6	-0.6	6.3
106-P-2-R-3-10-7-9	-100.0 %	-100.0 %	-100.0 %	909.898	6.1	173.3	-14.0	-0.0
101-P-2-R-3-5-7-7	-100.0 %	-100.0 %	-100.0 %	449.364	43.4	81.5	-24.0	15.4
111-TB-4-R-1-2-9-7	-100.0 %	-100.0 %	-100.0 %	194.046	4.7	26.3	-0.4	0.0
143-P-4-R-3-10-9-7	-100.0 %	-100.0 %	-100.0 %	192.624	76.7	46.3	0.0	0.0
98-TB-2-R-3-2-7-9	-100.0 %	-100.0 %	-100.0 %	845.807	117.2	104.4	-0.5	0.1
144-B-4-R-3-10-9-9	-100.0 %	-100.0 %	-100.0 %	484.094	18.7	121.1	-0.2	-0.0
106-TB-2-R-3-10-7-9	-100.0 %	-100.0 %	-100.0 %	7777.896	6.0	57.2	-0.2	-0.0
105-TB-2-R-3-10-7-7	-100.0 %	-100.0 %	-100.0 %	962.240	1.5	13.1	-0.0	0.0
103-B-2-R-3-5-9-7	-100.0 %	-99.9 %	-100.0 %	44.691	18.4	11.3	-0.7	-0.1
89-B-2-R-2-5-7-7	-100.0 %	-99.8 %	-100.0%	1.392	22.1	12.0	-1.8	-0.0
108-B-2-R-3-10-9-9	-100.0 %	-99.8 %	-100.0%	2.039	21.3	6.0	-1.0	-0.1
97-P-2-R-3-2-7-7	-99.9 %	-97.4 %	-100.0%	5.077	30.3	25.8	-5.2	0.0
127-TB-4-R-2-5-9-7	-99.9 %	-100.0 %	-100.0 %	13.595	4.4	0.8	0.0	0.0
128-P-4-R-2-5-9-9	-99.9 %	-99.9 %	-100.0%	-1.164	51.7	59.2	-1.3	-0.1
78-TB-2-R-1-5-7-9	-99.9 %	-99.2 %	-100.0%	0.952	8.0	21.7	1.0	-0.2
102-P-2-R-3-5-7-9	-99.9 %	-98.9 %	-99.9%	2.807	18.4	28.2	2.1	0.3
123-TB-4-R-2-2-9-7	-99.9 %	-100.0 %	-99.9 %	28.224	10.7	8.2	0.1	0.1
99-B-2-R-3-2-9-7	-99.9 %	-94.9 %	-100.0 %	18.180	97.3	46.8	-9.5	0.0
132-TB-4-R-2-10-9-9	-99.8 %	-100.0 %	-100.0 %	39.806	19.0	1.5	-0.0	-0.0
93-TB-2-R-2-10-7-7	-99.8 %	-98.6 %	-99.9%	2.451	19.8	28.2	1.4	0.9
103-P-2-R-3-5-9-7	-99.8 %	-97.1 %	-99.9%	2.451	17.9	21.3	2.0	0.2
139-P-4-R-3-5-9-7	-99.7 %	-97.9 %	-100.0%	9.095	28.5	15.8	8.8	0.2

Continued on next page

Table 4.2 Sorted by Stiffness Decrease – *Continued from previous page*

Filename	AAR+Shear			AAR Only				
	K	V_{ult}	V_{yld}	Δ_{ver}	σ^{lan}_{max}	σ^{tra}_{max}	σ^{lan}_{med}	σ^{tra}_{med}
		$\frac{(AAR+x)-x}{x} \times 100$		mm	MPa			
141-P-4-R-3-10-7-7	-99.7 %	-97.0 %	-100.0%	7.606	38.1	11.1	-2.4	-0.0
110-TB-4-R-1-2-7-9	-99.7 %	-99.9 %	-99.9%	-3.303	5.5	9.1	-0.7	-0.1
102-TB-2-R-3-5-7-9	-99.7 %	-99.0 %	-99.0%	7.393	56.0	36.8	10.3	1.9
102-B-2-R-3-5-7-9	-99.7 %	-90.6 %	-100.0 %	12.304	31.9	17.9	-3.2	0.0
98-P-2-R-3-2-7-9	-99.6 %	-98.9 %	-99.9%	1.768	89.8	30.4	-0.7	0.2
143-TB-4-R-3-10-9-7	-99.6 %	-99.9 %	-99.9%	5.547	12.1	1.4	-0.9	-0.0
133-P-4-R-3-2-7-7	-99.6 %	-99.6 %	-100.0%	6.311	67.8	46.9	-7.6	0.0
96-TB-2-R-2-10-9-9	-99.6 %	-99.6 %	-100.0%	0.689	10.7	1.8	0.1	0.0
131-TB-4-R-2-10-9-7	-99.5 %	-100.0 %	-99.9%	9.040	13.4	3.9	-0.1	-0.0
104-B-2-R-3-5-9-9	-99.5 %	-91.5 %	-99.9%	1.168	17.3	2.5	3.5	0.0
140-P-4-R-3-5-9-9	-99.5 %	-95.5 %	-99.5%	2.762	17.4	22.0	0.2	0.0
142-TB-4-R-3-10-7-9	-99.3 %	-98.4 %	-100.0%	2.371	8.9	2.4	0.7	0.0
134-P-4-R-3-2-7-9	-99.2 %	-99.1 %	-99.8%	4.324	91.4	24.9	17.8	-0.1
136-TB-4-R-3-2-9-9	-99.2 %	-99.8 %	-99.8%	4.826	54.5	39.8	3.2	0.2
101-B-2-R-3-5-7-7	-99.1 %	-88.3 %	-99.9%	4.075	100.2	36.5	-11.3	0.6
100-B-2-R-3-2-9-9	-99.0 %	-96.1 %	-100.0 %	12.123	67.0	81.5	-0.0	0.1
136-B-4-R-3-2-9-9	-98.8 %	-99.7 %	-99.4%	2.502	62.5	29.6	-0.5	-0.1
139-B-4-R-3-5-9-7	-98.8 %	-99.6 %	-99.5%	2.027	105.5	31.4	18.8	0.1
140-B-4-R-3-5-9-9	-98.8 %	-97.4 %	-99.7%	2.991	17.4	5.0	1.4	-0.0
121-TB-4-R-2-2-7-7	-98.7 %	-99.3 %	-100.0%	3.100	93.6	22.2	2.4	-0.5
104-TB-2-R-3-5-9-9	-98.5 %	-95.5 %	-100.0%	3.999	34.4	50.9	0.2	0.9
89-P-2-R-2-5-7-7	-98.4 %	-80.5 %	-99.0%	2.984	25.2	3.8	1.6	0.1
100-TB-2-R-3-2-9-9	-98.4 %	-98.4 %	-99.9%	1.122	45.0	43.7	-0.8	0.4
138-B-4-R-3-5-7-9	-97.7 %	-94.8 %	-99.1%	6.072	19.9	12.0	4.0	0.0
135-B-4-R-3-2-9-7	-97.5 %	-99.7 %	-98.8%	2.773	180.2	55.9	5.9	0.4
138-P-4-R-3-5-7-9	-97.5 %	-77.6 %	-96.9%	4.376	15.4	3.1	2.4	0.0
133-B-4-R-3-2-7-7	-97.0 %	-98.1 %	-100.0 %	13.490	43.3	21.4	14.0	-0.1
134-B-4-R-3-2-7-9	-95.7 %	-98.3 %	-98.1 %	17.384	71.0	19.7	17.0	0.0
⋮	⋮	⋮	⋮	⋮	⋮	⋮	⋮	
26-P-2-U-3-2-7-9	40.2 %	-25.6 %	-38.1%	0.847	1.1	239.2	-0.0	226.0
116-P-4-R-1-5-9-9	40.3 %	-6.3 %	-6.3%	0.760	0.1	0.0	0.0	0.0
85-P-2-R-2-2-7-7	40.3 %	-49.4 %	-34.3%	0.847	0.1	0.0	0.0	0.0
95-P-2-R-2-10-9-7	40.7 %	29.4 %	35.8%	0.855	0.1	0.0	0.0	0.0
115-P-4-R-1-5-9-7	40.8 %	-27.2 %	-27.2%	0.760	0.1	0.0	0.0	0.0
120-P-4-R-1-10-9-9	40.9 %	40.9 %	40.9%	0.760	0.1	0.0	0.0	0.0
32-P-2-U-3-5-9-9	41.3 %	18.7 %	14.1%	0.898	2.2	209.5	0.0	180.8
107-P-2-R-3-10-9-7	41.4 %	30.1 %	36.5%	1.352	0.2	0.0	0.0	0.0
79-P-2-R-1-5-9-7	41.5 %	11.8 %	11.8%	0.381	0.0	0.0	0.0	0.0
96-P-2-R-2-10-9-9	41.8 %	30.5 %	36.9%	0.855	0.1	0.0	0.0	0.0
13-P-2-U-2-2-7-7	42.2 %	-28.3 %	-57.3%	0.547	0.5	160.7	-0.0	153.2
14-P-2-U-2-2-7-9	42.2 %	-31.3 %	-55.2%	0.547	0.5	160.7	-0.0	153.2
108-P-2-R-3-10-9-9	42.5 %	31.2 %	37.6%	1.352	0.2	0.0	0.0	0.0
80-P-2-R-1-5-9-9	42.9 %	12.4 %	12.4%	0.381	0.0	0.0	0.0	0.0
27-P-2-U-3-2-9-7	42.9 %	-18.1 %	-73.3%	0.849	1.2	240.6	-0.0	228.0
111-P-4-R-1-2-9-7	43.7 %	-47.8 %	-77.2%	0.761	0.1	0.0	0.0	0.0
77-B-2-R-1-5-7-7	44.3 %	-19.7 %	-19.7%	0.376	0.0	0.0	0.0	0.0
78-B-2-R-1-5-7-9	44.6 %	-4.6 %	-4.6%	0.376	0.0	0.0	0.0	0.0
90-B-2-R-2-5-7-9	44.6 %	16.3 %	16.3%	0.846	0.1	0.0	0.0	0.0
112-P-4-R-1-2-9-9	45.5 %	-37.3 %	-76.9%	0.761	0.1	0.0	0.0	0.0
131-P-4-R-2-10-9-7	46.8 %	121.9 %	46.8%	1.705	0.4	0.1	0.0	0.0
144-P-4-R-3-10-9-9	48.5 %	48.5 %	48.5%	2.695	0.6	0.1	0.0	0.0

Continued on next page

Table 4.2 Sorted by Stiffness Decrease – *Continued from previous page*

Filename	AAR+Shear K	V_{ult}	V_{yld}	AAR Only Δ_{ver}	σ^{lan}_{max}	σ^{tra}_{max}	σ^{lan}_{med}	σ^{tra}_{med}
		$\frac{(AAR+x)-x}{x} \times 100$		mm	MPa			
127-P-4-R-2-5-9-7	48.8 %	-23.1 %	-23.1%	1.705	0.5	0.1	0.1	0.0
92-P-2-R-2-5-9-9	51.6 %	5.8 %	5.8%	0.855	0.1	0.0	0.0	0.0
75-P-2-R-1-2-9-7	52.3 %	-31.7 %	-69.5%	0.381	0.0	0.0	0.0	0.0
104-P-2-R-3-5-9-9	52.8 %	6.9 %	6.9%	1.353	0.1	0.0	0.0	0.0
83-B-2-R-1-10-9-7	53.4 %	49.3 %	49.3%	0.381	0.1	0.0	0.0	0.0
95-B-2-R-2-10-9-7	53.7 %	55.1 %	55.1%	0.853	0.2	0.1	0.0	0.0
76-P-2-R-1-2-9-9	54.2 %	-12.3 %	-69.5%	0.381	0.0	0.0	0.0	0.0
84-B-2-R-1-10-9-9	54.6 %	51.2 %	51.2%	0.381	0.1	0.0	0.0	0.0
107-B-2-R-3-10-9-7	55.7 %	57.0 %	57.0%	1.351	0.4	0.1	0.0	0.0
96-B-2-R-2-10-9-9	56.0 %	98.4 %	98.4%	0.853	0.2	0.1	0.0	-0.0
15-P-2-U-2-2-9-7	56.1 %	-21.0 %	-73.3%	0.548	0.5	161.8	-0.0	154.6
124-P-4-R-2-2-9-9	57.2 %	-33.4 %	-33.4%	1.704	0.5	0.2	0.1	0.0
123-P-4-R-2-2-9-7	57.5 %	-42.7 %	-42.7%	1.704	0.4	0.2	0.1	0.0
136-P-4-R-3-2-9-9	61.1 %	-31.9 %	-31.9%	2.694	1.2	0.3	0.1	0.0
28-P-2-U-3-2-9-9	62.5 %	-18.0 %	-25.9%	0.849	1.2	240.6	-0.0	228.0
87-P-2-R-2-2-9-7	64.7 %	-27.5 %	-13.9%	0.855	0.2	0.0	0.0	0.0
99-P-2-R-3-2-9-7	67.0 %	-41.1 %	-23.4%	1.352	0.3	0.0	0.0	0.0
88-P-2-R-2-2-9-9	67.9 %	-19.6 %	-9.3%	0.855	0.1	0.0	0.0	0.0
100-P-2-R-3-2-9-9	68.2 %	-18.6 %	-8.6%	1.353	0.3	0.0	0.0	0.0
98-B-2-R-3-2-7-9	73.3 %	-15.4 %	-22.5%	1.344	0.4	0.1	0.0	0.0
97-B-2-R-3-2-7-7	73.3 %	-25.2 %	-36.1%	1.344	0.4	0.1	0.0	0.0
73-B-2-R-1-2-7-7	74.3 %	-31.3 %	-43.5%	0.376	0.0	0.0	0.0	0.0
79-B-2-R-1-5-9-7	75.4 %	-20.4 %	-25.3%	0.381	0.1	0.0	0.0	0.0
86-B-2-R-2-2-7-9	76.7 %	-17.9 %	-30.4%	0.847	0.2	0.0	0.0	0.0
85-B-2-R-2-2-7-7	76.7 %	-23.7 %	-37.1%	0.847	0.2	0.0	0.0	0.0
74-B-2-R-1-2-7-9	76.8 %	-18.1 %	-42.9%	0.376	0.0	0.0	0.0	0.0
80-B-2-R-1-5-9-9	77.0 %	-6.8 %	-6.8%	0.381	0.1	0.0	0.0	0.0
92-B-2-R-2-5-9-9	78.6 %	-1.0 %	-1.0%	0.854	0.3	0.1	0.0	0.0
16-P-2-U-2-2-9-9	82.0 %	-22.8 %	-46.5%	0.548	0.5	161.8	-0.0	154.6
75-B-2-R-1-2-9-7	115.9 %	-32.0 %	-42.7%	0.381	0.1	0.0	0.0	0.0
76-B-2-R-1-2-9-9	118.3 %	-19.7 %	-42.5%	0.381	0.1	0.0	0.0	0.0
88-B-2-R-2-2-9-9	123.0 %	-20.2 %	-29.3%	0.853	0.3	0.1	0.1	0.0
72-B-4-U-3-10-9-9	166.7 %	-40.9 %	-87.6%	1.482	153.7	152.6	141.8	107.4
71-B-4-U-3-10-9-7	167.9 %	-27.8 %	-80.7%	1.489	153.2	152.0	141.8	106.4
70-B-4-U-3-10-7-9	295.6 %	-30.4 %	-75.7%	1.490	151.6	150.9	136.1	103.2

Table 4.3. Sorted by Ultimate Shear Stress Decrease

Filename	AAR+Shear K	V_{ult}	V_{yld}	AAR Only Δ_{ver}	σ^{lan}_{max}	σ^{tra}_{max}	σ^{lan}_{med}	σ^{tra}_{med}
		$\frac{(AAR+x)-x}{x} \times 100$		mm	MPa			
3-P-2-U-1-2-9-7	-100.1 %	-100.0 %	-100.0%	1.056	10.6	47.3	-1.8	3.3
97-TB-2-R-3-2-7-7	-100.0 %	-100.0 %	-100.0 %	11977.024	198.8	184.6	-0.6	6.3
111-TB-4-R-1-2-9-7	-100.0 %	-100.0 %	-100.0 %	194.046	4.7	26.3	-0.4	0.0
98-TB-2-R-3-2-7-9	-100.0 %	-100.0 %	-100.0 %	845.807	117.2	104.4	-0.5	0.1
101-P-2-R-3-5-7-7	-100.0 %	-100.0 %	-100.0 %	449.364	43.4	81.5	-24.0	15.4
106-P-2-R-3-10-7-9	-100.0 %	-100.0 %	-100.0 %	909.898	6.1	173.3	-14.0	-0.0

Continued on next page

Table 4.3 Sorted by Shear Strength Decrease – *Continued from previous page*

Filename	AAR+Shear			AAR Only				
	K	V_{ult}	V_{yld}	Δ_{ver}	σ^{lan}_{max}	σ^{tra}_{max}	σ^{lan}_{med}	σ^{tra}_{med}
	$\frac{(AAR+x)-x}{x} \times 100$			mm	MPa			
106-TB-2-R-3-10-7-9	-100.0 %	-100.0 %	-100.0 %	7777.896	6.0	57.2	-0.2	-0.0
4-P-2-U-1-2-9-9	-100.0 %	-100.0 %	-100.0 %	69.105	75.7	127.1	2.7	-0.1
105-TB-2-R-3-10-7-7	-100.0 %	-100.0 %	-100.0 %	962.240	1.5	13.1	-0.0	0.0
143-P-4-R-3-10-9-7	-100.0 %	-100.0 %	-100.0 %	192.624	76.7	46.3	0.0	0.0
144-B-4-R-3-10-9-9	-100.0 %	-100.0 %	-100.0 %	484.094	18.7	121.1	-0.2	-0.0
87-B-2-R-2-2-9-7	-100.0 %	-100.0 %	-100.0 %	26.360	45.7	36.4	-0.1	-0.1
91-B-2-R-2-5-9-7	-100.0 %	-100.0 %	-100.0 %	32.272	37.5	14.9	-0.4	-0.0
127-TB-4-R-2-5-9-7	-99.9 %	-100.0 %	-100.0 %	13.595	4.4	0.8	0.0	0.0
143-B-4-R-3-10-9-7	-100.4 %	-100.0 %	-100.0 %	14.468	13.3	5.5	-0.7	-0.0
139-TB-4-R-3-5-9-7	-100.0 %	-100.0 %	-100.0%	2.400	16.1	11.1	-0.1	-0.0
123-TB-4-R-2-2-9-7	-99.9 %	-100.0 %	-99.9 %	28.224	10.7	8.2	0.1	0.1
109-TB-4-R-1-2-7-7	-100.1 %	-100.0 %	-100.0%	-2.950	27.2	13.8	-0.5	-0.2
132-TB-4-R-2-10-9-9	-99.8 %	-100.0 %	-100.0 %	39.806	19.0	1.5	-0.0	-0.0
131-TB-4-R-2-10-9-7	-99.5 %	-100.0 %	-99.9%	9.040	13.4	3.9	-0.1	-0.0
135-P-4-R-3-2-9-7	-100.1 %	-100.0 %	-100.0%	5.299	38.5	22.9	1.2	-0.2
101-TB-2-R-3-5-7-7	-100.3 %	-99.9 %	-100.0%	2.390	11.3	16.0	-1.1	-0.1
110-TB-4-R-1-2-7-9	-99.7 %	-99.9 %	-99.9%	-3.303	5.5	9.1	-0.7	-0.1
128-P-4-R-2-5-9-9	-99.9 %	-99.9 %	-100.0%	-1.164	51.7	59.2	-1.3	-0.1
143-TB-4-R-3-10-9-7	-99.6 %	-99.9 %	-99.9%	5.547	12.1	1.4	-0.9	-0.0
103-B-2-R-3-5-9-7	-100.0 %	-99.9 %	-100.0 %	44.691	18.4	11.3	-0.7	-0.1
136-TB-4-R-3-2-9-9	-99.2 %	-99.8 %	-99.8%	4.826	54.5	39.8	3.2	0.2
91-P-2-R-2-5-9-7	-100.0 %	-99.8 %	-100.0%	3.999	12.4	7.0	-1.3	-0.0
108-B-2-R-3-10-9-9	-100.0 %	-99.8 %	-100.0%	2.039	21.3	6.0	-1.0	-0.1
89-B-2-R-2-5-7-7	-100.0 %	-99.8 %	-100.0%	1.392	22.1	12.0	-1.8	-0.0
135-B-4-R-3-2-9-7	-97.5 %	-99.7 %	-98.8%	2.773	180.2	55.9	5.9	0.4
136-B-4-R-3-2-9-9	-98.8 %	-99.7 %	-99.4%	2.502	62.5	29.6	-0.5	-0.1
96-TB-2-R-2-10-9-9	-99.6 %	-99.6 %	-100.0%	0.689	10.7	1.8	0.1	0.0
139-B-4-R-3-5-9-7	-98.8 %	-99.6 %	-99.5%	2.027	105.5	31.4	18.8	0.1
133-P-4-R-3-2-7-7	-99.6 %	-99.6 %	-100.0%	6.311	67.8	46.9	-7.6	0.0
121-TB-4-R-2-2-7-7	-98.7 %	-99.3 %	-100.0%	3.100	93.6	22.2	2.4	-0.5
132-P-4-R-2-10-9-9	-100.1 %	-99.3 %	-100.0%	-1.333	15.2	6.6	-0.7	0.0
78-TB-2-R-1-5-7-9	-99.9 %	-99.2 %	-100.0%	0.952	8.0	21.7	1.0	-0.2
134-TB-4-R-3-2-7-9	-100.4 %	-99.2 %	-100.0%	6.770	52.1	28.0	-10.3	0.3
134-P-4-R-3-2-7-9	-99.2 %	-99.1 %	-99.8%	4.324	91.4	24.9	17.8	-0.1
102-TB-2-R-3-5-7-9	-99.7 %	-99.0 %	-99.0%	7.393	56.0	36.8	10.3	1.9
102-P-2-R-3-5-7-9	-99.9 %	-98.9 %	-99.9%	2.807	18.4	28.2	2.1	0.3
98-P-2-R-3-2-7-9	-99.6 %	-98.9 %	-99.9%	1.768	89.8	30.4	-0.7	0.2
93-TB-2-R-2-10-7-7	-99.8 %	-98.6 %	-99.9%	2.451	19.8	28.2	1.4	0.9
142-TB-4-R-3-10-7-9	-99.3 %	-98.4 %	-100.0%	2.371	8.9	2.4	0.7	0.0
100-TB-2-R-3-2-9-9	-98.4 %	-98.4 %	-99.9%	1.122	45.0	43.7	-0.8	0.4
133-TB-4-R-3-2-7-7	-104.3 %	-98.4 %	-100.0%	7.678	74.9	23.9	6.7	0.8
134-B-4-R-3-2-7-9	-95.7 %	-98.3 %	-98.1 %	17.384	71.0	19.7	17.0	0.0
133-B-4-R-3-2-7-7	-97.0 %	-98.1 %	-100.0 %	13.490	43.3	21.4	14.0	-0.1
139-P-4-R-3-5-9-7	-99.7 %	-97.9 %	-100.0%	9.095	28.5	15.8	8.8	0.2
108-TB-2-R-3-10-9-9	-100.2 %	-97.9 %	-100.0%	8.963	38.4	20.4	2.2	1.7
105-P-2-R-3-10-7-7	-100.1 %	-97.5 %	-100.0%	2.865	12.0	8.5	1.5	0.1
140-B-4-R-3-5-9-9	-98.8 %	-97.4 %	-99.7%	2.991	17.4	5.0	1.4	-0.0
97-P-2-R-3-2-7-7	-99.9 %	-97.4 %	-100.0%	5.077	30.3	25.8	-5.2	0.0
103-P-2-R-3-5-9-7	-99.8 %	-97.1 %	-99.9%	2.451	17.9	21.3	2.0	0.2
141-P-4-R-3-10-7-7	-99.7 %	-97.0 %	-100.0%	7.606	38.1	11.1	-2.4	-0.0
100-B-2-R-3-2-9-9	-99.0 %	-96.1 %	-100.0 %	12.123	67.0	81.5	-0.0	0.1

Continued on next page

Table 4.3 Sorted by Shear Strength Decrease – *Continued from previous page*

Filename	AAR+Shear			AAR Only				
	K	V_{ult}	V_{yld}	Δ_{ver}	σ^{lan}_{max}	σ^{tra}_{max}	σ^{lan}_{med}	σ^{tra}_{med}
		$\frac{(AAR+x)-x}{x} \times 100$		mm	MPa			
104-TB-2-R-3-5-9-9	-98.5 %	-95.5 %	-100.0%	3.999	34.4	50.9	0.2	0.9
140-P-4-R-3-5-9-9	-99.5 %	-95.5 %	-99.5%	2.762	17.4	22.0	0.2	0.0
99-B-2-R-3-2-9-7	-99.9 %	-94.9 %	-100.0 %	18.180	97.3	46.8	-9.5	0.0
138-B-4-R-3-5-7-9	-97.7 %	-94.8 %	-99.1%	6.072	19.9	12.0	4.0	0.0
104-B-2-R-3-5-9-9	-99.5 %	-91.5 %	-99.9%	1.168	17.3	2.5	3.5	0.0
102-B-2-R-3-5-7-9	-99.7 %	-90.6 %	-100.0 %	12.304	31.9	17.9	-3.2	0.0
101-B-2-R-3-5-7-7	-99.1 %	-88.3 %	-99.9%	4.075	100.2	36.5	-11.3	0.6
89-P-2-R-2-5-7-7	-98.4 %	-80.5 %	-99.0%	2.984	25.2	3.8	1.6	0.1
⋮	⋮	⋮	⋮	⋮	⋮	⋮	⋮	
114-TB-4-R-1-5-7-9	-27.2 %	40.3 %	375.9%	0.751	0.1	0.1	0.0	0.0
120-P-4-R-1-10-9-9	40.9 %	40.9 %	40.9%	0.760	0.1	0.0	0.0	0.0
138-TB-4-R-3-5-7-9	-27.2 %	41.0 %	477.4%	2.679	0.4	0.4	0.1	0.0
135-TB-4-R-3-2-9-7	-12.1 %	41.1 %	488.7%	2.691	1.0	0.7	0.1	0.1
128-TB-4-R-2-5-9-9	-9.0 %	41.2 %	457.4%	1.706	0.4	0.2	0.1	0.0
120-B-4-R-1-10-9-9	-8.1 %	41.2 %	296.2%	0.759	0.2	0.1	0.1	0.0
114-B-4-R-1-5-7-9	-26.6 %	41.6 %	464.7%	0.751	0.2	0.1	0.1	0.0
126-TB-4-R-2-5-7-9	-27.2 %	42.1 %	460.4%	1.692	0.2	0.1	0.1	0.0
83-P-2-R-1-10-9-7	-10.9 %	43.5 %	-31.1%	0.381	0.0	0.0	0.0	0.0
116-B-4-R-1-5-9-9	-8.8 %	43.6 %	459.5%	0.759	0.3	0.1	0.1	0.0
144-TB-4-R-3-10-9-9	-8.4 %	43.8 %	317.0%	2.686	0.6	0.6	0.1	0.0
34-P-2-U-3-10-7-9	-10.5 %	44.2 %	-44.3%	0.946	5.3	165.0	-0.1	120.1
90-P-2-R-2-5-7-9	26.2 %	45.1 %	45.1%	0.847	0.0	0.0	0.0	0.0
126-B-4-R-2-5-7-9	-26.6 %	45.6 %	573.8%	1.685	0.9	0.5	0.1	-0.0
105-B-2-R-3-10-7-7	27.6 %	48.1 %	34.9%	1.344	0.2	0.1	0.0	-0.0
33-P-2-U-3-10-7-7	-12.4 %	48.2 %	-44.5%	0.946	4.0	164.7	-0.1	119.8
144-P-4-R-3-10-9-9	48.5 %	48.5 %	48.5%	2.695	0.6	0.1	0.0	0.0
22-P-2-U-2-10-7-9	-0.8 %	49.1 %	54.7%	0.597	1.5	120.5	-0.0	96.4
83-B-2-R-1-10-9-7	53.4 %	49.3 %	49.3%	0.381	0.1	0.0	0.0	0.0
21-P-2-U-2-10-7-7	-2.3 %	51.0 %	53.4%	0.596	1.4	120.5	0.0	96.1
84-B-2-R-1-10-9-9	54.6 %	51.2 %	51.2%	0.381	0.1	0.0	0.0	0.0
95-B-2-R-2-10-9-7	53.7 %	55.1 %	55.1%	0.853	0.2	0.1	0.0	0.0
24-P-2-U-2-10-9-9	-1.5 %	56.3 %	-28.4%	0.600	1.2	122.9	0.0	99.8
81-P-2-R-1-10-7-7	14.8 %	56.7 %	64.4%	0.376	0.0	0.0	0.0	0.0
107-B-2-R-3-10-9-7	55.7 %	57.0 %	57.0%	1.351	0.4	0.1	0.0	0.0
132-B-4-R-2-10-9-9	-8.1 %	57.3 %	341.3%	1.693	1.1	0.6	0.0	0.0
82-P-2-R-1-10-7-9	15.5 %	57.4 %	65.0%	0.376	0.0	0.0	0.0	0.0
94-P-2-R-2-10-7-9	17.0 %	57.5 %	65.2%	0.847	0.0	0.0	0.0	0.0
23-P-2-U-2-10-9-7	-3.2 %	62.9 %	-28.6%	0.599	1.2	122.9	-0.0	99.1
36-P-2-U-3-10-9-9	33.9 %	65.0 %	33.9%	0.949	3.7	168.4	-0.1	125.9
82-B-2-R-1-10-7-9	27.6 %	65.7 %	65.7%	0.376	0.0	0.0	0.0	0.0
122-TB-4-R-2-2-7-9	-31.7 %	69.4 %	468.1%	1.691	0.3	0.1	0.1	0.0
94-B-2-R-2-10-7-9	27.6 %	71.4 %	71.4%	0.847	0.1	0.0	0.0	-0.0
106-B-2-R-3-10-7-9	27.6 %	72.3 %	72.3%	1.344	0.2	0.1	0.0	0.0
112-TB-4-R-1-2-9-9	-12.1 %	77.2 %	385.5%	0.761	0.1	0.1	0.0	0.0
124-TB-4-R-2-2-9-9	-12.1 %	79.5 %	462.8%	1.700	0.4	0.4	0.1	0.0
130-B-4-R-2-10-7-9	-24.6 %	86.1 %	308.0%	1.690	0.6	0.5	0.1	-0.0
96-B-2-R-2-10-9-9	56.0 %	98.4 %	98.4%	0.853	0.2	0.1	0.0	-0.0
131-P-4-R-2-10-9-7	46.8 %	121.9 %	46.8%	1.705	0.4	0.1	0.0	0.0

Table 4.4. Sorted by Yield Shear Stress Decrease

Filename	AAR+Shear			AAR Only				
	K	V_{ult}	V_{yld}	Δ_{ver}	σ^{lan}_{max}	σ^{tra}_{max}	σ^{lan}_{med}	σ^{tra}_{med}
		$\frac{(AAR+x)-x}{x} \times 100$		mm	MPa			
3-P-2-U-1-2-9-7	-100.1 %	-100.0 %	-100.0%	1.056	10.6	47.3	-1.8	3.3
87-B-2-R-2-2-9-7	-100.0 %	-100.0 %	-100.0 %	26.360	45.7	36.4	-0.1	-0.1
91-B-2-R-2-5-9-7	-100.0 %	-100.0 %	-100.0 %	32.272	37.5	14.9	-0.4	-0.0
143-B-4-R-3-10-9-7	-100.4 %	-100.0 %	-100.0 %	14.468	13.3	5.5	-0.7	-0.0
139-TB-4-R-3-5-9-7	-100.0 %	-100.0 %	-100.0%	2.400	16.1	11.1	-0.1	-0.0
109-TB-4-R-1-2-7-7	-100.1 %	-100.0 %	-100.0%	-2.950	27.2	13.8	-0.5	-0.2
135-P-4-R-3-2-9-7	-100.1 %	-100.0 %	-100.0%	5.299	38.5	22.9	1.2	-0.2
101-TB-2-R-3-5-7-7	-100.3 %	-99.9 %	-100.0%	2.390	11.3	16.0	-1.1	-0.1
128-P-4-R-2-5-9-9	-99.9 %	-99.9 %	-100.0%	-1.164	51.7	59.2	-1.3	-0.1
103-B-2-R-3-5-9-7	-100.0 %	-99.9 %	-100.0 %	44.691	18.4	11.3	-0.7	-0.1
91-P-2-R-2-5-9-7	-100.0 %	-99.8 %	-100.0%	3.999	12.4	7.0	-1.3	-0.0
89-B-2-R-2-5-7-7	-100.0 %	-99.8 %	-100.0%	1.392	22.1	12.0	-1.8	-0.0
121-TB-4-R-2-2-7-7	-98.7 %	-99.3 %	-100.0%	3.100	93.6	22.2	2.4	-0.5
132-P-4-R-2-10-9-9	-100.1 %	-99.3 %	-100.0%	-1.333	15.2	6.6	-0.7	0.0
134-TB-4-R-3-2-7-9	-100.4 %	-99.2 %	-100.0%	6.770	52.1	28.0	-10.3	0.3
142-TB-4-R-3-10-7-9	-99.3 %	-98.4 %	-100.0%	2.371	8.9	2.4	0.7	0.0
133-TB-4-R-3-2-7-7	-104.3 %	-98.4 %	-100.0%	7.678	74.9	23.9	6.7	0.8
133-B-4-R-3-2-7-7	-97.0 %	-98.1 %	-100.0 %	13.490	43.3	21.4	14.0	-0.1
139-P-4-R-3-5-9-7	-99.7 %	-97.9 %	-100.0%	9.095	28.5	15.8	8.8	0.2
108-TB-2-R-3-10-9-9	-100.2 %	-97.9 %	-100.0%	8.963	38.4	20.4	2.2	1.7
105-P-2-R-3-10-7-7	-100.1 %	-97.5 %	-100.0%	2.865	12.0	8.5	1.5	0.1
97-P-2-R-3-2-7-7	-99.9 %	-97.4 %	-100.0%	5.077	30.3	25.8	-5.2	0.0
104-TB-2-R-3-5-9-9	-98.5 %	-95.5 %	-100.0%	3.999	34.4	50.9	0.2	0.9
99-B-2-R-3-2-9-7	-99.9 %	-94.9 %	-100.0 %	18.180	97.3	46.8	-9.5	0.0
4-P-2-U-1-2-9-9	-100.0 %	-100.0 %	-100.0 %	69.105	75.7	127.1	2.7	-0.1
97-TB-2-R-3-2-7-7	-100.0 %	-100.0 %	-100.0 %	11977.024	198.8	184.6	-0.6	6.3
106-P-2-R-3-10-7-9	-100.0 %	-100.0 %	-100.0 %	909.898	6.1	173.3	-14.0	-0.0
101-P-2-R-3-5-7-7	-100.0 %	-100.0 %	-100.0 %	449.364	43.4	81.5	-24.0	15.4
111-TB-4-R-1-2-9-7	-100.0 %	-100.0 %	-100.0 %	194.046	4.7	26.3	-0.4	0.0
144-B-4-R-3-10-9-9	-100.0 %	-100.0 %	-100.0 %	484.094	18.7	121.1	-0.2	-0.0
106-TB-2-R-3-10-7-9	-100.0 %	-100.0 %	-100.0 %	7777.896	6.0	57.2	-0.2	-0.0
98-TB-2-R-3-2-7-9	-100.0 %	-100.0 %	-100.0 %	845.807	117.2	104.4	-0.5	0.1
143-P-4-R-3-10-9-7	-100.0 %	-100.0 %	-100.0 %	192.624	76.7	46.3	0.0	0.0
105-TB-2-R-3-10-7-7	-100.0 %	-100.0 %	-100.0 %	962.240	1.5	13.1	-0.0	0.0
102-B-2-R-3-5-7-9	-99.7 %	-90.6 %	-100.0 %	12.304	31.9	17.9	-3.2	0.0
78-TB-2-R-1-5-7-9	-99.9 %	-99.2 %	-100.0%	0.952	8.0	21.7	1.0	-0.2
141-P-4-R-3-10-7-7	-99.7 %	-97.0 %	-100.0%	7.606	38.1	11.1	-2.4	-0.0
108-B-2-R-3-10-9-9	-100.0 %	-99.8 %	-100.0%	2.039	21.3	6.0	-1.0	-0.1
127-TB-4-R-2-5-9-7	-99.9 %	-100.0 %	-100.0 %	13.595	4.4	0.8	0.0	0.0
96-TB-2-R-2-10-9-9	-99.6 %	-99.6 %	-100.0%	0.689	10.7	1.8	0.1	0.0
132-TB-4-R-2-10-9-9	-99.8 %	-100.0 %	-100.0 %	39.806	19.0	1.5	-0.0	-0.0
133-P-4-R-3-2-7-7	-99.6 %	-99.6 %	-100.0%	6.311	67.8	46.9	-7.6	0.0
100-B-2-R-3-2-9-9	-99.0 %	-96.1 %	-100.0 %	12.123	67.0	81.5	-0.0	0.1
123-TB-4-R-2-2-9-7	-99.9 %	-100.0 %	-99.9 %	28.224	10.7	8.2	0.1	0.1
101-B-2-R-3-5-7-7	-99.1 %	-88.3 %	-99.9%	4.075	100.2	36.5	-11.3	0.6
110-TB-4-R-1-2-7-9	-99.7 %	-99.9 %	-99.9%	-3.303	5.5	9.1	-0.7	-0.1
143-TB-4-R-3-10-9-7	-99.6 %	-99.9 %	-99.9%	5.547	12.1	1.4	-0.9	-0.0
103-P-2-R-3-5-9-7	-99.8 %	-97.1 %	-99.9%	2.451	17.9	21.3	2.0	0.2
100-TB-2-R-3-2-9-9	-98.4 %	-98.4 %	-99.9%	1.122	45.0	43.7	-0.8	0.4
98-P-2-R-3-2-7-9	-99.6 %	-98.9 %	-99.9%	1.768	89.8	30.4	-0.7	0.2

Continued on next page

Table 4.4 Sorted by Shear Strength Decrease – *Continued from previous page*

Filename	AAR+Shear			AAR Only				
	K	V_{ult}	V_{yld}	Δ_{ver}	σ^{lan}_{max}	σ^{tra}_{max}	σ^{lan}_{med}	σ^{tra}_{med}
		$\frac{(AAR+x)-x}{x}\times 100$		mm	MPa			
102-P-2-R-3-5-7-9	-99.9 %	-98.9 %	-99.9%	2.807	18.4	28.2	2.1	0.3
131-TB-4-R-2-10-9-7	-99.5 %	-100.0 %	-99.9%	9.040	13.4	3.9	-0.1	-0.0
93-TB-2-R-2-10-7-7	-99.8 %	-98.6 %	-99.9%	2.451	19.8	28.2	1.4	0.9
104-B-2-R-3-5-9-9	-99.5 %	-91.5 %	-99.9%	1.168	17.3	2.5	3.5	0.0
134-P-4-R-3-2-7-9	-99.2 %	-99.1 %	-99.8%	4.324	91.4	24.9	17.8	-0.1
136-TB-4-R-3-2-9-9	-99.2 %	-99.8 %	-99.8%	4.826	54.5	39.8	3.2	0.2
140-B-4-R-3-5-9-9	-98.8 %	-97.4 %	-99.7%	2.991	17.4	5.0	1.4	-0.0
139-B-4-R-3-5-9-7	-98.8 %	-99.6 %	-99.5%	2.027	105.5	31.4	18.8	0.1
140-P-4-R-3-5-9-9	-99.5 %	-95.5 %	-99.5%	2.762	17.4	22.0	0.2	0.0
136-B-4-R-3-2-9-9	-98.8 %	-99.7 %	-99.4%	2.502	62.5	29.6	-0.5	-0.1
138-B-4-R-3-5-7-9	-97.7 %	-94.8 %	-99.1%	6.072	19.9	12.0	4.0	0.0
89-P-2-R-2-5-7-7	-98.4 %	-80.5 %	-99.0%	2.984	25.2	3.8	1.6	0.1
102-TB-2-R-3-5-7-9	-99.7 %	-99.0 %	-99.0%	7.393	56.0	36.8	10.3	1.9
135-B-4-R-3-2-9-7	-97.5 %	-99.7 %	-98.8%	2.773	180.2	55.9	5.9	0.4
134-B-4-R-3-2-7-9	-95.7 %	-98.3 %	-98.1 %	17.384	71.0	19.7	17.0	0.0
194-P-4-FR-2-2-7-9	-32.5 %	-0.7 %	-97.8%	0.945	35.6	31.9	0.4	4.4
199-P-4-FR-2-5-9-7	-15.5 %	8.8 %	-97.5%	0.950	28.5	23.1	0.4	4.0
185-P-4-FR-1-5-7-7	-31.9 %	-5.3 %	-97.1%	0.412	15.1	12.0	0.6	2.3
189-P-4-FR-1-10-7-7	-31.5 %	-1.7 %	-97.1%	0.413	11.9	8.5	0.7	1.9
190-P-4-FR-1-10-7-9	-33.2 %	6.9 %	-97.0%	0.413	11.8	8.5	0.7	1.9
181-P-4-FR-1-2-7-7	-32.2 %	-6.2 %	-96.9%	0.411	17.9	15.8	0.4	2.7
138-P-4-R-3-5-7-9	-97.5 %	-77.6 %	-96.9%	4.376	15.4	3.1	2.4	0.0
186-P-4-FR-1-5-7-9	-30.1 %	3.2 %	-96.9%	0.412	14.9	11.9	0.5	2.3
182-P-4-FR-1-2-7-9	-30.7 %	-0.4 %	-96.7%	0.411	17.8	15.6	0.4	2.7
187-P-4-FR-1-5-9-7	-14.1 %	1.5 %	-96.4%	0.418	15.4	12.4	0.4	2.2
191-P-4-FR-1-10-9-7	-13.6 %	7.3 %	-96.4%	0.419	12.4	8.9	0.6	1.9
201-P-4-FR-2-10-7-7	-51.3 %	3.1 %	-96.3%	0.948	20.9	15.1	0.7	3.6
216-P-4-FR-3-10-9-9	-46.9 %	13.7 %	-96.3%	1.459	27.1	20.9	0.8	5.7
183-P-4-FR-1-2-9-7	-13.6 %	-0.8 %	-96.1%	0.417	18.4	16.1	0.4	2.6
188-P-4-FR-1-5-9-9	-13.0 %	8.2 %	-96.1%	0.418	15.2	12.3	0.4	2.2
192-P-4-FR-1-10-9-9	-12.5 %	13.7 %	-96.1%	0.419	12.2	8.9	0.6	1.9
184-P-4-FR-1-2-9-9	-12.9 %	7.5 %	-95.8%	0.417	18.4	15.9	0.4	2.6
173-P-2-FR-3-5-7-7	-40.1 %	10.3 %	-95.6%	0.732	27.8	19.3	0.4	1.6
69-P-4-U-3-10-7-7	-43.5 %	-29.3 %	-95.6%	1.823	3.4	166.7	-0.0	106.2
173-TB-2-FR-3-5-7-7	-36.4 %	2.5 %	-95.4%	0.733	61.1	17.0	0.1	3.2
173-B-2-FR-3-5-7-7	-40.7 %	-15.1 %	-95.4%	0.729	40.4	8.2	-0.3	-0.0
177-TB-2-FR-3-10-7-7	-34.1 %	18.7 %	-95.4%	0.733	46.1	12.0	0.1	3.1
213-P-4-FR-3-10-7-7	-42.6 %	3.0 %	-95.0%	1.466	26.7	19.8	0.7	5.5
203-P-4-FR-2-10-9-7	-35.2 %	13.1 %	-94.9%	0.952	21.4	15.5	0.7	3.6
202-P-4-FR-2-10-7-9	-38.5 %	8.3 %	-94.9%	0.948	21.0	15.2	0.7	3.6
208-P-4-FR-3-2-9-9	-40.0 %	10.6 %	-94.9%	1.456	49.6	47.0	0.7	6.2
198-P-4-FR-2-5-7-9	-38.3 %	3.7 %	-94.6%	0.947	28.3	22.9	0.4	3.9
210-P-4-FR-3-5-7-9	-41.6 %	3.8 %	-94.6%	1.464	37.2	32.2	0.6	6.2
214-P-4-FR-3-10-7-9	-37.3 %	6.1 %	-94.4%	1.466	26.8	20.3	0.7	5.6
205-P-4-FR-3-2-7-7	-42.5 %	-0.3 %	-94.3%	1.463	50.1	47.0	0.7	6.0
212-P-4-FR-3-5-9-9	-32.8 %	14.1 %	-94.2%	1.457	37.4	32.7	0.7	6.3
206-P-4-FR-3-2-7-9	-38.8 %	-1.7 %	-94.0%	1.463	49.7	47.0	0.7	6.1
195-P-4-FR-2-2-9-7	-33.8 %	5.0 %	-94.0%	0.949	36.0	31.9	0.5	4.3
185-B-4-FR-1-5-7-7	-30.4 %	-1.0 %	-94.0%	0.411	15.9	5.7	-0.0	-0.3
174-P-2-FR-3-5-7-9	-32.7 %	24.4 %	-94.0%	0.732	27.8	19.3	0.4	1.6
204-P-4-FR-2-10-9-9	-25.2 %	15.0 %	-93.9%	0.952	21.3	15.7	0.7	3.6

Continued on next page

Table 4.4 Sorted by Shear Strength Decrease – *Continued from previous page*

Filename	AAR+Shear			AAR Only				
	K	V_{ult}	V_{yld}	Δ_{ver}	σ^{lan}_{max}	σ^{tra}_{max}	σ^{lan}_{med}	σ^{tra}_{med}
		$\frac{(AAR+x)-x}{x} \times 100$		mm	MPa			
209-P-4-FR-3-5-7-7	-34.2 %	-2.4 %	-93.7%	1.464	37.1	31.9	0.6	6.1
197-P-4-FR-2-5-7-7	-30.5 %	1.0 %	-93.6%	0.947	28.3	22.7	0.4	4.0
200-P-4-FR-2-5-9-9	-23.4 %	12.3 %	-93.4%	0.950	28.4	23.3	0.4	3.9
193-P-4-FR-2-2-7-7	-34.0 %	-0.7 %	-93.3%	0.945	35.9	31.9	0.4	4.4
69-B-4-U-3-10-7-7	21.8 %	-33.4 %	-93.3%	1.497	151.2	149.1	137.8	103.3
196-P-4-FR-2-2-9-9	-25.0 %	9.6 %	-93.1%	0.949	35.5	31.9	0.5	4.3
215-P-4-FR-3-10-9-7	-19.3 %	12.2 %	-92.6%	1.459	27.1	20.2	0.8	5.7
211-P-4-FR-3-5-9-7	-10.6 %	9.2 %	-91.4%	1.457	37.2	32.4	0.7	6.2
178-P-2-FR-3-10-7-9	-36.7 %	23.4 %	-91.4%	0.733	20.5	13.4	0.4	1.7
209-TB-4-FR-3-5-7-7	-34.6 %	-8.3 %	-91.1%	1.469	36.9	25.6	0.7	7.9
207-TB-4-FR-3-2-9-7	-13.4 %	0.5 %	-90.6%	1.462	50.1	37.1	0.8	8.8
207-P-4-FR-3-2-9-7	-27.8 %	1.4 %	-87.9%	1.456	49.9	46.9	0.7	6.1
72-B-4-U-3-10-9-9	166.7 %	-40.9 %	-87.6%	1.482	153.7	152.6	141.8	107.4
210-B-4-FR-3-5-7-9	-34.8 %	5.2 %	-83.7%	1.462	44.7	25.7	-0.1	-0.2
70-P-4-U-3-10-7-9	-39.1 %	-35.7 %	-83.0%	1.817	5.3	166.5	-0.0	106.3
71-B-4-U-3-10-9-7	167.9 %	-27.8 %	-80.7%	1.489	153.2	152.0	141.8	106.4
⋮	⋮	⋮	⋮	⋮	⋮	⋮	⋮	
120-P-4-R-1-10-9-9	40.9 %	40.9 %	40.9%	0.760	0.1	0.0	0.0	0.0
166-B-2-FR-2-10-7-9	-31.8 %	-4.6 %	40.9%	0.468	22.1	3.8	-0.2	-0.0
161-B-2-FR-2-5-7-7	-33.7 %	-11.4 %	41.8%	0.467	29.3	4.9	-0.2	0.0
149-B-2-FR-1-5-7-7	-33.2 %	-10.2 %	42.2%	0.206	14.9	3.4	-0.1	-0.1
153-P-2-FR-1-10-7-7	-31.0 %	1.0 %	42.3%	0.206	10.0	6.5	0.5	1.0
67-B-4-U-3-5-9-7	-8.9 %	8.7 %	42.3%	1.334	177.3	180.3	172.1	151.4
189-TB-4-FR-1-10-7-7	-31.8 %	10.2 %	42.6%	0.411	10.9	7.3	0.5	2.9
189-B-4-FR-1-10-7-7	-29.9 %	-2.3 %	42.9%	0.411	11.8	4.6	-0.0	-0.2
199-B-4-FR-2-5-9-7	-21.6 %	3.2 %	42.9%	0.942	33.1	13.1	-0.1	-0.0
153-TB-2-FR-1-10-7-7	-31.9 %	13.4 %	43.6%	0.205	9.7	5.8	0.4	1.7
203-B-4-FR-2-10-9-7	-20.9 %	2.6 %	43.7%	0.943	24.0	10.4	-0.1	-0.0
205-B-4-FR-3-2-7-7	-43.0 %	2.3 %	44.6%	1.460	60.3	29.3	-0.2	0.0
56-B-4-U-2-5-9-9	-9.0 %	10.7 %	44.6%	0.871	121.0	123.6	118.4	106.6
32-B-2-U-3-5-9-9	-9.5 %	-1.5 %	44.8%	0.674	177.6	181.5	173.2	163.4
90-P-2-R-2-5-7-9	26.2 %	45.1 %	45.1%	0.847	0.0	0.0	0.0	0.0
149-P-2-FR-1-5-7-7	-31.7 %	-1.8 %	45.1%	0.206	12.2	8.6	0.5	1.1
191-B-4-FR-1-10-9-7	-10.6 %	3.1 %	45.2%	0.417	12.6	4.7	-0.0	-0.2
65-B-4-U-3-5-7-7	-26.2 %	8.2 %	45.4%	1.330	175.9	178.4	170.4	147.8
53-B-4-U-2-5-7-7	-27.3 %	7.5 %	45.6%	0.872	120.2	122.4	117.4	105.0
31-B-2-U-3-5-9-7	-9.1 %	-0.7 %	45.9%	0.674	177.6	181.3	173.2	163.3
145-TB-2-FR-1-2-7-7	-31.2 %	-0.1 %	46.0%	0.205	17.4	9.5	0.4	1.9
157-B-2-FR-2-2-7-7	-33.8 %	-10.2 %	46.1%	0.467	37.4	5.8	-0.2	0.0
30-B-2-U-3-5-7-9	-26.8 %	-0.5 %	46.2%	0.675	176.3	180.1	171.9	161.4
71-P-4-U-3-10-9-7	-34.5 %	-22.9 %	46.3%	1.828	3.2	170.0	-0.1	109.8
54-B-4-U-2-5-7-9	-28.2 %	7.0 %	46.4%	0.872	120.1	122.7	117.4	105.1
131-P-4-R-2-10-9-7	46.8 %	121.9 %	46.8%	1.705	0.4	0.1	0.0	0.0
156-B-2-FR-1-10-9-9	-9.8 %	-4.4 %	46.9%	0.209	12.0	2.8	-0.1	-0.0
209-B-4-FR-3-5-7-7	-39.3 %	1.0 %	46.9%	1.466	44.7	24.9	-0.1	-0.2
151-B-2-FR-1-5-9-7	-9.8 %	-3.7 %	47.0%	0.209	15.5	3.3	-0.1	-0.1
149-TB-2-FR-1-5-7-7	-32.4 %	0.3 %	47.2%	0.205	13.3	7.6	0.4	1.7
201-B-4-FR-2-10-7-7	-40.7 %	0.1 %	47.4%	0.937	23.4	10.2	-0.1	-0.1
145-B-2-FR-1-2-7-7	-33.5 %	-9.0 %	47.8%	0.206	18.4	3.9	-0.1	-0.1
203-TB-4-FR-2-10-9-7	-11.6 %	14.4 %	47.9%	0.950	20.7	12.8	0.5	4.9
201-TB-4-FR-2-10-7-7	-32.6 %	14.5 %	48.0%	0.946	20.2	12.4	0.5	4.9

Continued on next page

Table 4.4 Sorted by Shear Strength Decrease – *Continued from previous page*

Filename	AAR+Shear			AAR Only				
	K	V_{ult}	V_{yld}	Δ_{ver}	σ^{lan}_{max}	σ^{tra}_{max}	σ^{lan}_{med}	σ^{tra}_{med}
	$\frac{(AAR+x)-x}{x}\times 100$			mm	MPa			
10-B-2-U-1-10-7-9	-24.6 %	-3.1 %	48.0%	0.222	56.4	57.8	55.1	50.6
187-B-4-FR-1-5-9-7	-11.0 %	9.5 %	48.2%	0.417	16.8	5.7	-0.0	-0.3
171-TB-2-FR-3-2-9-7	-10.6 %	15.0 %	48.5%	0.731	76.7	22.4	0.1	3.0
178-B-2-FR-3-10-7-9	-37.9 %	-6.6 %	48.5%	0.730	30.2	6.2	-0.3	0.0
144-P-4-R-3-10-9-9	48.5 %	48.5 %	48.5%	2.695	0.6	0.1	0.0	0.0
155-TB-2-FR-1-10-9-7	-14.7 %	17.4 %	48.6%	0.208	11.2	5.9	0.4	1.6
197-B-4-FR-2-5-7-7	-40.5 %	3.0 %	48.7%	0.937	32.6	12.9	-0.1	-0.0
197-TB-4-FR-2-5-7-7	-34.7 %	-2.1 %	49.2%	0.944	28.6	18.7	0.6	5.5
83-B-2-R-1-10-9-7	53.4 %	49.3 %	49.3%	0.381	0.1	0.0	0.0	0.0
165-P-2-FR-2-10-7-7	-30.8 %	6.6 %	49.6%	0.474	16.5	10.3	0.3	1.1
181-B-4-FR-1-2-7-7	-36.1 %	4.8 %	49.9%	0.411	20.3	6.7	-0.0	-0.4
186-B-4-FR-1-5-7-9	-29.4 %	0.5 %	50.1%	0.411	15.9	5.7	-0.0	-0.3
161-TB-2-FR-2-5-7-7	-29.4 %	2.3 %	50.2%	0.471	41.0	12.8	0.3	2.1
147-B-2-FR-1-2-9-7	-9.9 %	-0.5 %	50.3%	0.209	18.9	3.8	-0.1	-0.1
199-TB-4-FR-2-5-9-7	-12.4 %	-1.2 %	50.5%	0.949	28.9	19.1	0.6	5.4
68-B-4-U-3-5-9-9	-9.4 %	8.4 %	50.8%	1.340	177.4	180.8	172.5	152.4
187-TB-4-FR-1-5-9-7	-14.5 %	-1.0 %	50.9%	0.416	15.6	10.7	0.4	3.1
151-TB-2-FR-1-5-9-7	-15.0 %	2.9 %	51.0%	0.208	14.9	7.8	0.4	1.6
169-B-2-FR-3-2-7-7	-40.9 %	-14.3 %	51.0%	0.729	51.5	9.8	-0.4	-0.0
84-B-2-R-1-10-9-9	54.6 %	51.2 %	51.2%	0.381	0.1	0.0	0.0	0.0
215-TB-4-FR-3-10-9-7	-16.5 %	16.9 %	51.2%	1.466	25.5	16.6	0.8	6.9
163-B-2-FR-2-5-9-7	-15.9 %	-1.5 %	51.3%	0.470	29.7	5.0	-0.2	-0.0
168-B-2-FR-2-10-9-9	-15.7 %	0.1 %	51.4%	0.470	22.8	3.8	-0.2	-0.0
155-P-2-FR-1-10-9-7	-13.1 %	7.6 %	51.5%	0.210	10.2	6.6	0.4	0.9
185-TB-4-FR-1-5-7-7	-32.7 %	-0.6 %	51.5%	0.410	14.8	10.4	0.4	3.1
211-TB-4-FR-3-5-9-7	-16.9 %	-0.3 %	52.0%	1.465	36.7	26.0	0.8	8.0
167-TB-2-FR-2-10-9-7	-12.4 %	20.1 %	52.0%	0.473	32.5	9.5	0.3	2.3
165-TB-2-FR-2-10-7-7	-29.0 %	20.4 %	52.4%	0.471	31.1	9.3	0.3	2.3
212-B-4-FR-3-5-9-9	-26.8 %	22.6 %	52.7%	1.464	44.6	22.9	-0.1	-0.2
206-B-4-FR-3-2-7-9	-38.0 %	21.1 %	52.8%	1.464	60.3	27.7	-0.2	0.1
214-B-4-FR-3-10-7-9	-38.7 %	3.8 %	52.9%	1.462	31.6	18.8	-0.1	-0.1
191-TB-4-FR-1-10-9-7	-13.5 %	18.3 %	53.0%	0.417	11.6	7.6	0.4	2.9
207-B-4-FR-3-2-9-7	-26.8 %	19.5 %	53.3%	1.463	60.0	26.9	-0.1	0.2
21-P-2-U-2-10-7-7	-2.3 %	51.0 %	53.4%	0.596	1.4	120.5	0.0	96.1
215-B-4-FR-3-10-9-7	-21.9 %	4.4 %	53.7%	1.460	31.8	19.5	-0.1	-0.1
163-TB-2-FR-2-5-9-7	-11.3 %	5.0 %	54.1%	0.473	42.2	12.9	0.2	2.1
214-TB-4-FR-3-10-7-9	-28.1 %	19.5 %	54.5%	1.471	25.3	16.2	0.8	6.6
147-TB-2-FR-1-2-9-7	-15.3 %	5.7 %	54.6%	0.208	19.0	9.5	0.4	1.8
150-B-2-FR-1-5-7-9	-29.3 %	-7.6 %	54.6%	0.206	14.9	3.4	-0.1	-0.1
22-P-2-U-2-10-7-9	-0.8 %	49.1 %	54.7%	0.597	1.5	120.5	-0.0	96.4
193-B-4-FR-2-2-7-7	-41.5 %	5.9 %	54.9%	0.936	43.1	15.4	-0.1	0.0
95-B-2-R-2-10-9-7	53.7 %	55.1 %	55.1%	0.853	0.2	0.1	0.0	0.0
161-P-2-FR-2-5-7-7	-30.5 %	4.9 %	55.2%	0.474	22.0	14.4	0.5	0.9
47-B-4-U-1-10-9-7	-8.8 %	17.1 %	55.2%	0.440	57.3	58.2	55.7	48.2
190-B-4-FR-1-10-7-9	-28.9 %	5.4 %	55.3%	0.411	11.8	4.6	-0.0	-0.2
211-B-4-FR-3-5-9-7	-24.4 %	10.7 %	55.9%	1.462	44.7	22.2	-0.1	-0.2
216-TB-4-FR-3-10-9-9	-6.0 %	20.6 %	56.0%	1.466	25.4	16.7	0.8	6.9
188-B-4-FR-1-5-9-9	-10.0 %	12.4 %	56.1%	0.417	16.8	5.7	-0.0	-0.3
157-TB-2-FR-2-2-7-7	-30.1 %	6.8 %	56.2%	0.470	52.0	16.6	0.3	1.8
154-TB-2-FR-1-10-7-9	-31.4 %	23.4 %	56.2%	0.205	9.7	5.8	0.4	1.7
154-P-2-FR-1-10-7-9	-29.9 %	11.0 %	56.4%	0.206	9.9	6.5	0.5	1.0

Continued on next page

Table 4.4 Sorted by Shear Strength Decrease – *Continued from previous page*

Filename	AAR+Shear			AAR Only				
	K	V_{ult}	V_{yld}	Δ_{ver}	σ_{max}^{lan}	σ_{max}^{tra}	σ_{med}^{lan}	σ_{med}^{tra}
	$\frac{(AAR+x)-x}{x} \times 100$			mm	MPa			
180-B-2-FR-3-10-9-9	-21.0 %	-1.6 %	56.5%	0.729	30.4	6.6	-0.3	0.0
195-B-4-FR-2-2-9-7	-23.4 %	10.2 %	56.6%	0.942	43.3	15.3	-0.1	0.0
183-B-4-FR-1-2-9-7	-11.3 %	14.9 %	56.6%	0.417	21.0	6.6	-0.0	-0.4
167-P-2-FR-2-10-9-7	-13.1 %	11.4 %	56.6%	0.476	16.6	10.5	0.4	1.0
150-TB-2-FR-1-5-7-9	-32.0 %	6.7 %	56.6%	0.205	13.3	7.6	0.4	1.7
159-TB-2-FR-2-2-9-7	-10.6 %	13.2 %	56.6%	0.473	52.7	16.4	0.2	1.8
151-P-2-FR-1-5-9-7	-13.4 %	5.9 %	56.6%	0.209	12.4	8.7	0.4	1.0
146-TB-2-FR-1-2-7-9	-32.7 %	7.3 %	56.8%	0.205	17.4	9.5	0.4	1.9
175-B-2-FR-3-5-9-7	-26.3 %	-5.3 %	57.0%	0.729	40.4	8.5	-0.3	-0.0
107-B-2-R-3-10-9-7	55.7 %	57.0 %	57.0%	1.351	0.4	0.1	0.0	0.0
179-TB-2-FR-3-10-9-7	-20.0 %	24.5 %	57.6%	0.731	46.2	12.2	0.1	3.2
66-B-4-U-3-5-7-9	-27.7 %	10.4 %	57.8%	1.337	176.1	178.9	170.8	148.2
146-B-2-FR-1-2-7-9	-29.6 %	-6.0 %	57.8%	0.206	18.4	3.9	-0.1	-0.1
177-P-2-FR-3-10-7-7	-38.0 %	12.3 %	58.2%	0.733	20.6	13.4	0.4	1.8
171-B-2-FR-3-2-9-7	-25.7 %	-5.5 %	58.4%	0.729	51.1	10.1	-0.3	-0.1
150-P-2-FR-1-5-7-9	-30.7 %	7.6 %	59.0%	0.206	12.1	8.6	0.5	1.1
162-B-2-FR-2-5-7-9	-34.9 %	-6.6 %	59.3%	0.468	29.3	4.7	-0.2	-0.1
210-TB-4-FR-3-5-7-9	-35.5 %	4.6 %	59.4%	1.469	36.9	25.6	0.7	7.9
159-B-2-FR-2-2-9-7	-16.7 %	5.0 %	59.5%	0.470	37.4	5.8	-0.2	0.0
192-B-4-FR-1-10-9-9	-9.9 %	9.7 %	59.7%	0.417	12.6	4.7	-0.0	-0.2
182-B-4-FR-1-2-7-9	-29.9 %	12.4 %	59.8%	0.411	20.3	6.7	-0.0	-0.4
175-TB-2-FR-3-5-9-7	-12.7 %	8.9 %	59.9%	0.731	60.5	17.1	0.1	3.4
23-B-2-U-2-10-9-7	-8.7 %	-6.0 %	60.3%	0.466	109.3	111.8	106.0	96.3
166-TB-2-FR-2-10-7-9	-30.6 %	27.1 %	60.8%	0.471	30.7	9.3	0.3	2.2
202-TB-4-FR-2-10-7-9	-33.8 %	24.8 %	61.4%	0.946	20.2	12.4	0.5	4.9
174-TB-2-FR-3-5-7-9	-38.5 %	10.2 %	61.7%	0.733	59.8	17.1	0.1	3.2
162-TB-2-FR-2-5-7-9	-30.5 %	10.3 %	61.9%	0.471	40.5	12.8	0.3	2.1
156-TB-2-FR-1-10-9-9	-14.3 %	28.0 %	62.0%	0.208	11.2	5.9	0.4	1.6
148-B-2-FR-1-2-9-9	-10.2 %	2.2 %	62.0%	0.209	18.9	3.8	-0.1	-0.1
212-TB-4-FR-3-5-9-9	-22.0 %	6.6 %	62.6%	1.465	36.7	26.0	0.8	7.9
190-TB-4-FR-1-10-7-9	-29.9 %	25.7 %	62.6%	0.411	10.9	7.3	0.5	2.9
186-TB-4-FR-1-5-7-9	-30.7 %	6.7 %	62.7%	0.410	14.8	10.4	0.4	3.1
166-P-2-FR-2-10-7-9	-31.0 %	15.6 %	62.8%	0.474	16.4	10.2	0.3	1.0
170-TB-2-FR-3-2-7-9	-28.2 %	16.5 %	63.4%	0.732	76.7	22.6	0.1	2.9
184-B-4-FR-1-2-9-9	-10.7 %	20.6 %	63.5%	0.417	21.0	6.6	-0.0	-0.4
204-TB-4-FR-2-10-9-9	-13.4 %	26.6 %	63.8%	0.950	20.7	12.8	0.6	4.9
152-TB-2-FR-1-5-9-9	-14.6 %	11.7 %	63.9%	0.208	14.9	7.8	0.4	1.6
178-TB-2-FR-3-10-7-9	-29.9 %	29.6 %	64.0%	0.733	45.1	12.1	0.1	3.0
180-TB-2-FR-3-10-9-9	-10.7 %	36.1 %	64.2%	0.731	45.0	12.3	0.1	3.1
158-B-2-FR-2-2-7-9	-36.0 %	-4.9 %	64.2%	0.467	37.4	5.6	-0.2	0.0
164-B-2-FR-2-5-9-9	-17.0 %	3.0 %	64.3%	0.470	29.7	4.8	-0.2	-0.0
81-P-2-R-1-10-7-7	14.8 %	56.7 %	64.4%	0.376	0.0	0.0	0.0	0.0
82-P-2-R-1-10-7-9	15.5 %	57.4 %	65.0%	0.376	0.0	0.0	0.0	0.0
176-B-2-FR-3-5-9-9	-21.7 %	-0.3 %	65.2%	0.729	40.5	8.4	-0.3	-0.0
94-P-2-R-2-10-7-9	17.0 %	57.5 %	65.2%	0.847	0.0	0.0	0.0	0.0
174-B-2-FR-3-5-7-9	-40.1 %	-6.7 %	65.3%	0.730	40.5	8.0	-0.3	0.0
156-P-2-FR-1-10-9-9	-12.0 %	17.5 %	65.5%	0.210	10.1	6.6	0.4	0.9
82-B-2-R-1-10-7-9	27.6 %	65.7 %	65.7%	0.376	0.0	0.0	0.0	0.0
202-B-4-FR-2-10-7-9	-38.3 %	12.8 %	66.1%	0.938	23.3	10.1	-0.1	-0.1
192-TB-4-FR-1-10-9-9	-11.9 %	28.5 %	66.2%	0.417	11.6	7.6	0.4	2.9
198-B-4-FR-2-5-7-9	-40.5 %	11.7 %	66.8%	0.937	32.5	12.9	-0.1	-0.0

Continued on next page

Table 4.4 Sorted by Shear Strength Decrease – *Continued from previous page*

Filename	AAR+Shear			AAR Only				
	K	V_{ult}	V_{yld}	Δ_{ver}	σ^{lan}_{max}	σ^{tra}_{max}	σ^{lan}_{med}	σ^{tra}_{med}
		$\frac{(AAR+x)-x}{x} \times 100$		mm	MPa			
194-B-4-FR-2-2-7-9	-40.2 %	14.1 %	67.0%	0.936	43.0	15.3	-0.1	0.0
200-TB-4-FR-2-5-9-9	-13.7 %	9.6 %	67.1%	0.949	29.0	19.1	0.6	5.4
152-P-2-FR-1-5-9-9	-12.4 %	13.3 %	67.5%	0.209	12.3	8.7	0.4	1.0
179-P-2-FR-3-10-9-7	-16.8 %	21.8 %	67.6%	0.730	20.5	13.6	0.4	1.8
176-TB-2-FR-3-5-9-9	-10.8 %	19.1 %	67.9%	0.731	59.2	17.2	0.1	3.3
48-B-4-U-1-10-9-9	-9.3 %	20.1 %	67.9%	0.440	57.2	58.3	55.7	48.2
204-B-4-FR-2-10-9-9	-19.8 %	14.0 %	67.9%	0.944	24.0	10.4	-0.1	-0.0
148-TB-2-FR-1-2-9-9	-14.7 %	14.9 %	68.0%	0.208	19.0	9.5	0.4	1.8
168-TB-2-FR-2-10-9-9	-13.8 %	32.9 %	68.1%	0.473	32.0	9.4	0.3	2.2
172-B-2-FR-3-2-9-9	-23.1 %	-2.7 %	68.2%	0.729	51.2	10.0	-0.3	-0.0
170-B-2-FR-3-2-7-9	-44.9 %	-4.5 %	68.2%	0.730	51.6	9.7	-0.3	-0.0
152-B-2-FR-1-5-9-9	-10.1 %	-0.8 %	68.4%	0.209	15.5	3.3	-0.1	-0.1
163-P-2-FR-2-5-9-7	-13.8 %	14.0 %	68.6%	0.476	22.0	14.5	0.5	0.9
188-TB-4-FR-1-5-9-9	-12.2 %	10.6 %	68.6%	0.416	15.6	10.7	0.4	3.1
158-TB-2-FR-2-2-7-9	-30.4 %	15.4 %	68.8%	0.470	51.5	16.5	0.3	1.8
145-P-2-FR-1-2-7-7	-32.2 %	-7.1 %	69.6%	0.206	14.4	10.6	0.5	0.9
198-TB-4-FR-2-5-7-9	-35.2 %	11.4 %	69.8%	0.944	28.7	18.7	0.6	5.5
164-TB-2-FR-2-5-9-9	-13.6 %	15.7 %	69.8%	0.473	41.6	12.8	0.2	2.1
200-B-4-FR-2-5-9-9	-19.8 %	17.3 %	70.3%	0.943	33.1	13.0	-0.1	-0.0
205-TB-4-FR-3-2-7-7	-36.6 %	-6.8 %	70.3%	1.467	50.9	37.2	0.7	8.6
24-B-2-U-2-10-9-9	-8.1 %	-5.1 %	70.9%	0.466	109.2	112.1	106.0	96.6
160-B-2-FR-2-2-9-9	-16.4 %	5.3 %	71.0%	0.470	37.4	5.7	-0.2	-0.0
94-B-2-R-2-10-7-9	27.6 %	71.4 %	71.4%	0.847	0.1	0.0	0.0	-0.0
168-P-2-FR-2-10-9-9	-13.8 %	21.7 %	71.5%	0.476	16.5	10.4	0.4	1.0
175-P-2-FR-3-5-9-7	-12.0 %	19.9 %	71.9%	0.729	27.5	19.4	0.5	1.7
196-B-4-FR-2-2-9-9	-20.5 %	17.6 %	72.2%	0.942	43.2	15.3	-0.1	0.1
181-TB-4-FR-1-2-7-7	-33.4 %	-5.8 %	72.3%	0.409	18.7	13.8	0.4	3.7
106-B-2-R-3-10-7-9	27.6 %	72.3 %	72.3%	1.344	0.2	0.1	0.0	0.0
208-B-4-FR-3-2-9-9	-23.9 %	27.3 %	72.4%	1.464	60.2	28.0	-0.2	0.2
45-P-4-U-1-10-7-7	-25.9 %	-20.8 %	72.5%	0.547	0.4	65.9	-0.0	54.7
162-P-2-FR-2-5-7-9	-31.3 %	16.8 %	72.8%	0.474	22.0	14.3	0.5	0.9
21-B-2-U-2-10-7-7	-24.1 %	-4.5 %	73.1%	0.467	107.8	110.0	104.5	94.3
195-TB-4-FR-2-2-9-7	-14.9 %	-3.7 %	76.0%	0.948	38.1	26.2	0.5	6.0
147-P-2-FR-1-2-9-7	-13.6 %	-3.3 %	76.5%	0.209	14.7	10.7	0.4	0.8
172-TB-2-FR-3-2-9-9	-15.0 %	21.3 %	77.4%	0.731	75.2	22.5	0.1	2.9
45-B-4-U-1-10-7-7	-26.3 %	10.7 %	77.8%	0.442	56.4	57.3	54.8	47.1
160-TB-2-FR-2-2-9-9	-13.6 %	22.1 %	78.5%	0.473	52.1	16.4	0.3	1.8
59-P-4-U-2-10-9-7	-20.0 %	-15.2 %	78.8%	1.170	1.6	124.1	-0.1	90.8
157-P-2-FR-2-2-7-7	-28.9 %	-1.2 %	80.4%	0.473	27.9	18.9	0.6	0.4
193-TB-4-FR-2-2-7-7	-34.0 %	-0.7 %	81.5%	0.943	38.2	26.2	0.5	6.0
182-TB-4-FR-1-2-7-9	-31.2 %	-0.6 %	81.7%	0.409	18.7	13.8	0.4	3.7
46-P-4-U-1-10-7-9	-25.9 %	-18.3 %	82.7%	0.547	0.4	65.9	-0.0	54.7
208-TB-4-FR-3-2-9-9	-16.4 %	0.5 %	83.8%	1.462	50.1	37.1	0.9	8.8
164-P-2-FR-2-5-9-9	-13.8 %	24.8 %	84.5%	0.476	22.0	14.4	0.5	0.9
22-B-2-U-2-10-7-9	-24.4 %	-4.4 %	84.6%	0.467	107.7	110.4	104.5	94.6
183-TB-4-FR-1-2-9-7	-15.0 %	1.9 %	86.3%	0.415	19.3	14.0	0.4	3.6
159-P-2-FR-2-2-9-7	-14.0 %	3.6 %	87.0%	0.475	27.5	18.8	0.5	0.4
146-P-2-FR-1-2-7-9	-31.3 %	2.5 %	87.0%	0.206	14.4	10.6	0.5	0.9
180-P-2-FR-3-10-9-9	-10.6 %	33.2 %	87.5%	0.730	20.5	13.6	0.4	1.8
194-TB-4-FR-2-2-7-9	-31.6 %	3.3 %	88.9%	0.943	38.2	26.1	0.5	6.0
46-B-4-U-1-10-7-9	-26.4 %	13.5 %	89.8%	0.442	56.4	57.4	54.8	47.1

Continued on next page

Table 4.4 Sorted by Shear Strength Decrease – *Continued from previous page*

Filename	AAR+Shear			AAR Only				
	K	V_{ult}	V_{yld}	Δ_{ver}	σ^{lan}_{max}	σ^{tra}_{max}	σ^{lan}_{med}	σ^{tra}_{med}
	$\frac{(AAR+x)-x}{x} \times 100$			mm	MPa			
169-P-2-FR-3-2-7-7	-42.1 %	4.0 %	89.8%	0.732	36.5	26.1	0.6	1.4
34-B-2-U-3-10-7-9	-24.8 %	-5.6 %	92.3%	0.719	153.8	155.0	147.0	124.5
158-P-2-FR-2-2-7-9	-31.7 %	5.7 %	93.0%	0.473	27.9	18.6	0.6	0.4
148-P-2-FR-1-2-9-9	-12.7 %	5.7 %	93.0%	0.209	14.7	10.7	0.5	0.8
48-P-4-U-1-10-9-9	-8.6 %	-13.1 %	93.4%	0.548	0.4	67.2	-0.0	56.4
196-TB-4-FR-2-2-9-9	-14.2 %	5.9 %	93.5%	0.948	38.1	26.1	0.5	6.0
47-P-4-U-1-10-9-7	-8.6 %	-12.5 %	93.6%	0.548	0.4	67.2	-0.0	56.4
33-B-2-U-3-10-7-7	-26.5 %	-5.6 %	93.9%	0.719	153.8	154.4	146.7	124.1
35-B-2-U-3-10-9-7	-10.7 %	-4.6 %	94.7%	0.721	155.9	157.2	149.0	128.3
36-B-2-U-3-10-9-9	-9.6 %	-5.3 %	95.0%	0.722	155.9	157.9	149.4	129.4
176-P-2-FR-3-5-9-9	-13.1 %	32.3 %	95.6%	0.729	27.5	19.5	0.5	1.7
184-TB-4-FR-1-2-9-9	-12.5 %	7.3 %	96.1%	0.415	19.3	13.9	0.4	3.6
171-P-2-FR-3-2-9-7	-13.4 %	14.2 %	97.4%	0.729	35.9	25.9	0.6	1.4
96-B-2-R-2-10-9-9	56.0 %	98.4 %	98.4%	0.853	0.2	0.1	0.0	-0.0
172-P-2-FR-3-2-9-9	-10.9 %	28.3 %	99.4%	0.729	35.9	25.9	0.6	1.2
60-P-4-U-2-10-9-9	-21.8 %	-14.1 %	103.2%	1.171	2.5	124.0	-0.0	90.0
57-P-4-U-2-10-7-7	-37.8 %	-13.7 %	103.6%	1.164	2.4	121.3	-0.1	85.8
59-B-4-U-2-10-9-7	-8.2 %	33.8 %	109.6%	0.912	109.0	109.5	104.6	86.5
160-P-2-FR-2-2-9-9	-13.8 %	16.5 %	112.6%	0.475	27.6	18.6	0.5	0.4
60-B-4-U-2-10-9-9	-7.8 %	34.7 %	119.3%	0.913	109.0	109.8	104.8	86.5
57-B-4-U-2-10-7-7	-23.0 %	23.5 %	119.6%	0.909	107.3	107.3	102.5	83.8
81-TB-2-R-1-10-7-7	-26.0 %	-17.5 %	126.4%	0.376	0.0	0.0	0.0	0.0
58-B-4-U-2-10-7-9	-22.3 %	26.2 %	128.6%	0.918	107.6	107.8	103.2	84.3
41-P-4-U-1-5-7-7	-27.3 %	-32.7 %	135.8%	0.532	0.4	74.5	-0.0	66.3
83-TB-2-R-1-10-9-7	-10.2 %	-13.8 %	136.8%	0.381	0.0	0.0	0.0	0.0
95-TB-2-R-2-10-9-7	-10.1 %	-8.4 %	151.6%	0.855	0.1	0.0	0.0	0.0
44-P-4-U-1-5-9-9	-9.1 %	-15.3 %	157.3%	0.534	0.4	75.4	-0.0	67.6
107-TB-2-R-3-10-9-7	-10.1 %	-5.6 %	159.3%	1.352	0.1	0.0	0.0	0.0
42-P-4-U-1-5-7-9	-27.3 %	-26.3 %	161.0%	0.532	0.4	74.5	-0.0	66.3
43-P-4-U-1-5-9-7	-9.1 %	-23.6 %	163.1%	0.534	0.4	75.4	-0.0	67.6
66-P-4-U-3-5-7-9	-38.8 %	-35.0 %	163.4%	1.751	5.6	207.6	-0.1	160.2
56-P-4-U-2-5-9-9	-9.5 %	-17.8 %	163.7%	1.133	0.9	147.2	-0.0	129.4
68-P-4-U-3-5-9-9	-18.2 %	-27.9 %	167.1%	1.761	2.5	211.0	-0.1	166.2
65-P-4-U-3-5-7-7	-39.0 %	-34.0 %	167.3%	1.751	2.4	208.5	-0.1	162.1
53-P-4-U-2-5-7-7	-28.3 %	-22.7 %	167.4%	1.125	1.3	145.0	-0.0	120.0
67-P-4-U-3-5-9-7	-19.1 %	-26.0 %	170.2%	1.758	2.0	211.1	-0.1	166.1
54-P-4-U-2-5-7-9	-28.2 %	-22.3 %	173.6%	1.130	0.7	145.5	0.0	127.1
55-P-4-U-2-5-9-7	-10.2 %	-20.1 %	178.1%	1.130	0.8	146.9	-0.1	123.8
82-TB-2-R-1-10-7-9	-26.0 %	1.7 %	179.2%	0.376	0.0	0.0	0.0	0.0
84-TB-2-R-1-10-9-9	-10.2 %	3.6 %	184.6%	0.381	0.0	0.0	0.0	0.0
141-B-4-R-3-10-7-7	-50.8 %	3.1 %	189.3%	2.692	11.4	5.6	5.8	0.0
94-TB-2-R-2-10-7-9	-26.0 %	5.8 %	190.6%	0.847	0.0	0.0	0.0	0.0
77-TB-2-R-1-5-7-7	-27.5 %	-26.7 %	201.3%	0.376	0.0	0.0	0.0	0.0
49-P-4-U-2-2-7-7	-28.7 %	-33.2 %	201.8%	1.087	0.8	161.7	0.0	151.3
89-TB-2-R-2-5-7-7	-27.5 %	-23.4 %	215.0%	0.847	0.0	0.0	0.0	0.0
79-TB-2-R-1-5-9-7	-11.4 %	-22.6 %	218.2%	0.381	0.0	0.0	0.0	0.0
117-TB-4-R-1-10-7-7	-25.7 %	9.9 %	218.7%	0.751	0.1	0.0	0.0	0.0
62-P-4-U-3-2-7-9	-28.7 %	-26.6 %	219.1%	1.680	2.0	240.9	-0.0	223.3
142-B-4-R-3-10-7-9	-48.5 %	25.6 %	226.1%	2.731	14.2	4.5	6.5	-0.0
119-TB-4-R-1-10-9-7	-8.4 %	13.0 %	227.6%	0.760	0.1	0.1	0.0	0.0
61-P-4-U-3-2-7-7	-28.7 %	-28.0 %	230.3%	1.680	2.2	240.9	-0.0	223.2

Continued on next page

Table 4.4 Sorted by Shear Strength Decrease – *Continued from previous page*								
	AAR+Shear			AAR Only				
Filename	K	V_{ult}	V_{yld}	Δ_{ver}	σ^{lan}_{max}	σ^{tra}_{max}	σ^{lan}_{med}	σ^{tra}_{med}
	$\frac{(AAR+x)-x}{x} \times 100$			mm	MPa			
91-TB-2-R-2-5-9-7	-11.4 %	-19.4 %	231.4%	0.855	0.1	0.0	0.0	0.0
129-TB-4-R-2-10-7-7	-25.7 %	14.8 %	232.9%	1.690	0.2	0.1	0.0	0.0
103-TB-2-R-3-5-9-7	-11.3 %	-18.7 %	234.4%	1.352	0.1	0.1	0.0	0.0
37-P-4-U-1-2-7-7	-28.7 %	-31.6 %	238.0%	0.521	0.3	80.4	-0.0	76.2
141-TB-4-R-3-10-7-7	-25.7 %	18.1 %	242.4%	2.679	0.3	0.4	0.0	0.0
117-B-4-R-1-10-7-7	-24.6 %	22.4 %	243.4%	0.750	0.2	0.1	0.0	0.0
63-P-4-U-3-2-9-7	-9.6 %	-26.6 %	245.2%	1.684	2.7	242.3	-0.0	225.4
51-P-4-U-2-2-9-7	-9.6 %	-25.7 %	246.0%	1.090	0.7	162.7	0.0	152.8
64-P-4-U-3-2-9-9	-9.6 %	-24.4 %	248.5%	1.684	2.5	242.4	-0.0	225.4
137-B-4-R-3-5-7-7	-40.9 %	-6.9 %	254.6%	2.690	13.4	11.4	3.1	-0.0
52-P-4-U-2-2-9-9	-9.6 %	-25.5 %	256.8%	1.090	0.7	162.7	0.0	152.8
118-TB-4-R-1-10-7-9	-25.7 %	23.3 %	257.7%	0.751	0.1	0.0	0.0	0.0
50-P-4-U-2-2-7-9	-28.7 %	-28.7 %	263.1%	1.087	0.8	161.7	0.0	151.3
118-B-4-R-1-10-7-9	-24.6 %	31.4 %	268.5%	0.750	0.2	0.1	0.0	0.0
38-P-4-U-1-2-7-9	-28.7 %	-21.3 %	268.8%	0.521	0.3	80.4	-0.0	76.2
119-B-4-R-1-10-9-7	-8.1 %	31.6 %	269.2%	0.759	0.2	0.1	0.1	0.0
129-B-4-R-2-10-7-7	-24.6 %	31.8 %	269.8%	1.690	0.6	0.5	0.1	0.0
39-P-4-U-1-2-9-7	-9.6 %	-23.7 %	270.0%	0.522	0.3	80.9	-0.0	77.0
80-TB-2-R-1-5-9-9	-11.4 %	-5.0 %	275.1%	0.381	0.0	0.0	0.0	0.0
74-TB-2-R-1-2-7-9	-31.4 %	-10.1 %	275.6%	0.376	0.0	0.0	0.0	0.0
73-TB-2-R-1-2-7-7	-31.4 %	-29.4 %	276.3%	0.376	0.0	0.0	0.0	0.0
40-P-4-U-1-2-9-9	-9.6 %	-20.3 %	278.9%	0.522	0.3	80.9	-0.0	77.0
76-TB-2-R-1-2-9-9	-11.5 %	-6.2 %	281.3%	0.381	0.0	0.0	0.0	0.0
131-B-4-R-2-10-9-7	-8.1 %	37.2 %	284.9%	1.693	1.1	0.6	0.0	0.0
75-TB-2-R-1-2-9-7	-11.5 %	-27.9 %	287.4%	0.381	0.0	0.0	0.0	0.0
120-TB-4-R-1-10-9-9	-8.4 %	33.6 %	287.5%	0.760	0.1	0.1	0.0	0.0
90-TB-2-R-2-5-7-9	-27.5 %	-4.6 %	292.4%	0.847	0.0	0.0	0.0	0.0
120-B-4-R-1-10-9-9	-8.1 %	41.2 %	296.2%	0.759	0.2	0.1	0.1	0.0
92-TB-2-R-2-5-9-9	-11.4 %	-2.3 %	301.8%	0.855	0.1	0.0	0.0	0.0
130-TB-4-R-2-10-7-9	-25.7 %	38.7 %	302.3%	1.690	0.2	0.1	0.0	0.0
130-B-4-R-2-10-7-9	-24.6 %	86.1 %	308.0%	1.690	0.6	0.5	0.1	-0.0
144-TB-4-R-3-10-9-9	-8.4 %	43.8 %	317.0%	2.686	0.6	0.6	0.1	0.0
85-TB-2-R-2-2-7-7	-31.4 %	-28.8 %	324.8%	0.847	0.1	0.0	0.0	0.0
132-B-4-R-2-10-9-9	-8.1 %	57.3 %	341.3%	1.693	1.1	0.6	0.0	0.0
88-TB-2-R-2-2-9-9	-11.5 %	-6.0 %	345.2%	0.855	0.1	0.0	0.0	0.0
86-TB-2-R-2-2-7-9	-31.4 %	-7.8 %	347.1%	0.847	0.0	0.0	0.0	0.0
87-TB-2-R-2-2-9-7	-11.5 %	-25.0 %	347.6%	0.854	0.1	0.0	0.0	0.0
99-TB-2-R-3-2-9-7	-11.5 %	-24.7 %	349.8%	1.352	0.2	0.0	0.0	0.0
114-TB-4-R-1-5-7-9	-27.2 %	40.3 %	375.9%	0.751	0.1	0.1	0.0	0.0
113-TB-4-R-1-5-7-7	-27.2 %	4.8 %	376.3%	0.751	0.1	0.1	0.0	0.0
115-TB-4-R-1-5-9-7	-9.0 %	8.8 %	376.9%	0.760	0.1	0.1	0.0	0.0
116-TB-4-R-1-5-9-9	-9.0 %	38.7 %	379.0%	0.760	0.1	0.1	0.0	0.0
112-TB-4-R-1-2-9-9	-12.1 %	77.2 %	385.5%	0.761	0.1	0.1	0.0	0.0
125-TB-4-R-2-5-7-7	-27.2 %	9.5 %	403.4%	1.692	0.2	0.1	0.1	0.0
137-TB-4-R-3-5-7-7	-27.2 %	10.9 %	410.0%	2.680	0.3	0.4	0.1	0.0
110-B-4-R-1-2-7-9	-31.9 %	-1.3 %	430.9%	0.751	0.2	0.2	0.1	0.0
111-B-4-R-1-2-9-7	-12.5 %	-24.5 %	441.8%	0.759	0.3	0.1	0.1	-0.0
109-B-4-R-1-2-7-7	-31.9 %	-23.9 %	442.3%	0.751	0.2	0.2	0.1	0.0
128-TB-4-R-2-5-9-9	-9.0 %	41.2 %	457.4%	1.706	0.4	0.2	0.1	0.0
115-B-4-R-1-5-9-7	-8.8 %	6.5 %	457.7%	0.759	0.3	0.1	0.1	0.0
116-B-4-R-1-5-9-9	-8.8 %	43.6 %	459.5%	0.759	0.3	0.1	0.1	0.0

Continued on next page

Table 4.4 Sorted by Shear Strength Decrease – *Continued from previous page*

Filename	AAR+Shear			AAR Only				
	K	V_{ult}	V_{yld}	Δ_{ver}	σ^{lan}_{max}	σ^{tra}_{max}	σ^{lan}_{med}	σ^{tra}_{med}
	$\frac{(AAR+x)-x}{x}\times 100$			mm	MPa			
112-B-4-R-1-2-9-9	-12.5 %	0.0 %	459.6%	0.759	0.3	0.1	0.1	-0.0
126-TB-4-R-2-5-7-9	-27.2 %	42.1 %	460.4%	1.692	0.2	0.1	0.1	0.0
113-B-4-R-1-5-7-7	-26.6 %	6.1 %	461.4%	0.751	0.2	0.1	0.1	0.0
124-TB-4-R-2-2-9-9	-12.1 %	79.5 %	462.8%	1.700	0.4	0.4	0.1	0.0
114-B-4-R-1-5-7-9	-26.6 %	41.6 %	464.7%	0.751	0.2	0.1	0.1	0.0
122-TB-4-R-2-2-7-9	-31.7 %	69.4 %	468.1%	1.691	0.3	0.1	0.1	0.0
140-TB-4-R-3-5-9-9	-9.0 %	39.9 %	470.1%	2.686	0.7	0.8	0.1	0.0
138-TB-4-R-3-5-7-9	-27.2 %	41.0 %	477.4%	2.679	0.4	0.4	0.1	0.0
135-TB-4-R-3-2-9-7	-12.1 %	41.1 %	488.7%	2.691	1.0	0.7	0.1	0.1
127-B-4-R-2-5-9-7	-8.9 %	9.9 %	507.1%	1.703	1.3	1.0	0.2	-0.0
125-B-4-R-2-5-7-7	-26.6 %	10.8 %	512.1%	1.685	0.9	0.5	0.1	-0.0
124-B-4-R-2-2-9-9	-12.5 %	-7.4 %	550.4%	1.703	1.6	1.2	0.3	0.0
123-B-4-R-2-2-9-7	-12.5 %	-24.0 %	556.3%	1.703	1.6	1.2	0.3	0.0
121-B-4-R-2-2-7-7	-31.9 %	-20.8 %	559.0%	1.684	0.9	0.6	0.1	0.0
122-B-4-R-2-2-7-9	-31.9 %	-0.1 %	559.8%	1.684	0.9	0.6	0.1	0.0
128-B-4-R-2-5-9-9	-8.9 %	33.9 %	571.8%	1.703	1.3	1.0	0.2	-0.0
126-B-4-R-2-5-7-9	-26.6 %	45.6 %	573.8%	1.685	0.9	0.5	0.1	-0.0

Table 4.5. Sorted by Out of Plane displacement Decrease

Filename	AAR+Shear			AAR Only				
	K	V_{ult}	V_{yld}	Δ_{ver}	σ^{lan}_{max}	σ^{tra}_{max}	σ^{lan}_{med}	σ^{tra}_{med}
	$\frac{(AAR+x)-x}{x}\times 100$			mm	MPa			
97-TB-2-R-3-2-7-7	-100.0 %	-100.0 %	-100.0 %	11977.024	198.8	184.6	-0.6	6.3
106-TB-2-R-3-10-7-9	-100.0 %	-100.0 %	-100.0 %	7777.896	6.0	57.2	-0.2	-0.0
105-TB-2-R-3-10-7-7	-100.0 %	-100.0 %	-100.0 %	962.240	1.5	13.1	-0.0	0.0
106-P-2-R-3-10-7-9	-100.0 %	-100.0 %	-100.0 %	909.898	6.1	173.3	-14.0	-0.0
98-TB-2-R-3-2-7-9	-100.0 %	-100.0 %	-100.0 %	845.807	117.2	104.4	-0.5	0.1
144-B-4-R-3-10-9-9	-100.0 %	-100.0 %	-100.0 %	484.094	18.7	121.1	-0.2	-0.0
101-P-2-R-3-5-7-7	-100.0 %	-100.0 %	-100.0 %	449.364	43.4	81.5	-24.0	15.4
111-TB-4-R-1-2-9-7	-100.0 %	-100.0 %	-100.0 %	194.046	4.7	26.3	-0.4	0.0
143-P-4-R-3-10-9-7	-100.0 %	-100.0 %	-100.0 %	192.624	76.7	46.3	0.0	0.0
4-P-2-U-1-2-9-9	-100.0 %	-100.0 %	-100.0 %	69.105	75.7	127.1	2.7	-0.1
103-B-2-R-3-5-9-7	-100.0 %	-99.9 %	-100.0 %	44.691	18.4	11.3	-0.7	-0.1
132-TB-4-R-2-10-9-9	-99.8 %	-100.0 %	-100.0 %	39.806	19.0	1.5	-0.0	-0.0
91-B-2-R-2-5-9-7	-100.0 %	-100.0 %	-100.0 %	32.272	37.5	14.9	-0.4	-0.0
123-TB-4-R-2-2-9-7	-99.9 %	-100.0 %	-99.9 %	28.224	10.7	8.2	0.1	0.1
87-B-2-R-2-2-9-7	-100.0 %	-100.0 %	-100.0 %	26.360	45.7	36.4	-0.1	-0.1
99-B-2-R-3-2-9-7	-99.9 %	-94.9 %	-100.0 %	18.180	97.3	46.8	-9.5	0.0
134-B-4-R-3-2-7-9	-95.7 %	-98.3 %	-98.1 %	17.384	71.0	19.7	17.0	0.0
143-B-4-R-3-10-9-7	-100.4 %	-100.0 %	-100.0 %	14.468	13.3	5.5	-0.7	-0.0
127-TB-4-R-2-5-9-7	-99.9 %	-100.0 %	-100.0 %	13.595	4.4	0.8	0.0	0.0
133-B-4-R-3-2-7-7	-97.0 %	-98.1 %	-100.0 %	13.490	43.3	21.4	14.0	-0.1
102-B-2-R-3-5-7-9	-99.7 %	-90.6 %	-100.0 %	12.304	31.9	17.9	-3.2	0.0
100-B-2-R-3-2-9-9	-99.0 %	-96.1 %	-100.0 %	12.123	67.0	81.5	-0.0	0.1
139-P-4-R-3-5-9-7	-99.7 %	-97.9 %	-100.0%	9.095	28.5	15.8	8.8	0.2
131-TB-4-R-2-10-9-7	-99.5 %	-100.0 %	-99.9%	9.040	13.4	3.9	-0.1	-0.0

Continued on next page

Table 4.5 Sorted by Out of Plane displacement Decrease – *Continued from previous page*

Filename	AAR+Shear			AAR Only				
	K	V_{ult}	V_{yld}	Δ_{ver}	σ^{lan}_{max}	σ^{tra}_{max}	σ^{lan}_{med}	σ^{tra}_{med}
	$\frac{(AAR+x)-x}{x} \times 100$			mm	MPa			
108-TB-2-R-3-10-9-9	-100.2 %	-97.9 %	-100.0%	8.963	38.4	20.4	2.2	1.7
133-TB-4-R-3-2-7-7	-104.3 %	-98.4 %	-100.0%	7.678	74.9	23.9	6.7	0.8
141-P-4-R-3-10-7-7	-99.7 %	-97.0 %	-100.0%	7.606	38.1	11.1	-2.4	-0.0
102-TB-2-R-3-5-7-9	-99.7 %	-99.0 %	-99.0%	7.393	56.0	36.8	10.3	1.9
134-TB-4-R-3-2-7-9	-100.4 %	-99.2 %	-100.0%	6.770	52.1	28.0	-10.3	0.3
133-P-4-R-3-2-7-7	-99.6 %	-99.6 %	-100.0%	6.311	67.8	46.9	-7.6	0.0
138-B-4-R-3-5-7-9	-97.7 %	-94.8 %	-99.1%	6.072	19.9	12.0	4.0	0.0
143-TB-4-R-3-10-9-7	-99.6 %	-99.9 %	-99.9%	5.547	12.1	1.4	-0.9	-0.0
135-P-4-R-3-2-9-7	-100.1 %	-100.0 %	-100.0%	5.299	38.5	22.9	1.2	-0.2
97-P-2-R-3-2-7-7	-99.9 %	-97.4 %	-100.0%	5.077	30.3	25.8	-5.2	0.0
136-TB-4-R-3-2-9-9	-99.2 %	-99.8 %	-99.8%	4.826	54.5	39.8	3.2	0.2
138-P-4-R-3-5-7-9	-97.5 %	-77.6 %	-96.9%	4.376	15.4	3.1	2.4	0.0
134-P-4-R-3-2-7-9	-99.2 %	-99.1 %	-99.8%	4.324	91.4	24.9	17.8	-0.1
101-B-2-R-3-5-7-7	-99.1 %	-88.3 %	-99.9%	4.075	100.2	36.5	-11.3	0.6
104-TB-2-R-3-5-9-9	-98.5 %	-95.5 %	-100.0%	3.999	34.4	50.9	0.2	0.9
91-P-2-R-2-5-9-7	-100.0 %	-99.8 %	-100.0%	3.999	12.4	7.0	-1.3	-0.0
216-B-4-FR-3-10-9-9	-42.8 %	-4.1 %	29.9%	3.228	38.2	19.1	0.1	0.4
121-TB-4-R-2-2-7-7	-98.7 %	-99.3 %	-100.0%	3.100	93.6	22.2	2.4	-0.5
140-B-4-R-3-5-9-9	-98.8 %	-97.4 %	-99.7%	2.991	17.4	5.0	1.4	-0.0
89-P-2-R-2-5-7-7	-98.4 %	-80.5 %	-99.0%	2.984	25.2	3.8	1.6	0.1
105-P-2-R-3-10-7-7	-100.1 %	-97.5 %	-100.0%	2.865	12.0	8.5	1.5	0.1
102-P-2-R-3-5-7-9	-99.9 %	-98.9 %	-99.9%	2.807	18.4	28.2	2.1	0.3
135-B-4-R-3-2-9-7	-97.5 %	-99.7 %	-98.8%	2.773	180.2	55.9	5.9	0.4
140-P-4-R-3-5-9-9	-99.5 %	-95.5 %	-99.5%	2.762	17.4	22.0	0.2	0.0
142-B-4-R-3-10-7-9	-48.5 %	25.6 %	226.1%	2.731	14.2	4.5	6.5	-0.0
144-P-4-R-3-10-9-9	48.5 %	48.5 %	48.5%	2.695	0.6	0.1	0.0	0.0
136-P-4-R-3-2-9-9	61.1 %	-31.9 %	-31.9%	2.694	1.2	0.3	0.1	0.0
141-B-4-R-3-10-7-7	-50.8 %	3.1 %	189.3%	2.692	11.4	5.6	5.8	0.0
135-TB-4-R-3-2-9-7	-12.1 %	41.1 %	488.7%	2.691	1.0	0.7	0.1	0.1
137-B-4-R-3-5-7-7	-40.9 %	-6.9 %	254.6%	2.690	13.4	11.4	3.1	-0.0
144-TB-4-R-3-10-9-9	-8.4 %	43.8 %	317.0%	2.686	0.6	0.6	0.1	0.0
140-TB-4-R-3-5-9-9	-9.0 %	39.9 %	470.1%	2.686	0.7	0.8	0.1	0.0
142-P-4-R-3-10-7-9	21.9 %	21.9 %	21.9%	2.684	0.2	0.1	0.0	0.0
137-P-4-R-3-5-7-7	25.0 %	-7.8 %	-7.8%	2.684	0.5	0.1	0.0	0.0
137-TB-4-R-3-5-7-7	-27.2 %	10.9 %	410.0%	2.680	0.3	0.4	0.1	0.0
138-TB-4-R-3-5-7-9	-27.2 %	41.0 %	477.4%	2.679	0.4	0.4	0.1	0.0
141-TB-4-R-3-10-7-7	-25.7 %	18.1 %	242.4%	2.679	0.3	0.4	0.0	0.0
136-B-4-R-3-2-9-9	-98.8 %	-99.7 %	-99.4%	2.502	62.5	29.6	-0.5	-0.1
93-TB-2-R-2-10-7-7	-99.8 %	-98.6 %	-99.9%	2.451	19.8	28.2	1.4	0.9
103-P-2-R-3-5-9-7	-99.8 %	-97.1 %	-99.9%	2.451	17.9	21.3	2.0	0.2
139-TB-4-R-3-5-9-7	-100.0 %	-100.0 %	-100.0%	2.400	16.1	11.1	-0.1	-0.0
101-TB-2-R-3-5-7-7	-100.3 %	-99.9 %	-100.0%	2.390	11.3	16.0	-1.1	-0.1
142-TB-4-R-3-10-7-9	-99.3 %	-98.4 %	-100.0%	2.371	8.9	2.4	0.7	0.0
108-B-2-R-3-10-9-9	-100.0 %	-99.8 %	-100.0%	2.039	21.3	6.0	-1.0	-0.1
139-B-4-R-3-5-9-7	-98.8 %	-99.6 %	-99.5%	2.027	105.5	31.4	18.8	0.1
71-P-4-U-3-10-9-7	-34.5 %	-22.9 %	46.3%	1.828	3.2	170.0	-0.1	109.8
72-P-4-U-3-10-9-9	-30.1 %	-33.0 %	30.4%	1.825	3.9	169.8	-0.1	109.8
69-P-4-U-3-10-7-7	-43.5 %	-29.3 %	-95.6%	1.823	3.4	166.7	-0.0	106.2
70-P-4-U-3-10-7-9	-39.1 %	-35.7 %	-83.0%	1.817	5.3	166.5	-0.0	106.3
98-P-2-R-3-2-7-9	-99.6 %	-98.9 %	-99.9%	1.768	89.8	30.4	-0.7	0.2
68-P-4-U-3-5-9-9	-18.2 %	-27.9 %	167.1%	1.761	2.5	211.0	-0.1	166.2

Continued on next page

Table 4.5 Sorted by Out of Plane displacement Decrease – *Continued from previous page*

Filename	AAR+Shear			AAR Only				
	K	V_{ult}	V_{yld}	Δ_{ver}	σ^{lan}_{max}	σ^{tra}_{max}	σ^{lan}_{med}	σ^{tra}_{med}
	$\frac{(AAR+x)-x}{x} \times 100$			mm	MPa			
67-P-4-U-3-5-9-7	-19.1 %	-26.0 %	170.2%	1.758	2.0	211.1	-0.1	166.1
66-P-4-U-3-5-7-9	-38.8 %	-35.0 %	163.4%	1.751	5.6	207.6	-0.1	160.2
65-P-4-U-3-5-7-7	-39.0 %	-34.0 %	167.3%	1.751	2.4	208.5	-0.1	162.1
128-TB-4-R-2-5-9-9	-9.0 %	41.2 %	457.4%	1.706	0.4	0.2	0.1	0.0
131-P-4-R-2-10-9-7	46.8 %	121.9 %	46.8%	1.705	0.4	0.1	0.0	0.0
127-P-4-R-2-5-9-7	48.8 %	-23.1 %	-23.1%	1.705	0.5	0.1	0.1	0.0
123-P-4-R-2-2-9-7	57.5 %	-42.7 %	-42.7%	1.704	0.4	0.2	0.1	0.0
124-P-4-R-2-2-9-9	57.2 %	-33.4 %	-33.4%	1.704	0.5	0.2	0.1	0.0
124-B-4-R-2-2-9-9	-12.5 %	-7.4 %	550.4%	1.703	1.6	1.2	0.3	0.0
123-B-4-R-2-2-9-7	-12.5 %	-24.0 %	556.3%	1.703	1.6	1.2	0.3	0.0
128-B-4-R-2-5-9-9	-8.9 %	33.9 %	571.8%	1.703	1.3	1.0	0.2	-0.0
127-B-4-R-2-5-9-7	-8.9 %	9.9 %	507.1%	1.703	1.3	1.0	0.2	-0.0
124-TB-4-R-2-2-9-9	-12.1 %	79.5 %	462.8%	1.700	0.4	0.4	0.1	0.0
131-B-4-R-2-10-9-7	-8.1 %	37.2 %	284.9%	1.693	1.1	0.6	0.0	0.0
132-B-4-R-2-10-9-9	-8.1 %	57.3 %	341.3%	1.693	1.1	0.6	0.0	0.0
126-TB-4-R-2-5-7-9	-27.2 %	42.1 %	460.4%	1.692	0.2	0.1	0.1	0.0
125-TB-4-R-2-5-7-7	-27.2 %	9.5 %	403.4%	1.692	0.2	0.1	0.1	0.0
129-P-4-R-2-10-7-7	21.7 %	21.7 %	21.7%	1.692	0.2	0.0	0.0	0.0
125-P-4-R-2-5-7-7	24.4 %	-14.5 %	-14.5%	1.691	0.3	0.0	0.0	0.0
130-P-4-R-2-10-7-9	21.5 %	21.5 %	21.5%	1.691	0.2	0.0	0.0	0.0
126-P-4-R-2-5-7-9	24.7 %	-7.9 %	-7.9%	1.691	0.2	0.0	0.0	0.0
122-TB-4-R-2-2-7-9	-31.7 %	69.4 %	468.1%	1.691	0.3	0.1	0.1	0.0
121-P-4-R-2-2-7-7	33.6 %	-41.5 %	-41.5%	1.690	0.2	0.1	0.0	0.0
129-TB-4-R-2-10-7-7	-25.7 %	14.8 %	232.9%	1.690	0.2	0.1	0.0	0.0
130-TB-4-R-2-10-7-9	-25.7 %	38.7 %	302.3%	1.690	0.2	0.1	0.0	0.0
129-B-4-R-2-10-7-7	-24.6 %	31.8 %	269.8%	1.690	0.6	0.5	0.1	0.0
130-B-4-R-2-10-7-9	-24.6 %	86.1 %	308.0%	1.690	0.6	0.5	0.1	-0.0
122-P-4-R-2-2-7-9	34.5 %	-25.5 %	-39.1%	1.690	0.3	0.1	0.0	0.0
125-B-4-R-2-5-7-7	-26.6 %	10.8 %	512.1%	1.685	0.9	0.5	0.1	-0.0
126-B-4-R-2-5-7-9	-26.6 %	45.6 %	573.8%	1.685	0.9	0.5	0.1	-0.0
122-B-4-R-2-2-7-9	-31.9 %	-0.1 %	559.8%	1.684	0.9	0.6	0.1	0.0
121-B-4-R-2-2-7-7	-31.9 %	-20.8 %	559.0%	1.684	0.9	0.6	0.1	0.0
64-P-4-U-3-2-9-9	-9.6 %	-24.4 %	248.5%	1.684	2.5	242.4	-0.0	225.4
63-P-4-U-3-2-9-7	-9.6 %	-26.6 %	245.2%	1.684	2.7	242.3	-0.0	225.4
62-P-4-U-3-2-7-9	-28.7 %	-26.6 %	219.1%	1.680	2.0	240.9	-0.0	223.3
61-P-4-U-3-2-7-7	-28.7 %	-28.0 %	230.3%	1.680	2.2	240.9	-0.0	223.2
⋮	⋮	⋮	⋮	⋮	⋮	⋮	⋮	
84-P-2-R-1-10-9-9	37.7 %	26.7 %	32.9%	0.381	0.0	0.0	0.0	0.0
76-P-2-R-1-2-9-9	54.2 %	-12.3 %	-69.5%	0.381	0.0	0.0	0.0	0.0
75-P-2-R-1-2-9-7	52.3 %	-31.7 %	-69.5%	0.381	0.0	0.0	0.0	0.0
83-P-2-R-1-10-9-7	-10.9 %	43.5 %	-31.1%	0.381	0.0	0.0	0.0	0.0
79-P-2-R-1-5-9-7	41.5 %	11.8 %	11.8%	0.381	0.0	0.0	0.0	0.0
80-P-2-R-1-5-9-9	42.9 %	12.4 %	12.4%	0.381	0.0	0.0	0.0	0.0
84-TB-2-R-1-10-9-9	-10.2 %	3.6 %	184.6%	0.381	0.0	0.0	0.0	0.0
76-TB-2-R-1-2-9-9	-11.5 %	-6.2 %	281.3%	0.381	0.0	0.0	0.0	0.0
83-TB-2-R-1-10-9-7	-10.2 %	-13.8 %	136.8%	0.381	0.0	0.0	0.0	0.0
80-TB-2-R-1-5-9-9	-11.4 %	-5.0 %	275.1%	0.381	0.0	0.0	0.0	0.0
79-TB-2-R-1-5-9-7	-11.4 %	-22.6 %	218.2%	0.381	0.0	0.0	0.0	0.0
75-TB-2-R-1-2-9-7	-11.5 %	-27.9 %	287.4%	0.381	0.0	0.0	0.0	0.0
83-B-2-R-1-10-9-7	53.4 %	49.3 %	49.3%	0.381	0.1	0.0	0.0	0.0
84-B-2-R-1-10-9-9	54.6 %	51.2 %	51.2%	0.381	0.1	0.0	0.0	0.0

Continued on next page

Table 4.5 Sorted by Out of Plane displacement Decrease – *Continued from previous page*

Filename	AAR+Shear			AAR Only				
	K	V_{ult}	V_{yld}	Δ_{ver}	σ^{lan}_{max}	σ^{tra}_{max}	σ^{lan}_{med}	σ^{tra}_{med}
	$\frac{(AAR+x)-x}{x} \times 100$			mm	MPa			
75-B-2-R-1-2-9-7	115.9 %	-32.0 %	-42.7%	0.381	0.1	0.0	0.0	0.0
76-B-2-R-1-2-9-9	118.3 %	-19.7 %	-42.5%	0.381	0.1	0.0	0.0	0.0
79-B-2-R-1-5-9-7	75.4 %	-20.4 %	-25.3%	0.381	0.1	0.0	0.0	0.0
80-B-2-R-1-5-9-9	77.0 %	-6.8 %	-6.8%	0.381	0.1	0.0	0.0	0.0
81-P-2-R-1-10-7-7	14.8 %	56.7 %	64.4%	0.376	0.0	0.0	0.0	0.0
82-P-2-R-1-10-7-9	15.5 %	57.4 %	65.0%	0.376	0.0	0.0	0.0	0.0
73-P-2-R-1-2-7-7	32.0 %	-25.8 %	-27.3%	0.376	0.0	0.0	0.0	0.0
81-TB-2-R-1-10-7-7	-26.0 %	-17.5 %	126.4%	0.376	0.0	0.0	0.0	0.0
74-TB-2-R-1-2-7-9	-31.4 %	-10.1 %	275.6%	0.376	0.0	0.0	0.0	0.0
73-TB-2-R-1-2-7-7	-31.4 %	-29.4 %	276.3%	0.376	0.0	0.0	0.0	0.0
82-TB-2-R-1-10-7-9	-26.0 %	1.7 %	179.2%	0.376	0.0	0.0	0.0	0.0
77-TB-2-R-1-5-7-7	-27.5 %	-26.7 %	201.3%	0.376	0.0	0.0	0.0	0.0
78-P-2-R-1-5-7-9	23.0 %	38.1 %	38.1%	0.376	0.0	0.0	0.0	0.0
77-P-2-R-1-5-7-7	24.6 %	16.4 %	16.4%	0.376	0.0	0.0	0.0	0.0
74-P-2-R-1-2-7-9	33.0 %	-8.4 %	-27.1%	0.376	0.0	0.0	0.0	0.0
81-B-2-R-1-10-7-7	27.5 %	28.3 %	28.3%	0.376	0.0	0.0	0.0	0.0
82-B-2-R-1-10-7-9	27.6 %	65.7 %	65.7%	0.376	0.0	0.0	0.0	0.0
78-B-2-R-1-5-7-9	44.6 %	-4.6 %	-4.6%	0.376	0.0	0.0	0.0	0.0
77-B-2-R-1-5-7-7	44.3 %	-19.7 %	-19.7%	0.376	0.0	0.0	0.0	0.0
73-B-2-R-1-2-7-7	74.3 %	-31.3 %	-43.5%	0.376	0.0	0.0	0.0	0.0
74-B-2-R-1-2-7-9	76.8 %	-18.1 %	-42.9%	0.376	0.0	0.0	0.0	0.0
12-P-2-U-1-10-9-9	-19.7 %	34.9 %	-28.4%	0.277	0.3	66.2	-0.0	58.2
11-P-2-U-1-10-9-7	-23.9 %	33.4 %	-28.4%	0.277	0.3	66.2	-0.0	58.2
10-P-2-U-1-10-7-9	-20.7 %	24.1 %	-44.3%	0.276	0.3	64.8	-0.0	56.5
9-P-2-U-1-10-7-7	-20.8 %	26.3 %	-44.3%	0.276	0.3	64.8	-0.0	56.5
8-P-2-U-1-5-9-9	-1.2 %	-6.1 %	-59.1%	0.269	0.3	74.7	-0.0	69.0
7-P-2-U-1-5-9-7	0.6 %	-9.2 %	-59.1%	0.269	0.3	74.7	-0.0	69.0
6-P-2-U-1-5-7-9	23.7 %	-9.5 %	-35.5%	0.268	0.3	73.7	-0.0	67.8
5-P-2-U-1-5-7-7	23.6 %	-14.2 %	-35.6%	0.268	0.3	73.7	-0.0	67.8
1-P-2-U-1-2-7-7	26.0 %	-50.6 %	-50.6%	0.262	0.2	80.0	-0.0	76.9
2-P-2-U-1-2-7-9	27.9 %	-39.7 %	-39.7%	0.262	0.2	80.0	-0.0	76.9
10-B-2-U-1-10-7-9	-24.6 %	-3.1 %	48.0%	0.222	56.4	57.8	55.1	50.6
9-B-2-U-1-10-7-7	-24.5 %	-2.3 %	35.4%	0.222	56.4	57.8	55.1	50.6
10-TB-2-U-1-10-7-9	-25.7 %	-33.3 %	-16.2%	0.222	56.2	57.7	55.0	47.6
9-TB-2-U-1-10-7-7	-25.7 %	-41.6 %	-26.6%	0.222	56.2	57.7	55.0	47.6
11-B-2-U-1-10-9-7	-10.6 %	-2.4 %	28.2%	0.222	57.2	58.6	56.0	51.7
12-B-2-U-1-10-9-9	-8.1 %	-4.0 %	35.6%	0.222	57.2	58.6	56.0	51.7
12-TB-2-U-1-10-9-9	-8.5 %	-26.2 %	-7.3%	0.221	57.0	58.5	55.8	48.8
11-TB-2-U-1-10-9-7	-9.2 %	-35.1 %	-18.5%	0.221	57.0	58.5	55.8	48.8
6-B-2-U-1-5-7-9	-26.9 %	-0.7 %	17.1%	0.213	61.5	62.3	60.5	57.7
5-B-2-U-1-5-7-7	-26.9 %	-5.9 %	7.8%	0.213	61.5	62.3	60.5	57.7
5-TB-2-U-1-5-7-7	-27.4 %	-21.2 %	6.5%	0.213	61.3	62.5	60.4	55.6
6-TB-2-U-1-5-7-9	-27.4 %	-8.8 %	8.1%	0.213	61.3	62.5	60.4	55.6
7-B-2-U-1-5-9-7	-8.9 %	-5.3 %	3.7%	0.213	61.9	62.7	61.0	58.4
8-B-2-U-1-5-9-9	-8.9 %	-6.9 %	13.9%	0.213	61.9	62.7	61.0	58.4
7-TB-2-U-1-5-9-7	-9.6 %	-14.6 %	7.0%	0.213	61.8	62.9	60.9	56.4
8-TB-2-U-1-5-9-9	-9.1 %	-0.6 %	5.5%	0.213	61.8	62.9	60.9	56.4
156-P-2-FR-1-10-9-9	-12.0 %	17.5 %	65.5%	0.210	10.1	6.6	0.4	0.9
155-P-2-FR-1-10-9-7	-13.1 %	7.6 %	51.5%	0.210	10.2	6.6	0.4	0.9
152-P-2-FR-1-5-9-9	-12.4 %	13.3 %	67.5%	0.209	12.3	8.7	0.4	1.0
151-P-2-FR-1-5-9-7	-13.4 %	5.9 %	56.6%	0.209	12.4	8.7	0.4	1.0

Continued on next page

Table 4.5 Sorted by Out of Plane displacement Decrease – *Continued from previous page*

Filename	AAR+Shear			AAR Only				
	K	V_{ult}	V_{yld}	Δ_{ver}	σ^{lan}_{max}	σ^{tra}_{max}	σ^{lan}_{med}	σ^{tra}_{med}
		$\frac{(AAR+x)-x}{x}\times 100$		mm	MPa			
148-P-2-FR-1-2-9-9	-12.7 %	5.7 %	93.0%	0.209	14.7	10.7	0.5	0.8
147-P-2-FR-1-2-9-7	-13.6 %	-3.3 %	76.5%	0.209	14.7	10.7	0.4	0.8
156-B-2-FR-1-10-9-9	-9.8 %	-4.4 %	46.9%	0.209	12.0	2.8	-0.1	-0.0
155-B-2-FR-1-10-9-7	-9.7 %	-6.4 %	28.9%	0.209	12.0	2.8	-0.1	-0.0
152-B-2-FR-1-5-9-9	-10.1 %	-0.8 %	68.4%	0.209	15.5	3.3	-0.1	-0.1
151-B-2-FR-1-5-9-7	-9.8 %	-3.7 %	47.0%	0.209	15.5	3.3	-0.1	-0.1
148-B-2-FR-1-2-9-9	-10.2 %	2.2 %	62.0%	0.209	18.9	3.8	-0.1	-0.1
147-B-2-FR-1-2-9-7	-9.9 %	-0.5 %	50.3%	0.209	18.9	3.8	-0.1	-0.1
156-TB-2-FR-1-10-9-9	-14.3 %	28.0 %	62.0%	0.208	11.2	5.9	0.4	1.6
155-TB-2-FR-1-10-9-7	-14.7 %	17.4 %	48.6%	0.208	11.2	5.9	0.4	1.6
151-TB-2-FR-1-5-9-7	-15.0 %	2.9 %	51.0%	0.208	14.9	7.8	0.4	1.6
152-TB-2-FR-1-5-9-9	-14.6 %	11.7 %	63.9%	0.208	14.9	7.8	0.4	1.6
147-TB-2-FR-1-2-9-7	-15.3 %	5.7 %	54.6%	0.208	19.0	9.5	0.4	1.8
148-TB-2-FR-1-2-9-9	-14.7 %	14.9 %	68.0%	0.208	19.0	9.5	0.4	1.8
1-B-2-U-1-2-7-7	-28.7 %	-3.8 %	-2.8%	0.207	64.6	65.0	64.1	62.9
2-B-2-U-1-2-7-9	-28.7 %	7.0 %	8.1%	0.207	64.6	65.0	64.1	62.9
1-TB-2-U-1-2-7-7	-29.4 %	-2.3 %	-2.5%	0.207	64.5	65.2	64.0	61.7
2-TB-2-U-1-2-7-9	-29.4 %	-8.2 %	0.3%	0.207	64.5	65.2	64.0	61.7
4-B-2-U-1-2-9-9	-12.2 %	13.9 %	15.1%	0.207	64.8	65.1	64.3	63.2
3-B-2-U-1-2-9-7	-12.2 %	-2.2 %	-1.2%	0.207	64.8	65.1	64.3	63.2
3-TB-2-U-1-2-9-7	-9.6 %	3.4 %	-4.9%	0.207	64.7	65.3	64.3	62.2
4-TB-2-U-1-2-9-9	-9.6 %	-1.8 %	-1.0%	0.207	64.7	65.3	64.3	62.2
154-P-2-FR-1-10-7-9	-29.9 %	11.0 %	56.4%	0.206	9.9	6.5	0.5	1.0
153-P-2-FR-1-10-7-7	-31.0 %	1.0 %	42.3%	0.206	10.0	6.5	0.5	1.0
150-P-2-FR-1-5-7-9	-30.7 %	7.6 %	59.0%	0.206	12.1	8.6	0.5	1.1
149-P-2-FR-1-5-7-7	-31.7 %	-1.8 %	45.1%	0.206	12.2	8.6	0.5	1.1
146-P-2-FR-1-2-7-9	-31.3 %	2.5 %	87.0%	0.206	14.4	10.6	0.5	0.9
145-P-2-FR-1-2-7-7	-32.2 %	-7.1 %	69.6%	0.206	14.4	10.6	0.5	0.9
153-B-2-FR-1-10-7-7	-32.7 %	-13.3 %	28.9%	0.206	11.4	2.9	-0.1	-0.1
154-B-2-FR-1-10-7-9	-28.8 %	-12.0 %	39.9%	0.206	11.4	2.9	-0.1	-0.1
150-B-2-FR-1-5-7-9	-29.3 %	-7.6 %	54.6%	0.206	14.9	3.4	-0.1	-0.1
149-B-2-FR-1-5-7-7	-33.2 %	-10.2 %	42.2%	0.206	14.9	3.4	-0.1	-0.1
146-B-2-FR-1-2-7-9	-29.6 %	-6.0 %	57.8%	0.206	18.4	3.9	-0.1	-0.1
145-B-2-FR-1-2-7-7	-33.5 %	-9.0 %	47.8%	0.206	18.4	3.9	-0.1	-0.1
153-TB-2-FR-1-10-7-7	-31.9 %	13.4 %	43.6%	0.205	9.7	5.8	0.4	1.7
154-TB-2-FR-1-10-7-9	-31.4 %	23.4 %	56.2%	0.205	9.7	5.8	0.4	1.7
149-TB-2-FR-1-5-7-7	-32.4 %	0.3 %	47.2%	0.205	13.3	7.6	0.4	1.7
150-TB-2-FR-1-5-7-9	-32.0 %	6.7 %	56.6%	0.205	13.3	7.6	0.4	1.7
146-TB-2-FR-1-2-7-9	-32.7 %	7.3 %	56.8%	0.205	17.4	9.5	0.4	1.9
145-TB-2-FR-1-2-7-7	-31.2 %	-0.1 %	46.0%	0.205	17.4	9.5	0.4	1.9
128-P-4-R-2-5-9-9	-99.9 %	-99.9 %	-100.0%	-1.164	51.7	59.2	-1.3	-0.1
132-P-4-R-2-10-9-9	-100.1 %	-99.3 %	-100.0%	-1.333	15.2	6.6	-0.7	0.0
109-TB-4-R-1-2-7-7	-100.1 %	-100.0 %	-100.0%	-2.950	27.2	13.8	-0.5	-0.2
110-TB-4-R-1-2-7-9	-99.7 %	-99.9 %	-99.9%	-3.303	5.5	9.1	-0.7	-0.1

Table 4.6. Sorted by Maximum Longitudinal Reinforcement Stress

Filename	AAR+Shear			AAR Only				
	K	V_{yld}	V_{ult}	Δ_{ver}	σ^{lan}_{max}	σ^{tra}_{max}	σ^{lan}_{med}	σ^{tra}_{med}
		$\frac{(AAR+x)-x}{x} \times 100$		mm	MPa			
97-TB-2-R-3-2-7-7	-100.0 %	-100.0 %	-100.0 %	11977.024	198.8	184.6	-0.6	6.3
64-TB-4-U-3-2-9-9	-9.5 %	-9.9 %	1.9%	1.268	191.6	195.0	188.4	175.8
63-TB-4-U-3-2-9-7	-9.4 %	-3.4 %	-3.5%	1.268	191.6	195.0	188.5	175.6
64-B-4-U-3-2-9-9	-9.7 %	24.3 %	24.3%	1.267	191.4	194.2	188.6	178.1
63-B-4-U-3-2-9-7	-9.6 %	9.7 %	9.7%	1.267	191.4	194.2	188.6	178.1
28-B-2-U-3-2-9-9	-12.3 %	26.5 %	27.7%	0.635	191.3	193.2	188.9	184.1
27-B-2-U-3-2-9-7	-10.0 %	19.4 %	20.6%	0.635	191.3	193.2	188.9	184.1
62-TB-4-U-3-2-7-9	-28.2 %	-11.3 %	-3.3%	1.269	191.1	194.5	187.7	174.4
61-TB-4-U-3-2-7-7	-29.4 %	-8.3 %	0.3%	1.269	191.1	194.5	187.9	174.1
28-TB-2-U-3-2-9-9	-9.8 %	-0.6 %	-9.6%	0.635	191.1	194.1	188.7	180.0
27-TB-2-U-3-2-9-7	-9.8 %	8.5 %	-10.0%	0.635	191.1	194.1	188.7	179.9
61-B-4-U-3-2-7-7	-29.1 %	9.4 %	9.4%	1.268	190.8	193.7	188.0	176.8
62-B-4-U-3-2-7-9	-28.6 %	23.3 %	23.3%	1.268	190.7	193.7	188.0	176.8
25-B-2-U-3-2-7-7	-30.1 %	17.9 %	19.1%	0.636	190.7	192.7	188.2	183.3
26-B-2-U-3-2-7-9	-28.6 %	23.4 %	24.7%	0.636	190.7	192.7	188.2	183.3
26-TB-2-U-3-2-7-9	-28.7 %	1.5 %	-9.3%	0.636	190.5	193.6	188.1	178.9
25-TB-2-U-3-2-7-7	-29.2 %	6.6 %	-12.1%	0.636	190.5	193.6	188.1	178.9
135-B-4-R-3-2-9-7	-97.5 %	-99.7 %	-98.8%	2.773	180.2	55.9	5.9	0.4
32-B-2-U-3-5-9-9	-9.5 %	-1.5 %	44.8%	0.674	177.6	181.5	173.2	163.4
31-B-2-U-3-5-9-7	-9.1 %	-0.7 %	45.9%	0.674	177.6	181.3	173.2	163.3
68-TB-4-U-3-5-9-9	-10.2 %	-13.5 %	-2.6%	1.339	177.5	182.2	172.0	143.8
67-TB-4-U-3-5-9-7	-9.9 %	-15.4 %	-2.3%	1.338	177.5	181.9	171.9	142.6
68-B-4-U-3-5-9-9	-9.4 %	8.4 %	50.8%	1.340	177.4	180.8	172.5	152.4
67-B-4-U-3-5-9-7	-8.9 %	8.7 %	42.3%	1.334	177.3	180.3	172.1	151.4
32-TB-2-U-3-5-9-9	-9.8 %	-4.9 %	-8.3%	0.675	177.0	181.8	172.8	155.0
31-TB-2-U-3-5-9-7	-10.3 %	-11.5 %	-16.2%	0.674	176.9	181.6	172.7	154.4
66-TB-4-U-3-5-7-9	-26.5 %	-17.4 %	-2.5%	1.344	176.3	180.5	170.6	141.1
30-B-2-U-3-5-7-9	-26.8 %	-0.5 %	46.2%	0.675	176.3	180.1	171.9	161.4
29-B-2-U-3-5-7-7	-28.4 %	-5.7 %	38.6%	0.675	176.3	179.8	171.9	161.4
65-TB-4-U-3-5-7-7	-27.7 %	-21.0 %	-1.1%	1.339	176.1	180.2	170.6	139.6
66-B-4-U-3-5-7-9	-27.7 %	10.4 %	57.8%	1.337	176.1	178.9	170.8	148.2
65-B-4-U-3-5-7-7	-26.2 %	8.2 %	45.4%	1.330	175.9	178.4	170.4	147.8
30-TB-2-U-3-5-7-9	-28.8 %	-9.4 %	-13.5%	0.676	175.8	180.5	171.6	152.9
29-TB-2-U-3-5-7-7	-27.9 %	-19.4 %	-21.3%	0.675	175.6	180.2	171.4	152.3
⋮	⋮	⋮	⋮	⋮	⋮	⋮	⋮	
111-TB-4-R-1-2-9-7	-100.0 %	-100.0 %	-100.0 %	194.046	4.7	26.3	-0.4	0.0
127-TB-4-R-2-5-9-7	-99.9 %	-100.0 %	-100.0 %	13.595	4.4	0.8	0.0	0.0
33-P-2-U-3-10-7-7	-12.4 %	48.2 %	-44.5%	0.946	4.0	164.7	-0.1	119.8
72-P-4-U-3-10-9-9	-30.1 %	-33.0 %	30.4%	1.825	3.9	169.8	-0.1	109.8
36-P-2-U-3-10-9-9	33.9 %	65.0 %	33.9%	0.949	3.7	168.4	-0.1	125.9
69-P-4-U-3-10-7-7	-43.5 %	-29.3 %	-95.6%	1.823	3.4	166.7	-0.0	106.2
35-P-2-U-3-10-9-7	-1.9 %	-4.8 %	-39.1%	0.949	3.2	168.1	-0.1	124.3
71-P-4-U-3-10-9-7	-34.5 %	-22.9 %	46.3%	1.828	3.2	170.0	-0.1	109.8
58-P-4-U-2-10-7-9	-33.3 %	-15.6 %	39.3%	1.164	3.1	121.2	-0.0	85.2
63-P-4-U-3-2-9-7	-9.6 %	-26.6 %	245.2%	1.684	2.7	242.3	-0.0	225.4
68-P-4-U-3-5-9-9	-18.2 %	-27.9 %	167.1%	1.761	2.5	211.0	-0.1	166.2
60-P-4-U-2-10-9-9	-21.8 %	-14.1 %	103.2%	1.171	2.5	124.0	-0.0	90.0
64-P-4-U-3-2-9-9	-9.6 %	-24.4 %	248.5%	1.684	2.5	242.4	-0.0	225.4
57-P-4-U-2-10-7-7	-37.8 %	-13.7 %	103.6%	1.164	2.4	121.3	-0.1	85.8

Continued on next page

Table 4.6 Sorted by Maximum Longitudinal Reinforcement Stress – *Continued from previous page*

Filename	AAR+Shear			AAR Only				
	K	V_{ult}	V_{yld}	Δ_{ver}	σ^{lan}_{max}	σ^{tra}_{max}	σ^{lan}_{med}	σ^{tra}_{med}
	$\frac{(AAR+x)-x}{x} \times 100$			mm	MPa			
65-P-4-U-3-5-7-7	-39.0 %	-34.0 %	167.3%	1.751	2.4	208.5	-0.1	162.1
32-P-2-U-3-5-9-9	41.3 %	18.7 %	14.1%	0.898	2.2	209.5	0.0	180.8
31-P-2-U-3-5-9-7	21.1 %	18.0 %	-59.3%	0.897	2.2	209.4	0.0	179.3
61-P-4-U-3-2-7-7	-28.7 %	-28.0 %	230.3%	1.680	2.2	240.9	-0.0	223.2
62-P-4-U-3-2-7-9	-28.7 %	-26.6 %	219.1%	1.680	2.0	240.9	-0.0	223.3
30-P-2-U-3-5-7-9	18.3 %	5.9 %	-6.5%	0.896	2.0	207.1	0.0	176.4
29-P-2-U-3-5-7-7	11.6 %	15.3 %	-10.0%	0.895	2.0	207.1	0.0	175.4
67-P-4-U-3-5-9-7	-19.1 %	-26.0 %	170.2%	1.758	2.0	211.1	-0.1	166.1
59-P-4-U-2-10-9-7	-20.0 %	-15.2 %	78.8%	1.170	1.6	124.1	-0.1	90.8
124-B-4-R-2-2-9-9	-12.5 %	-7.4 %	550.4%	1.703	1.6	1.2	0.3	0.0
123-B-4-R-2-2-9-7	-12.5 %	-24.0 %	556.3%	1.703	1.6	1.2	0.3	0.0
105-TB-2-R-3-10-7-7	-100.0 %	-100.0 %	-100.0 %	962.240	1.5	13.1	-0.0	0.0
22-P-2-U-2-10-7-9	-0.8 %	49.1 %	54.7%	0.597	1.5	120.5	-0.0	96.4
21-P-2-U-2-10-7-7	-2.3 %	51.0 %	53.4%	0.596	1.4	120.5	0.0	96.1
128-B-4-R-2-5-9-9	-8.9 %	33.9 %	571.8%	1.703	1.3	1.0	0.2	-0.0
127-B-4-R-2-5-9-7	-8.9 %	9.9 %	507.1%	1.703	1.3	1.0	0.2	-0.0
53-P-4-U-2-5-7-7	-28.3 %	-22.7 %	167.4%	1.125	1.3	145.0	-0.0	120.0
28-P-2-U-3-2-9-9	62.5 %	-18.0 %	-25.9%	0.849	1.2	240.6	-0.0	228.0
24-P-2-U-2-10-9-9	-1.5 %	56.3 %	-28.4%	0.600	1.2	122.9	0.0	99.8
27-P-2-U-3-2-9-7	42.9 %	-18.1 %	-73.3%	0.849	1.2	240.6	-0.0	228.0
136-P-4-R-3-2-9-9	61.1 %	-31.9 %	-31.9%	2.694	1.2	0.3	0.1	0.0
23-P-2-U-2-10-9-7	-3.2 %	62.9 %	-28.6%	0.599	1.2	122.9	-0.0	99.1
131-B-4-R-2-10-9-7	-8.1 %	37.2 %	284.9%	1.693	1.1	0.6	0.0	0.0
132-B-4-R-2-10-9-9	-8.1 %	57.3 %	341.3%	1.693	1.1	0.6	0.0	0.0
26-P-2-U-3-2-7-9	40.2 %	-25.6 %	-38.1%	0.847	1.1	239.2	-0.0	226.0
25-P-2-U-3-2-7-7	36.1 %	-18.4 %	-39.2%	0.847	1.1	239.2	-0.0	226.0
135-TB-4-R-3-2-9-7	-12.1 %	41.1 %	488.7%	2.691	1.0	0.7	0.1	0.1
122-B-4-R-2-2-7-9	-31.9 %	-0.1 %	559.8%	1.684	0.9	0.6	0.1	0.0
121-B-4-R-2-2-7-7	-31.9 %	-20.8 %	559.0%	1.684	0.9	0.6	0.1	0.0
56-P-4-U-2-5-9-9	-9.5 %	-17.8 %	163.7%	1.133	0.9	147.2	-0.0	129.4
125-B-4-R-2-5-7-7	-26.6 %	10.8 %	512.1%	1.685	0.9	0.5	0.1	-0.0
126-B-4-R-2-5-7-9	-26.6 %	45.6 %	573.8%	1.685	0.9	0.5	0.1	-0.0
55-P-4-U-2-5-9-7	-10.2 %	-20.1 %	178.1%	1.130	0.8	146.9	-0.1	123.8
20-P-2-U-2-5-9-9	11.0 %	7.7 %	-59.1%	0.573	0.8	145.3	-0.0	132.1
50-P-4-U-2-2-7-9	-28.7 %	-28.7 %	263.1%	1.087	0.8	161.7	0.0	151.3
49-P-4-U-2-2-7-7	-28.7 %	-33.2 %	201.8%	1.087	0.8	161.7	0.0	151.3
19-P-2-U-2-5-9-7	13.0 %	16.9 %	-59.1%	0.573	0.7	145.3	-0.0	131.9
140-TB-4-R-3-5-9-9	-9.0 %	39.9 %	470.1%	2.686	0.7	0.8	0.1	0.0
54-P-4-U-2-5-7-9	-28.2 %	-22.3 %	173.6%	1.130	0.7	145.5	0.0	127.1
52-P-4-U-2-2-9-9	-9.6 %	-25.5 %	256.8%	1.090	0.7	162.7	0.0	152.8
51-P-4-U-2-2-9-7	-9.6 %	-25.7 %	246.0%	1.090	0.7	162.7	0.0	152.8
130-B-4-R-2-10-7-9	-24.6 %	86.1 %	308.0%	1.690	0.6	0.5	0.1	-0.0
129-B-4-R-2-10-7-7	-24.6 %	31.8 %	269.8%	1.690	0.6	0.5	0.1	0.0
18-P-2-U-2-5-7-9	15.6 %	0.7 %	-7.9%	0.571	0.6	143.6	-0.0	129.8
17-P-2-U-2-5-7-7	13.7 %	1.2 %	-8.9%	0.571	0.6	143.6	-0.0	129.8
144-P-4-R-3-10-9-9	48.5 %	48.5 %	48.5%	2.695	0.6	0.1	0.0	0.0
144-TB-4-R-3-10-9-9	-8.4 %	43.8 %	317.0%	2.686	0.6	0.6	0.1	0.0
127-P-4-R-2-5-9-7	48.8 %	-23.1 %	-23.1%	1.705	0.5	0.1	0.1	0.0
137-P-4-R-3-5-7-7	25.0 %	-7.8 %	-7.8%	2.684	0.5	0.1	0.0	0.0
14-P-2-U-2-2-7-9	42.2 %	-31.3 %	-55.2%	0.547	0.5	160.7	-0.0	153.2
13-P-2-U-2-2-7-7	42.2 %	-28.3 %	-57.3%	0.547	0.5	160.7	-0.0	153.2

Continued on next page

Table 4.6 Sorted by Maximum Longitudinal Reinforcement Stress – *Continued from previous page*

Filename	AAR+Shear			AAR Only				
	K	V_{ult}	V_{yld}	Δ_{ver}	σ^{lan}_{max}	σ^{tra}_{max}	σ^{lan}_{med}	σ^{tra}_{med}
	$\frac{(AAR+x)-x}{x} \times 100$			mm	MPa			
124-P-4-R-2-2-9-9	57.2 %	-33.4 %	-33.4%	1.704	0.5	0.2	0.1	0.0
16-P-2-U-2-2-9-9	82.0 %	-22.8 %	-46.5%	0.548	0.5	161.8	-0.0	154.6
15-P-2-U-2-2-9-7	56.1 %	-21.0 %	-73.3%	0.548	0.5	161.8	-0.0	154.6
131-P-4-R-2-10-9-7	46.8 %	121.9 %	46.8%	1.705	0.4	0.1	0.0	0.0
107-B-2-R-3-10-9-7	55.7 %	57.0 %	57.0%	1.351	0.4	0.1	0.0	0.0
97-B-2-R-3-2-7-7	73.3 %	-25.2 %	-36.1%	1.344	0.4	0.1	0.0	0.0
123-P-4-R-2-2-9-7	57.5 %	-42.7 %	-42.7%	1.704	0.4	0.2	0.1	0.0
138-TB-4-R-3-5-7-9	-27.2 %	41.0 %	477.4%	2.679	0.4	0.4	0.1	0.0
124-TB-4-R-2-2-9-9	-12.1 %	79.5 %	462.8%	1.700	0.4	0.4	0.1	0.0
48-P-4-U-1-10-9-9	-8.6 %	-13.1 %	93.4%	0.548	0.4	67.2	-0.0	56.4
47-P-4-U-1-10-9-7	-8.6 %	-12.5 %	93.6%	0.548	0.4	67.2	-0.0	56.4
43-P-4-U-1-5-9-7	-9.1 %	-23.6 %	163.1%	0.534	0.4	75.4	-0.0	67.6
44-P-4-U-1-5-9-9	-9.1 %	-15.3 %	157.3%	0.534	0.4	75.4	-0.0	67.6
46-P-4-U-1-10-7-9	-25.9 %	-18.3 %	82.7%	0.547	0.4	65.9	-0.0	54.7
45-P-4-U-1-10-7-7	-25.9 %	-20.8 %	72.5%	0.547	0.4	65.9	-0.0	54.7
98-B-2-R-3-2-7-9	73.3 %	-15.4 %	-22.5%	1.344	0.4	0.1	0.0	0.0
41-P-4-U-1-5-7-7	-27.3 %	-32.7 %	135.8%	0.532	0.4	74.5	-0.0	66.3
42-P-4-U-1-5-7-9	-27.3 %	-26.3 %	161.0%	0.532	0.4	74.5	-0.0	66.3
128-TB-4-R-2-5-9-9	-9.0 %	41.2 %	457.4%	1.706	0.4	0.2	0.1	0.0
137-TB-4-R-3-5-7-7	-27.2 %	10.9 %	410.0%	2.680	0.3	0.4	0.1	0.0
40-P-4-U-1-2-9-9	-9.6 %	-20.3 %	278.9%	0.522	0.3	80.9	-0.0	77.0
39-P-4-U-1-2-9-7	-9.6 %	-23.7 %	270.0%	0.522	0.3	80.9	-0.0	77.0
38-P-4-U-1-2-7-9	-28.7 %	-21.3 %	268.8%	0.521	0.3	80.4	-0.0	76.2
37-P-4-U-1-2-7-7	-28.7 %	-31.6 %	238.0%	0.521	0.3	80.4	-0.0	76.2
112-B-4-R-1-2-9-9	-12.5 %	0.0 %	459.6%	0.759	0.3	0.1	0.1	-0.0
111-B-4-R-1-2-9-7	-12.5 %	-24.5 %	441.8%	0.759	0.3	0.1	0.1	-0.0
99-P-2-R-3-2-9-7	67.0 %	-41.1 %	-23.4%	1.352	0.3	0.0	0.0	0.0
88-B-2-R-2-2-9-9	123.0 %	-20.2 %	-29.3%	0.853	0.3	0.1	0.1	0.0
125-P-4-R-2-5-7-7	24.4 %	-14.5 %	-14.5%	1.691	0.3	0.0	0.0	0.0
122-TB-4-R-2-2-7-9	-31.7 %	69.4 %	468.1%	1.691	0.3	0.1	0.1	0.0
100-P-2-R-3-2-9-9	68.2 %	-18.6 %	-8.6%	1.353	0.3	0.0	0.0	0.0
92-B-2-R-2-5-9-9	78.6 %	-1.0 %	-1.0%	0.854	0.3	0.1	0.0	0.0
12-P-2-U-1-10-9-9	-19.7 %	34.9 %	-28.4%	0.277	0.3	66.2	-0.0	58.2
11-P-2-U-1-10-9-7	-23.9 %	33.4 %	-28.4%	0.277	0.3	66.2	-0.0	58.2
10-P-2-U-1-10-7-9	-20.7 %	24.1 %	-44.3%	0.276	0.3	64.8	-0.0	56.5
9-P-2-U-1-10-7-7	-20.8 %	26.3 %	-44.3%	0.276	0.3	64.8	-0.0	56.5
8-P-2-U-1-5-9-9	-1.2 %	-6.1 %	-59.1%	0.269	0.3	74.7	-0.0	69.0
7-P-2-U-1-5-9-7	0.6 %	-9.2 %	-59.1%	0.269	0.3	74.7	-0.0	69.0
6-P-2-U-1-5-7-9	23.7 %	-9.5 %	-35.5%	0.268	0.3	73.7	-0.0	67.8
5-P-2-U-1-5-7-7	23.6 %	-14.2 %	-35.6%	0.268	0.3	73.7	-0.0	67.8
115-B-4-R-1-5-9-7	-8.8 %	6.5 %	457.7%	0.759	0.3	0.1	0.1	0.0
116-B-4-R-1-5-9-9	-8.8 %	43.6 %	459.5%	0.759	0.3	0.1	0.1	0.0
141-TB-4-R-3-10-7-7	-25.7 %	18.1 %	242.4%	2.679	0.3	0.4	0.0	0.0
122-P-4-R-2-2-7-9	34.5 %	-25.5 %	-39.1%	1.690	0.3	0.1	0.0	0.0
142-P-4-R-3-10-7-9	21.9 %	21.9 %	21.9%	2.684	0.2	0.1	0.0	0.0
126-TB-4-R-2-5-7-9	-27.2 %	42.1 %	460.4%	1.692	0.2	0.1	0.1	0.0
126-P-4-R-2-5-7-9	24.7 %	-7.9 %	-7.9%	1.691	0.2	0.0	0.0	0.0
85-B-2-R-2-2-7-7	76.7 %	-23.7 %	-37.1%	0.847	0.2	0.0	0.0	0.0
1-P-2-U-1-2-7-7	26.0 %	-50.6 %	-50.6%	0.262	0.2	80.0	-0.0	76.9
2-P-2-U-1-2-7-9	27.9 %	-39.7 %	-39.7%	0.262	0.2	80.0	-0.0	76.9
125-TB-4-R-2-5-7-7	-27.2 %	9.5 %	403.4%	1.692	0.2	0.1	0.1	0.0

Continued on next page

Table 4.6 Sorted by Maximum Longitudinal Reinforcement Stress – *Continued from previous page*

Filename	AAR+Shear			AAR Only				
	K	V_{ult}	V_{yld}	Δ_{ver}	σ_{max}^{lan}	σ_{max}^{tra}	σ_{med}^{lan}	σ_{med}^{tra}
		$\frac{(AAR+x)-x}{x} \times 100$		mm	MPa			
119-B-4-R-1-10-9-7	-8.1 %	31.6 %	269.2%	0.759	0.2	0.1	0.1	0.0
120-B-4-R-1-10-9-9	-8.1 %	41.2 %	296.2%	0.759	0.2	0.1	0.1	0.0
109-B-4-R-1-2-7-7	-31.9 %	-23.9 %	442.3%	0.751	0.2	0.2	0.1	0.0
110-B-4-R-1-2-7-9	-31.9 %	-1.3 %	430.9%	0.751	0.2	0.2	0.1	0.0
86-B-2-R-2-2-7-9	76.7 %	-17.9 %	-30.4%	0.847	0.2	0.0	0.0	0.0
106-B-2-R-3-10-7-9	27.6 %	72.3 %	72.3%	1.344	0.2	0.1	0.0	0.0
95-B-2-R-2-10-9-7	53.7 %	55.1 %	55.1%	0.853	0.2	0.1	0.0	0.0
117-B-4-R-1-10-7-7	-24.6 %	22.4 %	243.4%	0.750	0.2	0.1	0.0	0.0
118-B-4-R-1-10-7-9	-24.6 %	31.4 %	268.5%	0.750	0.2	0.1	0.0	0.0
121-P-4-R-2-2-7-7	33.6 %	-41.5 %	-41.5%	1.690	0.2	0.1	0.0	0.0
105-B-2-R-3-10-7-7	27.6 %	48.1 %	34.9%	1.344	0.2	0.1	0.0	-0.0
96-B-2-R-2-10-9-9	56.0 %	98.4 %	98.4%	0.853	0.2	0.1	0.0	-0.0
130-TB-4-R-2-10-7-9	-25.7 %	38.7 %	302.3%	1.690	0.2	0.1	0.0	0.0
129-TB-4-R-2-10-7-7	-25.7 %	14.8 %	232.9%	1.690	0.2	0.1	0.0	0.0
99-TB-2-R-3-2-9-7	-11.5 %	-24.7 %	349.8%	1.352	0.2	0.0	0.0	0.0
129-P-4-R-2-10-7-7	21.7 %	21.7 %	21.7%	1.692	0.2	0.0	0.0	0.0
114-B-4-R-1-5-7-9	-26.6 %	41.6 %	464.7%	0.751	0.2	0.1	0.1	0.0
113-B-4-R-1-5-7-7	-26.6 %	6.1 %	461.4%	0.751	0.2	0.1	0.1	0.0
130-P-4-R-2-10-7-9	21.5 %	21.5 %	21.5%	1.691	0.2	0.0	0.0	0.0
107-P-2-R-3-10-9-7	41.4 %	30.1 %	36.5%	1.352	0.2	0.0	0.0	0.0
108-P-2-R-3-10-9-9	42.5 %	31.2 %	37.6%	1.352	0.2	0.0	0.0	0.0
87-P-2-R-2-2-9-7	64.7 %	-27.5 %	-13.9%	0.855	0.2	0.0	0.0	0.0
104-P-2-R-3-5-9-9	52.8 %	6.9 %	6.9%	1.353	0.1	0.0	0.0	0.0
93-B-2-R-2-10-7-7	27.6 %	30.6 %	30.6%	0.847	0.1	0.0	0.0	-0.0
94-B-2-R-2-10-7-9	27.6 %	71.4 %	71.4%	0.847	0.1	0.0	0.0	-0.0
112-P-4-R-1-2-9-9	45.5 %	-37.3 %	-76.9%	0.761	0.1	0.0	0.0	0.0
111-P-4-R-1-2-9-7	43.7 %	-47.8 %	-77.2%	0.761	0.1	0.0	0.0	0.0
103-TB-2-R-3-5-9-7	-11.3 %	-18.7 %	234.4%	1.352	0.1	0.1	0.0	0.0
90-B-2-R-2-5-7-9	44.6 %	16.3 %	16.3%	0.846	0.1	0.0	0.0	0.0
112-TB-4-R-1-2-9-9	-12.1 %	77.2 %	385.5%	0.761	0.1	0.1	0.0	0.0
115-TB-4-R-1-5-9-7	-9.0 %	8.8 %	376.9%	0.760	0.1	0.1	0.0	0.0
116-TB-4-R-1-5-9-9	-9.0 %	38.7 %	379.0%	0.760	0.1	0.1	0.0	0.0
88-P-2-R-2-2-9-9	67.9 %	-19.6 %	-9.3%	0.855	0.1	0.0	0.0	0.0
120-P-4-R-1-10-9-9	40.9 %	40.9 %	40.9%	0.760	0.1	0.0	0.0	0.0
119-P-4-R-1-10-9-7	26.6 %	26.6 %	-23.9%	0.760	0.1	0.0	0.0	0.0
116-P-4-R-1-5-9-9	40.3 %	-6.3 %	-6.3%	0.760	0.1	0.0	0.0	0.0
115-P-4-R-1-5-9-7	40.8 %	-27.2 %	-27.2%	0.760	0.1	0.0	0.0	0.0
119-TB-4-R-1-10-9-7	-8.4 %	13.0 %	227.6%	0.760	0.1	0.1	0.0	0.0
120-TB-4-R-1-10-9-9	-8.4 %	33.6 %	287.5%	0.760	0.1	0.1	0.0	0.0
107-TB-2-R-3-10-9-7	-10.1 %	-5.6 %	159.3%	1.352	0.1	0.0	0.0	0.0
88-TB-2-R-2-2-9-9	-11.5 %	-6.0 %	345.2%	0.855	0.1	0.0	0.0	0.0
92-P-2-R-2-5-9-9	51.6 %	5.8 %	5.8%	0.855	0.1	0.0	0.0	0.0
114-TB-4-R-1-5-7-9	-27.2 %	40.3 %	375.9%	0.751	0.1	0.1	0.0	0.0
113-TB-4-R-1-5-7-7	-27.2 %	4.8 %	376.3%	0.751	0.1	0.1	0.0	0.0
87-TB-2-R-2-2-9-7	-11.5 %	-25.0 %	347.6%	0.854	0.1	0.0	0.0	0.0
95-P-2-R-2-10-9-7	40.7 %	29.4 %	35.8%	0.855	0.1	0.0	0.0	0.0
96-P-2-R-2-10-9-9	41.8 %	30.5 %	36.9%	0.855	0.1	0.0	0.0	0.0
91-TB-2-R-2-5-9-7	-11.4 %	-19.4 %	231.4%	0.855	0.1	0.0	0.0	0.0
114-P-4-R-1-5-7-9	21.0 %	0.9 %	0.9%	0.752	0.1	0.0	0.0	0.0
113-P-4-R-1-5-7-7	20.4 %	-17.1 %	-17.1%	0.752	0.1	0.0	0.0	0.0
110-P-4-R-1-2-7-9	25.1 %	-36.5 %	-44.3%	0.752	0.1	0.0	0.0	0.0

Continued on next page

Table 4.6 Sorted by Maximum Longitudinal Reinforcement Stress – *Continued from previous page*

Filename	AAR+Shear			AAR Only				
	K	V_{ult}	V_{yld}	Δ_{ver}	σ^{lan}_{max}	σ^{tra}_{max}	σ^{lan}_{med}	σ^{tra}_{med}
	$\frac{(AAR+x)-x}{x} \times 100$			mm	MPa			
109-P-4-R-1-2-7-7	26.8 %	-45.6 %	-45.6%	0.752	0.1	0.0	0.0	0.0
117-P-4-R-1-10-7-7	20.1 %	20.1 %	20.1%	0.752	0.1	0.0	0.0	0.0
118-P-4-R-1-10-7-9	20.4 %	20.4 %	20.4%	0.752	0.1	0.0	0.0	0.0
118-TB-4-R-1-10-7-9	-25.7 %	23.3 %	257.7%	0.751	0.1	0.0	0.0	0.0
117-TB-4-R-1-10-7-7	-25.7 %	9.9 %	218.7%	0.751	0.1	0.0	0.0	0.0
75-B-2-R-1-2-9-7	115.9 %	-32.0 %	-42.7%	0.381	0.1	0.0	0.0	0.0
76-B-2-R-1-2-9-9	118.3 %	-19.7 %	-42.5%	0.381	0.1	0.0	0.0	0.0
95-TB-2-R-2-10-9-7	-10.1 %	-8.4 %	151.6%	0.855	0.1	0.0	0.0	0.0
92-TB-2-R-2-5-9-9	-11.4 %	-2.3 %	301.8%	0.855	0.1	0.0	0.0	0.0
79-B-2-R-1-5-9-7	75.4 %	-20.4 %	-25.3%	0.381	0.1	0.0	0.0	0.0
80-B-2-R-1-5-9-9	77.0 %	-6.8 %	-6.8%	0.381	0.1	0.0	0.0	0.0
83-B-2-R-1-10-9-7	53.4 %	49.3 %	49.3%	0.381	0.1	0.0	0.0	0.0
85-TB-2-R-2-2-7-7	-31.4 %	-28.8 %	324.8%	0.847	0.1	0.0	0.0	0.0
84-B-2-R-1-10-9-9	54.6 %	51.2 %	51.2%	0.381	0.1	0.0	0.0	0.0
85-P-2-R-2-2-7-7	40.3 %	-49.4 %	-34.3%	0.847	0.1	0.0	0.0	0.0
90-P-2-R-2-5-7-9	26.2 %	45.1 %	45.1%	0.847	0.0	0.0	0.0	0.0
94-P-2-R-2-10-7-9	17.0 %	57.5 %	65.2%	0.847	0.0	0.0	0.0	0.0
93-P-2-R-2-10-7-7	16.6 %	7.3 %	12.6%	0.847	0.0	0.0	0.0	0.0
86-TB-2-R-2-2-7-9	-31.4 %	-7.8 %	347.1%	0.847	0.0	0.0	0.0	0.0
89-TB-2-R-2-5-7-7	-27.5 %	-23.4 %	215.0%	0.847	0.0	0.0	0.0	0.0
90-TB-2-R-2-5-7-9	-27.5 %	-4.6 %	292.4%	0.847	0.0	0.0	0.0	0.0
73-B-2-R-1-2-7-7	74.3 %	-31.3 %	-43.5%	0.376	0.0	0.0	0.0	0.0
74-B-2-R-1-2-7-9	76.8 %	-18.1 %	-42.9%	0.376	0.0	0.0	0.0	0.0
78-B-2-R-1-5-7-9	44.6 %	-4.6 %	-4.6%	0.376	0.0	0.0	0.0	0.0
77-B-2-R-1-5-7-7	44.3 %	-19.7 %	-19.7%	0.376	0.0	0.0	0.0	0.0
75-P-2-R-1-2-9-7	52.3 %	-31.7 %	-69.5%	0.381	0.0	0.0	0.0	0.0
76-P-2-R-1-2-9-9	54.2 %	-12.3 %	-69.5%	0.381	0.0	0.0	0.0	0.0
80-P-2-R-1-5-9-9	42.9 %	12.4 %	12.4%	0.381	0.0	0.0	0.0	0.0
79-P-2-R-1-5-9-7	41.5 %	11.8 %	11.8%	0.381	0.0	0.0	0.0	0.0
94-TB-2-R-2-10-7-9	-26.0 %	5.8 %	190.6%	0.847	0.0	0.0	0.0	0.0
81-B-2-R-1-10-7-7	27.5 %	28.3 %	28.3%	0.376	0.0	0.0	0.0	0.0
82-B-2-R-1-10-7-9	27.6 %	65.7 %	65.7%	0.376	0.0	0.0	0.0	0.0
73-P-2-R-1-2-7-7	32.0 %	-25.8 %	-27.3%	0.376	0.0	0.0	0.0	0.0
75-TB-2-R-1-2-9-7	-11.5 %	-27.9 %	287.4%	0.381	0.0	0.0	0.0	0.0
84-P-2-R-1-10-9-9	37.7 %	26.7 %	32.9%	0.381	0.0	0.0	0.0	0.0
76-TB-2-R-1-2-9-9	-11.5 %	-6.2 %	281.3%	0.381	0.0	0.0	0.0	0.0
74-P-2-R-1-2-7-9	33.0 %	-8.4 %	-27.1%	0.376	0.0	0.0	0.0	0.0
83-P-2-R-1-10-9-7	-10.9 %	43.5 %	-31.1%	0.381	0.0	0.0	0.0	0.0
77-P-2-R-1-5-7-7	24.6 %	16.4 %	16.4%	0.376	0.0	0.0	0.0	0.0
78-P-2-R-1-5-7-9	23.0 %	38.1 %	38.1%	0.376	0.0	0.0	0.0	0.0
80-TB-2-R-1-5-9-9	-11.4 %	-5.0 %	275.1%	0.381	0.0	0.0	0.0	0.0
79-TB-2-R-1-5-9-7	-11.4 %	-22.6 %	218.2%	0.381	0.0	0.0	0.0	0.0
74-TB-2-R-1-2-7-9	-31.4 %	-10.1 %	275.6%	0.376	0.0	0.0	0.0	0.0
81-P-2-R-1-10-7-7	14.8 %	56.7 %	64.4%	0.376	0.0	0.0	0.0	0.0
82-P-2-R-1-10-7-9	15.5 %	57.4 %	65.0%	0.376	0.0	0.0	0.0	0.0
77-TB-2-R-1-5-7-7	-27.5 %	-26.7 %	201.3%	0.376	0.0	0.0	0.0	0.0
73-TB-2-R-1-2-7-7	-31.4 %	-29.4 %	276.3%	0.376	0.0	0.0	0.0	0.0
84-TB-2-R-1-10-9-9	-10.2 %	3.6 %	184.6%	0.381	0.0	0.0	0.0	0.0
83-TB-2-R-1-10-9-7	-10.2 %	-13.8 %	136.8%	0.381	0.0	0.0	0.0	0.0
82-TB-2-R-1-10-7-9	-26.0 %	1.7 %	179.2%	0.376	0.0	0.0	0.0	0.0
81-TB-2-R-1-10-7-7	-26.0 %	-17.5 %	126.4%	0.376	0.0	0.0	0.0	0.0

Table 4.7. Sorted by Maximum Transverse Reinforcement Stress

Filename	AAR+Shear			AAR Only				
	K	V_{yld}	V_{ult}	Δ_{ver}	σ^{lan}_{max}	σ^{tra}_{max}	σ^{lan}_{med}	σ^{tra}_{med}
	$\frac{(AAR+V)-V}{V} \times 100$			mm	MPa			
64-P-4-U-3-2-9-9	-9.6 %	-24.4 %	248.5%	1.684	2.5	242.4	-0.0	225.4
63-P-4-U-3-2-9-7	-9.6 %	-26.6 %	245.2%	1.684	2.7	242.3	-0.0	225.4
61-P-4-U-3-2-7-7	-28.7 %	-28.0 %	230.3%	1.680	2.2	240.9	-0.0	223.2
62-P-4-U-3-2-7-9	-28.7 %	-26.6 %	219.1%	1.680	2.0	240.9	-0.0	223.3
28-P-2-U-3-2-9-9	62.5 %	-18.0 %	-25.9%	0.849	1.2	240.6	-0.0	228.0
27-P-2-U-3-2-9-7	42.9 %	-18.1 %	-73.3%	0.849	1.2	240.6	-0.0	228.0
26-P-2-U-3-2-7-9	40.2 %	-25.6 %	-38.1%	0.847	1.1	239.2	-0.0	226.0
25-P-2-U-3-2-7-7	36.1 %	-18.4 %	-39.2%	0.847	1.1	239.2	-0.0	226.0
67-P-4-U-3-5-9-7	-19.1 %	-26.0 %	170.2%	1.758	2.0	211.1	-0.1	166.1
68-P-4-U-3-5-9-9	-18.2 %	-27.9 %	167.1%	1.761	2.5	211.0	-0.1	166.2
32-P-2-U-3-5-9-9	41.3 %	18.7 %	14.1%	0.898	2.2	209.5	0.0	180.8
31-P-2-U-3-5-9-7	21.1 %	18.0 %	-59.3%	0.897	2.2	209.4	0.0	179.3
65-P-4-U-3-5-7-7	-39.0 %	-34.0 %	167.3%	1.751	2.4	208.5	-0.1	162.1
66-P-4-U-3-5-7-9	-38.8 %	-35.0 %	163.4%	1.751	5.6	207.6	-0.1	160.2
30-P-2-U-3-5-7-9	18.3 %	5.9 %	-6.5%	0.896	2.0	207.1	0.0	176.4
29-P-2-U-3-5-7-7	11.6 %	15.3 %	-10.0%	0.895	2.0	207.1	0.0	175.4
64-TB-4-U-3-2-9-9	-9.5 %	-9.9 %	1.9%	1.268	191.6	195.0	188.4	175.8
63-TB-4-U-3-2-9-7	-9.4 %	-3.4 %	-3.5%	1.268	191.6	195.0	188.5	175.6
62-TB-4-U-3-2-7-9	-28.2 %	-11.3 %	-3.3%	1.269	191.1	194.5	187.7	174.4
61-TB-4-U-3-2-7-7	-29.4 %	-8.3 %	0.3%	1.269	191.1	194.5	187.9	174.1
64-B-4-U-3-2-9-9	-9.7 %	24.3 %	24.3%	1.267	191.4	194.2	188.6	178.1
63-B-4-U-3-2-9-7	-9.6 %	9.7 %	9.7%	1.267	191.4	194.2	188.6	178.1
28-TB-2-U-3-2-9-9	-9.8 %	-0.6 %	-9.6%	0.635	191.1	194.1	188.7	180.0
27-TB-2-U-3-2-9-7	-9.8 %	8.5 %	-10.0%	0.635	191.1	194.1	188.7	179.9
61-B-4-U-3-2-7-7	-29.1 %	9.4 %	9.4%	1.268	190.8	193.7	188.0	176.8
62-B-4-U-3-2-7-9	-28.6 %	23.3 %	23.3%	1.268	190.7	193.7	188.0	176.8
26-TB-2-U-3-2-7-9	-28.7 %	1.5 %	-9.3%	0.636	190.5	193.6	188.1	178.9
25-TB-2-U-3-2-7-7	-29.2 %	6.6 %	-12.1%	0.636	190.5	193.6	188.1	178.9
28-B-2-U-3-2-9-9	-12.3 %	26.5 %	27.7%	0.635	191.3	193.2	188.9	184.1
27-B-2-U-3-2-9-7	-10.0 %	19.4 %	20.6%	0.635	191.3	193.2	188.9	184.1
25-B-2-U-3-2-7-7	-30.1 %	17.9 %	19.1%	0.636	190.7	192.7	188.2	183.3
26-B-2-U-3-2-7-9	-28.6 %	23.4 %	24.7%	0.636	190.7	192.7	188.2	183.3
97-TB-2-R-3-2-7-7	-100.0 %	-100.0 %	-100.0 %	11977.024	198.8	184.6	-0.6	6.3
68-TB-4-U-3-5-9-9	-10.2 %	-13.5 %	-2.6%	1.339	177.5	182.2	172.0	143.8
67-TB-4-U-3-5-9-7	-9.9 %	-15.4 %	-2.3%	1.338	177.5	181.9	171.9	142.6
32-TB-2-U-3-5-9-9	-9.8 %	-4.9 %	-8.3%	0.675	177.0	181.8	172.8	155.0
31-TB-2-U-3-5-9-7	-10.3 %	-11.5 %	-16.2%	0.674	176.9	181.6	172.7	154.4
32-B-2-U-3-5-9-9	-9.5 %	-1.5 %	44.8%	0.674	177.6	181.5	173.2	163.4
31-B-2-U-3-5-9-7	-9.1 %	-0.7 %	45.9%	0.674	177.6	181.3	173.2	163.3
68-B-4-U-3-5-9-9	-9.4 %	8.4 %	50.8%	1.340	177.4	180.8	172.5	152.4
66-TB-4-U-3-5-7-9	-26.5 %	-17.4 %	-2.5%	1.344	176.3	180.5	170.6	141.1
30-TB-2-U-3-5-7-9	-28.8 %	-9.4 %	-13.5%	0.676	175.8	180.5	171.6	152.9
67-B-4-U-3-5-9-7	-8.9 %	8.7 %	42.3%	1.334	177.3	180.3	172.1	151.4
65-TB-4-U-3-5-7-7	-27.7 %	-21.0 %	-1.1%	1.339	176.1	180.2	170.6	139.6
29-TB-2-U-3-5-7-7	-27.9 %	-19.4 %	-21.3%	0.675	175.6	180.2	171.4	152.3
30-B-2-U-3-5-7-9	-26.8 %	-0.5 %	46.2%	0.675	176.3	180.1	171.9	161.4
29-B-2-U-3-5-7-7	-28.4 %	-5.7 %	38.6%	0.675	176.3	179.8	171.9	161.4
66-B-4-U-3-5-7-9	-27.7 %	10.4 %	57.8%	1.337	176.1	178.9	170.8	148.2
65-B-4-U-3-5-7-7	-26.2 %	8.2 %	45.4%	1.330	175.9	178.4	170.4	147.8
106-P-2-R-3-10-7-9	-100.0 %	-100.0 %	-100.0 %	909.898	6.1	173.3	-14.0	-0.0

Continued on next page

Table 4.7 Sorted by Maximum Transverse Reinforcement Stress – *Continued from previous page*

Filename	AAR+Shear			AAR Only				
	K	V_{ult}	V_{yld}	Δ_{ver}	σ^{lan}_{max}	σ^{tra}_{max}	σ^{lan}_{med}	σ^{tra}_{med}
	$\frac{(AAR+x)-x}{x} \times 100$			mm	MPa			
71-P-4-U-3-10-9-7	-34.5 %	-22.9 %	46.3%	1.828	3.2	170.0	-0.1	109.8
72-P-4-U-3-10-9-9	-30.1 %	-33.0 %	30.4%	1.825	3.9	169.8	-0.1	109.8
36-P-2-U-3-10-9-9	33.9 %	65.0 %	33.9%	0.949	3.7	168.4	-0.1	125.9
35-P-2-U-3-10-9-7	-1.9 %	-4.8 %	-39.1%	0.949	3.2	168.1	-0.1	124.3
69-P-4-U-3-10-7-7	-43.5 %	-29.3 %	-95.6%	1.823	3.4	166.7	-0.0	106.2
70-P-4-U-3-10-7-9	-39.1 %	-35.7 %	-83.0%	1.817	5.3	166.5	-0.0	106.3
34-P-2-U-3-10-7-9	-10.5 %	44.2 %	-44.3%	0.946	5.3	165.0	-0.1	120.1
33-P-2-U-3-10-7-7	-12.4 %	48.2 %	-44.5%	0.946	4.0	164.7	-0.1	119.8
52-P-4-U-2-2-9-9	-9.6 %	-25.5 %	256.8%	1.090	0.7	162.7	0.0	152.8
51-P-4-U-2-2-9-7	-9.6 %	-25.7 %	246.0%	1.090	0.7	162.7	0.0	152.8
16-P-2-U-2-2-9-9	82.0 %	-22.8 %	-46.5%	0.548	0.5	161.8	-0.0	154.6
15-P-2-U-2-2-9-7	56.1 %	-21.0 %	-73.3%	0.548	0.5	161.8	-0.0	154.6
50-P-4-U-2-2-7-9	-28.7 %	-28.7 %	263.1%	1.087	0.8	161.7	0.0	151.3
49-P-4-U-2-2-7-7	-28.7 %	-33.2 %	201.8%	1.087	0.8	161.7	0.0	151.3
14-P-2-U-2-2-7-9	42.2 %	-31.3 %	-55.2%	0.547	0.5	160.7	-0.0	153.2
13-P-2-U-2-2-7-7	42.2 %	-28.3 %	-57.3%	0.547	0.5	160.7	-0.0	153.2
⋮	⋮	⋮	⋮	⋮	⋮	⋮	⋮	
163-B-2-FR-2-5-9-7	-15.9 %	-1.5 %	51.3%	0.470	29.7	5.0	-0.2	-0.0
161-B-2-FR-2-5-7-7	-33.7 %	-11.4 %	41.8%	0.467	29.3	4.9	-0.2	0.0
164-B-2-FR-2-5-9-9	-17.0 %	3.0 %	64.3%	0.470	29.7	4.8	-0.2	-0.0
162-B-2-FR-2-5-7-9	-34.9 %	-6.6 %	59.3%	0.468	29.3	4.7	-0.2	-0.1
192-B-4-FR-1-10-9-9	-9.9 %	9.7 %	59.7%	0.417	12.6	4.7	-0.0	-0.2
191-B-4-FR-1-10-9-7	-10.6 %	3.1 %	45.2%	0.417	12.6	4.7	-0.0	-0.2
190-B-4-FR-1-10-7-9	-28.9 %	5.4 %	55.3%	0.411	11.8	4.6	-0.0	-0.2
189-B-4-FR-1-10-7-7	-29.9 %	-2.3 %	42.9%	0.411	11.8	4.6	-0.0	-0.2
142-B-4-R-3-10-7-9	-48.5 %	25.6 %	226.1%	2.731	14.2	4.5	6.5	-0.0
167-B-2-FR-2-10-9-7	-16.4 %	-3.1 %	34.8%	0.470	22.8	4.0	-0.2	-0.0
165-B-2-FR-2-10-7-7	-33.7 %	-13.9 %	29.0%	0.468	22.1	3.9	-0.2	-0.0
146-B-2-FR-1-2-7-9	-29.6 %	-6.0 %	57.8%	0.206	18.4	3.9	-0.1	-0.1
145-B-2-FR-1-2-7-7	-33.5 %	-9.0 %	47.8%	0.206	18.4	3.9	-0.1	-0.1
131-TB-4-R-2-10-9-7	-99.5 %	-100.0 %	-99.9%	9.040	13.4	3.9	-0.1	-0.0
168-B-2-FR-2-10-9-9	-15.7 %	0.1 %	51.4%	0.470	22.8	3.8	-0.2	-0.0
89-P-2-R-2-5-7-7	-98.4 %	-80.5 %	-99.0%	2.984	25.2	3.8	1.6	0.1
166-B-2-FR-2-10-7-9	-31.8 %	-4.6 %	40.9%	0.468	22.1	3.8	-0.2	-0.0
148-B-2-FR-1-2-9-9	-10.2 %	2.2 %	62.0%	0.209	18.9	3.8	-0.1	-0.1
147-B-2-FR-1-2-9-7	-9.9 %	-0.5 %	50.3%	0.209	18.9	3.8	-0.1	-0.1
150-B-2-FR-1-5-7-9	-29.3 %	-7.6 %	54.6%	0.206	14.9	3.4	-0.1	-0.1
149-B-2-FR-1-5-7-7	-33.2 %	-10.2 %	42.2%	0.206	14.9	3.4	-0.1	-0.1
152-B-2-FR-1-5-9-9	-10.1 %	-0.8 %	68.4%	0.209	15.5	3.3	-0.1	-0.1
151-B-2-FR-1-5-9-7	-9.8 %	-3.7 %	47.0%	0.209	15.5	3.3	-0.1	-0.1
138-P-4-R-3-5-7-9	-97.5 %	-77.6 %	-96.9%	4.376	15.4	3.1	2.4	0.0
153-B-2-FR-1-10-7-7	-32.7 %	-13.3 %	28.9%	0.206	11.4	2.9	-0.1	-0.1
154-B-2-FR-1-10-7-9	-28.8 %	-12.0 %	39.9%	0.206	11.4	2.9	-0.1	-0.1
156-B-2-FR-1-10-9-9	-9.8 %	-4.4 %	46.9%	0.209	12.0	2.8	-0.1	-0.0
155-B-2-FR-1-10-9-7	-9.7 %	-6.4 %	28.9%	0.209	12.0	2.8	-0.1	-0.0
104-B-2-R-3-5-9-9	-99.5 %	-91.5 %	-99.9%	1.168	17.3	2.5	3.5	0.0
142-TB-4-R-3-10-7-9	-99.3 %	-98.4 %	-100.0%	2.371	8.9	2.4	0.7	0.0
96-TB-2-R-2-10-9-9	-99.6 %	-99.6 %	-100.0%	0.689	10.7	1.8	0.1	0.0
132-TB-4-R-2-10-9-9	-99.8 %	-100.0 %	-100.0 %	39.806	19.0	1.5	-0.0	-0.0
143-TB-4-R-3-10-9-7	-99.6 %	-99.9 %	-99.9%	5.547	12.1	1.4	-0.9	-0.0
124-B-4-R-2-2-9-9	-12.5 %	-7.4 %	550.4%	1.703	1.6	1.2	0.3	0.0

Continued on next page

Table 4.7 Sorted by Maximum Transverse Reinforcement Stress – *Continued from previous page*

Filename	AAR+Shear			AAR Only				
	K	V_{ult}	V_{yld}	Δ_{ver}	σ^{lan}_{max}	σ^{tra}_{max}	σ^{lan}_{med}	σ^{tra}_{med}
	$\frac{(AAR+x)-x}{x}\times 100$			mm	MPa			
123-B-4-R-2-2-9-7	-12.5 %	-24.0 %	556.3%	1.703	1.6	1.2	0.3	0.0
128-B-4-R-2-5-9-9	-8.9 %	33.9 %	571.8%	1.703	1.3	1.0	0.2	-0.0
127-B-4-R-2-5-9-7	-8.9 %	9.9 %	507.1%	1.703	1.3	1.0	0.2	-0.0
140-TB-4-R-3-5-9-9	-9.0 %	39.9 %	470.1%	2.686	0.7	0.8	0.1	0.0
127-TB-4-R-2-5-9-7	-99.9 %	-100.0 %	-100.0 %	13.595	4.4	0.8	0.0	0.0
135-TB-4-R-3-2-9-7	-12.1 %	41.1 %	488.7%	2.691	1.0	0.7	0.1	0.1
132-B-4-R-2-10-9-9	-8.1 %	57.3 %	341.3%	1.693	1.1	0.6	0.0	0.0
131-B-4-R-2-10-9-7	-8.1 %	37.2 %	284.9%	1.693	1.1	0.6	0.0	0.0
144-TB-4-R-3-10-9-9	-8.4 %	43.8 %	317.0%	2.686	0.6	0.6	0.1	0.0
122-B-4-R-2-2-7-9	-31.9 %	-0.1 %	559.8%	1.684	0.9	0.6	0.1	0.0
121-B-4-R-2-2-7-7	-31.9 %	-20.8 %	559.0%	1.684	0.9	0.6	0.1	0.0
125-B-4-R-2-5-7-7	-26.6 %	10.8 %	512.1%	1.685	0.9	0.5	0.1	-0.0
126-B-4-R-2-5-7-9	-26.6 %	45.6 %	573.8%	1.685	0.9	0.5	0.1	-0.0
129-B-4-R-2-10-7-7	-24.6 %	31.8 %	269.8%	1.690	0.6	0.5	0.1	0.0
130-B-4-R-2-10-7-9	-24.6 %	86.1 %	308.0%	1.690	0.6	0.5	0.1	-0.0
138-TB-4-R-3-5-7-9	-27.2 %	41.0 %	477.4%	2.679	0.4	0.4	0.1	0.0
124-TB-4-R-2-2-9-9	-12.1 %	79.5 %	462.8%	1.700	0.4	0.4	0.1	0.0
137-TB-4-R-3-5-7-7	-27.2 %	10.9 %	410.0%	2.680	0.3	0.4	0.1	0.0
141-TB-4-R-3-10-7-7	-25.7 %	18.1 %	242.4%	2.679	0.3	0.4	0.0	0.0
136-P-4-R-3-2-9-9	61.1 %	-31.9 %	-31.9%	2.694	1.2	0.3	0.1	0.0
128-TB-4-R-2-5-9-9	-9.0 %	41.2 %	457.4%	1.706	0.4	0.2	0.1	0.0
109-B-4-R-1-2-7-7	-31.9 %	-23.9 %	442.3%	0.751	0.2	0.2	0.1	0.0
110-B-4-R-1-2-7-9	-31.9 %	-1.3 %	430.9%	0.751	0.2	0.2	0.1	0.0
123-P-4-R-2-2-9-7	57.5 %	-42.7 %	-42.7%	1.704	0.4	0.2	0.1	0.0
124-P-4-R-2-2-9-9	57.2 %	-33.4 %	-33.4%	1.704	0.5	0.2	0.1	0.0
114-B-4-R-1-5-7-9	-26.6 %	41.6 %	464.7%	0.751	0.2	0.1	0.1	0.0
113-B-4-R-1-5-7-7	-26.6 %	6.1 %	461.4%	0.751	0.2	0.1	0.1	0.0
125-TB-4-R-2-5-7-7	-27.2 %	9.5 %	403.4%	1.692	0.2	0.1	0.1	0.0
126-TB-4-R-2-5-7-9	-27.2 %	42.1 %	460.4%	1.692	0.2	0.1	0.1	0.0
122-TB-4-R-2-2-7-9	-31.7 %	69.4 %	468.1%	1.691	0.3	0.1	0.1	0.0
127-P-4-R-2-5-9-7	48.8 %	-23.1 %	-23.1%	1.705	0.5	0.1	0.1	0.0
115-B-4-R-1-5-9-7	-8.8 %	6.5 %	457.7%	0.759	0.3	0.1	0.1	0.0
116-B-4-R-1-5-9-9	-8.8 %	43.6 %	459.5%	0.759	0.3	0.1	0.1	0.0
144-P-4-R-3-10-9-9	48.5 %	48.5 %	48.5%	2.695	0.6	0.1	0.0	0.0
112-B-4-R-1-2-9-9	-12.5 %	0.0 %	459.6%	0.759	0.3	0.1	0.1	-0.0
111-B-4-R-1-2-9-7	-12.5 %	-24.5 %	441.8%	0.759	0.3	0.1	0.1	-0.0
107-B-2-R-3-10-9-7	55.7 %	57.0 %	57.0%	1.351	0.4	0.1	0.0	0.0
131-P-4-R-2-10-9-7	46.8 %	121.9 %	46.8%	1.705	0.4	0.1	0.0	0.0
117-B-4-R-1-10-7-7	-24.6 %	22.4 %	243.4%	0.750	0.2	0.1	0.0	0.0
118-B-4-R-1-10-7-9	-24.6 %	31.4 %	268.5%	0.750	0.2	0.1	0.0	0.0
137-P-4-R-3-5-7-7	25.0 %	-7.8 %	-7.8%	2.684	0.5	0.1	0.0	0.0
119-B-4-R-1-10-9-7	-8.1 %	31.6 %	269.2%	0.759	0.2	0.1	0.1	0.0
120-B-4-R-1-10-9-9	-8.1 %	41.2 %	296.2%	0.759	0.2	0.1	0.1	0.0
92-B-2-R-2-5-9-9	78.6 %	-1.0 %	-1.0%	0.854	0.3	0.1	0.0	0.0
122-P-4-R-2-2-7-9	34.5 %	-25.5 %	-39.1%	1.690	0.3	0.1	0.0	0.0
97-B-2-R-3-2-7-7	73.3 %	-25.2 %	-36.1%	1.344	0.4	0.1	0.0	0.0
142-P-4-R-3-10-7-9	21.9 %	21.9 %	21.9%	2.684	0.2	0.1	0.0	0.0
130-TB-4-R-2-10-7-9	-25.7 %	38.7 %	302.3%	1.690	0.2	0.1	0.0	0.0
129-TB-4-R-2-10-7-7	-25.7 %	14.8 %	232.9%	1.690	0.2	0.1	0.0	0.0
121-P-4-R-2-2-7-7	33.6 %	-41.5 %	-41.5%	1.690	0.2	0.1	0.0	0.0
88-B-2-R-2-2-9-9	123.0 %	-20.2 %	-29.3%	0.853	0.3	0.1	0.1	0.0

Continued on next page

Table 4.7 Sorted by Maximum Transverse Reinforcement Stress – *Continued from previous page*

Filename	AAR+Shear			AAR Only				
	K	V_{ult}	V_{yld}	Δ_{ver}	σ^{lan}_{max}	σ^{tra}_{max}	σ^{lan}_{med}	σ^{tra}_{med}
		$\frac{(AAR+x)-x}{x} \times 100$		mm		MPa		
98-B-2-R-3-2-7-9	73.3 %	-15.4 %	-22.5%	1.344	0.4	0.1	0.0	0.0
95-B-2-R-2-10-9-7	53.7 %	55.1 %	55.1%	0.853	0.2	0.1	0.0	0.0
103-TB-2-R-3-5-9-7	-11.3 %	-18.7 %	234.4%	1.352	0.1	0.1	0.0	0.0
106-B-2-R-3-10-7-9	27.6 %	72.3 %	72.3%	1.344	0.2	0.1	0.0	0.0
115-TB-4-R-1-5-9-7	-9.0 %	8.8 %	376.9%	0.760	0.1	0.1	0.0	0.0
116-TB-4-R-1-5-9-9	-9.0 %	38.7 %	379.0%	0.760	0.1	0.1	0.0	0.0
119-TB-4-R-1-10-9-7	-8.4 %	13.0 %	227.6%	0.760	0.1	0.1	0.0	0.0
105-B-2-R-3-10-7-7	27.6 %	48.1 %	34.9%	1.344	0.2	0.1	0.0	-0.0
120-TB-4-R-1-10-9-9	-8.4 %	33.6 %	287.5%	0.760	0.1	0.1	0.0	0.0
112-TB-4-R-1-2-9-9	-12.1 %	77.2 %	385.5%	0.761	0.1	0.1	0.0	0.0
96-B-2-R-2-10-9-9	56.0 %	98.4 %	98.4%	0.853	0.2	0.1	0.0	-0.0
113-TB-4-R-1-5-7-7	-27.2 %	4.8 %	376.3%	0.751	0.1	0.1	0.0	0.0
114-TB-4-R-1-5-7-9	-27.2 %	40.3 %	375.9%	0.751	0.1	0.1	0.0	0.0
99-TB-2-R-3-2-9-7	-11.5 %	-24.7 %	349.8%	1.352	0.2	0.0	0.0	0.0
86-B-2-R-2-2-7-9	76.7 %	-17.9 %	-30.4%	0.847	0.2	0.0	0.0	0.0
85-B-2-R-2-2-7-7	76.7 %	-23.7 %	-37.1%	0.847	0.2	0.0	0.0	0.0
125-P-4-R-2-5-7-7	24.4 %	-14.5 %	-14.5%	1.691	0.3	0.0	0.0	0.0
107-TB-2-R-3-10-9-7	-10.1 %	-5.6 %	159.3%	1.352	0.1	0.0	0.0	0.0
87-TB-2-R-2-2-9-7	-11.5 %	-25.0 %	347.6%	0.854	0.1	0.0	0.0	0.0
129-P-4-R-2-10-7-7	21.7 %	21.7 %	21.7%	1.692	0.2	0.0	0.0	0.0
118-TB-4-R-1-10-7-9	-25.7 %	23.3 %	257.7%	0.751	0.1	0.0	0.0	0.0
117-TB-4-R-1-10-7-7	-25.7 %	9.9 %	218.7%	0.751	0.1	0.0	0.0	0.0
91-TB-2-R-2-5-9-7	-11.4 %	-19.4 %	231.4%	0.855	0.1	0.0	0.0	0.0
100-P-2-R-3-2-9-9	68.2 %	-18.6 %	-8.6%	1.353	0.3	0.0	0.0	0.0
93-B-2-R-2-10-7-7	27.6 %	30.6 %	30.6%	0.847	0.1	0.0	0.0	-0.0
95-TB-2-R-2-10-9-7	-10.1 %	-8.4 %	151.6%	0.855	0.1	0.0	0.0	0.0
94-B-2-R-2-10-7-9	27.6 %	71.4 %	71.4%	0.847	0.1	0.0	0.0	-0.0
126-P-4-R-2-5-7-9	24.7 %	-7.9 %	-7.9%	1.691	0.2	0.0	0.0	0.0
76-B-2-R-1-2-9-9	118.3 %	-19.7 %	-42.5%	0.381	0.1	0.0	0.0	0.0
88-TB-2-R-2-2-9-9	-11.5 %	-6.0 %	345.2%	0.855	0.1	0.0	0.0	0.0
75-B-2-R-1-2-9-7	115.9 %	-32.0 %	-42.7%	0.381	0.1	0.0	0.0	0.0
112-P-4-R-1-2-9-9	45.5 %	-37.3 %	-76.9%	0.761	0.1	0.0	0.0	0.0
111-P-4-R-1-2-9-7	43.7 %	-47.8 %	-77.2%	0.761	0.1	0.0	0.0	0.0
120-P-4-R-1-10-9-9	40.9 %	40.9 %	40.9%	0.760	0.1	0.0	0.0	0.0
119-P-4-R-1-10-9-7	26.6 %	26.6 %	-23.9%	0.760	0.1	0.0	0.0	0.0
79-B-2-R-1-5-9-7	75.4 %	-20.4 %	-25.3%	0.381	0.1	0.0	0.0	0.0
80-B-2-R-1-5-9-9	77.0 %	-6.8 %	-6.8%	0.381	0.1	0.0	0.0	0.0
92-TB-2-R-2-5-9-9	-11.4 %	-2.3 %	301.8%	0.855	0.1	0.0	0.0	0.0
90-B-2-R-2-5-7-9	44.6 %	16.3 %	16.3%	0.846	0.1	0.0	0.0	0.0
83-B-2-R-1-10-9-7	53.4 %	49.3 %	49.3%	0.381	0.1	0.0	0.0	0.0
99-P-2-R-3-2-9-7	67.0 %	-41.1 %	-23.4%	1.352	0.3	0.0	0.0	0.0
84-B-2-R-1-10-9-9	54.6 %	51.2 %	51.2%	0.381	0.1	0.0	0.0	0.0
130-P-4-R-2-10-7-9	21.5 %	21.5 %	21.5%	1.691	0.2	0.0	0.0	0.0
115-P-4-R-1-5-9-7	40.8 %	-27.2 %	-27.2%	0.760	0.1	0.0	0.0	0.0
116-P-4-R-1-5-9-9	40.3 %	-6.3 %	-6.3%	0.760	0.1	0.0	0.0	0.0
86-TB-2-R-2-2-7-9	-31.4 %	-7.8 %	347.1%	0.847	0.0	0.0	0.0	0.0
89-TB-2-R-2-5-7-7	-27.5 %	-23.4 %	215.0%	0.847	0.0	0.0	0.0	0.0
107-P-2-R-3-10-9-7	41.4 %	30.1 %	36.5%	1.352	0.2	0.0	0.0	0.0
108-P-2-R-3-10-9-9	42.5 %	31.2 %	37.6%	1.352	0.2	0.0	0.0	0.0
104-P-2-R-3-5-9-9	52.8 %	6.9 %	6.9%	1.353	0.1	0.0	0.0	0.0
113-P-4-R-1-5-7-7	20.4 %	-17.1 %	-17.1%	0.752	0.1	0.0	0.0	0.0

Continued on next page

Table 4.7 Sorted by Maximum Transverse Reinforcement Stress – *Continued from previous page*

Filename	AAR+Shear			AAR Only				
	K	V_{ult}	V_{yld}	Δ_{ver}	σ^{lan}_{max}	σ^{tra}_{max}	σ^{lan}_{med}	σ^{tra}_{med}
		$\frac{(AAR+x)-x}{x} \times 100$		mm	MPa			
114-P-4-R-1-5-7-9	21.0 %	0.9 %	0.9%	0.752	0.1	0.0	0.0	0.0
109-P-4-R-1-2-7-7	26.8 %	-45.6 %	-45.6%	0.752	0.1	0.0	0.0	0.0
110-P-4-R-1-2-7-9	25.1 %	-36.5 %	-44.3%	0.752	0.1	0.0	0.0	0.0
85-TB-2-R-2-2-7-7	-31.4 %	-28.8 %	324.8%	0.847	0.1	0.0	0.0	0.0
88-P-2-R-2-2-9-9	67.9 %	-19.6 %	-9.3%	0.855	0.1	0.0	0.0	0.0
90-TB-2-R-2-5-7-9	-27.5 %	-4.6 %	292.4%	0.847	0.0	0.0	0.0	0.0
117-P-4-R-1-10-7-7	20.1 %	20.1 %	20.1%	0.752	0.1	0.0	0.0	0.0
118-P-4-R-1-10-7-9	20.4 %	20.4 %	20.4%	0.752	0.1	0.0	0.0	0.0
94-TB-2-R-2-10-7-9	-26.0 %	5.8 %	190.6%	0.847	0.0	0.0	0.0	0.0
87-P-2-R-2-2-9-7	64.7 %	-27.5 %	-13.9%	0.855	0.2	0.0	0.0	0.0
92-P-2-R-2-5-9-9	51.6 %	5.8 %	5.8%	0.855	0.1	0.0	0.0	0.0
78-B-2-R-1-5-7-9	44.6 %	-4.6 %	-4.6%	0.376	0.0	0.0	0.0	0.0
77-B-2-R-1-5-7-7	44.3 %	-19.7 %	-19.7%	0.376	0.0	0.0	0.0	0.0
73-B-2-R-1-2-7-7	74.3 %	-31.3 %	-43.5%	0.376	0.0	0.0	0.0	0.0
74-B-2-R-1-2-7-9	76.8 %	-18.1 %	-42.9%	0.376	0.0	0.0	0.0	0.0
96-P-2-R-2-10-9-9	41.8 %	30.5 %	36.9%	0.855	0.1	0.0	0.0	0.0
79-TB-2-R-1-5-9-7	-11.4 %	-22.6 %	218.2%	0.381	0.0	0.0	0.0	0.0
95-P-2-R-2-10-9-7	40.7 %	29.4 %	35.8%	0.855	0.1	0.0	0.0	0.0
75-TB-2-R-1-2-9-7	-11.5 %	-27.9 %	287.4%	0.381	0.0	0.0	0.0	0.0
82-B-2-R-1-10-7-9	27.6 %	65.7 %	65.7%	0.376	0.0	0.0	0.0	0.0
76-TB-2-R-1-2-9-9	-11.5 %	-6.2 %	281.3%	0.381	0.0	0.0	0.0	0.0
85-P-2-R-2-2-7-7	40.3 %	-49.4 %	-34.3%	0.847	0.1	0.0	0.0	0.0
81-B-2-R-1-10-7-7	27.5 %	28.3 %	28.3%	0.376	0.0	0.0	0.0	0.0
74-TB-2-R-1-2-7-9	-31.4 %	-10.1 %	275.6%	0.376	0.0	0.0	0.0	0.0
80-TB-2-R-1-5-9-9	-11.4 %	-5.0 %	275.1%	0.381	0.0	0.0	0.0	0.0
84-TB-2-R-1-10-9-9	-10.2 %	3.6 %	184.6%	0.381	0.0	0.0	0.0	0.0
83-TB-2-R-1-10-9-7	-10.2 %	-13.8 %	136.8%	0.381	0.0	0.0	0.0	0.0
90-P-2-R-2-5-7-9	26.2 %	45.1 %	45.1%	0.847	0.0	0.0	0.0	0.0
73-TB-2-R-1-2-7-7	-31.4 %	-29.4 %	276.3%	0.376	0.0	0.0	0.0	0.0
94-P-2-R-2-10-7-9	17.0 %	57.5 %	65.2%	0.847	0.0	0.0	0.0	0.0
93-P-2-R-2-10-7-7	16.6 %	7.3 %	12.6%	0.847	0.0	0.0	0.0	0.0
77-TB-2-R-1-5-7-7	-27.5 %	-26.7 %	201.3%	0.376	0.0	0.0	0.0	0.0
82-TB-2-R-1-10-7-9	-26.0 %	1.7 %	179.2%	0.376	0.0	0.0	0.0	0.0
80-P-2-R-1-5-9-9	42.9 %	12.4 %	12.4%	0.381	0.0	0.0	0.0	0.0
79-P-2-R-1-5-9-7	41.5 %	11.8 %	11.8%	0.381	0.0	0.0	0.0	0.0
81-TB-2-R-1-10-7-7	-26.0 %	-17.5 %	126.4%	0.376	0.0	0.0	0.0	0.0
76-P-2-R-1-2-9-9	54.2 %	-12.3 %	-69.5%	0.381	0.0	0.0	0.0	0.0
75-P-2-R-1-2-9-7	52.3 %	-31.7 %	-69.5%	0.381	0.0	0.0	0.0	0.0
81-P-2-R-1-10-7-7	14.8 %	56.7 %	64.4%	0.376	0.0	0.0	0.0	0.0
84-P-2-R-1-10-9-9	37.7 %	26.7 %	32.9%	0.381	0.0	0.0	0.0	0.0
78-P-2-R-1-5-7-9	23.0 %	38.1 %	38.1%	0.376	0.0	0.0	0.0	0.0
74-P-2-R-1-2-7-9	33.0 %	-8.4 %	-27.1%	0.376	0.0	0.0	0.0	0.0
83-P-2-R-1-10-9-7	-10.9 %	43.5 %	-31.1%	0.381	0.0	0.0	0.0	0.0
82-P-2-R-1-10-7-9	15.5 %	57.4 %	65.0%	0.376	0.0	0.0	0.0	0.0
77-P-2-R-1-5-7-7	24.6 %	16.4 %	16.4%	0.376	0.0	0.0	0.0	0.0
73-P-2-R-1-2-7-7	32.0 %	-25.8 %	-27.3%	0.376	0.0	0.0	0.0	0.0

4.1 INDIVIDUAL RESULTS

4.1.1 BEAM

4.1.1.1 Analysis: 1-B-2-U-1-2-7-7

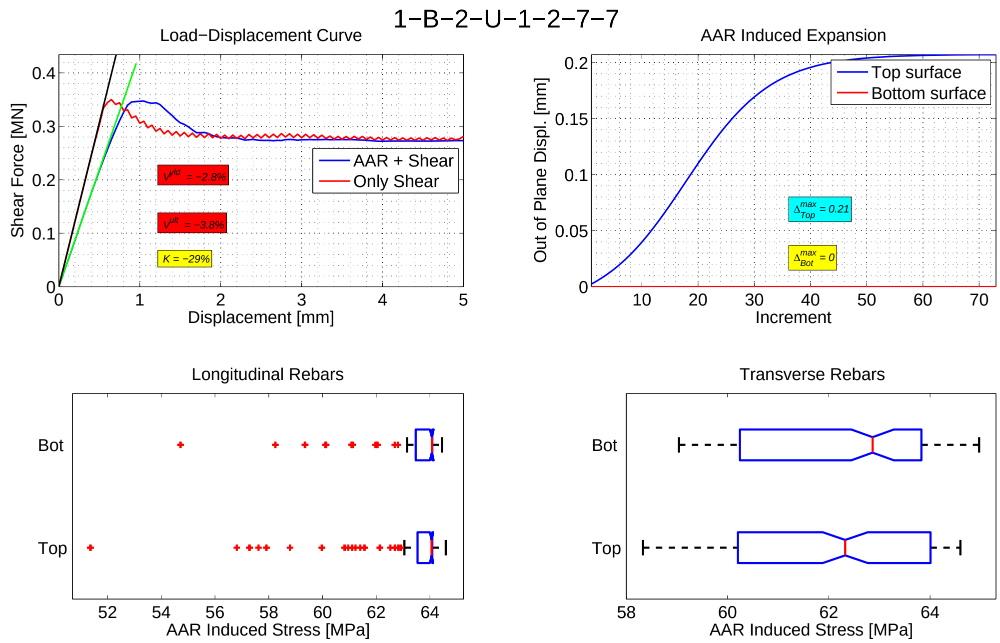

4.1.1.2 Analysis: 2-B-2-U-1-2-7-9

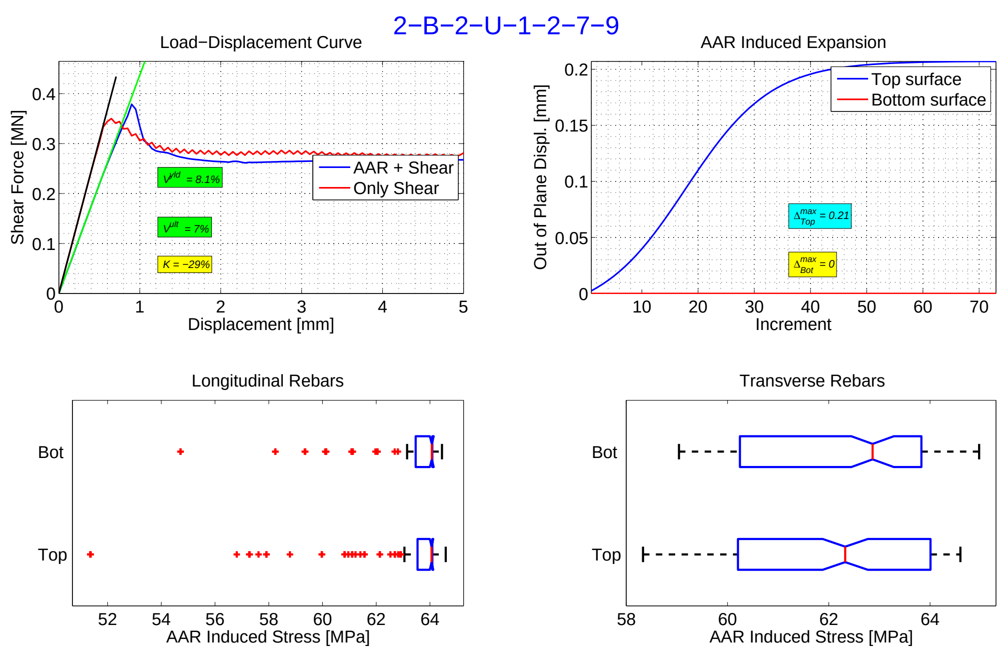

4.1.1.3 Analysis: 3-B-2-U-1-2-9-7

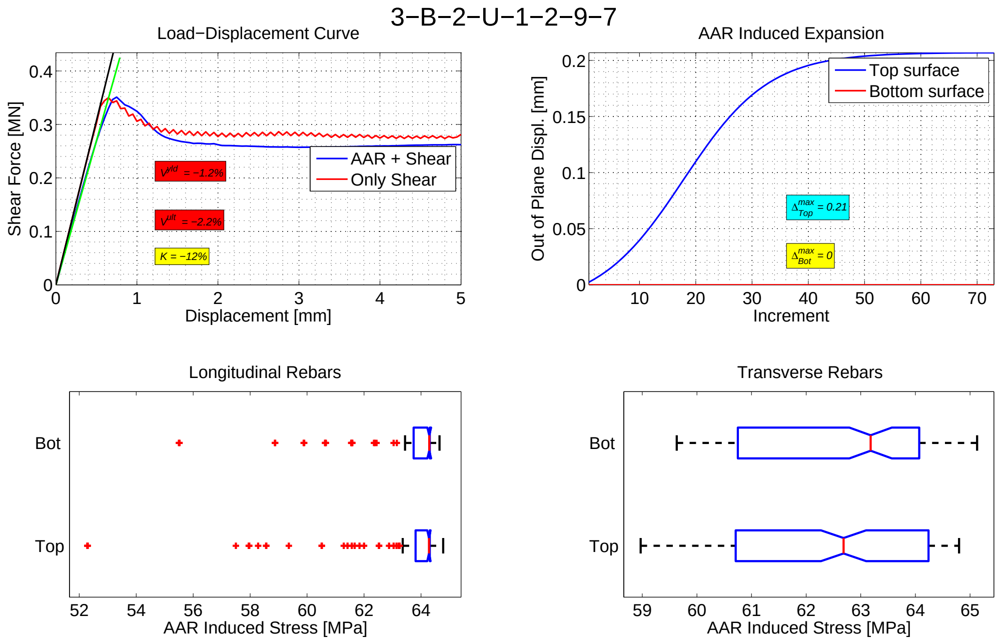

4.1.1.4 Analysis: 4-B-2-U-1-2-9-9

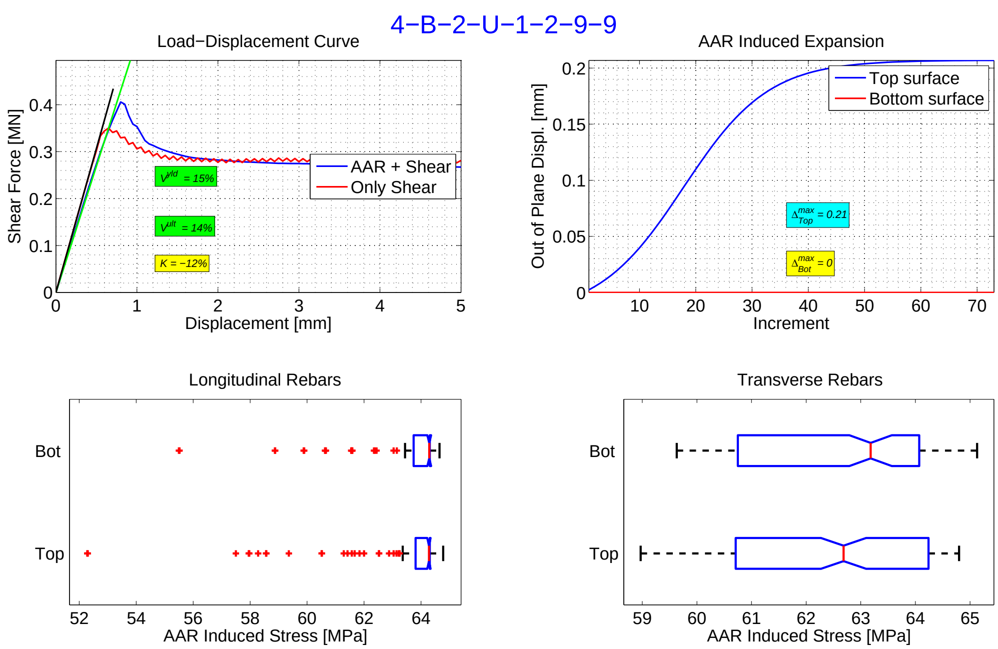

4.1.1.5 Analysis: 5-B-2-U-1-5-7-7

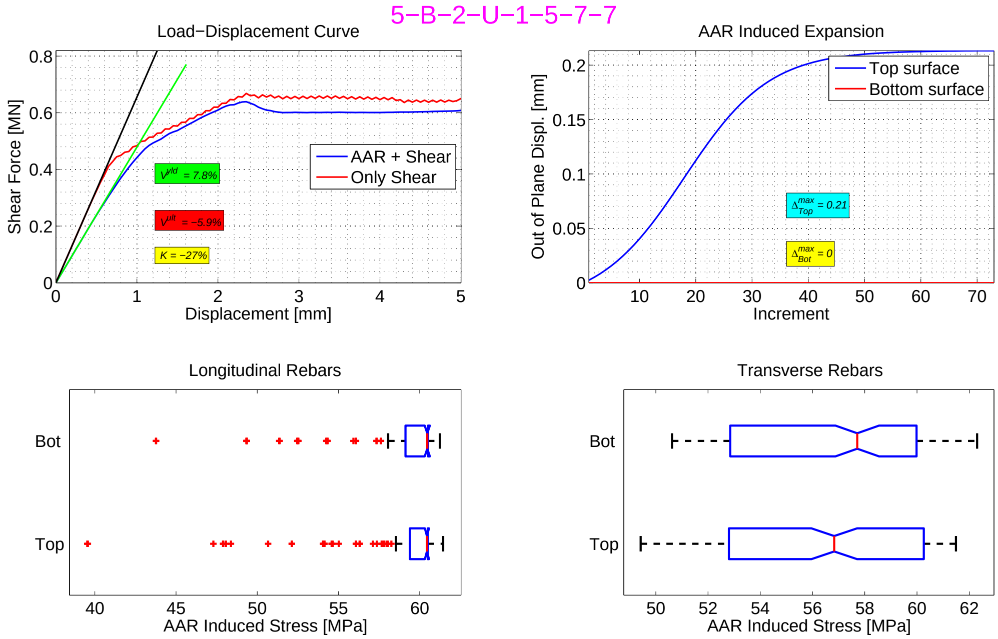

4.1.1.6 Analysis: 6-B-2-U-1-5-7-9

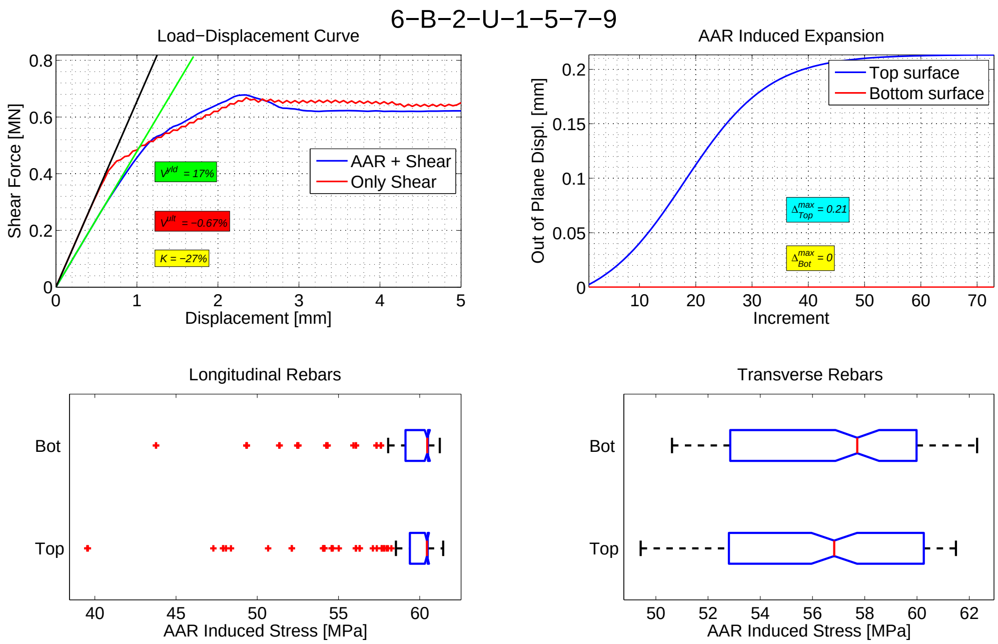

4.1.1.7 Analysis: 7-B-2-U-1-5-9-7

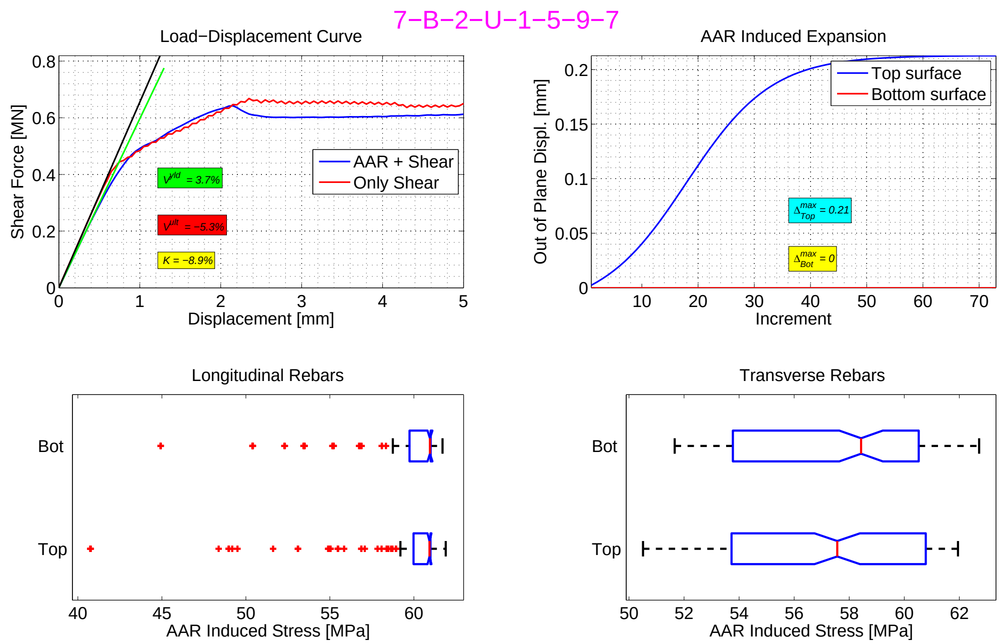

4.1.1.8 Analysis: 8-B-2-U-1-5-9-9

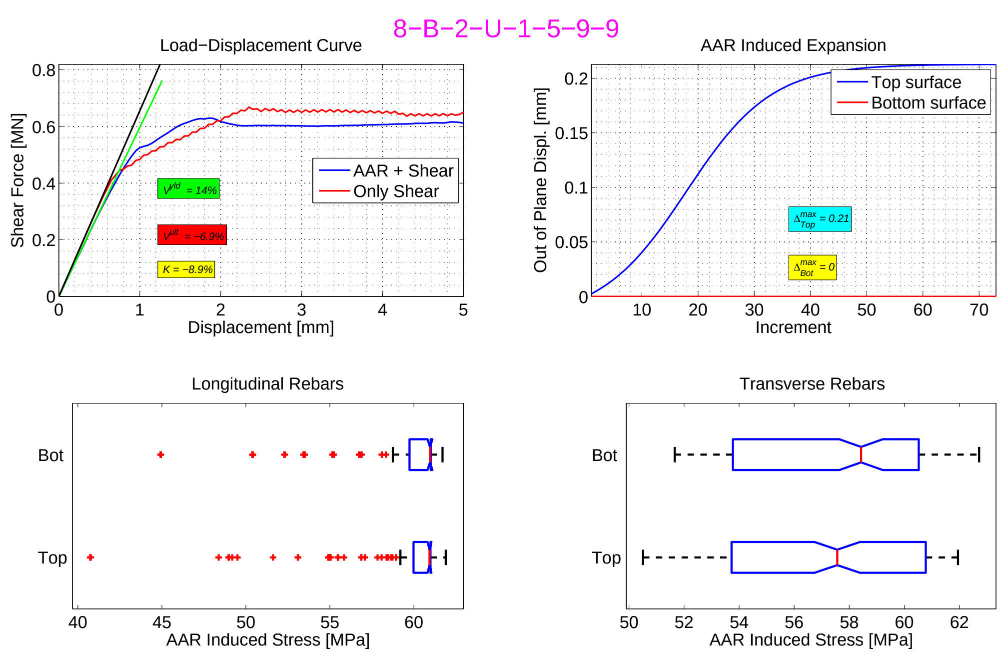

4.1.1.9 Analysis: 9-B-2-U-1-10-7-7

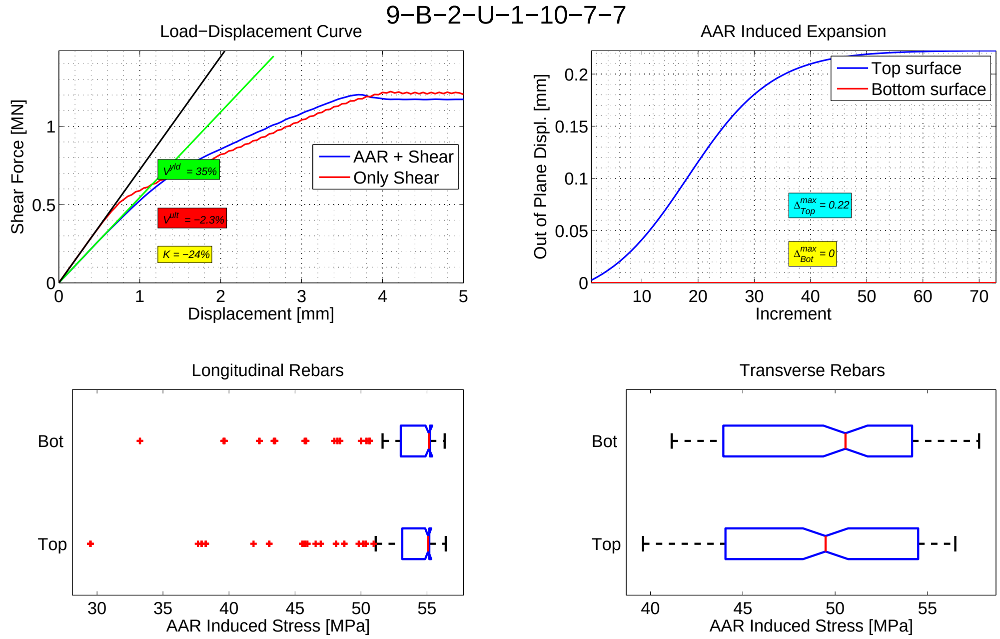

4.1.1.10 Analysis: 10-B-2-U-1-10-7-9

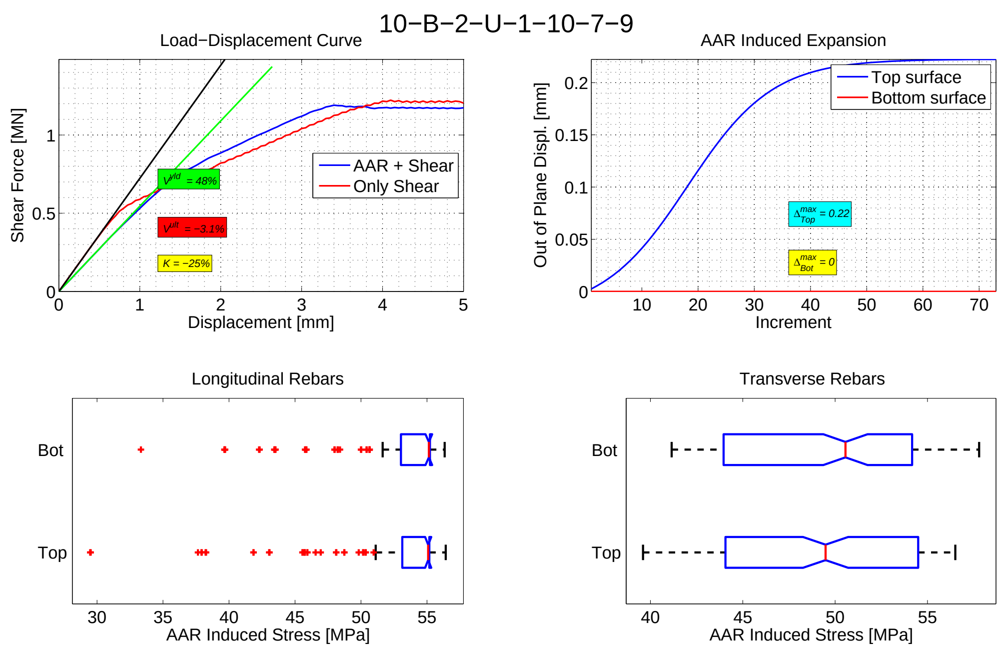

4.1.1.11 Analysis: 11-B-2-U-1-10-9-7

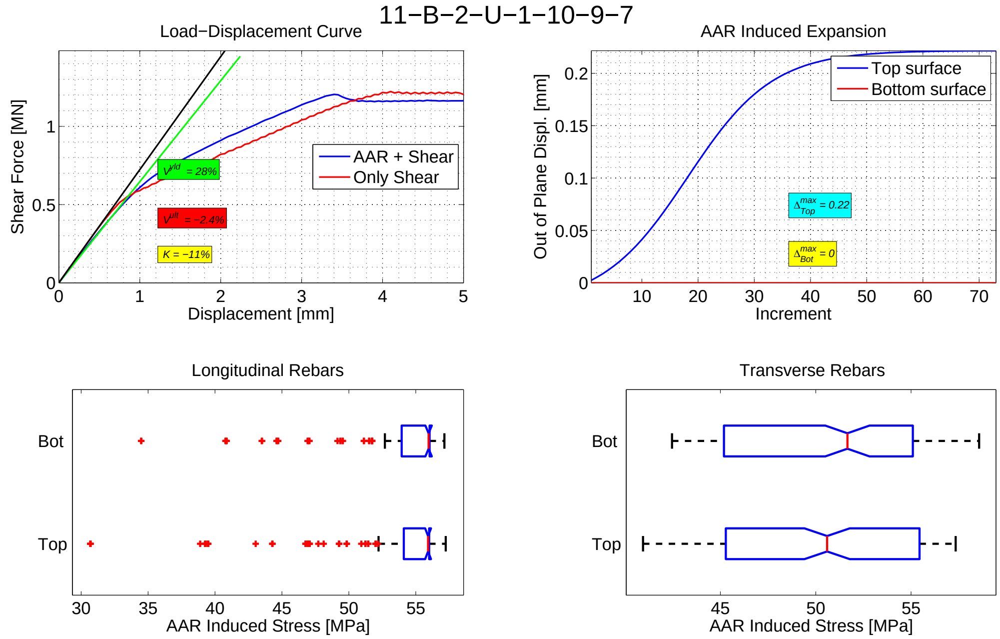

4.1.1.12 Analysis: 12-B-2-U-1-10-9-9

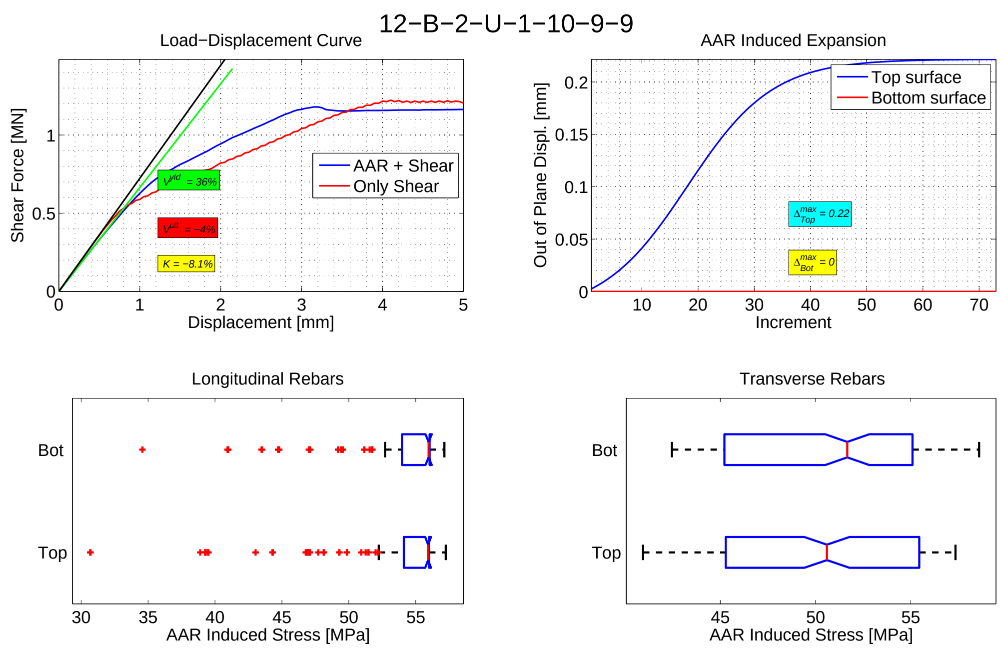

4.1.1.13 Analysis: 13-B-2-U-2-2-7-7

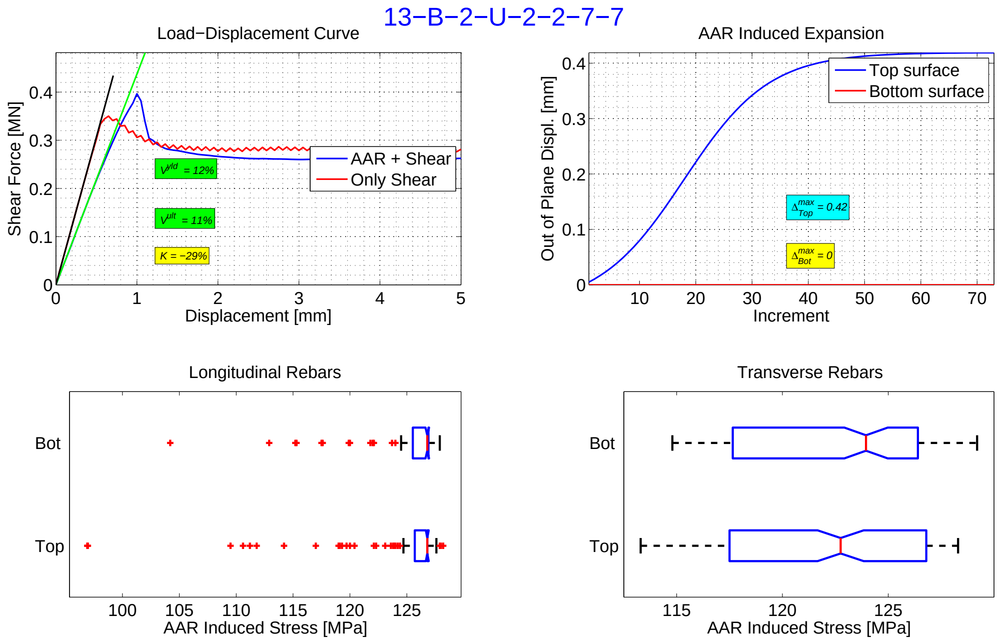

4.1.1.14 Analysis: 14-B-2-U-2-2-7-9

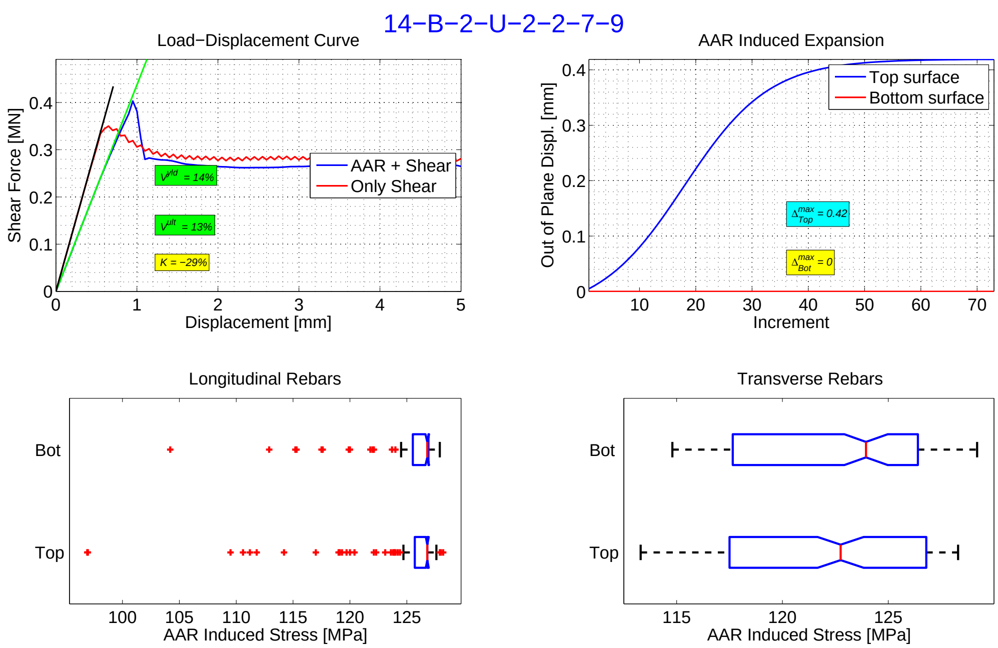

4.1.1.15 Analysis: 15-B-2-U-2-2-9-7

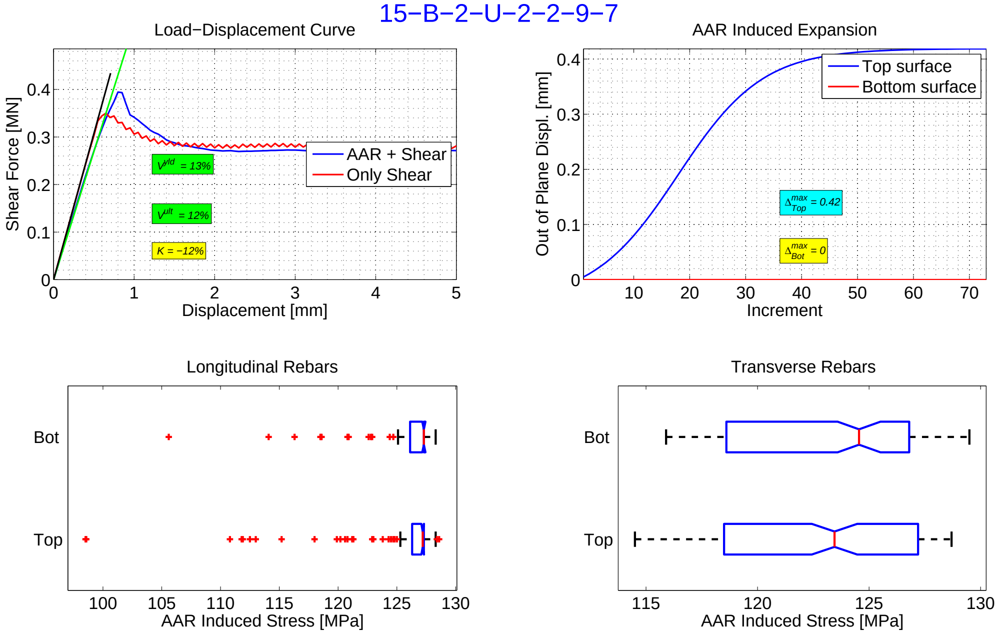

4.1.1.16 Analysis: 16-B-2-U-2-2-9-9

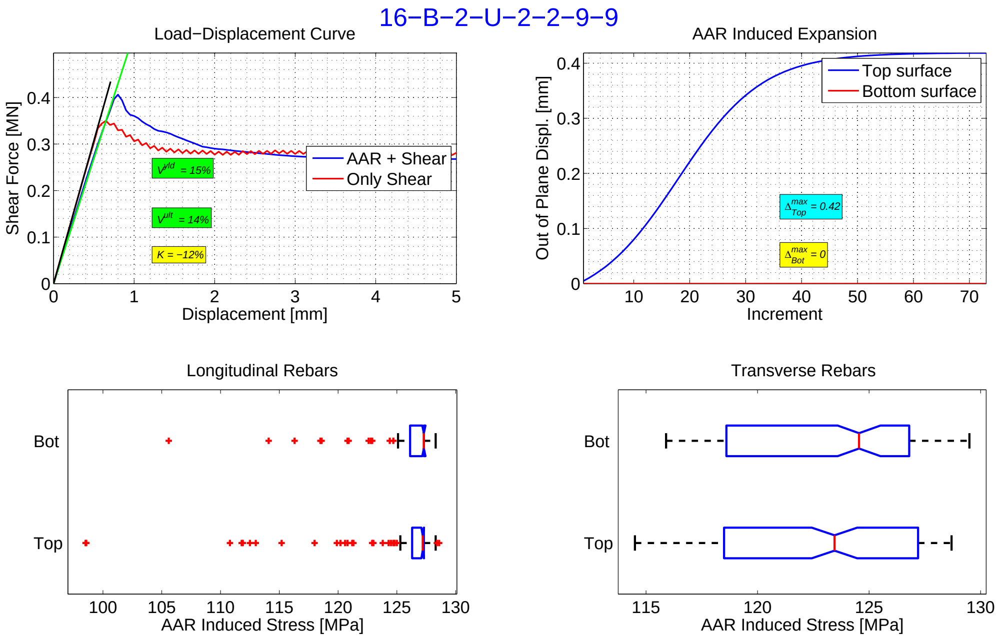

4.1.1.17 Analysis: 17-B-2-U-2-5-7-7

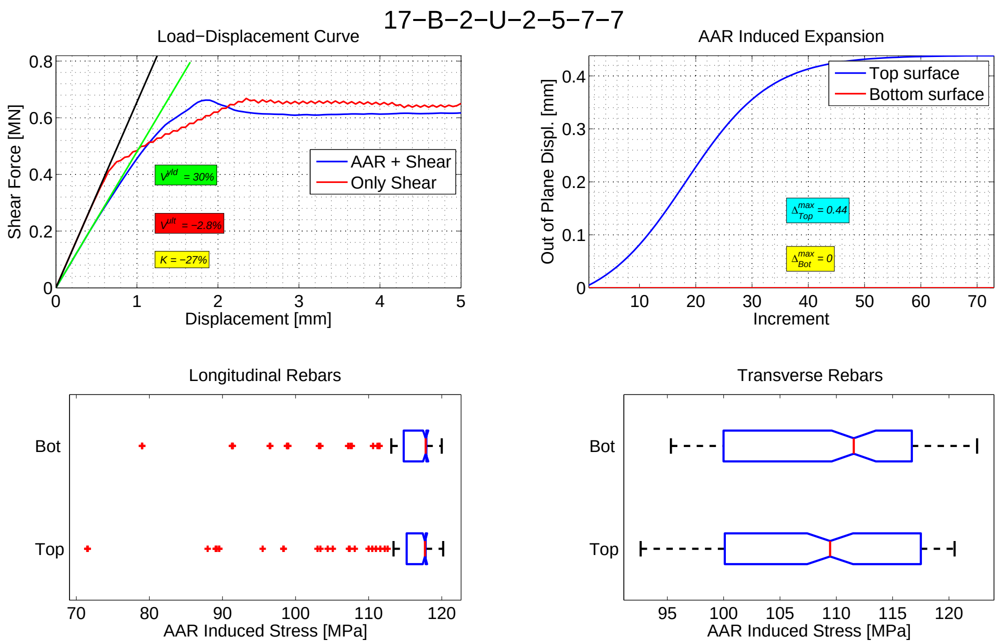

4.1.1.18 Analysis: 18-B-2-U-2-5-7-9

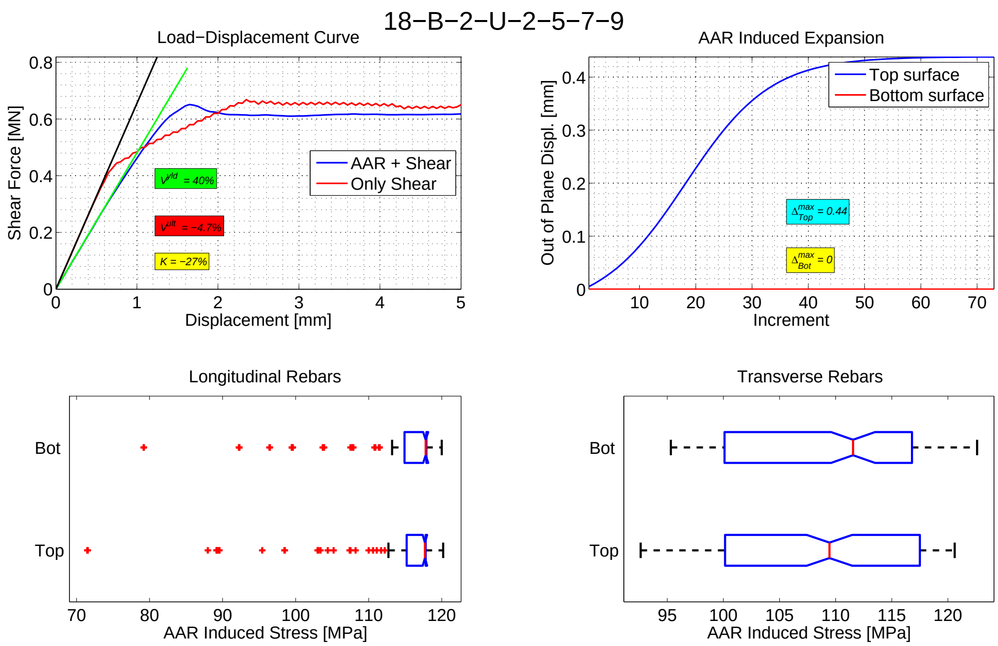

4.1.1.19 Analysis: 19-B-2-U-2-5-9-7

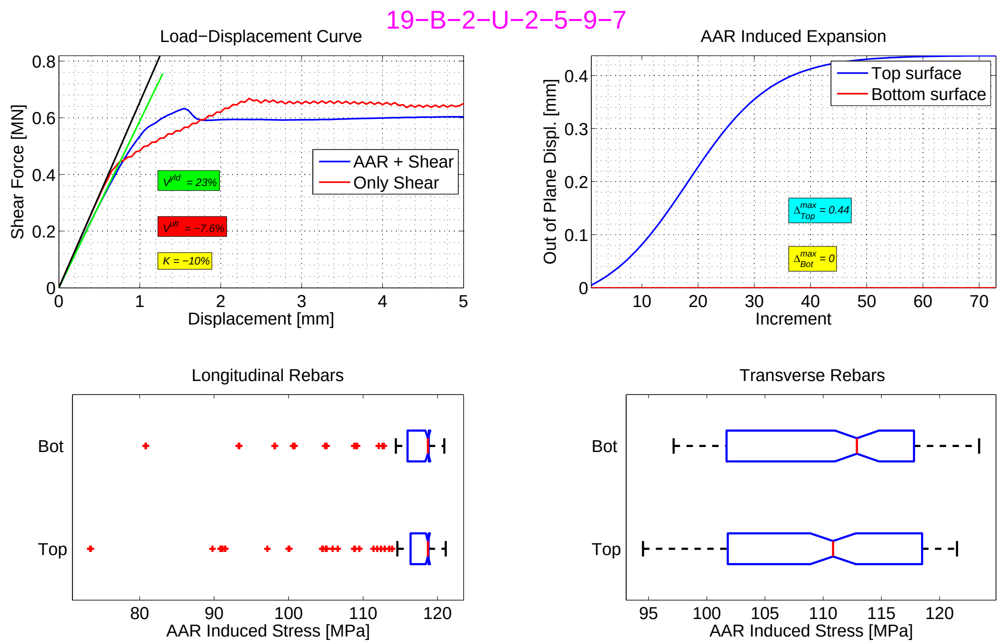

4.1.1.20 Analysis: 20-B-2-U-2-5-9-9

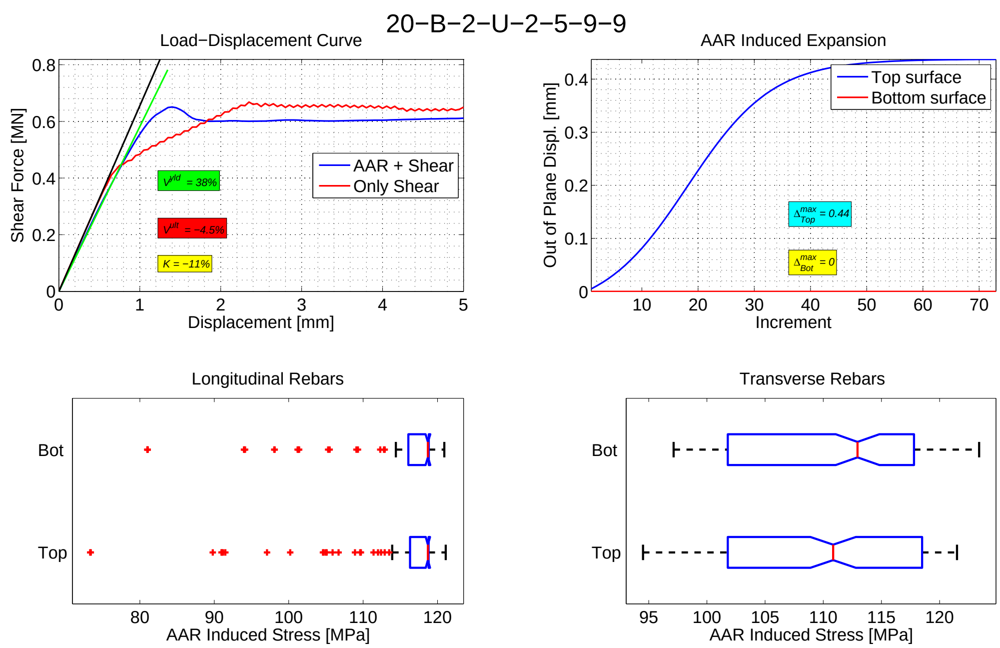

4.1.1.21 Analysis: 21-B-2-U-2-10-7-7

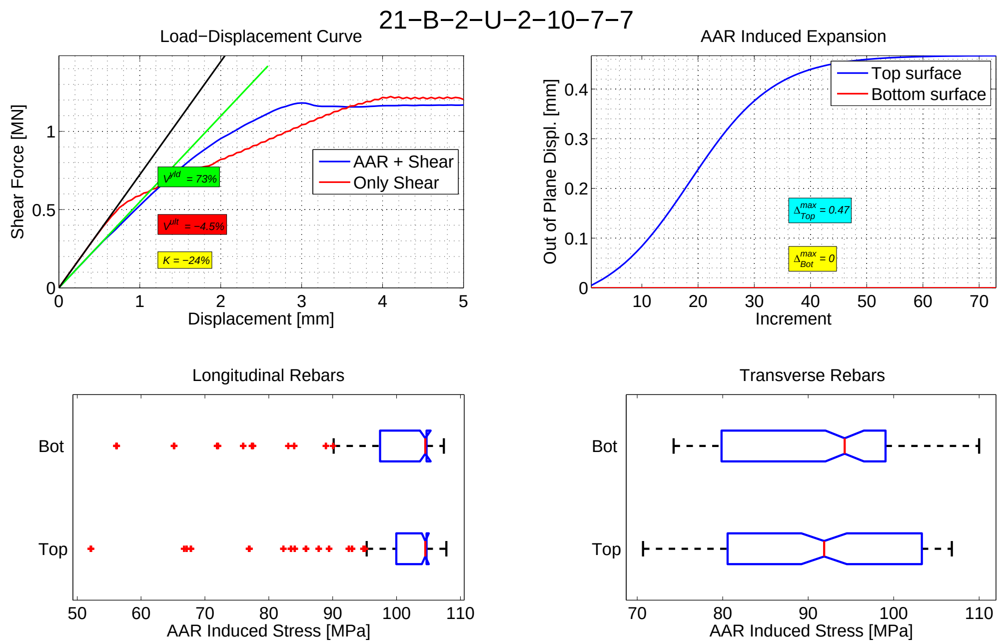

4.1.1.22 Analysis: 22-B-2-U-2-10-7-9

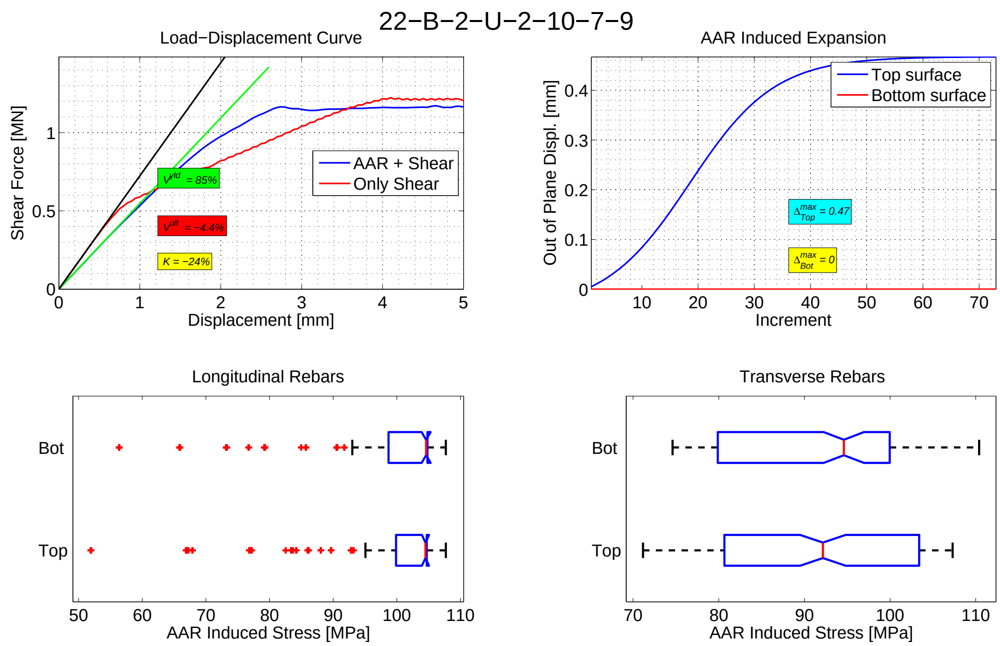

4.1.1.23 Analysis: 23-B-2-U-2-10-9-7

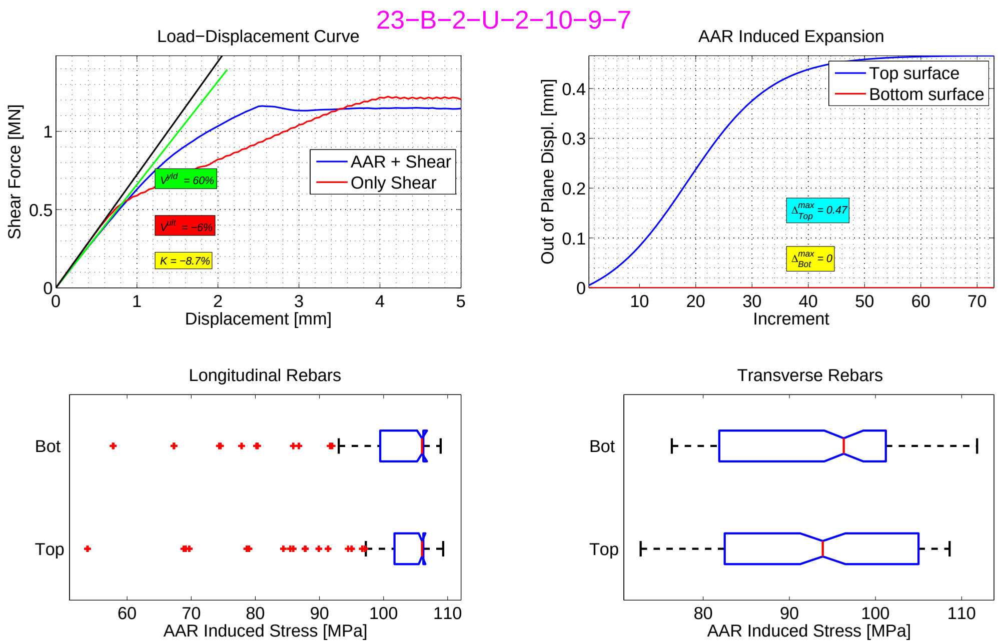

4.1.1.24 Analysis: 24-B-2-U-2-10-9-9

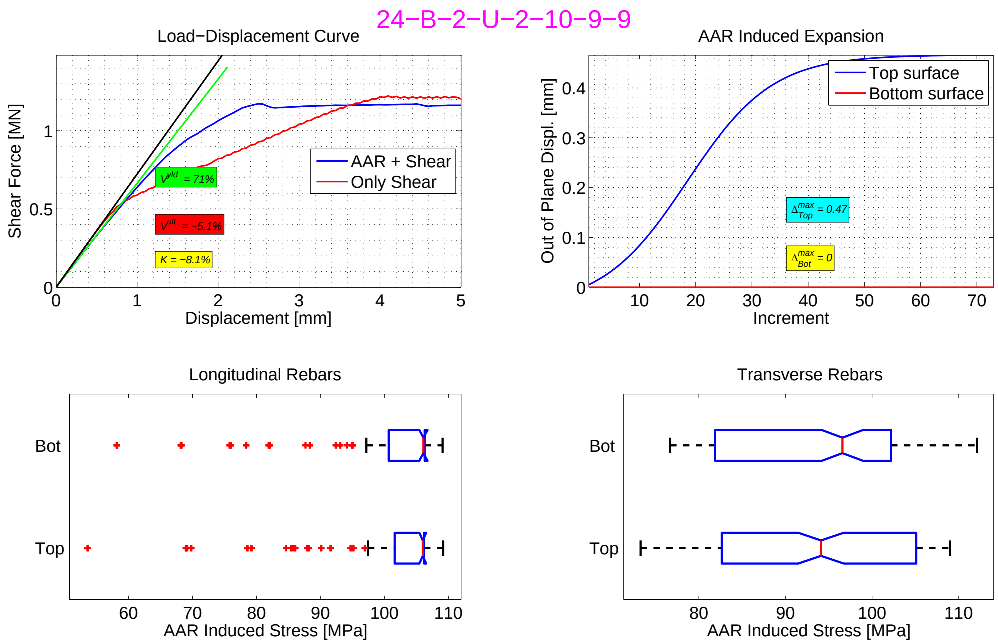

4.1.1.25 Analysis: 25-B-2-U-3-2-7-7

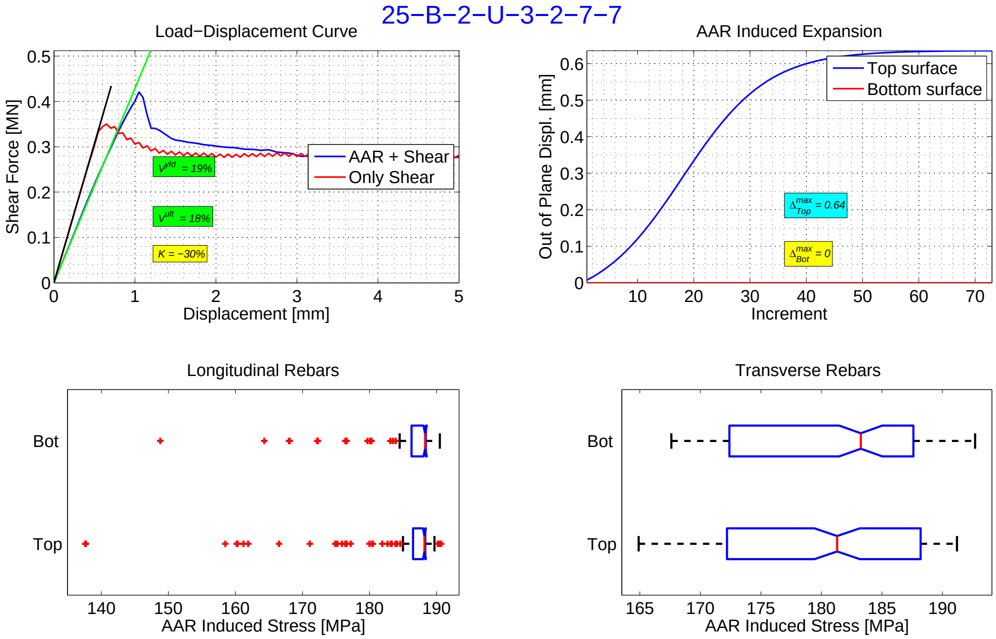

4.1.1.26 Analysis: 26-B-2-U-3-2-7-9

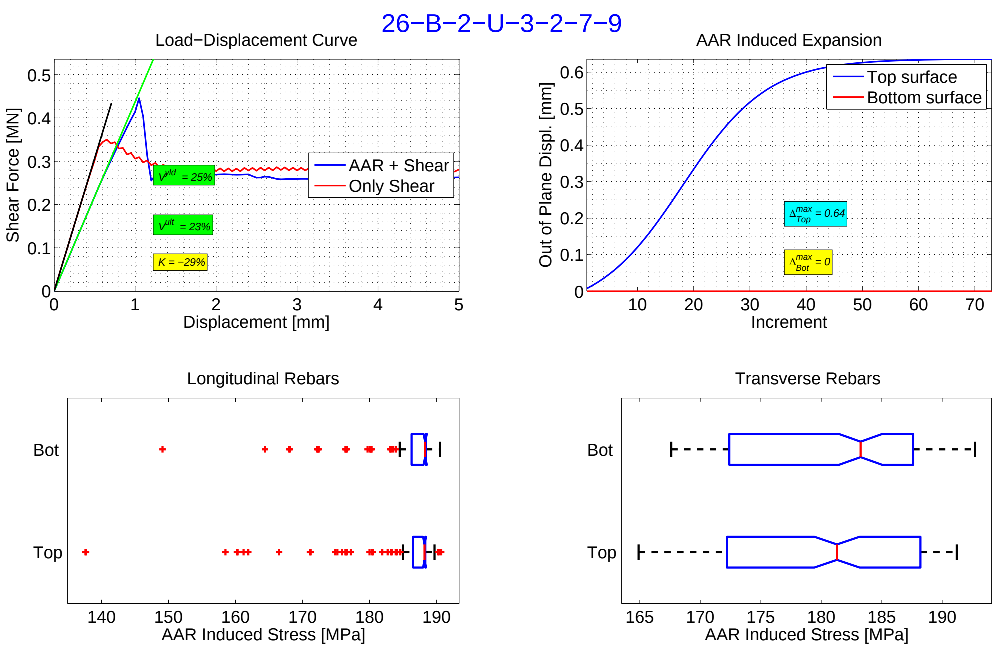

4.1.1.27 Analysis: 27-B-2-U-3-2-9-7

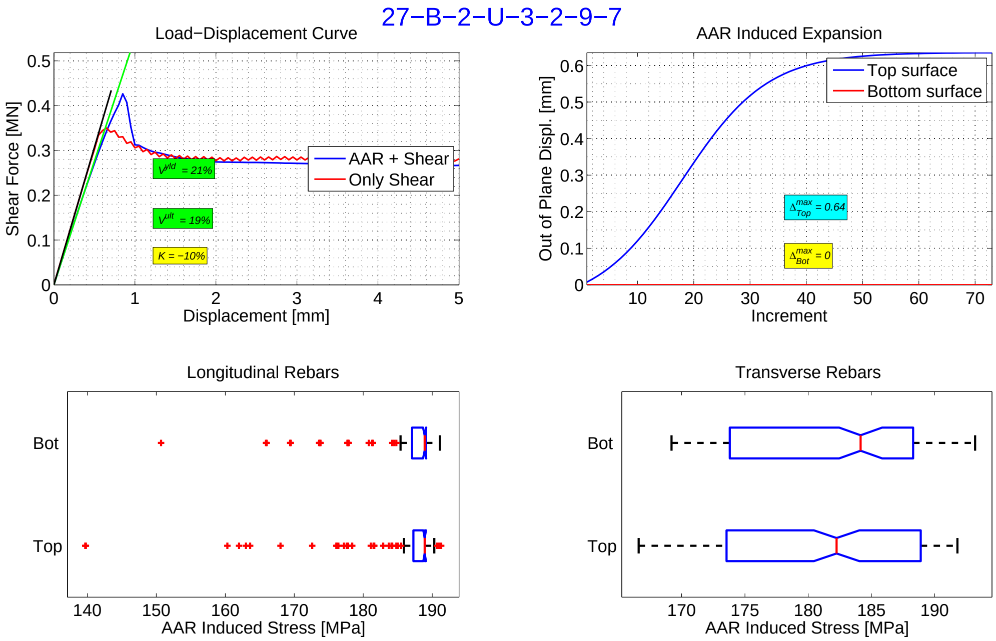

4.1.1.28 Analysis: 28-B-2-U-3-2-9-9

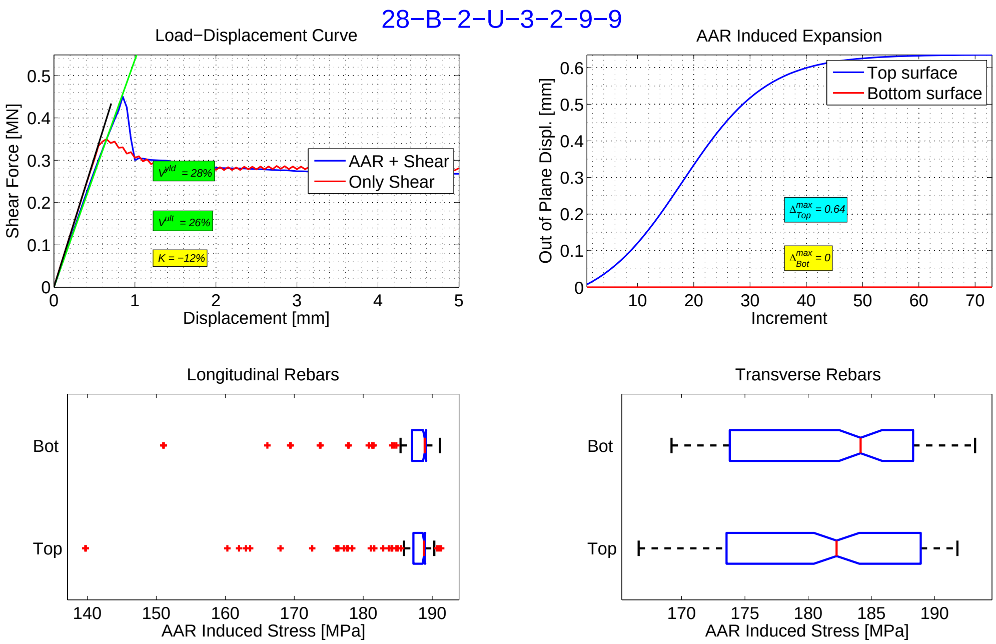

4.1.1.29 Analysis: 29-B-2-U-3-5-7-7

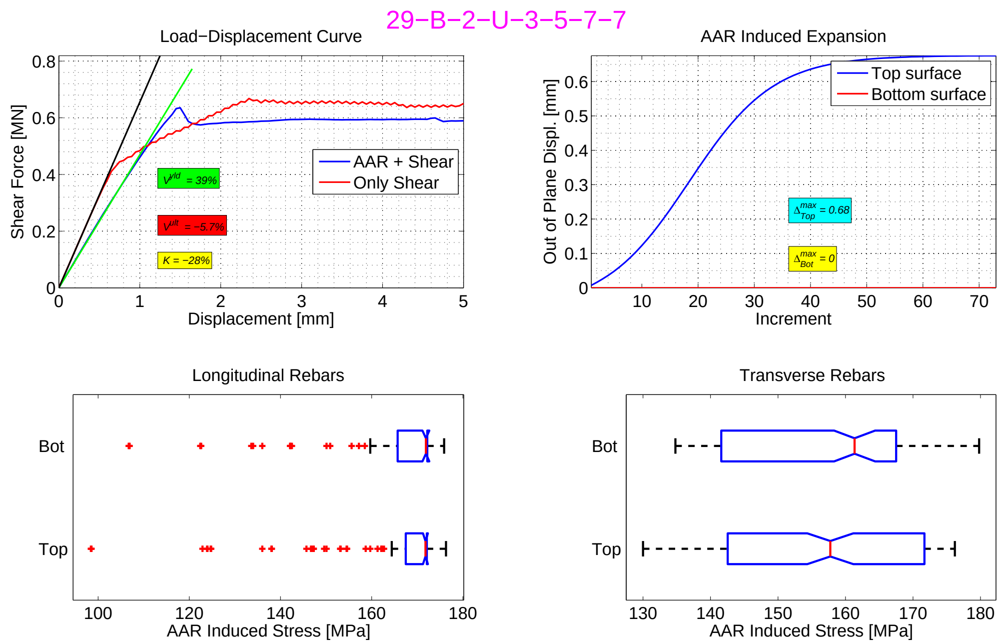

4.1.1.30 Analysis: 30-B-2-U-3-5-7-9

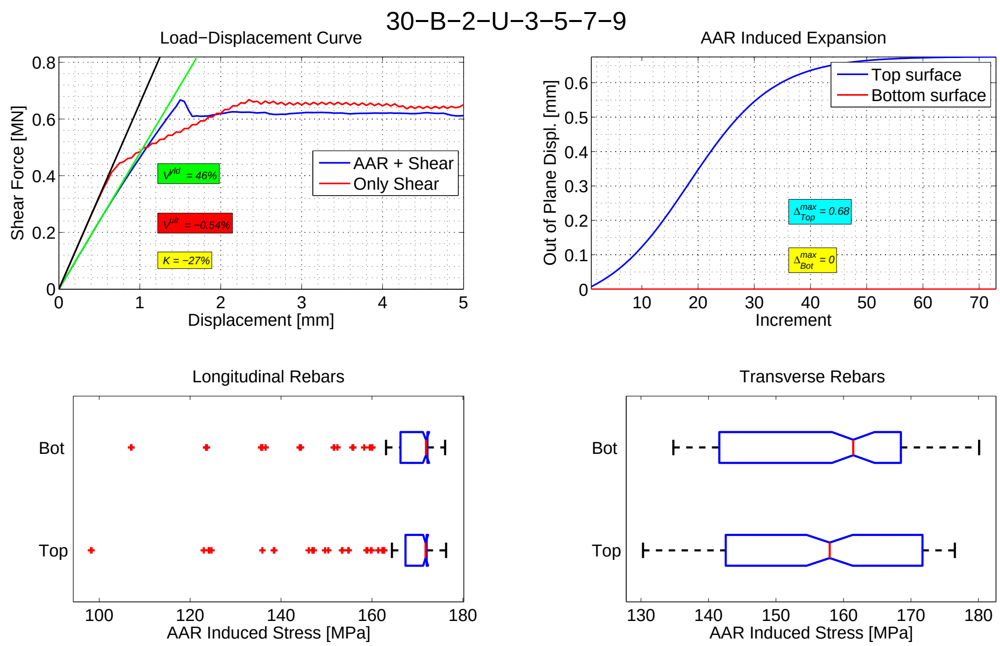

4.1.1.31 Analysis: 31-B-2-U-3-5-9-7

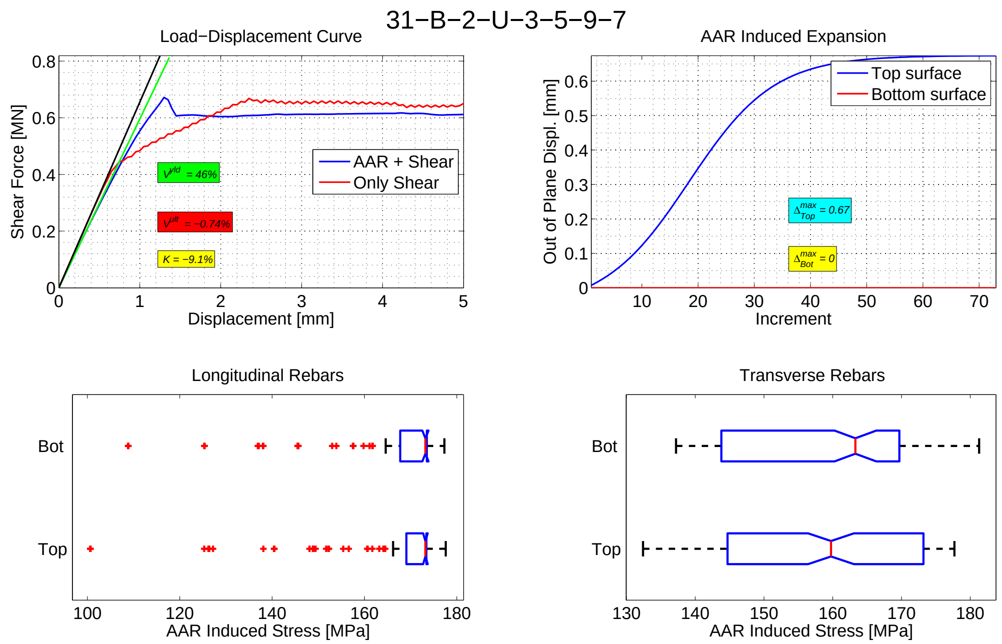

4.1.1.32 Analysis: 32-B-2-U-3-5-9-9

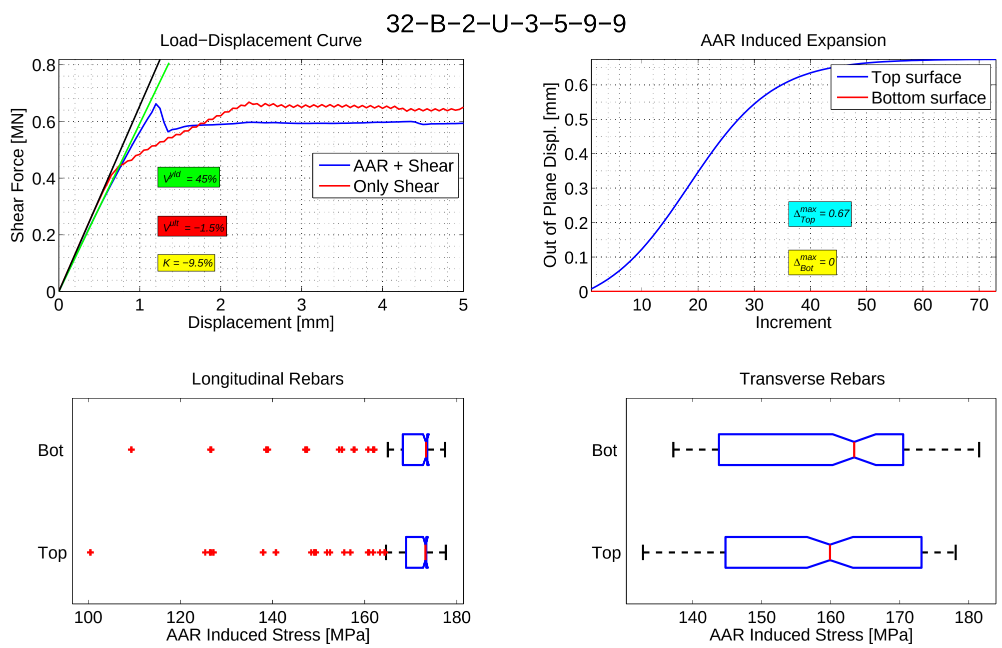

4.1.1.33 Analysis: 33-B-2-U-3-10-7-7

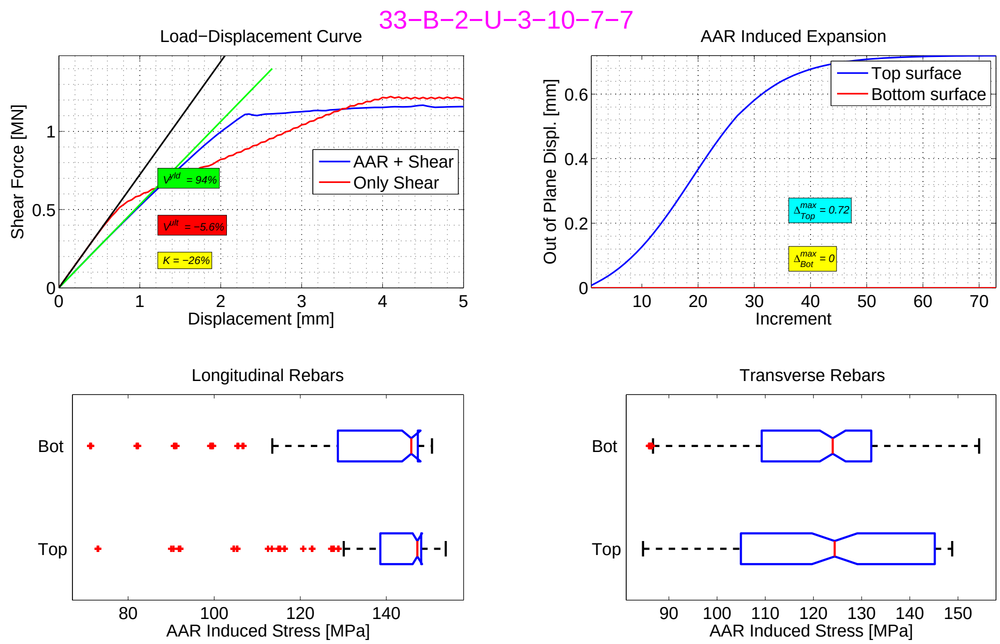

4.1.1.34 Analysis: 34-B-2-U-3-10-7-9

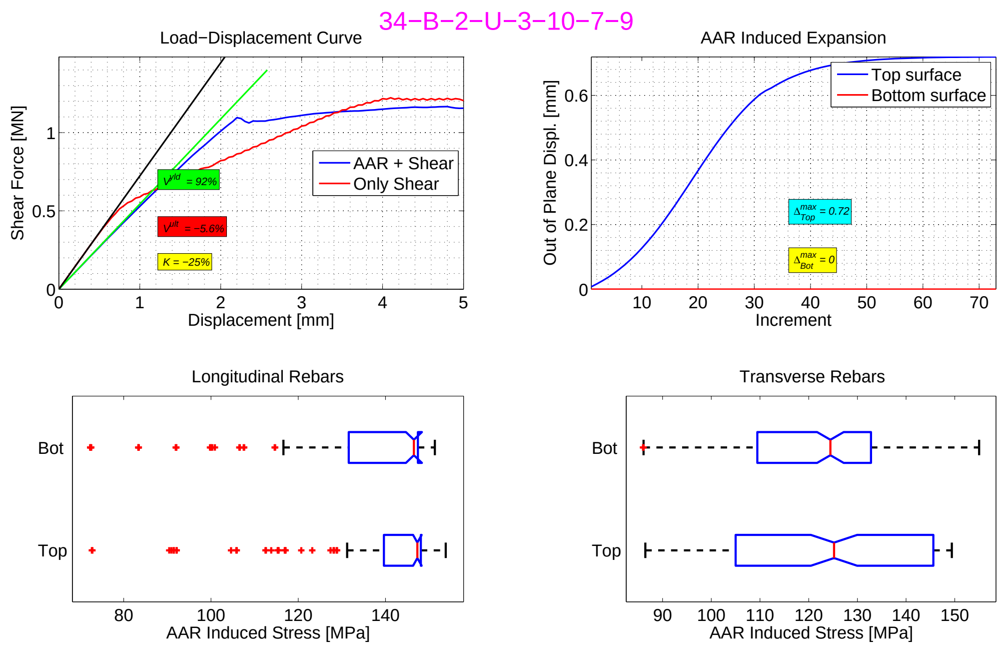

4.1.1.35 Analysis: 35-B-2-U-3-10-9-7

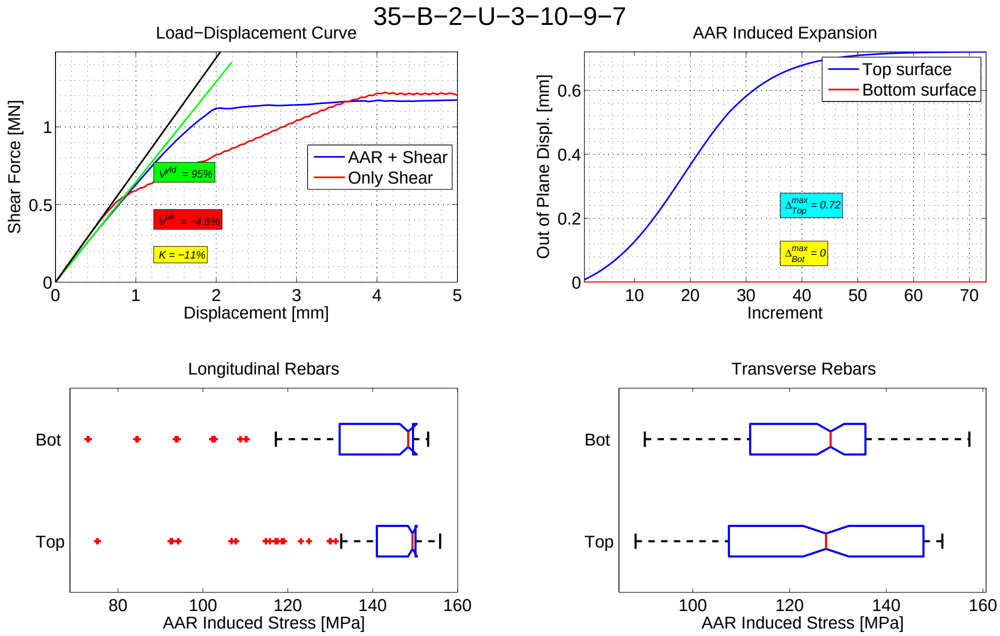

4.1.1.36 Analysis: 36-B-2-U-3-10-9-9

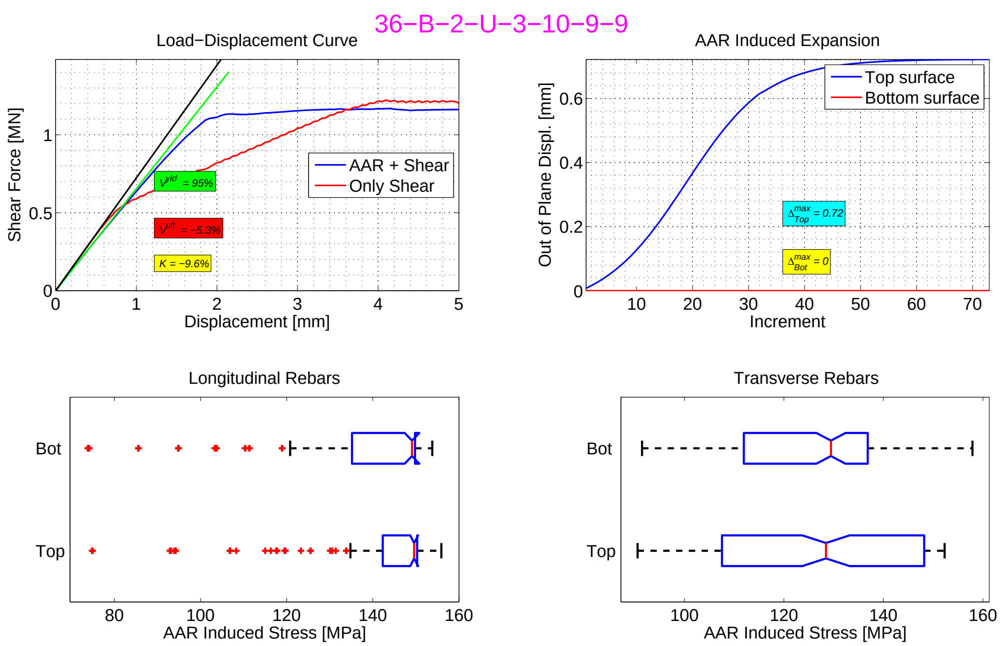

4.1.1.37 Analysis: 37-B-4-U-1-2-7-7

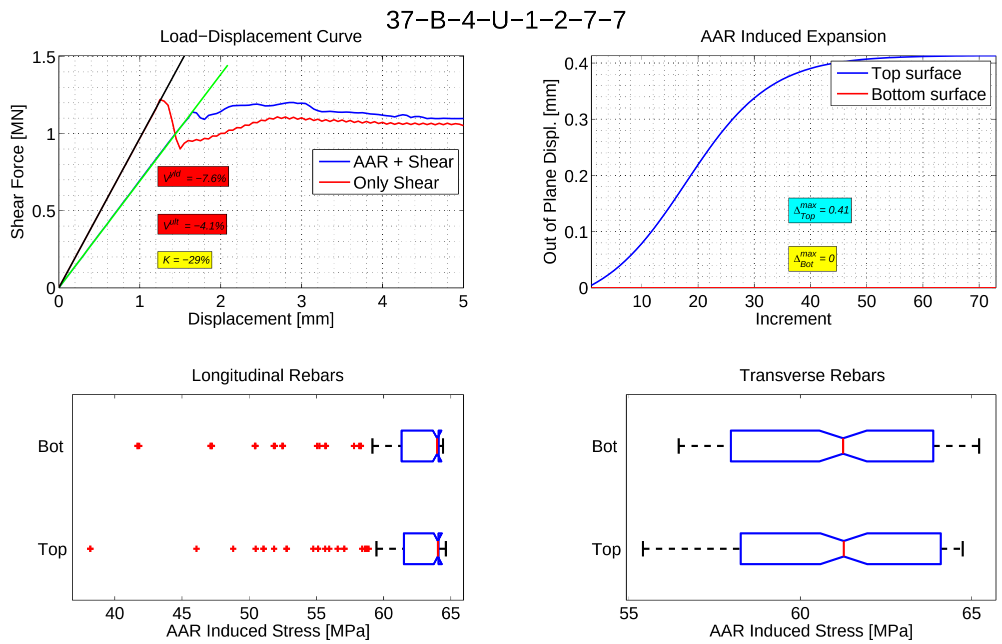

4.1.1.38 Analysis: 38-B-4-U-1-2-7-9

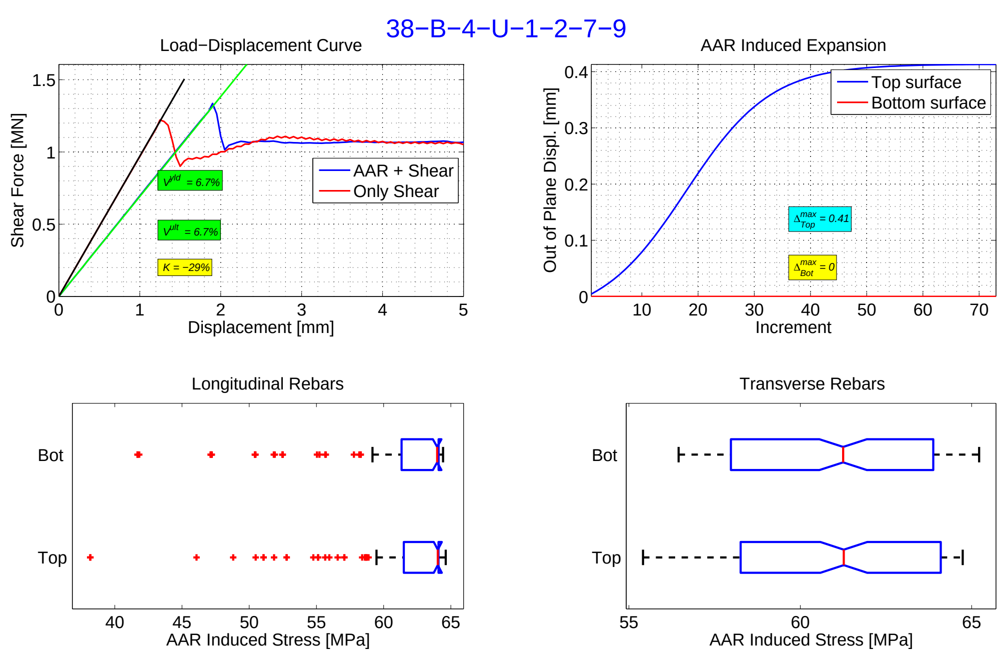

4.1.1.39 Analysis: 39-B-4-U-1-2-9-7

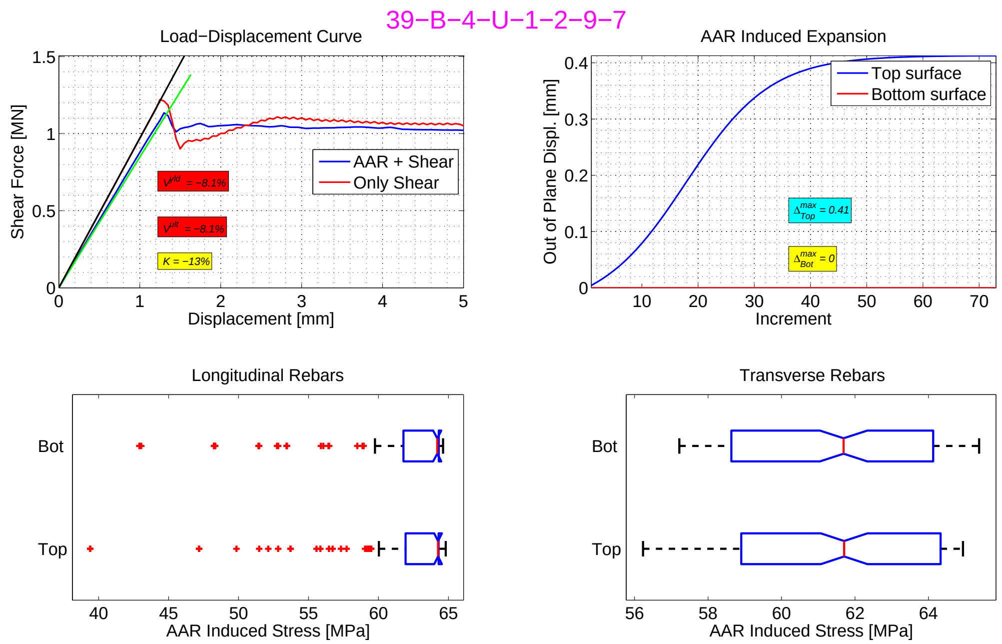

4.1.1.40 Analysis: 40-B-4-U-1-2-9-9

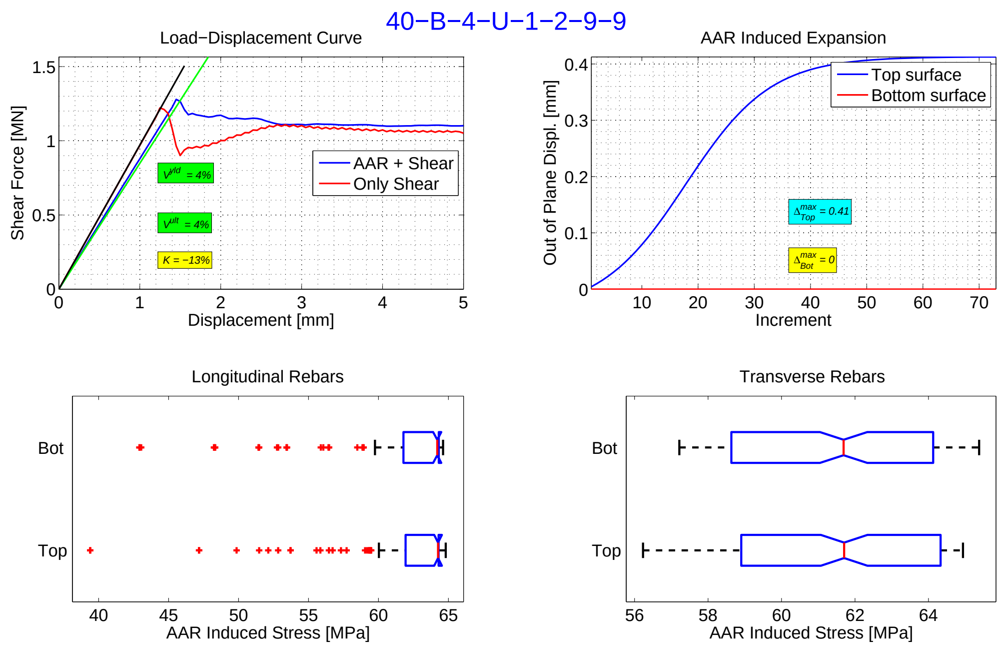

4.1.1.41 Analysis: 41-B-4-U-1-5-7-7

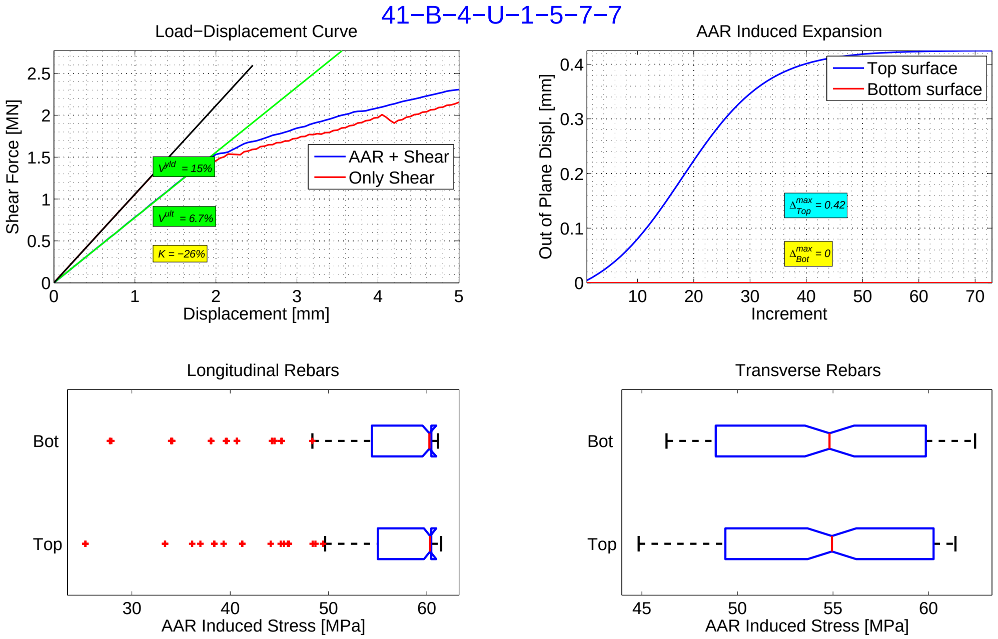

4.1.1.42 Analysis: 42-B-4-U-1-5-7-9

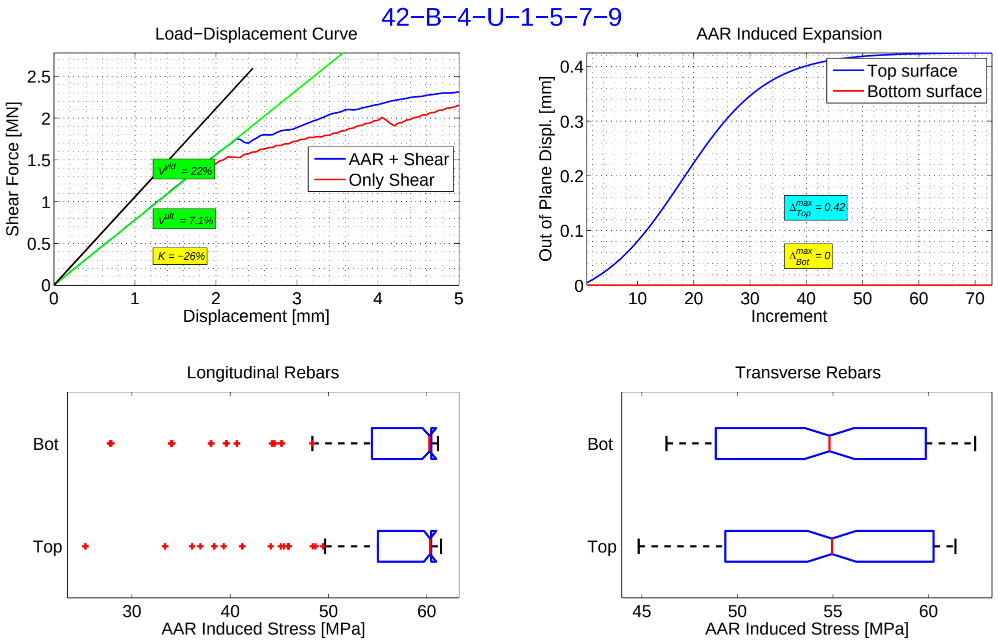

4.1.1.43 Analysis: 43-B-4-U-1-5-9-7

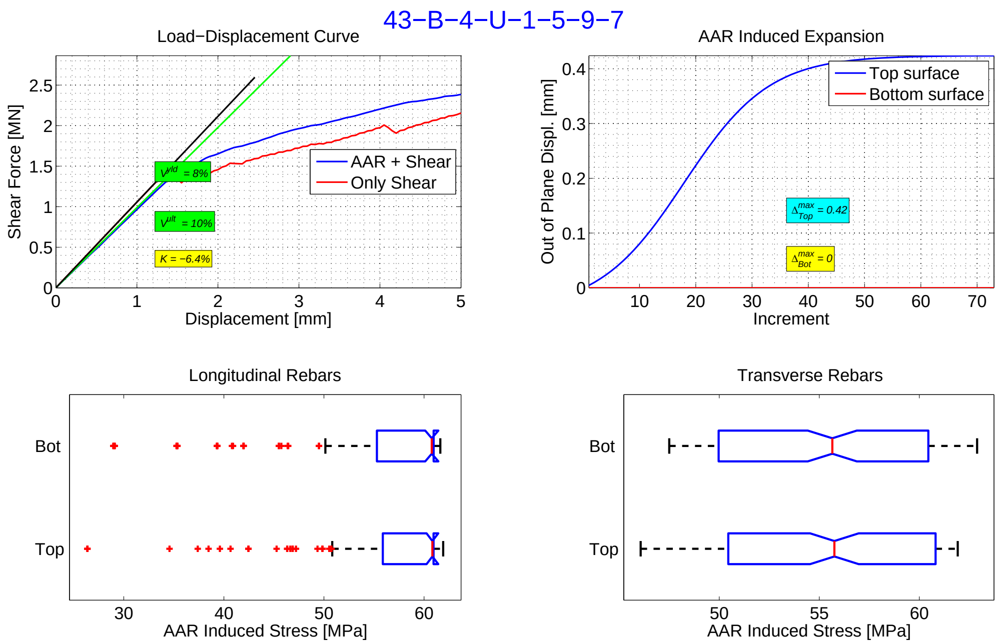

4.1.1.44 Analysis: 44-B-4-U-1-5-9-9

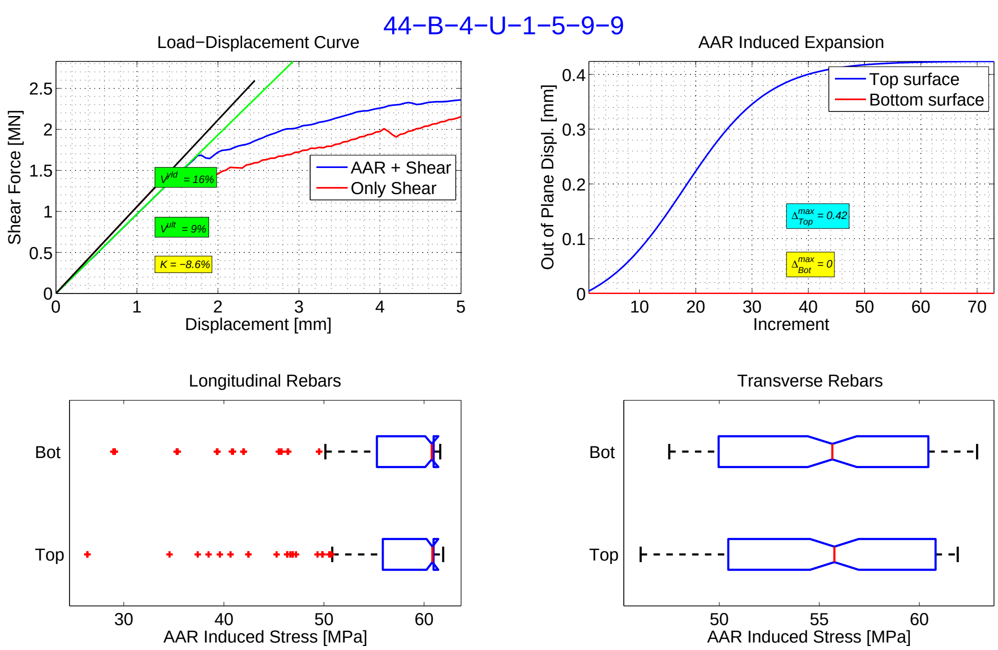

4.1.1.45 Analysis: 45-B-4-U-1-10-7-7

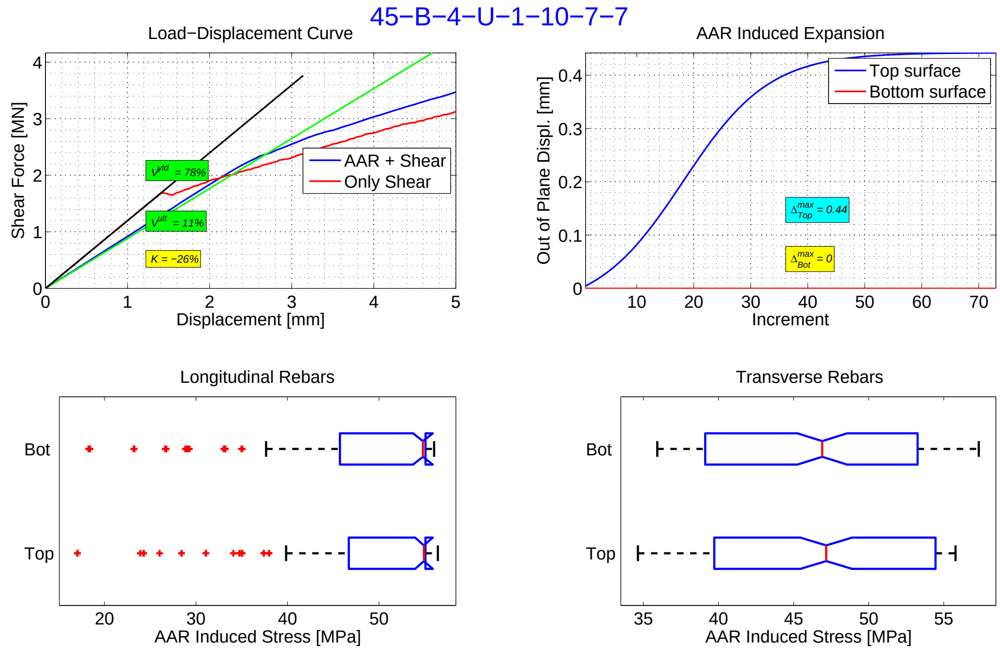

4.1.1.46 Analysis: 46-B-4-U-1-10-7-9

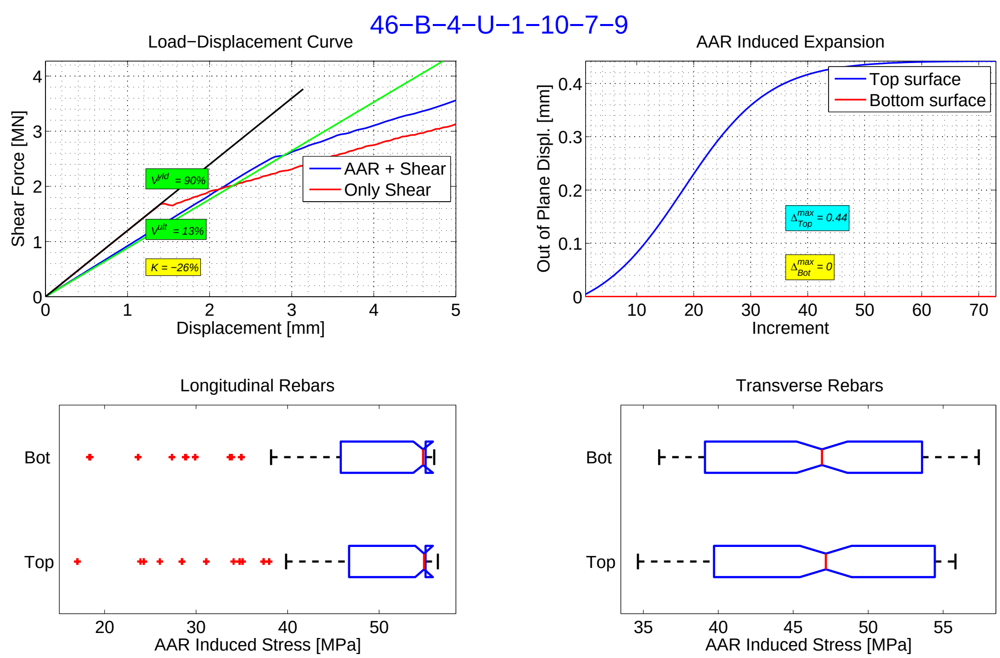

4.1.1.47 Analysis: 47-B-4-U-1-10-9-7

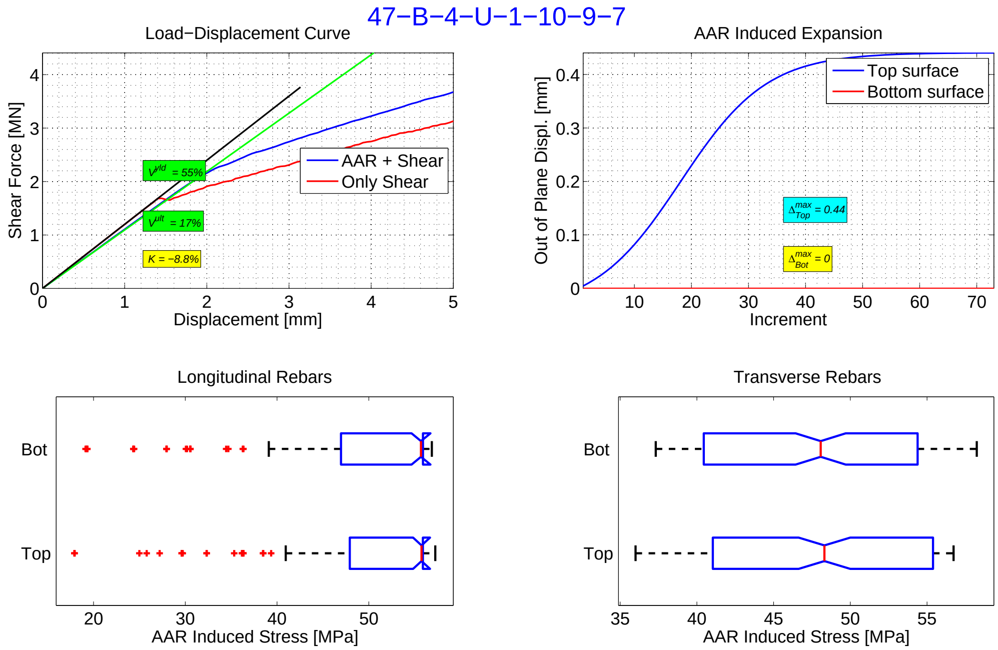

4.1.1.48 Analysis: 48-B-4-U-1-10-9-9

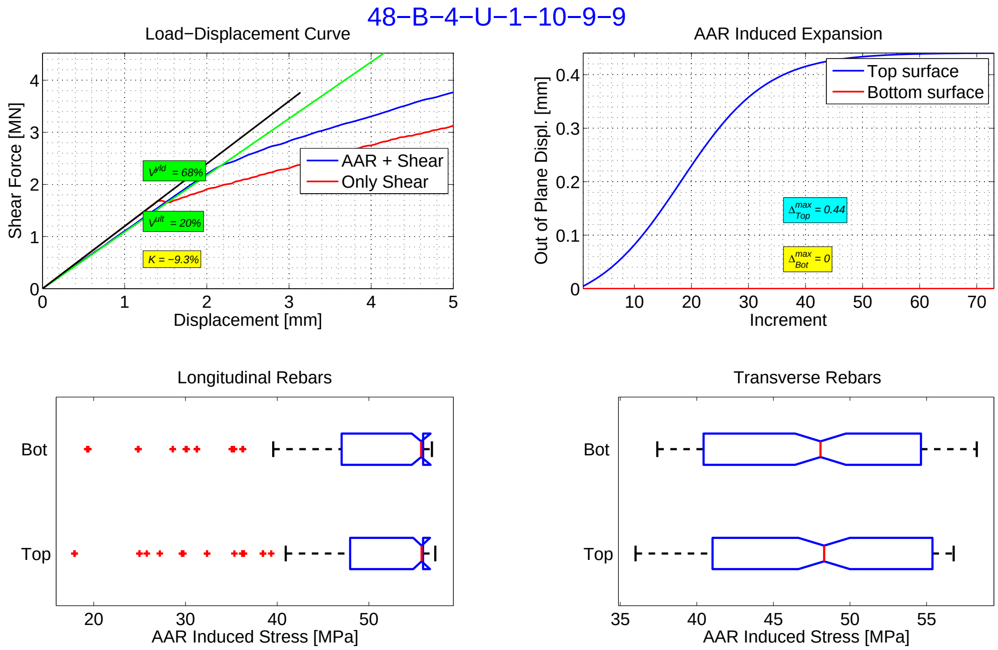

4.1.1.49 Analysis: 49-B-4-U-2-2-7-7

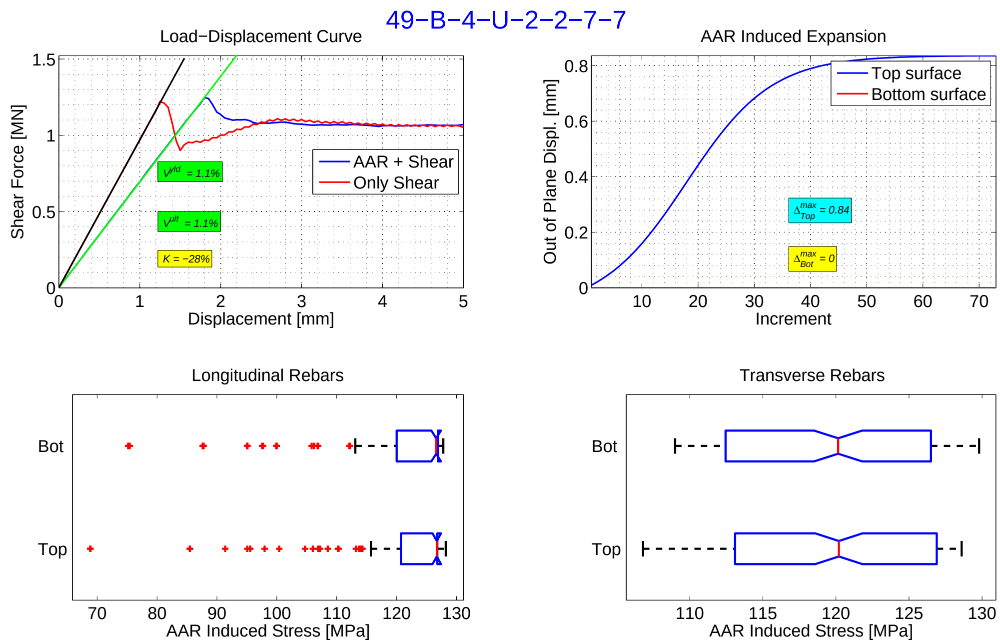

4.1.1.50 Analysis: 50-B-4-U-2-2-7-9

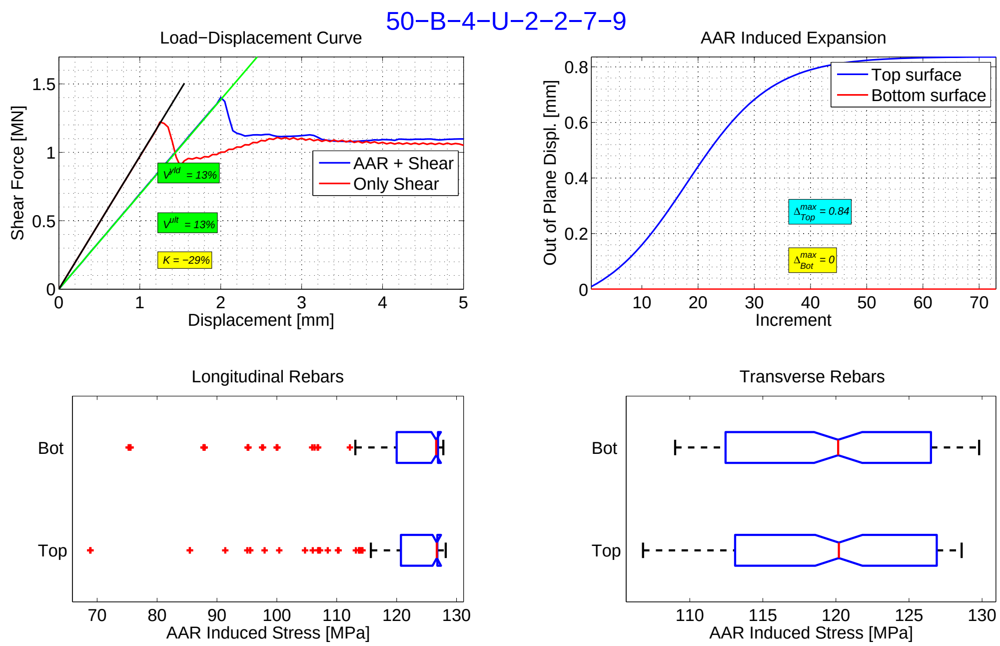

4.1.1.51 Analysis: 51-B-4-U-2-2-9-7

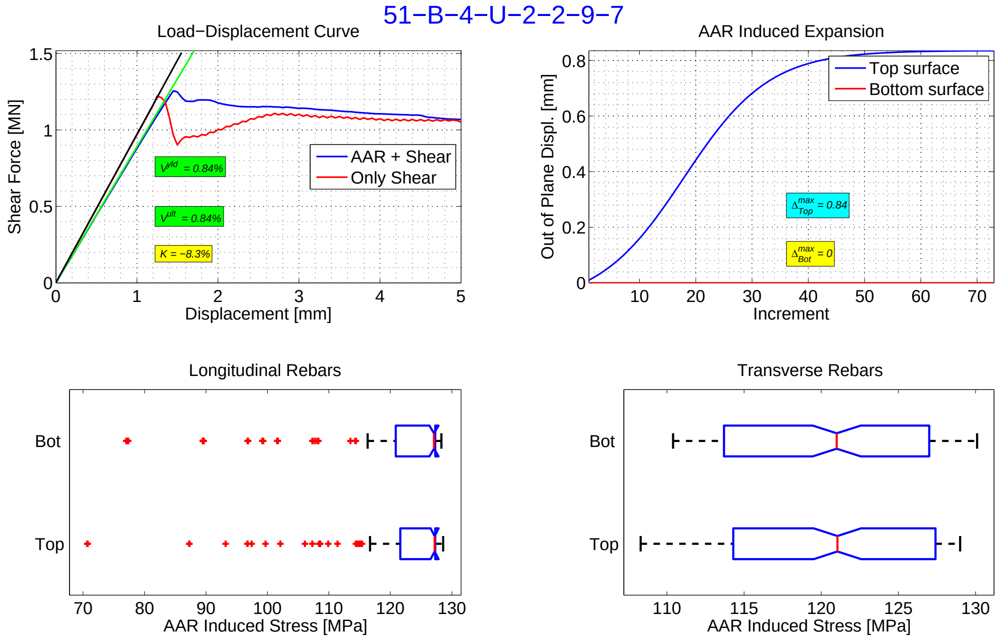

4.1.1.52 Analysis: 52-B-4-U-2-2-9-9

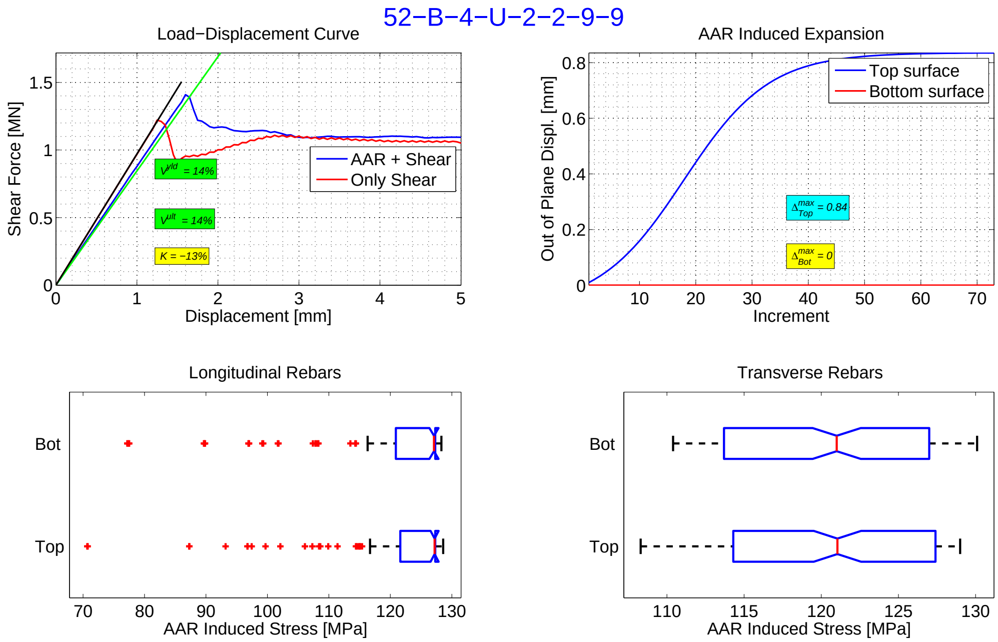

4.1.1.53 Analysis: 53-B-4-U-2-5-7-7

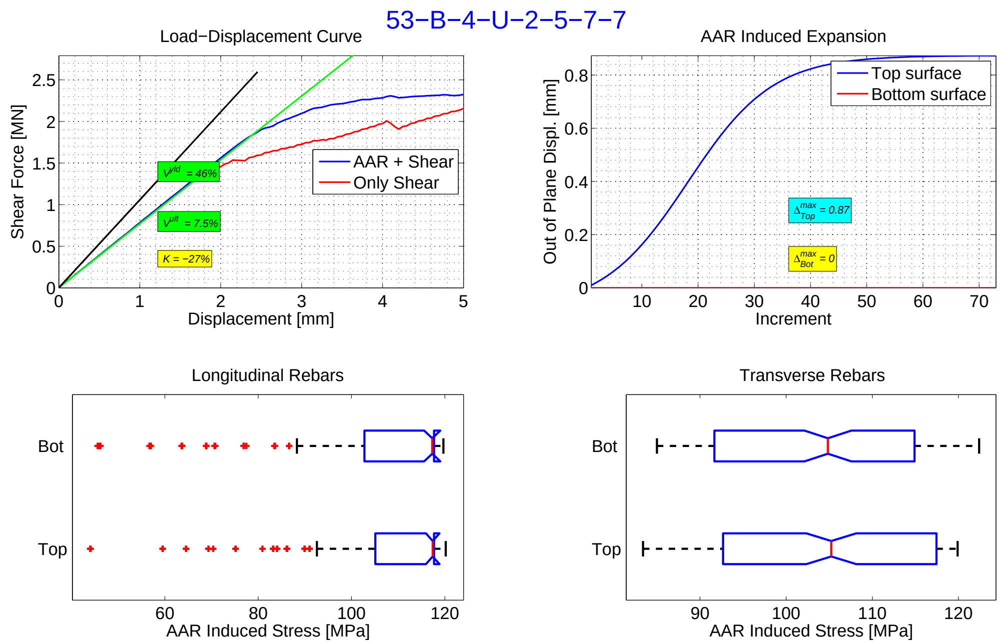

4.1.1.54 Analysis: 54-B-4-U-2-5-7-9

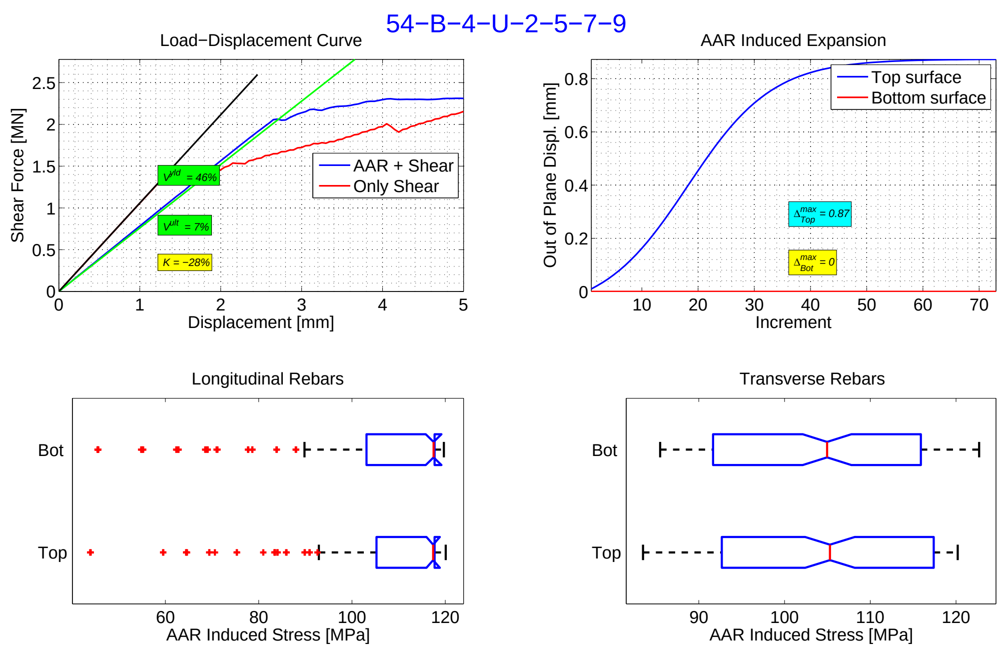

4.1.1.55 Analysis: 55-B-4-U-2-5-9-7

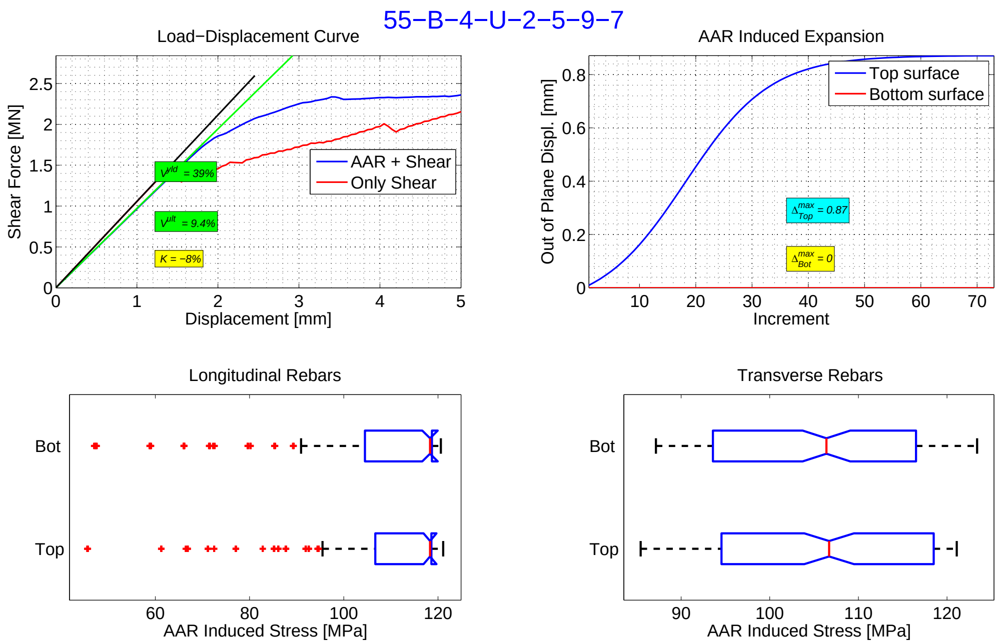

4.1.1.56 Analysis: 56-B-4-U-2-5-9-9

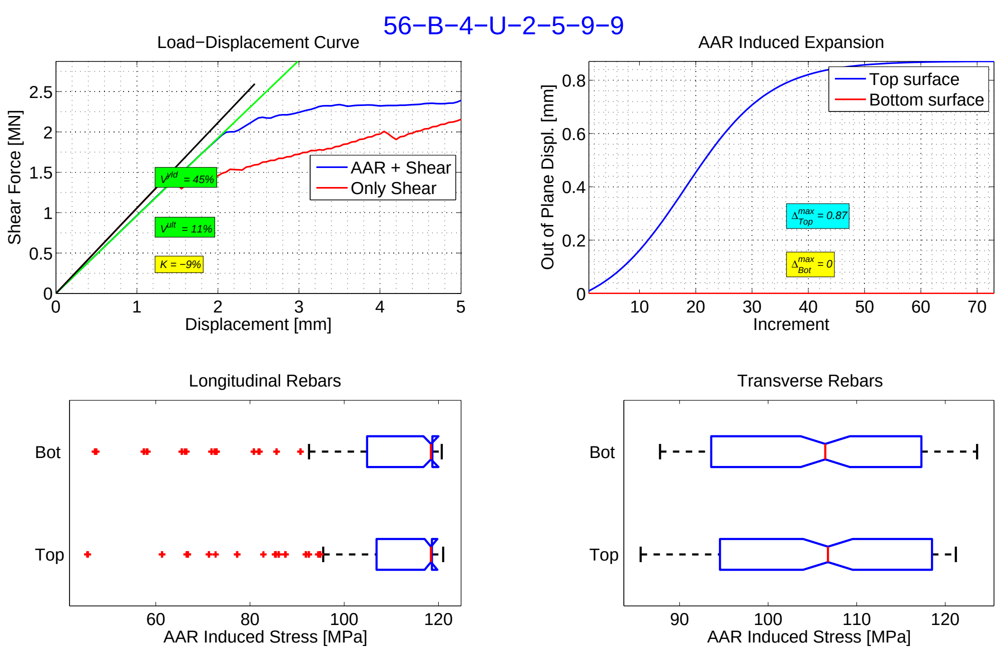

4.1.1.57 Analysis: 57-B-4-U-2-10-7-7

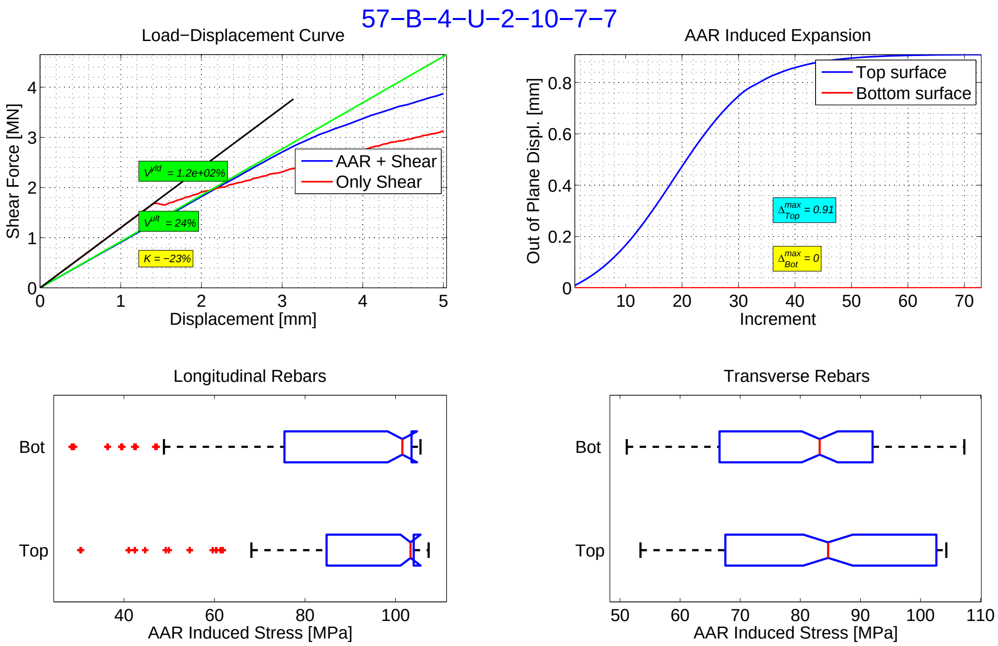

4.1.1.58 Analysis: 58-B-4-U-2-10-7-9

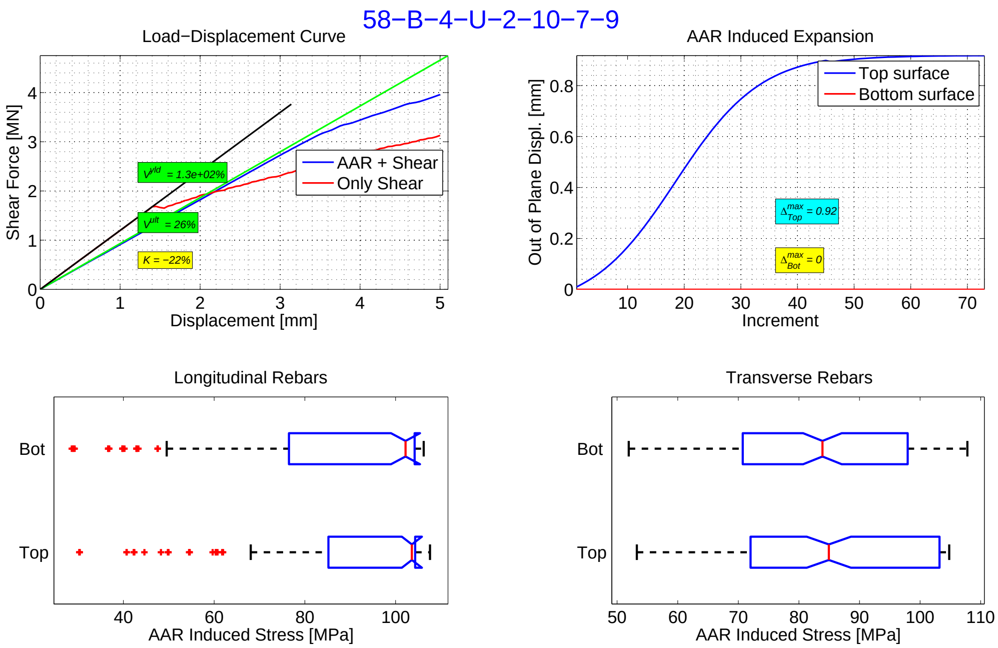

4.1.1.59 Analysis: 59-B-4-U-2-10-9-7

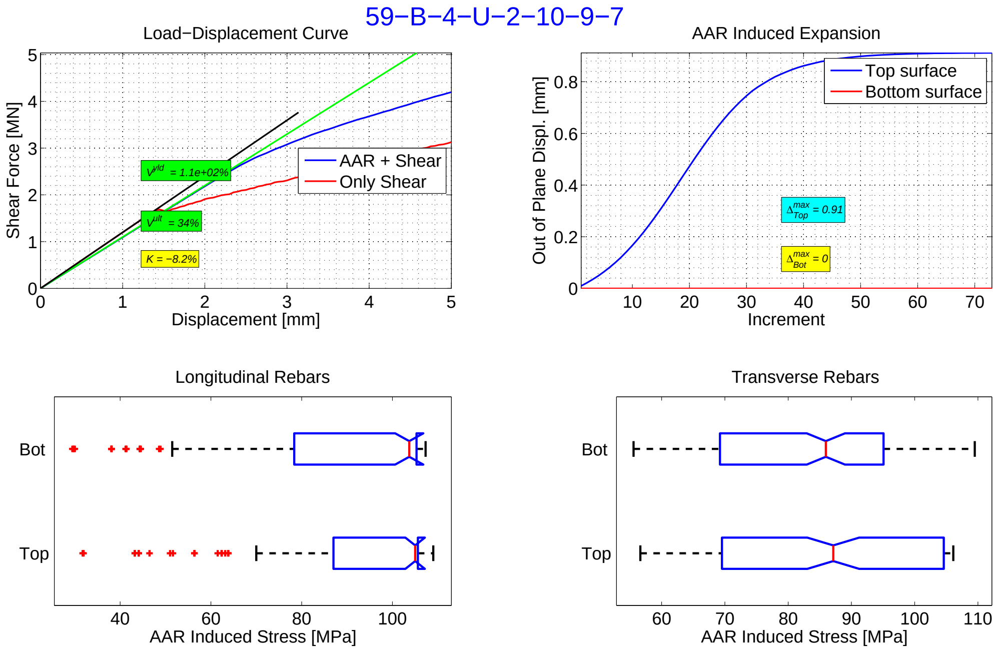

4.1.1.60 Analysis: 60-B-4-U-2-10-9-9

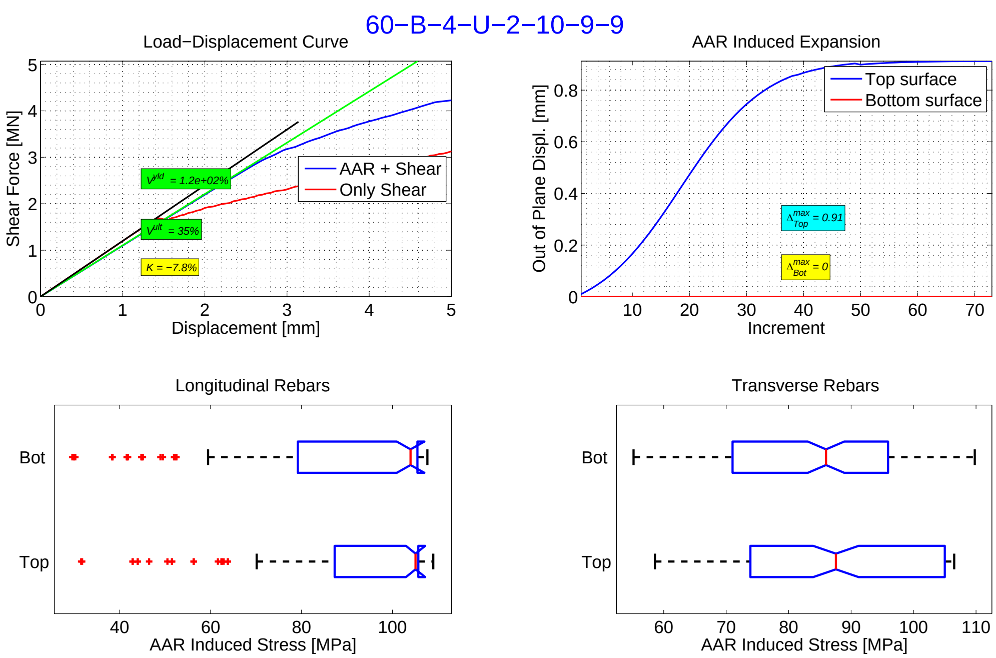

4.1.1.61 Analysis: 61-B-4-U-3-2-7-7

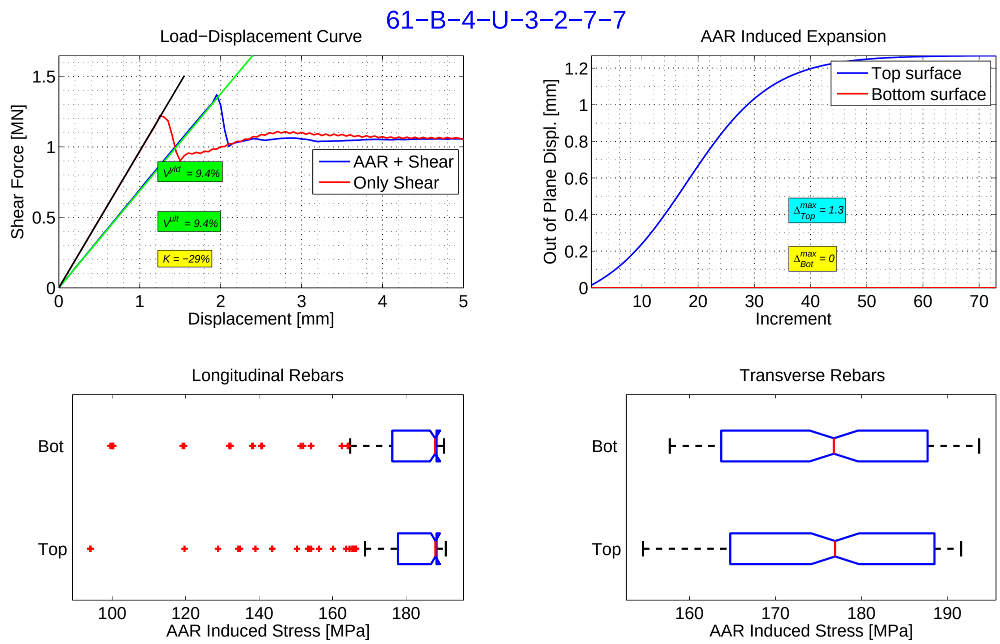

4.1.1.62 Analysis: 62-B-4-U-3-2-7-9

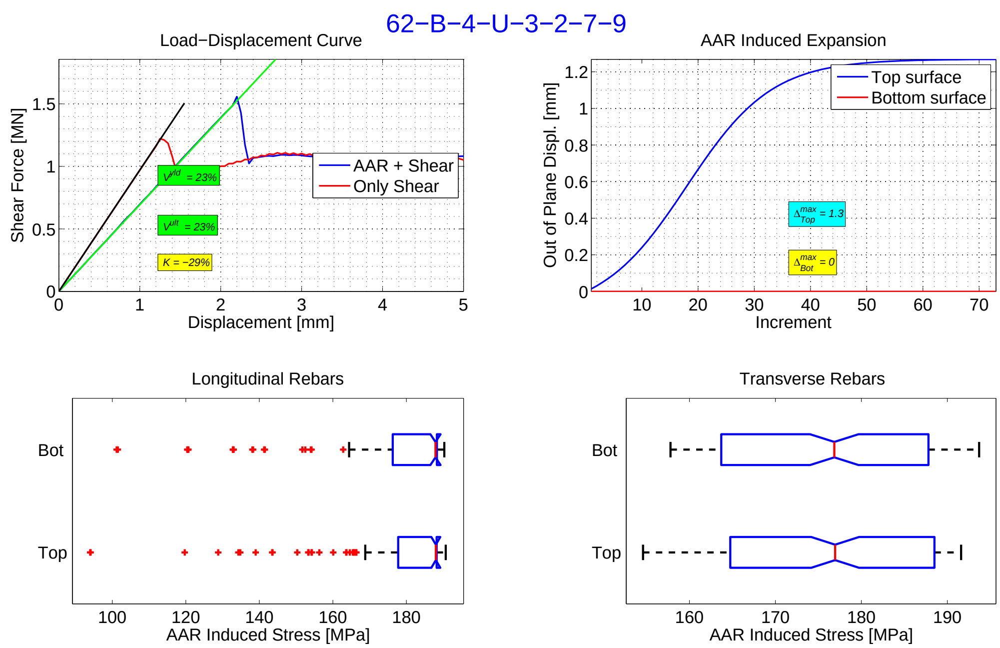

4.1.1.63 Analysis: 63-B-4-U-3-2-9-7

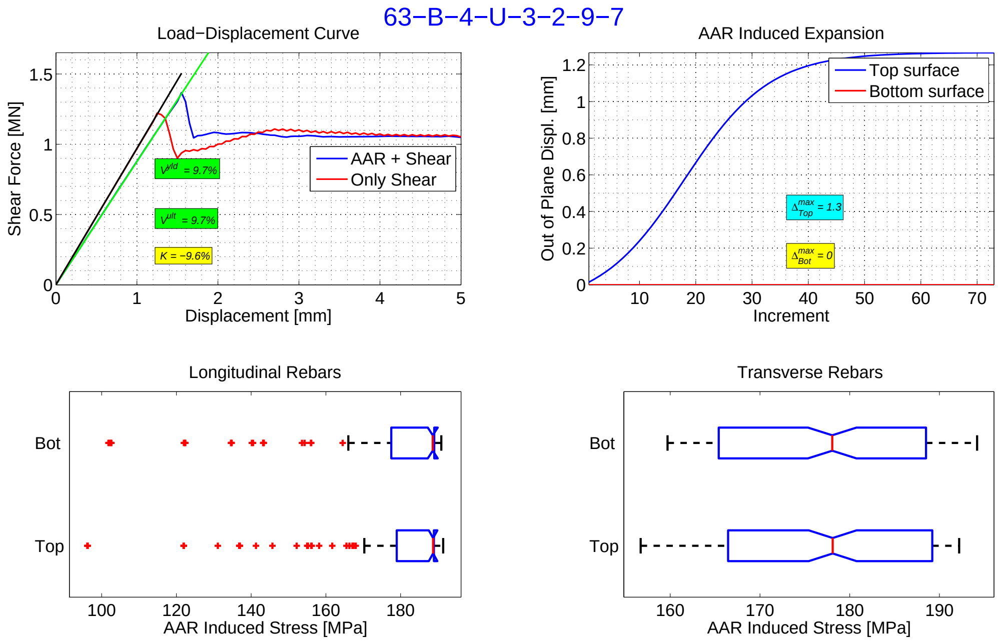

4.1.1.64 Analysis: 64-B-4-U-3-2-9-9

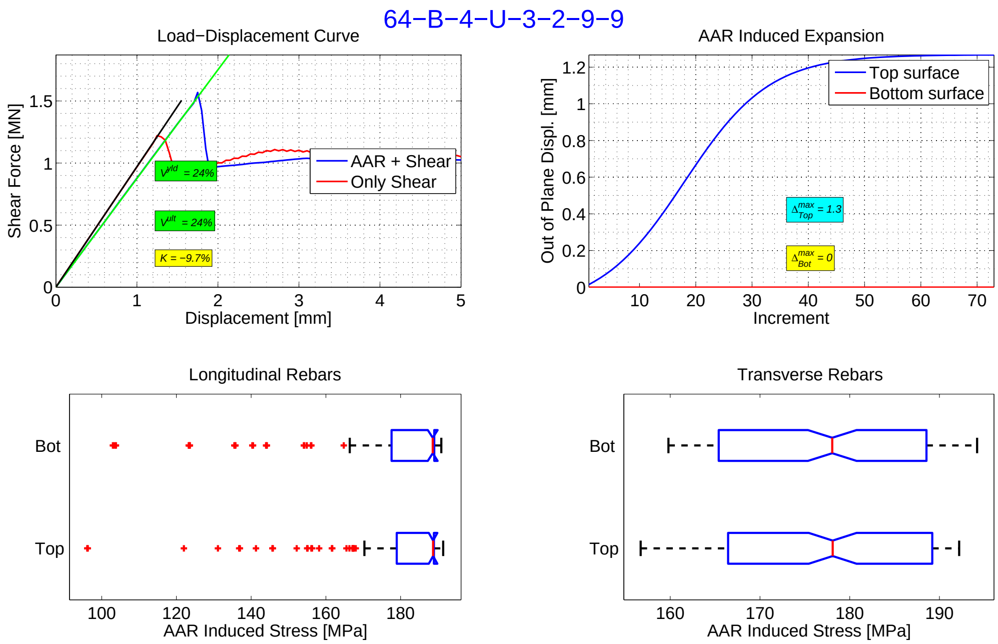

4.1.1.65 Analysis: 65-B-4-U-3-5-7-7

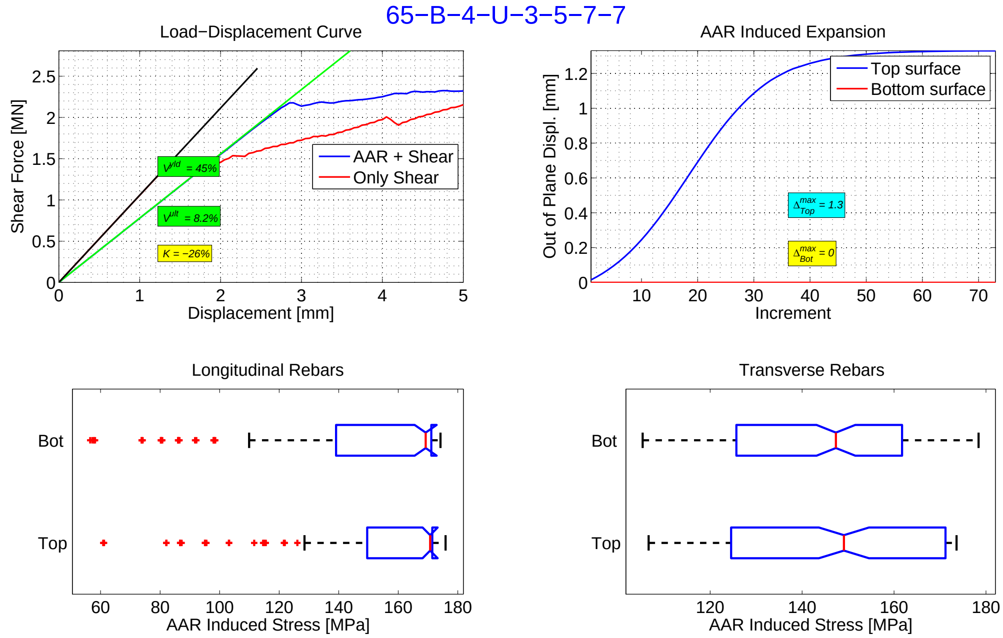

4.1.1.66 Analysis: 66-B-4-U-3-5-7-9

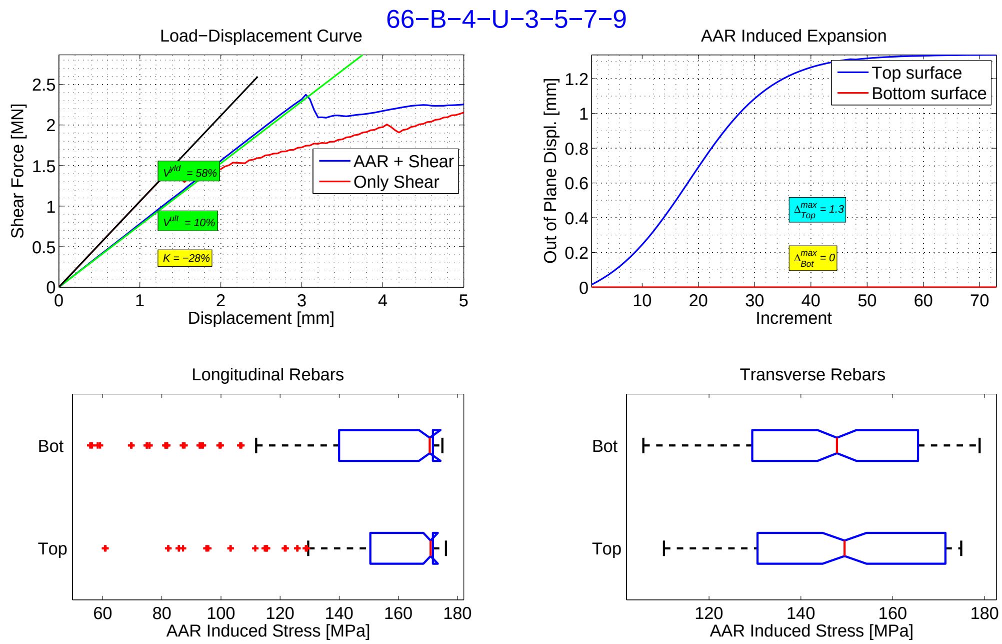

4.1.1.67 Analysis: 67-B-4-U-3-5-9-7

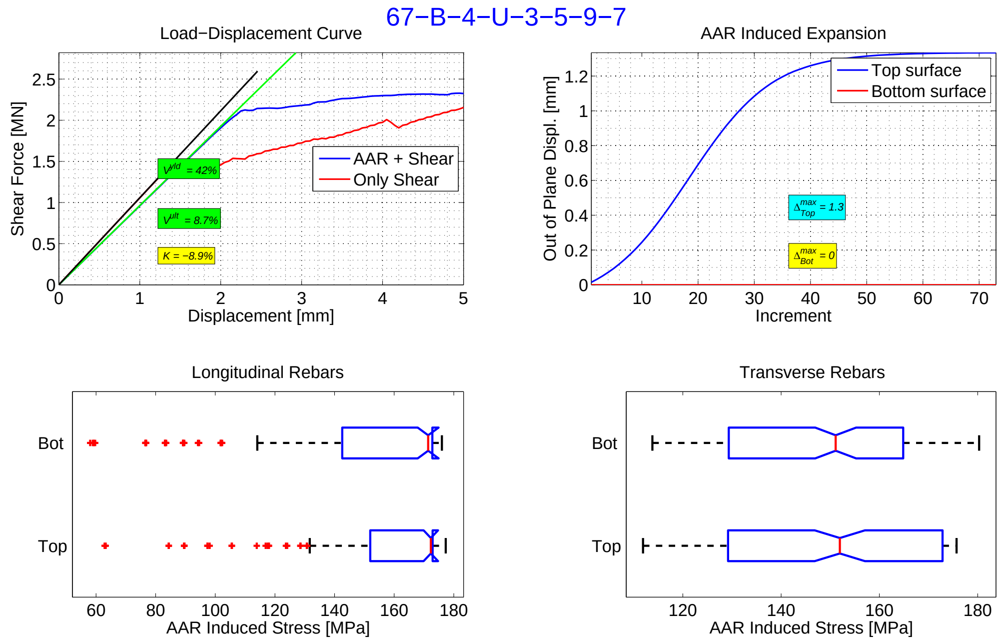

4.1.1.68 Analysis: 68-B-4-U-3-5-9-9

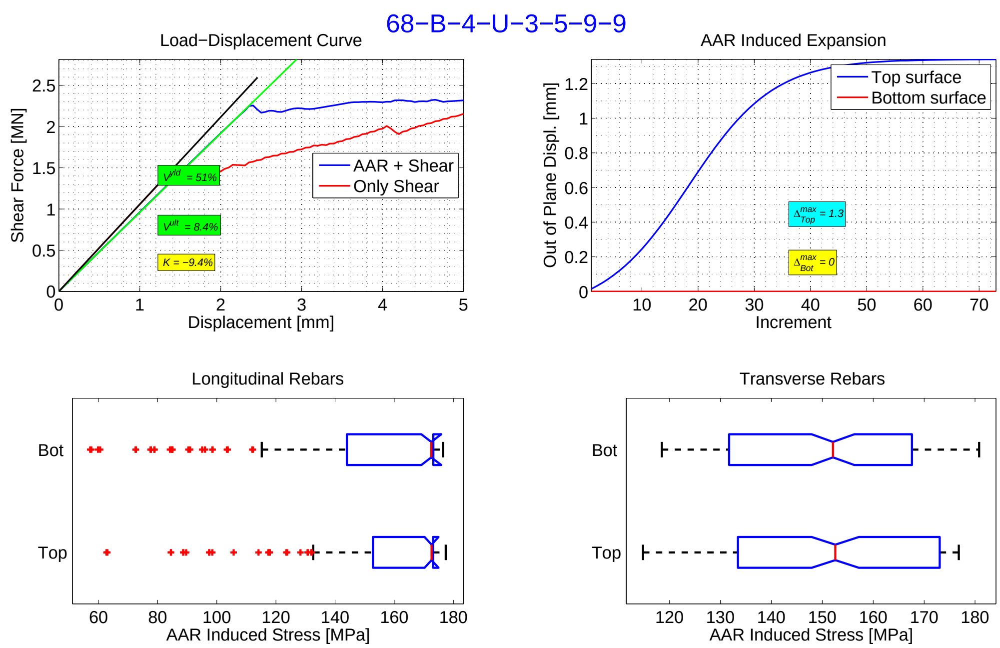

4.1.1.69 Analysis: 69-B-4-U-3-10-7-7

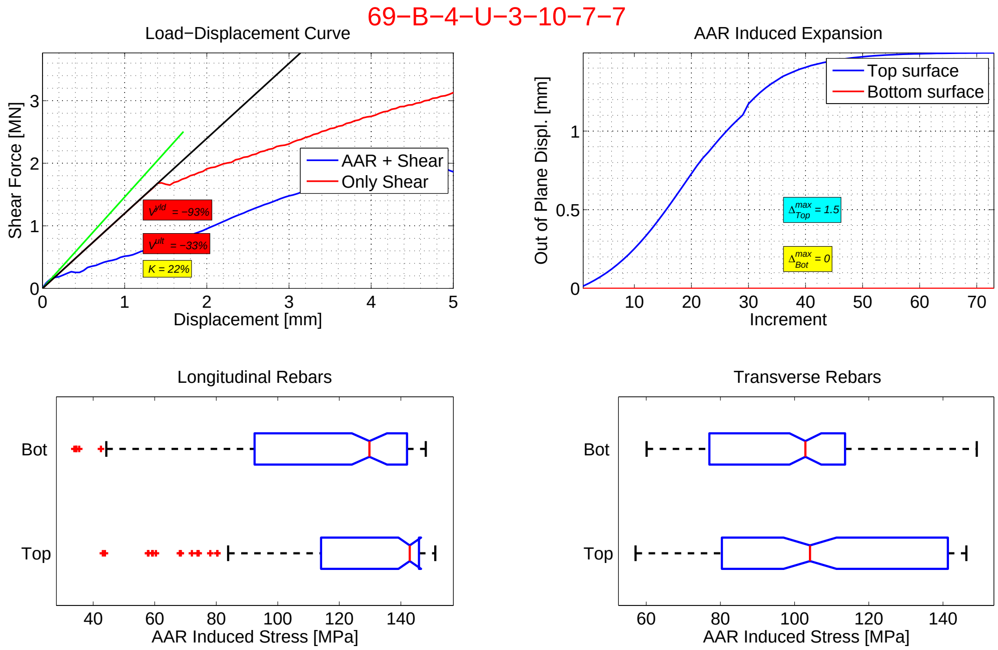

4.1.1.70 Analysis: 70-B-4-U-3-10-7-9

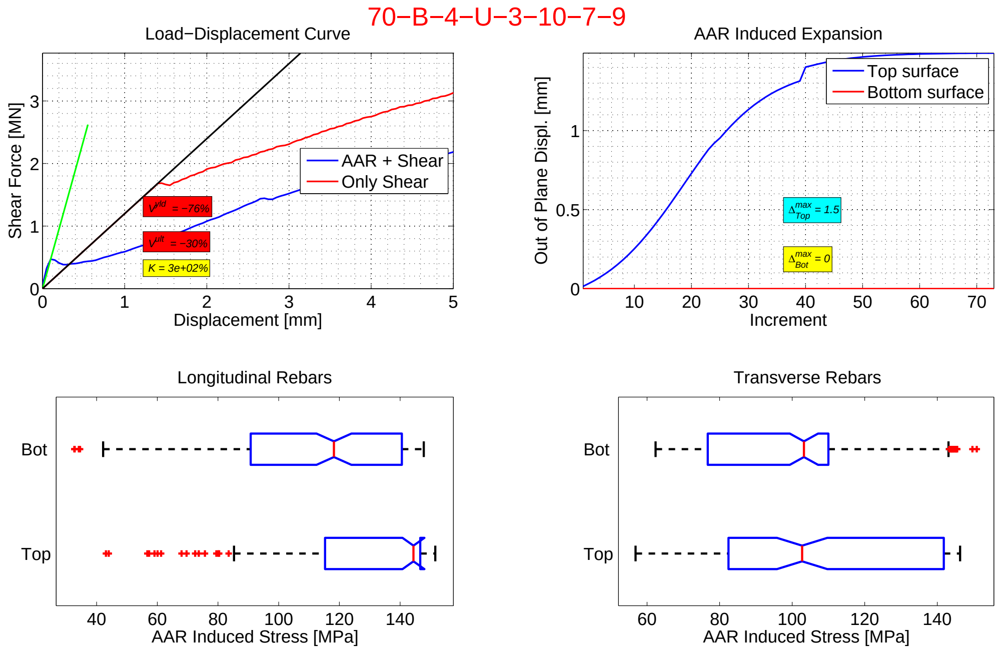

4.1.1.71 Analysis: 71-B-4-U-3-10-9-7

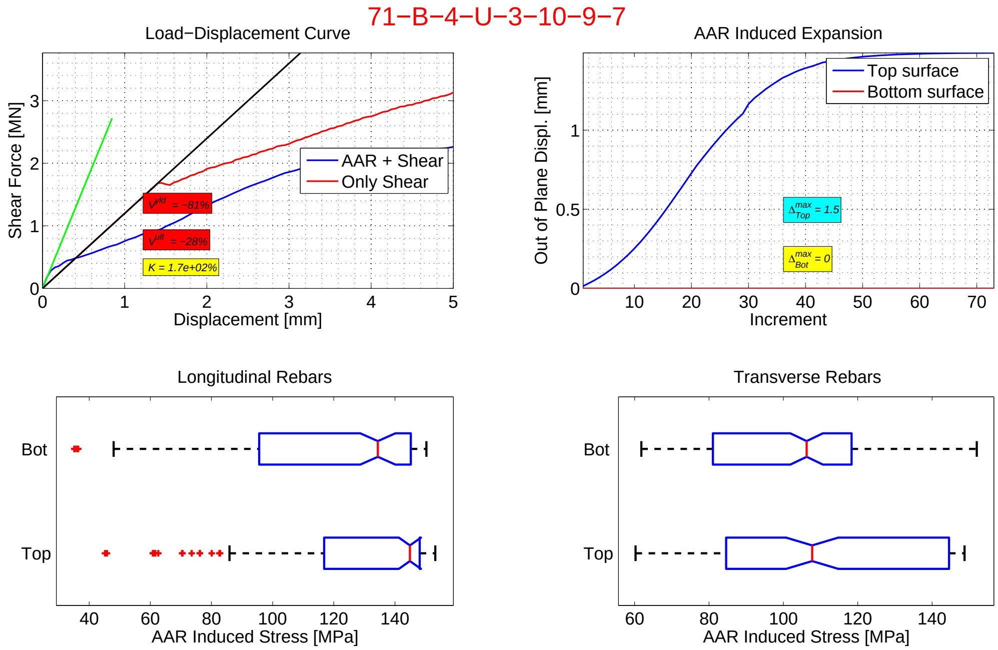

4.1.1.72 Analysis: 72-B-4-U-3-10-9-9

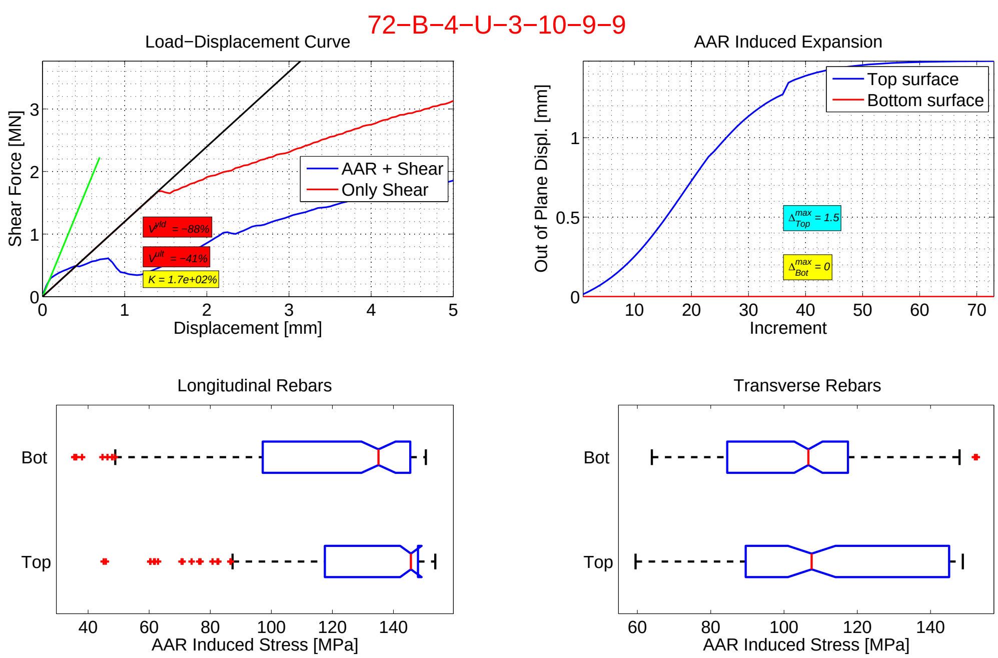

4.1.1.73 Analysis: 73-B-2-R-1-2-7-7

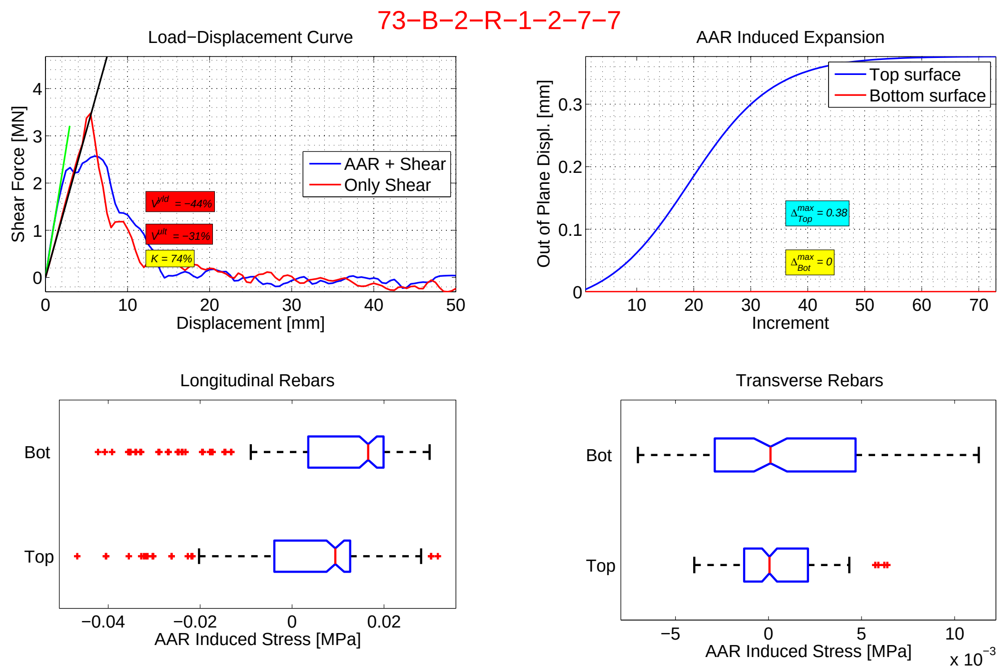

4.1.1.74 Analysis: 74-B-2-R-1-2-7-9

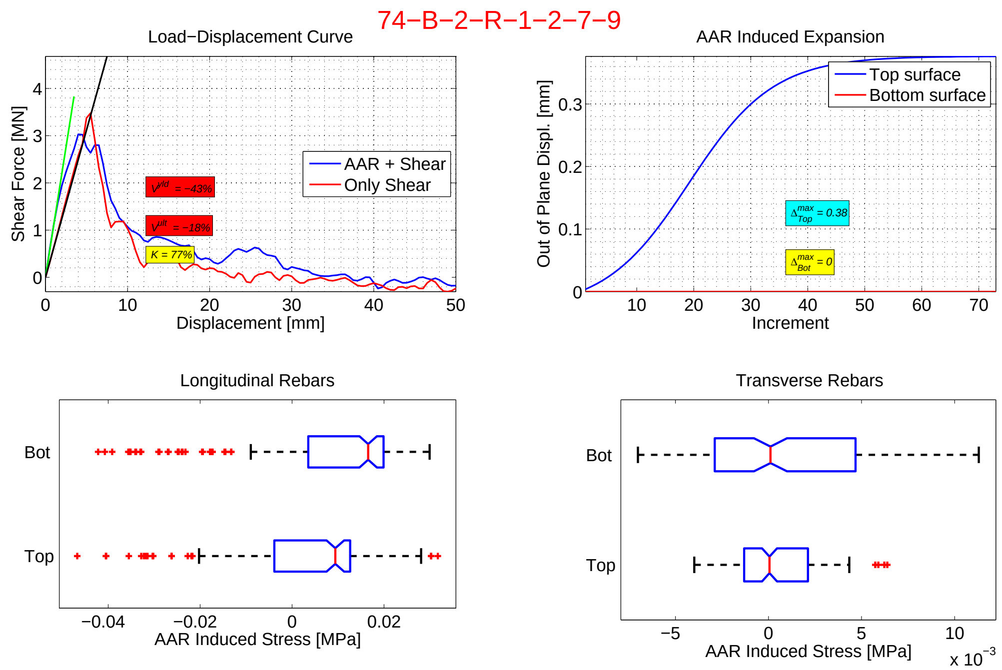

4.1.1.75 Analysis: 75-B-2-R-1-2-9-7

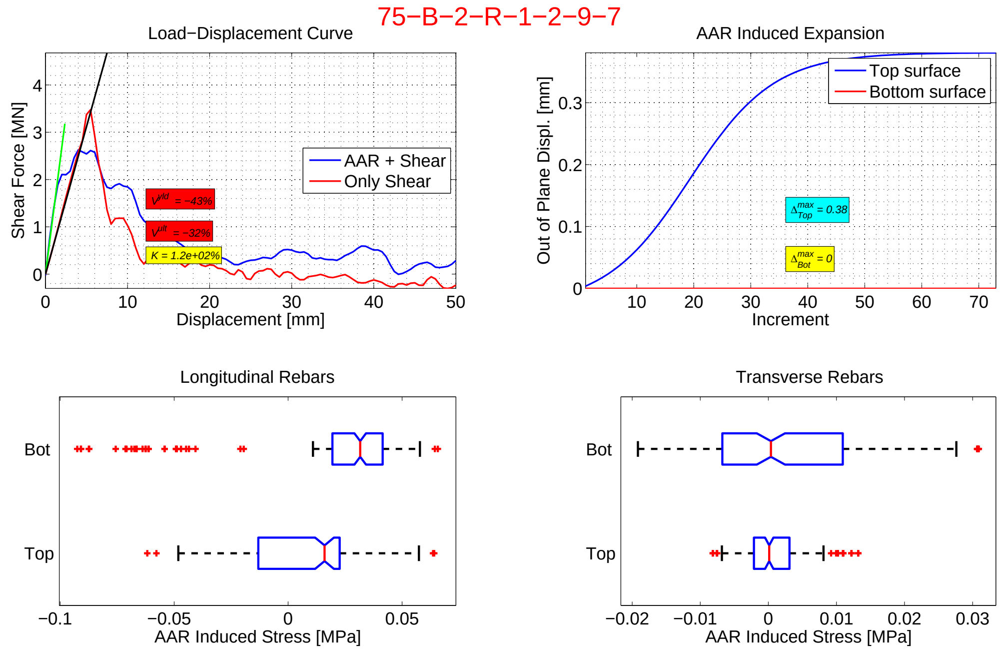

4.1.1.76 Analysis: 76-B-2-R-1-2-9-9

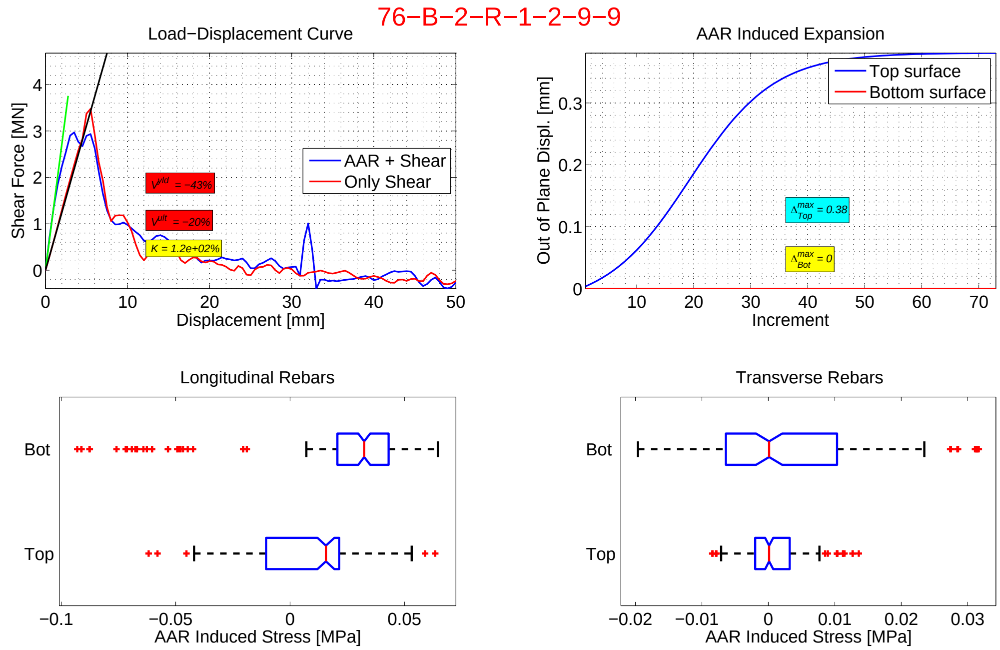

4.1.1.77 Analysis: 77-B-2-R-1-5-7-7

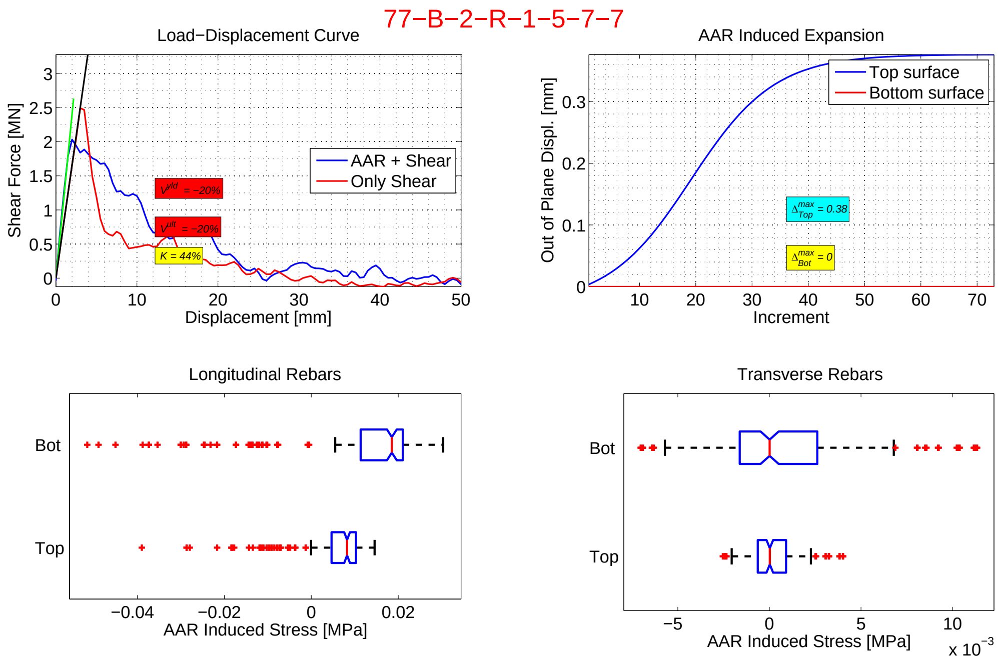

4.1.1.78 Analysis: 78-B-2-R-1-5-7-9

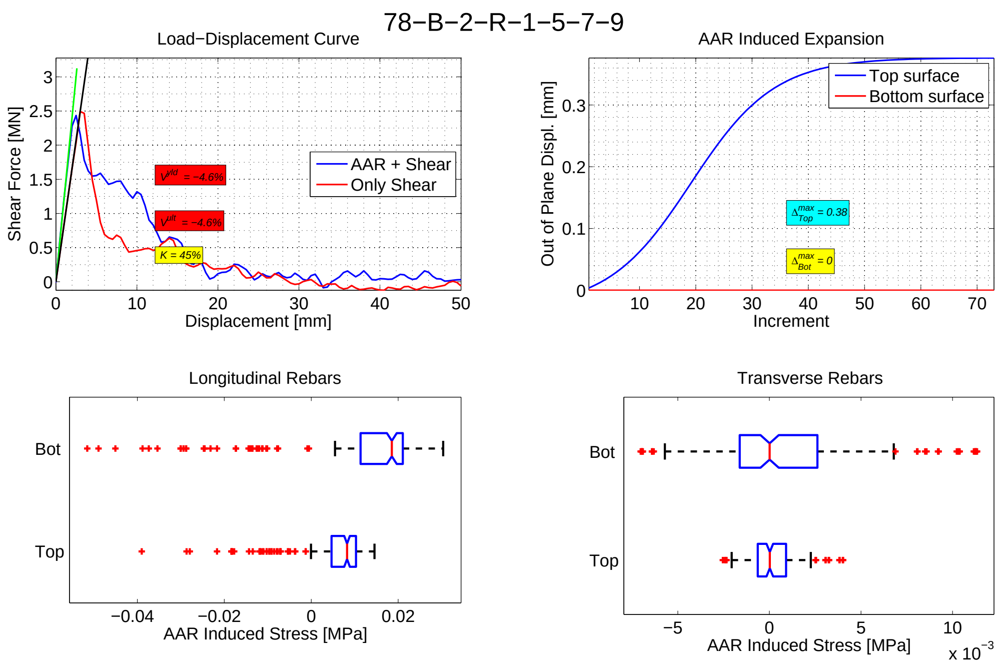

4.1.1.79 Analysis: 79-B-2-R-1-5-9-7

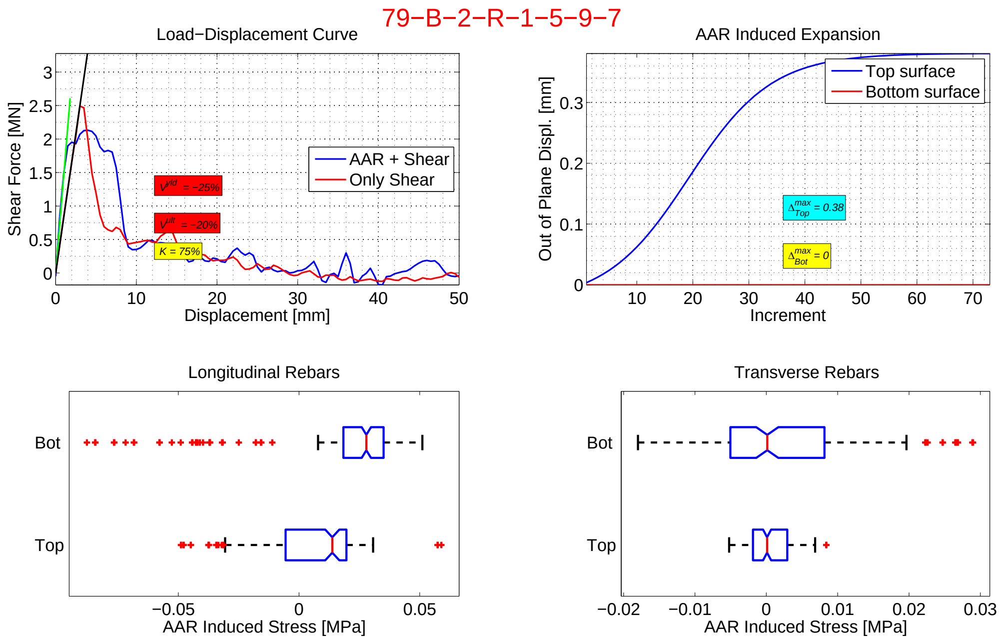

4.1.1.80 Analysis: 80-B-2-R-1-5-9-9

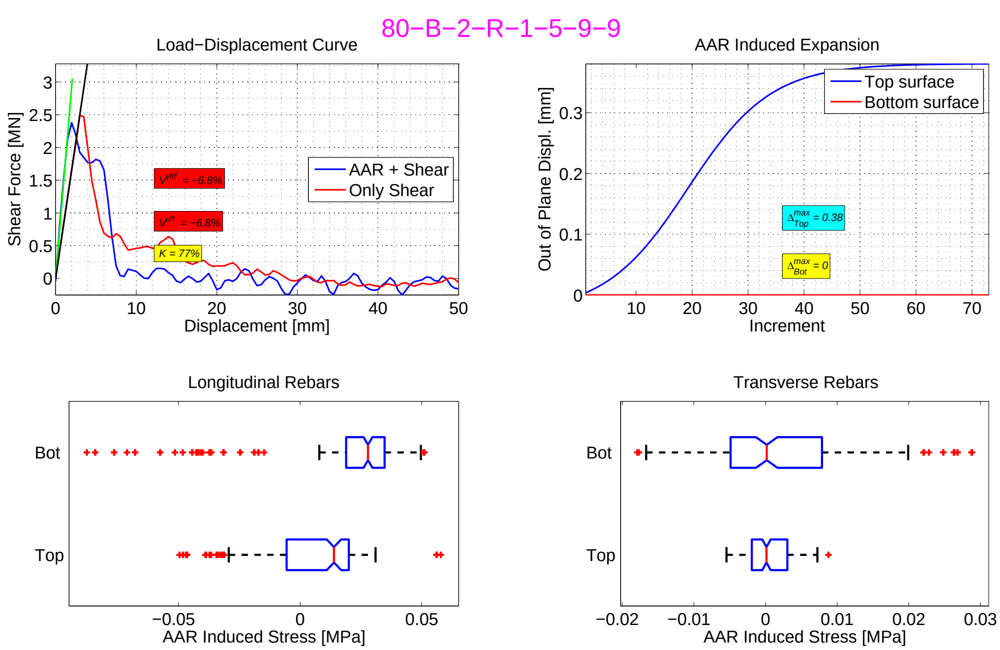

4.1.1.81 Analysis: 81-B-2-R-1-10-7-7

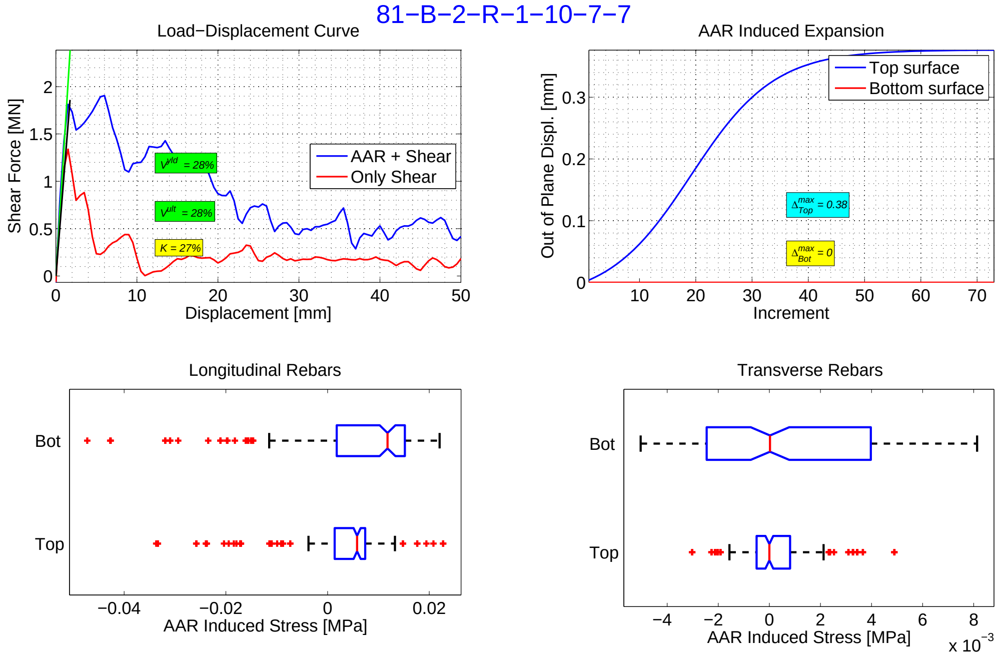

4.1.1.82 Analysis: 82-B-2-R-1-10-7-9

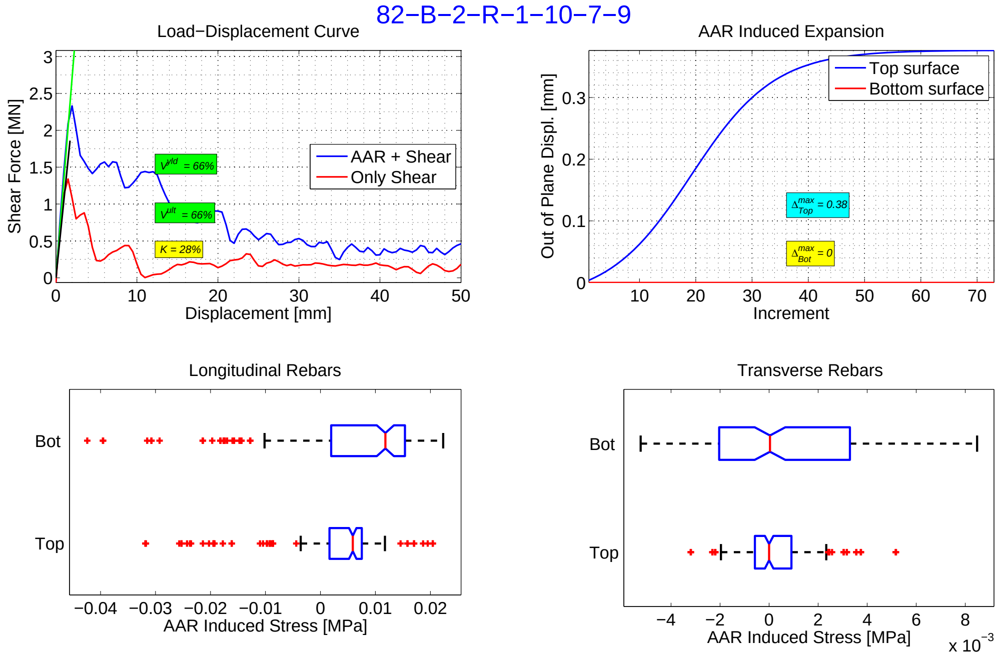

4.1.1.83 Analysis: 83-B-2-R-1-10-9-7

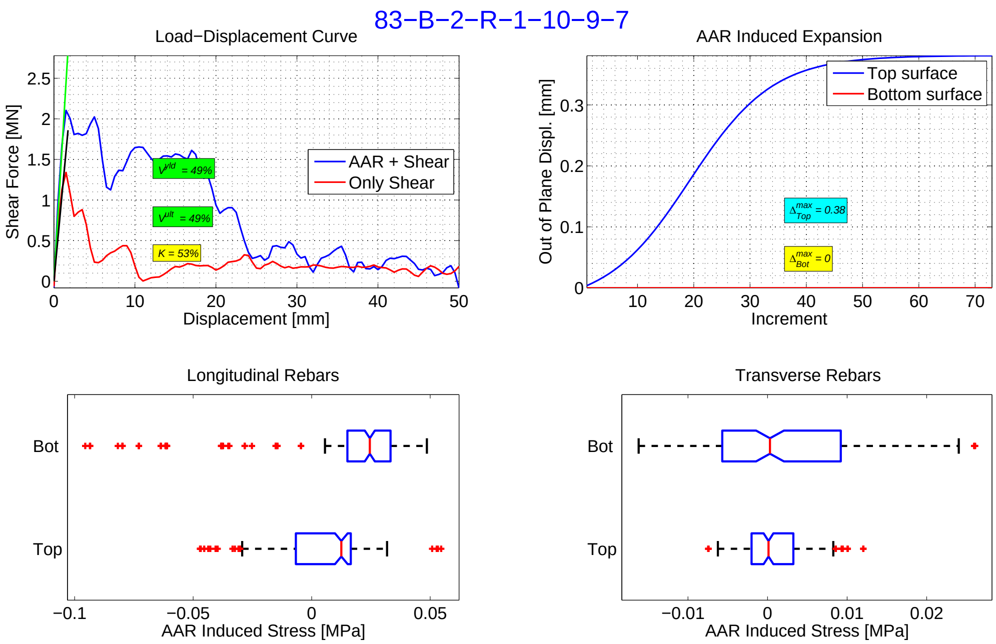

4.1.1.84 Analysis: 84-B-2-R-1-10-9-9

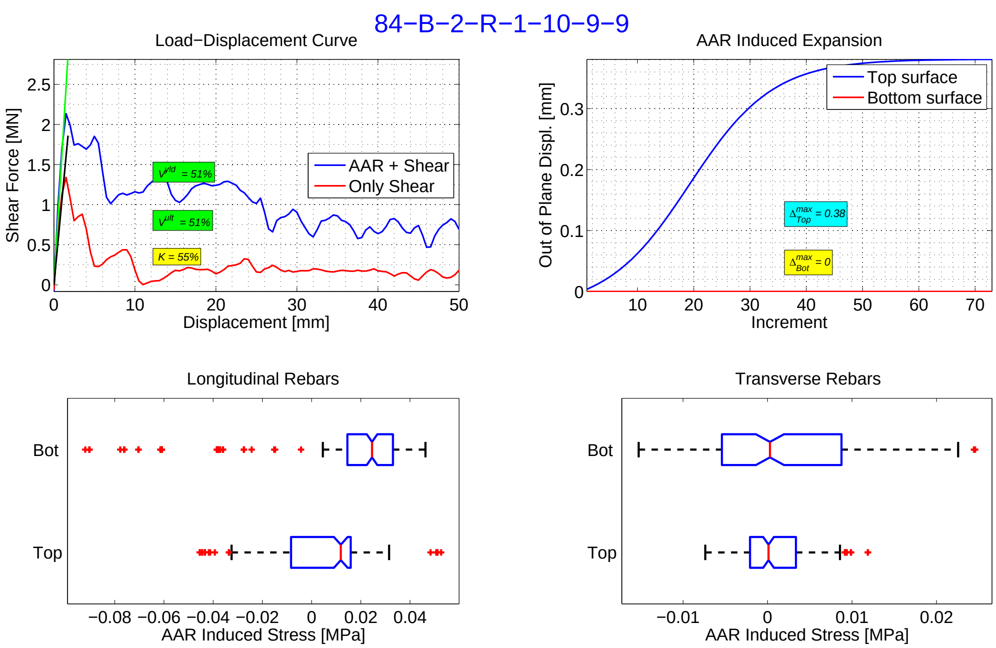

4.1.1.85 Analysis: 85-B-2-R-2-2-7-7

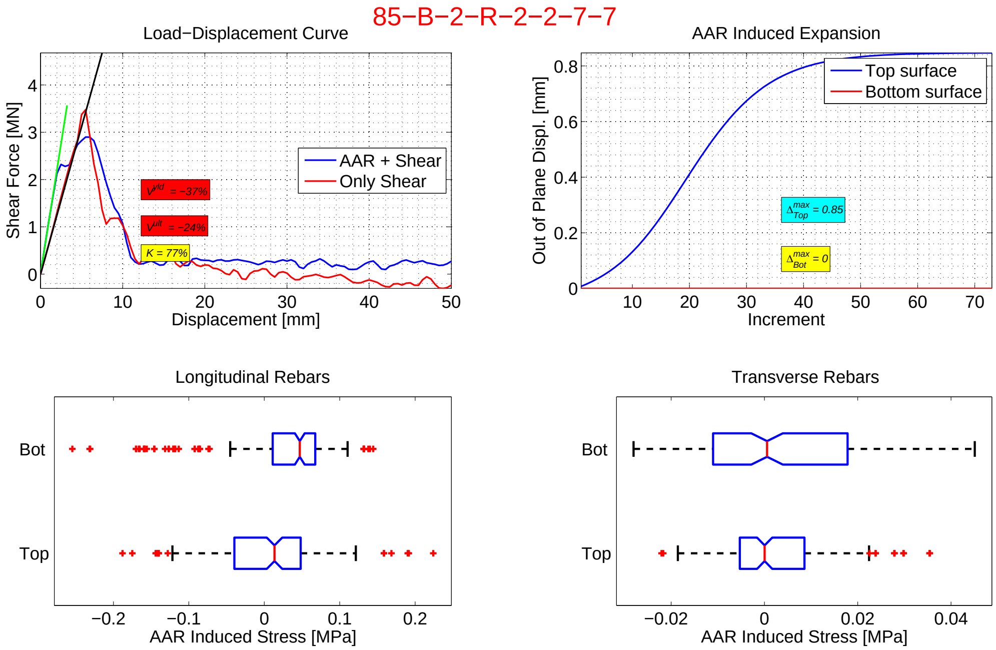

4.1.1.86 Analysis: 86-B-2-R-2-2-7-9

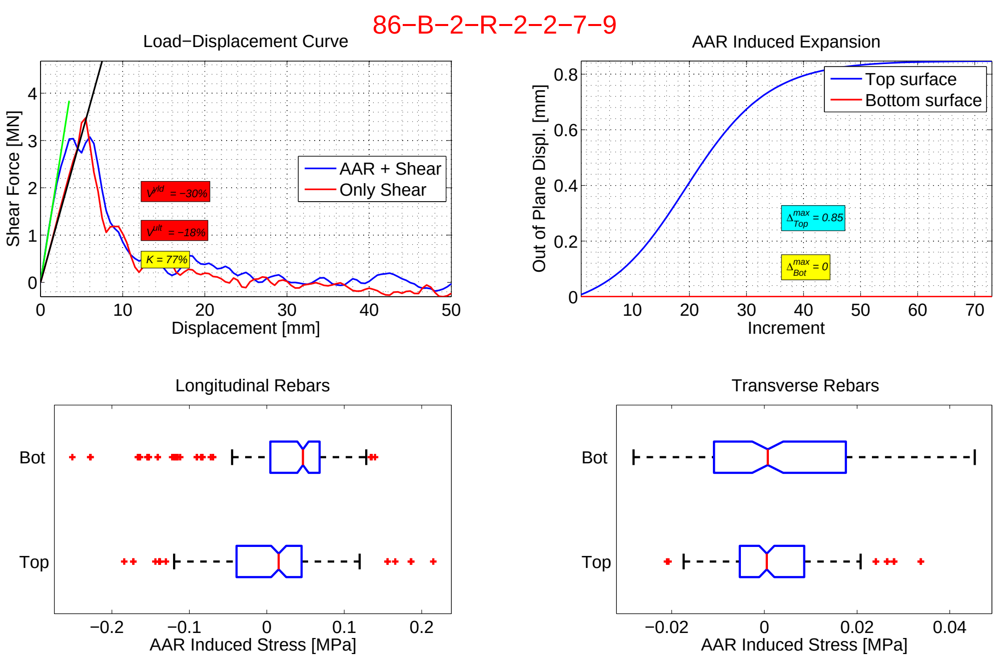

4.1.1.87 Analysis: 87-B-2-R-2-2-9-7

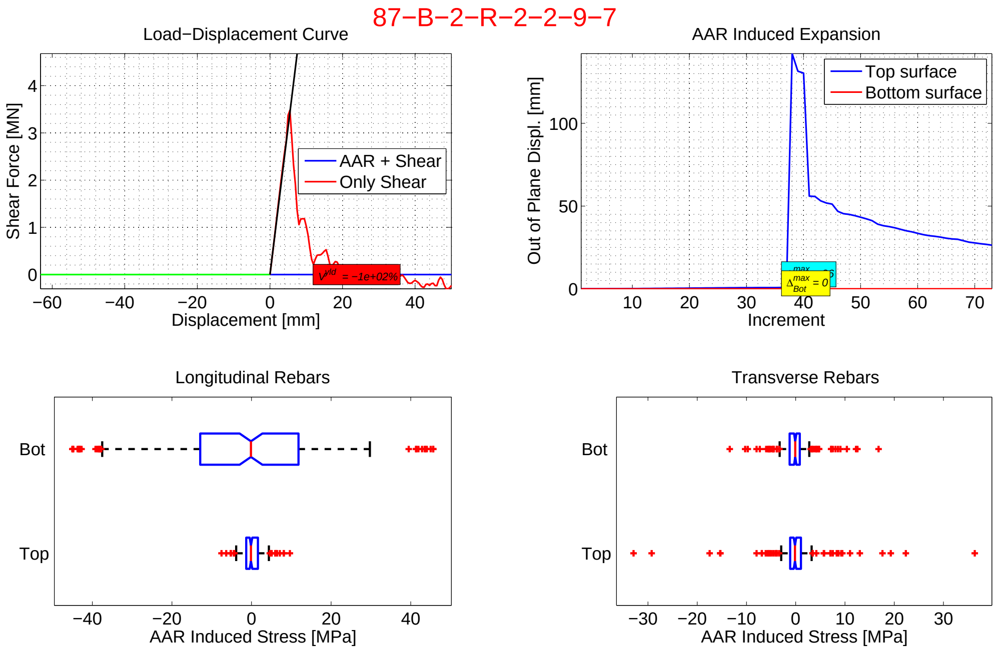

4.1.1.88 Analysis: 88-B-2-R-2-2-9-9

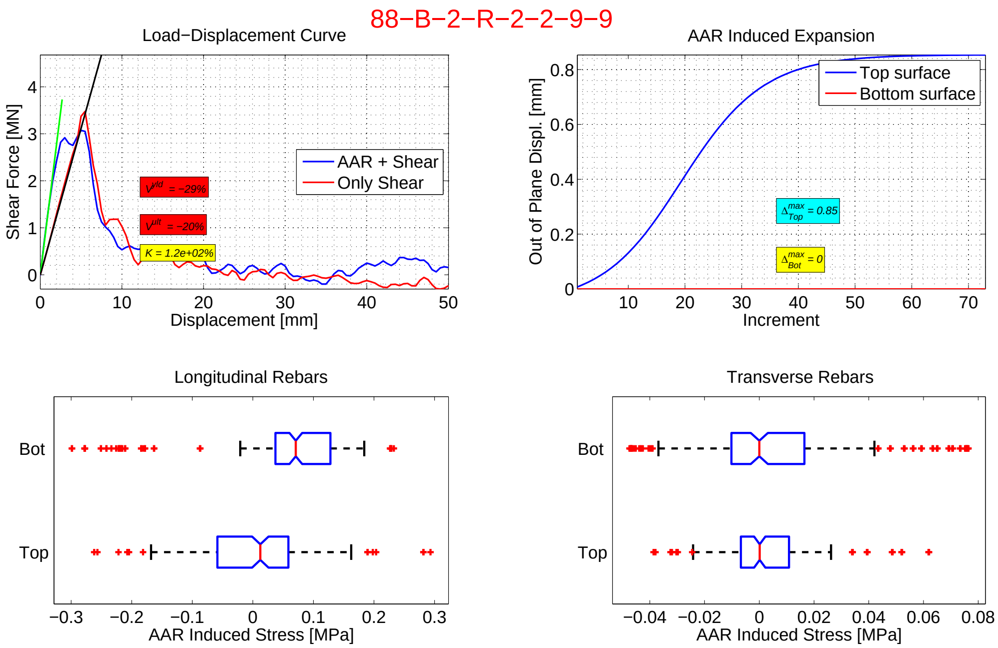

4.1.1.89 Analysis: 89-B-2-R-2-5-7-7

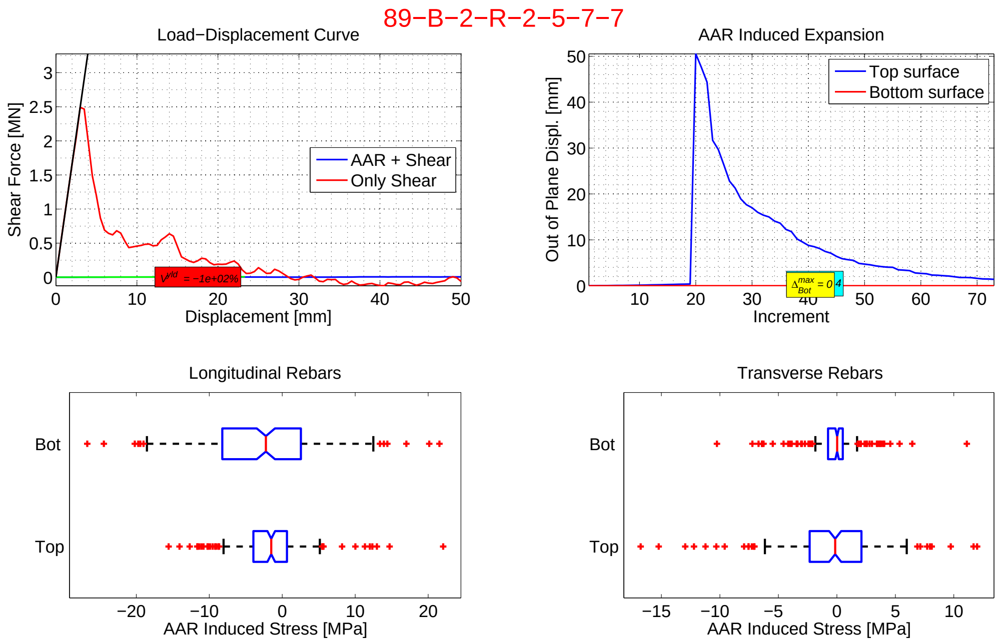

4.1.1.90 Analysis: 90-B-2-R-2-5-7-9

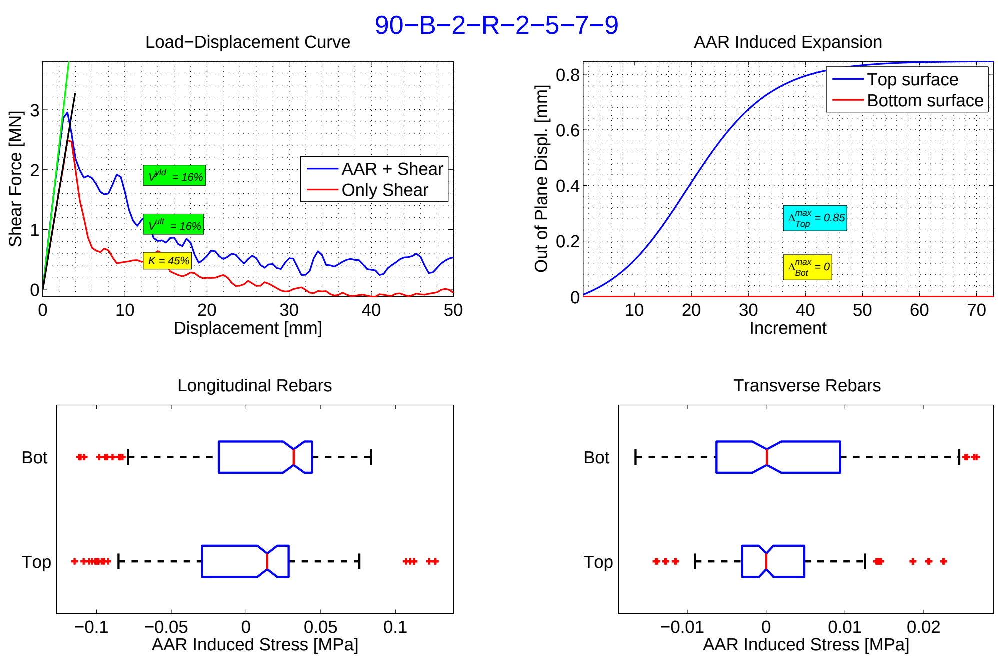

4.1.1.91 Analysis: 91-B-2-R-2-5-9-7

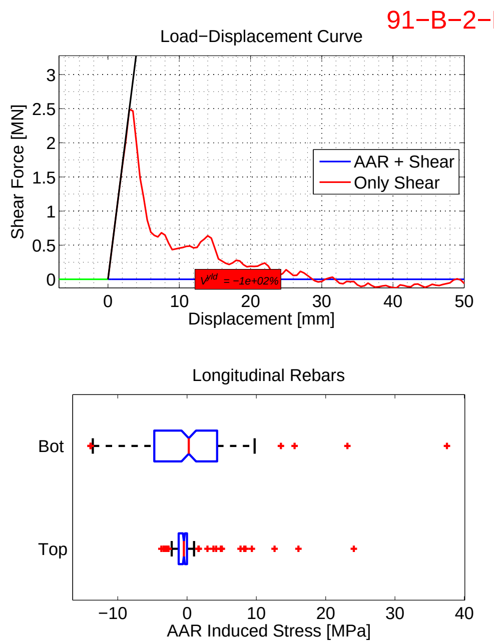

4.1.1.92 Analysis: 92-B-2-R-2-5-9-9

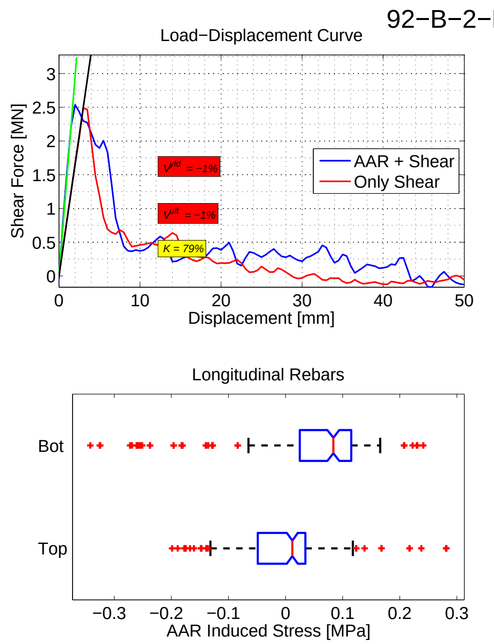

4.1.1.93 Analysis: 93-B-2-R-2-10-7-7

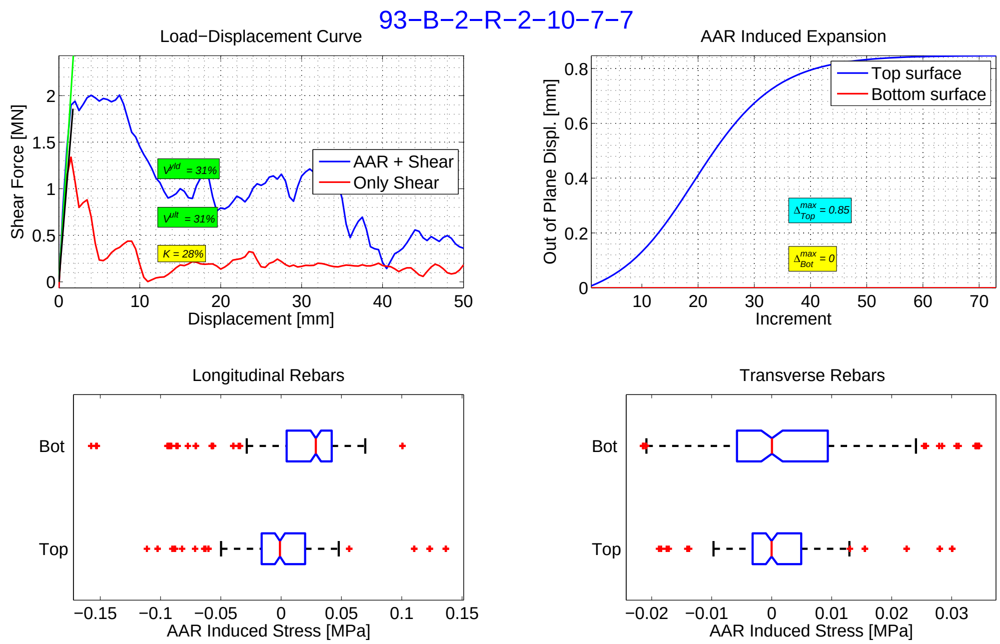

4.1.1.94 Analysis: 94-B-2-R-2-10-7-9

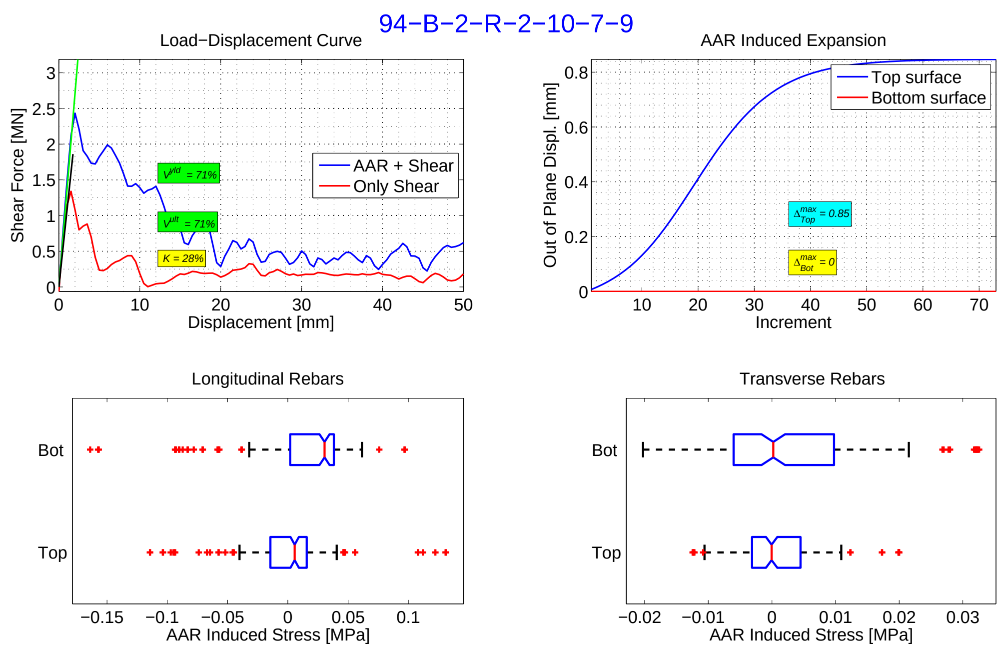

4.1.1.95 Analysis: 95-B-2-R-2-10-9-7

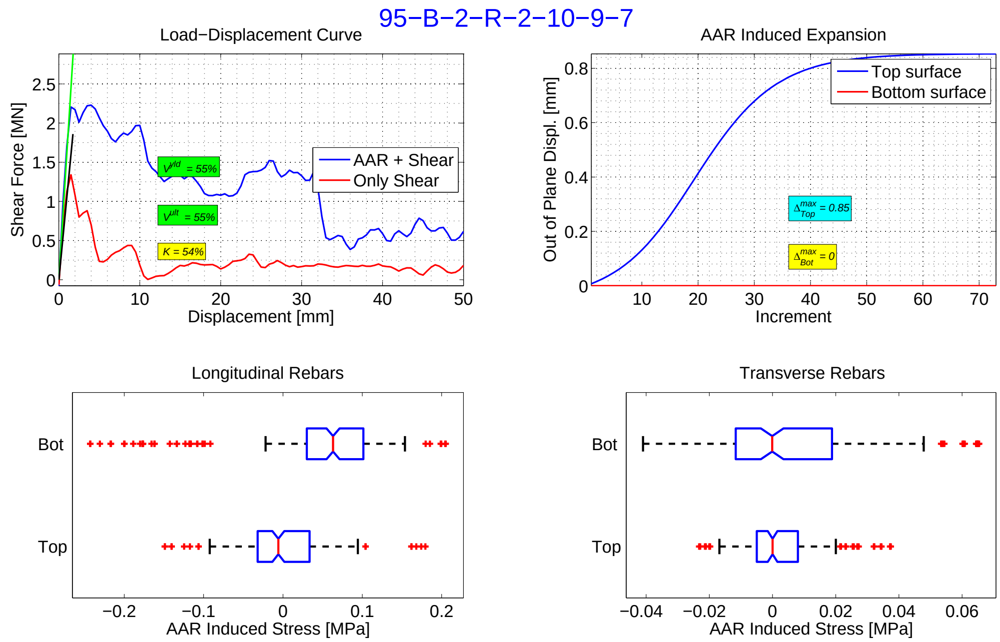

4.1.1.96 Analysis: 96-B-2-R-2-10-9-9

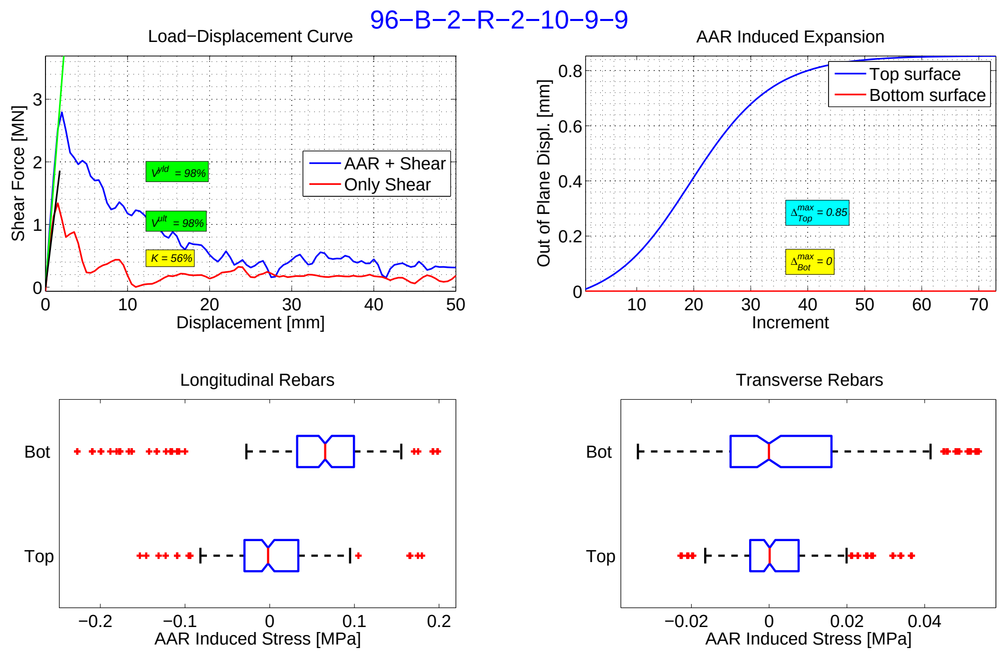

4.1.1.97 Analysis: 97-B-2-R-3-2-7-7

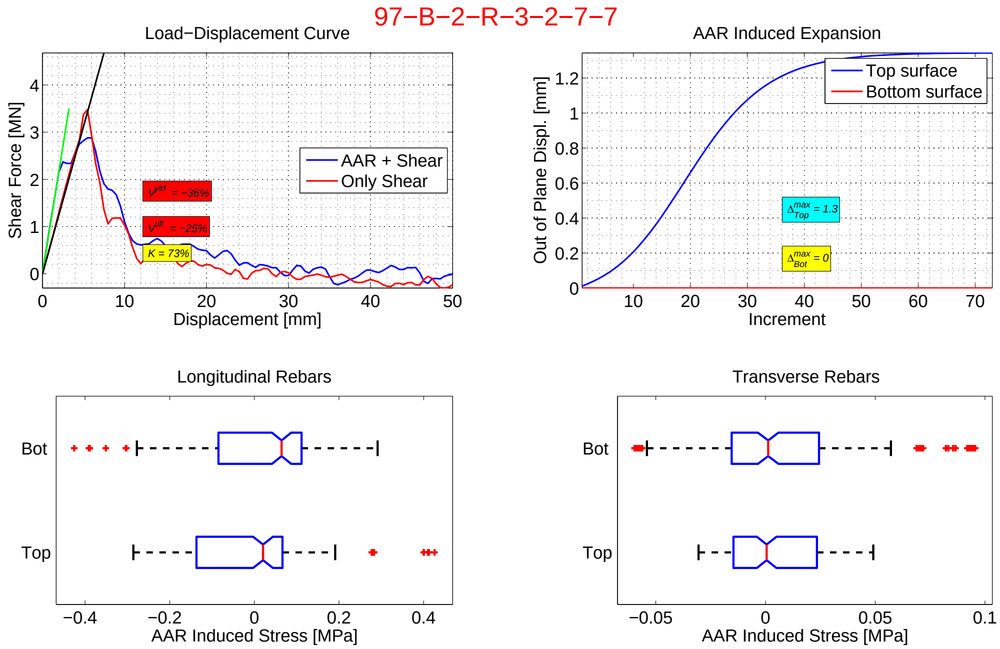

4.1.1.98 Analysis: 98-B-2-R-3-2-7-9

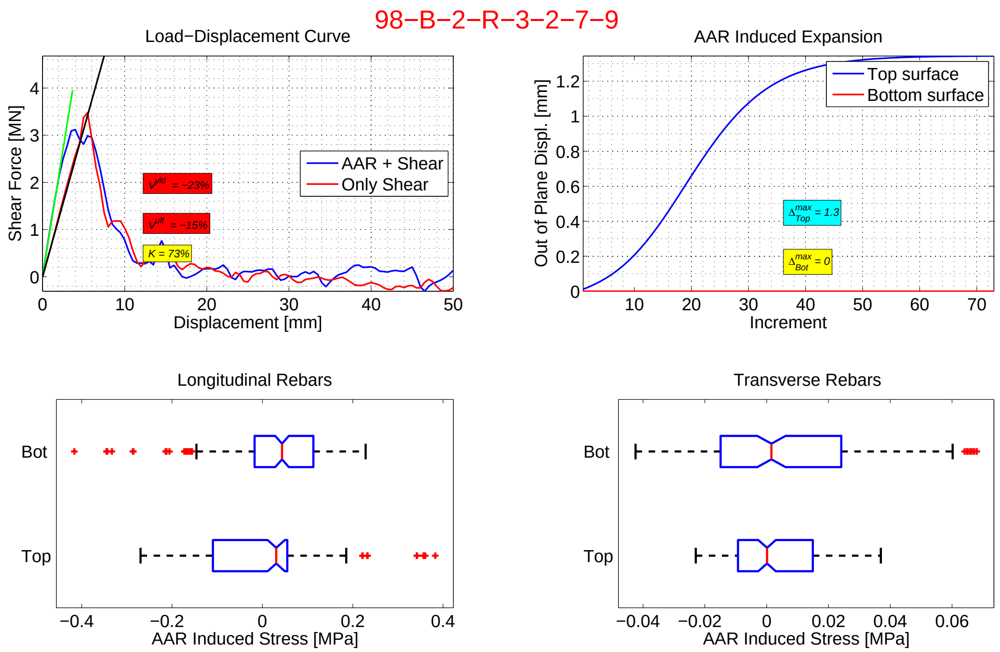

4.1.1.99 Analysis: 99-B-2-R-3-2-9-7

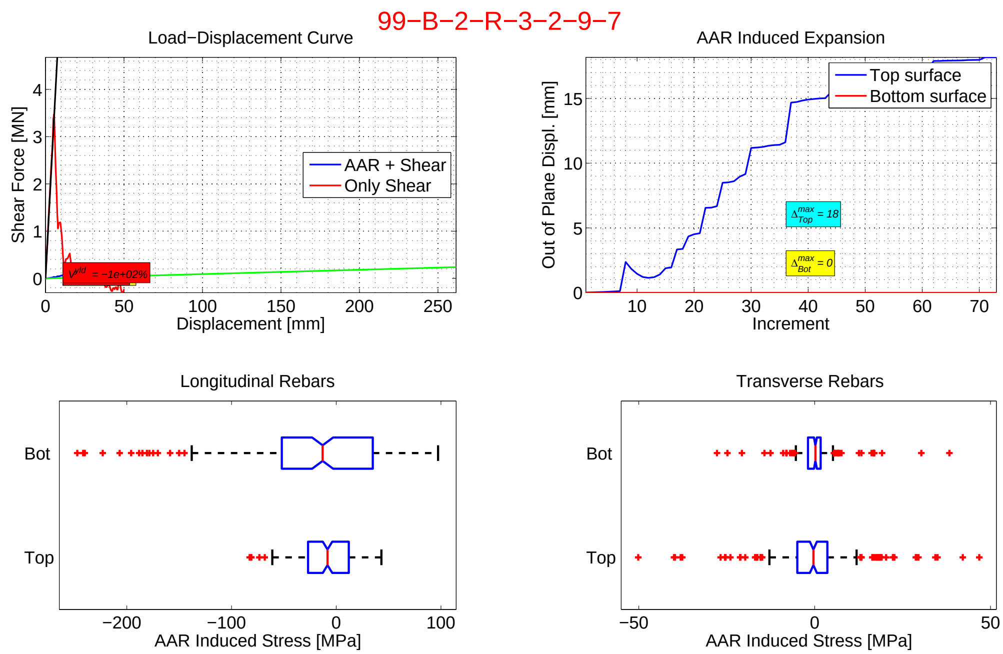

4.1.1.100 Analysis: 100-B-2-R-3-2-9-9

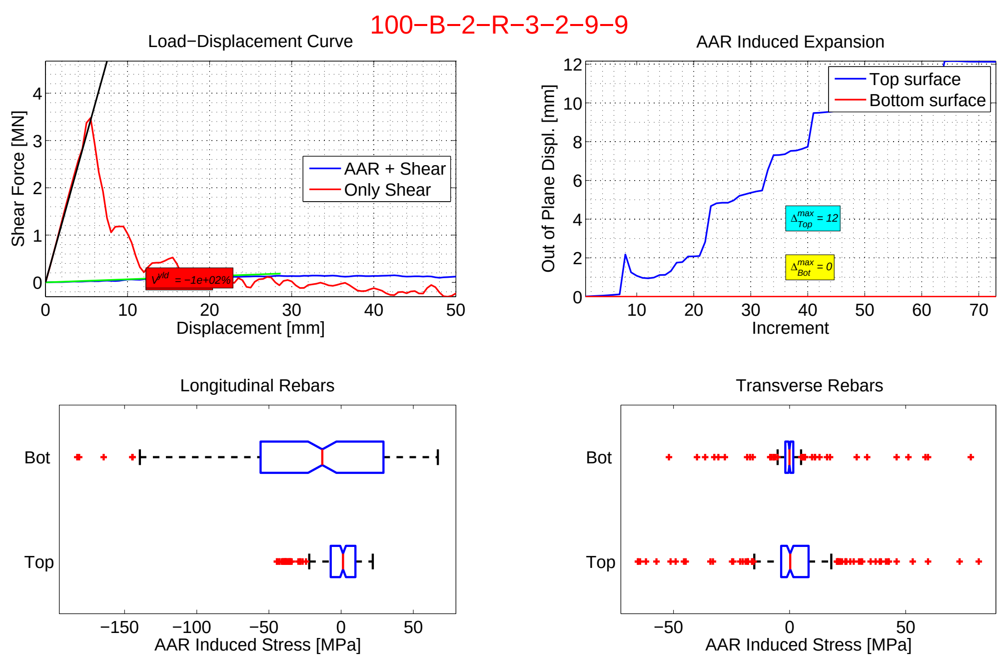

4.1.1.101 Analysis: 101-B-2-R-3-5-7-7

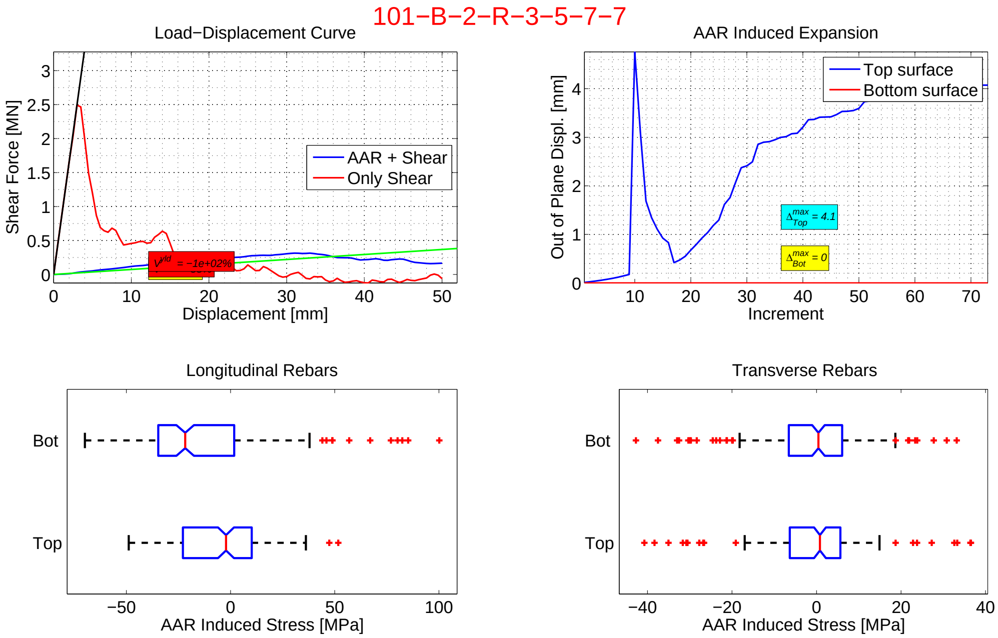

4.1.1.102 Analysis: 102-B-2-R-3-5-7-9

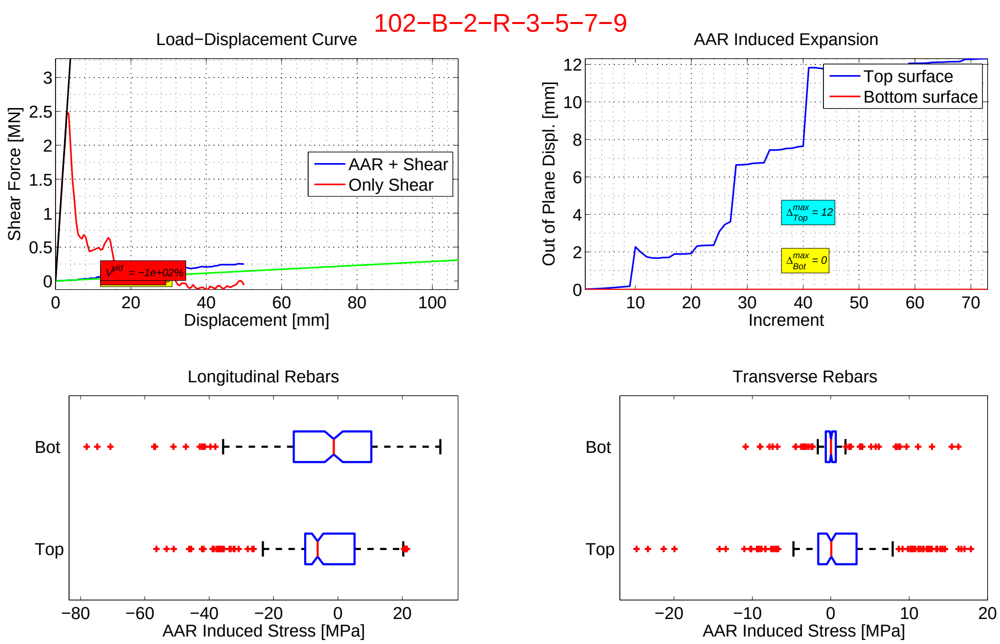

4.1.1.103 Analysis: 103-B-2-R-3-5-9-7

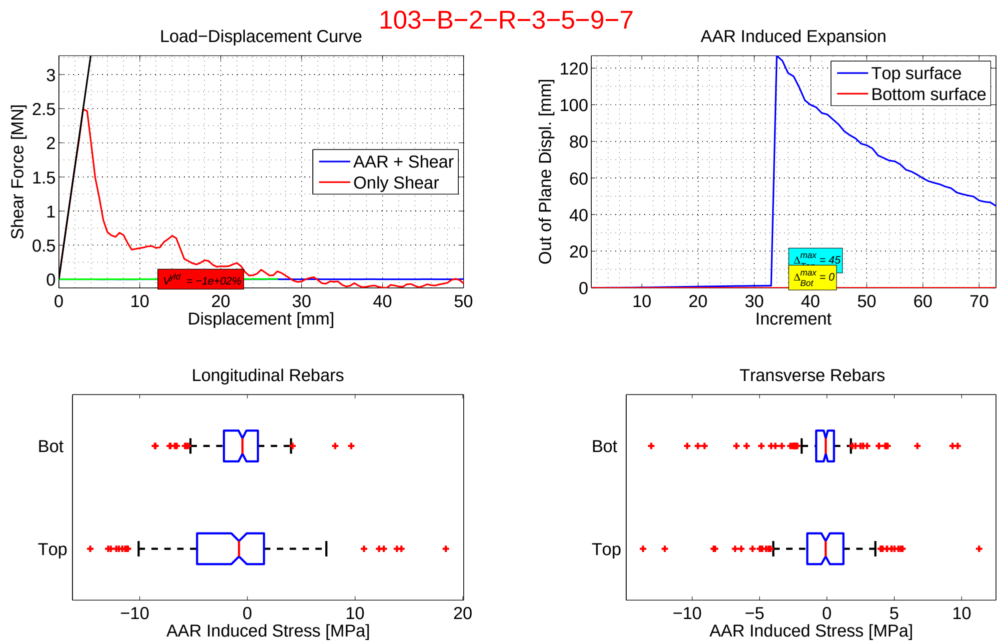

4.1.1.104 Analysis: 104-B-2-R-3-5-9-9

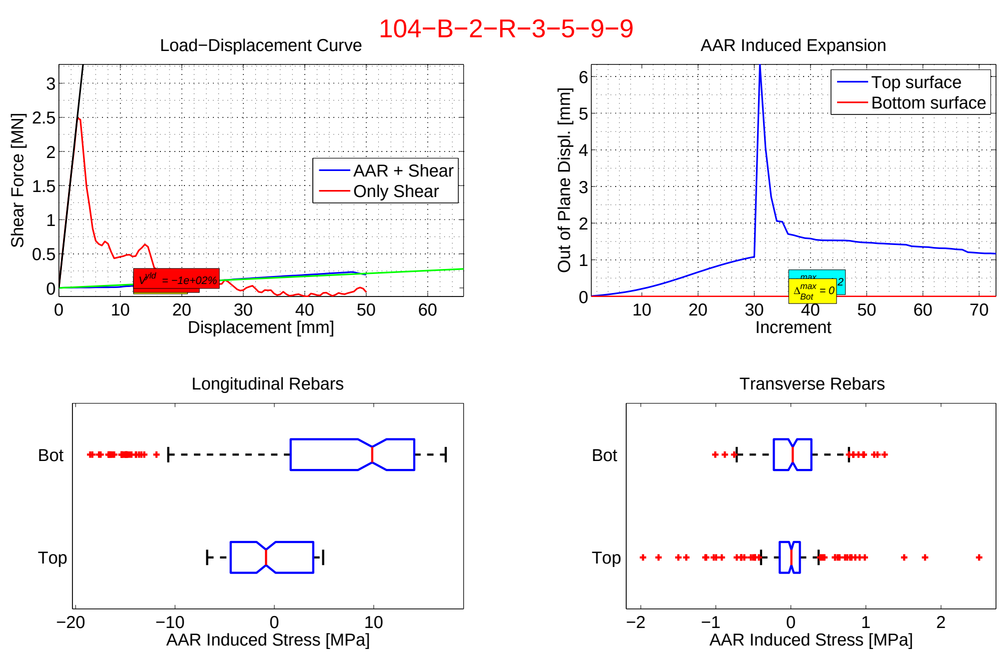

4.1.1.105 Analysis: 105-B-2-R-3-10-7-7

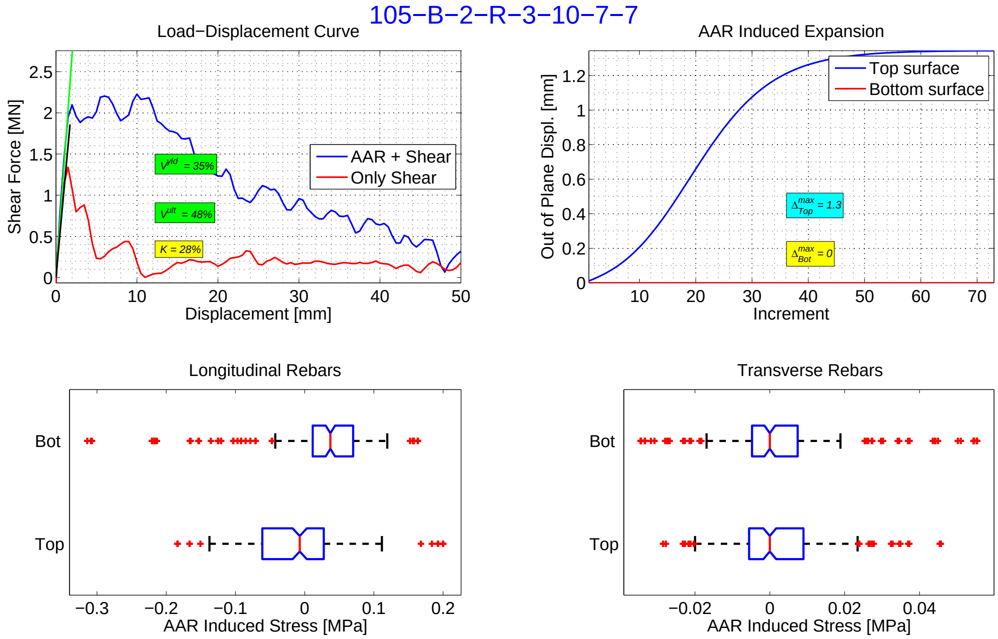

4.1.1.106 Analysis: 106-B-2-R-3-10-7-9

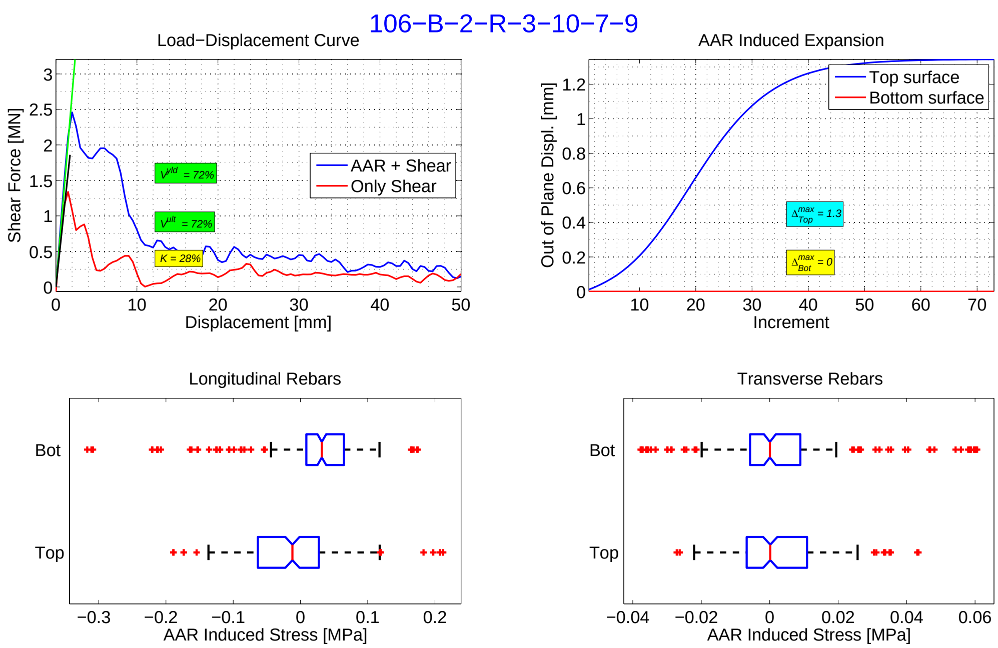

4.1.1.107 Analysis: 107-B-2-R-3-10-9-7

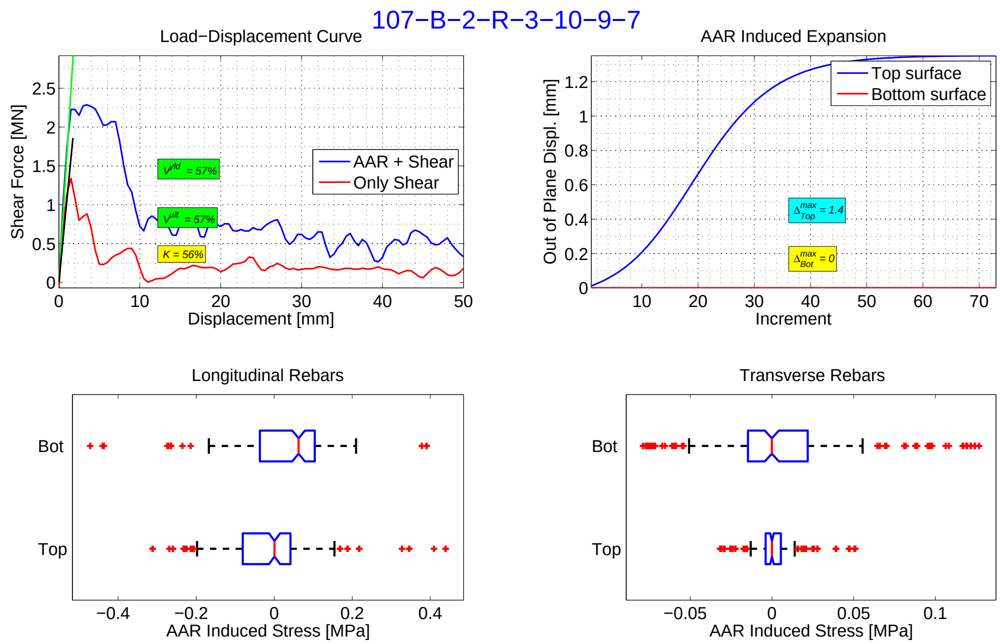

4.1.1.108 Analysis: 108-B-2-R-3-10-9-9

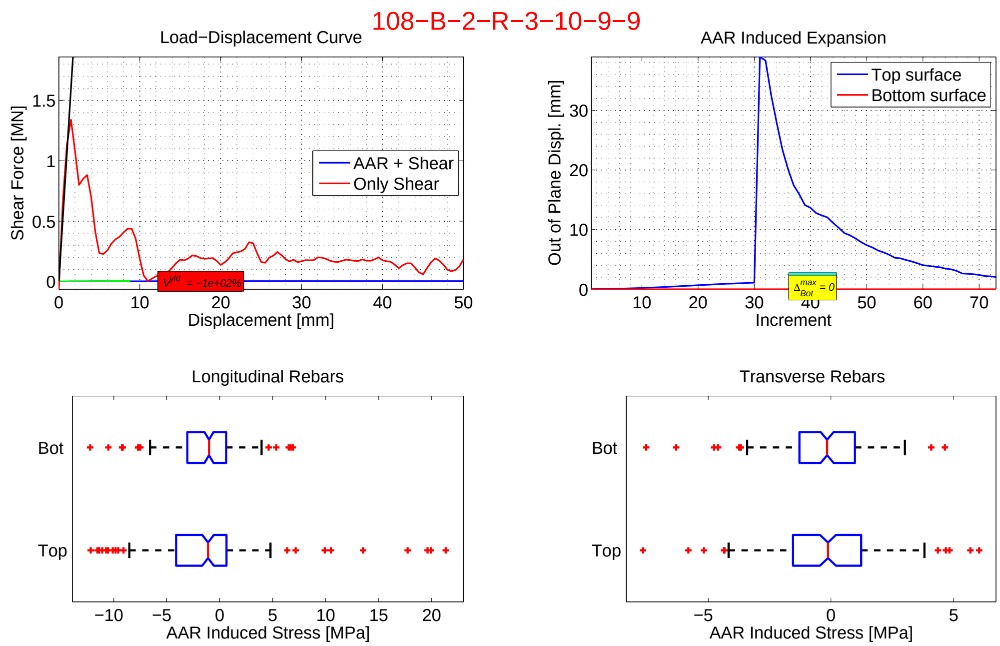

4.1.1.109 Analysis: 109-B-4-R-1-2-7-7

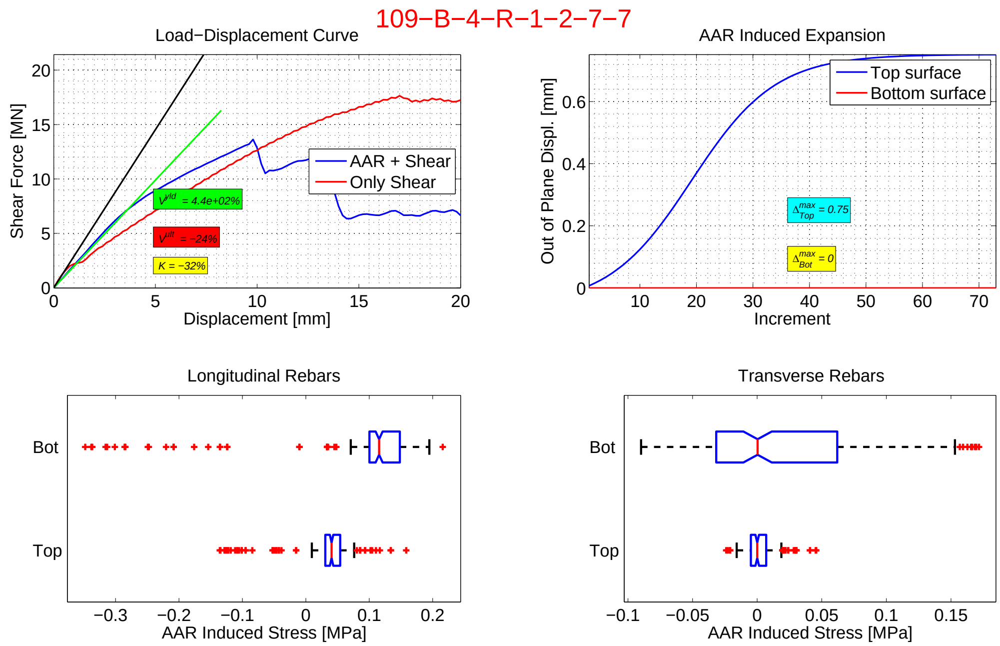

4.1.1.110 Analysis: 110-B-4-R-1-2-7-9

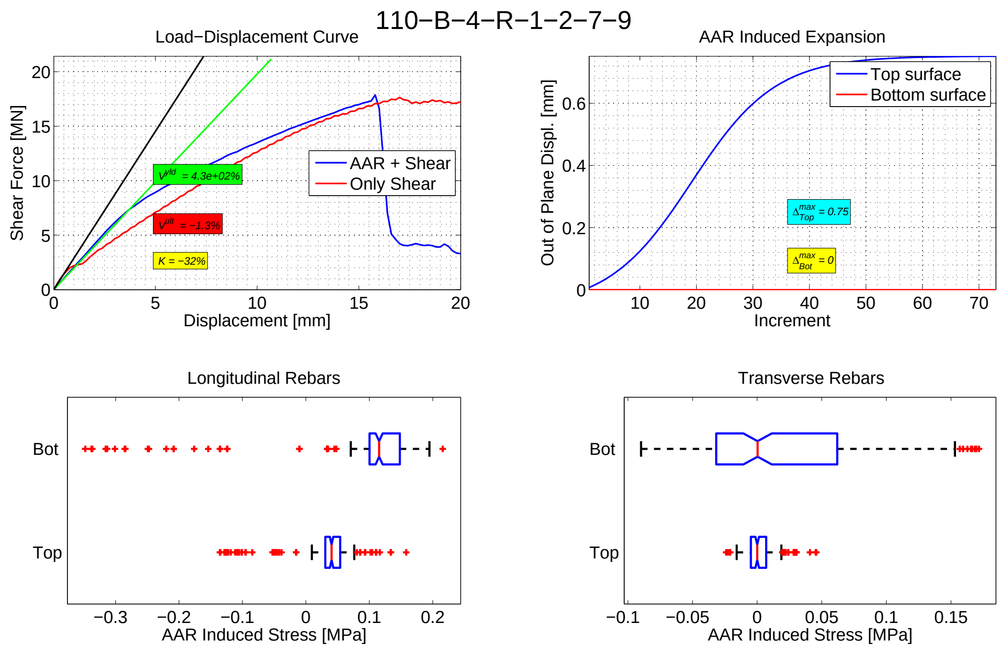

4.1.1.111 Analysis: 111-B-4-R-1-2-9-7

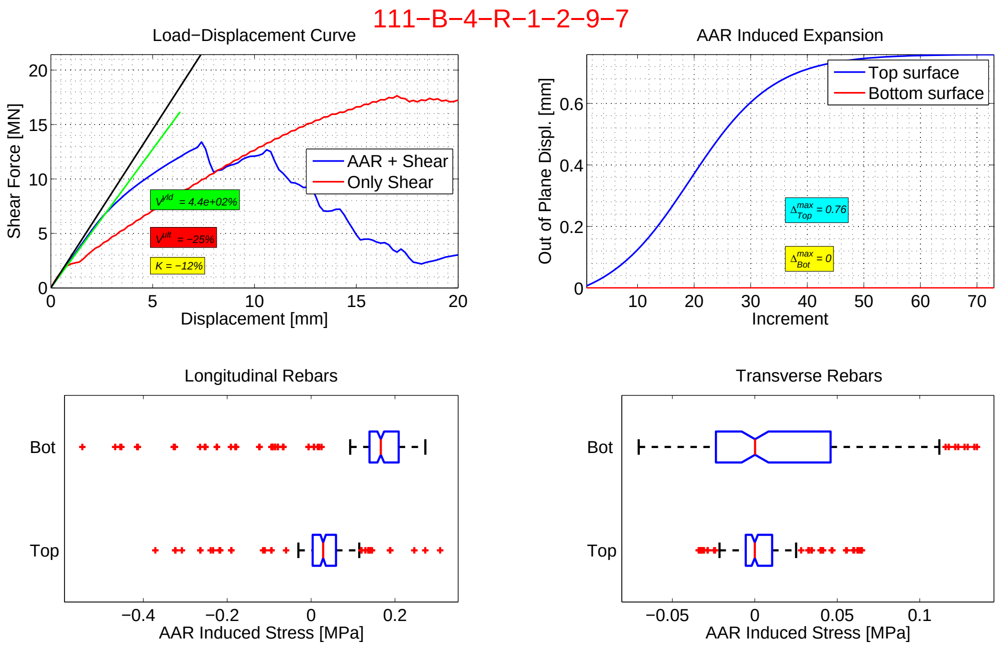

4.1.1.112 Analysis: 112-B-4-R-1-2-9-9

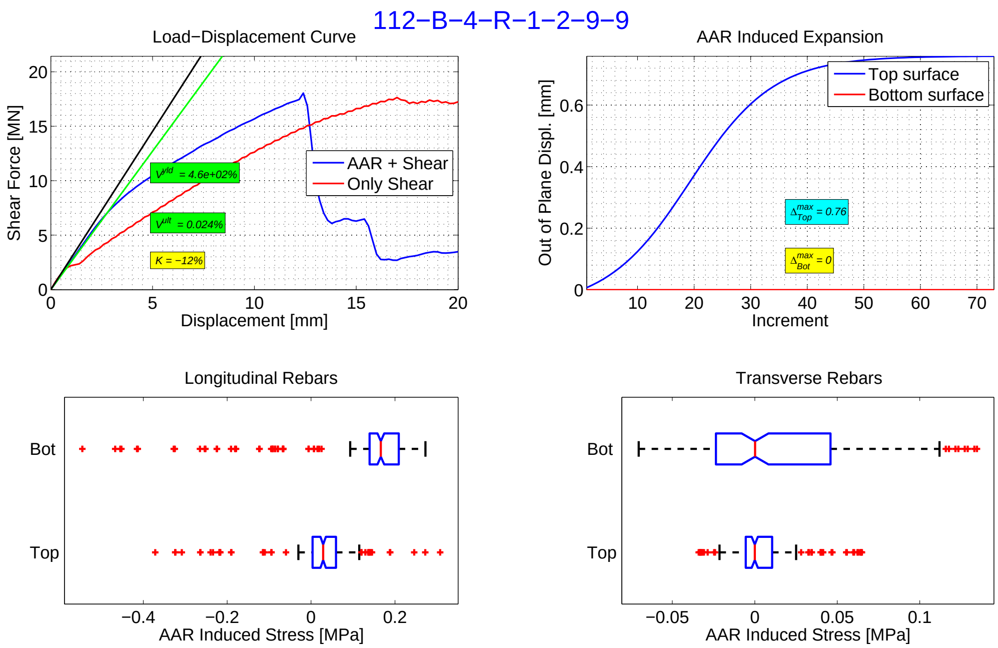

4.1.1.113 Analysis: 113-B-4-R-1-5-7-7

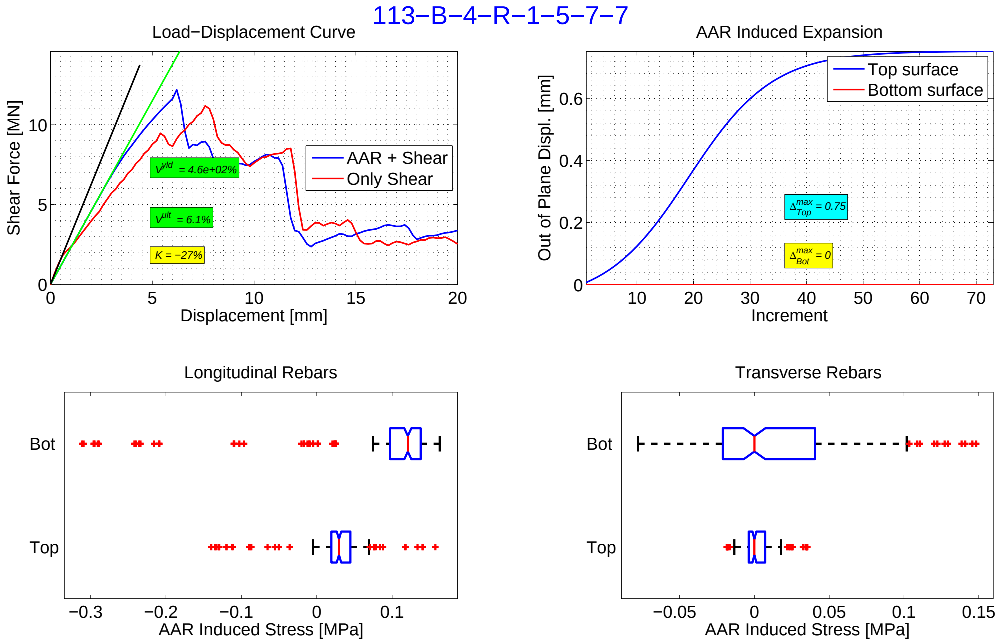

4.1.1.114 Analysis: 114-B-4-R-1-5-7-9

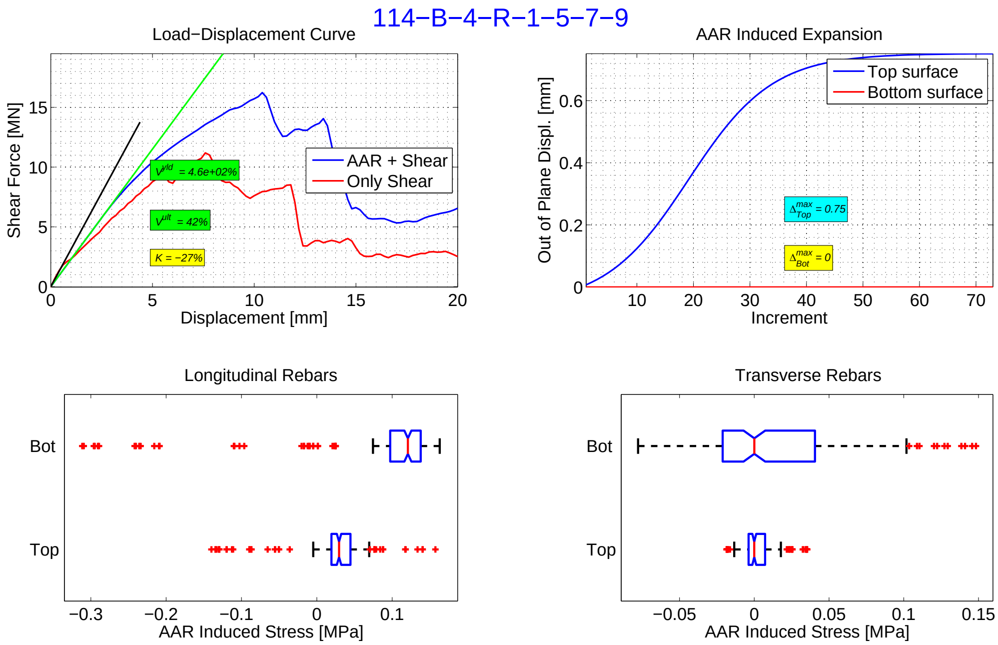

4.1.1.115 Analysis: 115-B-4-R-1-5-9-7

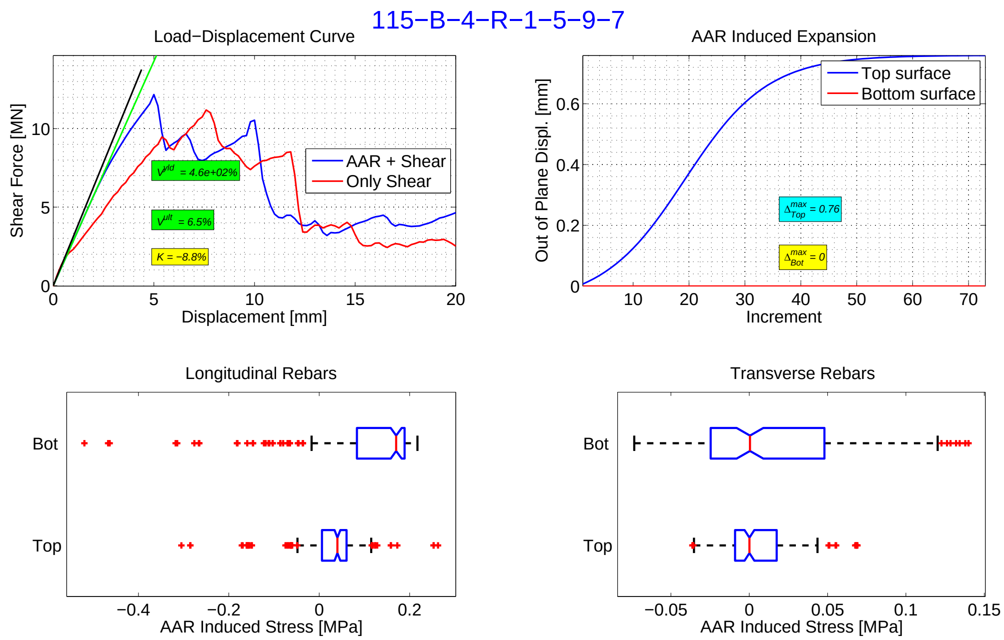

4.1.1.116 Analysis: 116-B-4-R-1-5-9-9

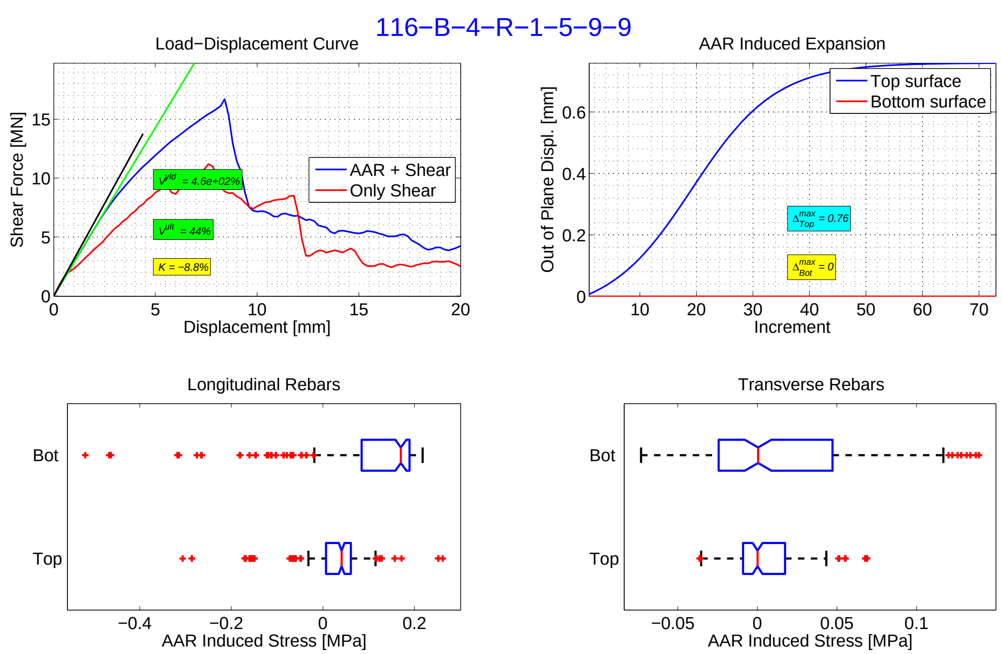

4.1.1.117 Analysis: 117-B-4-R-1-10-7-7

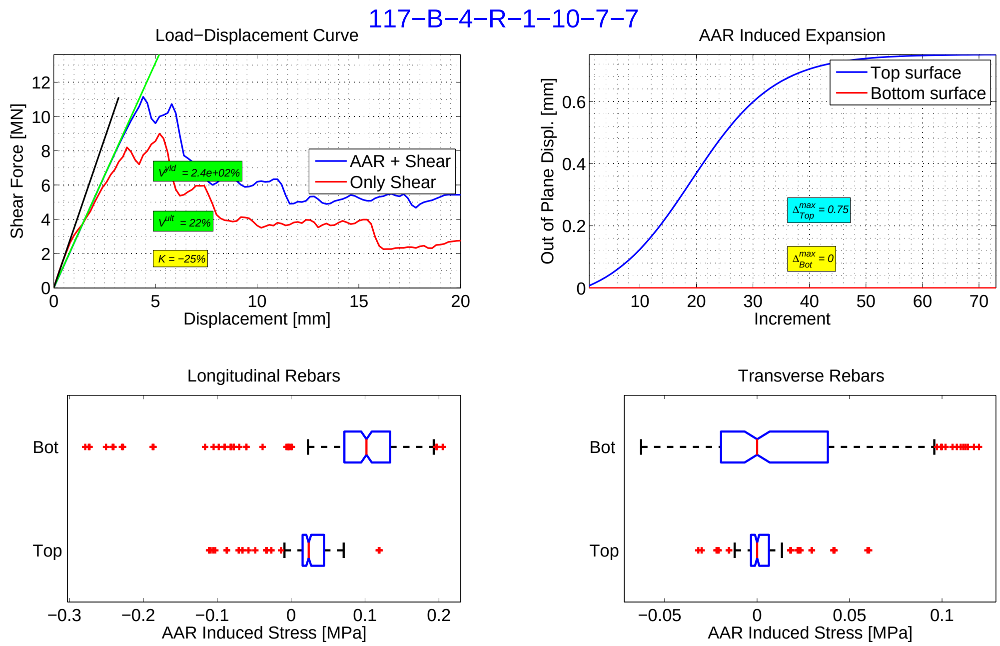

4.1.1.118 Analysis: 118-B-4-R-1-10-7-9

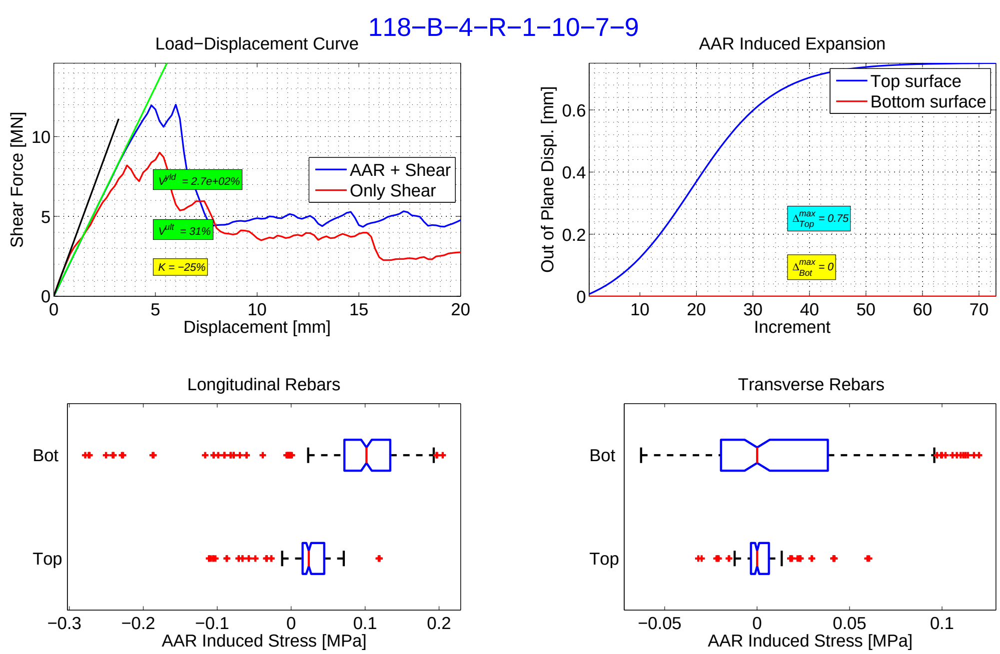

4.1.1.119 Analysis: 119-B-4-R-1-10-9-7

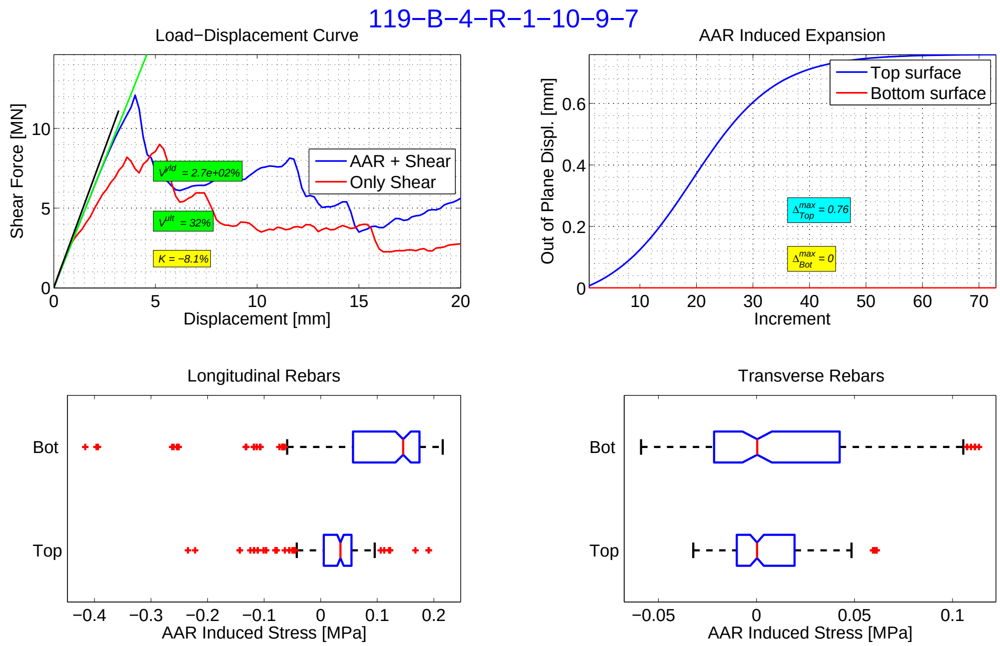

4.1.1.120 Analysis: 120-B-4-R-1-10-9-9

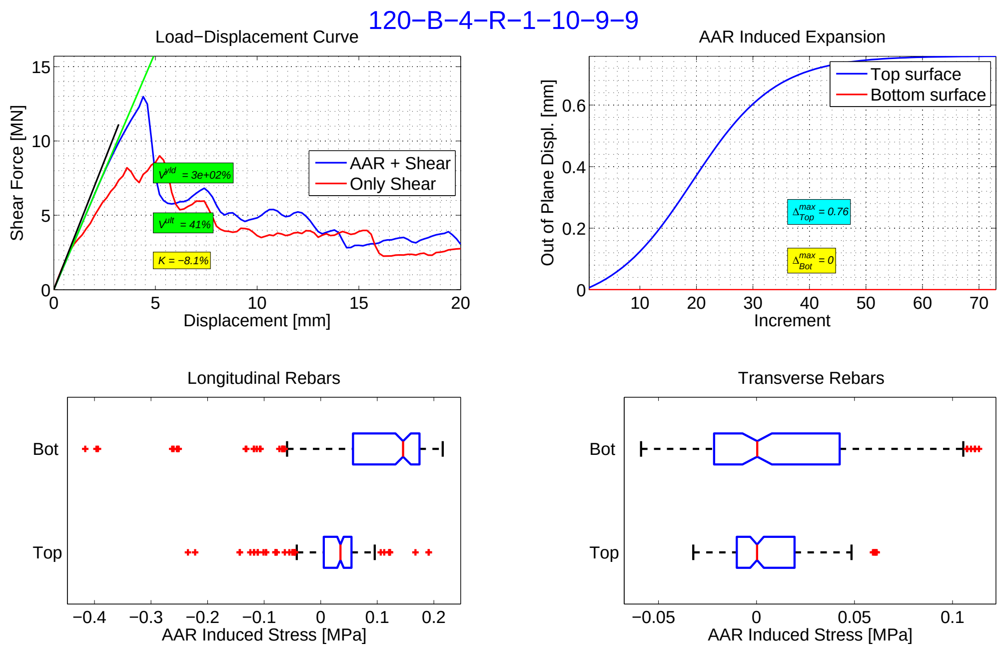

4.1.1.121 Analysis: 121-B-4-R-2-2-7-7

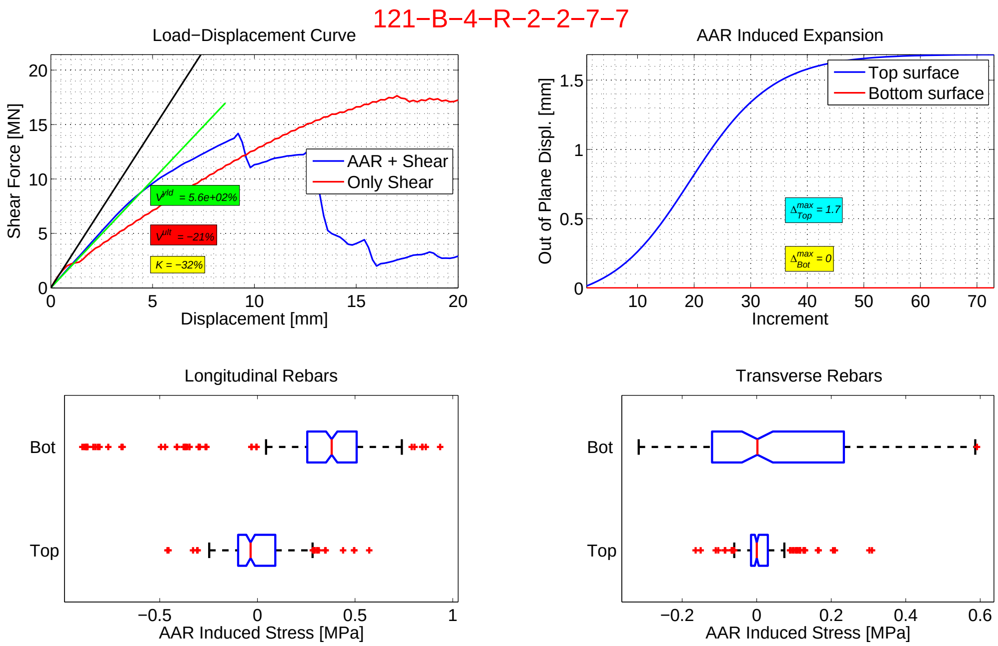

4.1.1.122 Analysis: 122-B-4-R-2-2-7-9

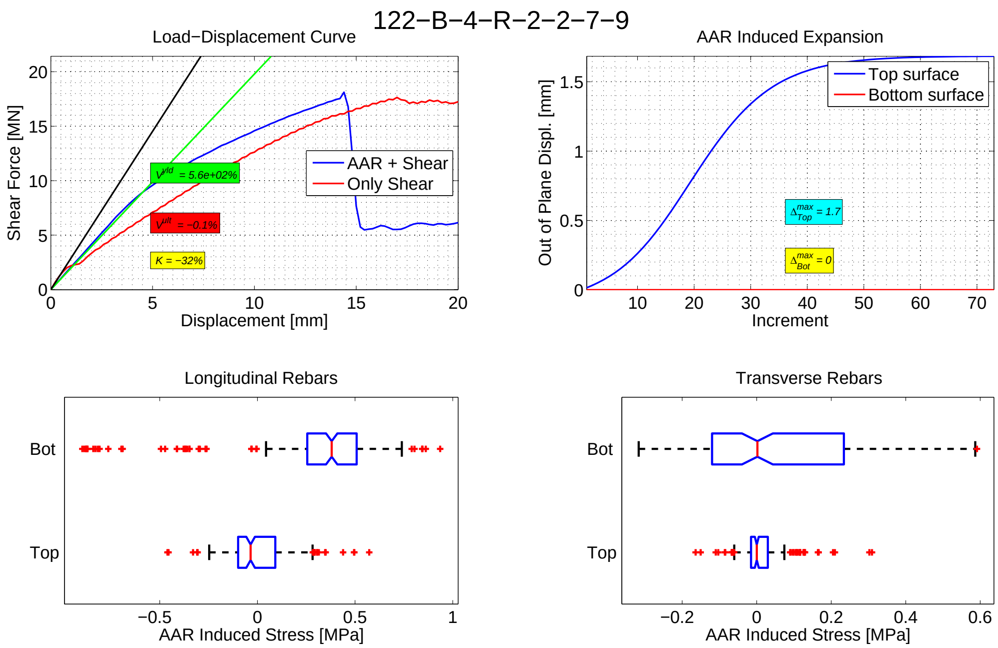

4.1.1.123 Analysis: 123-B-4-R-2-2-9-7

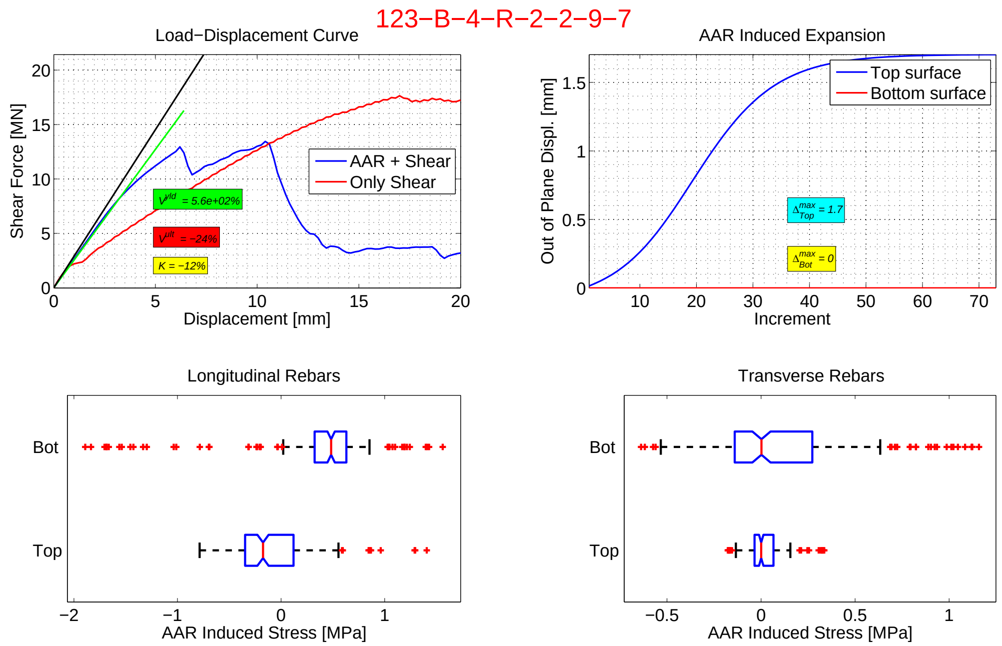

4.1.1.124 Analysis: 124-B-4-R-2-2-9-9

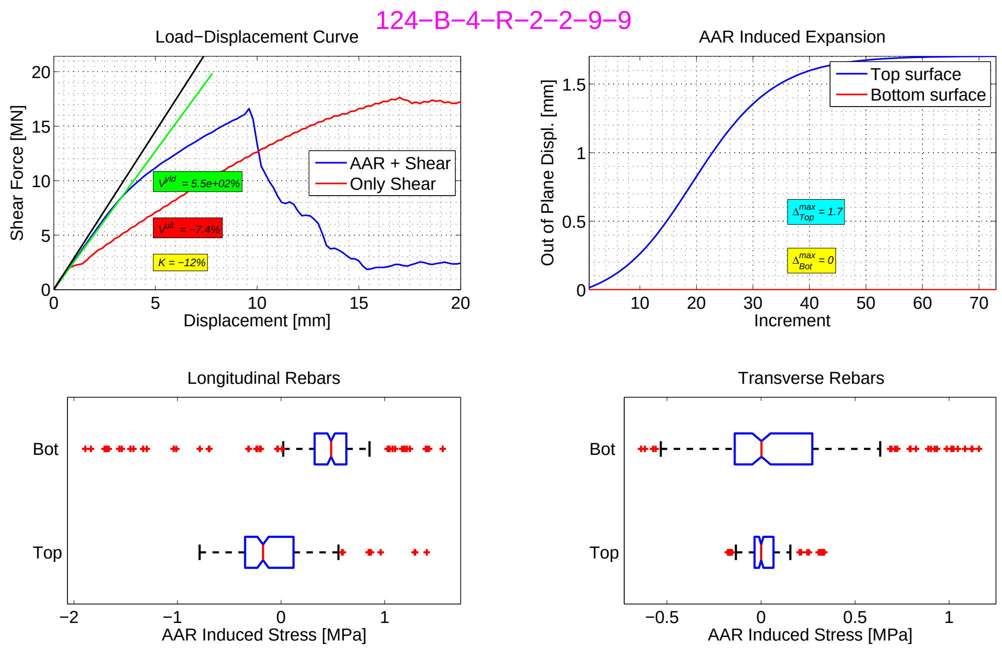

4.1.1.125 Analysis: 125-B-4-R-2-5-7-7

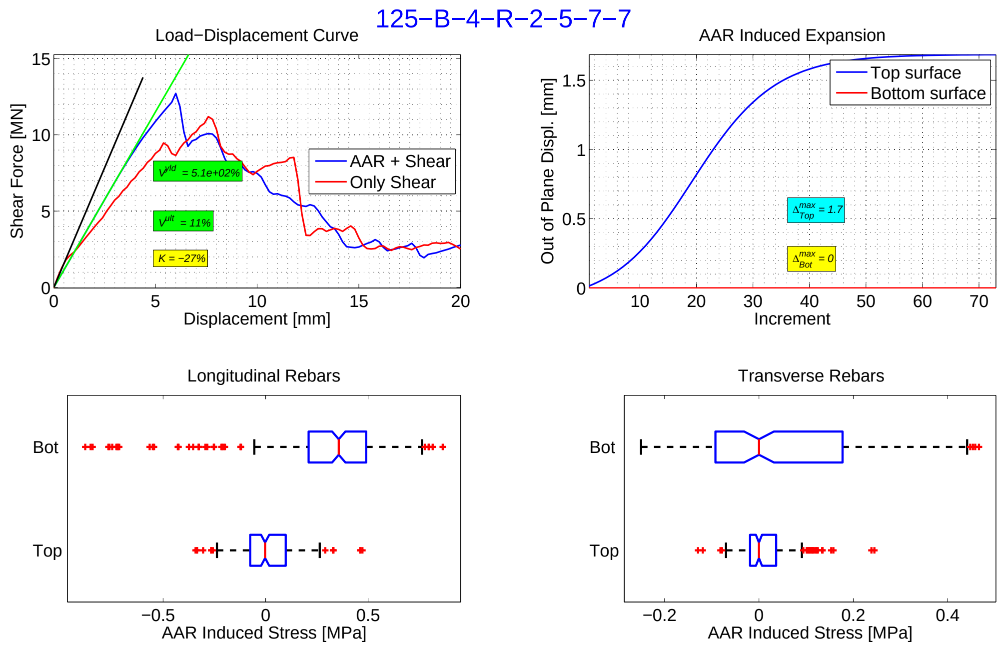

4.1.1.126 Analysis: 126-B-4-R-2-5-7-9

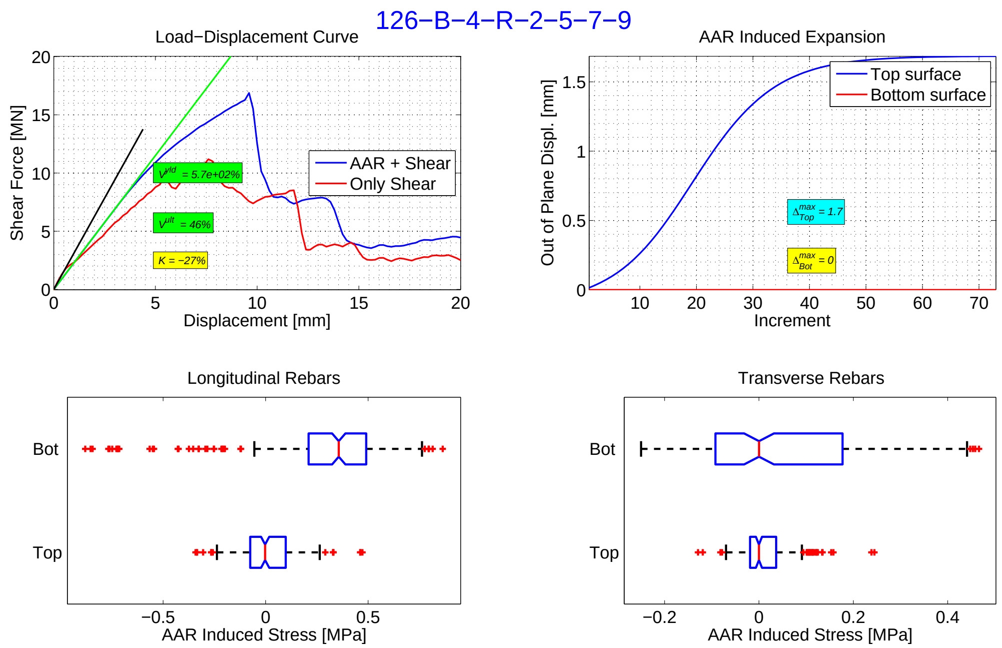

4.1.1.127 Analysis: 127-B-4-R-2-5-9-7

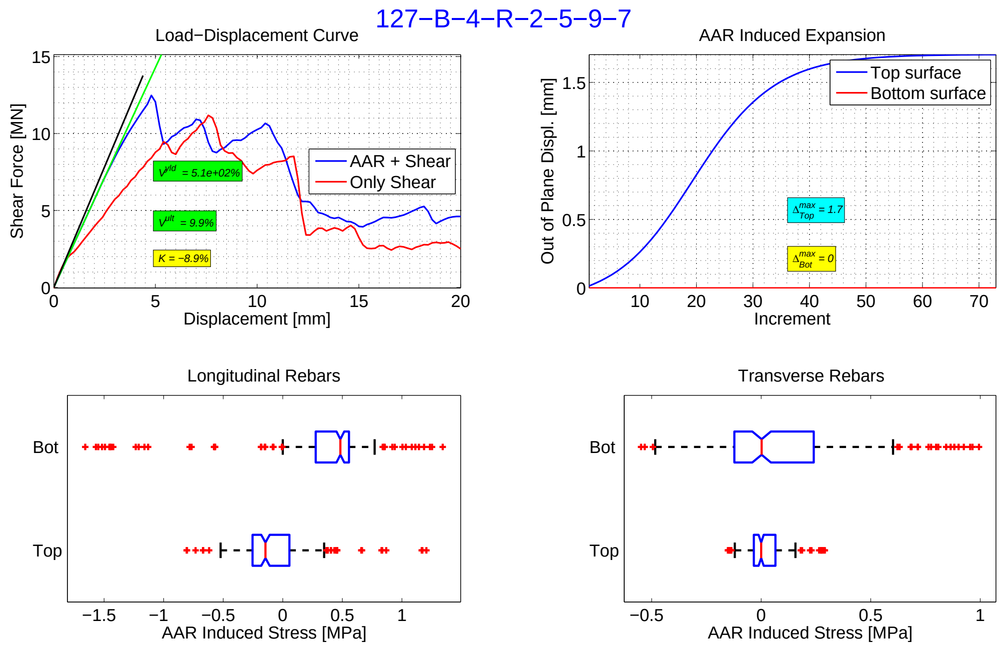

4.1.1.128 Analysis: 128-B-4-R-2-5-9-9

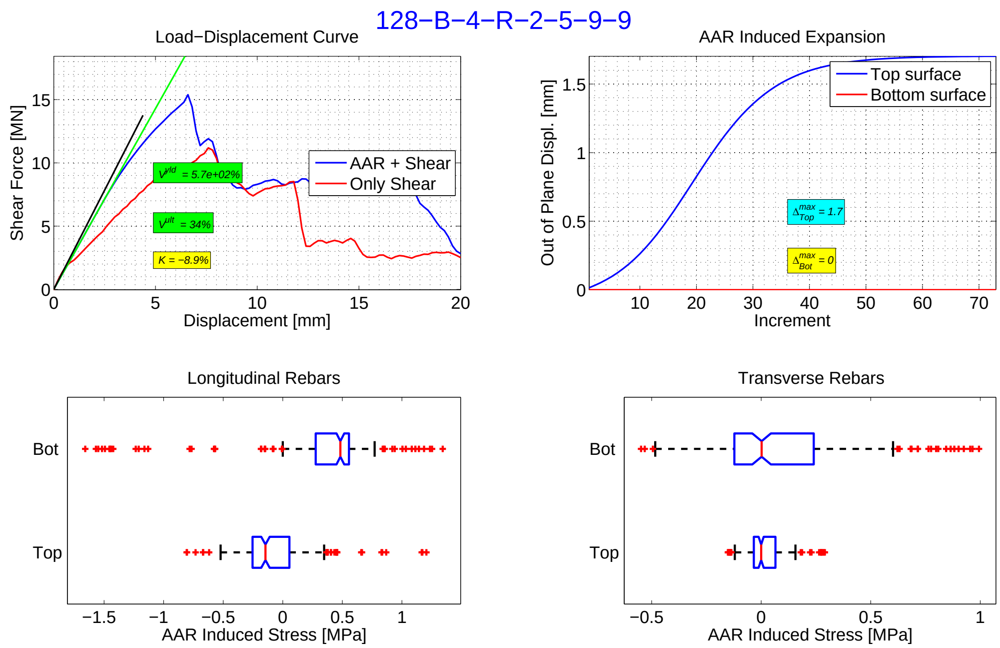

4.1.1.129 Analysis: 129-B-4-R-2-10-7-7

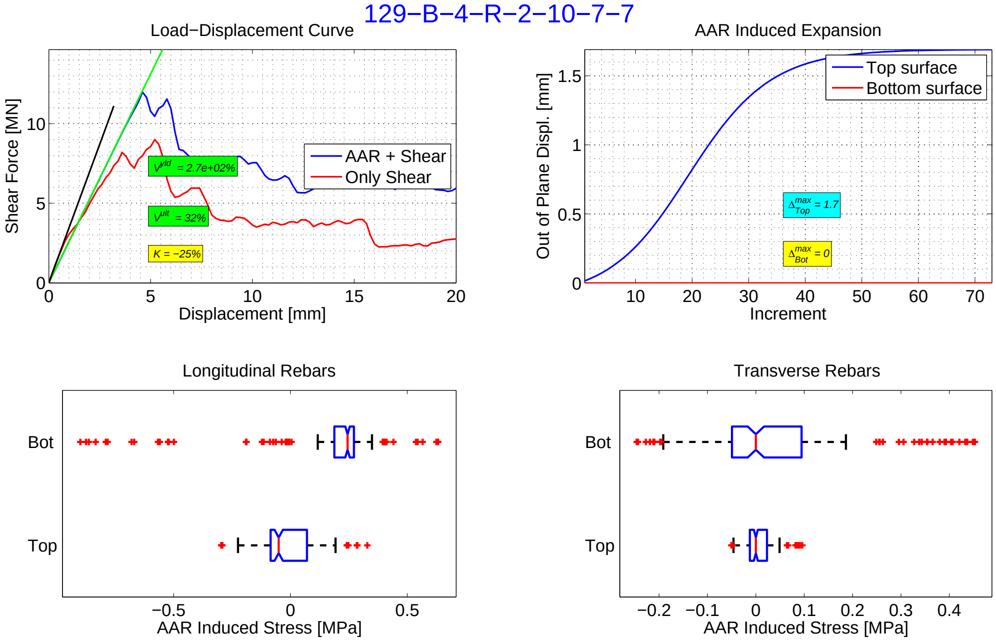

4.1.1.130 Analysis: 130-B-4-R-2-10-7-9

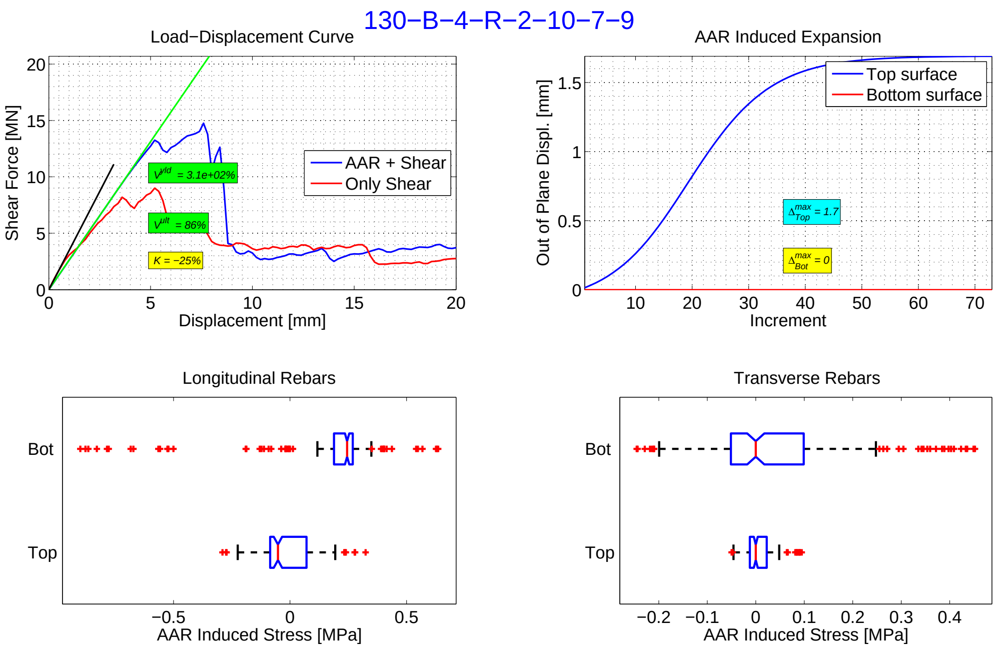

4.1.1.131 Analysis: 131-B-4-R-2-10-9-7

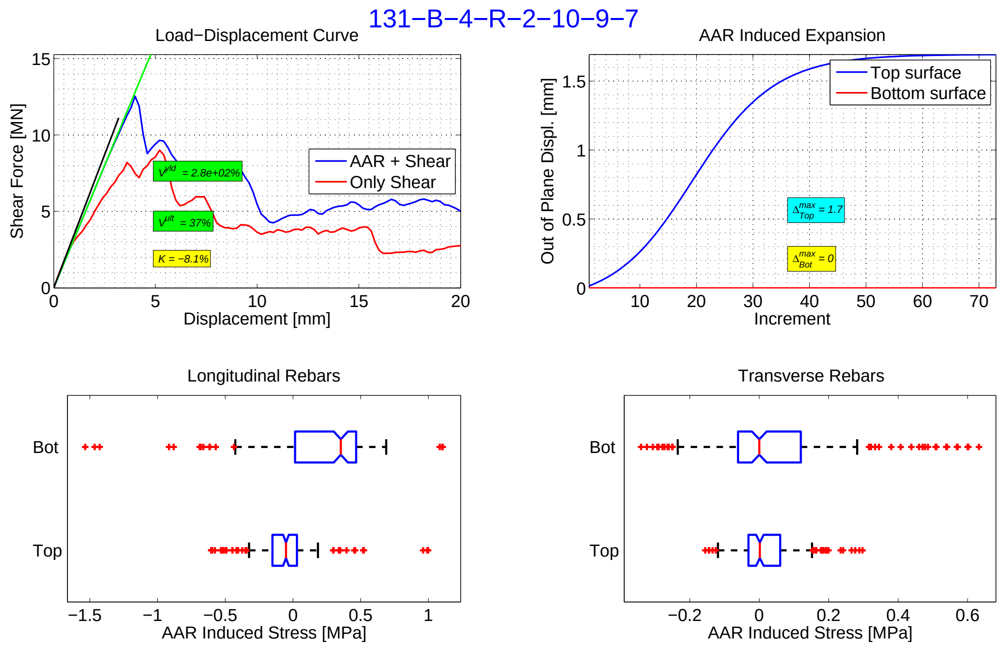

4.1.1.132 Analysis: 132-B-4-R-2-10-9-9

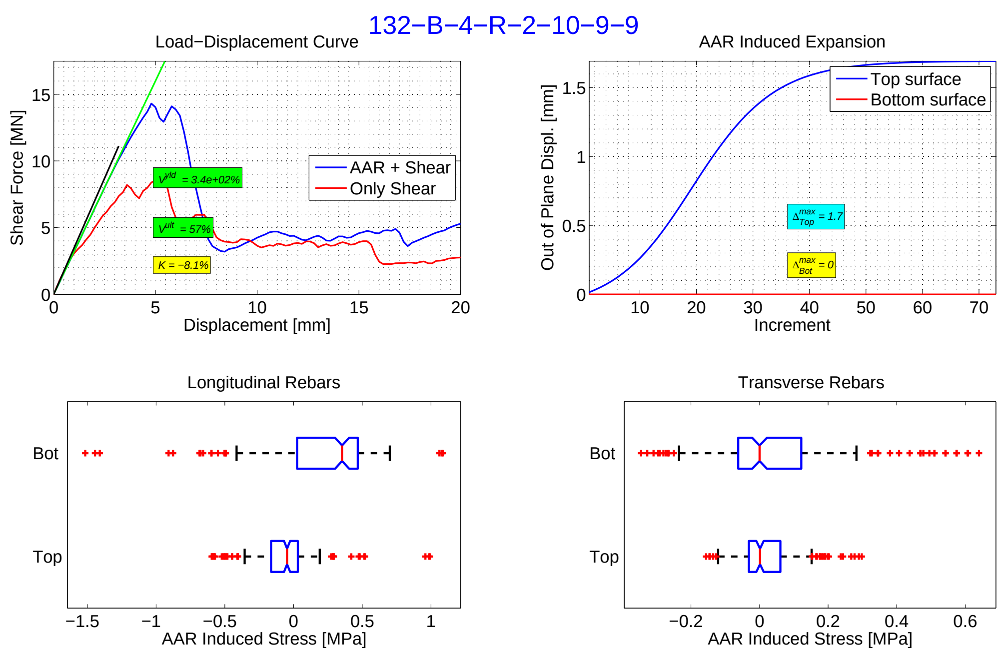

4.1.1.133 Analysis: 133-B-4-R-3-2-7-7

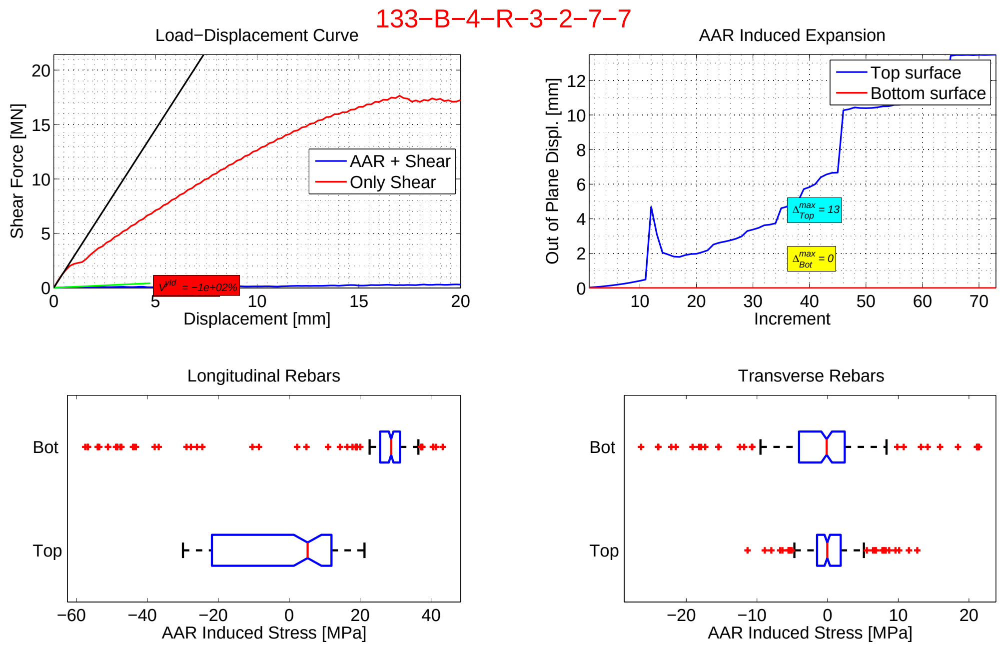

4.1.1.134 Analysis: 134-B-4-R-3-2-7-9

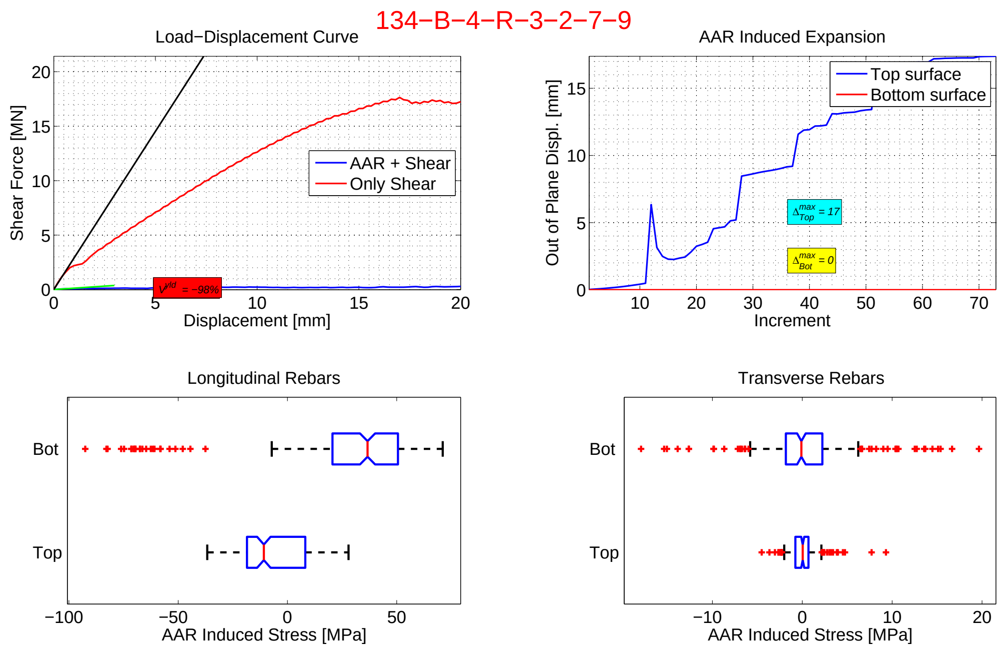

4.1.1.135 Analysis: 135-B-4-R-3-2-9-7

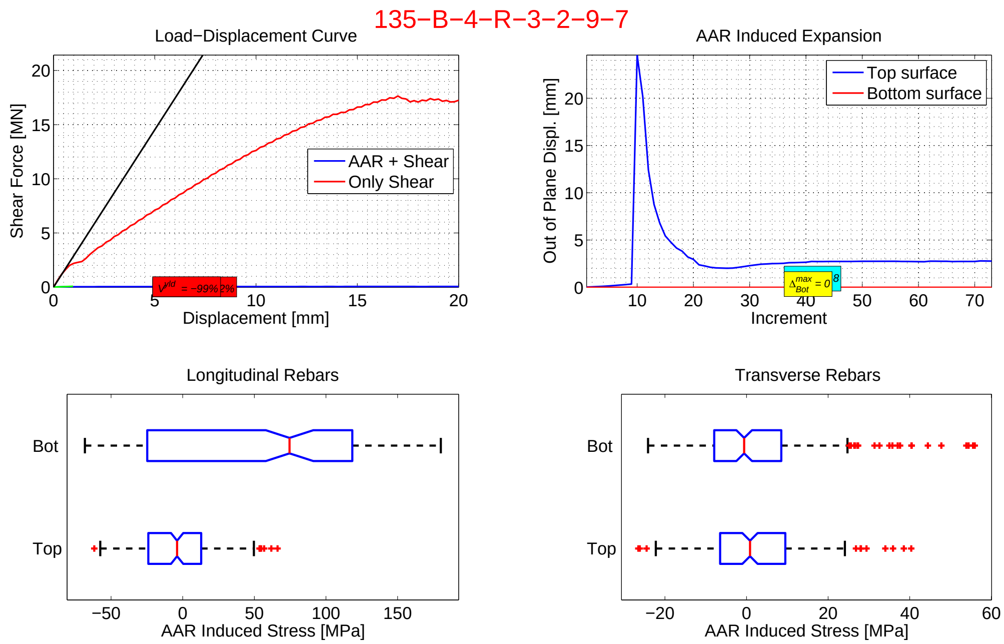

4.1.1.136 Analysis: 136-B-4-R-3-2-9-9

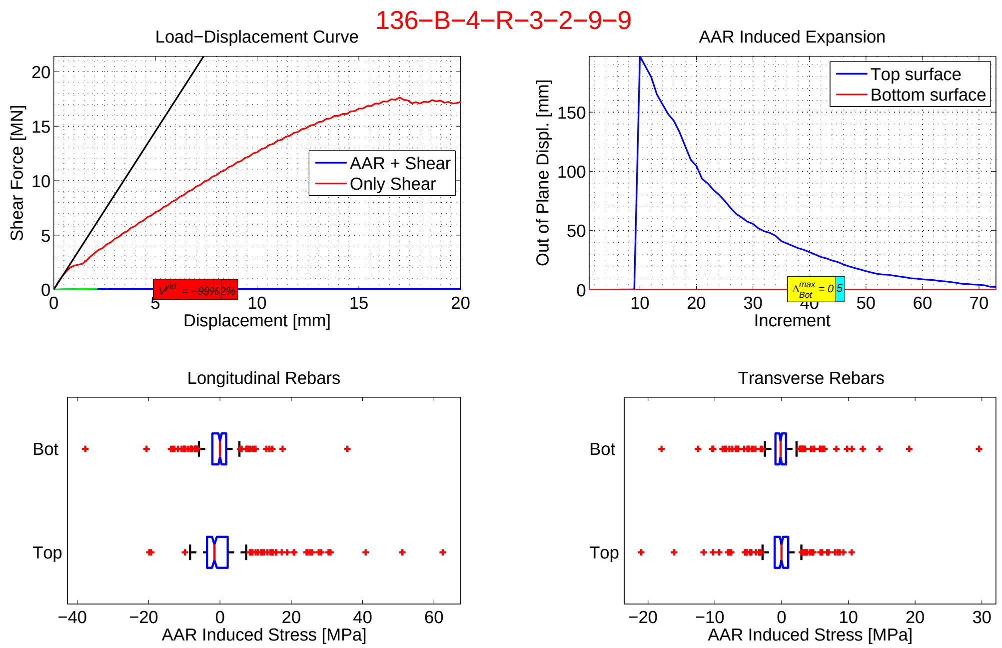

4.1.1.137 Analysis: 137-B-4-R-3-5-7-7

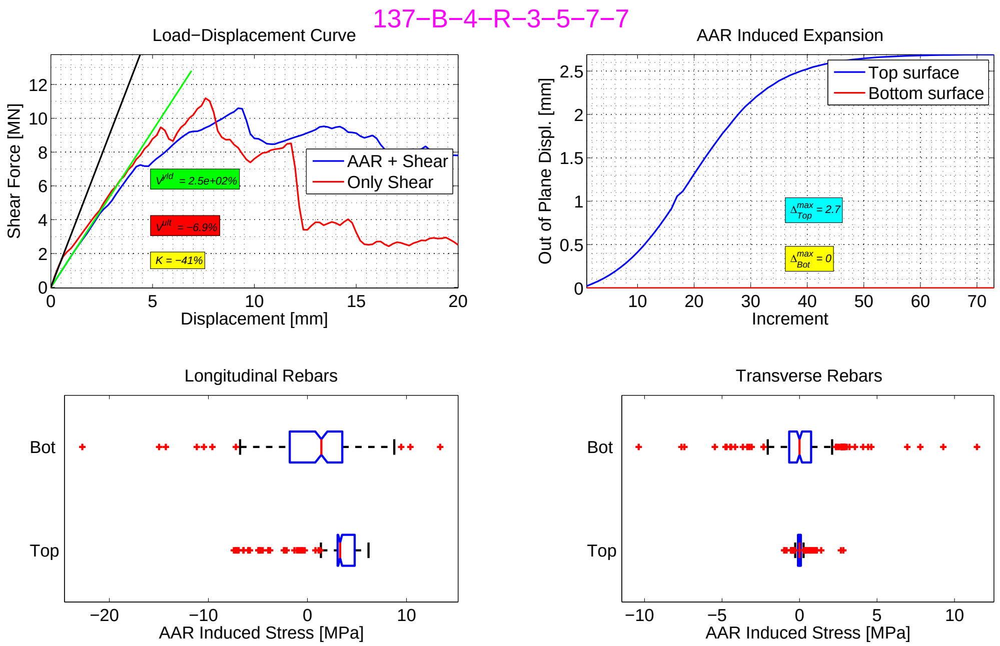

4.1.1.138 Analysis: 138-B-4-R-3-5-7-9

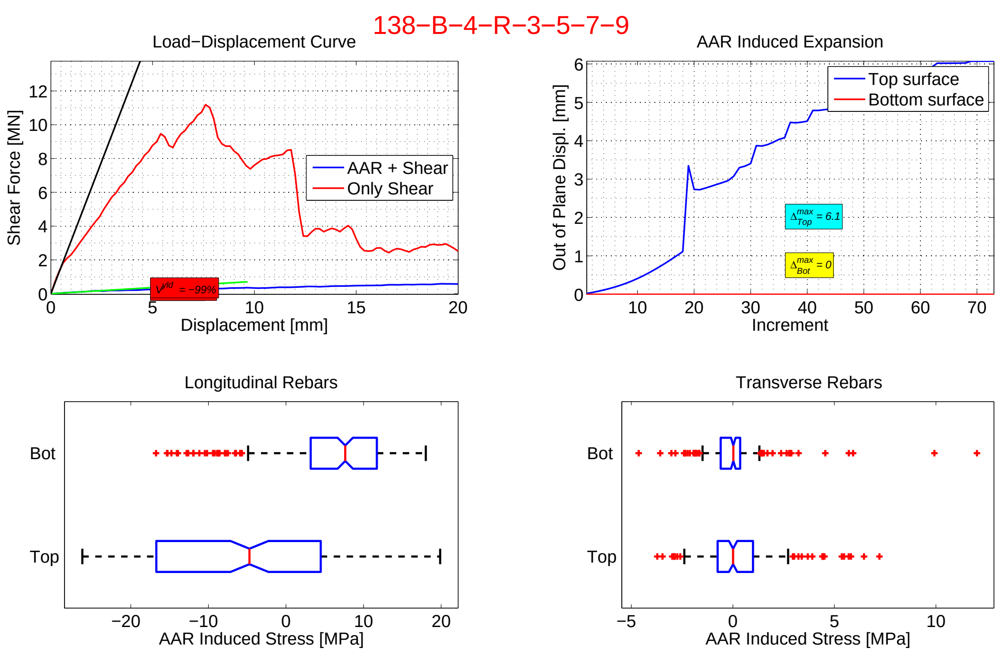

4.1.1.139 Analysis: 139-B-4-R-3-5-9-7

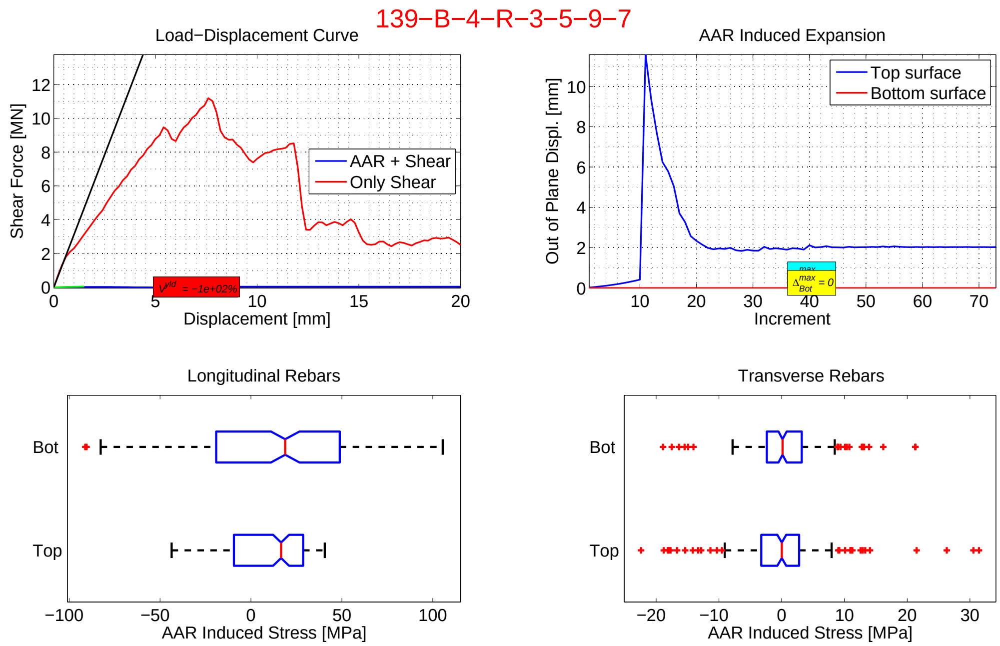

4.1.1.140 Analysis: 140-B-4-R-3-5-9-9

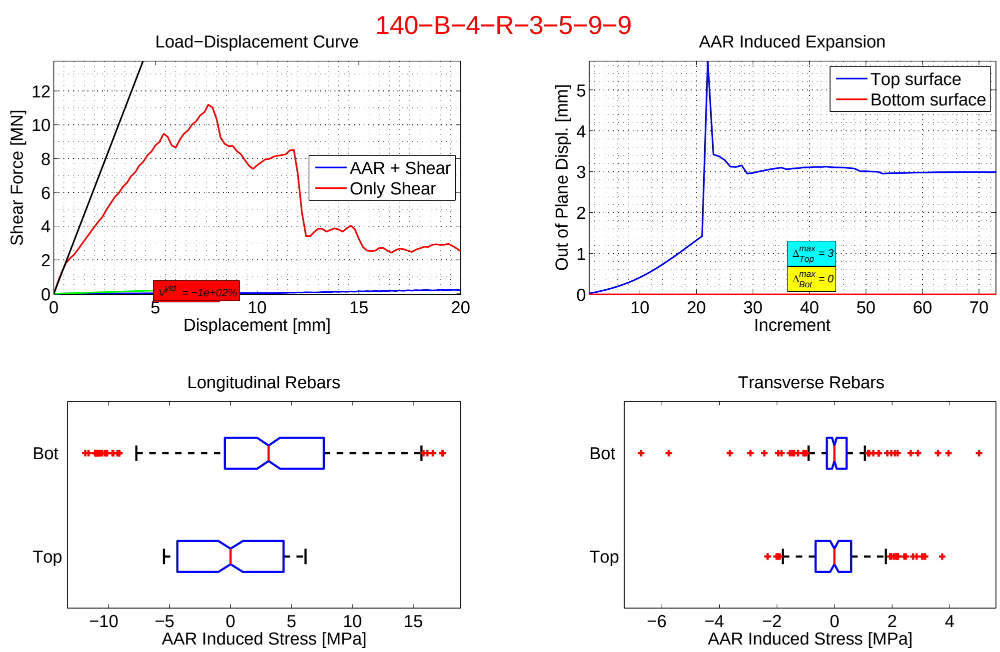

4.1.1.141 Analysis: 141-B-4-R-3-10-7-7

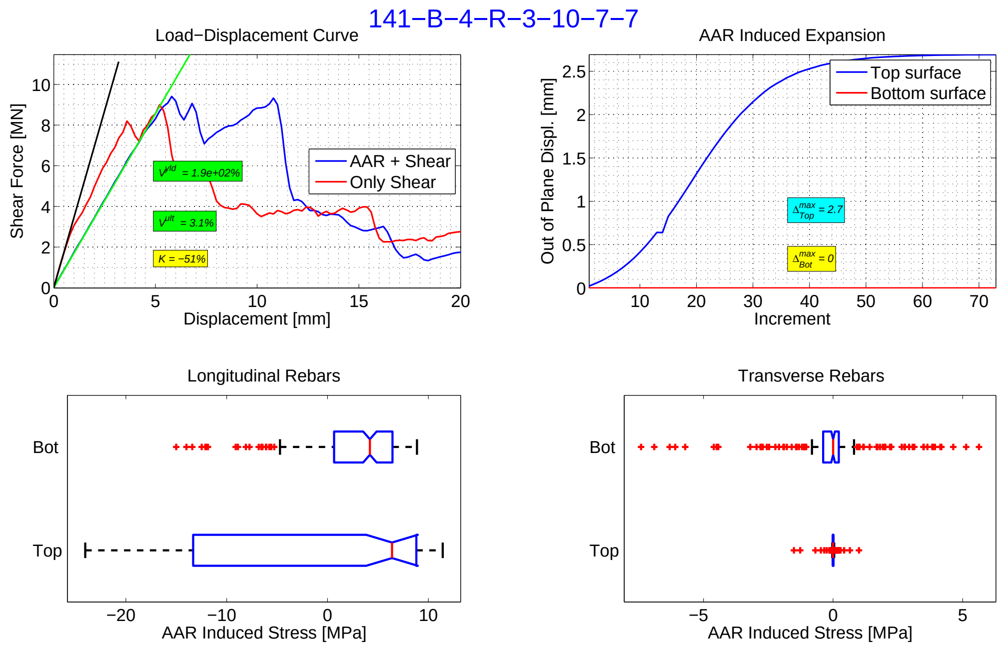

4.1.1.142 Analysis: 142-B-4-R-3-10-7-9

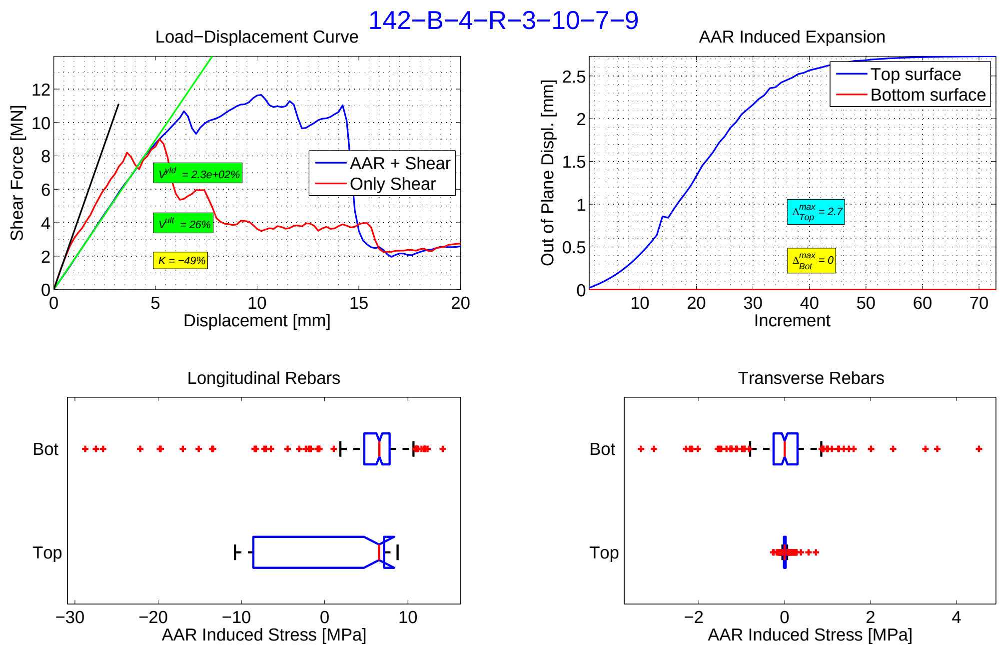

4.1.1.143 Analysis: 143-B-4-R-3-10-9-7

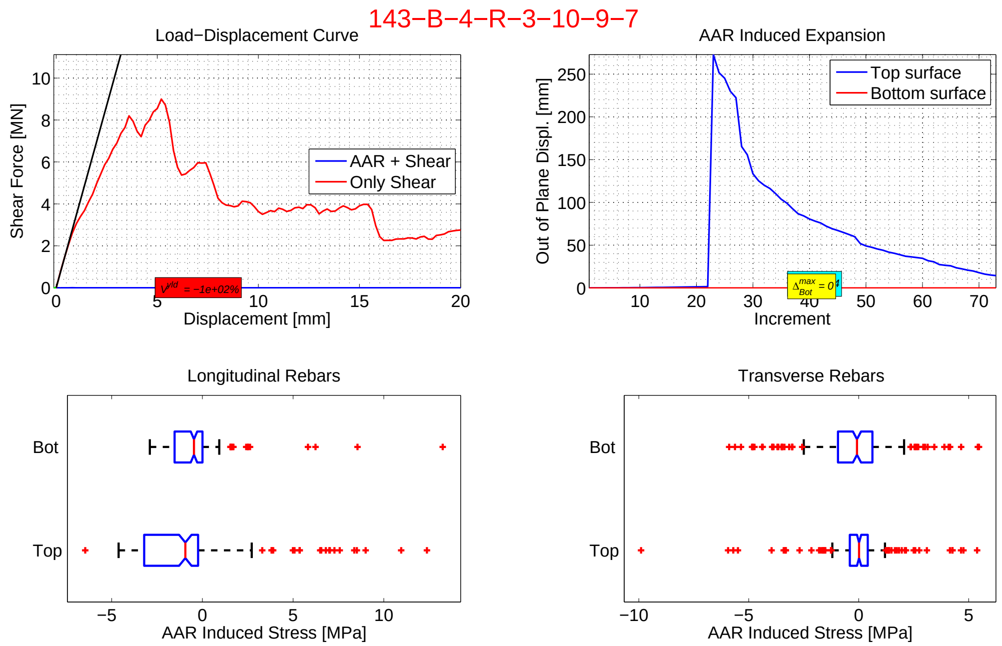

4.1.1.144 Analysis: 144-B-4-R-3-10-9-9

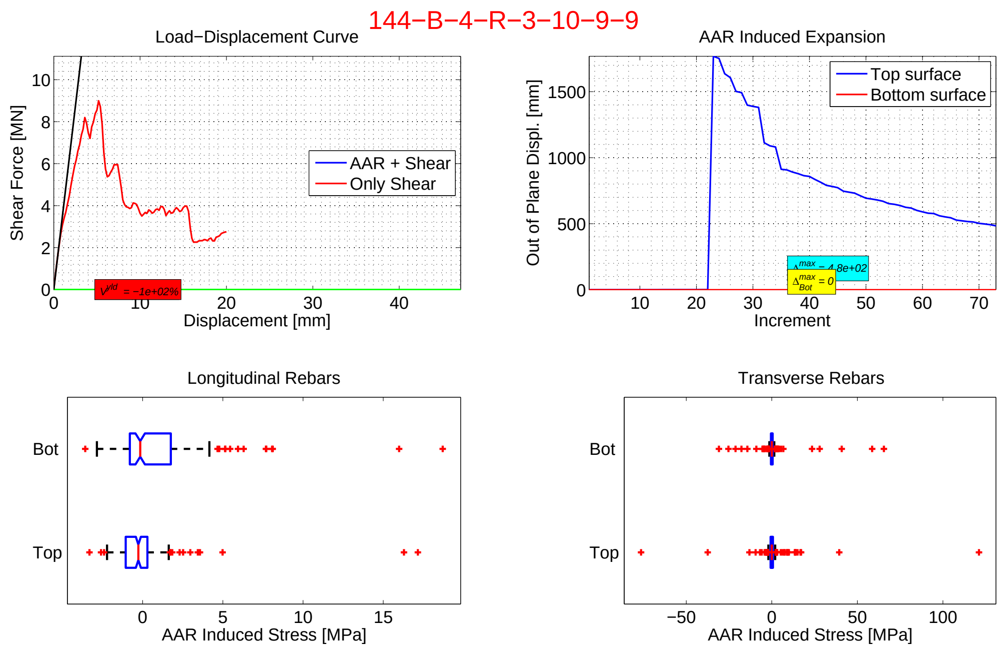

4.1.1.145 Analysis: 145-B-2-FR-1-2-7-7

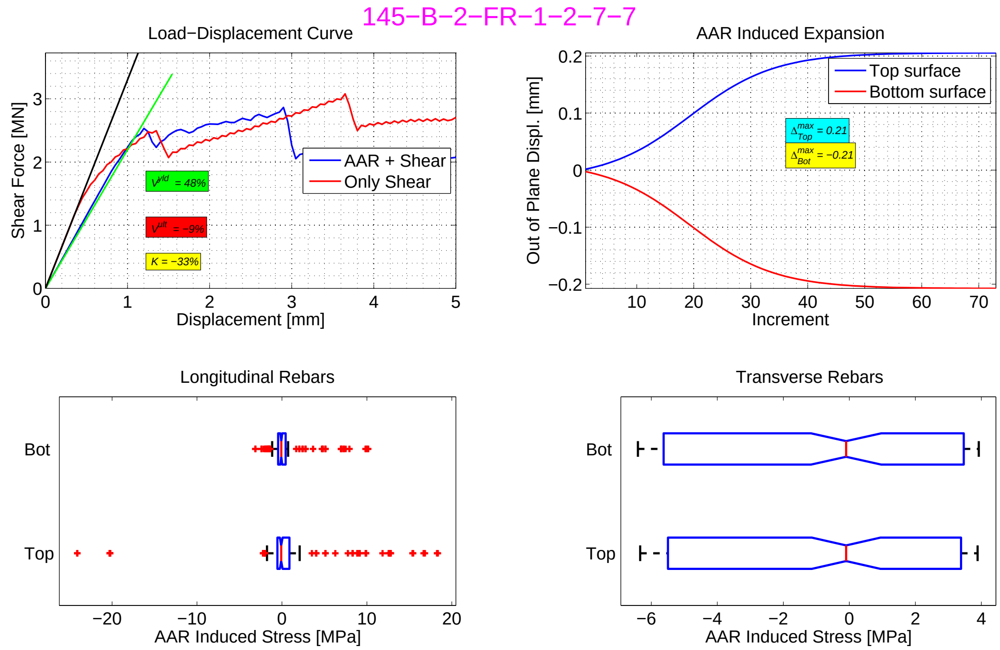

4.1.1.146 Analysis: 146-B-2-FR-1-2-7-9

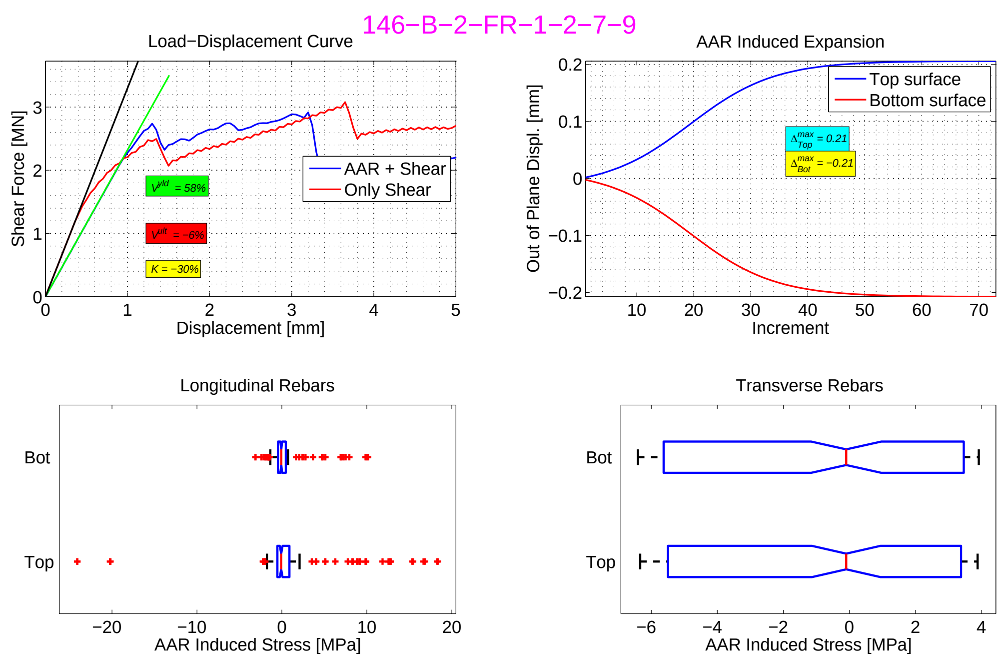

4.1.1.147 Analysis: 147-B-2-FR-1-2-9-7

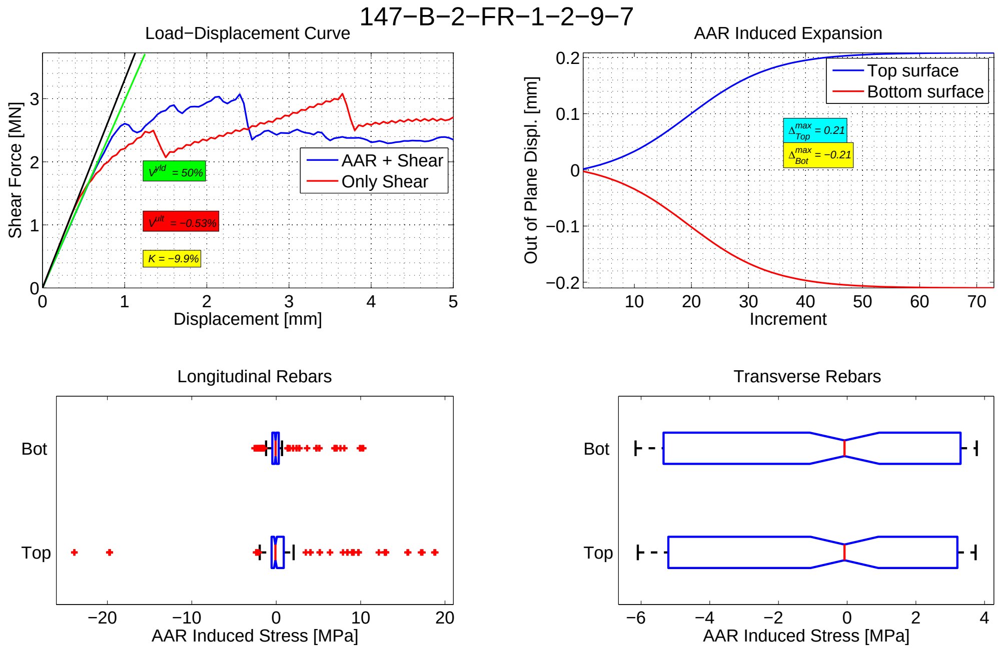

4.1.1.148 Analysis: 148-B-2-FR-1-2-9-9

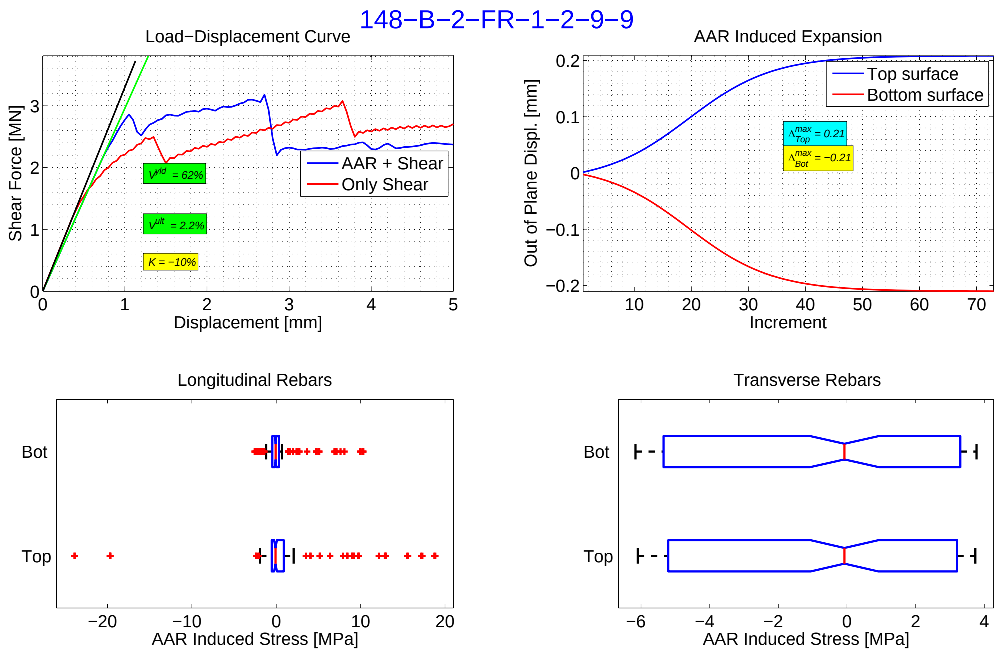

4.1.1.149 Analysis: 149-B-2-FR-1-5-7-7

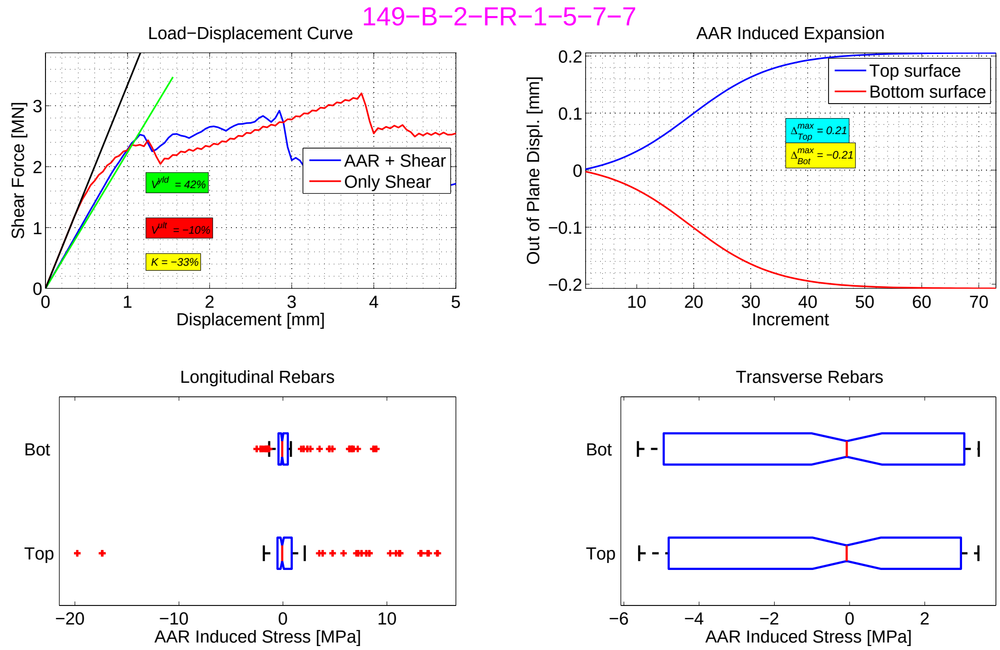

4.1.1.150 Analysis: 150-B-2-FR-1-5-7-9

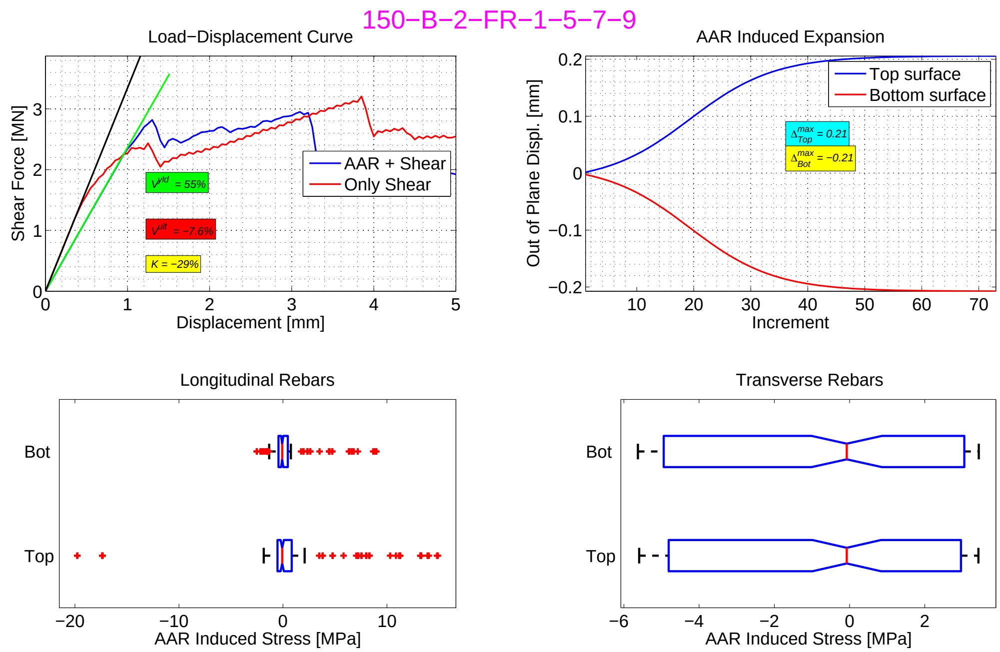

4.1.1.151 Analysis: 151-B-2-FR-1-5-9-7

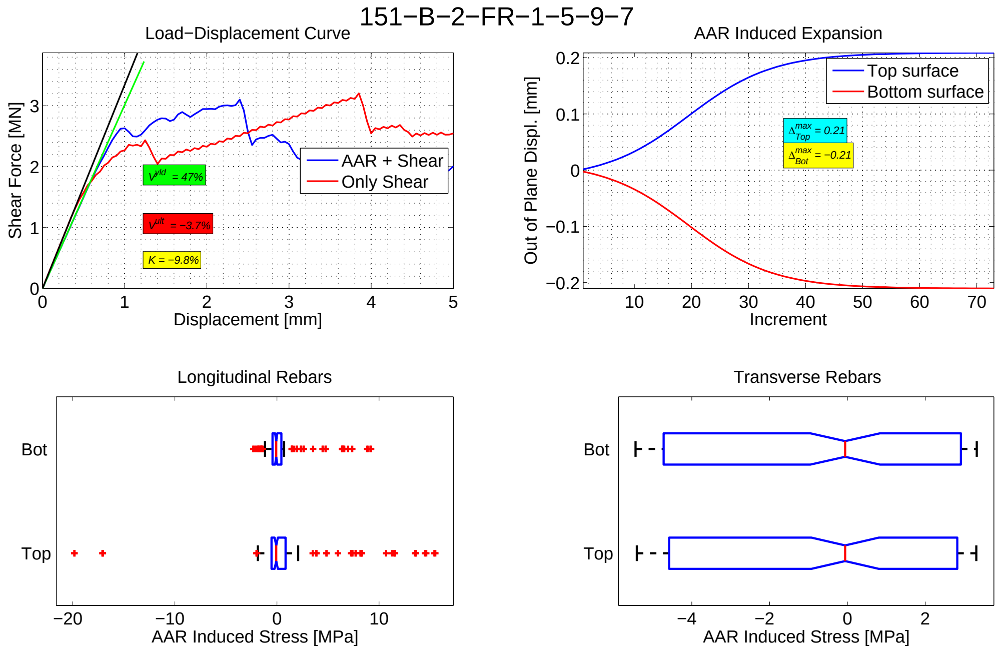

4.1.1.152 Analysis: 152-B-2-FR-1-5-9-9

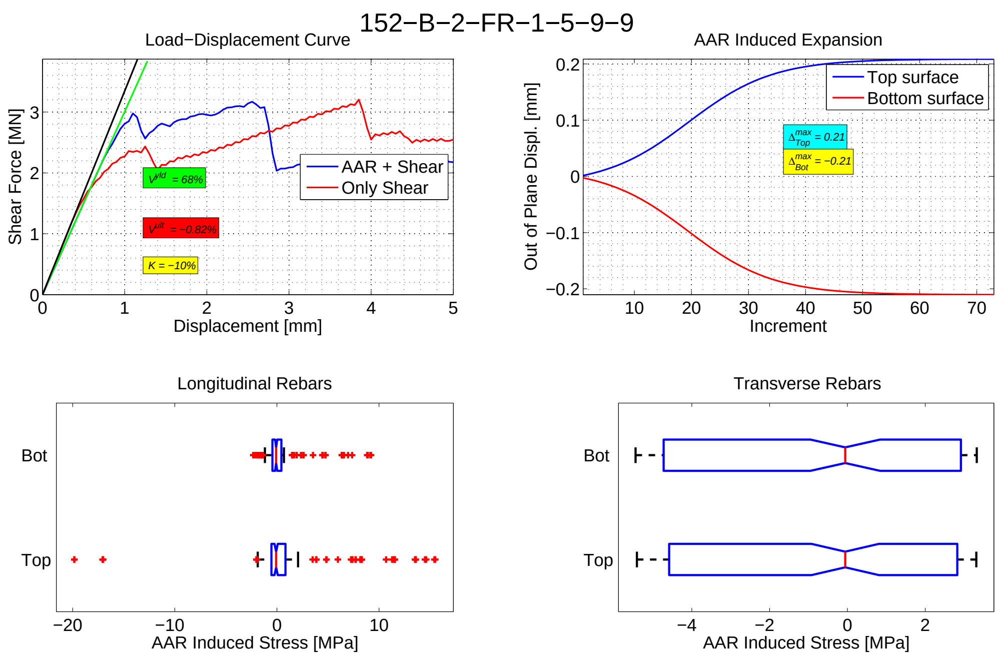

4.1.1.153 Analysis: 153-B-2-FR-1-10-7-7

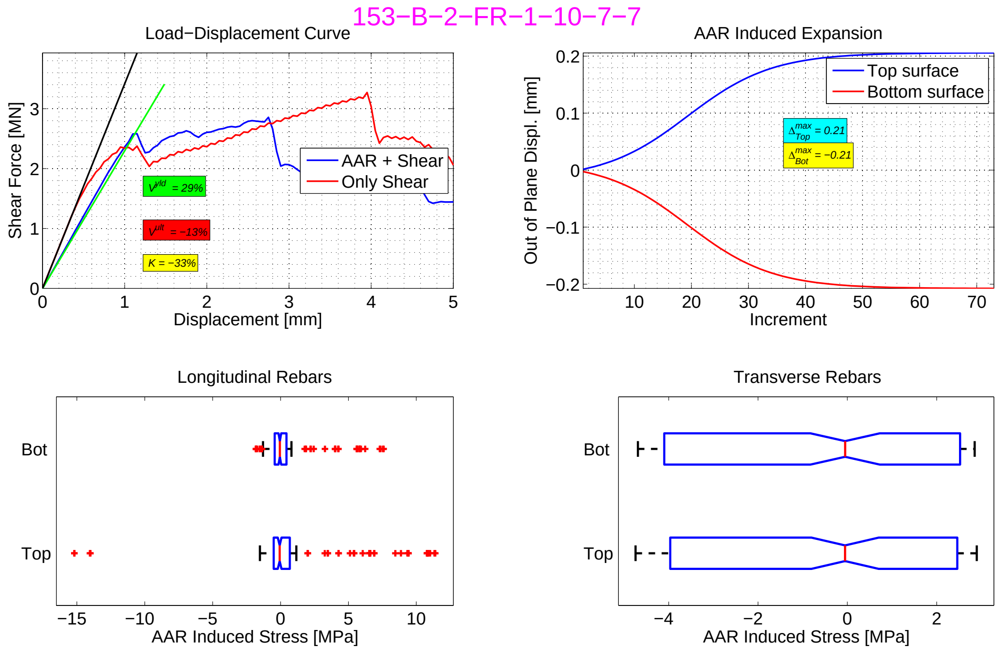

4.1.1.154 Analysis: 154-B-2-FR-1-10-7-9

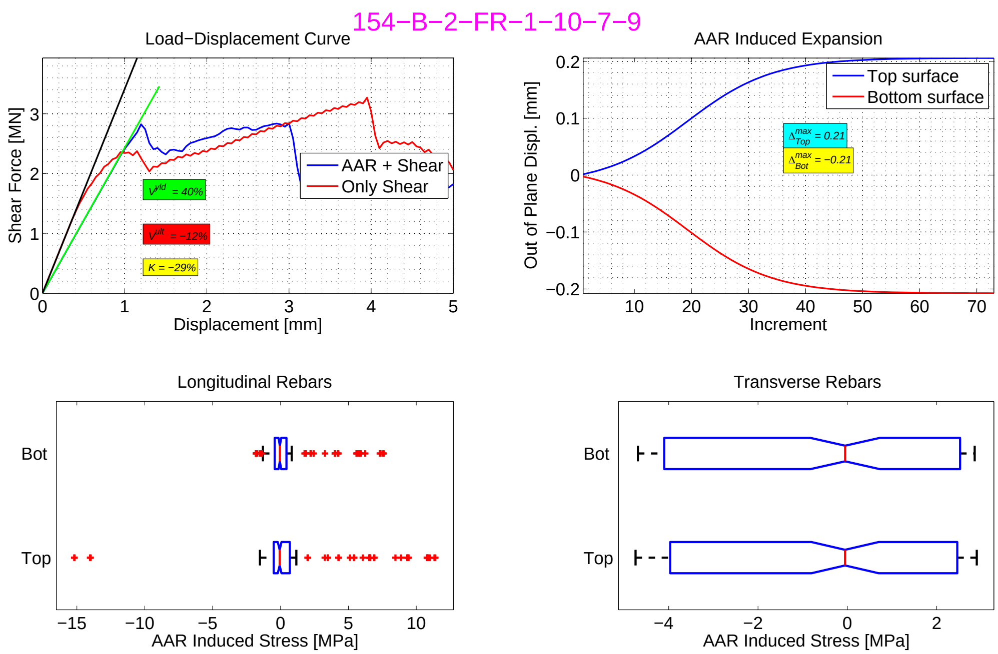

4.1.1.155 Analysis: 155-B-2-FR-1-10-9-7

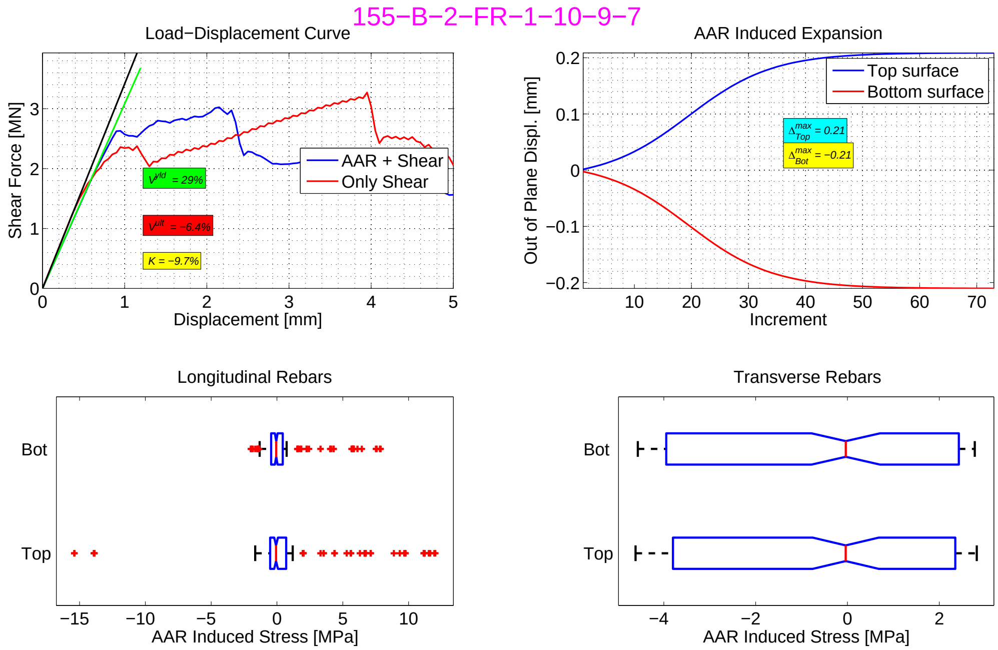

4.1.1.156 Analysis: 156-B-2-FR-1-10-9-9

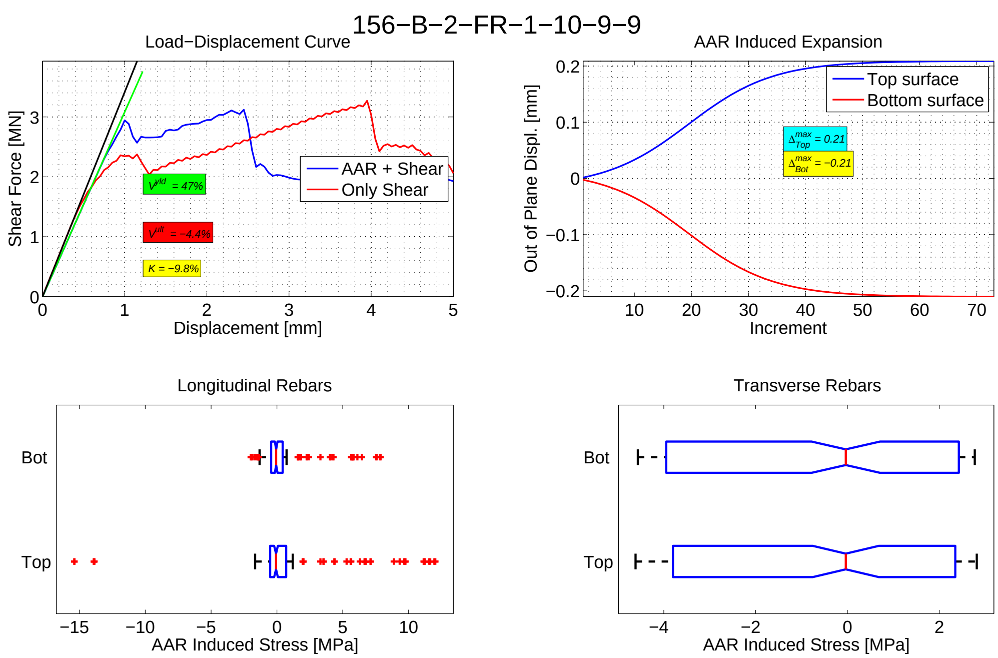

4.1.1.157 Analysis: 157-B-2-FR-2-2-7-7

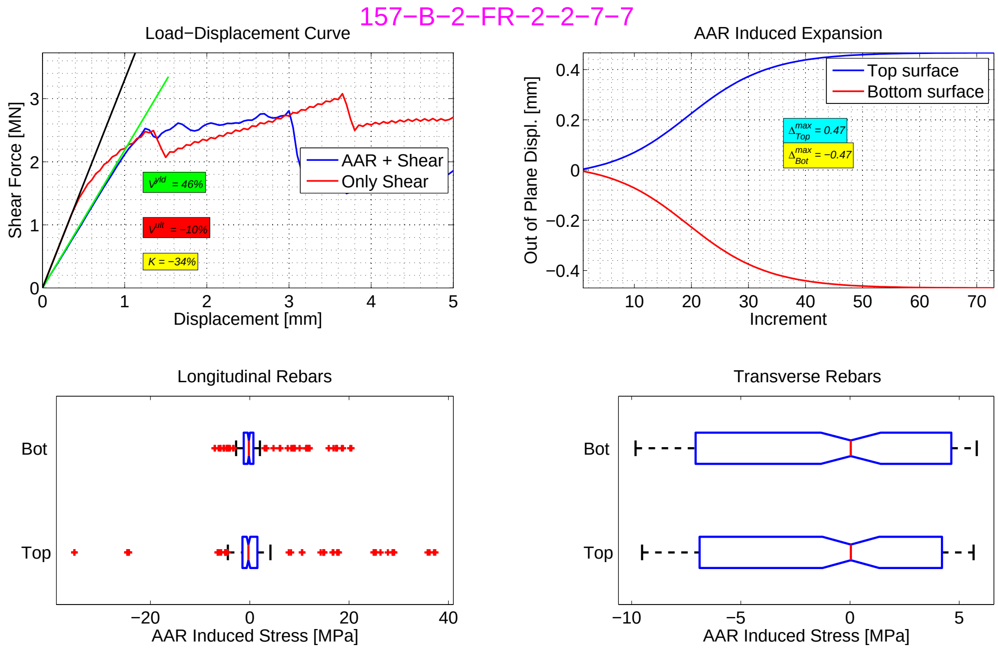

4.1.1.158 Analysis: 158-B-2-FR-2-2-7-9

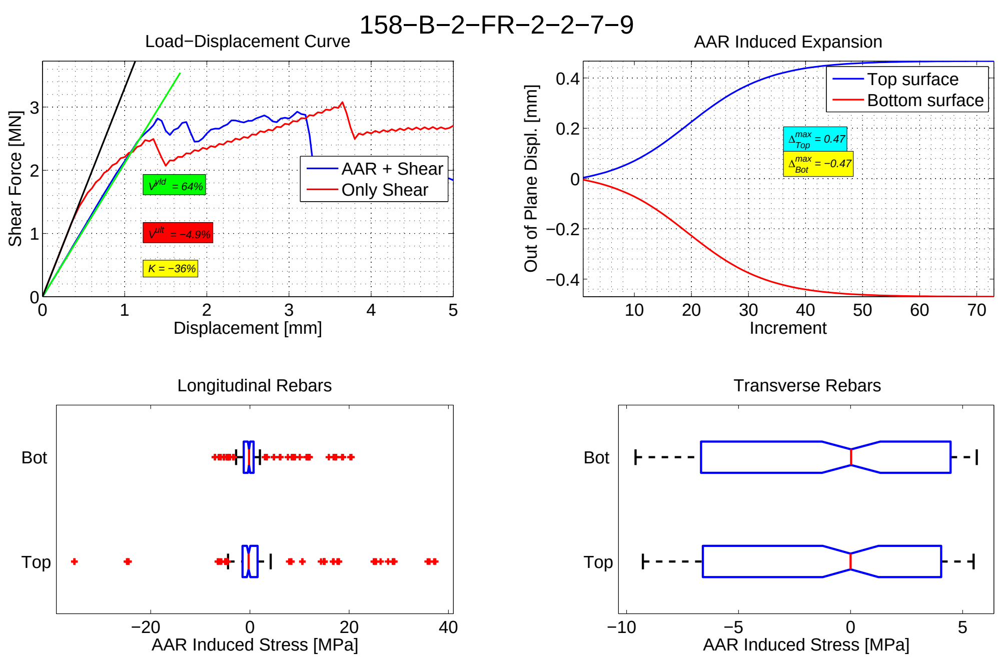

4.1.1.159 Analysis: 159-B-2-FR-2-2-9-7

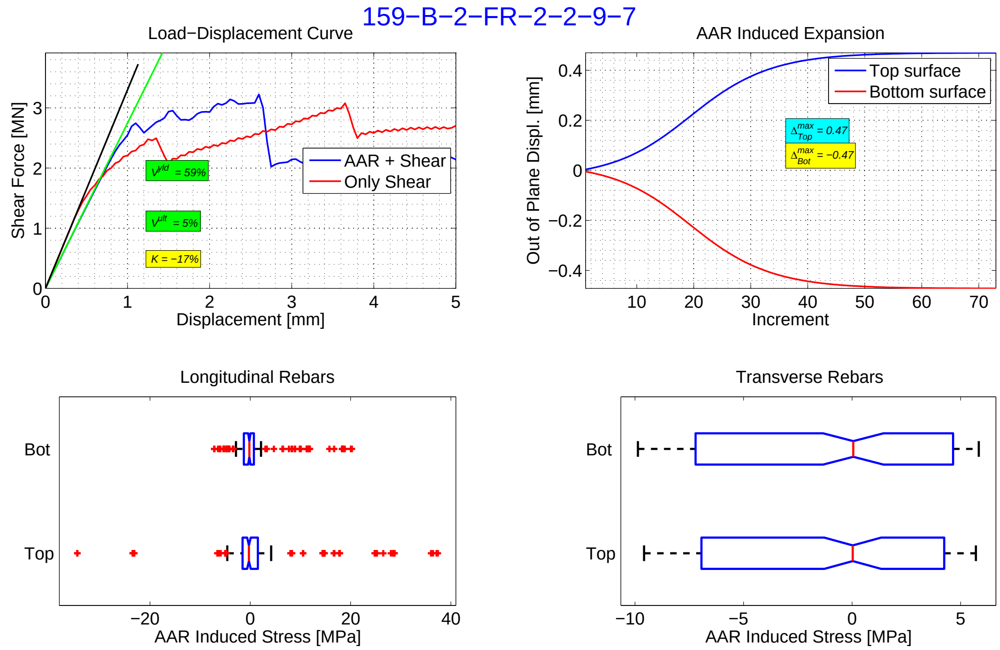

4.1.1.160 Analysis: 160-B-2-FR-2-2-9-9

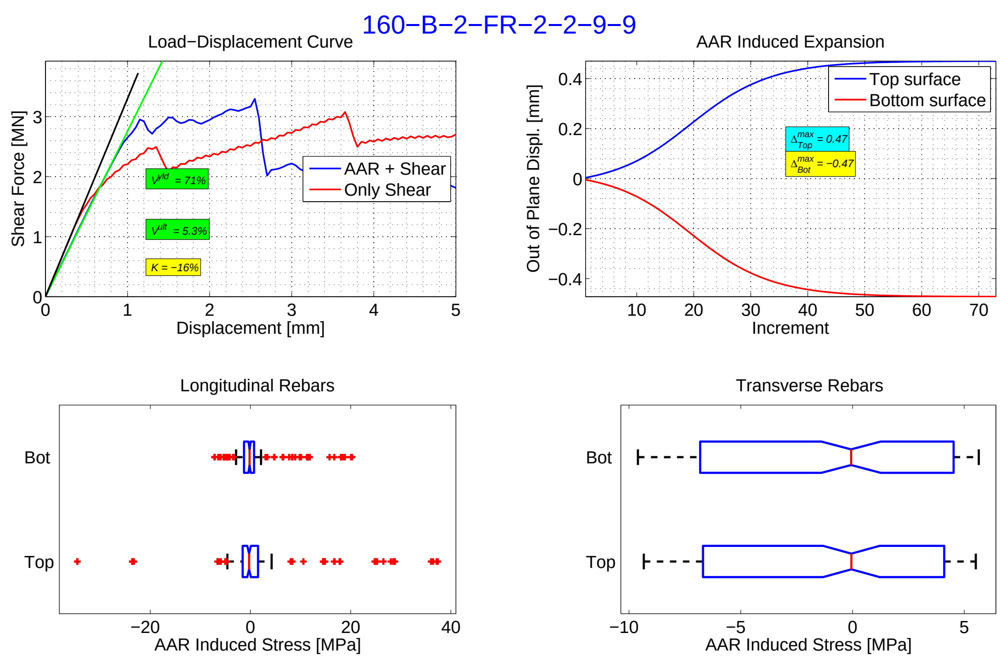

4.1.1.161 Analysis: 161-B-2-FR-2-5-7-7

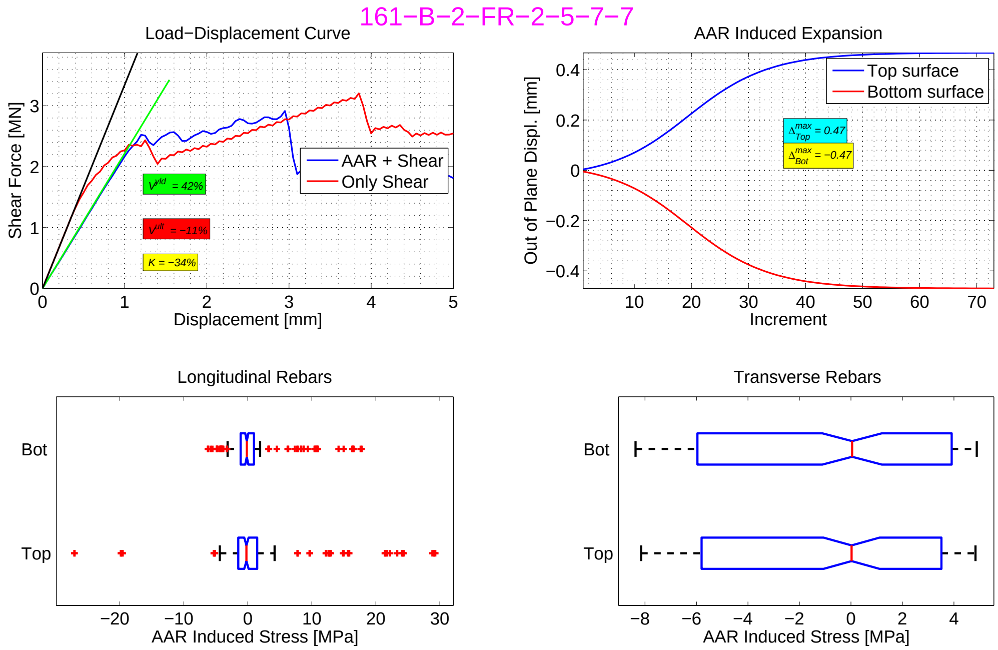

4.1.1.162 Analysis: 162-B-2-FR-2-5-7-9

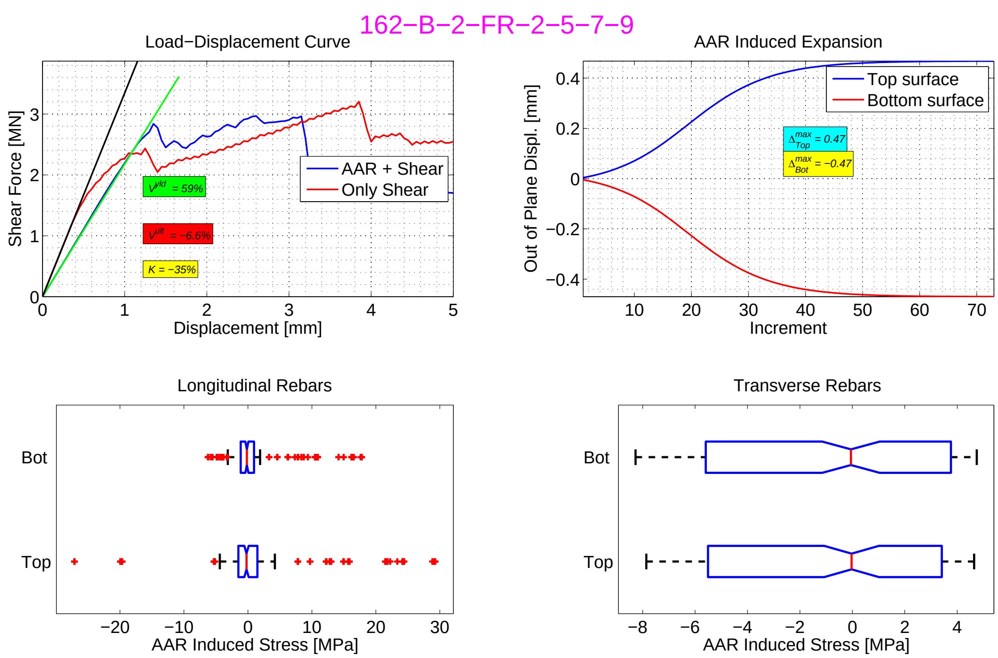

4.1.1.163 Analysis: 163-B-2-FR-2-5-9-7

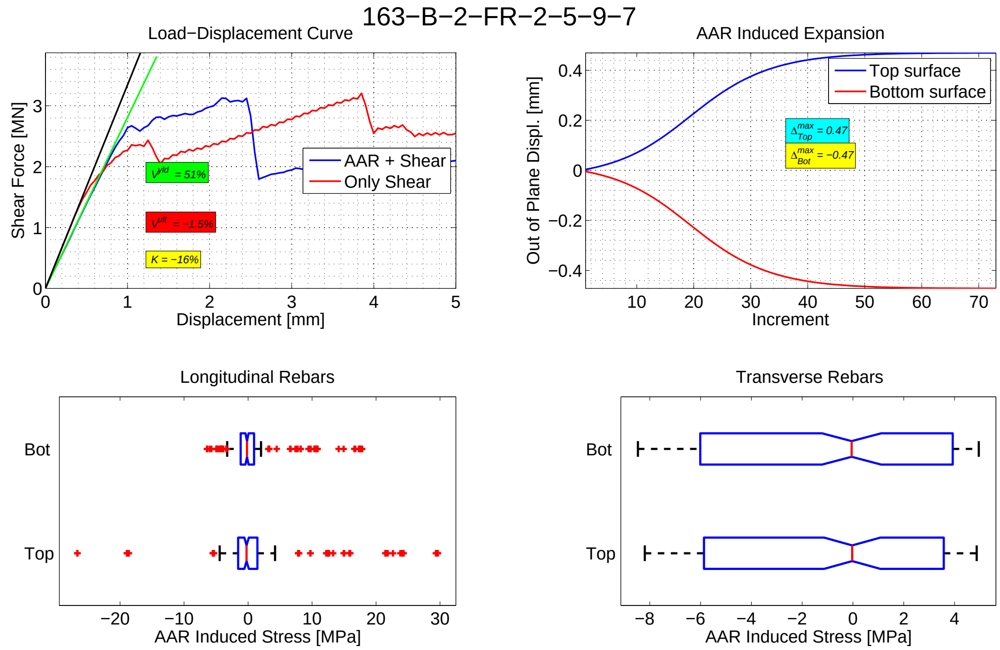

4.1.1.164 Analysis: 164-B-2-FR-2-5-9-9

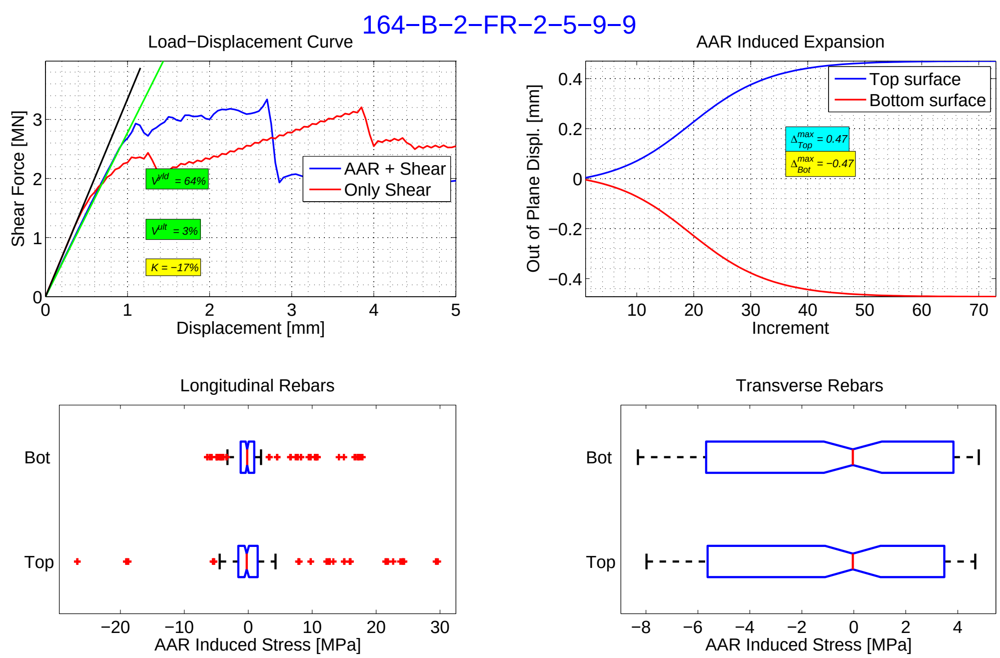

4.1.1.165 Analysis: 165-B-2-FR-2-10-7-7

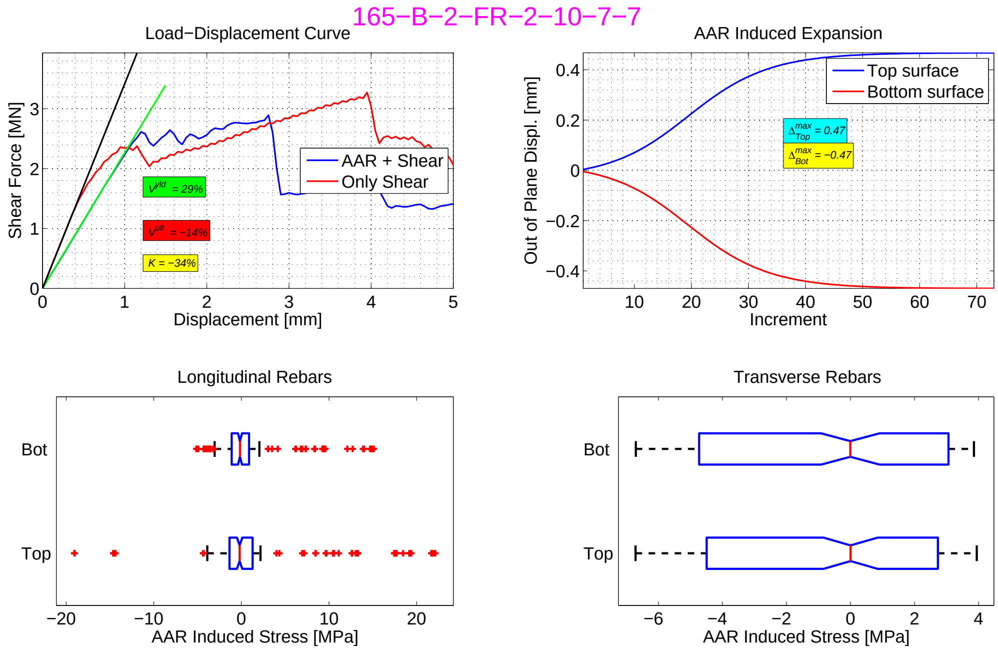

4.1.1.166 Analysis: 166-B-2-FR-2-10-7-9

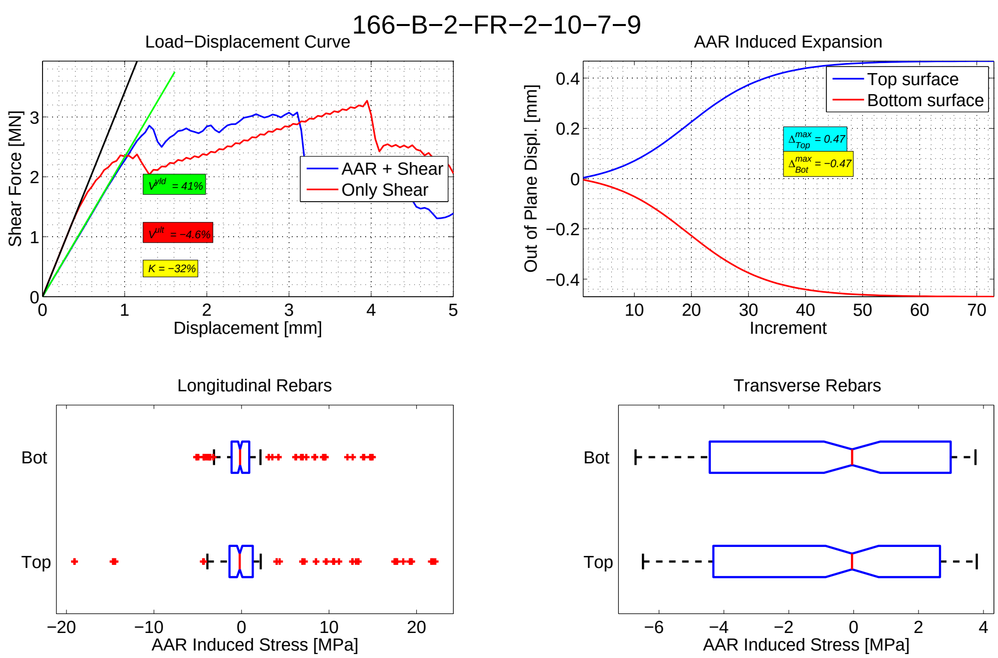

4.1.1.167 Analysis: 167-B-2-FR-2-10-9-7

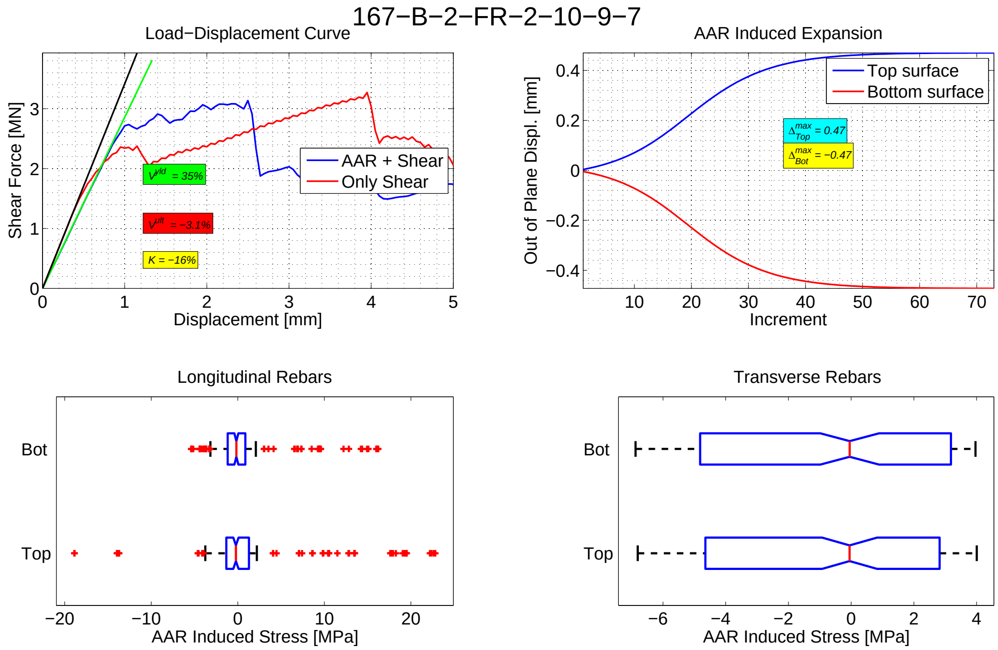

4.1.1.168 Analysis: 168-B-2-FR-2-10-9-9

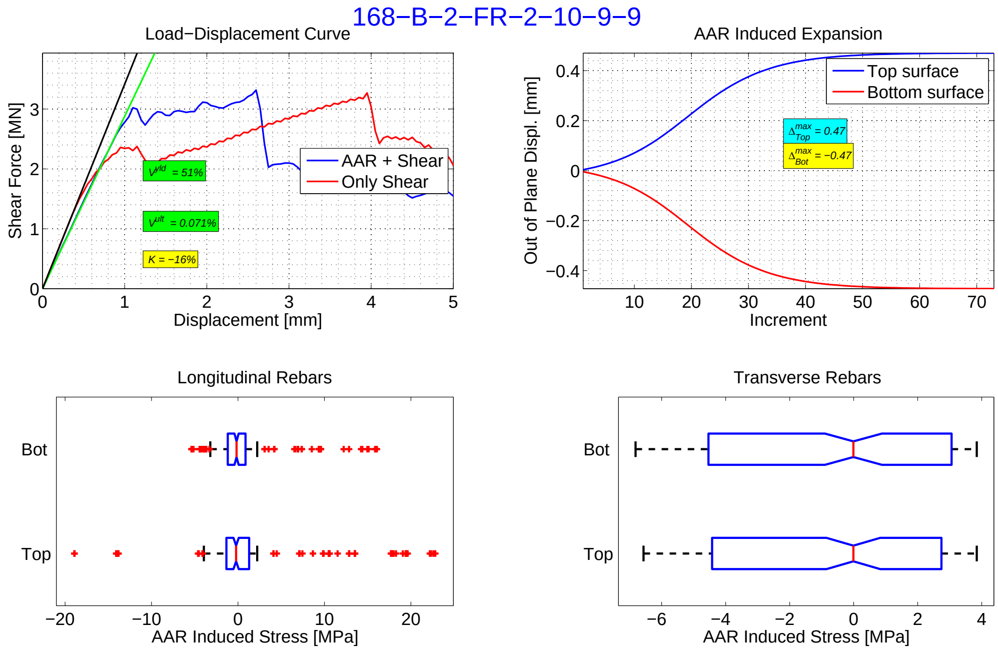

4.1.1.169 Analysis: 169-B-2-FR-3-2-7-7

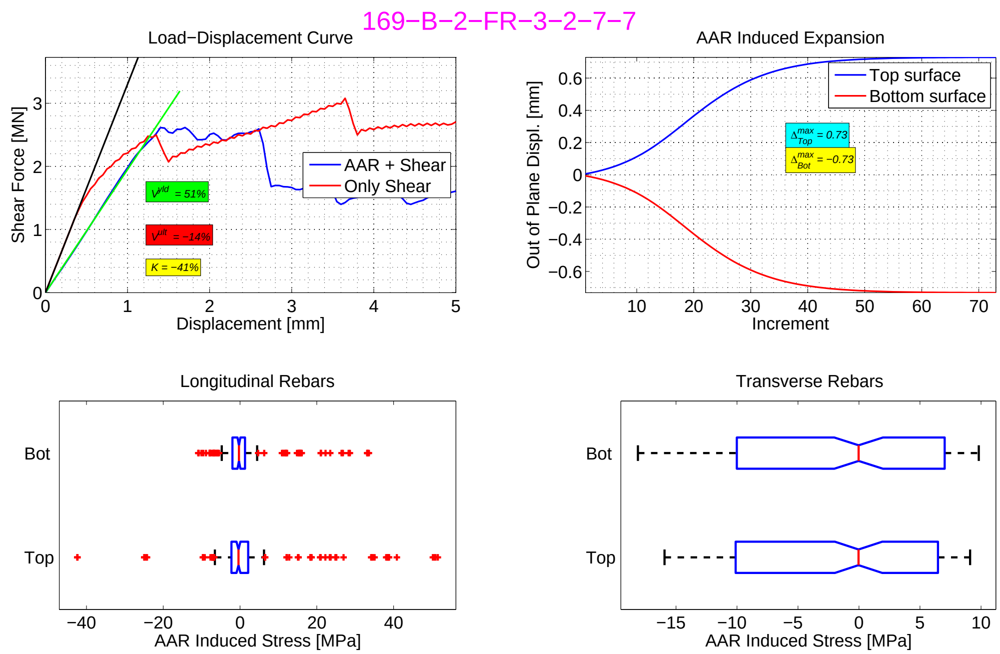

4.1.1.170 Analysis: 170-B-2-FR-3-2-7-9

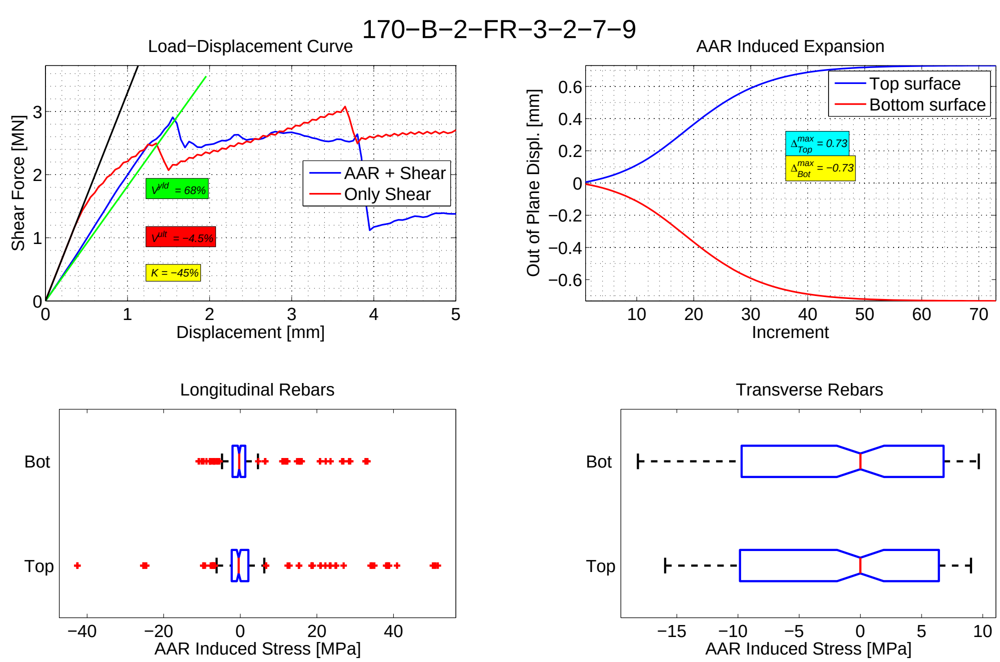

4.1.1.171 Analysis: 171-B-2-FR-3-2-9-7

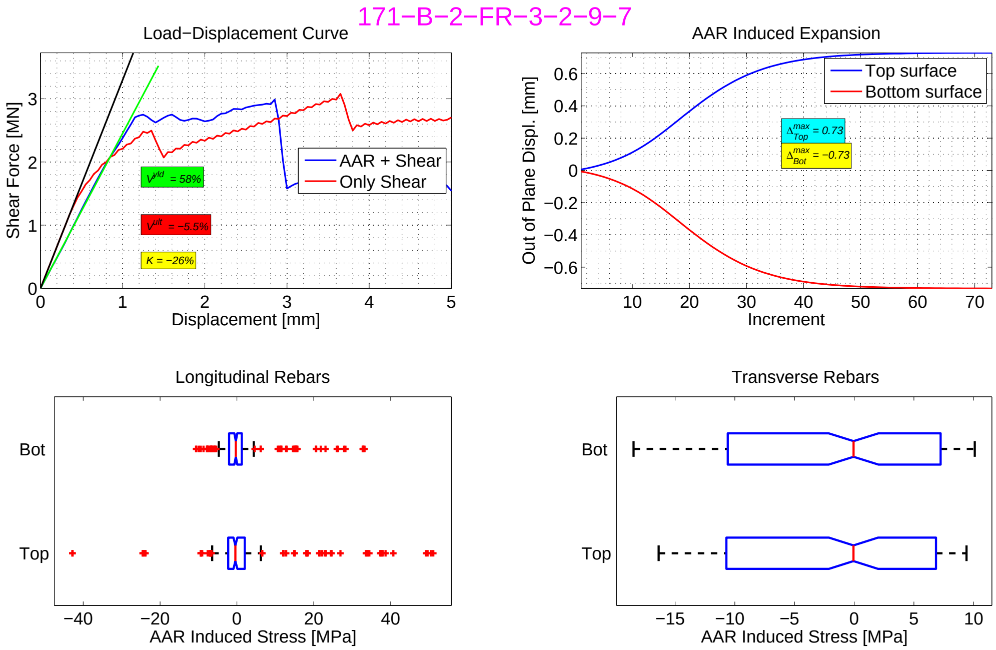

4.1.1.172 Analysis: 172-B-2-FR-3-2-9-9

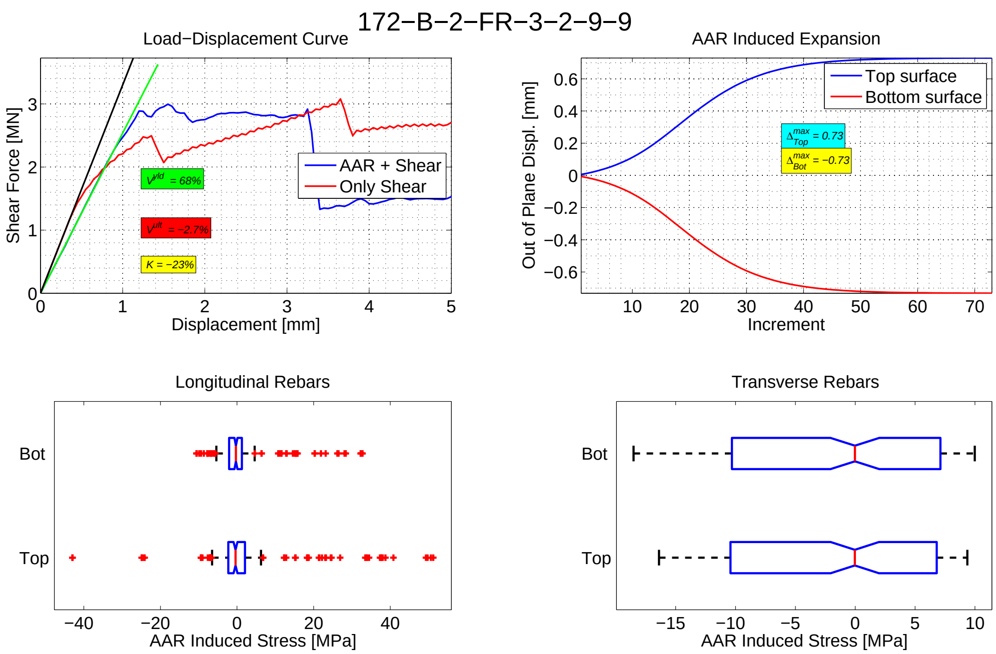

4.1.1.173 Analysis: 173-B-2-FR-3-5-7-7

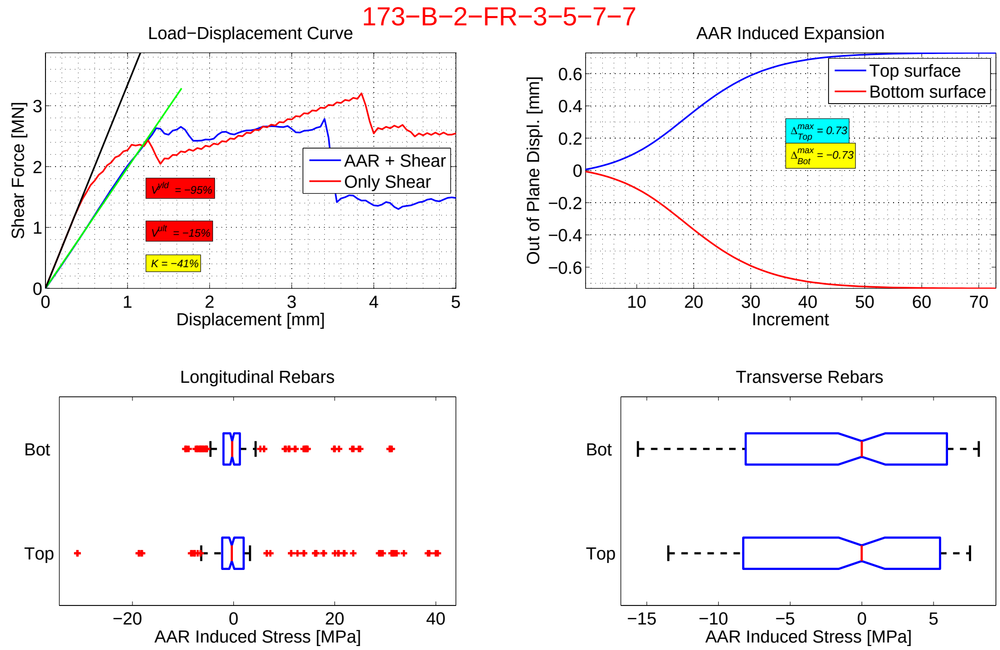

4.1.1.174 Analysis: 174-B-2-FR-3-5-7-9

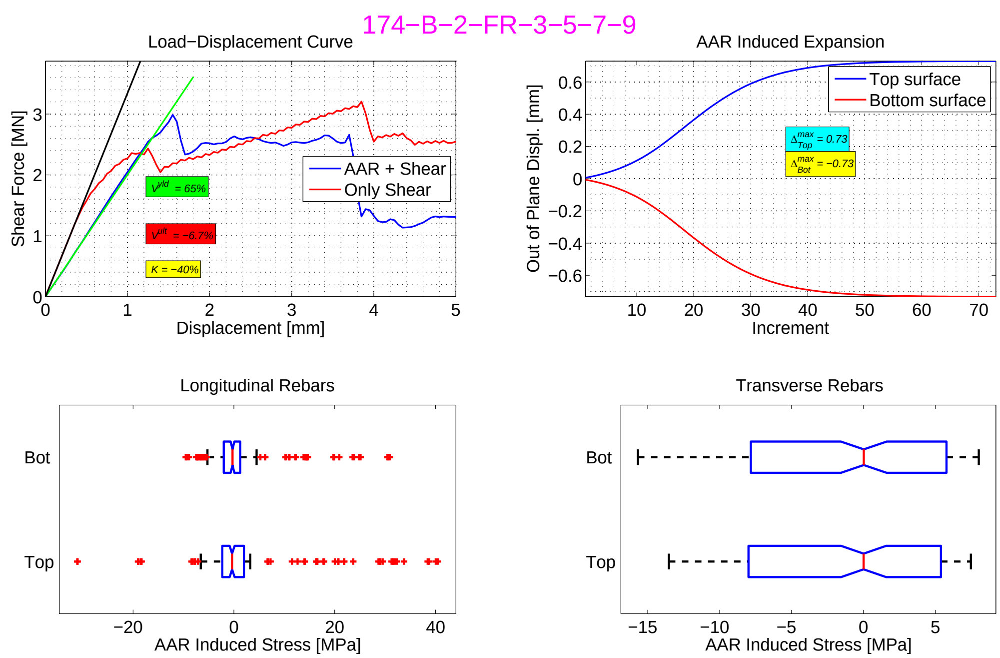

4.1.1.175 Analysis: 175-B-2-FR-3-5-9-7

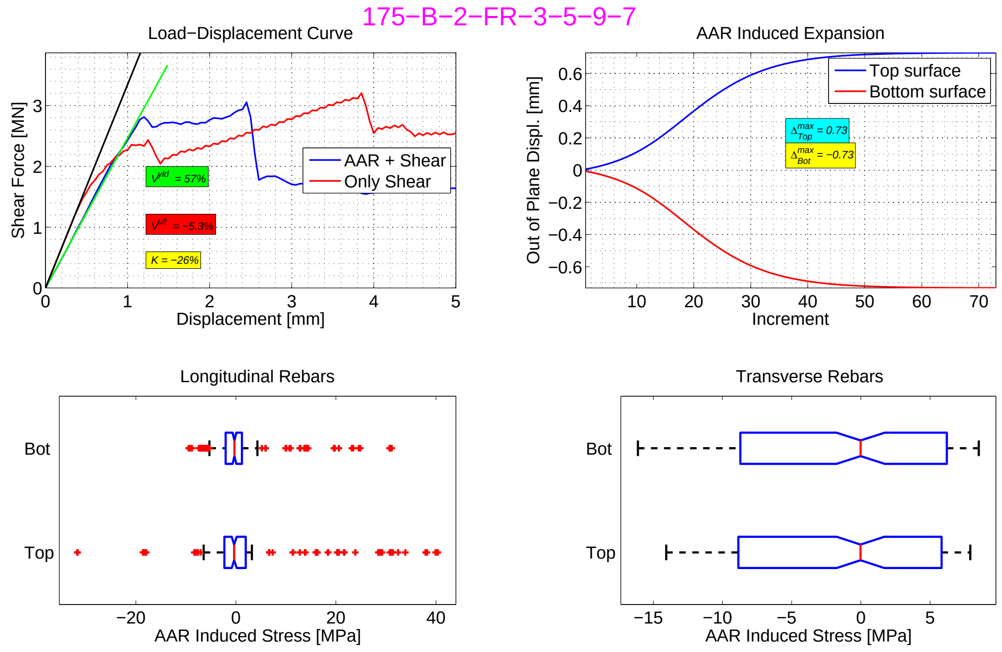

4.1.1.176 Analysis: 176-B-2-FR-3-5-9-9

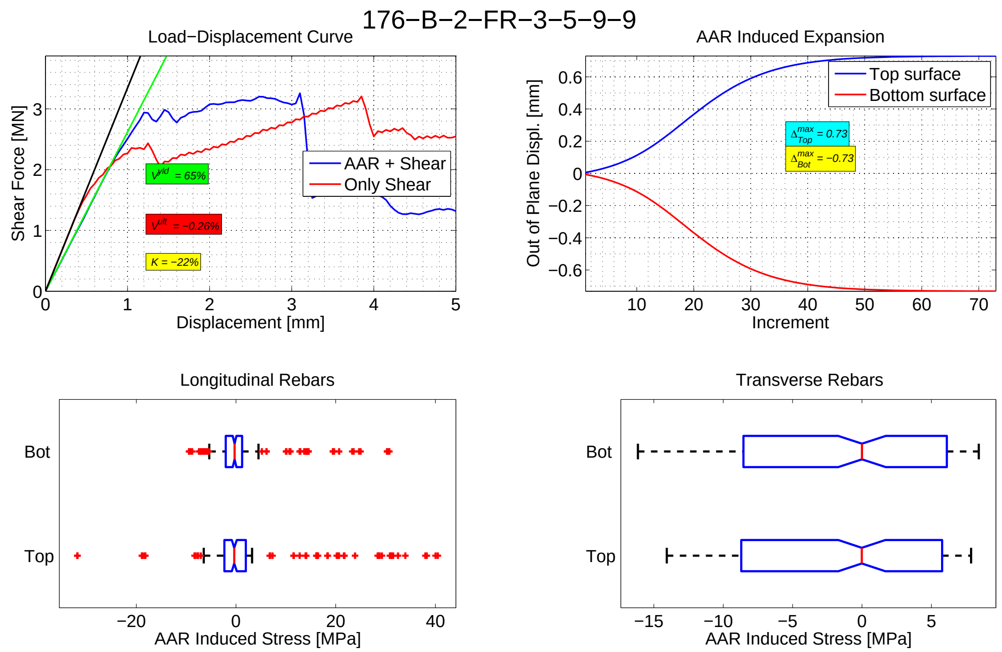

4.1.1.177 Analysis: 177-B-2-FR-3-10-7-7

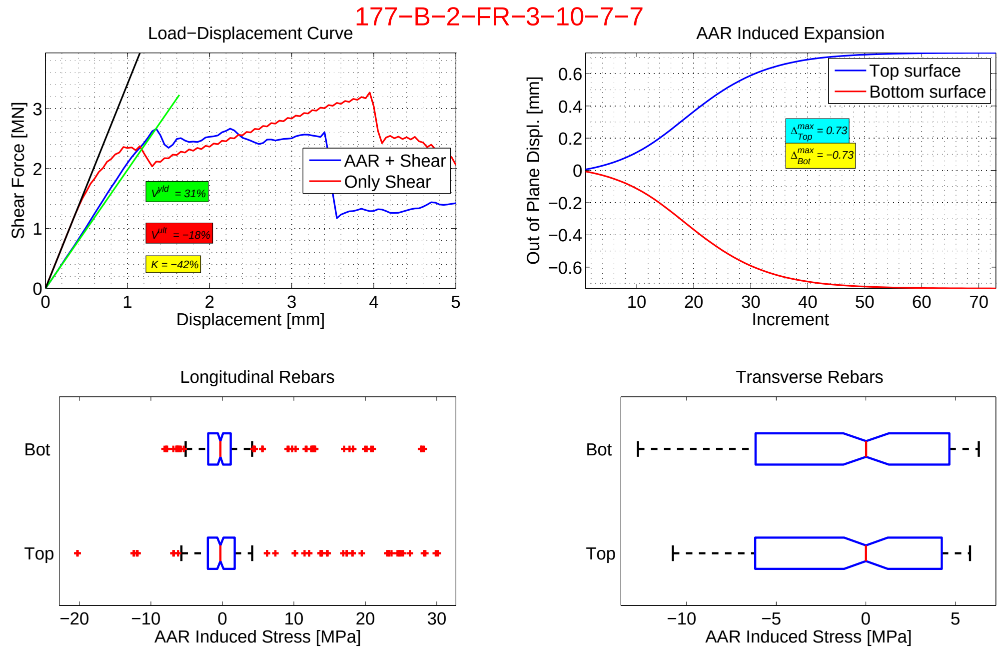

4.1.1.178 Analysis: 178-B-2-FR-3-10-7-9

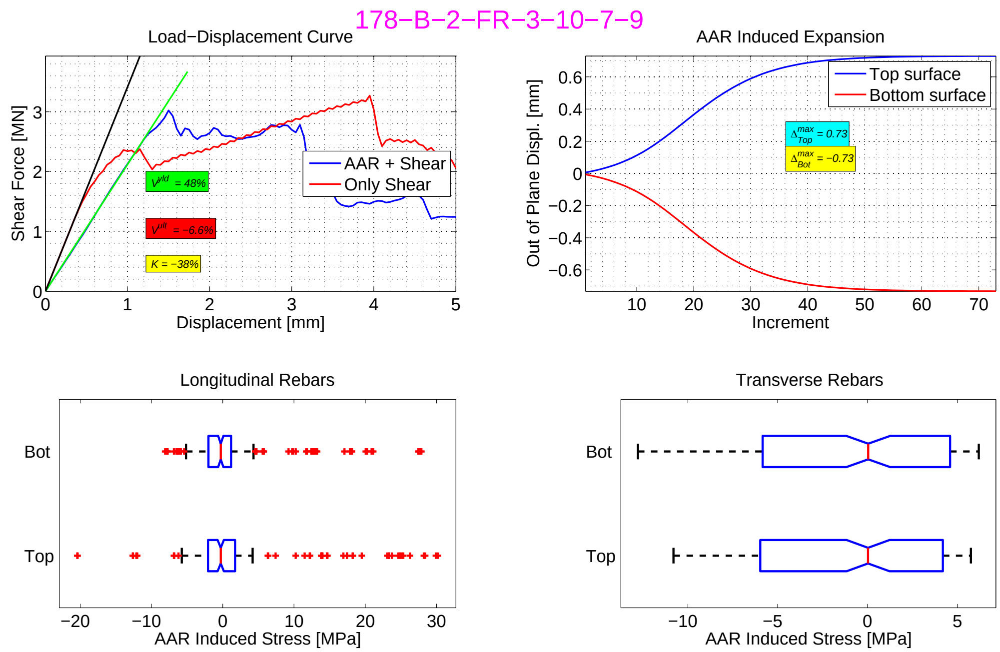

4.1.1.179 Analysis: 179-B-2-FR-3-10-9-7

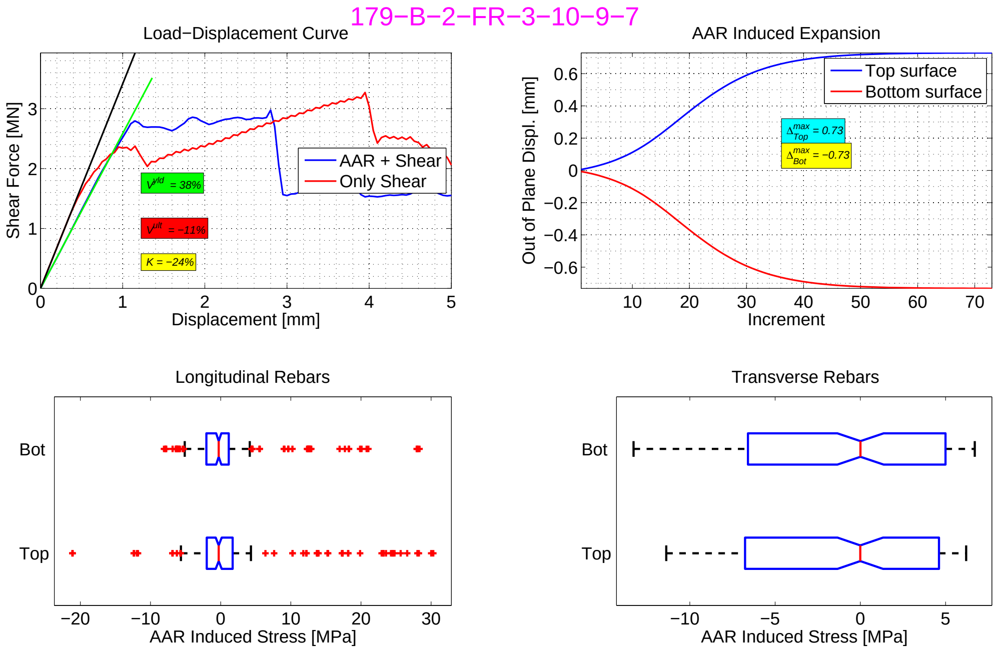

4.1.1.180 Analysis: 180-B-2-FR-3-10-9-9

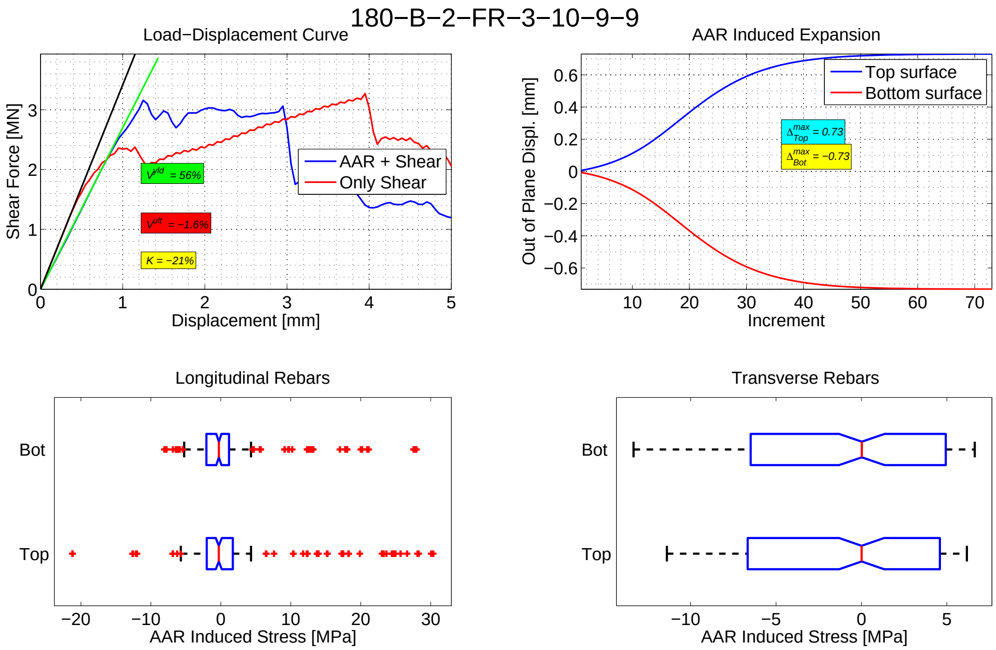

4.1.1.181 Analysis: 181-B-4-FR-1-2-7-7

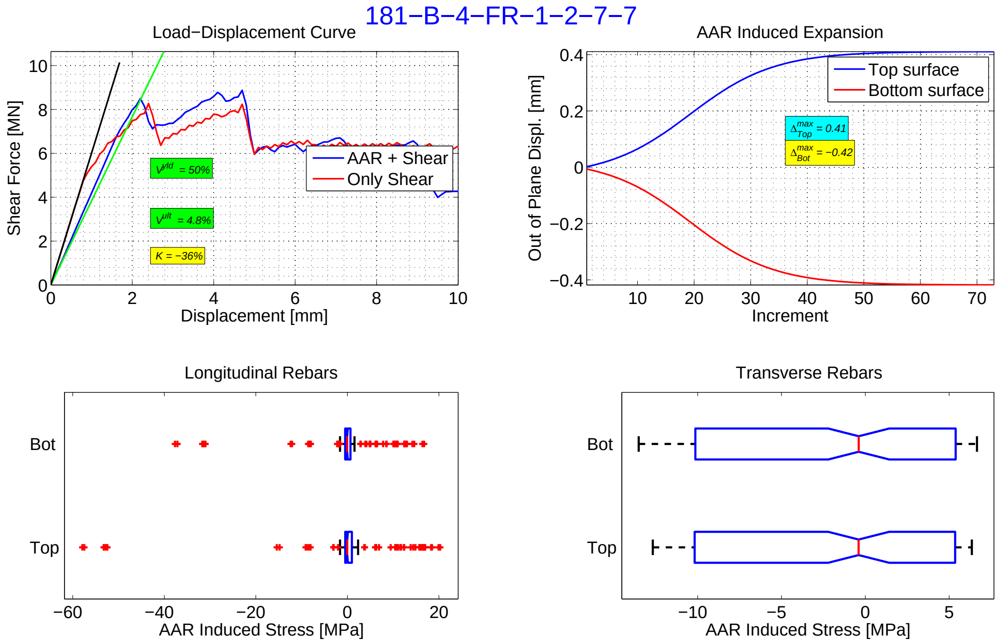

4.1.1.182 Analysis: 182-B-4-FR-1-2-7-9

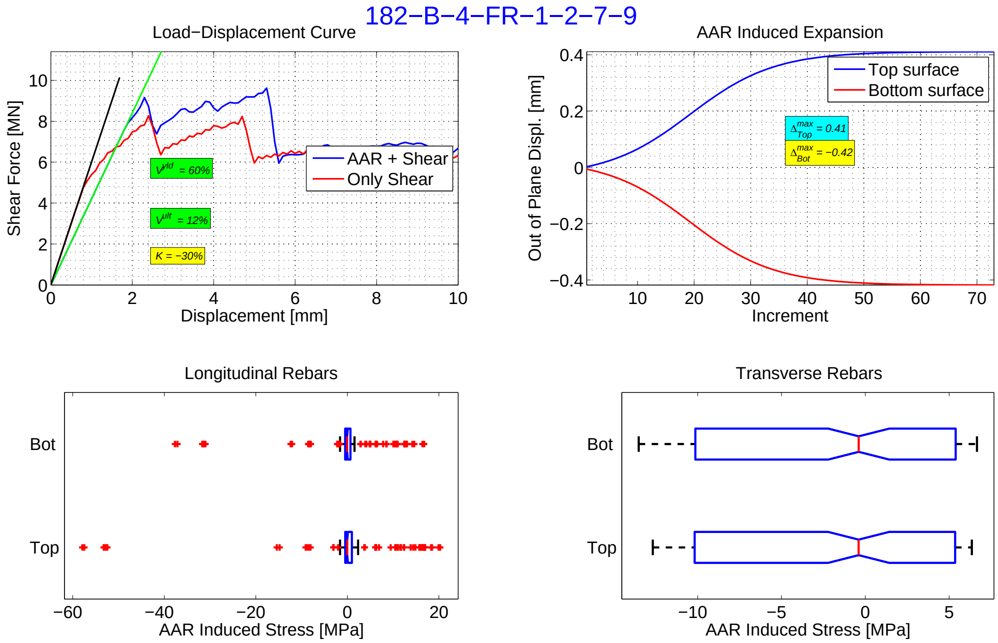

4.1.1.183 Analysis: 183-B-4-FR-1-2-9-7

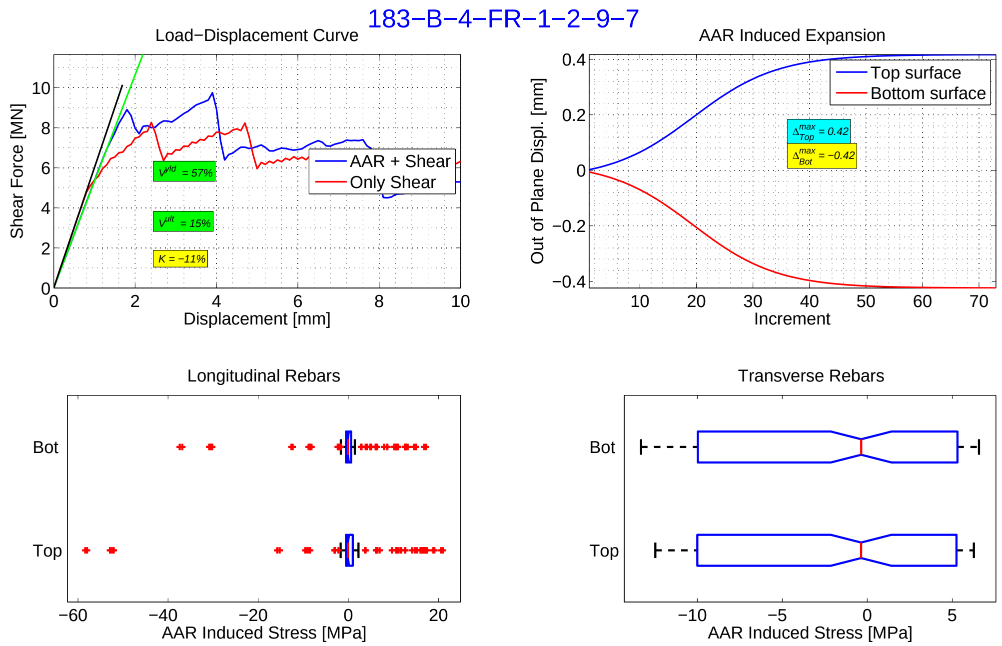

4.1.1.184 Analysis: 184-B-4-FR-1-2-9-9

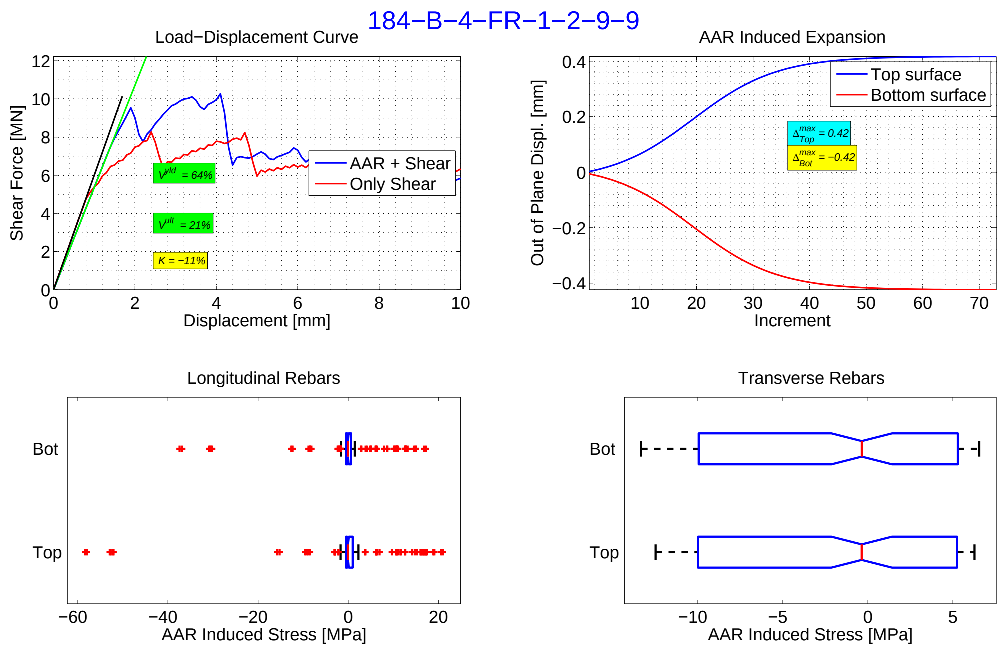

4.1.1.185 Analysis: 185-B-4-FR-1-5-7-7

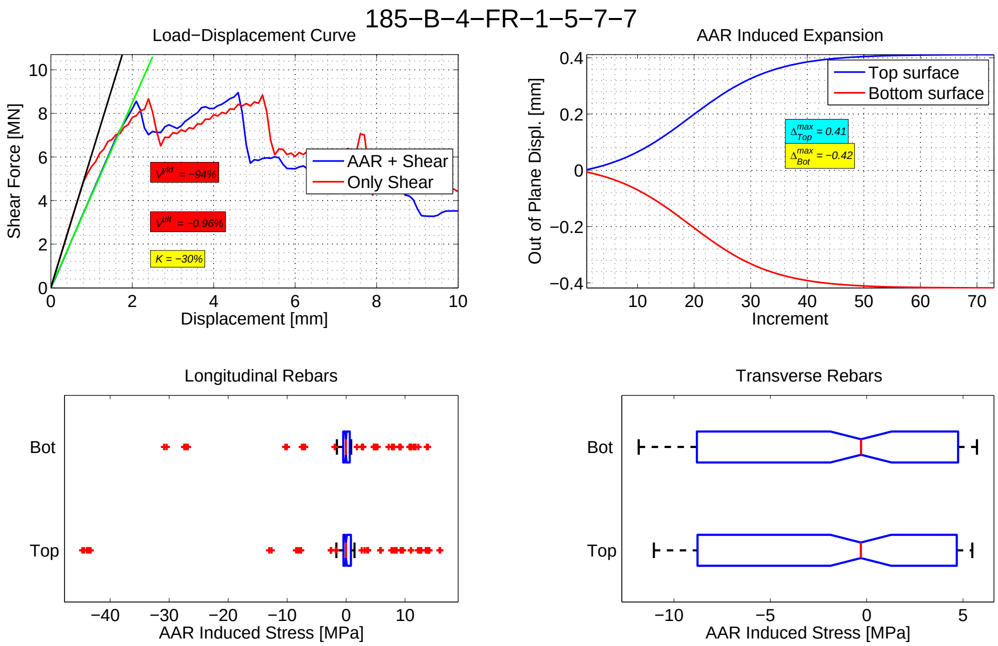

4.1.1.186 Analysis: 186-B-4-FR-1-5-7-9

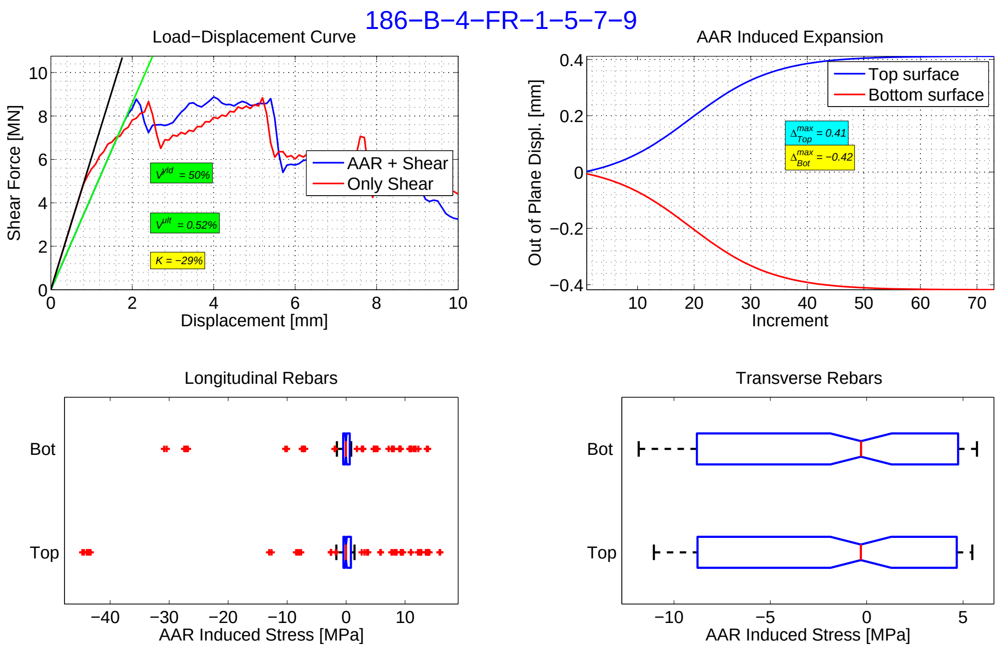

4.1.1.187 Analysis: 187-B-4-FR-1-5-9-7

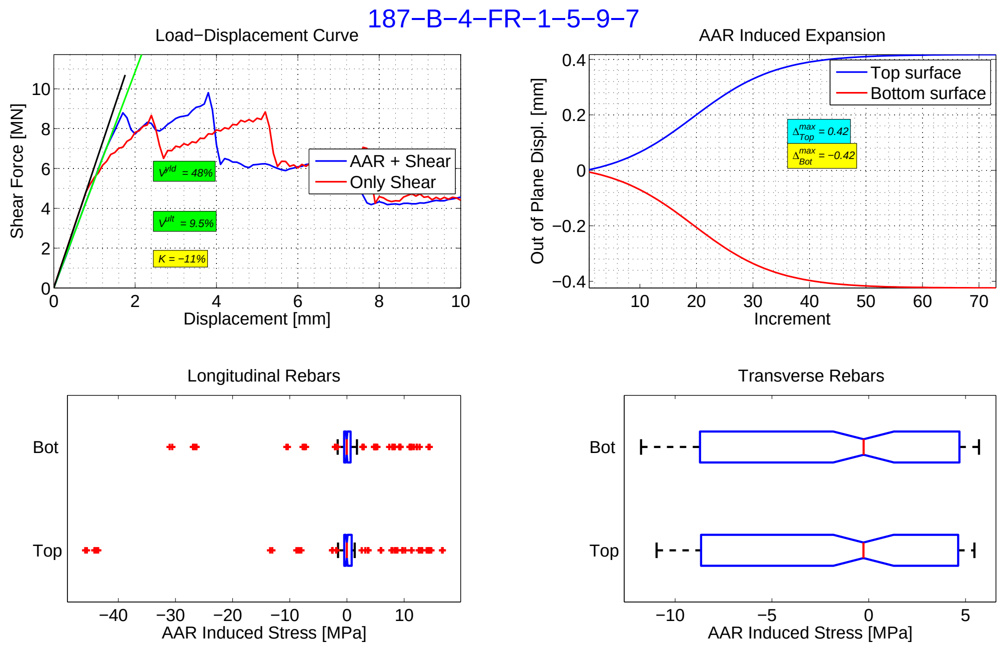

4.1.1.188 Analysis: 188-B-4-FR-1-5-9-9

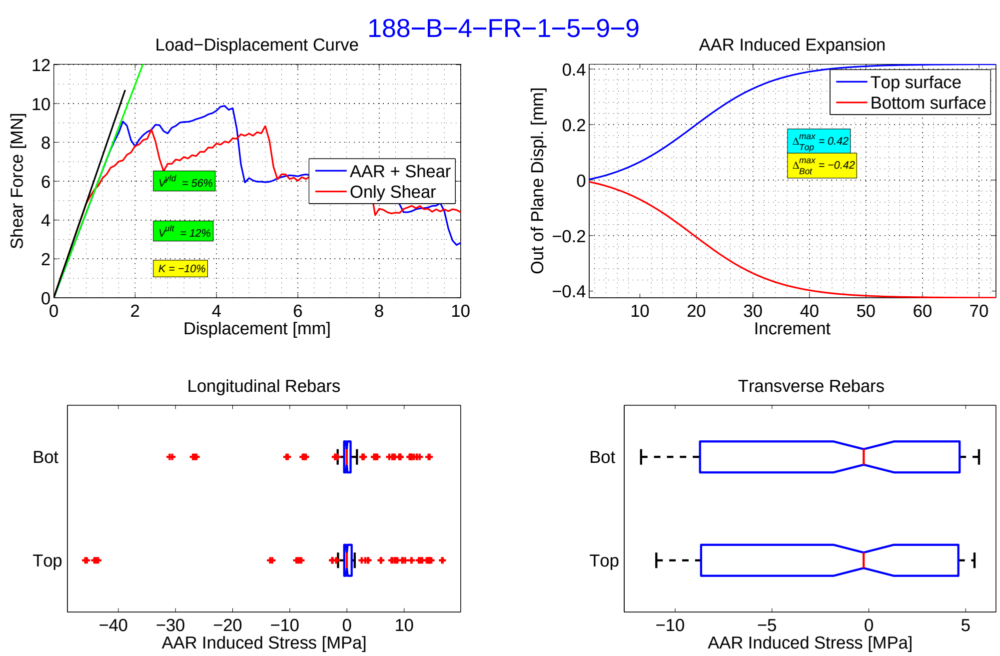

4.1.1.189 Analysis: 189-B-4-FR-1-10-7-7

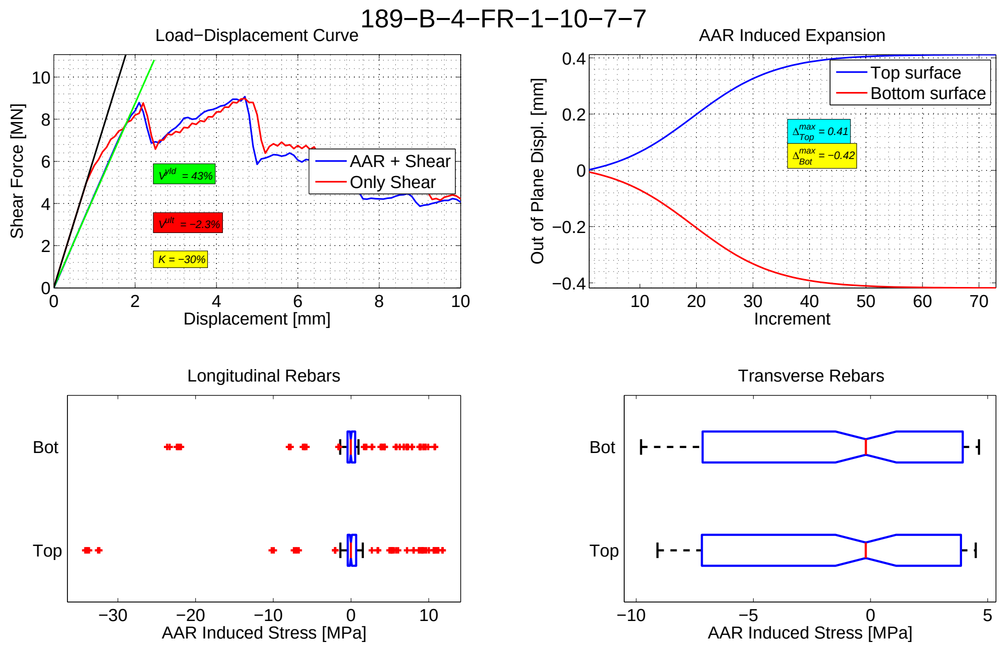

4.1.1.190 Analysis: 190-B-4-FR-1-10-7-9

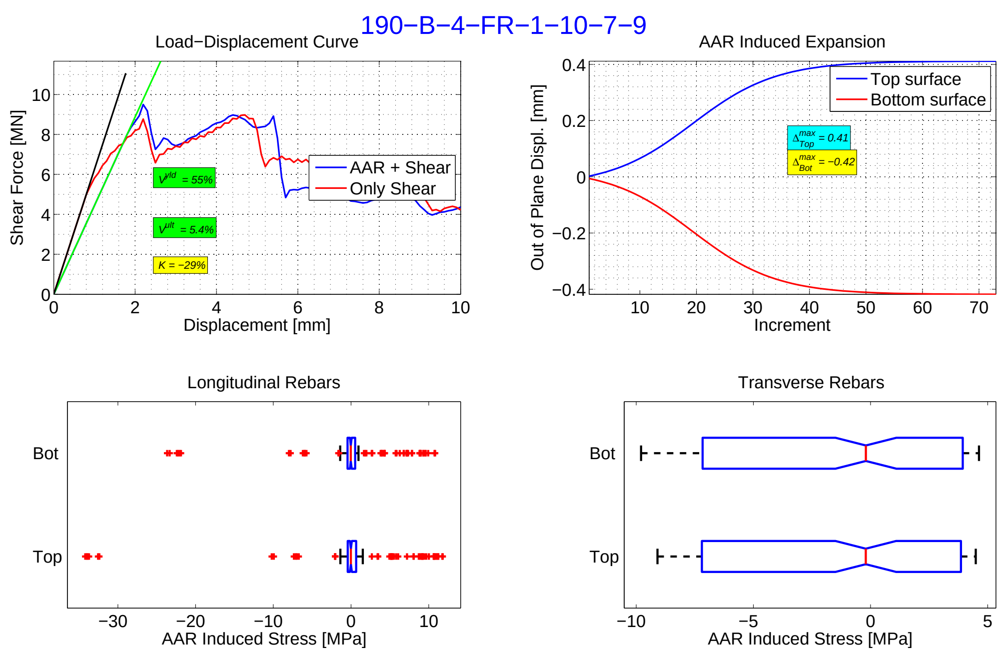

4.1.1.191 Analysis: 191-B-4-FR-1-10-9-7

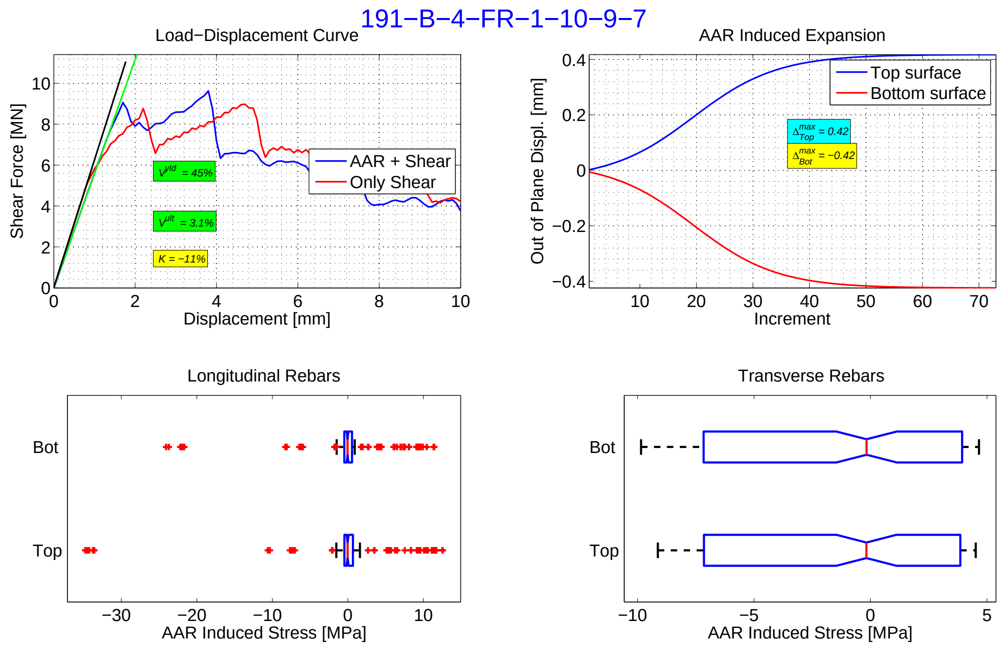

4.1.1.192 Analysis: 192-B-4-FR-1-10-9-9

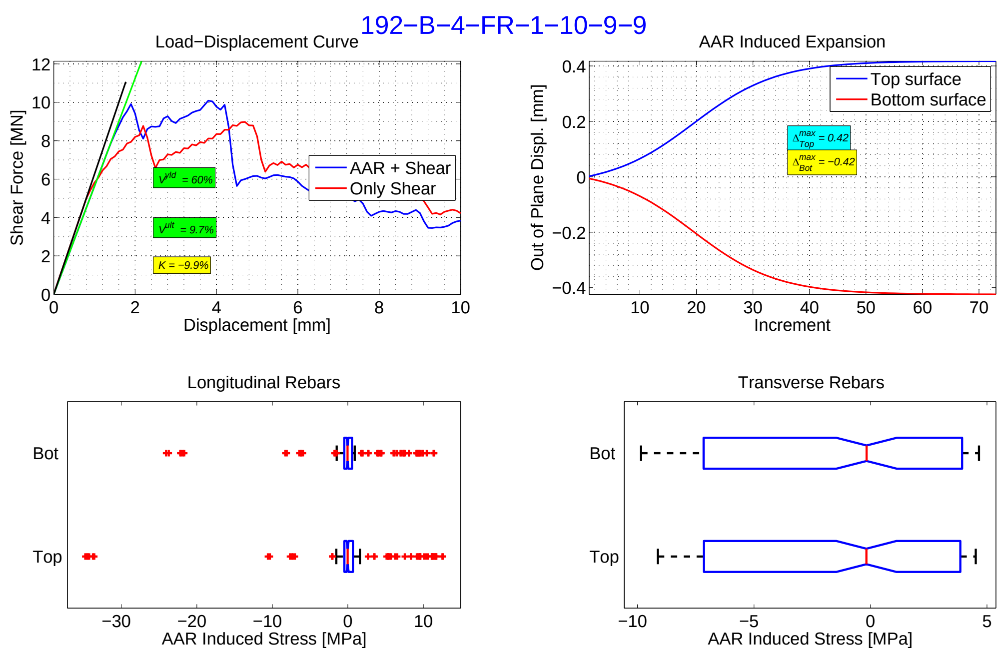

4.1.1.193 Analysis: 193-B-4-FR-2-2-7-7

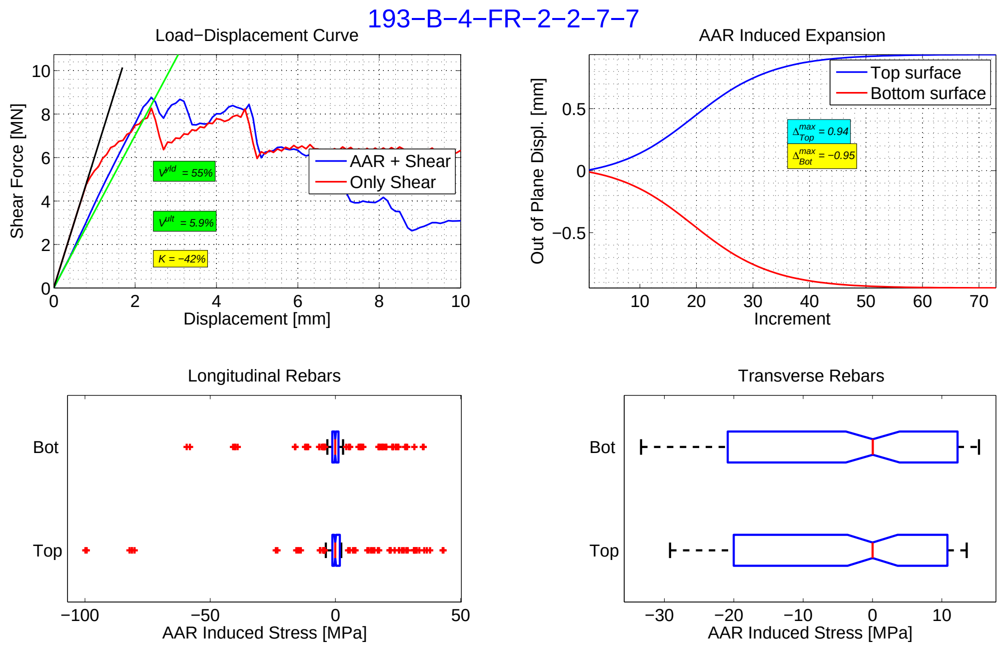

4.1.1.194 Analysis: 194-B-4-FR-2-2-7-9

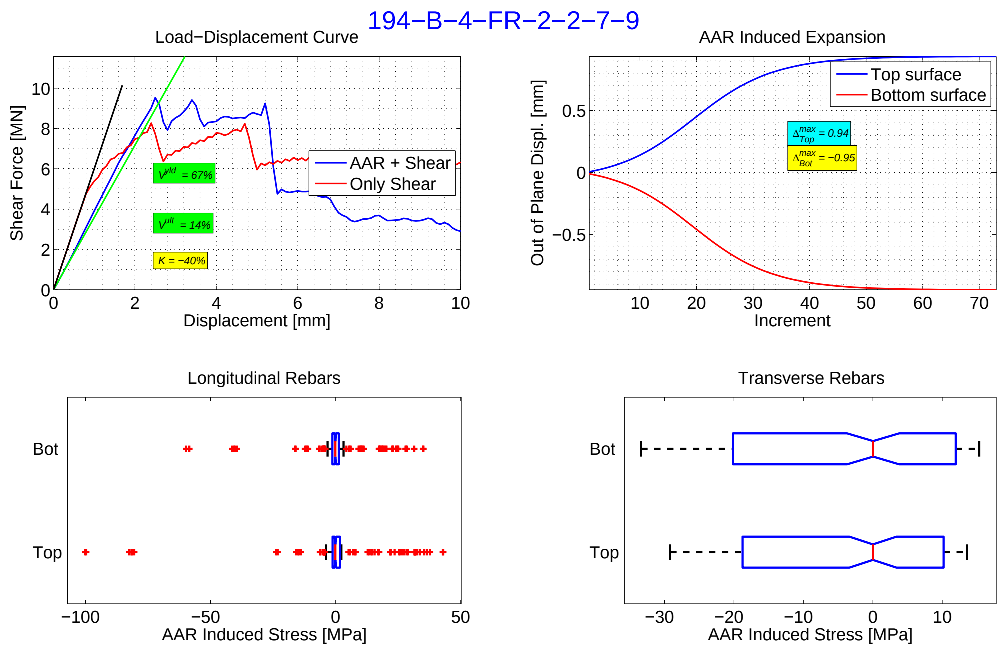

4.1.1.195 Analysis: 195-B-4-FR-2-2-9-7

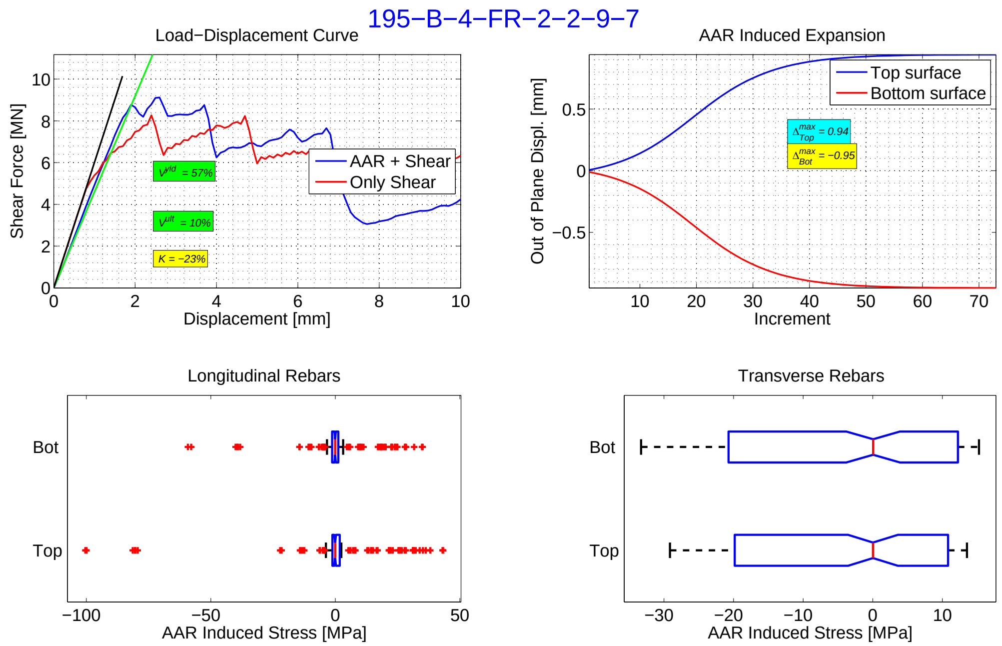

4.1.1.196 Analysis: 196-B-4-FR-2-2-9-9

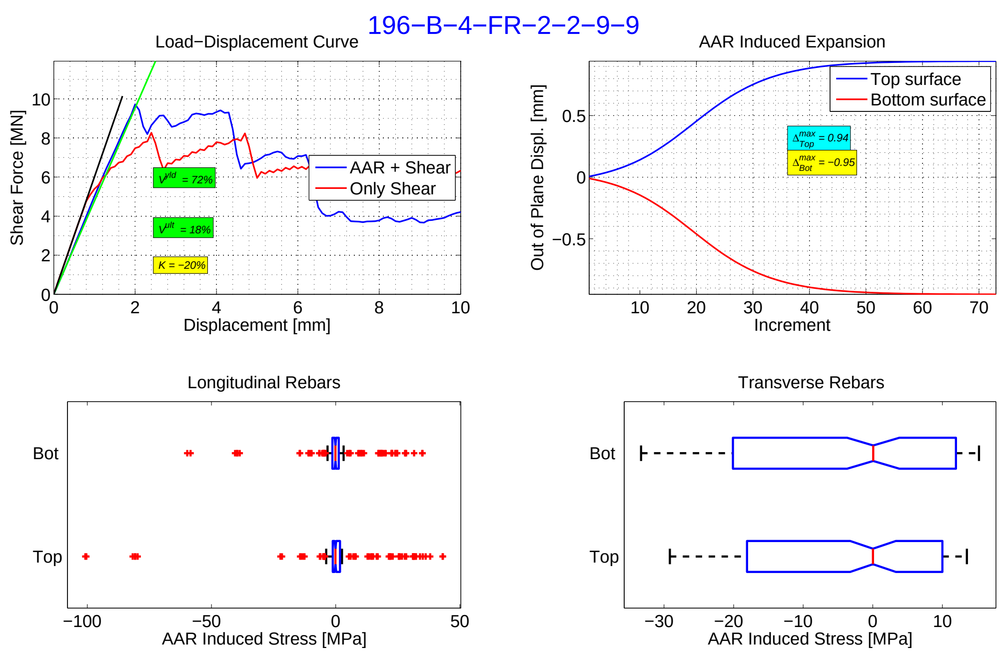

4.1.1.197 Analysis: 197-B-4-FR-2-5-7-7

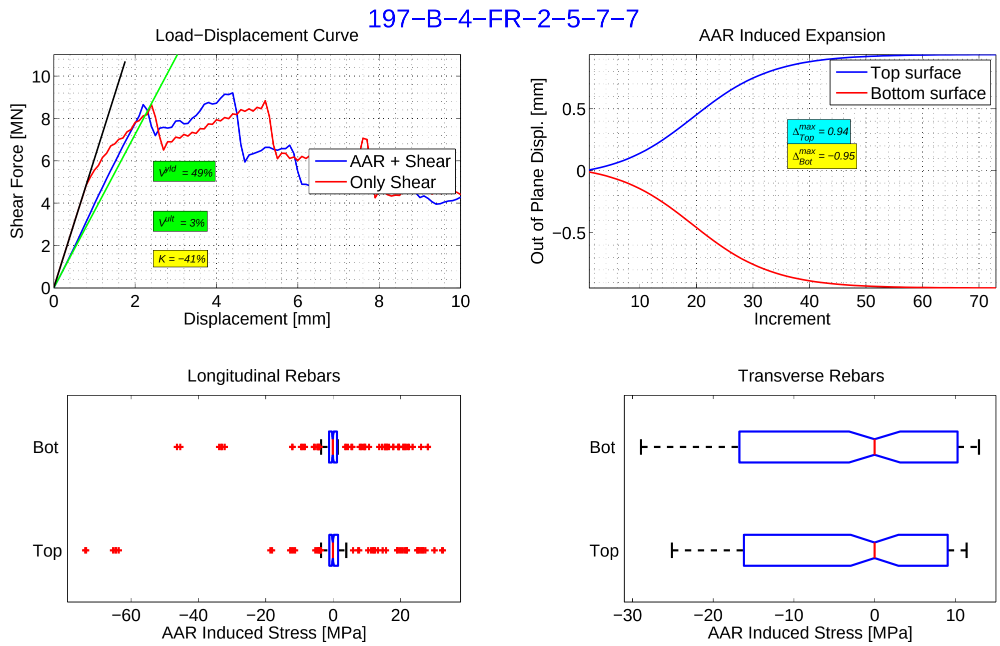

4.1.1.198 Analysis: 198-B-4-FR-2-5-7-9

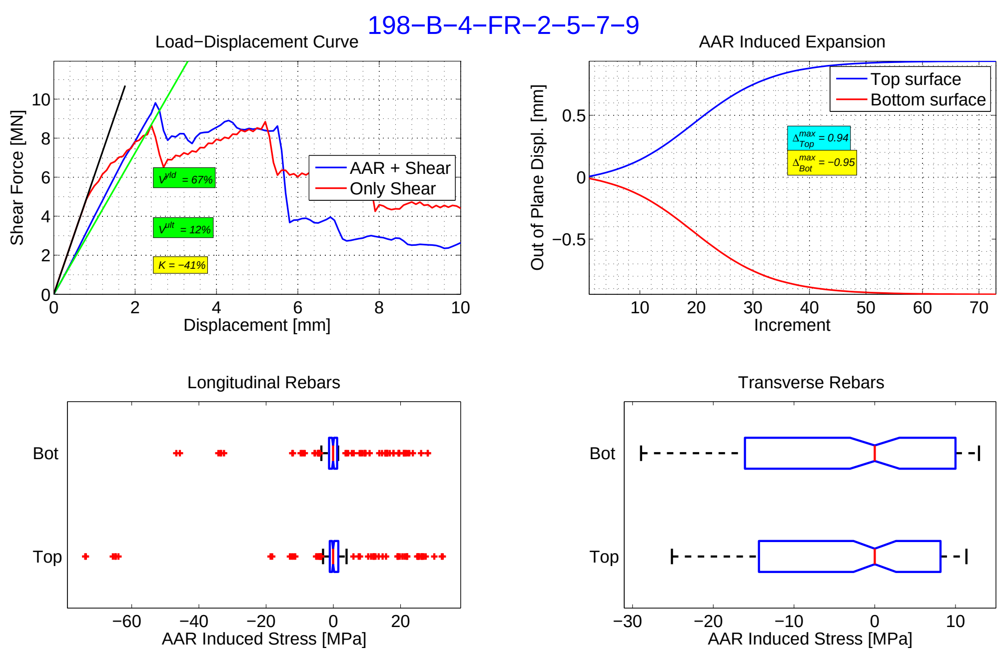

4.1.1.199 Analysis: 199-B-4-FR-2-5-9-7

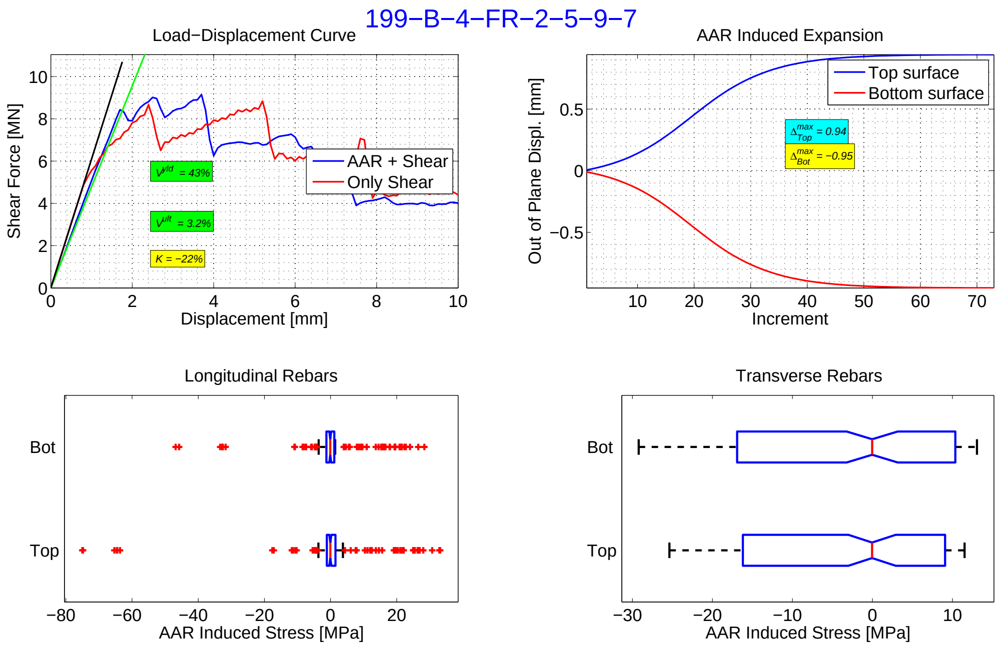

4.1.1.200 Analysis: 200-B-4-FR-2-5-9-9

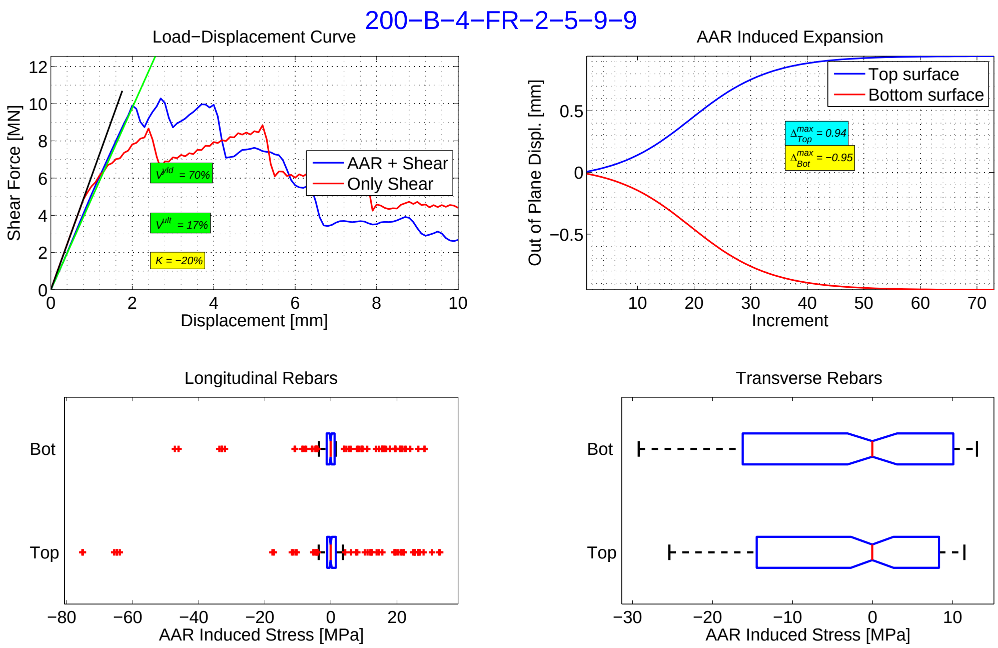

4.1.1.201 Analysis: 201-B-4-FR-2-10-7-7

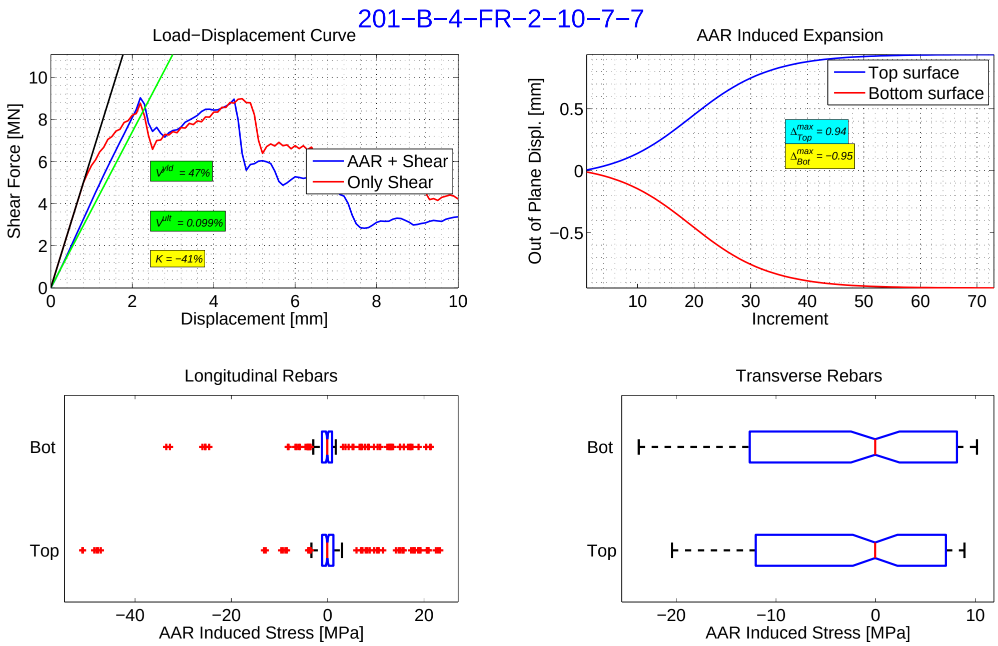

4.1.1.202 Analysis: 202-B-4-FR-2-10-7-9

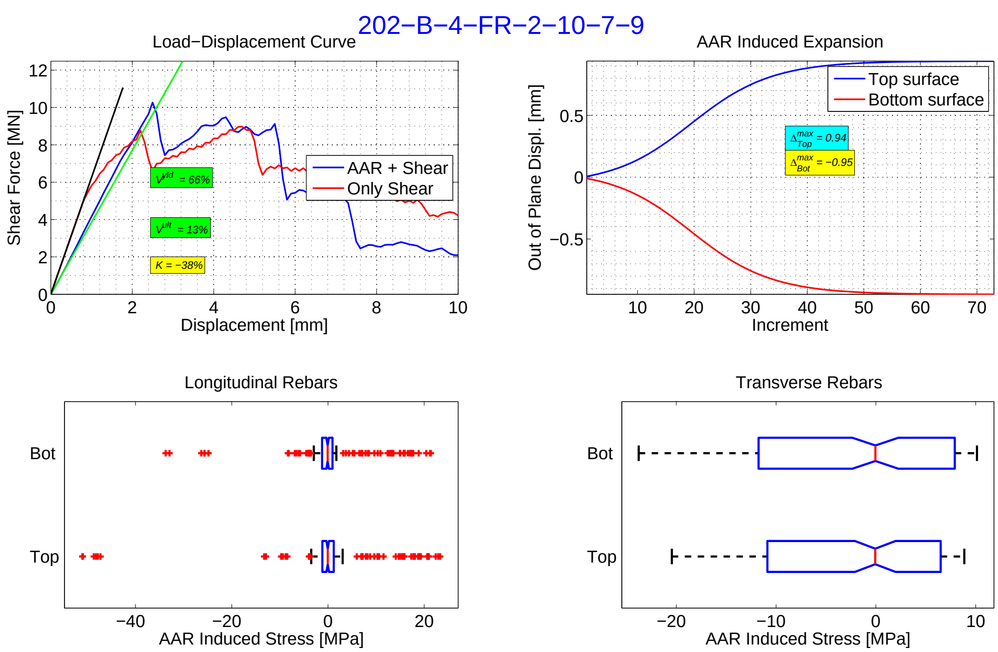

4.1.1.203 Analysis: 203-B-4-FR-2-10-9-7

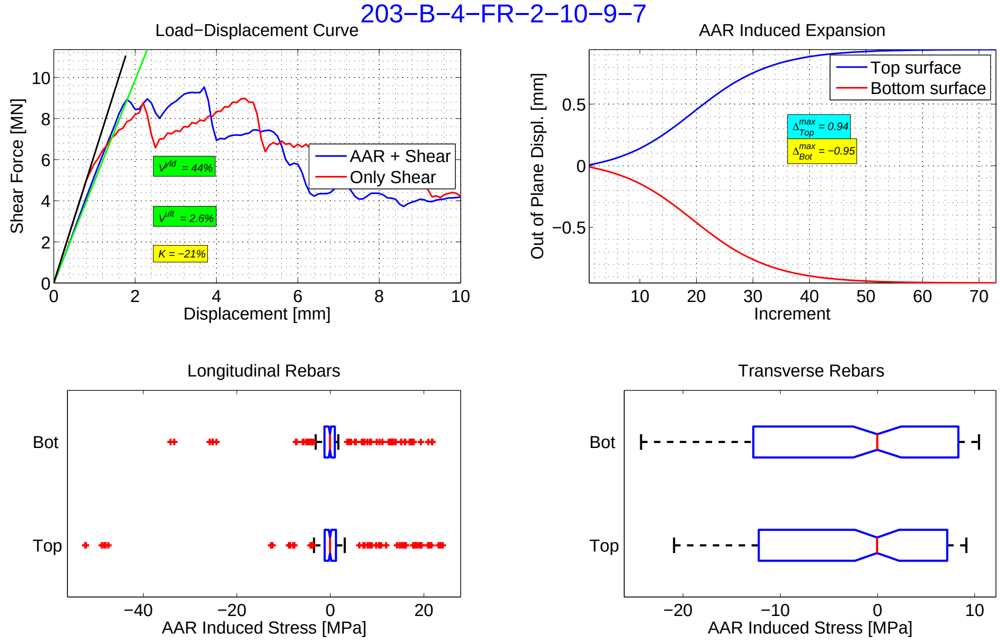

4.1.1.204 Analysis: 204-B-4-FR-2-10-9-9

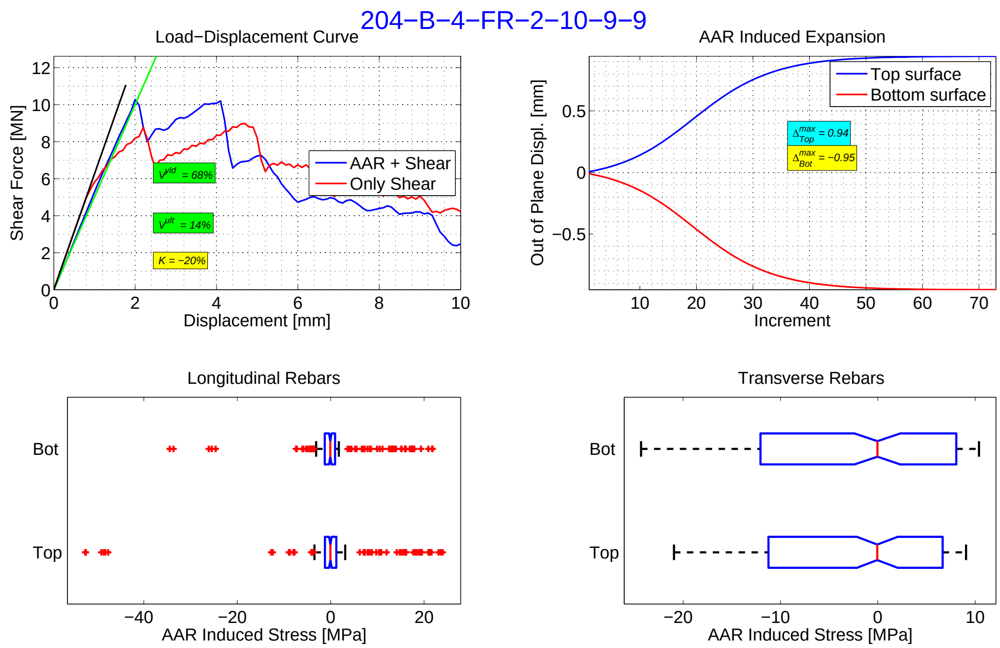

4.1.1.205 Analysis: 205-B-4-FR-3-2-7-7

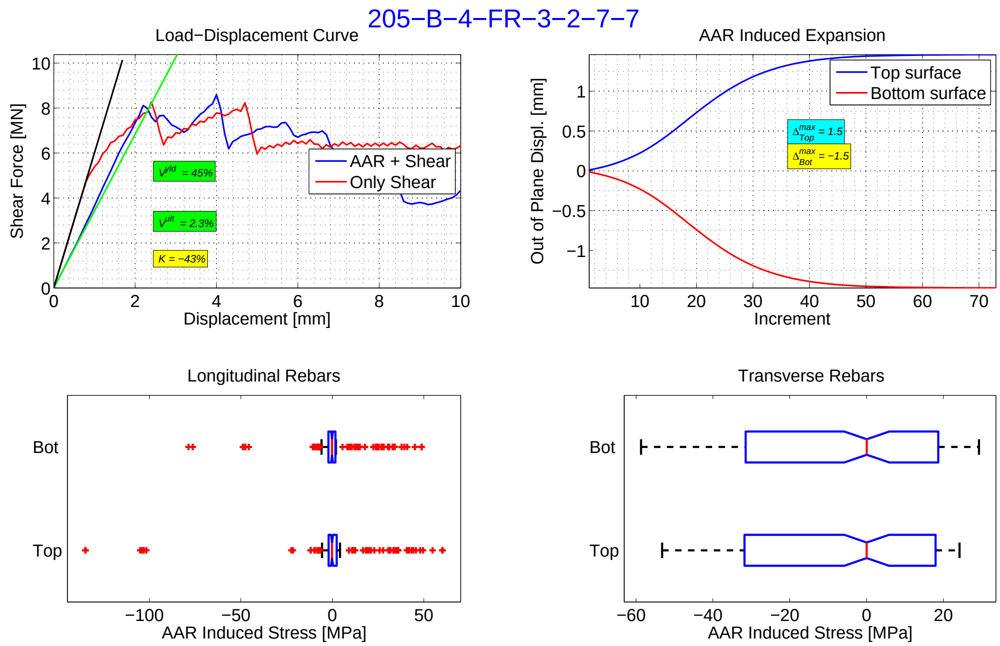

4.1.1.206 Analysis: 206-B-4-FR-3-2-7-9

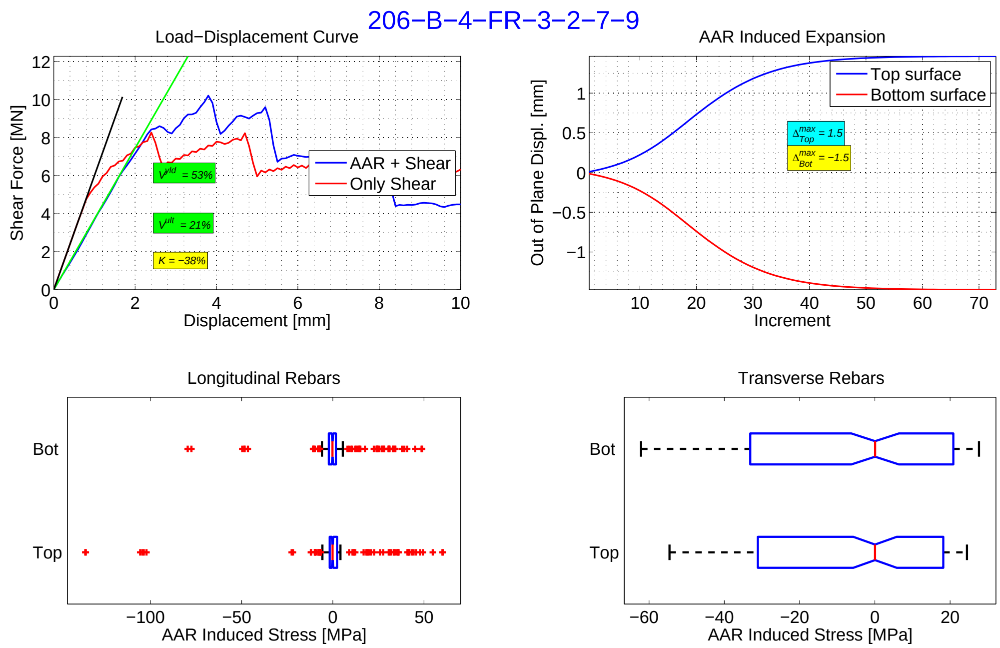

4.1.1.207 Analysis: 207-B-4-FR-3-2-9-7

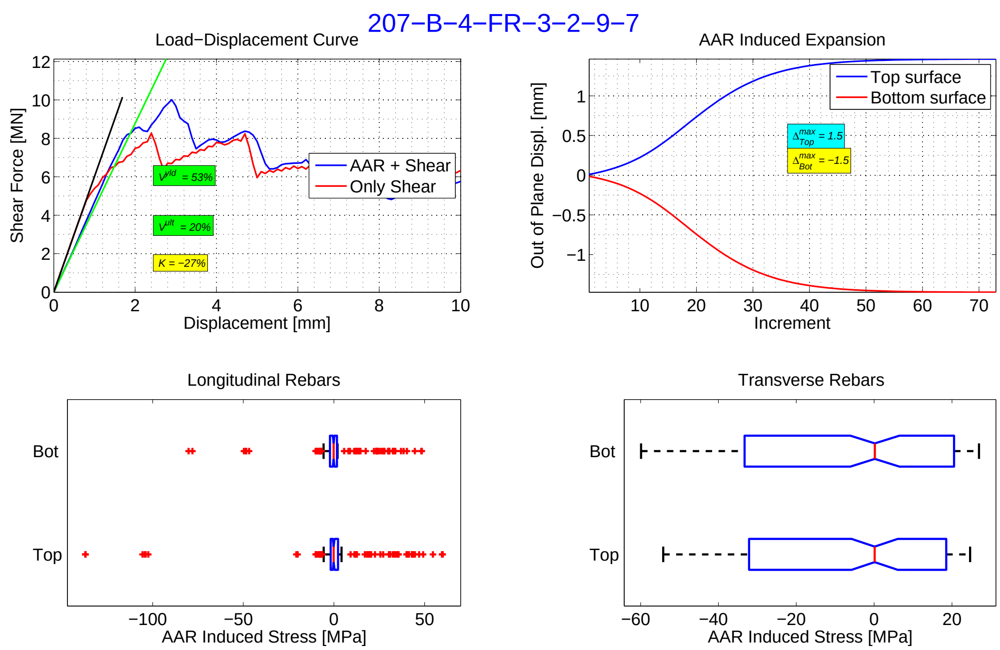

4.1.1.208 Analysis: 208-B-4-FR-3-2-9-9

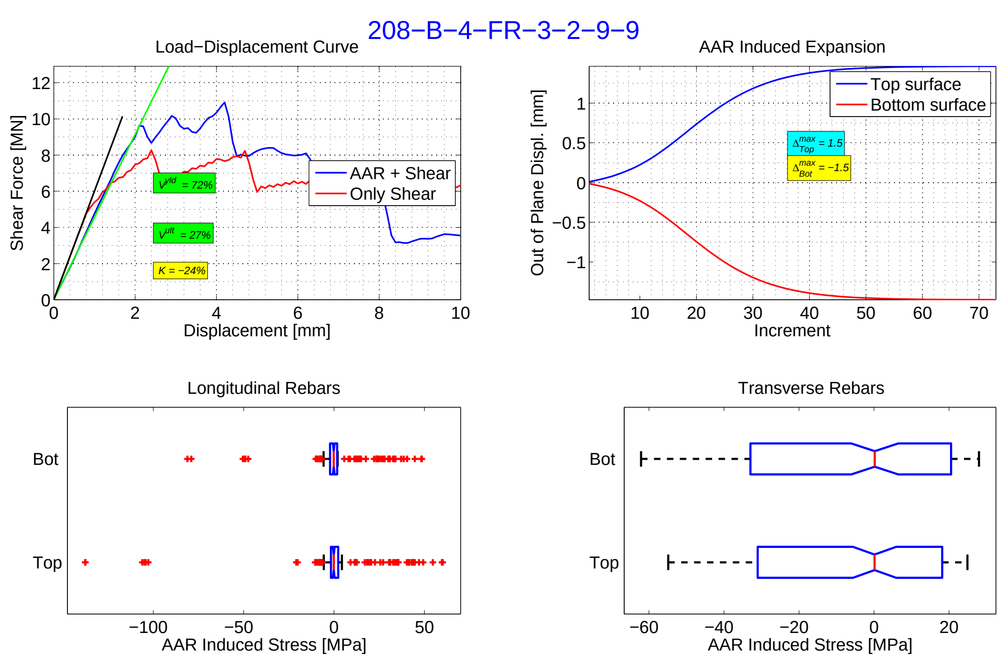

4.1.1.209 Analysis: 209-B-4-FR-3-5-7-7

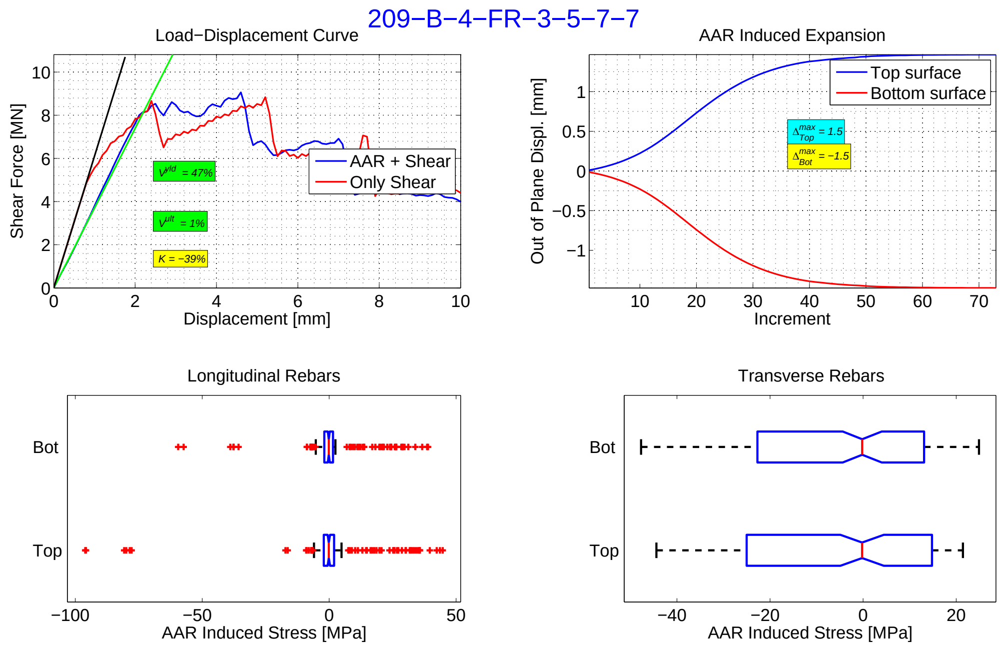

4.1.1.210 Analysis: 210-B-4-FR-3-5-7-9

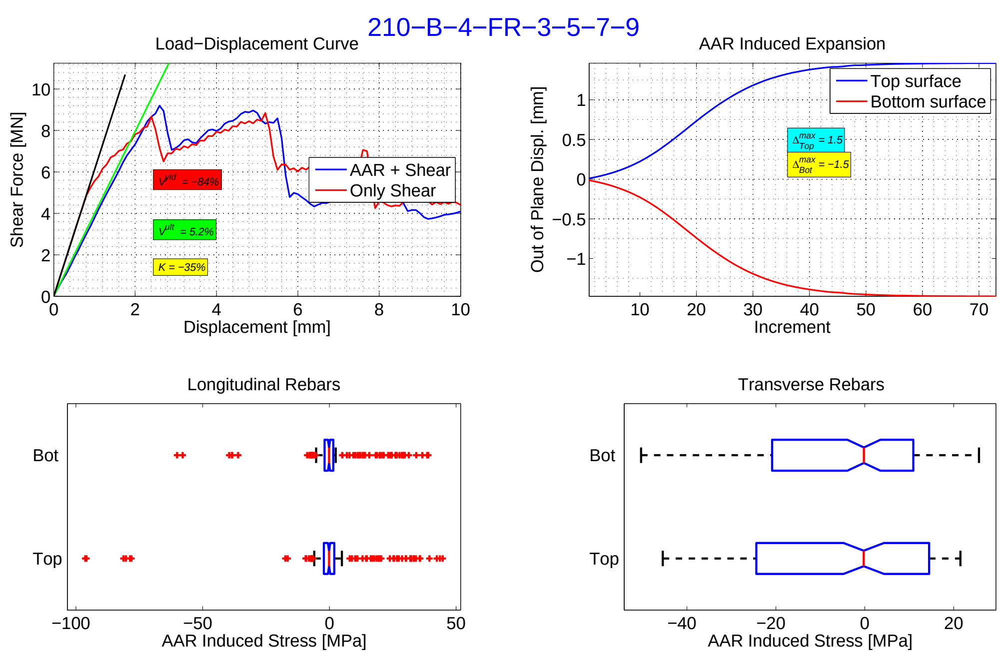

4.1.1.211 Analysis: 211-B-4-FR-3-5-9-7

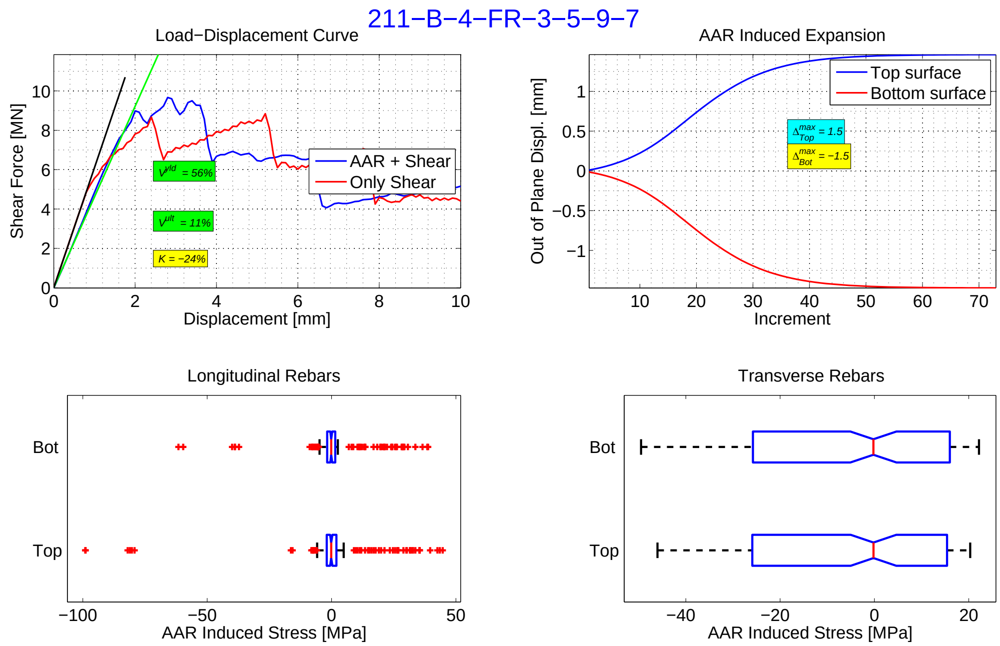

4.1.1.212 Analysis: 212-B-4-FR-3-5-9-9

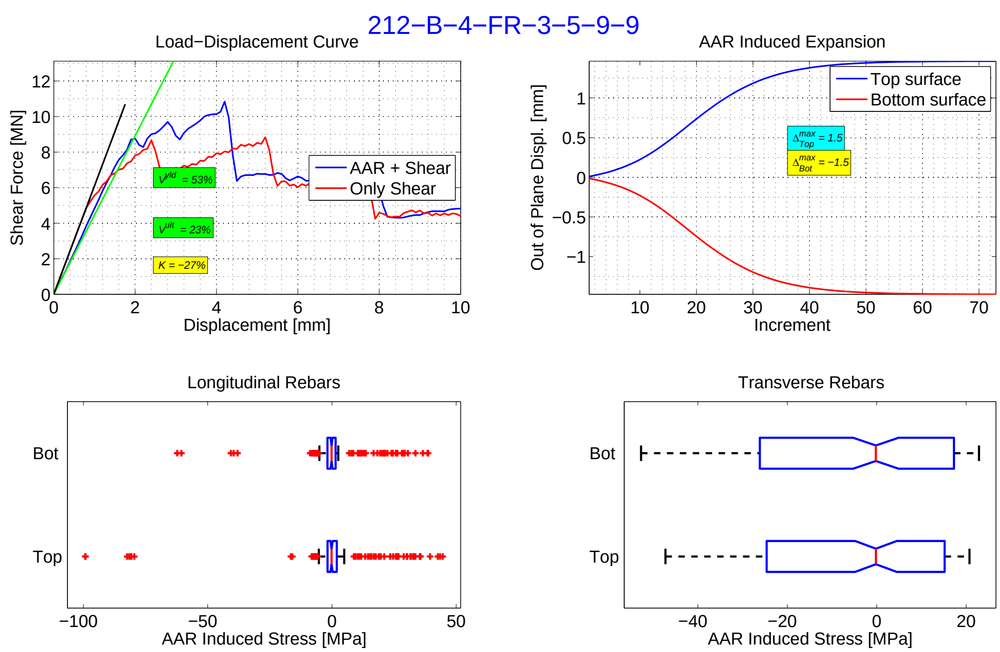

4.1.1.213 Analysis: 213-B-4-FR-3-10-7-7

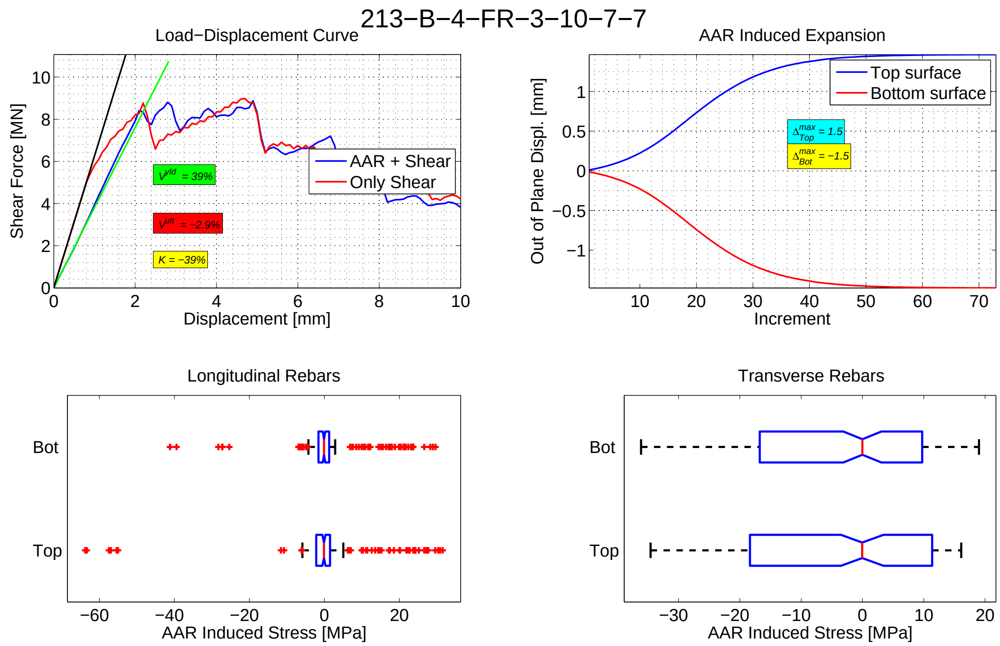

4.1.1.214 Analysis: 214-B-4-FR-3-10-7-9

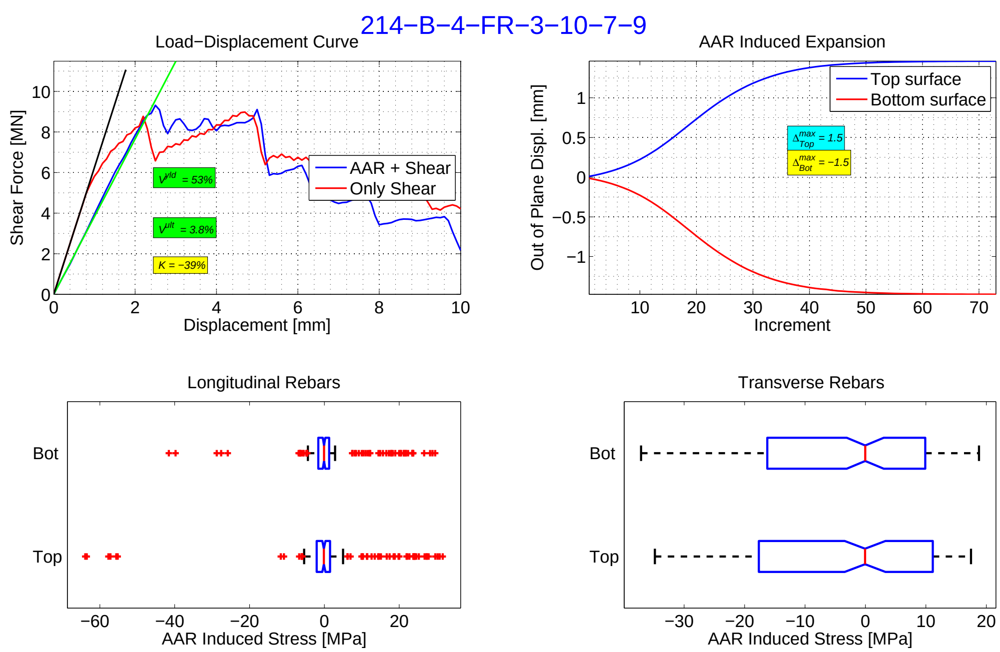

4.1.1.215 Analysis: 215-B-4-FR-3-10-9-7

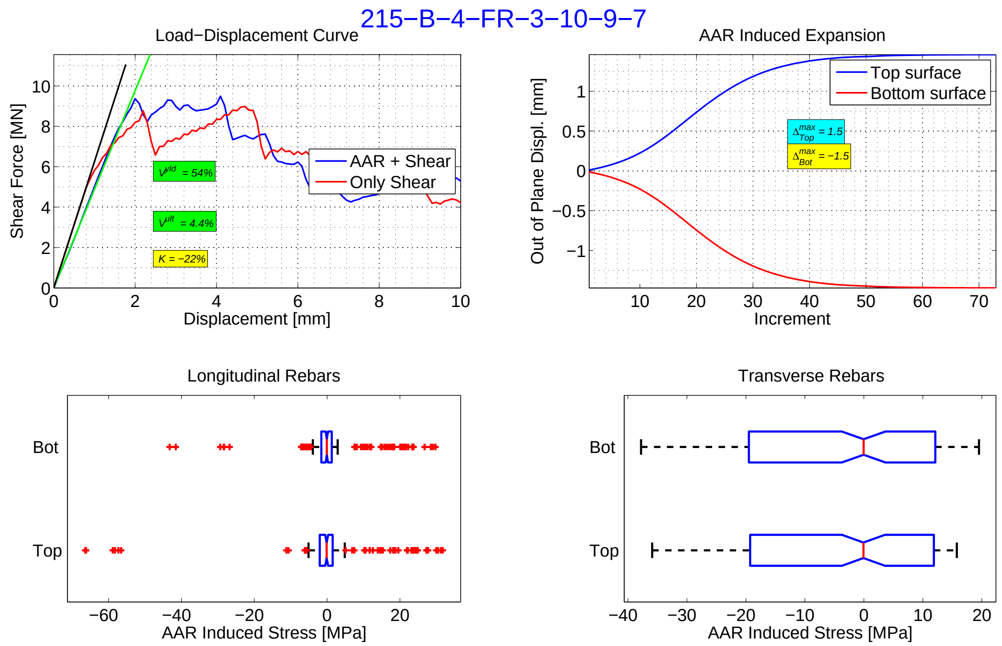

4.1.1.216 Analysis: 216-B-4-FR-3-10-9-9

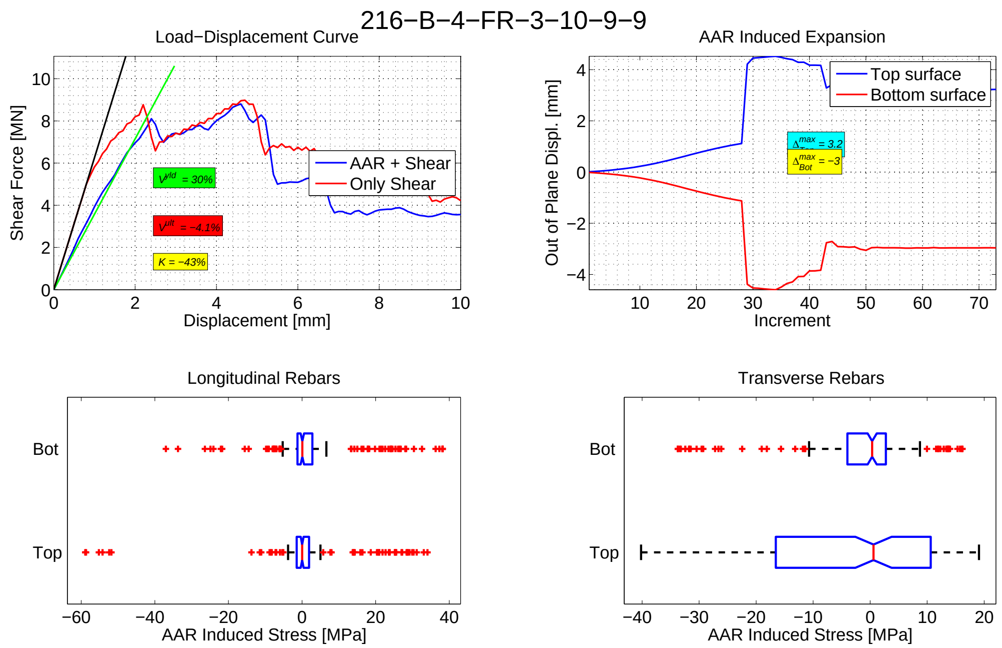

4.1.2 TRUNCATED BEAM

4.1.2.1 Analysis: 1-TB-2-U-1-2-7-7

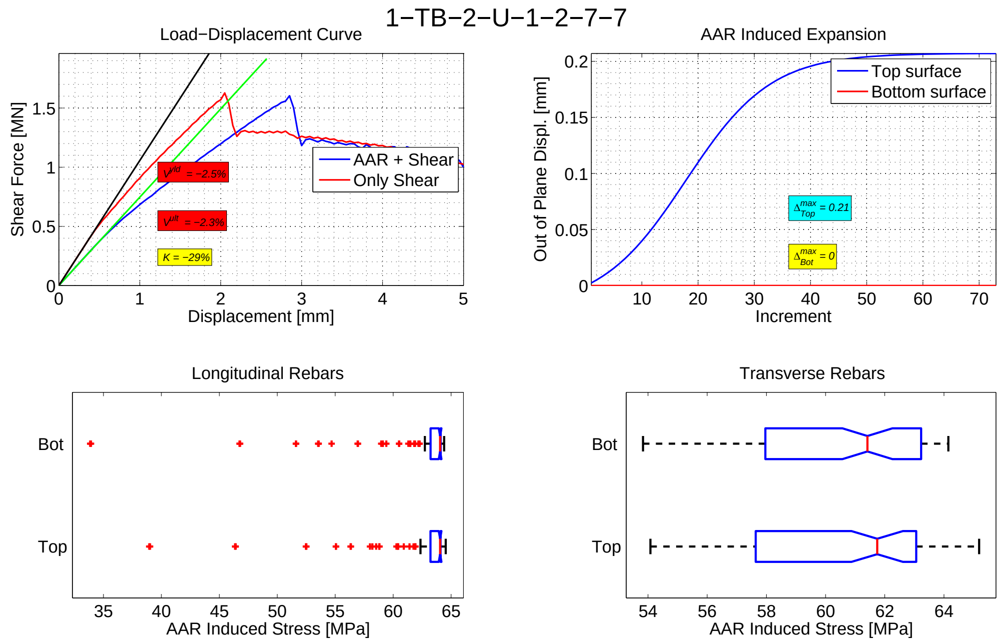

4.1.2.2 Analysis: 2-TB-2-U-1-2-7-9

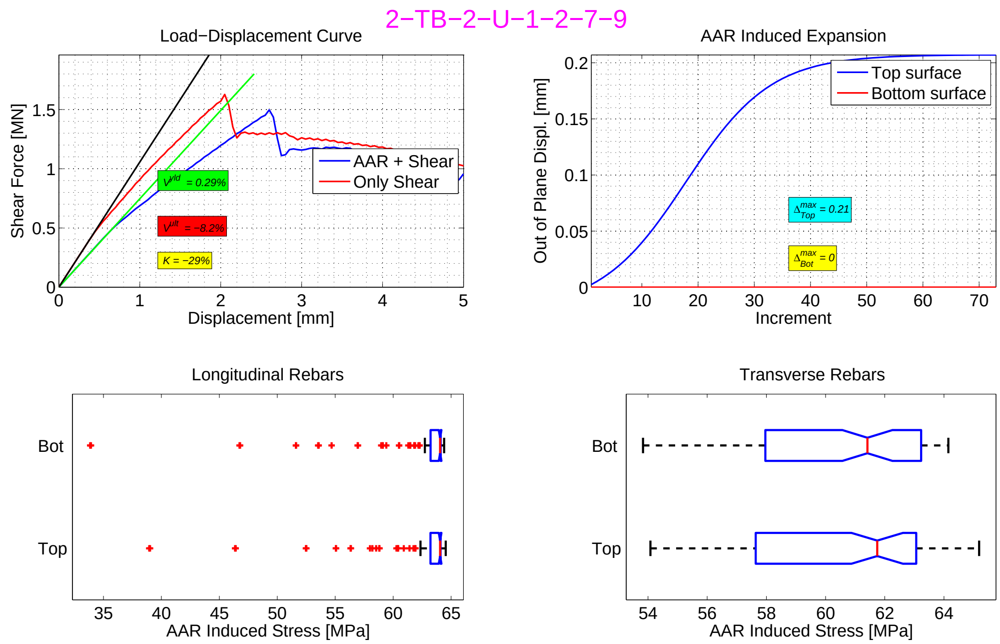

4.1.2.3 Analysis: 3-TB-2-U-1-2-9-7

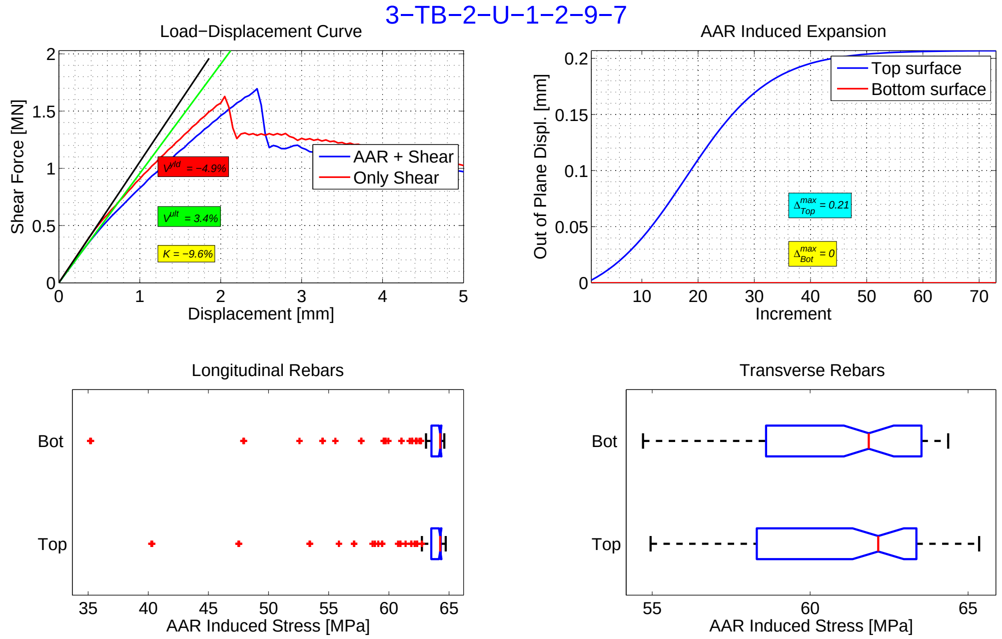

4.1.2.4 Analysis: 4-TB-2-U-1-2-9-9

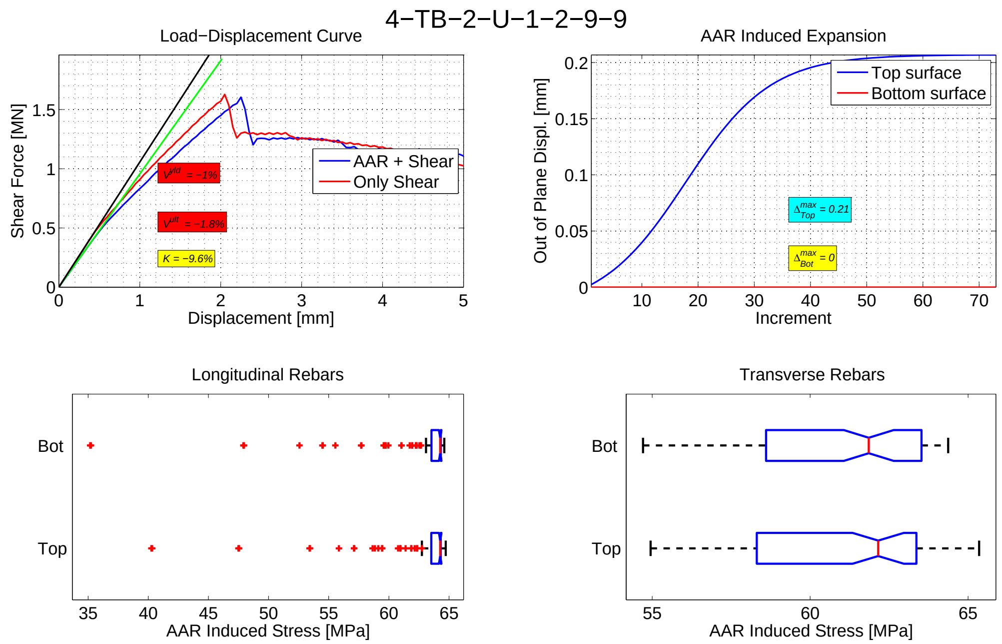

4.1.2.5 Analysis: 5-TB-2-U-1-5-7-7

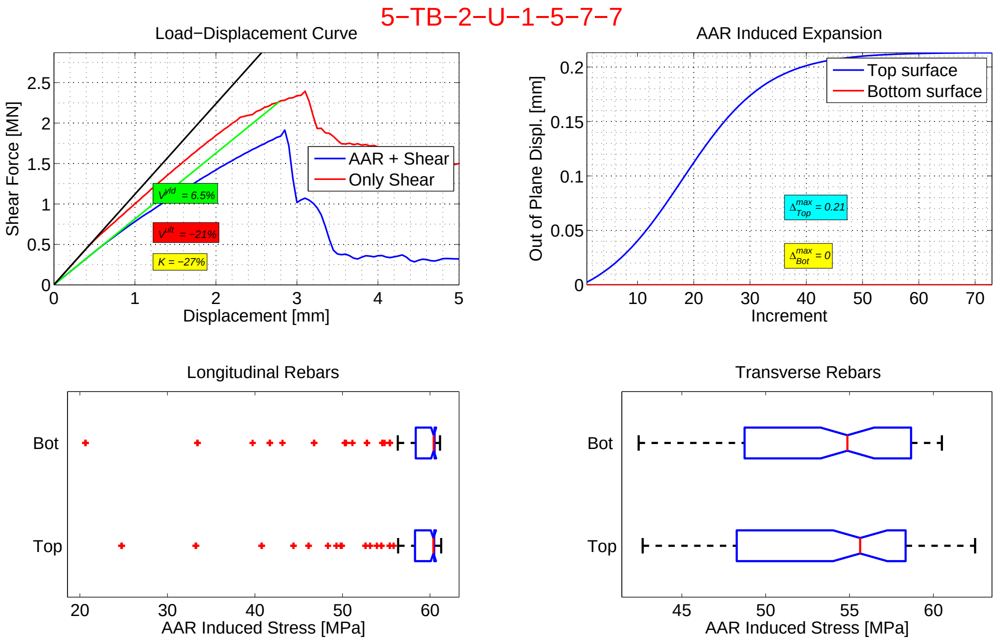

4.1.2.6 Analysis: 6-TB-2-U-1-5-7-9

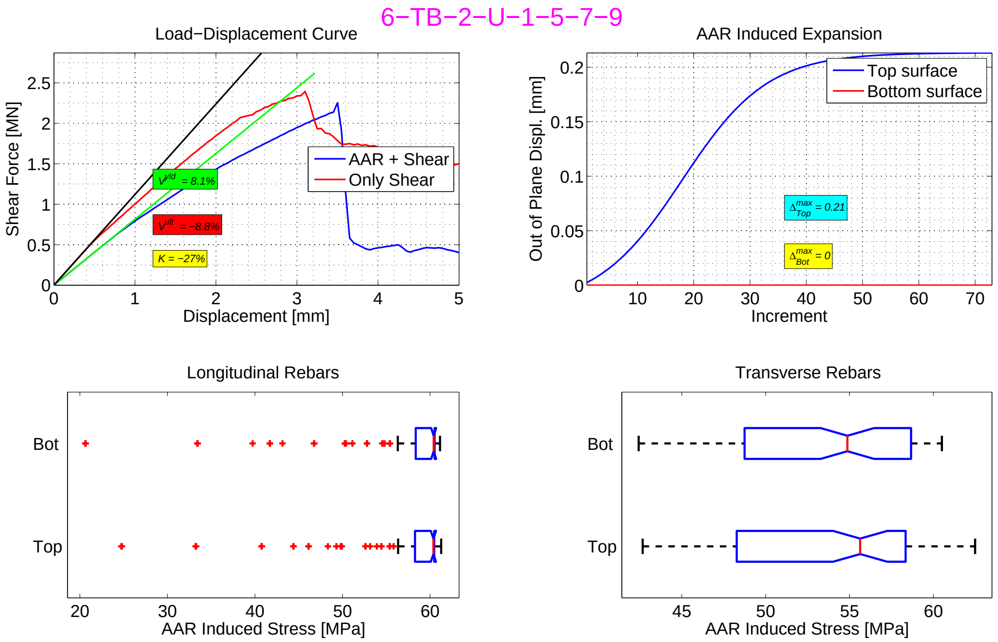

4.1.2.7 Analysis: 7-TB-2-U-1-5-9-7

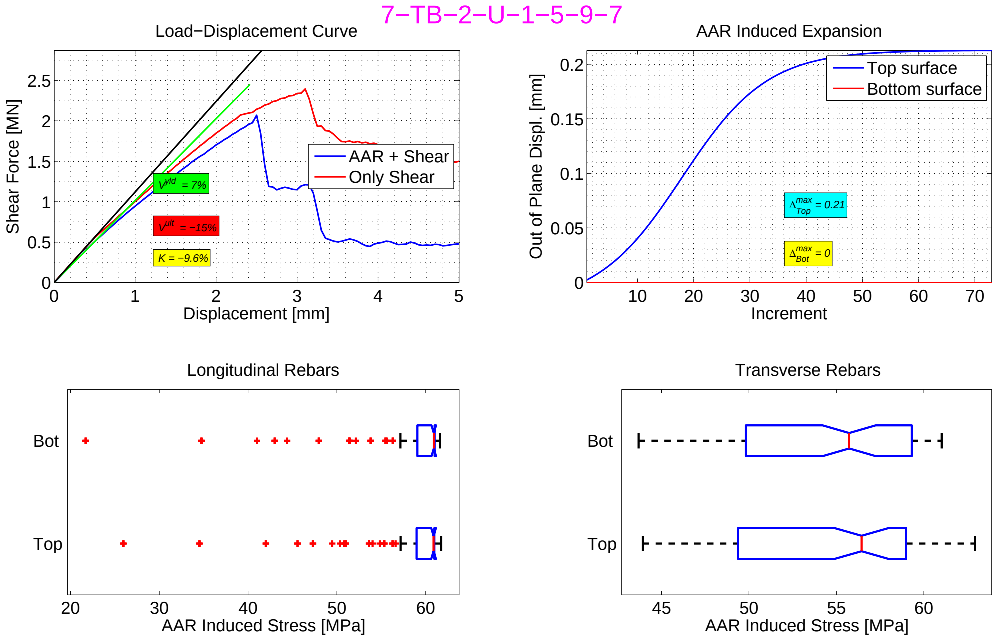

4.1.2.8 Analysis: 8-TB-2-U-1-5-9-9

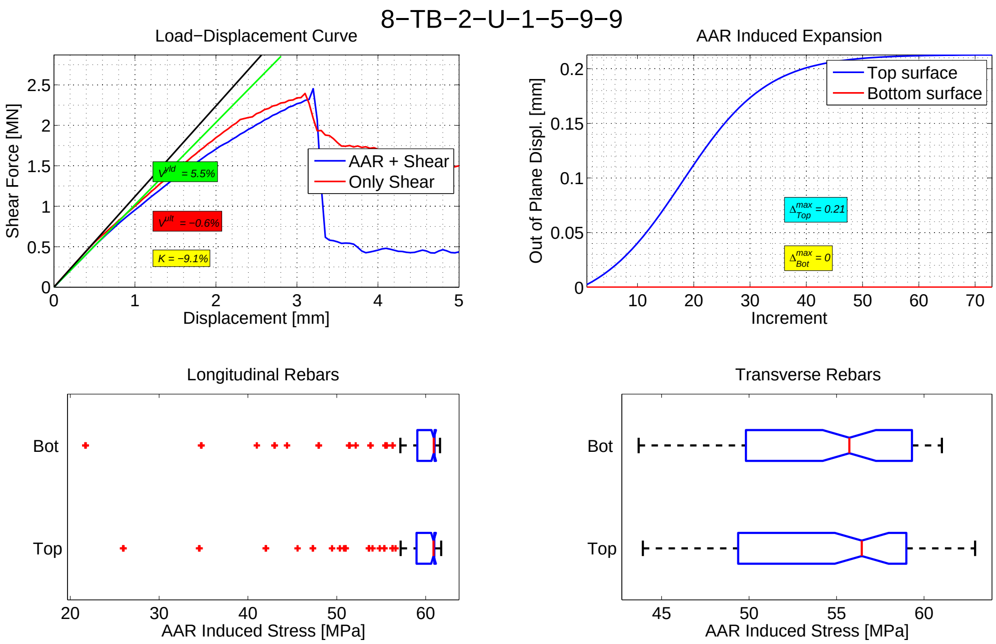

4.1.2.9 Analysis: 9-TB-2-U-1-10-7-7

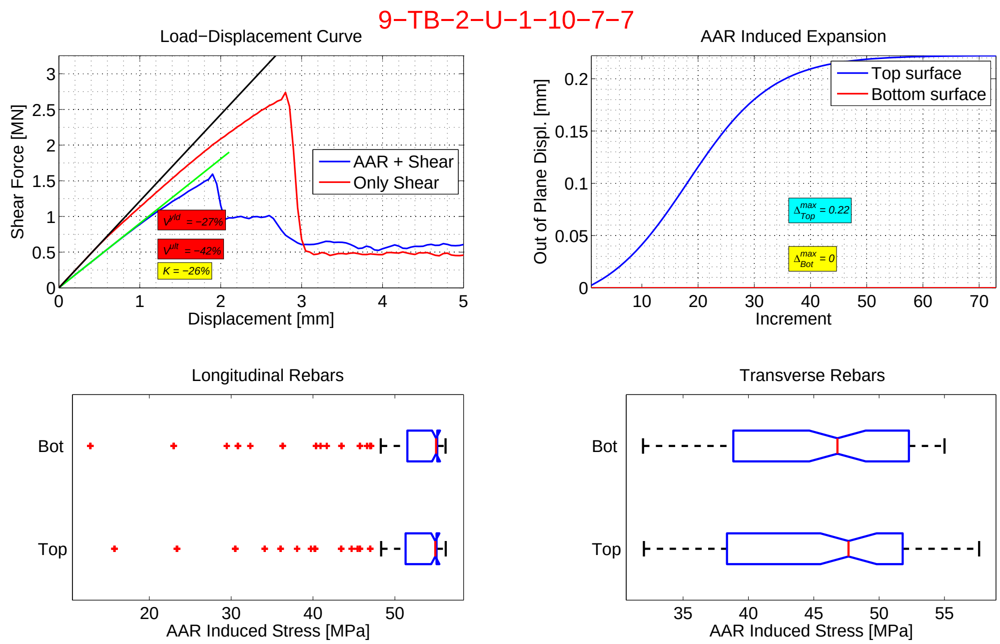

4.1.2.10 Analysis: 10-TB-2-U-1-10-7-9

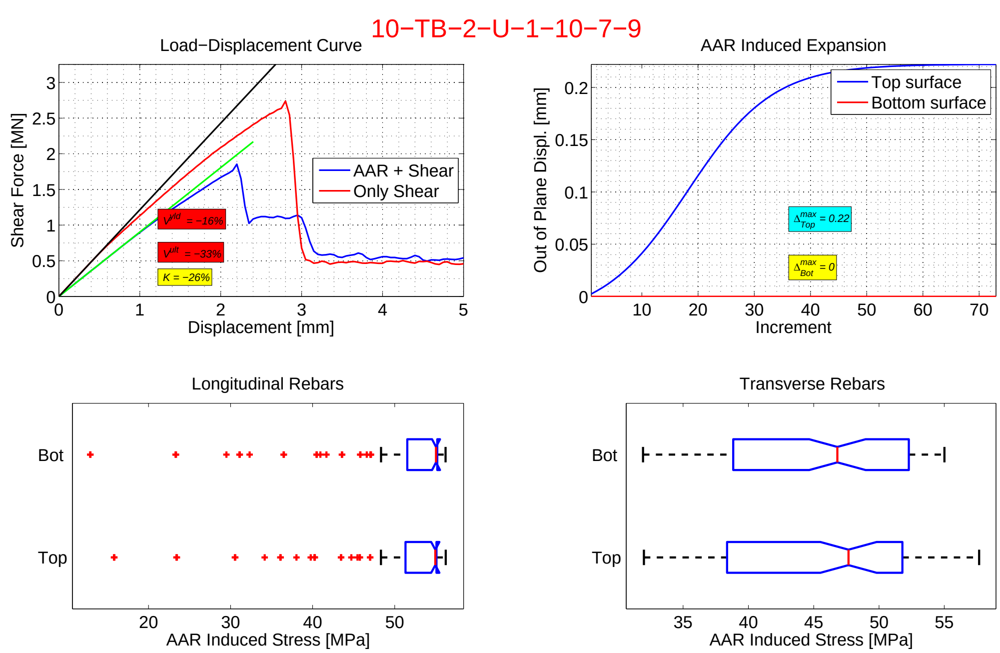

4.1.2.11 Analysis: 11-TB-2-U-1-10-9-7

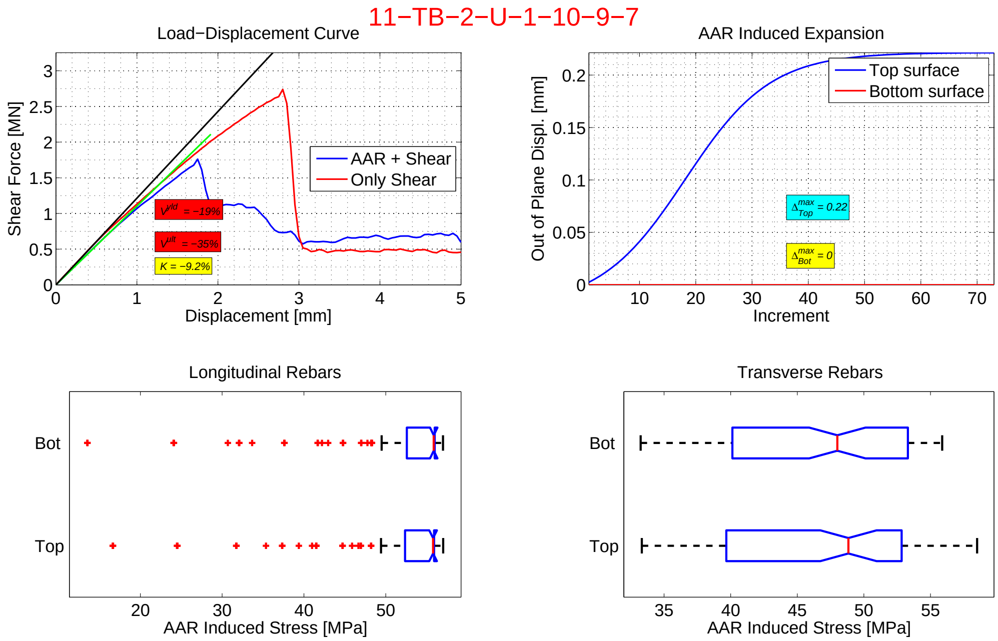

4.1.2.12 Analysis: 12-TB-2-U-1-10-9-9

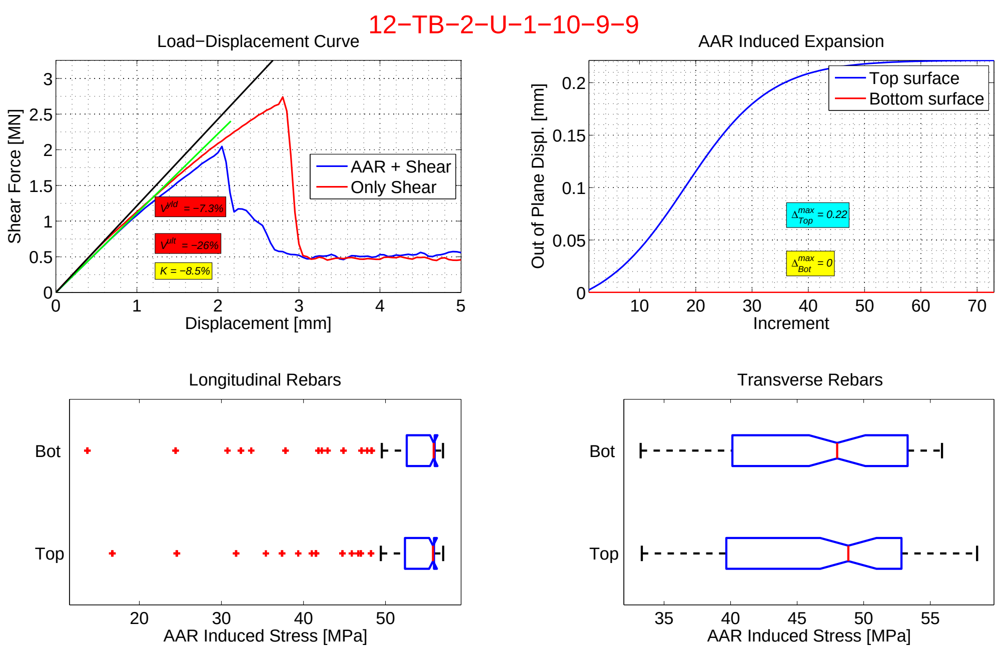

4.1.2.13 Analysis: 13-TB-2-U-2-2-7-7

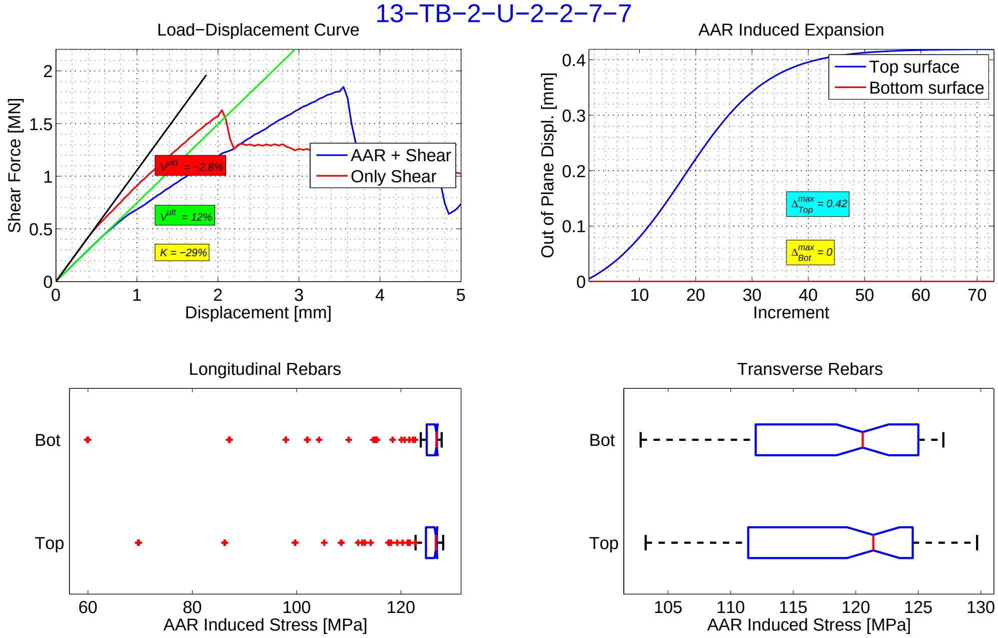

4.1.2.14 Analysis: 14-TB-2-U-2-2-7-9

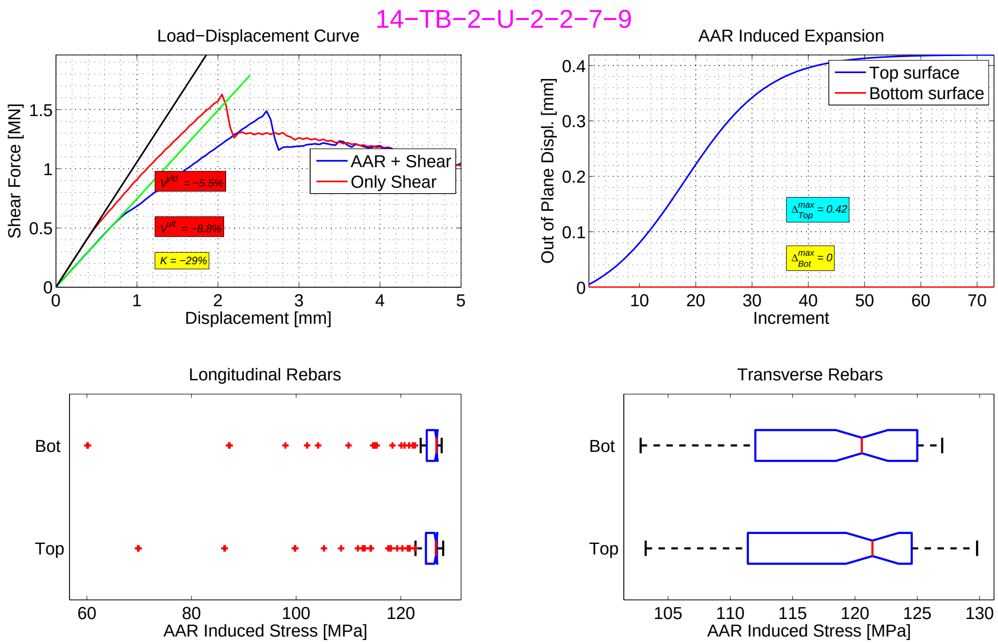

4.1.2.15 Analysis: 15-TB-2-U-2-2-9-7

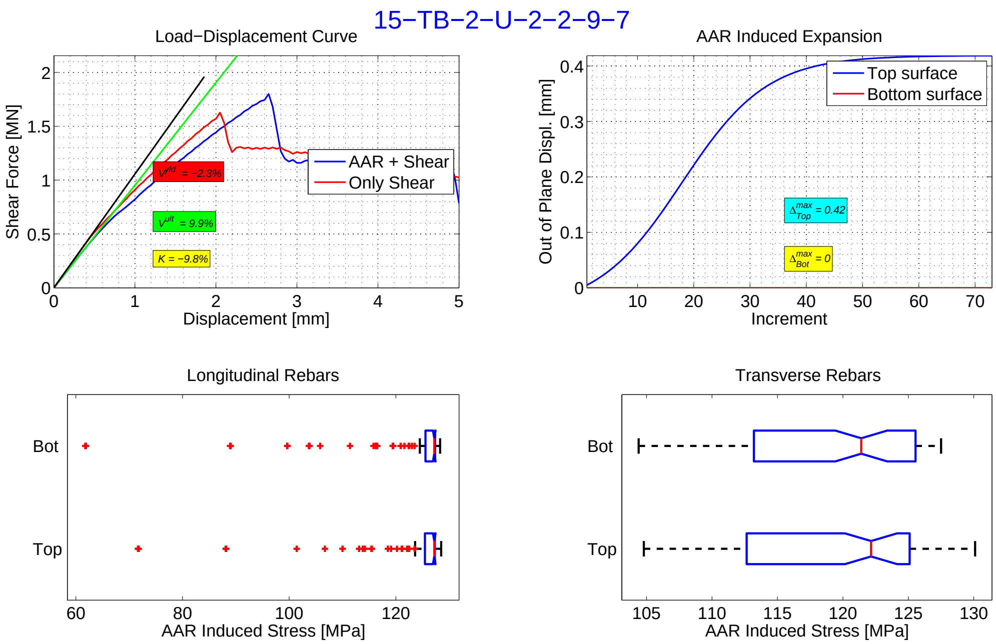

4.1.2.16 Analysis: 16-TB-2-U-2-2-9-9

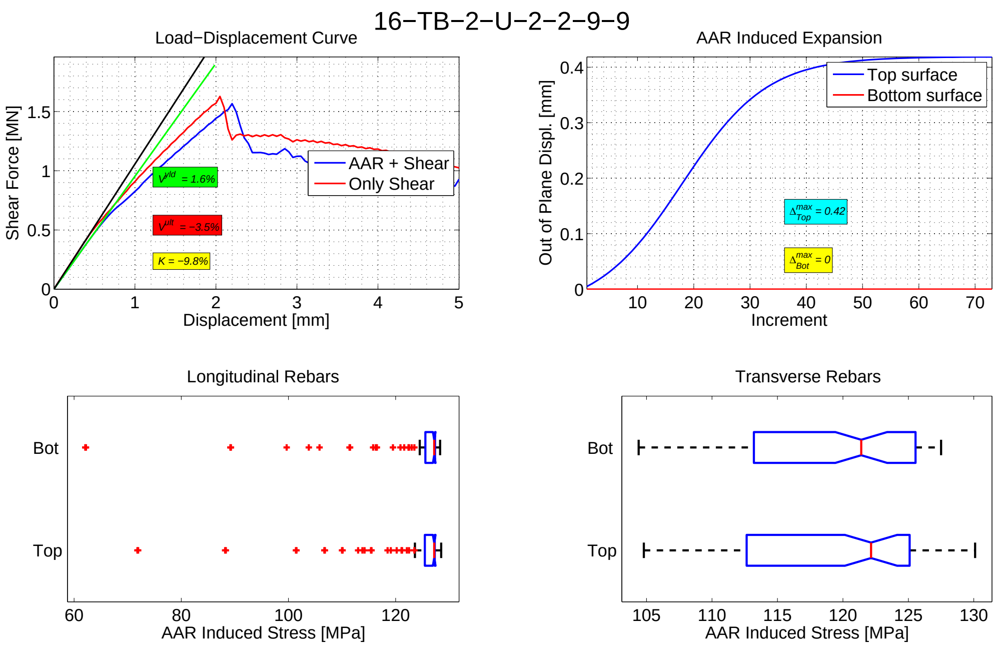

4.1.2.17 Analysis: 17-TB-2-U-2-5-7-7

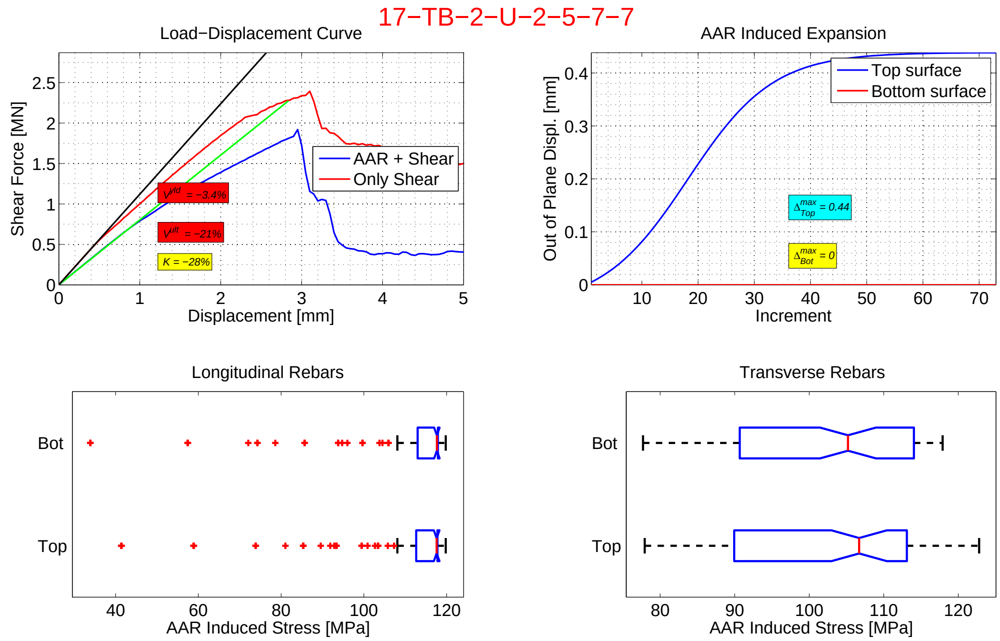

4.1.2.18 Analysis: 18-TB-2-U-2-5-7-9

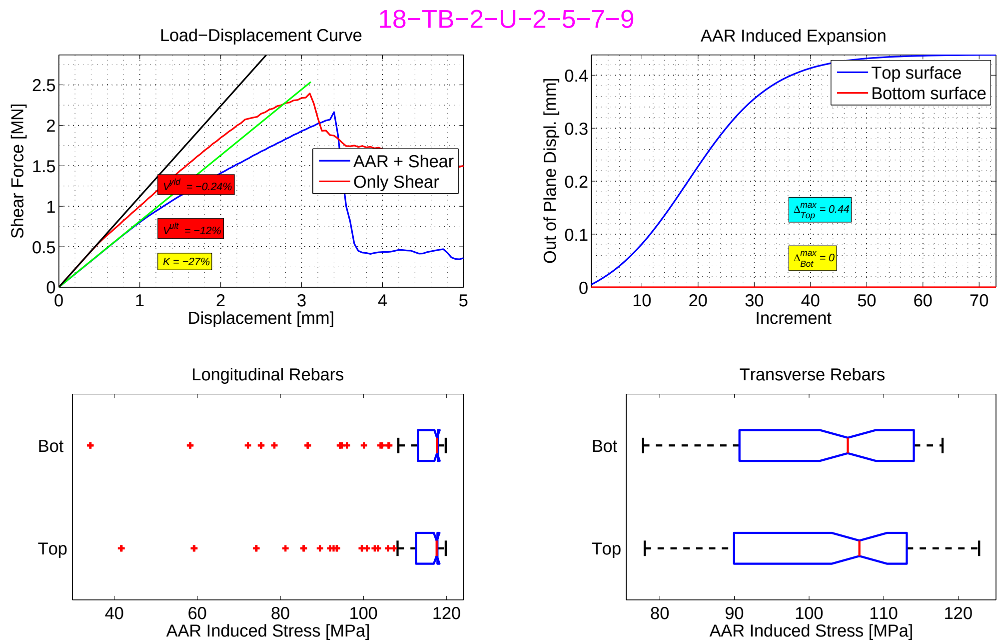

4.1.2.19 Analysis: 19-TB-2-U-2-5-9-7

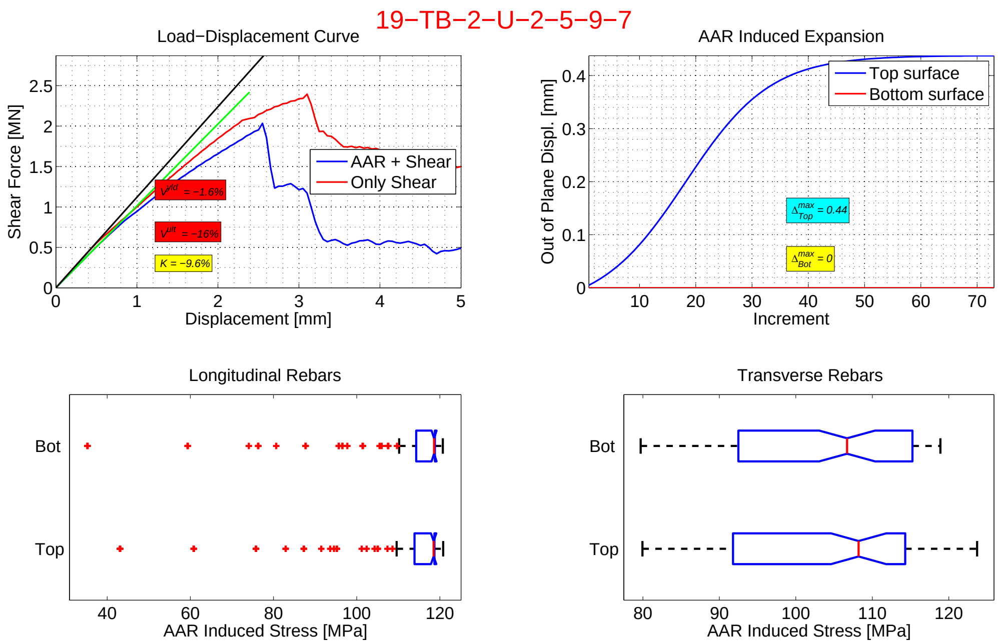

4.1.2.20 Analysis: 20-TB-2-U-2-5-9-9

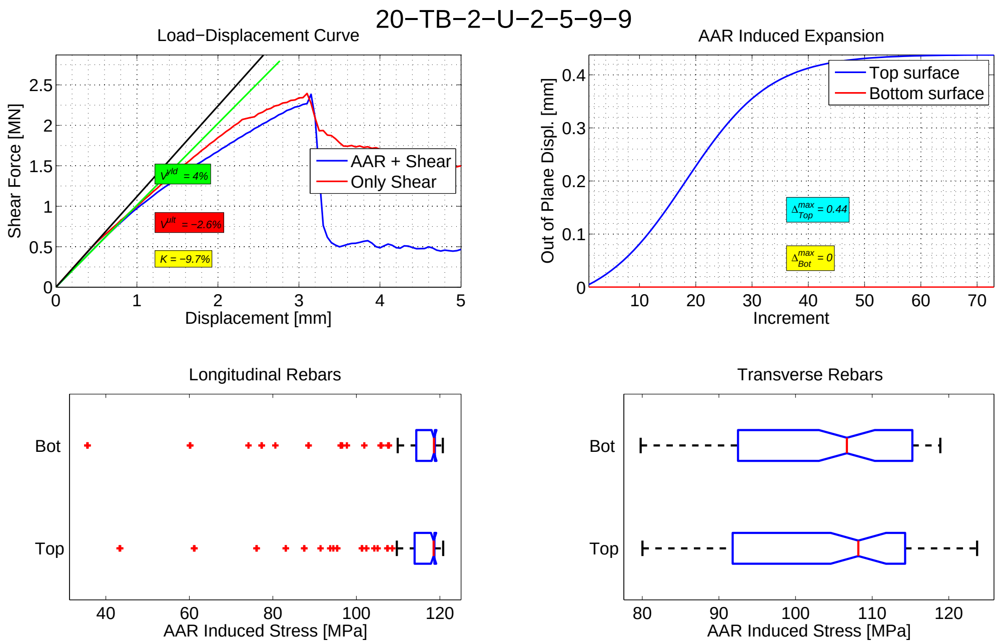

4.1.2.21 Analysis: 21-TB-2-U-2-10-7-7

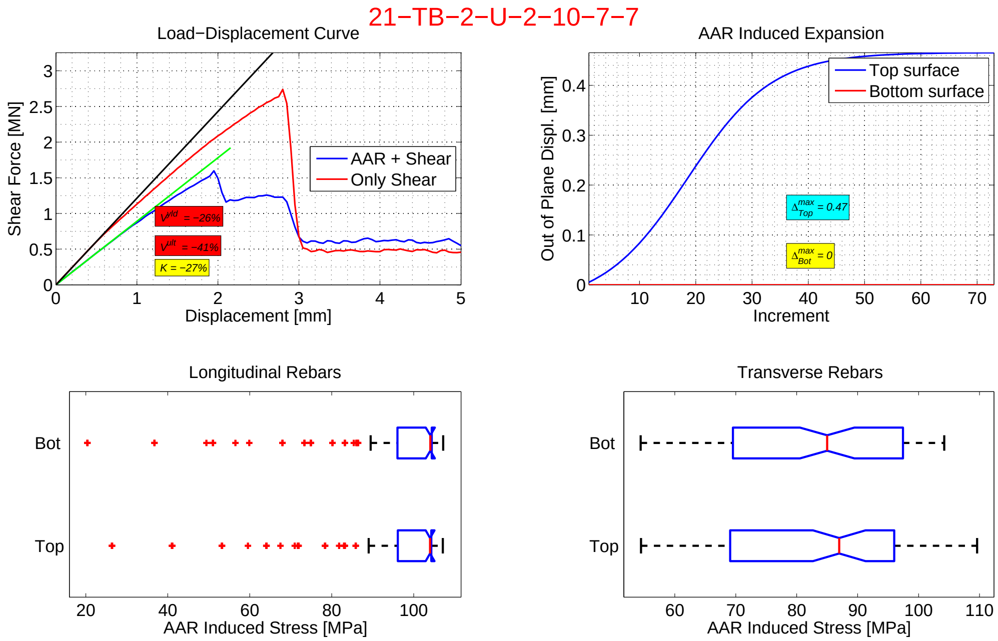

4.1.2.22 Analysis: 22-TB-2-U-2-10-7-9

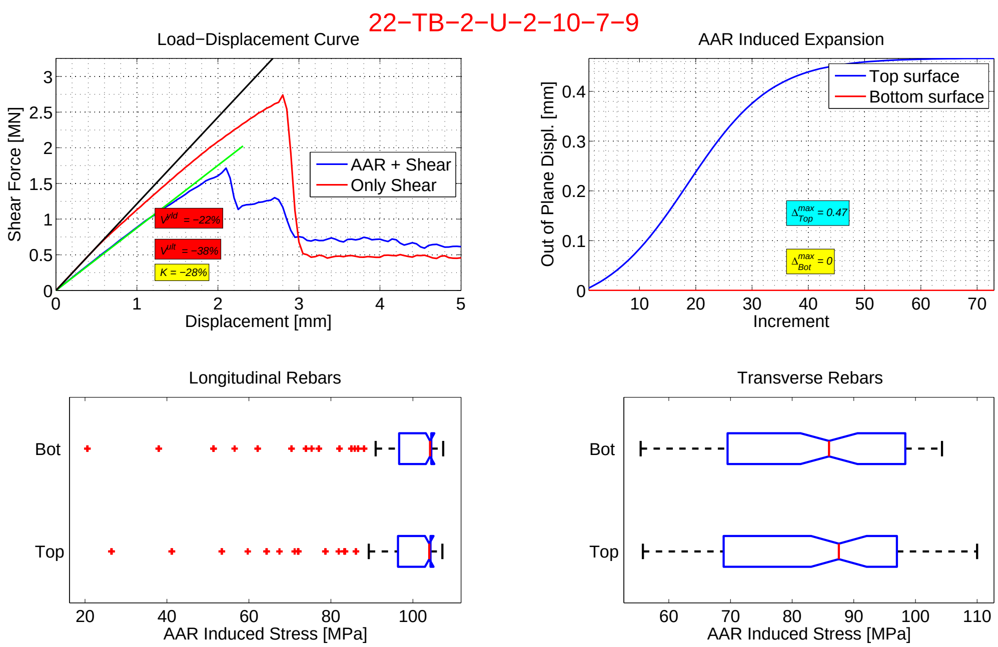

4.1.2.23 Analysis: 23-TB-2-U-2-10-9-7

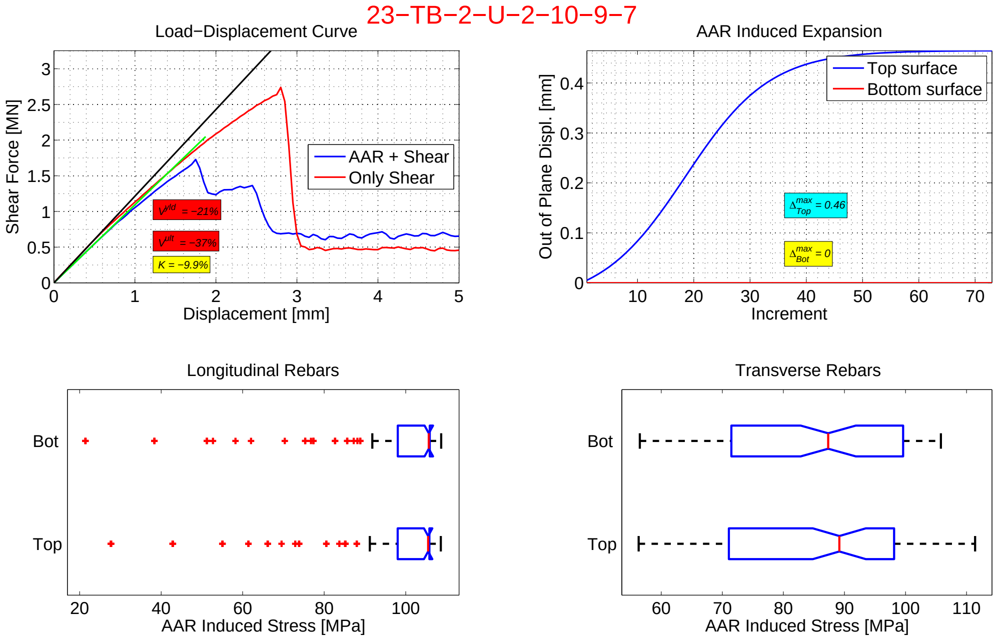

4.1.2.24 Analysis: 24-TB-2-U-2-10-9-9

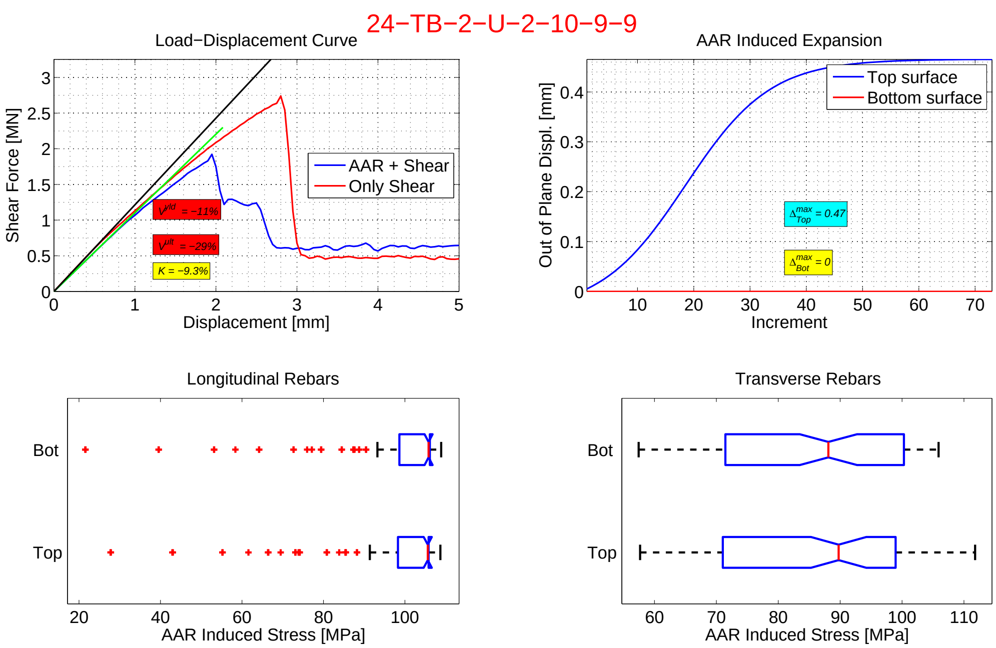

4.1.2.25 Analysis: 25-TB-2-U-3-2-7-7

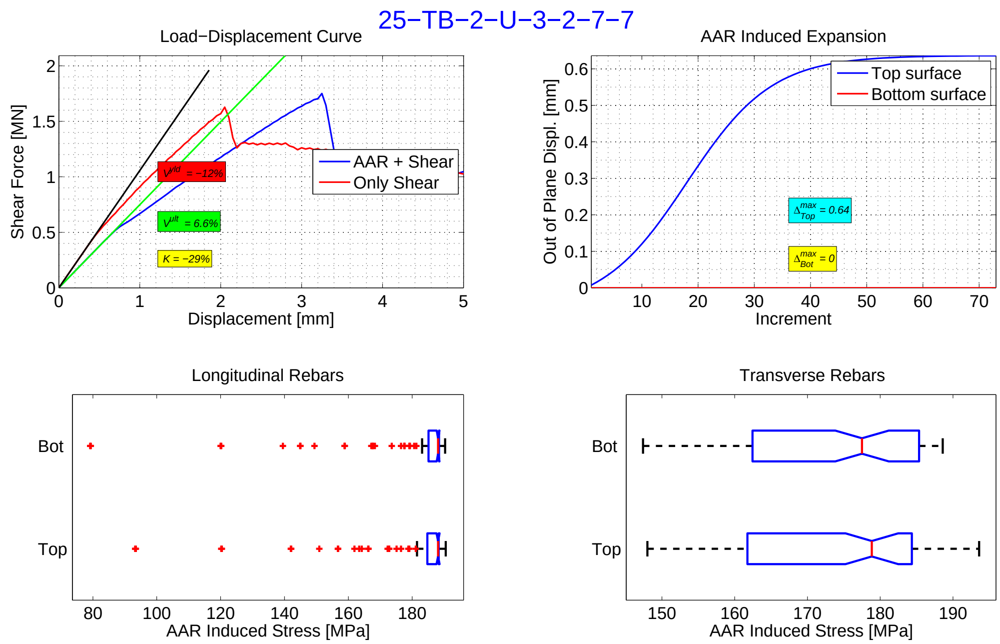

4.1.2.26 Analysis: 26-TB-2-U-3-2-7-9

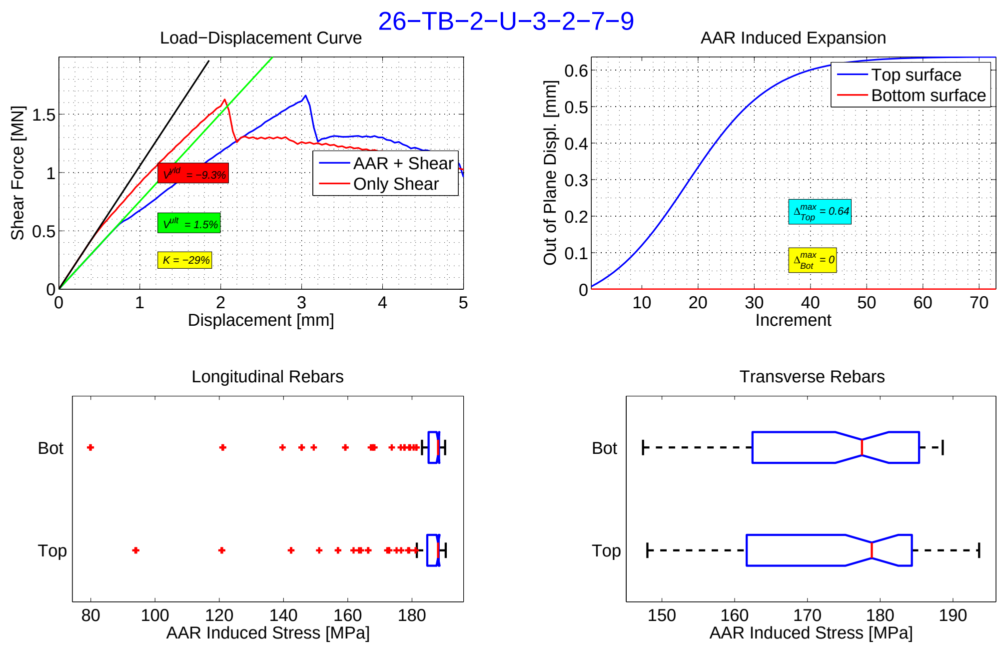

4.1.2.27 Analysis: 27-TB-2-U-3-2-9-7

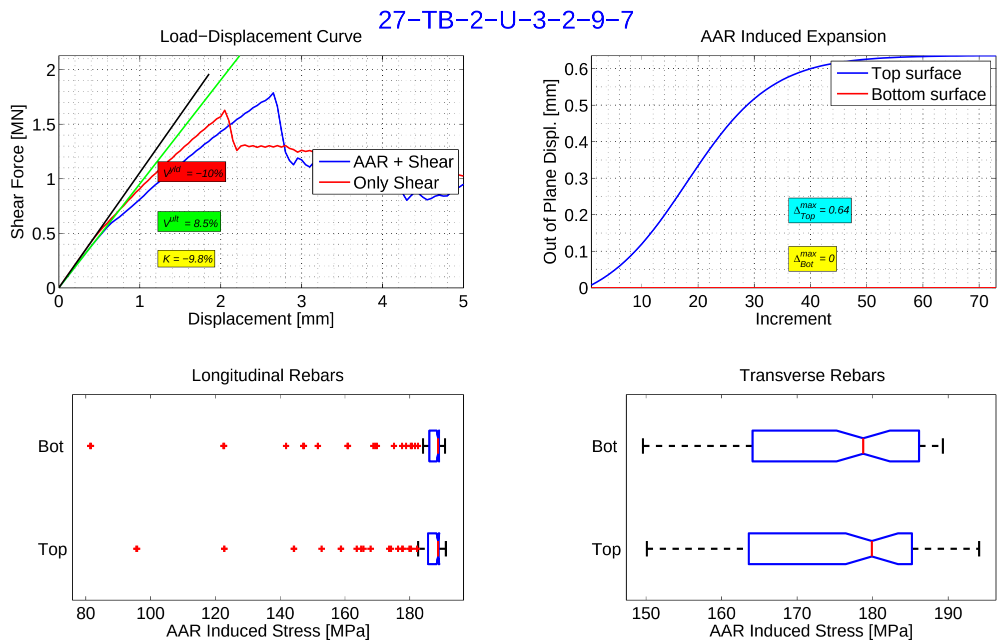

4.1.2.28 Analysis: 28-TB-2-U-3-2-9-9

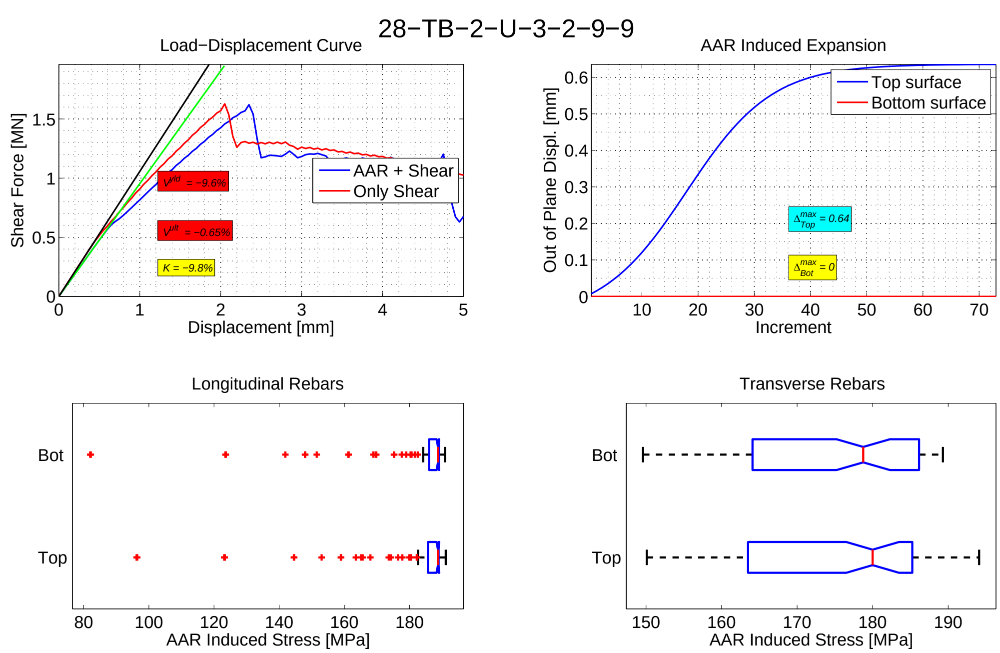

4.1.2.29 Analysis: 29-TB-2-U-3-5-7-7

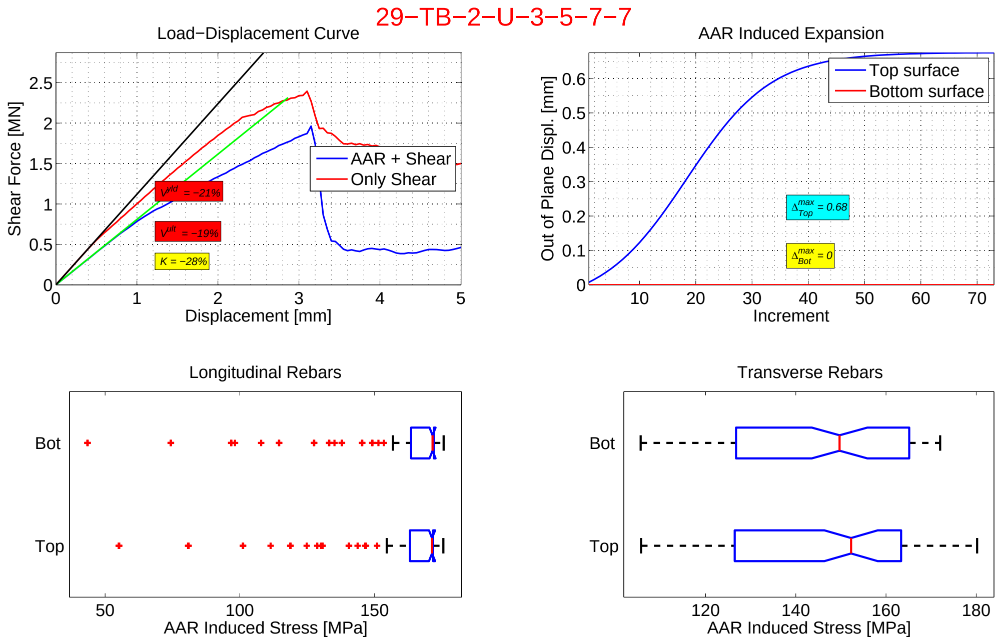

4.1.2.30 Analysis: 30-TB-2-U-3-5-7-9

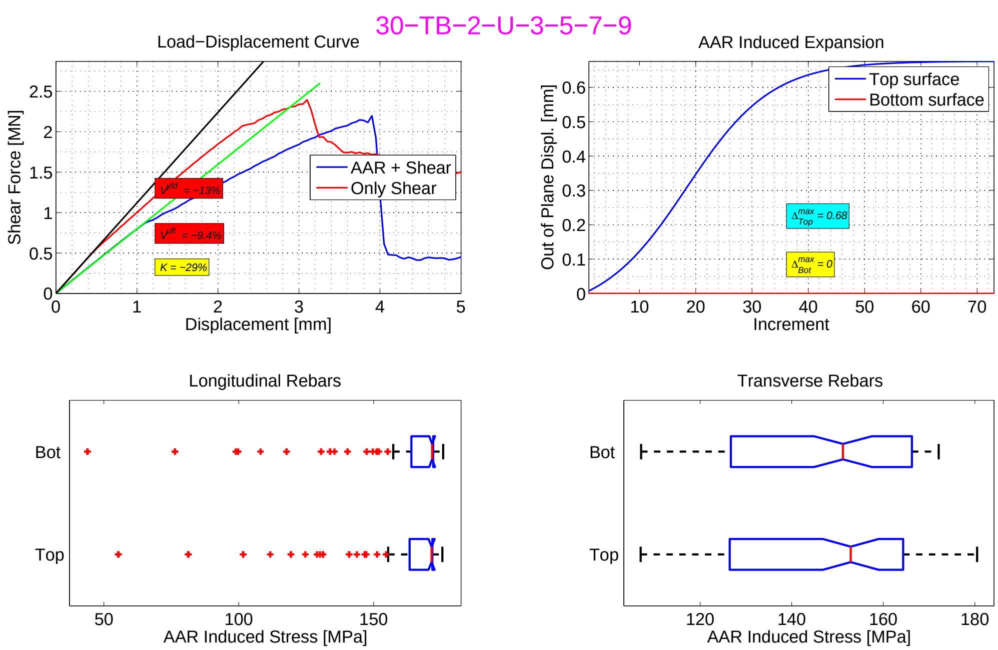

4.1.2.31 Analysis: 31-TB-2-U-3-5-9-7

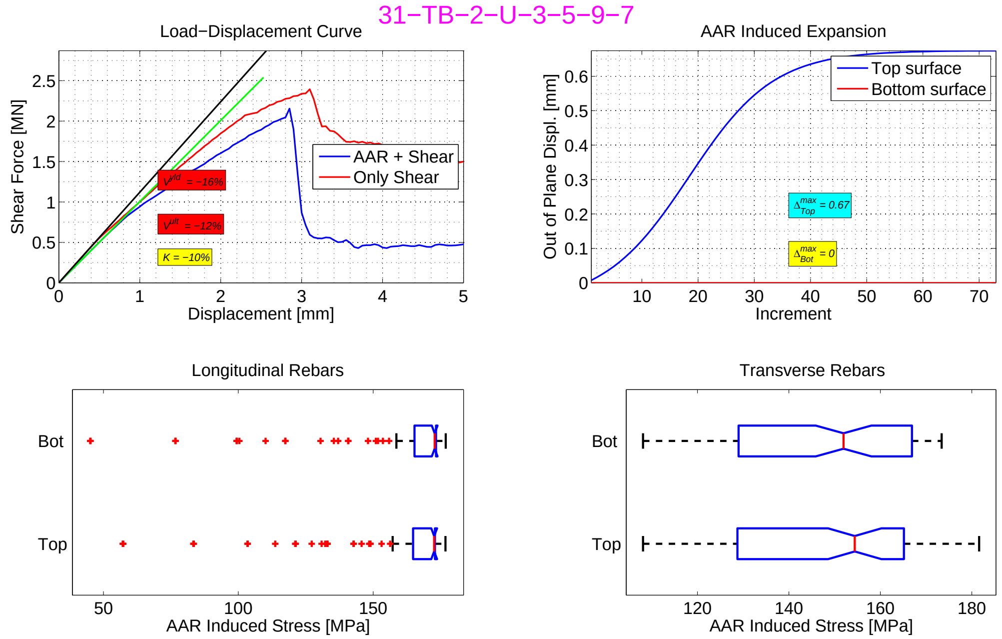

4.1.2.32 Analysis: 32-TB-2-U-3-5-9-9

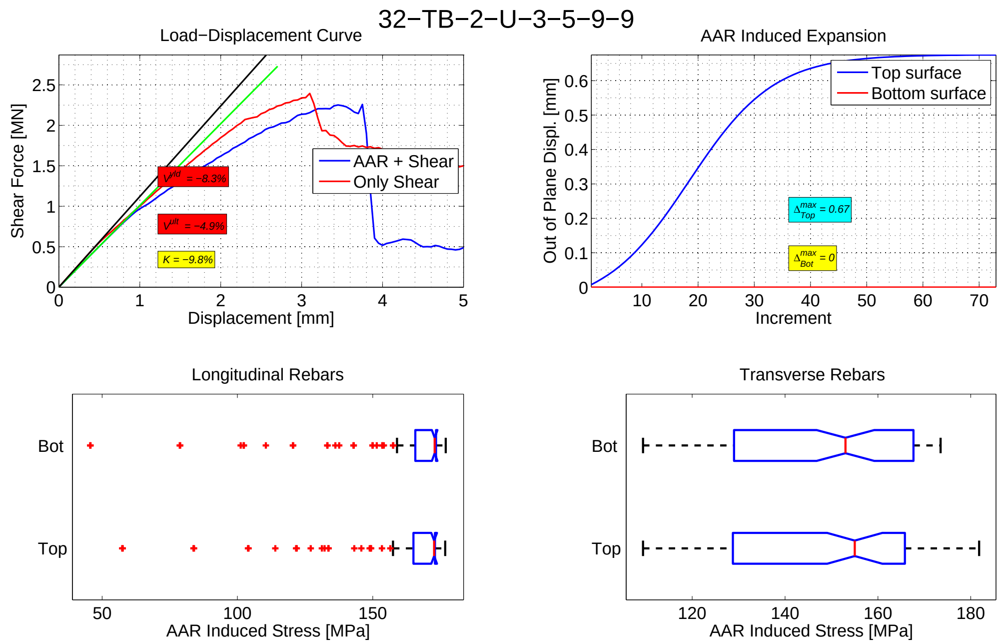

4.1.2.33 Analysis: 33-TB-2-U-3-10-7-7

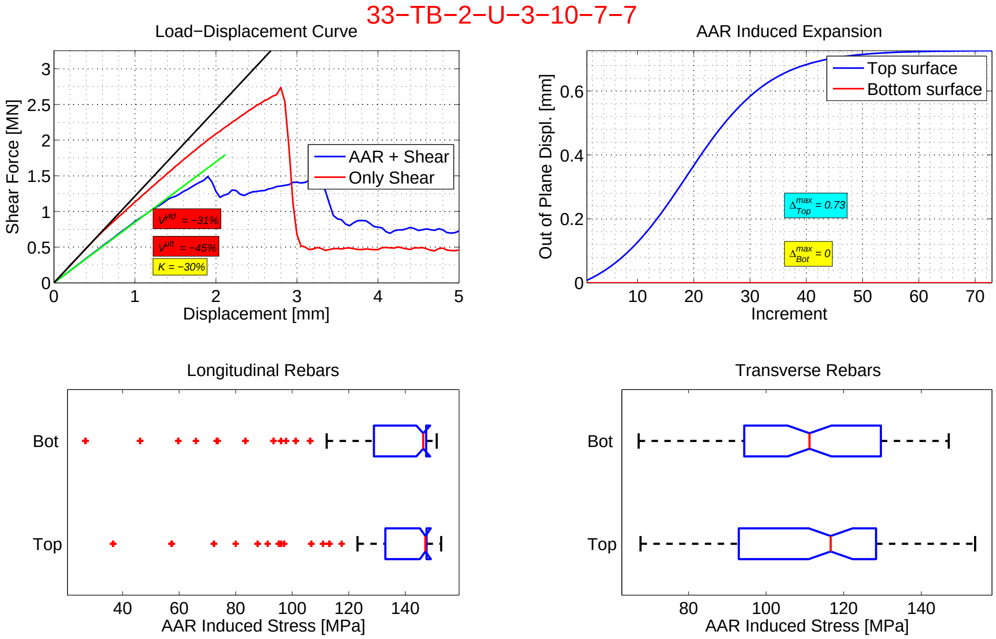

4.1.2.34 Analysis: 34-TB-2-U-3-10-7-9

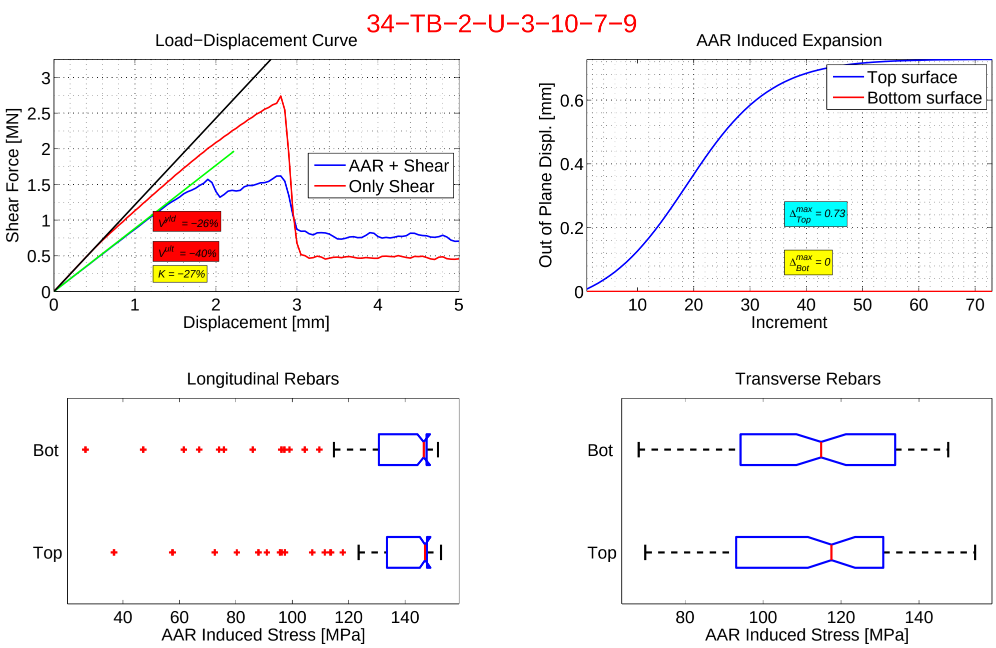

4.1.2.35 Analysis: 35-TB-2-U-3-10-9-7

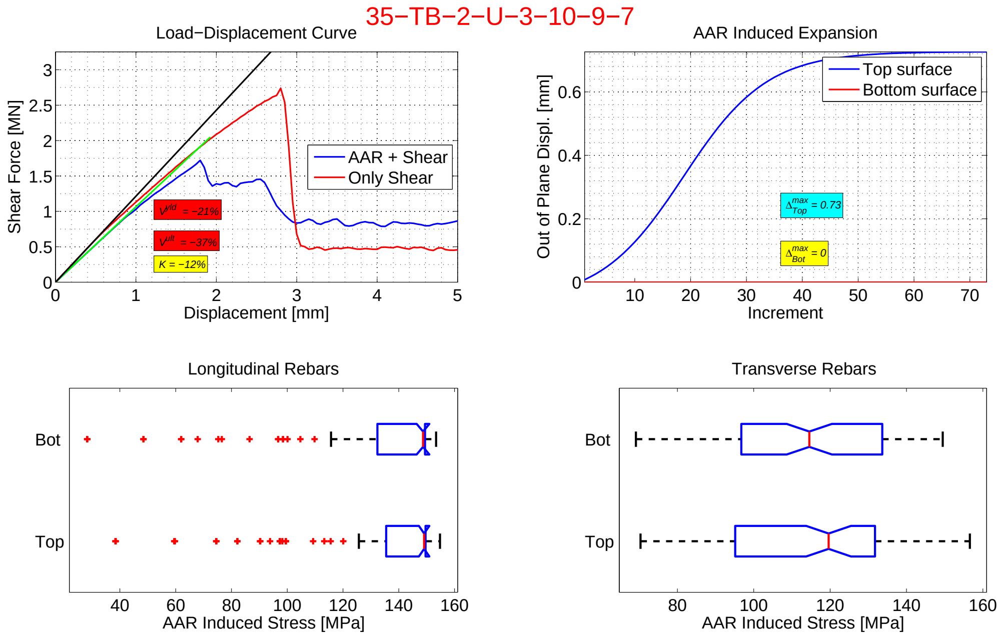

4.1.2.36 Analysis: 36-TB-2-U-3-10-9-9

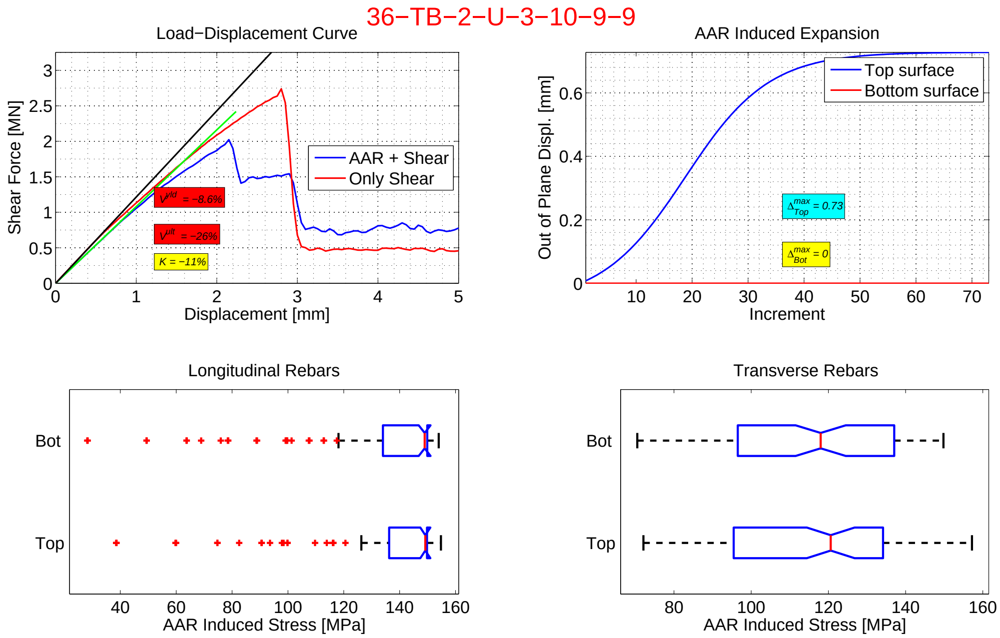

4.1.2.37 Analysis: 37-TB-4-U-1-2-7-7

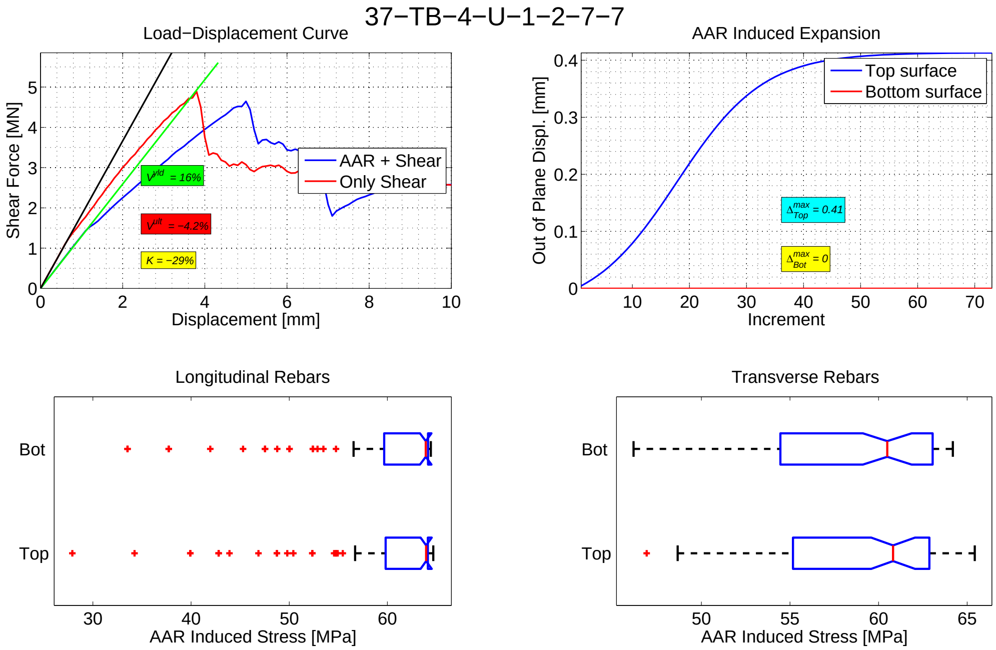

4.1.2.38 Analysis: 38-TB-4-U-1-2-7-9

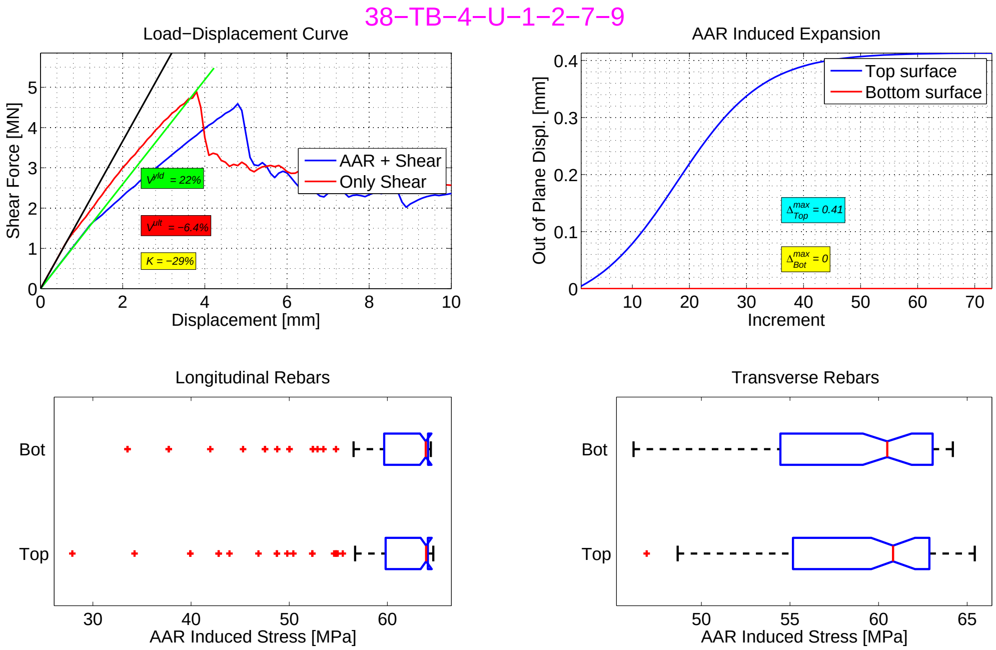

4.1.2.39 Analysis: 39-TB-4-U-1-2-9-7

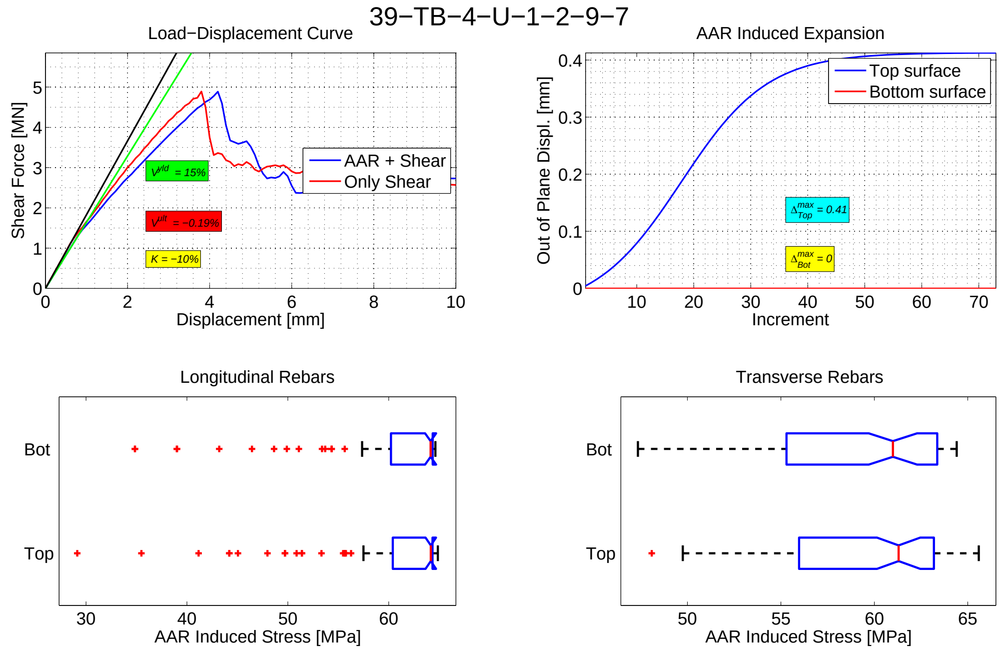

4.1.2.40 Analysis: 40-TB-4-U-1-2-9-9

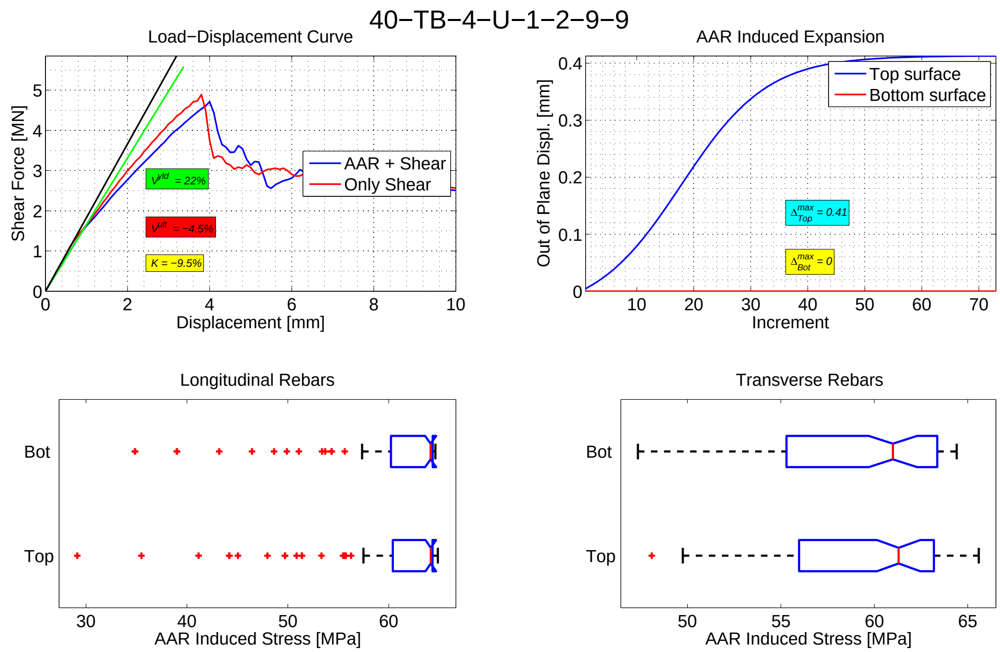

4.1.2.41 Analysis: 41-TB-4-U-1-5-7-7

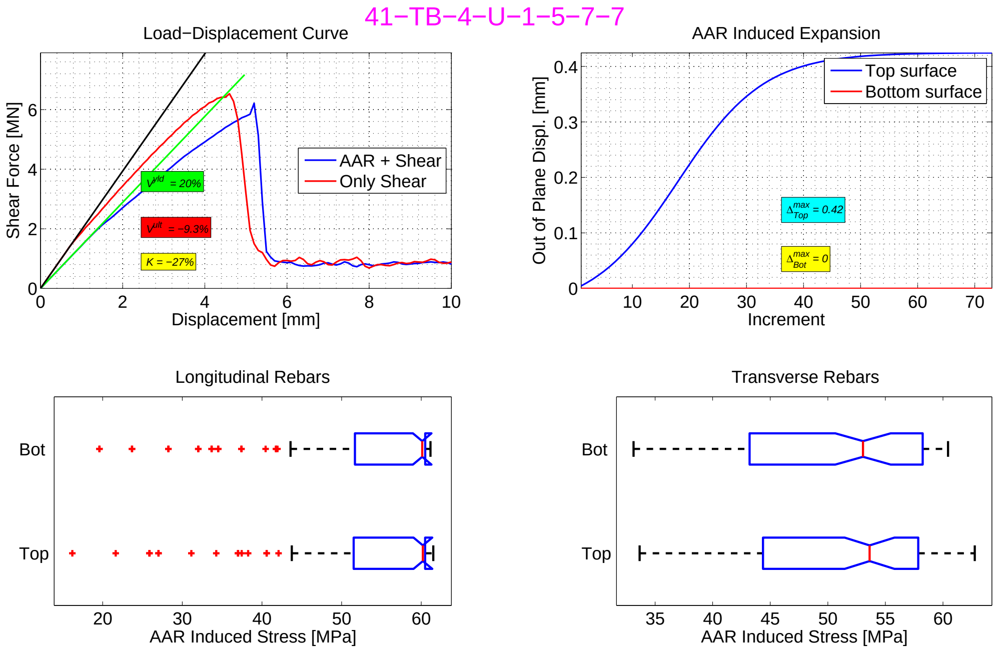

4.1.2.42 Analysis: 42-TB-4-U-1-5-7-9

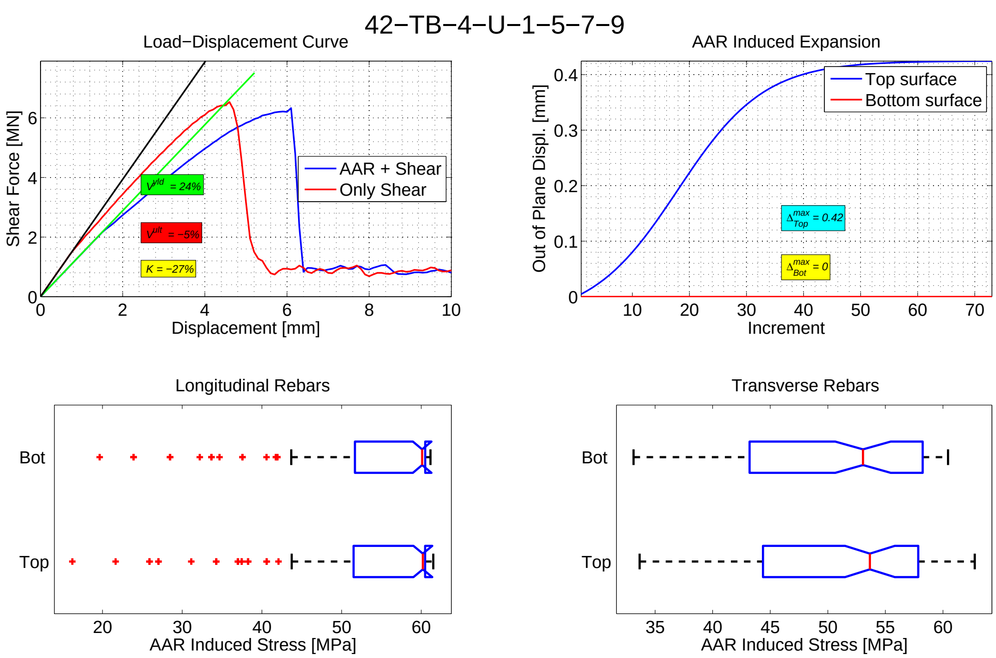

4.1.2.43 Analysis: 43-TB-4-U-1-5-9-7

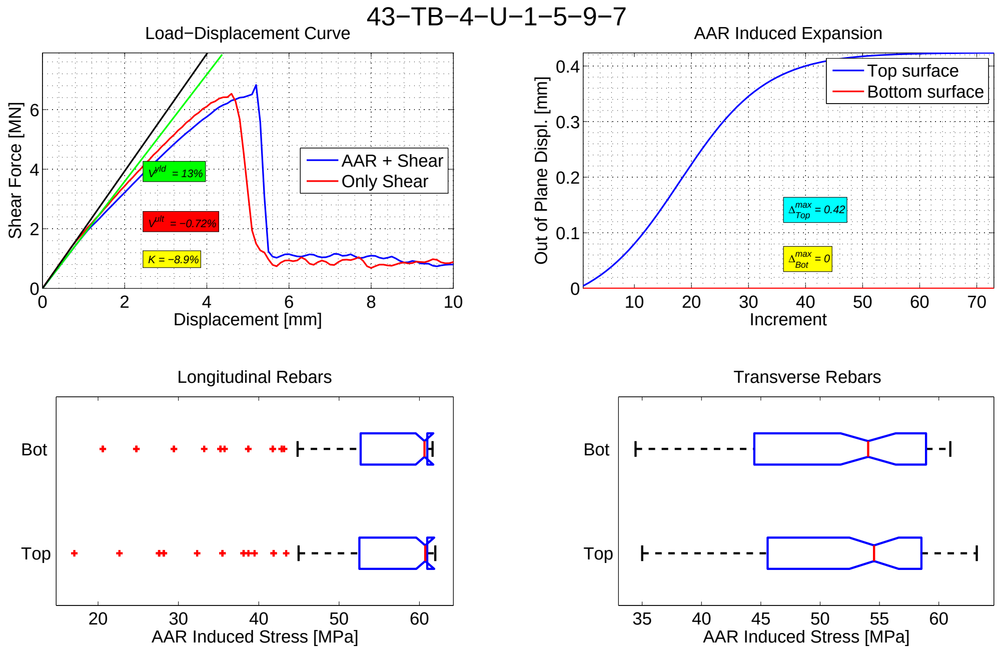

4.1.2.44 Analysis: 44-TB-4-U-1-5-9-9

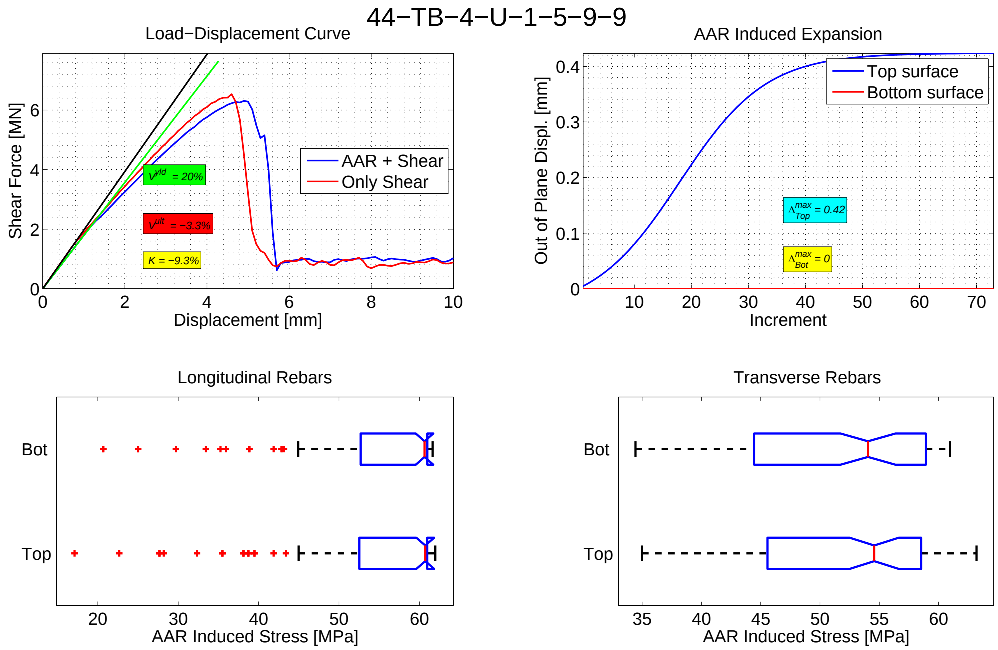

4.1.2.45 Analysis: 45-TB-4-U-1-10-7-7

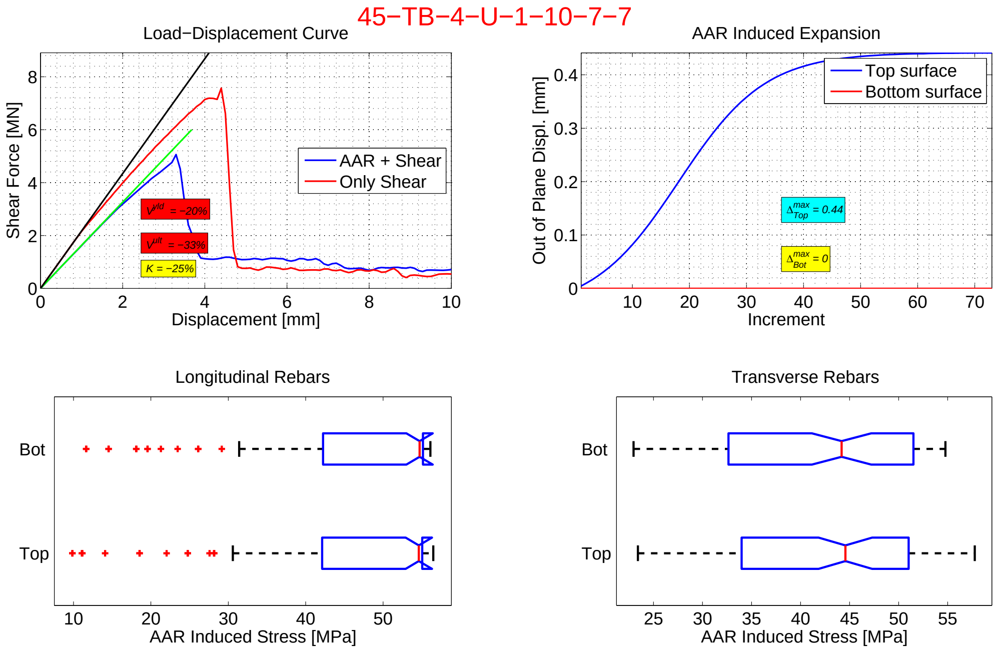

4.1.2.46 Analysis: 46-TB-4-U-1-10-7-9

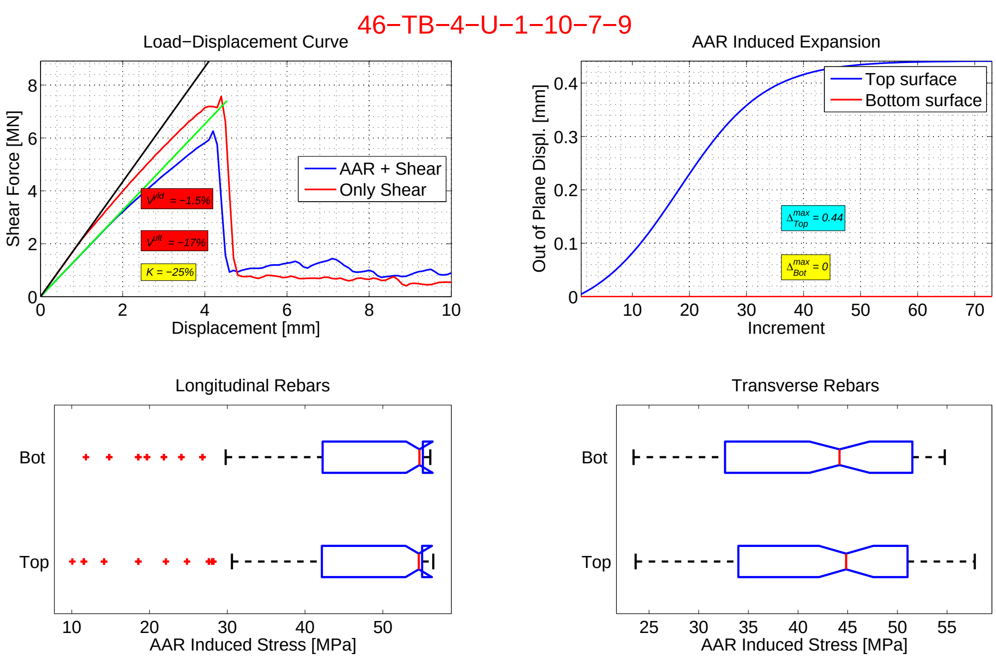

4.1.2.47 Analysis: 47-TB-4-U-1-10-9-7

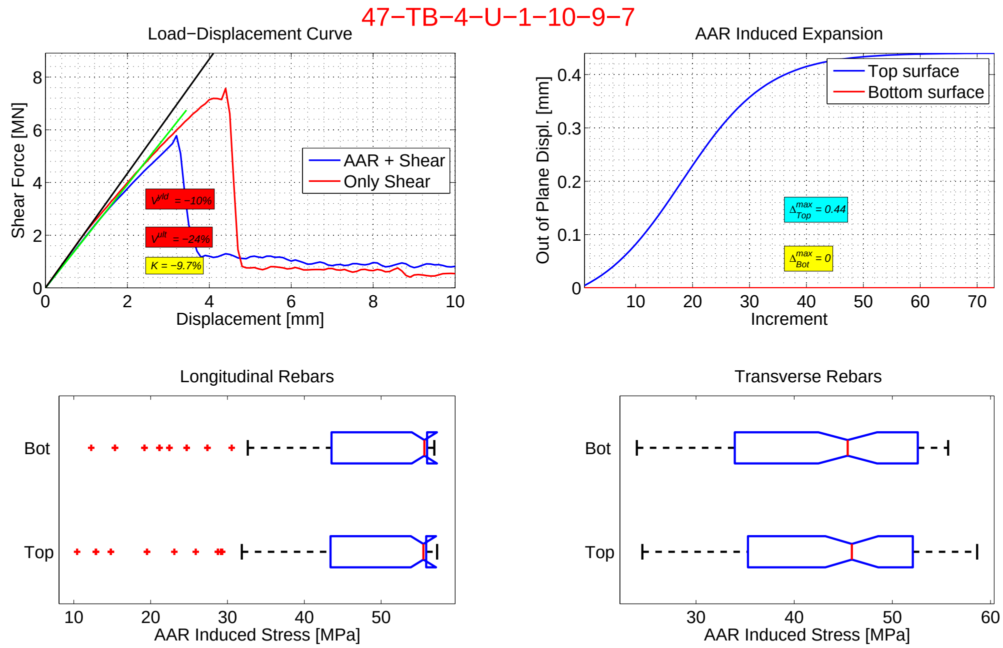

4.1.2.48 Analysis: 48-TB-4-U-1-10-9-9

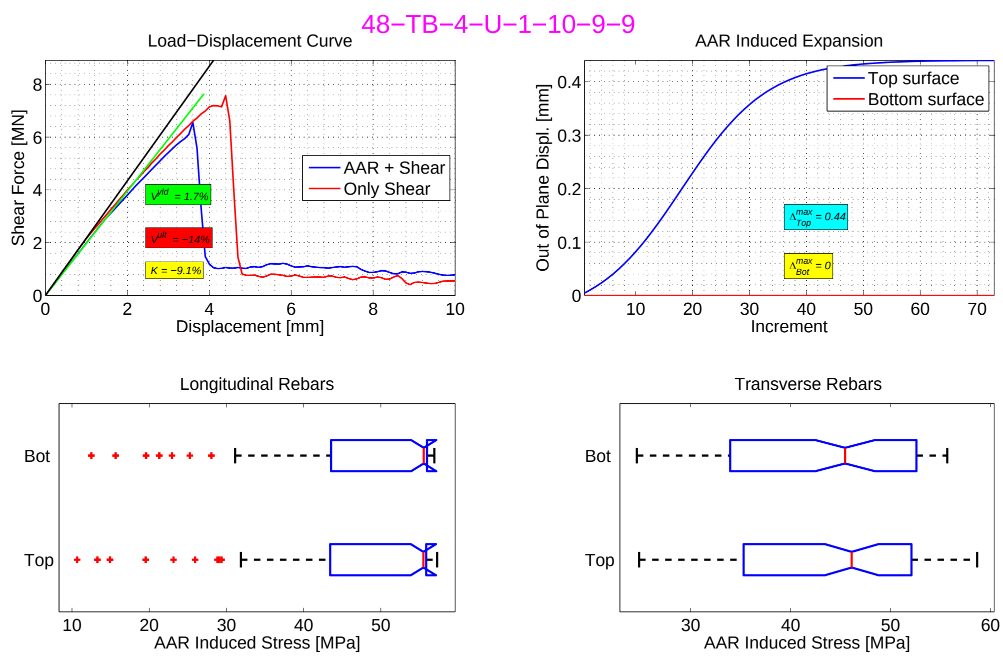

4.1.2.49 Analysis: 49-TB-4-U-2-2-7-7

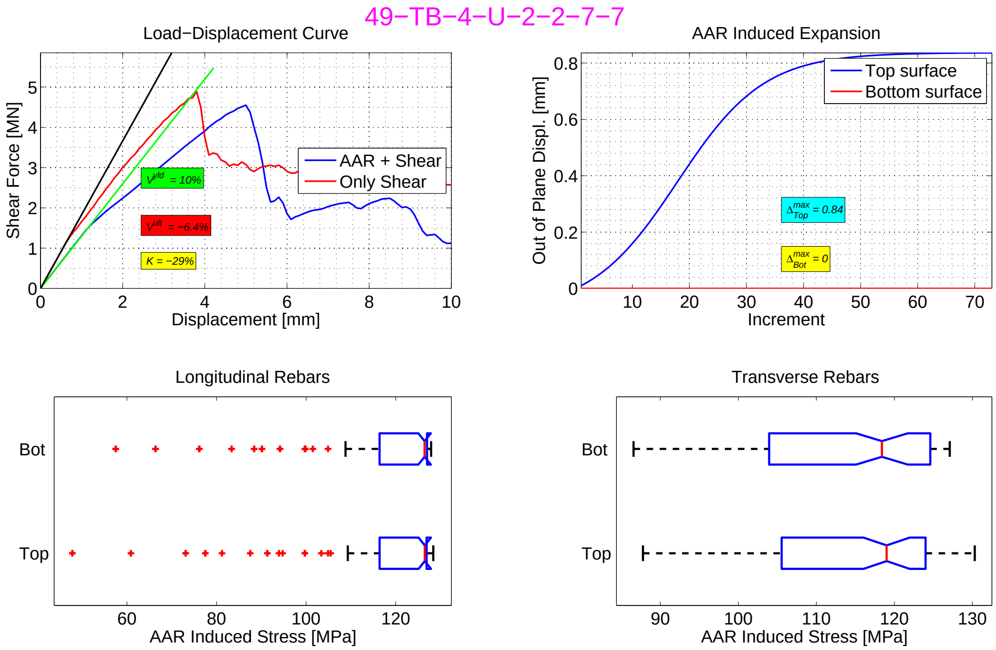

4.1.2.50 Analysis: 50-TB-4-U-2-2-7-9

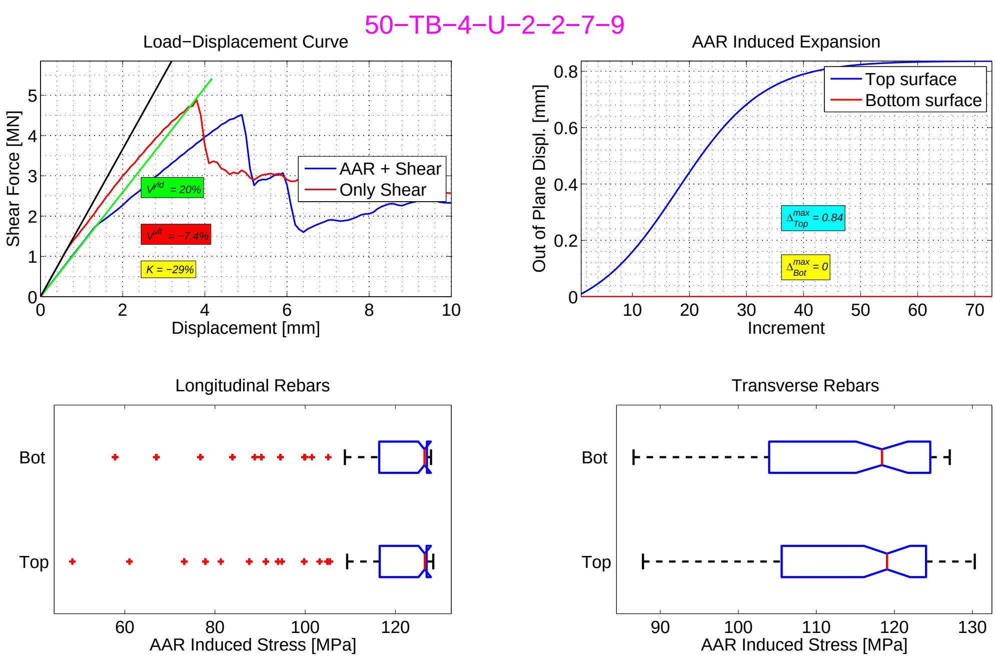

4.1.2.51 Analysis: 51-TB-4-U-2-2-9-7

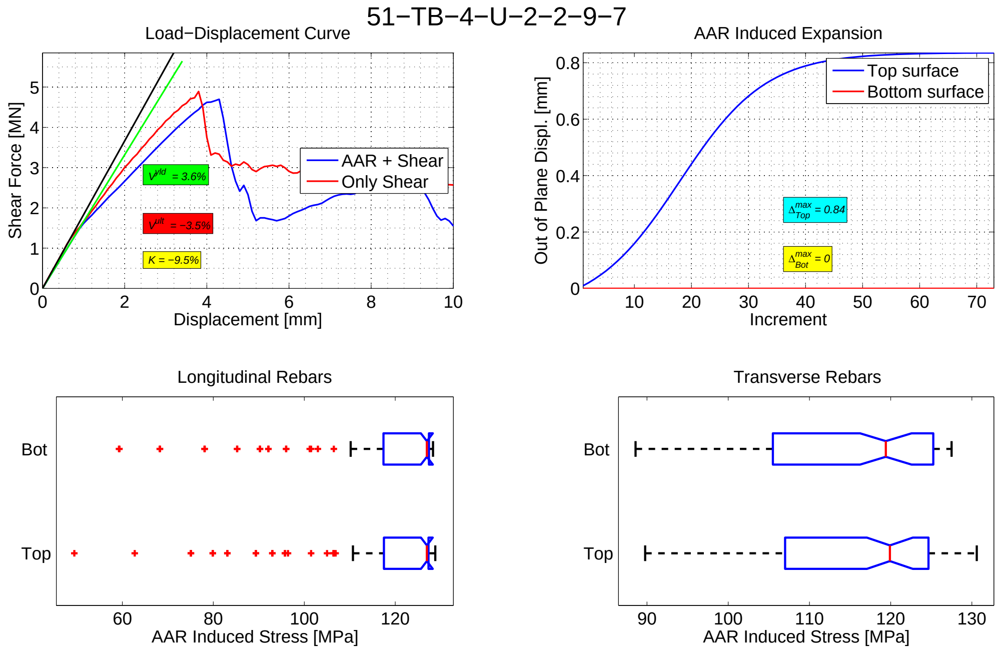

4.1.2.52 Analysis: 52-TB-4-U-2-2-9-9

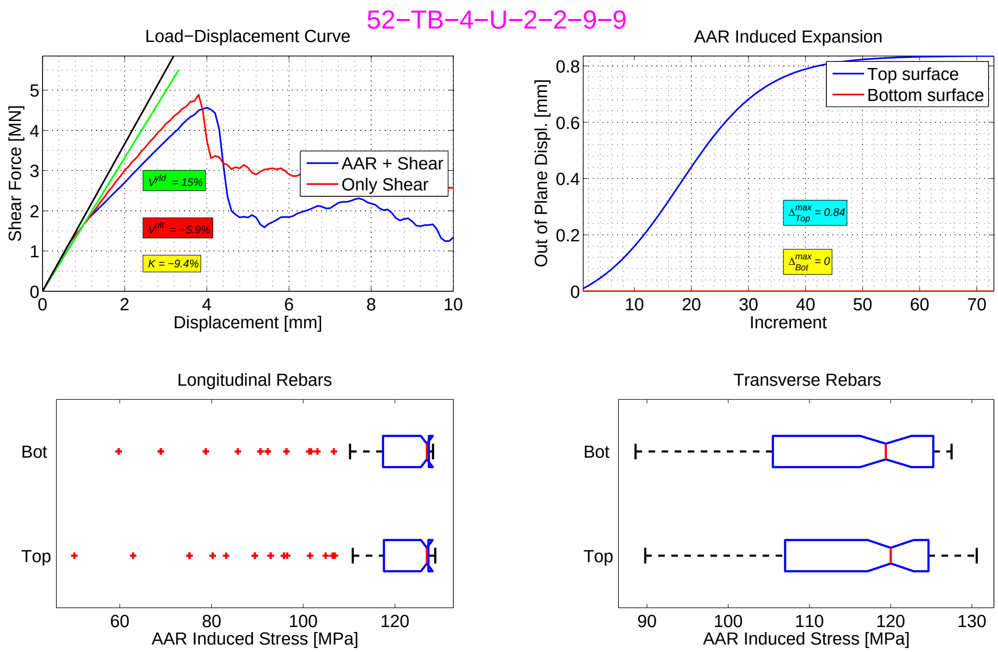

4.1.2.53 Analysis: 53-TB-4-U-2-5-7-7

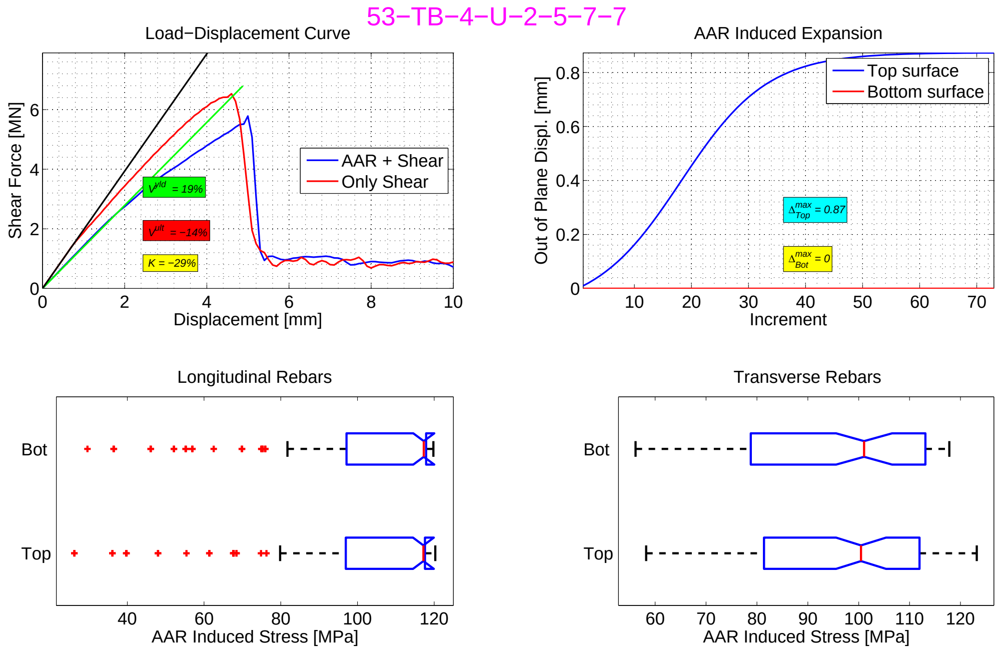

4.1.2.54 Analysis: 54-TB-4-U-2-5-7-9

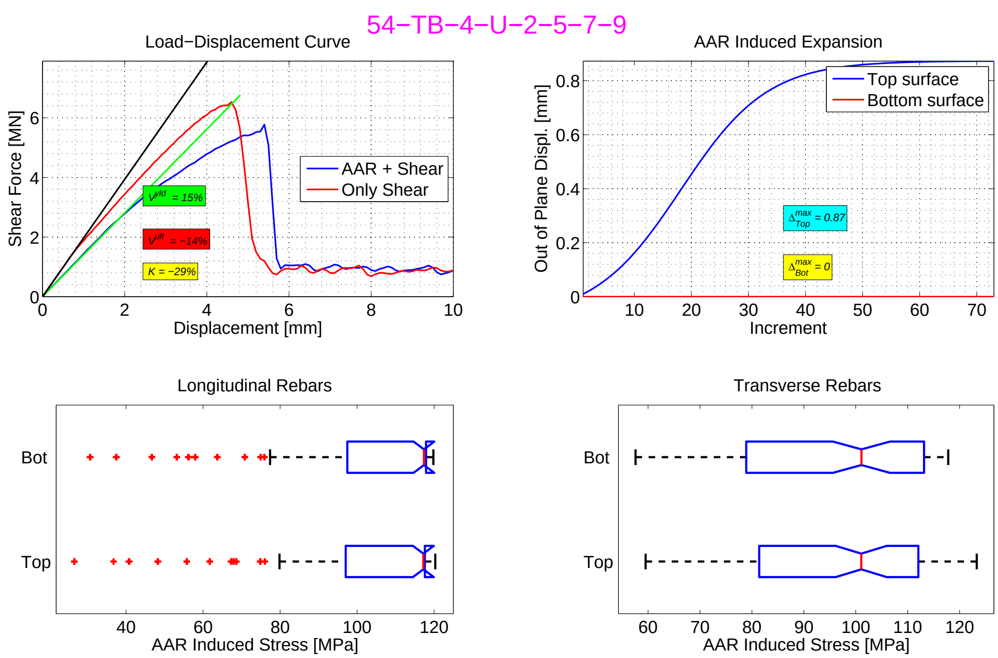

4.1.2.55 Analysis: 55-TB-4-U-2-5-9-7

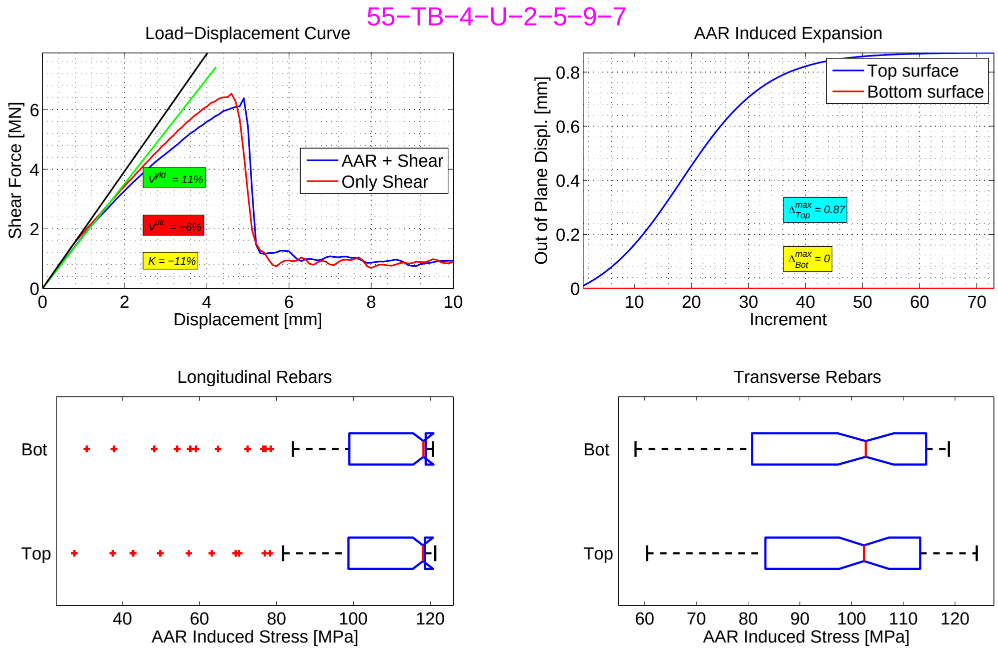

4.1.2.56 Analysis: 56-TB-4-U-2-5-9-9

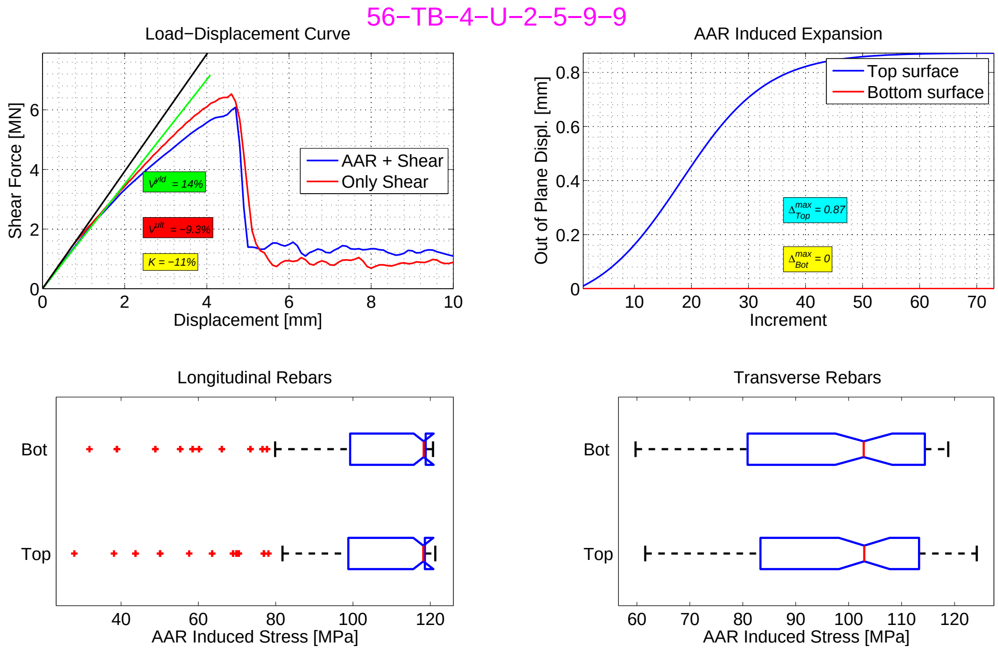

4.1.2.57 Analysis: 57-TB-4-U-2-10-7-7

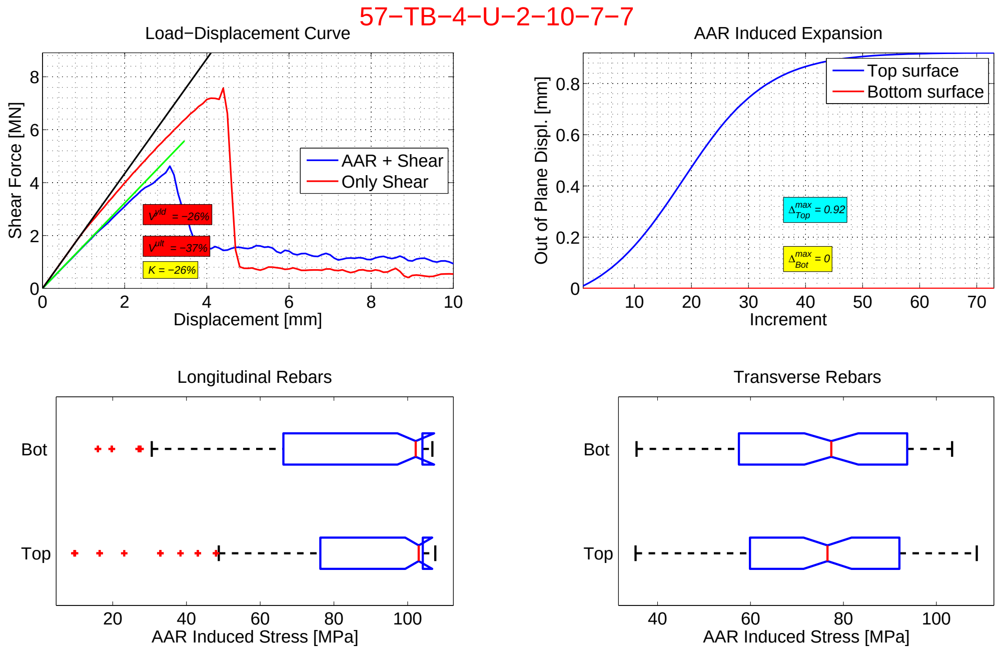

4.1.2.58 Analysis: 58-TB-4-U-2-10-7-9

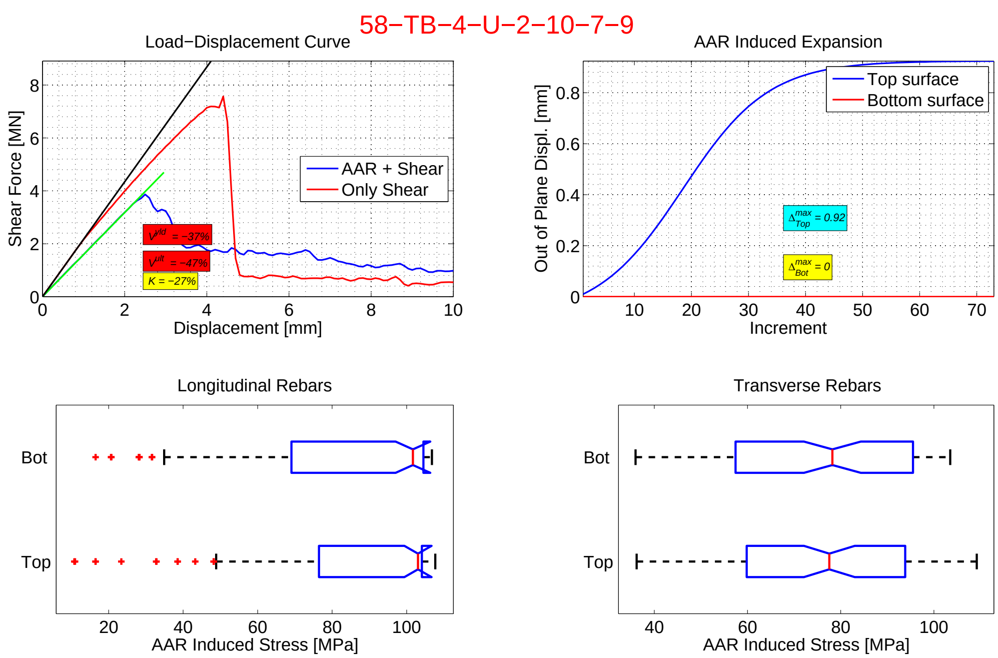

4.1.2.59 Analysis: 59-TB-4-U-2-10-9-7

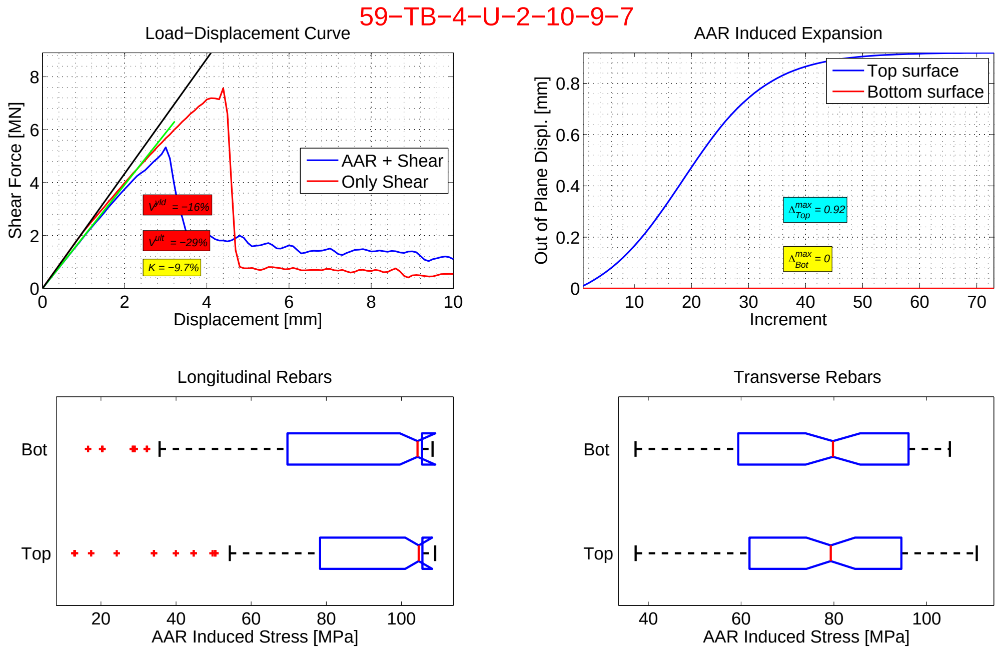

4.1.2.60 Analysis: 60-TB-4-U-2-10-9-9

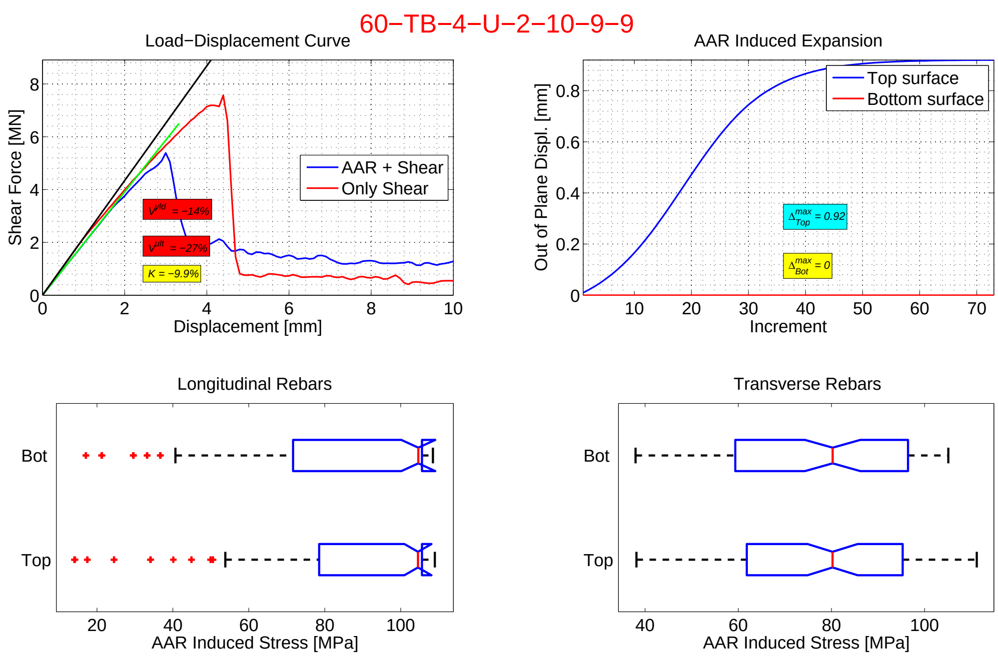

4.1.2.61 Analysis: 61-TB-4-U-3-2-7-7

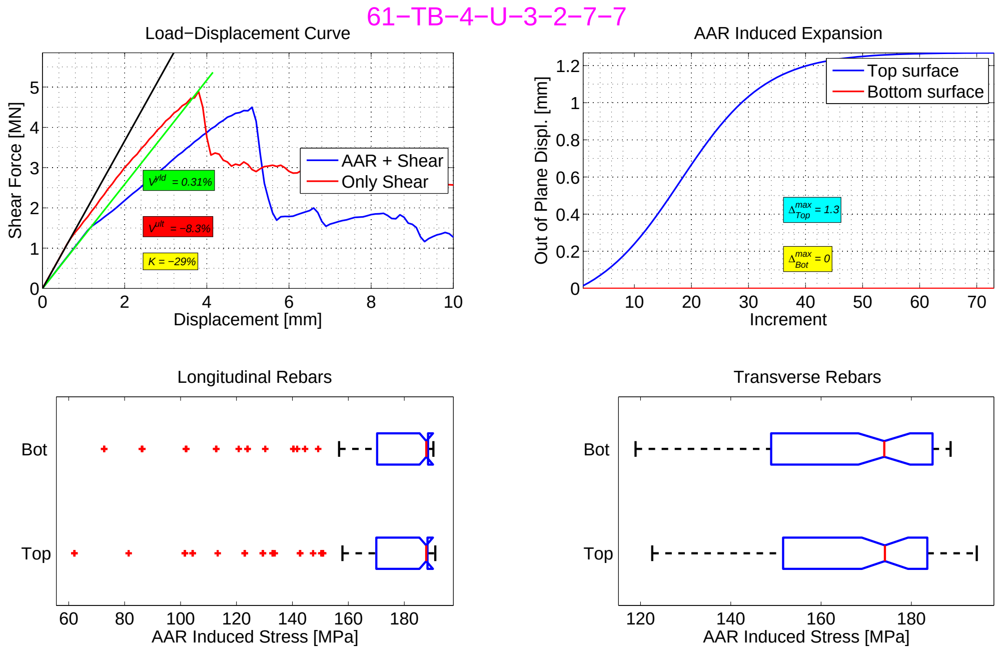

4.1.2.62 Analysis: 62-TB-4-U-3-2-7-9

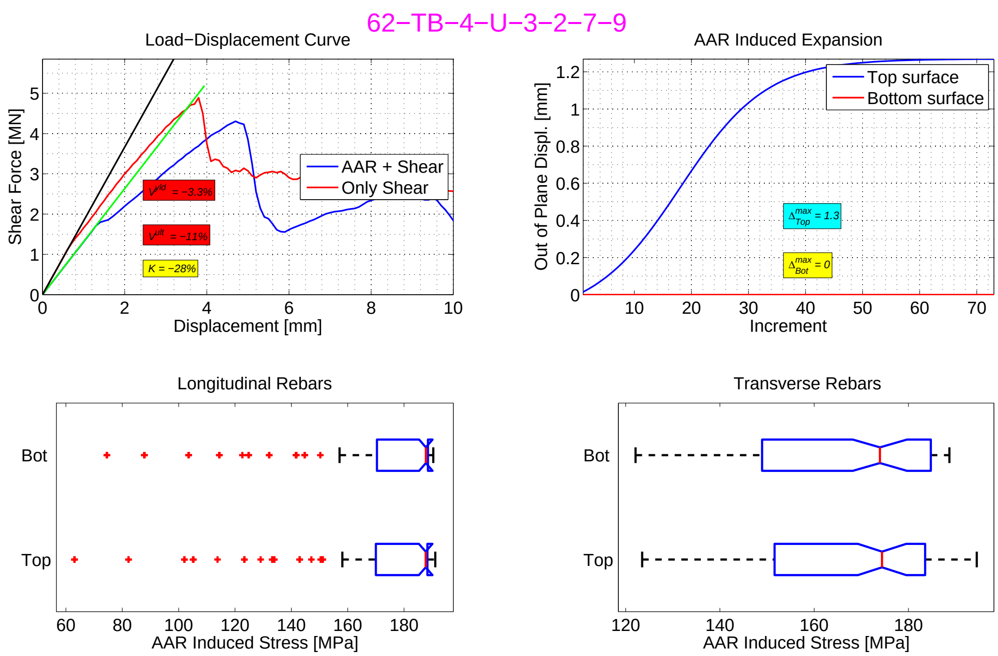

4.1.2.63 Analysis: 63-TB-4-U-3-2-9-7

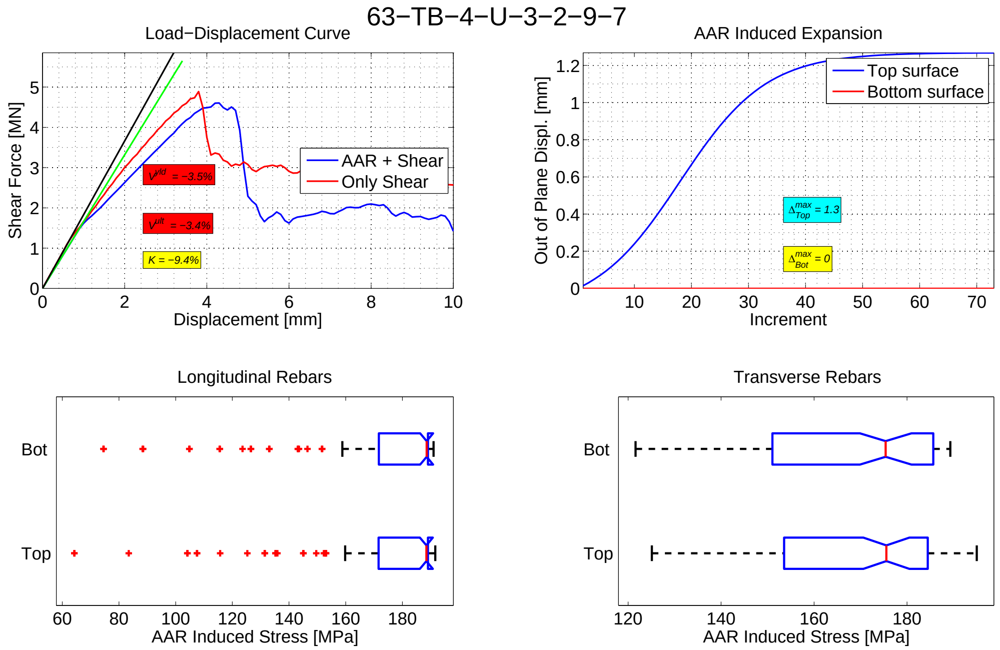

4.1.2.64 Analysis: 64-TB-4-U-3-2-9-9

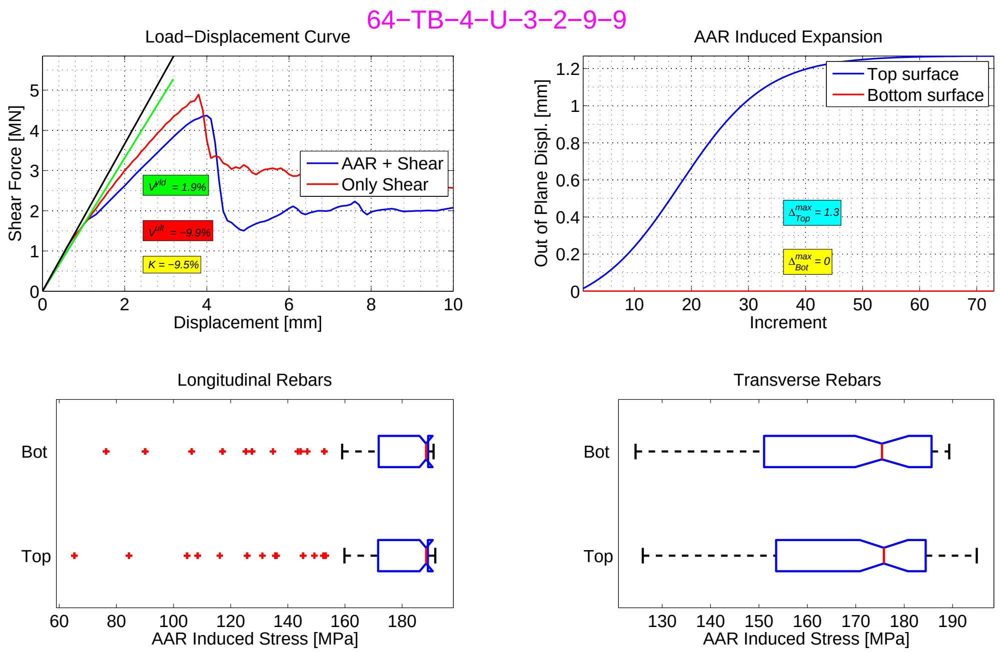

4.1.2.65 Analysis: 65-TB-4-U-3-5-7-7

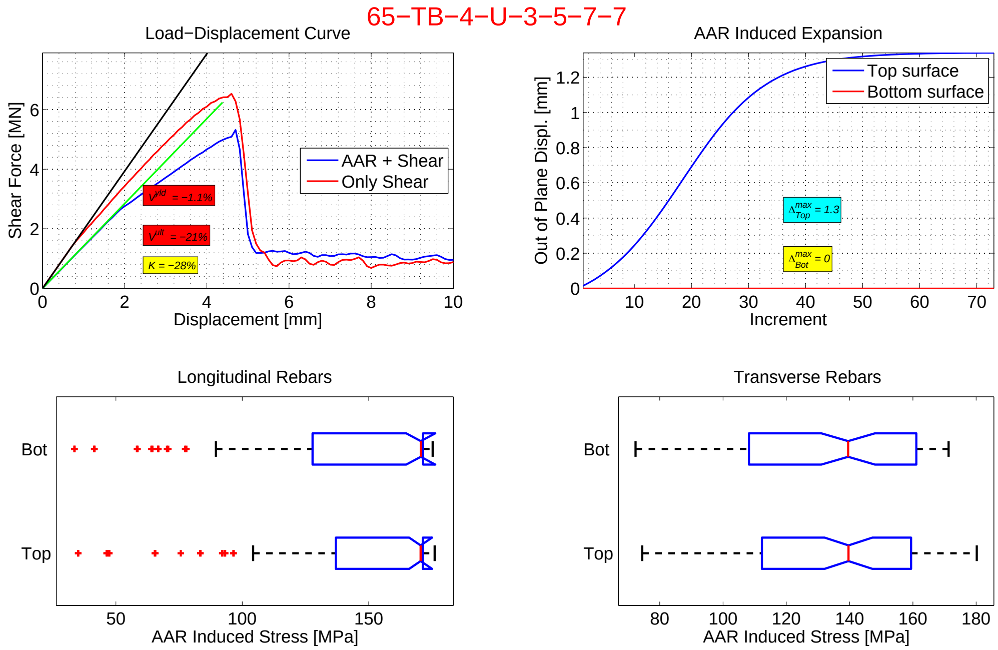

4.1.2.66 Analysis: 66-TB-4-U-3-5-7-9

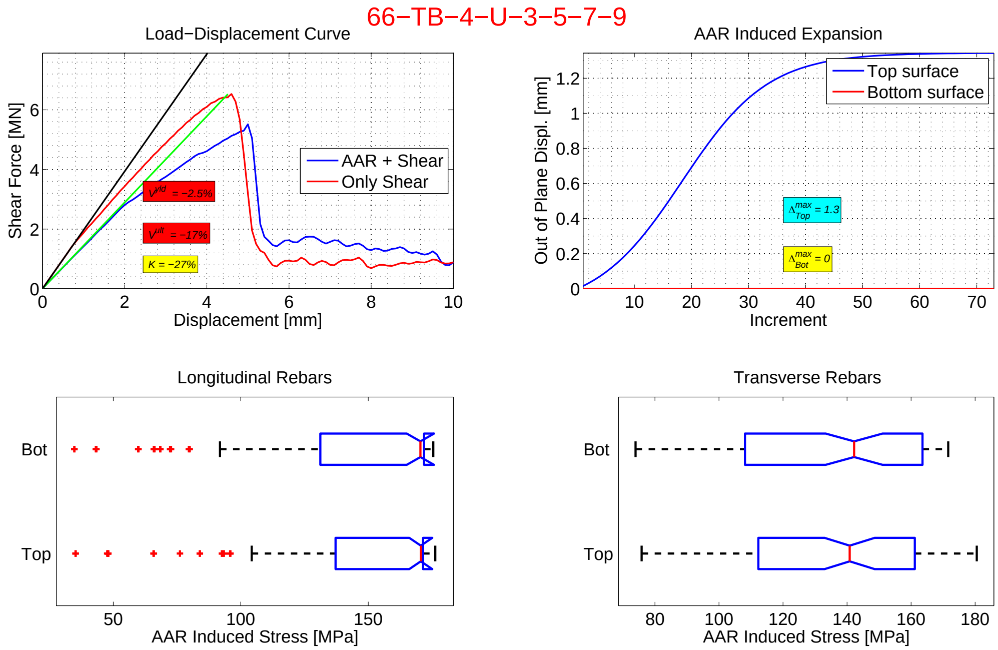

4.1.2.67 Analysis: 67-TB-4-U-3-5-9-7

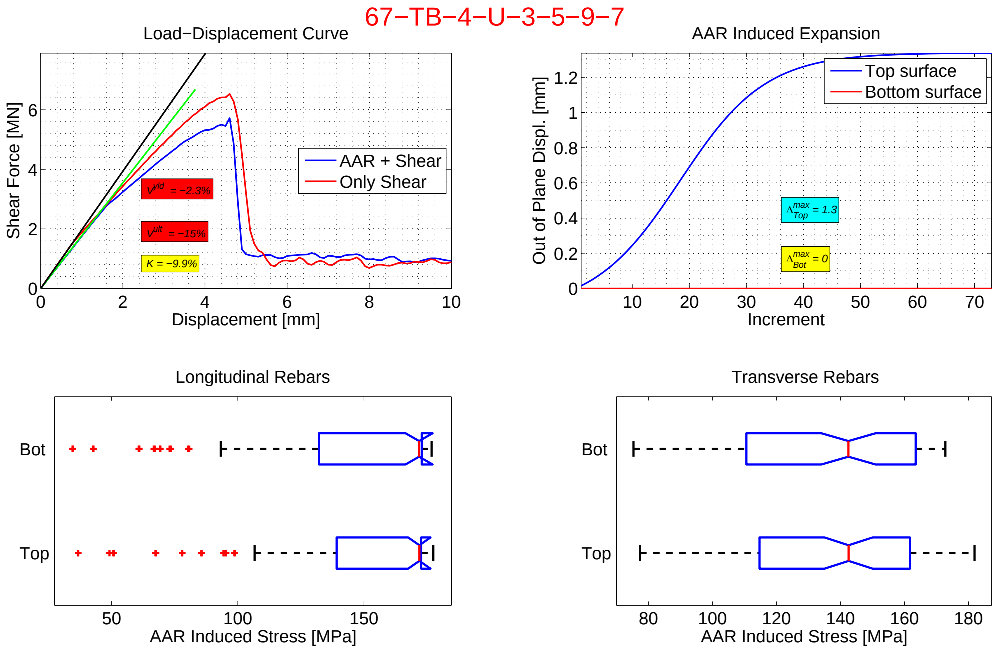

4.1.2.68 Analysis: 68-TB-4-U-3-5-9-9

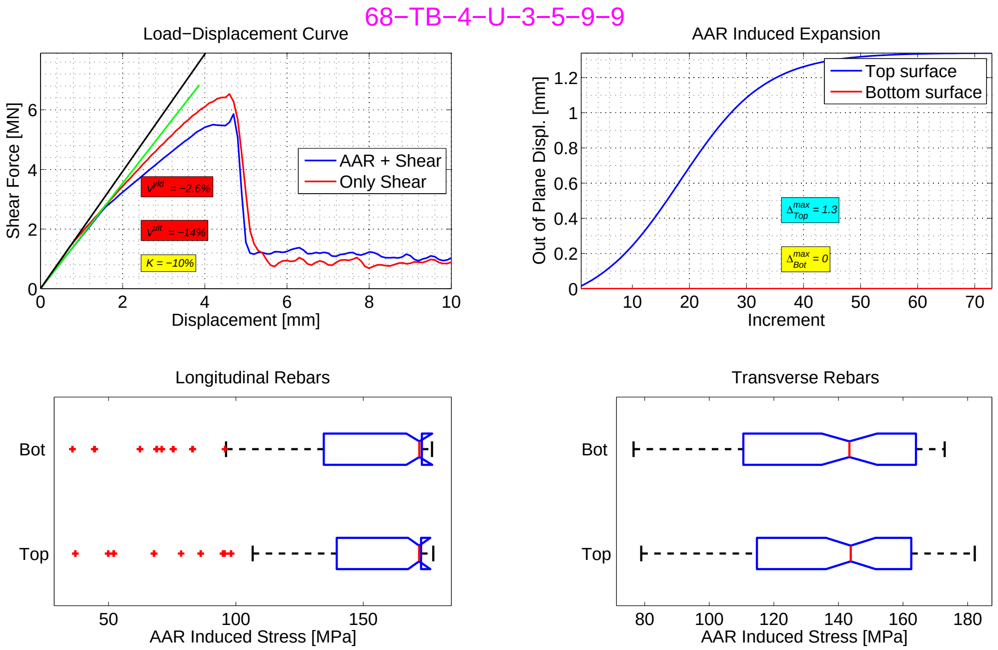

4.1.2.69 Analysis: 69-TB-4-U-3-10-7-7

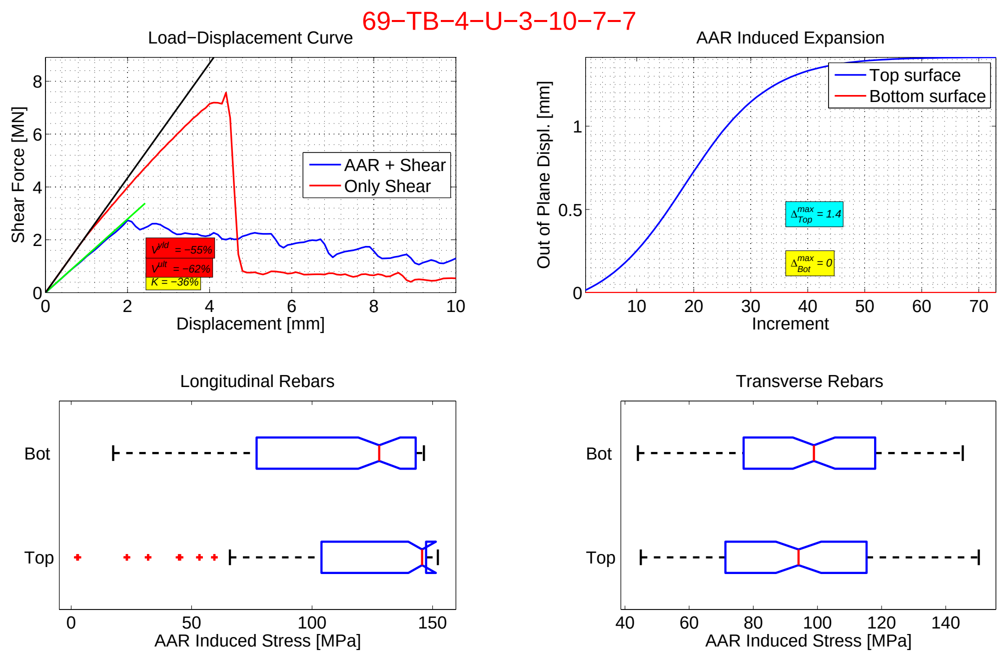

4.1.2.70 Analysis: 70-TB-4-U-3-10-7-9

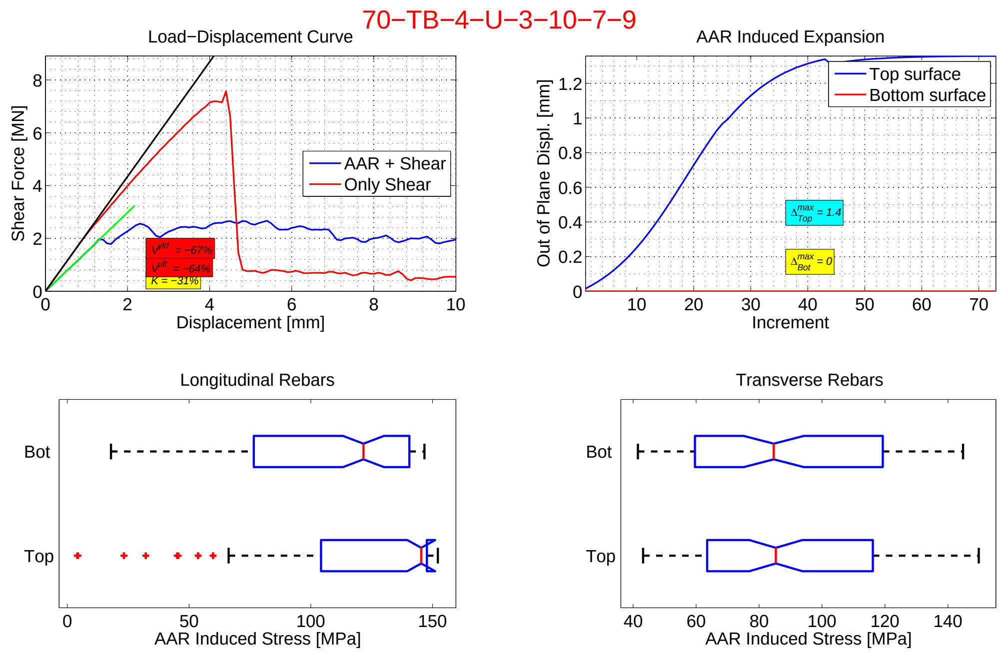

4.1.2.71 Analysis: 71-TB-4-U-3-10-9-7

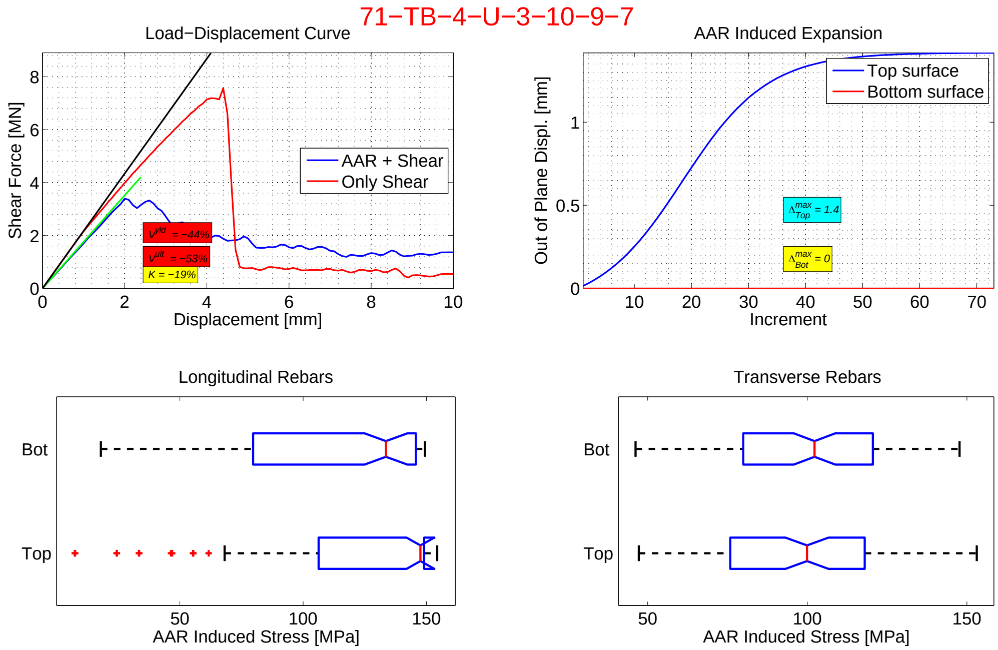

4.1.2.72 Analysis: 72-TB-4-U-3-10-9-9

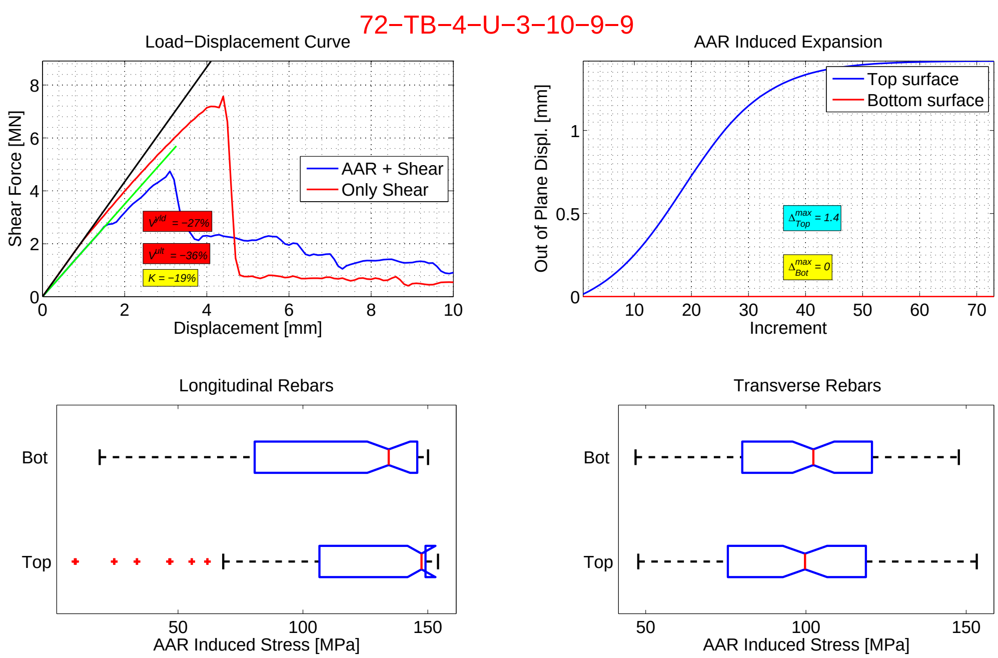

4.1.2.73 Analysis: 73-TB-2-R-1-2-7-7

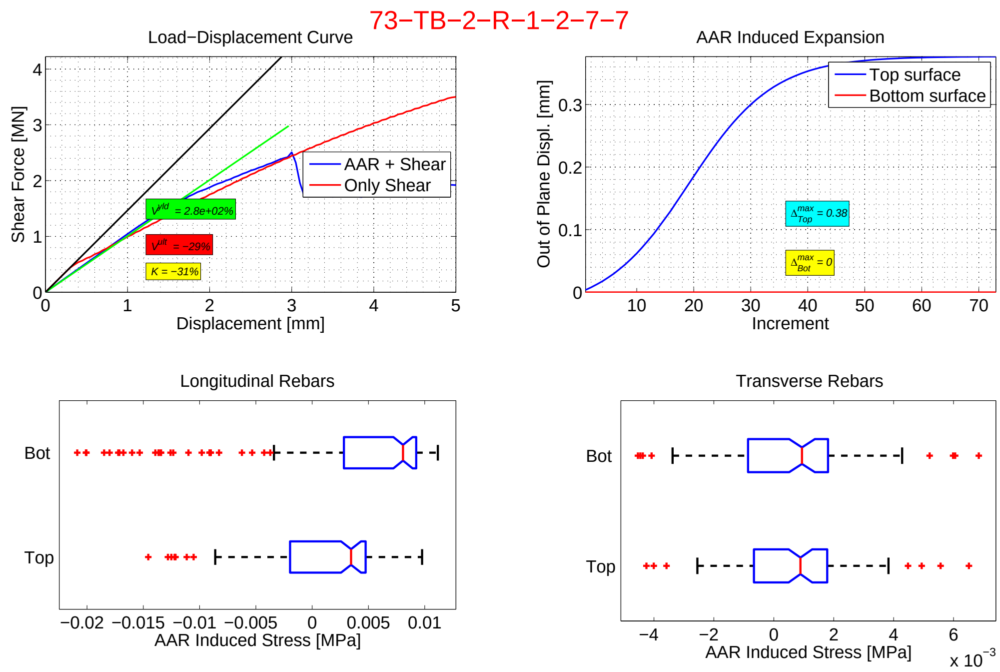

4.1.2.74 Analysis: 74-TB-2-R-1-2-7-9

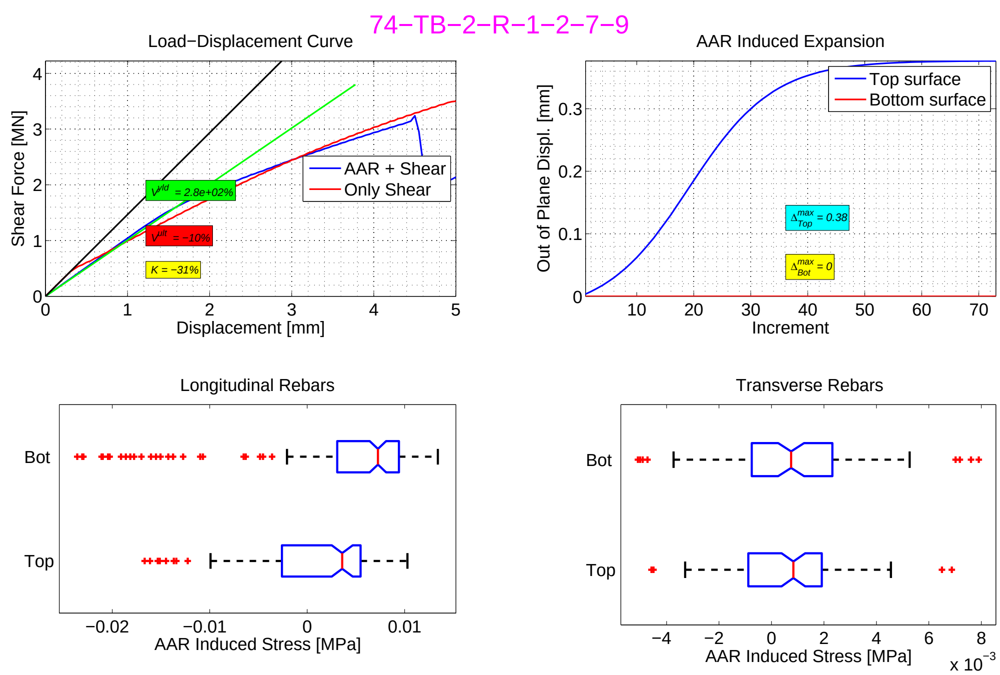

4.1.2.75 Analysis: 75-TB-2-R-1-2-9-7

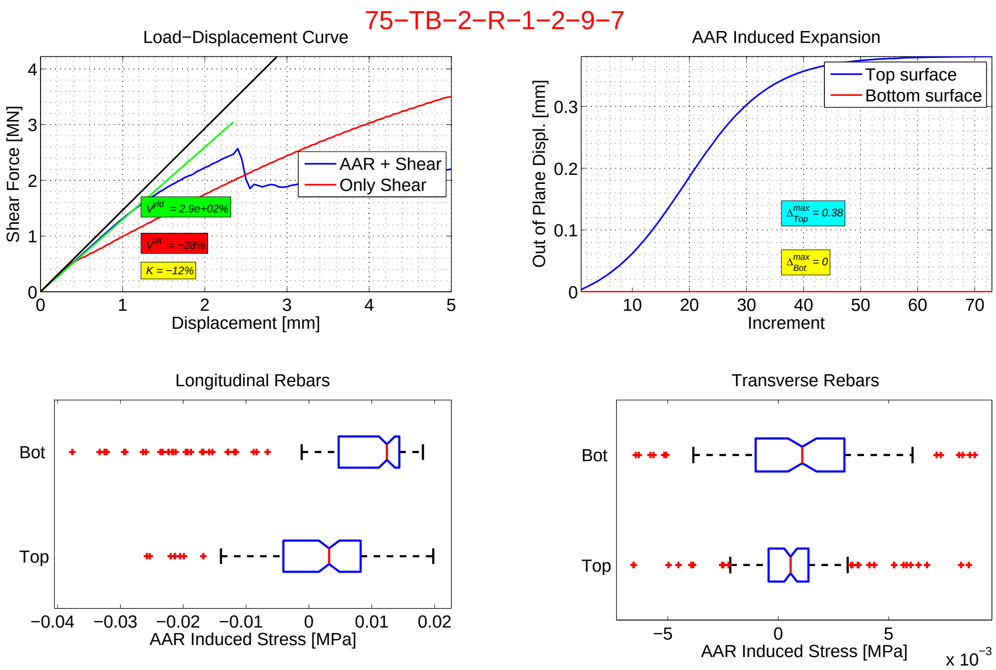

4.1.2.76 Analysis: 76-TB-2-R-1-2-9-9

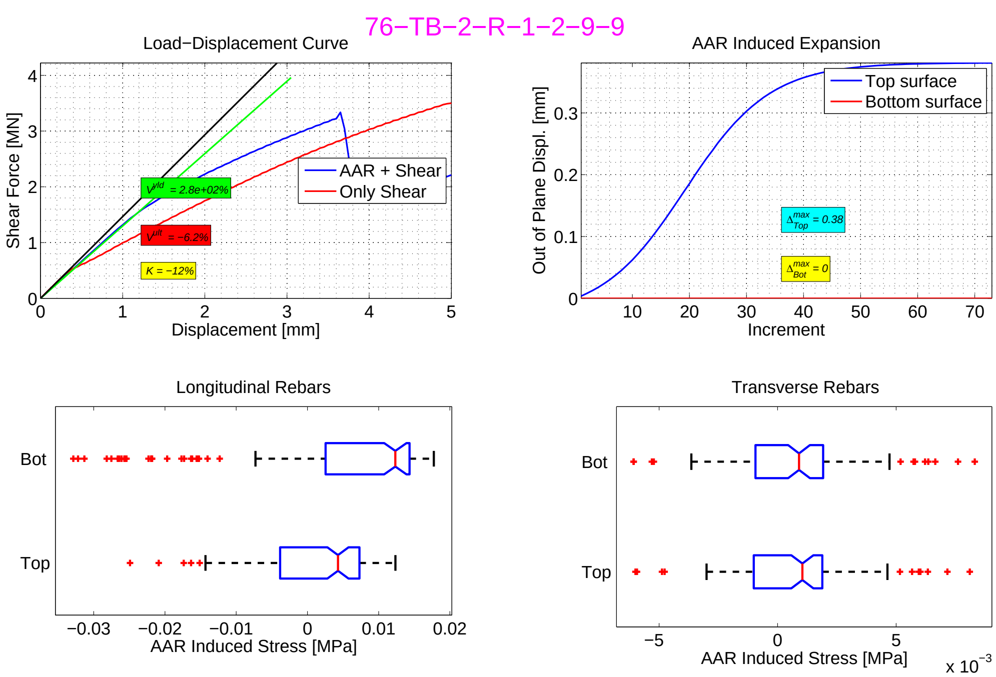

4.1.2.77 Analysis: 77-TB-2-R-1-5-7-7

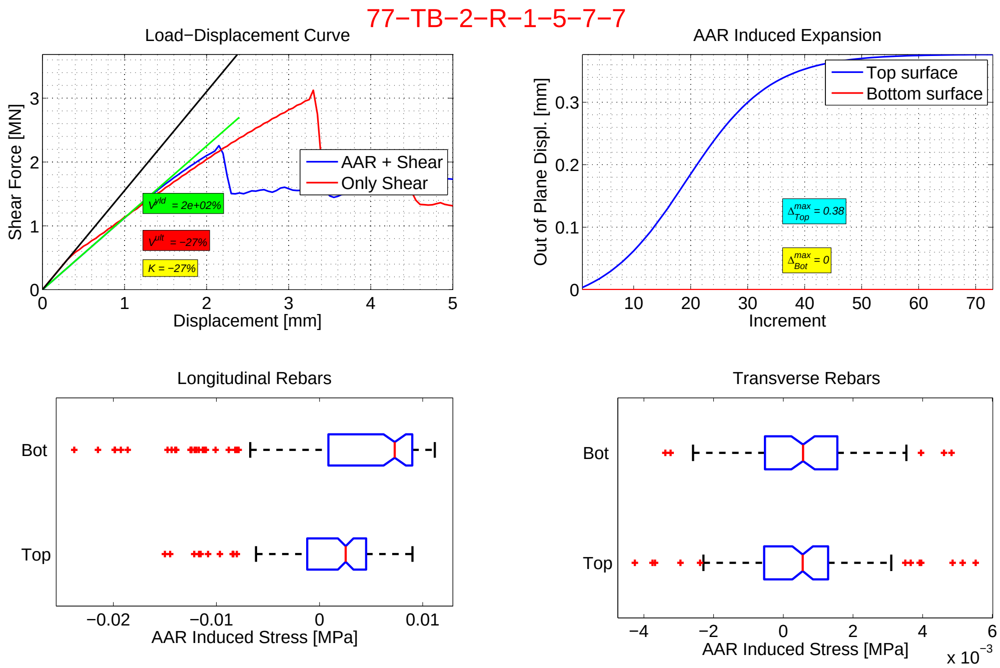

4.1.2.78 Analysis: 78-TB-2-R-1-5-7-9

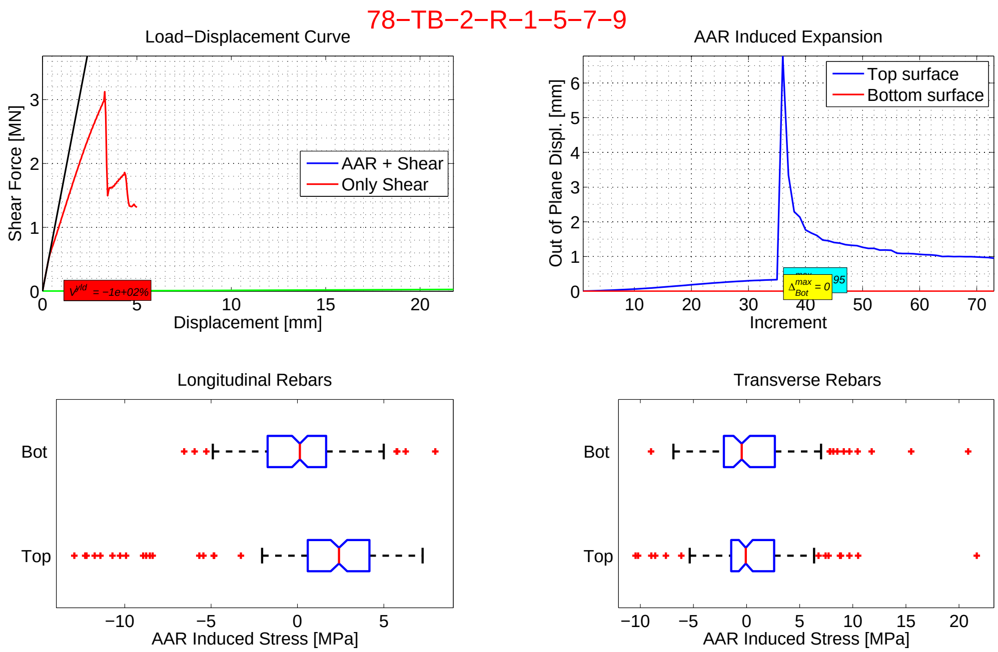

4.1.2.79 Analysis: 79-TB-2-R-1-5-9-7

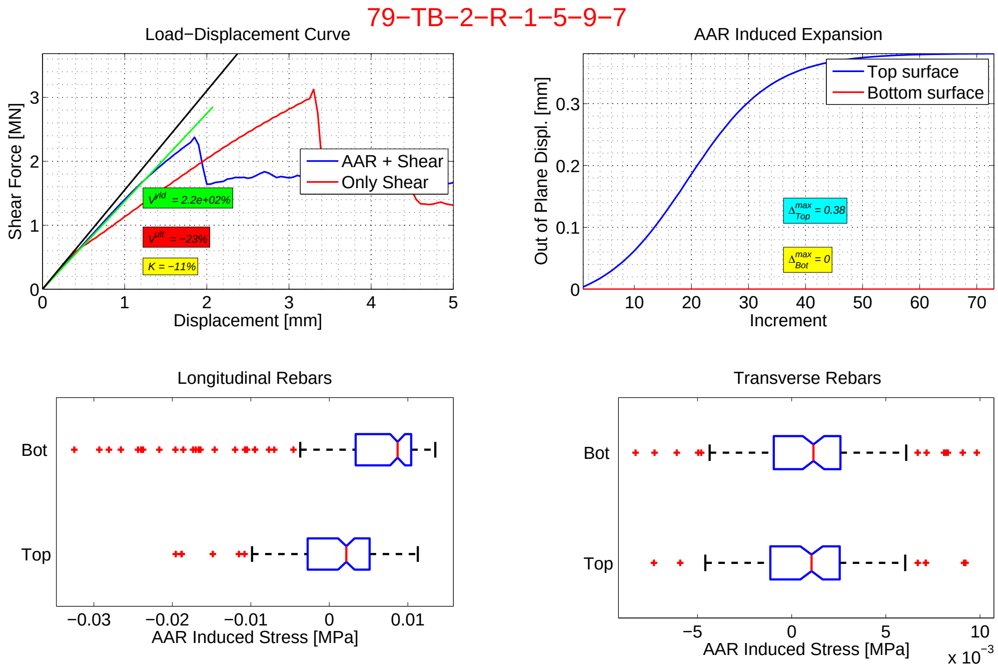

4.1.2.80 Analysis: 80-TB-2-R-1-5-9-9

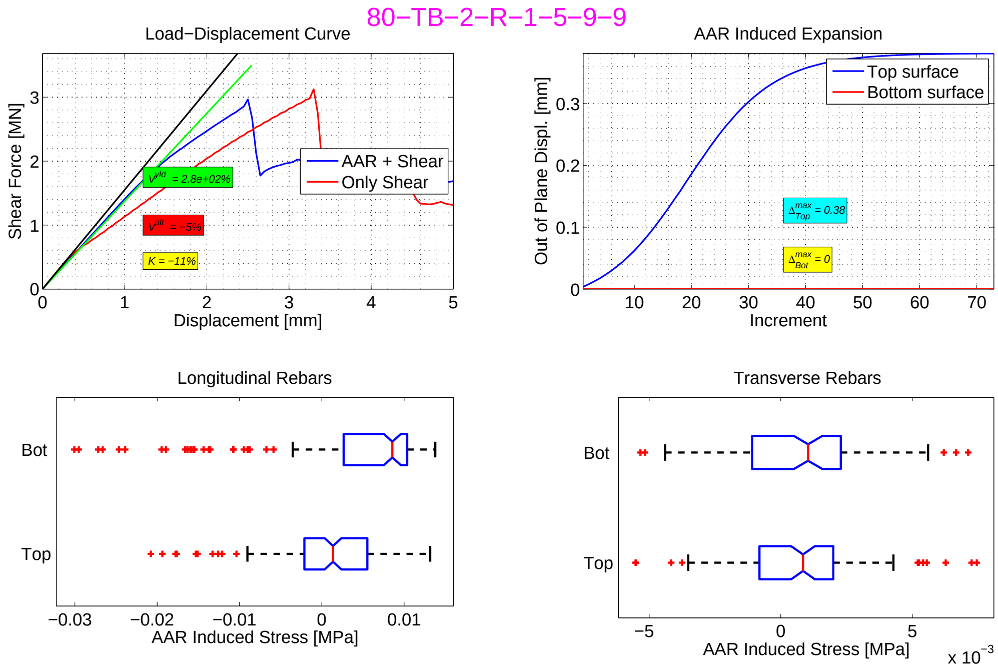

4.1.2.81 Analysis: 81-TB-2-R-1-10-7-7

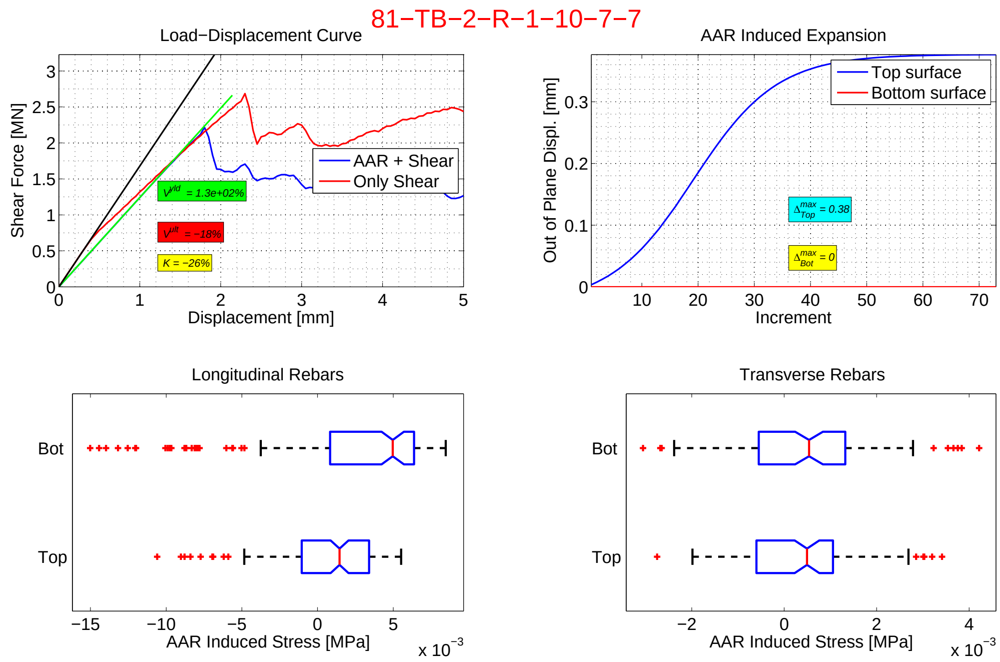

4.1.2.82 Analysis: 82-TB-2-R-1-10-7-9

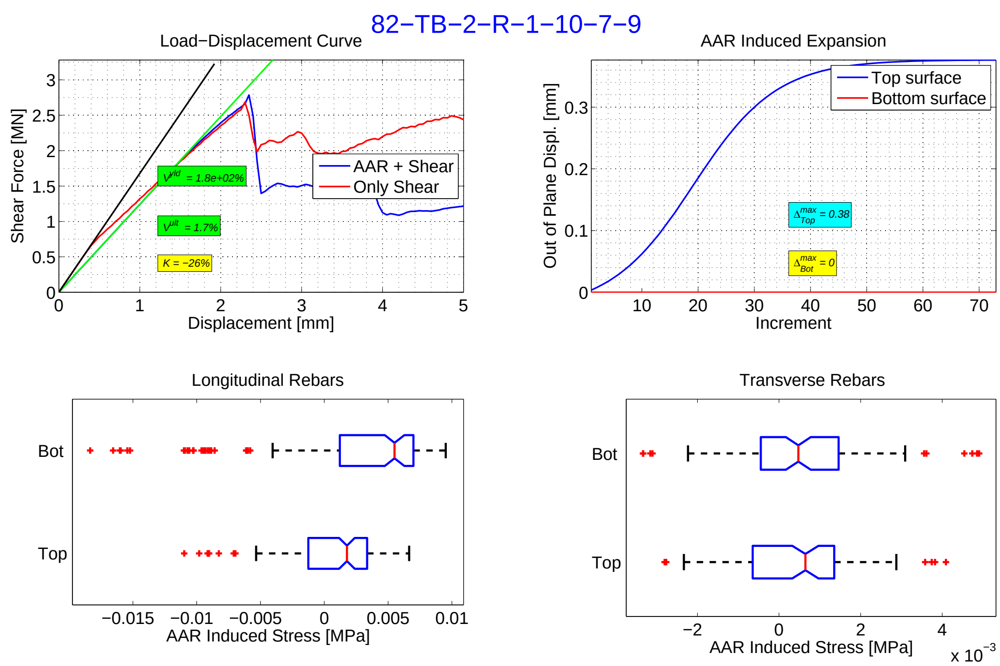

4.1.2.83 Analysis: 83-TB-2-R-1-10-9-7

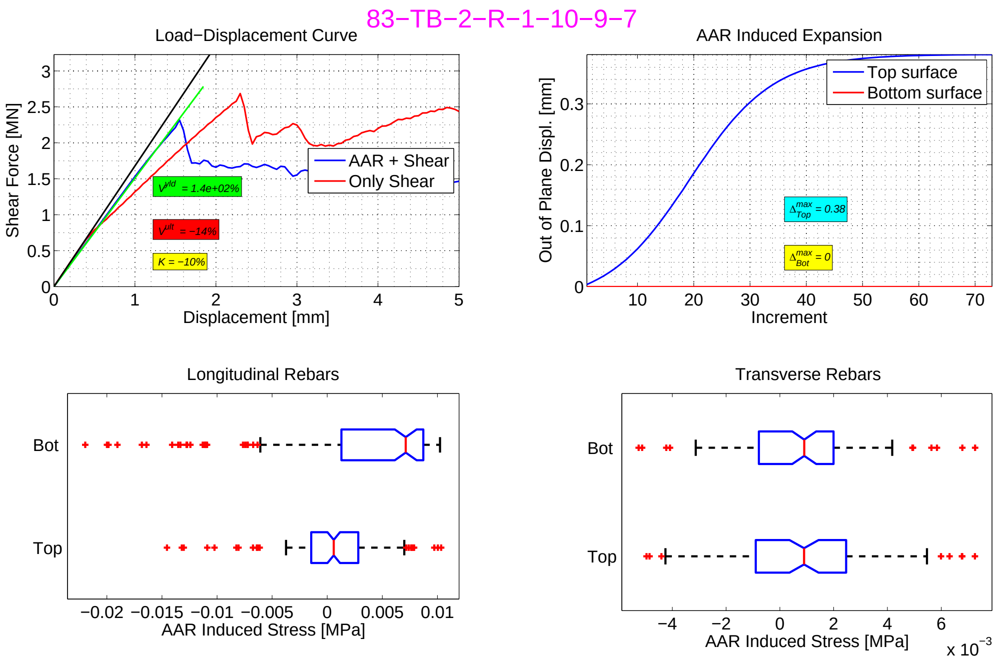

4.1.2.84 Analysis: 84-TB-2-R-1-10-9-9

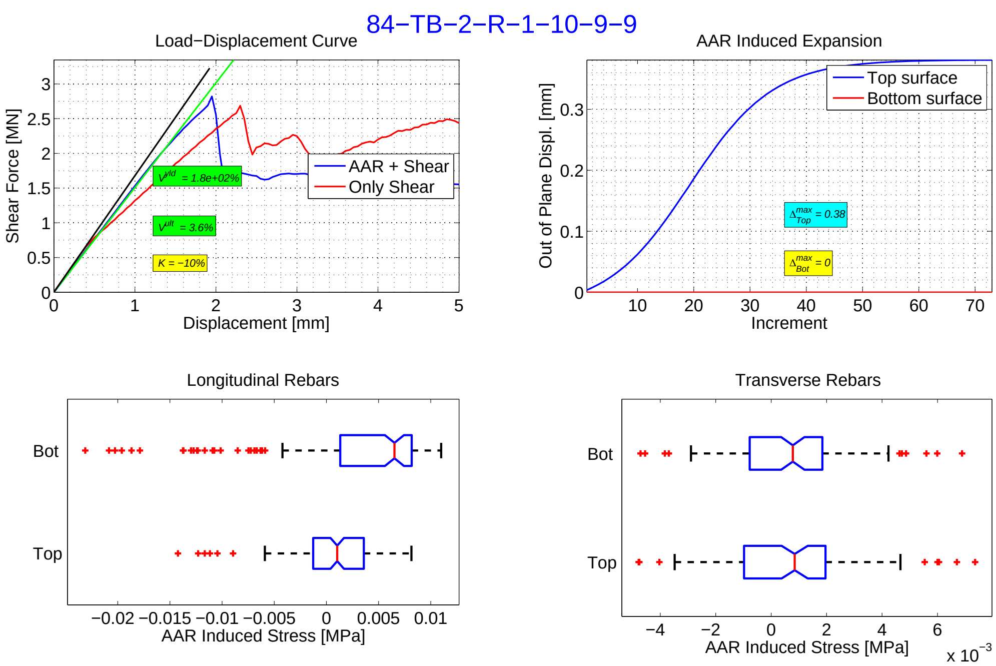

4.1.2.85 Analysis: 85-TB-2-R-2-2-7-7

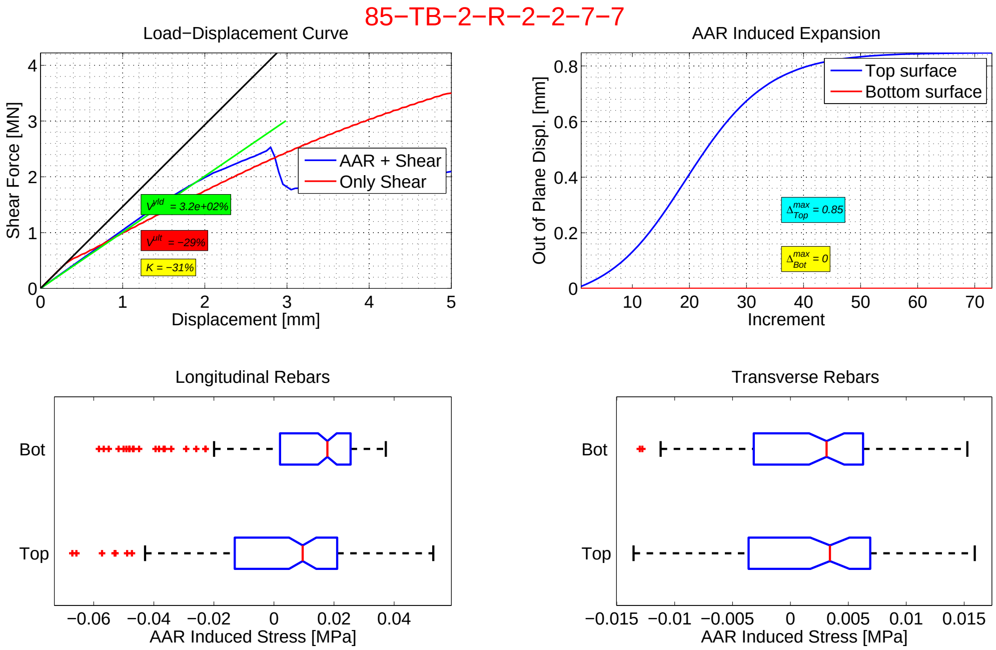

4.1.2.86 Analysis: 86-TB-2-R-2-2-7-9

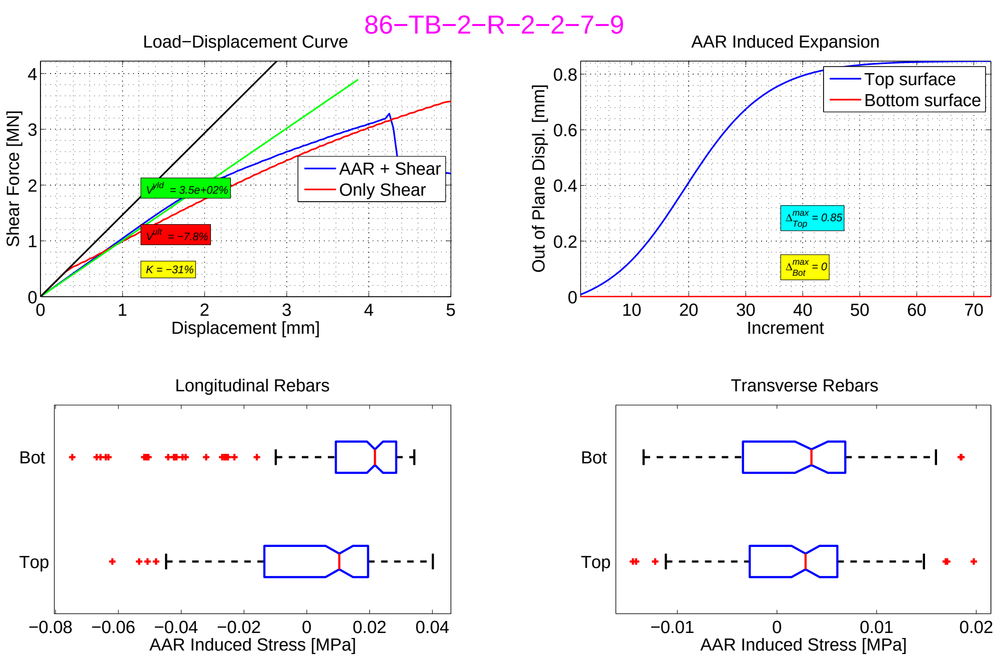

4.1.2.87 Analysis: 87-TB-2-R-2-2-9-7

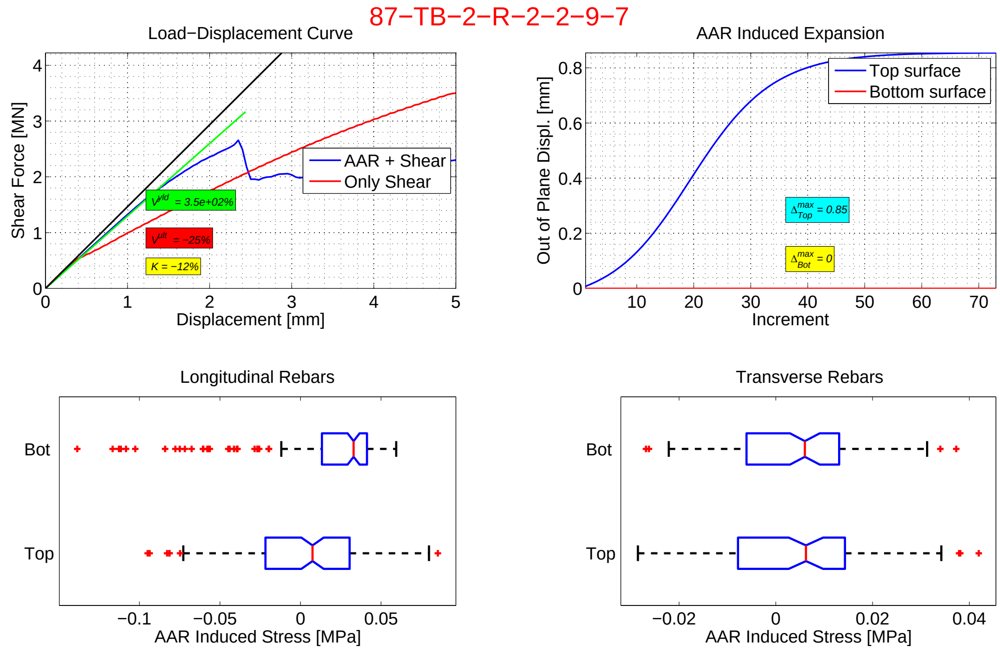

4.1.2.88 Analysis: 88-TB-2-R-2-2-9-9

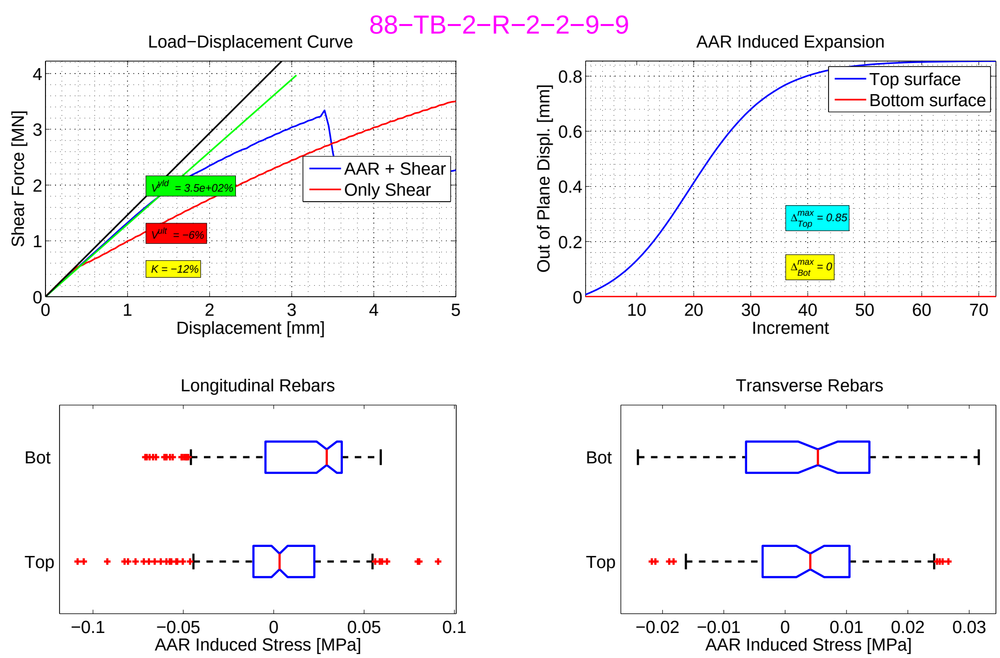

4.1.2.89 Analysis: 89-TB-2-R-2-5-7-7

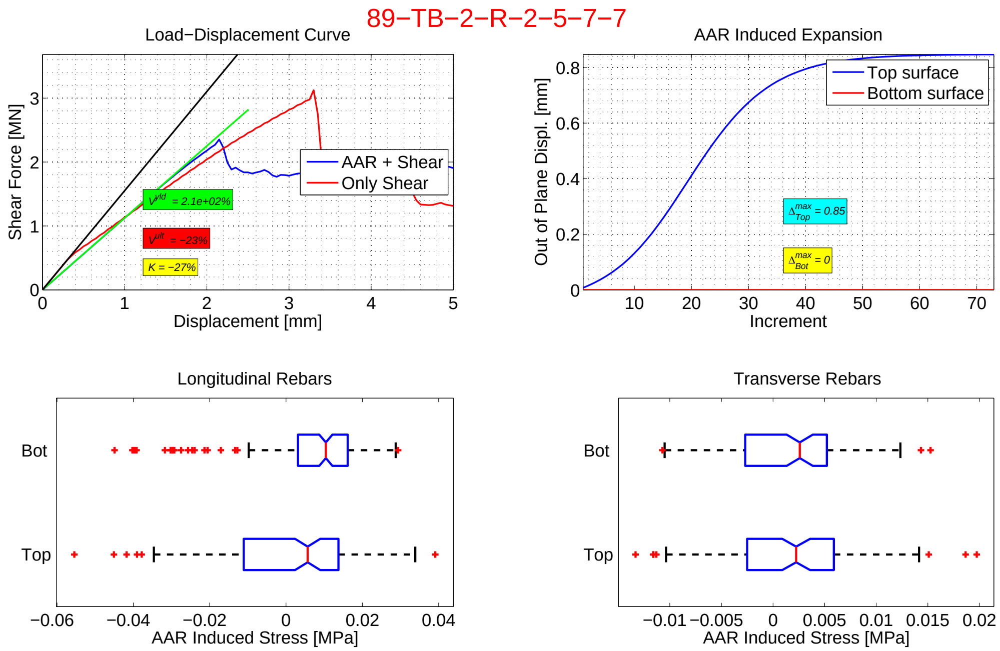

4.1.2.90 Analysis: 90-TB-2-R-2-5-7-9

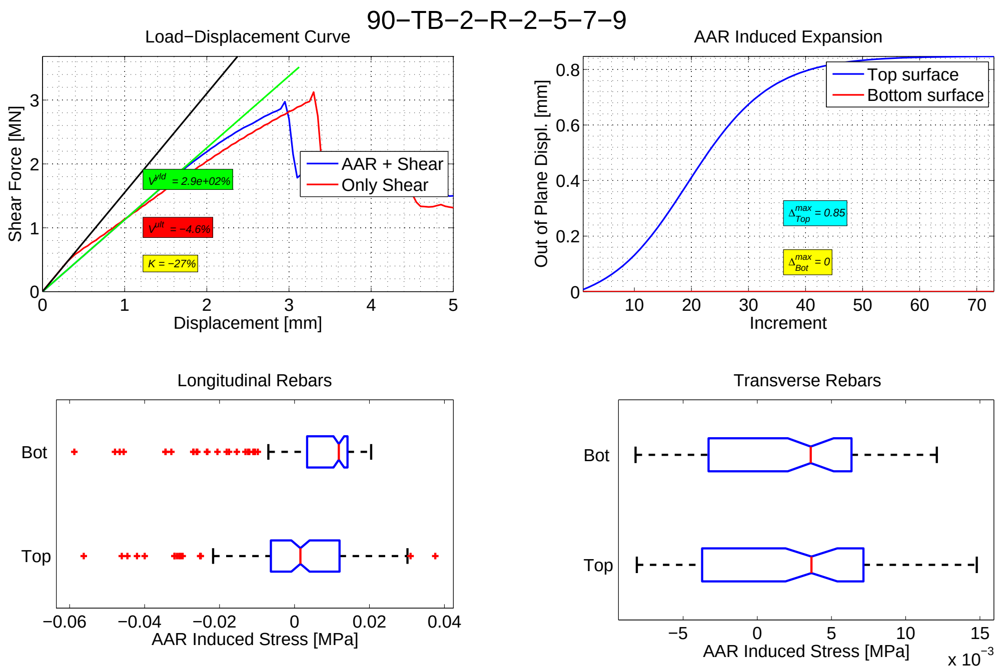

4.1.2.91 Analysis: 91-TB-2-R-2-5-9-7

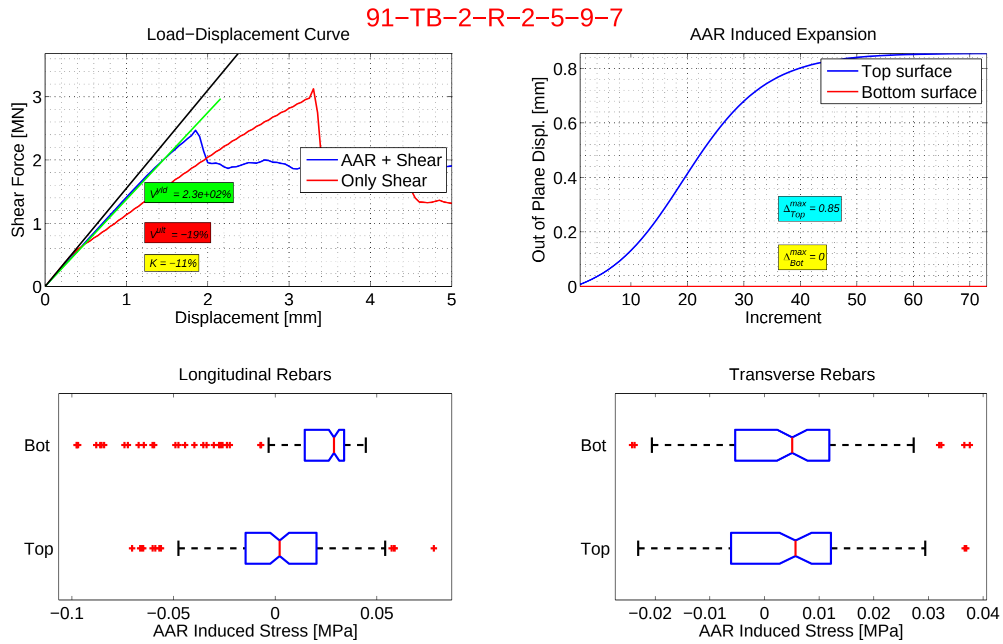

4.1.2.92 Analysis: 92-TB-2-R-2-5-9-9

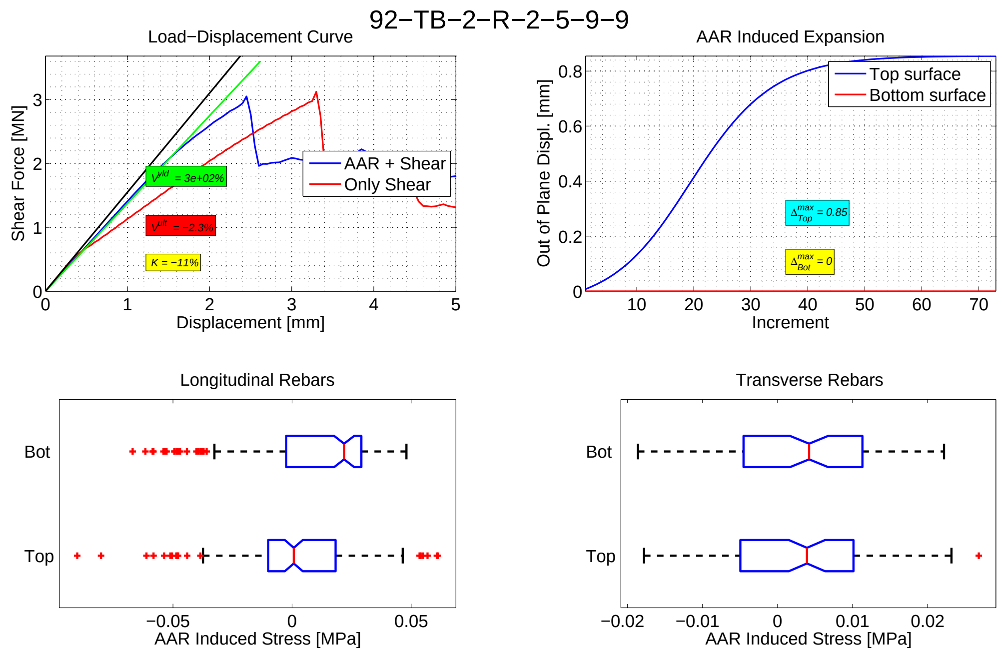

4.1.2.93 Analysis: 93-TB-2-R-2-10-7-7

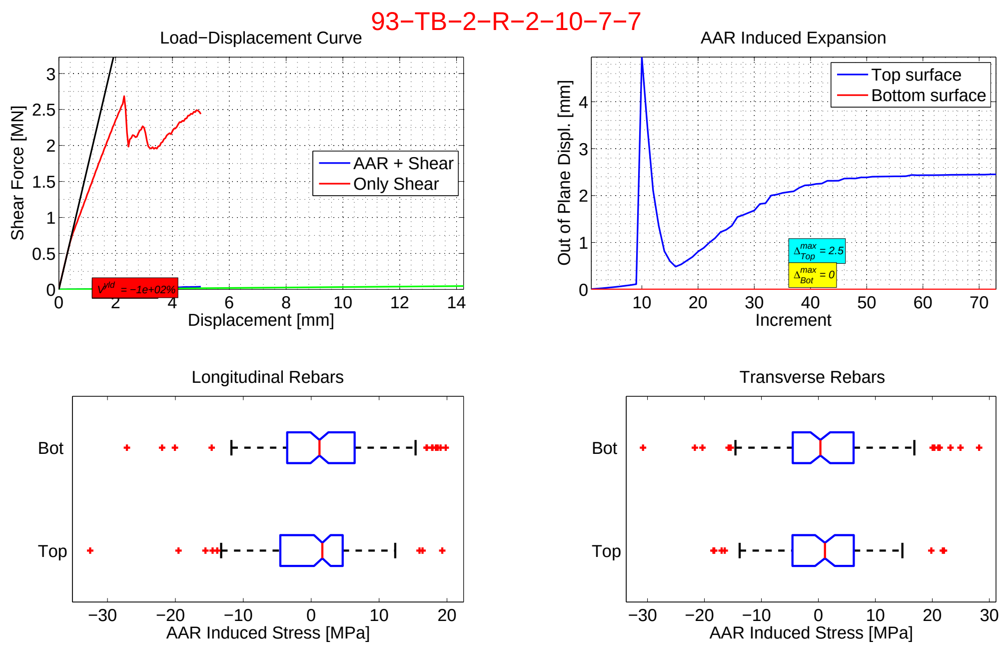

4.1.2.94 Analysis: 94-TB-2-R-2-10-7-9

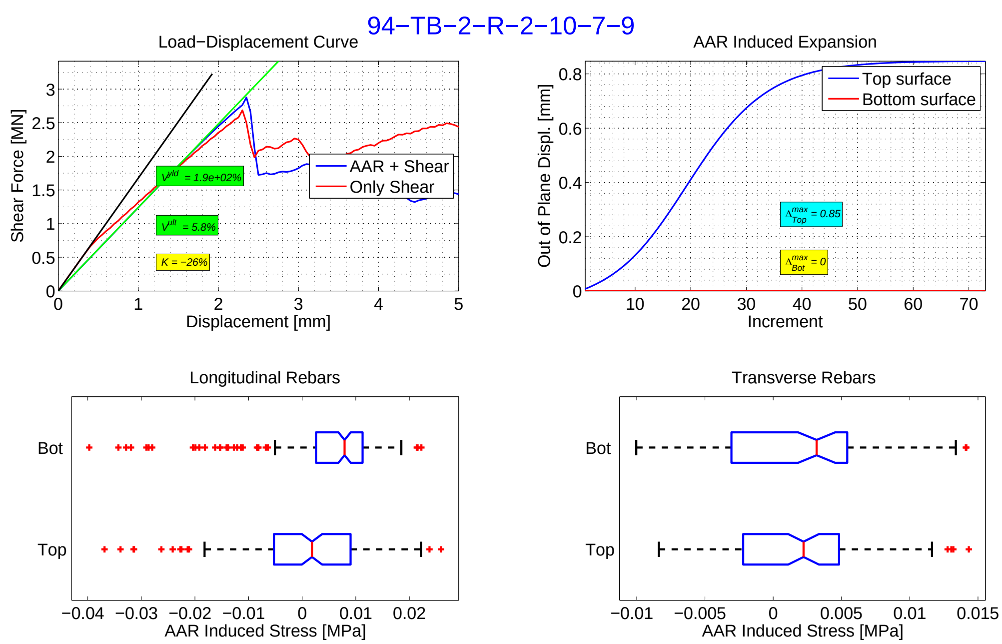

4.1.2.95 Analysis: 95-TB-2-R-2-10-9-7

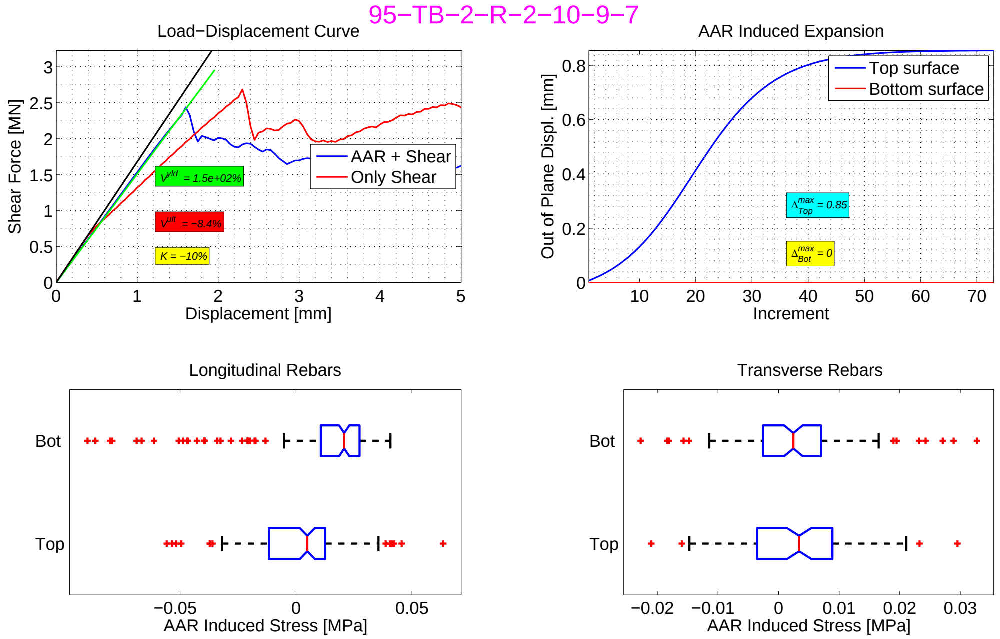

4.1.2.96 Analysis: 96-TB-2-R-2-10-9-9

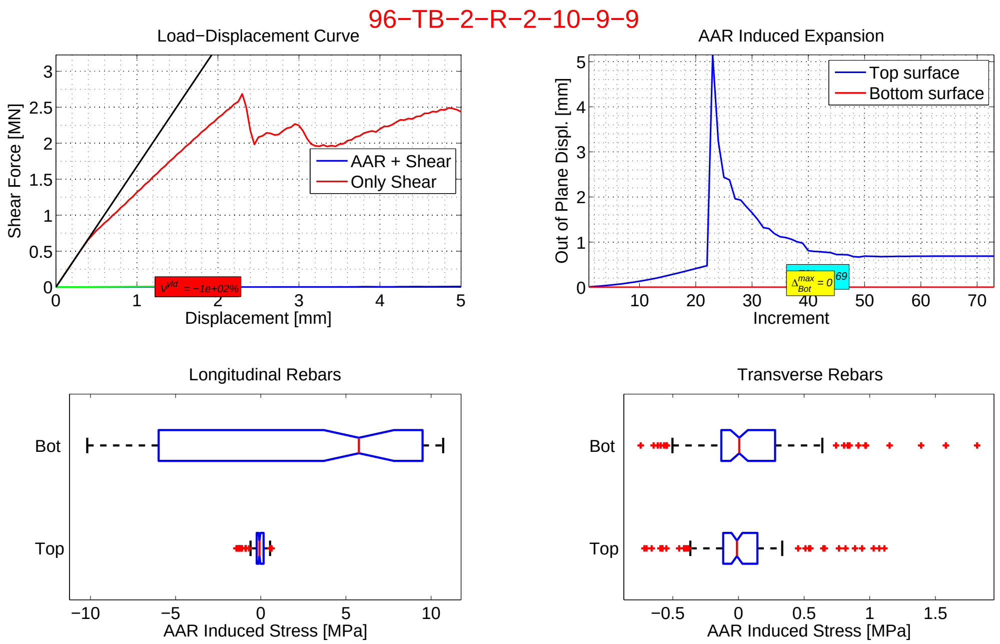

4.1.2.97 Analysis: 97-TB-2-R-3-2-7-7

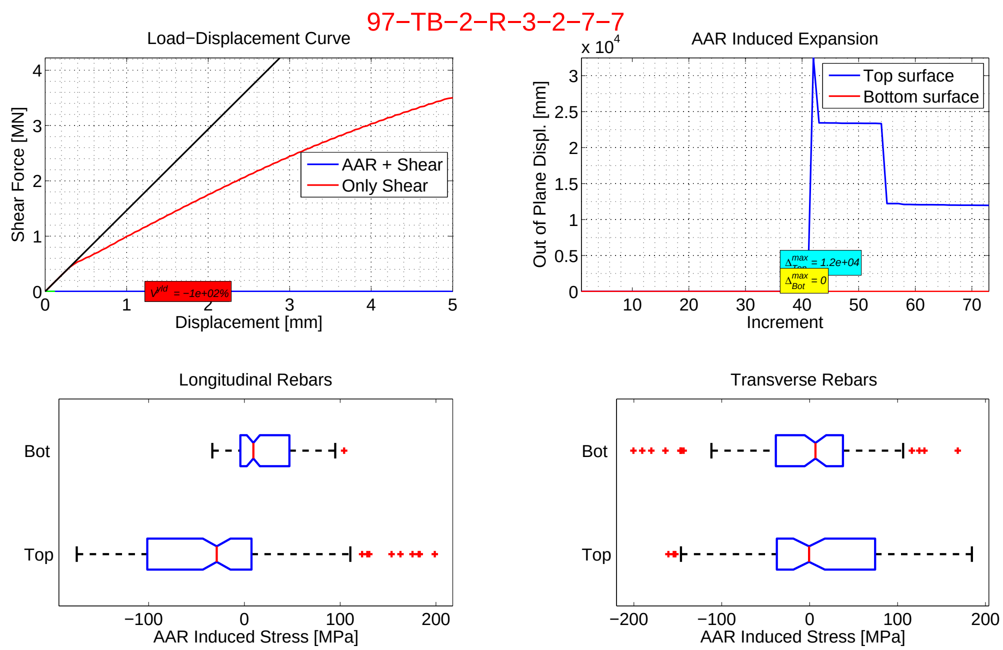

4.1.2.98 Analysis: 98-TB-2-R-3-2-7-9

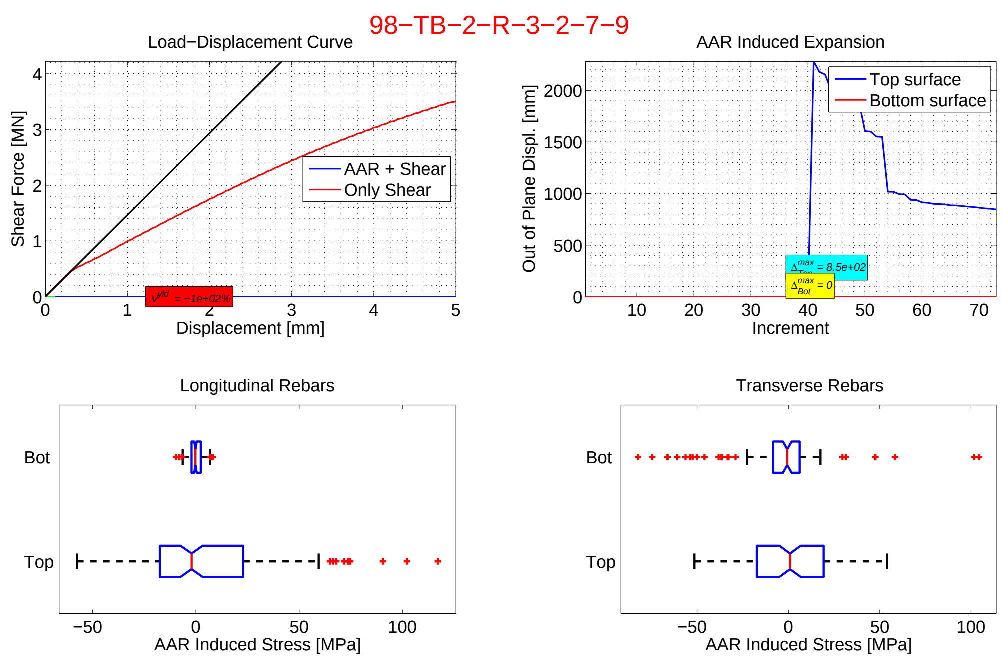

4.1.2.99 Analysis: 99-TB-2-R-3-2-9-7

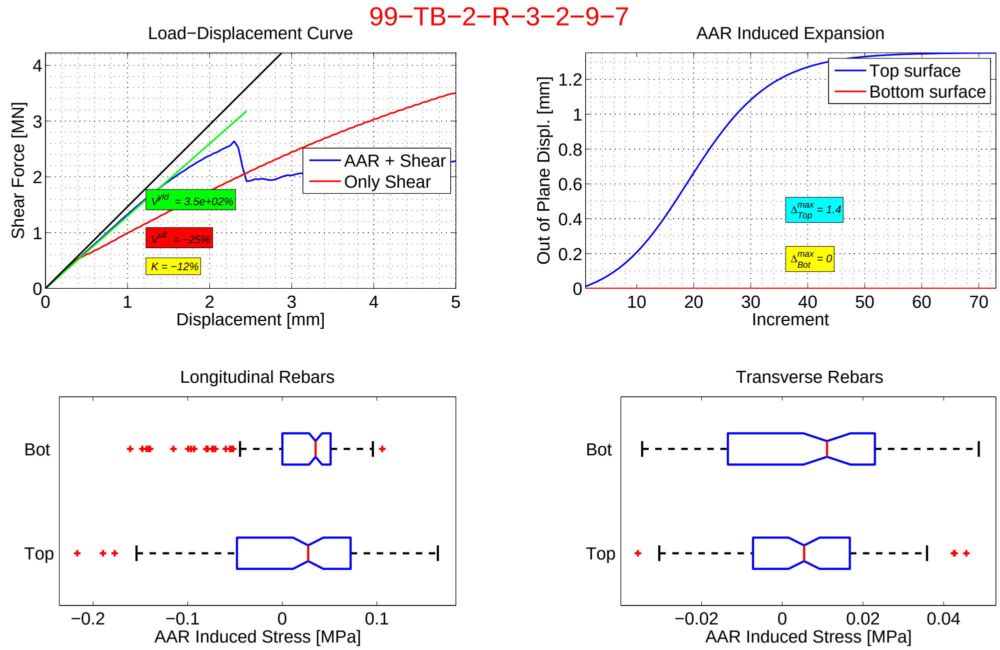

4.1.2.100 Analysis: 100-TB-2-R-3-2-9-9

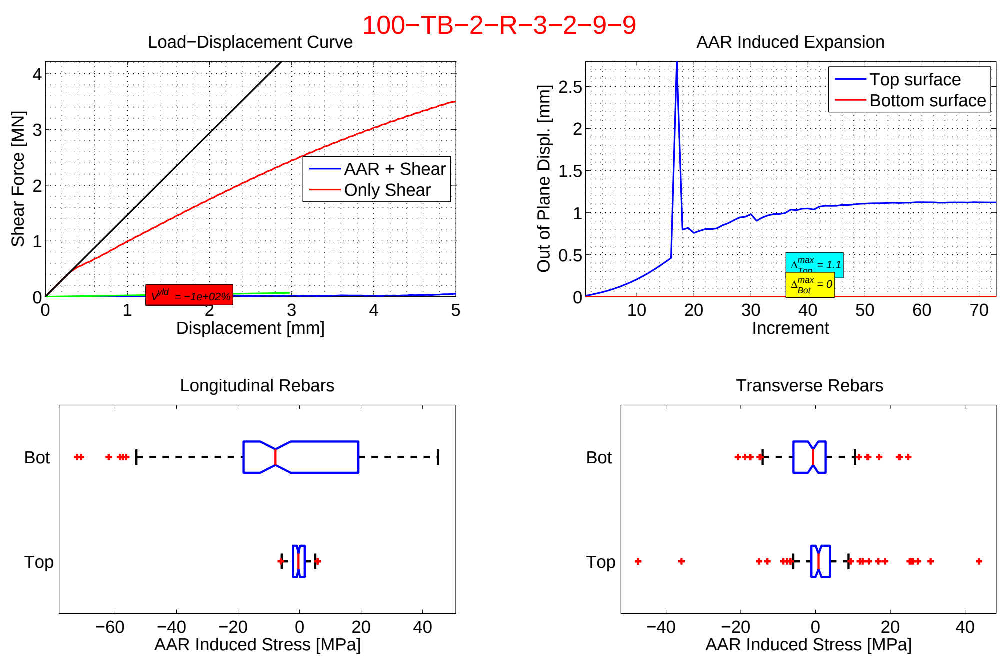

4.1.2.101 Analysis: 101-TB-2-R-3-5-7-7

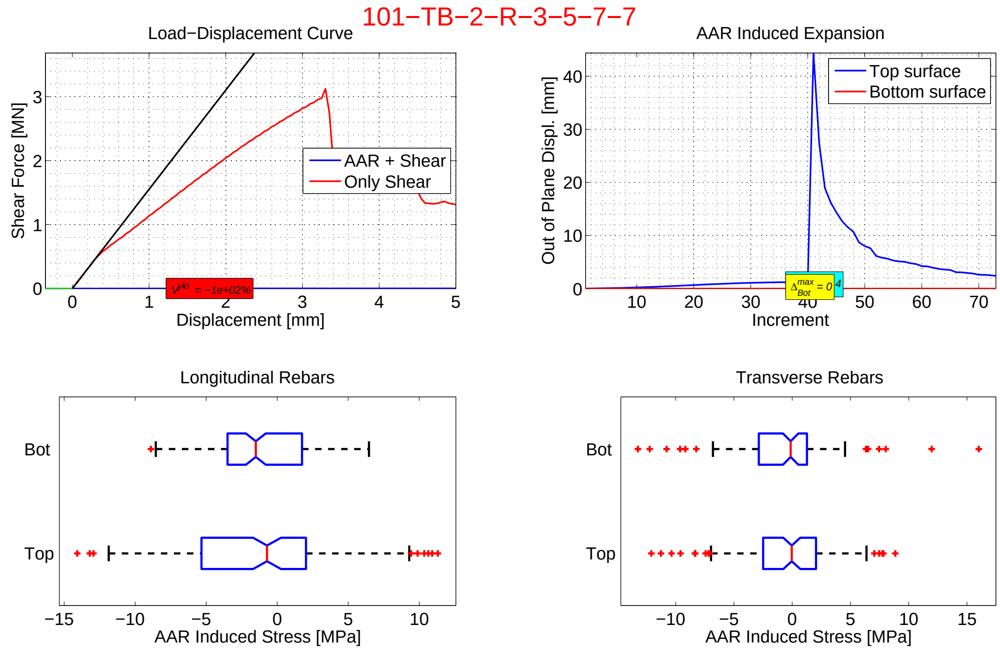

4.1.2.102 Analysis: 102-TB-2-R-3-5-7-9

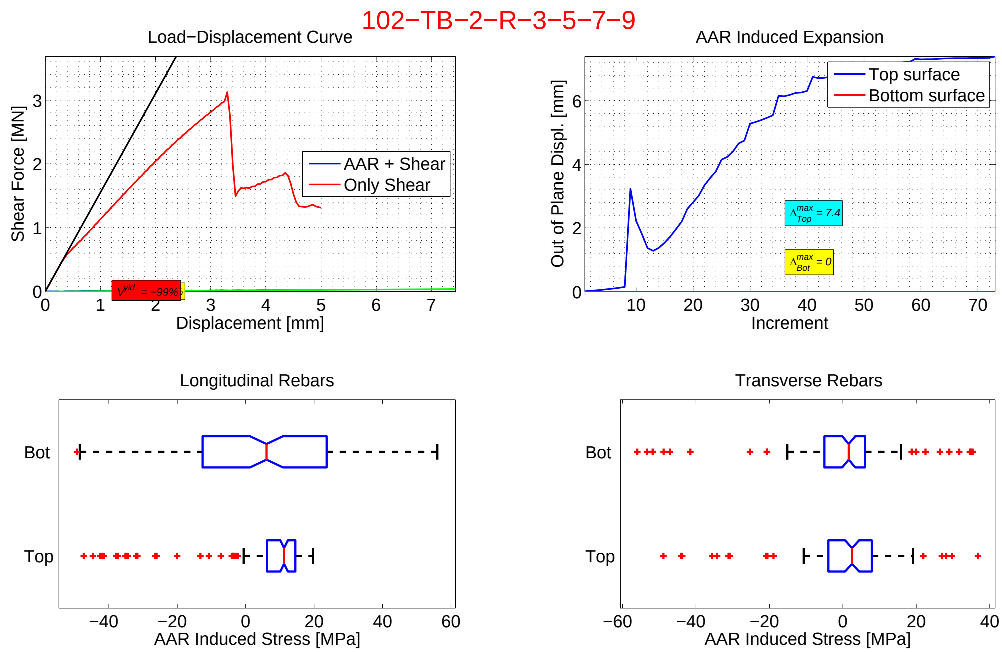

4.1.2.103 Analysis: 103-TB-2-R-3-5-9-7

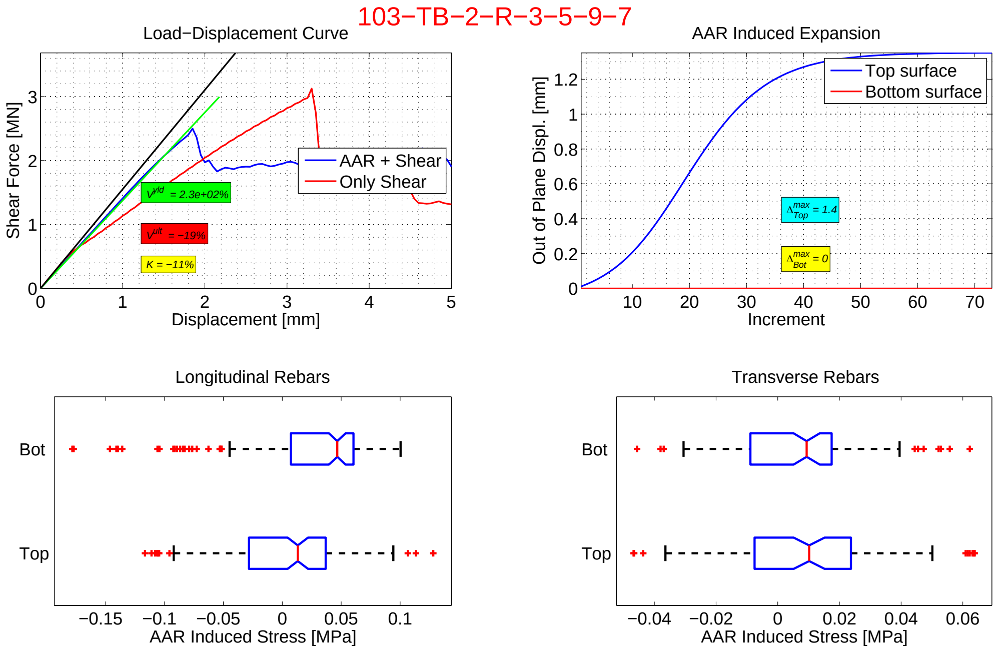

4.1.2.104 Analysis: 104-TB-2-R-3-5-9-9

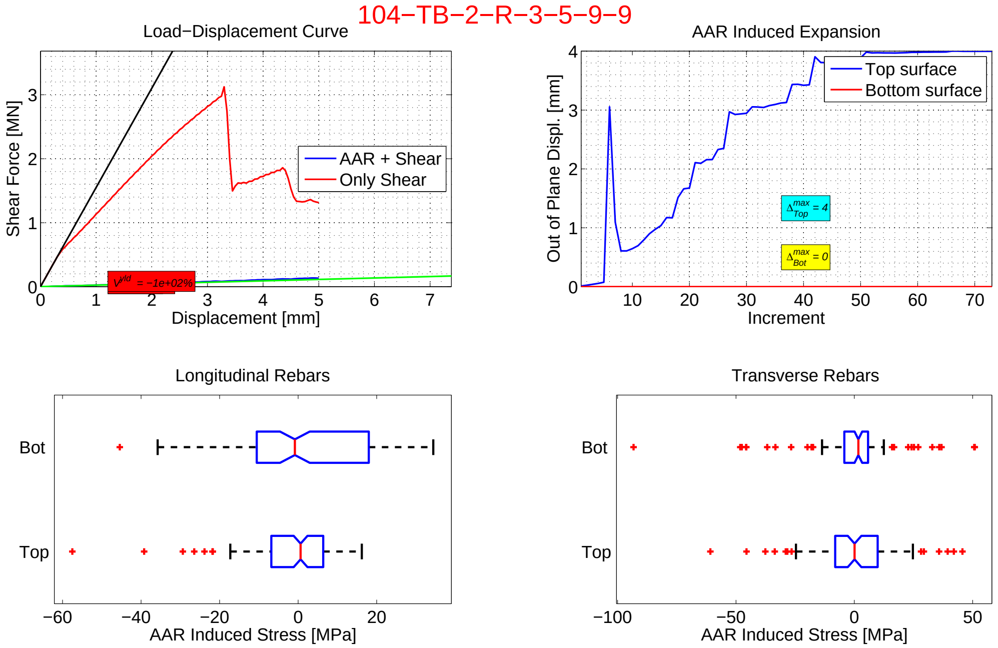

4.1.2.105 Analysis: 105-TB-2-R-3-10-7-7

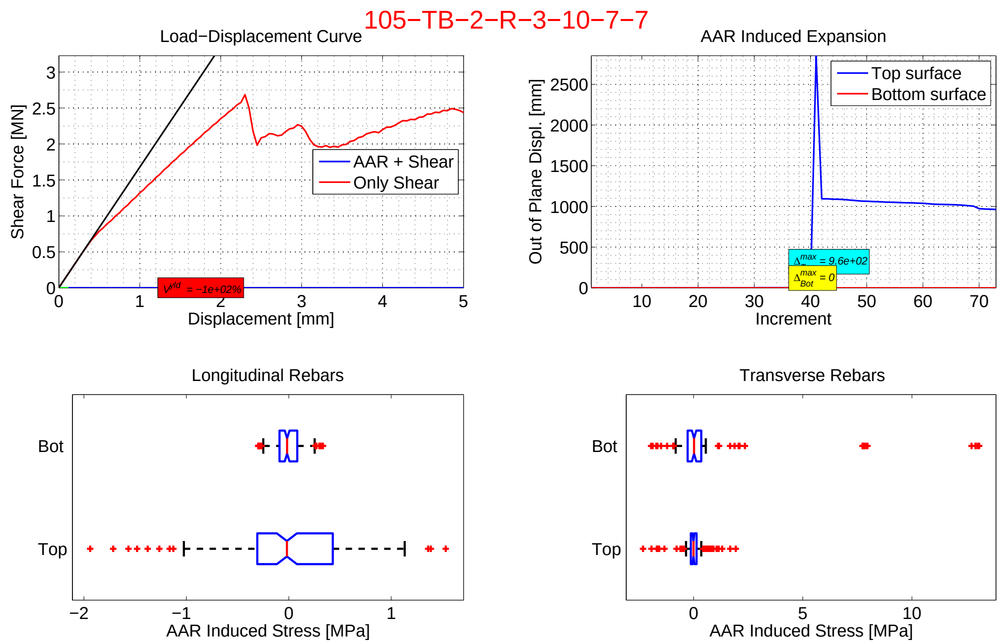

4.1.2.106 Analysis: 106-TB-2-R-3-10-7-9

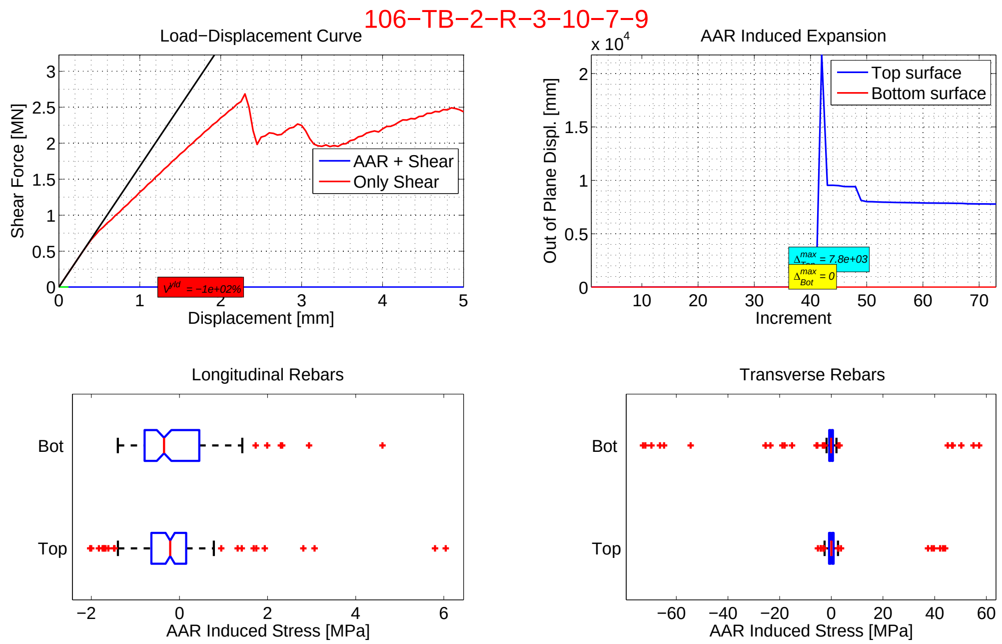

4.1.2.107 Analysis: 107-TB-2-R-3-10-9-7

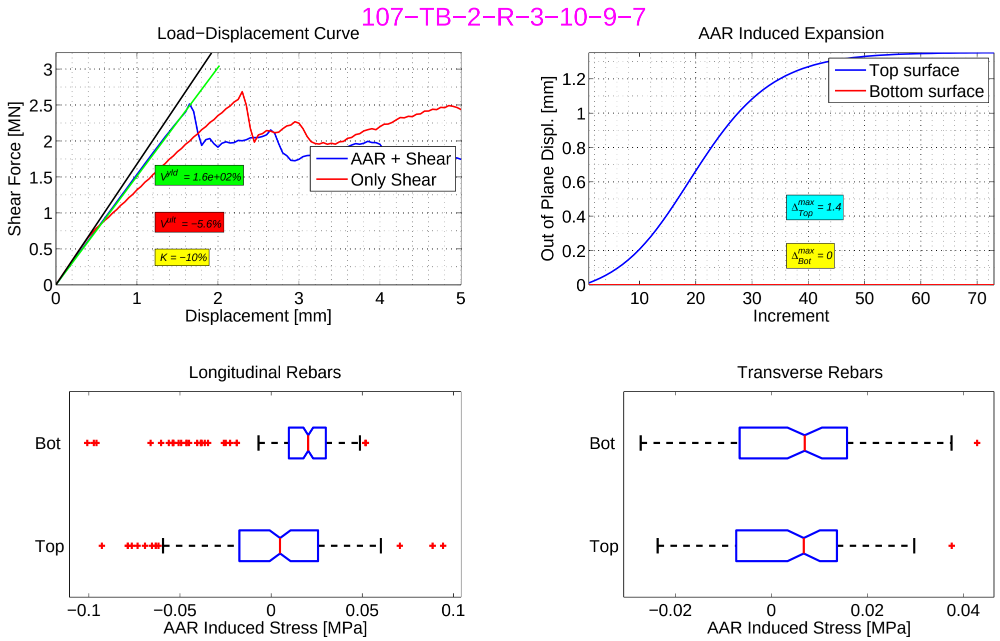

4.1.2.108 Analysis: 108-TB-2-R-3-10-9-9

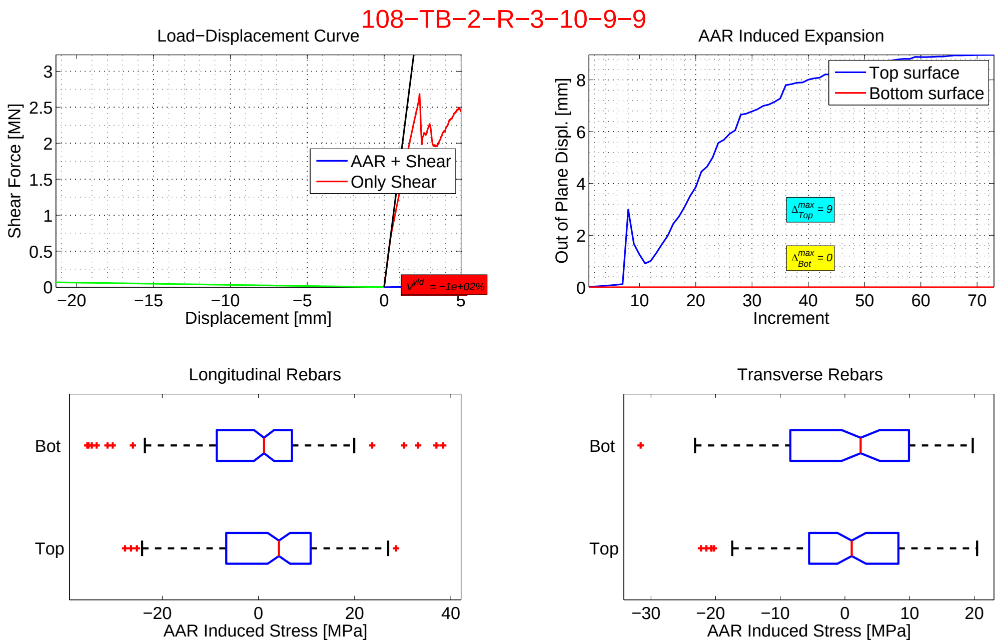

4.1.2.109 Analysis: 109-TB-4-R-1-2-7-7

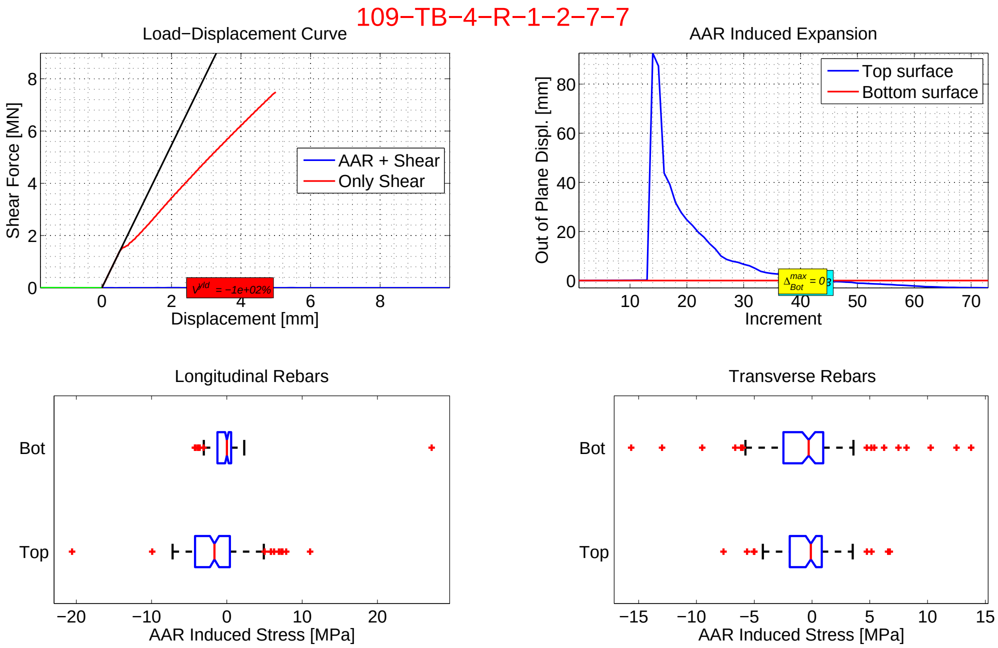

4.1.2.110 Analysis: 110-TB-4-R-1-2-7-9

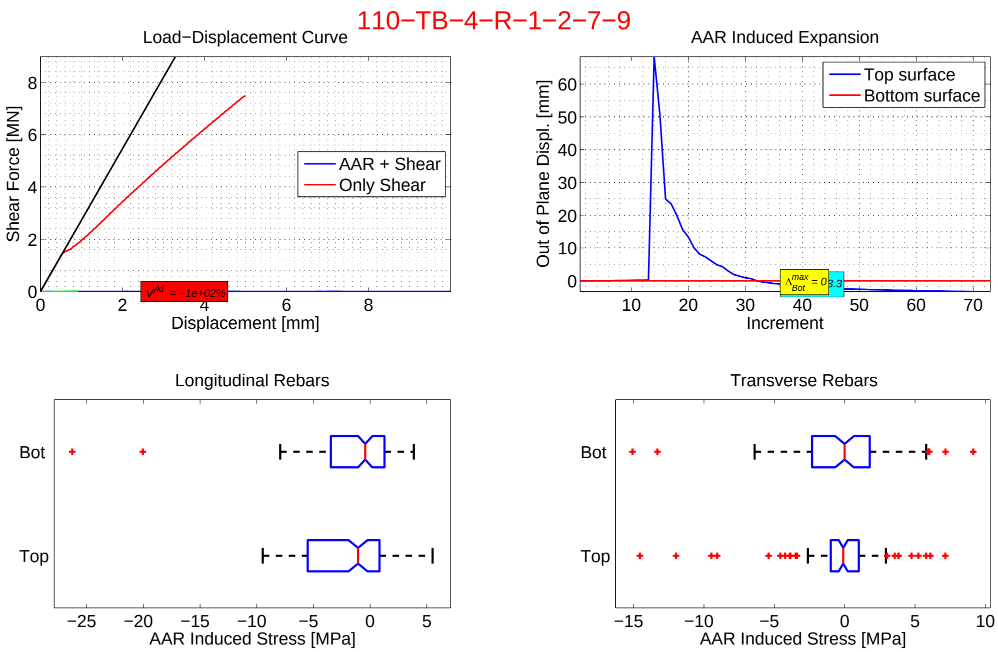

4.1.2.111 Analysis: 111-TB-4-R-1-2-9-7

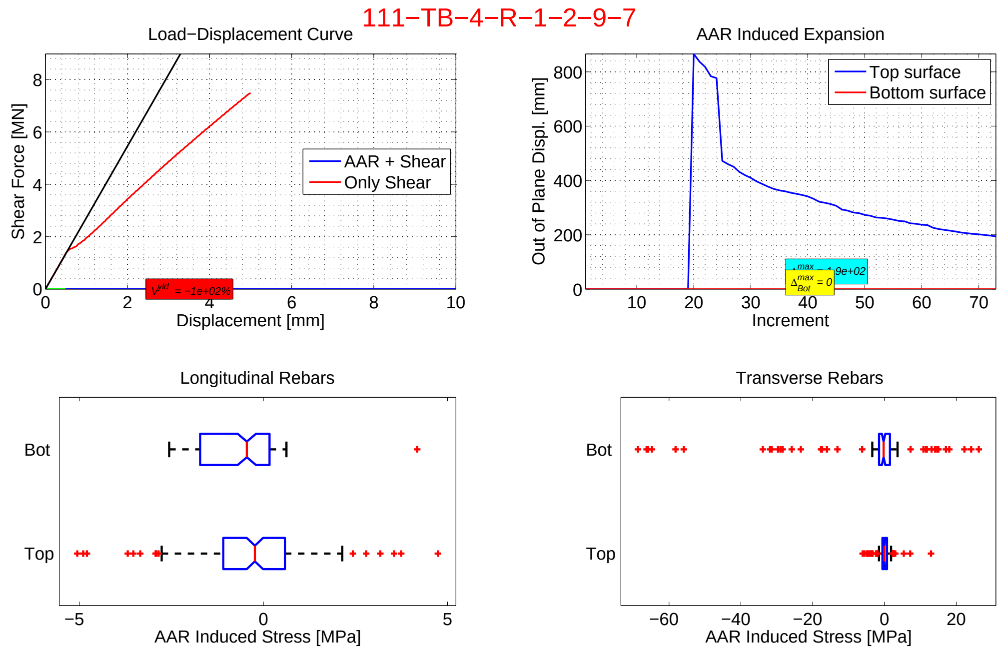

4.1.2.112 Analysis: 112-TB-4-R-1-2-9-9

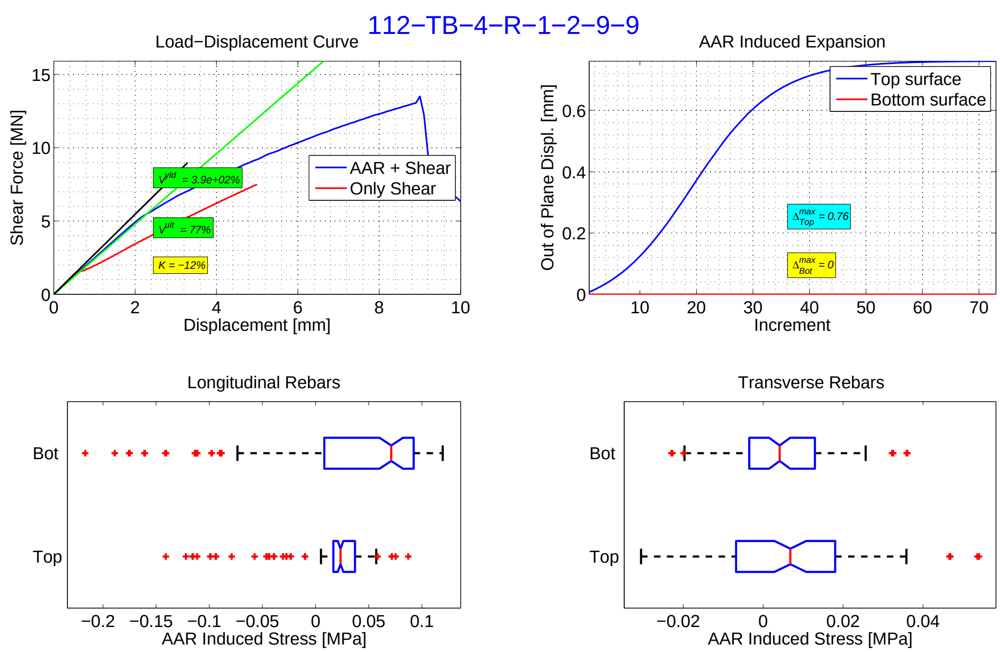

4.1.2.113 Analysis: 113-TB-4-R-1-5-7-7

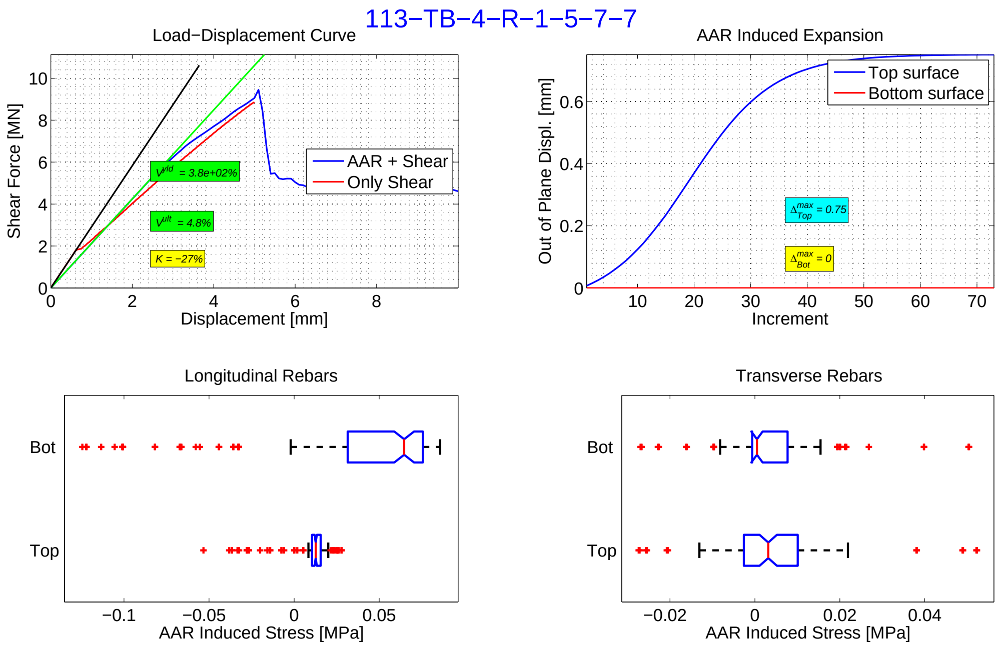

4.1.2.114 Analysis: 114-TB-4-R-1-5-7-9

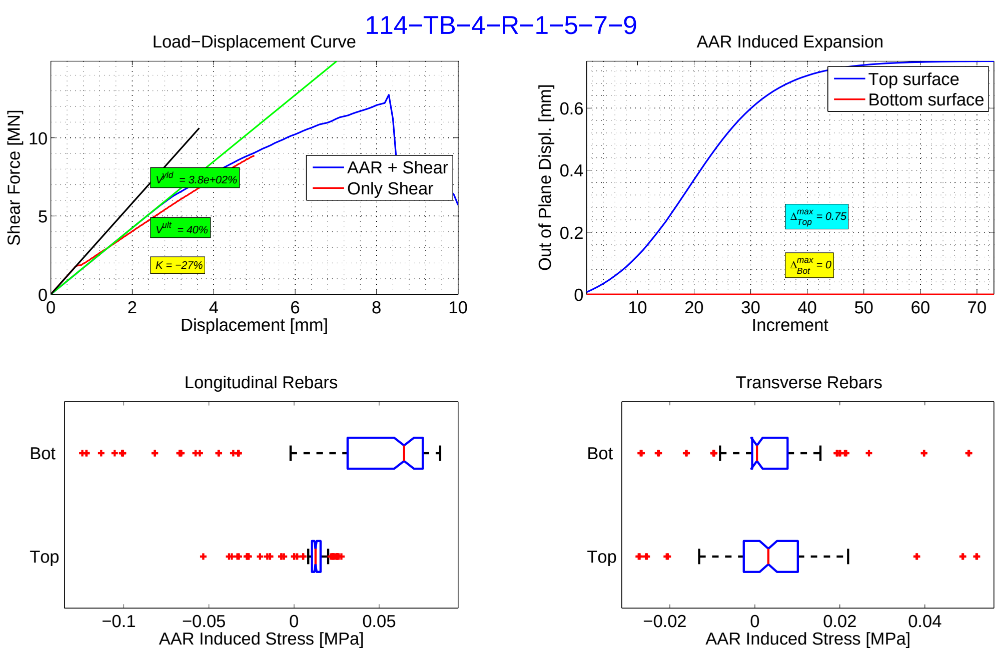

4.1.2.115 Analysis: 115-TB-4-R-1-5-9-7

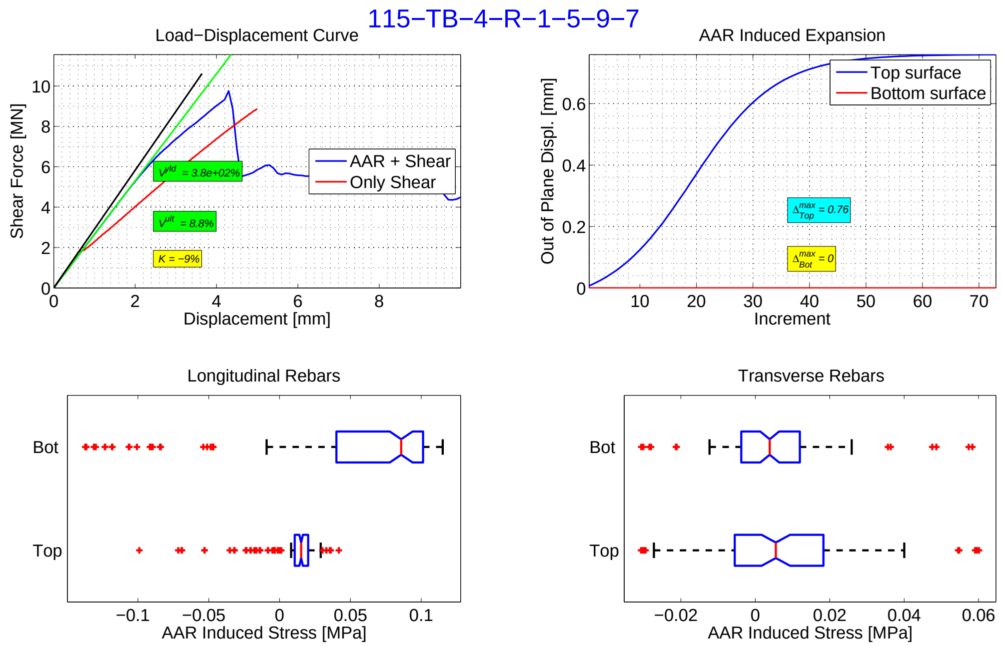

4.1.2.116 Analysis: 116-TB-4-R-1-5-9-9

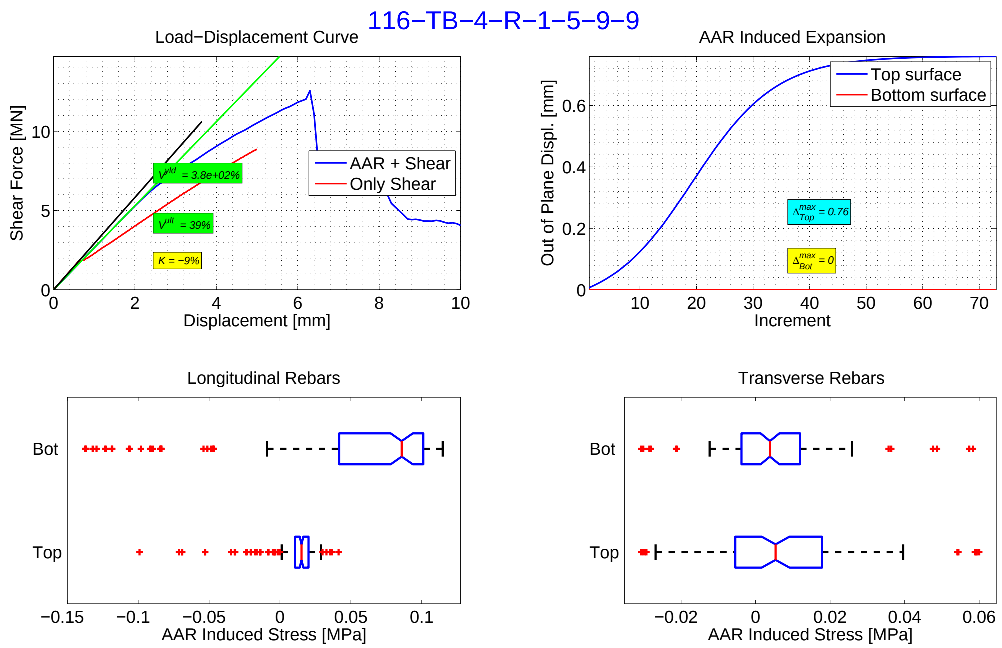

4.1.2.117 Analysis: 117-TB-4-R-1-10-7-7

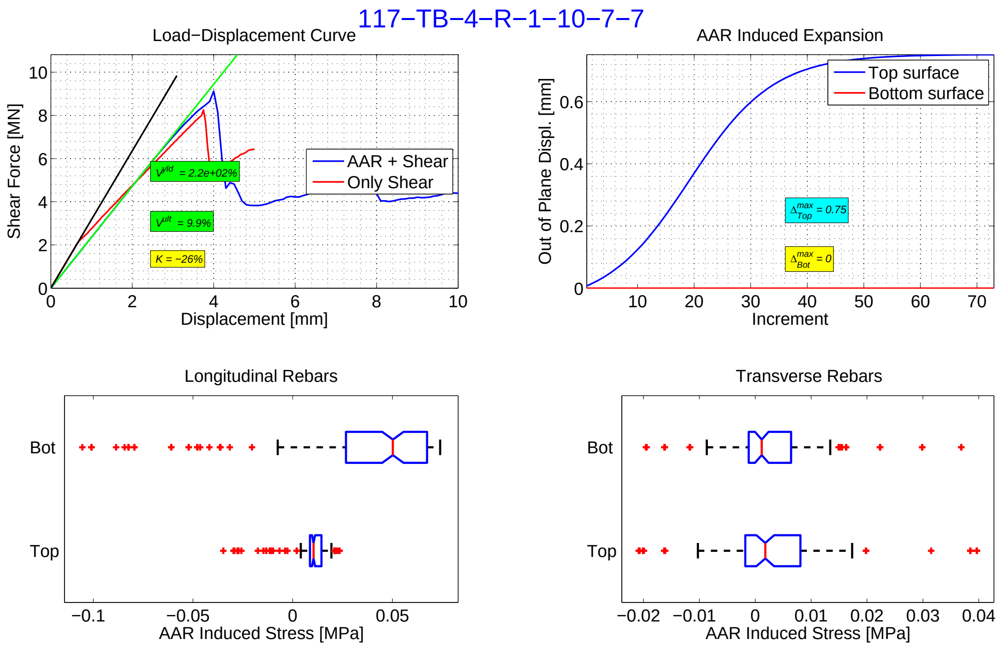

4.1.2.118 Analysis: 118-TB-4-R-1-10-7-9

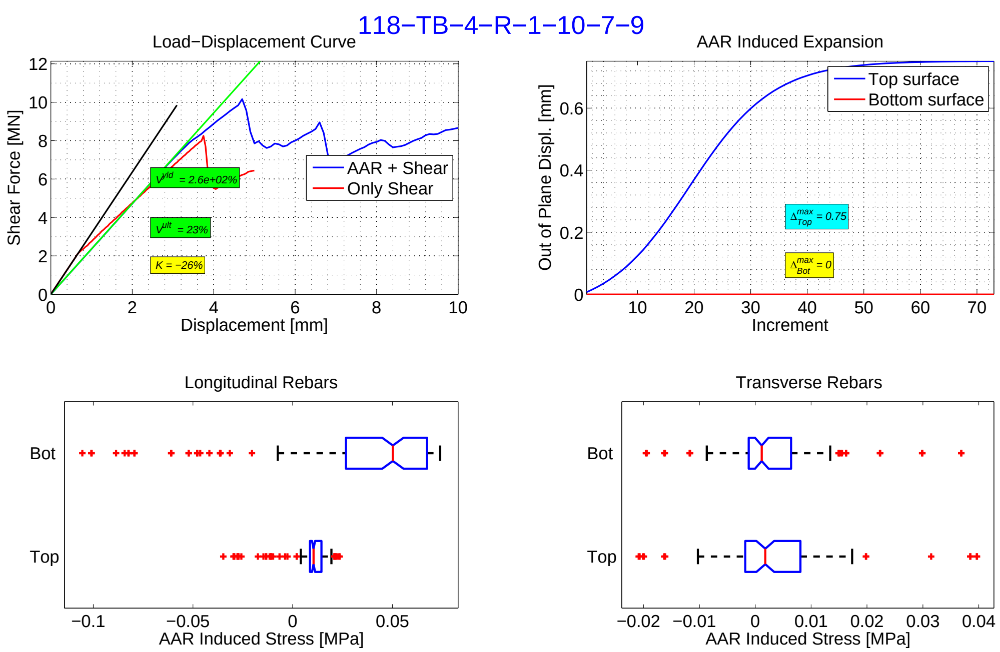

4.1.2.119 Analysis: 119-TB-4-R-1-10-9-7

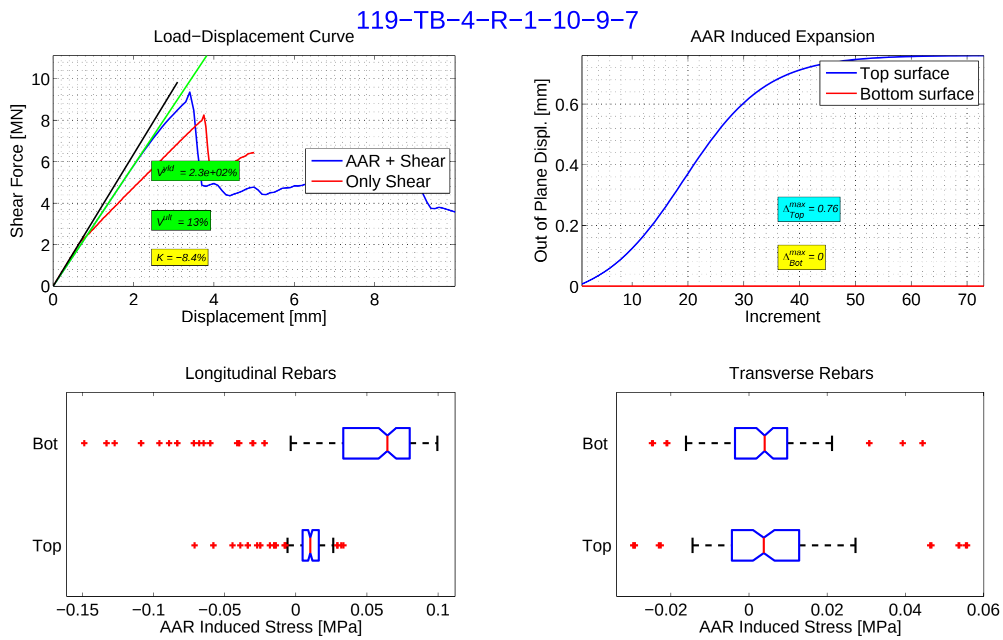

4.1.2.120 Analysis: 120-TB-4-R-1-10-9-9

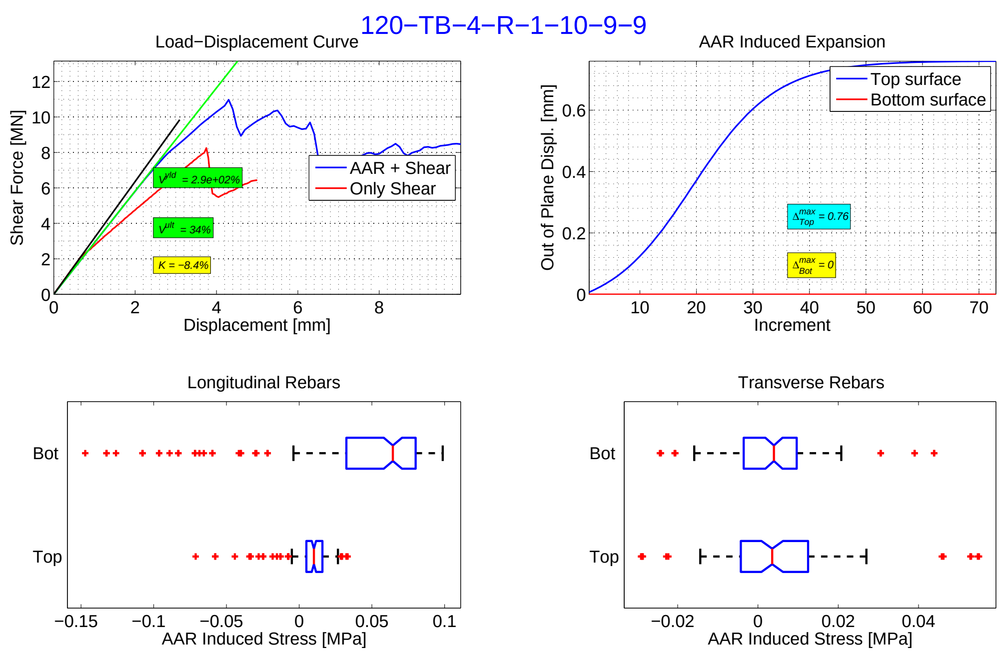

4.1.2.121 Analysis: 121-TB-4-R-2-2-7-7

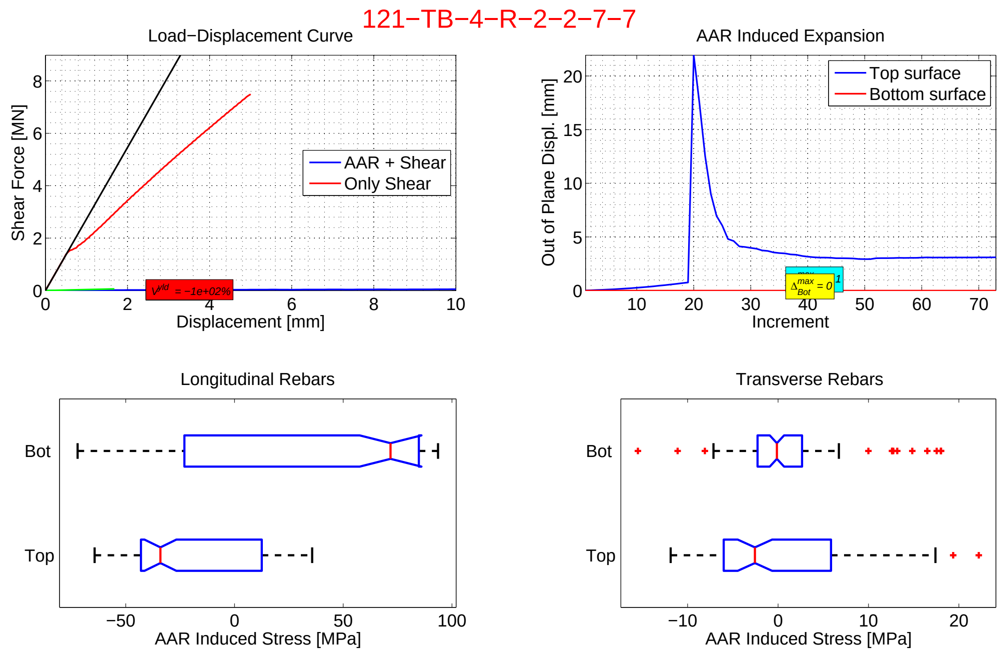

4.1.2.122 Analysis: 122-TB-4-R-2-2-7-9

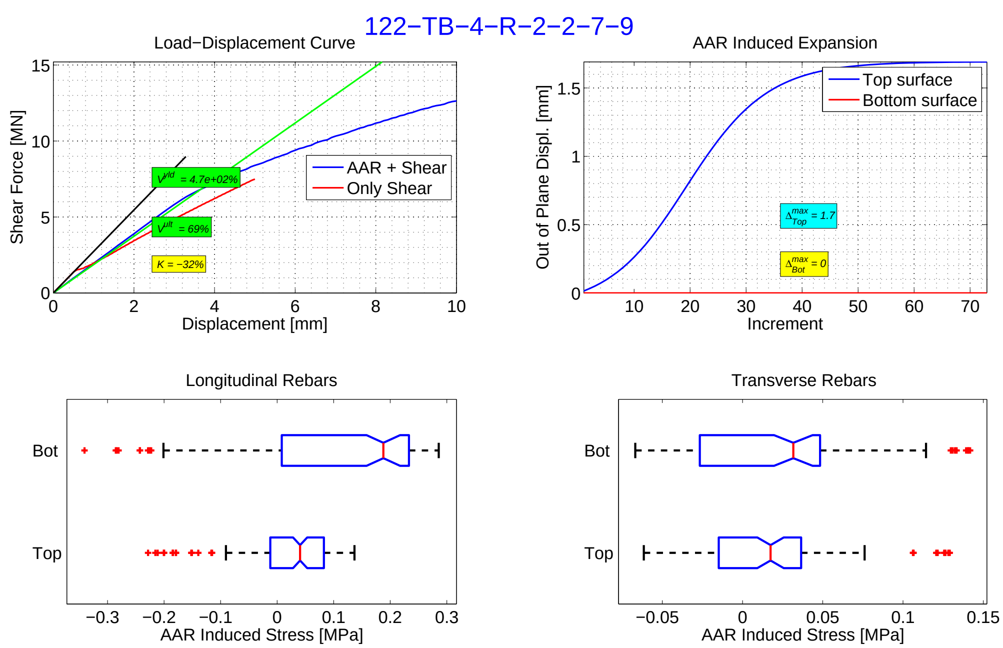

4.1.2.123 Analysis: 123-TB-4-R-2-2-9-7

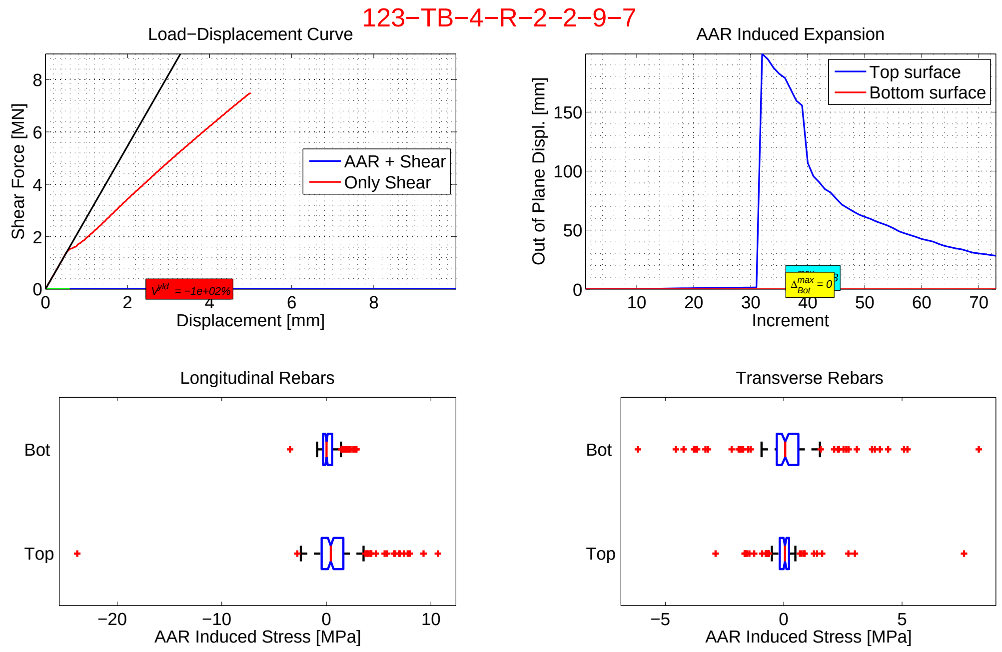

4.1.2.124 Analysis: 124-TB-4-R-2-2-9-9

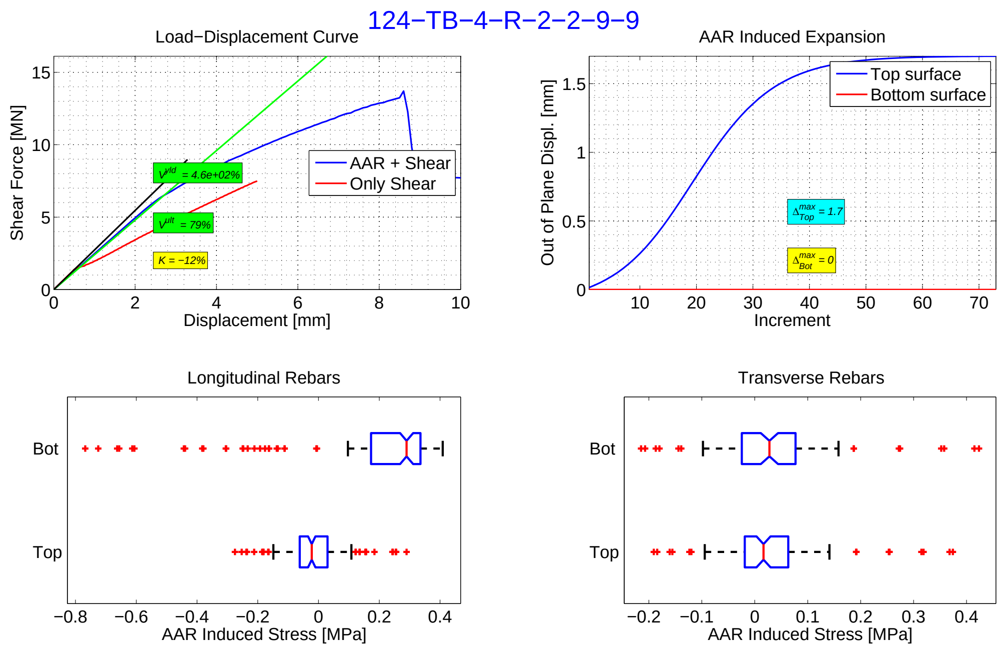

4.1.2.125 Analysis: 125-TB-4-R-2-5-7-7

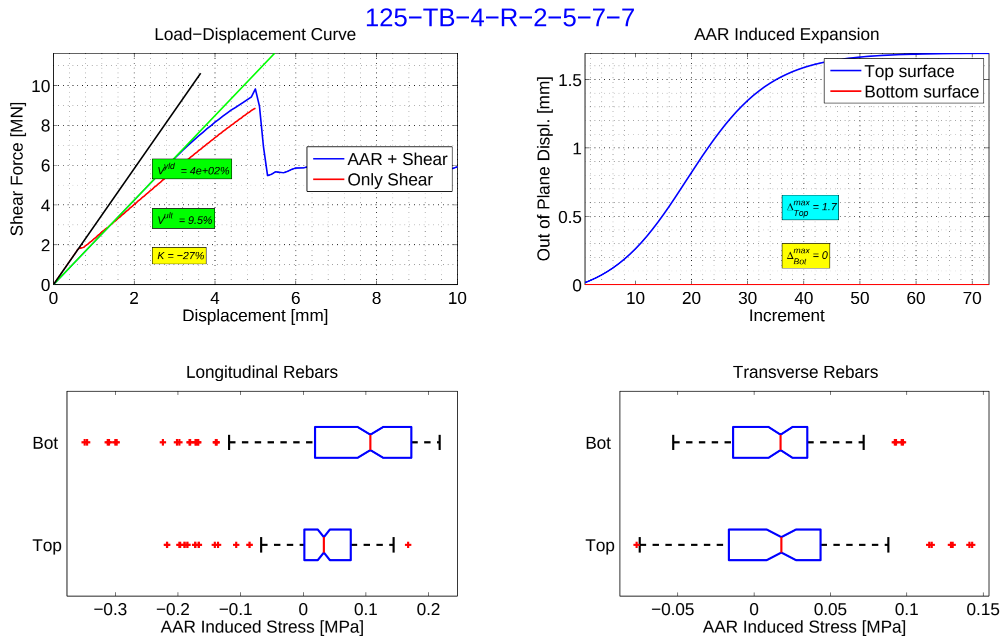

4.1.2.126 Analysis: 126-TB-4-R-2-5-7-9

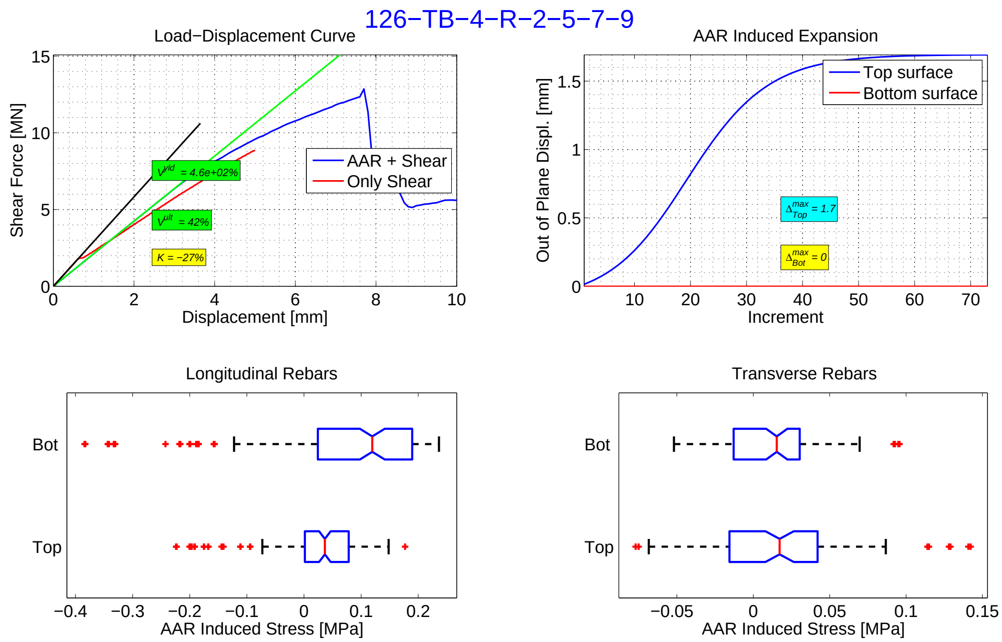

4.1.2.127 Analysis: 127-TB-4-R-2-5-9-7

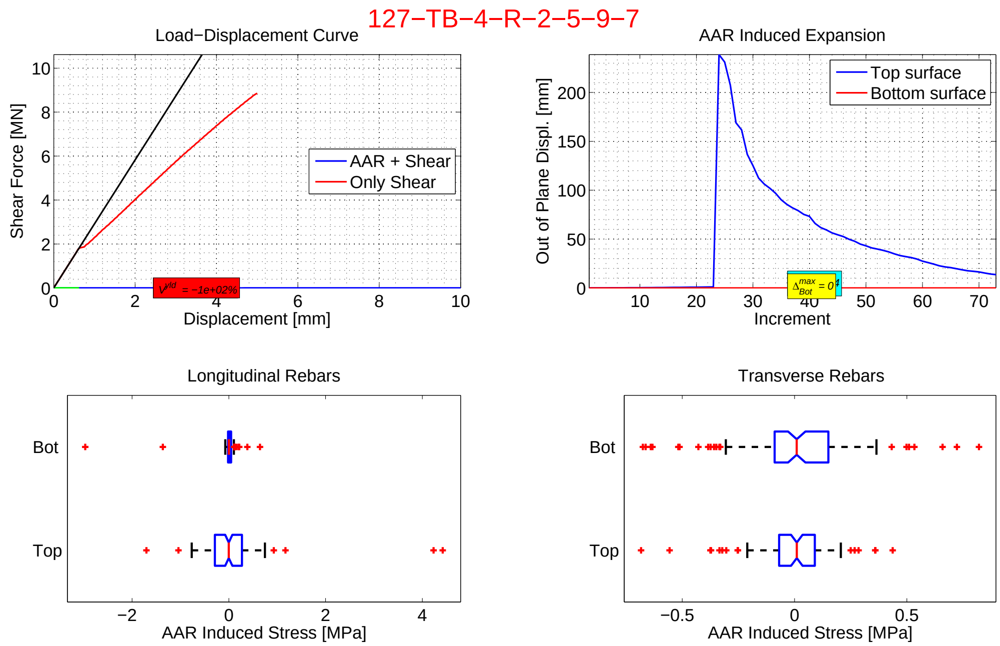

4.1.2.128 Analysis: 128-TB-4-R-2-5-9-9

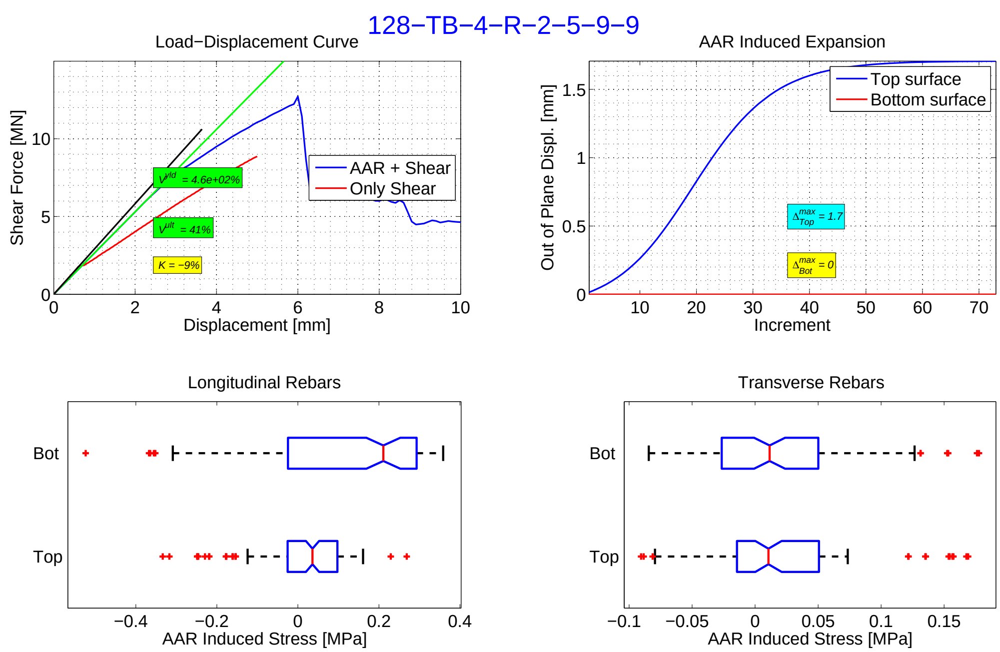

4.1.2.129 Analysis: 129-TB-4-R-2-10-7-7

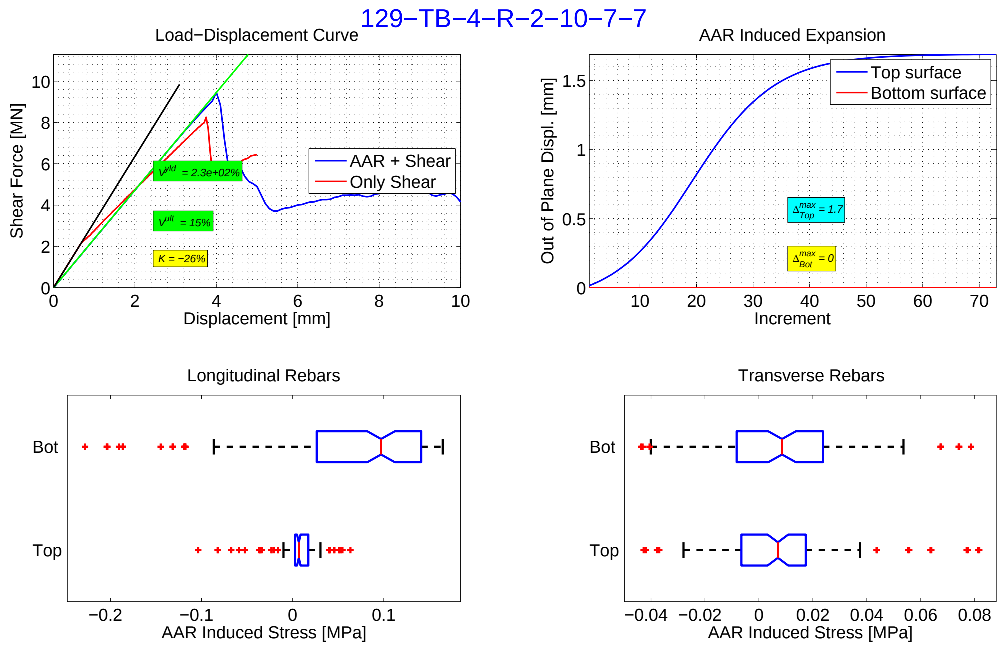

4.1.2.130 Analysis: 130-TB-4-R-2-10-7-9

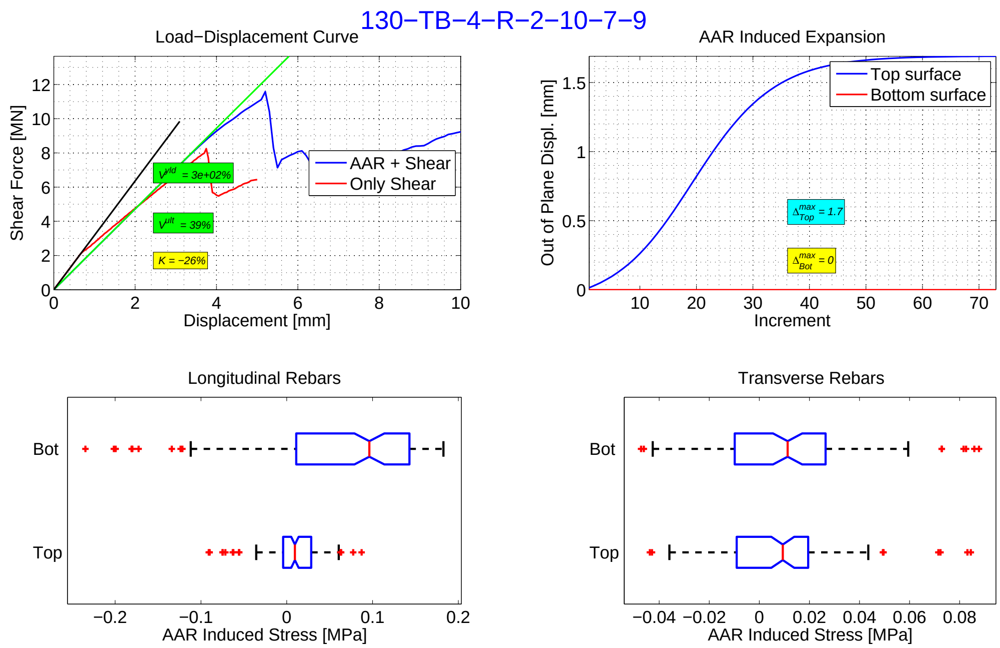

4.1.2.131 Analysis: 131-TB-4-R-2-10-9-7

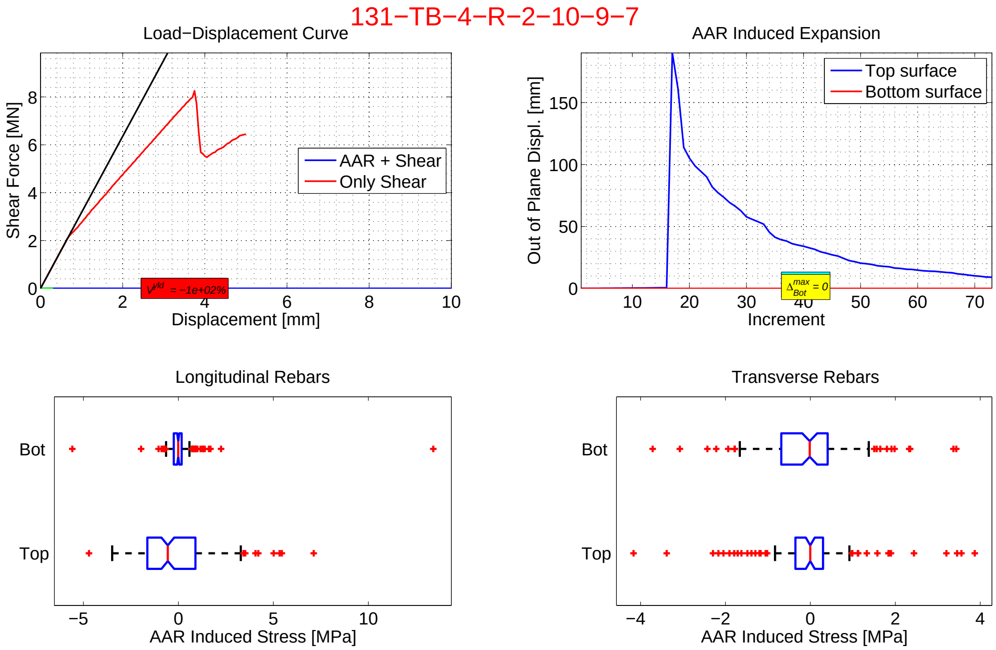

4.1.2.132 Analysis: 132-TB-4-R-2-10-9-9

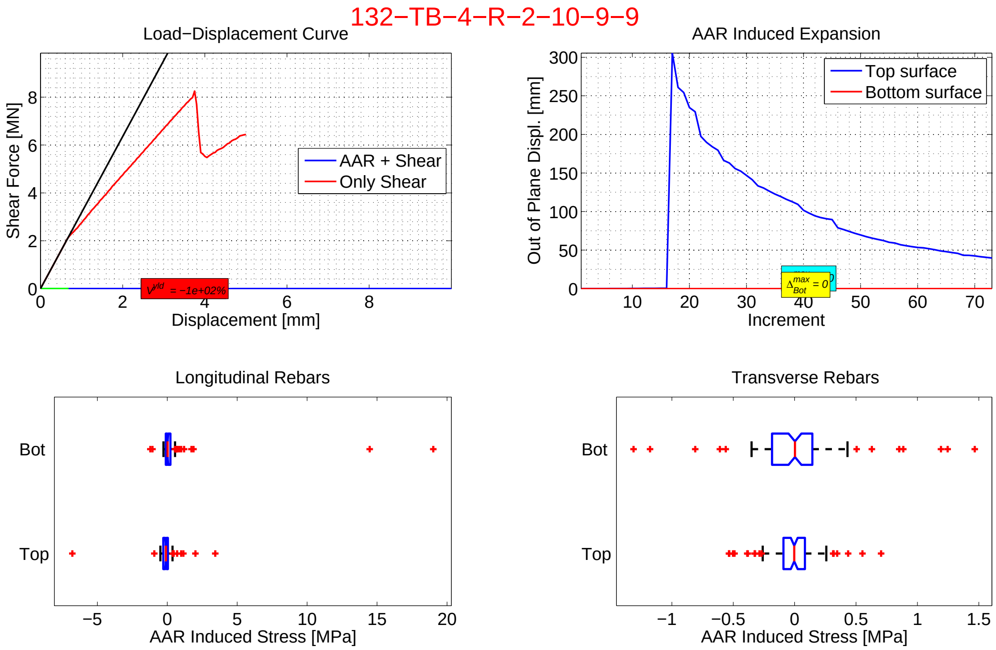

4.1.2.133 Analysis: 133-TB-4-R-3-2-7-7

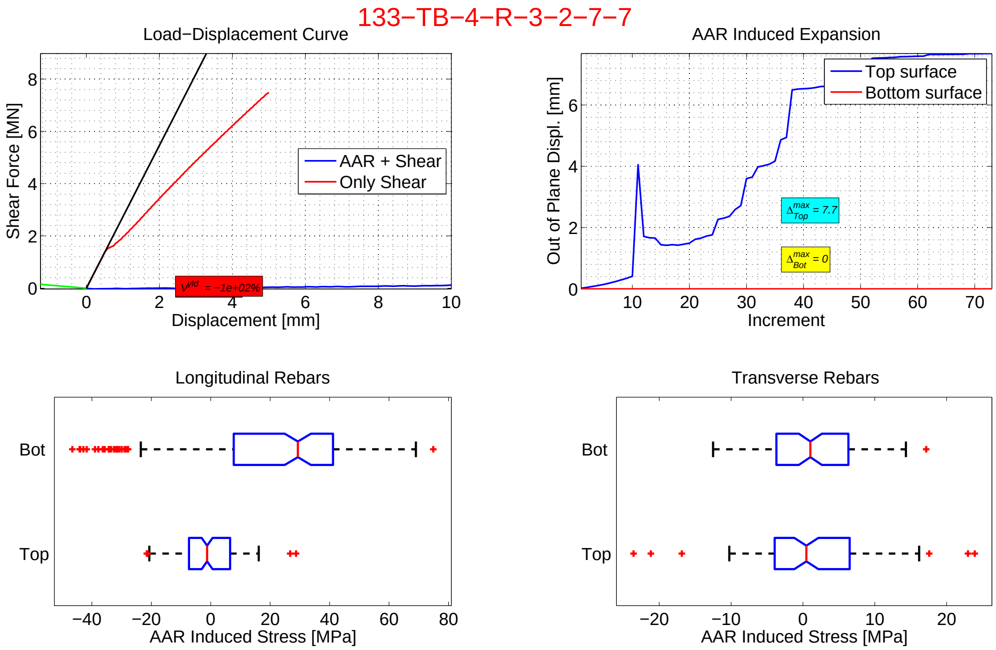

4.1.2.134 Analysis: 134-TB-4-R-3-2-7-9

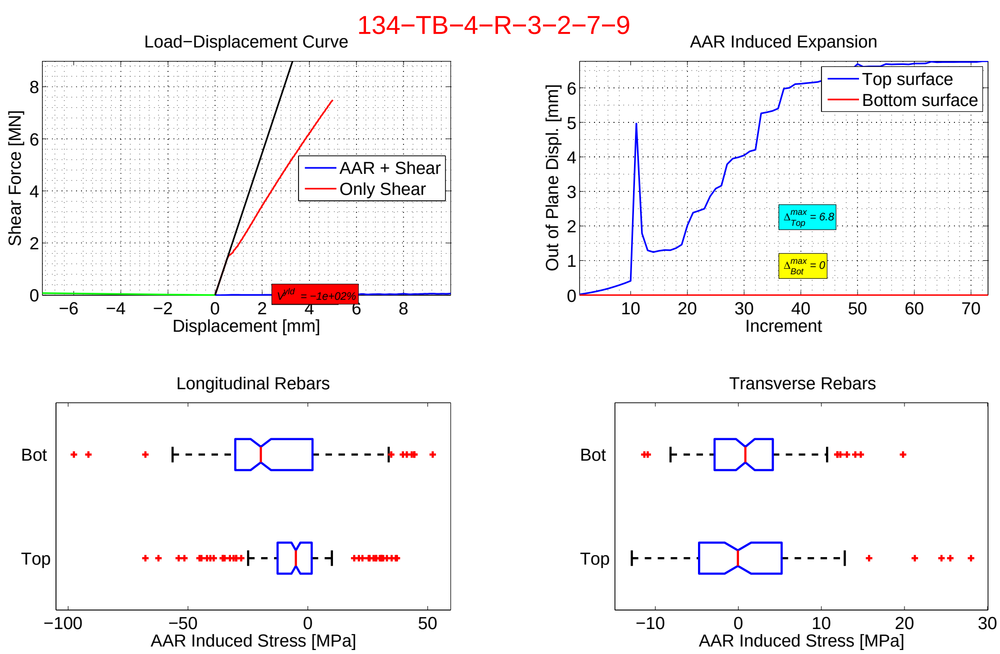

4.1.2.135 Analysis: 135-TB-4-R-3-2-9-7

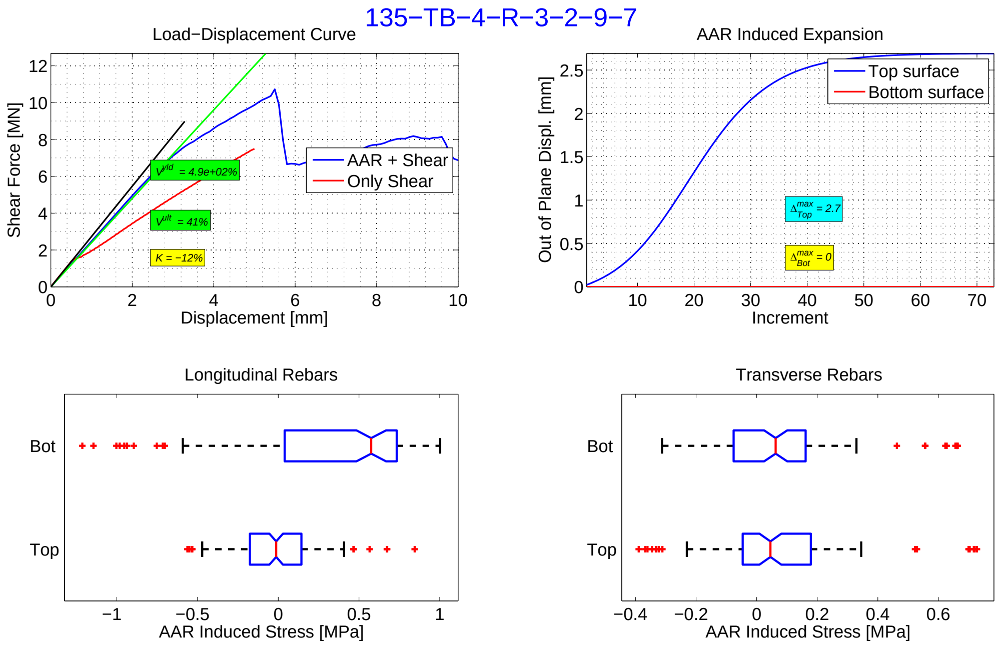

4.1.2.136 Analysis: 136-TB-4-R-3-2-9-9

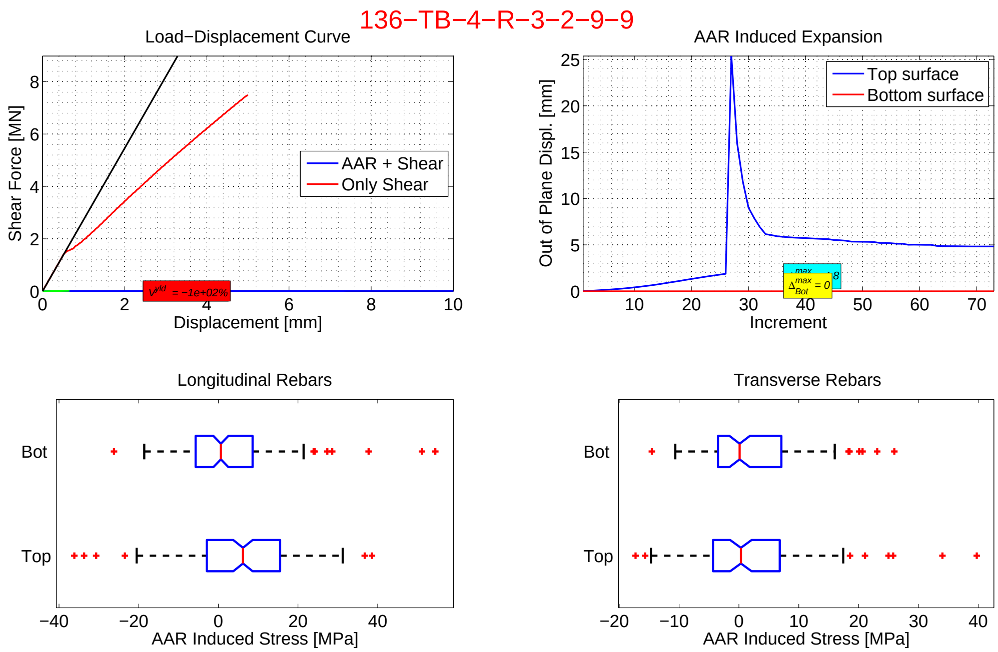

4.1.2.137 Analysis: 137-TB-4-R-3-5-7-7

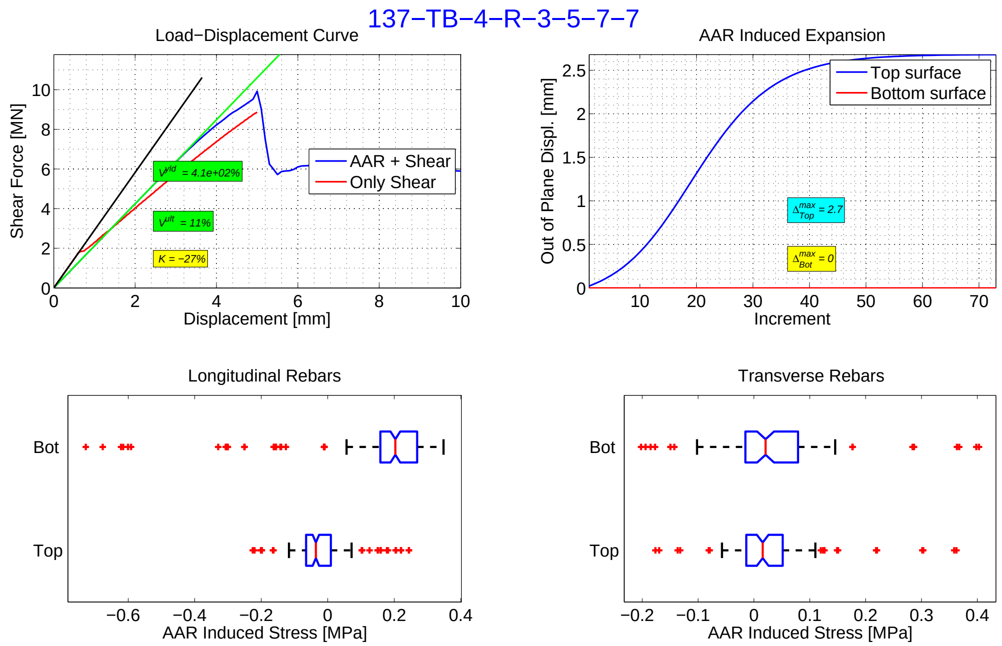

4.1.2.138 Analysis: 138-TB-4-R-3-5-7-9

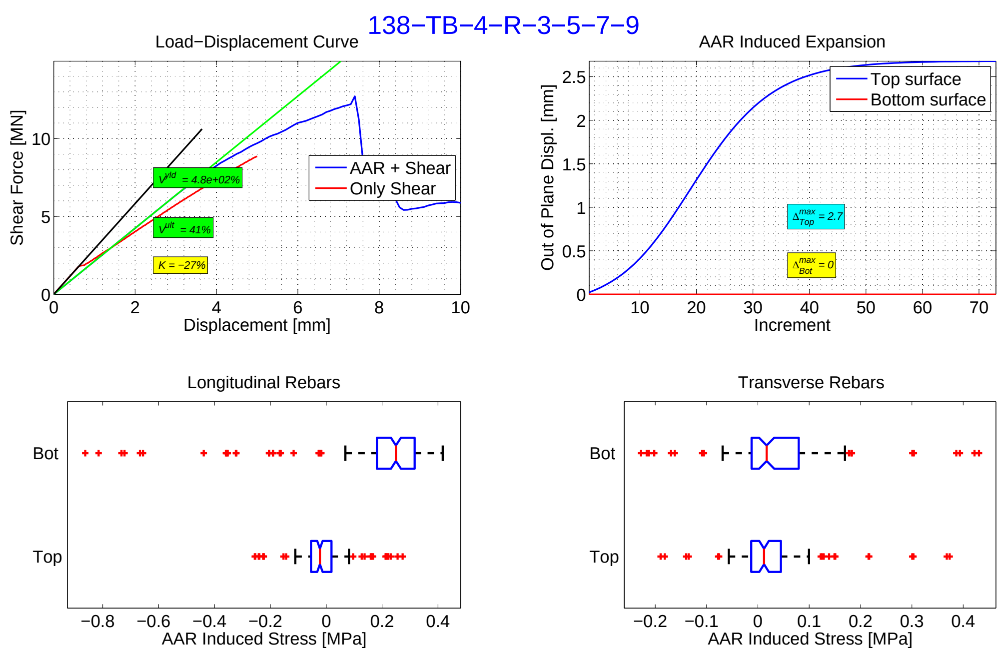

4.1.2.139 Analysis: 139-TB-4-R-3-5-9-7

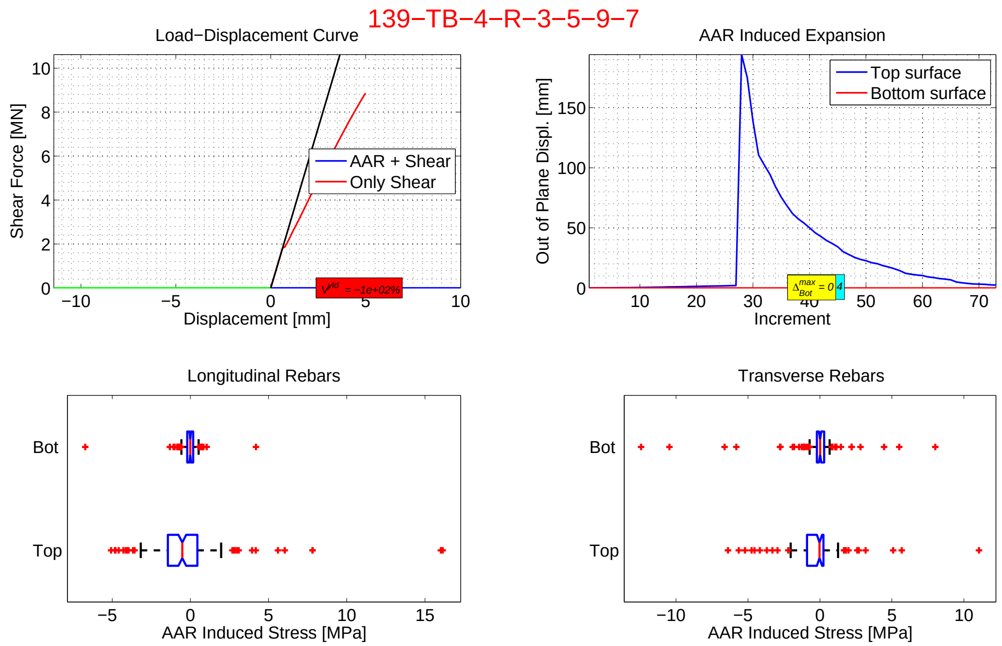

4.1.2.140 Analysis: 140-TB-4-R-3-5-9-9

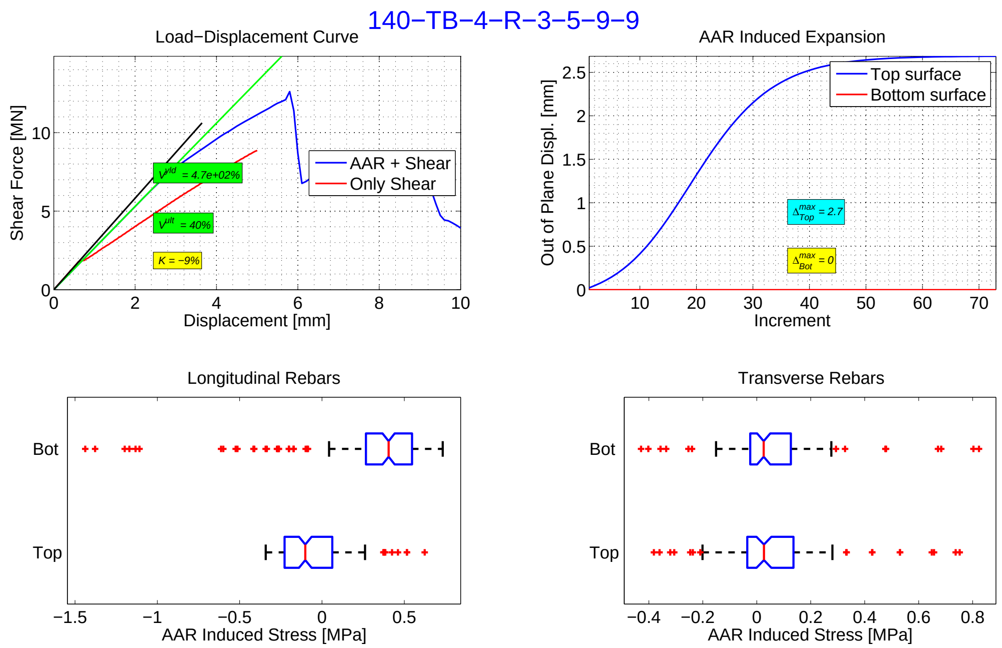

4.1.2.141 Analysis: 141-TB-4-R-3-10-7-7

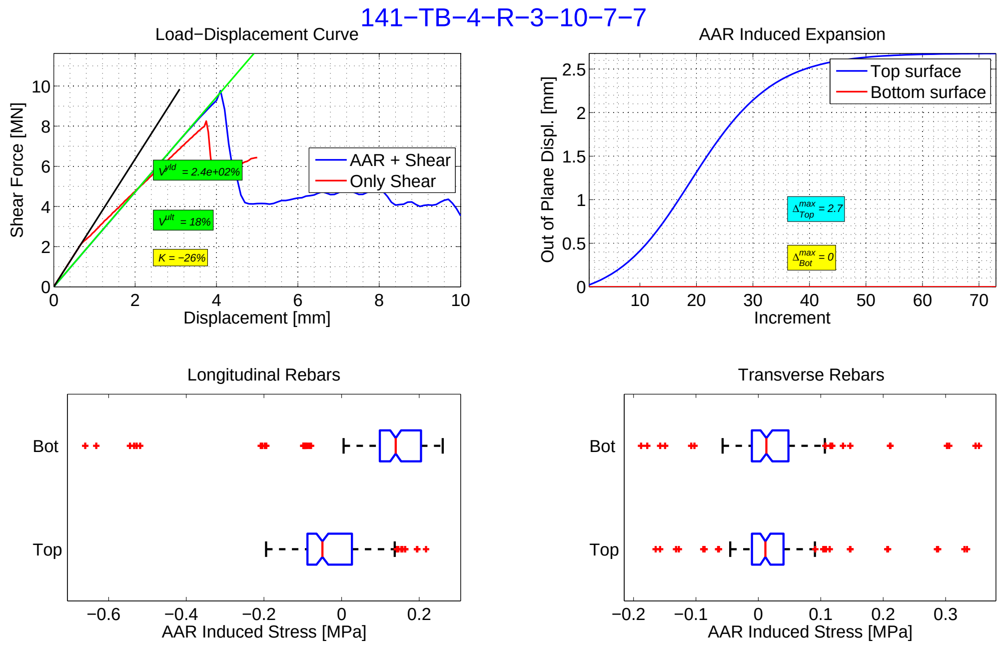

4.1.2.142 Analysis: 142-TB-4-R-3-10-7-9

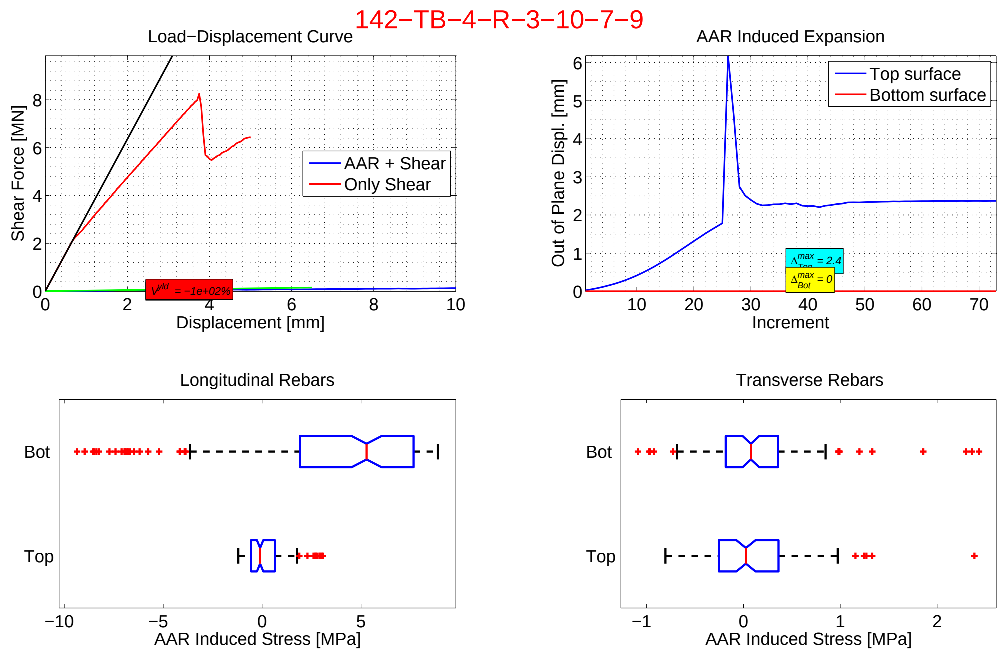

4.1.2.143 Analysis: 143-TB-4-R-3-10-9-7

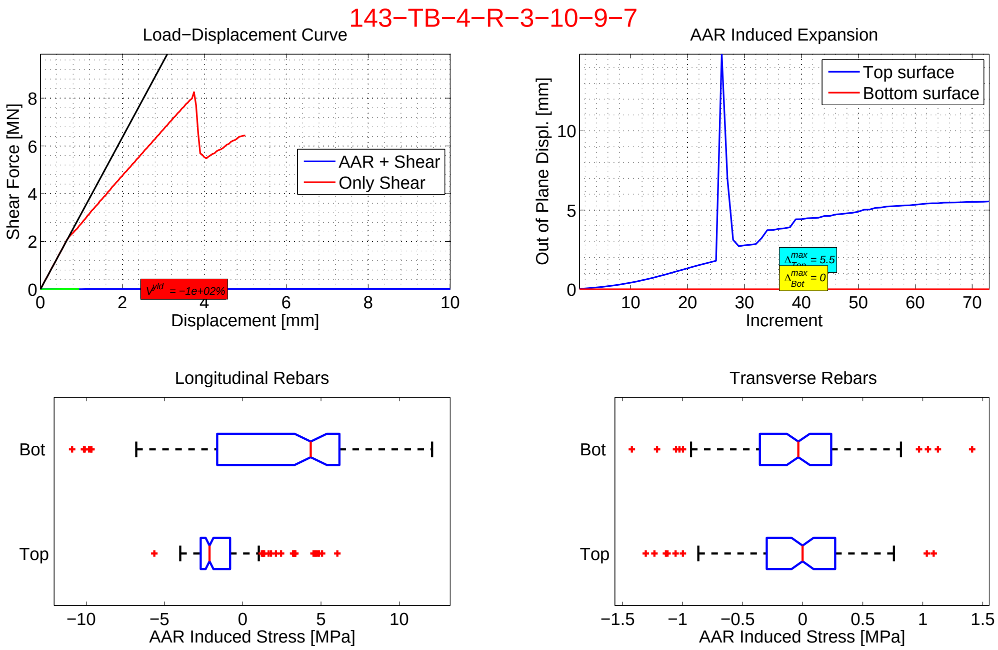

4.1.2.144 Analysis: 144-TB-4-R-3-10-9-9

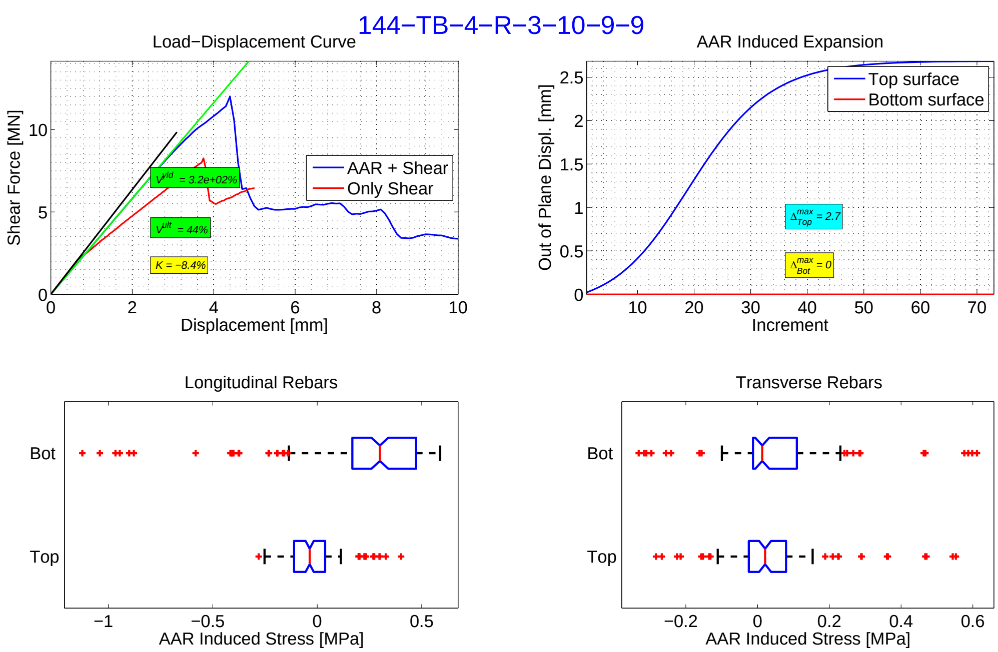

4.1.2.145 Analysis: 145-TB-2-FR-1-2-7-7

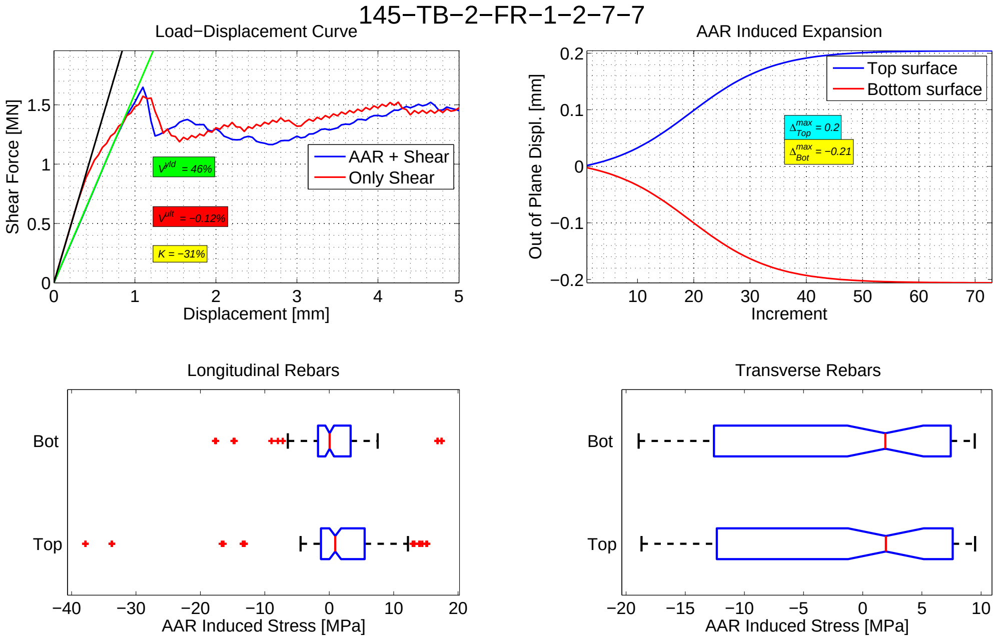

4.1.2.146 Analysis: 146-TB-2-FR-1-2-7-9

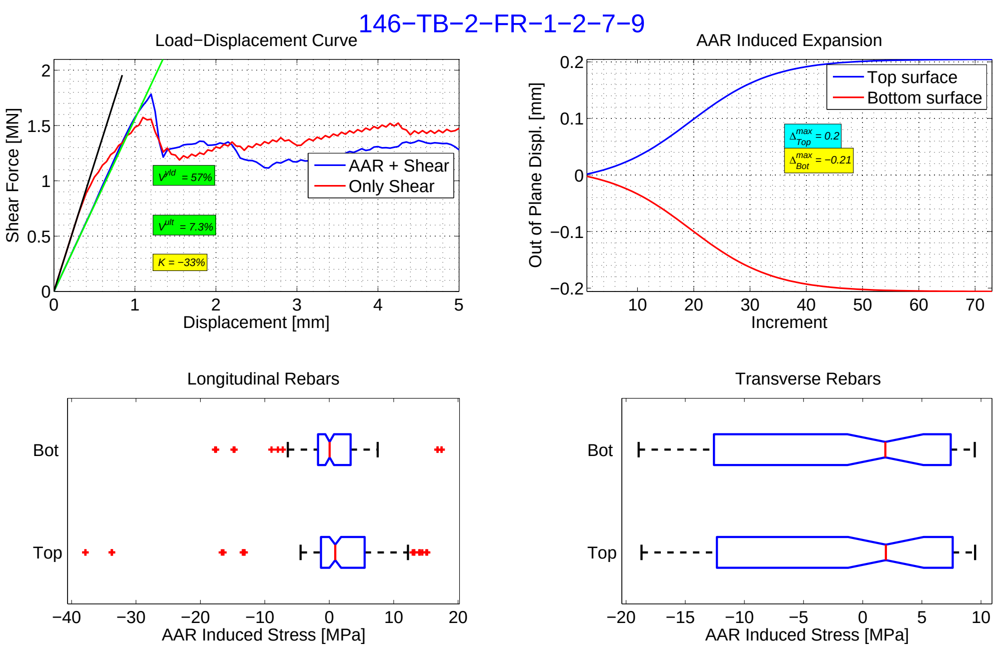

4.1.2.147 Analysis: 147-TB-2-FR-1-2-9-7

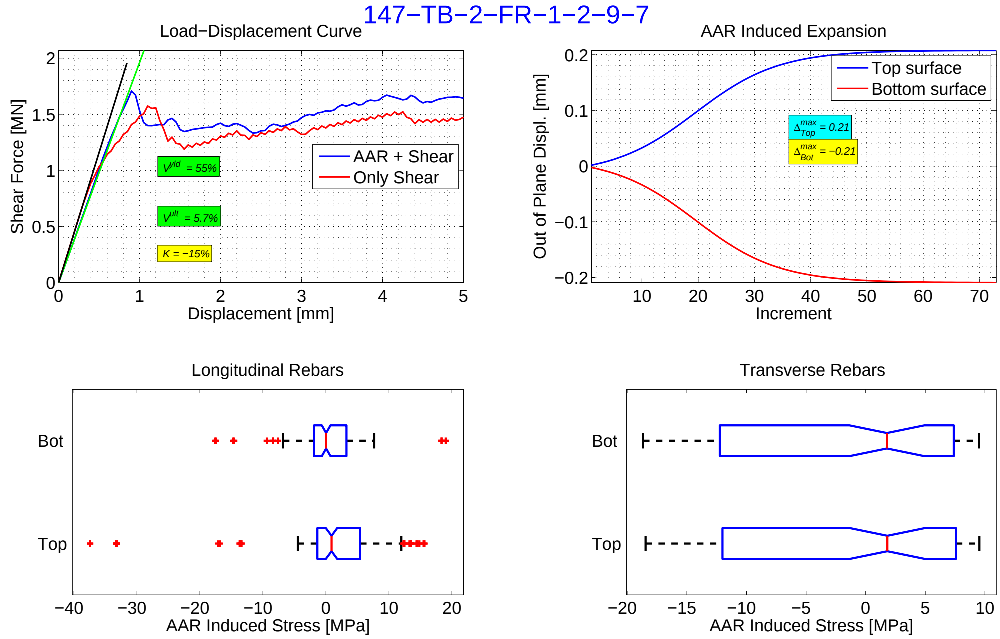

4.1.2.148 Analysis: 148-TB-2-FR-1-2-9-9

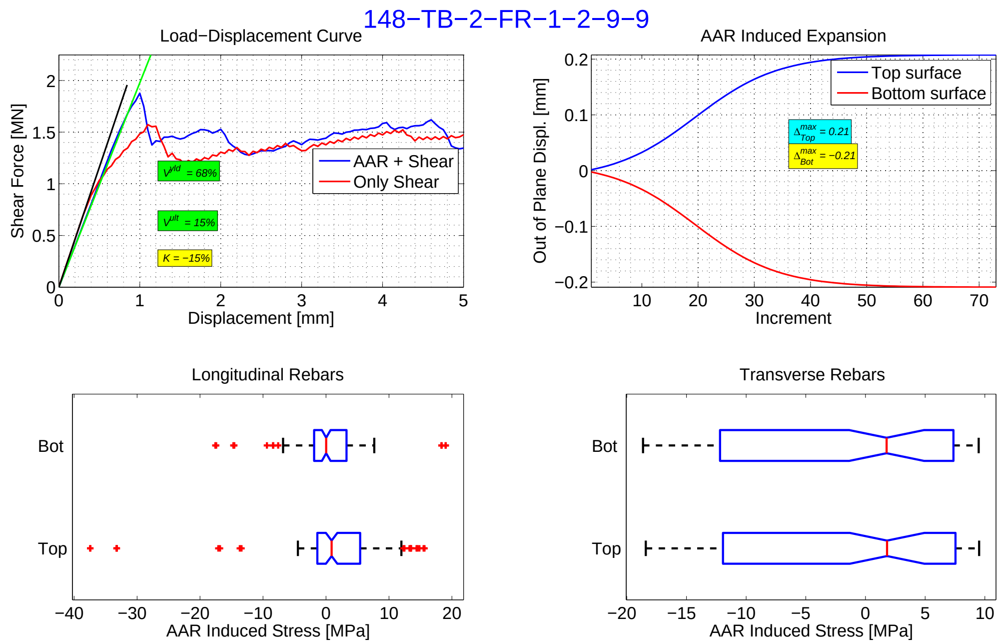

4.1.2.149 Analysis: 149-TB-2-FR-1-5-7-7

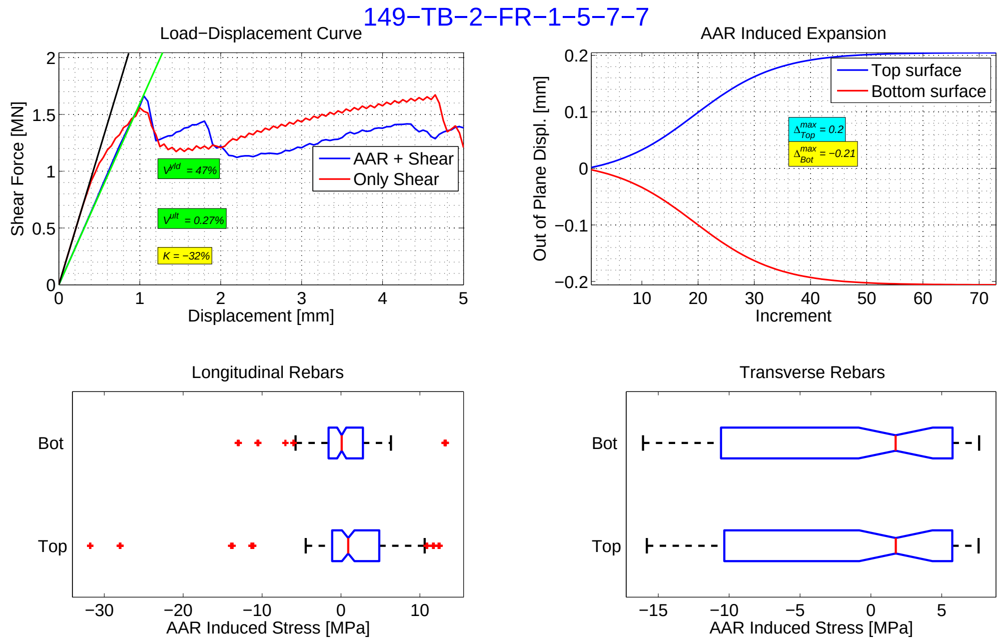

4.1.2.150 Analysis: 150-TB-2-FR-1-5-7-9

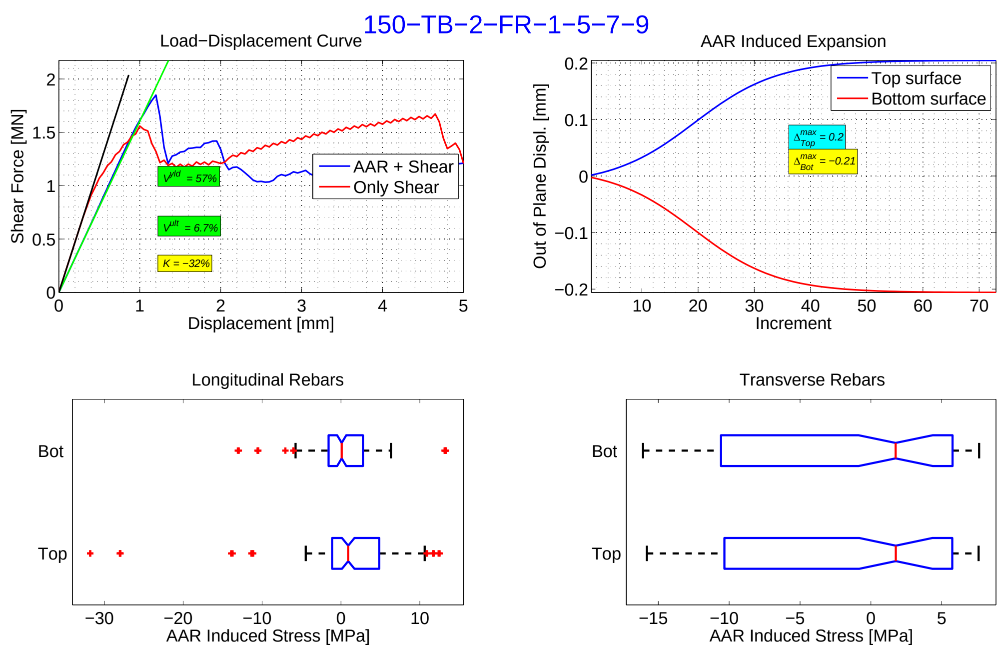

4.1.2.151 Analysis: 151-TB-2-FR-1-5-9-7

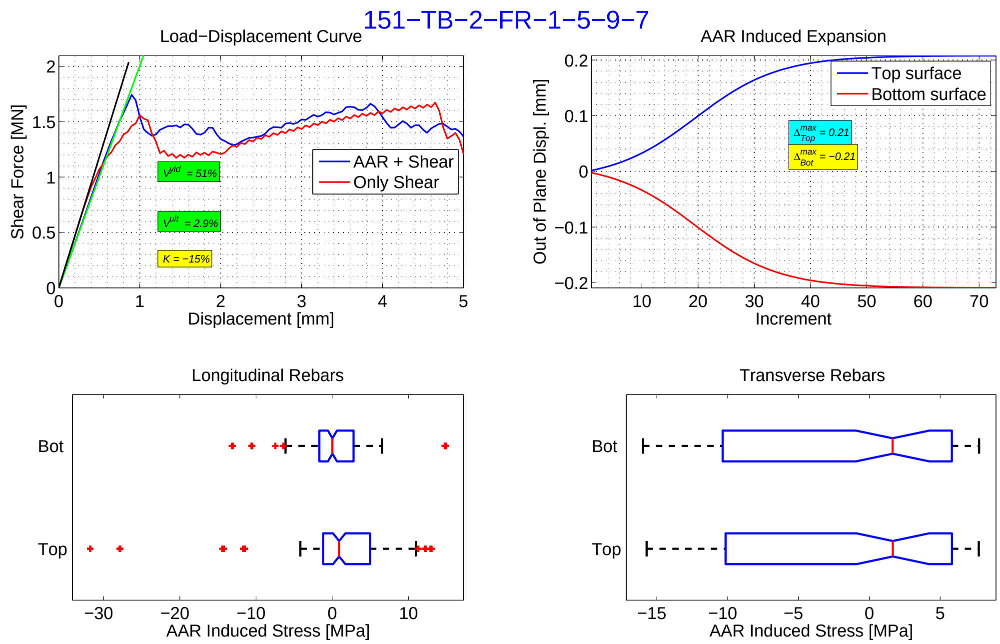

4.1.2.152 Analysis: 152-TB-2-FR-1-5-9-9

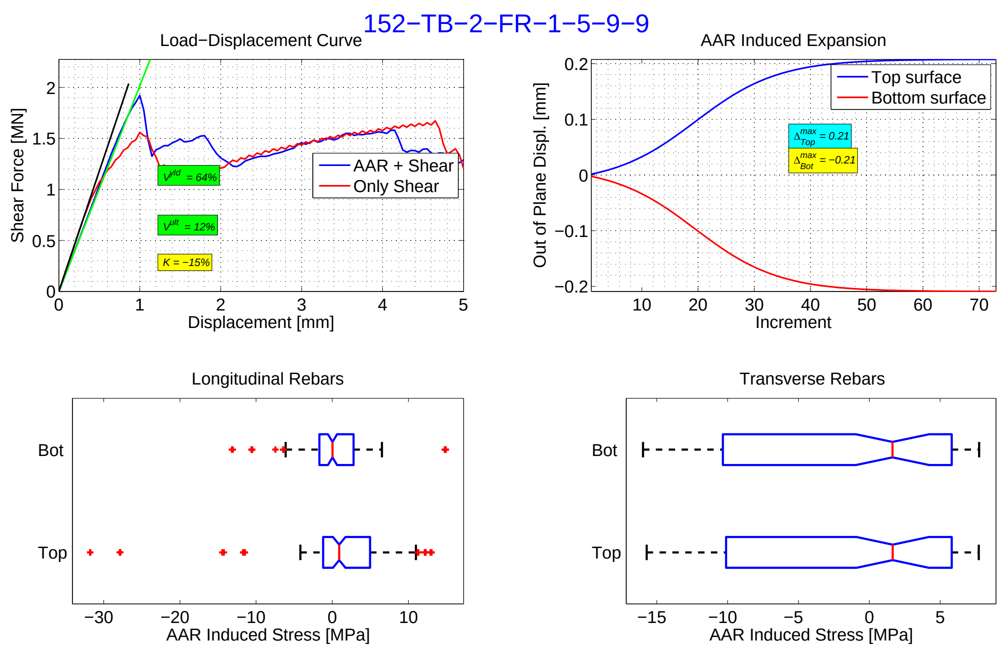

4.1.2.153 Analysis: 153-TB-2-FR-1-10-7-7

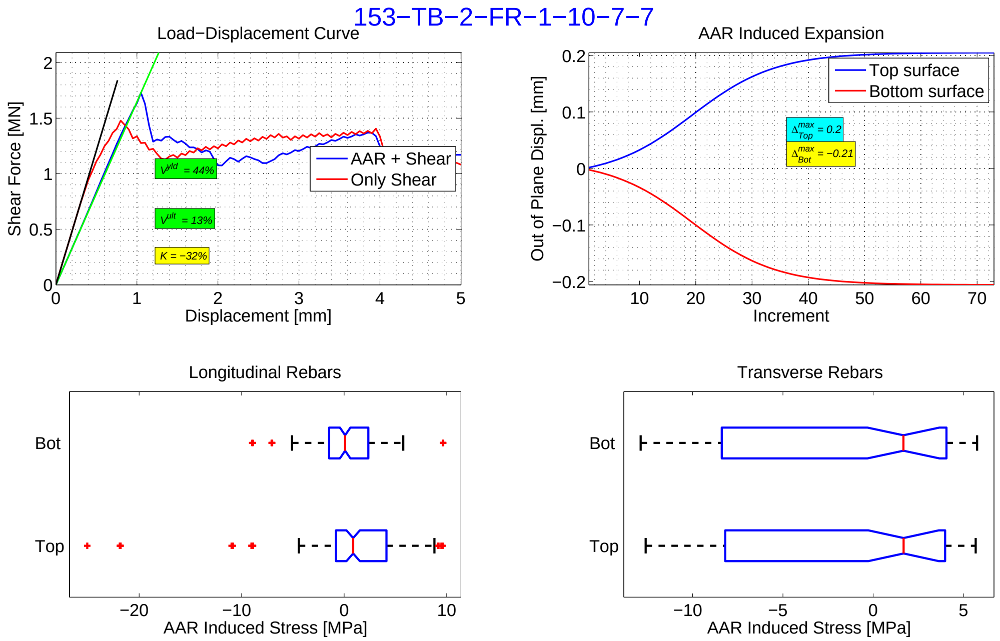

4.1.2.154 Analysis: 154-TB-2-FR-1-10-7-9

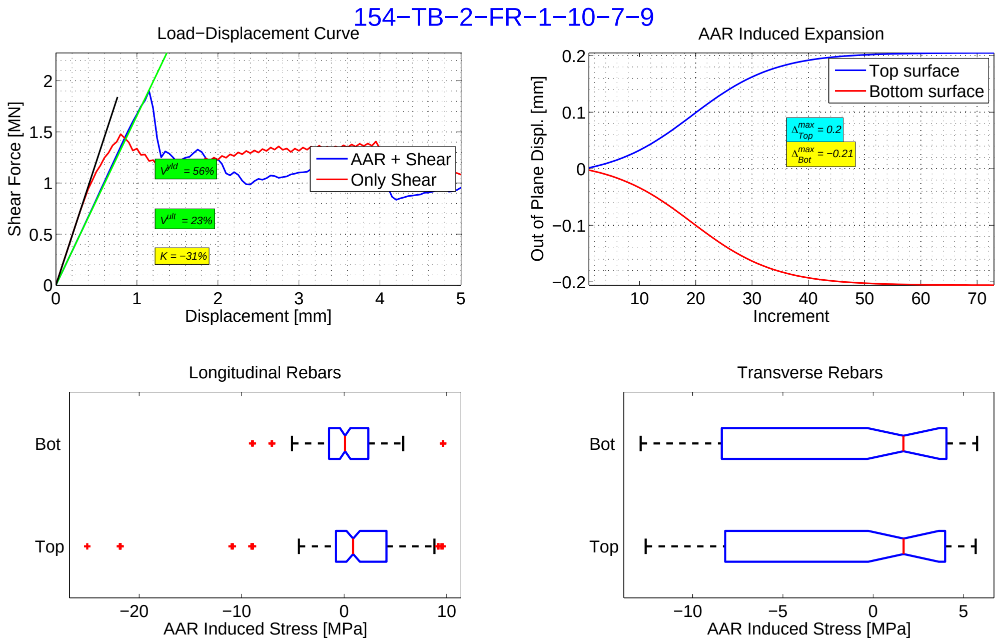

4.1.2.155 Analysis: 155-TB-2-FR-1-10-9-7

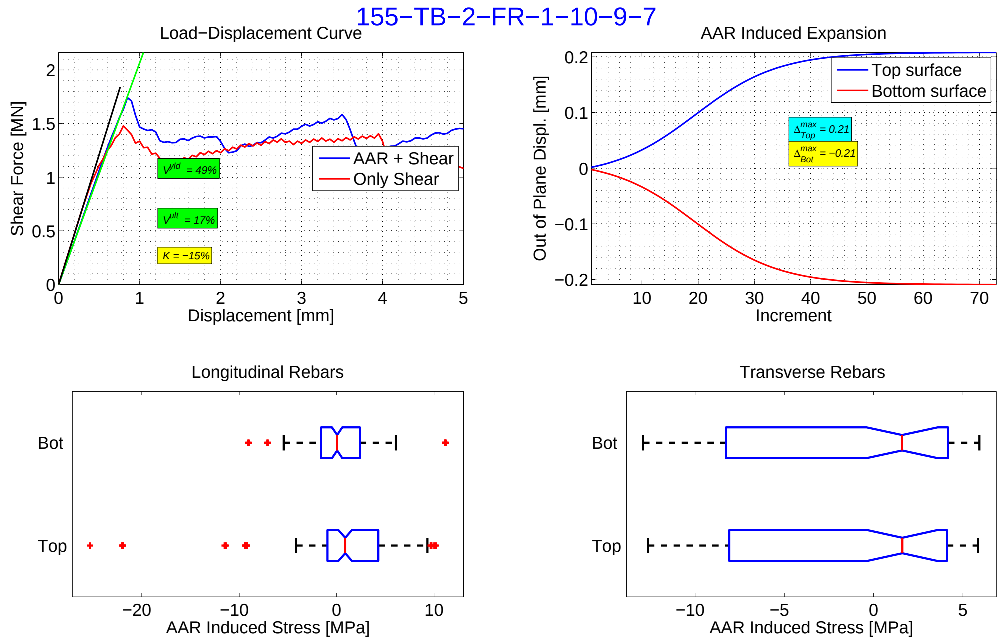

4.1.2.156 Analysis: 156-TB-2-FR-1-10-9-9

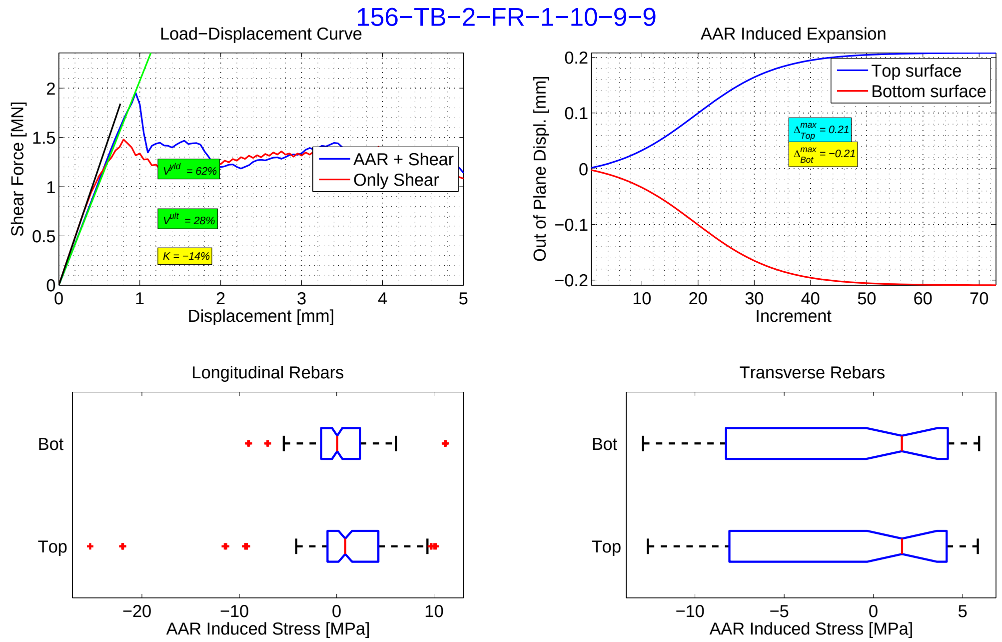

4.1.2.157 Analysis: 157-TB-2-FR-2-2-7-7

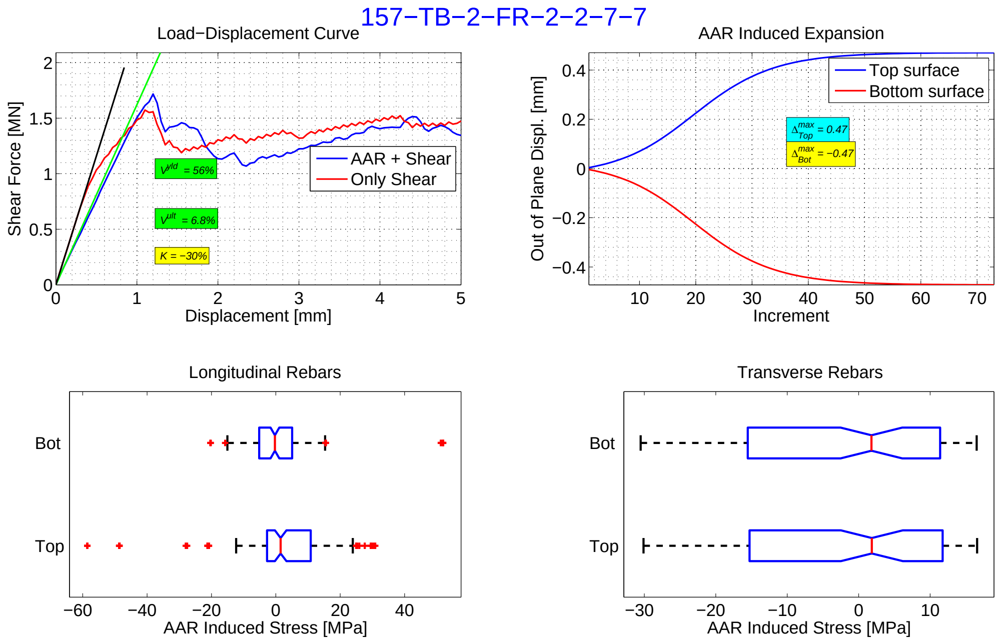

4.1.2.158 Analysis: 158-TB-2-FR-2-2-7-9

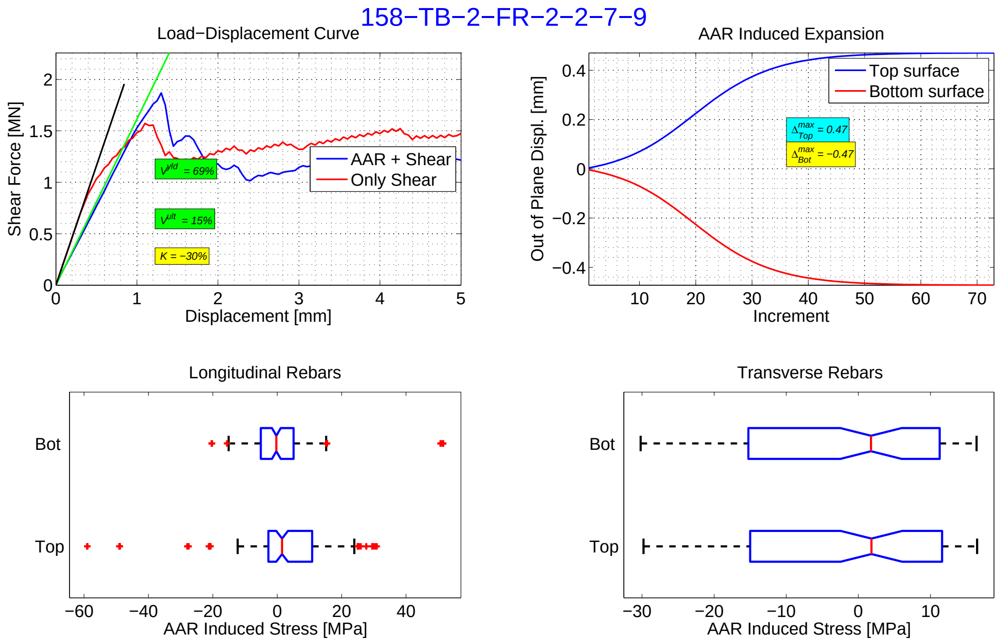

4.1.2.159 Analysis: 159-TB-2-FR-2-2-9-7

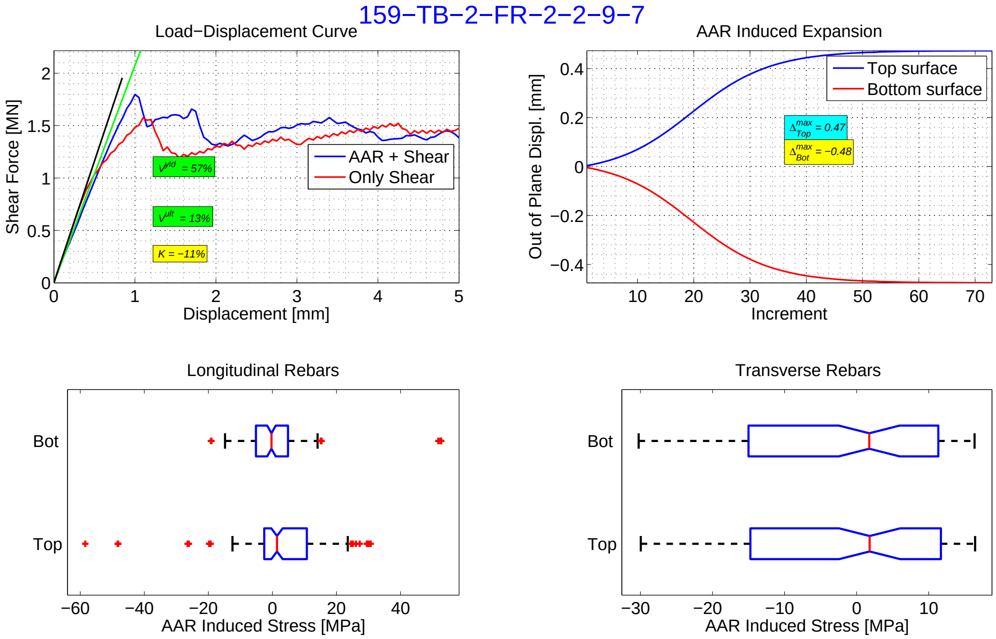

4.1.2.160 Analysis: 160-TB-2-FR-2-2-9-9

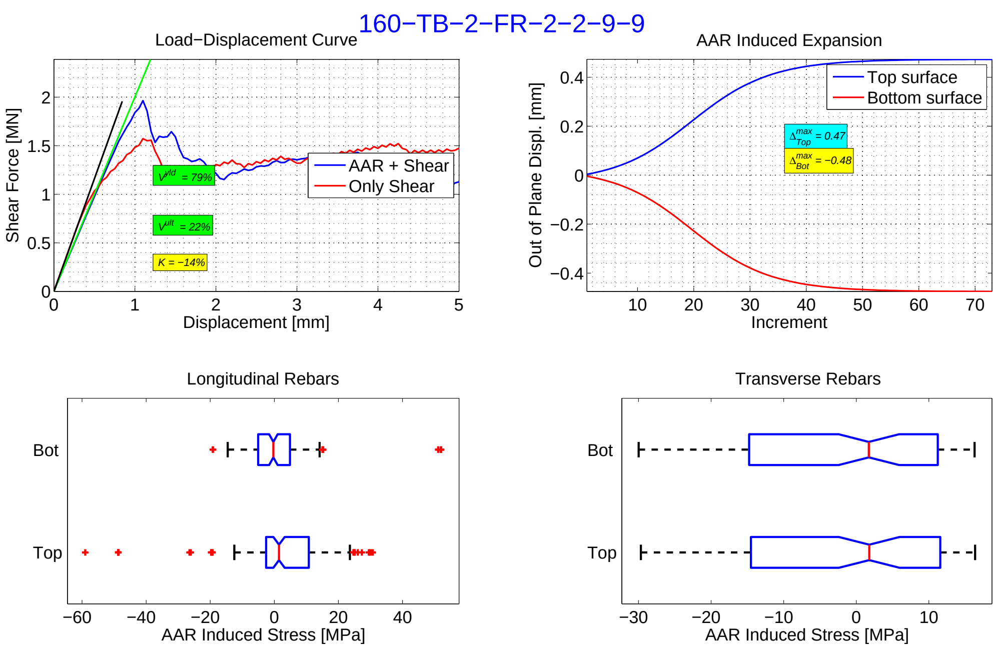

4.1.2.161 Analysis: 161-TB-2-FR-2-5-7-7

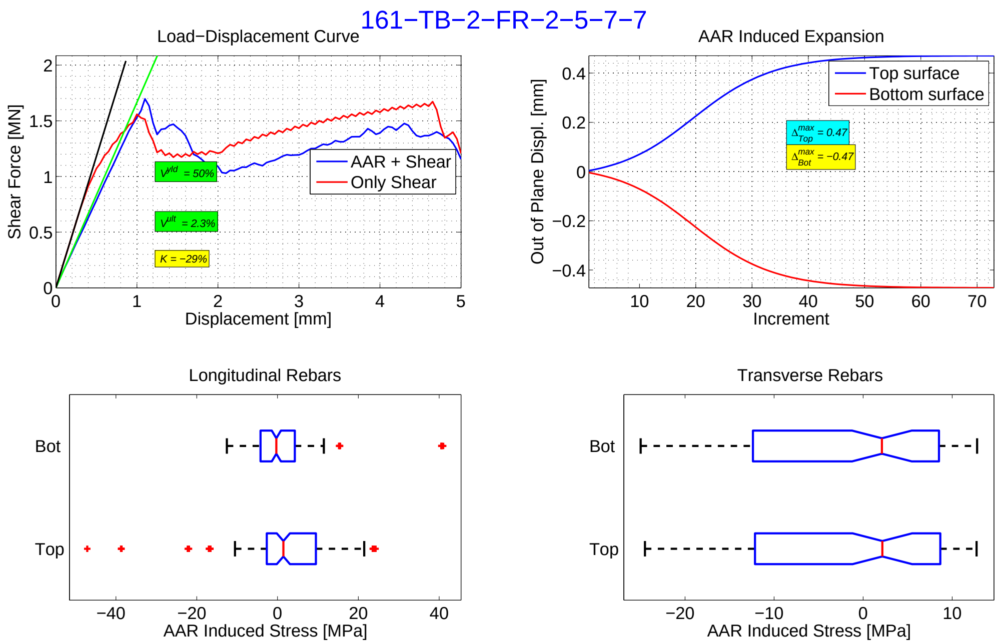

4.1.2.162 Analysis: 162-TB-2-FR-2-5-7-9

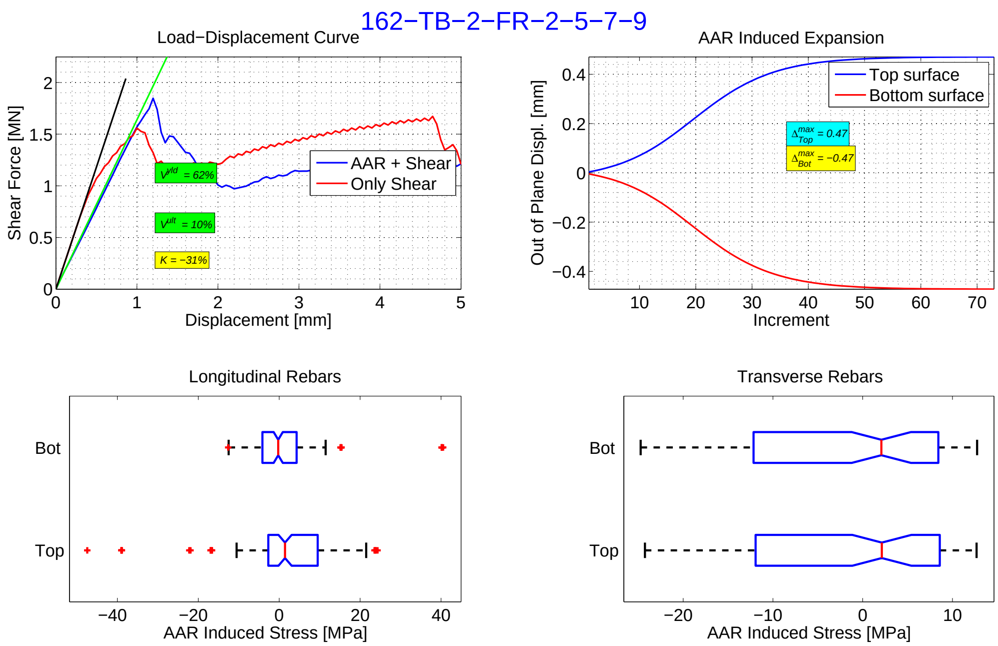

4.1.2.163 Analysis: 163-TB-2-FR-2-5-9-7

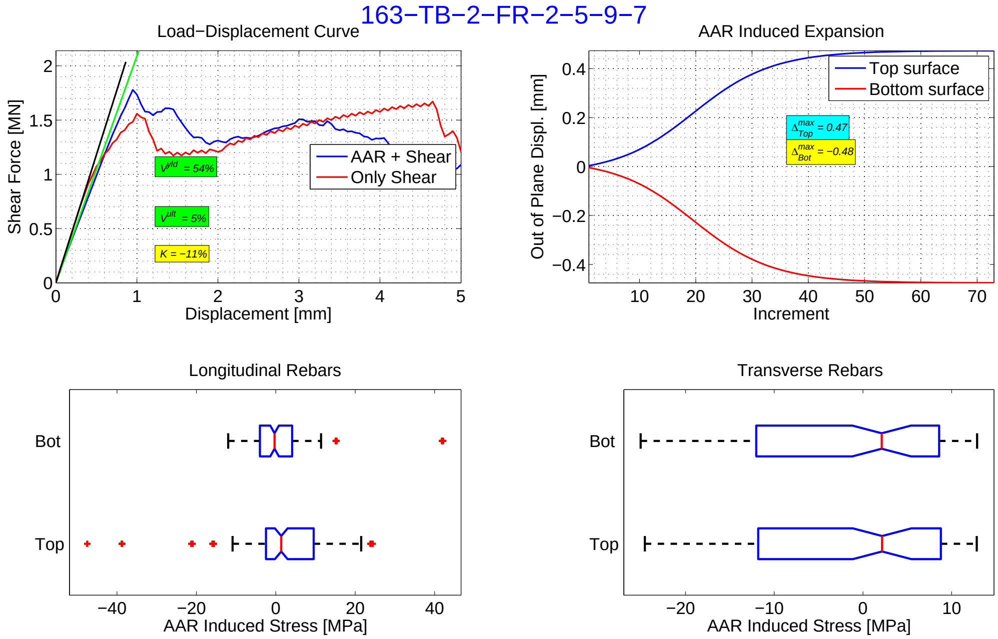

4.1.2.164 Analysis: 164-TB-2-FR-2-5-9-9

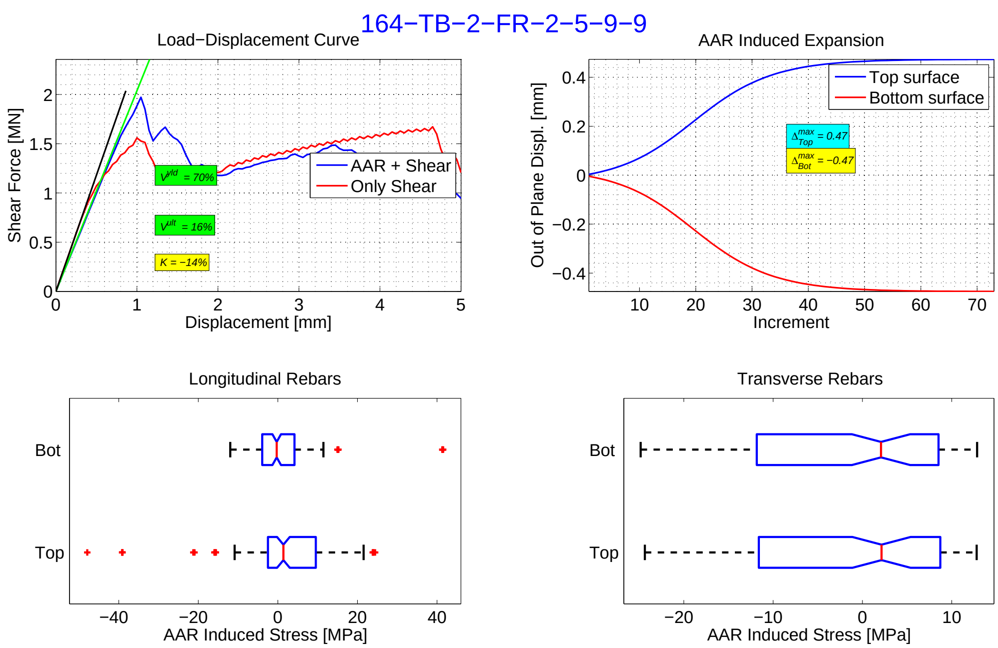

4.1.2.165 Analysis: 165-TB-2-FR-2-10-7-7

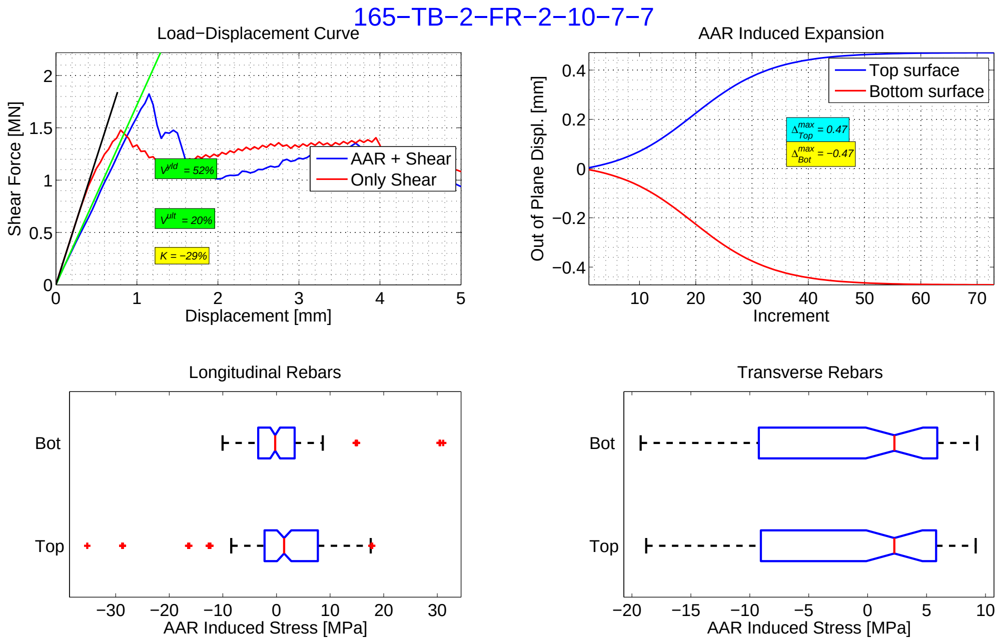

4.1.2.166 Analysis: 166-TB-2-FR-2-10-7-9

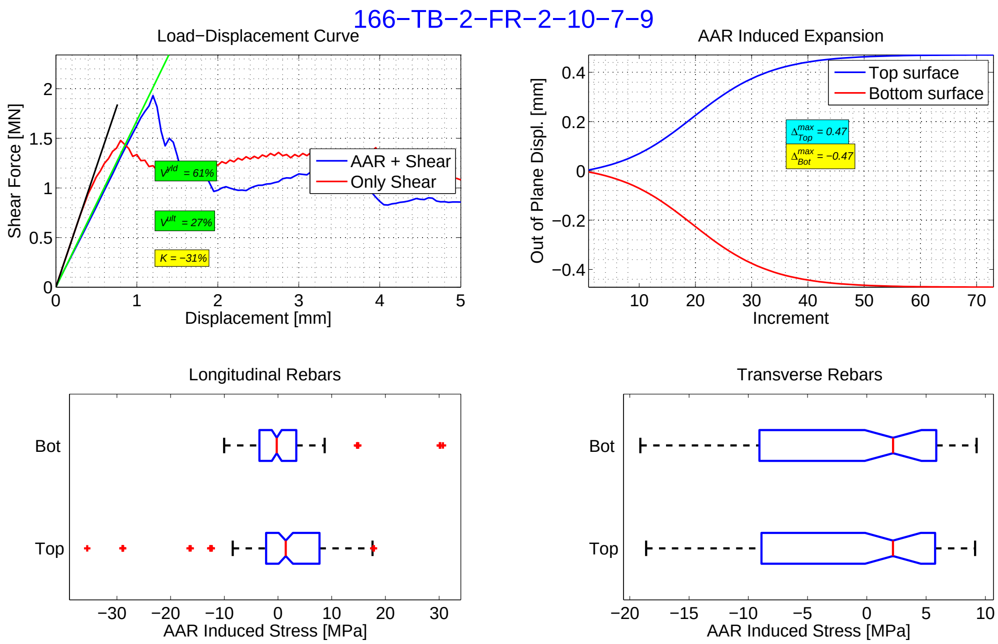

4.1.2.167 Analysis: 167-TB-2-FR-2-10-9-7

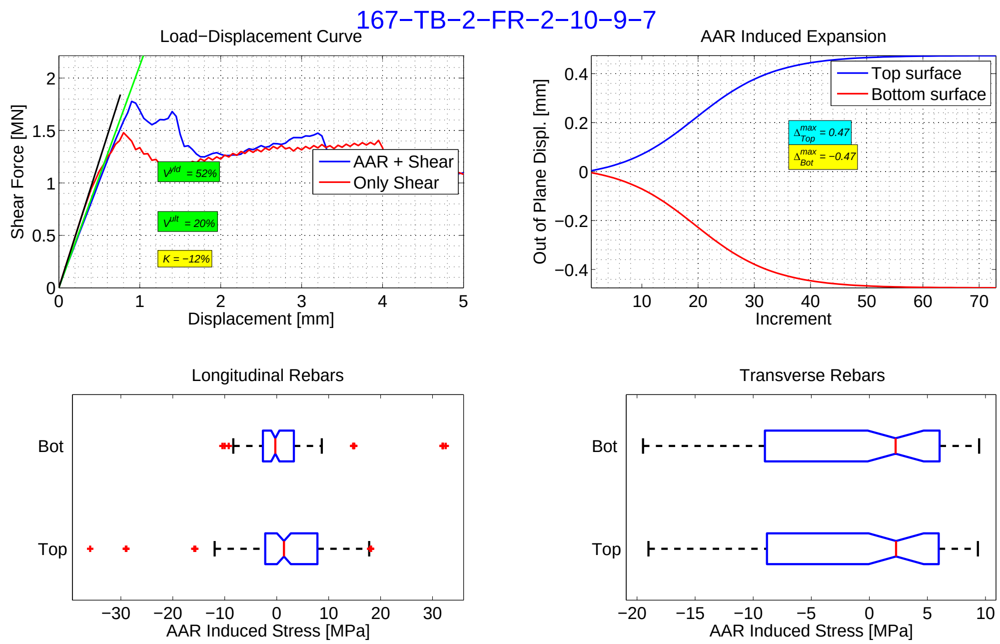

4.1.2.168 Analysis: 168-TB-2-FR-2-10-9-9

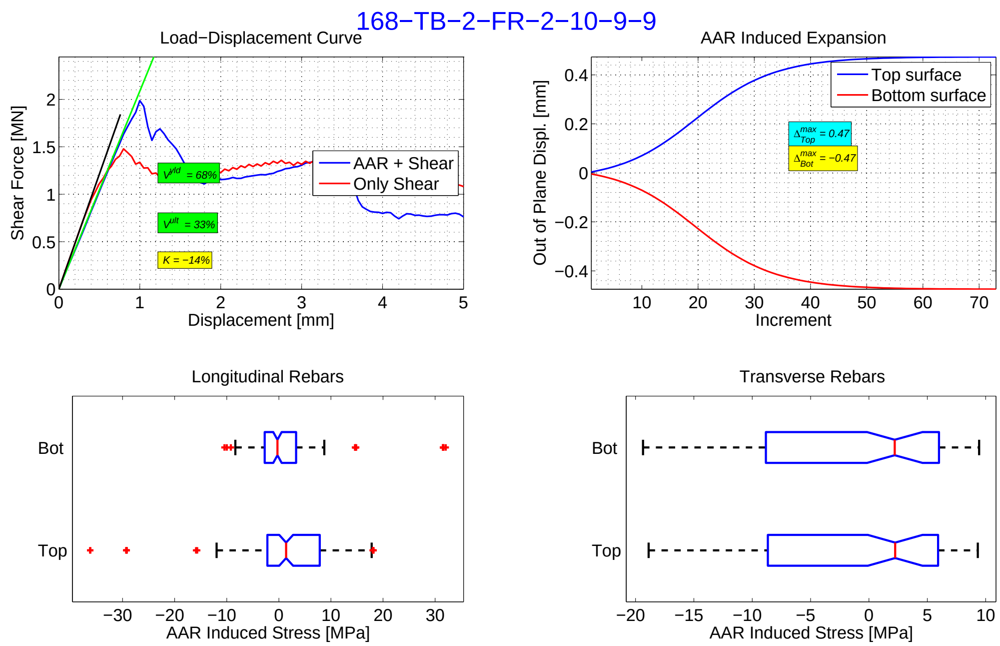

4.1.2.169 Analysis: 169-TB-2-FR-3-2-7-7

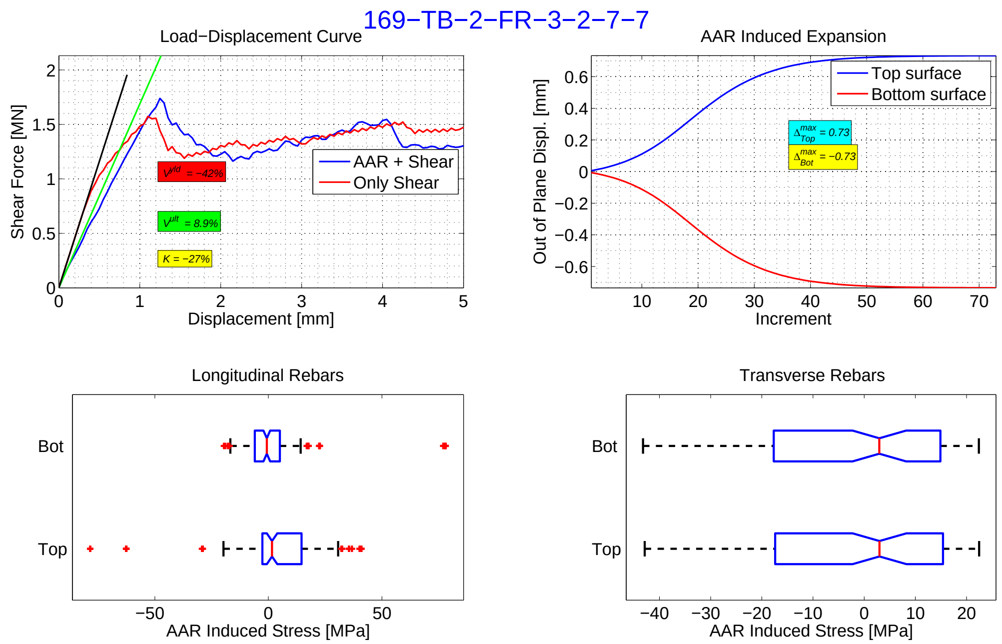

4.1.2.170 Analysis: 170-TB-2-FR-3-2-7-9

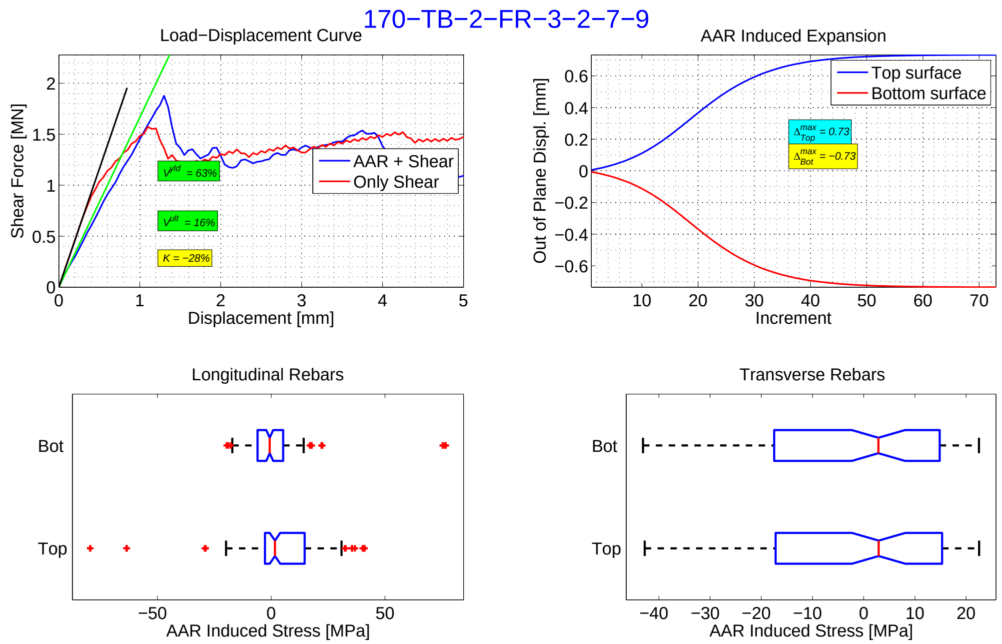

4.1.2.171 Analysis: 171-TB-2-FR-3-2-9-7

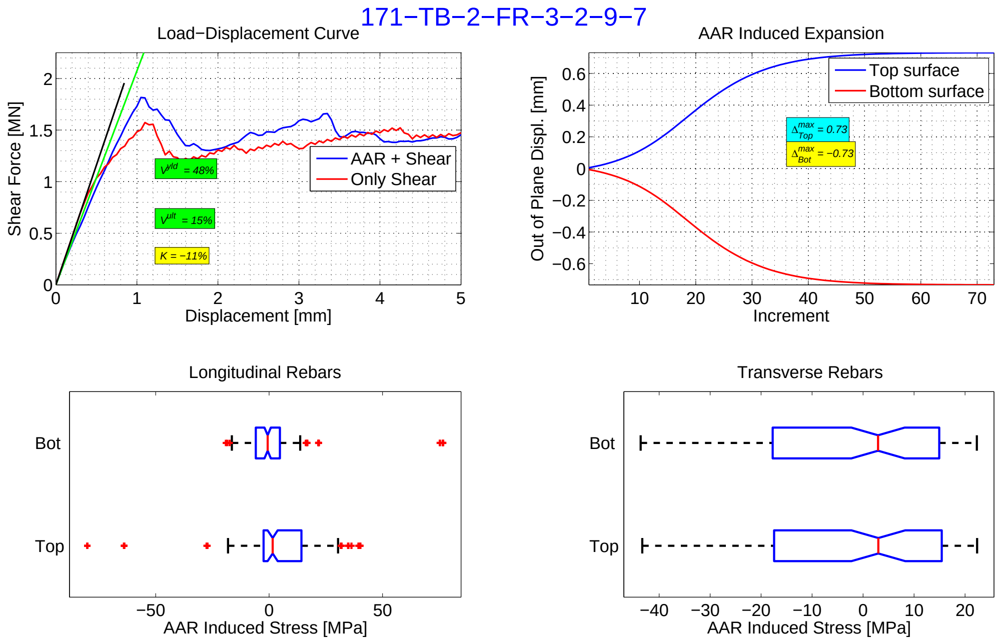

4.1.2.172 Analysis: 172-TB-2-FR-3-2-9-9

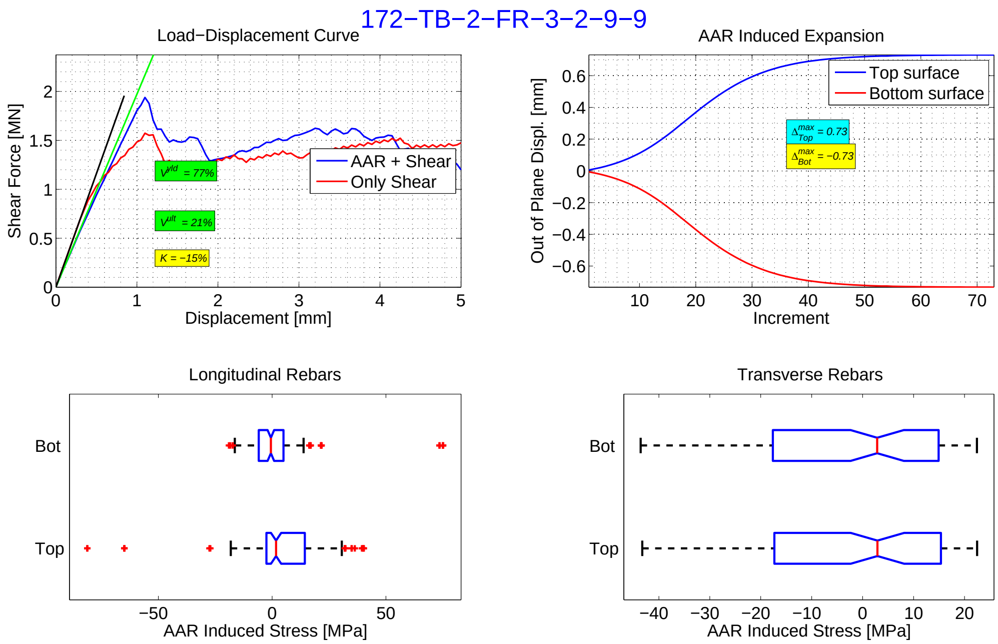

4.1.2.173 Analysis: 173-TB-2-FR-3-5-7-7

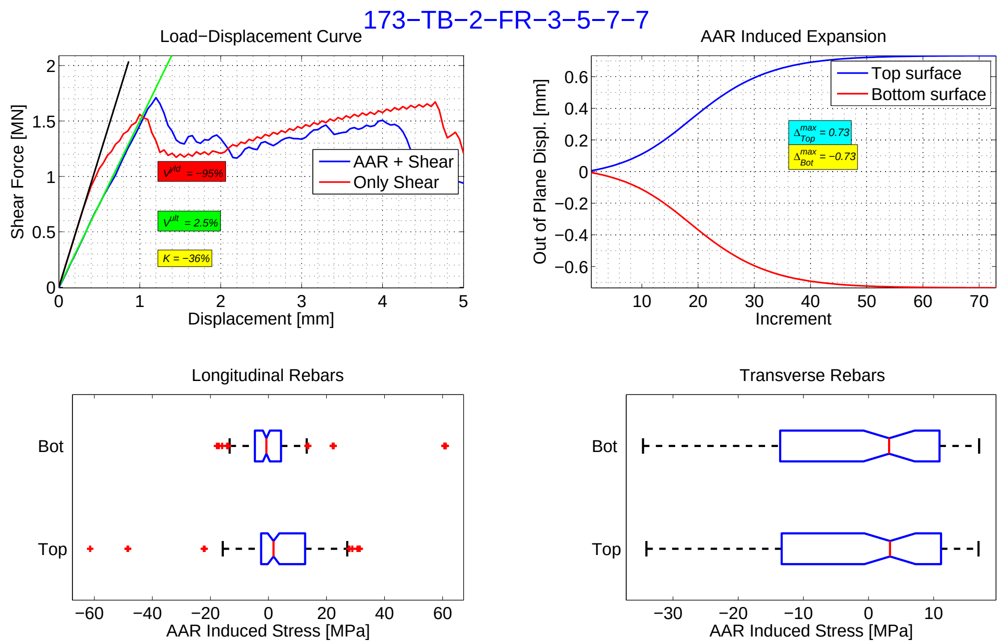

4.1.2.174 Analysis: 174-TB-2-FR-3-5-7-9

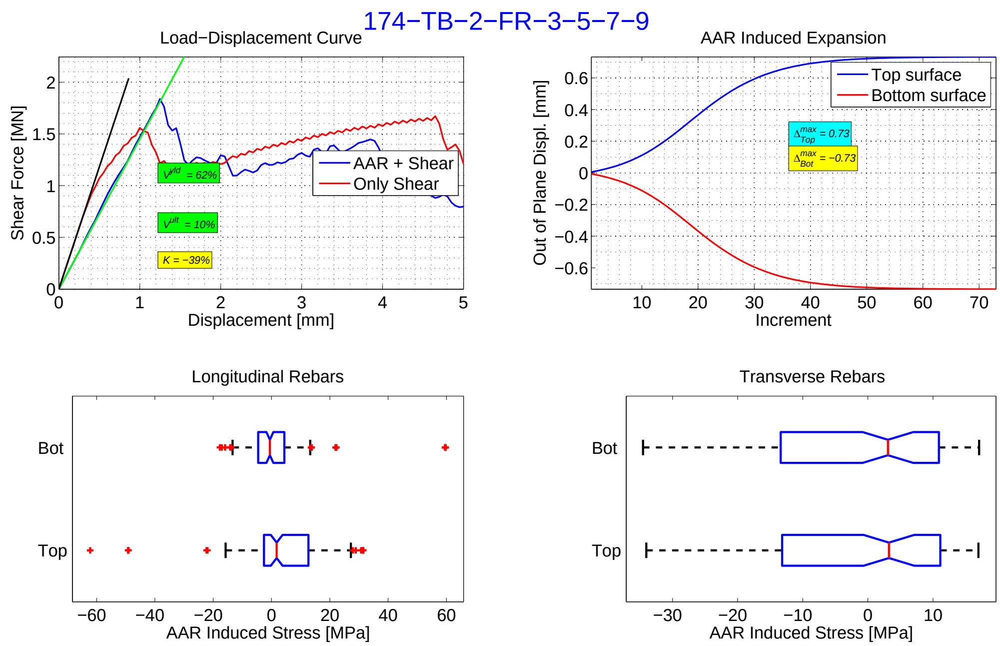

4.1.2.175 Analysis: 175-TB-2-FR-3-5-9-7

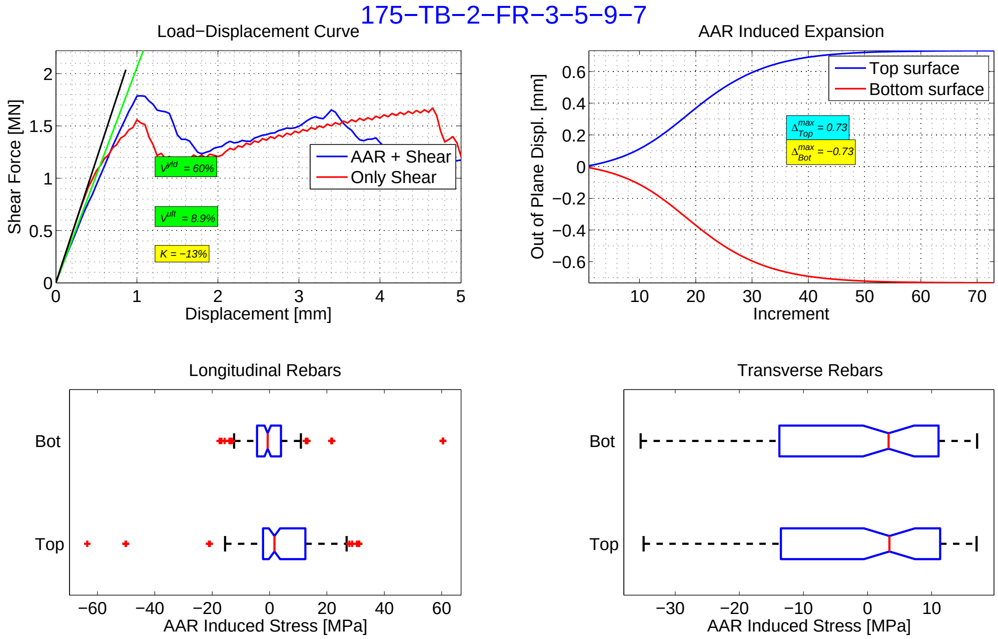

4.1.2.176 Analysis: 176-TB-2-FR-3-5-9-9

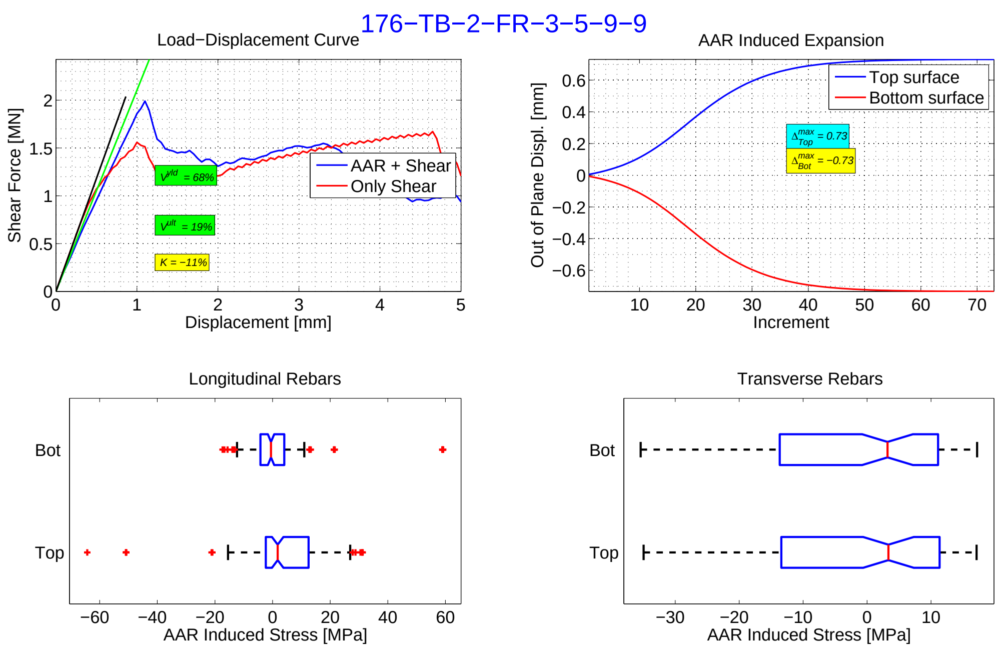

4.1.2.177 Analysis: 177-TB-2-FR-3-10-7-7

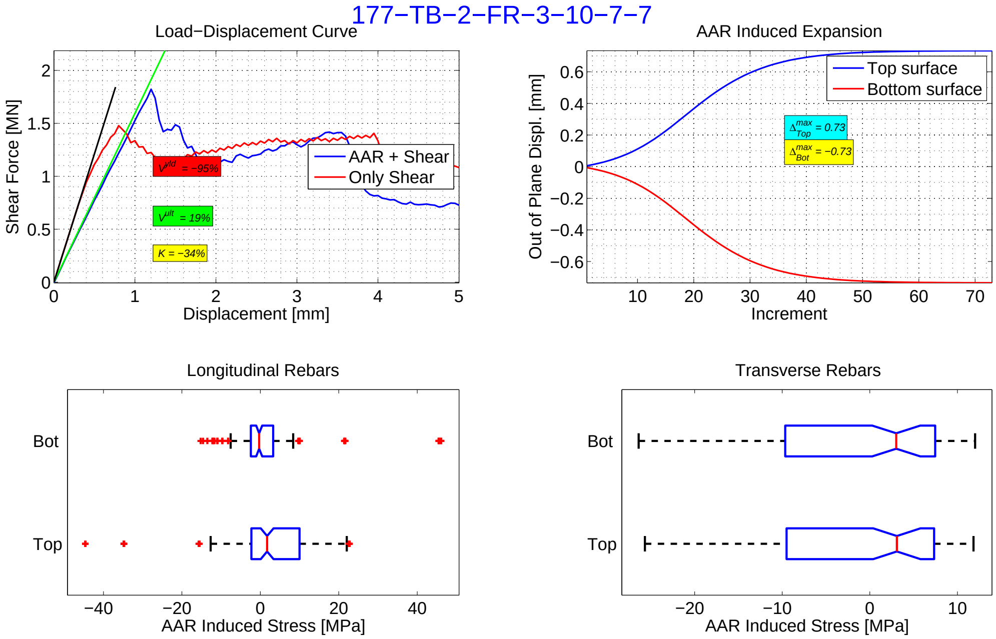

4.1.2.178 Analysis: 178-TB-2-FR-3-10-7-9

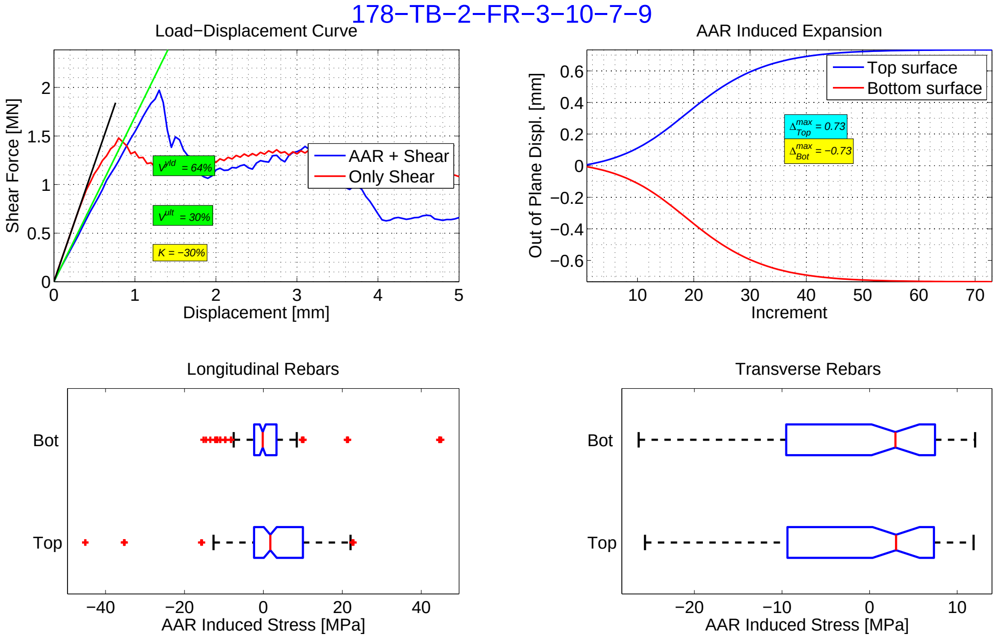

4.1.2.179 Analysis: 179-TB-2-FR-3-10-9-7

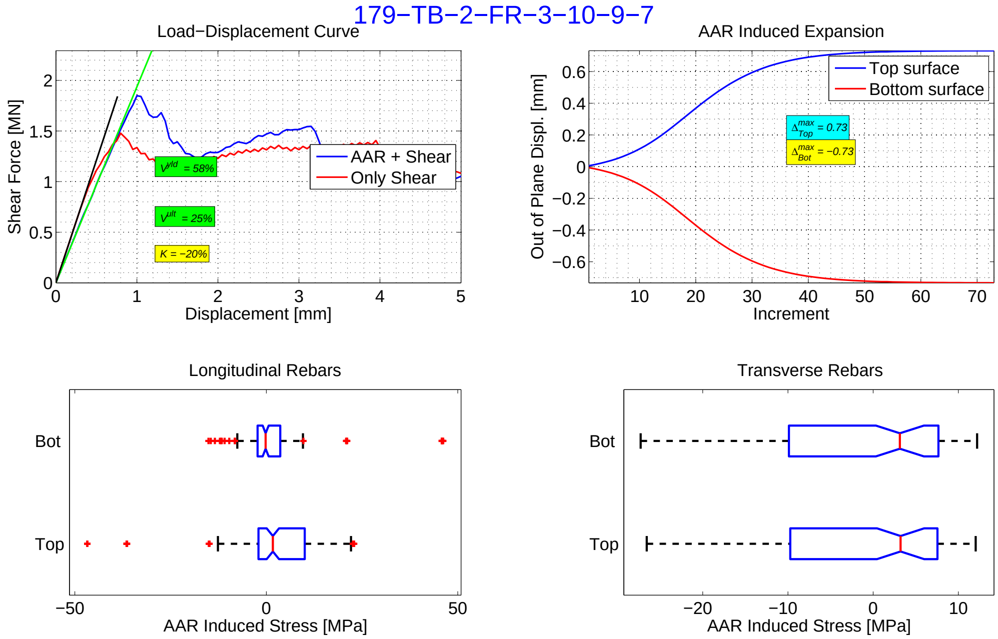

4.1.2.180 Analysis: 180-TB-2-FR-3-10-9-9

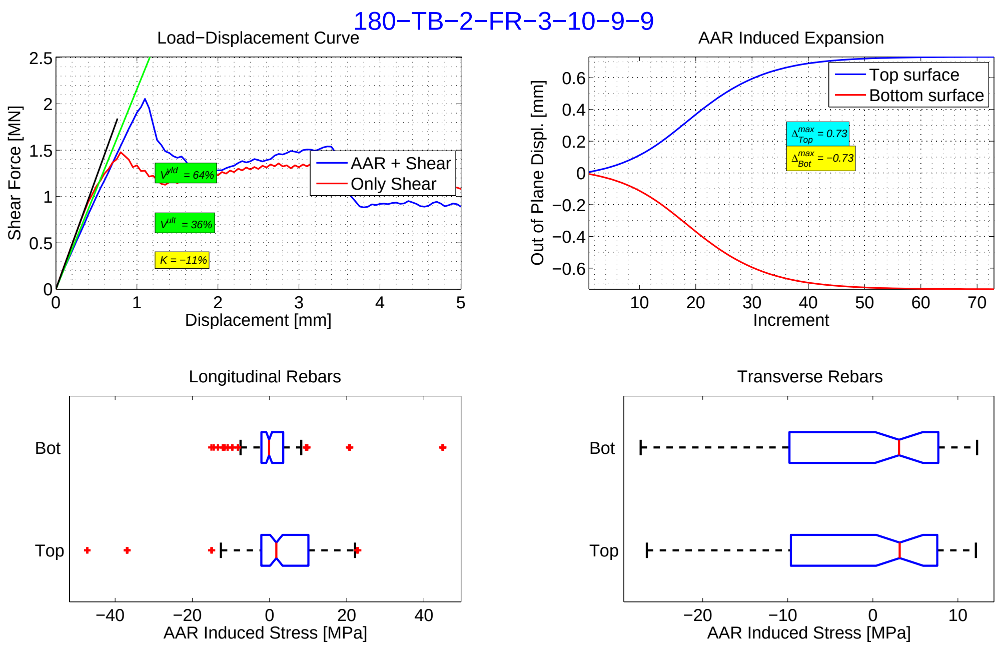

4.1.2.181 Analysis: 181-TB-4-FR-1-2-7-7

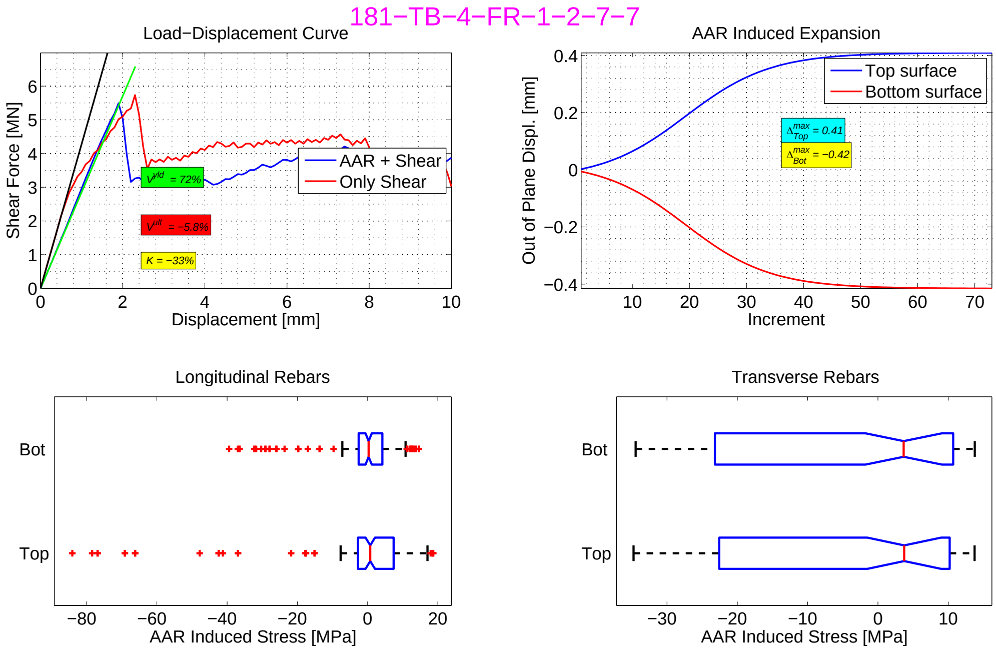

4.1.2.182 Analysis: 182-TB-4-FR-1-2-7-9

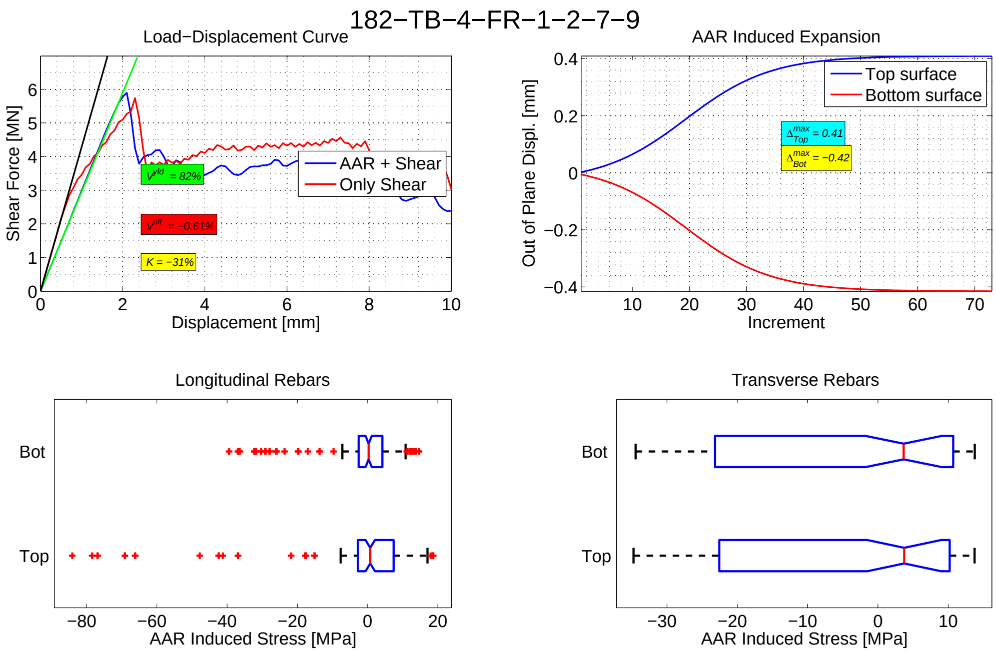

4.1.2.183 Analysis: 183-TB-4-FR-1-2-9-7

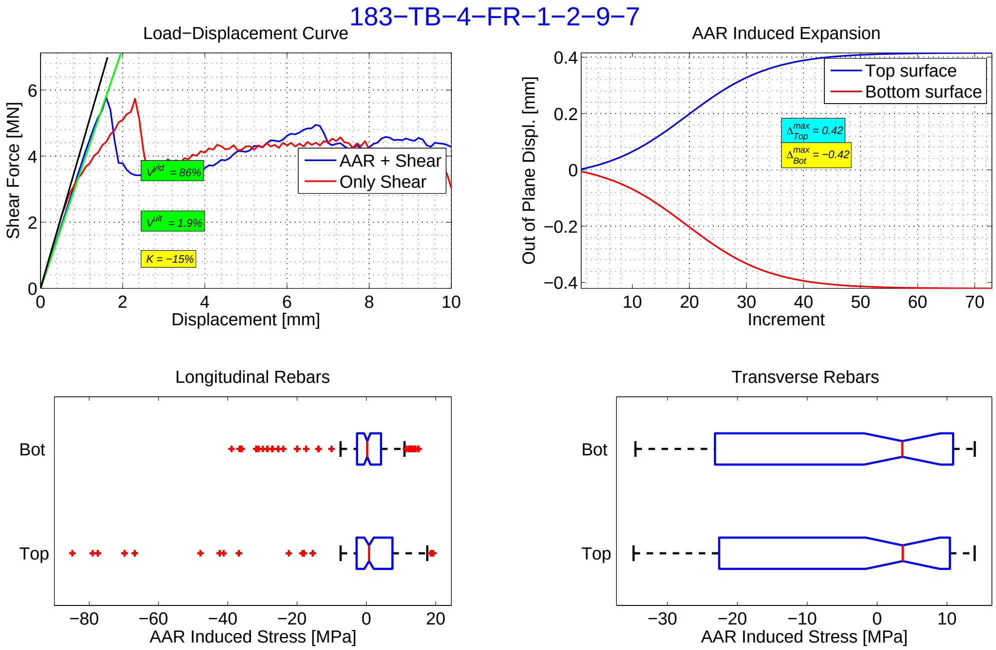

4.1.2.184 Analysis: 184-TB-4-FR-1-2-9-9

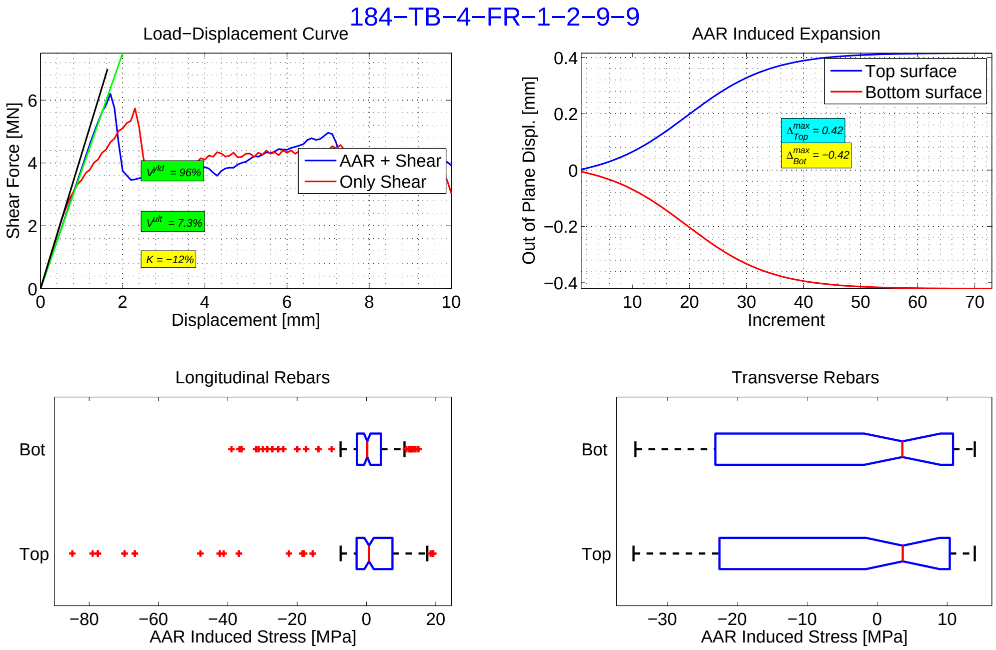

4.1.2.185 Analysis: 185-TB-4-FR-1-5-7-7

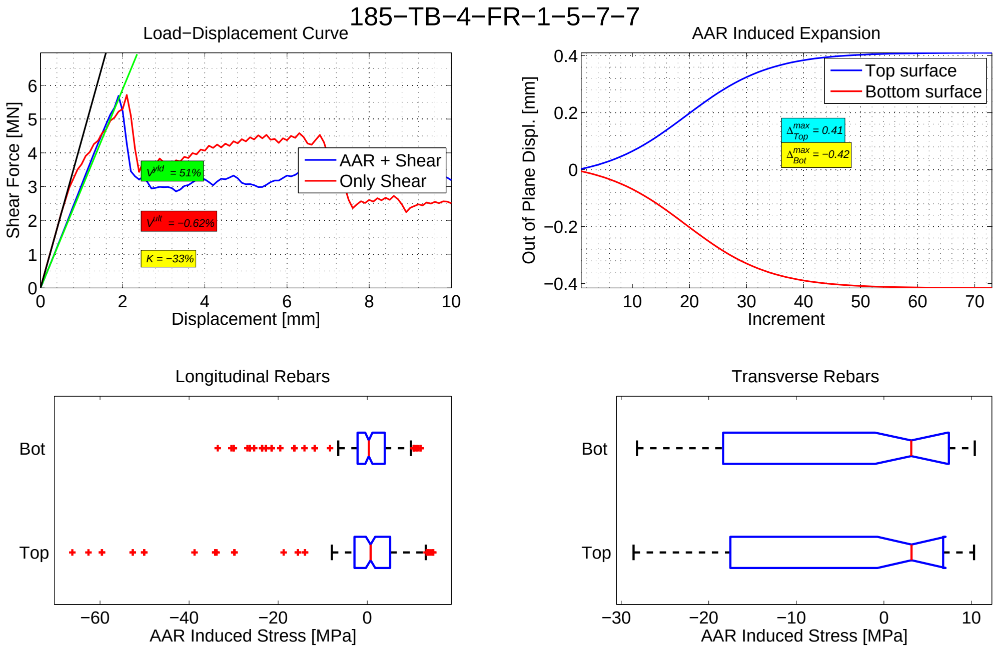

4.1.2.186 Analysis: 186-TB-4-FR-1-5-7-9

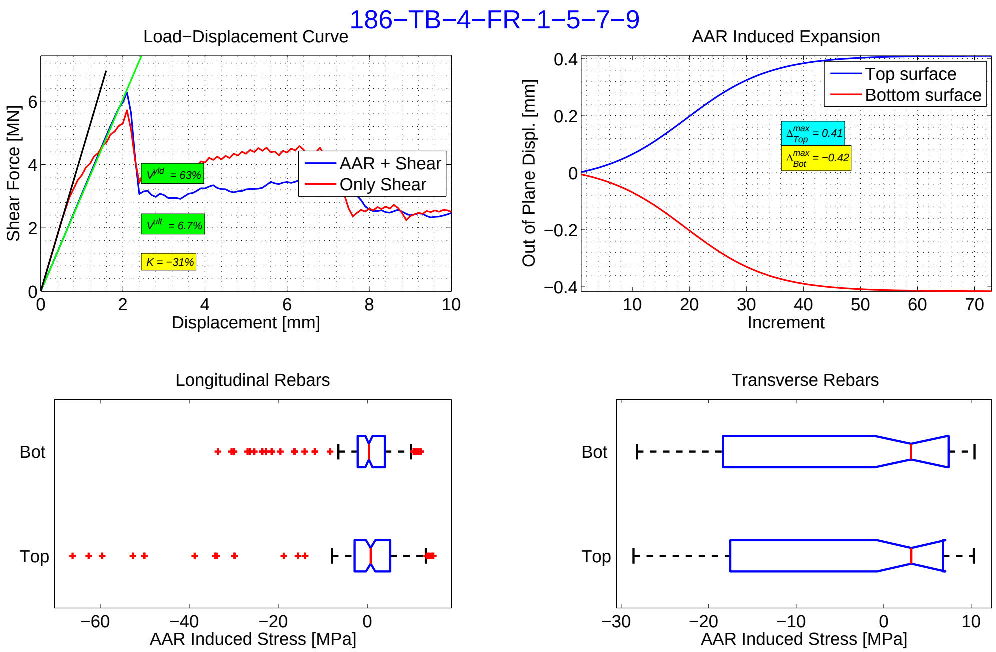

4.1.2.187 Analysis: 187-TB-4-FR-1-5-9-7

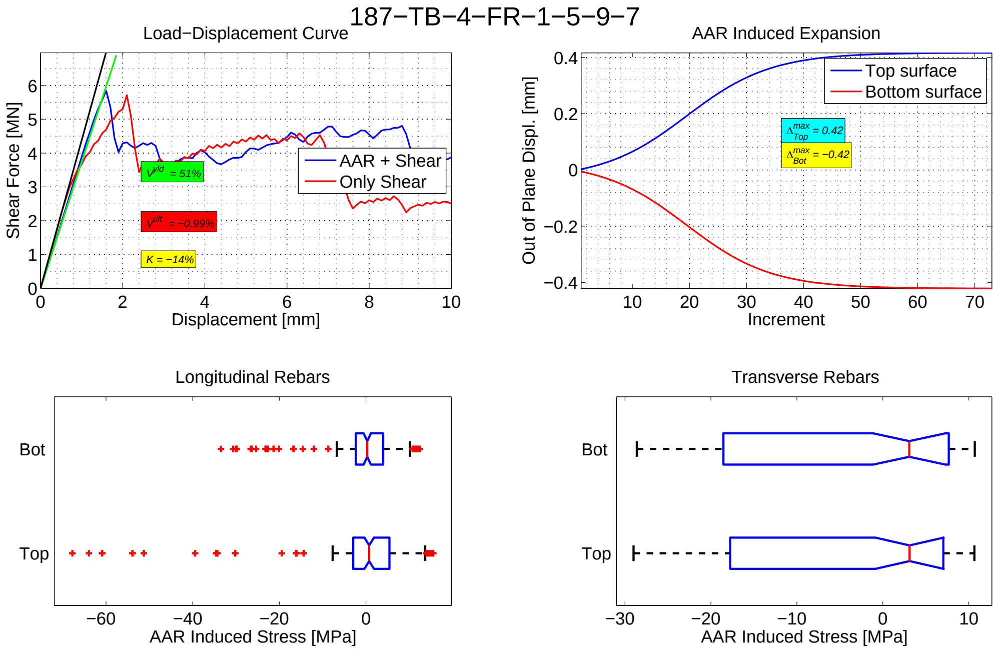

4.1.2.188 Analysis: 188-TB-4-FR-1-5-9-9

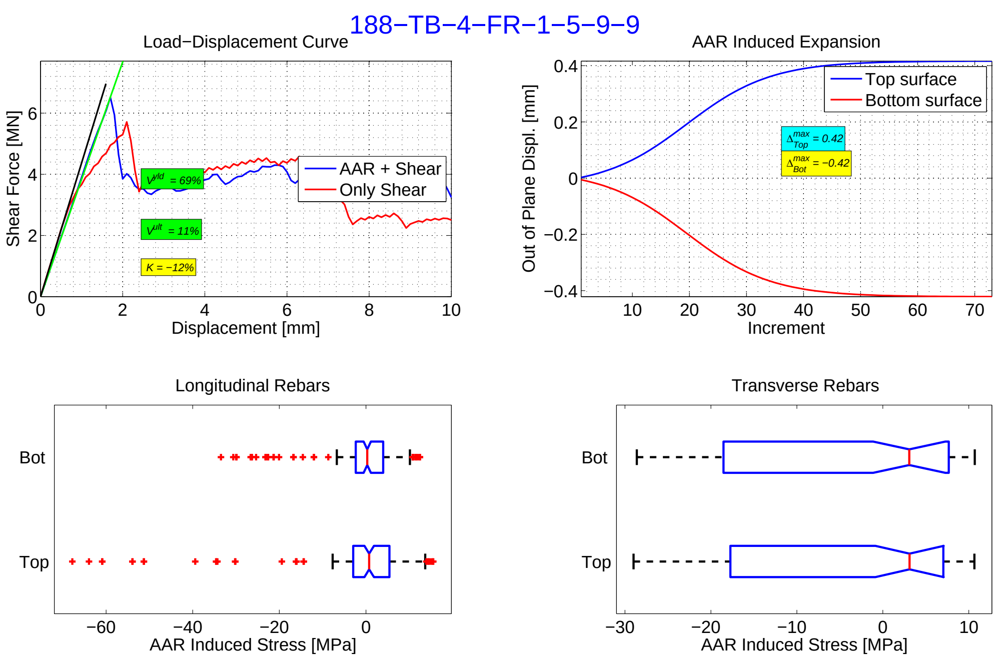

4.1.2.189 Analysis: 189-TB-4-FR-1-10-7-7

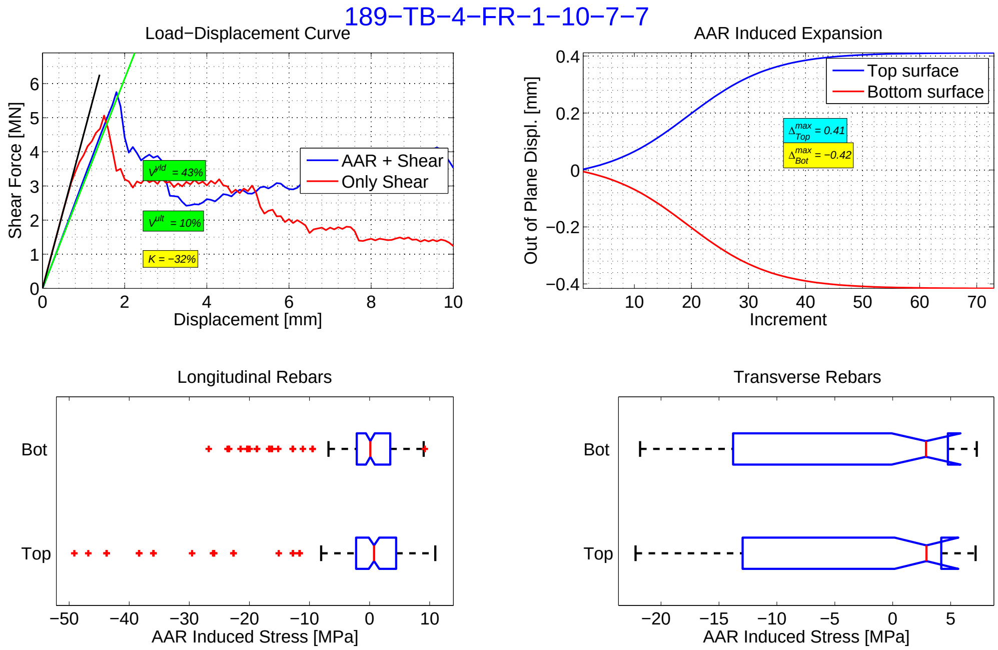

4.1.2.190 Analysis: 190-TB-4-FR-1-10-7-9

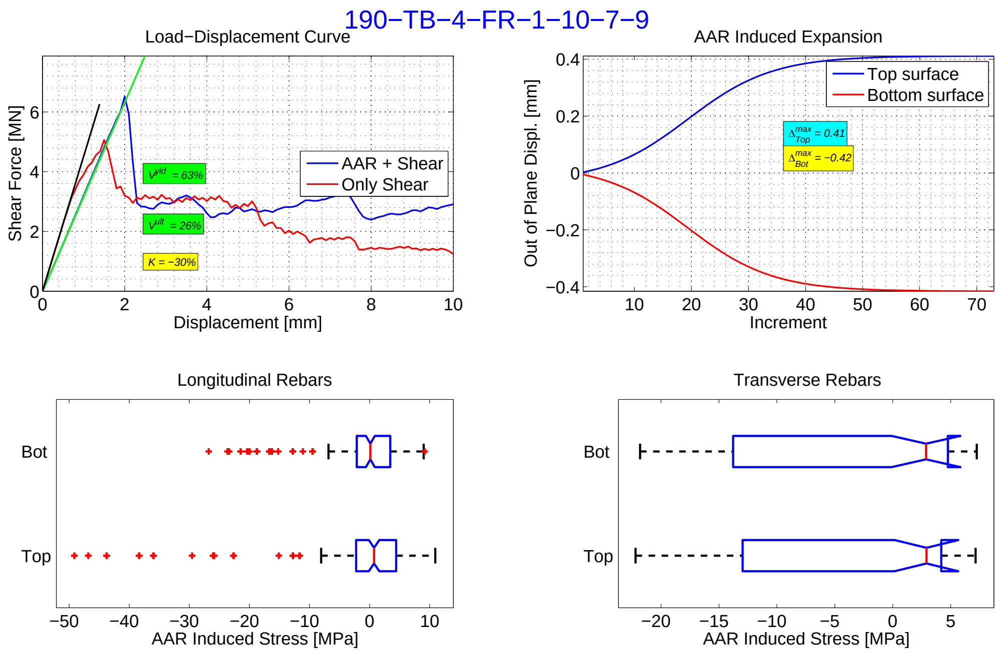

4.1.2.191 Analysis: 191-TB-4-FR-1-10-9-7

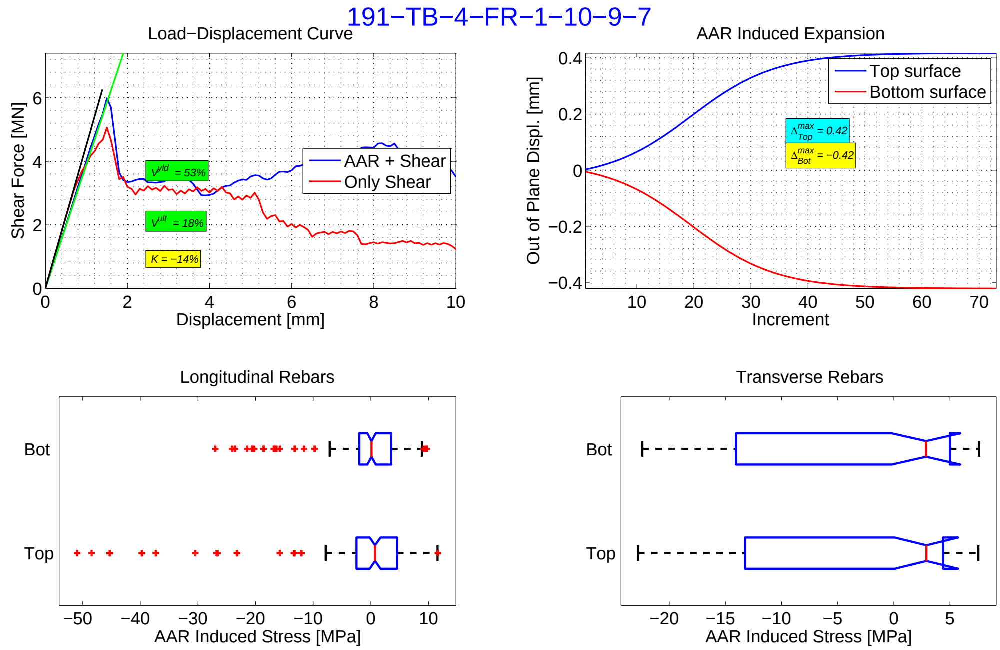

4.1.2.192 Analysis: 192-TB-4-FR-1-10-9-9

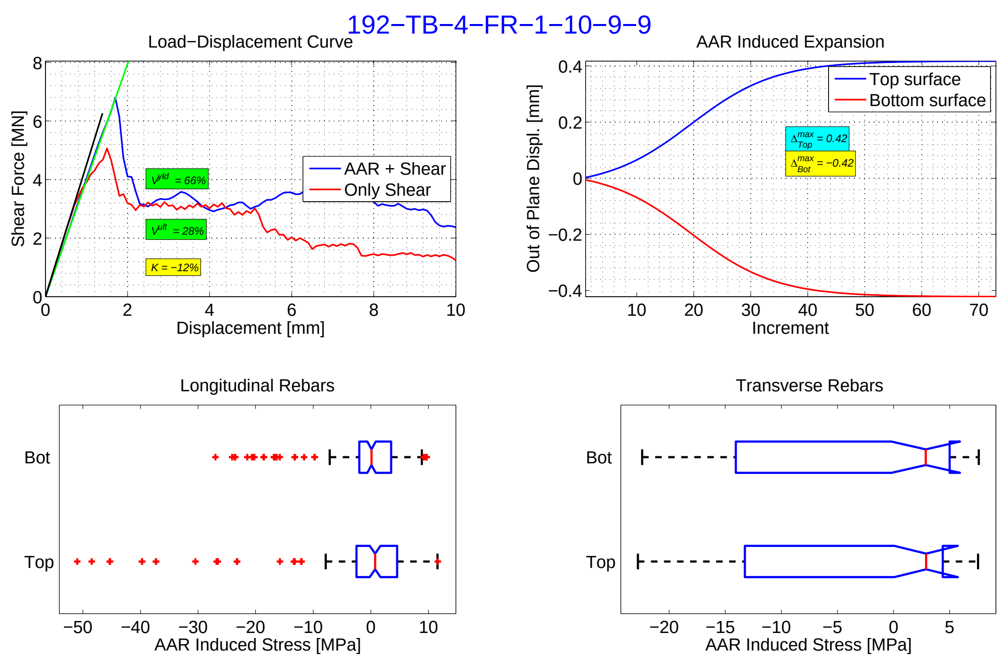

4.1.2.193 Analysis: 193-TB-4-FR-2-2-7-7

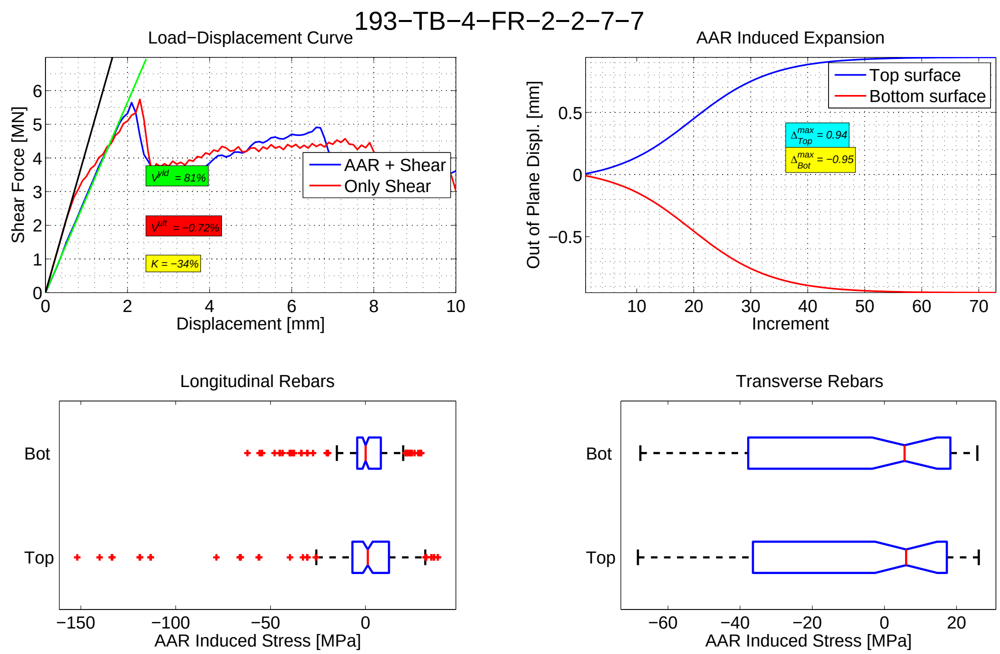

4.1.2.194 Analysis: 194-TB-4-FR-2-2-7-9

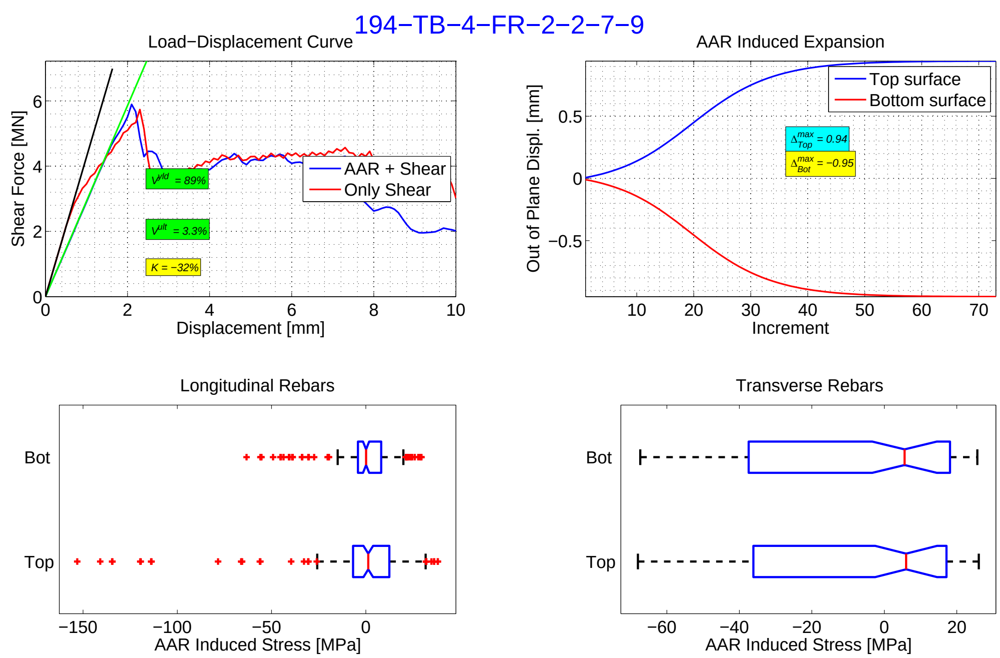

4.1.2.195 Analysis: 195-TB-4-FR-2-2-9-7

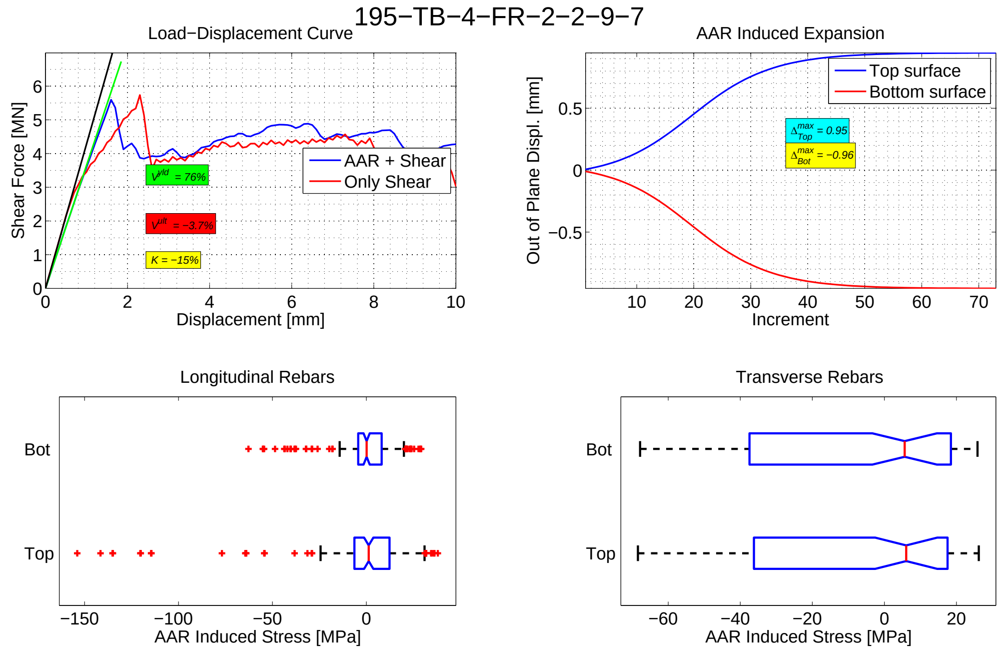

4.1.2.196 Analysis: 196-TB-4-FR-2-2-9-9

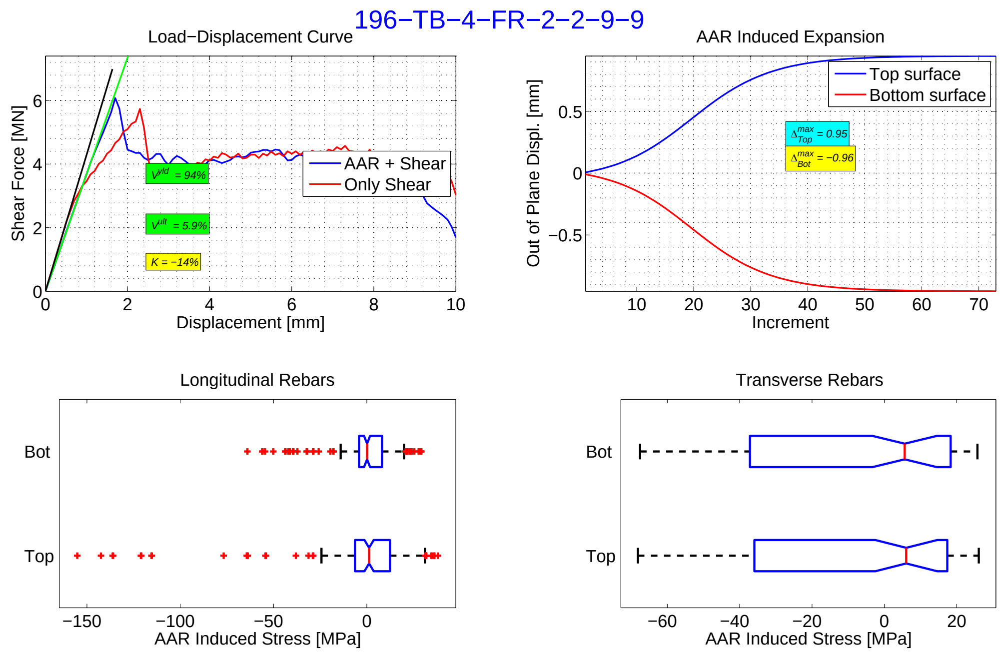

4.1.2.197 Analysis: 197-TB-4-FR-2-5-7-7

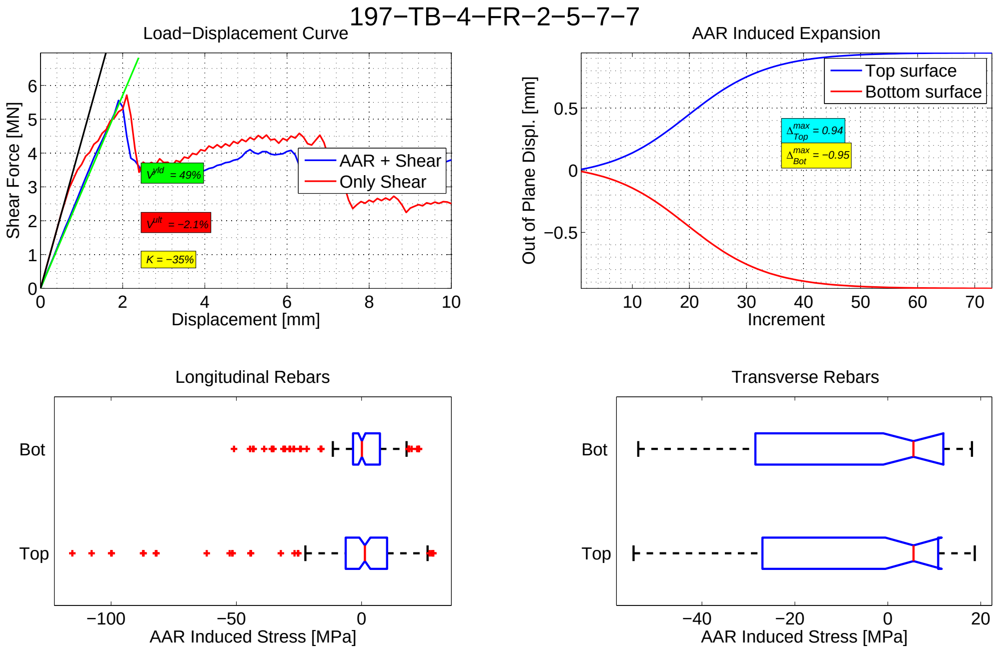

4.1.2.198 Analysis: 198-TB-4-FR-2-5-7-9

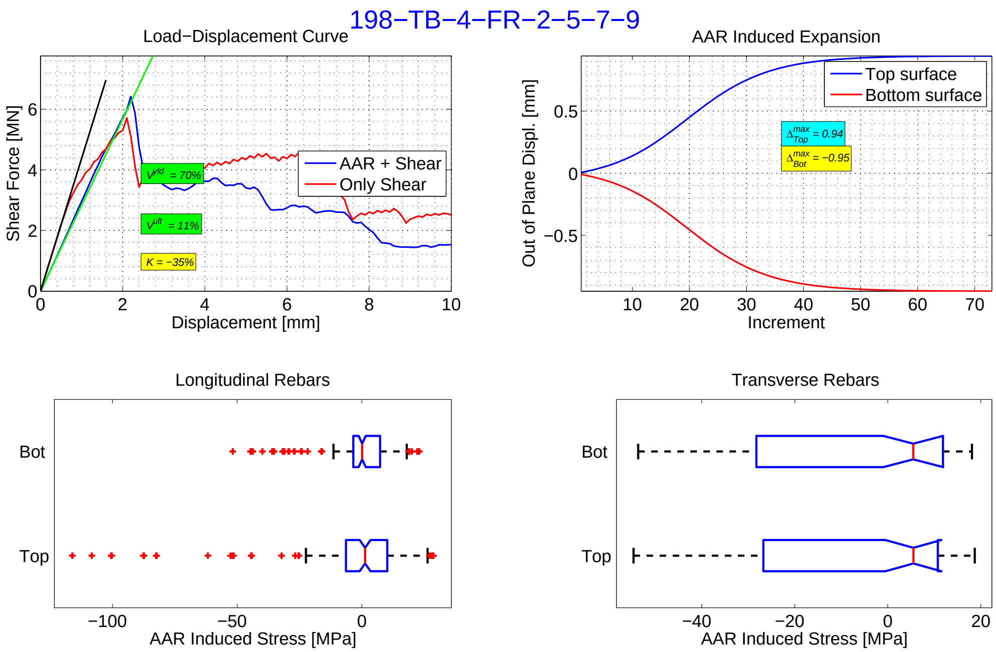

4.1.2.199 Analysis: 199-TB-4-FR-2-5-9-7

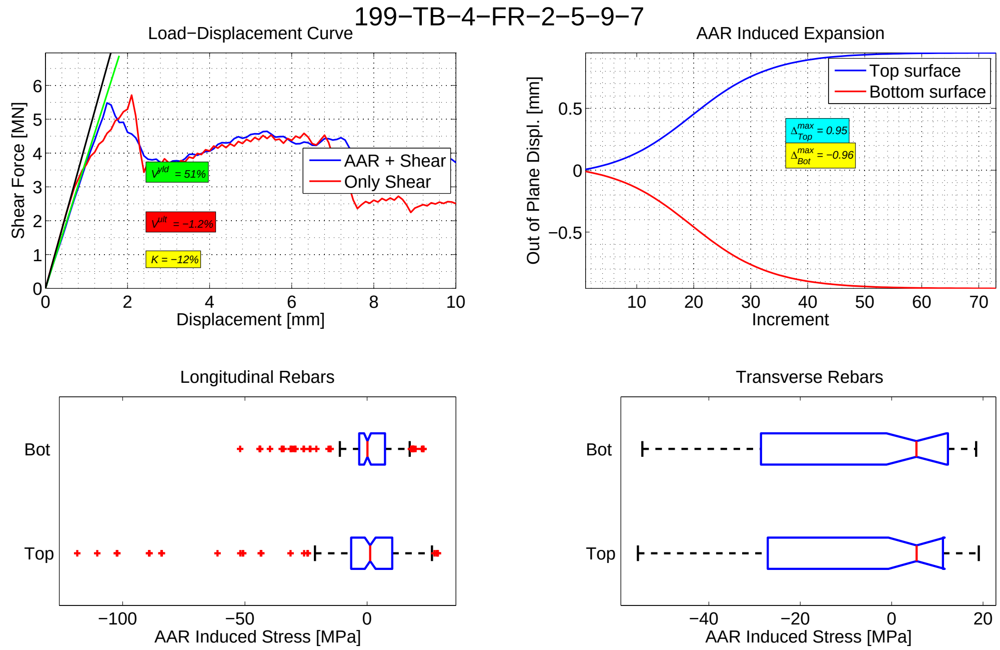

4.1.2.200 Analysis: 200-TB-4-FR-2-5-9-9

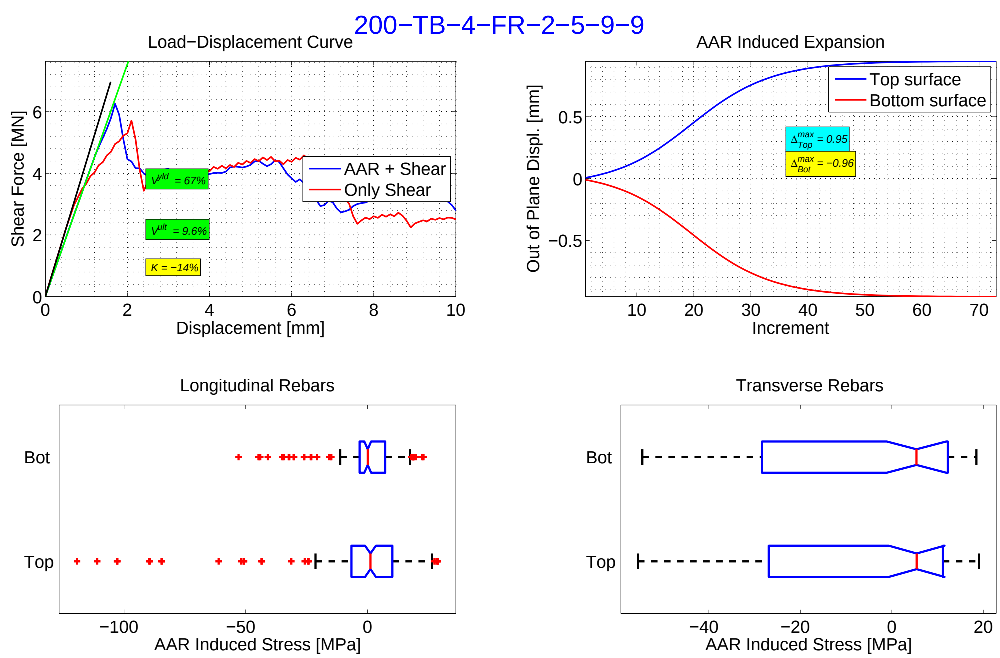

4.1.2.201 Analysis: 201-TB-4-FR-2-10-7-7

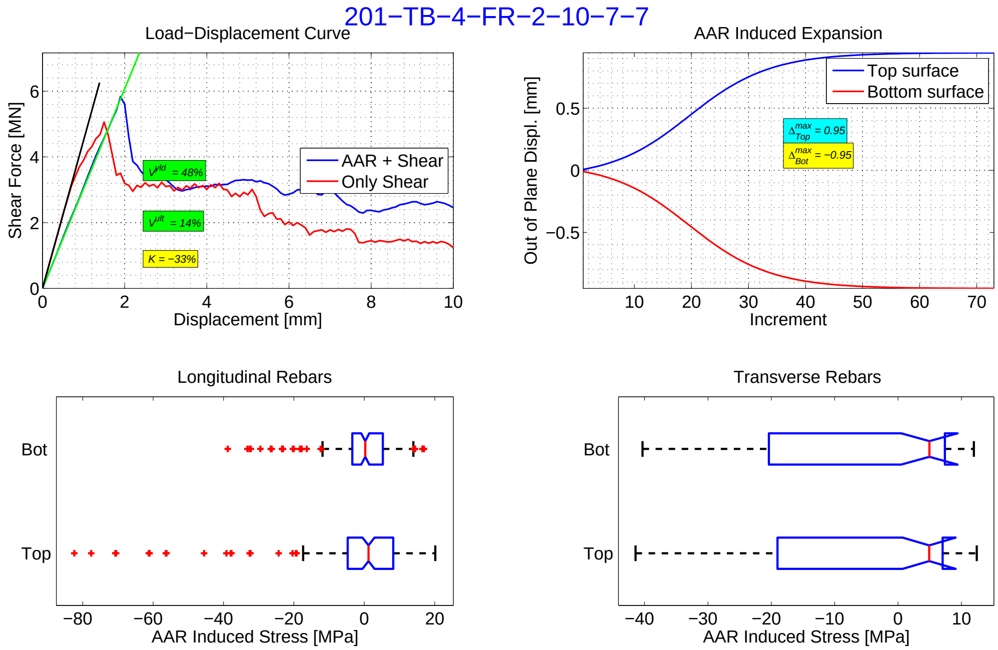

4.1.2.202 Analysis: 202-TB-4-FR-2-10-7-9

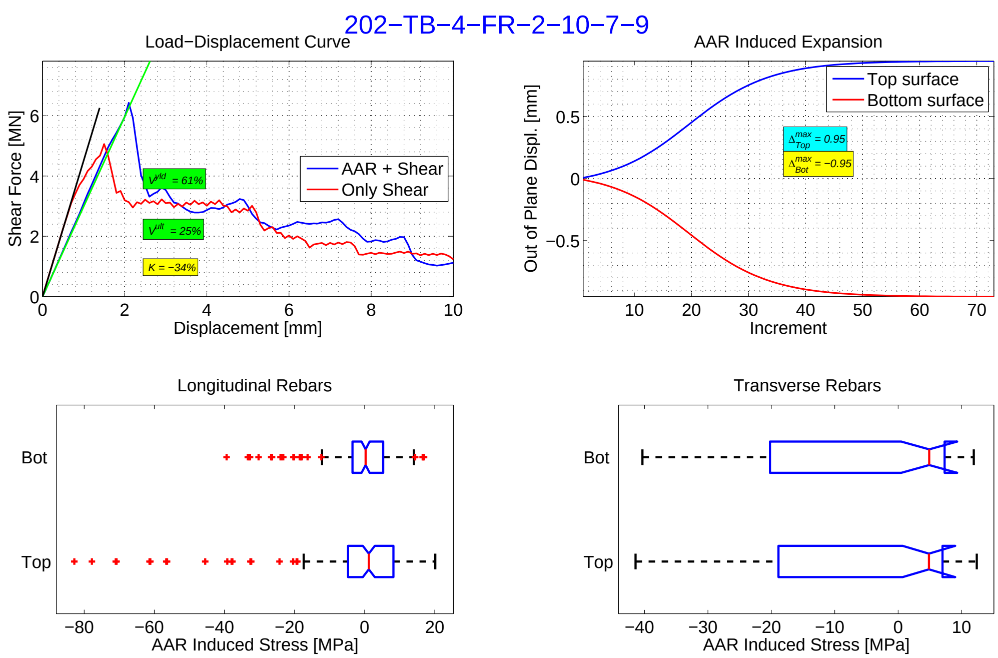

4.1.2.203 Analysis: 203-TB-4-FR-2-10-9-7

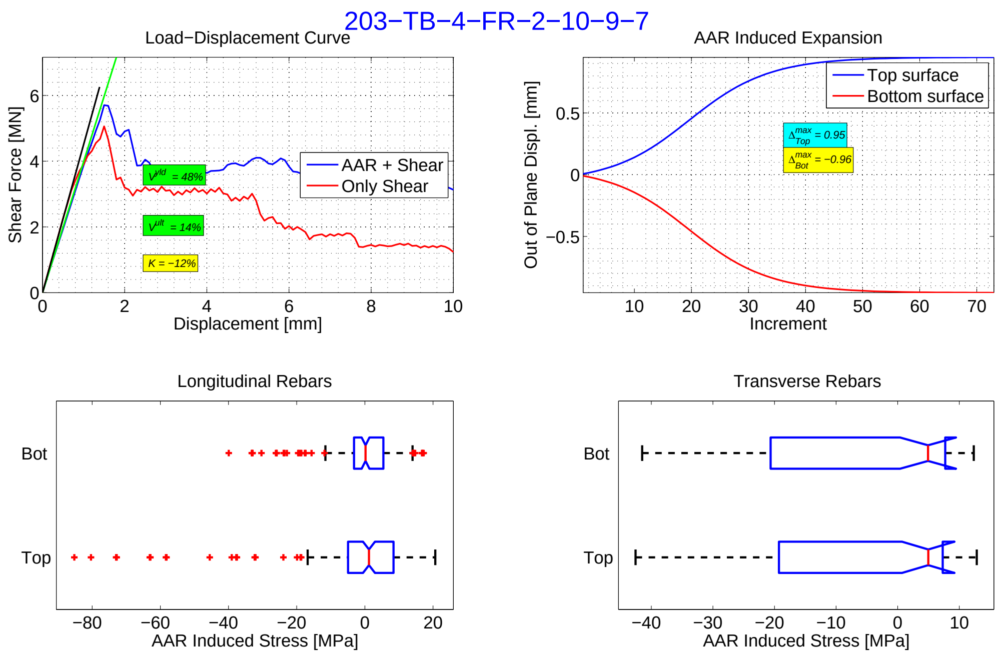

4.1.2.204 Analysis: 204-TB-4-FR-2-10-9-9

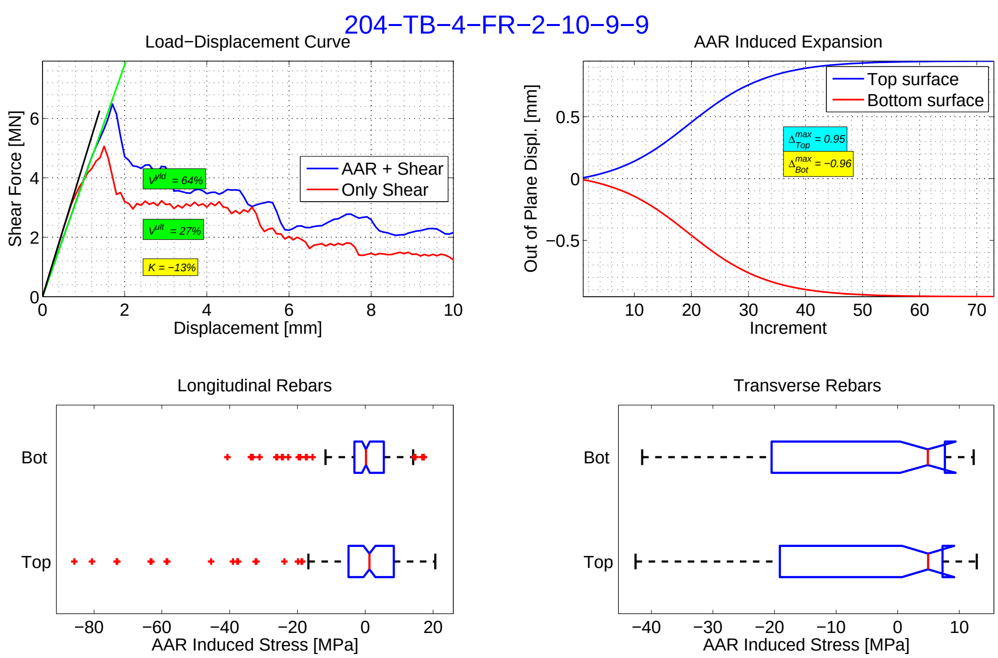

4.1.2.205 Analysis: 205-TB-4-FR-3-2-7-7

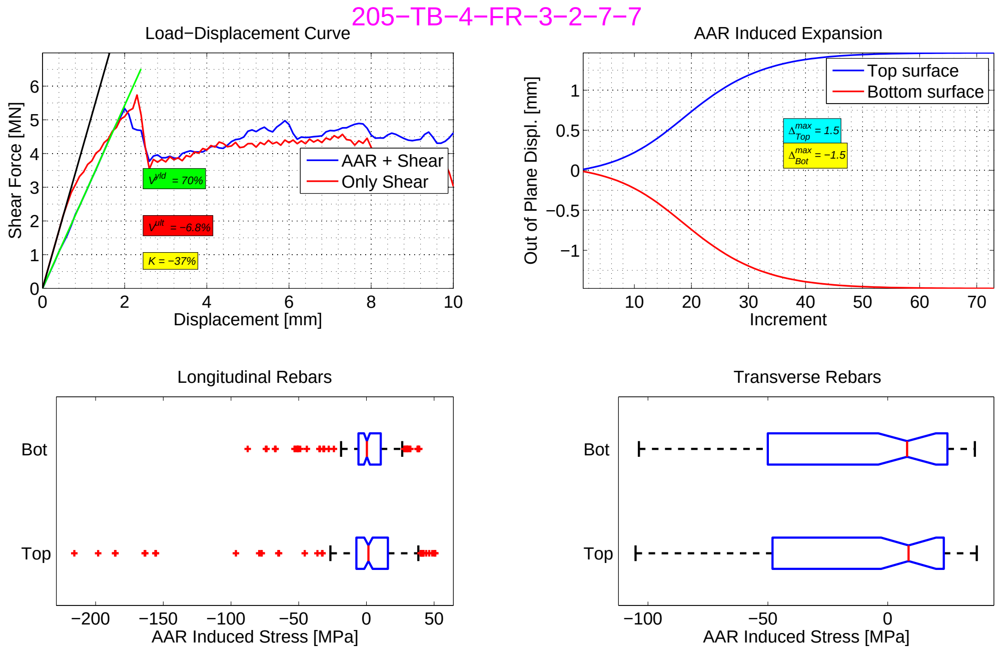

4.1.2.206 Analysis: 206-TB-4-FR-3-2-7-9

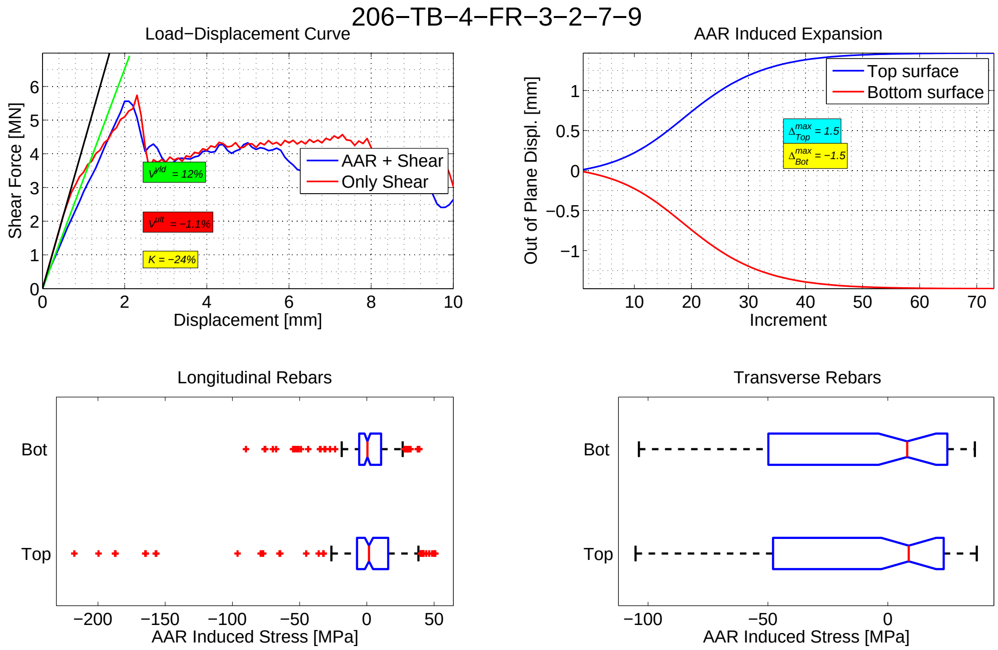

4.1.2.207 Analysis: 207-TB-4-FR-3-2-9-7

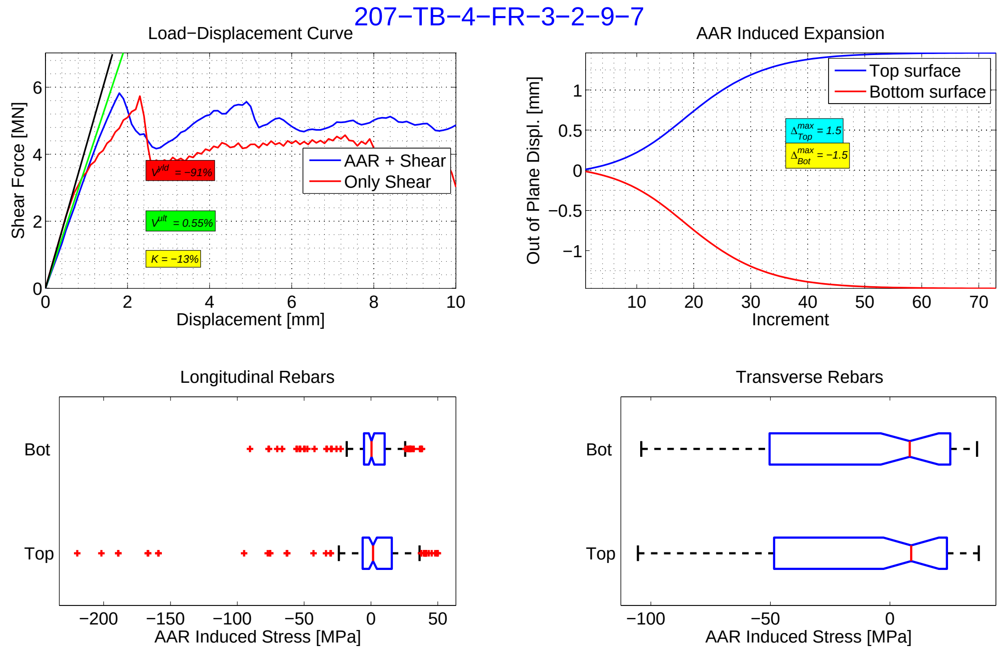

4.1.2.208 Analysis: 208-TB-4-FR-3-2-9-9

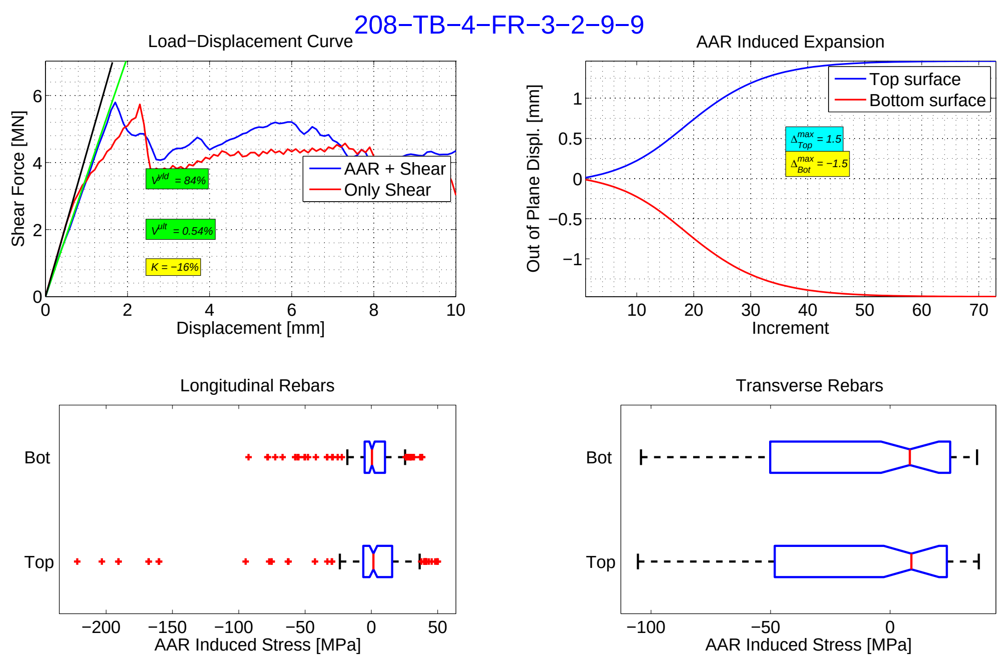

4.1.2.209 Analysis: 209-TB-4-FR-3-5-7-7

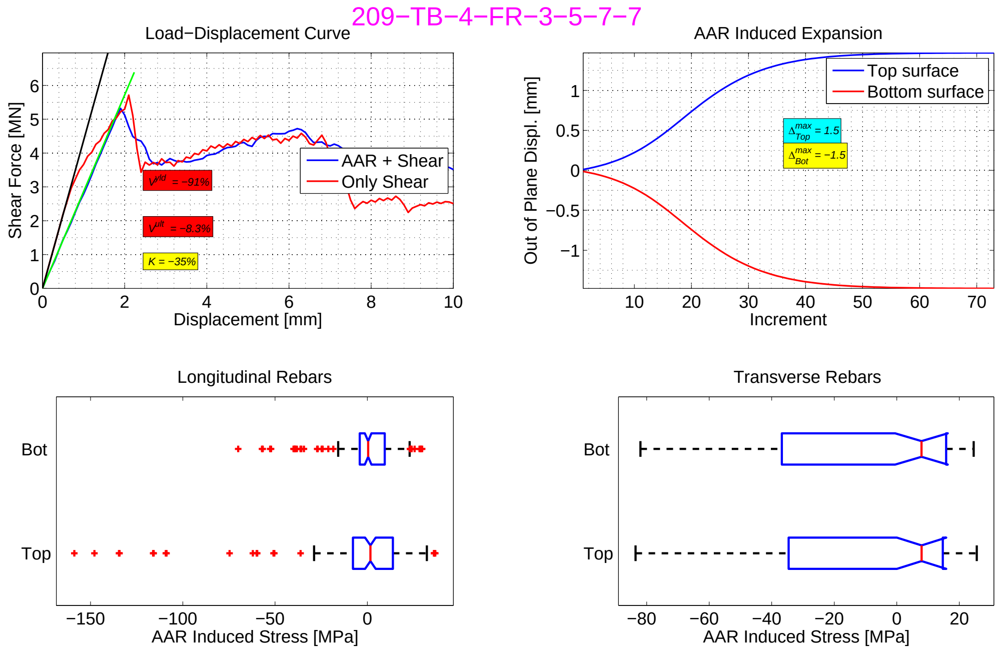

4.1.2.210 Analysis: 210-TB-4-FR-3-5-7-9

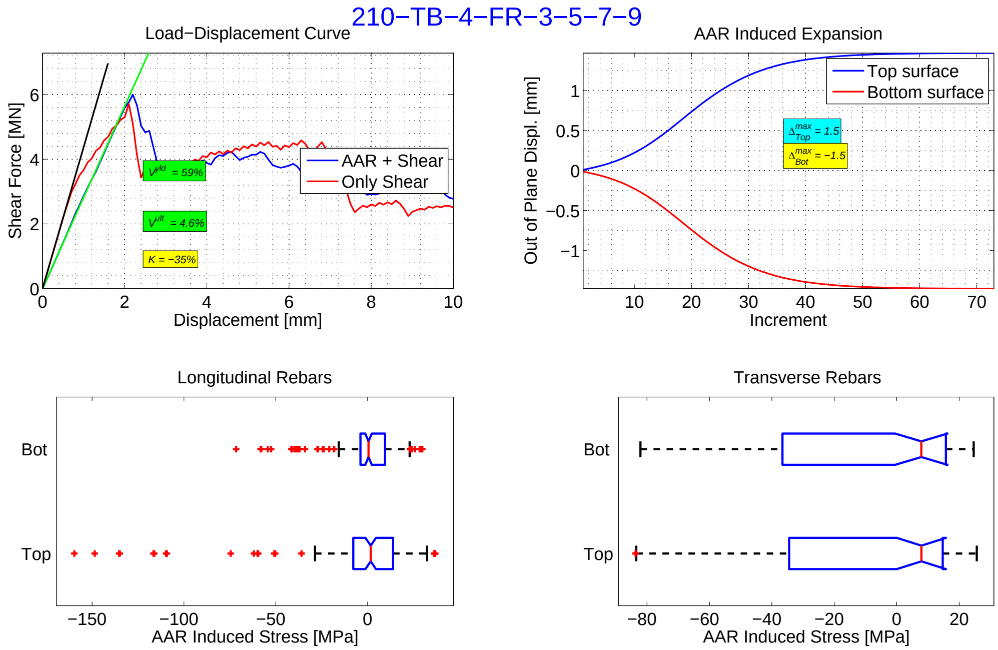

4.1.2.211 Analysis: 211-TB-4-FR-3-5-9-7

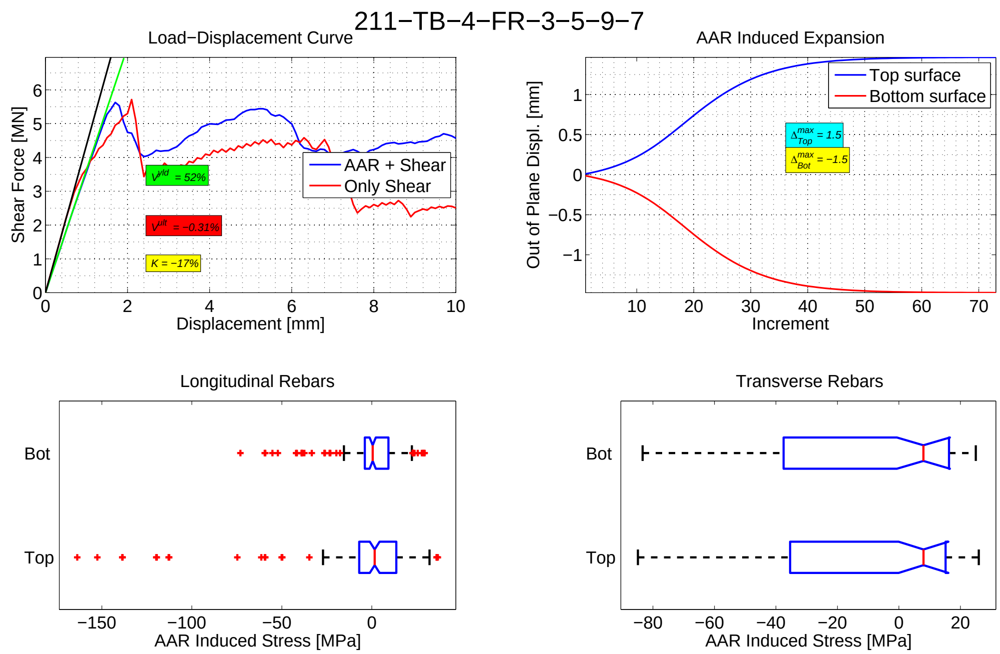

4.1.2.212 Analysis: 212-TB-4-FR-3-5-9-9

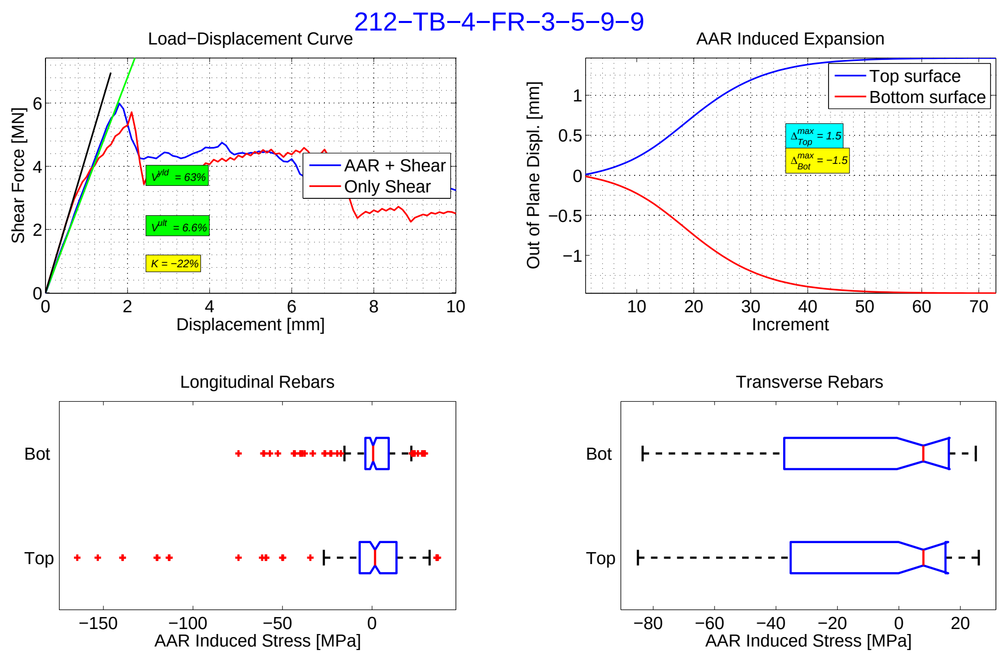

4.1.2.213 Analysis: 213-TB-4-FR-3-10-7-7

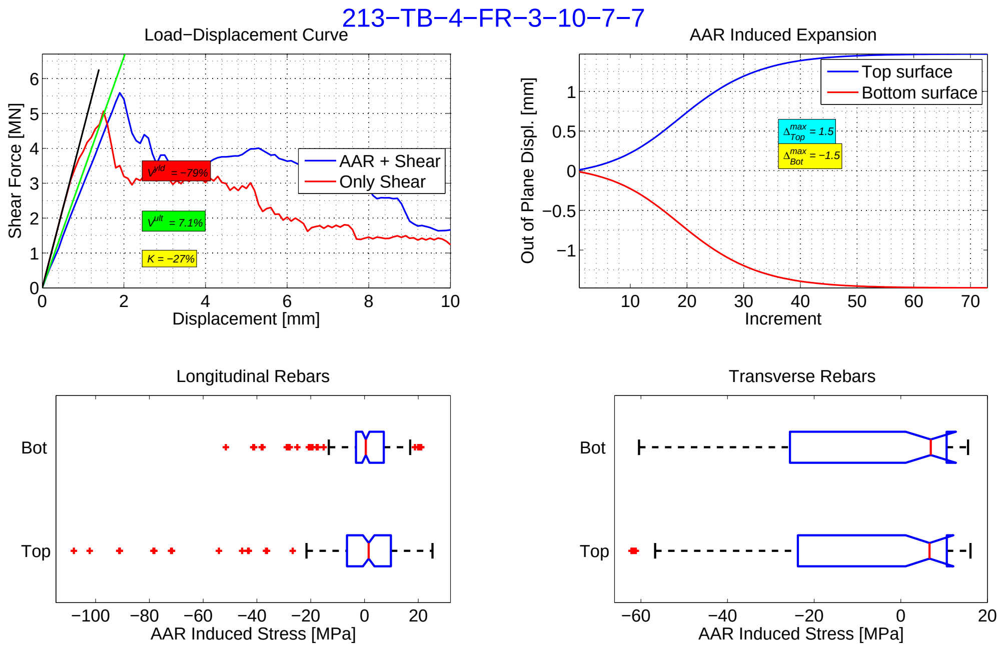

4.1.2.214 Analysis: 214-TB-4-FR-3-10-7-9

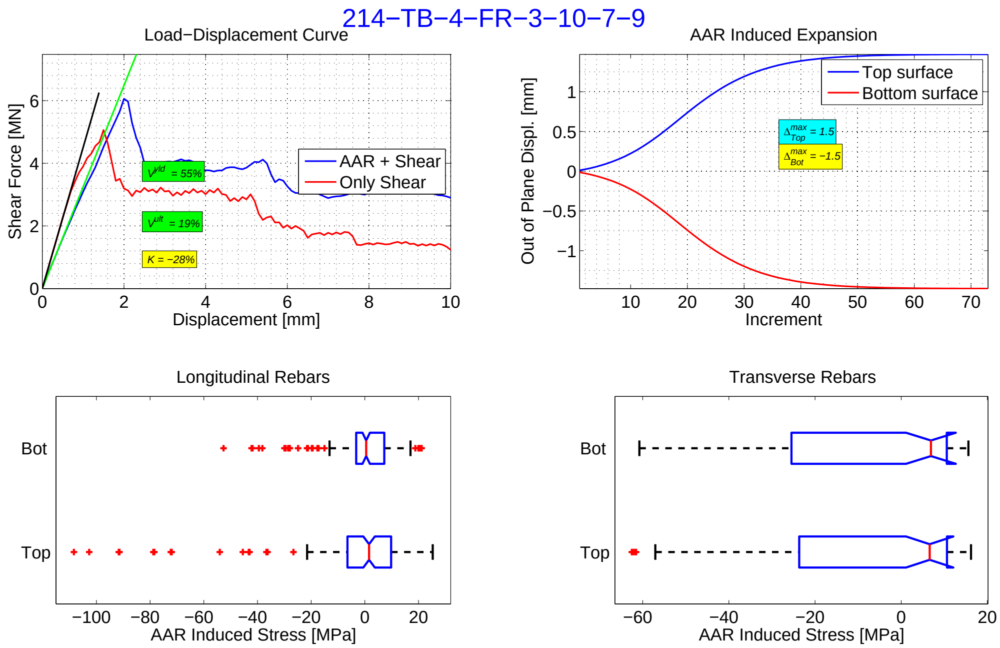

4.1.2.215 Analysis: 215-TB-4-FR-3-10-9-7

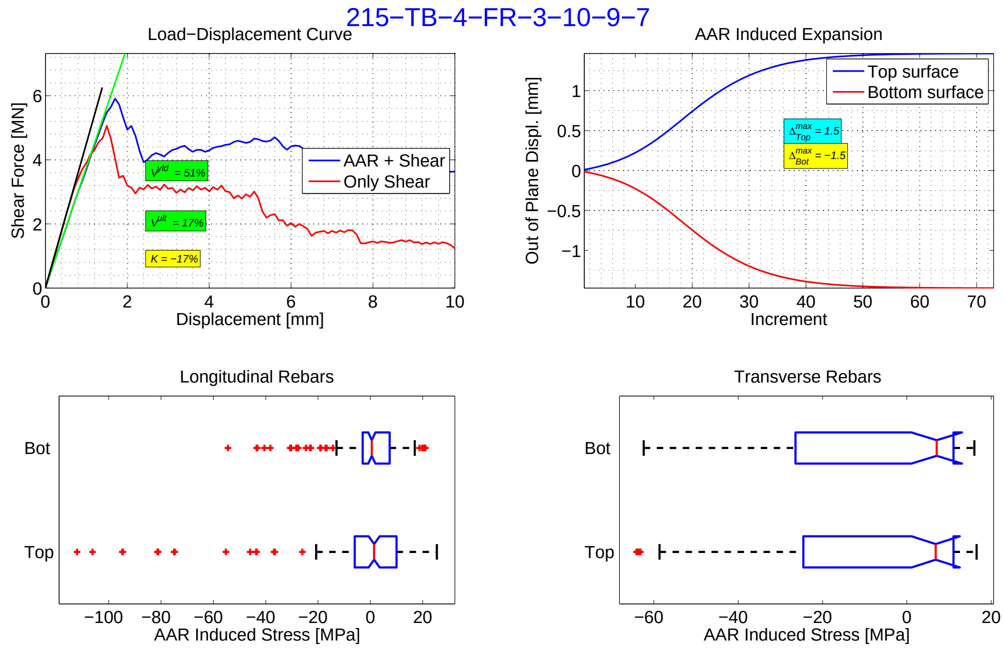

4.1.2.216 Analysis: 216-TB-4-FR-3-10-9-9

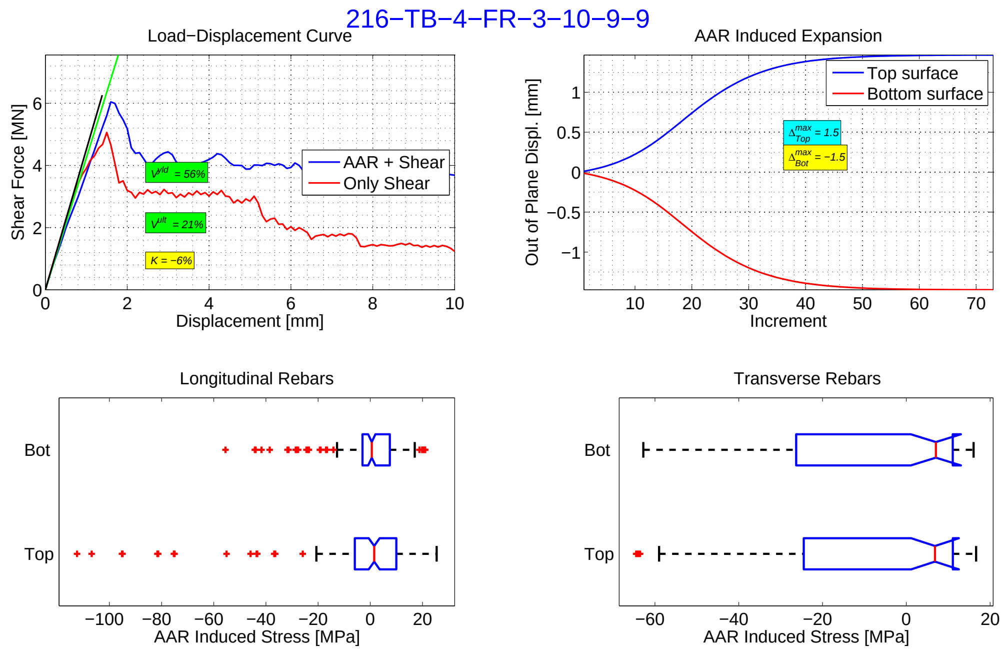

4.1.3 PANEL

4.1.3.1 Analysis: 1-P-2-U-1-2-7-7

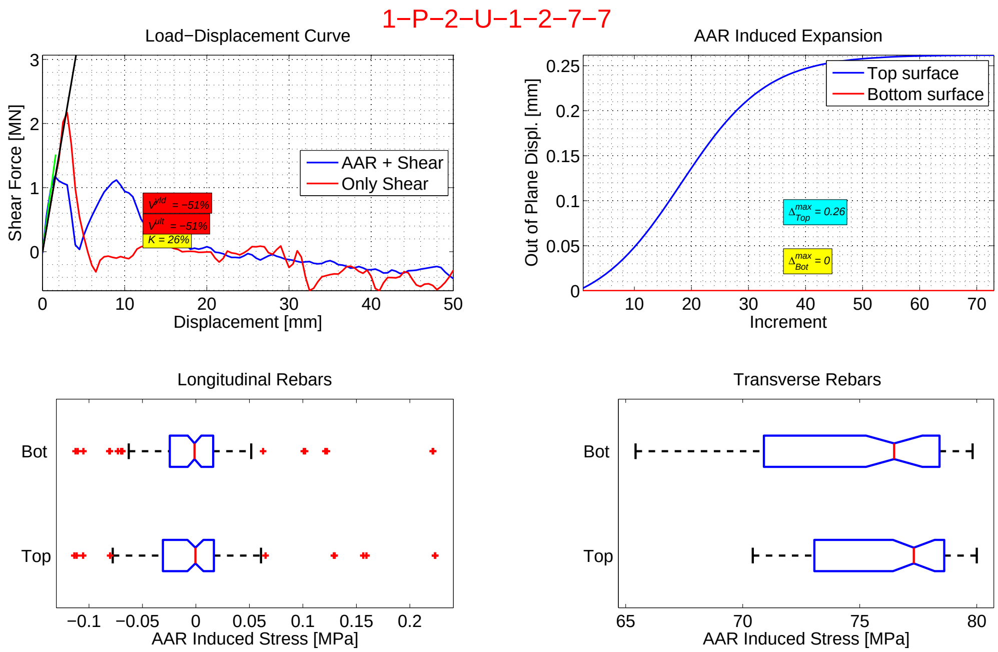

4.1.3.2 Analysis: 2-P-2-U-1-2-7-9

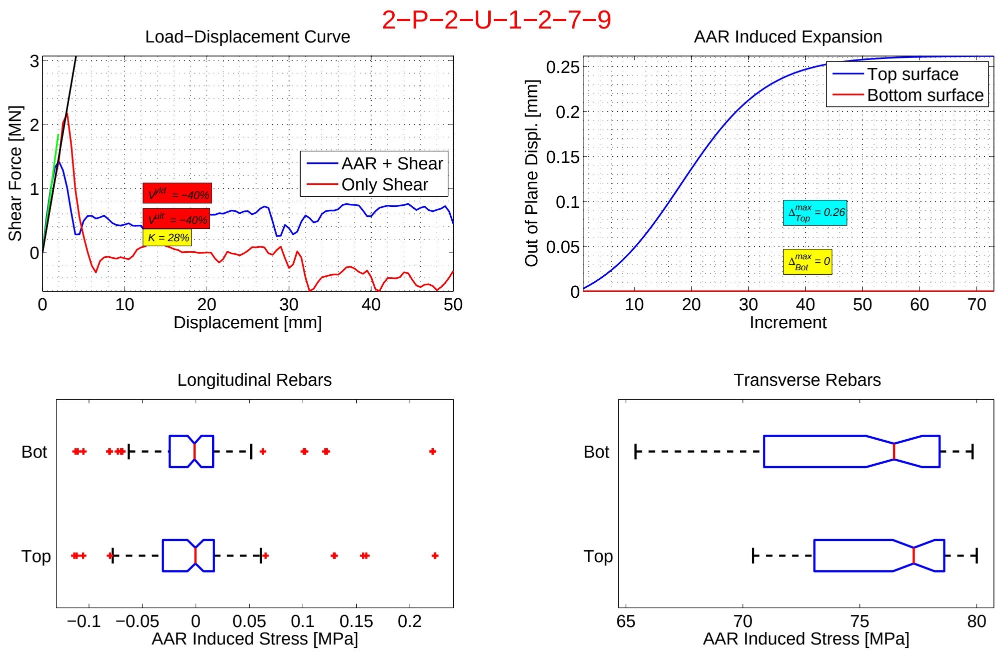

4.1.3.3 Analysis: 3-P-2-U-1-2-9-7

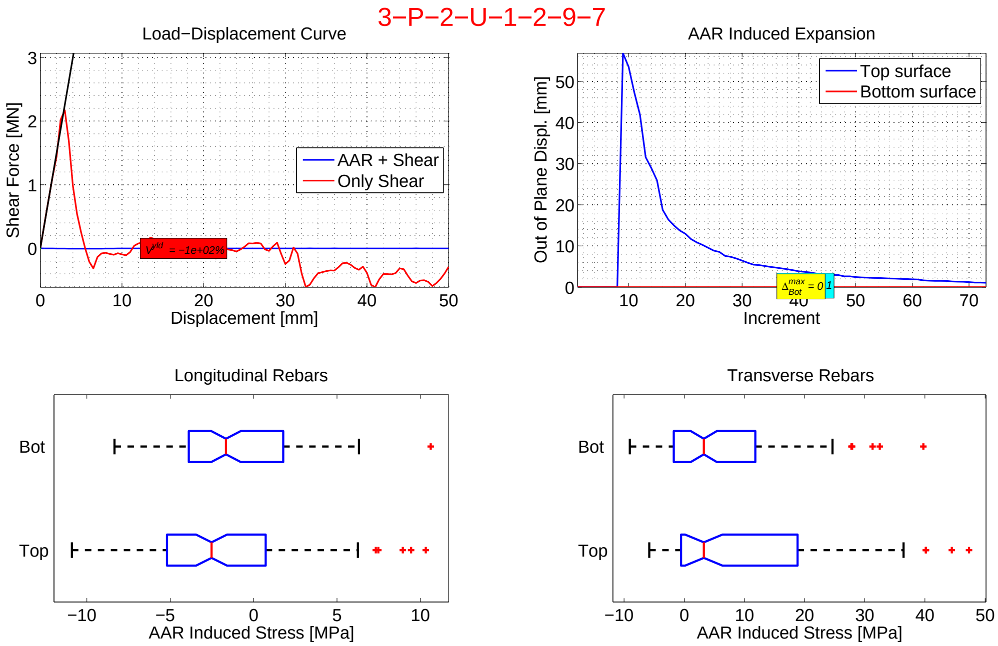

4.1.3.4 Analysis: 4-P-2-U-1-2-9-9

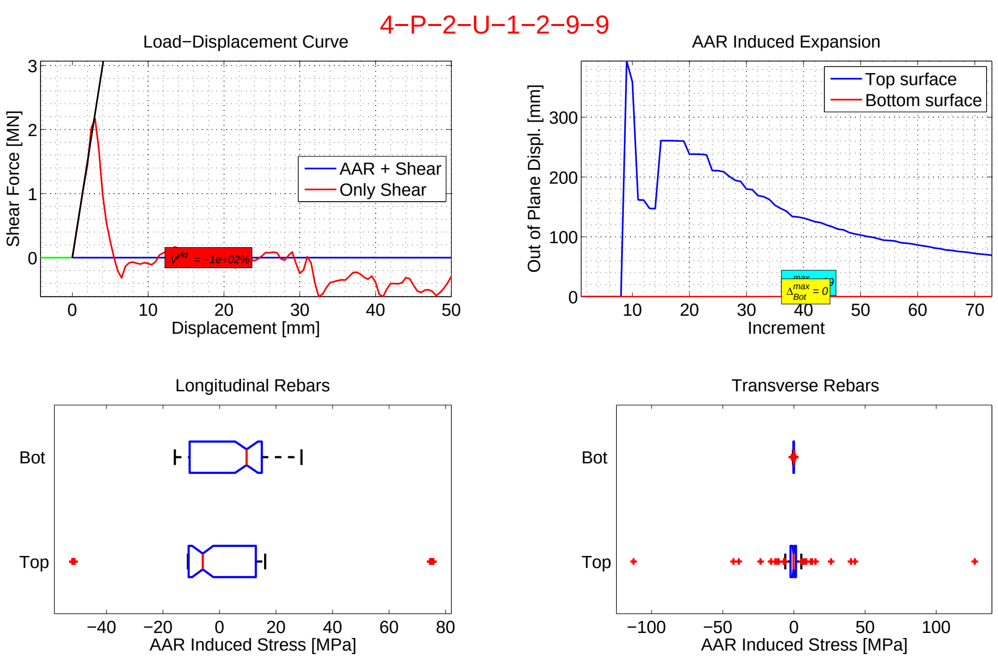

4.1.3.5 Analysis: 5-P-2-U-1-5-7-7

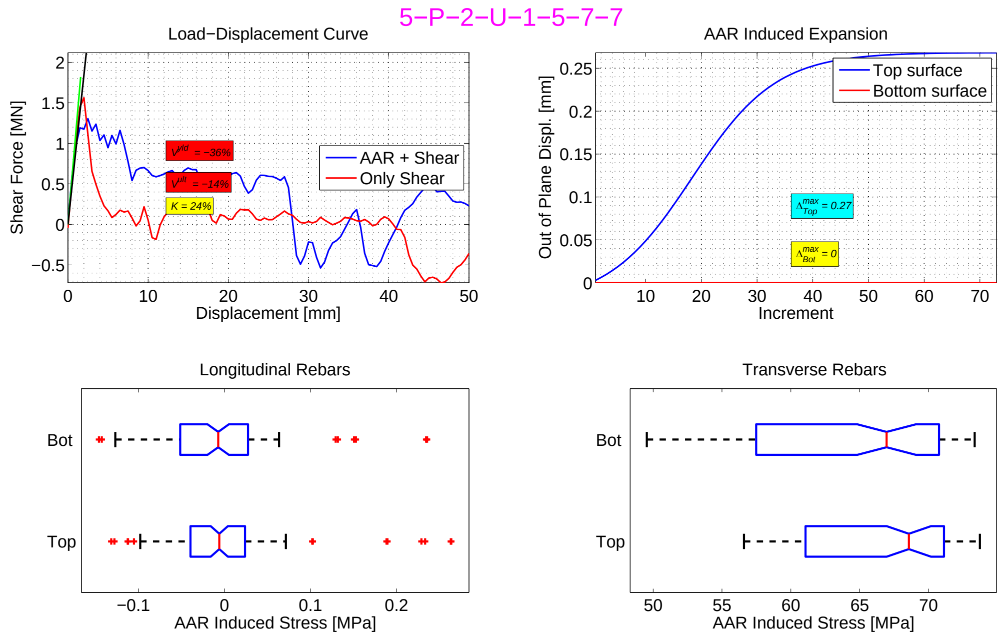

4.1.3.6 Analysis: 6-P-2-U-1-5-7-9

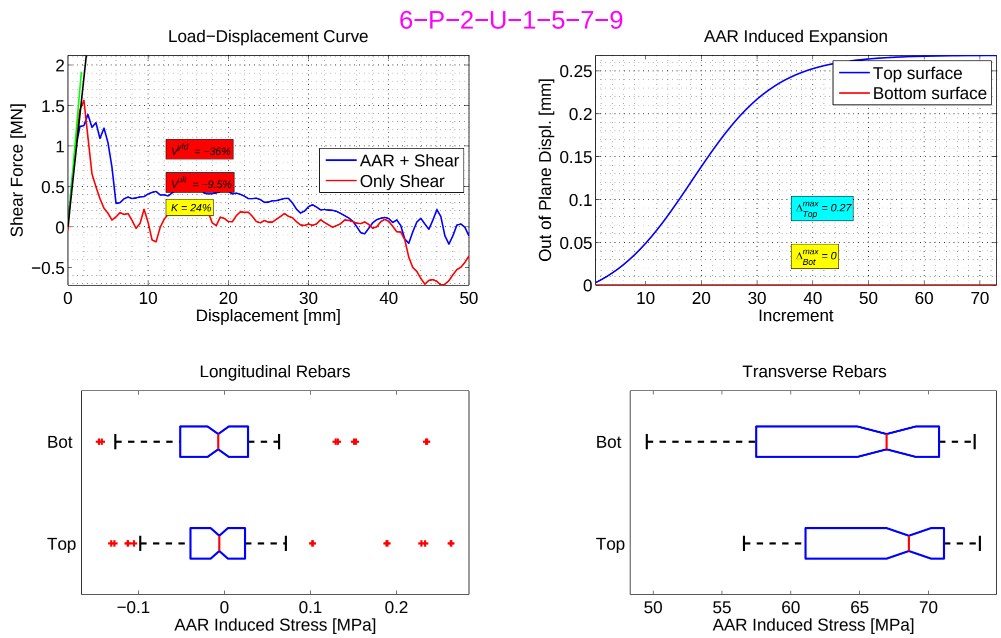

4.1.3.7 Analysis: 7-P-2-U-1-5-9-7

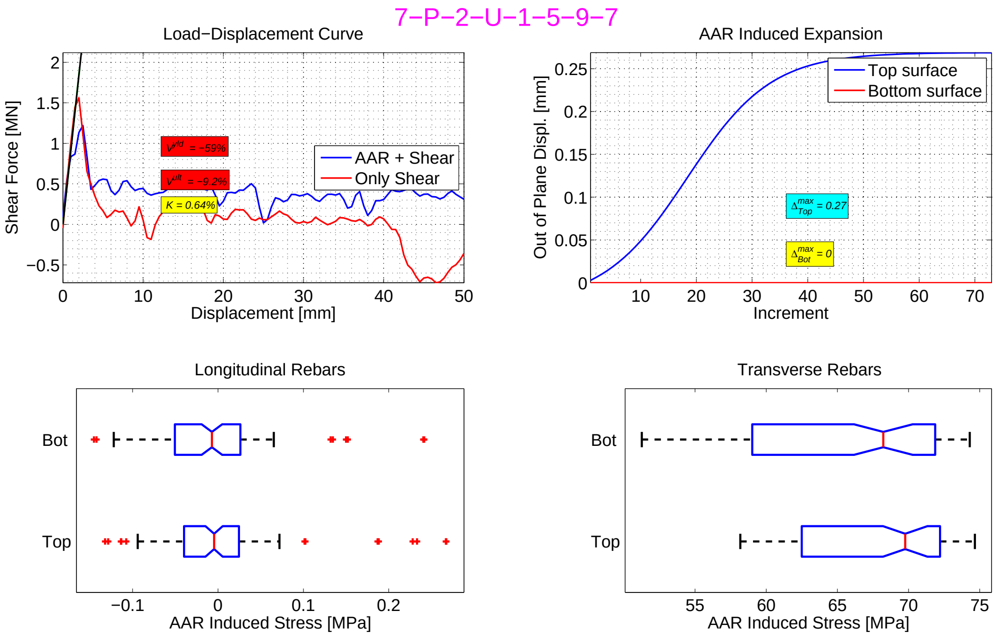

4.1.3.8 Analysis: 8-P-2-U-1-5-9-9

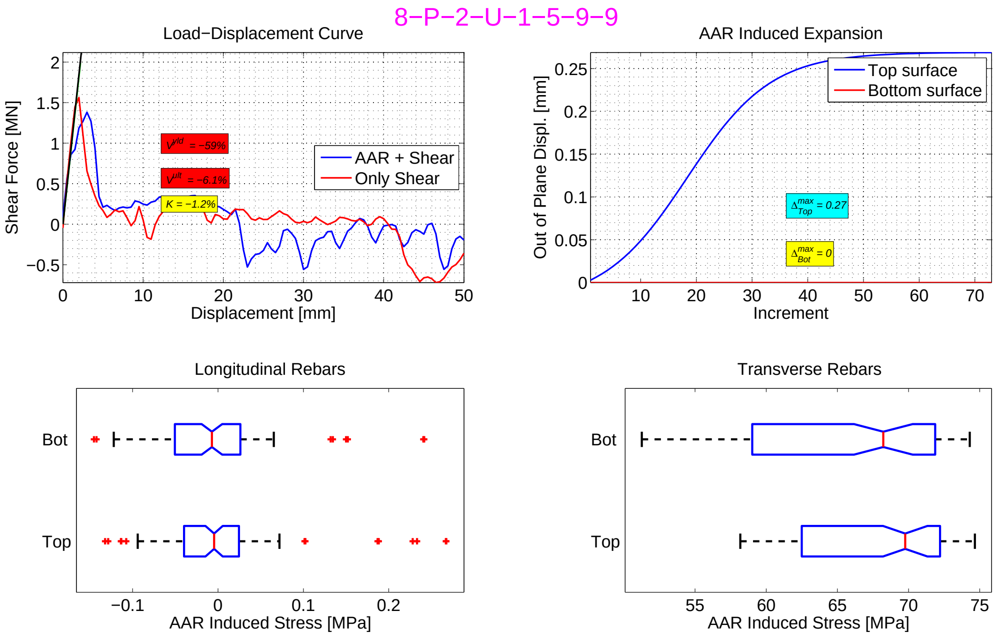

4.1.3.9 Analysis: 9-P-2-U-1-10-7-7

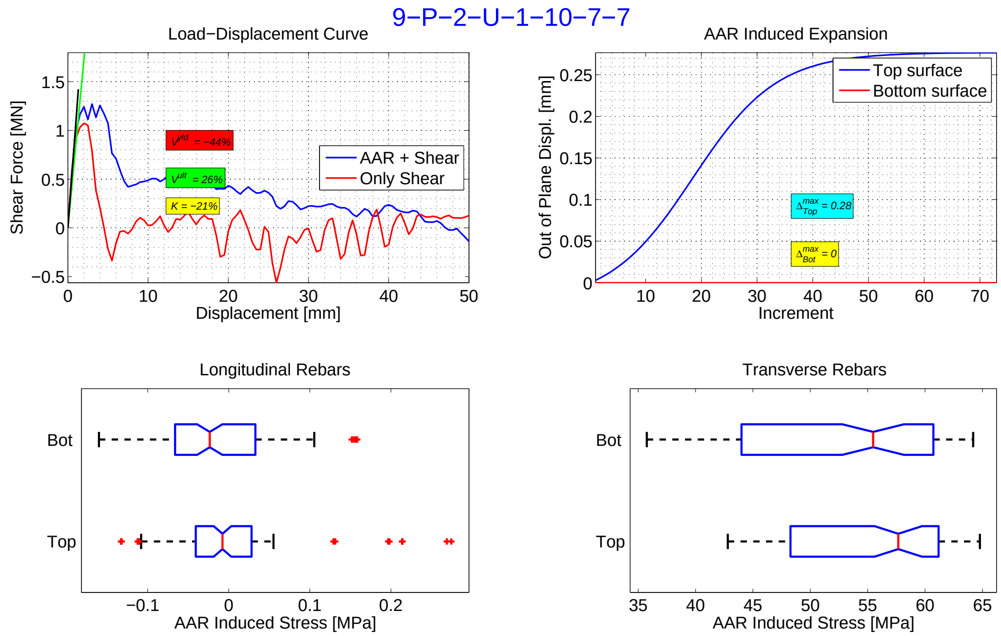

4.1.3.10 Analysis: 10-P-2-U-1-10-7-9

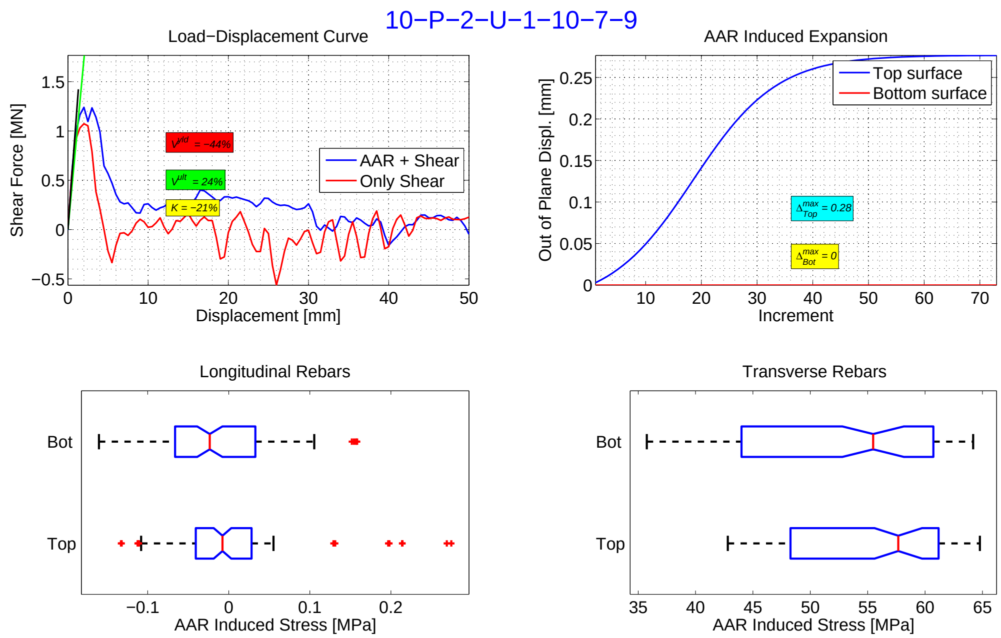

4.1.3.11 Analysis: 11-P-2-U-1-10-9-7

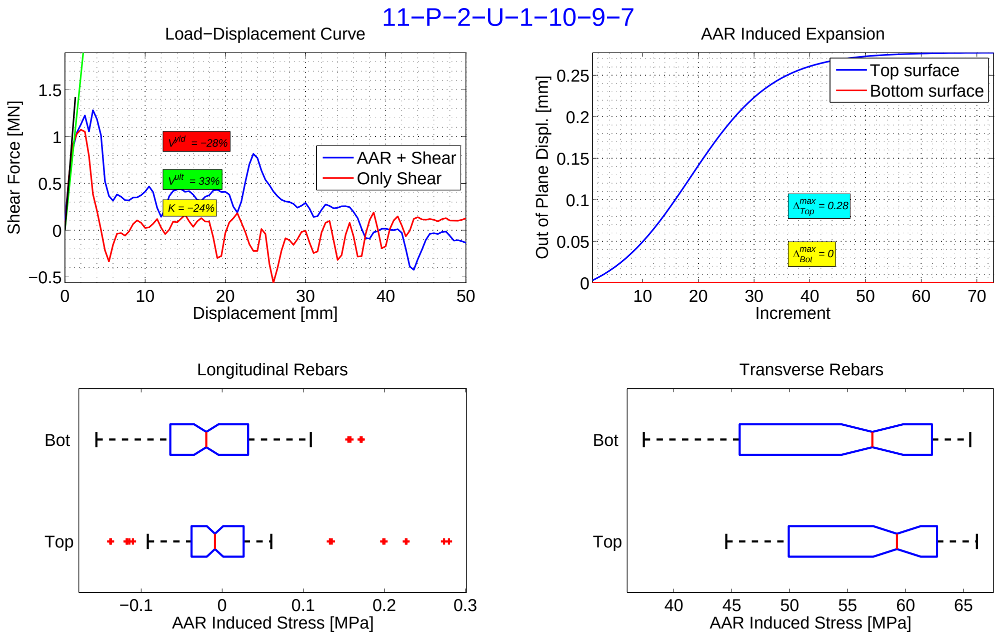

4.1.3.12 Analysis: 12-P-2-U-1-10-9-9

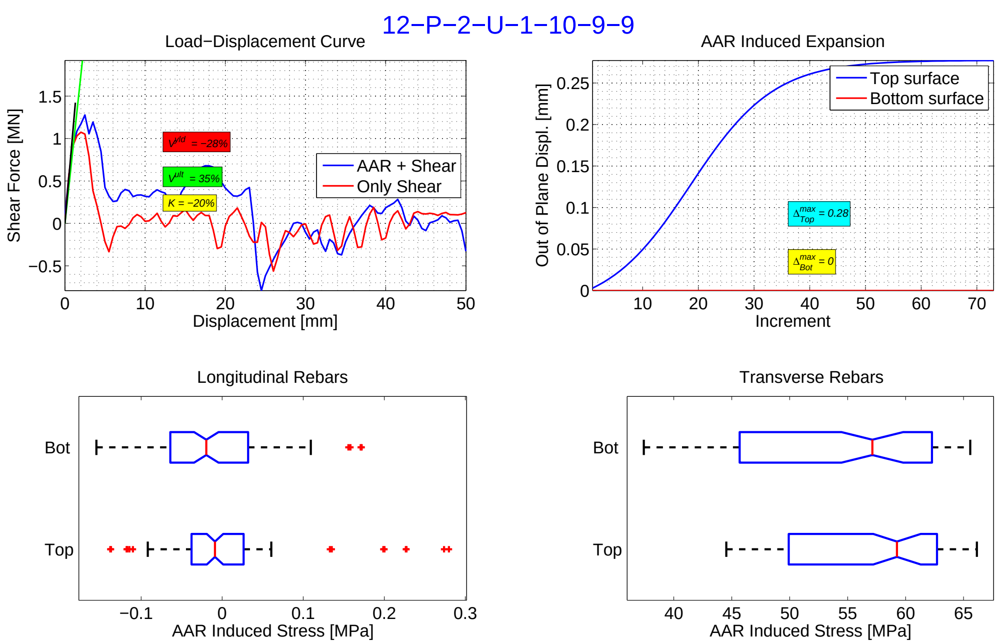

4.1.3.13 Analysis: 13-P-2-U-2-2-7-7

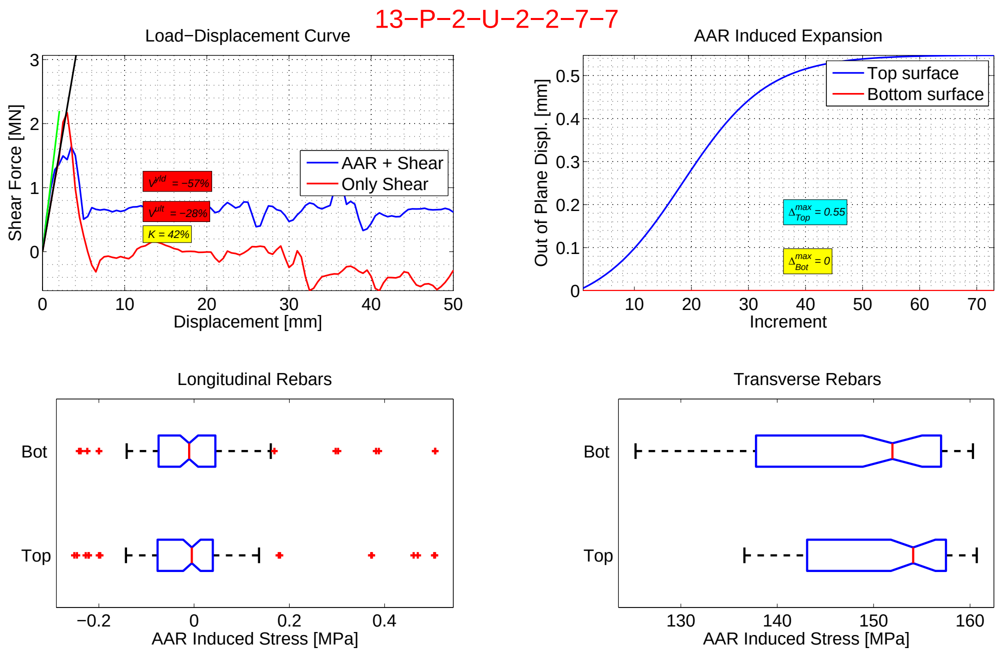

4.1.3.14 Analysis: 14-P-2-U-2-2-7-9

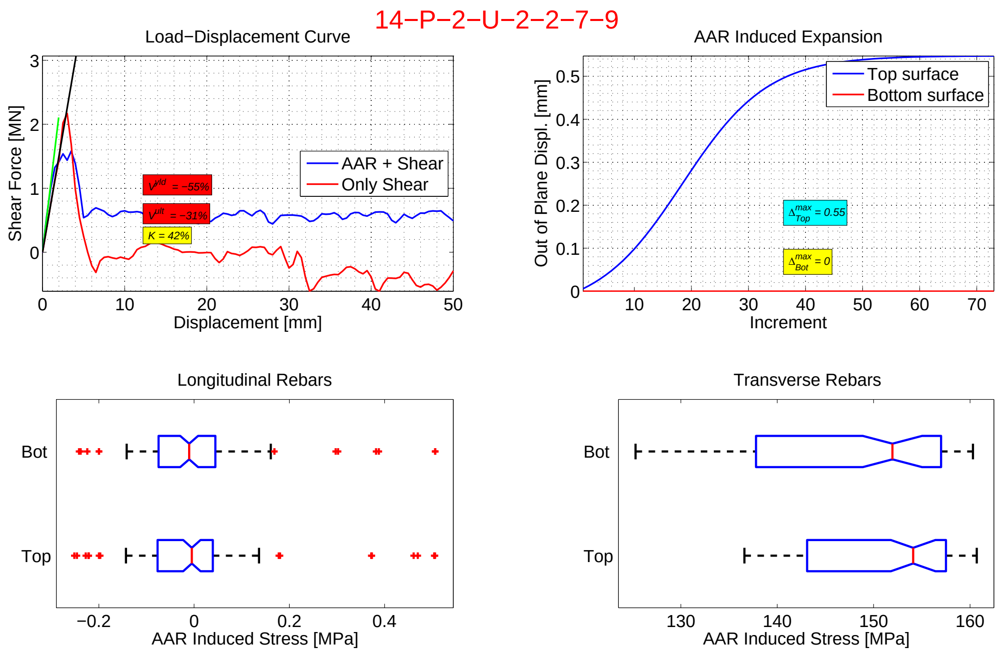

4.1.3.15 Analysis: 15-P-2-U-2-2-9-7

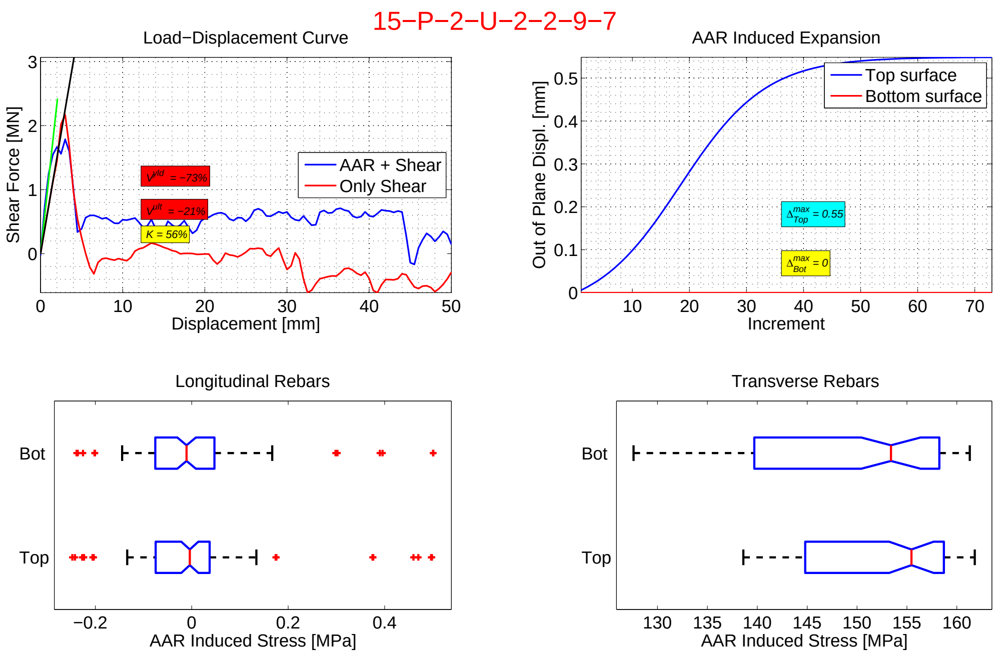

4.1.3.16 Analysis: 16-P-2-U-2-2-9-9

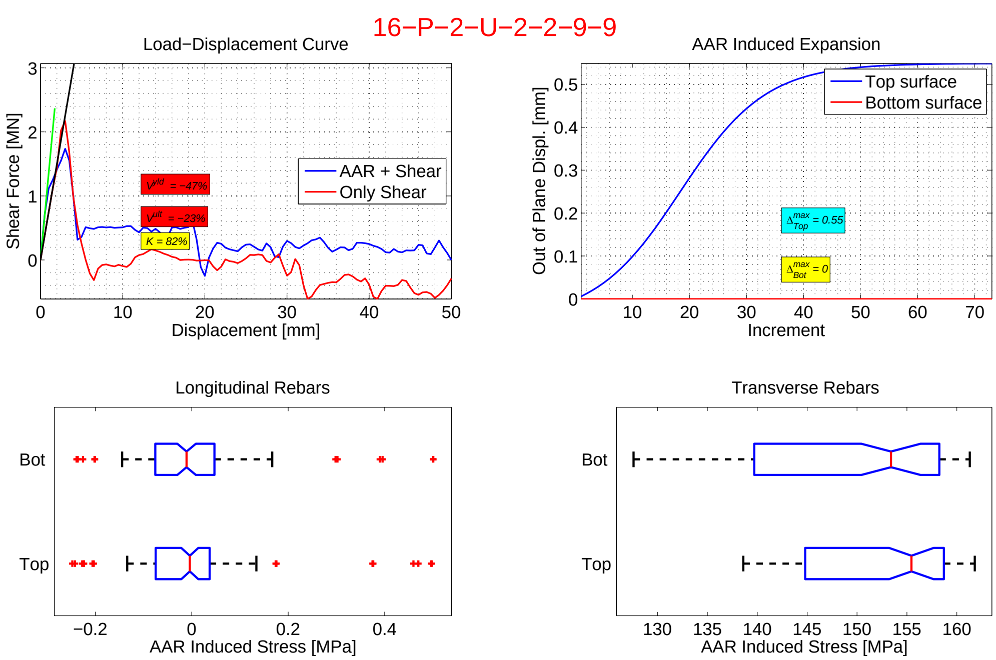

4.1.3.17 Analysis: 17-P-2-U-2-5-7-7

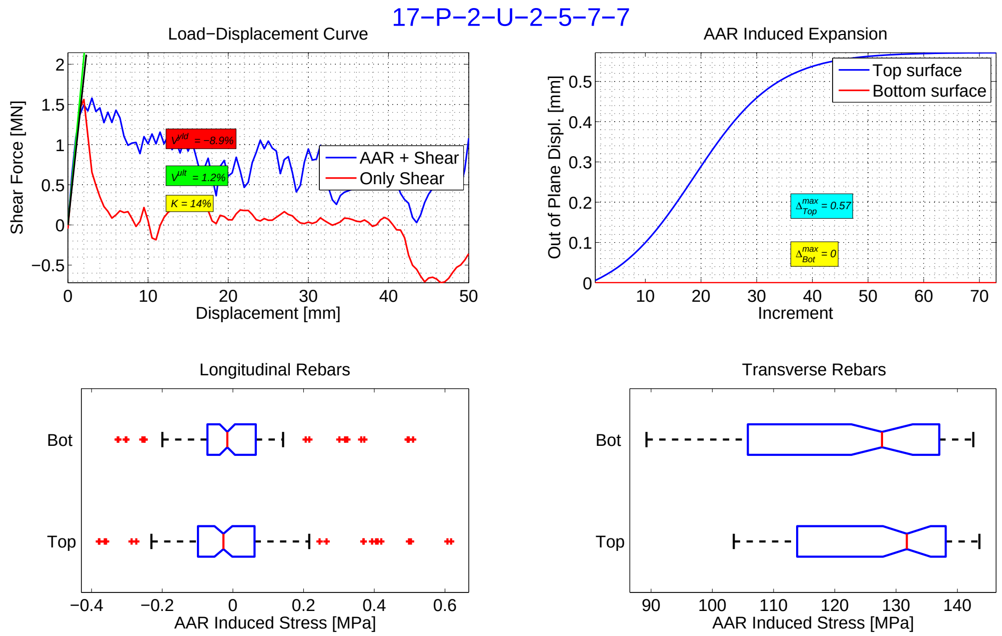

4.1.3.18 Analysis: 18-P-2-U-2-5-7-9

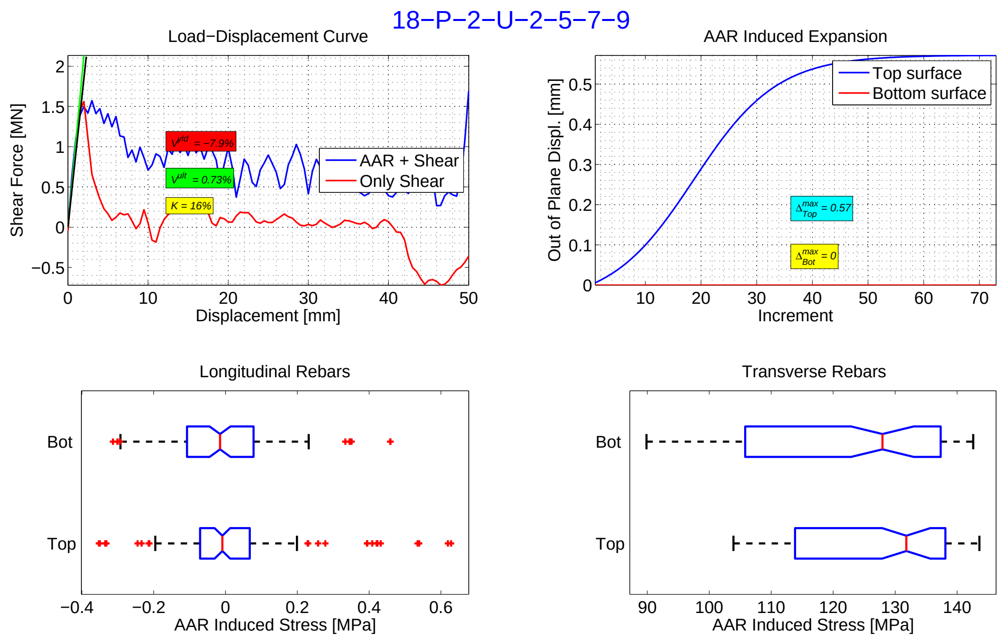

4.1.3.19 Analysis: 19-P-2-U-2-5-9-7

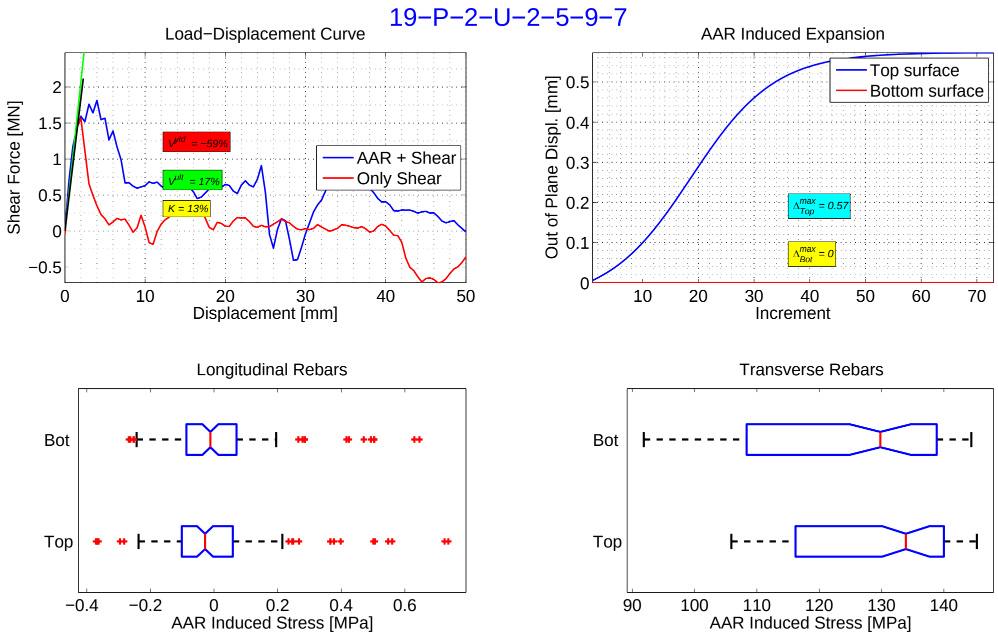

4.1.3.20 Analysis: 20-P-2-U-2-5-9-9

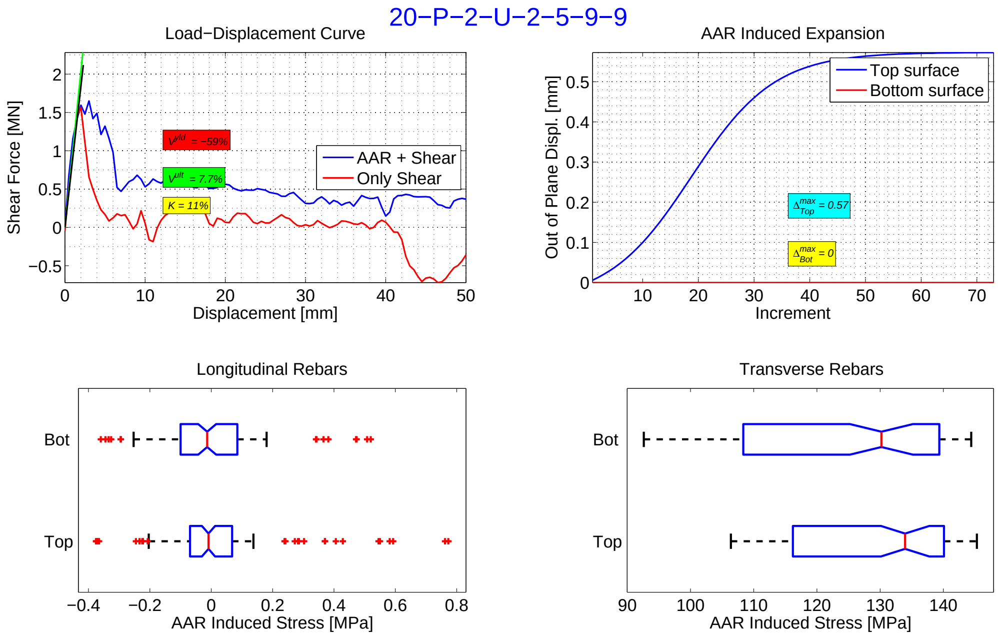

4.1.3.21 Analysis: 21-P-2-U-2-10-7-7

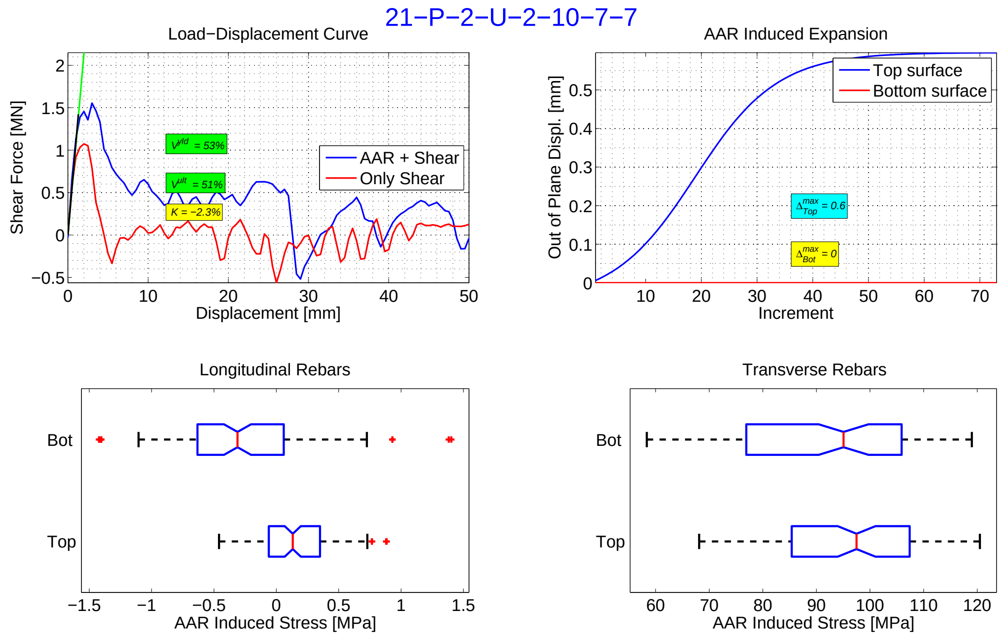

4.1.3.22 Analysis: 22-P-2-U-2-10-7-9

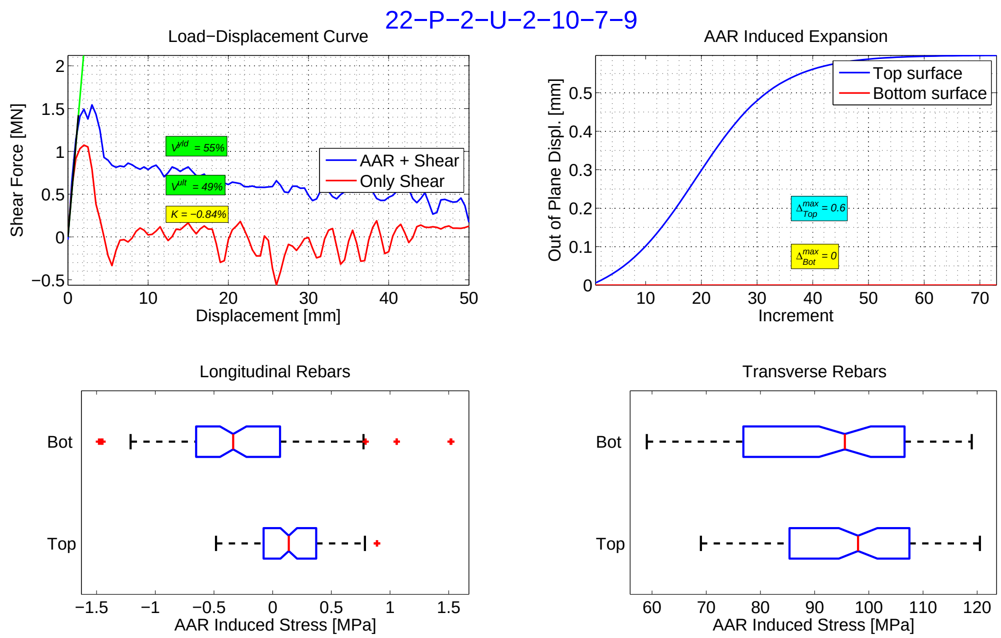

4.1.3.23 Analysis: 23-P-2-U-2-10-9-7

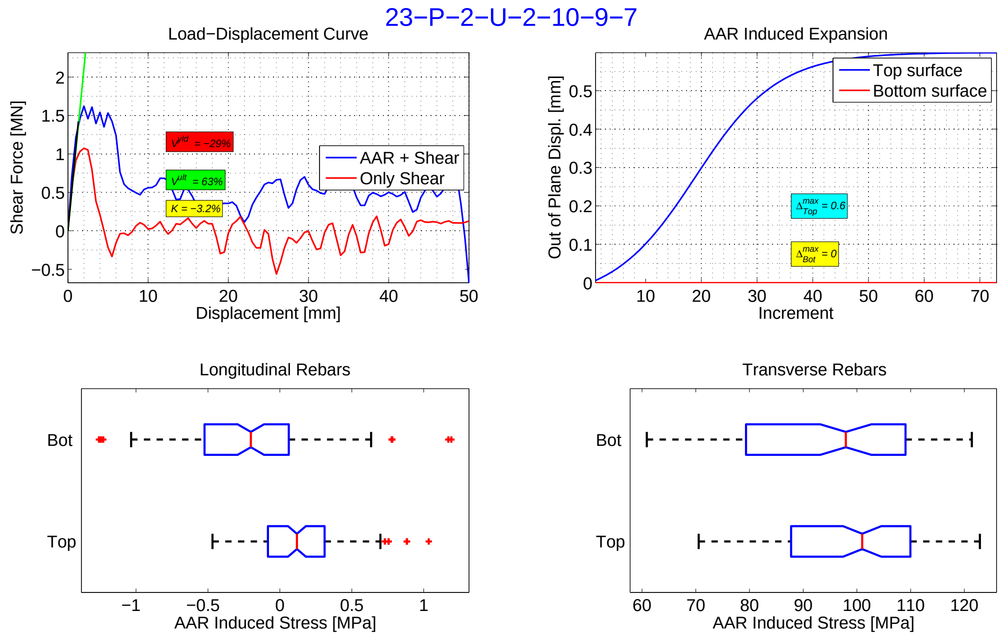

4.1.3.24 Analysis: 24-P-2-U-2-10-9-9

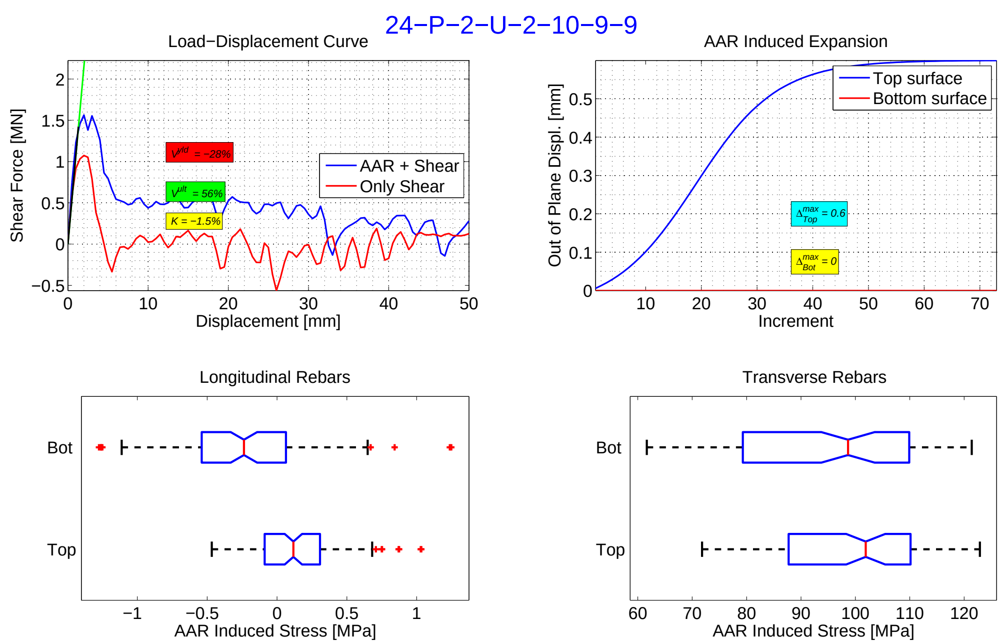

4.1.3.25 Analysis: 25-P-2-U-3-2-7-7

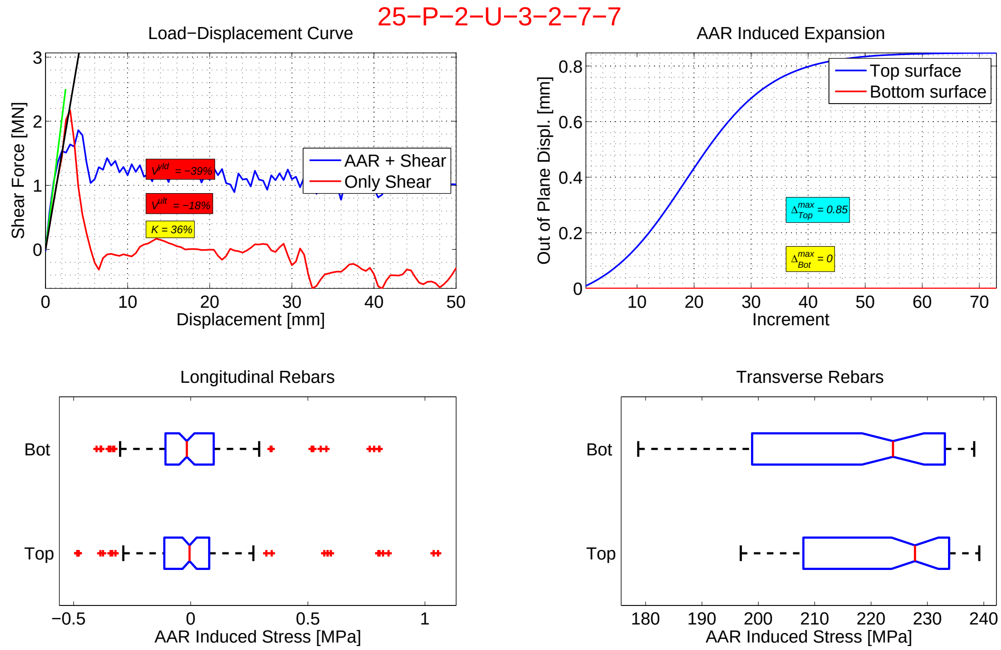

4.1.3.26 Analysis: 26-P-2-U-3-2-7-9

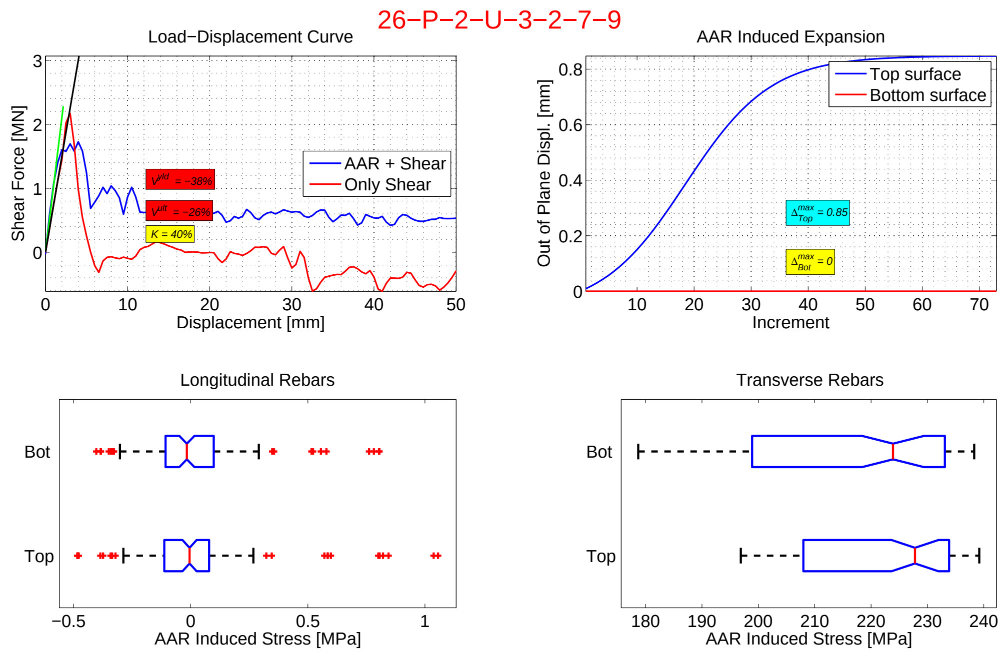

4.1.3.27 Analysis: 27-P-2-U-3-2-9-7

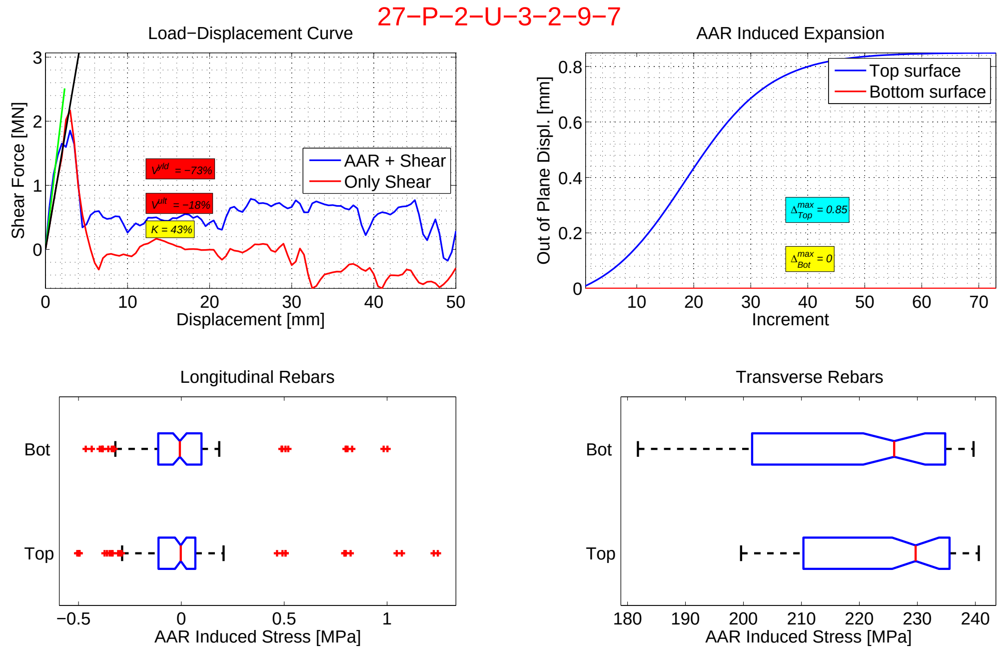

4.1.3.28 Analysis: 28-P-2-U-3-2-9-9

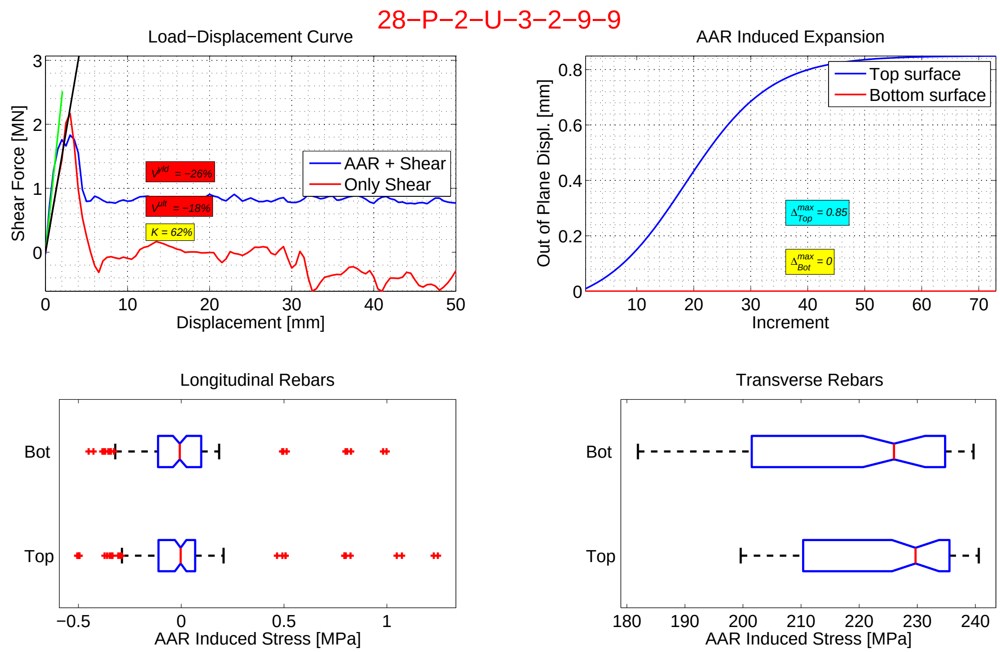

4.1.3.29 Analysis: 29-P-2-U-3-5-7-7

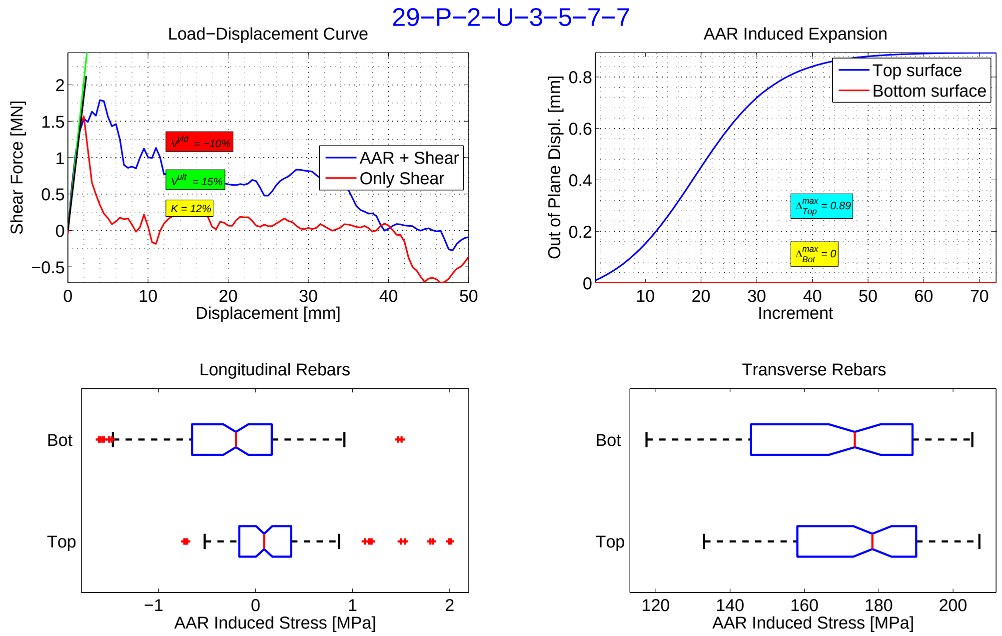

4.1.3.30 Analysis: 30-P-2-U-3-5-7-9

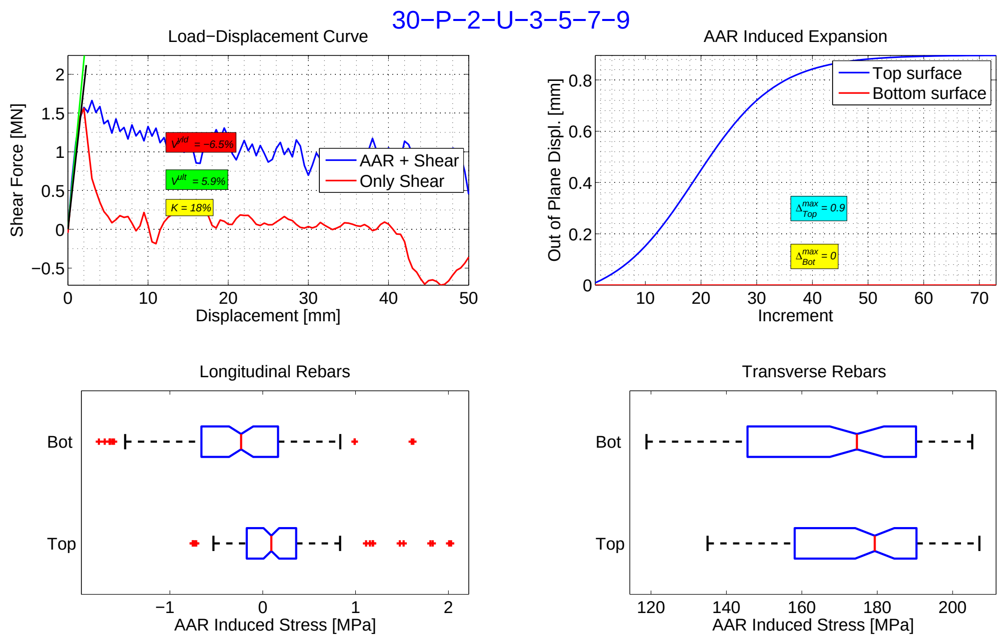

4.1.3.31 Analysis: 31-P-2-U-3-5-9-7

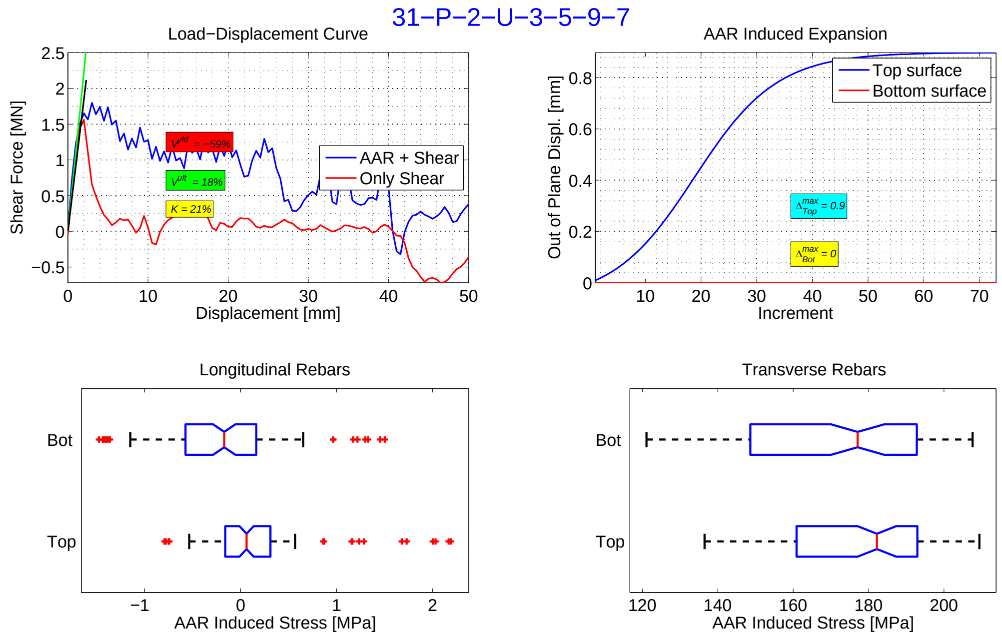

4.1.3.32 Analysis: 32-P-2-U-3-5-9-9

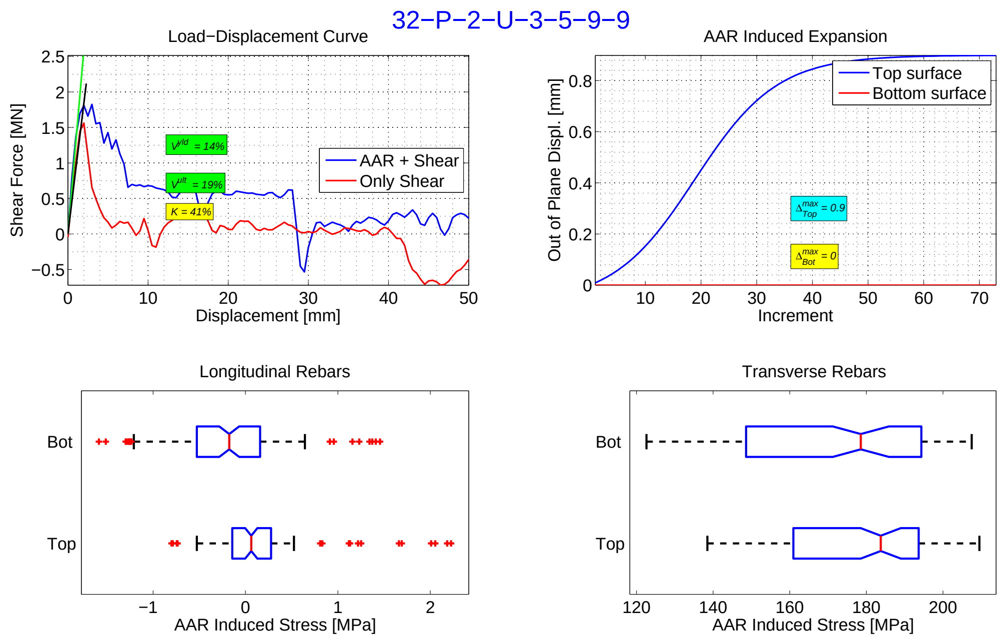

4.1.3.33 Analysis: 33-P-2-U-3-10-7-7

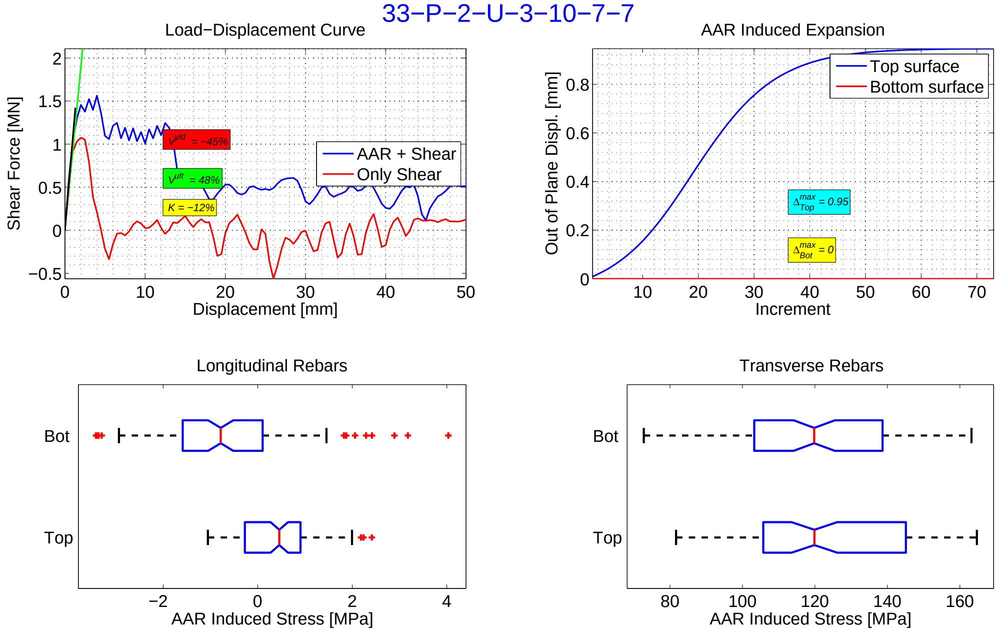

4.1.3.34 Analysis: 34-P-2-U-3-10-7-9

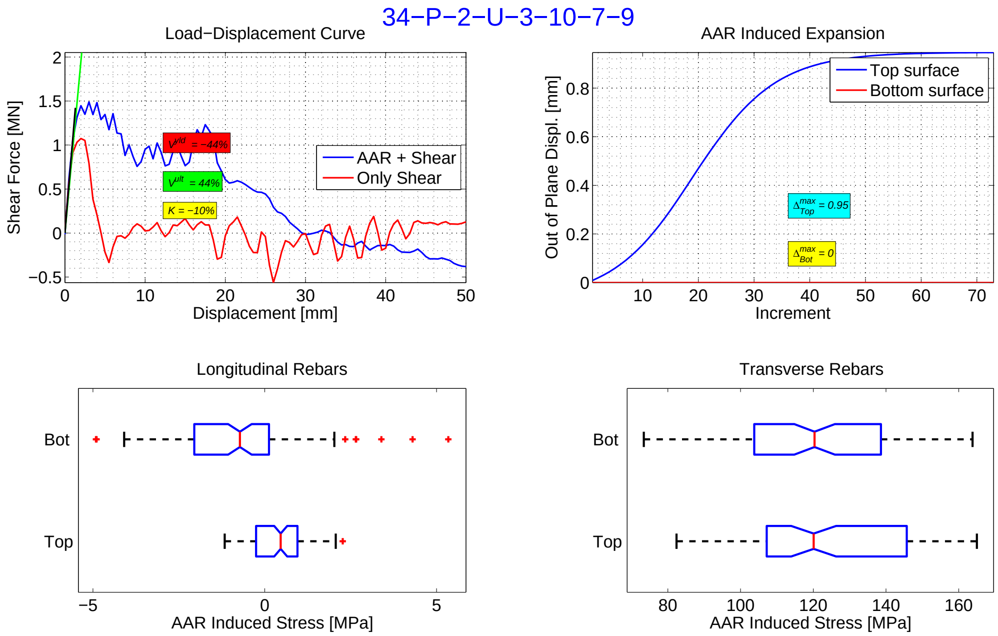

4.1.3.35 Analysis: 35-P-2-U-3-10-9-7

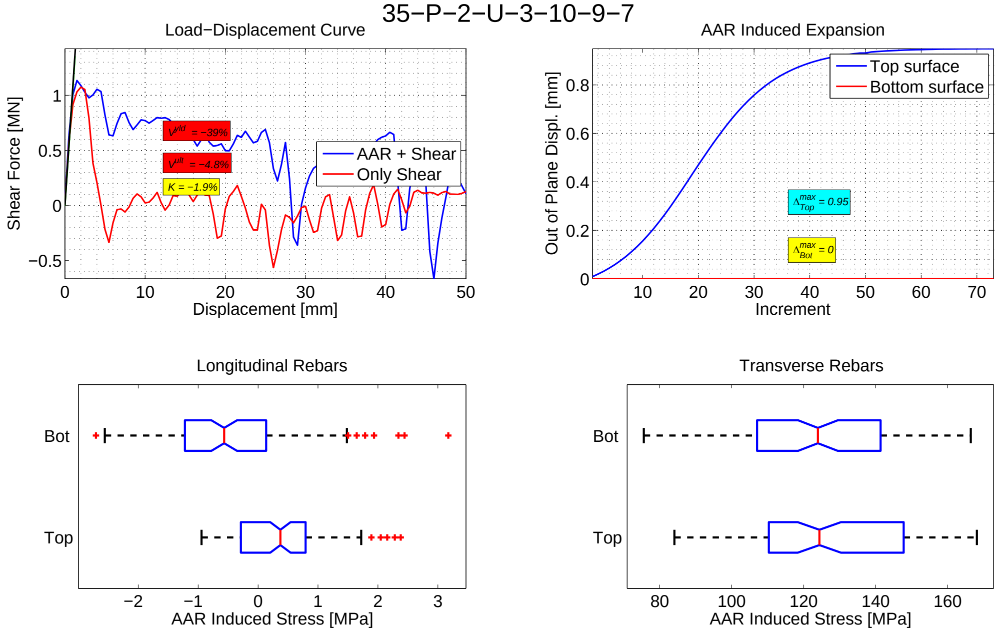

4.1.3.36 Analysis: 36-P-2-U-3-10-9-9

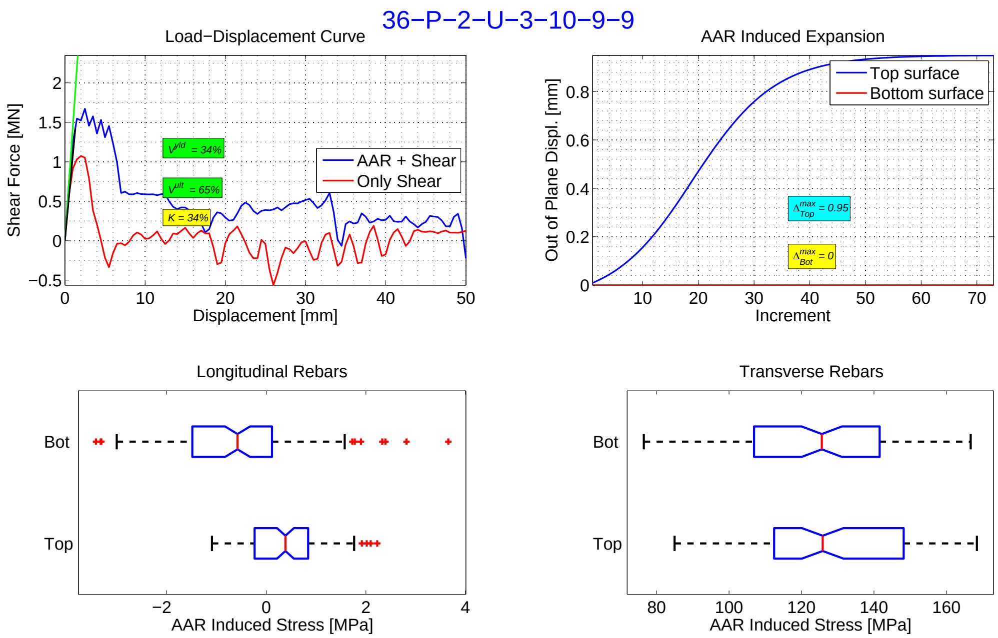

4.1.3.37 Analysis: 37-P-4-U-1-2-7-7

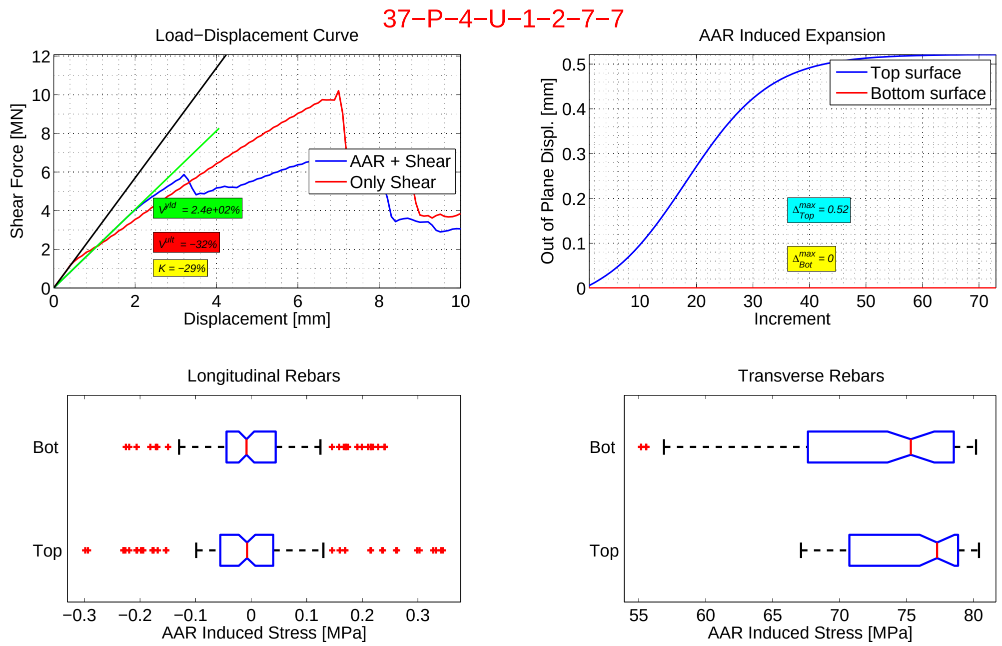

4.1.3.38 Analysis: 38-P-4-U-1-2-7-9

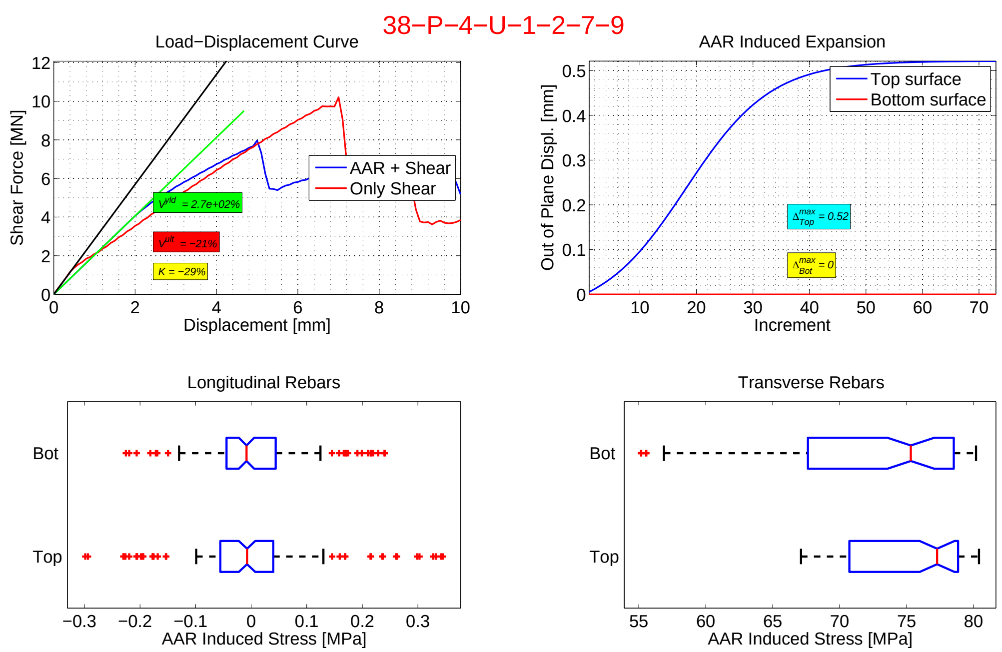

4.1.3.39 Analysis: 39-P-4-U-1-2-9-7

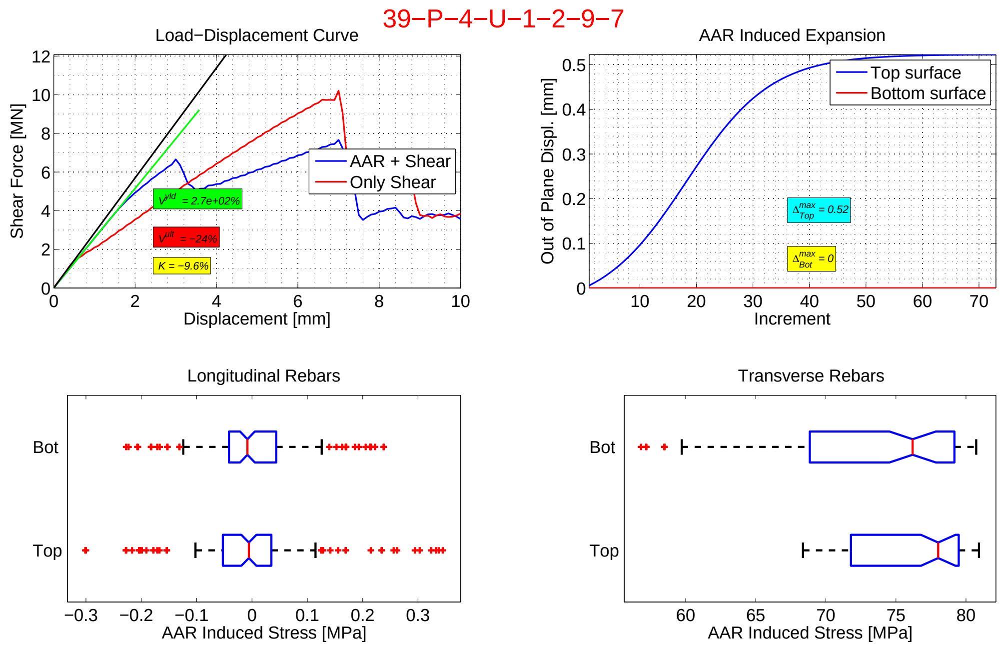

4.1.3.40 Analysis: 40-P-4-U-1-2-9-9

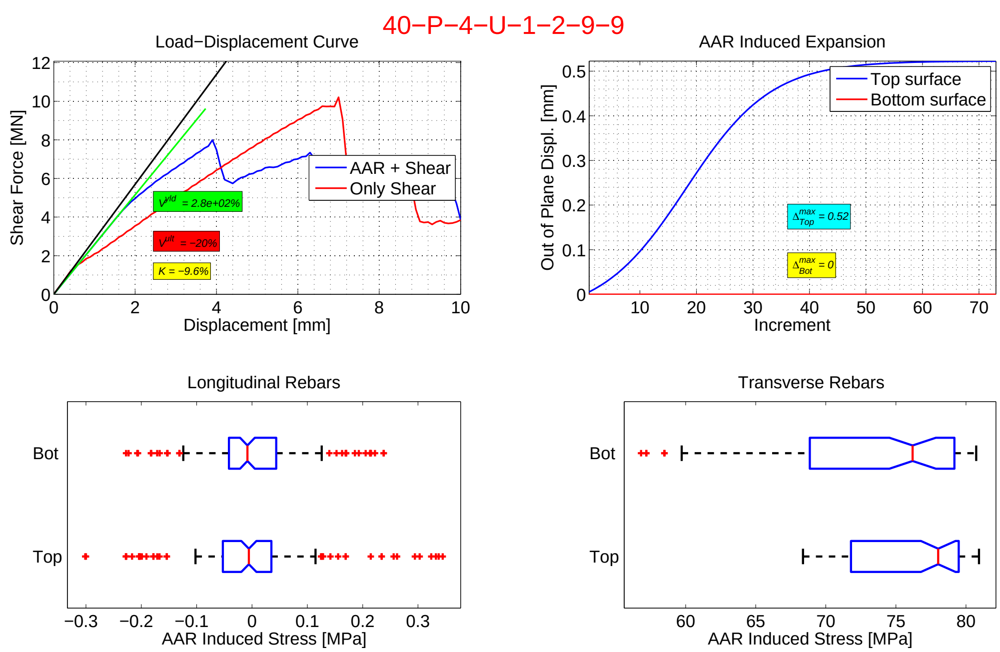

4.1.3.41 Analysis: 41-P-4-U-1-5-7-7

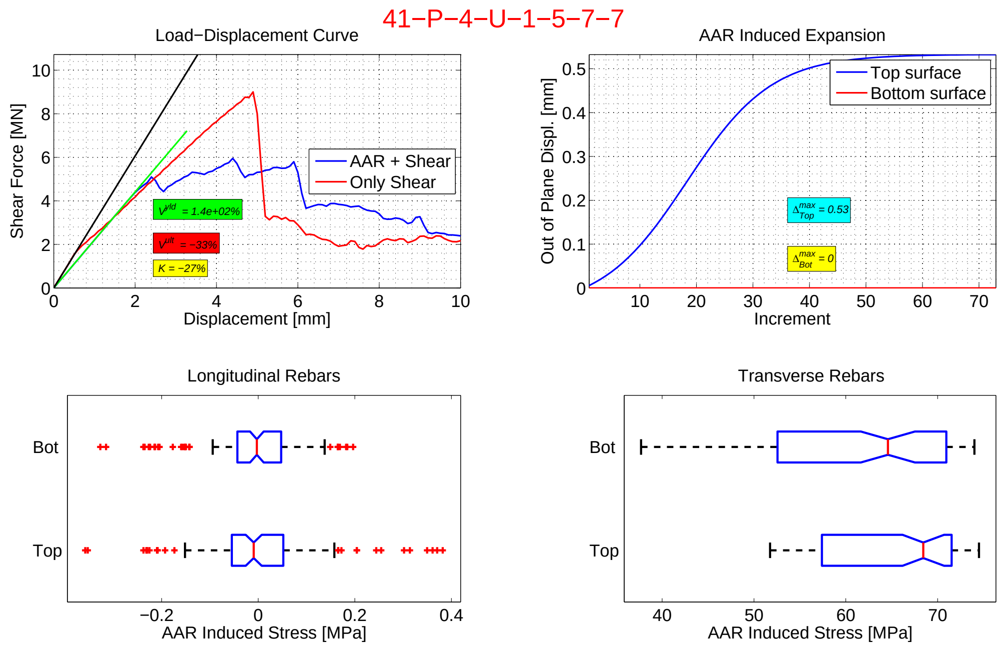

4.1.3.42 Analysis: 42-P-4-U-1-5-7-9

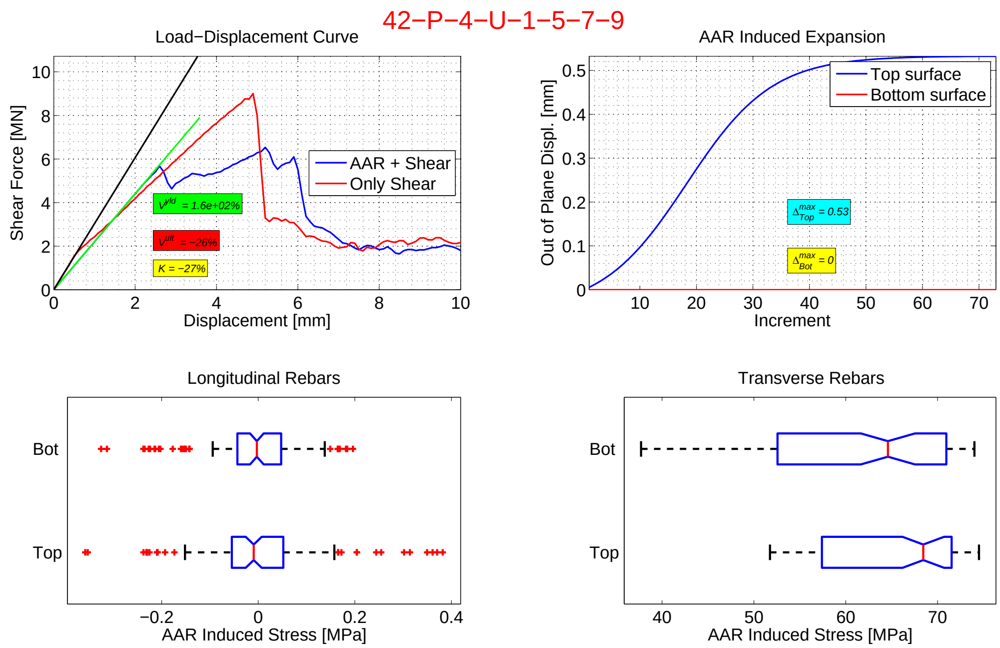

4.1.3.43 Analysis: 43-P-4-U-1-5-9-7

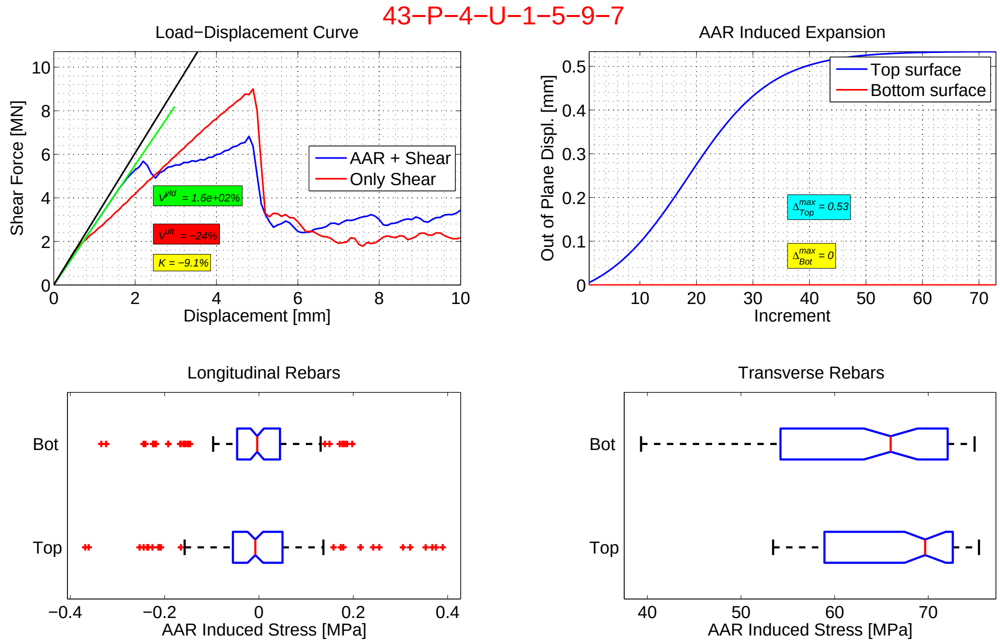

4.1.3.44 Analysis: 44-P-4-U-1-5-9-9

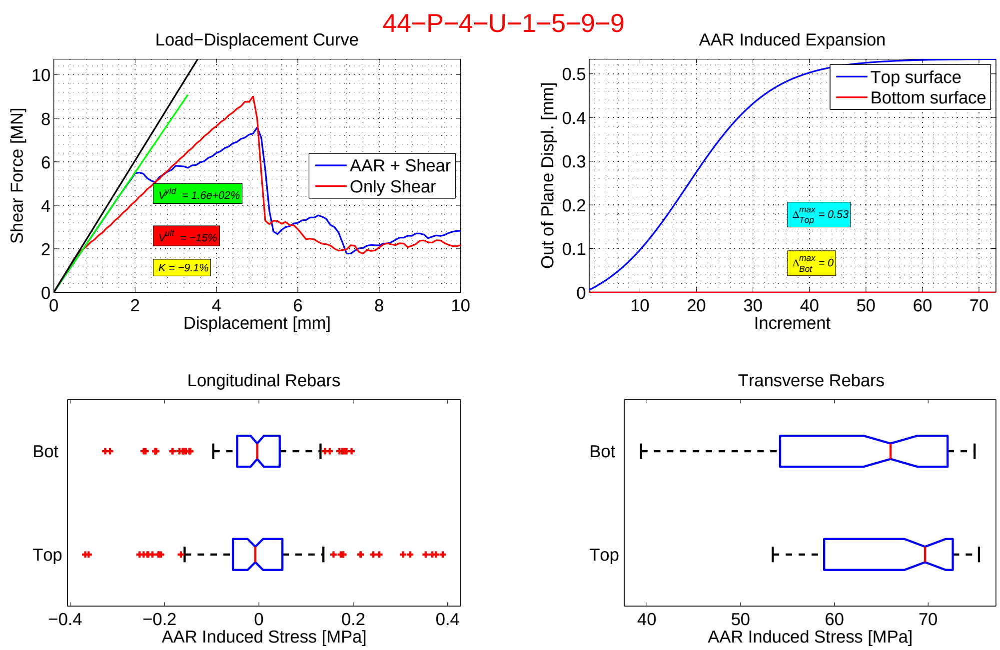

4.1.3.45 Analysis: 45-P-4-U-1-10-7-7

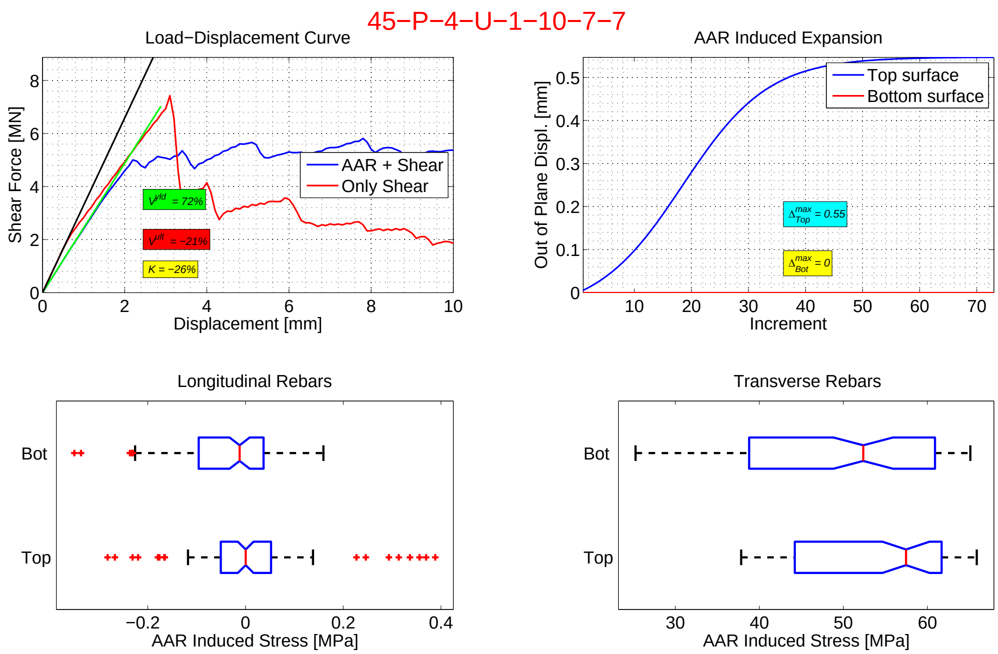

4.1.3.46 Analysis: 46-P-4-U-1-10-7-9

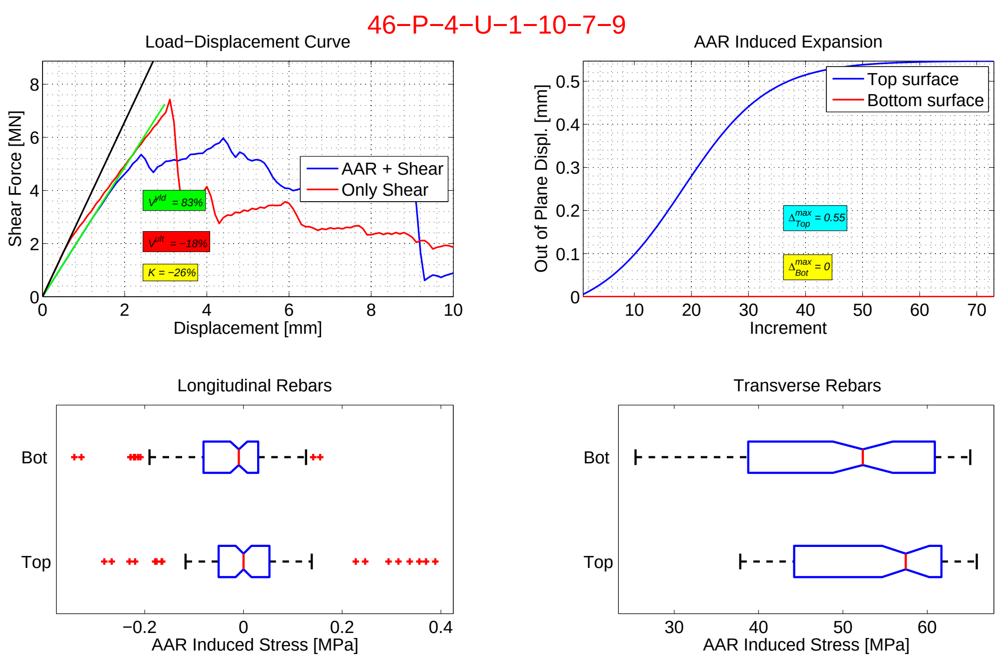

4.1.3.47 Analysis: 47-P-4-U-1-10-9-7

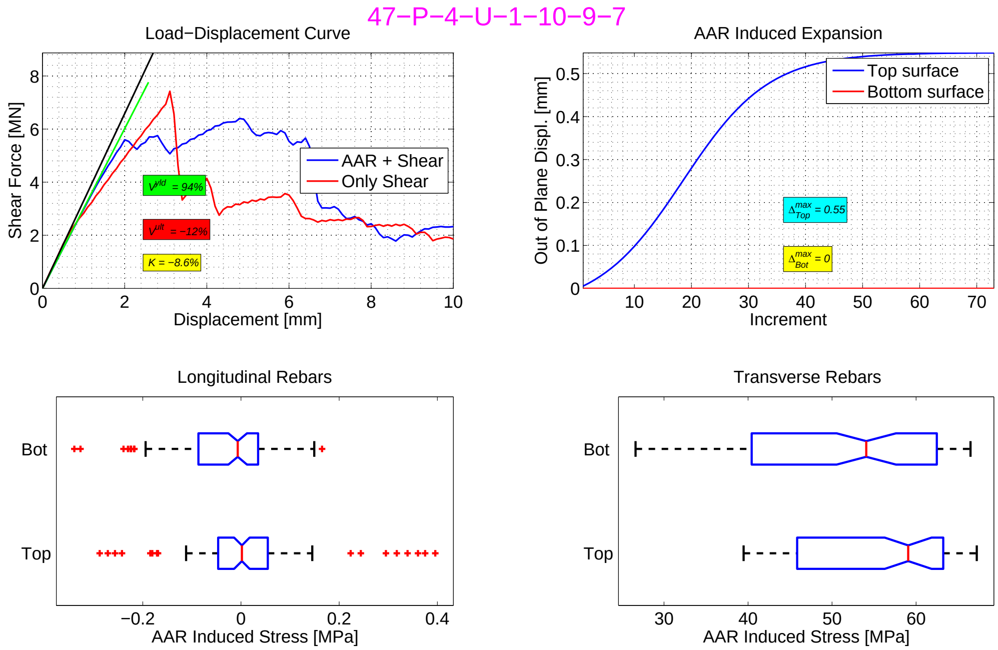

4.1.3.48 Analysis: 48-P-4-U-1-10-9-9

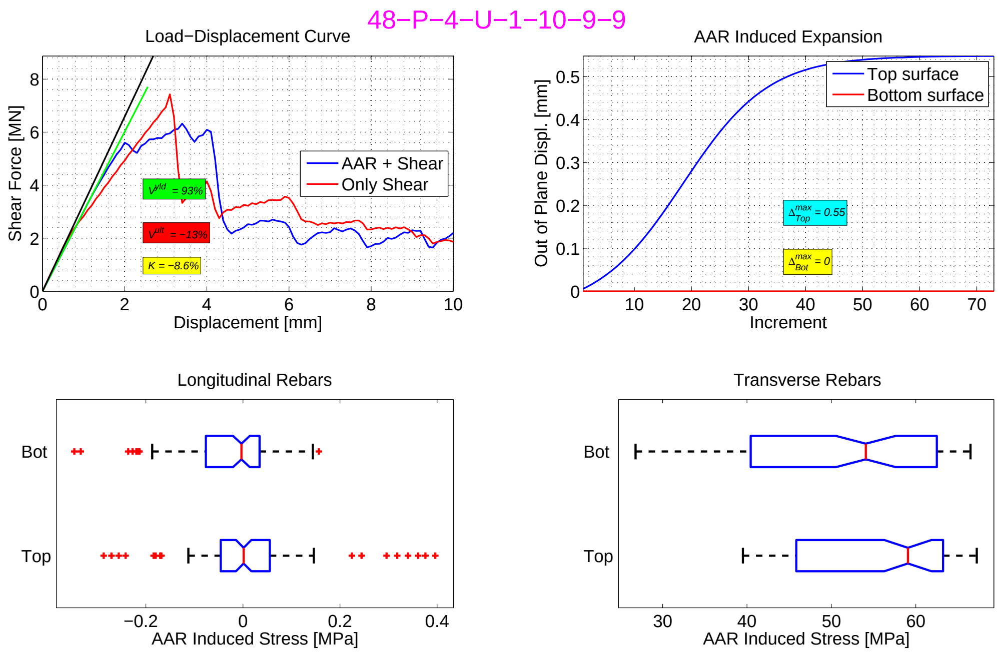

4.1.3.49 Analysis: 49-P-4-U-2-2-7-7

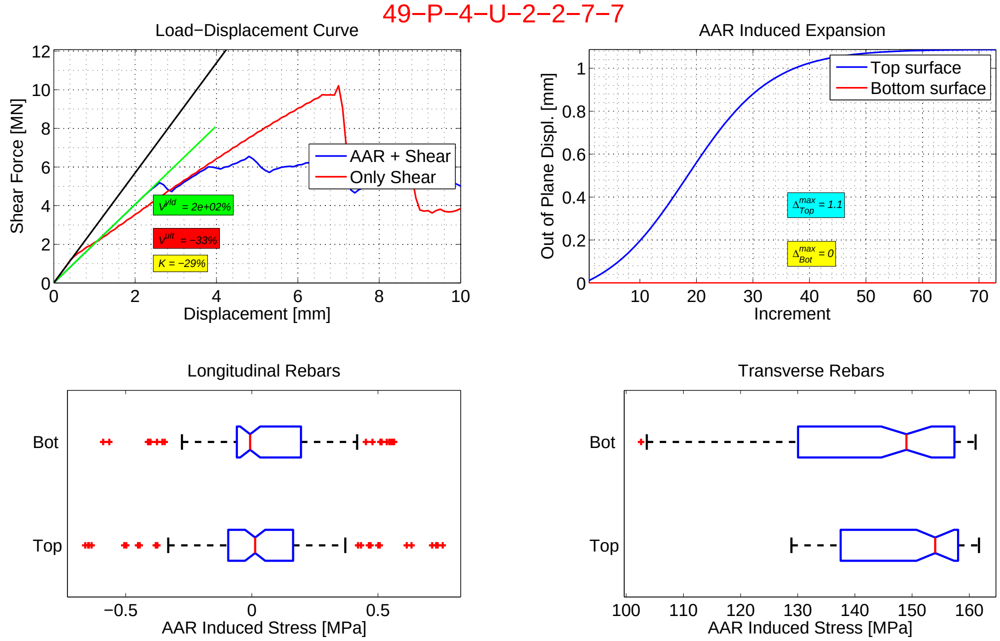

4.1.3.50 Analysis: 50-P-4-U-2-2-7-9

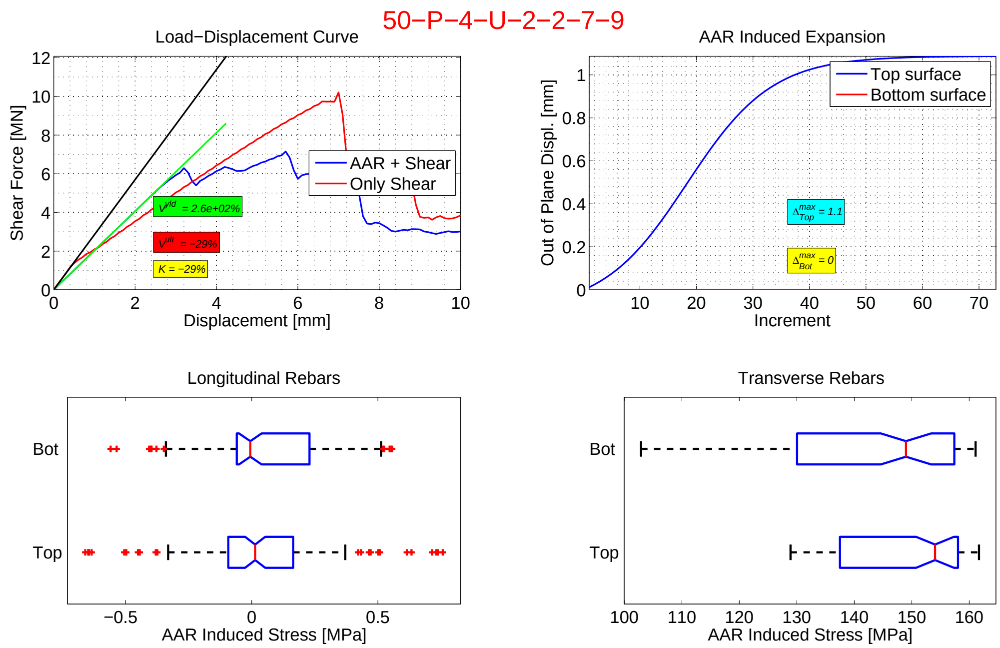

4.1.3.51 Analysis: 51-P-4-U-2-2-9-7

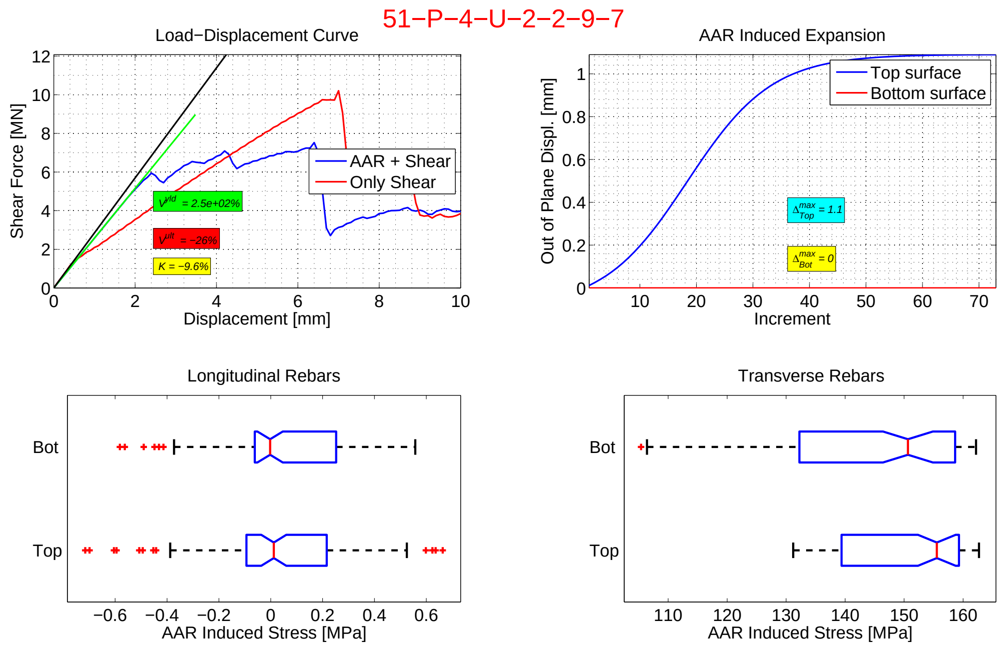

4.1.3.52 Analysis: 52-P-4-U-2-2-9-9

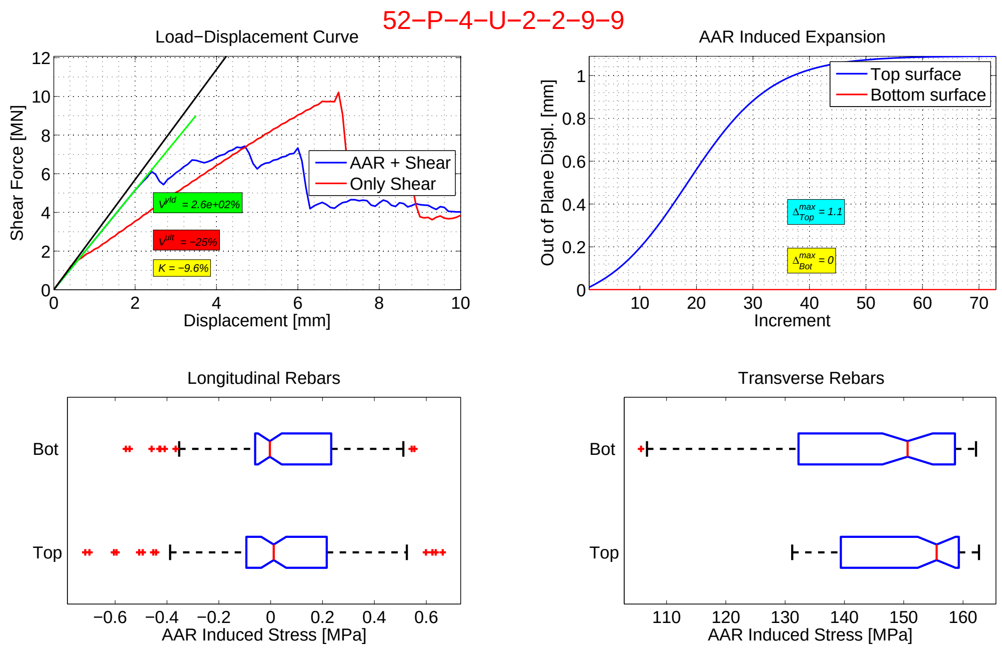

4.1.3.53 Analysis: 53-P-4-U-2-5-7-7

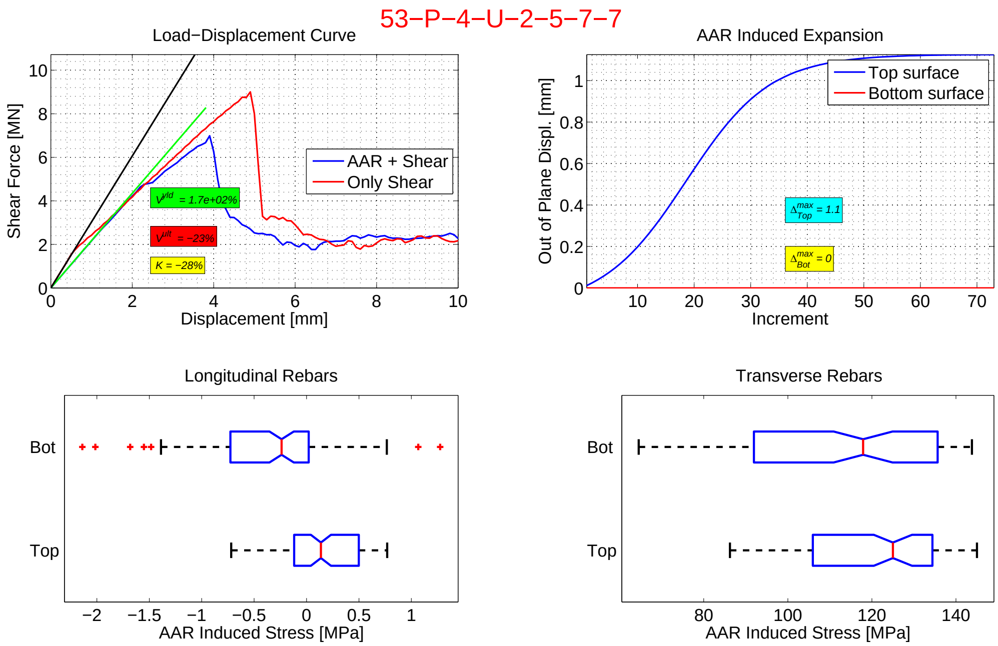

4.1.3.54 Analysis: 54-P-4-U-2-5-7-9

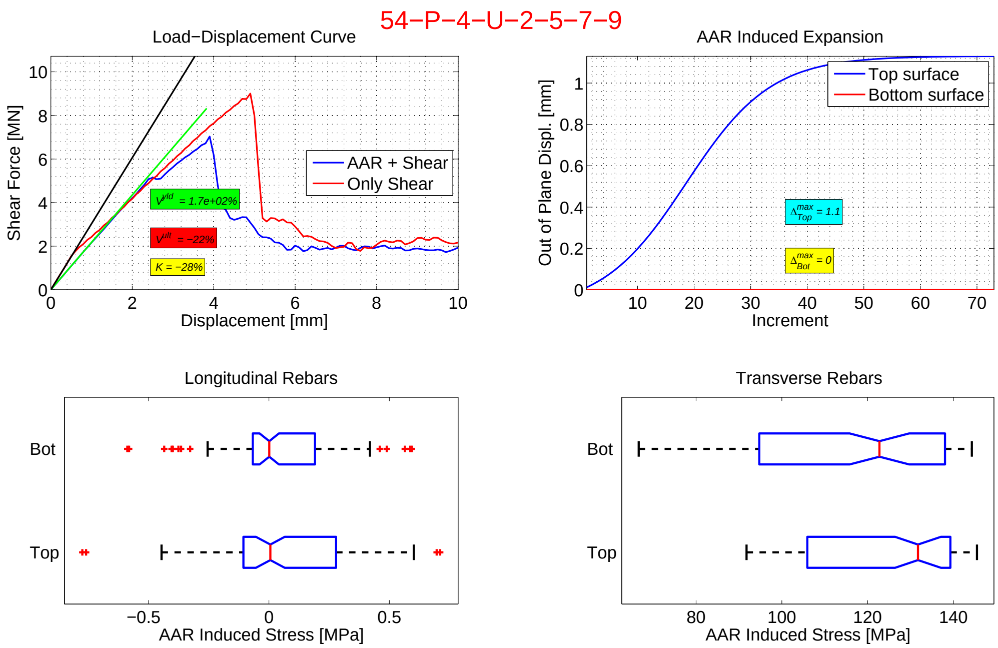

4.1.3.55 Analysis: 55-P-4-U-2-5-9-7

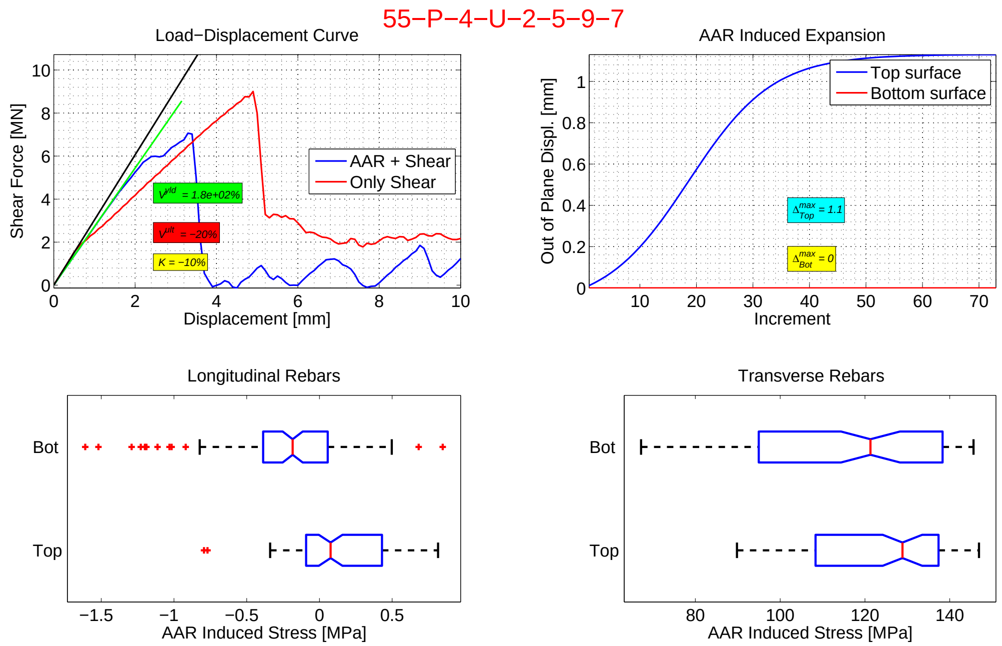

4.1.3.56 Analysis: 56-P-4-U-2-5-9-9

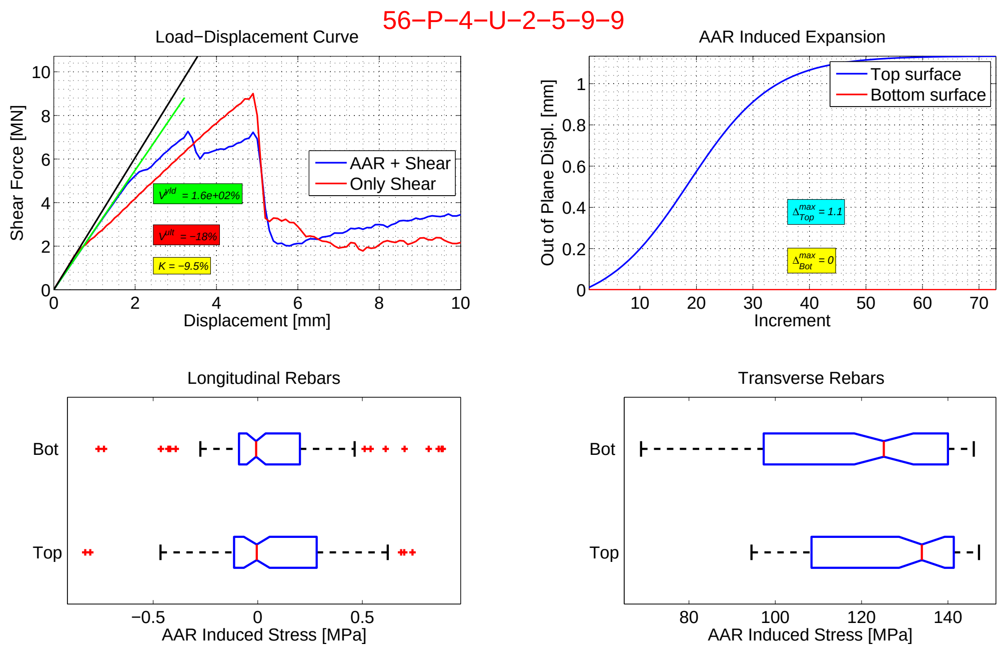

4.1.3.57 Analysis: 57-P-4-U-2-10-7-7

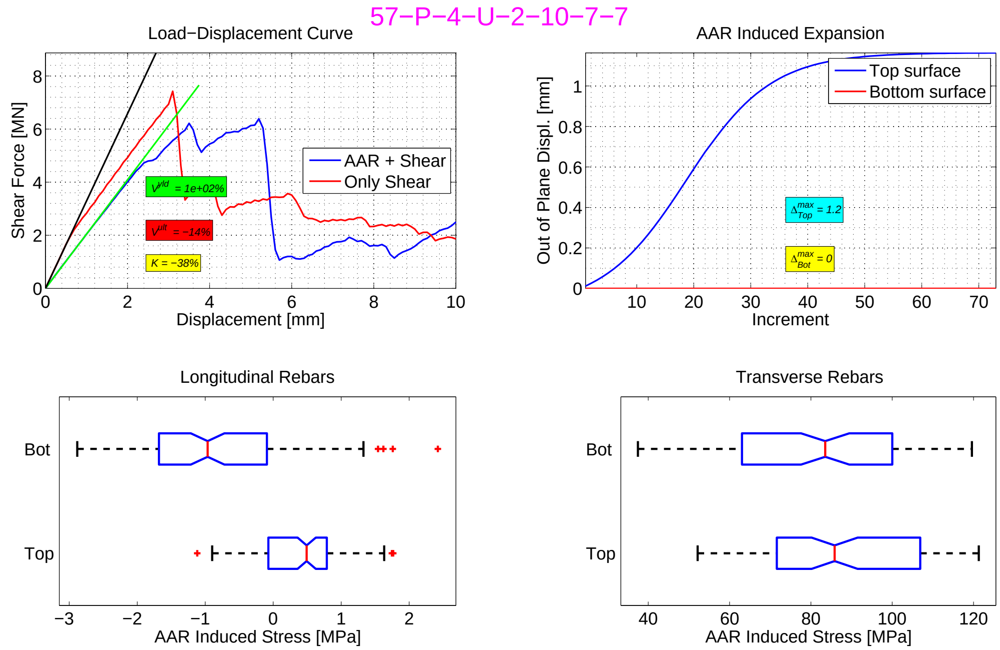

4.1.3.58 Analysis: 58-P-4-U-2-10-7-9

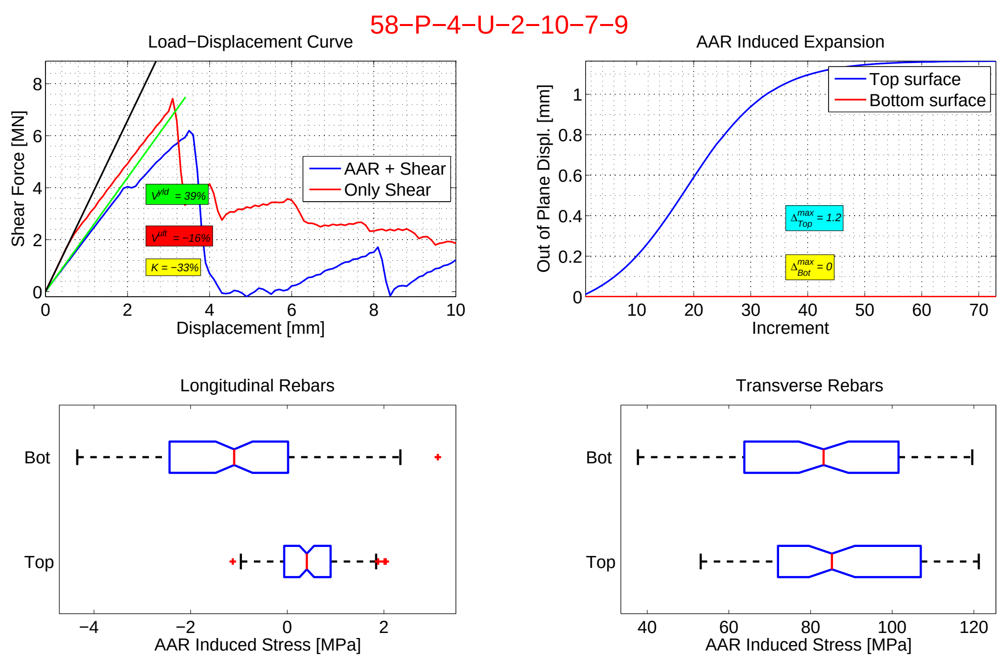

4.1.3.59 Analysis: 59-P-4-U-2-10-9-7

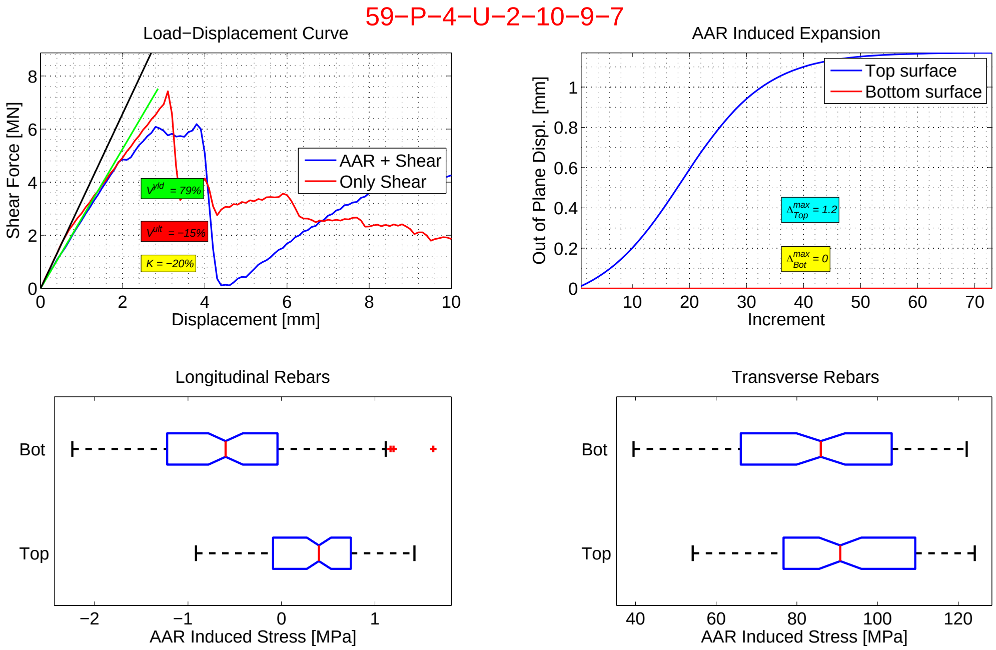

4.1.3.60 Analysis: 60-P-4-U-2-10-9-9

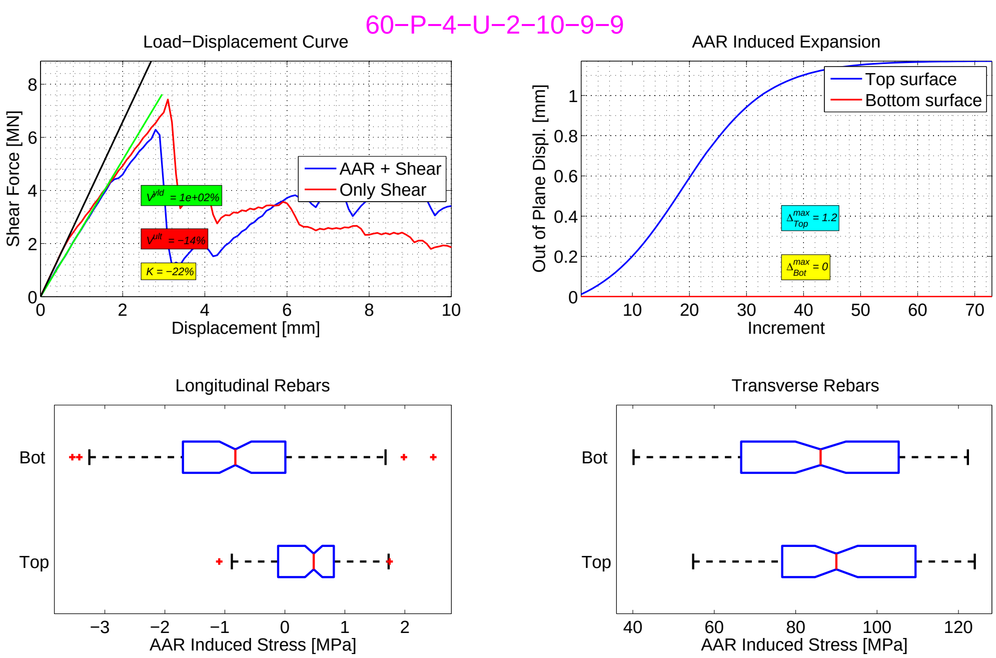

4.1.3.61 Analysis: 61-P-4-U-3-2-7-7

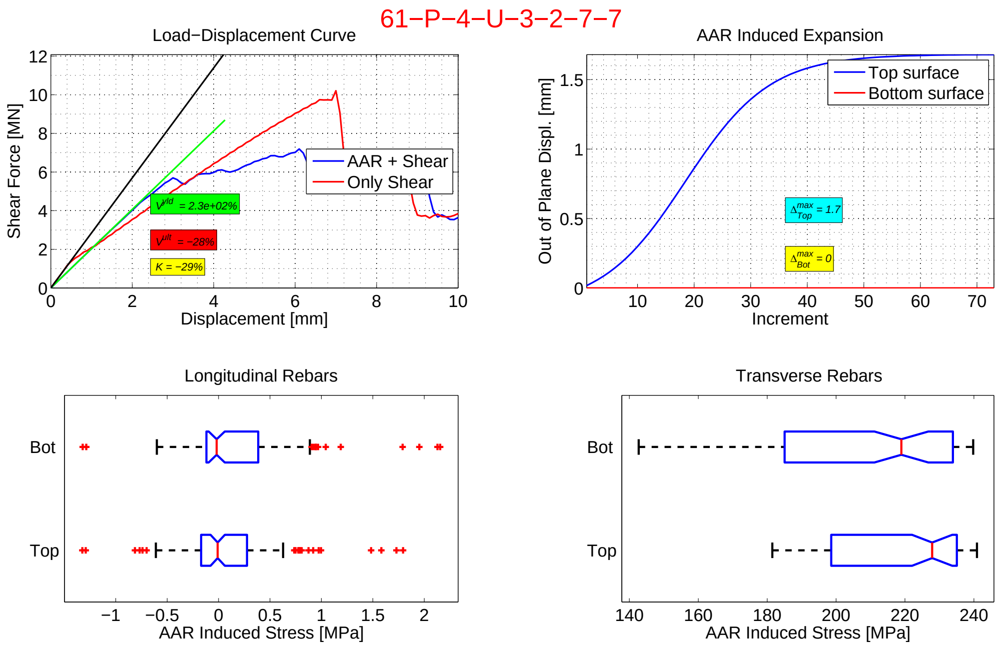

4.1.3.62 Analysis: 62-P-4-U-3-2-7-9

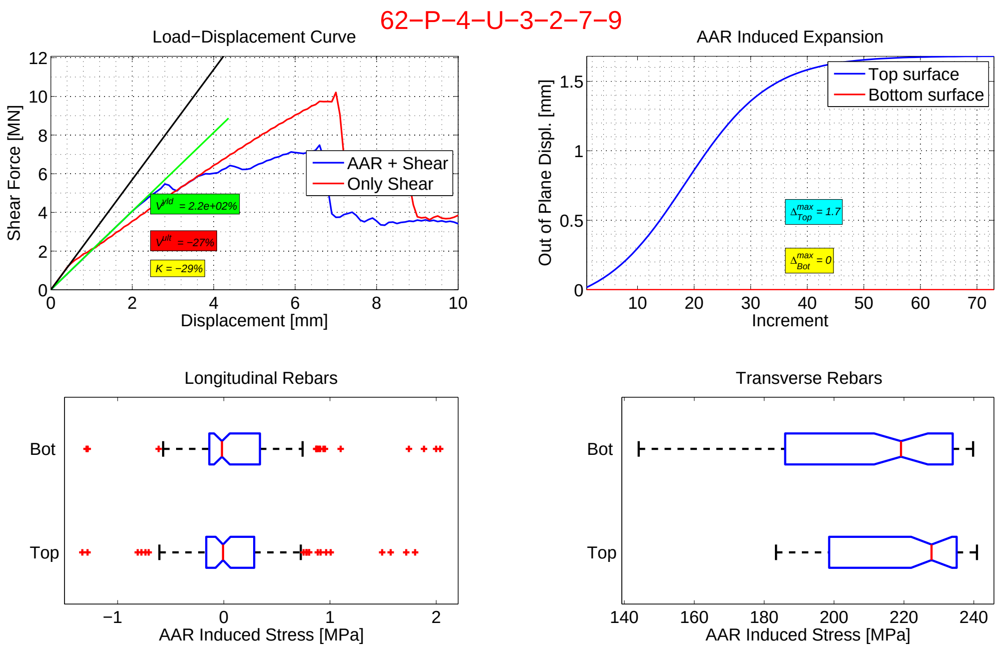

4.1.3.63 Analysis: 63-P-4-U-3-2-9-7

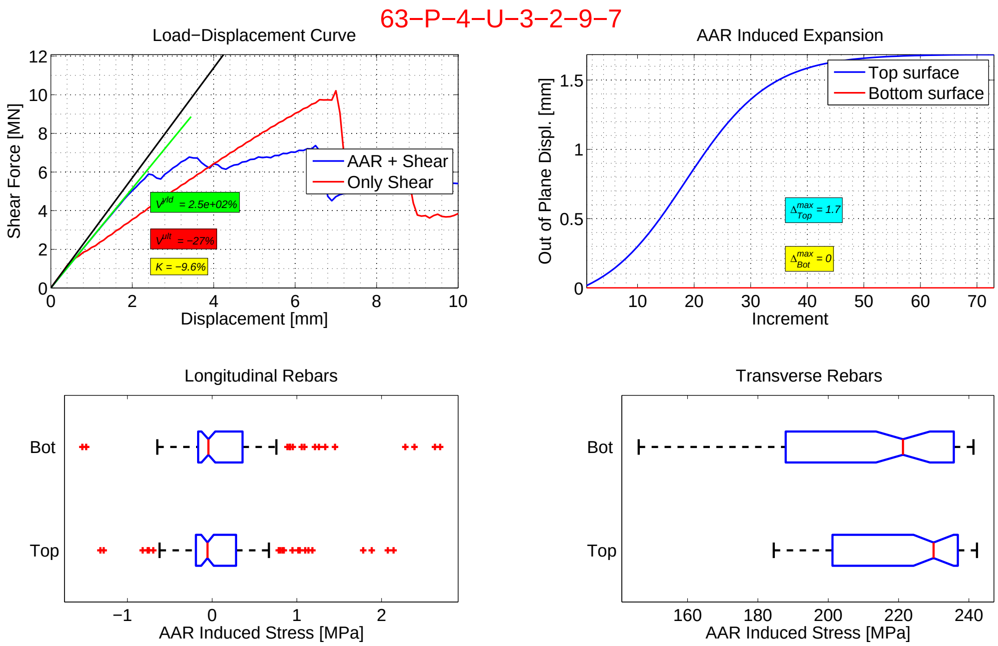

4.1.3.64 Analysis: 64-P-4-U-3-2-9-9

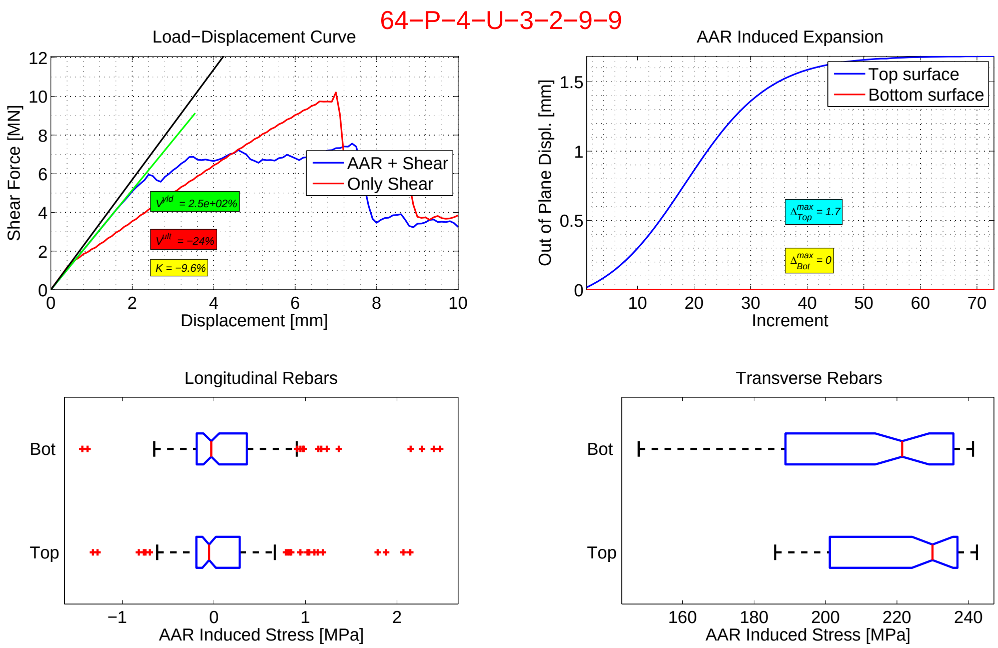

4.1.3.65 Analysis: 65-P-4-U-3-5-7-7

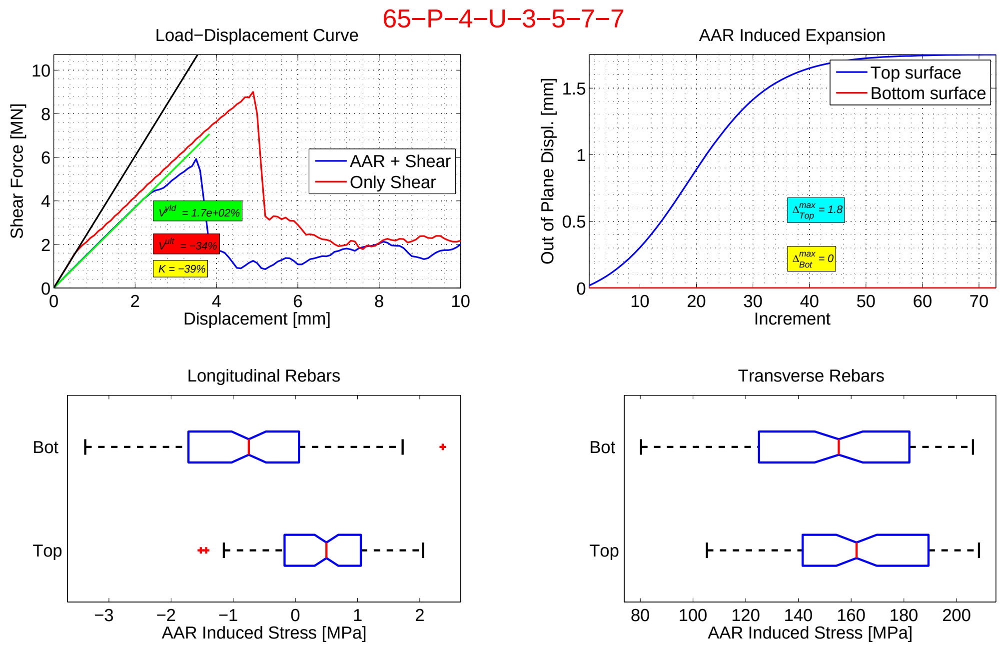

4.1.3.66 Analysis: 66-P-4-U-3-5-7-9

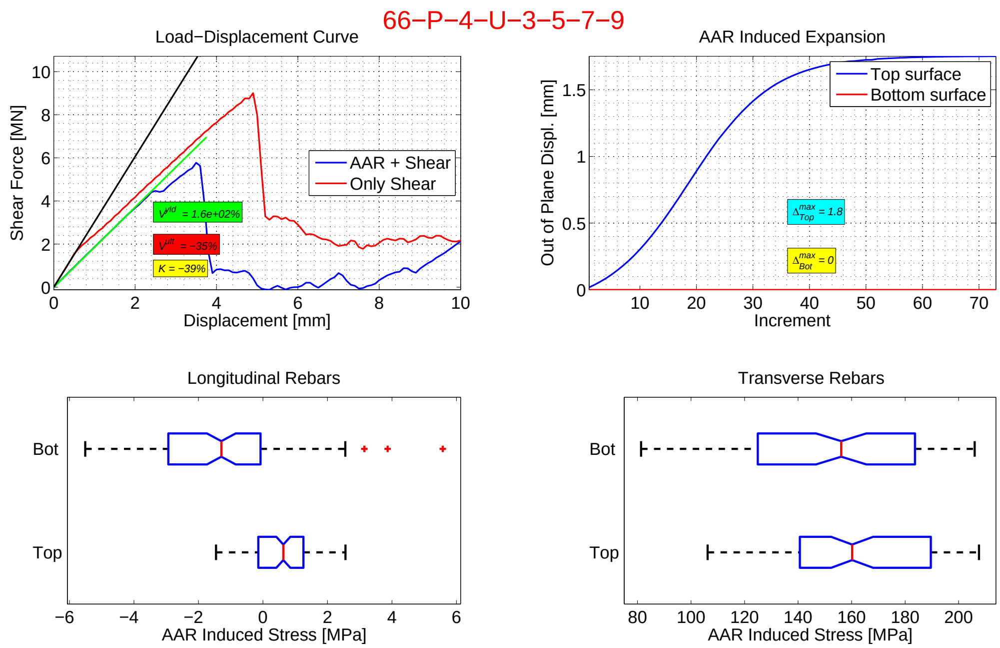

4.1.3.67 Analysis: 67-P-4-U-3-5-9-7

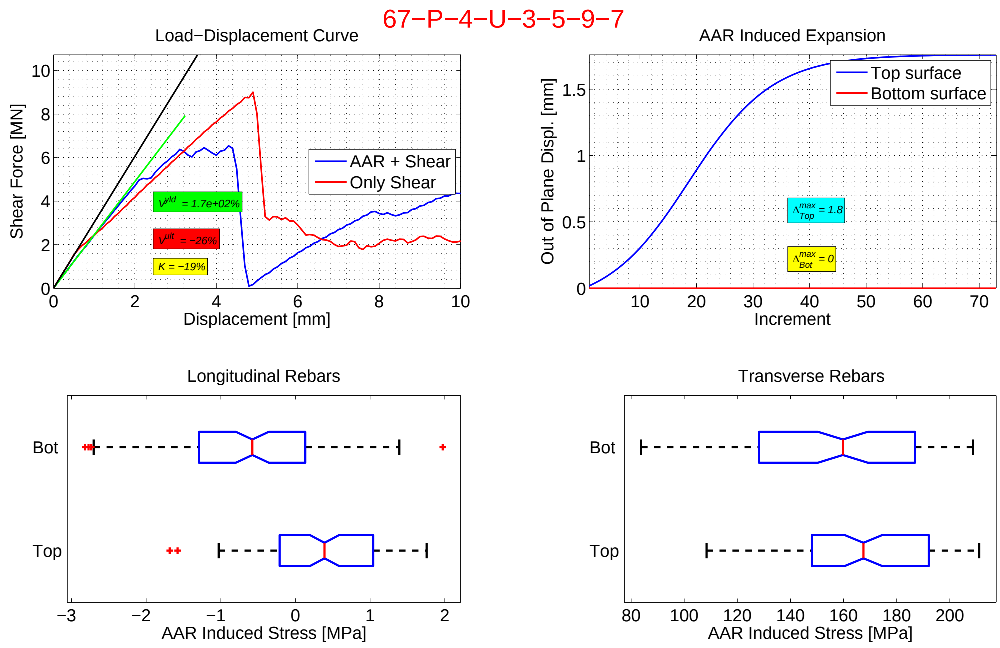

4.1.3.68 Analysis: 68-P-4-U-3-5-9-9

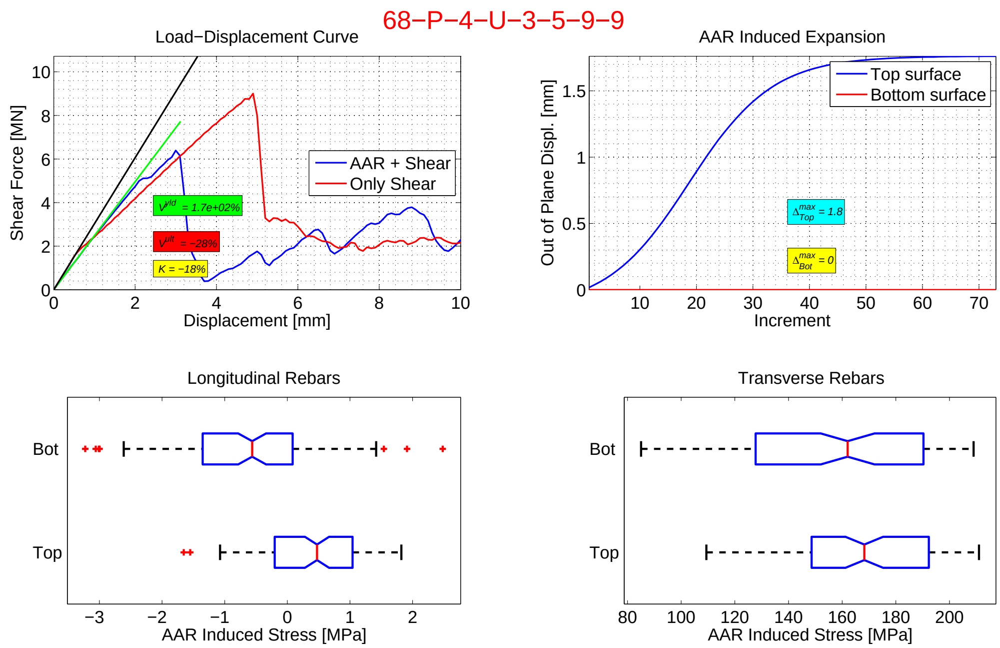

4.1.3.69 Analysis: 69-P-4-U-3-10-7-7

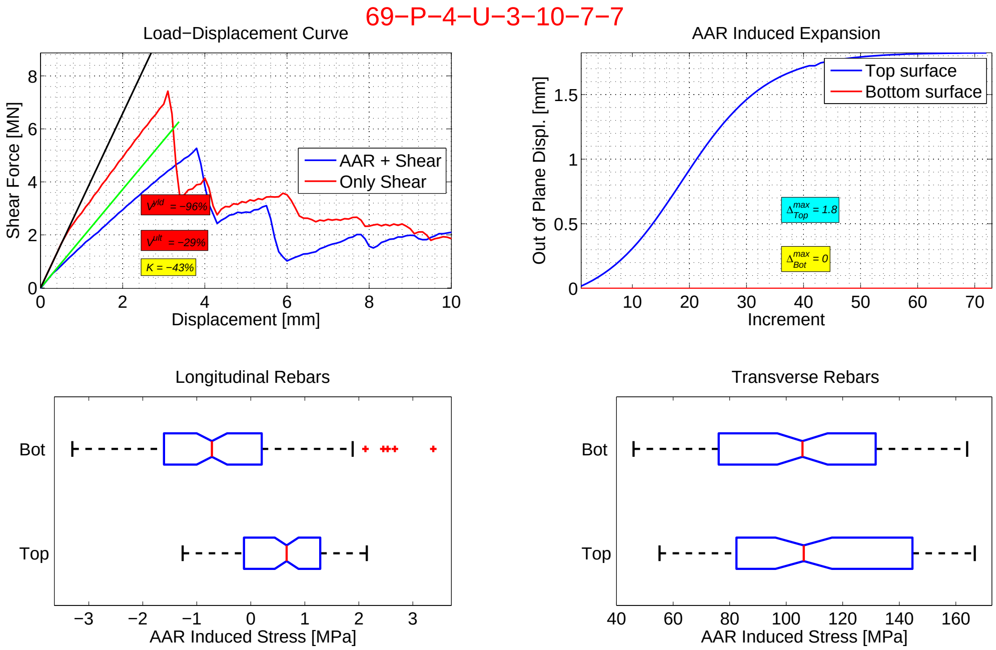

4.1.3.70 Analysis: 70-P-4-U-3-10-7-9

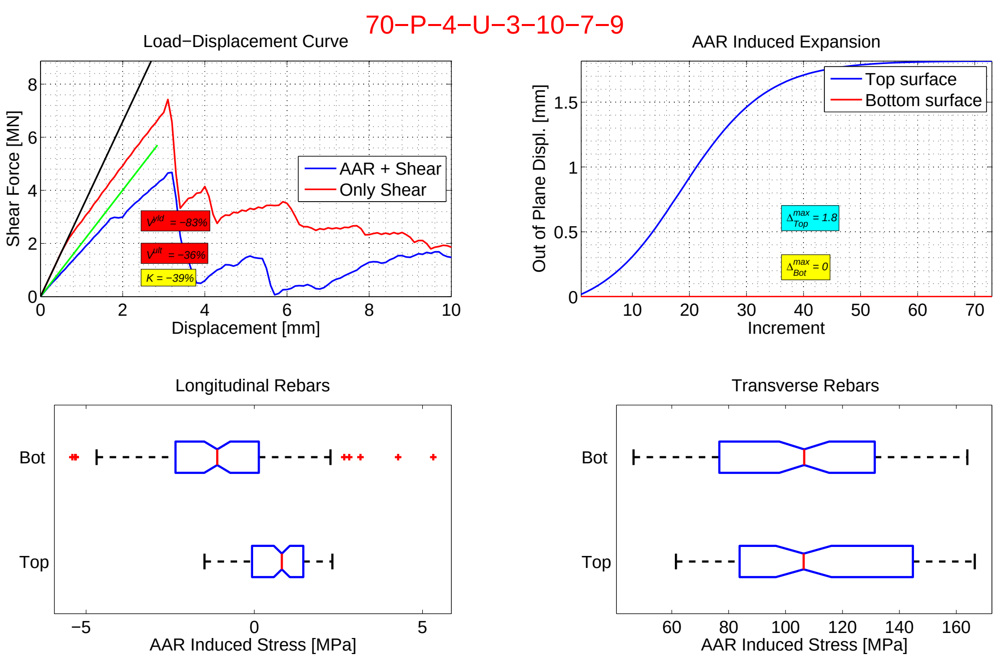

4.1.3.71 Analysis: 71-P-4-U-3-10-9-7

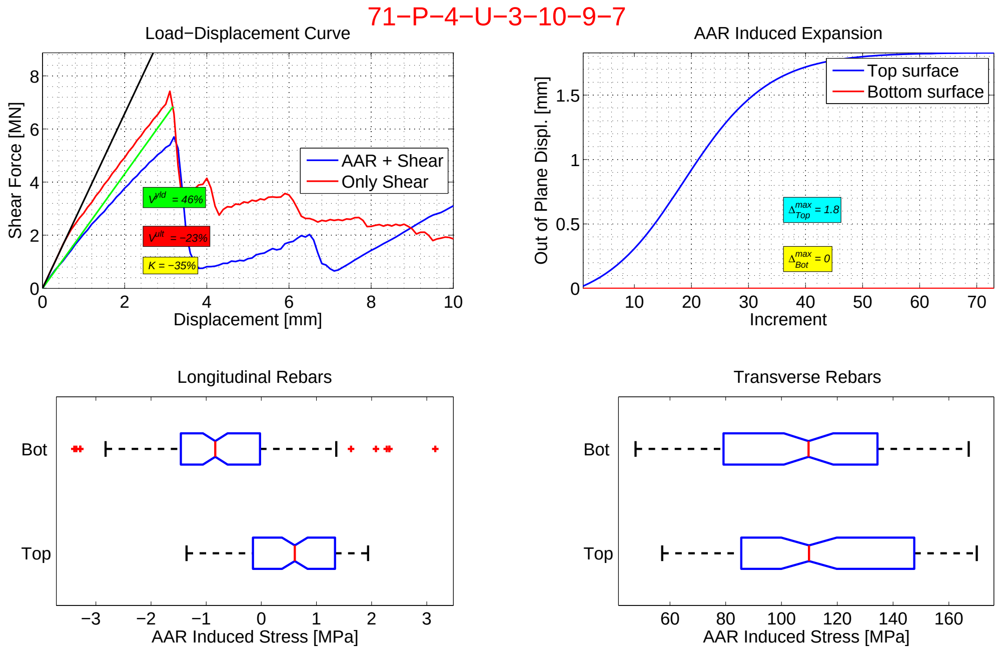

4.1.3.72 Analysis: 72-P-4-U-3-10-9-9

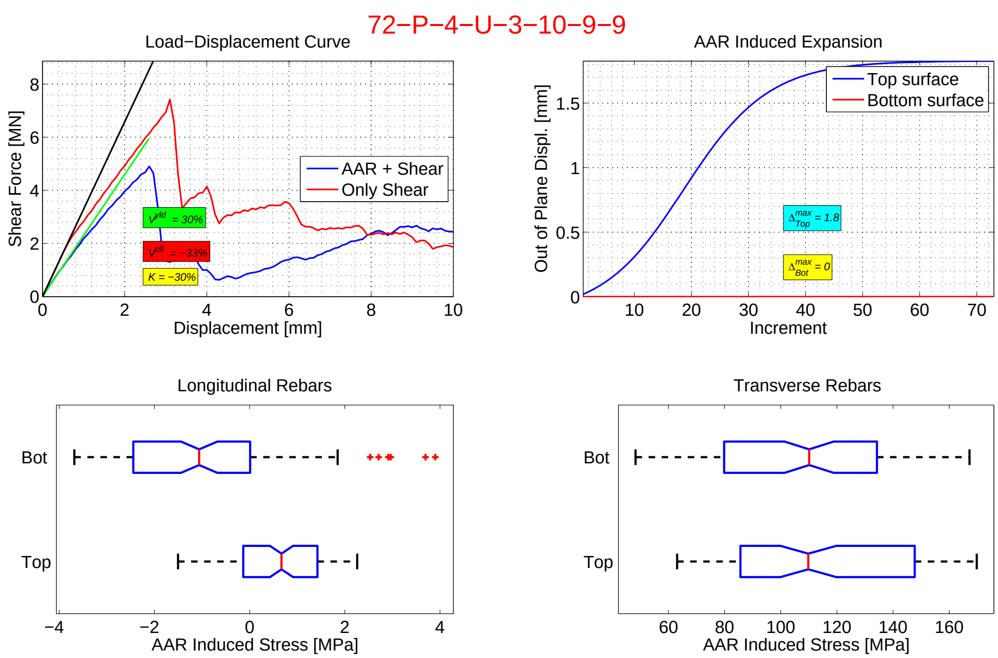

4.1.3.73 Analysis: 73-P-2-R-1-2-7-7

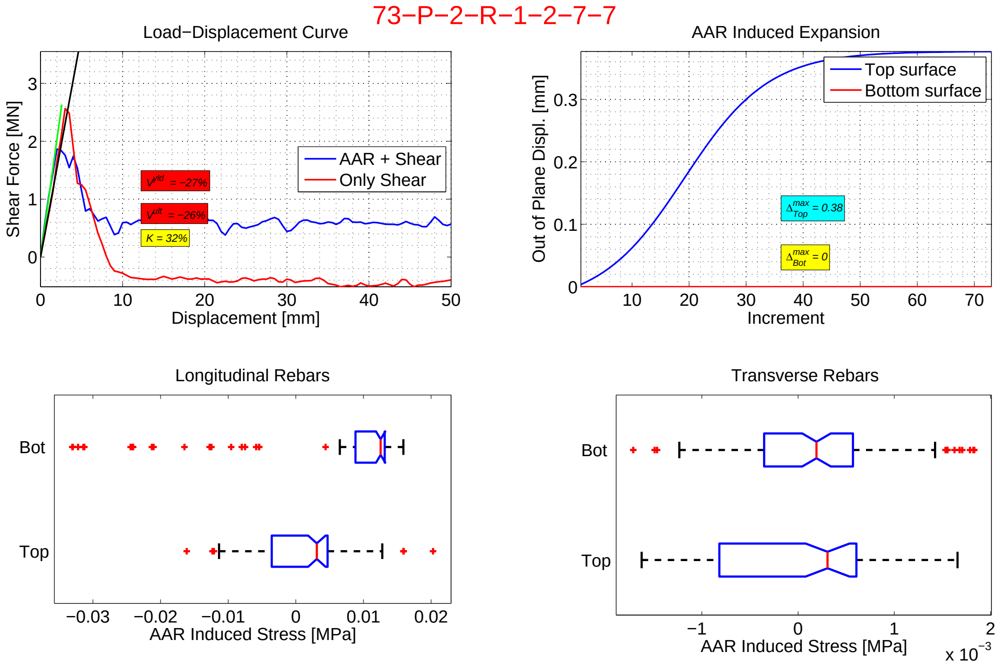

4.1.3.74 Analysis: 74-P-2-R-1-2-7-9

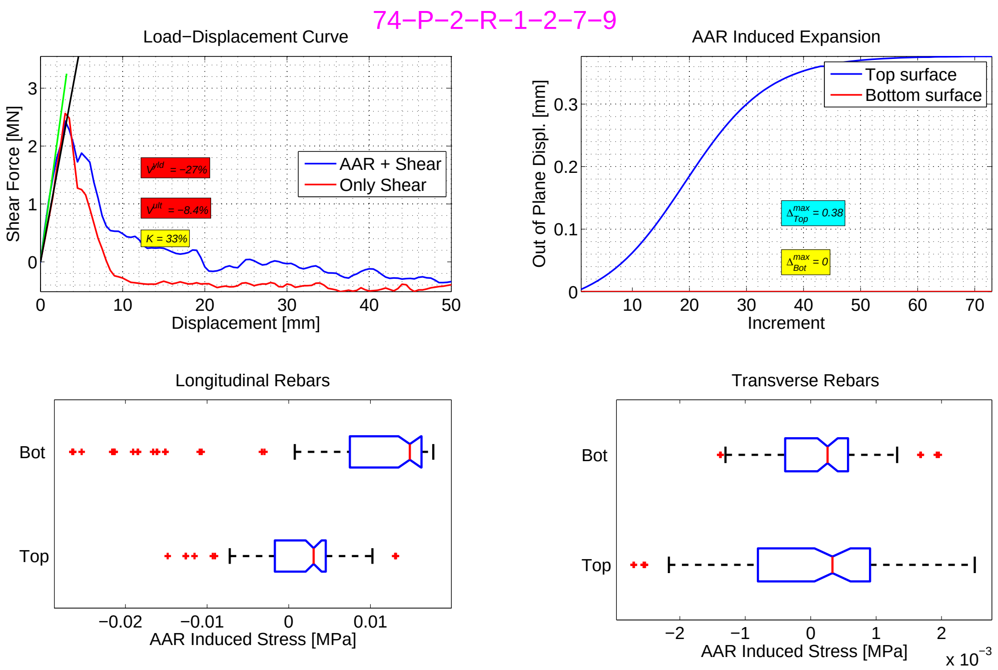

4.1.3.75 Analysis: 75-P-2-R-1-2-9-7

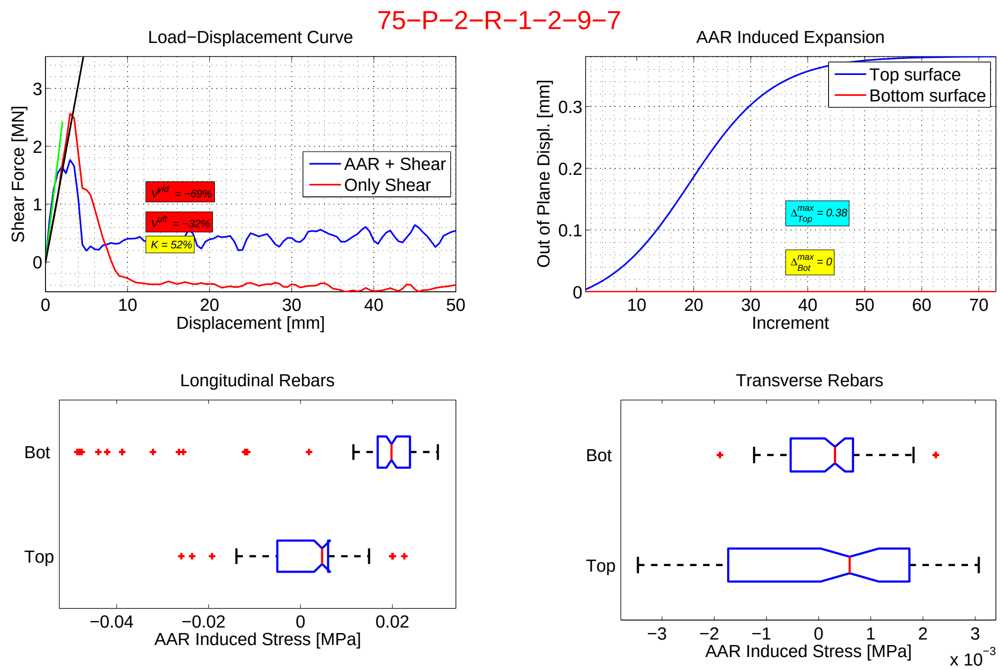

4.1.3.76 Analysis: 76-P-2-R-1-2-9-9

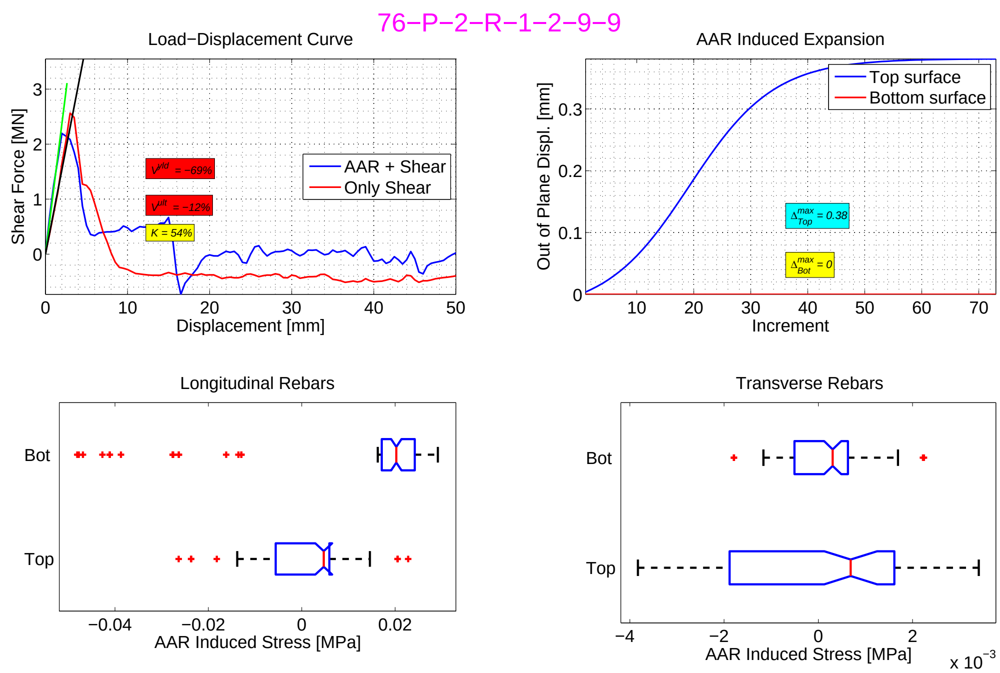

4.1.3.77 Analysis: 77-P-2-R-1-5-7-7

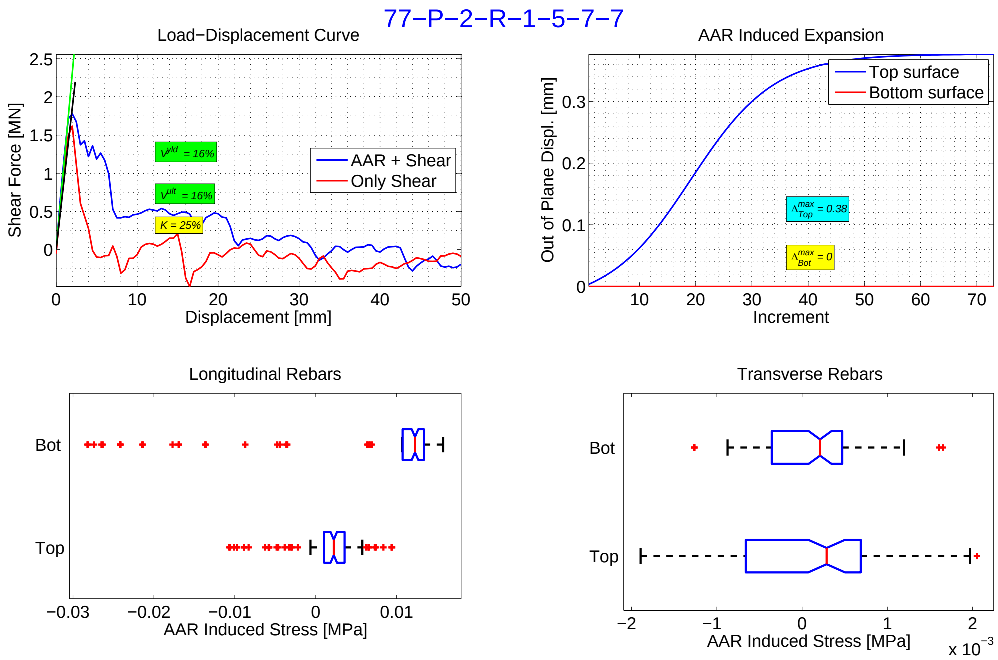

4.1.3.78 Analysis: 78-P-2-R-1-5-7-9

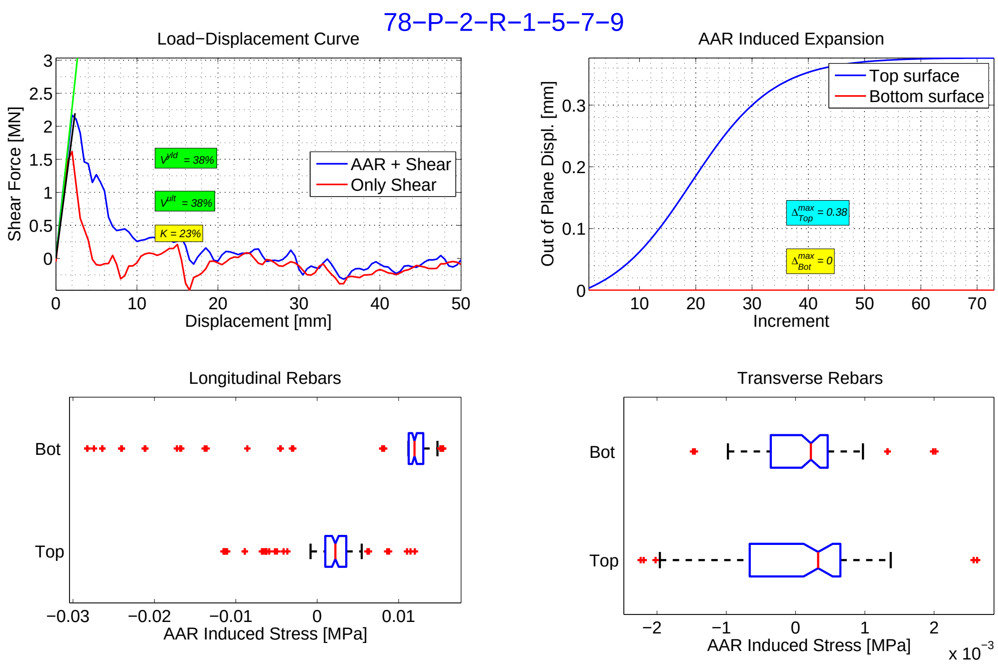

4.1.3.79 Analysis: 79-P-2-R-1-5-9-7

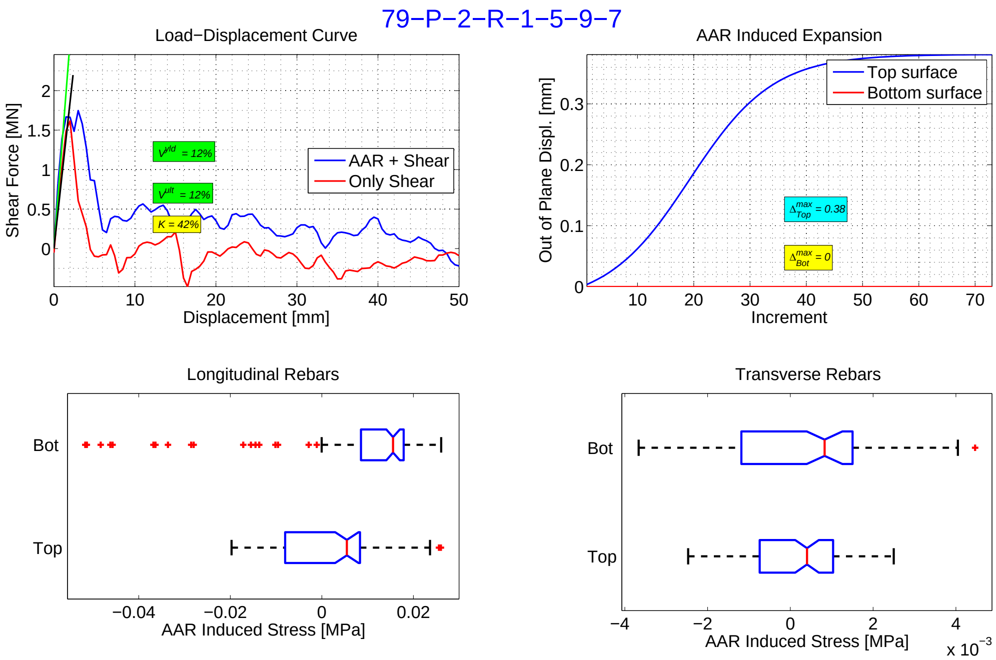

4.1.3.80 Analysis: 80-P-2-R-1-5-9-9

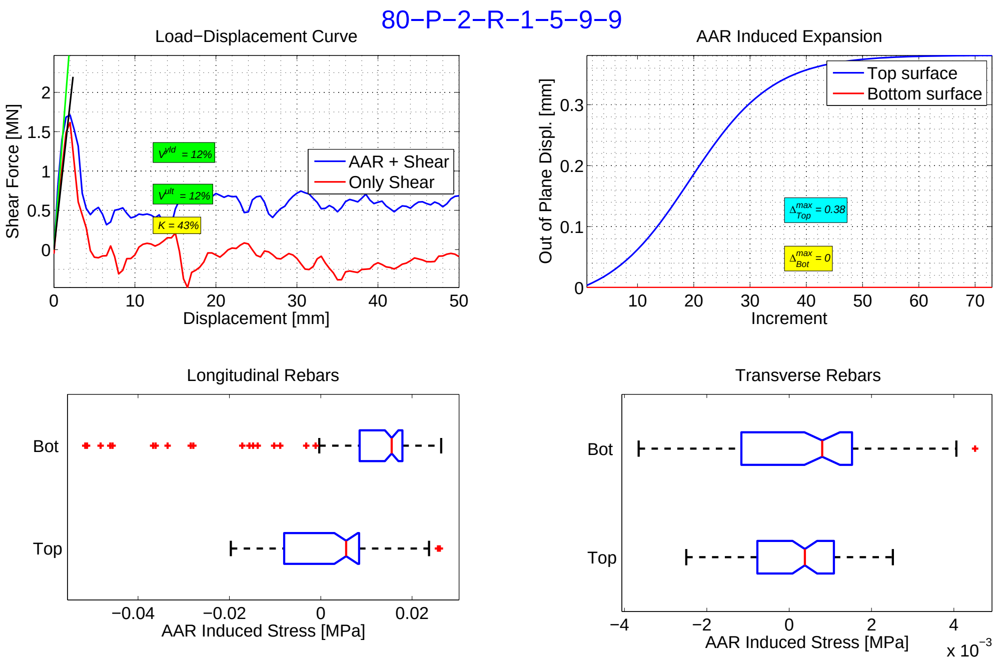

4.1.3.81 Analysis: 81-P-2-R-1-10-7-7

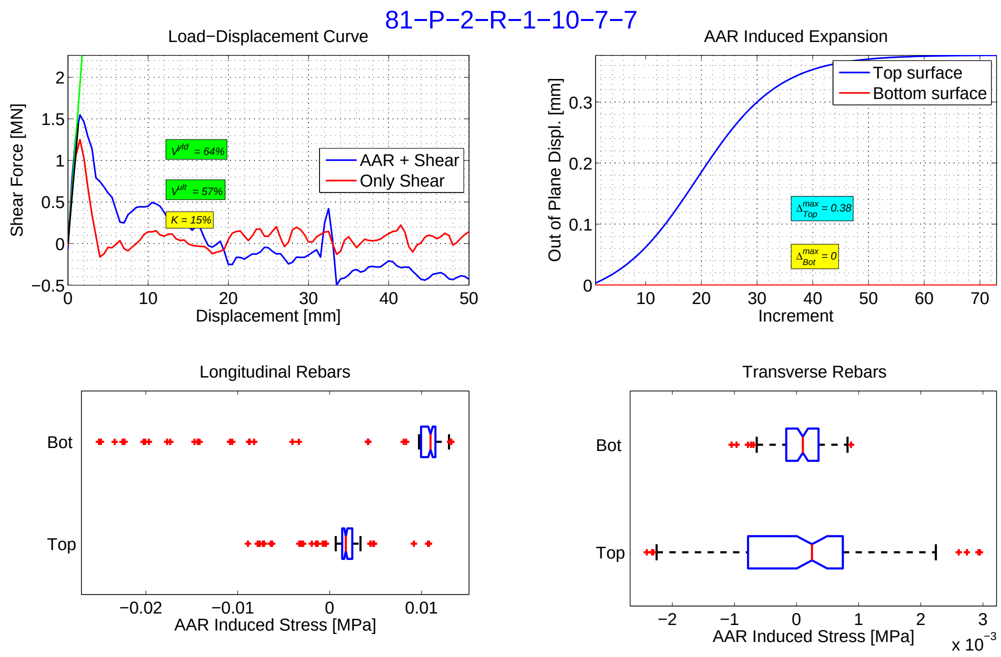

4.1.3.82 Analysis: 82-P-2-R-1-10-7-9

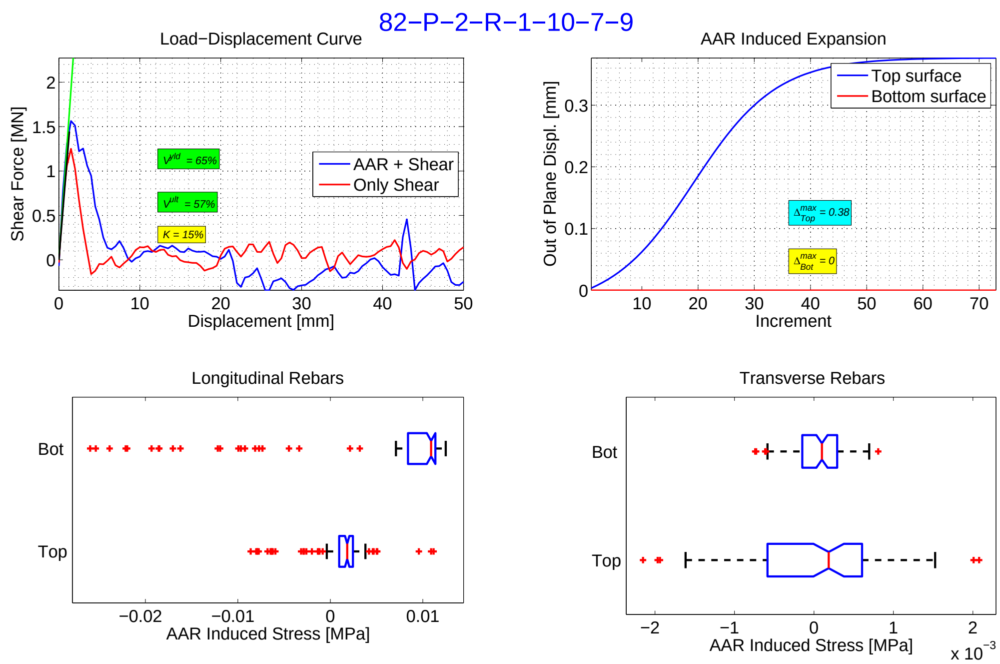

4.1.3.83 Analysis: 83-P-2-R-1-10-9-7

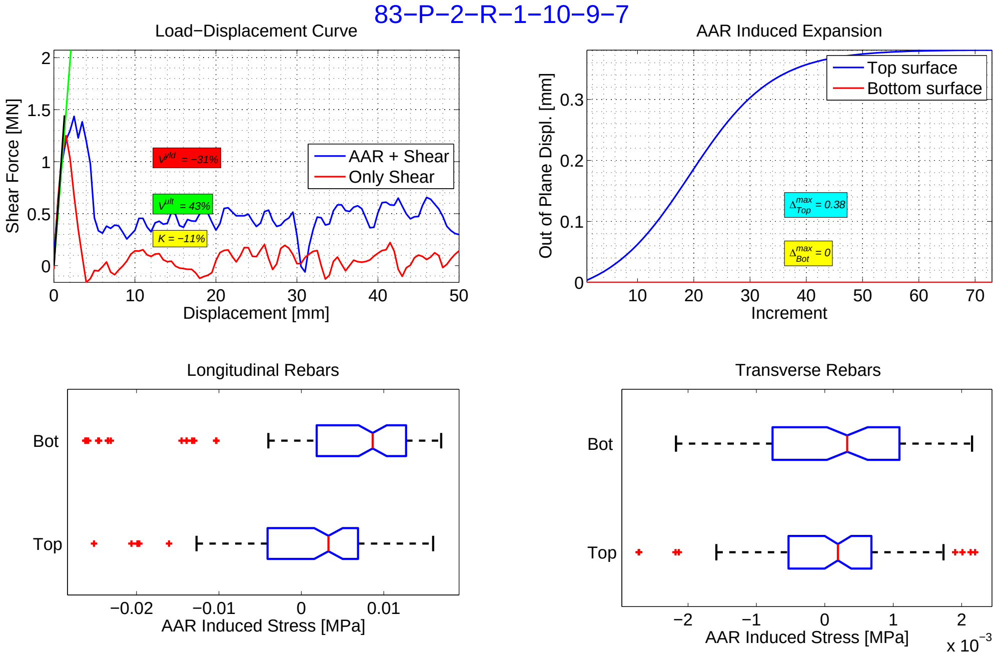

4.1.3.84 Analysis: 84-P-2-R-1-10-9-9

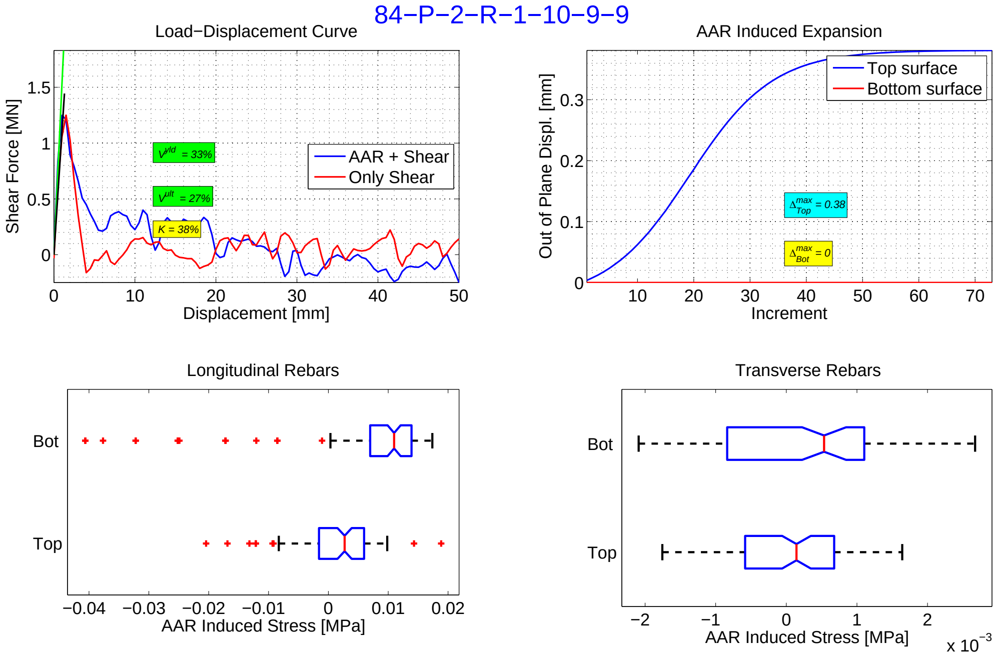

4.1.3.85 Analysis: 85-P-2-R-2-2-7-7

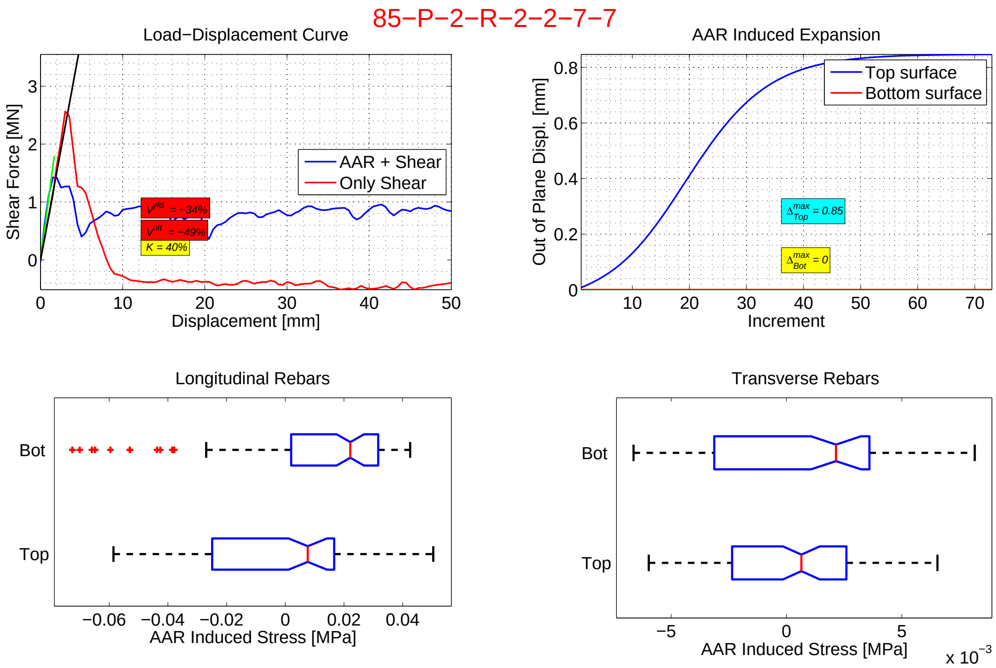

4.1.3.86 Analysis: 86-P-2-R-2-2-7-9

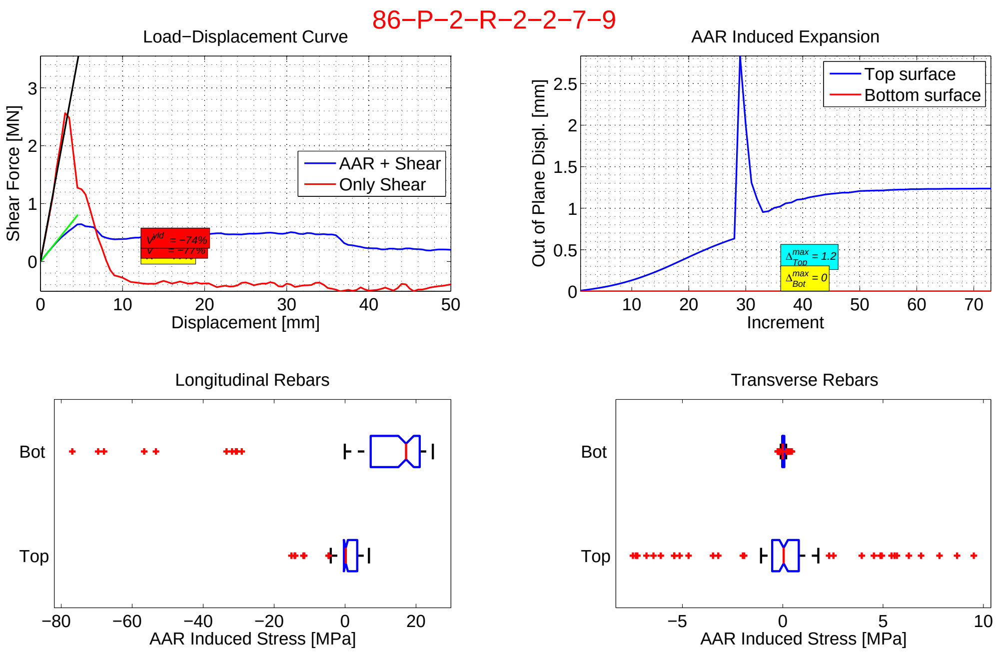

4.1.3.87 Analysis: 87-P-2-R-2-2-9-7

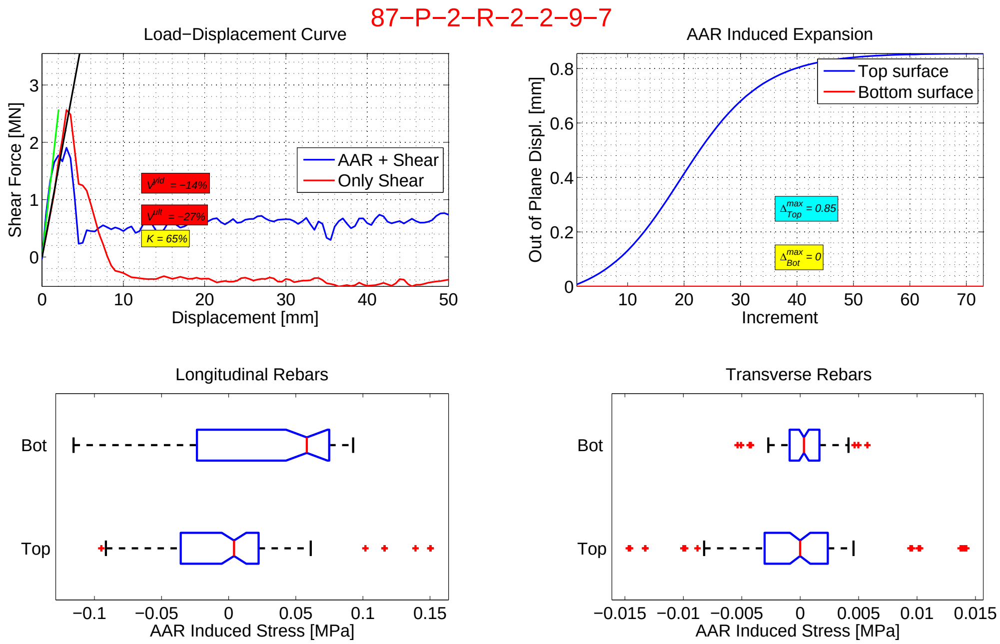

4.1.3.88 Analysis: 88-P-2-R-2-2-9-9

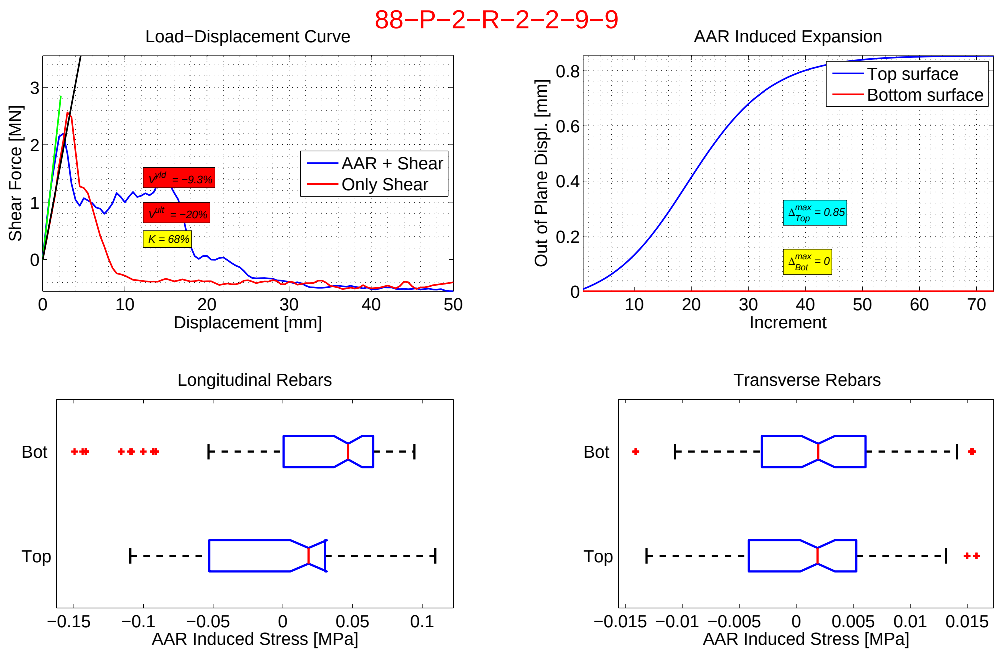

4.1.3.89 Analysis: 89-P-2-R-2-5-7-7

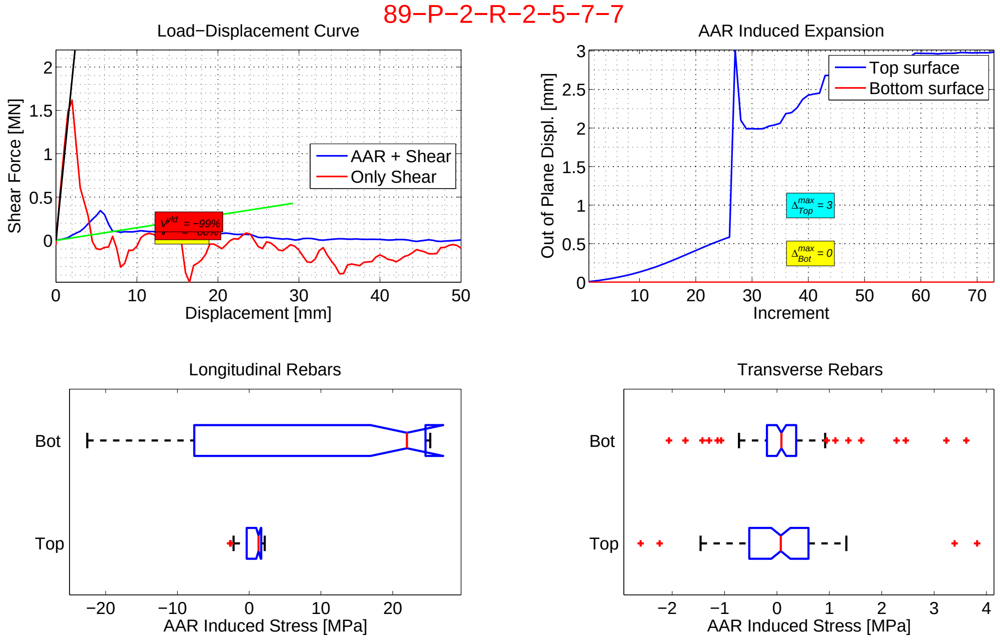

4.1.3.90 Analysis: 90-P-2-R-2-5-7-9

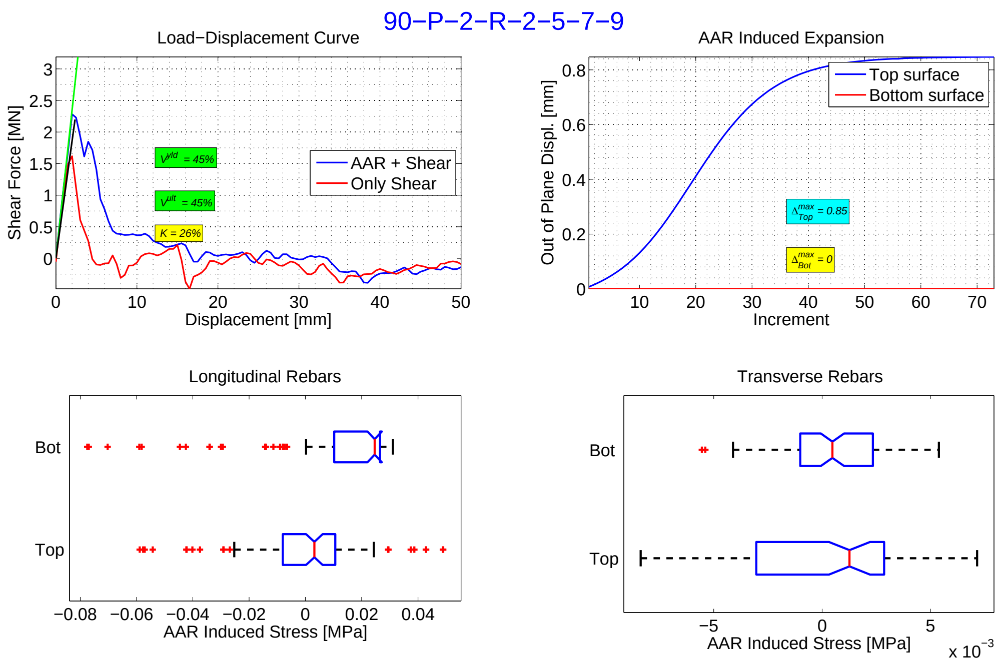

4.1.3.91 Analysis: 91-P-2-R-2-5-9-7

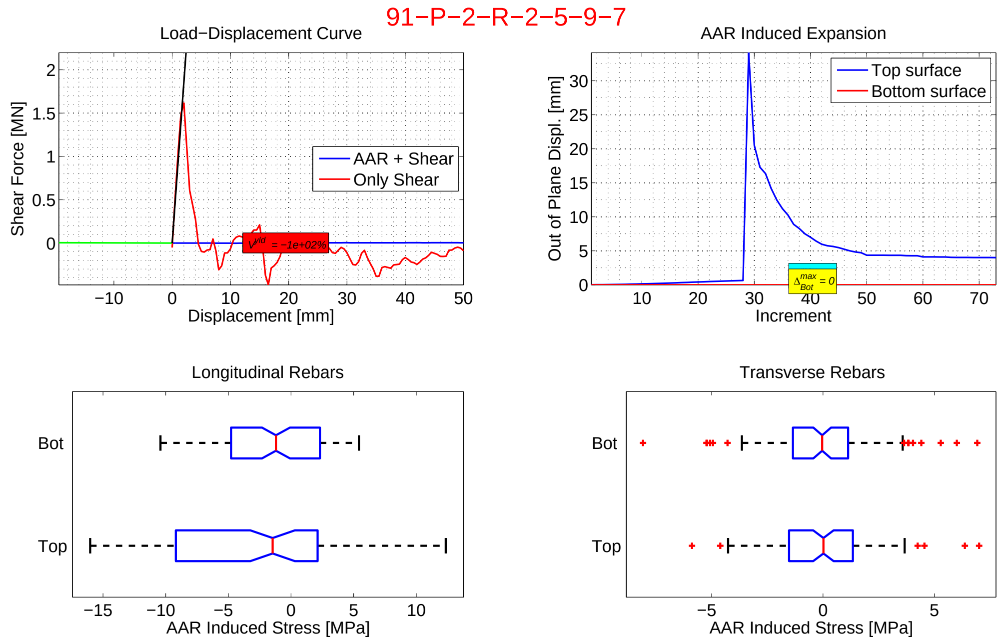

4.1.3.92 Analysis: 92-P-2-R-2-5-9-9

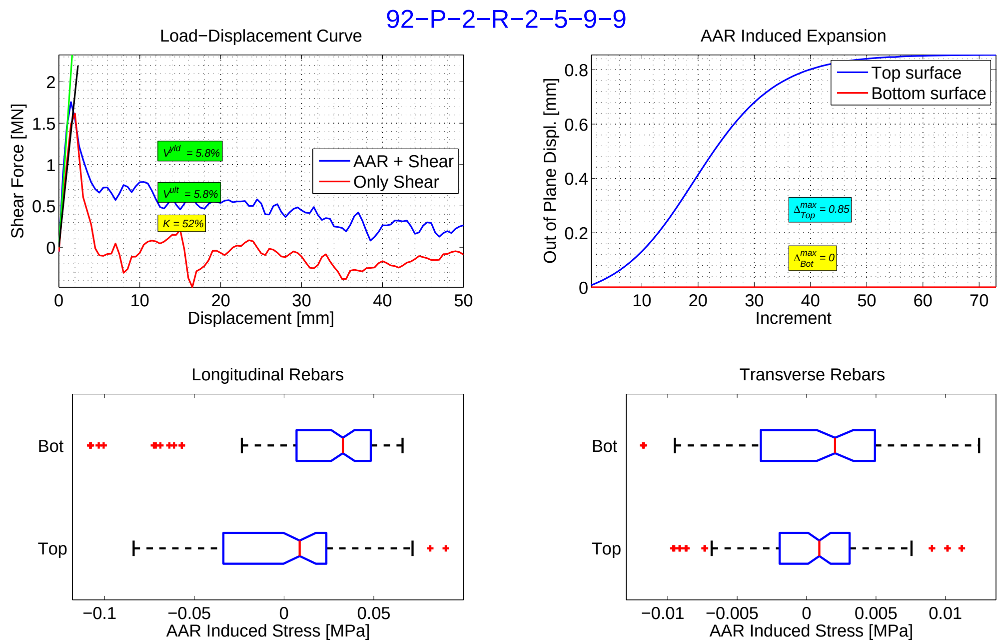

4.1.3.93 Analysis: 93-P-2-R-2-10-7-7

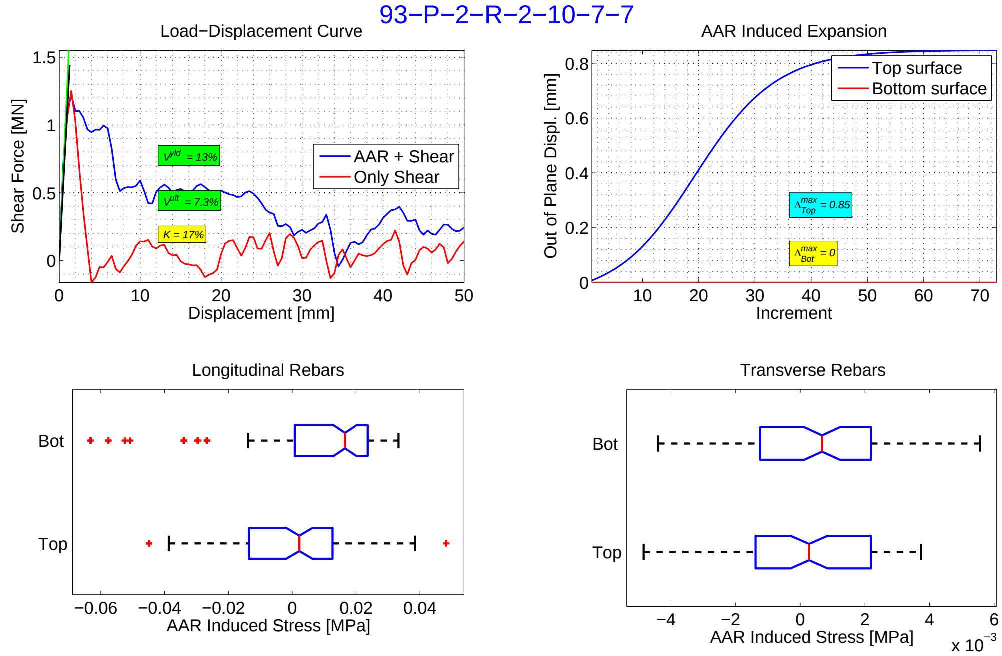

4.1.3.94 Analysis: 94-P-2-R-2-10-7-9

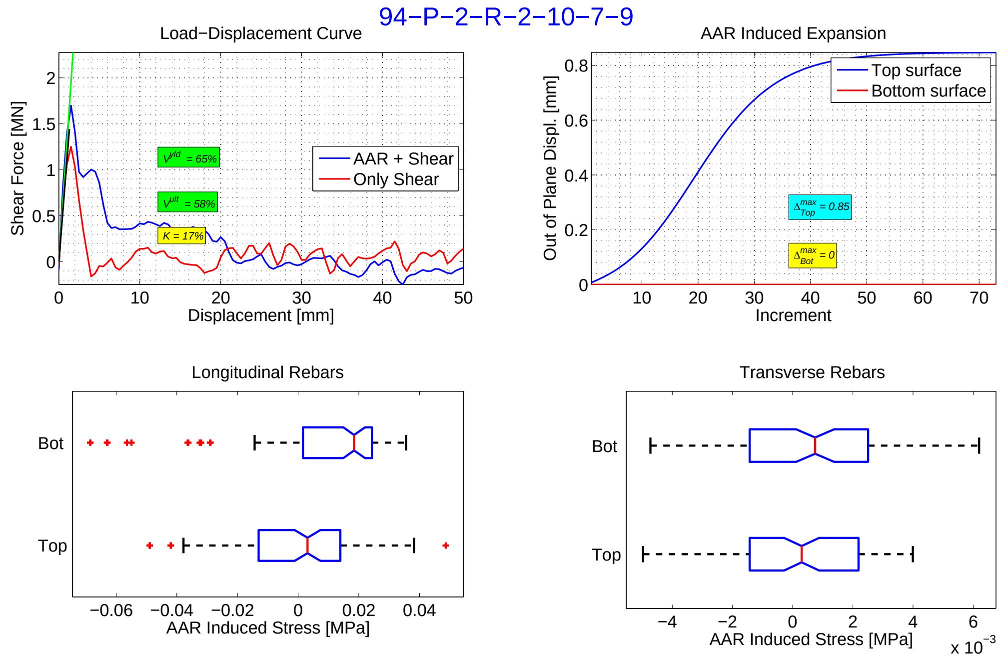

4.1.3.95 Analysis: 95-P-2-R-2-10-9-7

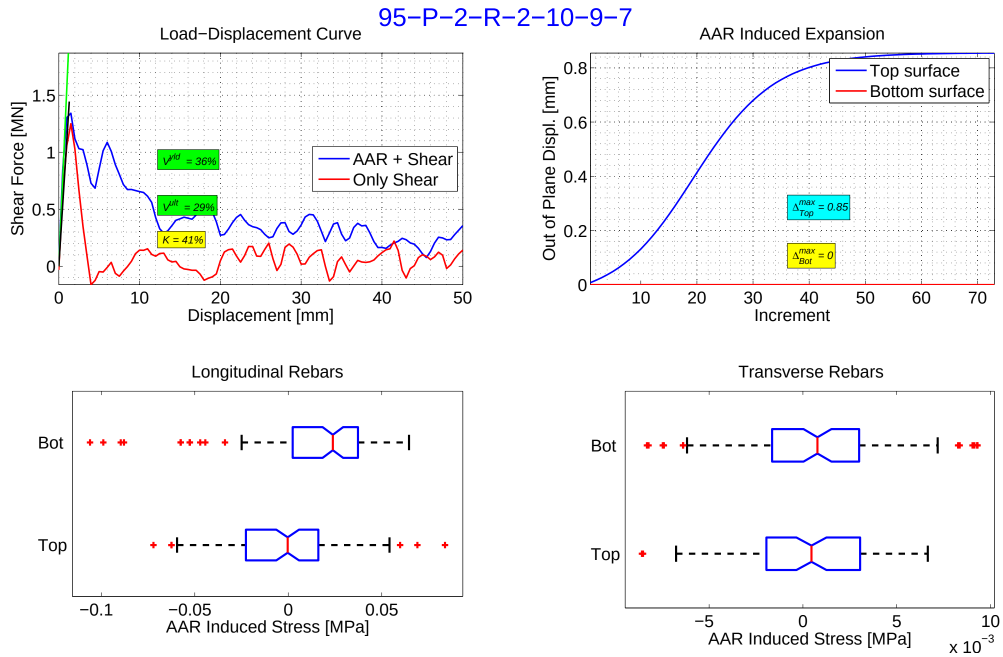

4.1.3.96 Analysis: 96-P-2-R-2-10-9-9

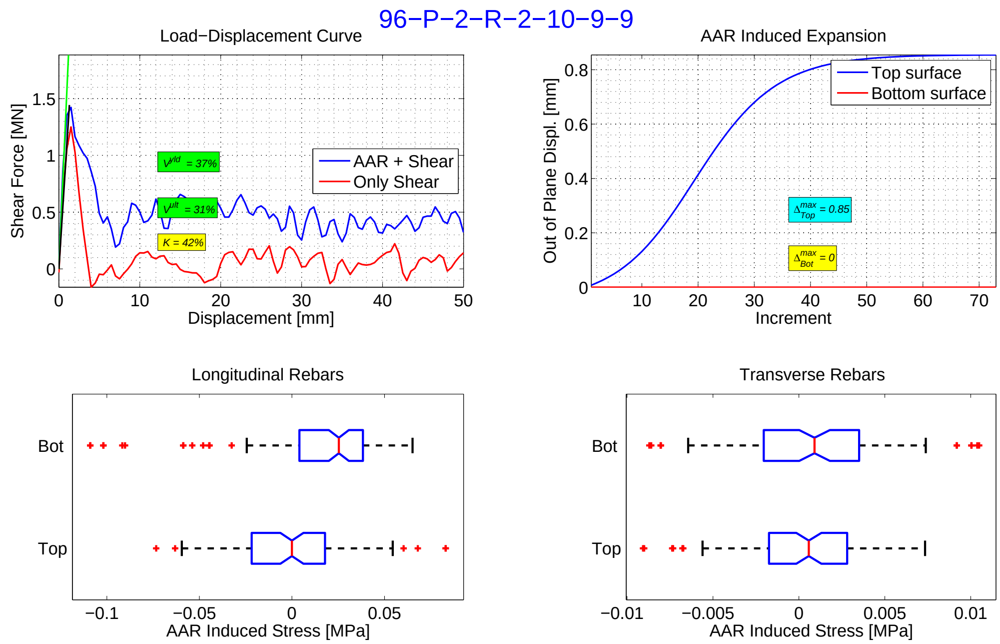

4.1.3.97 Analysis: 97-P-2-R-3-2-7-7

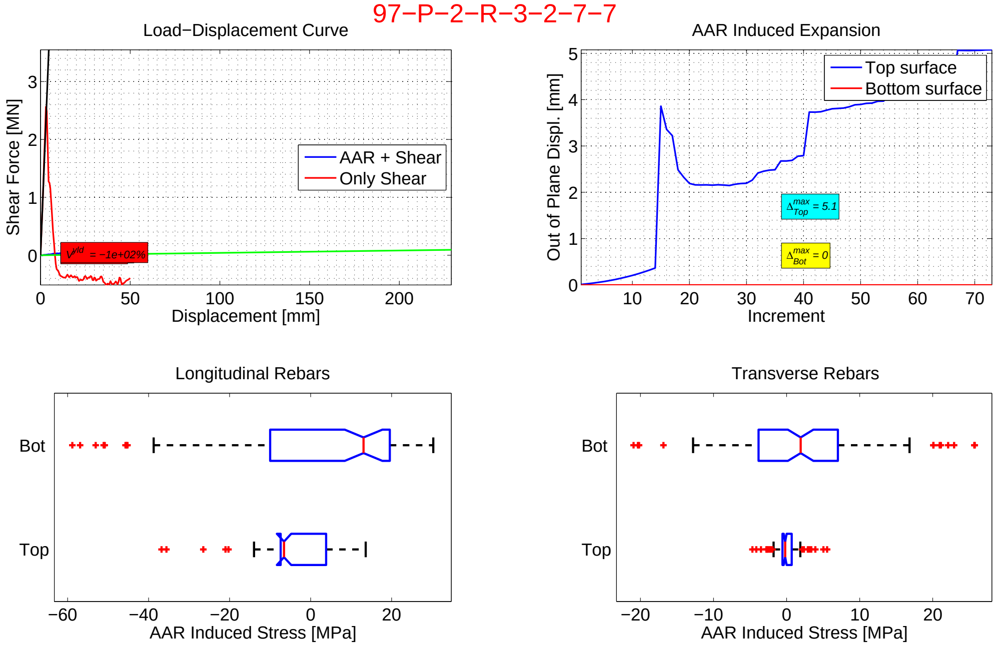

4.1.3.98 Analysis: 98-P-2-R-3-2-7-9

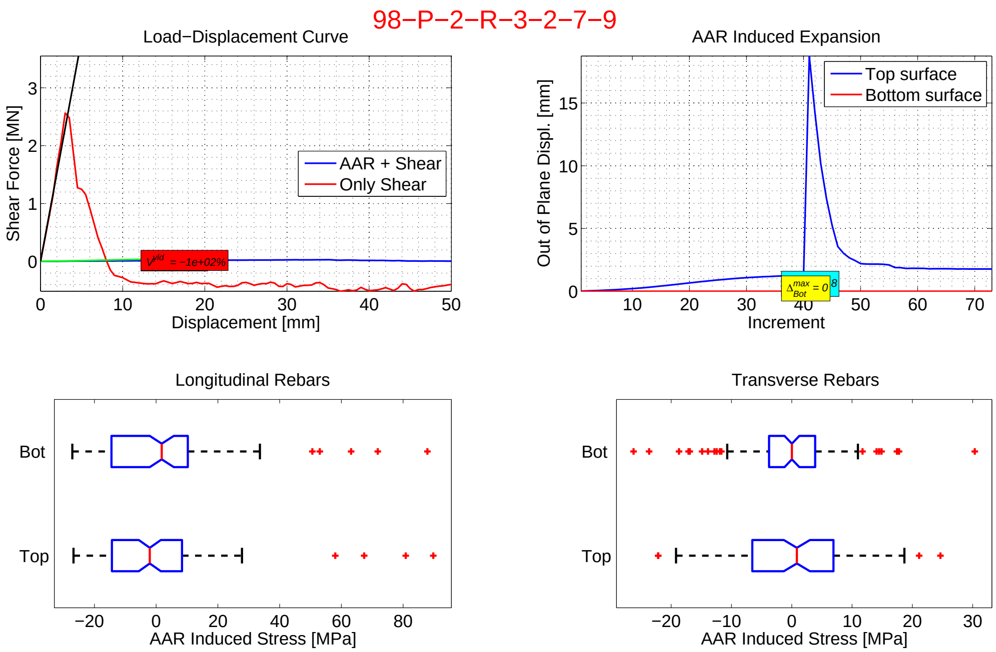

4.1.3.99 Analysis: 99-P-2-R-3-2-9-7

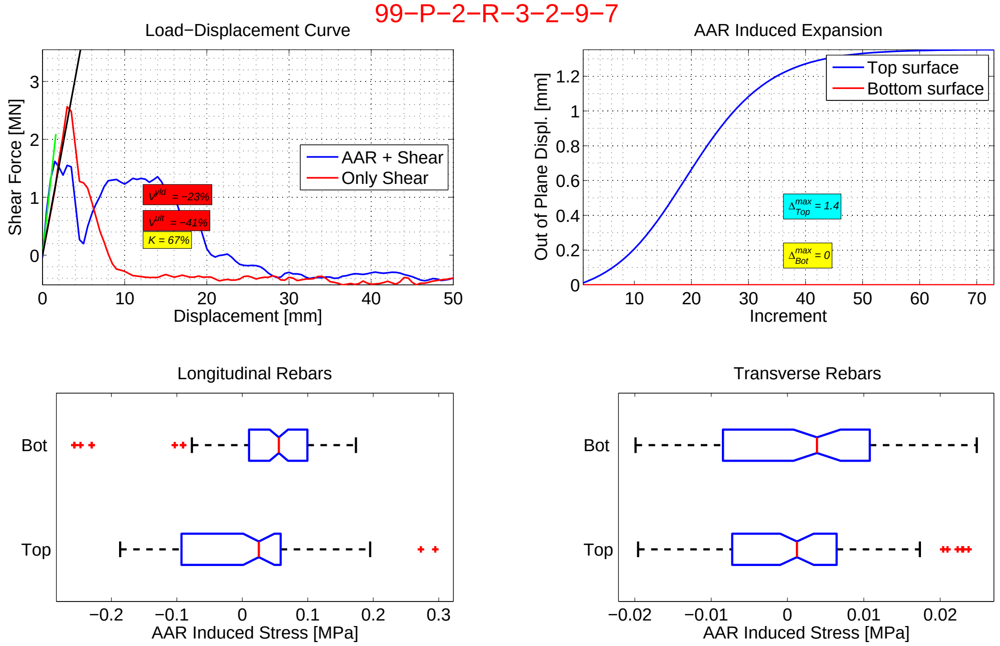

4.1.3.100 Analysis: 100-P-2-R-3-2-9-9

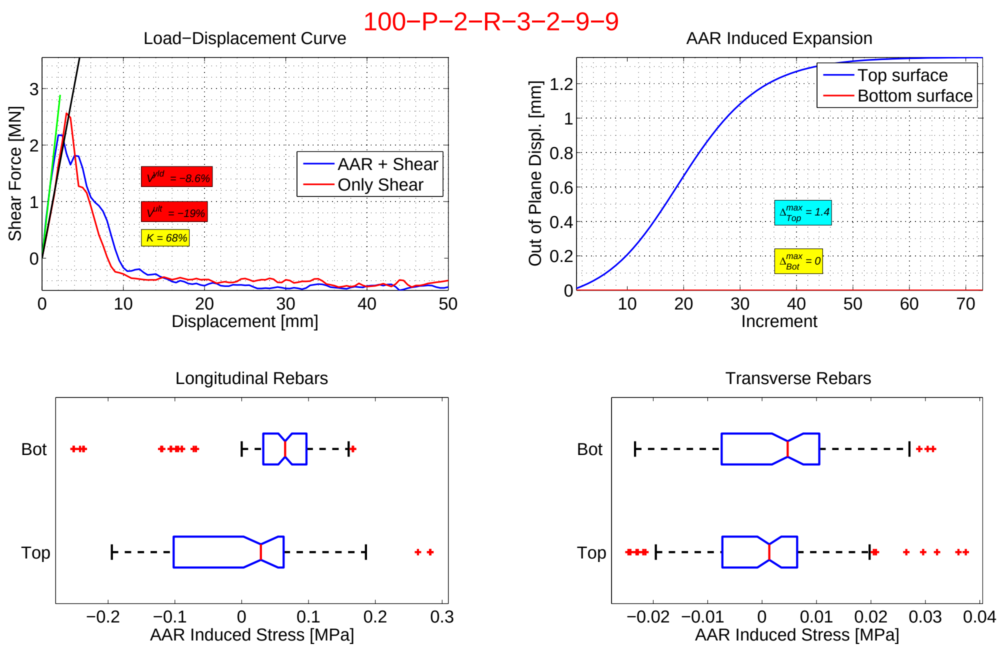

4.1.3.101 Analysis: 101-P-2-R-3-5-7-7

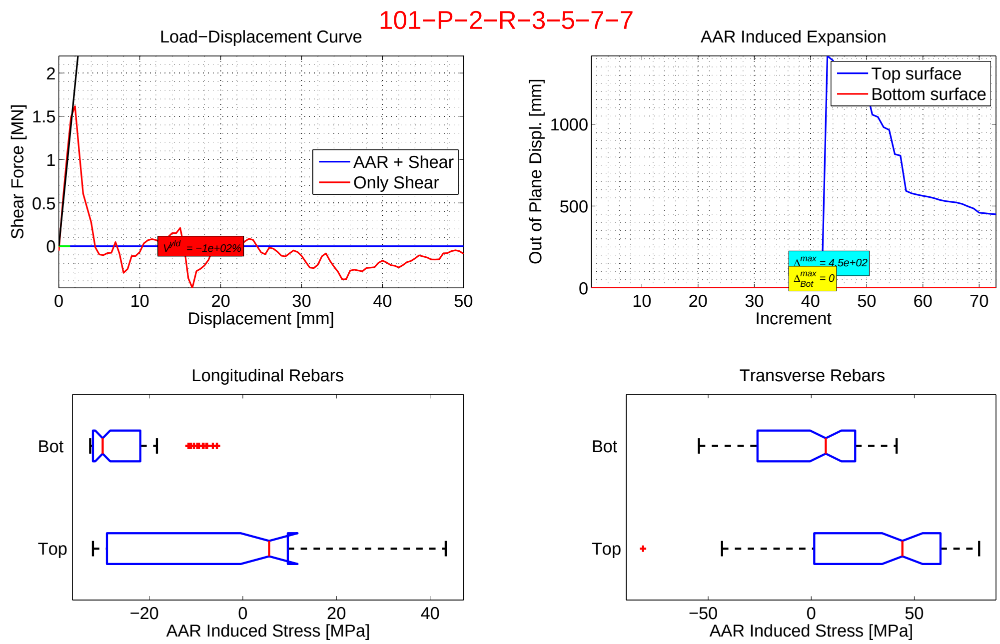

4.1.3.102 Analysis: 102-P-2-R-3-5-7-9

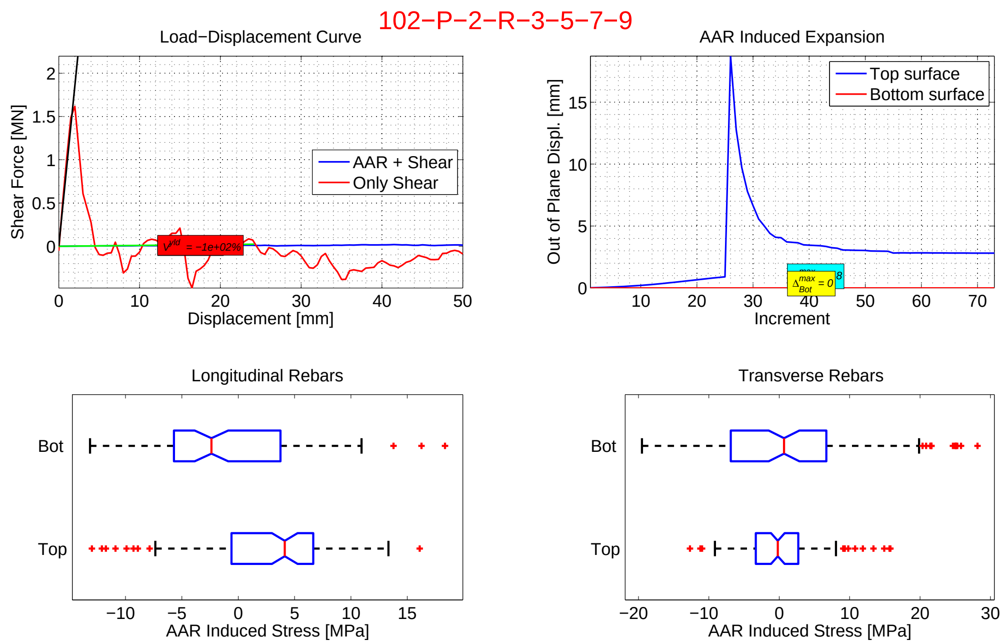

4.1.3.103 Analysis: 103-P-2-R-3-5-9-7

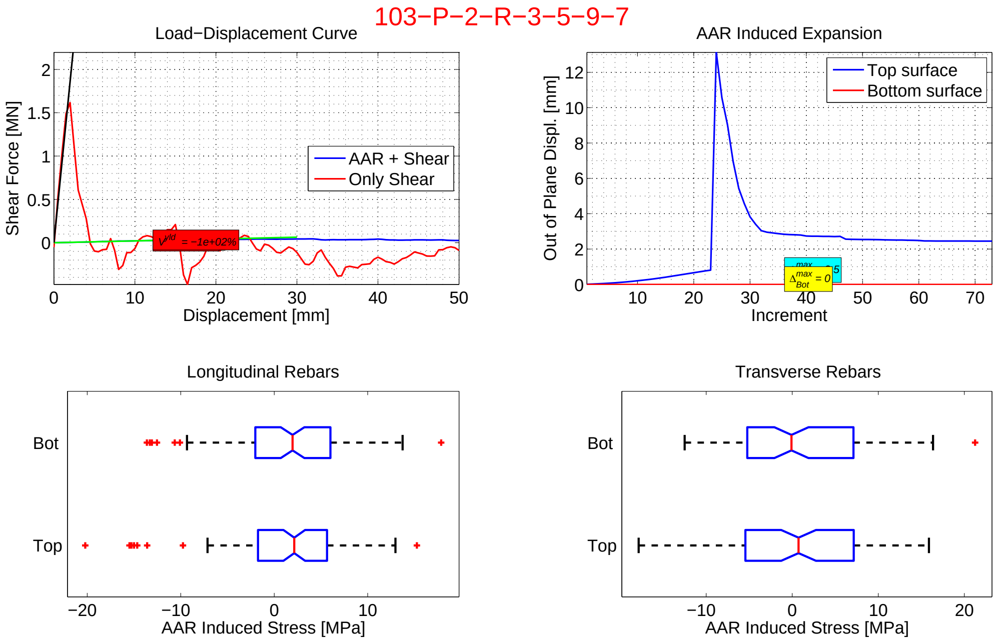

4.1.3.104 Analysis: 104-P-2-R-3-5-9-9

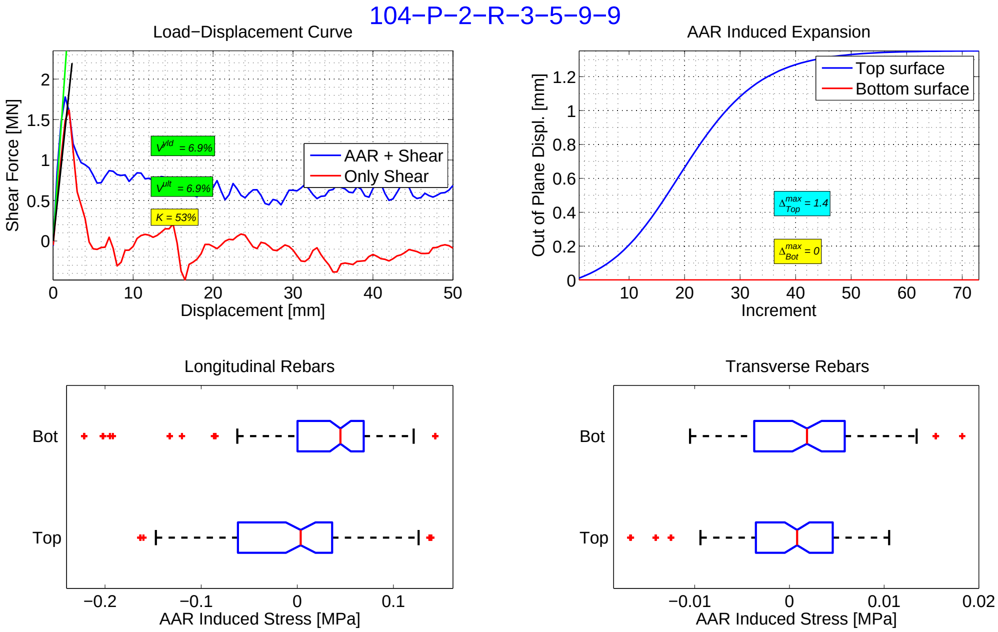

4.1.3.105 Analysis: 105-P-2-R-3-10-7-7

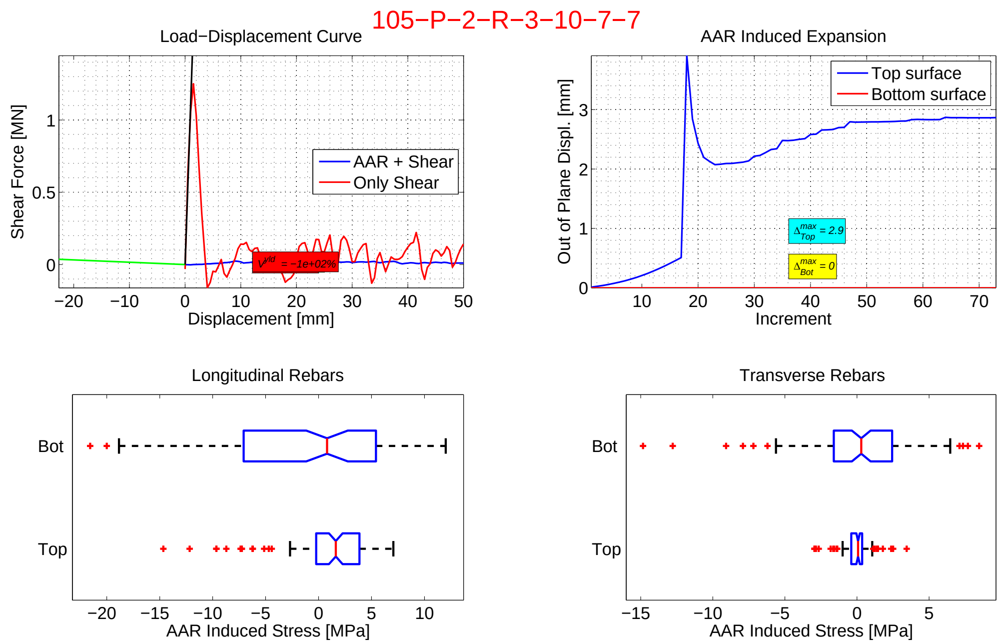

4.1.3.106 Analysis: 106-P-2-R-3-10-7-9

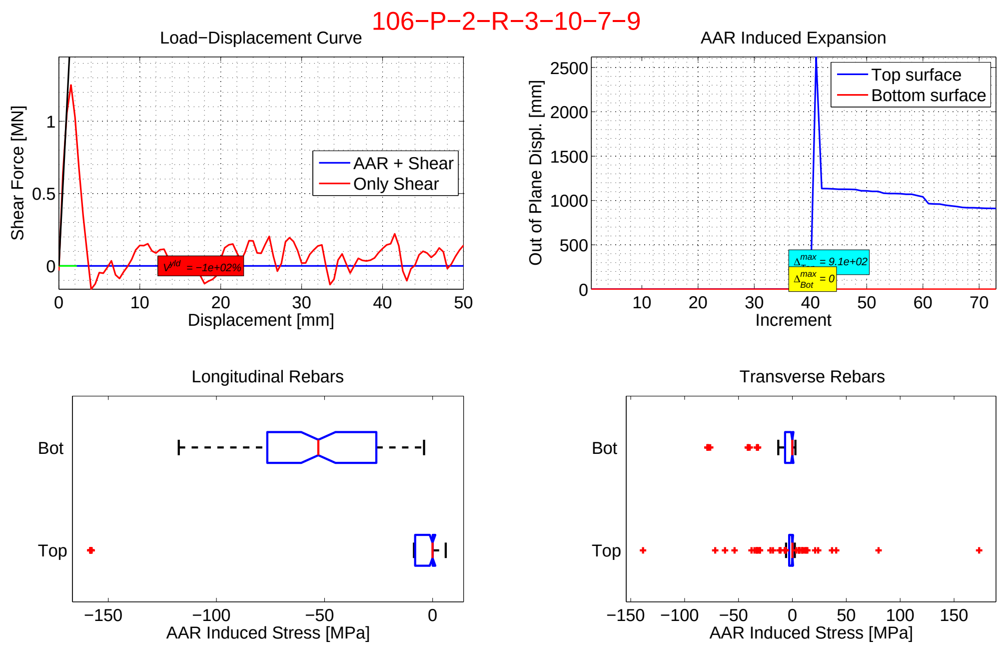

4.1.3.107 Analysis: 107-P-2-R-3-10-9-7

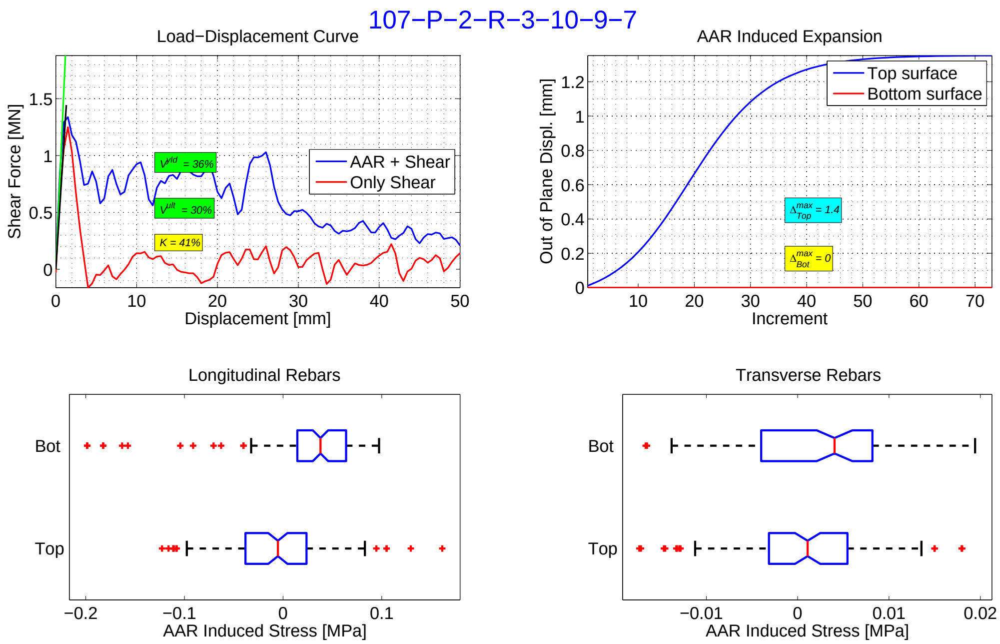

4.1.3.108 Analysis: 108-P-2-R-3-10-9-9

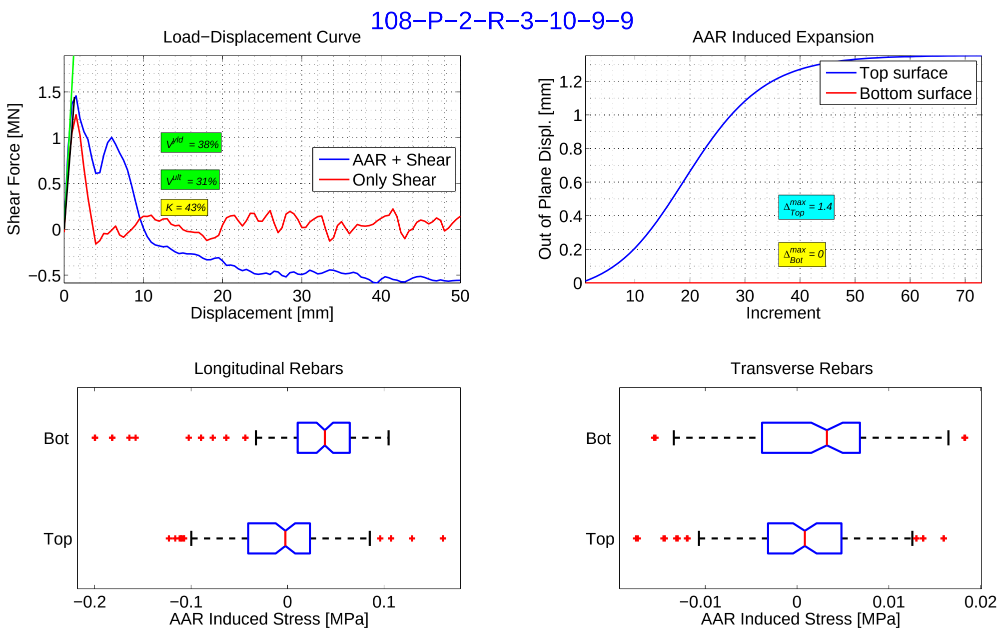

4.1.3.109 Analysis: 109-P-4-R-1-2-7-7

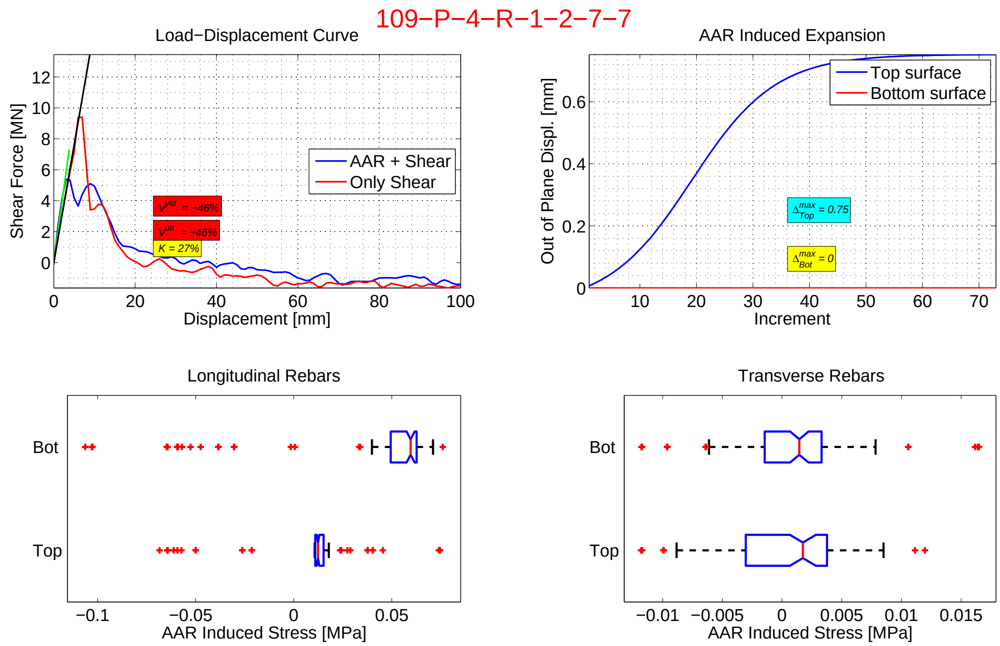

4.1.3.110 Analysis: 110-P-4-R-1-2-7-9

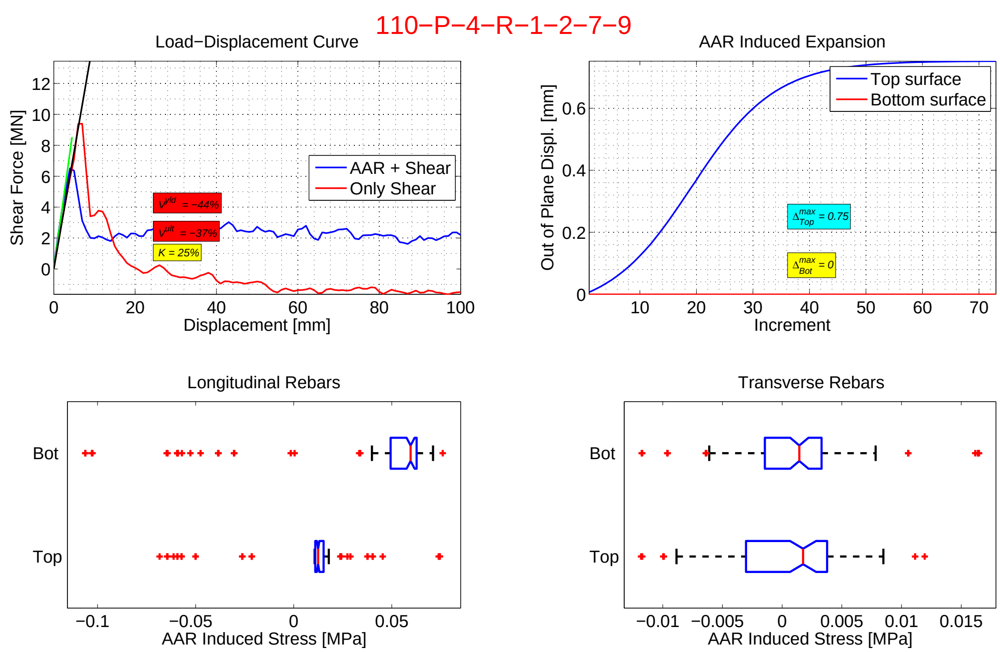

4.1.3.111 Analysis: 111-P-4-R-1-2-9-7

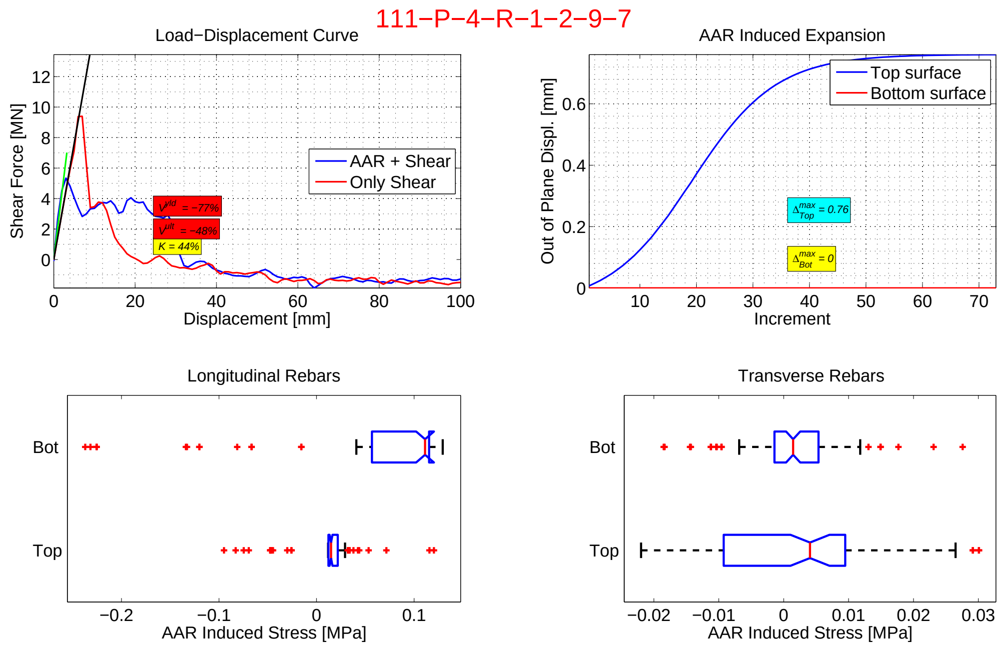

4.1.3.112 Analysis: 112-P-4-R-1-2-9-9

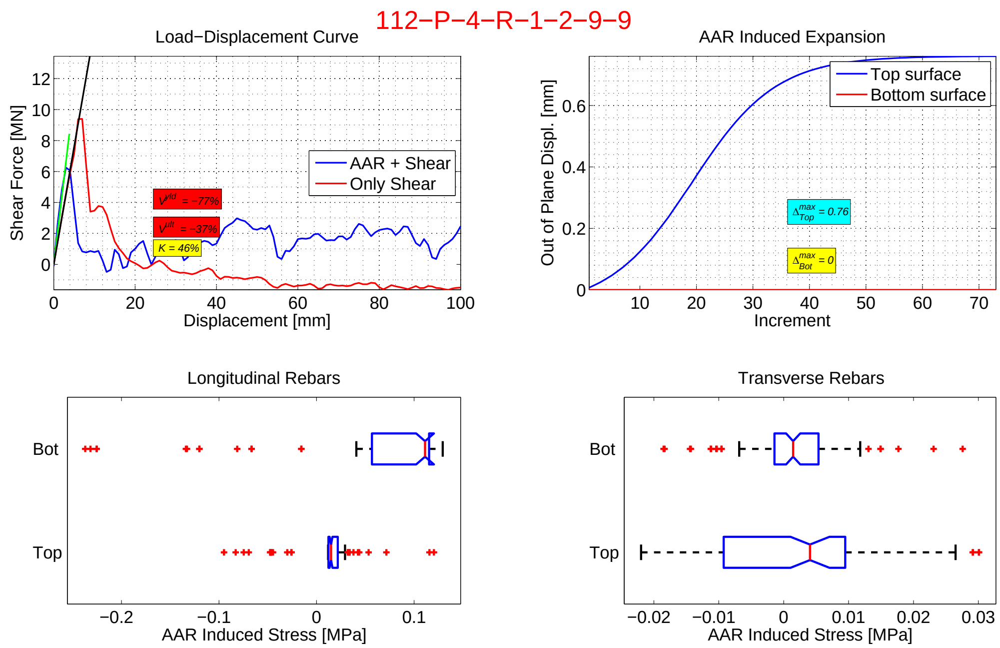

4.1.3.113 Analysis: 113-P-4-R-1-5-7-7

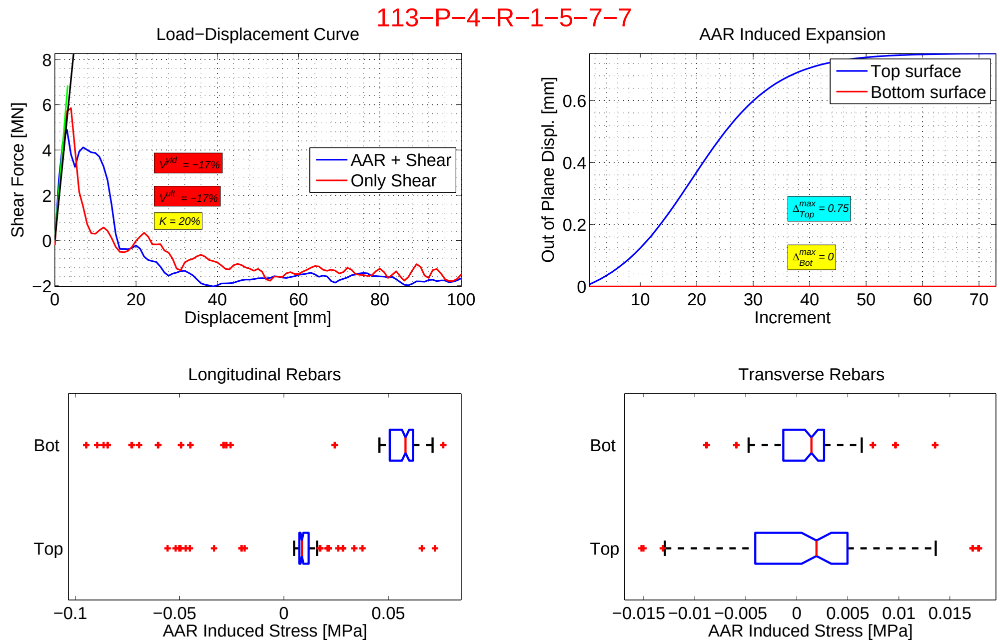

4.1.3.114 Analysis: 114-P-4-R-1-5-7-9

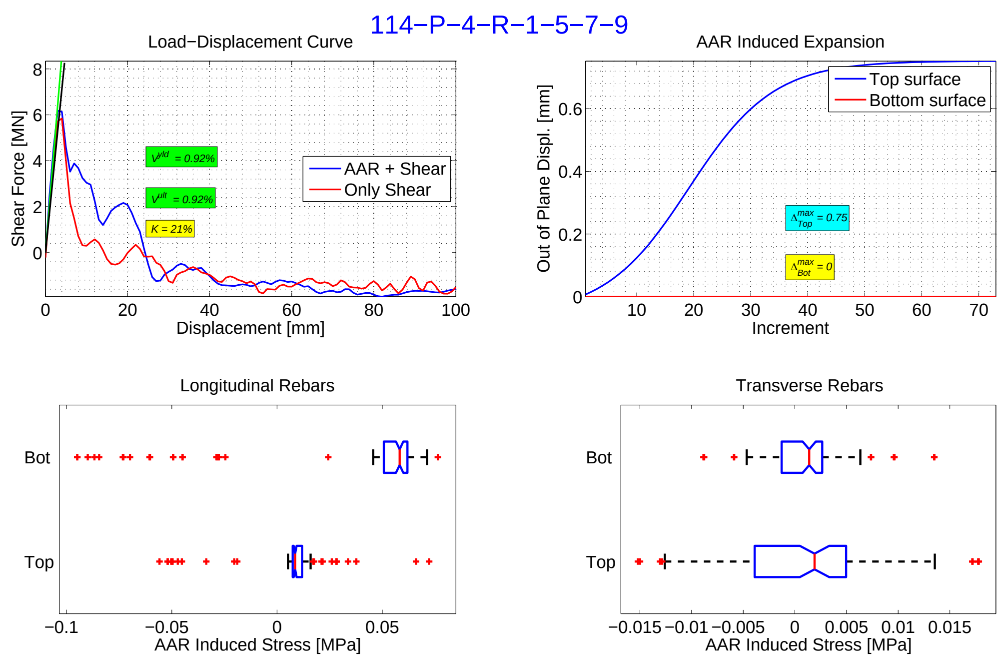

4.1.3.115 Analysis: 115-P-4-R-1-5-9-7

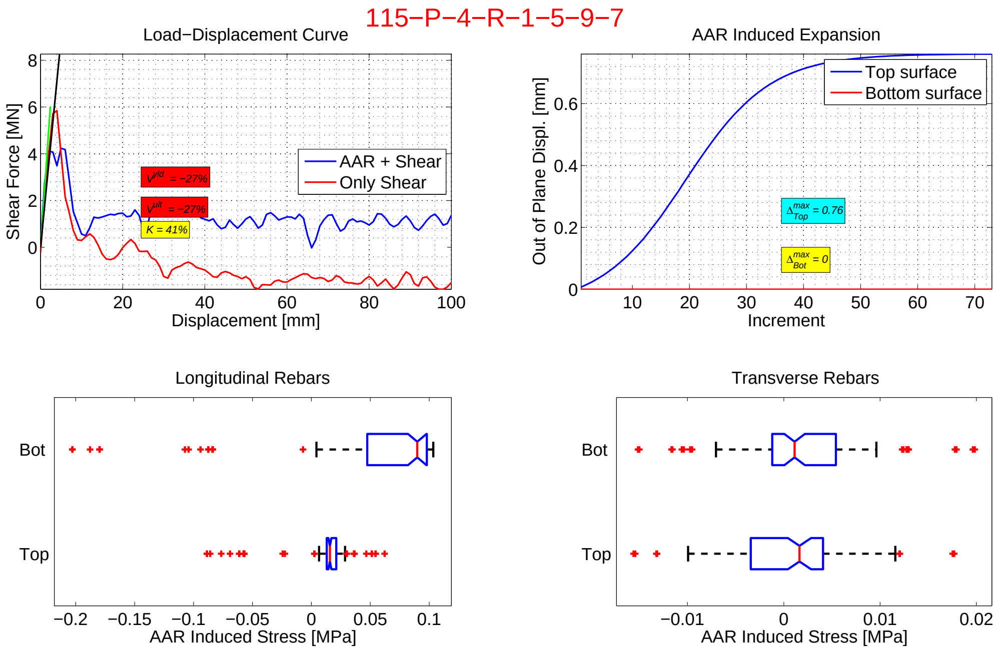

4.1.3.116 Analysis: 116-P-4-R-1-5-9-9

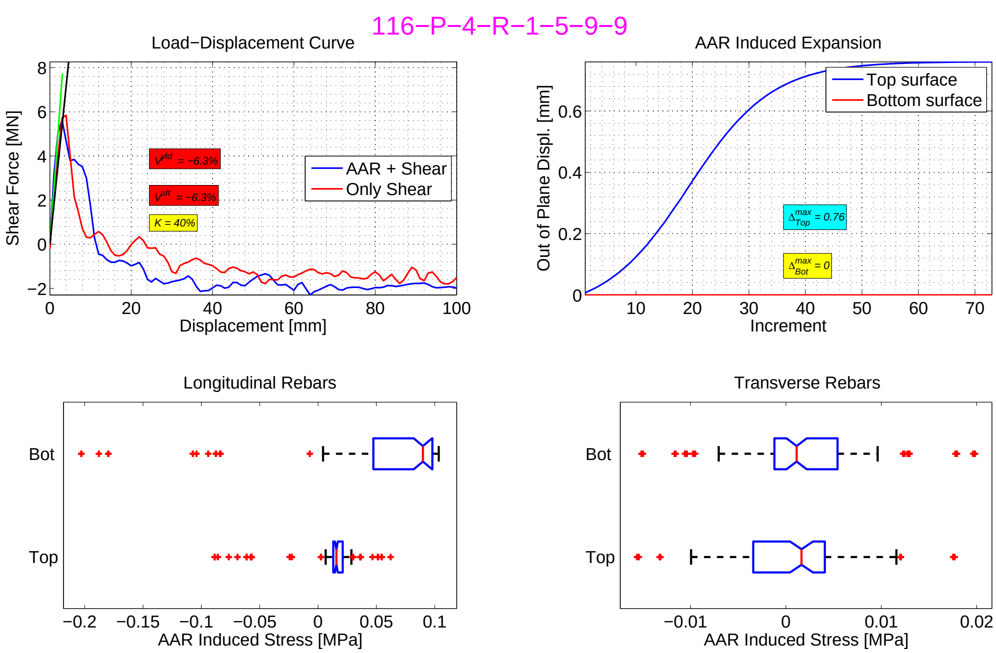

4.1.3.117 Analysis: 117-P-4-R-1-10-7-7

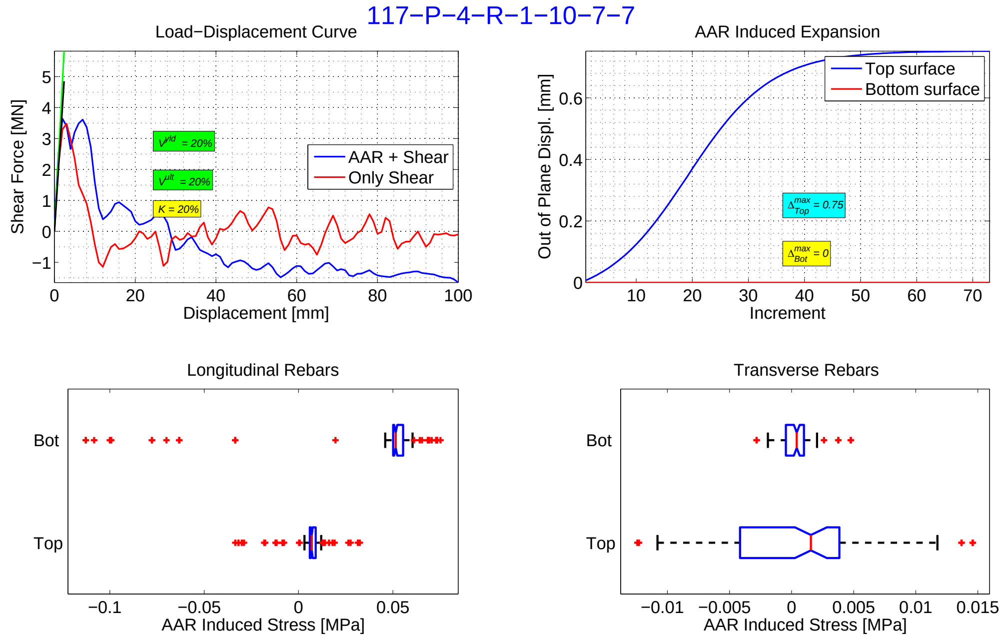

4.1.3.118 Analysis: 118-P-4-R-1-10-7-9

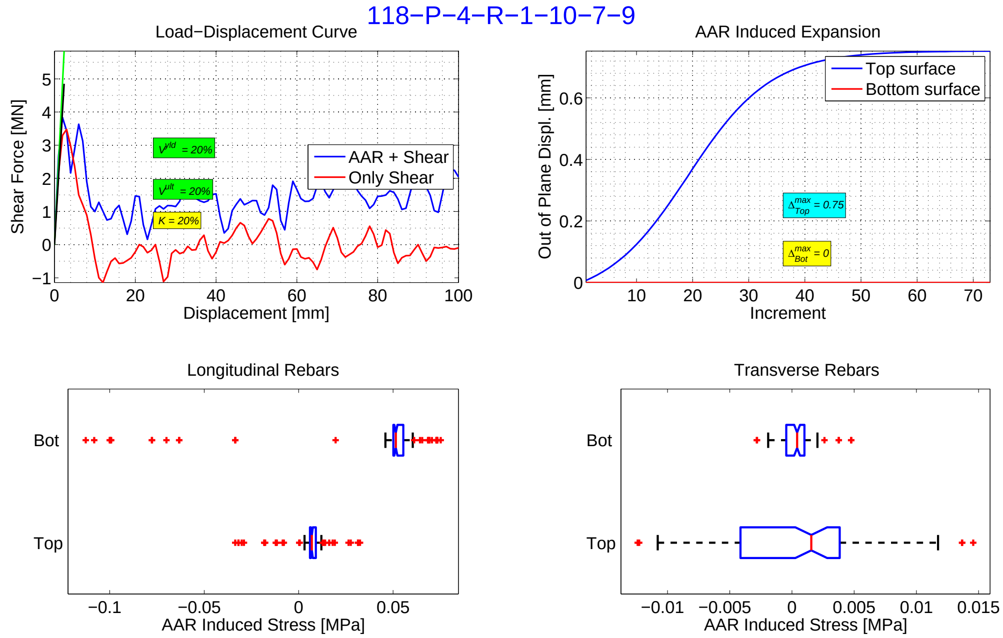

4.1.3.119 Analysis: 119-P-4-R-1-10-9-7

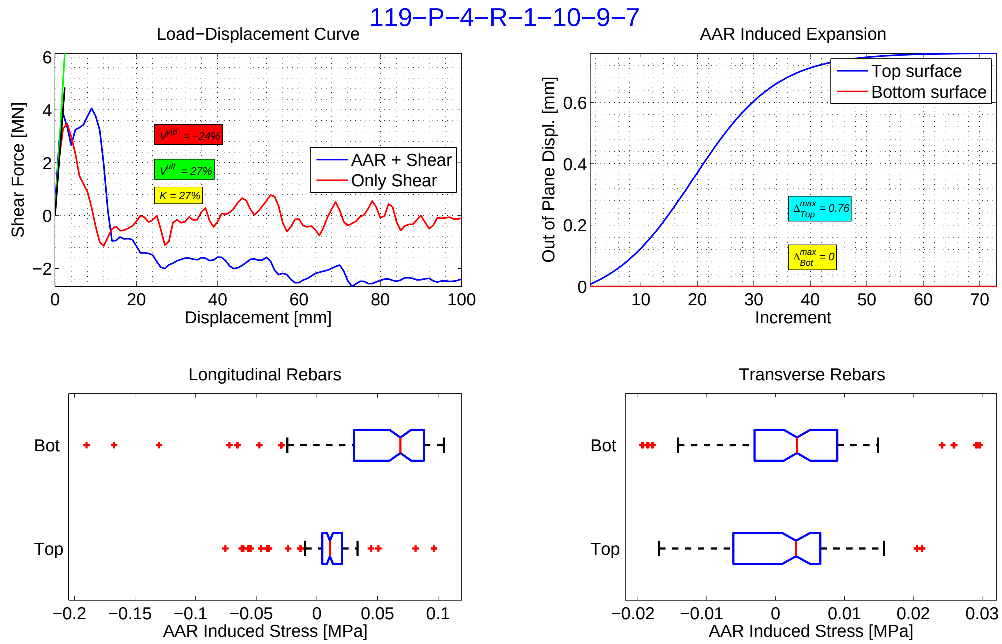

4.1.3.120 Analysis: 120-P-4-R-1-10-9-9

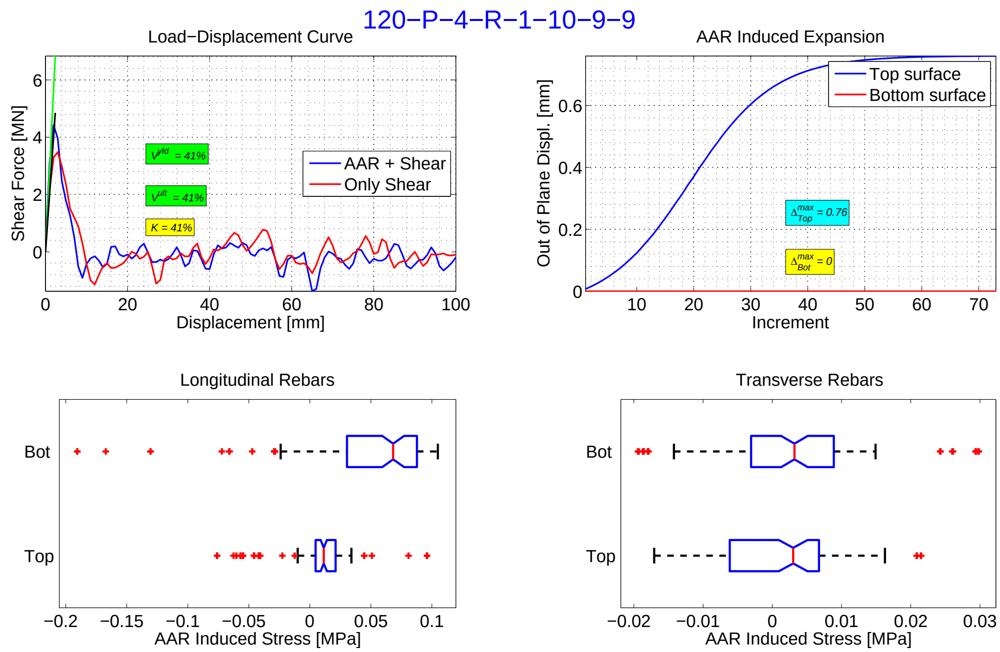

4.1.3.121 Analysis: 121-P-4-R-2-2-7-7

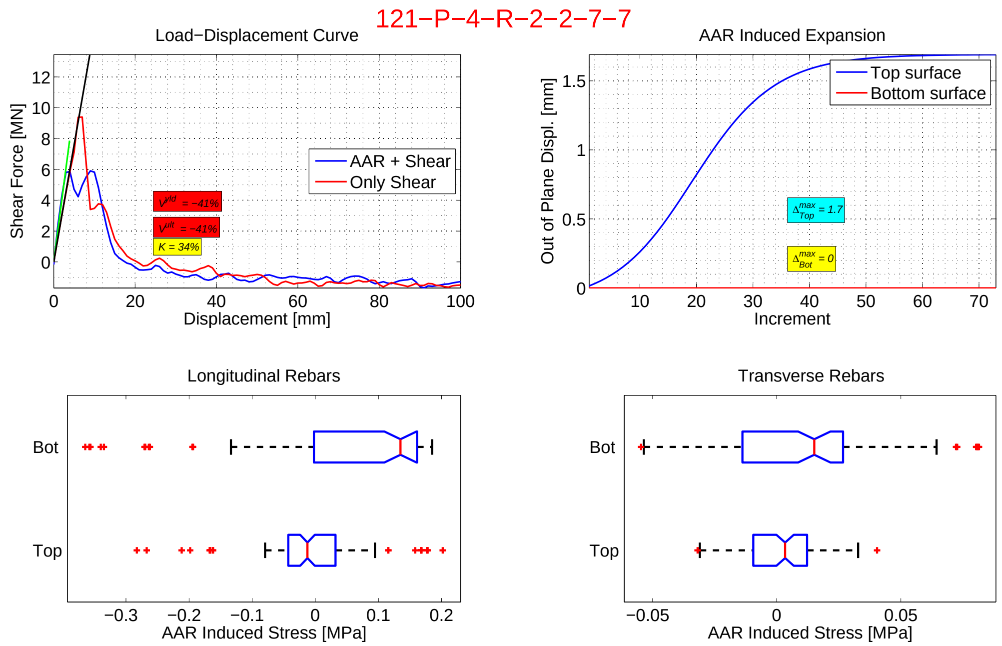

4.1.3.122 Analysis: 122-P-4-R-2-2-7-9

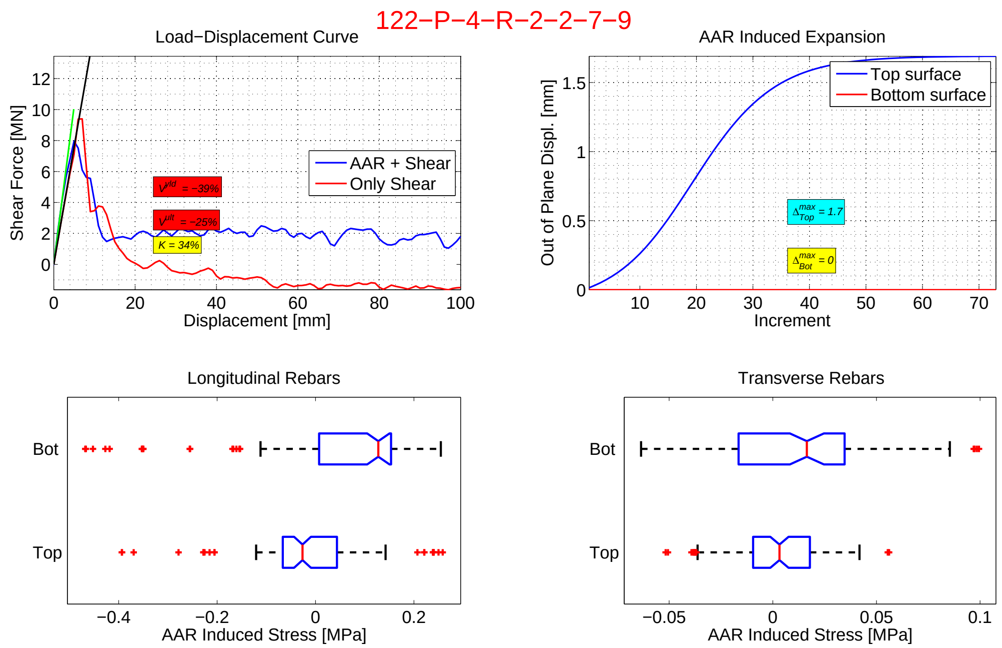

4.1.3.123 Analysis: 123-P-4-R-2-2-9-7

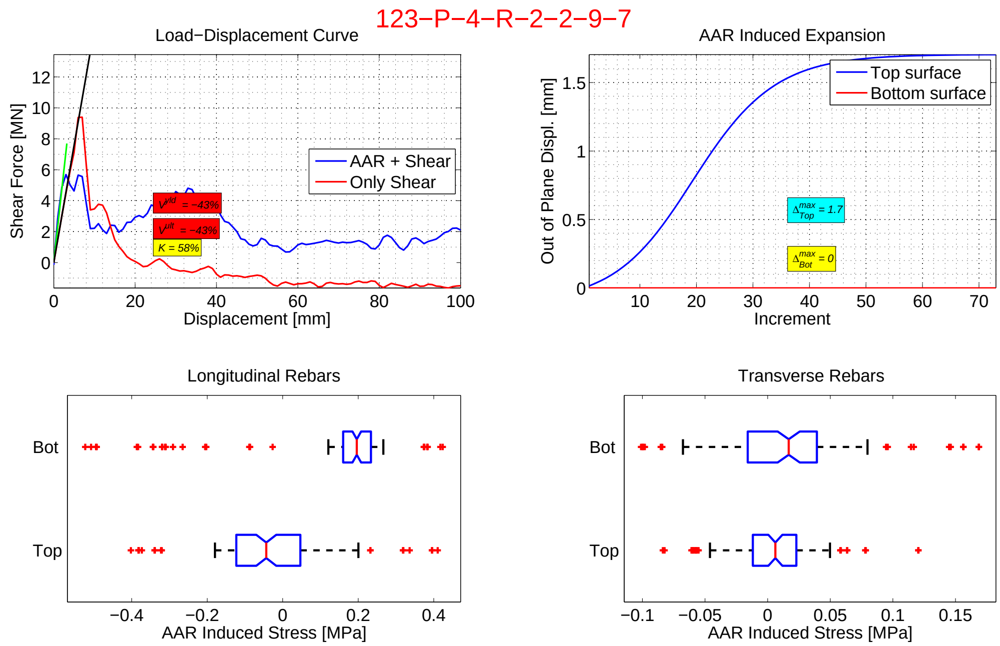

4.1.3.124 Analysis: 124-P-4-R-2-2-9-9

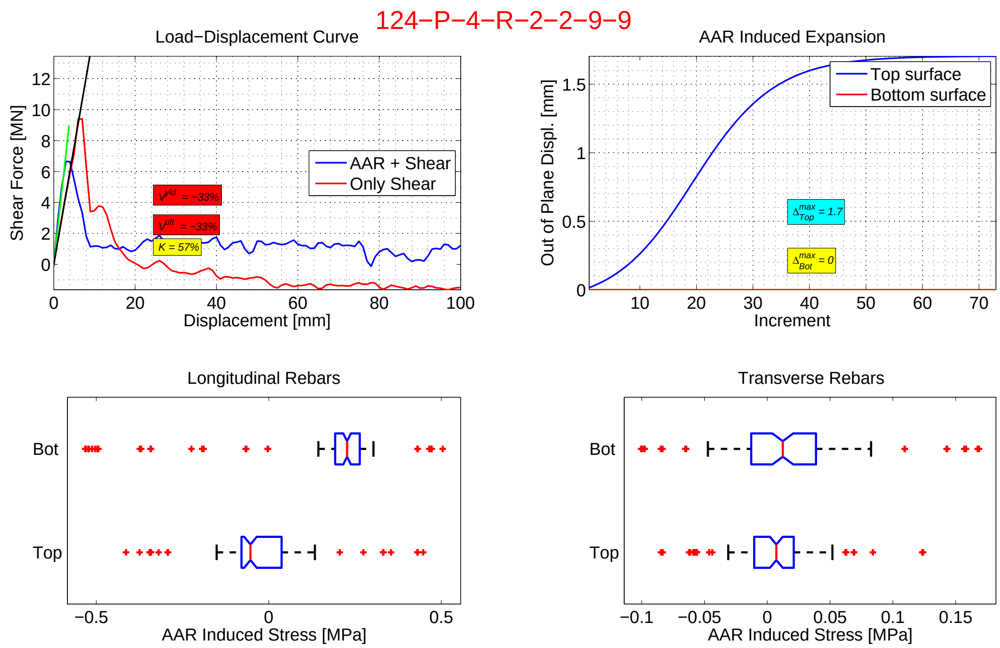

4.1.3.125 Analysis: 125-P-4-R-2-5-7-7

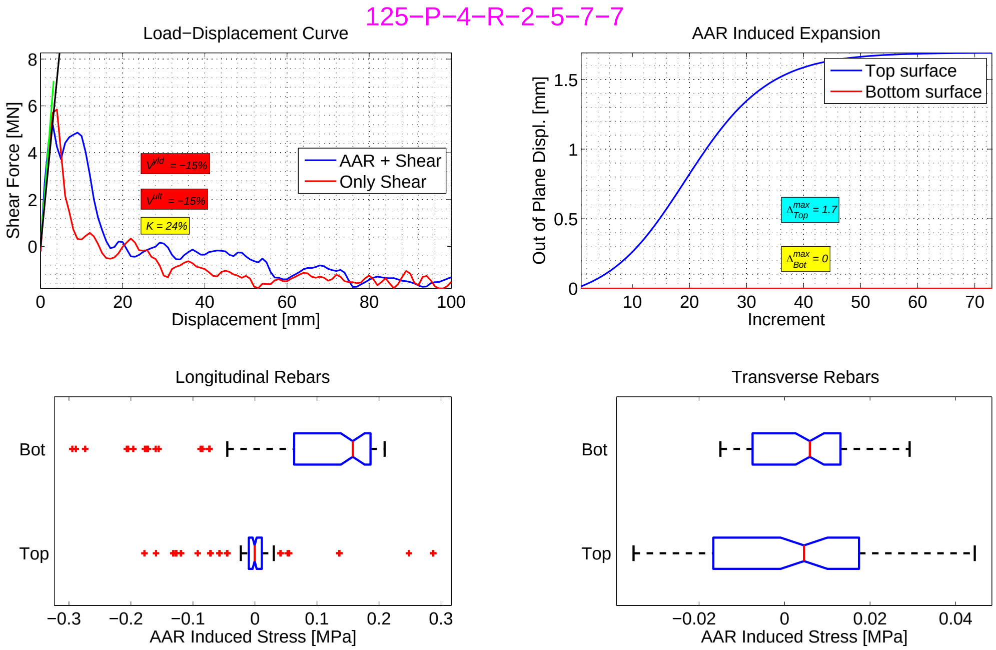

4.1.3.126 Analysis: 126-P-4-R-2-5-7-9

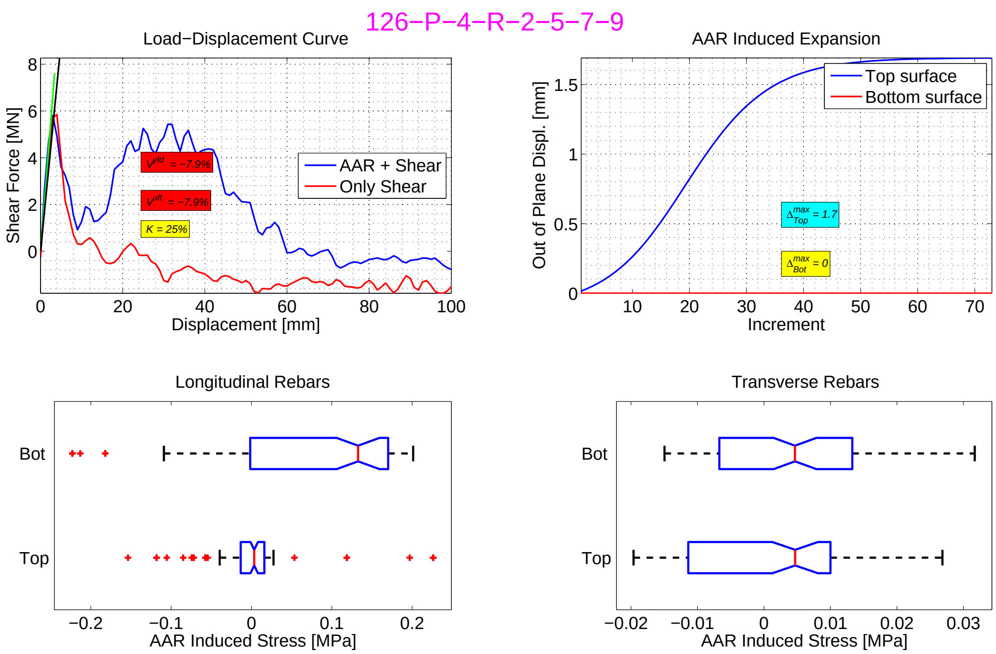

4.1.3.127 Analysis: 127-P-4-R-2-5-9-7

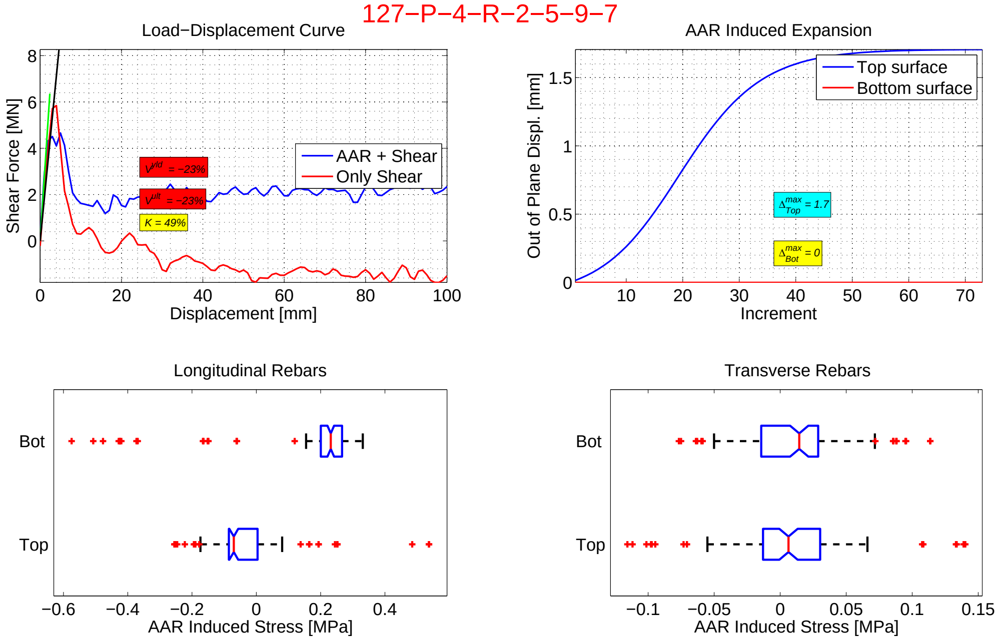

4.1.3.128 Analysis: 128-P-4-R-2-5-9-9

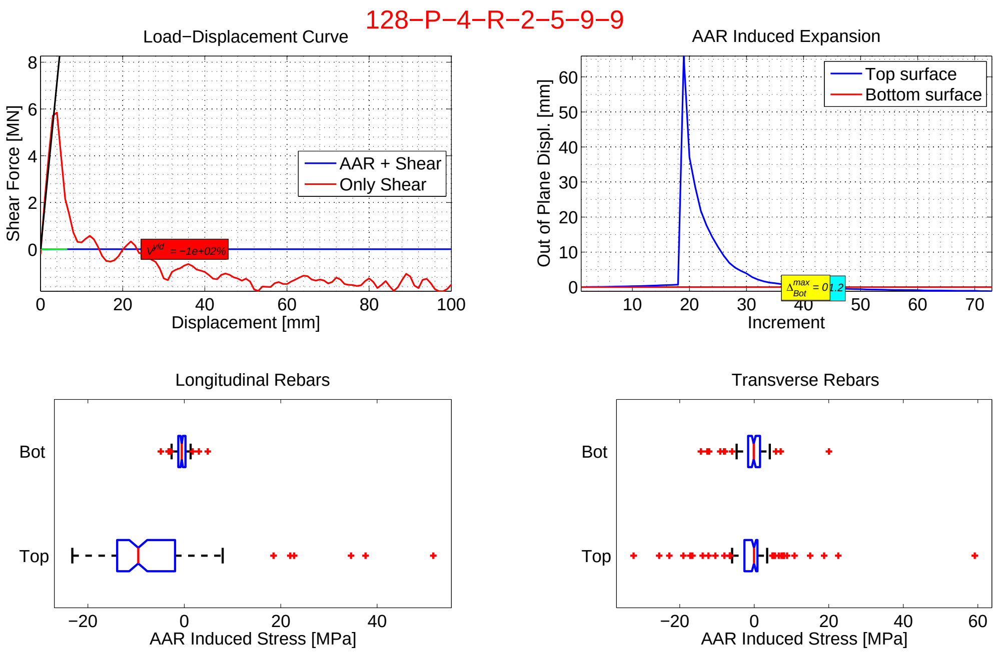

4.1.3.129 Analysis: 129-P-4-R-2-10-7-7

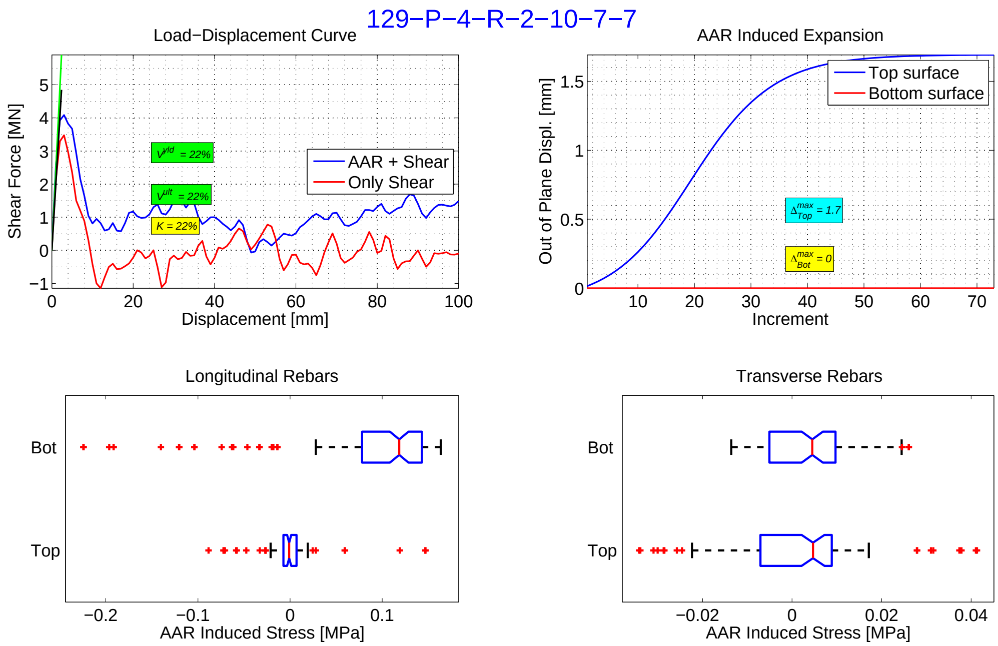

4.1.3.130 Analysis: 130-P-4-R-2-10-7-9

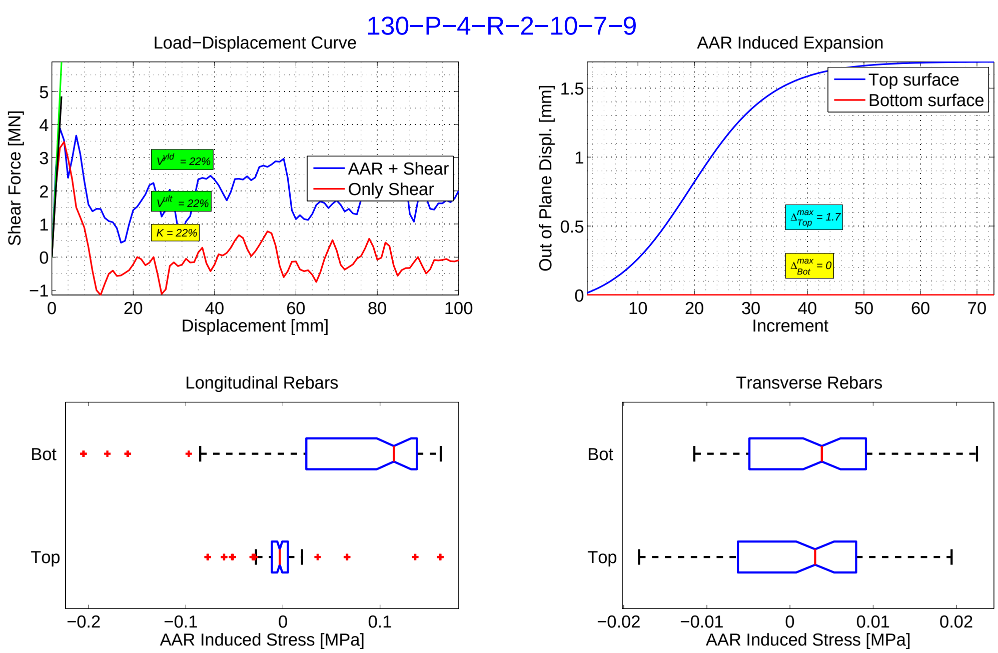

4.1.3.131 Analysis: 131-P-4-R-2-10-9-7

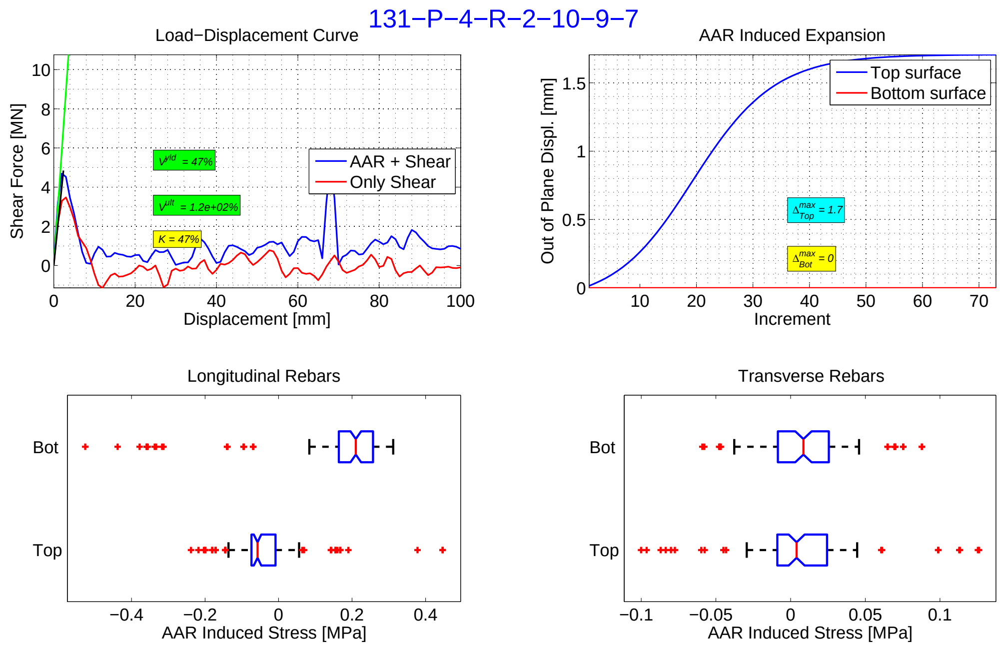

4.1.3.132 Analysis: 132-P-4-R-2-10-9-9

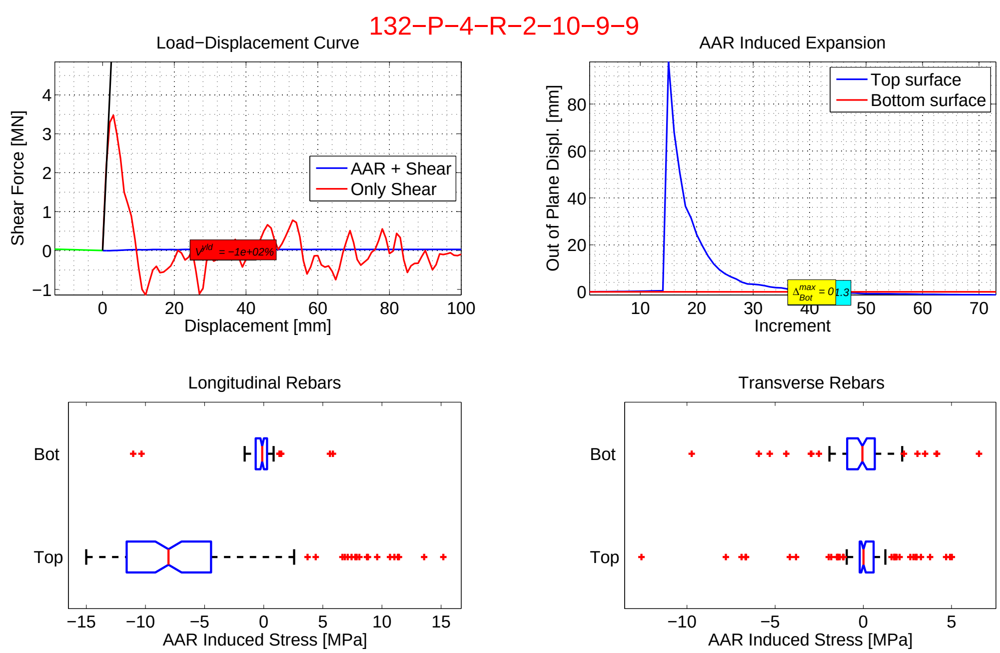

4.1.3.133 Analysis: 133-P-4-R-3-2-7-7

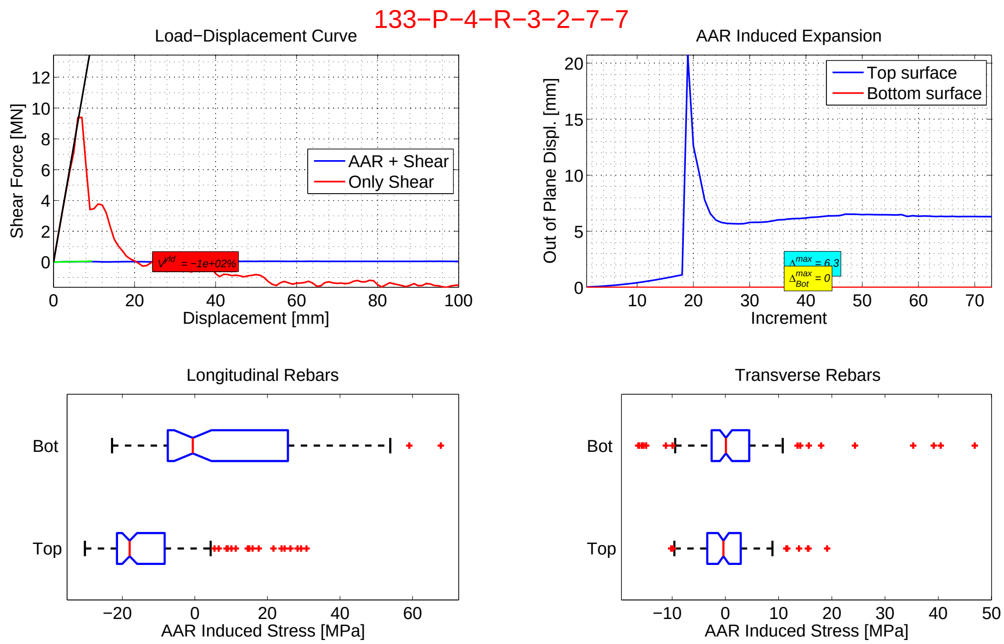

4.1.3.134 Analysis: 134-P-4-R-3-2-7-9

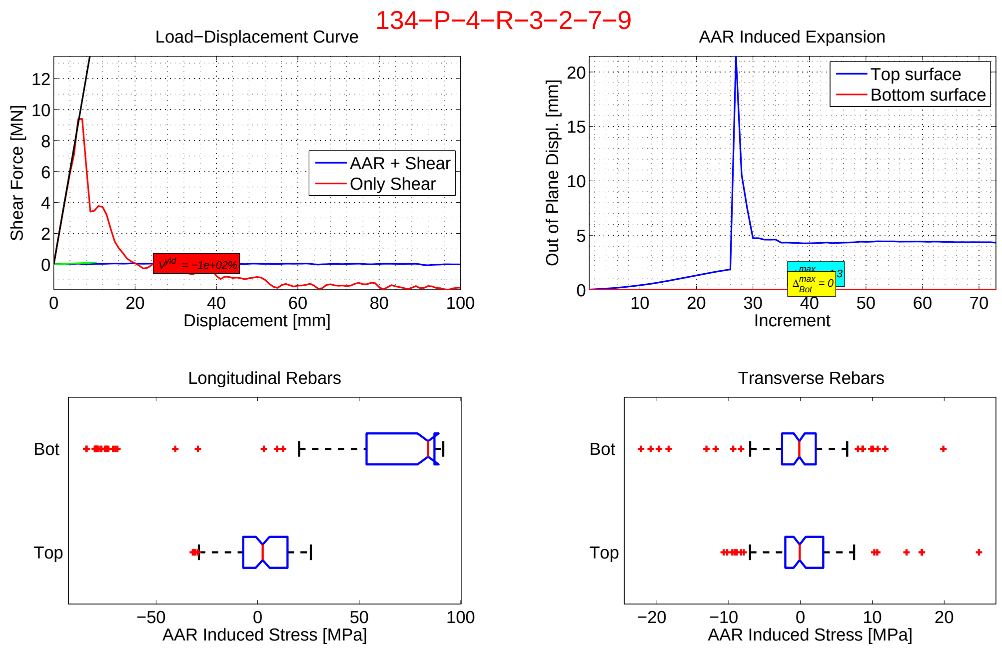

4.1.3.135 Analysis: 135-P-4-R-3-2-9-7

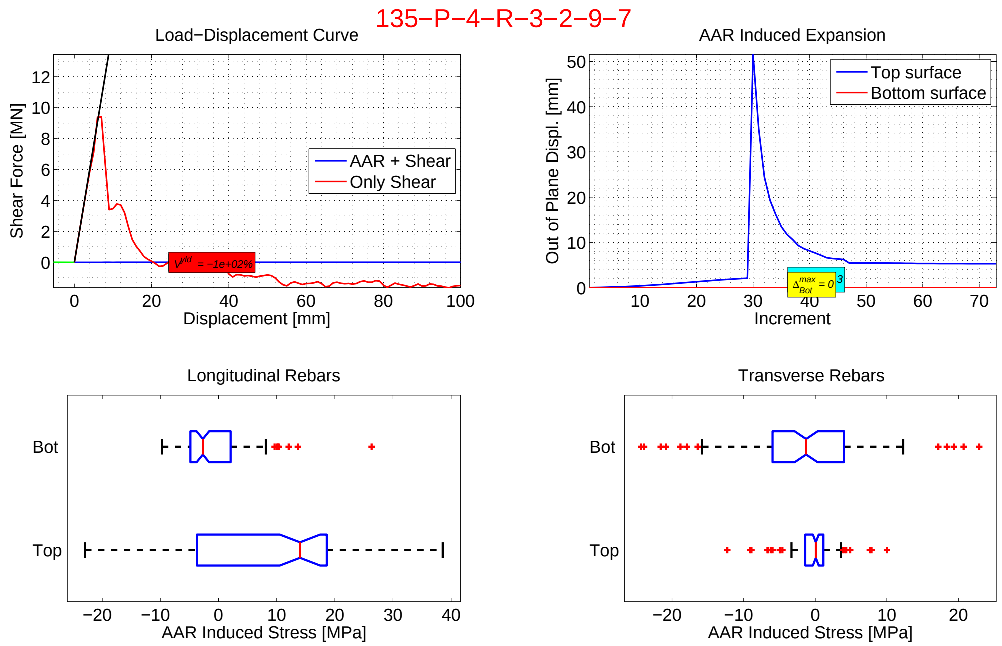

4.1.3.136 Analysis: 136-P-4-R-3-2-9-9

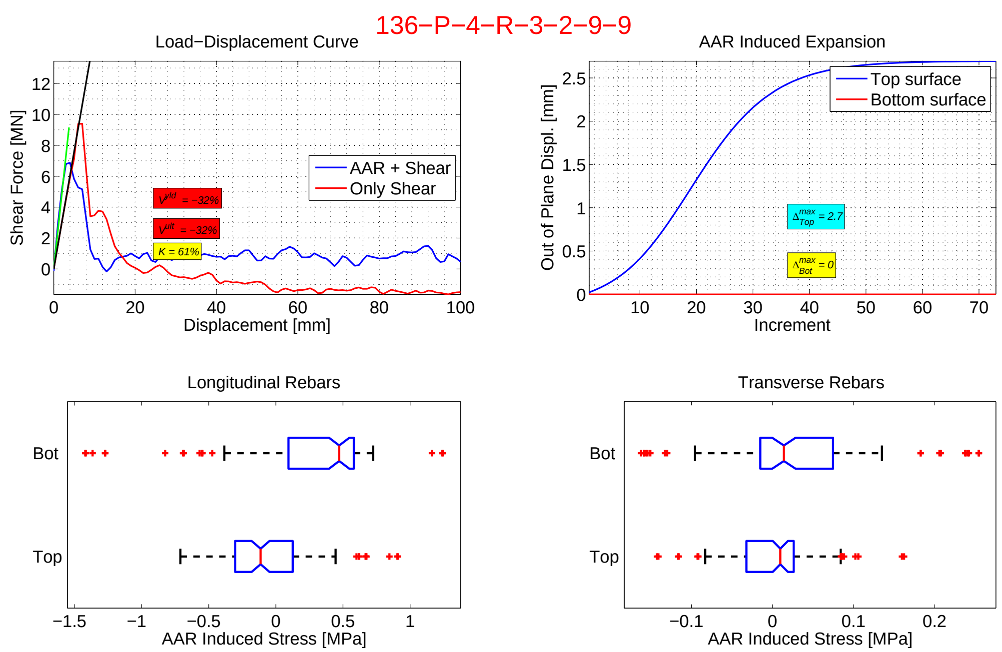

4.1.3.137 Analysis: 137-P-4-R-3-5-7-7

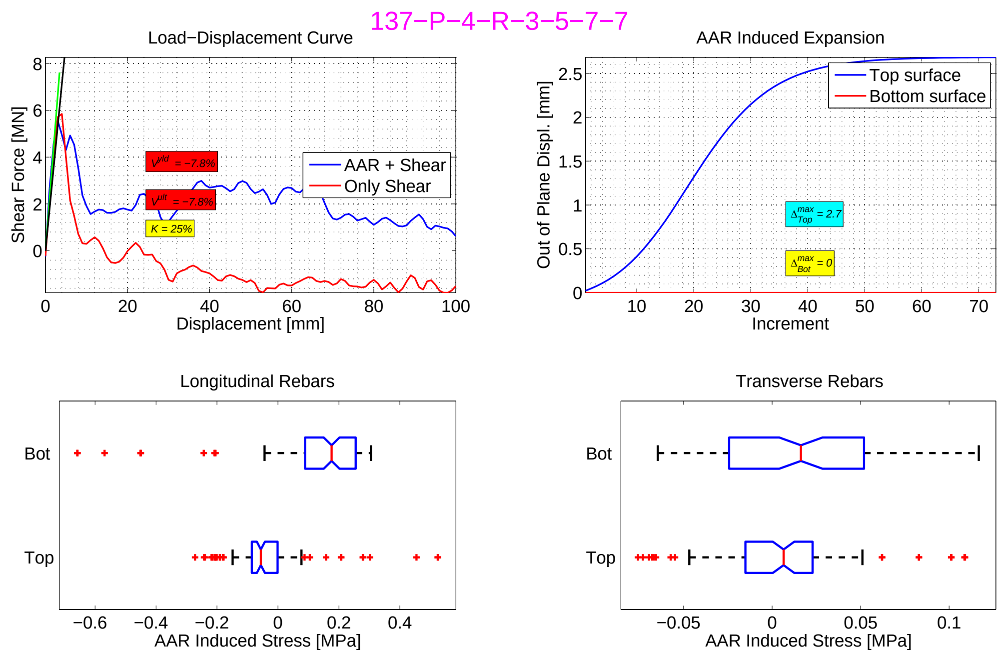

4.1.3.138 Analysis: 138-P-4-R-3-5-7-9

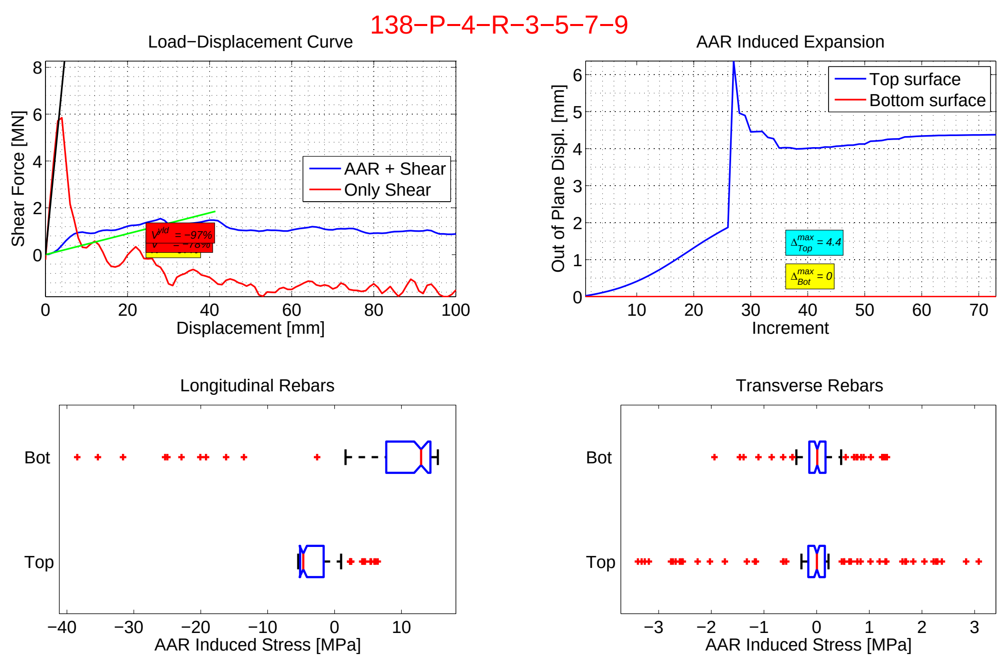

4.1.3.139 Analysis: 139-P-4-R-3-5-9-7

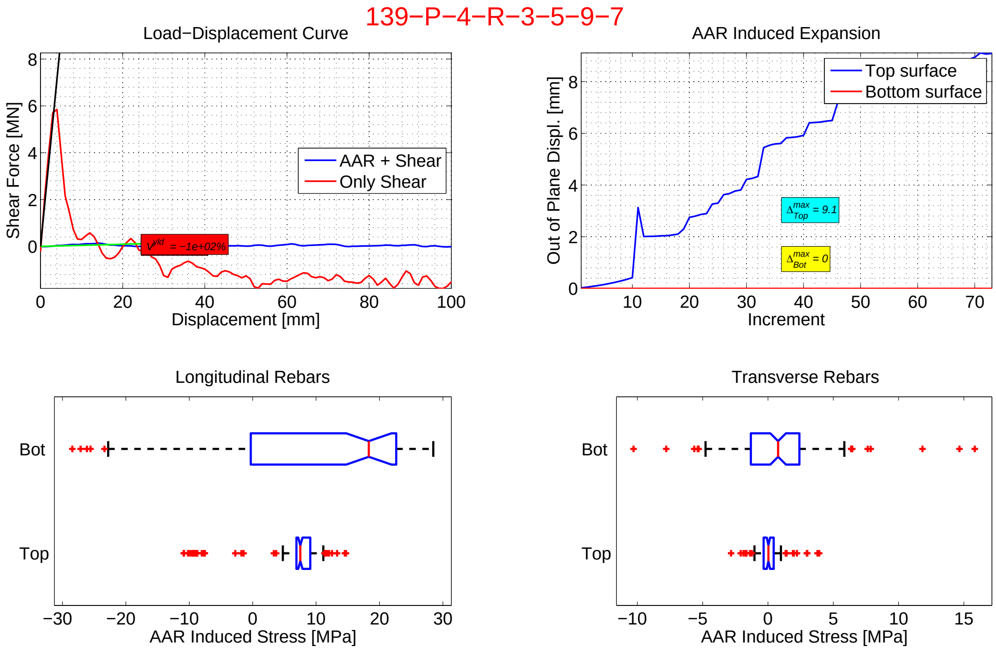

4.1.3.140 Analysis: 140-P-4-R-3-5-9-9

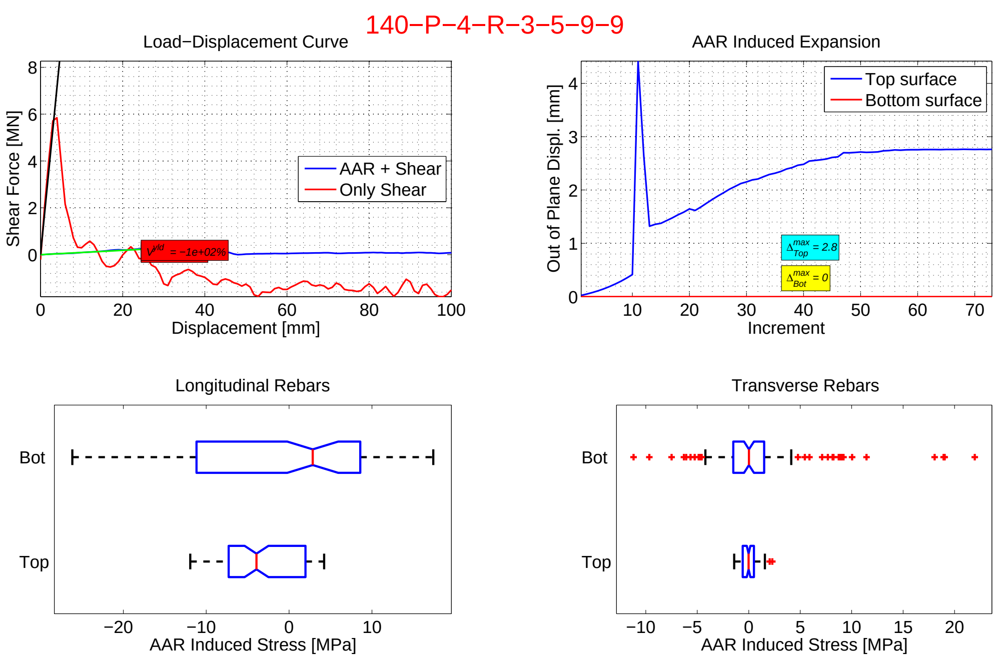

4.1.3.141 Analysis: 141-P-4-R-3-10-7-7

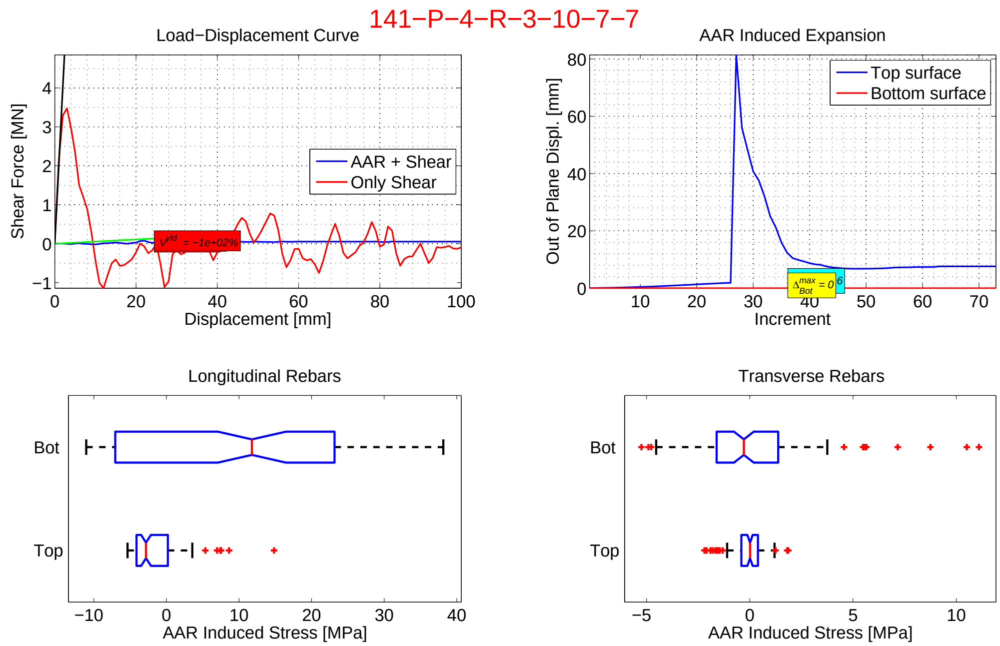

4.1.3.142 Analysis: 142-P-4-R-3-10-7-9

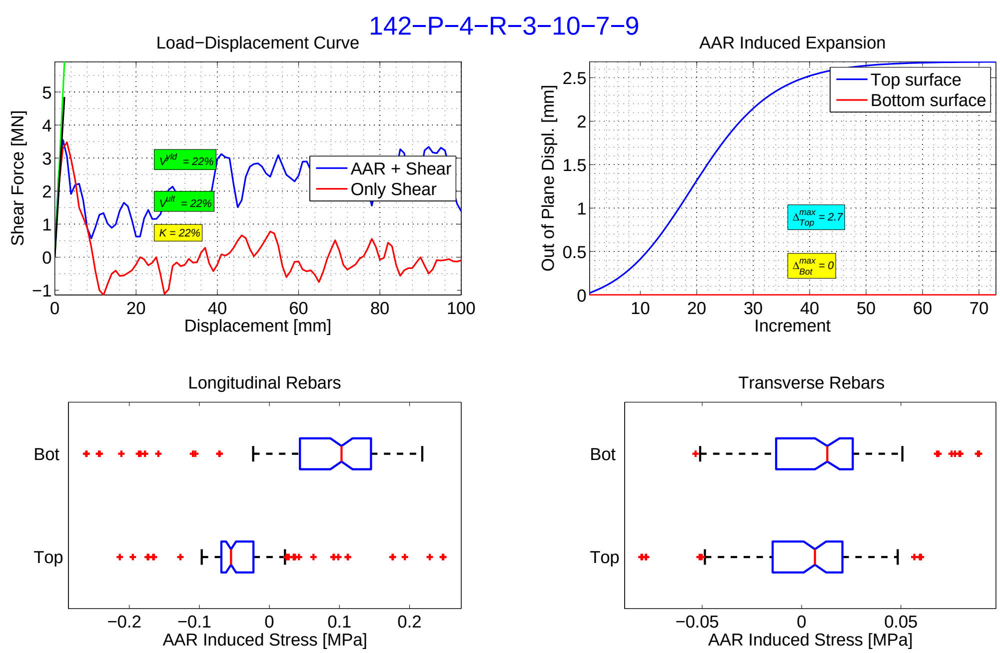

4.1.3.143 Analysis: 143-P-4-R-3-10-9-7

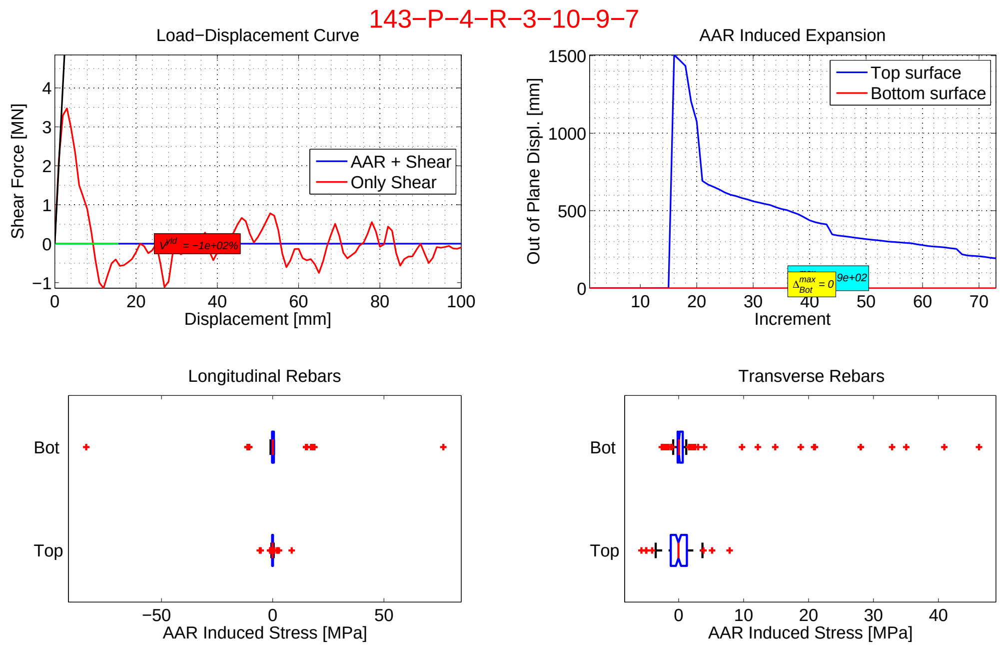

4.1.3.144 Analysis: 144-P-4-R-3-10-9-9

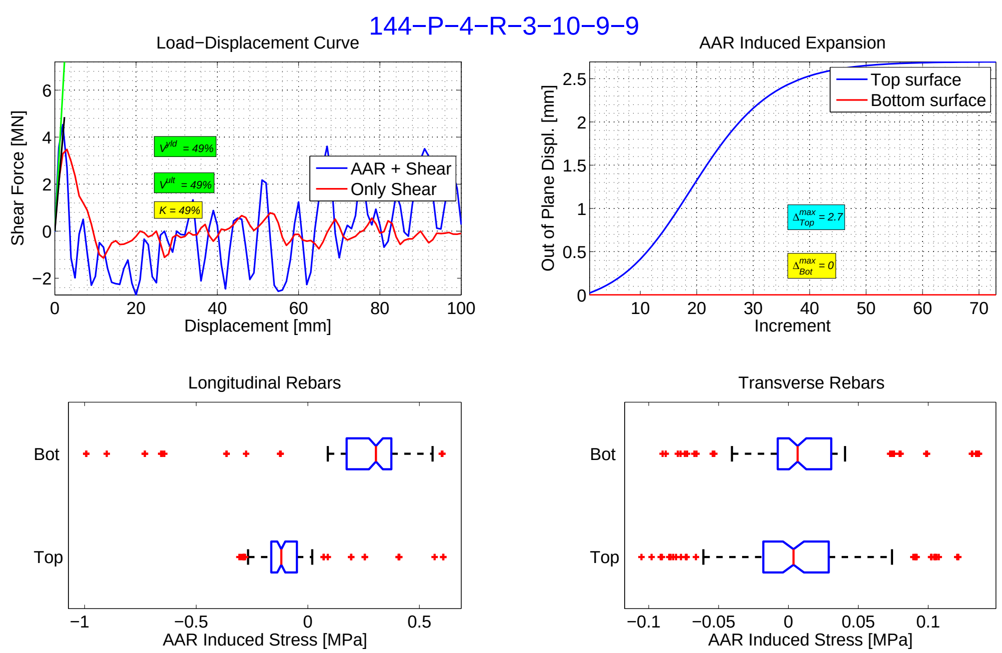

4.1.3.145 Analysis: 145-P-2-FR-1-2-7-7

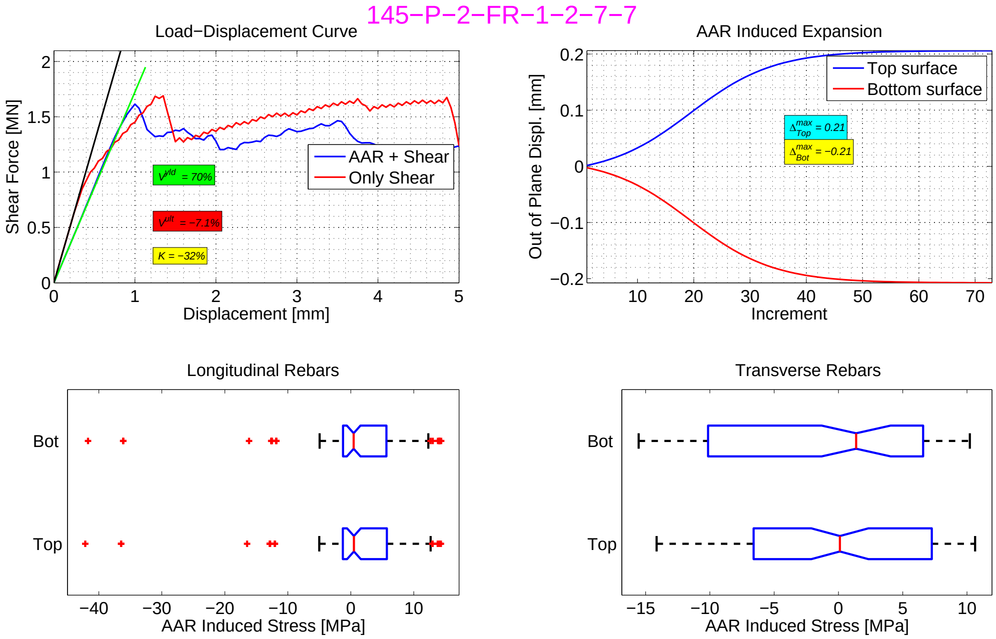

4.1.3.146 Analysis: 146-P-2-FR-1-2-7-9

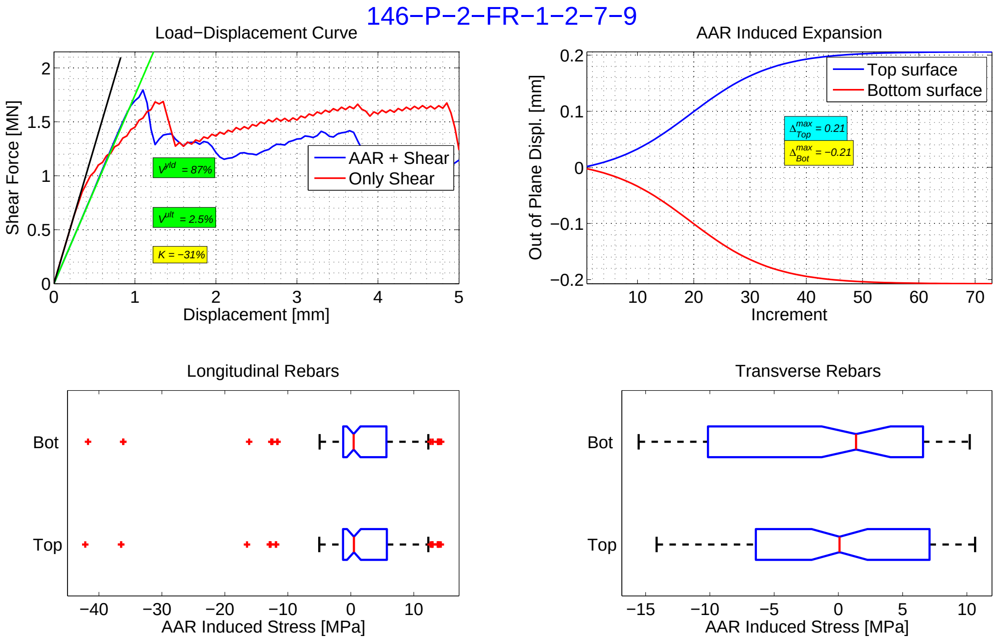

4.1.3.147 Analysis: 147-P-2-FR-1-2-9-7

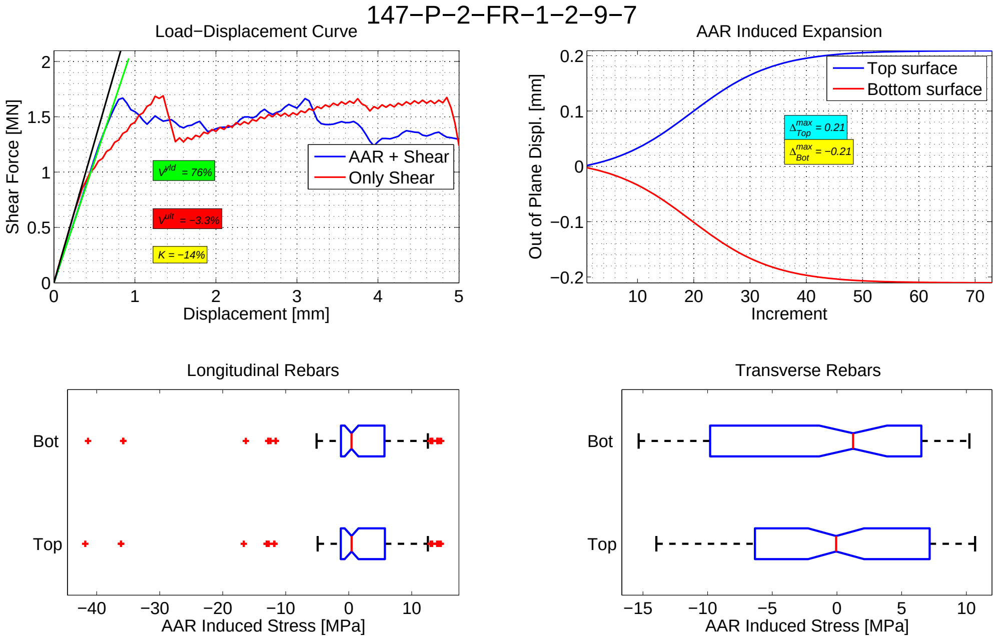

4.1.3.148 Analysis: 148-P-2-FR-1-2-9-9

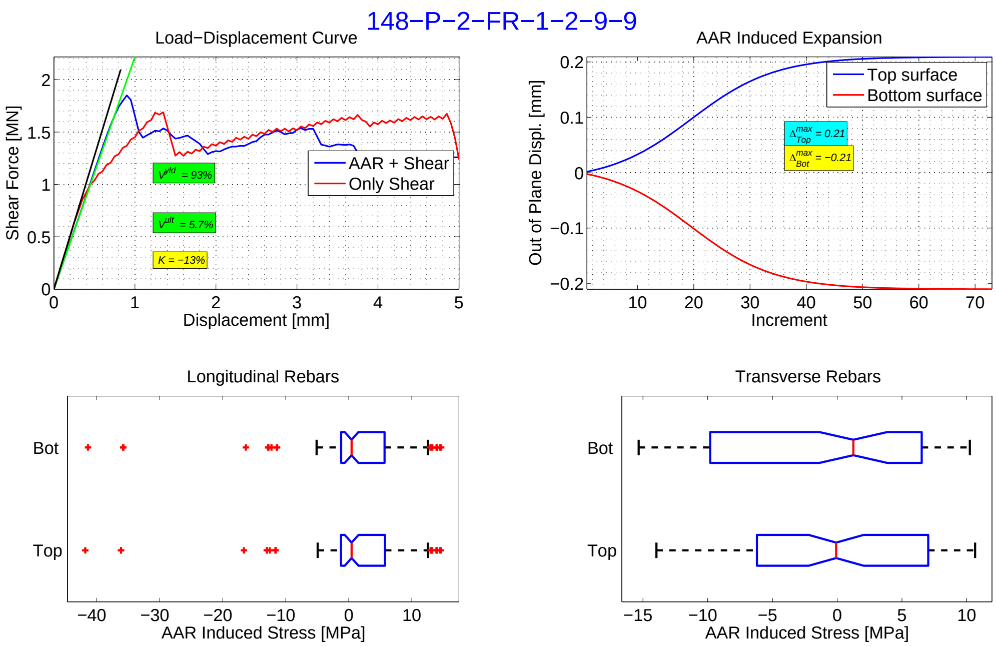

4.1.3.149 Analysis: 149-P-2-FR-1-5-7-7

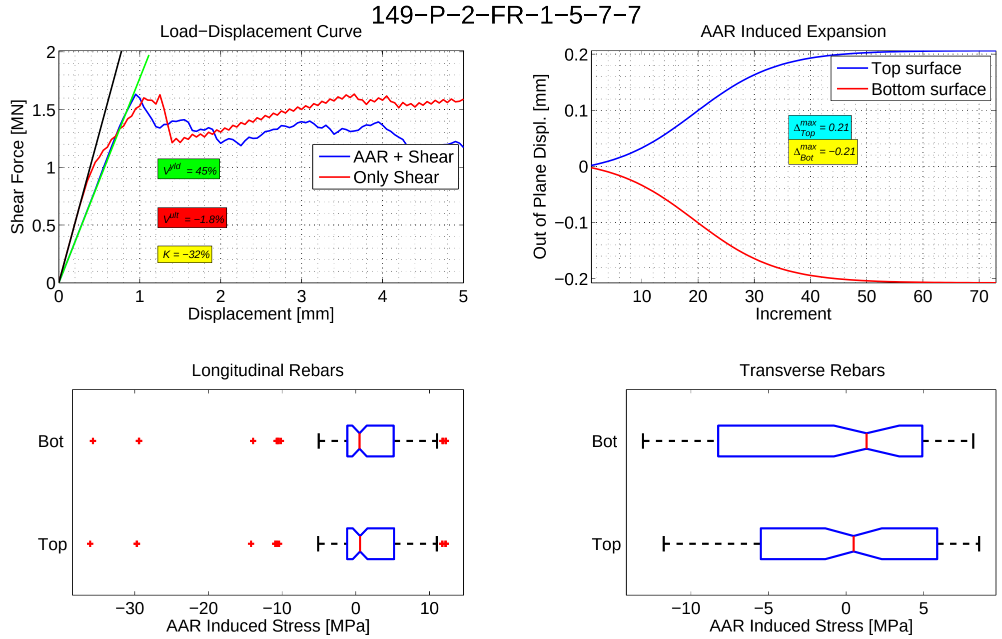

4.1.3.150 Analysis: 150-P-2-FR-1-5-7-9

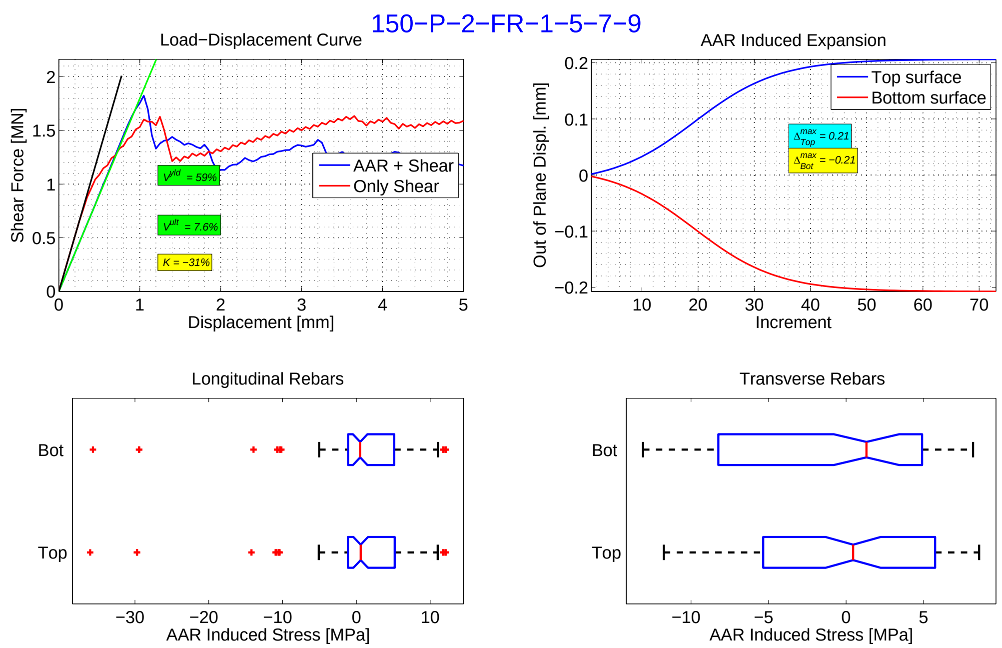

4.1.3.151 Analysis: 151-P-2-FR-1-5-9-7

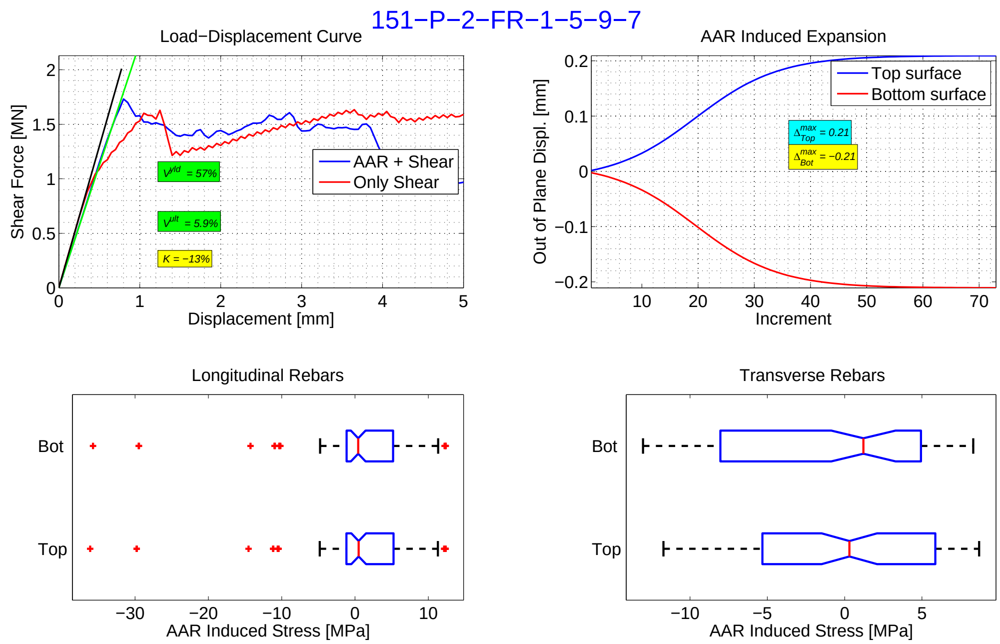

4.1.3.152 Analysis: 152-P-2-FR-1-5-9-9

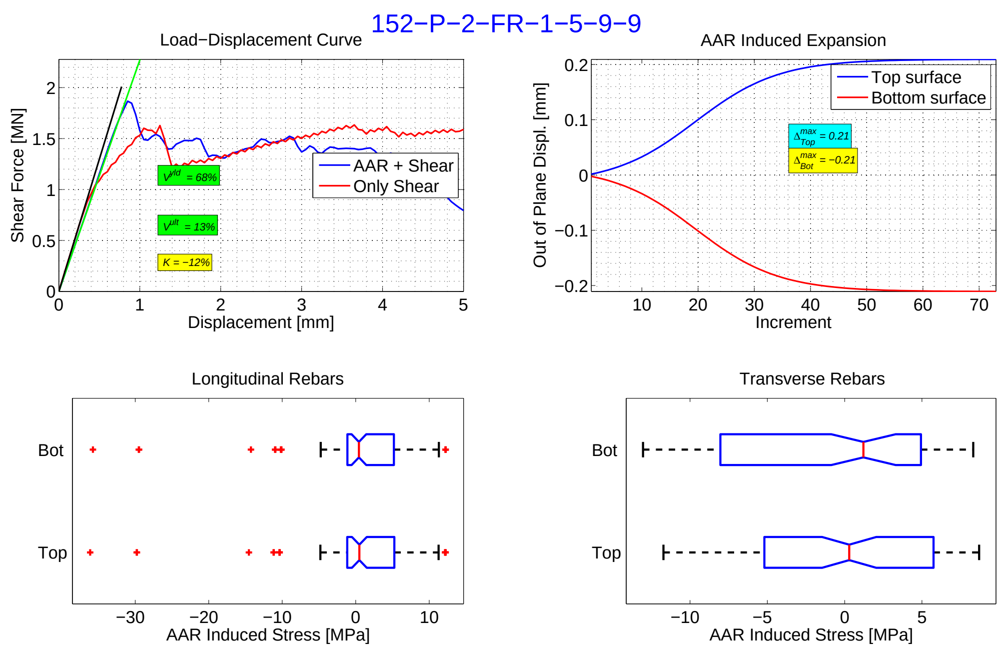

4.1.3.153 Analysis: 153-P-2-FR-1-10-7-7

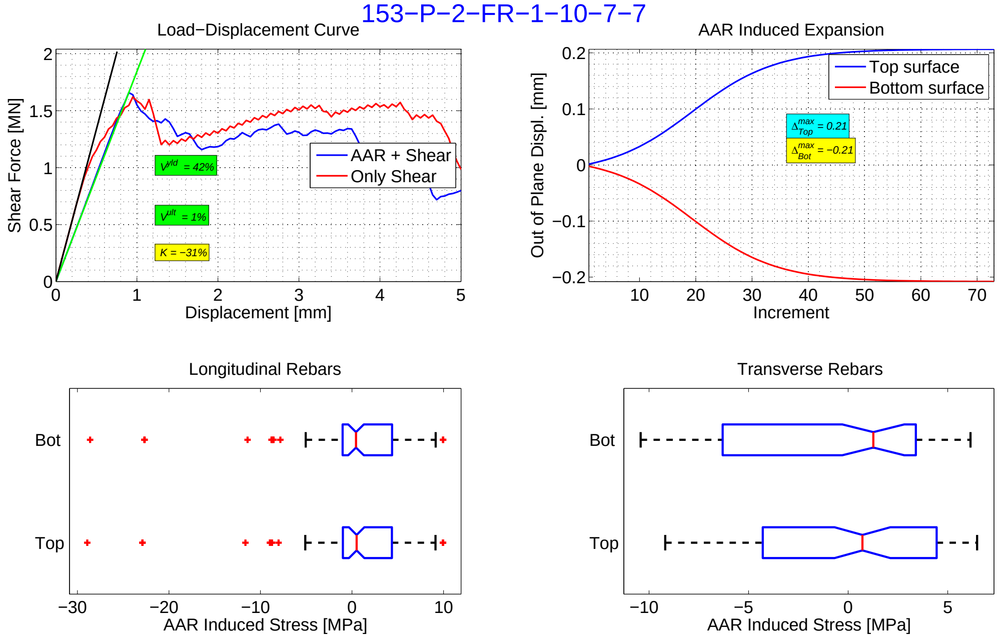

4.1.3.154 Analysis: 154-P-2-FR-1-10-7-9

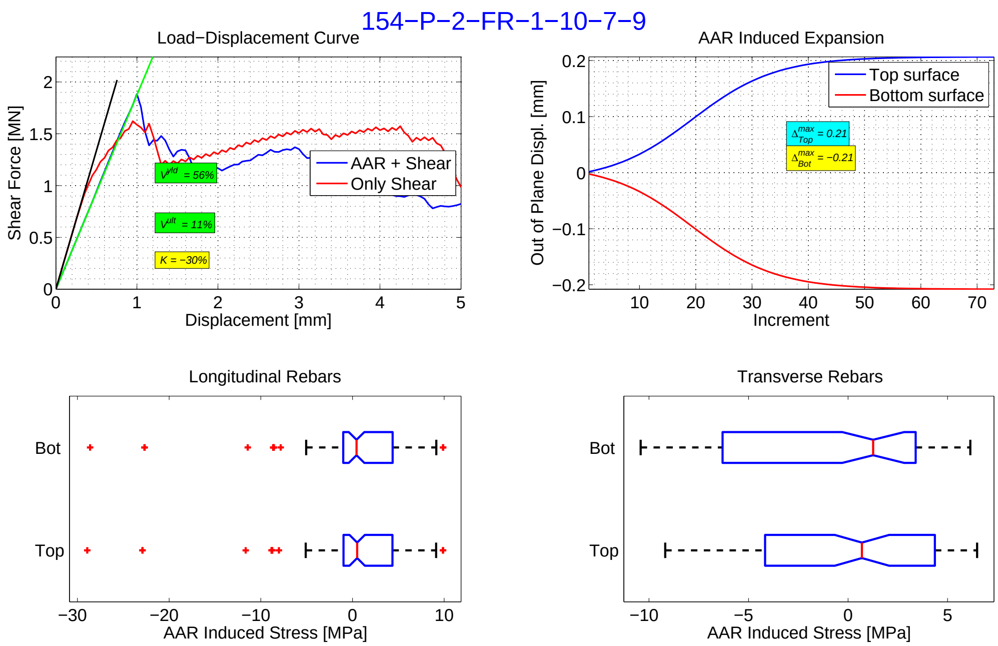

4.1.3.155 Analysis: 155-P-2-FR-1-10-9-7

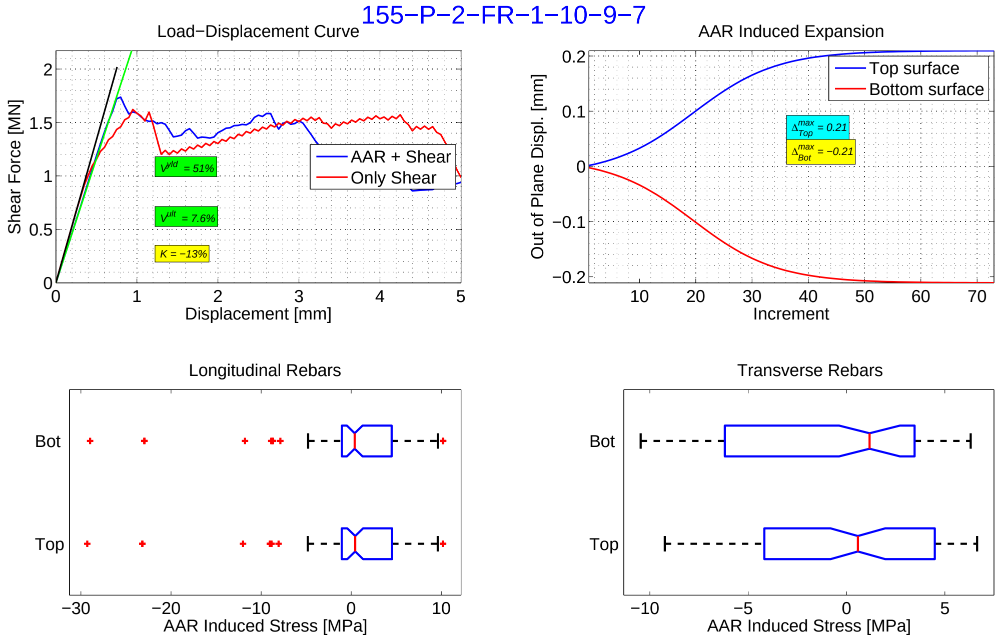

4.1.3.156 Analysis: 156-P-2-FR-1-10-9-9

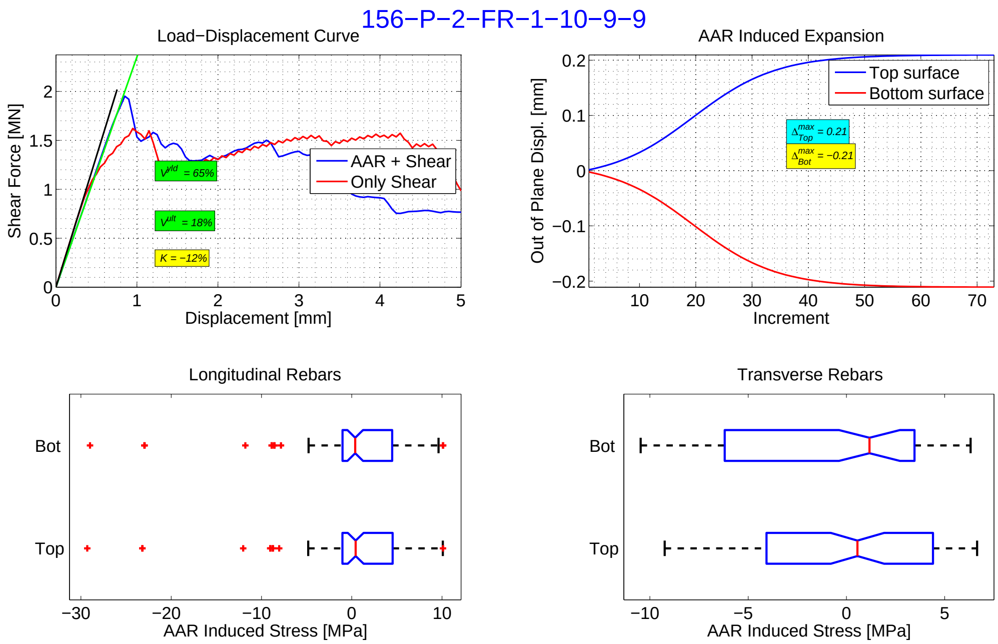

4.1.3.157 Analysis: 157-P-2-FR-2-2-7-7

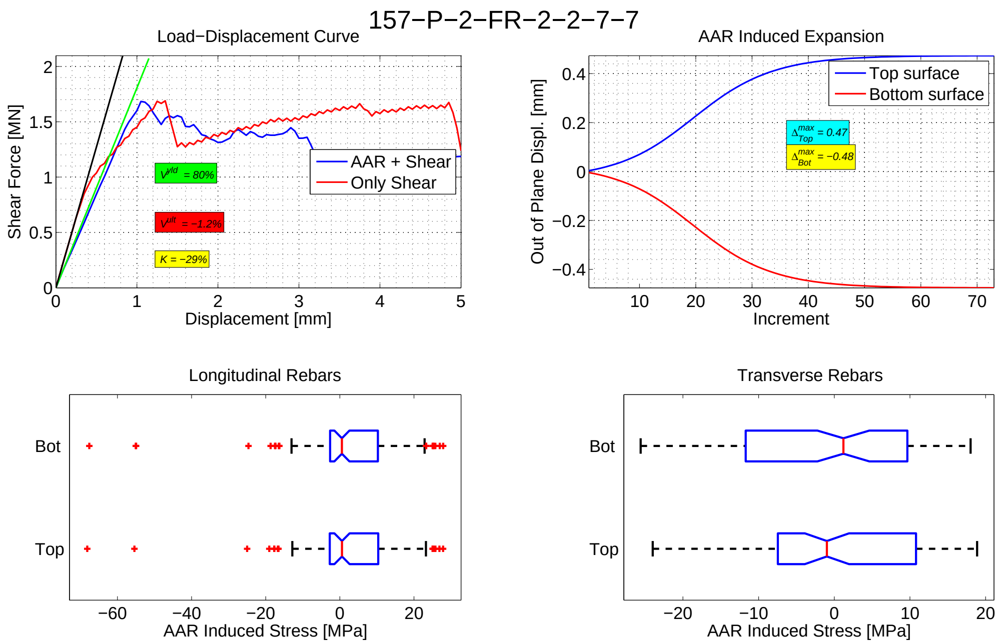

4.1.3.158 Analysis: 158-P-2-FR-2-2-7-9

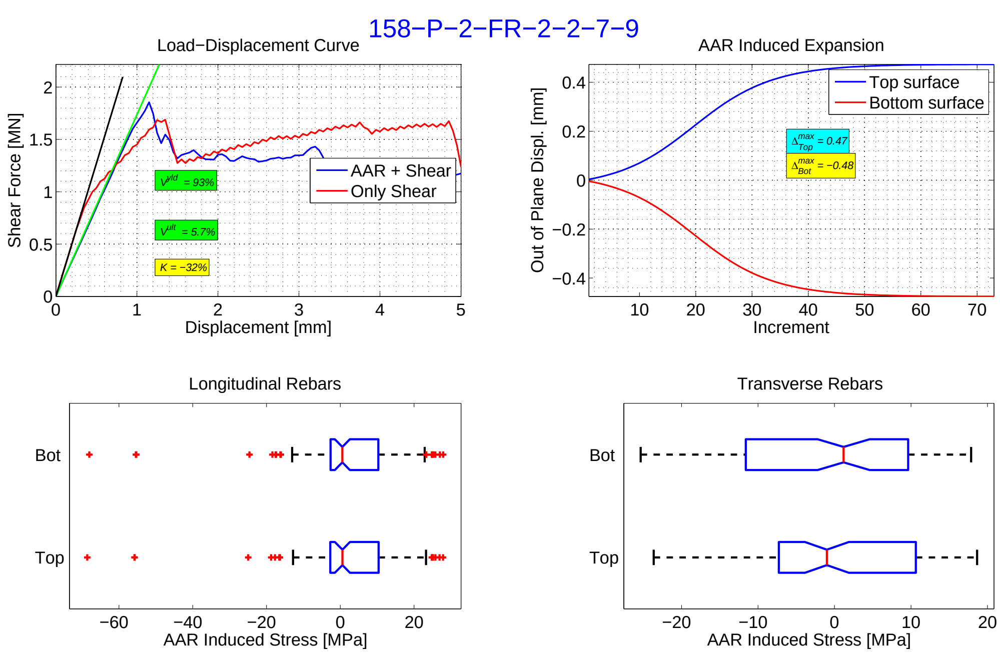

4.1.3.159 Analysis: 159-P-2-FR-2-2-9-7

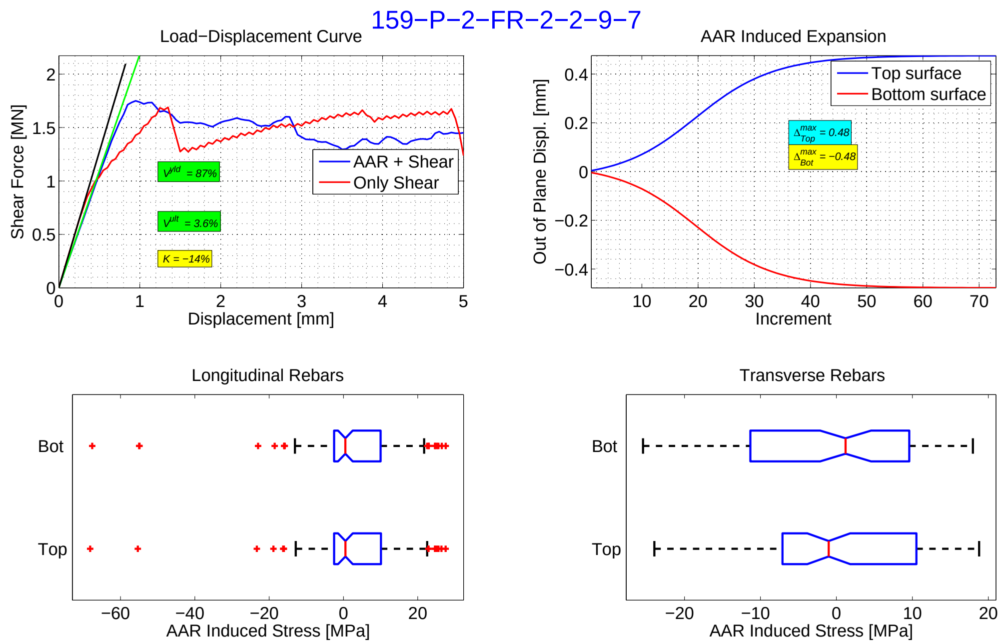

4.1.3.160 Analysis: 160-P-2-FR-2-2-9-9

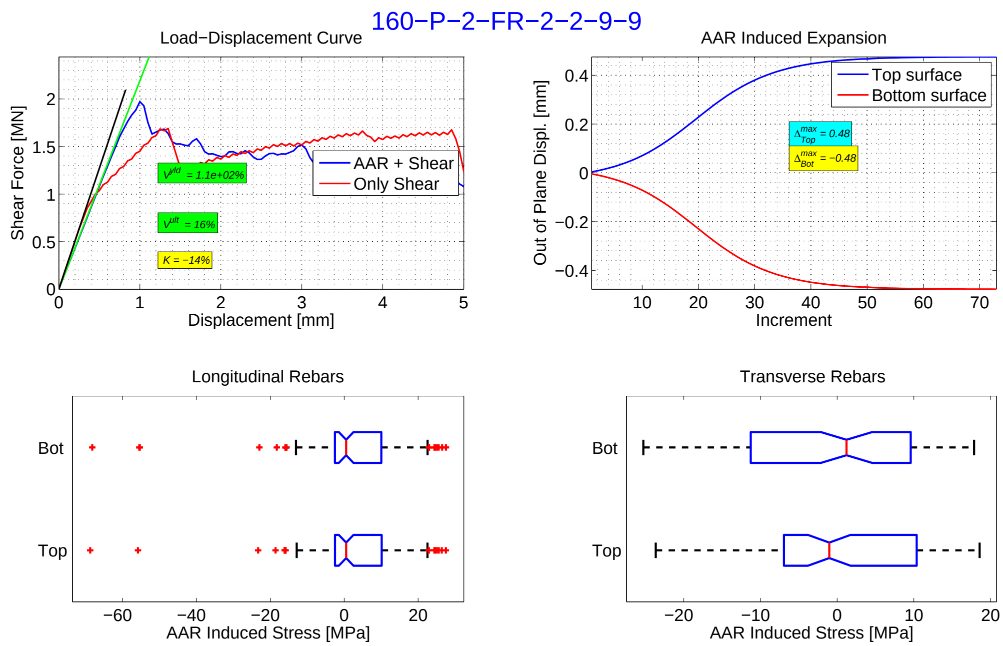

4.1.3.161 Analysis: 161-P-2-FR-2-5-7-7

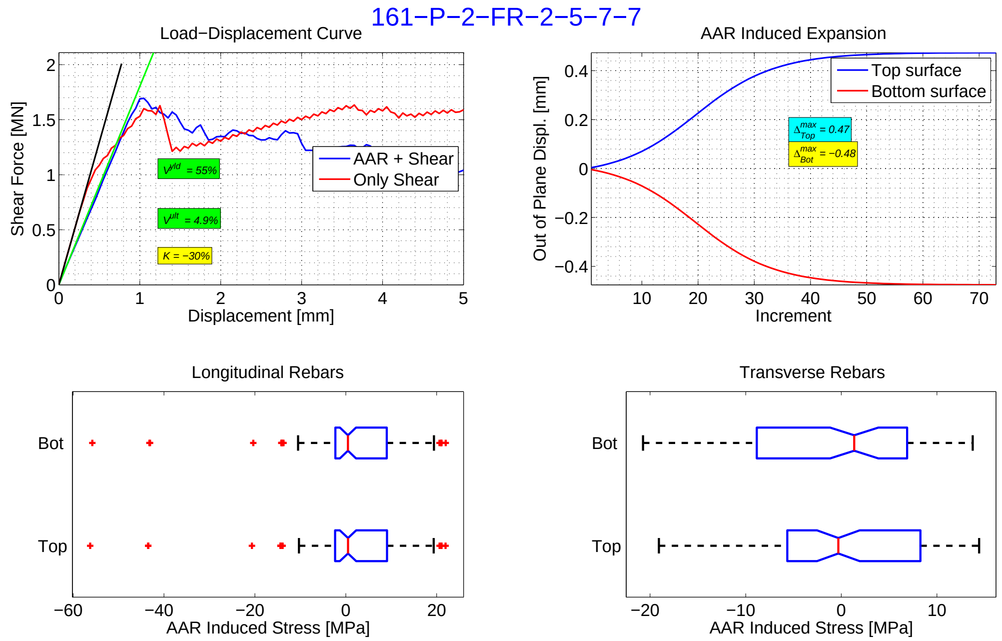

4.1.3.162 Analysis: 162-P-2-FR-2-5-7-9

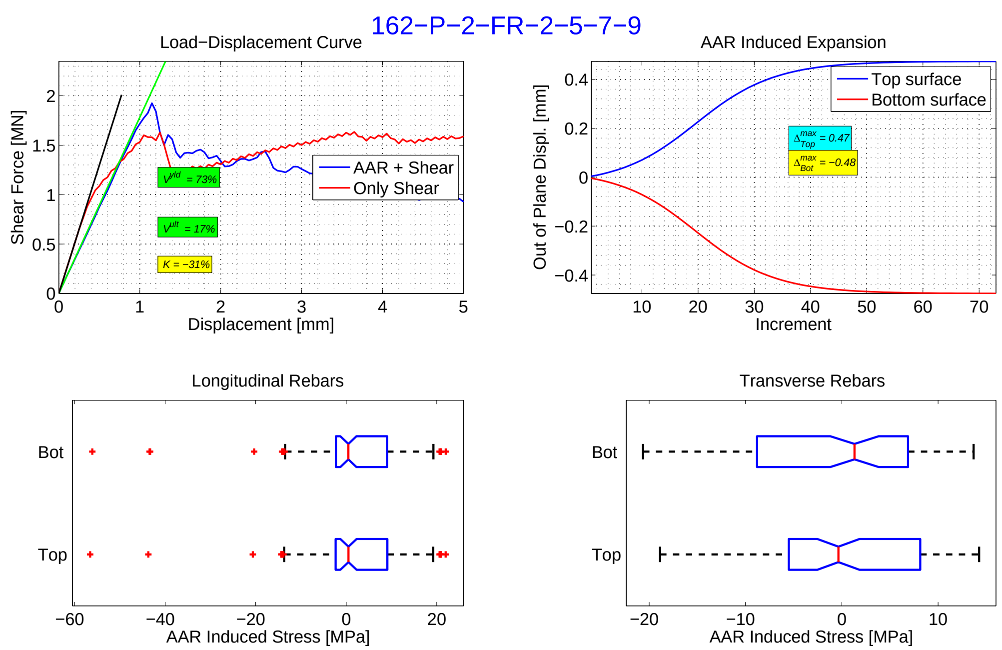

4.1.3.163 Analysis: 163-P-2-FR-2-5-9-7

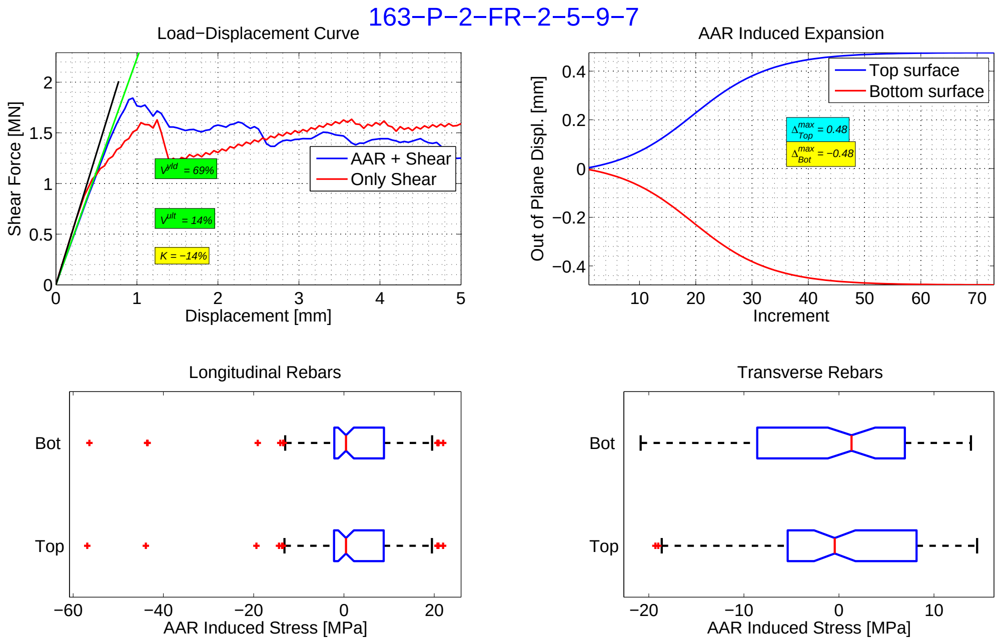

4.1.3.164 Analysis: 164-P-2-FR-2-5-9-9

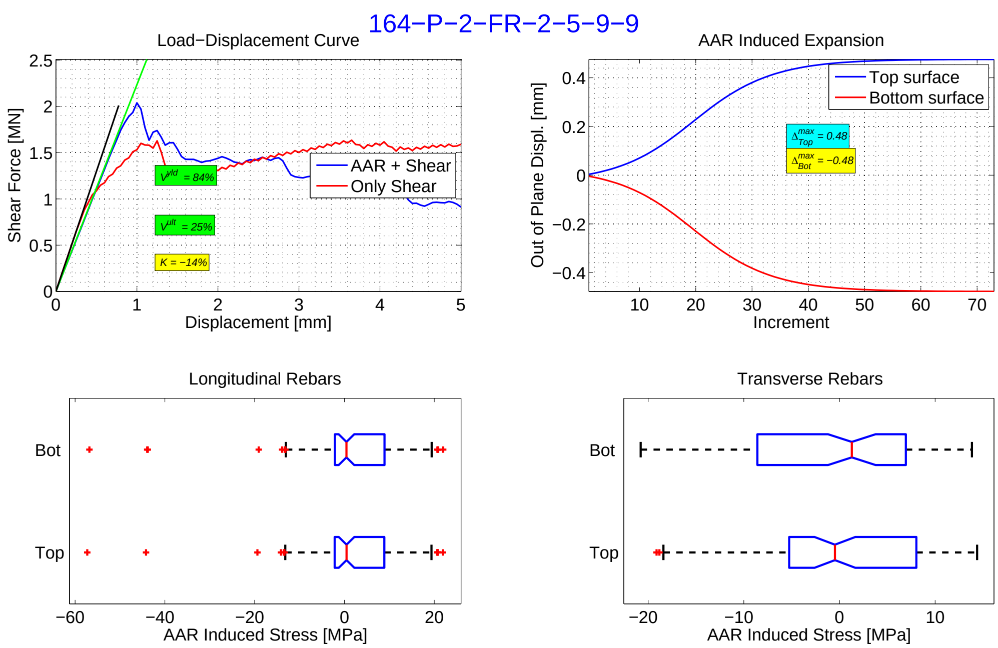

4.1.3.165 Analysis: 165-P-2-FR-2-10-7-7

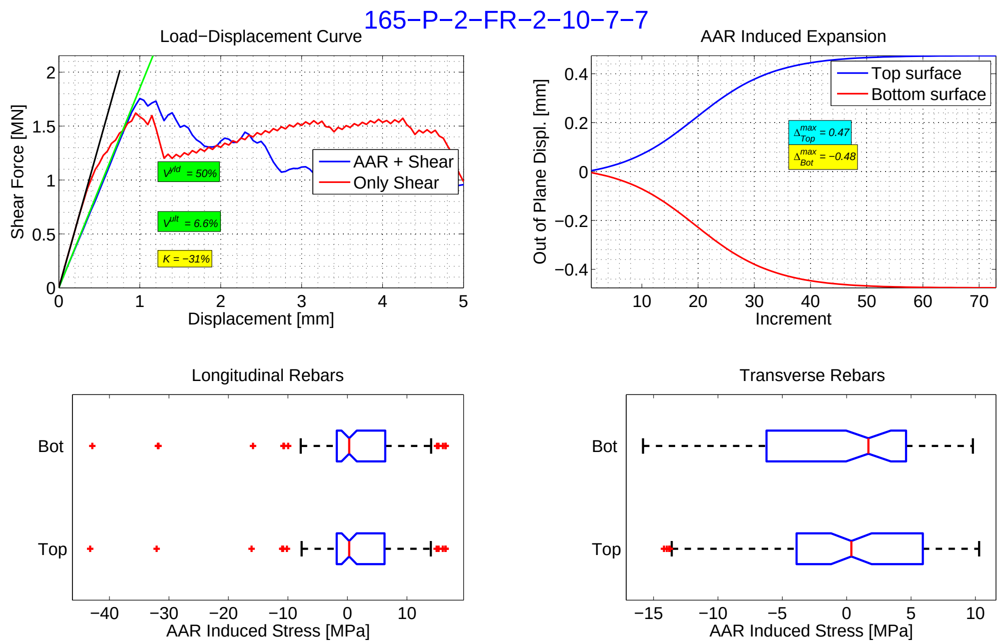

4.1.3.166 Analysis: 166-P-2-FR-2-10-7-9

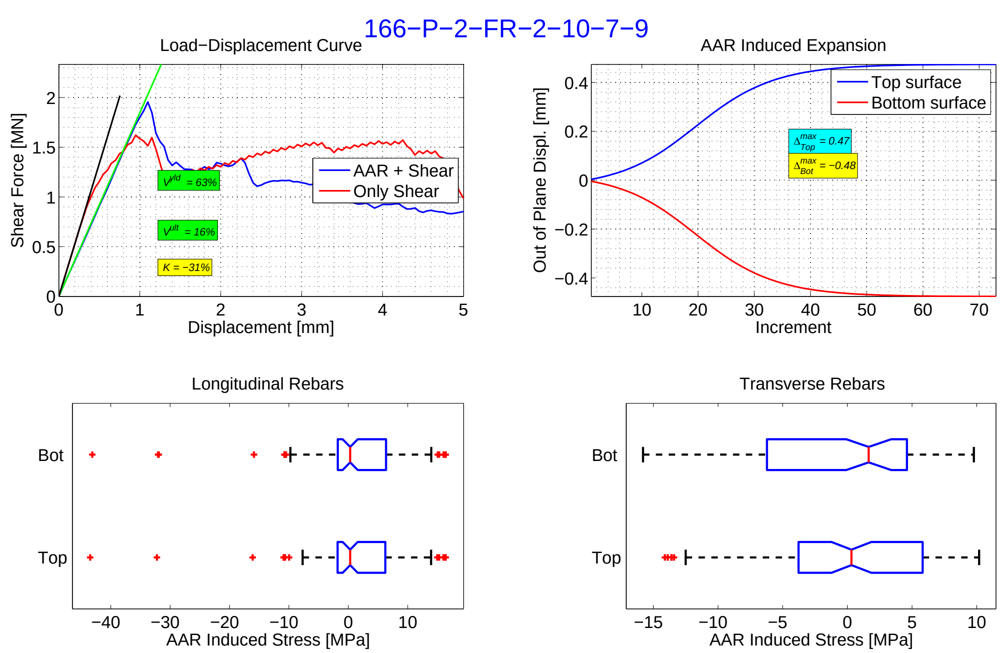

4.1.3.167 Analysis: 167-P-2-FR-2-10-9-7

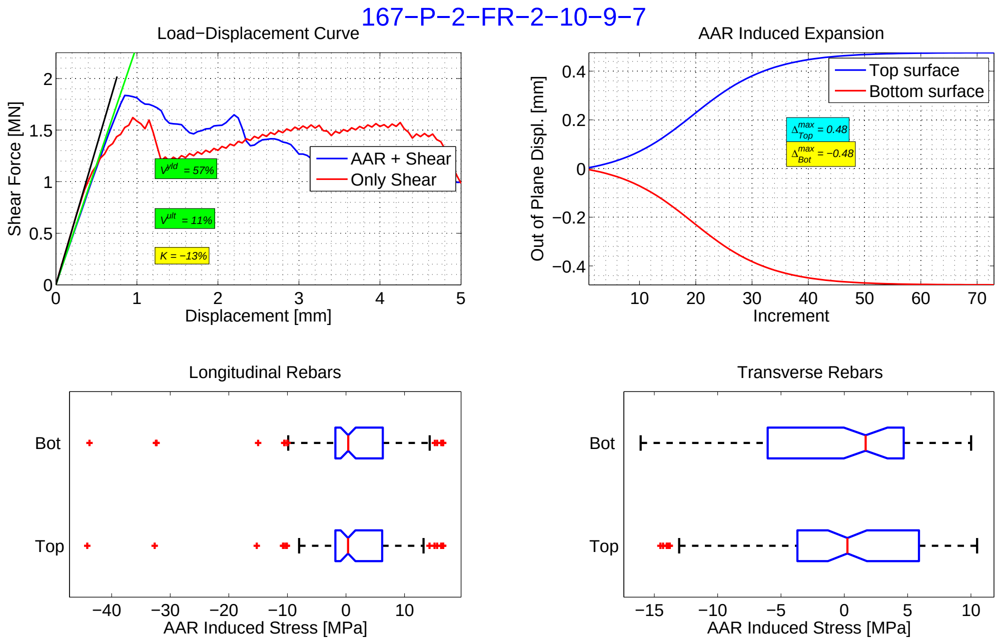

4.1.3.168 Analysis: 168-P-2-FR-2-10-9-9

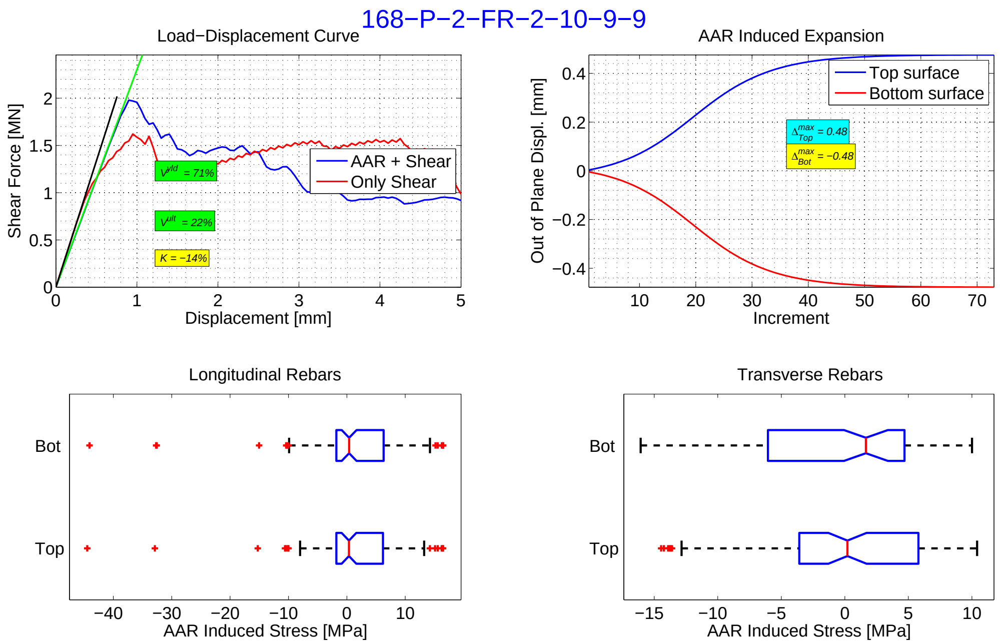

4.1.3.169 Analysis: 169-P-2-FR-3-2-7-7

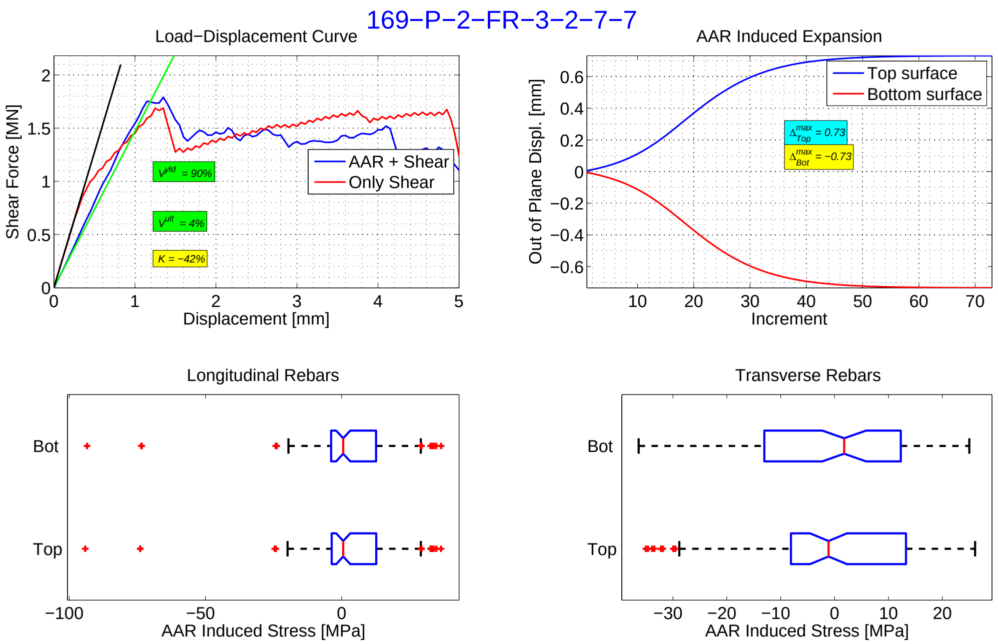

4.1.3.170 Analysis: 170-P-2-FR-3-2-7-9

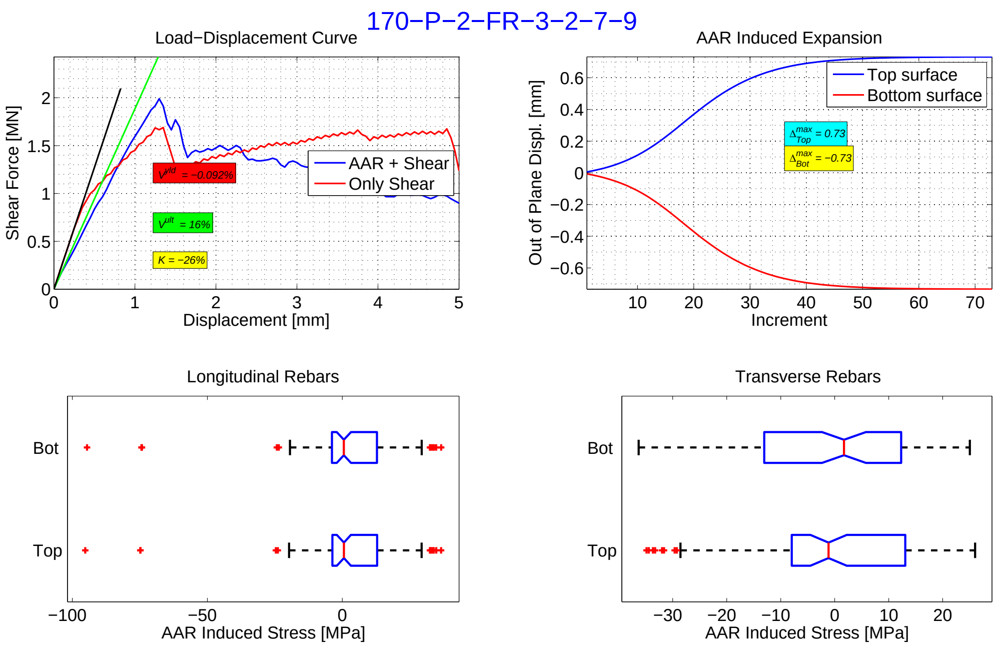

4.1.3.171 Analysis: 171-P-2-FR-3-2-9-7

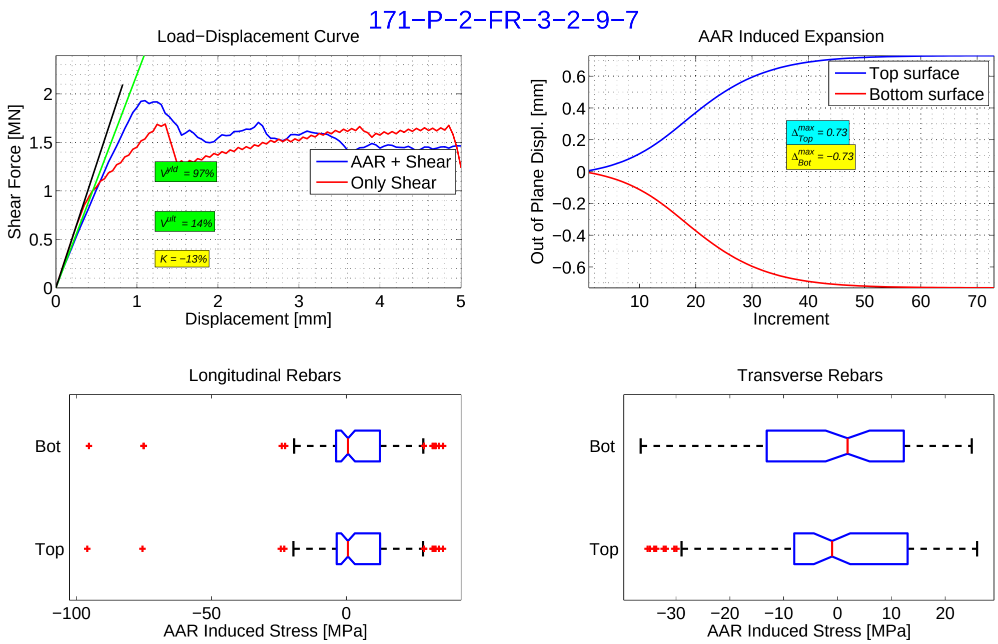

4.1.3.172 Analysis: 172-P-2-FR-3-2-9-9

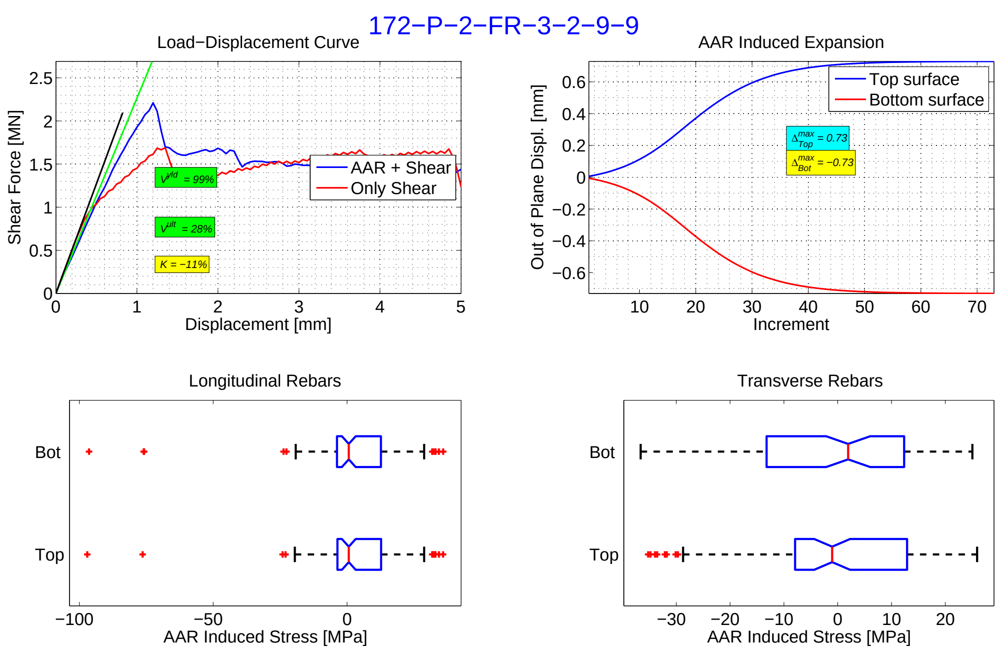

4.1.3.173 Analysis: 173-P-2-FR-3-5-7-7

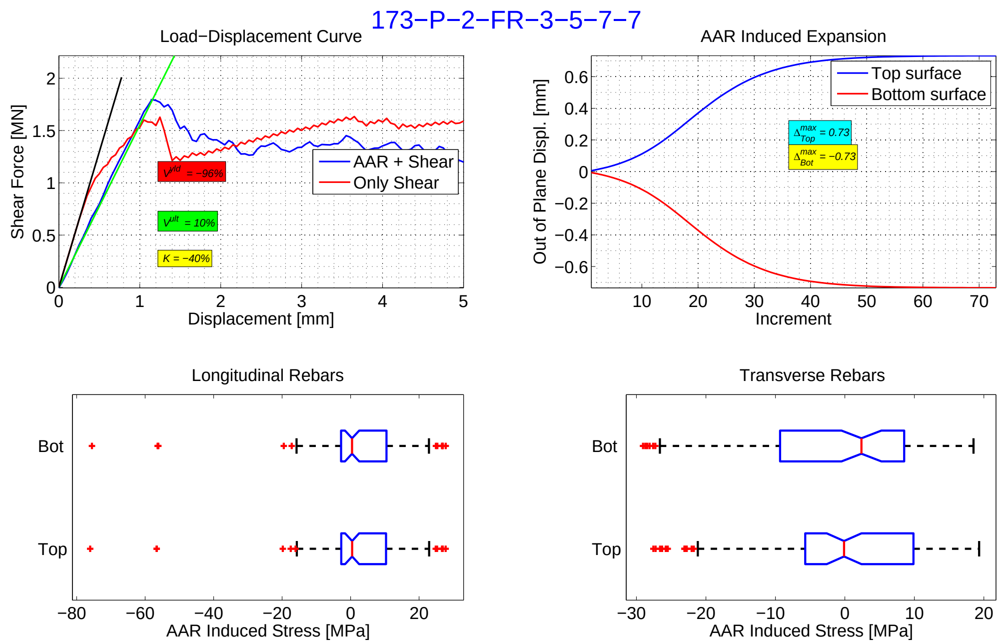

4.1.3.174 Analysis: 174-P-2-FR-3-5-7-9

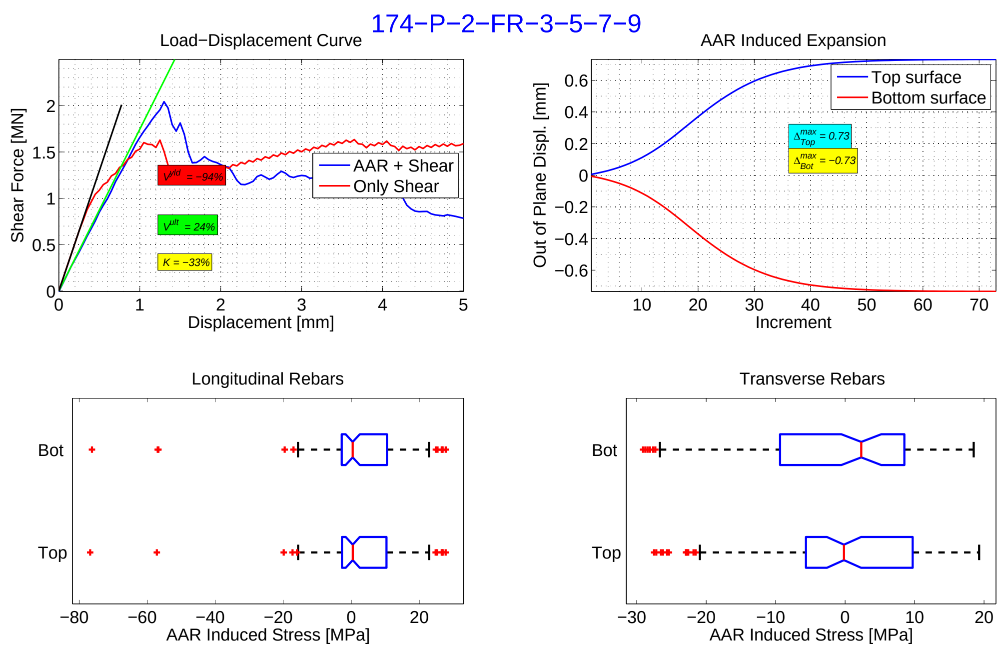

4.1.3.175 Analysis: 175-P-2-FR-3-5-9-7

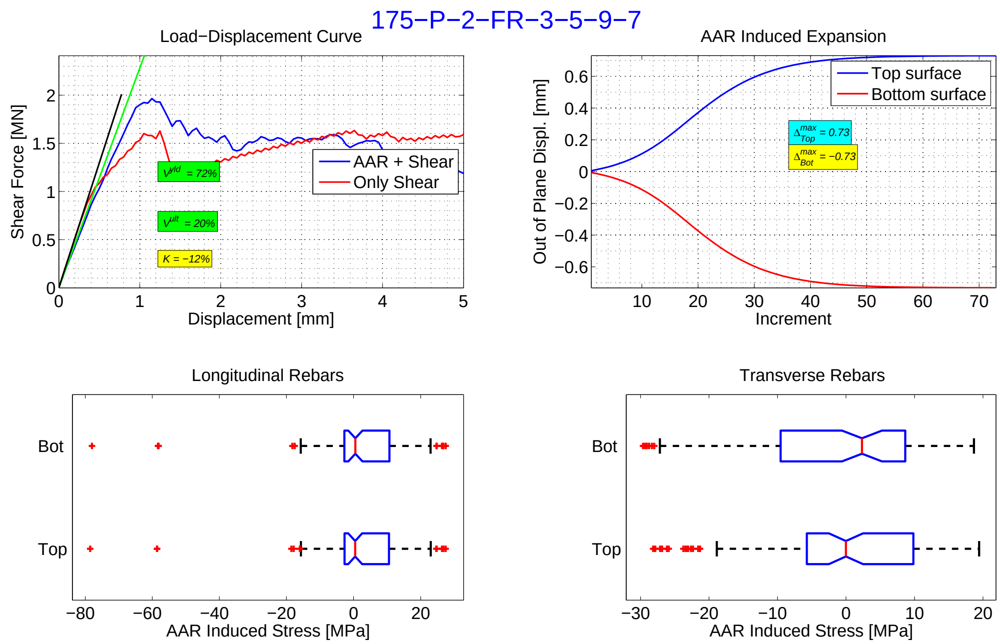

4.1.3.176 Analysis: 176-P-2-FR-3-5-9-9

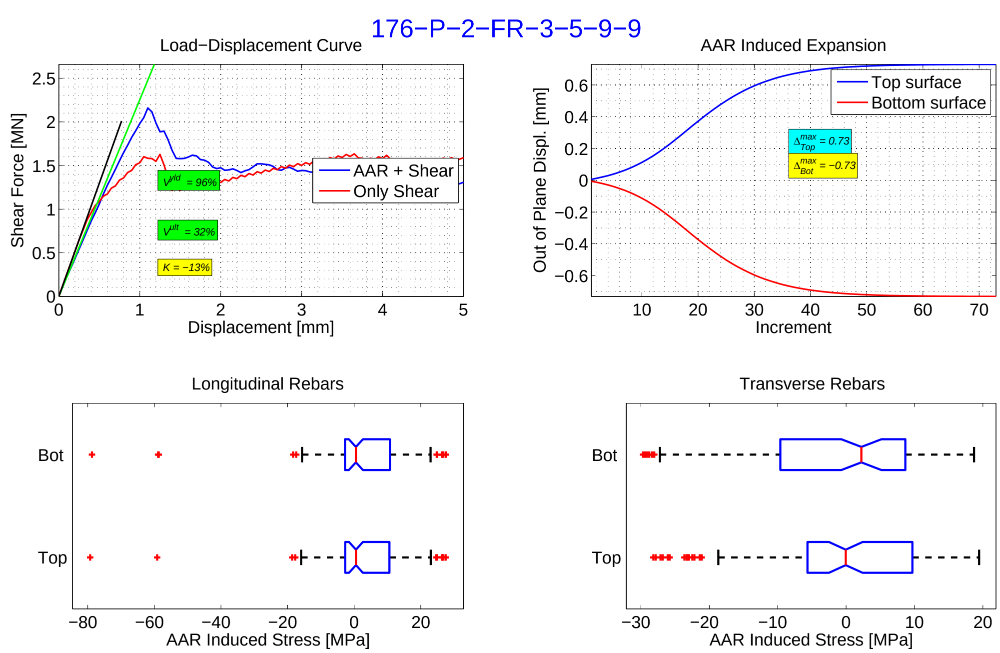

4.1.3.177 Analysis: 177-P-2-FR-3-10-7-7

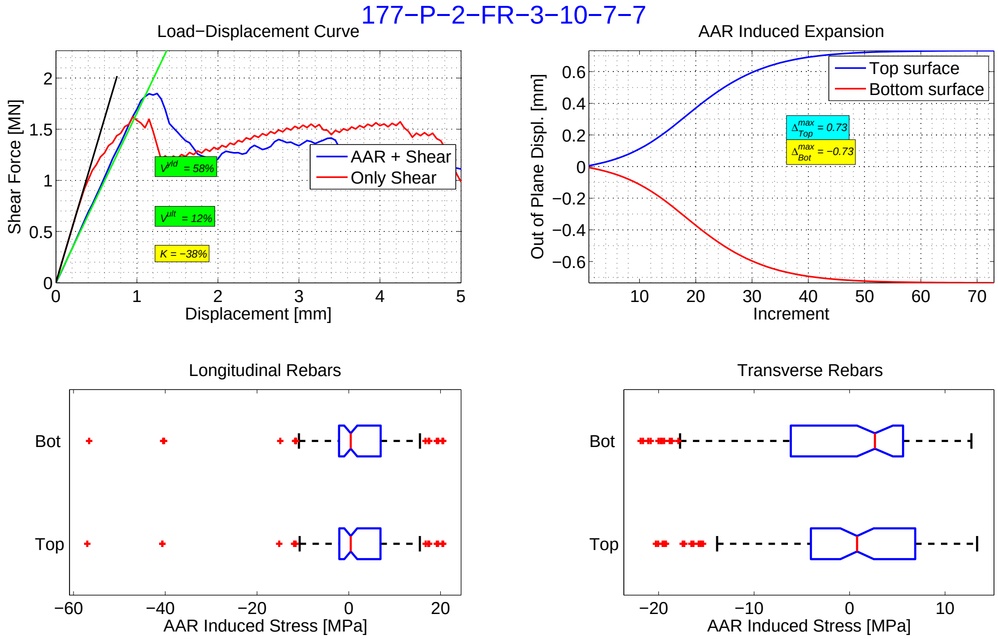

4.1.3.178 Analysis: 178-P-2-FR-3-10-7-9

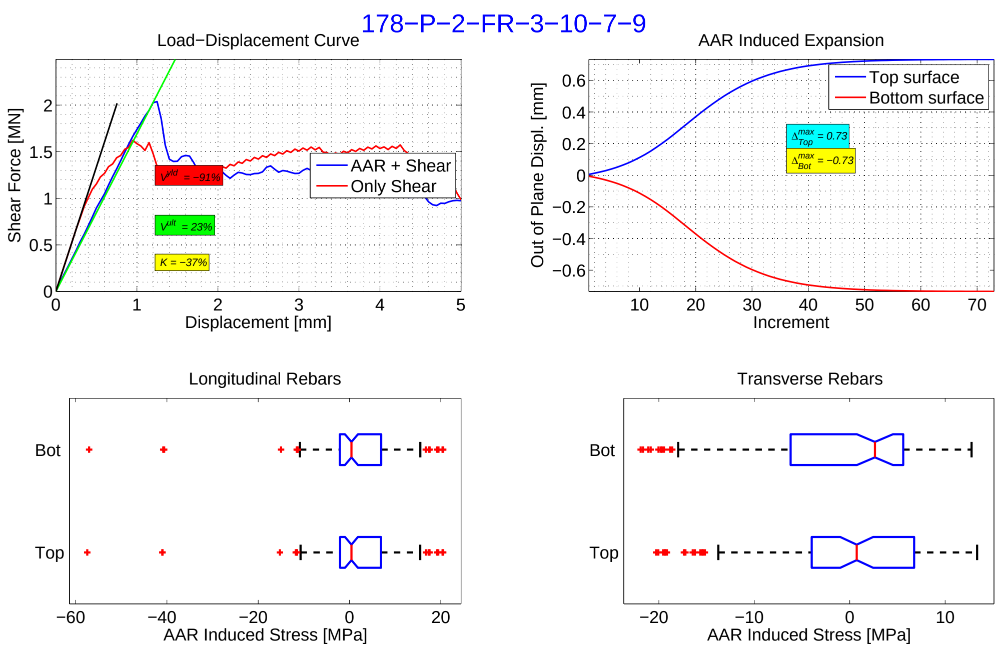

4.1.3.179 Analysis: 179-P-2-FR-3-10-9-7

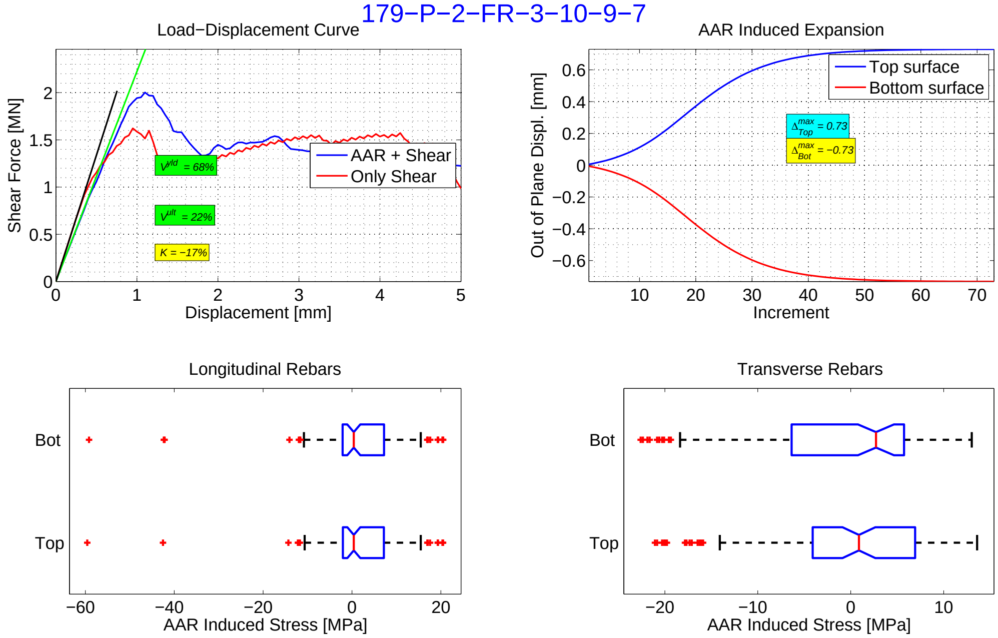

4.1.3.180 Analysis: 180-P-2-FR-3-10-9-9

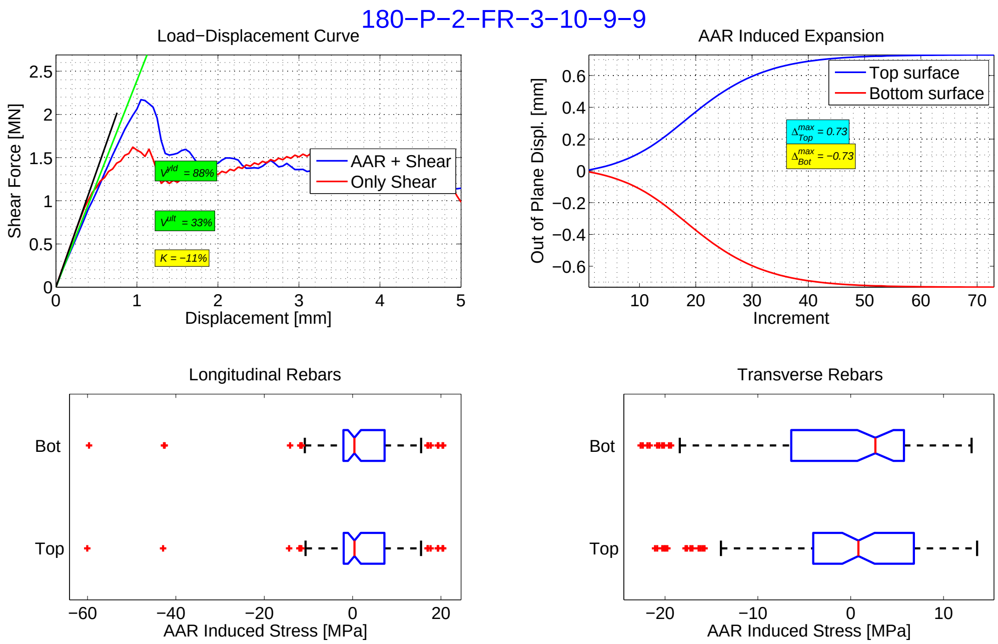

4.1.3.181 Analysis: 181-P-4-FR-1-2-7-7

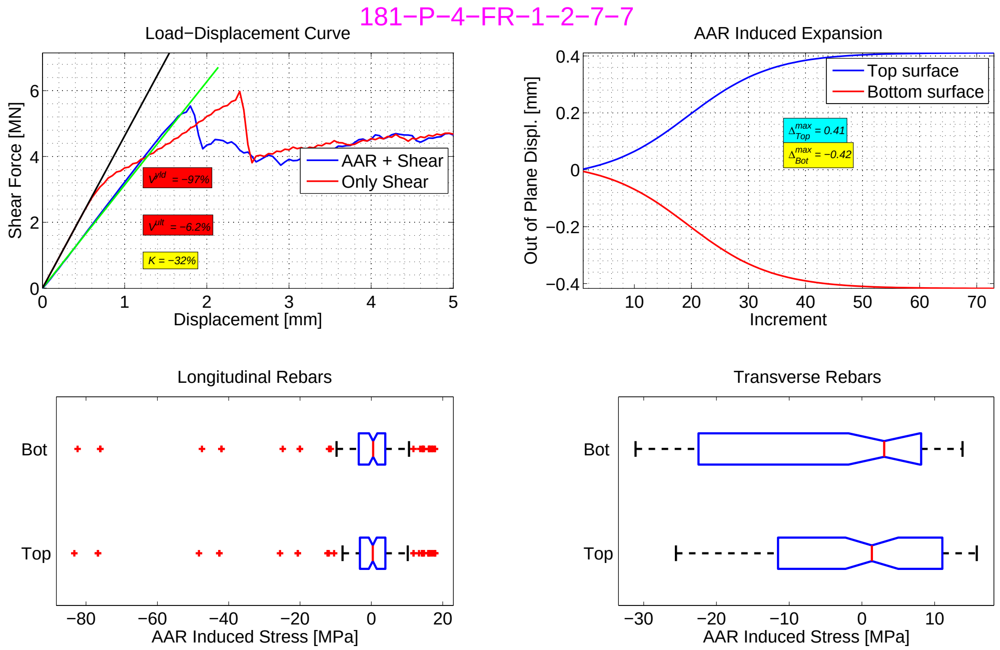

4.1.3.182 Analysis: 182-P-4-FR-1-2-7-9

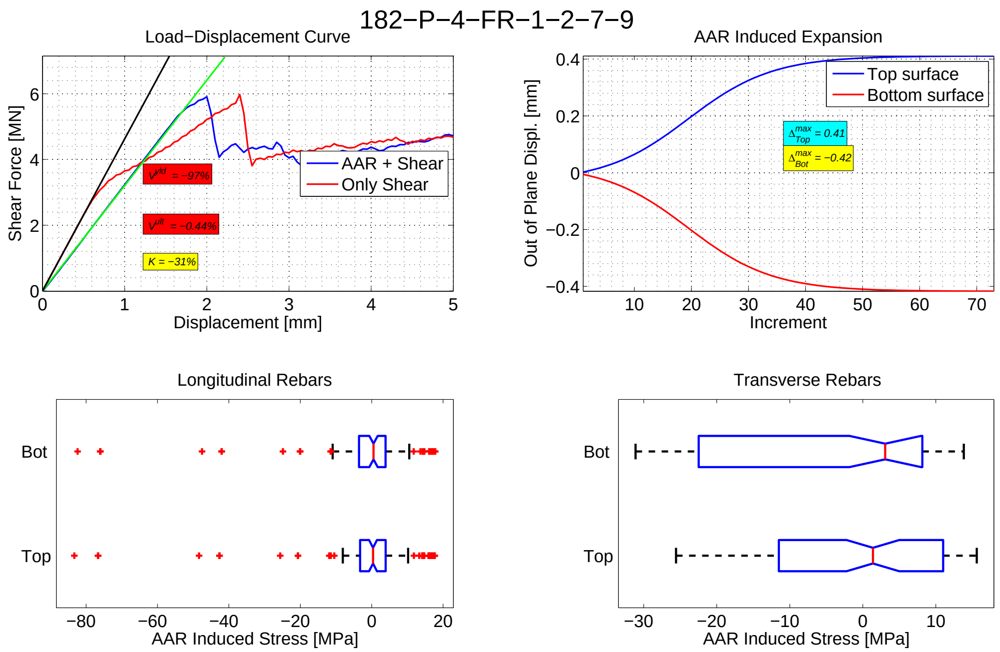

4.1.3.183 Analysis: 183-P-4-FR-1-2-9-7

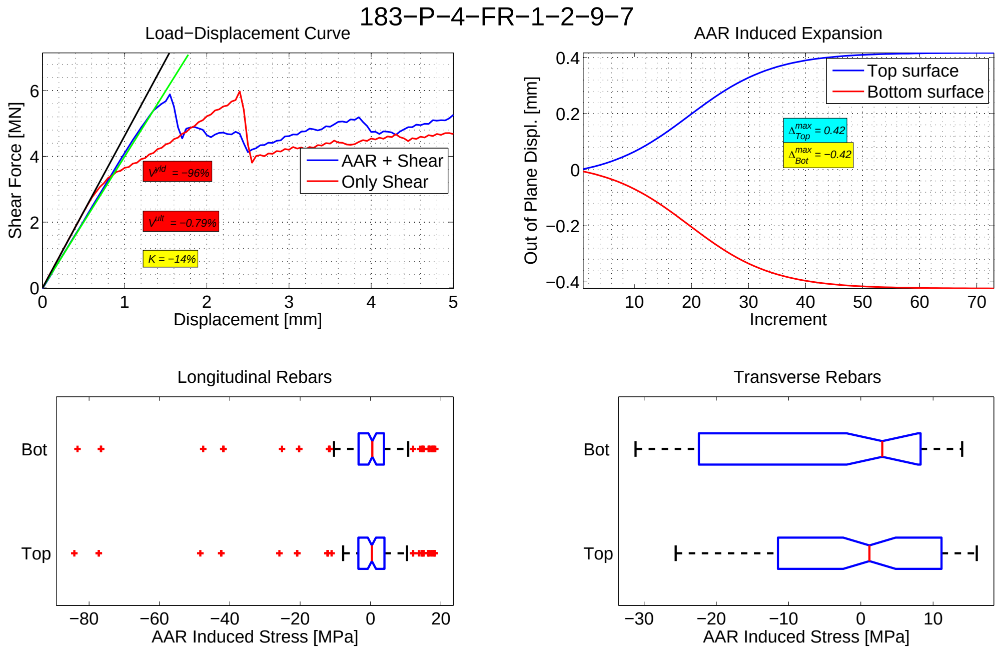

4.1.3.184 Analysis: 184-P-4-FR-1-2-9-9

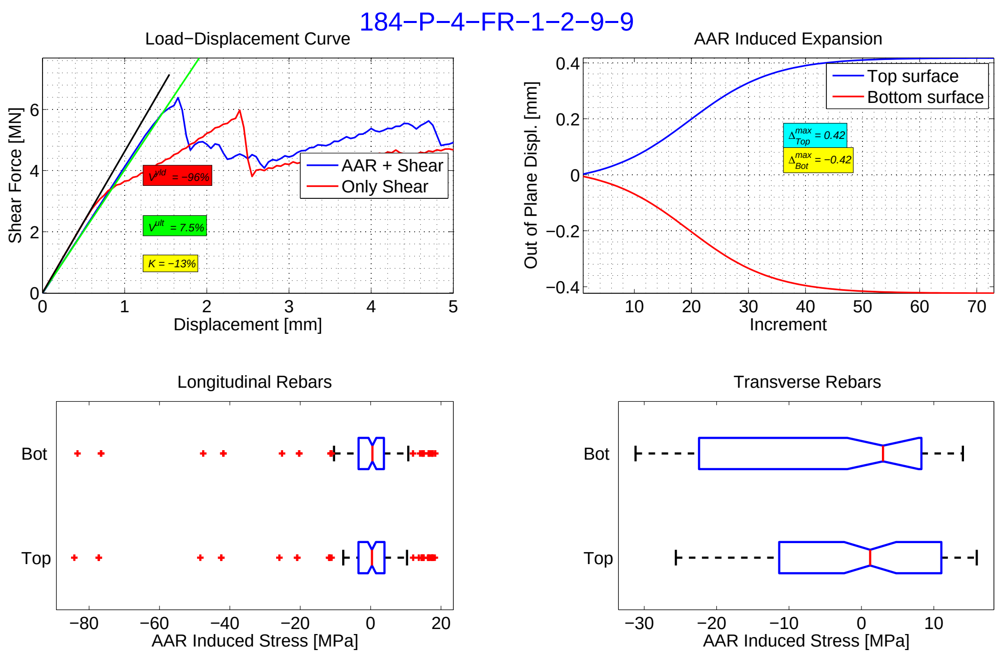

4.1.3.185 Analysis: 185-P-4-FR-1-5-7-7

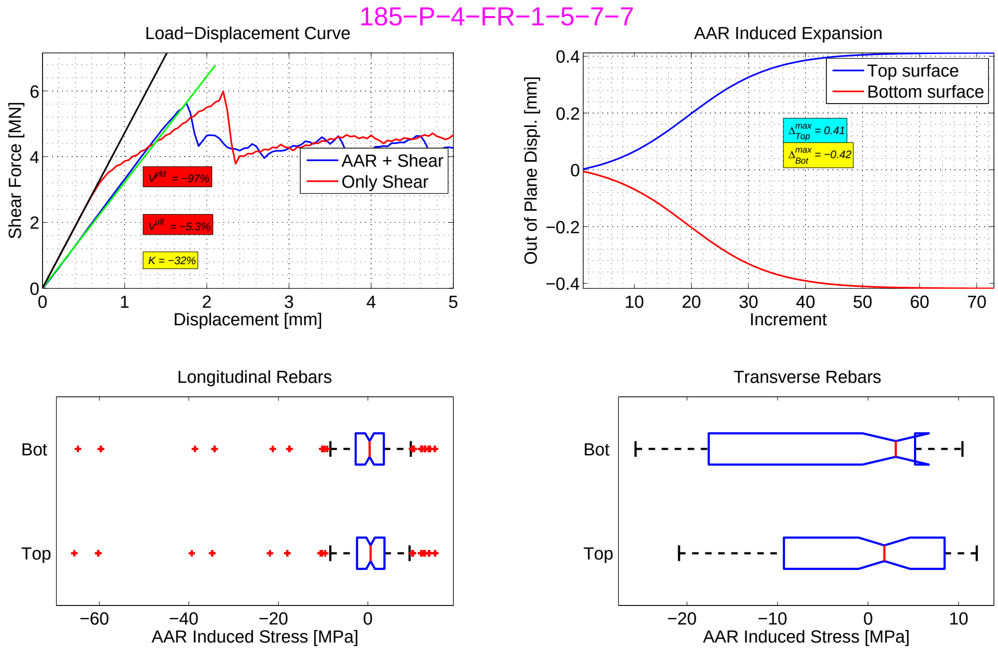

4.1.3.186 Analysis: 186-P-4-FR-1-5-7-9

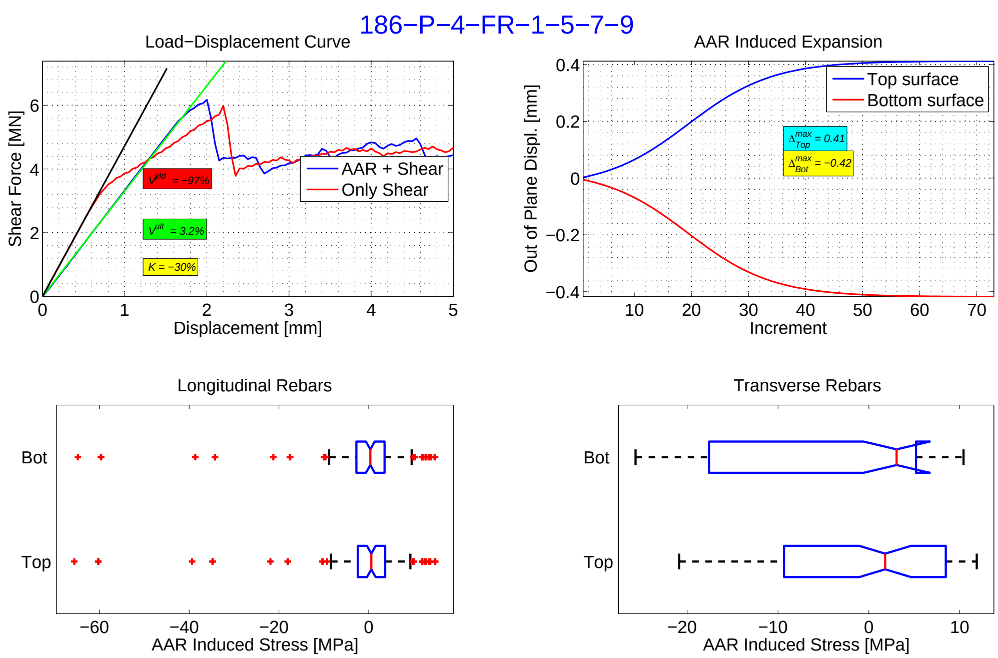

4.1.3.187 Analysis: 187-P-4-FR-1-5-9-7

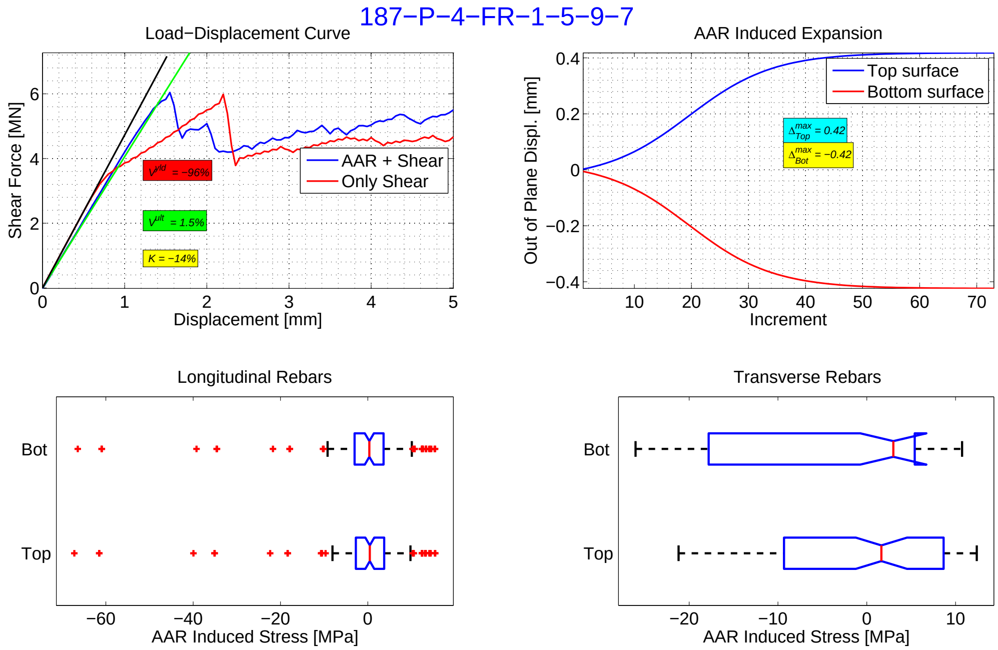

4.1.3.188 Analysis: 188-P-4-FR-1-5-9-9

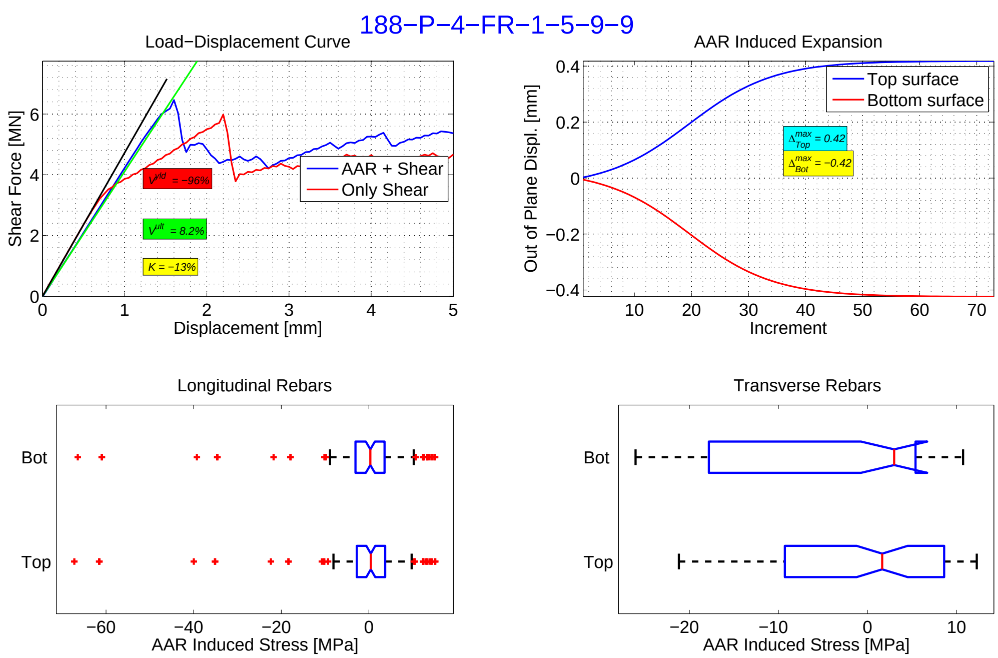

4.1.3.189 Analysis: 189-P-4-FR-1-10-7-7

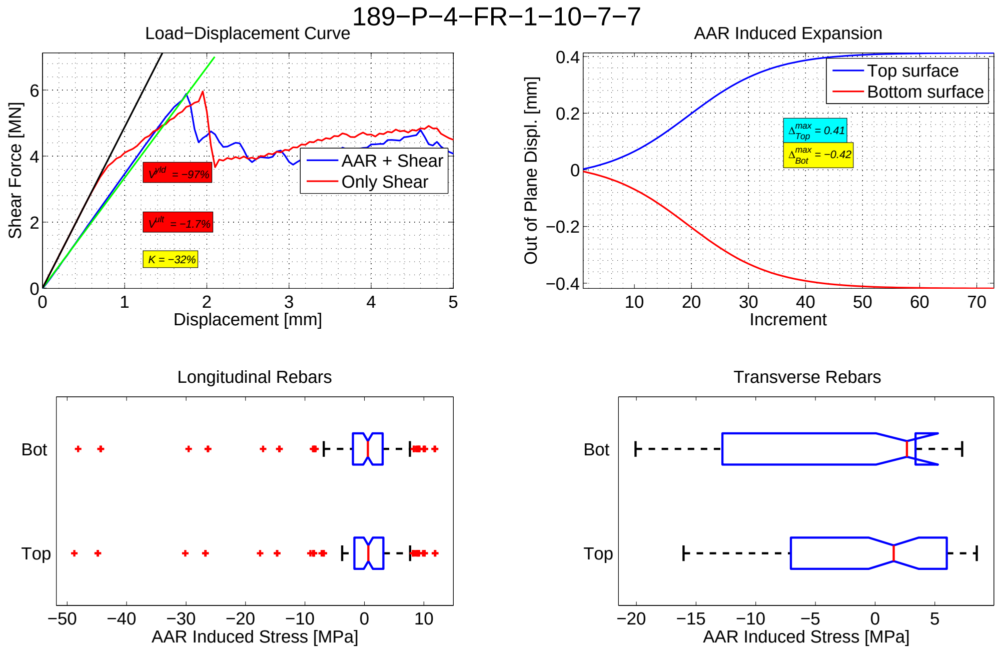

4.1.3.190 Analysis: 190-P-4-FR-1-10-7-9

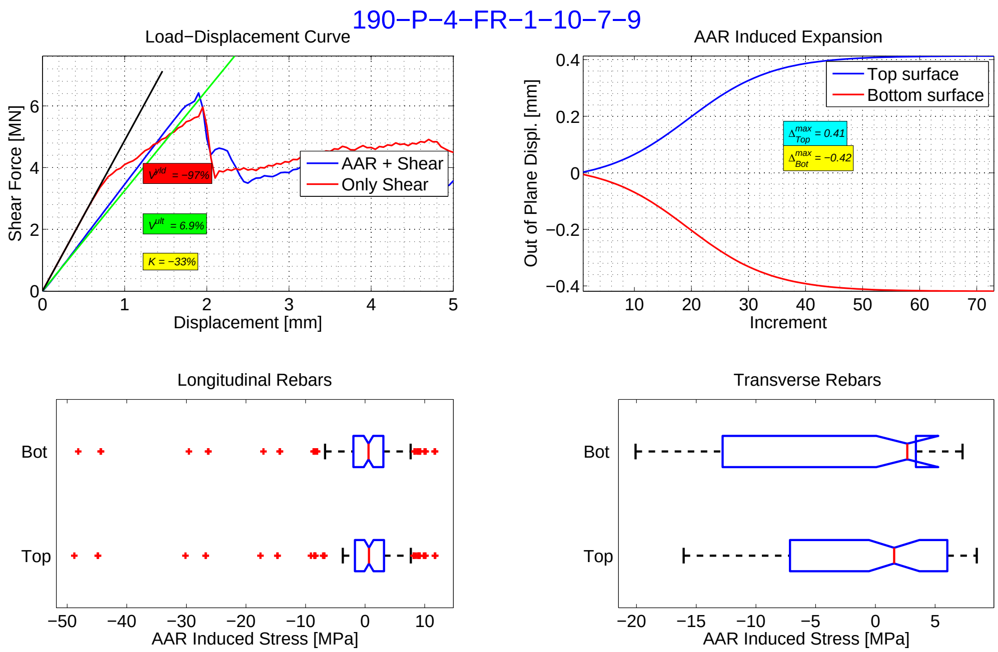

4.1.3.191 Analysis: 191-P-4-FR-1-10-9-7

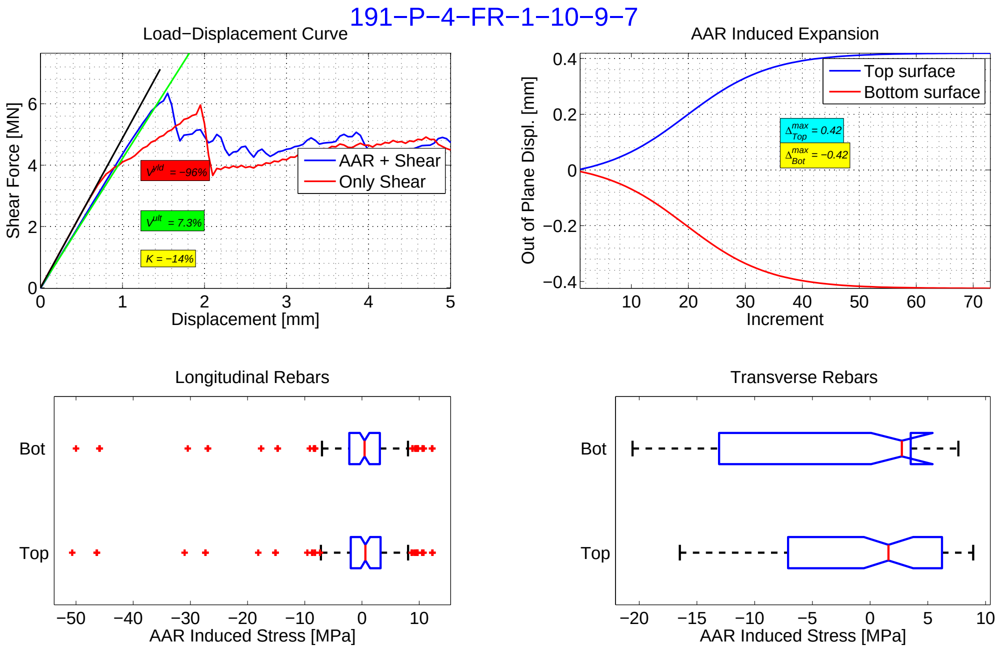

4.1.3.192 Analysis: 192-P-4-FR-1-10-9-9

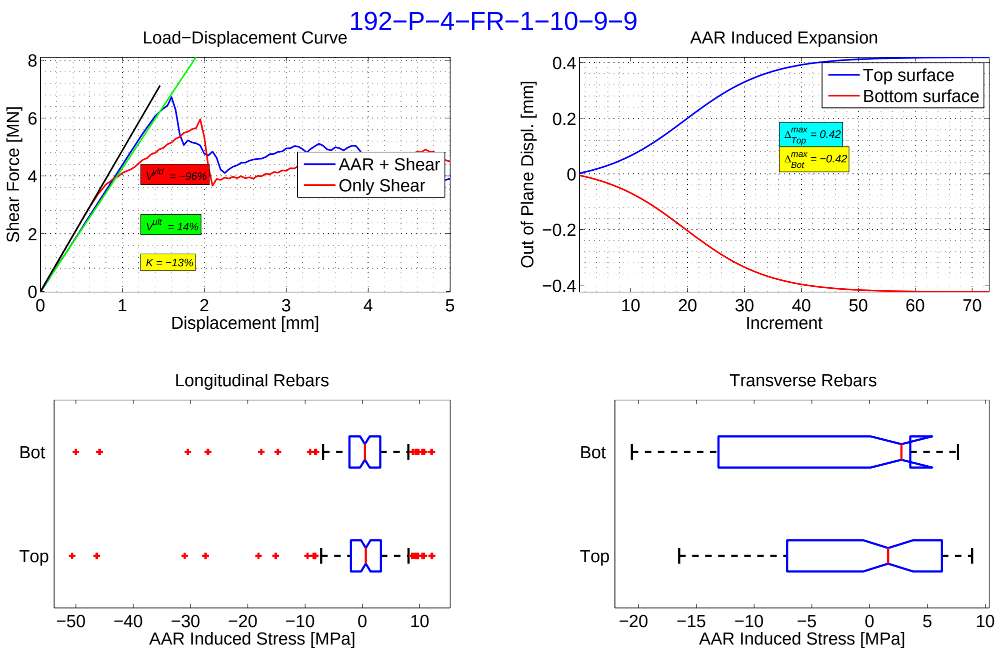

4.1.3.193 Analysis: 193-P-4-FR-2-2-7-7

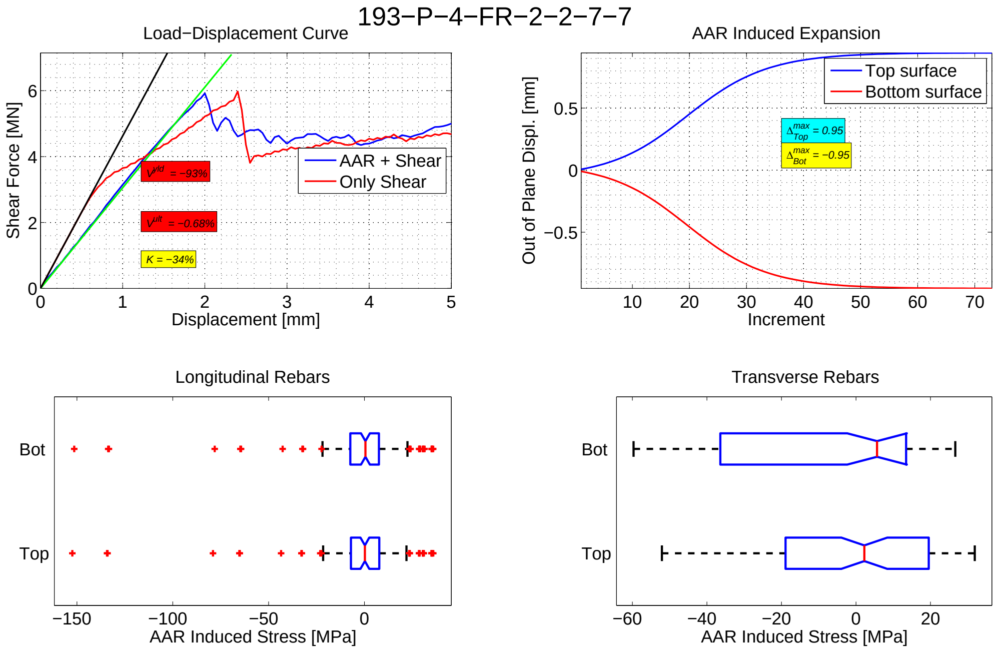

4.1.3.194 Analysis: 194-P-4-FR-2-2-7-9

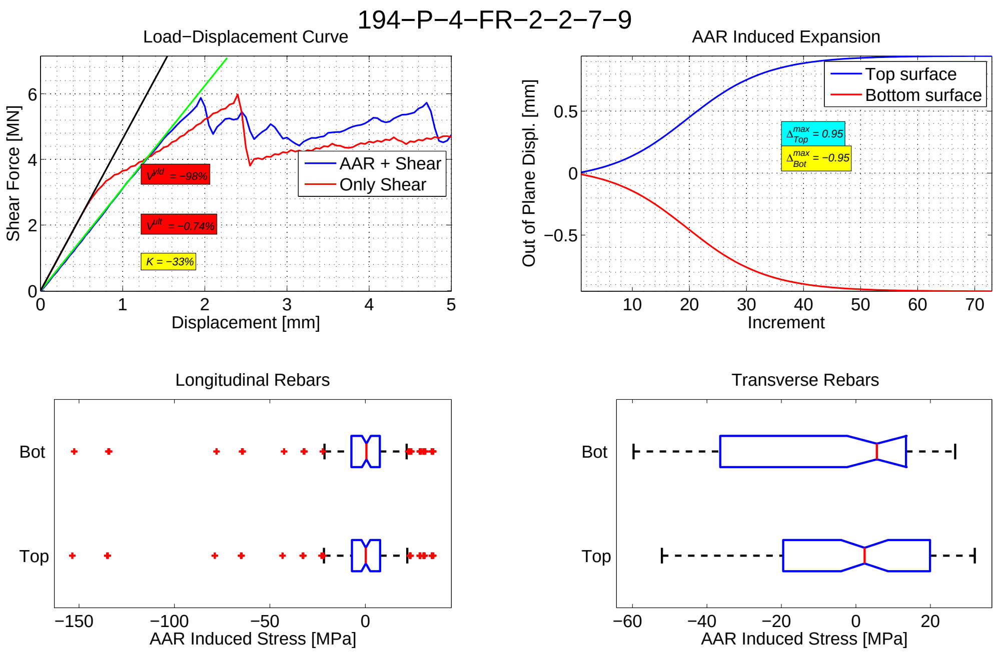

4.1.3.195 Analysis: 195-P-4-FR-2-2-9-7

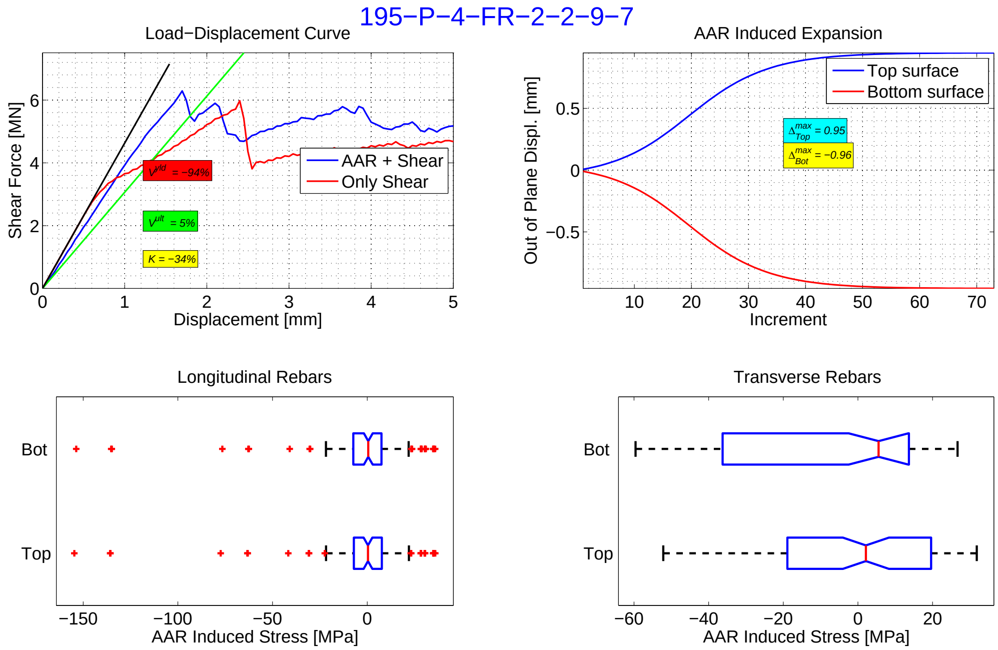

4.1.3.196 Analysis: 196-P-4-FR-2-2-9-9

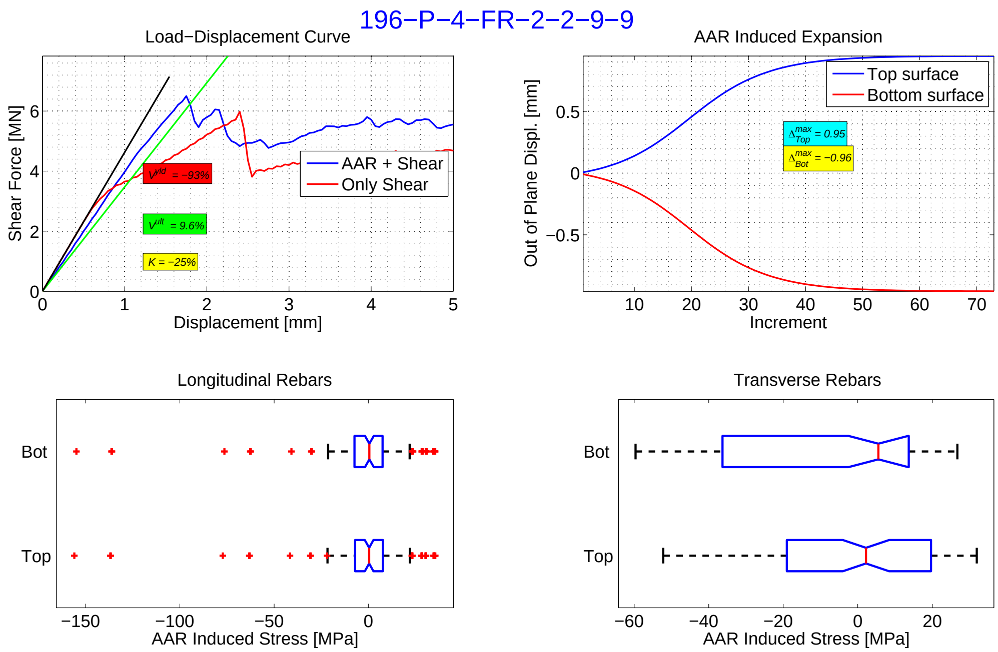

4.1.3.197 Analysis: 197-P-4-FR-2-5-7-7

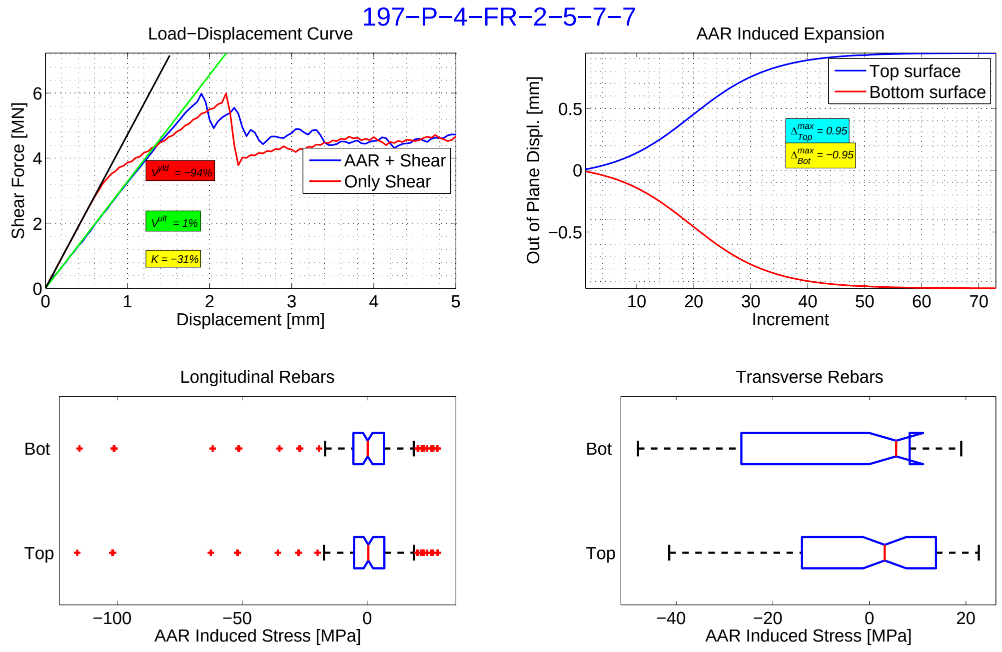

4.1.3.198 Analysis: 198-P-4-FR-2-5-7-9

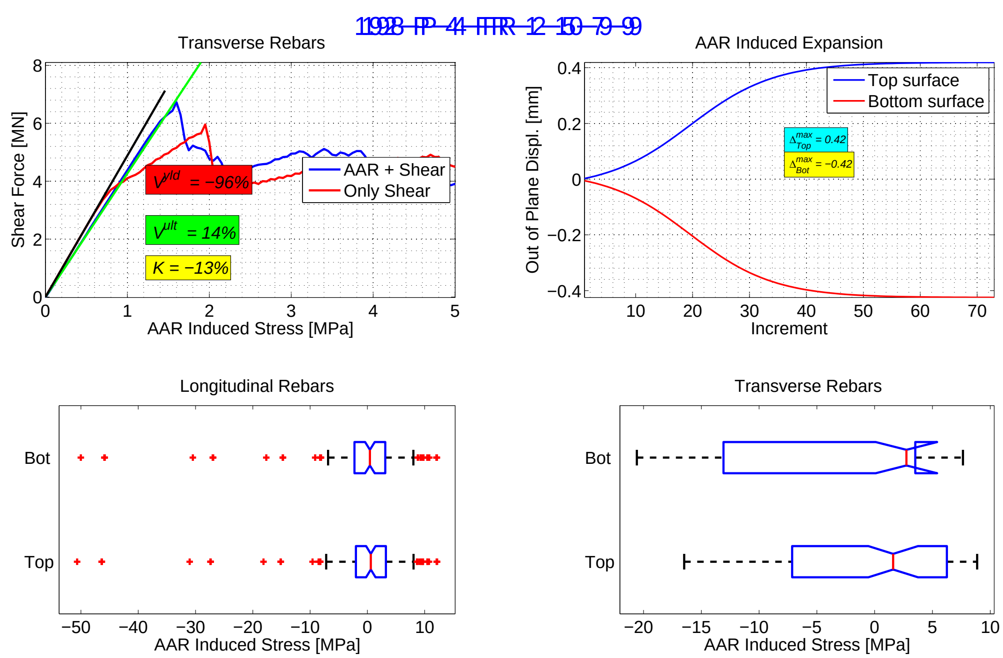

4.1.3.199 Analysis: 199-P-4-FR-2-5-9-7

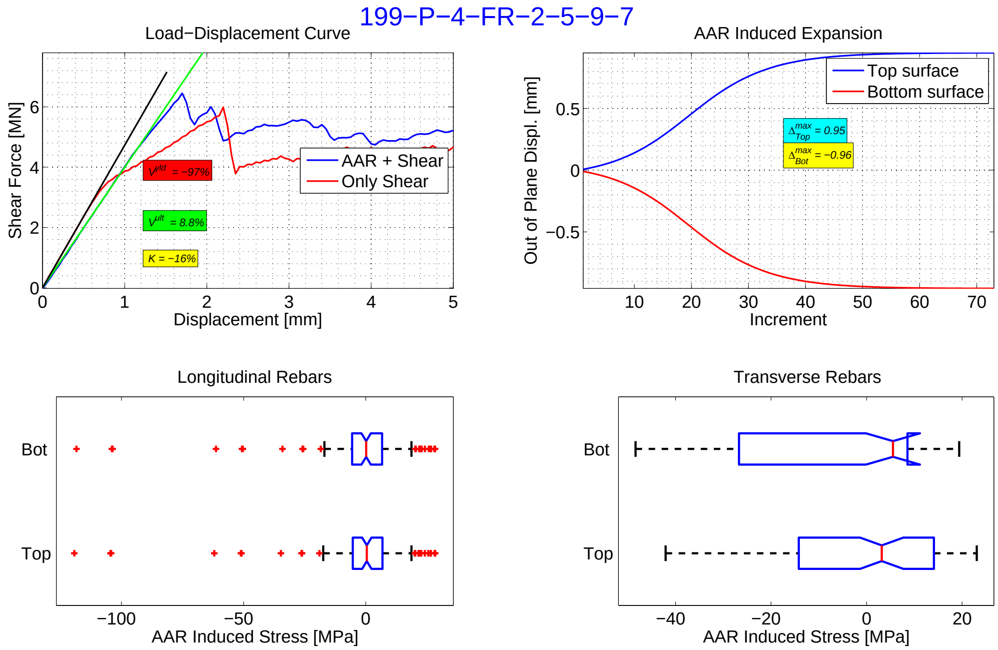

4.1.3.200 Analysis: 200-P-4-FR-2-5-9-9

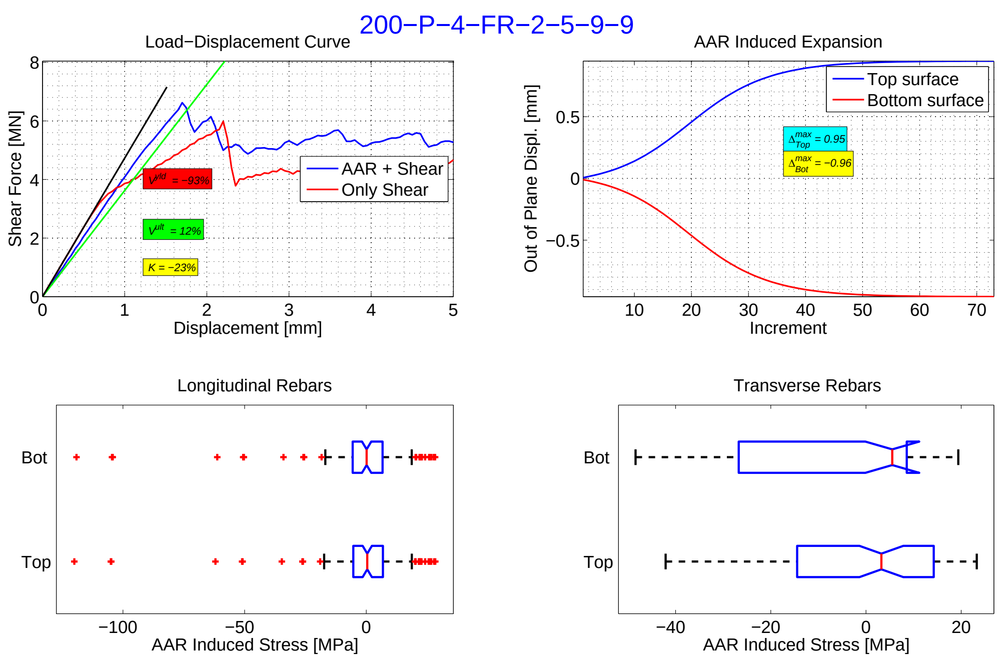

4.1.3.201 Analysis: 201-P-4-FR-2-10-7-7

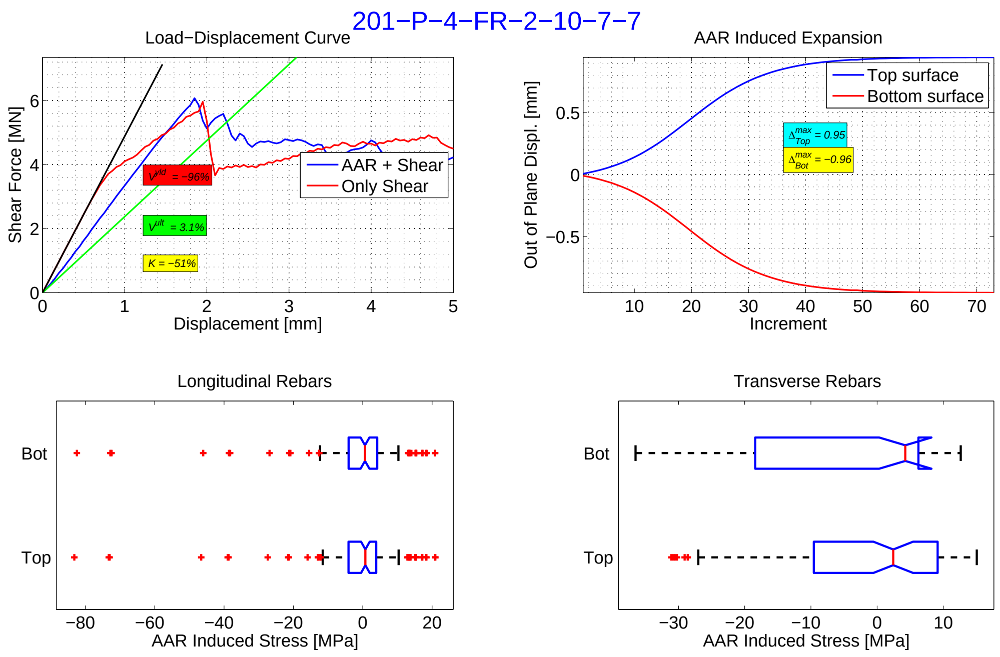

4.1.3.202 Analysis: 202-P-4-FR-2-10-7-9

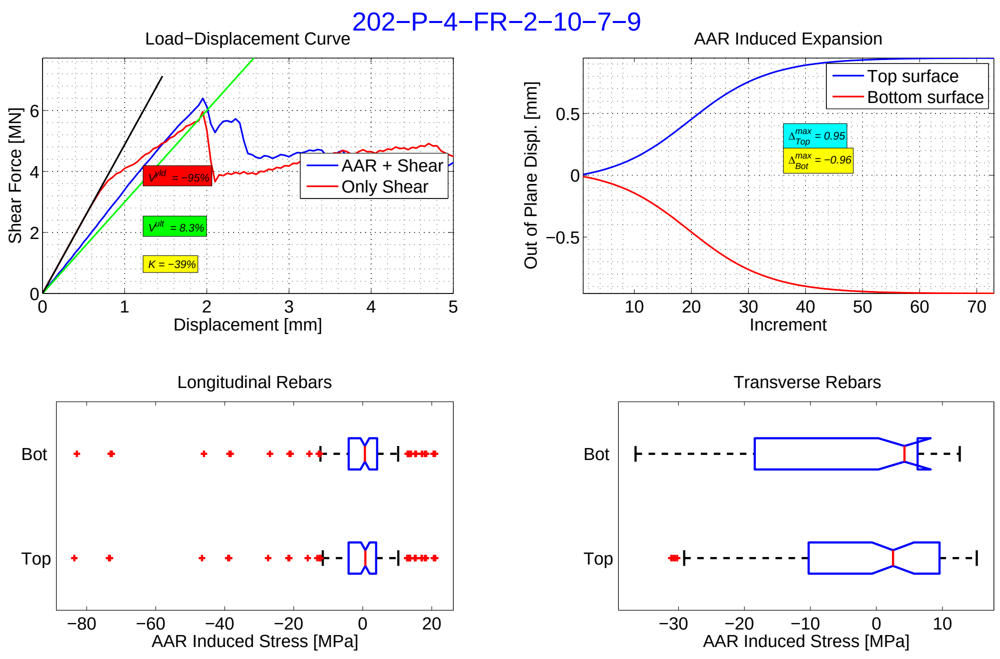

4.1.3.203 Analysis: 203-P-4-FR-2-10-9-7

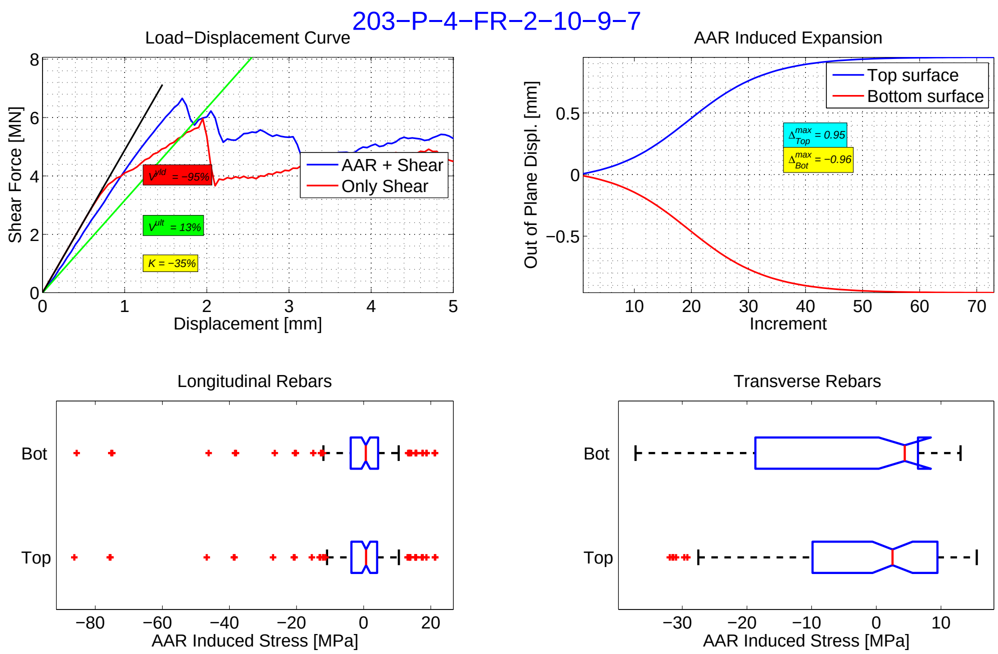

4.1.3.204 Analysis: 204-P-4-FR-2-10-9-9

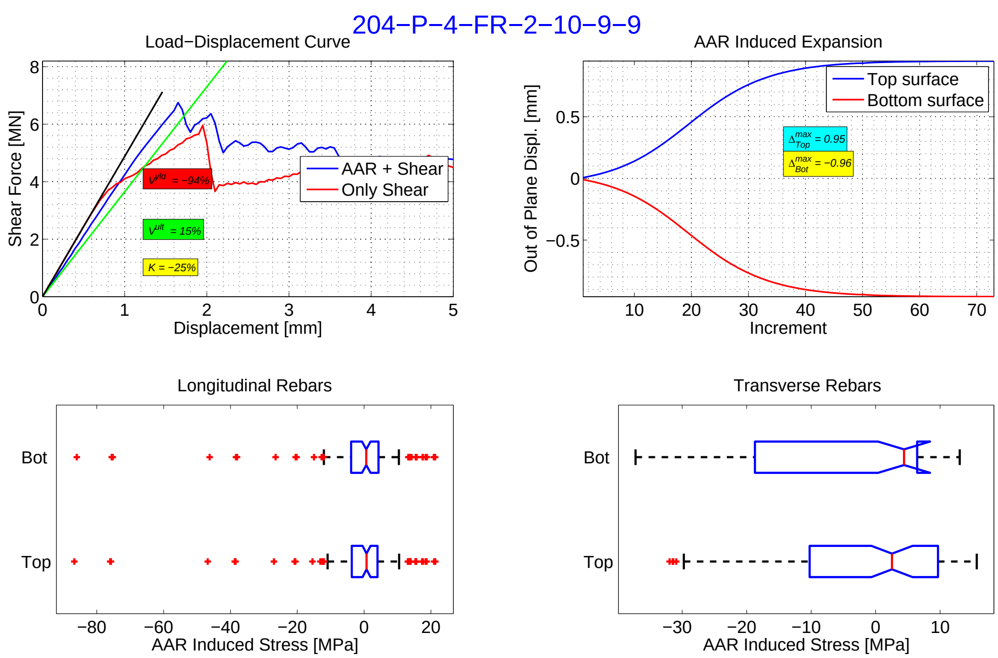

4.1.3.205 Analysis: 205-P-4-FR-3-2-7-7

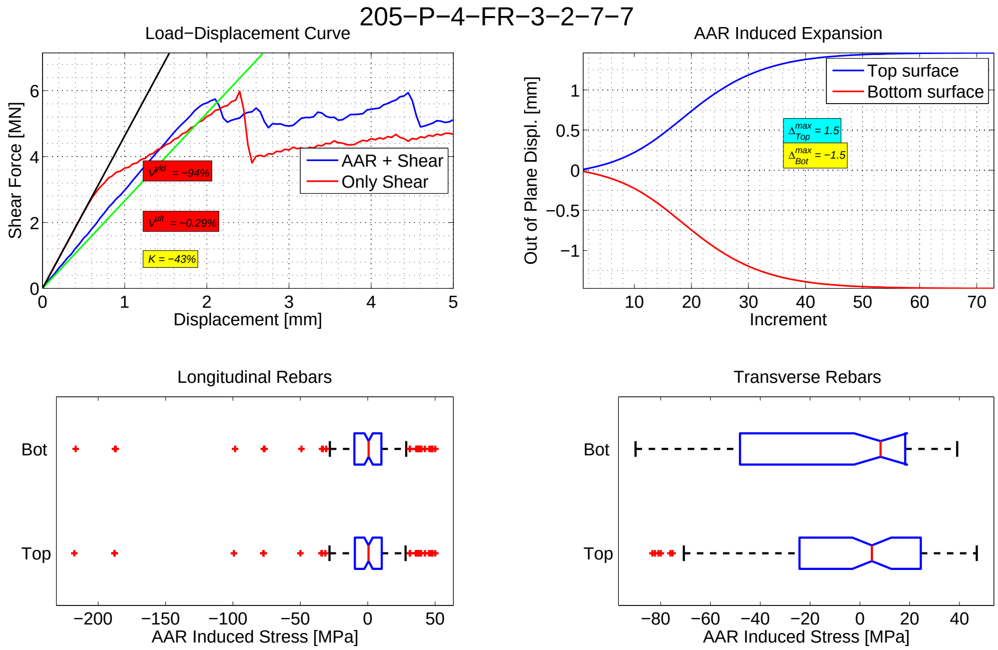

4.1.3.206 Analysis: 206-P-4-FR-3-2-7-9

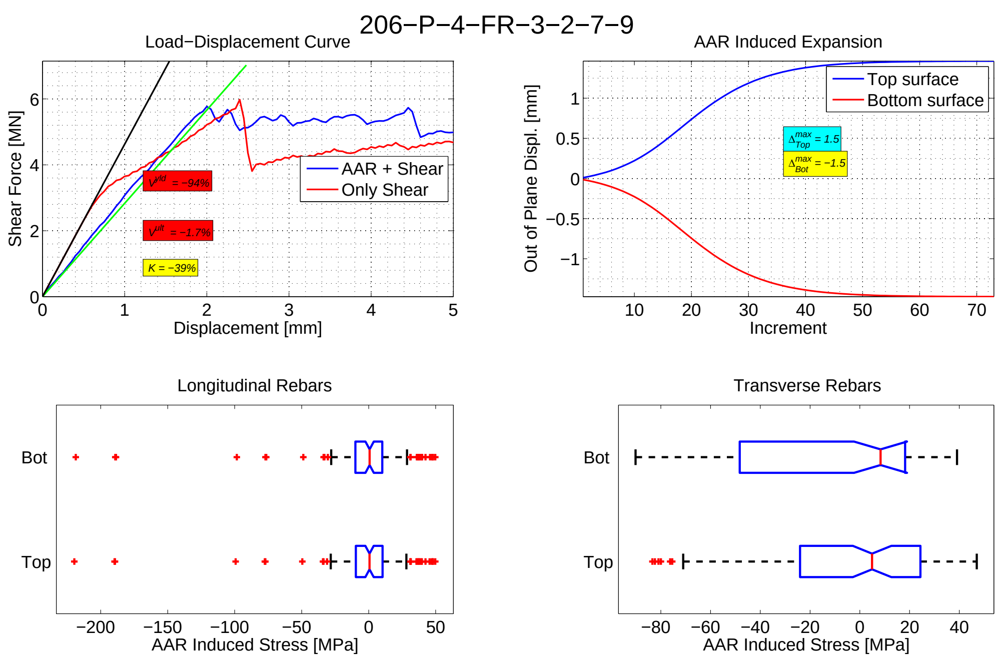

4.1.3.207 Analysis: 207-P-4-FR-3-2-9-7

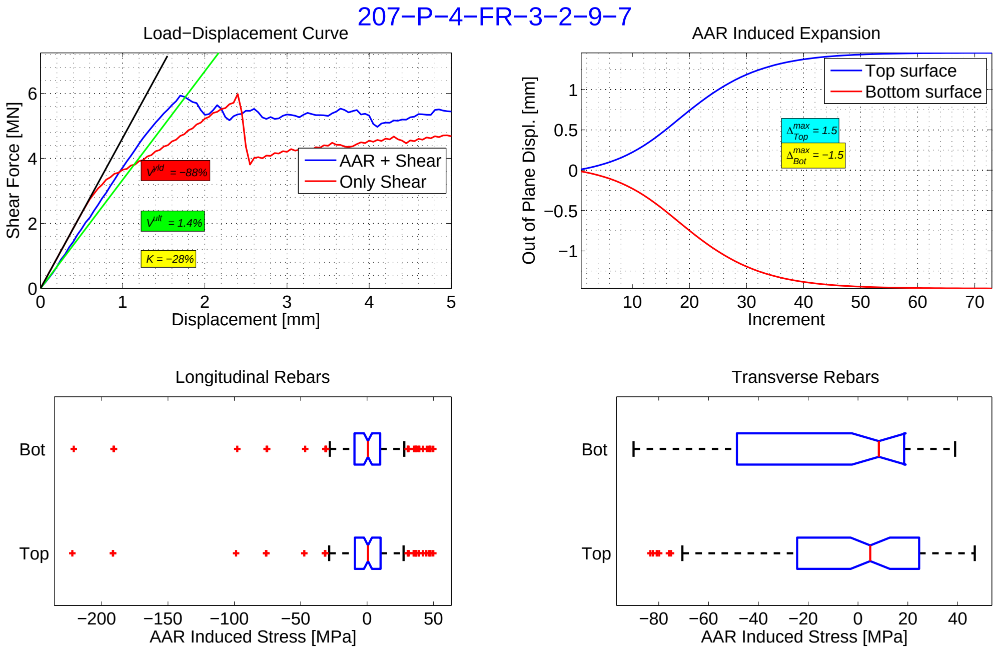

4.1.3.208 Analysis: 208-P-4-FR-3-2-9-9

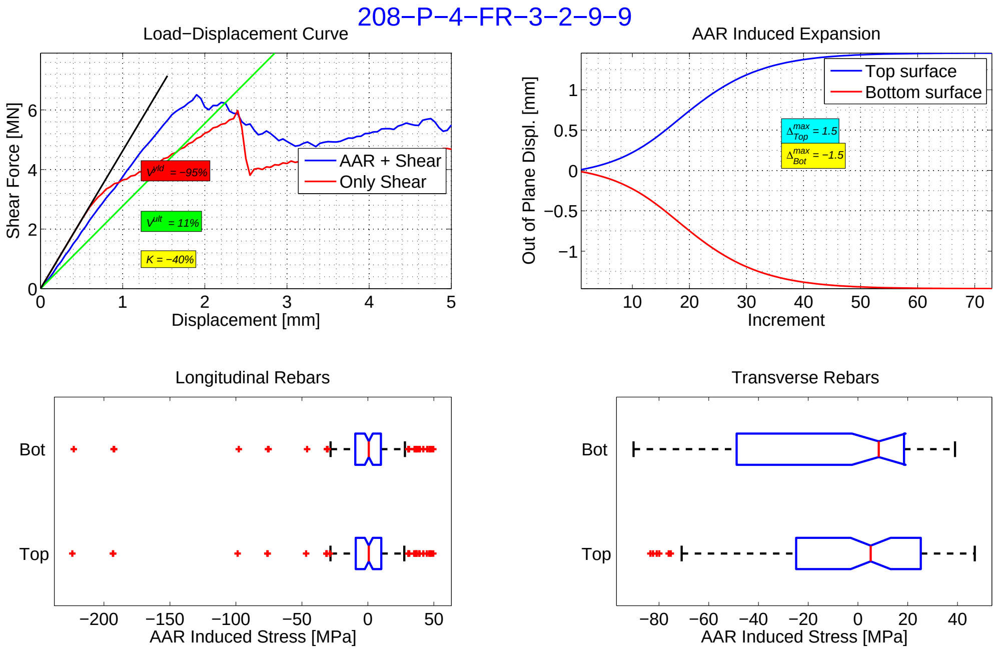

4.1.3.209 Analysis: 209-P-4-FR-3-5-7-7

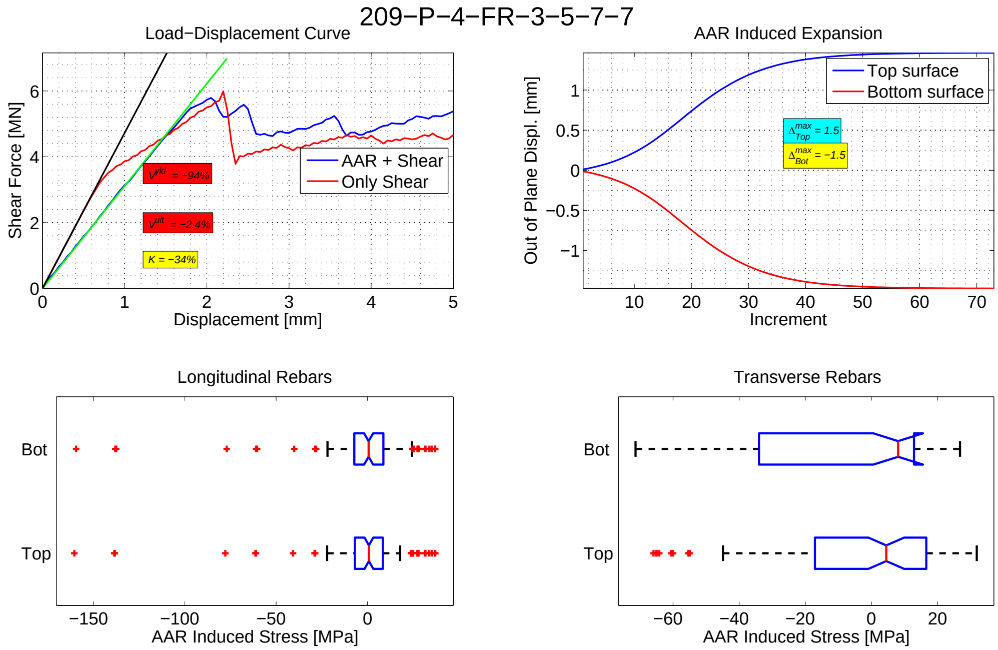

4.1.3.210 Analysis: 210-P-4-FR-3-5-7-9

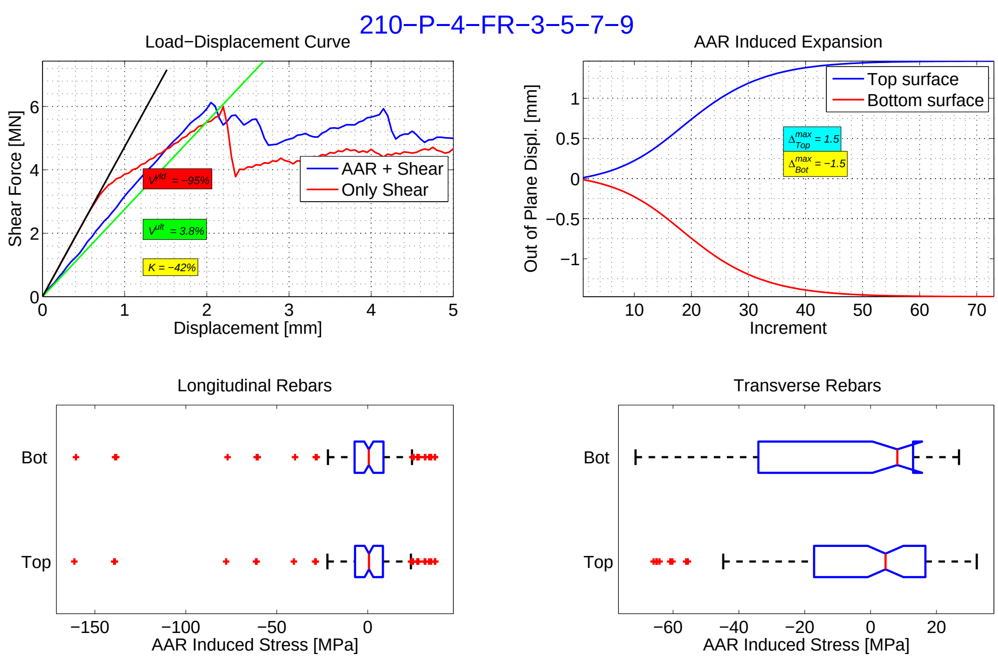

4.1.3.211 Analysis: 211-P-4-FR-3-5-9-7

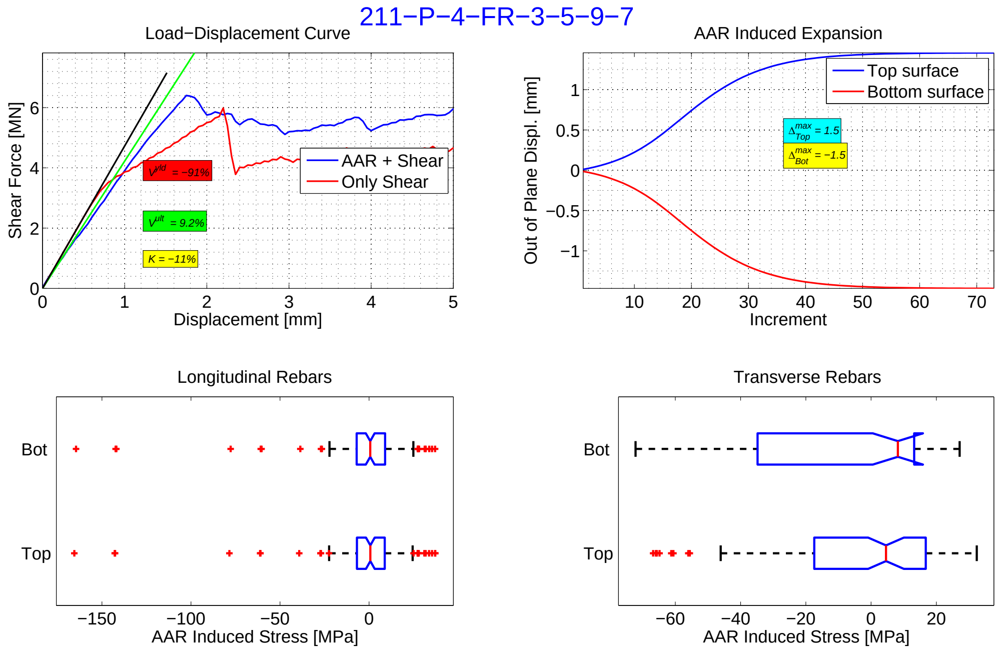

4.1.3.212 Analysis: 212-P-4-FR-3-5-9-9

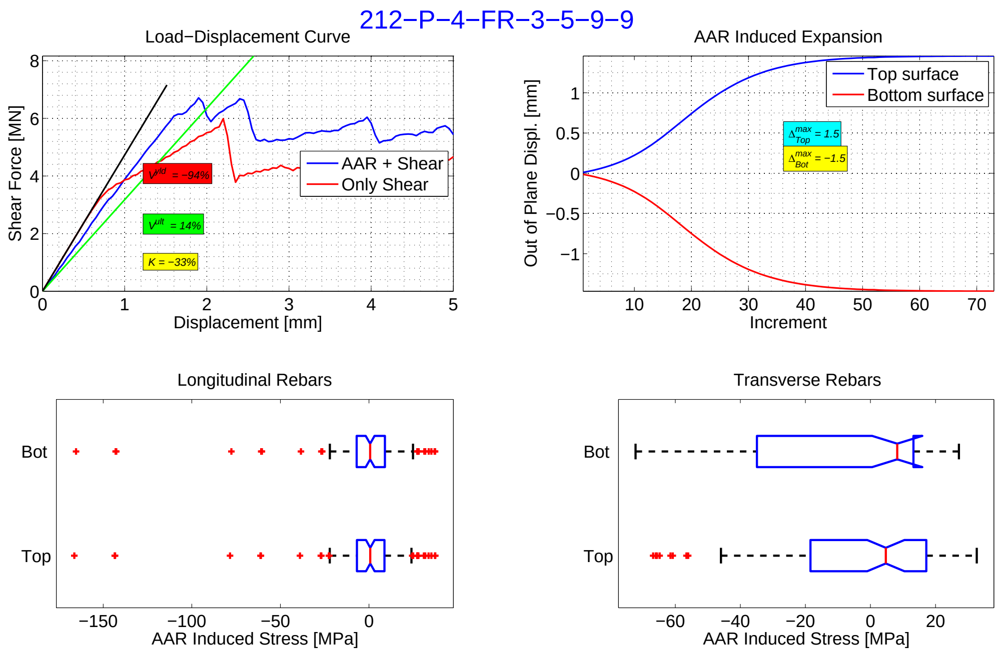

4.1.3.213 Analysis: 213-P-4-FR-3-10-7-7

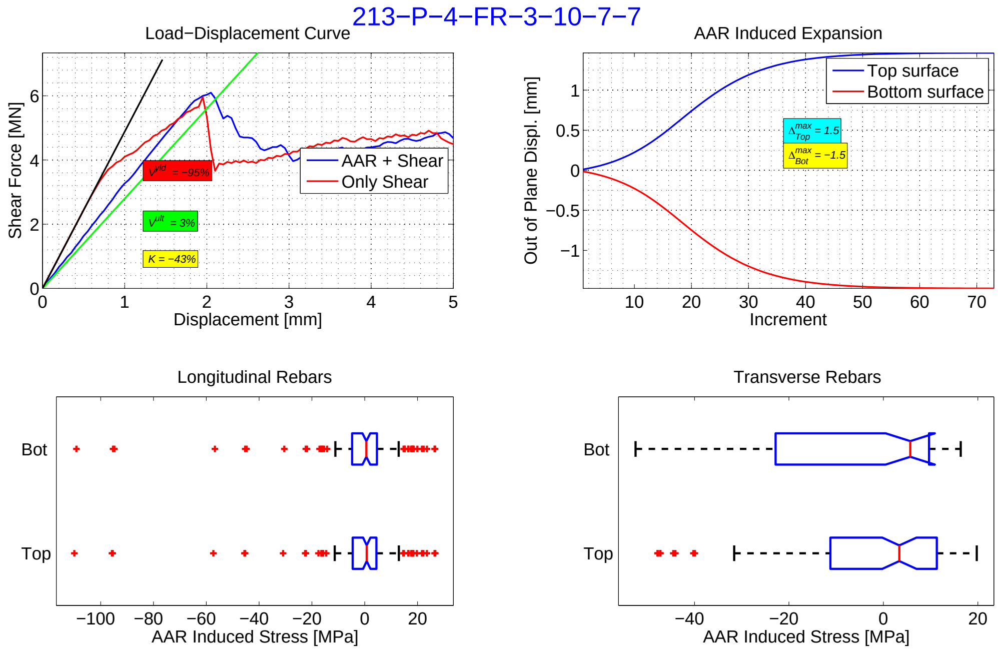

4.1.3.214 Analysis: 214-P-4-FR-3-10-7-9

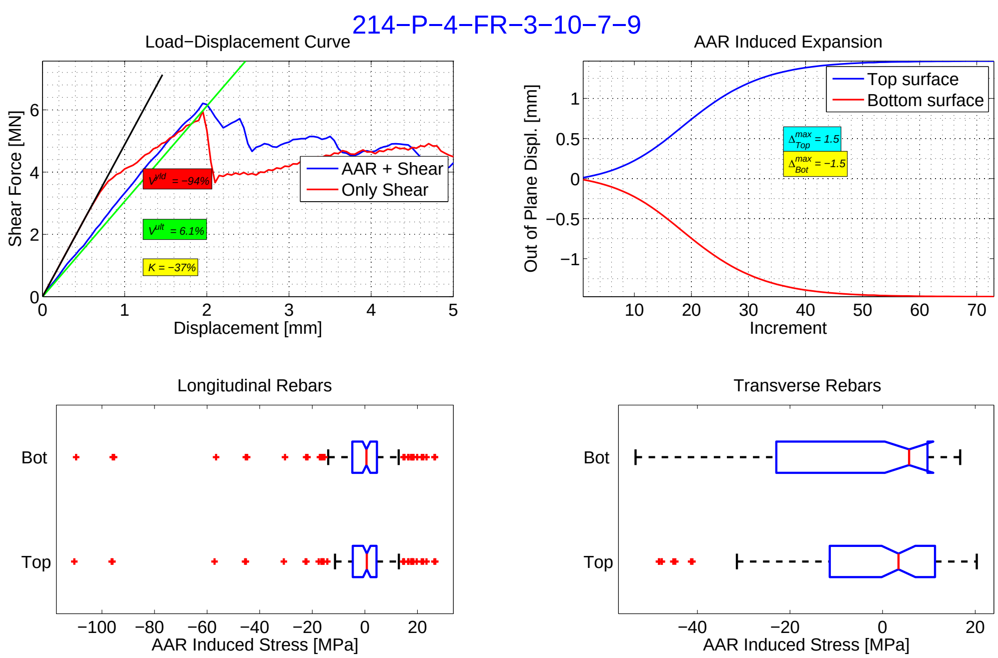

4.1.3.215 Analysis: 215-P-4-FR-3-10-9-7

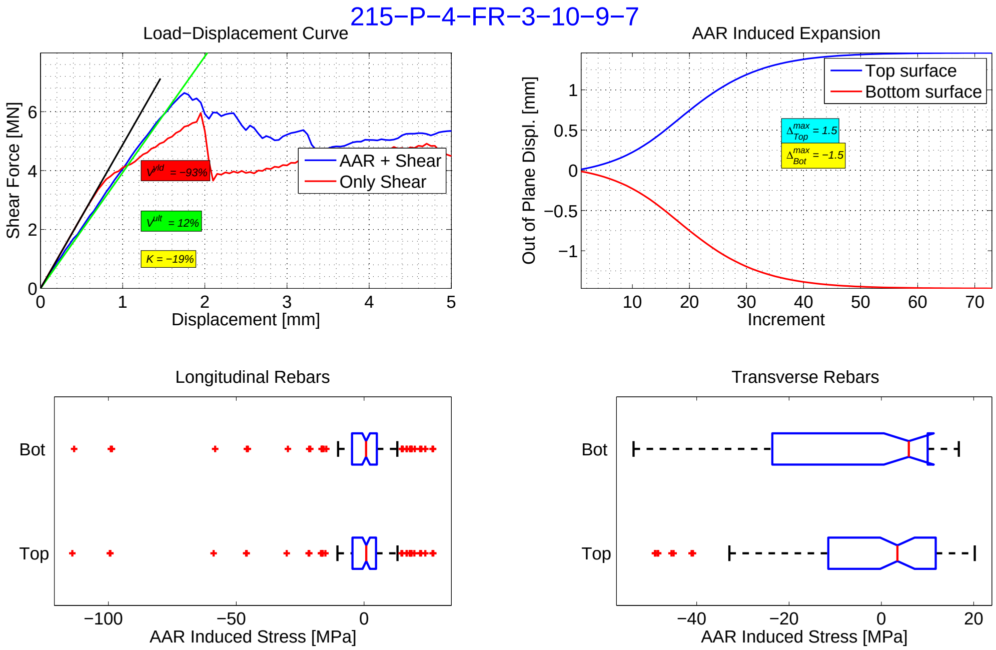

4.1.3.216 Analysis: 216-P-4-FR-3-10-9-9

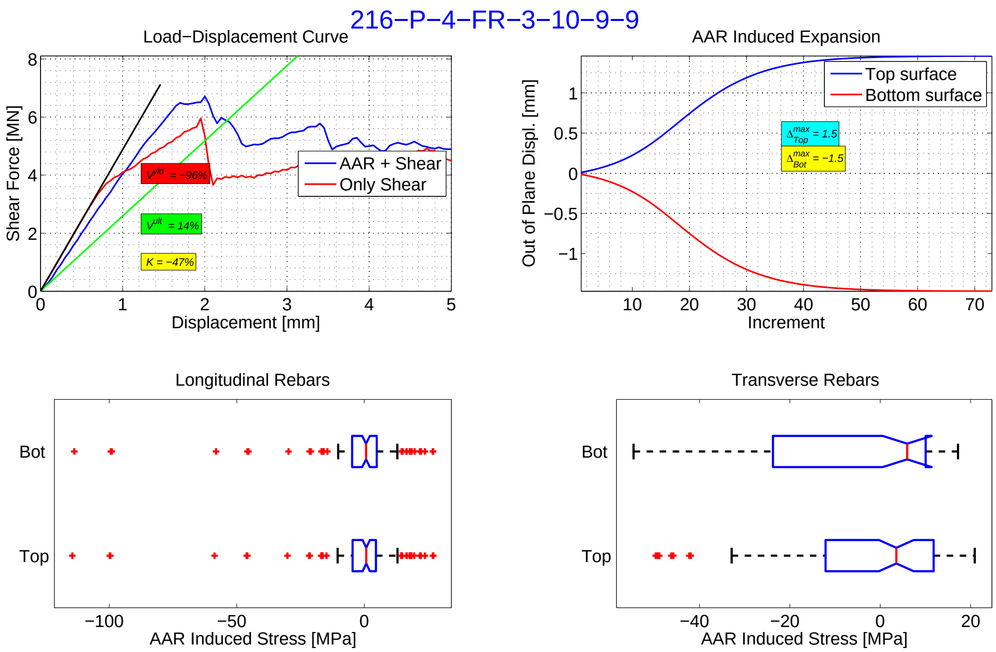

4.2 3D PLOTS

4.2.1 ANALYSIS: DEPTH=2; ρ=0.02;β_E=0.7; β_{FT}=0.7

Depth = 2; ρ = 0.02; β_E = 0.7; β_{ft} = 0.7

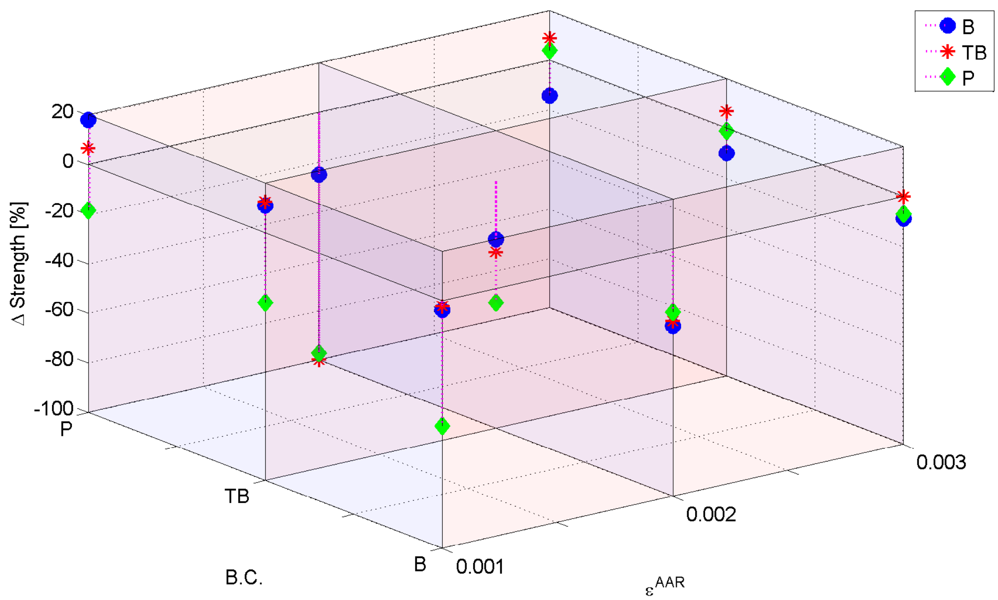

Depth = 2; ρ = 0.02; β_E = 0.7; β_{ft} = 0.7

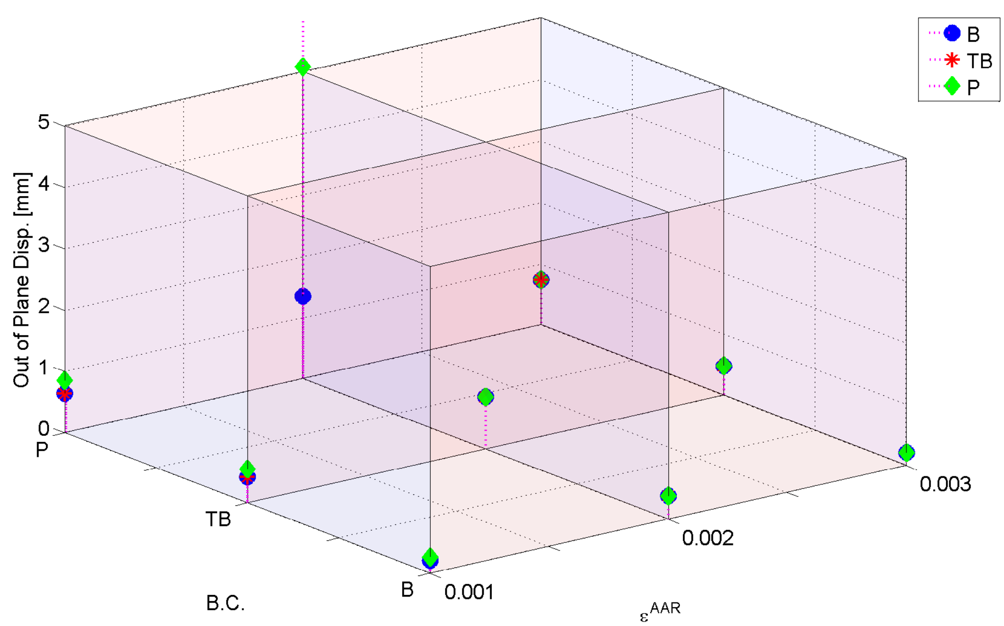

4.2.2 ANALYSIS: DEPTH=2; ρ=0.02;β_E=0.7; β_{FT}=0.9

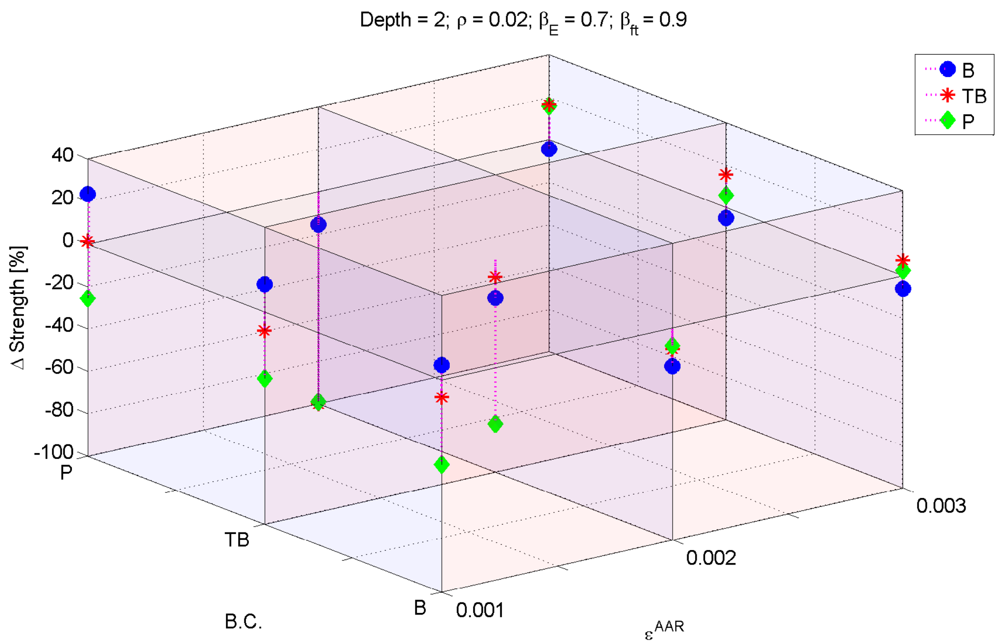

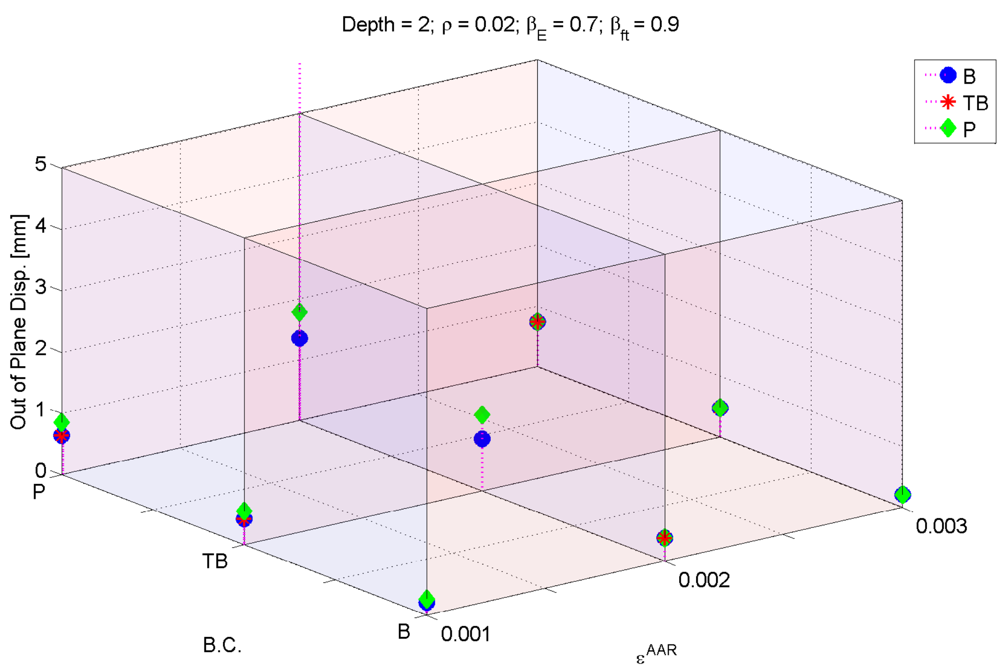

4.2.3 ANALYSIS: DEPTH=2; ρ=0.02;β_E=0.9; β_{FT}=0.7

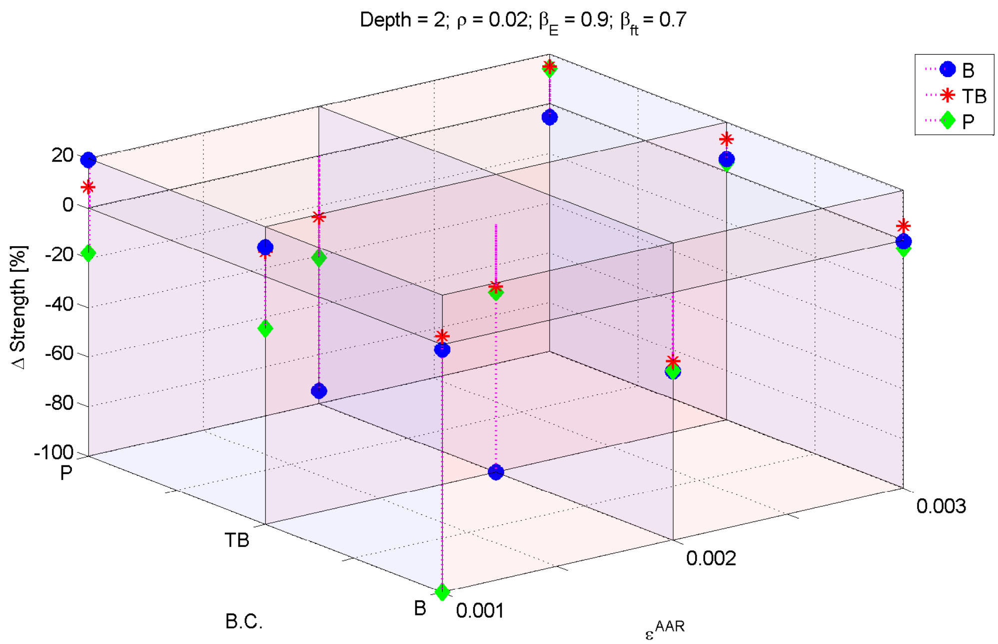

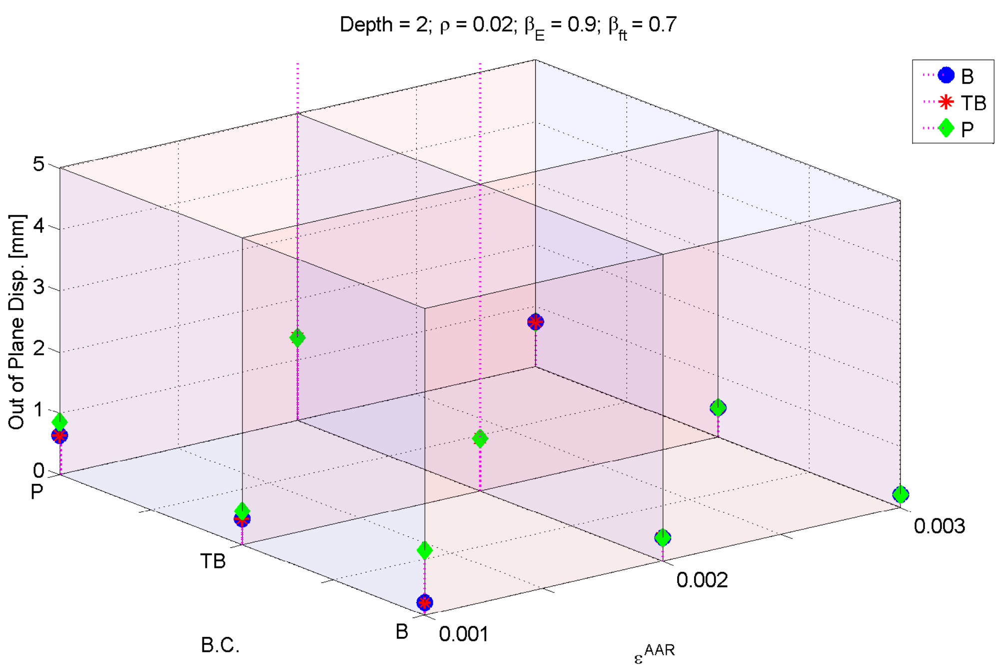

4.2.4 ANALYSIS: DEPTH=2; ρ=0.02;β_E=0.9; β_{FT}=0.9

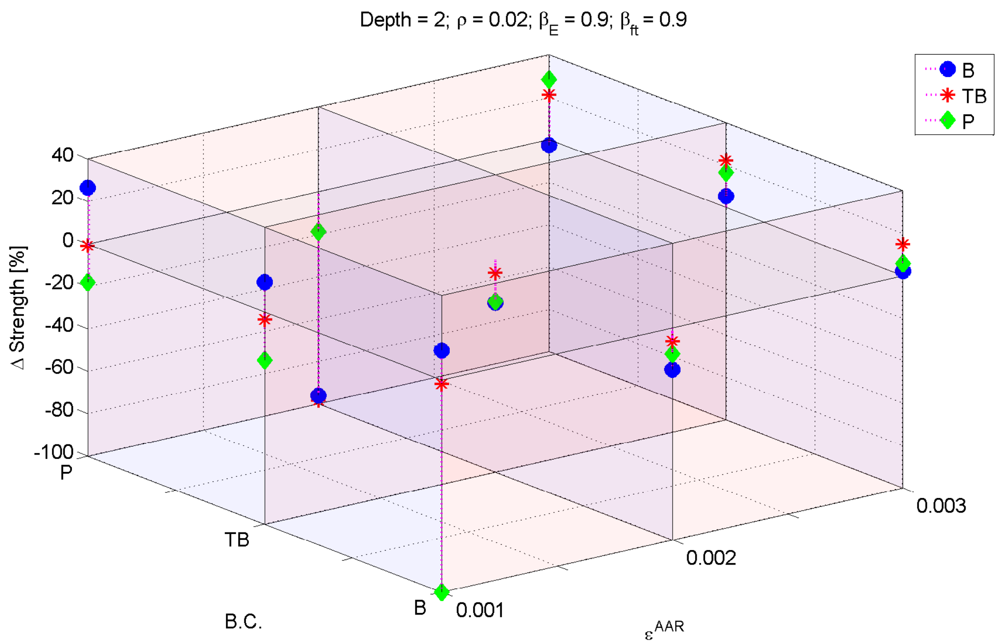

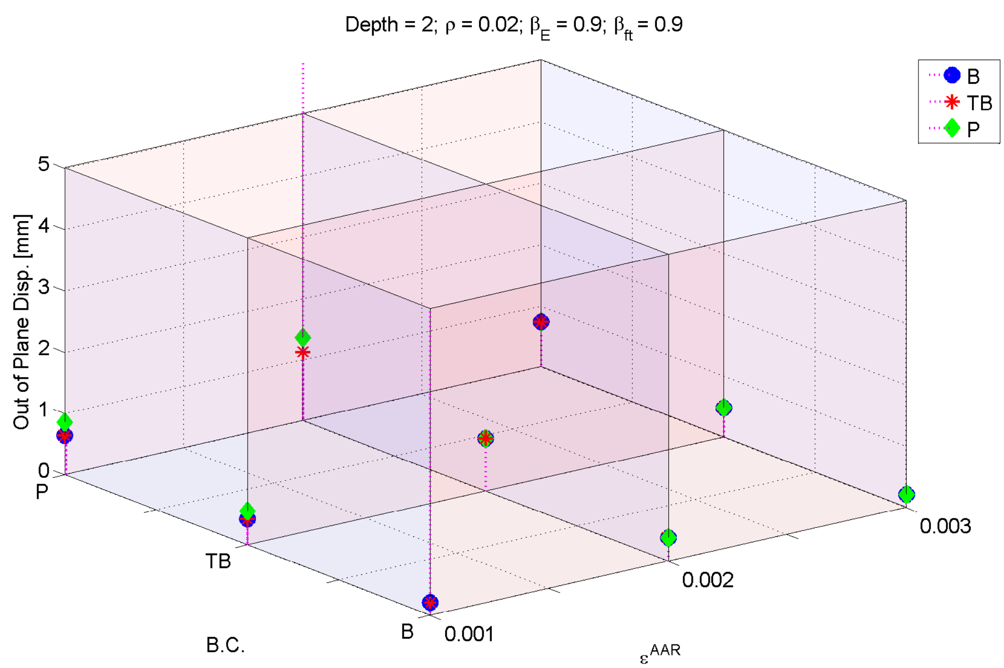

4.2.5 ANALYSIS: DEPTH=2; ρ=0.05;β_E=0.7; β_{FT}=0.7

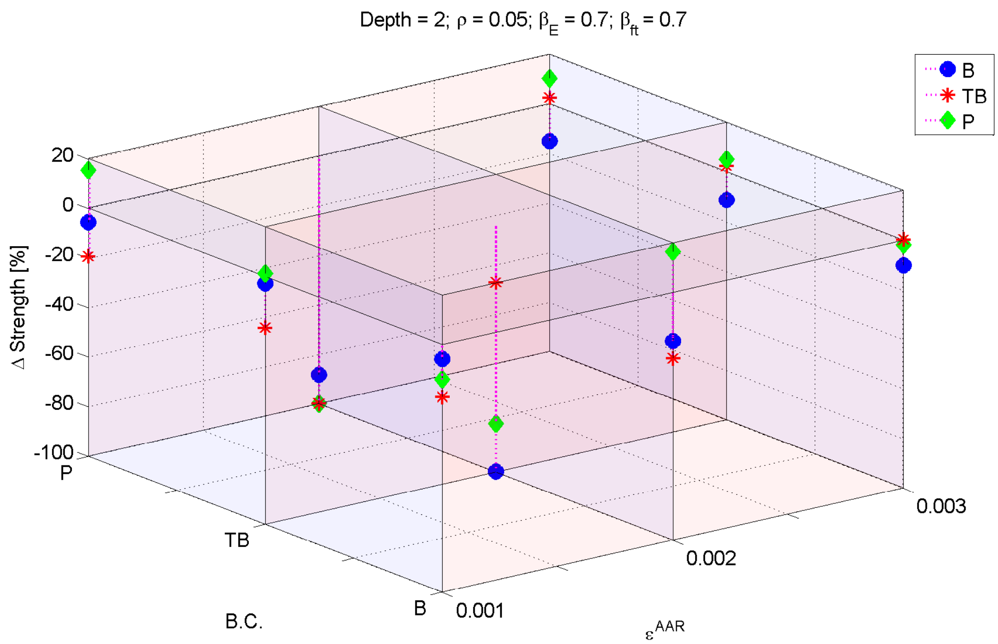

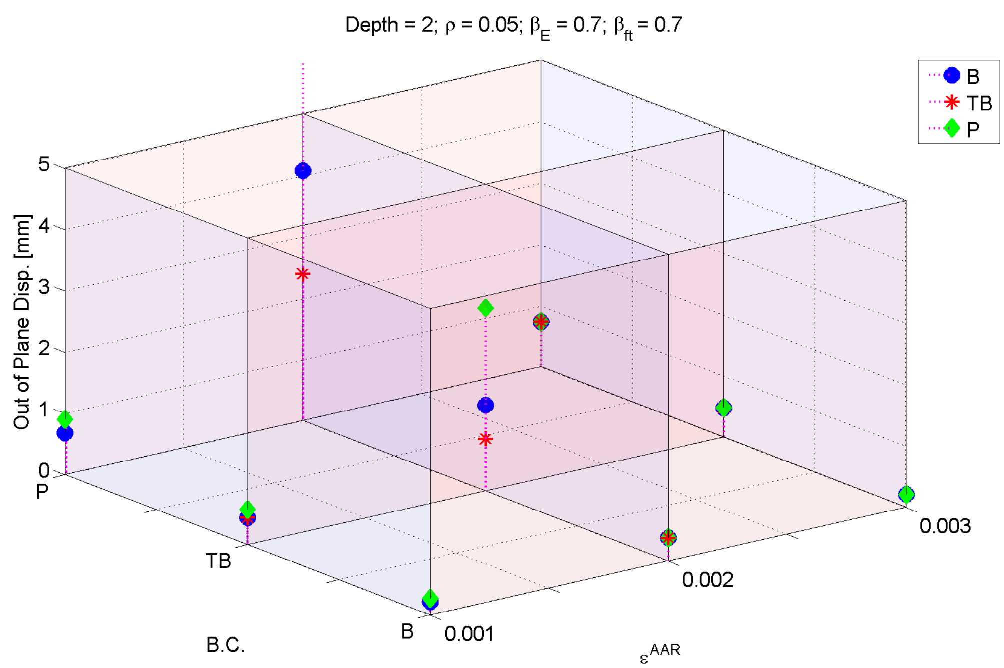

4.2.6 ANALYSIS: DEPTH=2; ρ=0.05;β_E=0.7; β_{FT}=0.9

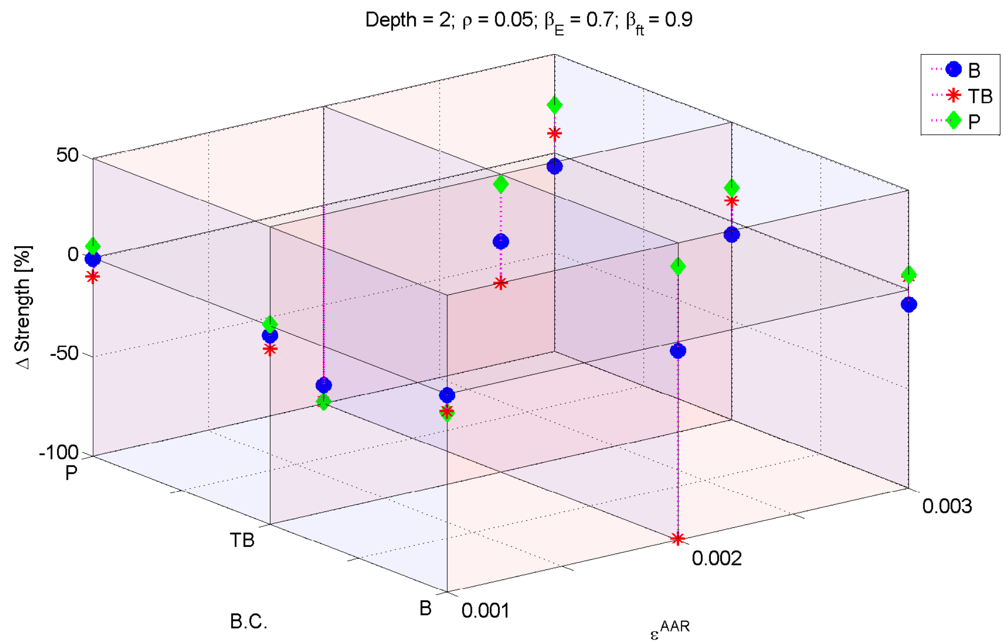

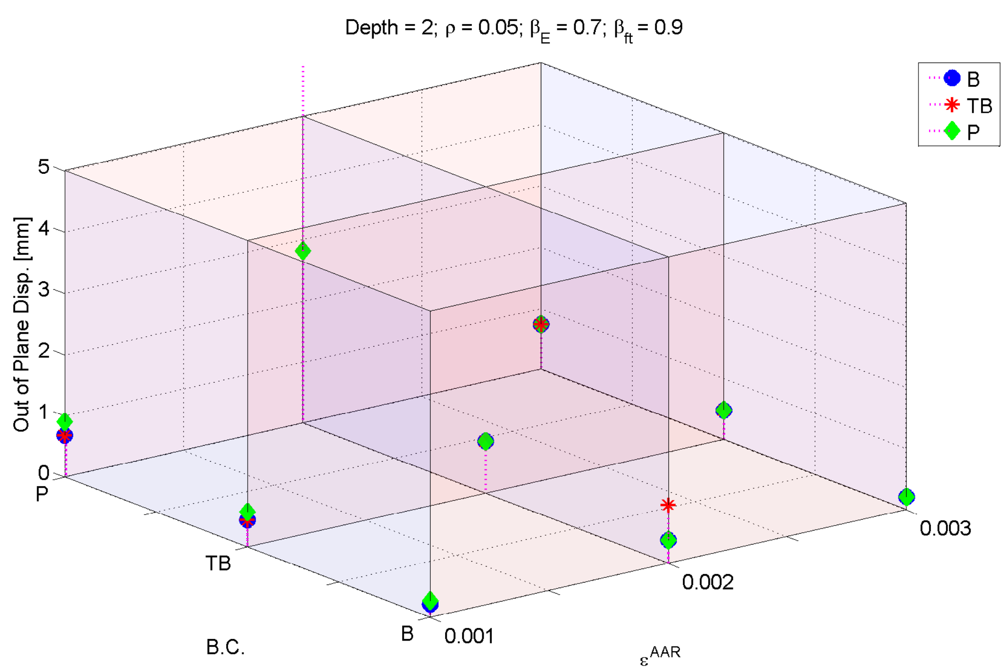

4.2.7 ANALYSIS: DEPTH=2; ρ=0.05;β_E=0.9; β_{FT}=0.7

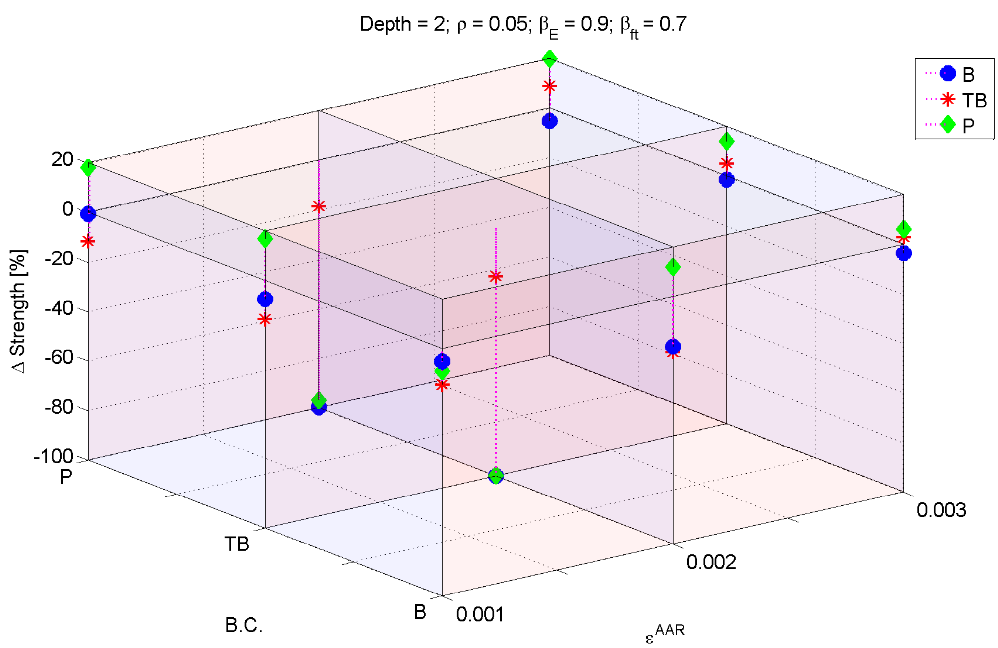

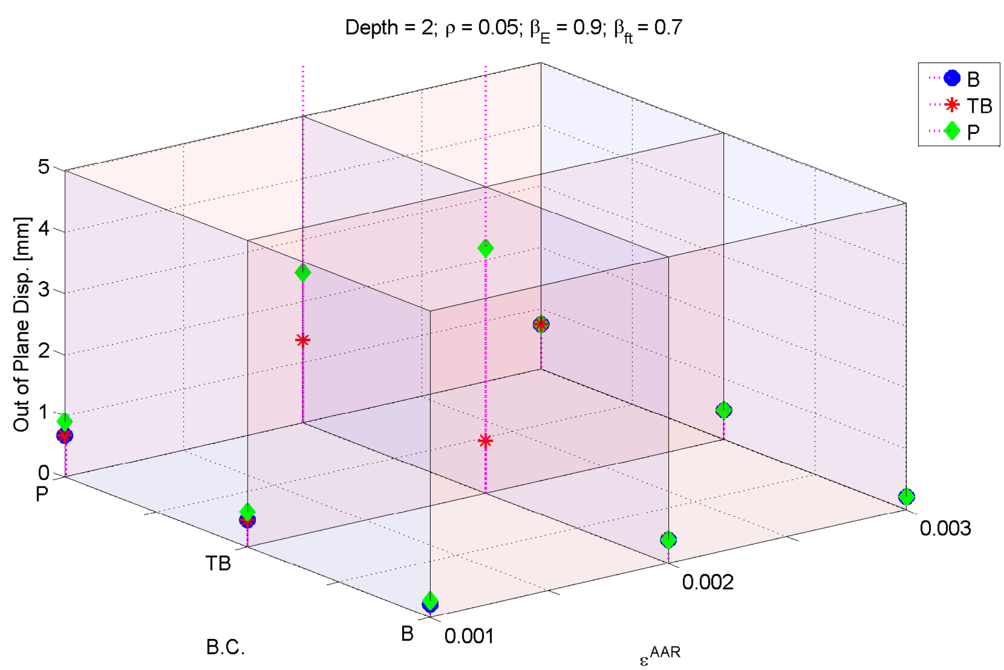

4.2.8 ANALYSIS: DEPTH=2; ρ=0.05;β_E=0.9; β_{FT}=0.9

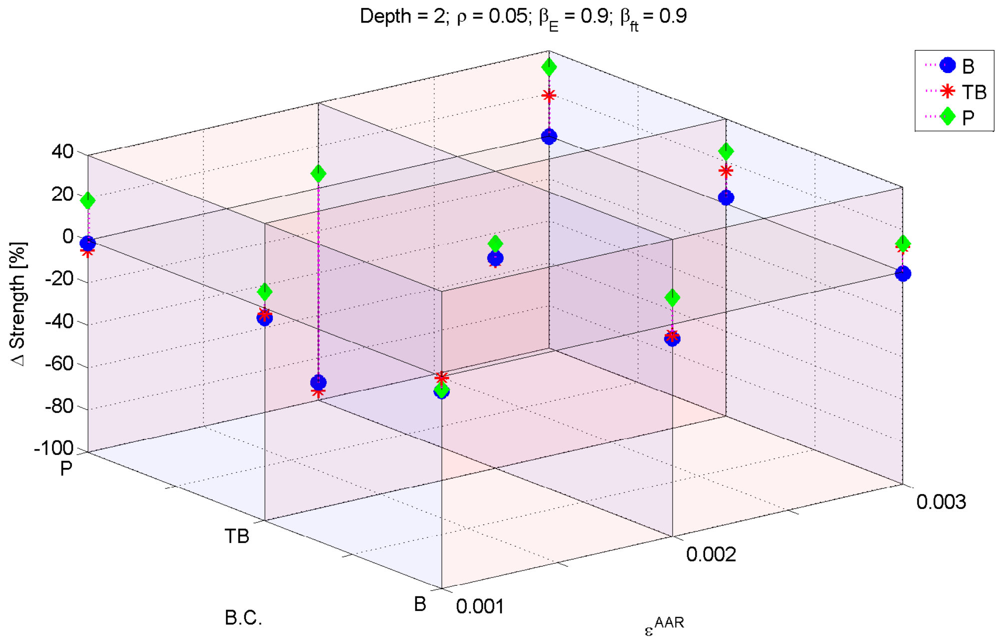

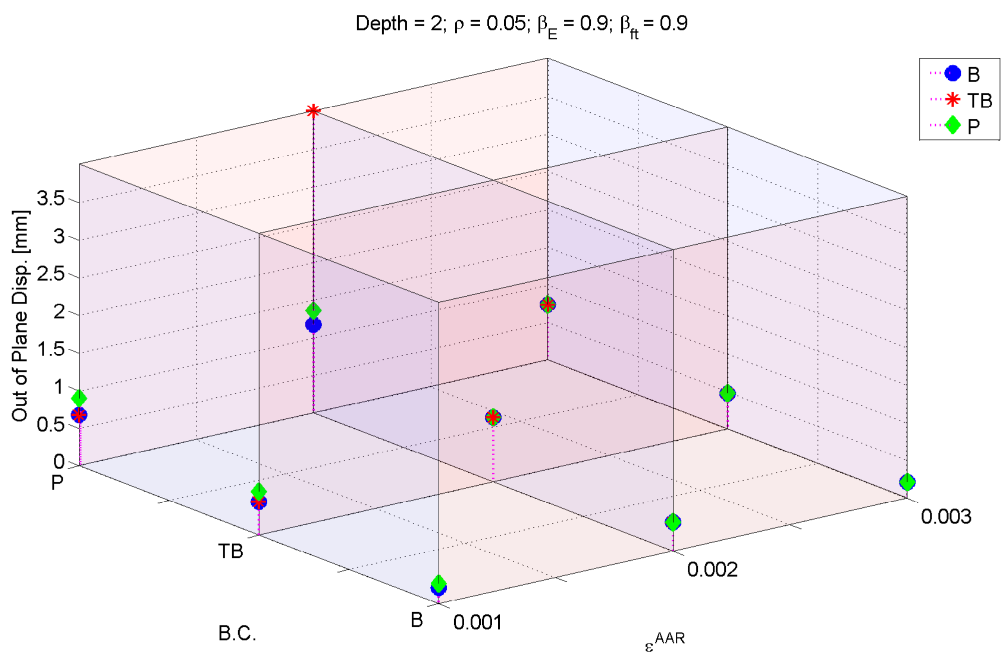

4.2.9 ANALYSIS: DEPTH=2; ρ=0.1;β_E=0.7; β_{FT}=0.7

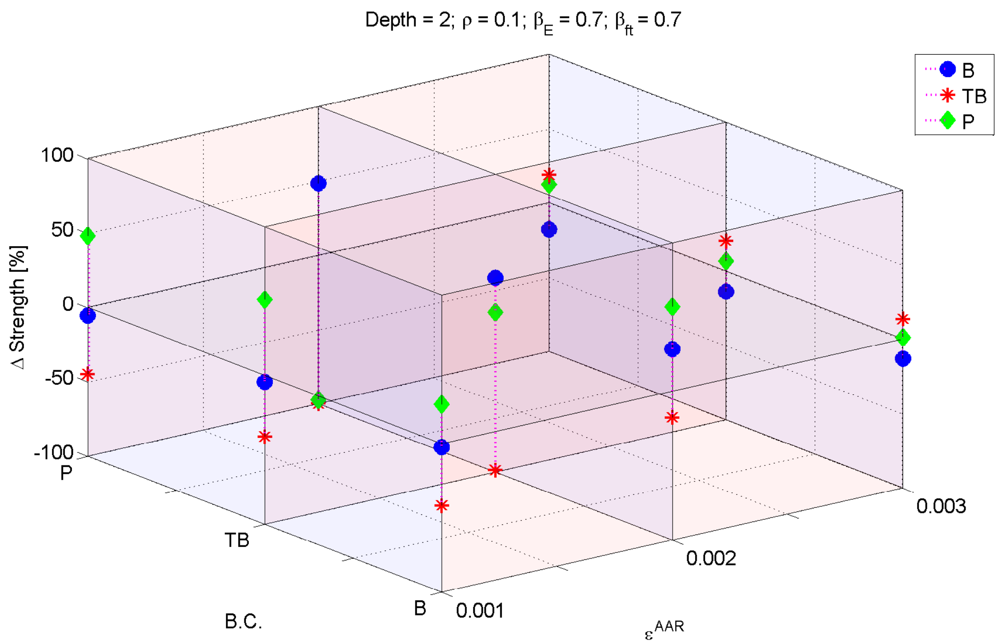

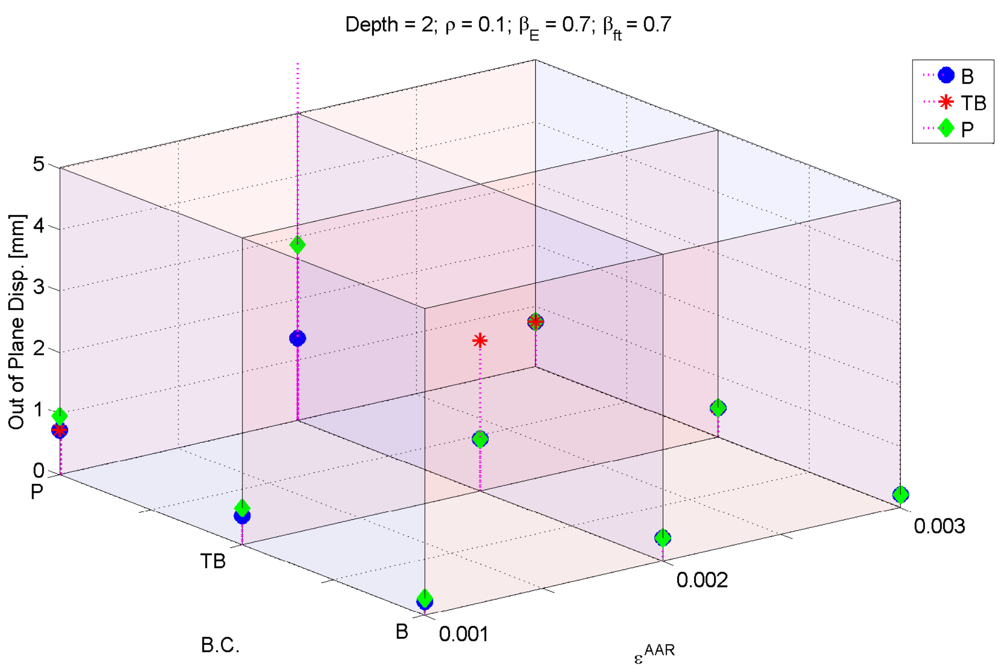

4.2.10 ANALYSIS: DEPTH=2; ρ=0.1;β_E=0.7; β_{FT}=0.9

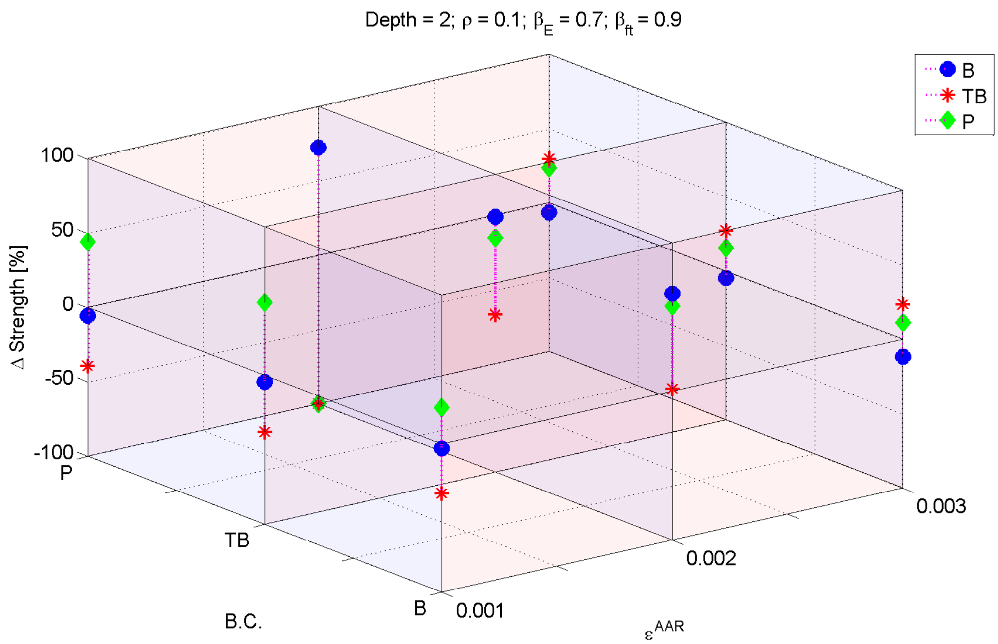

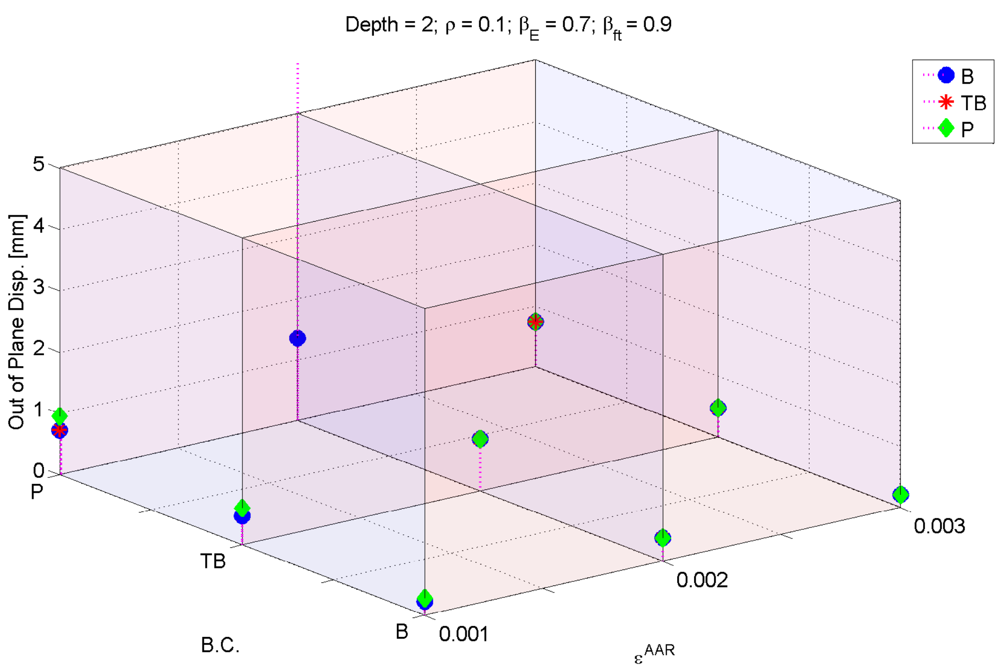

4.2.11 ANALYSIS: DEPTH=2; ρ=0.1;β_E=0.9; β_{FT}=0.7

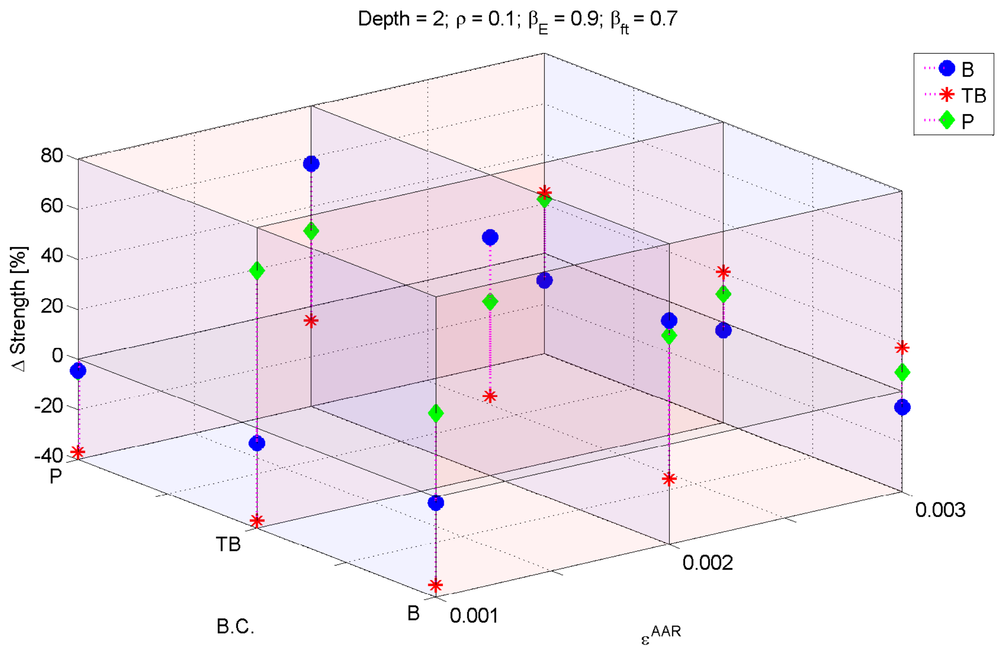

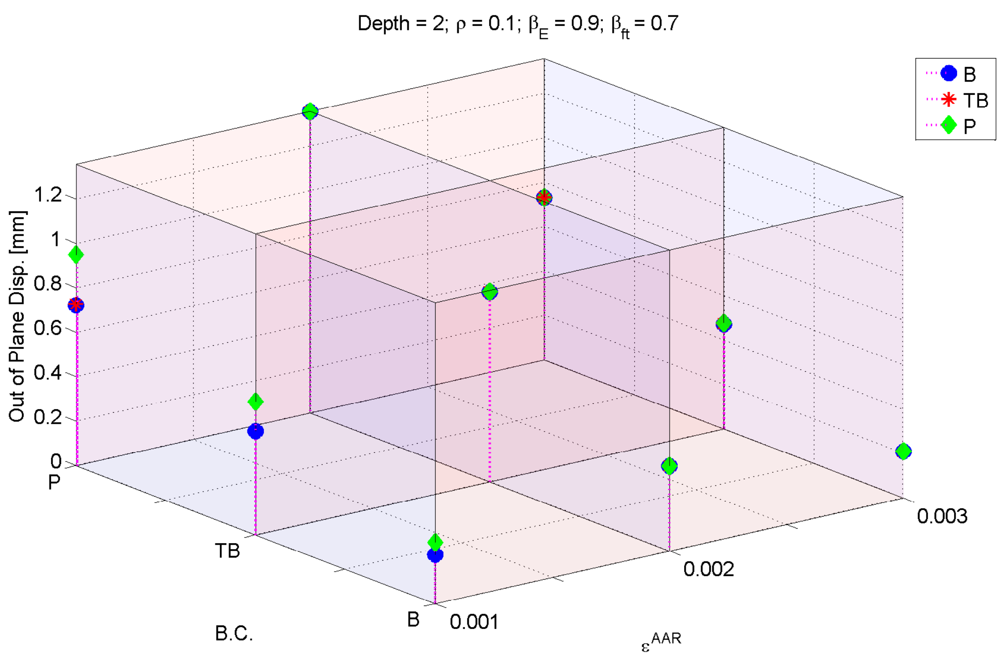

4.2.12 ANALYSIS: DEPTH=2; ρ=0.1;β_E=0.9; β_{FT}=0.9

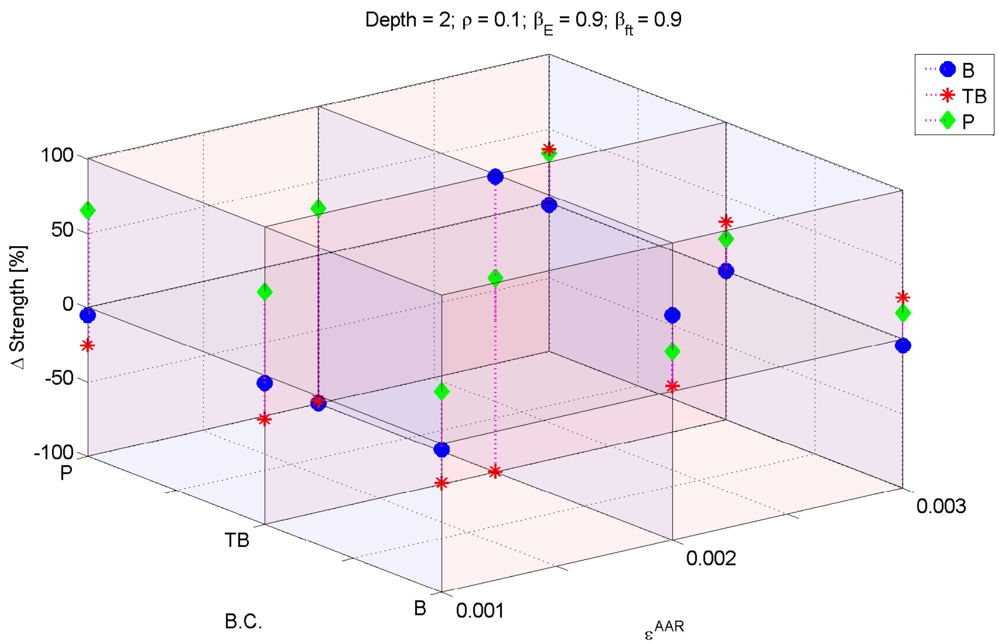

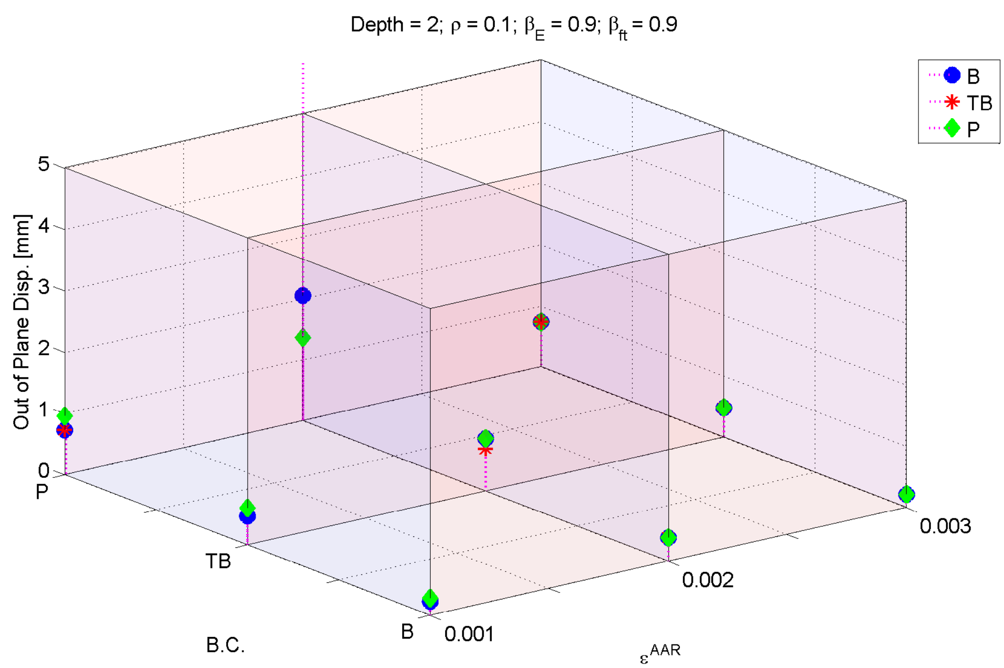

4.2.13 ANALYSIS: DEPTH=4; ρ=0.02;β_E=0.7; β_{FT}=0.7

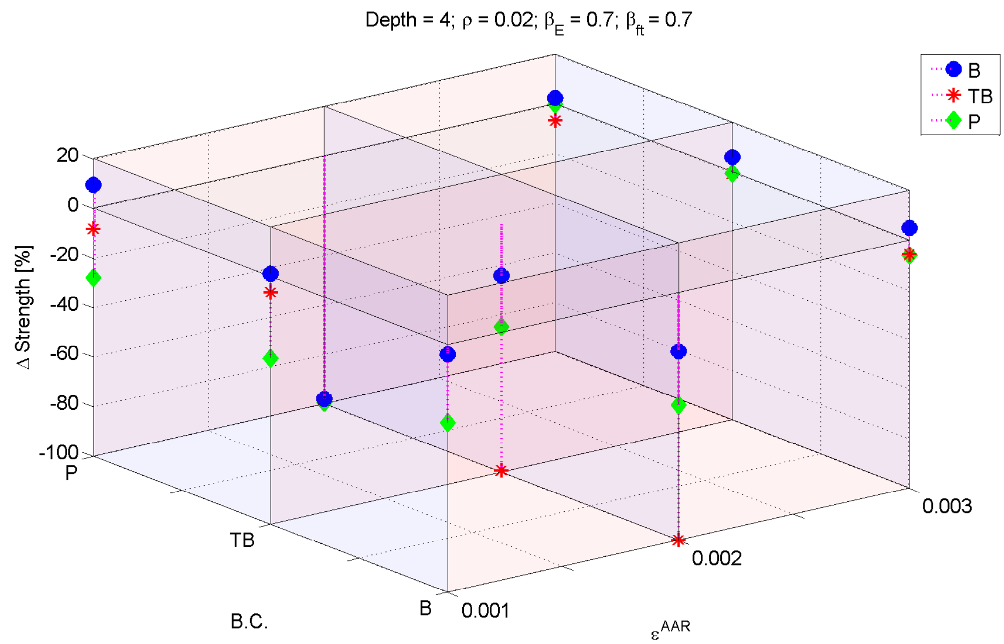

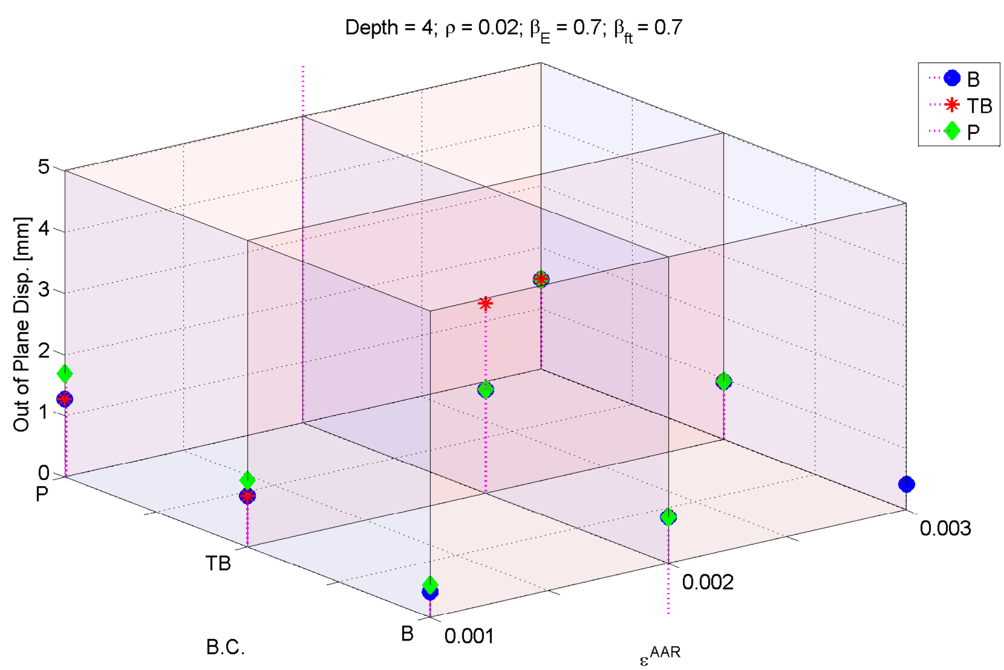

4.2.14 ANALYSIS: DEPTH=4; ρ=0.02;β_E=0.7; β_{FT}=0.9

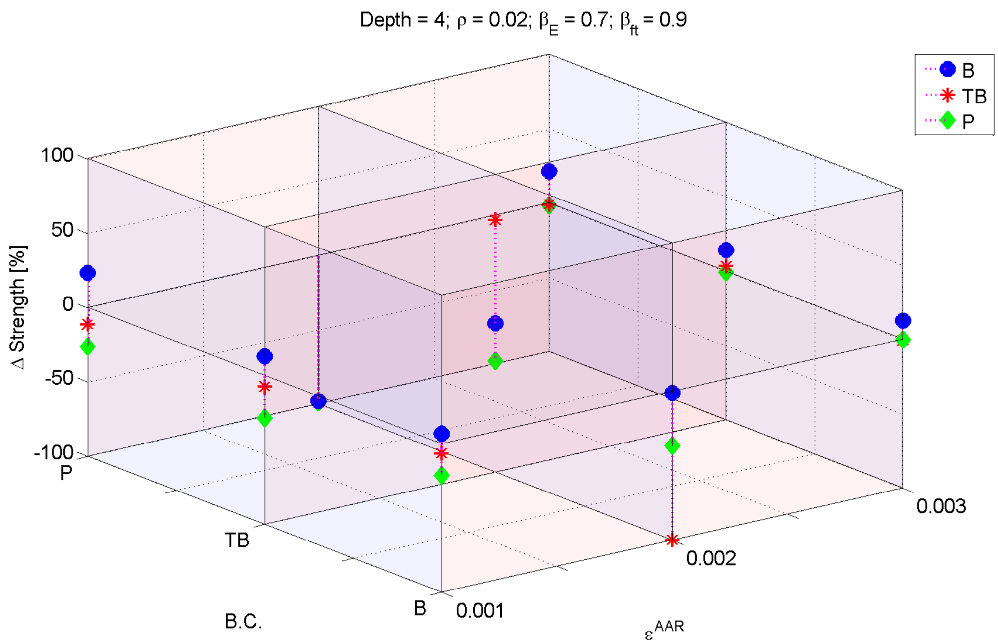

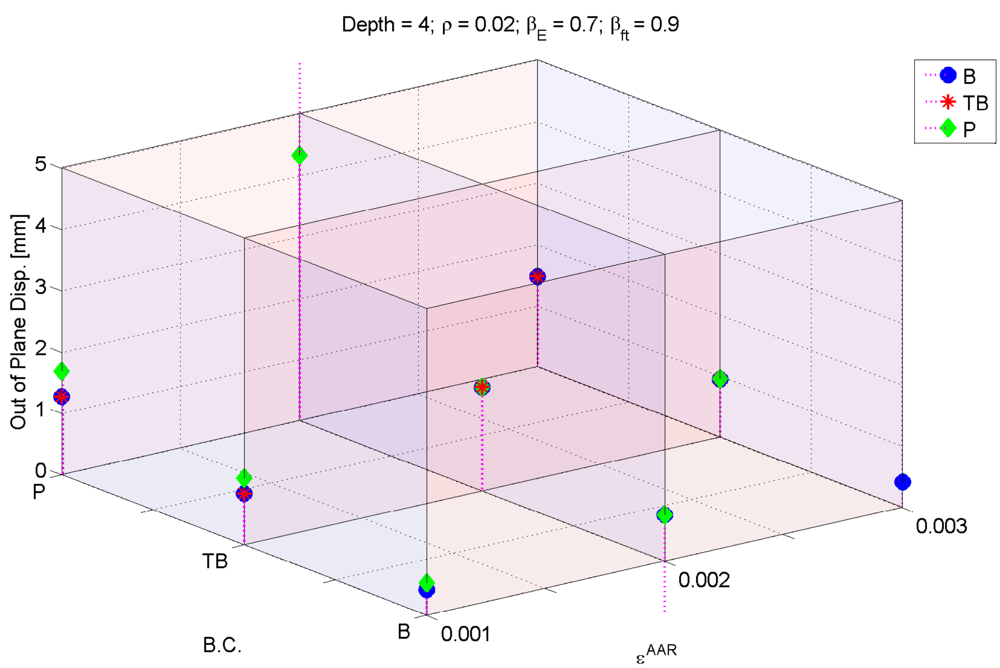

4.2.15 ANALYSIS: DEPTH=4; ρ=0.02;β_E=0.9; β_{FT}=0.7

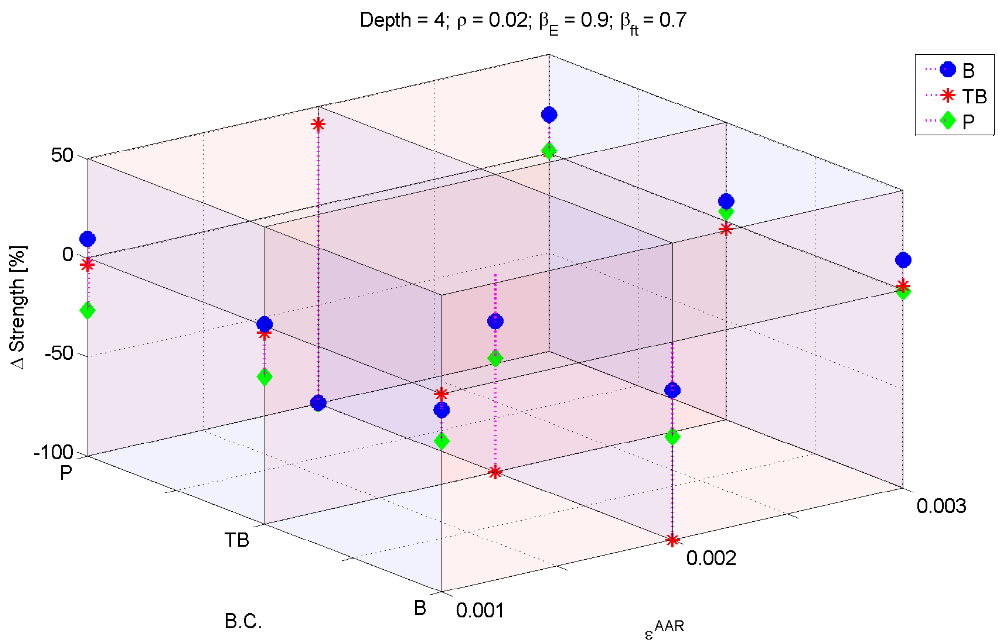

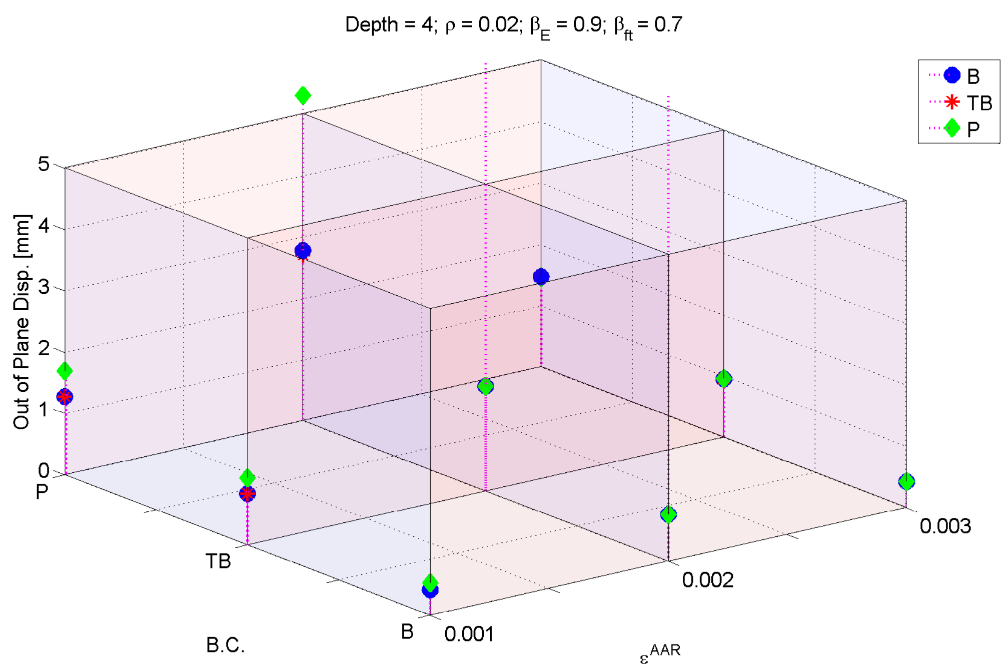

4.2.16 ANALYSIS: DEPTH=4; ρ=0.02;β_E=0.9; β_{FT}=0.9

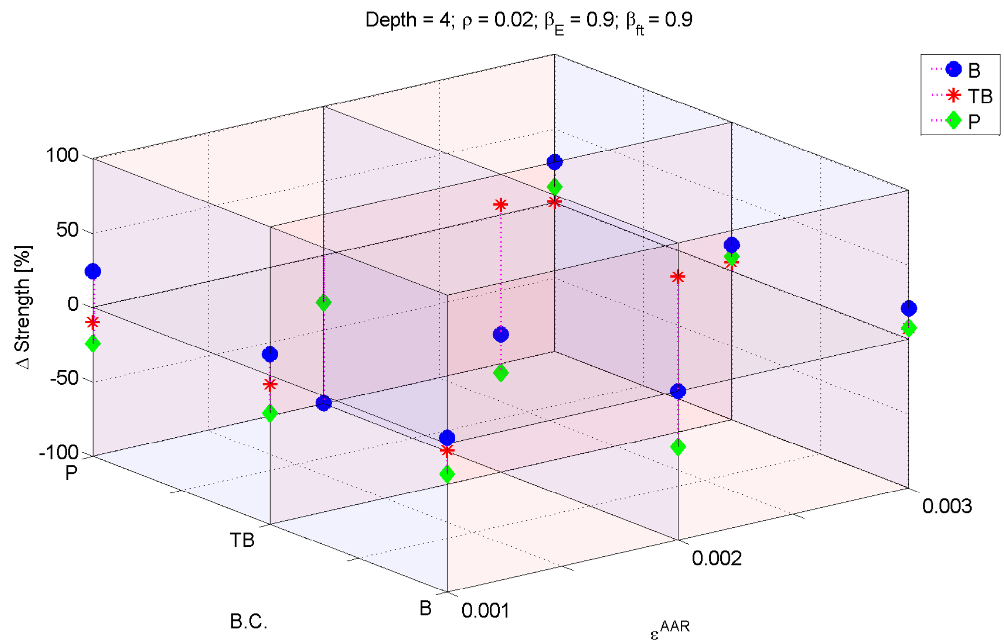

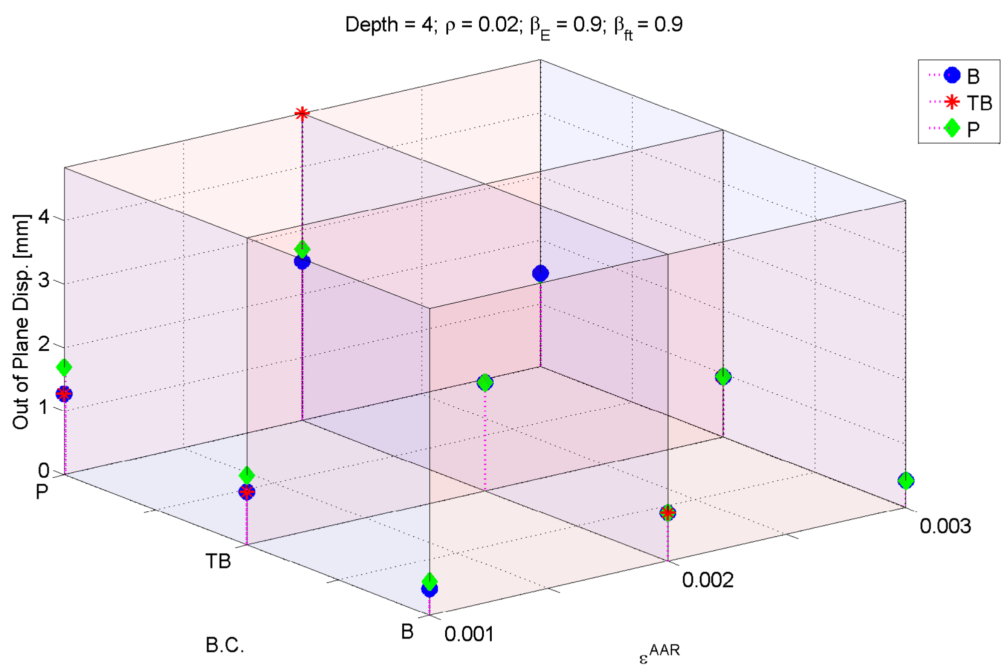

4.2.17 ANALYSIS: DEPTH=4; ρ=0.05;β_E=0.7; β_{FT}=0.7

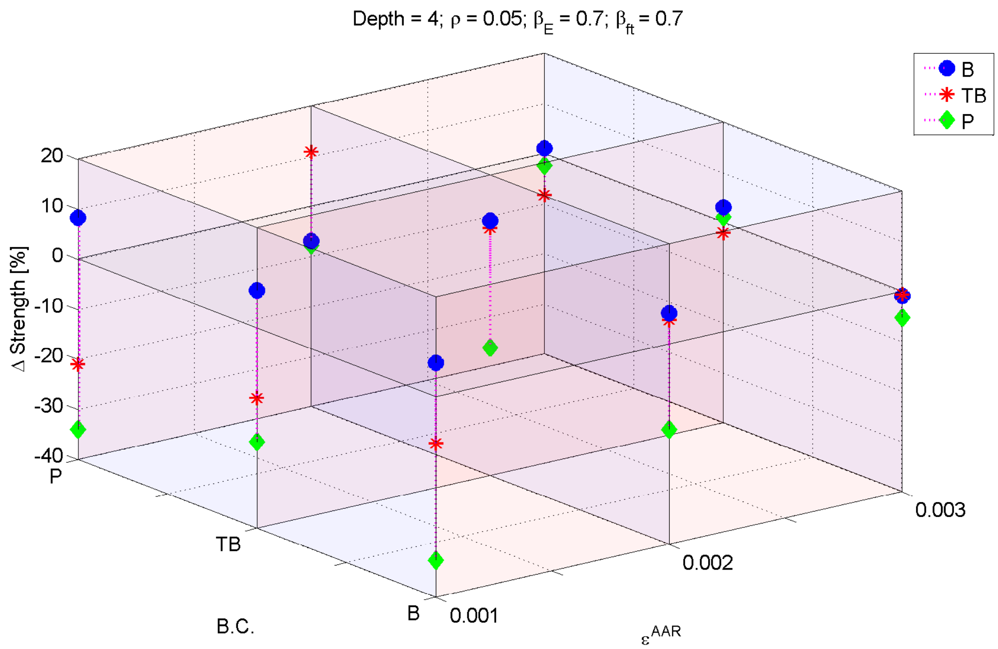

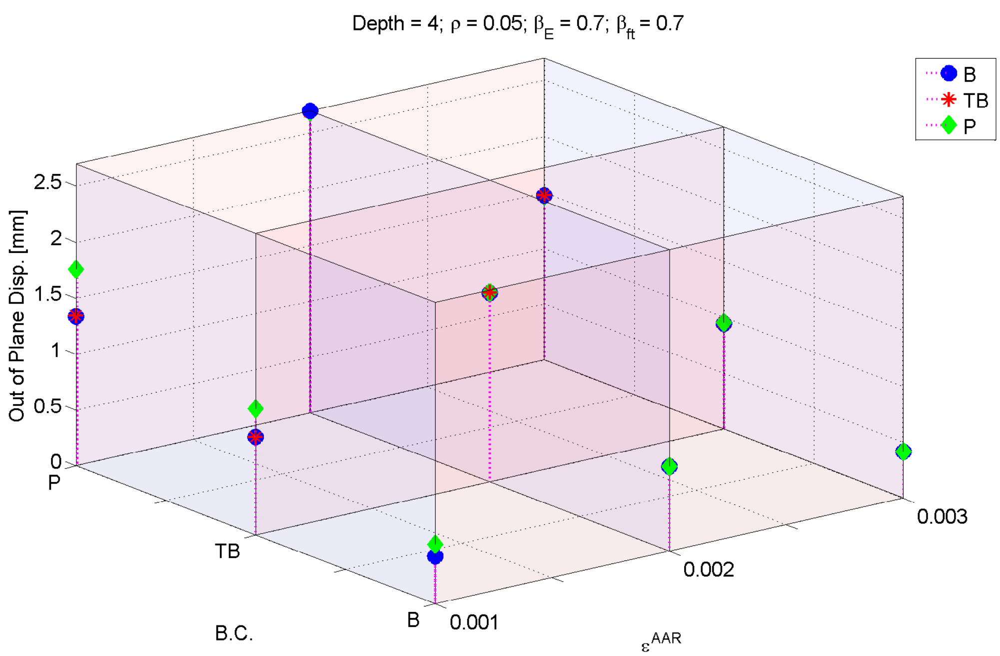

4.2.18 ANALYSIS: DEPTH=4; ρ=0.05;β_E=0.7; β_{FT}=0.9

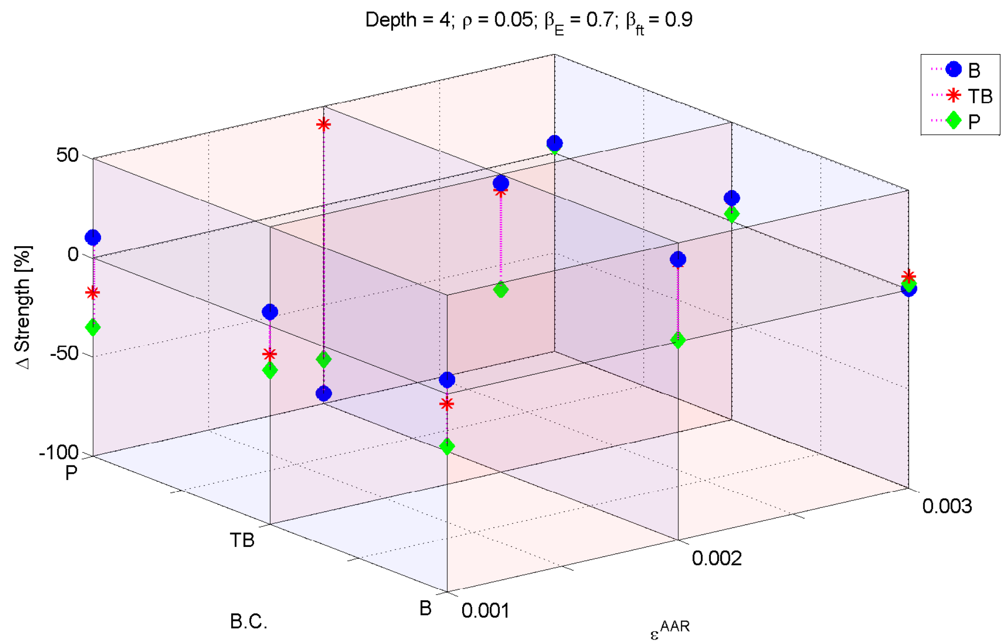

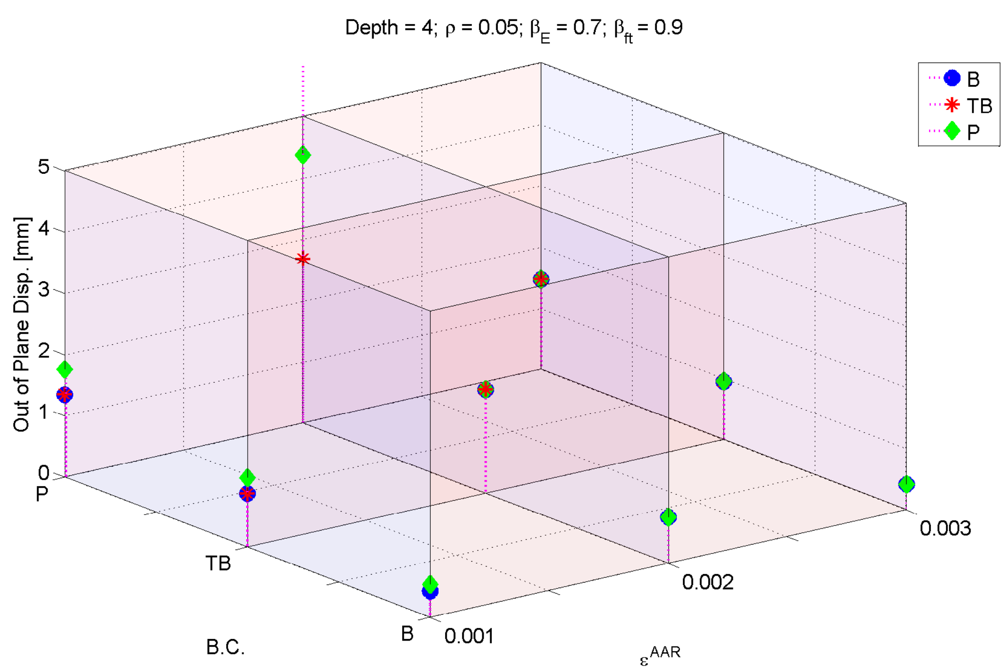

4.2.19 ANALYSIS: DEPTH=4; ρ=0.05;β_E=0.9; β_{FT}=0.7

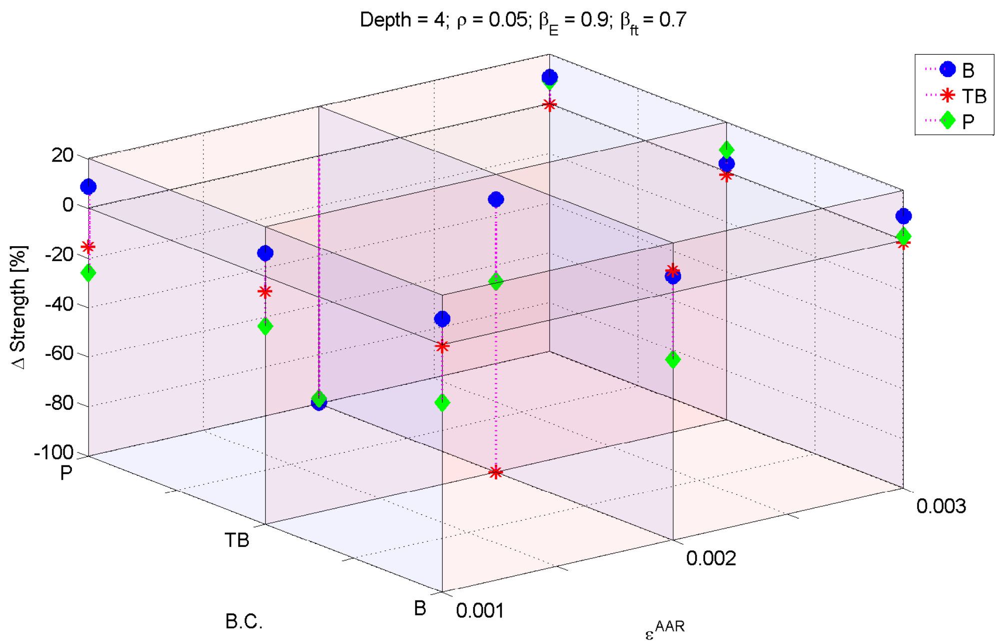

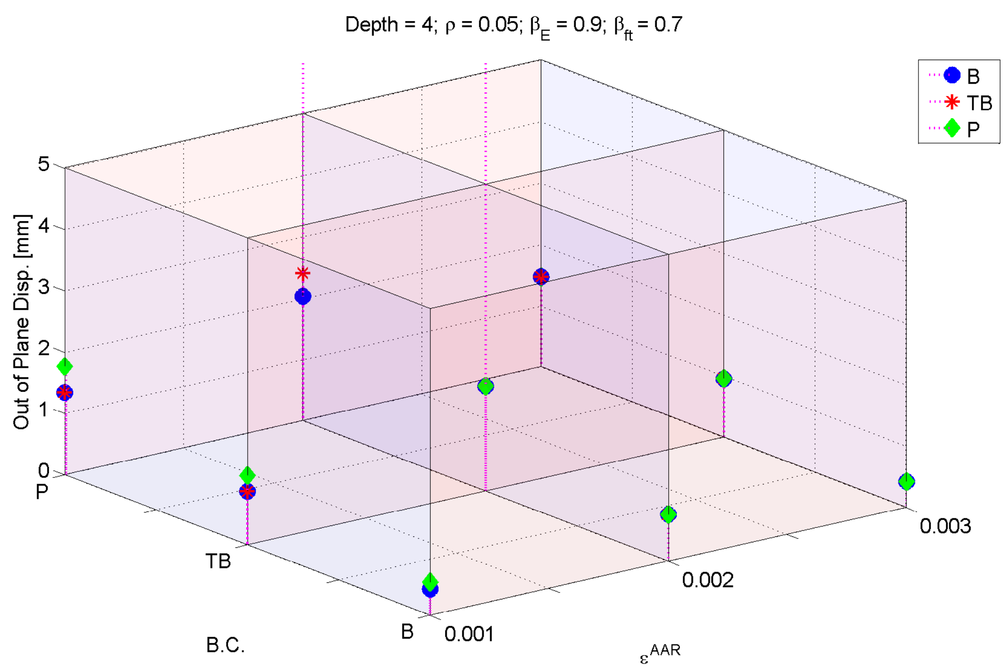

4.2.20 ANALYSIS: DEPTH=4; ρ=0.05;β_E=0.9; β_{FT}=0.9

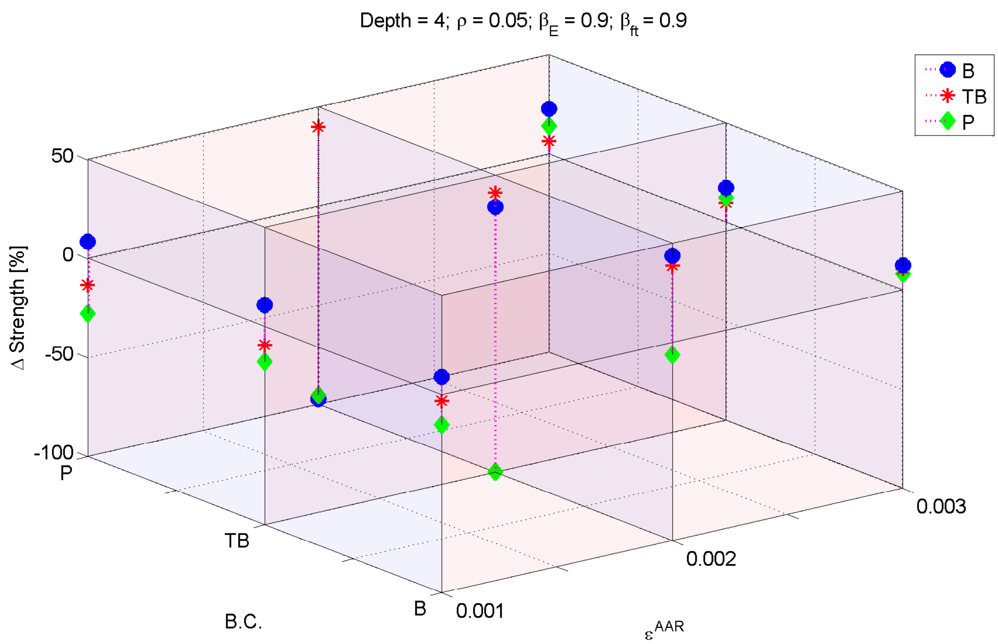

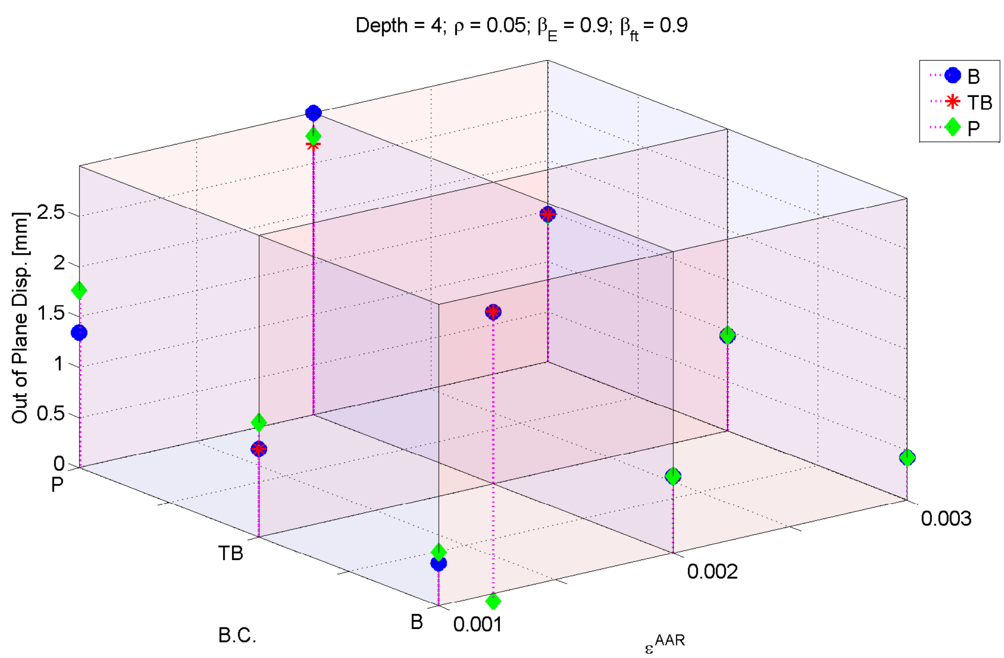

4.2.21 ANALYSIS: DEPTH=4; ρ=0.1;β_E=0.7; β_{FT}=0.7

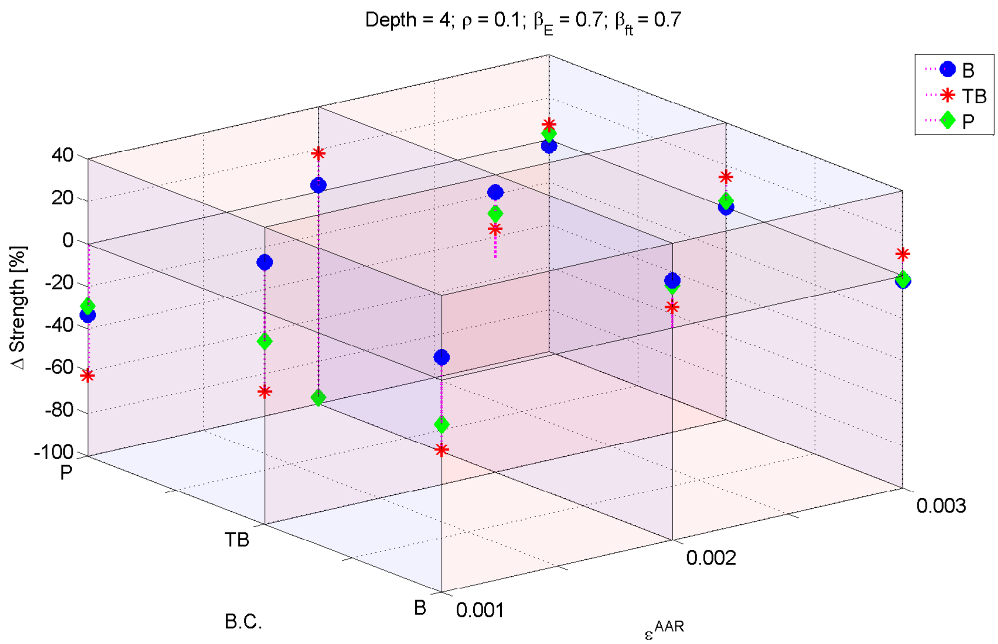

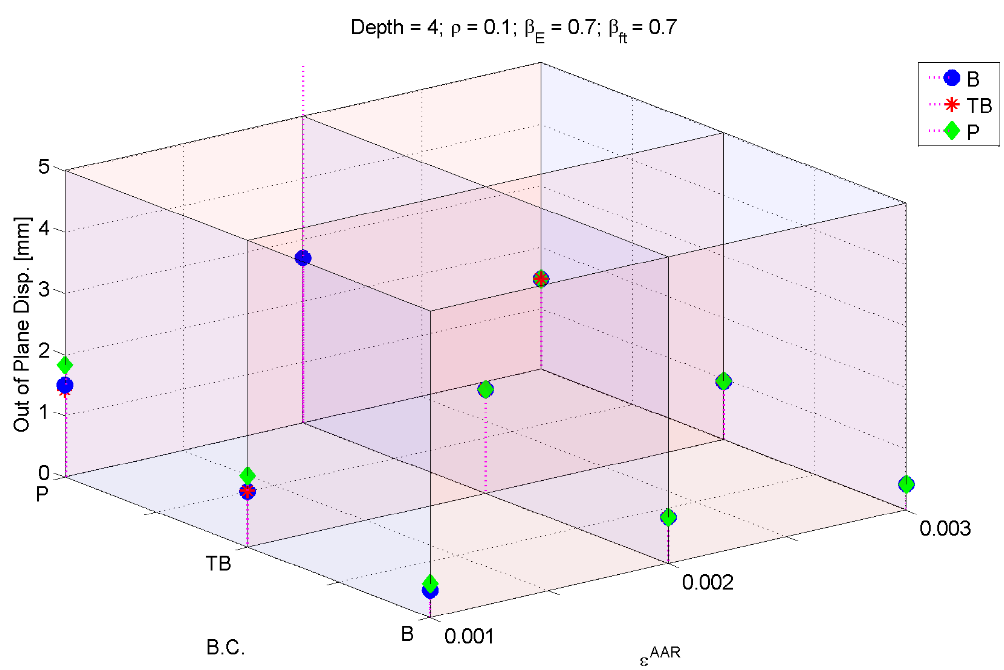

4.2.22 ANALYSIS: DEPTH=4; ρ=0.1;β_E=0.7; β_{FT}=0.9

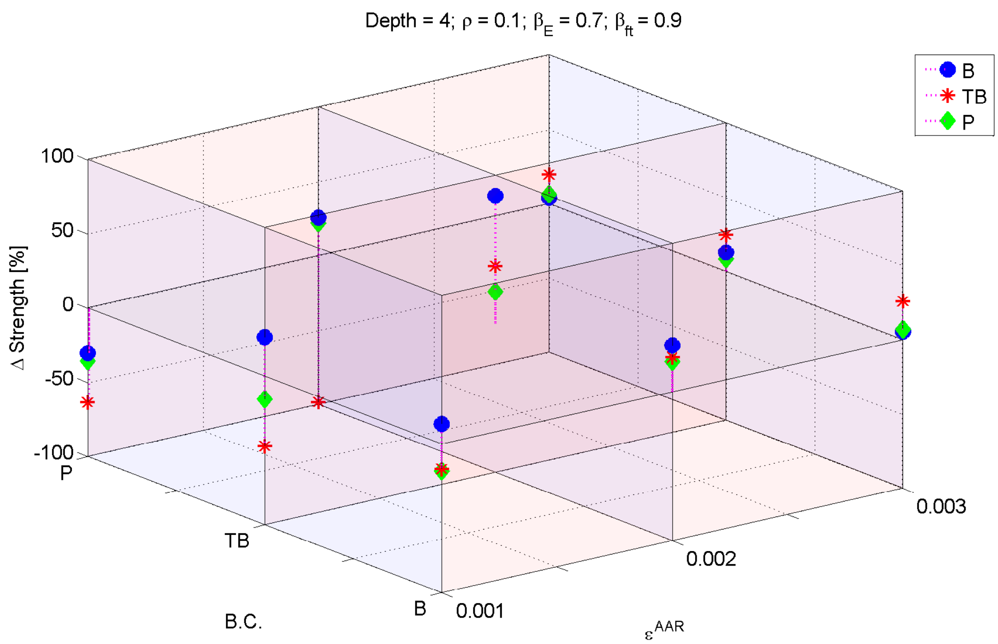

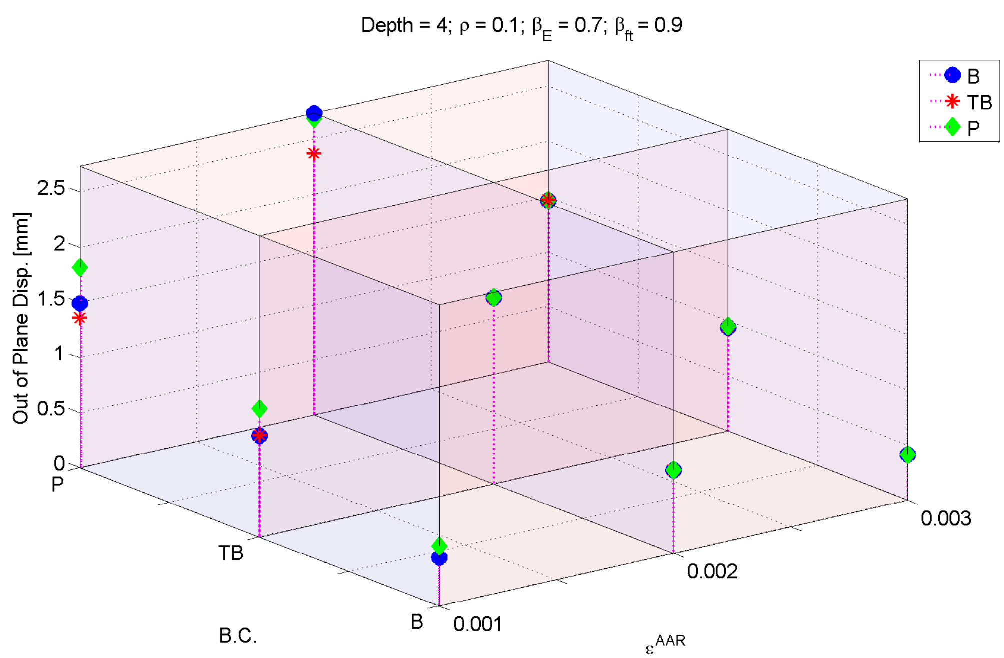

4.2.23 ANALYSIS: DEPTH=4; ρ=0.1;β_E=0.9; β_{FT}=0.7

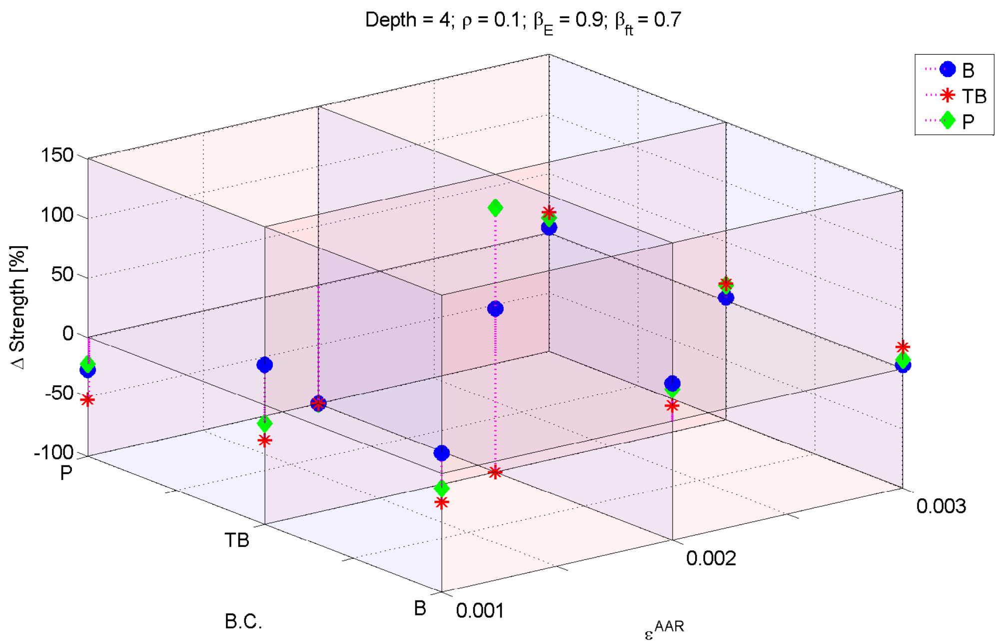

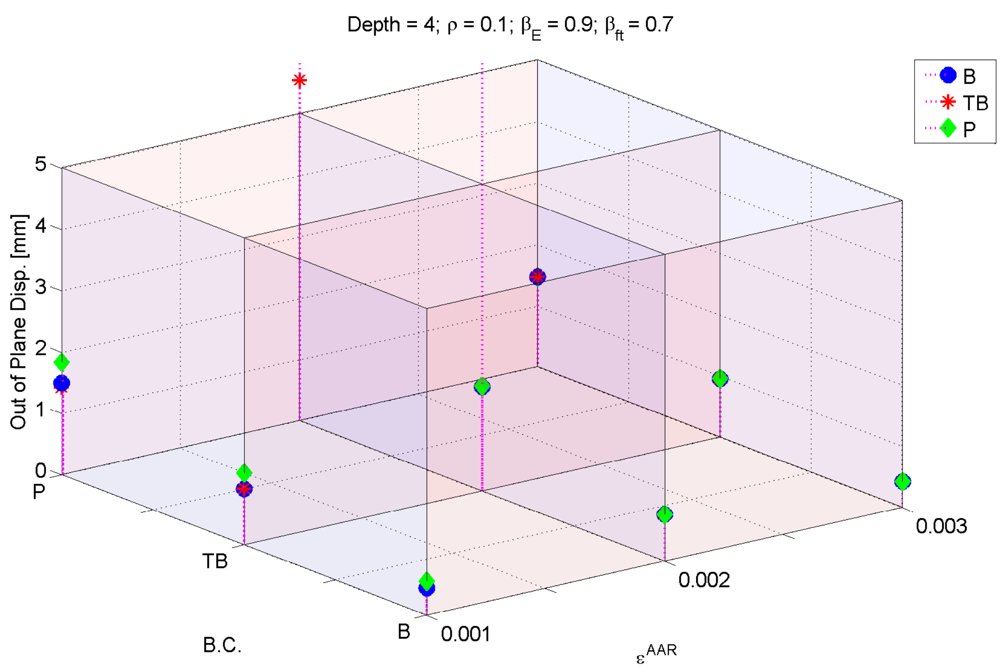

4.2.24 ANALYSIS: DEPTH=4; ρ=0.1;β_E=0.9; β_{FT}=0.9